UNIVERSITY
OF COLOGNE

Tridentate N^C^N Ligands in Cyclometalated Organo-nickel(II) Complexes for C–C Cross Coupling Catalysis

Inaugural Dissertation

for the attainment of the

Doctoral Degree (Dr. rer. nat.)

University of Cologne

Department of Chemistry

Institute for Inorganic Chemistry

Research Group of Prof. Dr. Axel Klein

Submitted by

Lukas Daniel Kletsch (*M. Sc.*)

From Cologne

Cologne, July 2024

Referees:	Prof. Dr. Axel Klein
	Prof. Dr. Dr. (h.c.) Sanjay Mathur
Chair:	Prof. Dr. Stephanie Kath-Schorr
Date of Submission:	05th May 2024
Date of Examination:	17th July 2024

The experimental studies of this thesis were carried out from June 2020 to May 2024 in the Department of Chemistry at University of Cologne under supervision of Prof. Dr. Axel Klein.

“Nickel ist halt kein Palladium…”

Prof. Dr. Axel Klein, **2020**

Danksagung

Ich danke / I would like to thank

Herrn Prof. Dr. Axel Klein sehr herzlich für die Möglichkeit der Promotion. Ich danke Ihnen für die Bereitstellung des sehr spannenden Themas, für die großartige Zusammenarbeit, sowie das stets offene Ohr bei diversen Problemstellungen.

Herrn Prof. Dr. Mathias Wickleder für die Zweitbetreuung. Auch bei Ihnen fand ich stets hilfreiche Ratschläge und fühlte mich bei Ihnen immer willkommen.

Herrn Prof. Dr. Dr. (h.c.) Sanjay Mathur herzlich für die Bereitschaft zur Anfertigung des Zweitgutachtens.

dem Cusanuswerk e.V. für die finanzielle und ideelle Unterstützung seit 2013. Ich bin sehr froh darüber, auch in Zukunft ein (Alt-)Cusaner sein zu dürfen und trage dies in Ehren.

Dr. Nicolas Vogt und Dr. Simon Krakor ganz besonders für die Begeisterung zur Nickelchemie und die Ebnung meines Wegs in den Arbeitskreis Klein.

dem ehemaligen Arbeitskreis Klein: Dr. Maren Krause, Dr. Natalia Arefyeva, Dr. René von der Stück, Dr. Alexander Haseloer, Dr. Aaron Sandleben und Dr. Simon Garbe. Ihr habt mich herzlich aufgenommen und mich in jeder Angelegenheit unterstützt.

dem aktuellen Arbeitskreis, besonders meinen Laborkollegen in 320, Leo Payen, Vladimir Kjartan Stojadinovic und Sascha Schäfer für die gemeinsame Zeit, den Zusammenhalt und den offenen Ideenaustausch und die gemeinsame Bewältigung alltäglicher Hindernisse. Danke an das Platin-Labor, Johannes Hohnsen und Joshua Friedel, für alle gemeinsamen Momente. Danke dem Ecklabor, besonders Rose Jordan für die TD-DFT Rechnungen zu den gemeinsamen Publikationen und die großartige Zusammenarbeit und Maryam Niazi und Eric Anthony Tobechukwu für die bereichernden Einblicke in das Leben im Iran und in Nigeria. Ich danke auch Tobias Greven für die vielen gemeinsamen Wochenenden.

meinen PraktikantInnen und AbsolventInnen: Alicia Köcher, André Zenz, Daniele Cuzzupè, Julian Strippel, Katharina Klupsch, Madalina Iovanica, Basile Roufosse, Manuel Neubauer, Moritz Wyrtki, Sebastian Tenten, Tom Köneke und Tristan Krüger. Ihr wart spitze - Vielen Dank für eure Hingabe zu diesem Thema!

Silke Kremer und Dr. Ingo Pantenburg für die Messung meiner Einkristallproben und Dr. David van Gerven, Tobias Rennebaum und Sean Sebastian Sebastian für die zahlreichen kristallografischen Hilfestellungen.

Dirk Pullem für die Elementaranalysen, Astrid Baum und Gamze Gömec für die Messung der Massenspektren und der Chemikalienausgabe, Ingo Müller, Nihad el Ghachtoun und Sylvia Rakovac.

Prof. Dr. David Vicic for the opportunity to visit Lehigh University to perform catalytic tests in his lab and to learn a lot about life in the US. I would like to thank the wonderful people, that took care of me during my research stay as well: Dr. Wendy Breyer for the possibility of using the instrumentation, Luc Mauro and his family for taking care of me during my stay, also outside the lab, Lydia Emswiler, Cherry Mae Ravidas, Josie Rojo and Shane Hall for all the time (and ice cream), we shared. I also thank the Young Group very much, especially Domenica Fertal, for taking me to all the nice events. You really made me feel home in Bethlehem, PA!

Maike Badorrek ganz herzlich für den liebevollen und stets geduldvollen Umgang mit mir. Ein großer Dank gilt auch unserem gemeinsamen Hund Cocco für stets gespitzten Ohren zum Entladen meiner Sorgen und viel frische Luft beim täglichen Gassigehen. Danke auch an Dietmar, Gaby und Jan für die stetige Unterstützung.

Kai Ostrowski für eine ewig währende Freundschaft. Danke auch an Domenik Schumacher und unser gemeinsames Bandprojekt *Portlux*.

ganz besonders Mama Marlene, Papa Josef und meiner Schwester Laura. Eure Unterstützung hat es mir erst ermöglicht mein Studium und meine Promotion zu bewältigen.

Abstract

New cyclometalated nickel(II) complexes [Ni(N^C^N)X] containing the tridentate N^C^N binding ligands and X coligands were synthesized, characterized and studied in *Negishi* type C–C cross coupling catalytic reactions.

For more than 30 years palladium had been the choice for these important organic transformation reactions. In recent years efforts to replace the expensive and rare palladium through abundant metals has put a focus on nickel due to its chemical similarity. Although a big number of nickel catalysts are meanwhile reported, many mechanistic questions remained open and very reactive or very stable catalysts are still sought for. This project aimed to introduce these new cyclometalated complexes with an anionic N^C^N$^-$ binding motive, representing a very stable ligand scaffold and donating electron density to the nickel atom, thus inducing a strong ligand field and leading to a rather nucleophilic reaction center. Also, these ligands allow subtle finetuning of the reactivity through substitution and replacement of individual groups. The biggest challenge of the project is the development of synthesis procedures to access a very broad variety of ligands and complex structures with the [Ni(N^C^N)X] motive, with X representing the so-called ancillary ligand (or coligand).

Starting from the prototypical N^HC^N protoligand (ligand precursor) 1,3-di(2-pyridyl)benzene, a variety of substituted N^HC^N molecules was synthesized and studied, in which the electronic properties of the central anionic phenide ring were varied using electron withdrawing and electron donating groups and the peripheric pyridines replaced by other *N*-containing aromatic rings. These substitutions generated limitations of the recently published and very versatile base-assisted C–H activation of the N^HC^N protoligands for the complex synthesis which made halide (X = Cl, Br, or I) substitution at the central C position necessary (N^XC^N). The protoligands were successfully converted to the target complexes through C–H activation or oxidative addition and a large variety of so far unreported organometallic Ni(II) complexes were obtained, which were characterized by various spectroscopic and electrochemical methods. For selected examples, the full triad of nickel, palladium and platinum complexes of the type [M(II)(N^C^N)X] was synthesized for the first time, replacing a previously reported undesirable method used highly toxic organomercury intermediates. First attempts to vary the coligands X were successful for all halides and NCS. In addition, a variety of carboxylates, alkoxides, perfluorinated alkylides, and the literary-known carbazolate were introduced as coligands either directly by using the corresponding organic Ni(II) salts $Ni(ER)_2$ (E = C, O or N) or by exchanging the halide coligand from an isolated [Ni(Py(Ph)Py)X] complex with the use of Ag(I)- or Li(I) salts. A new route of using the nitrato complexes as a precursor for coligand exchange reactions was a breakthrough for more possible coligands on [Ni(N^C^N)(ER)] complexes.

First tests of this broad variety of Ni(II) complexes in C–C cross coupling reactions under *Negishi* conditions gave the target products selectively in good yields.

Table of Content

1 Introduction

Since the past few decades, C–C cross coupling reactions became more and more popular and indispensable for modern organic synthetic chemistry. Very prominent examples of highly selective and effective cross coupling reactions are represented through the *Stille*-,[1] *Kumada*-,[2] *Hiyama*-,[3] *Suzuki-Miyaura*-,[4] and *Negishi* [5] cross coupling reactions. To underline the importance of these reactions, *Akira Suzuki*, *Ei-ichi Negishi*, and *Richard Heck*,[6] originator of the Heck-Reaction, a cross coupling reaction for a direct olefination of aryl bromides, were honored through the Nobel Prize in 2010.[7] In the above mentioned cases, it is essential to use a catalyst, which often is reported to be of an organometallic transition metal compound, specifically as palladium (pre)catalysts.[6, 8-11] The low natural abundance of palladium [12, 13] and its broad application in various types of catalysis,[14-17] has massively increased its value and price in the past three decades.[18] In recent years, attempts have been made to replace the expensive palladium through its lighter and cheaper congener nickel[19-22] or neighbouring 3d metals, such as iron,[23-25] or cobalt.[19, 26, 27]

The cross coupling reaction mechanism (Figure 1-1) for palladium-based catalysts is postulated to start with the formation of the active catalyst [Pd(L)$_2$] gets undergoing an oxidative addition, in which the catalyst inserts into an organohalide R–X bond of an alkyl or arylhalogenide and increases its oxidation state from 0 to +II (alternatively from +II to +IV).

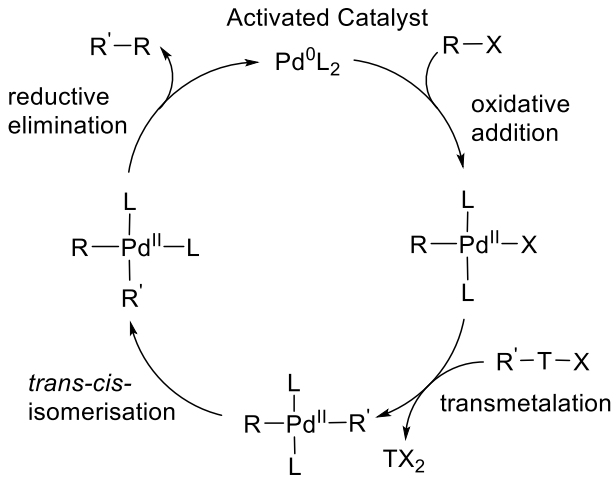

Figure 1-1 Postulated mechanism for C–C cross coupling reactions with the use of a transmetalating agent R'–T–X. Reproduced from [4].

For the next step, a transmetalating agent R'–T–X exchanges the halide ligand X by the second organic function R' at the catalyst metal center and releases an inorganic halide salt. A

trans-*cis*-isomerization follows, bringing the two carbanionic ligands into a *cis* position to each other, which allows to form the coupling product R–R' in a reductive elimination step, restoring the active Pd(0) catalyst. The above-named reactions show essentially the same mechanism and only differ in the transmetalating agent R'–T–X, as summarized in Table 1-1.

Table 1-1 Types of C–C cross coupling reactions, defined by their transmetalating agent R'–T–X.

Cross coupling reaction	**Transmetalating agent *R'–T–X***
Stille	R'–SnR_3
Kumada (mainly Ni-catalyzed)	R'–MgX
Hiyama	R'–SiR_3
Suzuki-Miyaura	R'–$B(OR)_2$
Negishi	R'-ZnX

Established palladium catalysts, that are used in these reactions mostly bear a palladium(0) or palladium(II) metal center. Pd(II) compounds are usually considered as pre-catalysts. In the presence of bases such as NEt_3 and water, they undergo reduction to the active Pd(0) catalysts.[28-34] An early and very popular example is the *tetrakis*-triphenylphosphine palladium(0) catalyst [$Pd(PPh_3)_4$], that was first synthesized in 1957 by *Malatesia et al.*[35] by a reduction of Pd(II) chloride with hydrazine in presence of triphenylphosphine. In 1984 the Pd(II) complex [$Pd(dppf)Cl_2$] (dppf = *bis*(diphenylphosphino)ferrocene) was added to the broad series of palladium catalysts for C–C cross coupling reactions.[36]

In view of the analogous electronic d^8 configuration, the replacement of Pd(II) by Ni(II) looks. Indeed, for both elements, the oxidation state +II allow for a similar square planar coordination for organometallic Ni and Pd complexes. However, while reduction of Pd(II) almost inevitably leads to Pd(0),[28-34] reduction of Ni(II) leads in many cases to Ni(I) complexes.[37-40] The same is true for oxidized species, which are frequently Pd(IV), but Ni(III).[41-53] Pd(III) is considered as an exotic oxidation state,[49, 54-58] while Ni(IV) can only be stabilized using strong σ-donor ligands.[42, 46, 59-65] Thus, while Pd prefers 2-electron steps with the stable oxidation states 0, +II and +IV, Ni usually undergoes single electron transfer reaction connecting Ni(0), Ni(I), Ni(II), Ni(III), and in some cases Ni(IV).

The journey of nickel, as a catalyst for C–C cross coupling reactions goes back to 1954 and was firstly reported by *Kharasch et al.*,[66] in which Ni(0) was used for aryl- and alkyl halide cross coupling reaction (Figure 1-2).

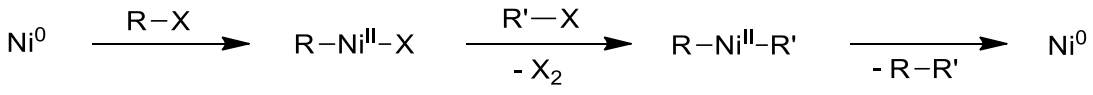

Figure 1-2 Postulated mechanism for C–C cross coupling reactions by *Kharasch et al.* using Ni(0) as a catalyst. Reproduced from [66].

In this early work it was also found that the ligand plays a decisive role for the catalytic performance.[45, 67] For phosphine ligands, the mechanism shown in Figure 1-1 seems to operate. Single reduction of Ni(II) leads to Ni(I) which disproportionates to Ni(0) - the active catalyst - and Ni(II). In contrast to this, bidentate *α*-diimine ligands such as 2,2'-bipyridine (bpy) stabilize the Ni(I) oxidation state through charge transfer to the diimine π*-system. Such formal Ni(I) species undergo oxidative addition to Ni(III) species (Figure 1-3).[45, 67-69]

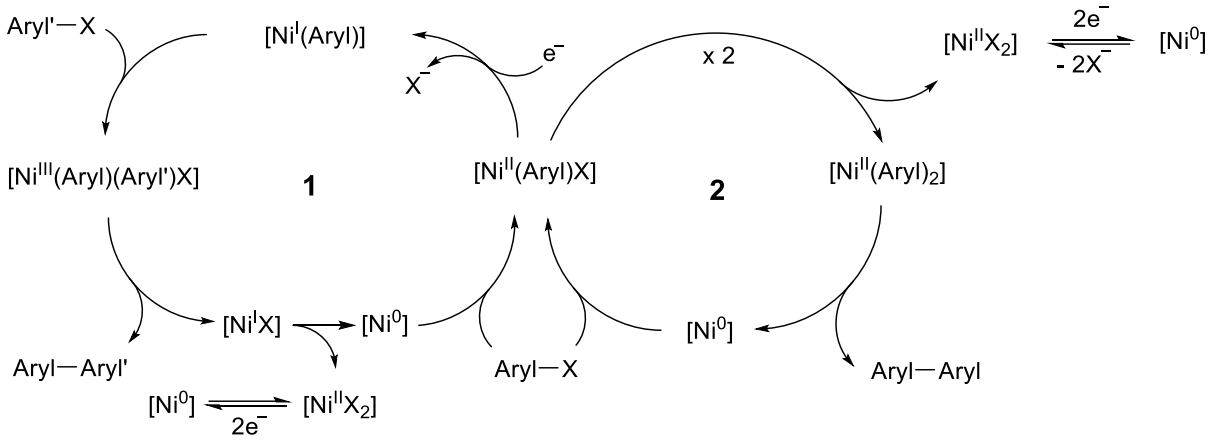

Figure 1-3 Postulated electrocatalytic mechanism of a nickel bipyridine complex in a C–C cross coupling reaction; X = halides. Reproduced from [67, 69].

However, there are further differences to the Pd-based cycle. Starting from the [Ni(II)(Aryl)X] catalyst (shown in the center in Figure 1-3), two competing catalytic cycles have to be considered. In cycle 1, it gets reduced to a Ni(I) species leading to an elimination of a halide. Next, it is followed by an oxidative addition of an Aryl'-halide forming a Ni(III) compound. This intermediate can eliminate the cross coupling product, returning to a Ni(I) species, that might undergo a disproportionation to Ni(0) and Ni(II). The Ni(0) product can undergo in an oxidative addition to form the [Ni(II)(Aryl)X] species. Cycle 2 shows the possible self-transmetalation reaction of the complex [Ni(II)(Aryl)X] leading to [Ni(II)X_2] and [Ni(II)(Aryl)$_2$]. The latter can undergo the unwanted reductive elimination of the homocoupling product Aryl–Aryl. The resulting Ni(0) species can undergo an oxidative addition reforming the starting catalyst.

The problem of lacking selectivity in cross coupling reactions with [Ni(bpy)X_2] (bpy = 2,2' bipyridine) complexes, could be improved by using 2,2':6',2''-terpyridine (terpy). Terpy, like bpy, represents the vast group of oligopyridine ligands.[70-72] Its synthesis and the first transformations to the corresponding Ni(II) complexes were published in the early 30s by *Morgan* and *Burstall*.[73, 74]

Terpyridine nickel complexes of the type [Ni(terpy)X_2] show catalytic activity with regard to the attachment of carbon–carbon and carbon–heteroatom bonds under *Negishi* conditions and in electrocatalysed coupling reactions. [75-79] The group of *Vicic* focused on different terpyridine

systems.[80-83] They found that reduced complexes [Ni(terpy)X] (X = halides or CH_3), which are either described as [Ni(I)(terpy)(X)] or [Ni(II)(terpy^{-})(X)],[82, 83] are able to perform the coupling of a primary zinc organyl with non-activated alkyl halides.[84] The postulated mechanism of the cross coupling catalysis is shown in Figure 1-4 for the example of [Ni(terpy)I].[80, 85]

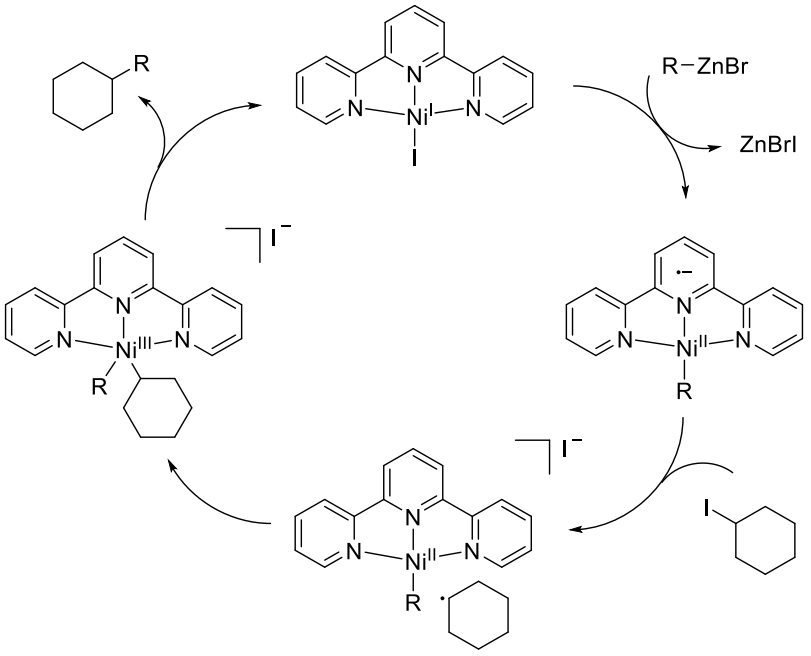

Figure 1-4 Postulated catalytic cycle for cross coupling reactions using [Ni(terpy)X] complexes as catalyst. Reproduced from [80, 83, 85].

As detailed mechanistic studies showed, in the first step, the starting reduced Ni complex undergoes a transmetalation reaction with a zinc organyl RZnBr (with R = alkyl group), forming the corresponding complex reduced [Ni(terpy)R] complex, in which the terpy ligand is present in its radical anionic form [Ni(II)(terpy^{-})R]. In the second step an electron is transferred from the terpy^{-} ligand to the iodo cyclohexane forming an iodide anion and a cyclohexyl radical, which then adds to the cationic Ni(II) species [Ni(II)(terpy)R]$^{+}$ forming [Ni(III)(terpy)R(*c*hex)]$^{+}$. In a last step, the coupling product cyclohexane–R can be formed through a reductive elimination and the starting reduced complex gets regenerated. The pentacoordinate Ni(II) precatalysts [Ni(terpy)X_2] are stable compounds[86] and upon reduction yield the reduced complexes [Ni(terpy)X] which are soluble in organic solvents. However, the positive charge of the cationic Ni(II) species [Ni(II)(terpy)R]$^{+}$ and [Ni(III)(terpy)R(*c*hex)]$^{+}$ might lead to solubility issues in organic solvents. This led to the idea of substituting one pyridine in the N^N^N tridentate terpy ligand by a carbanionic phenide unit producing cyclometalated anionic $^{-}$C^N^N or N^C^{-}^N ligands for neutral tetracoordinated Ni(II) catalyst precursors [Ni(C^N^N)X] or [Ni(N^C^N)X].[86-92]

Early work by *Klein et al.* featured the complexes [Ni(bpy)(Mes)X] [90] (Mes = 2,4,6-trimethyl-phenyl), which showed good solubility in organic solvents and were active in various types of cross coupling catalysis.[45, 93-98] Combining the structural motives of the complexes [Ni(bpy)(Mes)X] and the terpy derivatives $[Ni(terpy)X]^+$ leads straight to the cyclometalated complexes [Ni(Phbpy)X] containing the carbanionic $^-$Phbpy ligand (HPhbpy = 6-phenyl-2,2'-bipyridine).[89, 91, 99-101] The C^N^N protoligand 6-phenyl-2,2'-bipyridine (HPhbpy) was synthesized the first time by *Knott* and *Breckenridge* in 1954.[102] *Constable et al.* published the first cyclometalated Pt(II) and Pd(II) (but also Ru(II), Rh(III) and Au(III)) complexes in 1990, in which the ligand system $^-$Phbpy was applied for the first time.[103, 104] The first [Ni(Phbpy)X] complex followed 24 years later (Figure 1-5) through oxidative addition of the Ni(0) precursor $[Ni(COD)_2]$ into a Br–C bond of the Br–Phbpy protoligand to produce [Ni(Phbpy)Br].[99] The nickel centre is coordinated in a tridentate manner by the aromatic ligand and the coordination sphere is saturated by a bromide coligand.

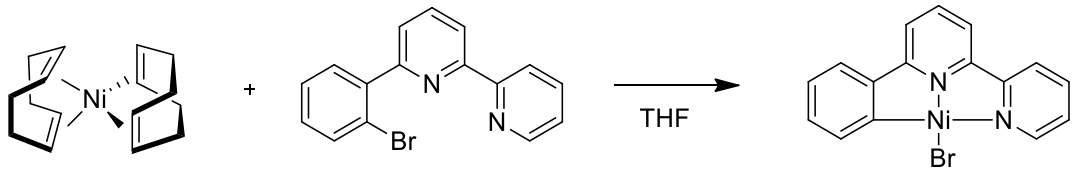

Figure 1-5 First synthesis of [Ni(Phbpy)Br] through an oxidative addition of $[Ni(COD)_2]$ into the C–Br bond. Reproduced from [99].

The [Ni(Phbpy)X] compounds showed essential advantages compared with the $[Ni(terpy)X]^+$ complexes, e.g. their solubility in organic solvents due to the neutral charge. Further, the electronic structure at the phenyl unit can be modified independently of the bipyridine unit, due to the asymmetric character of the ligand. Through electron donating groups at the phenyl unit, the *Lewis*-basicity of the ligand can be enhanced leading to an increased electron density at the nickel centre. The π-acceptor function of the bipyridine unit can be increased by electron withdrawing groups.[105, 106] A number of Ni(II) complex derivatives have been produced, differing in their coligands but also in their ligand backbone (Figure 1-6).

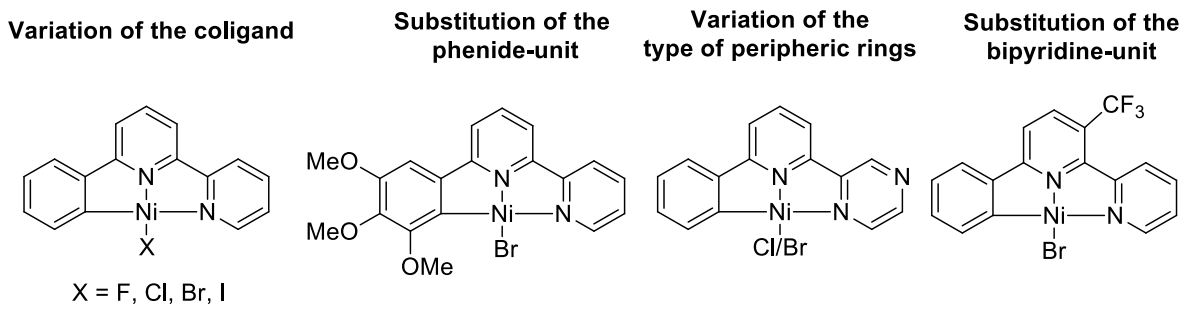

Figure 1-6 Examples of reported cyclometalated [Ni(C^N^N)X] complexes. Reproduced from [89, 91, 99-101]

Far simpler than the oxidative addition of C–X ligand derivatives to Ni(0) precursors in terms of the required ligands is the direct C–H nickelation using a Ni(II) precursor and the simple protoligand. This reaction occurs readily for Pd and Pt[104] either as base-assisted deprotonation-metalation or electrophilic substitution.[107] In 2020 the *Klein et al.* published first ground-breaking results.[101] It showed, that it indeed is possible to force a direct C–H activation to form the complex [Ni(Phbpy)Br] by heating Ni(II) bromide and the protoligand HPhbpy in non-protic solvents in the presence of the bases K_2CO_3 and KOAc. Quantitative yields were obtained starting from the precursor complex [Ni(HPhbpy)Br_2] (Figure 1-7).[101]

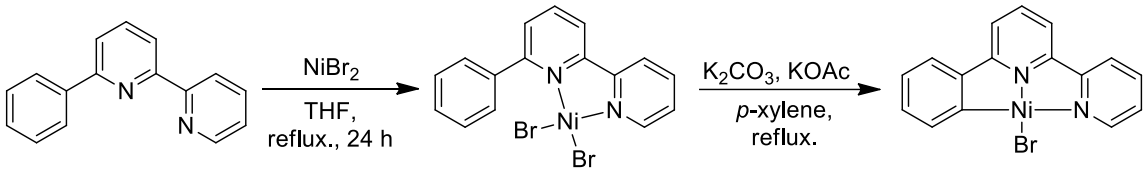

Figure 1-7 Synthesis of [Ni(Phbpy)Br]. The base-assisted C–H activation with KOAc/K_2CO_3 in *p*-xylene. Reproduced from [101].

During the research on the exchange of coligands, a central problem was identified with methyl- [99], fluoro- [91] and pentafluorophenyl- [91] derivatives. These complexes undergo an elimination reaction in solution, reverting to a N^N-bidentate coordination (Figure 1-8). The rapid elimination occurs presumably due to the *cis*-configuration of the carbanion with the cleaving X group. However, a recent publication reports the isolation of [Ni(Phbpy)CN] in poor yields and compared it to the Pd and Pt analogues, which were way easier to handle and to isolate.[108]

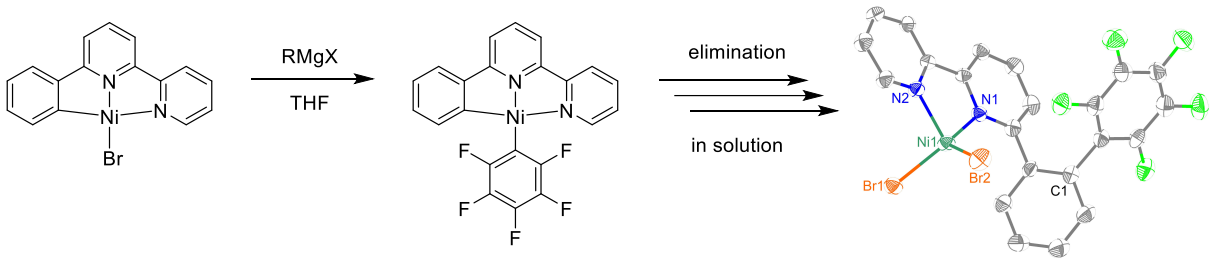

Figure 1-8 Reductive elimination from [Ni(Phbpy)C_6F_5] in solution. (CCDC: 1484538). Reproduced from [91, 109].

Nevertheless, the successfully synthesized [Ni(C^N^N)X] (X = F, Cl, Br, I) complexes were investigated for their catalytic properties in two different *Negishi*-like C–C cross coupling reactions (Figure 1-9).[109] In both, a sp^2 hybridized carbon atom was coupled with a sp^3 hybridized carbon atom.

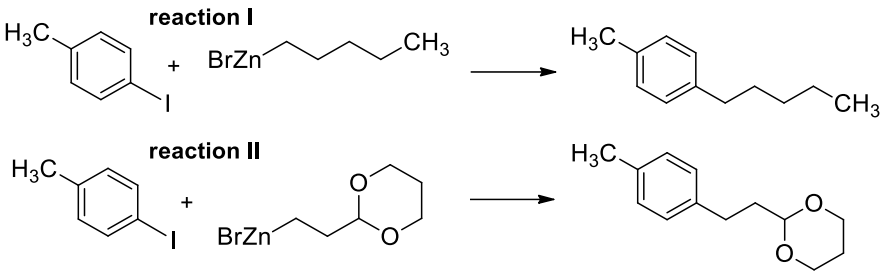

Figure 1-9 Investigated *Negishi*-like cross coupling reactions for catalytic tests of [Ni(C^N^N)X] complexes. Reproduced from [109].

[Ni(C^N^N)X] complexes appeared to be very useful for this purpose and shows overall yields of up to 74%. The conversion and selectivity are observed to be harshly influenced by the electronic properties of the tridentate ligand, which was changed within the first series of catalysts by introducing electron-withdrawing and -donating groups on the σ-donating site and on the π-accepting bipyridine unit. The most effective catalyst is [Ni(3-MeOPhbpy)Br] with a selective heterocoupling of 45%. The coligand plays a crucial role in this aspect as well and shifts the total yield in both reactions between 43 and 64% (Figure 1-10).[109]

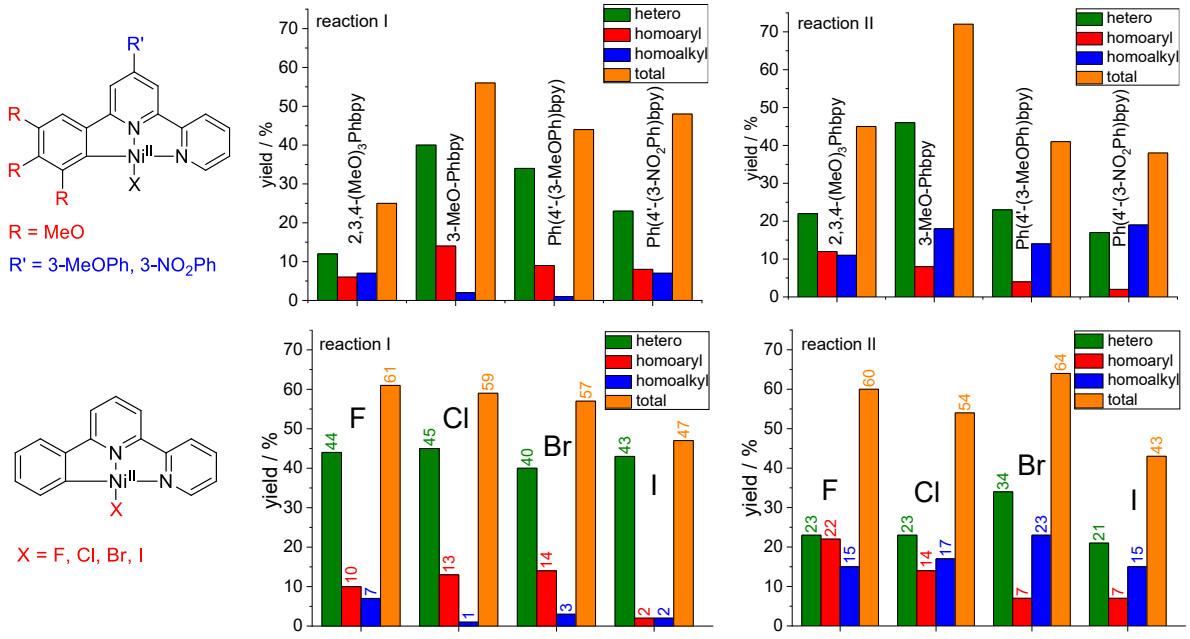

Figure 1-10 Yields of *Negishi*-type reactions of [Ni(C^N^N)X] catalysts. From [109].

Unfortunately, the small number of different catalysts, especially in regard of the coligand, in view of the largely varying yields and selectivity do not allow a structure-activity correlation at this stage.

To increase the number of potential catalysts by e.g. solving the problem of an elimination, the change of the cyclometalated position needed to be considered. Since 2014, research

established a N^C^N coordination on a nickel(II) centre, forming [Ni(N^C^N)X] complexes. First Ni(II) complexes have been reported by *van Koten* [110-112] and *Zargarian* (Figure 1-11).[113]

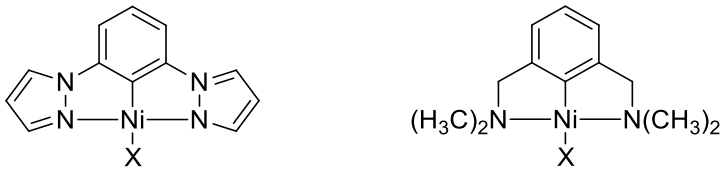

Figure 1-11 Two literary known types of [Ni(N^C^N)X]complexes. Reproduced from [99, 110-113].

To synthesize the N^C^N analogues complexes to the previously synthesized C^N^N systems, the ligand 1,3-di(2-pyridyl)benzene (PyHPhPy) needs to be introduced. PyHPhPy was firstly synthesised by the research group of *Sauvage* in 1991[114] following the synthesis of 1,3-di(2-pyridyl)benzene (PyHPhPy) published by *Bönnemann* in 1974.[115] In this report Ru(II) complexes were synthesized and characterized. By using [Ru(tterpy)Cl_3] (tterpy = 4'-*p*-tolyl-2,2',6',2''-terpyridine) and $AgBF_4$ as a dechlorinating agent, then adding PyHPhPy and heating it in acetone, the first complex carrying PyPh–Py as a tridentate ligand was synthesized, defined as [Ru(tterpy)(PyPhPy)]BF_4, in which the Ru centre is octahedrally coordinated. The first square planar complexes of the type [M(PyPhPy)X] were synthesized in 1999 by *Carmen et. al*.[116], in which $K_2[PtCl_4]$ was added to the protonated ligand PyHPhPy in acetic acid, which led to the desired complex [Pt(PyPhPy)Cl] (Figure 1-12).

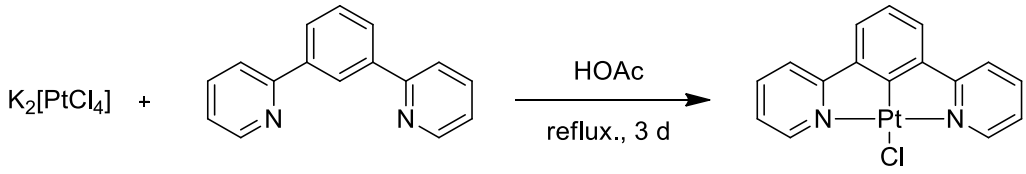

Figure 1-12 First synthesis of [Pt(PyPhPy)Cl] *via* direct C–H activation in HOAc. Reproduced from [116].

These species grew in interest because of their luminescent properties so researchers, especially the group of *Williams*, focused on these systems during the past decades and found many of these easily accessible, highly emissive and easy tuneable compounds.[117-121]

Six years later the group of *Sansoni* [122] published the first Pd(II) derivative. The ligand PyHPhPy was precoordinated to Hg(II) acetate with the aid of LiCl in methanol in a first step leading to the precursor [Hg(PyPhPy)Cl], in which the Hg(II) centre is bound monodentately to the carbanionic phenyl unit. In a second step this precursor gets transmetalated with Pd(II) acetate under addition of a lithium salt LiX to produce the target complex [Pd(PyPhPy)X]. Hereby, the bromido, chlorido, and iodido complex could be successfully synthesized (Figure 1-13).

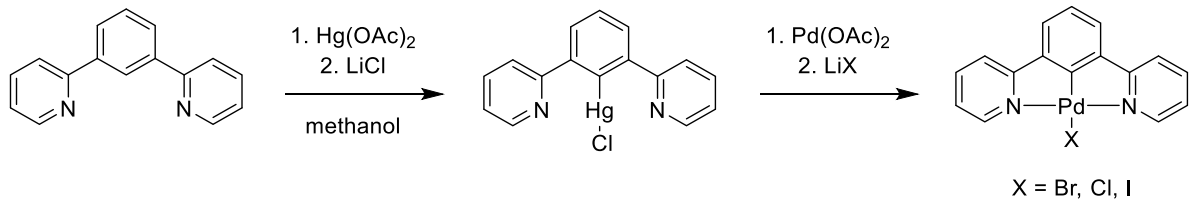

Figure 1-13 Synthesis of [Pd(PyPhPy)X] *via* transmetalation of an intermediary isolated organomercury species. Reproduced from [122].

These species did not become as popular as their Pt(II) analogues, which might be reasoned by the toxicity of the intermediate and therefore hard accessibility of these species. The relevance of this intermediary isolated organomercury species is explained by a different preferred cyclometalation for the reaction of a Pd(II) salt with the protoligand in acetic acid, firstly found by *Cardenas et al.* in 1999.[116] Nevertheless, these species might be auspicious candidates for luminescent applications as well and therefore a handful of research groups still focussed on their investigations.[123-126]

The reawakening of this topic happened in 2020, in which three independent research groups published synthetic routes for the nickel analogues, which were not known up to then (Figure 1-14).[92, 127, 128]

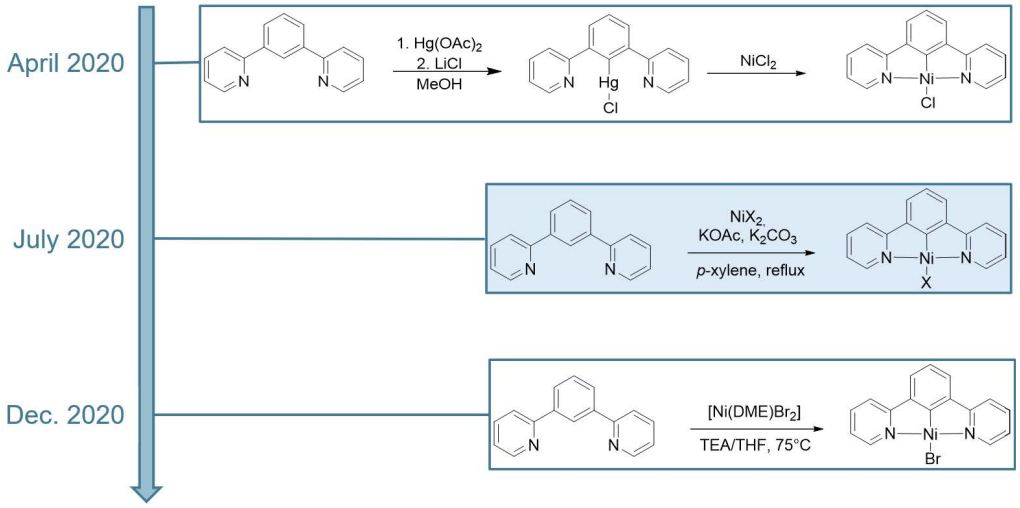

Figure 1-14 Chronology of the first publications of [Ni(PyPhPy)X] from April to December 2020. *Top*: Transmetalation from an organomercury compound by *Yam et al. Middle*: Base-assisted C–H activation in *p*-xylene by *Klein et al. Bottom*: Use of a strong base and a soluble Ni(II) precursor for the C–H activation. Reproduced from [92, 127, 128].

In April 2020, *Yam et al.* published the first [Ni(PyPhPy)X] compounds, that were accessed through the same synthetic route as their Pd(II) analogues, namely the transmetalation *via* an intermediary formed and highly toxic organomercury compound.[122] These species were investigated for their luminescent properties and it turned out that [Ni(PyPhPy)R] complexes

might be interesting candidates for photoluminescence, as [Ni(PyPhPy)Carbazolate] already showed.[127] These results were followed immediately by another synthetic route for these species by *Klein et al.* in July 2020,[92] which successfully omitted the use of highly toxic organomercury species and used commercially available and cheap chemicals. This C–H activation method was assisted by the combination of bases KOAc and K_2CO_3, which already led to a successful C–H activation for [Ni(Phbpy)X] as well.[101] The key was to find a aprotic nonpolar and easy dryable solvent with a high boiling point and therefore *p*-xylene was the optimum choice for this purpose. Lastly, a third approach was published by *Wendt et al.*,[128] in December 2020, where a soluble Ni(II) precursor [Ni(DME)Br_2] and NEt_3 were used in THF to synthesize the desired compound for an application in *Kumada*-like C–C cross coupling reactions (selective heterocoupling yield for [Ni(PyPhPy)Br]: 47%).

From 2020 onwards, [Ni(N^C^N)X] complexes gained attention from different research groups again, since an easy access was found now. Our work founded a new field of research, which published results showed different interesting properties for these compounds, like luminescence of C–F bond activations.[129-132]

2 Aim of this Work

Starting from the initial synthesis of the [Ni(PyPhPy)X] (X = Cl, Br, I) in 2020,[92] the scope of this dissertation was the synthesis and characterization of novel [Ni(N^C^N)X] derivatives and the search for trends within their optical and electrochemical properties. The initial di(2-pyridyl)benzene ligand will be substituted firstly by introducing substituents on the central phenide unit, which represents essentially a variation of the electron density in the σ-donor carbanionic C function of the ligand. This function is essential for the electron inventory of the Ni(II) center and variation will probably have an impact on the highest occupied molecular orbitals (HOMO) of the complexes and the electrochemical oxidation potentials which are assumed to be due to Ni(II)/Ni(III) redox processes, as inferred from our early studies.[92] This will be followed by a variation of the π-accepting units by exchanging the pyridyl functions by other *N*-heteroaromatic units. They are forming the electron-accepting part of the complex and constitute the lowest unoccupied molecular orbital. Variations in these parts will have an impact on the ligand-centered electrochemical reduction potentials.[101] In combination, the σ-donating and the π-accepting part will very probably determine the optical properties of the complexes, as from previous studies, metal-to-ligand charge transfer (MLCT) transitions, in addition to ligand-centered π–π* (LC) transition dominate the electronic absorptions. Finally, the coligand will be varied in this work. Remarkably, this was not possible for [Ni(C^N^N)X] analogues,[109] but the trans-position of the carbanion to the X coligand might facilitate the exchange (Figure 2-1).

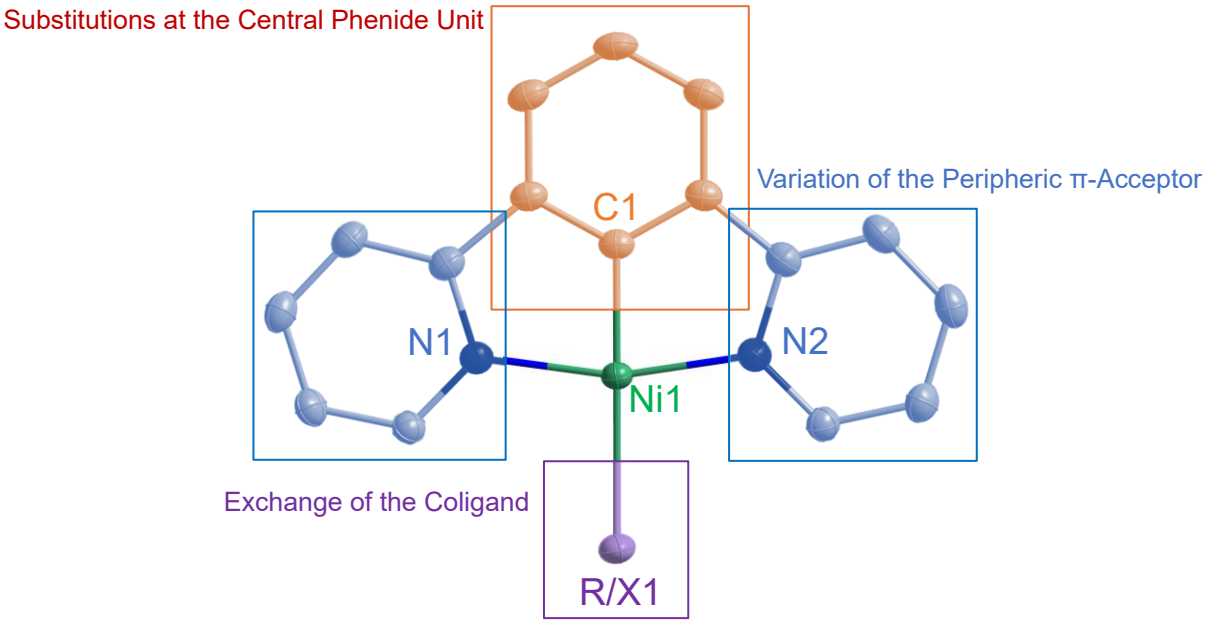

Figure 2-1 Structural variations on the complexes [Ni(N^C^N)X]: Substitutions at the central (C1) phenide unit, the variation of the peripheral (N1 and N2) π-acceptor units and the exchange of the coligand (R/X1).

Some of these changes were already investigated for [Pt(N^C^N)X] complexes by *Wang et al.*,[117] which would allow a direct comparison of these properties with directly correlating platinum derivatives.

The synthesis of the ligands should mainly be performed using the recently improved *Negishi* cross coupling synthesis [92] in which the reactive species is the 2-pyridyl zinc chloride (2-PyZnCl). This reaction will possibly be the first choice for the synthesis of central ring substituted N^C^N protoligands. With the variation of the peripheric *N*-heteroaromats, problems might occur depending on the stability of the intermediary present and highly reactive zinc organyls. In such cases a different C–C cross coupling method needs to be considered. The idea of the use of phenylene-1,3-diboronic acid and the respective bromoaryl under *Suzuki-Miyaura* conditions inverts the reactivity towards the phenyl unit and might be the right choice for these problems (Figure 2-2).

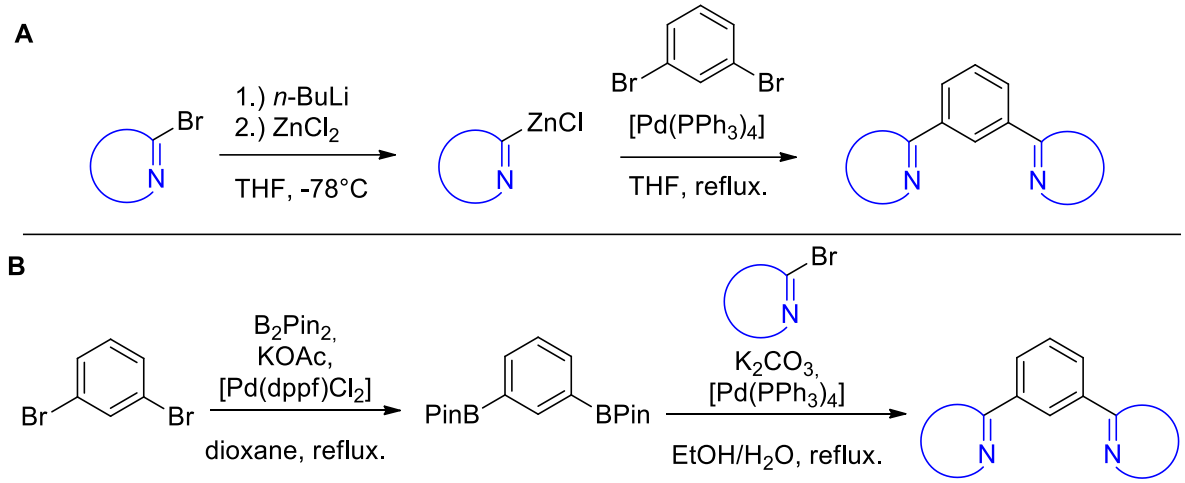

Figure 2-2 *Negishi* (A) vs. *Suzuki-Miyaura* (B) cross coupling used for the synthesis of peripheric ring substituted N^C^N protoligands.

The synthesis of the complexes should be performed basing on recent results using the base-assisted C–H activation by *Klein et al.* [92] with the addition, that the oxidative addition, which perfectly worked for [Ni(Phbpy)X],[99] might be a fourth synthetic pathway for the synthesis of [Ni(N^C^N)X]. The benefit would be the mild but effective reaction conditions for a cyclonickelation, which might be important for less stable N^C^N ligand systems (Figure 2-3).

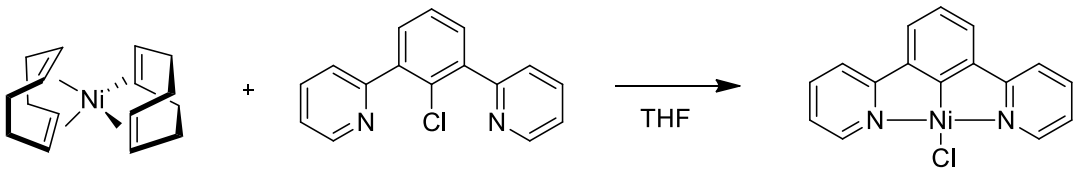

Figure 2-3 Postulated reaction for a cyclonickelation of N^CCl^N ligands *via* oxidative addition.

All the synthesized and fully characterized compounds should then be taken to *Lehigh University,* PA, USA. The expertise of *Prof. Dr. D. A. Vicic* for catalytic experiments should help to investigate these compounds for their performance in *Negishi*-like C–C cross coupling reactions. These experiments should be performed analogously to the ones, that were performed by [Ni(C^N^N)X] complexes, to allow to draw conclusions in comparison to these derivatives.[109] Therefore two different reaction should be performed by novel [Ni(N^C^N)X] compounds (Figure 2-4) and the conversion yields should be determined using GC-MS.

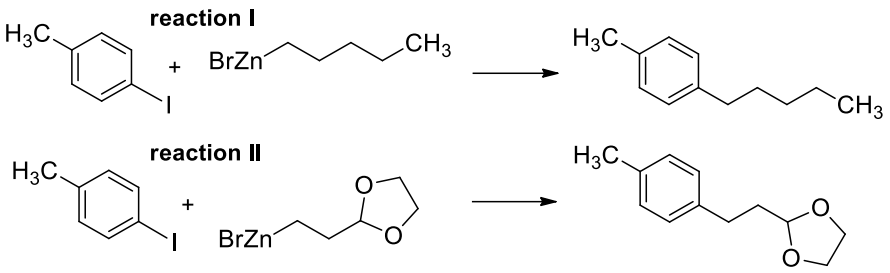

Figure 2-4 Planned *Negishi*-like cross coupling reactions for catalytic tests of [Ni(N^C^N)X] complexes.

3 Results and Discussion

3.1 Central C-ring Substituted [Ni(Py(Ph)Py)Br] Complexes

3.1.1 Synthesis and Characterization of the Protoligands N^CH^N

In the course of the investigation of central ring substituted [Ni(N^C^N)X/R] complexes, a number of substituted N^CH^N protoligands (ligand precursors) were synthesized. Based on a *Negishi* cross coupling reaction[5] for the synthesis of the unsubstituted (standard) ligand 1,3-di(2-pyridyl) benzene Py(HPh)Py by *Klein et al.* in 2020,[92] the decision for the same route for central ring substituted derivatives was made. In all cases, the reaction sequences started with a lithiation and transmetalation of 2-bromopyridine, yielding the reactive intermediate 2-pyridyl zinc chloride. This was *in situ* used in a reaction with a substituted 1,3-dibromo-benzene derivative in a 2:1 ratio, catalyzed by Pd(0) (Figure 3-1). After purification *via* column chromatography, the products analyzed by ^{1}H NMR spectroscopy, mass spectrometry (MS) and elemental analysis (for details, see Experimental Section, Chapter 5.2.2).

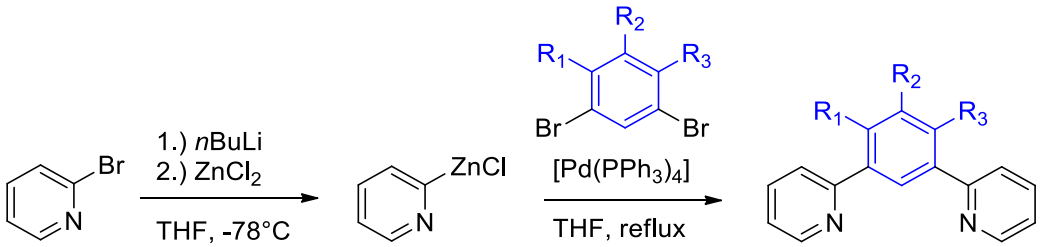

Figure 3-1 *Negishi*-type cross coupling reaction for a substitution of the central phenide unit of the tridentate N^CH^N protoligands.[92]

Most substituted 1,3-dibromobenzene derivatives were commercially available (see Materials and Methods, Chapter 5.1). 1,3-dibromo-4,5,6-trimethoxybenzene was synthesized starting from 1,2,3-trimethoxybenzene in a bromination reaction using 1,3-dibromo-5,5'-dimethyl-hydantoin (DBH), adapted from *Matsumoto et al.*,[133] with a yield of 67% (Figure 3-2, details in the Experimental Section, Chapter 5.2.1).

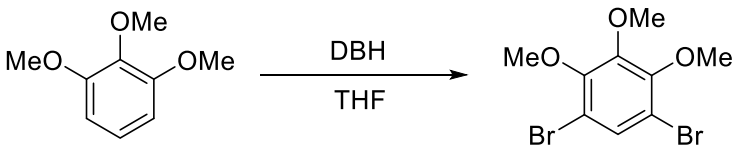

Figure 3-2 Bromination reaction of 1,2,3-Trimethoxybenzene using DBH yielding 1,3-dibromo-4,5,6-trimethoxy-benzene (DBH = 1,3-dibromo-5,5'-dimethylhydantoin).[133]

In total eleven different protoligands bearing electron-withdrawing groups (EWGs), as well as electron-donating groups (EDGs) R_1 to R_3 were synthesized in yields ranging from 48 to 97% as off-white solids (Table 3-1).

Table 3-1 Synthesized N^C^N protoligands bearing a substituted phenide ring with each isolated yield.

	EWG substituted protoligands		**EDG substituted protoligands**	
Monosubstituted N^C^N ligands	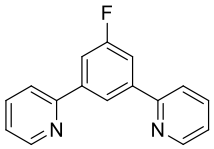 **A:** Py(**5F**PhH)Py Yield: 80%	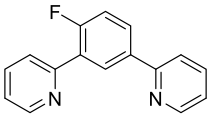 **B:** Py(**4F**PhH)Py Yield: 86%	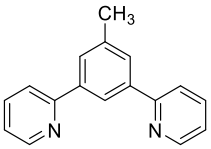 **C:** Py(5**Me**PhH)Py Yield: 93%	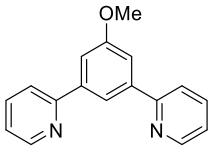 **D:** Py(**5MeO**PhH)Py Yield: 96%
	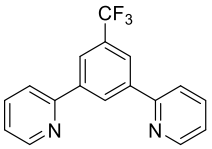 **E:** Py(**5CF$_3$**PhH)Py Yield: 97%	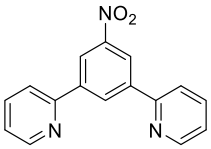 **F:** Py(**5NO$_2$**PhH)Py Yield: 41%	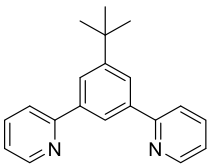 **G:** Py(**5BuPh**H)Py Yield: 91%	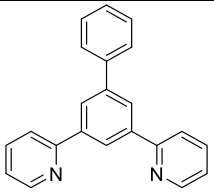 **H:** Py(**5Ph**PhH)Py Yield: 87%
Disubstituted N^C^N ligands	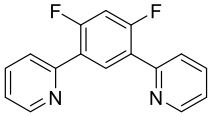 **I:** Py(**4,6FPh**H)Py Yield: 71%		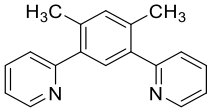 **J:** Py(**4,6MePh**H)Py Yield: 84%	
Trisubstituted and other N^C^N ligands	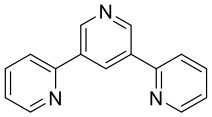 **K:** Py**Py**HPy Yield: 71%		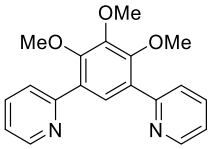 **L:** Py(**4,5,6MeOPh**H)Py Yield: 30%	

The synthesis and characterization for Ligands A – D, I and J, were published [117, 121, 134] using a *Stille* cross coupling analogously to *Cardenas et al.* from 1999 [116] synthesis to access those and use them in Pt(II) complexes. Ligand C – E were known earlier by preparation using *Negishi* conditions.[135-137] Ligands G and K were firstly synthesized *via Suzuki-Miyaura* conditions.[138, 139] And ligands F, H and L are literary unknown.

Colorless single crystals of Py(5BuPhH)Py (Left), Py(5PhPhH)Py (Central), Py(4,5,6MeOPhH)Py (Right) for single-crystal XRD (SC-XRD) were obtained from saturated solutions after column chromatography (Figure 3-3).

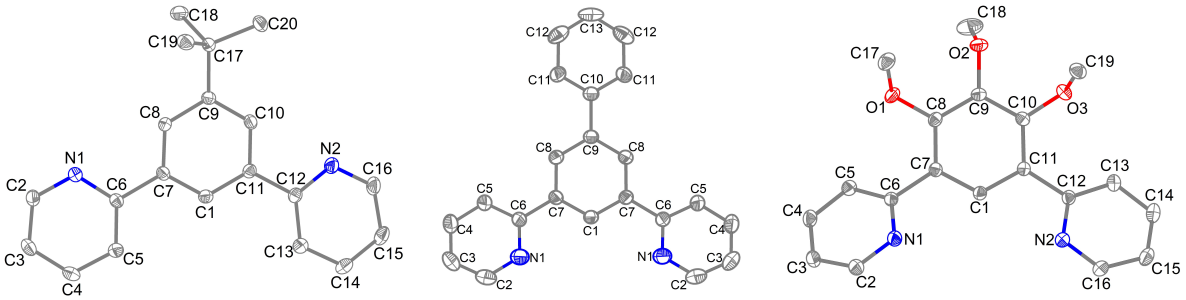

Figure 3-3 Molecular structures of selected central C-ring substituted N^C^N ligands. *Left:* Py(5BuPhH)Py; *Middle:* Py(5PhPhH)Py; *Right:* Py(4,5,6MeOPhH)Py. Ellipsoids are shown with a 50% probability. Hydrogen atoms are omitted for clarity.

These three compounds crystallized in a primitive lattice with four units per unit cell each (all values are summarized in Table 3-2). While the asymmetric unit of the 5-*tert*-butyl substituted ligand (Figure 3-3, left) is formed by one full molecule, the one of the 5-phenyl substituted one (Figure 3-3, central) has a C_2 axis through the central biphenyl unit and therefore only half of the molecule forms the asymmetric unit. For the trimethoxy substituted ligand (Figure 3-3, right) two molecules constitute the asymmetric unit. The crystal structures (see Chapter 7.3.1 to 6.3.3) were investigated for π-stacking interactions showing a Py–Py distance of 3.98 Å for the 5-*tert*-butyl, a Ph–Ph distance of 4.15 Å for the 5-phenyl and a Py–Py distance of 4.15 Å for the 4,5,6-trimethoxy substituted ligand, all exceeding the definition of *Janiak* for π–π interactions. The torsion angles between a pyridyl- and the central phenyl unit (C1–C7–C6–C5/N1) are 24° for Py(5PhPhH)Py, 30° for Py(5BuPhH)Py and 38° Py(4,5,6MeOPhH)Py. The latter two show a double *cis*-N–C conformation at the C6–C7 and C11–C12 bonds, appropriate for coordination, which is supported by intramolecular (N1···C1–H···N2) hydrogen bonding. In contrast to this, the Py(5PhPhH)Py derivative has a double *trans*-N-C conformation and no hydrogen bonding. However, the C6–C7 and C11–C12 bond are obviously easy to rotate to adopt the final configuration for coordination.

Table 3-2 Crystallographic data for Py(5BuPhH)Py, Py(5PhPhH)Py and Py(4,5,6MeOPhH)Py.

Identification code	**Py(5BuPhH)Py**	**Py(5PhPhH)Py**	**Py(4,5,6MeOPhH)Py**
Empirical formula	$C_{20}H_{20}N_2$	$C_{22}H_{16}N_2$	$C_{19}H_{18}N_2O_3$
Temperature/K	293(2)	293(2)	100.0
Crystal system	monoclinic	orthorhombic	triclinic
Space group	$P2_1/n$	$Pbcn$	$P\bar{1}$
a/Å	12.0960(4)	16.2755(5)	9.977(1)
b/Å	10.2452(4)	11.3410(3)	11.243(1)
c/Å	13.2431(5)	8.2673(2)	16.590(2)
α/°	90	90	72.200(4)
β/°	109.074(1)	90	76.003(4)

γ/°	90	90	65.595(3)
Volume/Å^3	1551.1(1)	1525.98(7)	1599.1(3)
Z	4	4	4
ρ_{calc}g/cm^3	1.235	1.342	1.339
F(000)	616.0	648.0	680.0
Radiation	MoKα (λ = 0.71073)	MoKα (λ = 0.71073)	MoKα (λ = 0.71073)
2Θ range for data collection/°	3.964 to 56.588	4.378 to 58.374	4.09 to 60.528
Index ranges	–16 ≤ h ≤ 16, –13 ≤ k ≤ 13, –17 ≤ l ≤ 17	–22 ≤ h ≤ 22, –15 ≤ k ≤ 15, –10 ≤ l ≤ 11	–14 ≤ h ≤ 13, –15 ≤ k ≤ 15, –23 ≤ l ≤ 23
Reflections collected	67917	22441	114489
Independent reflections	3820 [R_{int} = 0.0798, R_{sigma} = 0.0287]	2064 [R_{int} = 0.0700, R_{sigma} = 0.0259]	9416 [R_{int} = 0.0660, R_{sigma} = 0.0306]
Data/restr./parameters	3820/0/203	2064/0/112	9416/0/440
Goodness-of-fit on F^2	1.093	1.179	1.120
Final *R* indexes [*I*>=2σ (*I*)]	R_1 = 0.0493, wR_2 = 0.1239	R_1 = 0.0684, wR_2 = 0.1850	R_1 = 0.0537, wR_2 = 0.1318
Final *R* indexes [all data]	R_1 = 0.0638, wR_2 = 0.1357	R_1 = 0.0698, wR_2 = 0.1862	R_1 = 0.0623, wR_2 = 0.1391
Largest diff. peak/hole/ e Å^{-3}	0.41/–0.25	0.31/–0.52	0.91/–0.62
CCDC	2343505	2343500	2343506

Cyclic voltammograms of the protoligands (Figure 3-4 and 3-5) show substantial variations in the reduction potentials in comparison to the standard ligand PyHPhPy (E_{red1} = –2.83 V, E_{red2} = –3.31 V; Table 3-3).

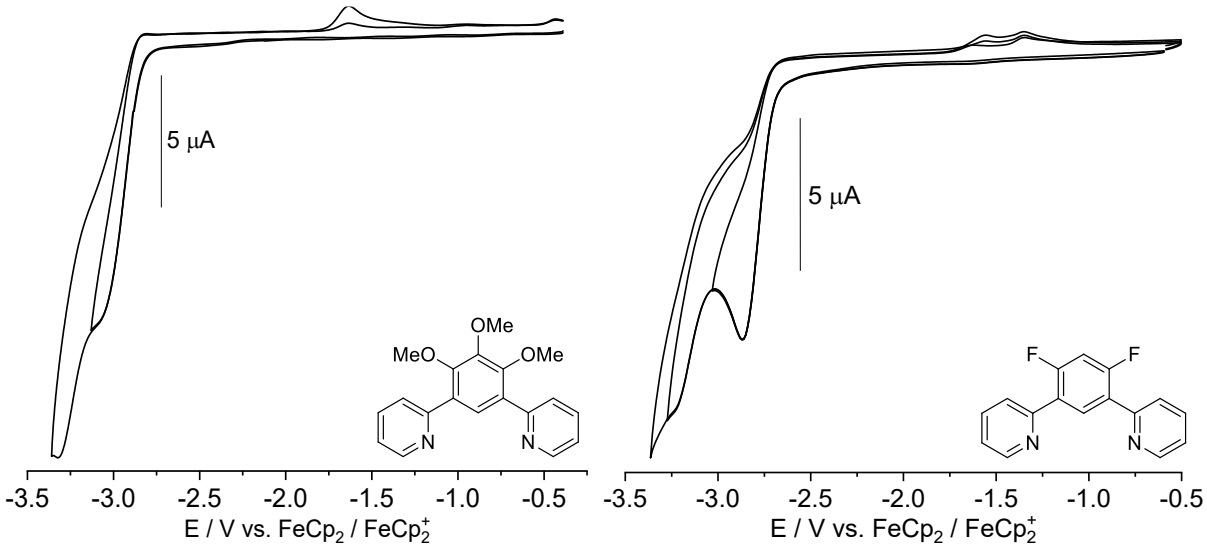

Figure 3-4 Cyclic voltammograms of Py(4,5,6MeOPhH)Py (left) and Py(4,6FPhH)Py (right), measured in a 0.1M nBu$_4$PF$_6$ solution in THF at rt with a scan rate of 100 mV/s.

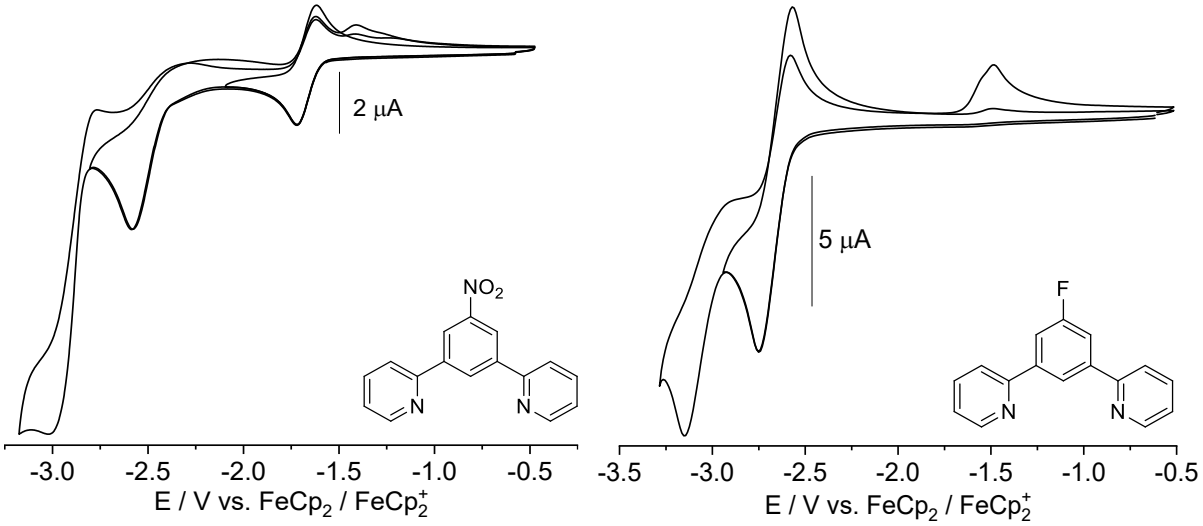

Figure 3-5 Cyclic voltammograms of Py(5NO_2PhH)Py (left) and Py(5FPhH)Py (right), measured in a 0.1M *n*Bu_4PF_6 solution in THF at rt with a scan rate of 100 mV/s.

EDG-substituted ligands show cathodic shifts compared with PyHPhPy, while EWG-substituted derivatives shift to lower reduction potentials. Generally, the shifts are not very large, as the main acceptor for the electron-uptake are the two pyridyl groups, as has been found previously.[92, 117, 136, 138, 140] This is also in line with the conclusion from UV/Vis absorption spectroscopy, that chromophore is essentially localized on the pyridine units.

Table 3-3 Reduction potentials of all central ring substituted N^CH^N ligands.

	***E* Red1**	**E Red2 (E_{pc})**
PyPhHPy[a]	–2.83 ($E_{1/2}$)	–3.31
Py(4,5,6MeOPhH)Py	–3.05 (E_{pc})	–3.33
Py(5BuPhH)Py	–2.87 ($E_{1/2}$)	-
Py(4,6FPhH)Py	–2.87 (E_{pc})	–3.27
Py(5MePhH)Py	–2.84 ($E_{1/2}$)	-
Py(5MeOPhH)Py	–2.81 ($E_{1/2}$)	-
Py(5PhPhH)Py	–2.77 (E_{pc})	–3.07
Py(4FPhH)Py	–2.77 ($E_{1/2}$)	–3.33
Py(5CF_3PhH)Py	–2.74 (E_{pc})	–2.97
Py(5FPhH)Py	–2.66 ($E_{1/2}$)	–3.15
Py(4,6MePhH)Py[b]	–1.77 (E_{pc})	–2.03
Py(5NO_2PhH)Py	–1.67 ($E_{1/2}$)	–2.58

Measured in a 0.1M *n*Bu_4PF_6 solution in THF at rt with a scan rate of 100 mV/s. All potentials in V. E_{pc} = Cathodic Peak Potential, $E_{1/2}$ = Half-Step Potential. a = From ref.[92]. b = Red3 at –2.22 V (E_{pc}). c = Red3 at –3.03 V (E_{pc}).

UV/Vis absorption spectra, recorded in dry THF at rt all show two absorption maxima in the range 230 to 300 nm (Figure 3-6), very similar to the standard ligand Py(HPh)Py, which

absorbs at 245 and 280 nm (see Table 3-4).[92] The absorptions can be assigned to π–π* transitions based on previous work.[89, 91, 92, 117, 121, 134-139] Some ligands show a third band at lower energy (300 – 350 nm), that presumably represent n–π* transitions.

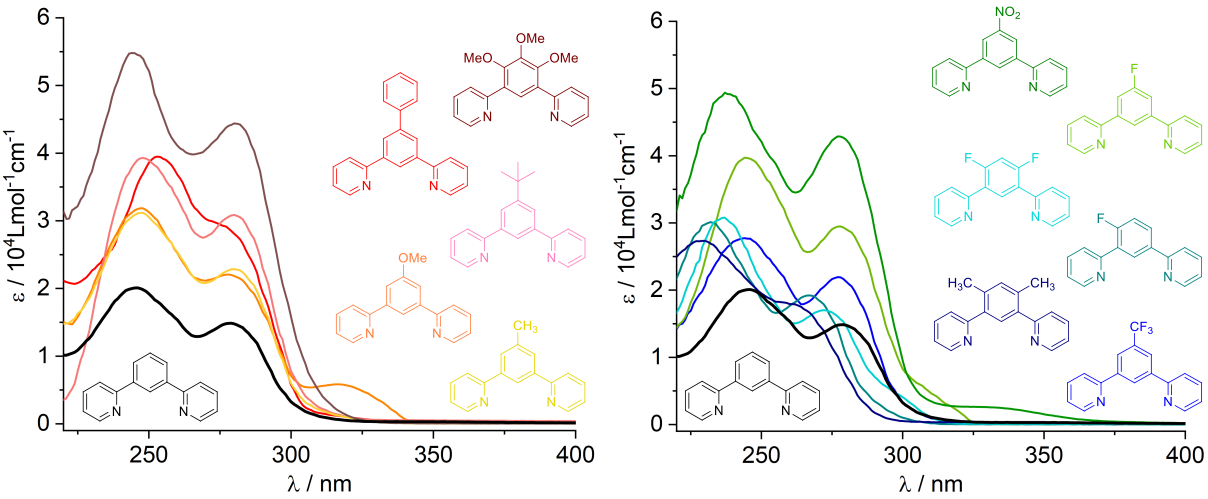

Figure 3-6 UV/vis absorption spectra of C-ring substituted N^CH^N protoligands measured in THF at rt. *Left:* Electron-donating groups (EDGs). *Right:* Electron-withdrawing groups (EWGs).

Table 3-4 Absorption maxima and extinction coeff. of central ring substituted N^C^N ligands.

	Absorption Max. λ_x in nm (Ext. Coeff. ε in 1000 · Lmol^{-1}cm^{-1})		
	λ_3	**λ_2**	**λ_1**
PyPhHPy[a]	-	279 (14.9)	245 (20.1)
Py(4,5,6MeOPhH)Py	-	281 (44.4)	245 (54.9)
Py(5MePhH)Py	-	281 (22.8)	247 (31.1)
Py(5BuPhH)Py	-	280 (30.9)	248 (39.4)
Py(5PhPhH)Py	-	278 (29.5)^{sh}	253 (39.5)
Py(5MeOPhH)Py	316 (5.9)	279 (22.0)	247 (31.9)
Py(4,6MePhH)Py	-	260 (19.8)^{sh}	228 (28.0)
Py(4FPhH)Py	-	267 (19.4)	231 (30.2)
Py(4,6FPhH)Py	-	272 (17.1)	236 (31.0)
Py(5NO$_2$PhH)Py	324 (2.5)^{sh}	277 (42.9)	237 (49.2)
Py(5CF$_3$PhH)Py	-	277 (22.0)	244 (27.8)
Py(5FPhH)Py	306 (6.1)^{sh}	278 (29.7)	245 (39.8)

Measured in THF at rt. sh = shoulder. a = From ref. [92]

Overall, the impact of the central C-unit substitution is small, which agrees with the idea, that the main chromophore of these ligands is localized in the two pyridyl units and not in the central C-ring.[92, 117, 136, 138, 140]

3.1.2 Synthesis and Characterization of the Ni(II) Complexes

All protoligands were successfully transformed into the target Ni(II) complexes [Ni(N^C^N)X] starting from the anhydrous halides NiX_2 (X = Cl, Br) in yields between 50 and 94% (Figure 3-7) using the base-assisted nickelation, initially developed for HC^N^N protoligands.[92, 101]

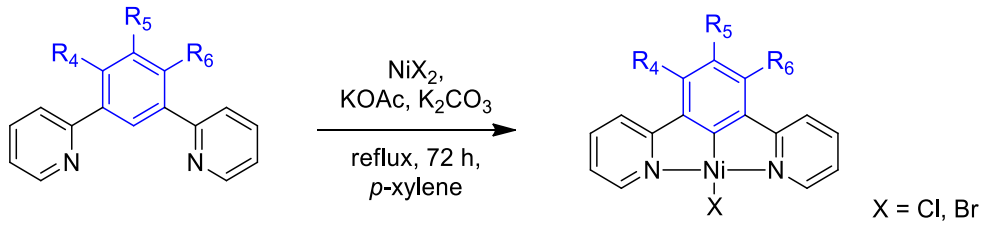

Figure 3-7 Synthesis of central ring substituted complexes *via* C–H activation by *Klein et al.* from 2020.[92, 101]

The complexes can be classified into four different groups (A-D, Figure 3-8), depending on the substitution pattern. Within this study, the terpyridine complex D was also synthesized and investigated.[141]

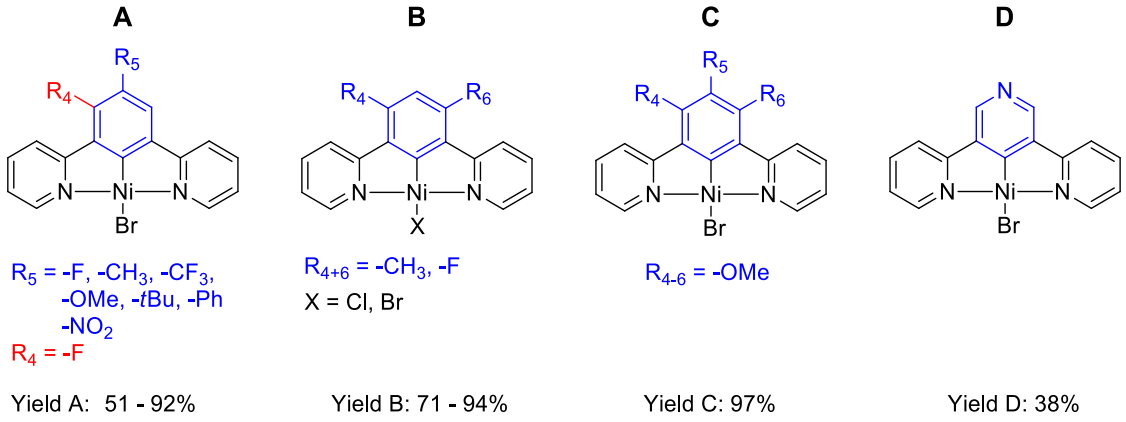

Figure 3-8 Synthesized [Ni(N^C^N)X] (X = Cl, Br) complex derivatives carrying a substituted central phenide unit with the respective yields.

The ultimate proof for the successful synthesis of the complexes comes from ^{1}H NMR spectra of the complexes, with the central C–H function of the protoligand metalated to C–Ni and the corresponding H signal missing in the spectra (full ^{1}H NMR data in the Experimental Section 5.4.1). The diamagnetic character of the complexes is in line with the square planar geometry around the d^8 configured metal center expected from the strong ligand field and the tridentate ligand. ^{13}C NMR spectroscopy was impeded by the low solubility of the complexes in common organic solvents.

The square-planar coordination was confirmed by SC-XRD for [Ni(Py(5BuPh)Py)Br] and [Ni(Py(5CF$_3$Ph)Py)Br] (Figure 3-9). These species were crystallized by an isothermic evaporation of saturated THF solutions of the complexes at 3°C.

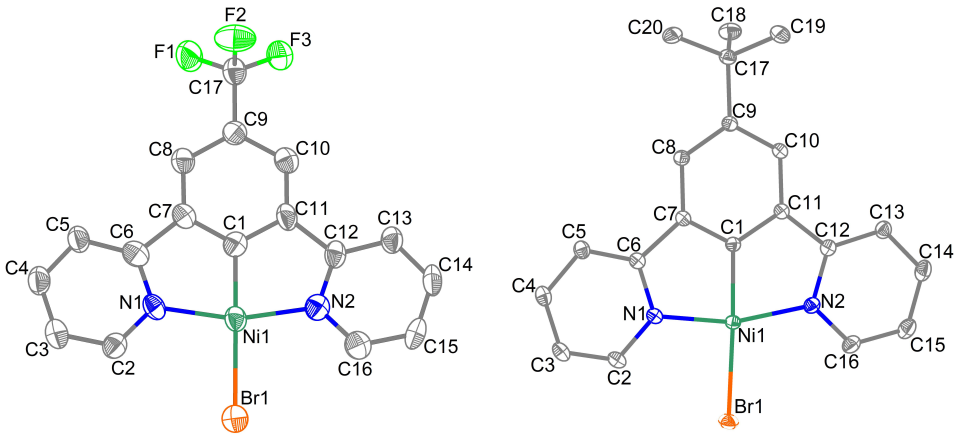

Figure 3-9 Molecular structures of [Ni(Py(5CF$_3$Ph)Py)Br] (*left*) and [Ni(Py(5BuPh)Py)Br] (*right*). Ellipsoids are shown with a 50% probability. Hydrogen atoms are omitted for clarity.

The trifluoromethyl substituted complex crystallized in the orthorhombic space group *P*bca, whereas the *tert*-butyl substituted derivative was solved in the monoclinic space group *P*2$_1$/c, each with eight units per unit cell. The asymmetric unit of [Ni(Py(5BuPh)Py)Br] contains two crystallographically independent molecules (Table 3-5).

Table 3-5 Crystallographic data for [Ni(Py(5CF$_3$Ph)Py)Br] and [Ni(Py(5BuPh)Py)Br].

Identification code	**[Ni(Py(5CF$_3$Ph)Py)Br]**	**[Ni(Py(5BuPh)Py)Br]**
Empirical formula	$C_{17}H_{10}BrF_3N_2Ni$	$C_{20}H_{19}BrN_2Ni$
Temperature/K	293(2)	100.0
Crystal system	orthorhombic	monoclinic
Space group	*P*bca	*P*2$_1$/c
a/Å	16.7845(1)	7.0878(4)
b/Å	8.1115(4)	21.5386(1)
c/Å	21.5990(9)	22.4094(1)
β/°	90	93.866(2)
Volume/Å^3	2940.6(3)	3413.2(4)
Z	8	8
ρ_{calc}g/cm^3	1.978	1.658
F(000)	1728.0	1728.0
Radiation	MoKα (λ = 0.71073)	MoKα (λ = 0.71073)
2Θ range for data collection/°	3.772 to 53.752	4.104 to 70.192
Index ranges	–21 ≤ h ≤ 21, –10 ≤ k ≤ 10, –25 ≤ l ≤ 27	–11 ≤ h ≤ 11, –34 ≤ k ≤ 34, –36 ≤ l ≤ 36

Reflections collected	31791	249355
Independent reflections	3149 [R_{int} = 0.2621, R_{sigma} = 0.1094]	15097 [R_{int} = 0.0671, R_{sigma} = 0.0266]
Data/restraints/parameters	3149/0/218	15097/0/440
Goodness-of-fit on F^2	0.885	1.084
Final R indexes [I>=2σ (I)]	R_1 = 0.0547, wR_2 = 0.1234	R_1 = 0.0291, wR_2 = 0.0627
Final R indexes [all data]	R_1 = 0.1256, wR_2 = 0.1529	R_1 = 0.0386, wR_2 = 0.0663
Largest diff. peak/hole / e Å^{-3}	0.78/–0.82	0.78/–0.87
CCDC	2343479	2343484

Overall, the bond lengths and angles around Ni are very similar to those previously reported for Ni(II) complexes of the tridentate ligands PyPhPy[92] and Py4,6MePhPy.[140] A detailed view shows that the aromatic moieties of the tridentate N^C^N ligands in the two new complexes are almost perfectly co-planar in the structures, with torsion angles between 1.9° (C5–C6–C7–C8) and 3.2° (C10–C11–C12–C13) for [Ni(Py(5CF$_3$Ph)Py)Br] and 1.9° (C30–C31–C32–C33) and 4.1° (C25–C26–C27–C28) for [Ni(Py(5BuPh)Py)Br] (for full tables, see Chapter 7.3.4 and 6.3.5). Nevertheless, the coordination is not perfectly square-planar with N$_1$–Ni–N$_2$ angles of around 163°.

This is due to the chelate bite-angles of around 82° of the two five-membered chelate rings N–C–C–C–Ni and is typical for such tridentate N^C^N, C^N^N or C^N^C ligands in transition metal complexes.[89, 91, 92, 99, 100, 104, 108, 116, 117, 122, 123, 127, 140-147] Compared with the previously reported complex [Ni(PyPhPy)Br] containing the standard PyPhPy ligand, the C$_1$–Ni–Br angles in the two new derivatives are markedly deviating from the ideal 180°.[92]

Table 3-6 Angles and bond lengths of [Ni(Py(5CF$_3$Ph)Py)Br], [Ni(Py(5BuPh)Py)Br] and [Ni(Py(Ph)Py)Br].

	[Ni(PyPhPy)Br]^a	**[Ni(Py(5CF$_3$Ph)Py)Br]**	**[Ni(Py(5BuPh)Py)Br]**
Distances / Å			
Ni–C1	1.8298(2)	1.826(7)	1.822(1)
Ni–N1	1.9489(1)	1.933(6)	1.943(1)
Ni–N2	1.9536(1)	1.941(6)	1.941(1)
Ni–Br1	2.3963(3)	2.382(1)	2.394(2)
Angles / °			
C1–Ni1–N1	81.94(7)	81.8(3)	81.83(5)
C1–Ni–N2	81.85(7)	82.0(3)	81.88(5)
N1–Ni–Br1	97.83(4)	97.8(2)	98.20(3)
N2–Ni–Br1	98.39(4)	98.6(2)	98.12(3)
Sum / °	360.0	360.2	360.0

C1–Ni–Br1	179.48(5)	173.7(2)	172.71(4)
N1–Ni–N2	163.78(6)	163.5(3)	163.72(5)

a = From ref. [92].

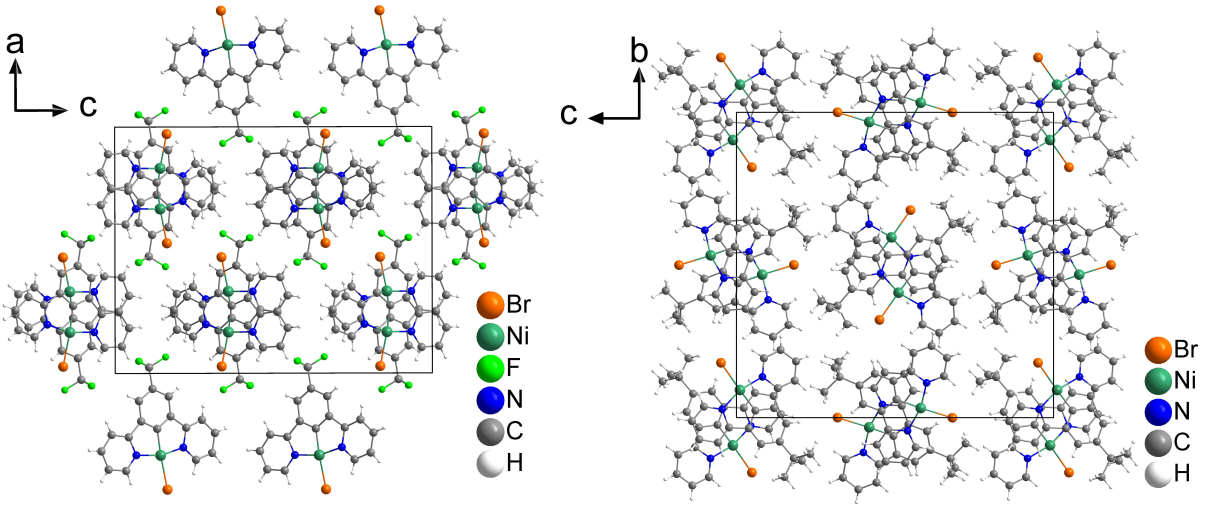

Figure 3-10 Crystal structure of [Ni(Py(5CF$_3$Ph)Py)Br] viewed along the crystallographic *b*-axis (left) and [Ni(Py(5BuPh)Py)Br] viewed along the *a*-axis (right).

As shown in Figure 3-10, both structures show a head-to-tail π-stacking arrangement, in which the coligand of two neighboring complexes point into the opposite direction, as it is typical for similar structures.[92, 99, 140, 148] However, the packing differs in that in the structure of the *tert*-butyl substituted complex the phenyl-pyridyl unit of one complex overlaps with the one of the neighboring complex. The distance between the two units of 3.77 Å at an angle of 20° is at the limit of *Janiak's* definition and therefore a very weak π-stacking.[149]

In the structure of the trifluoromethyl substituted complex, the distance between both units is 3.93 Å, which already exceeds the border of *Janiak's* definition by this distance.

Cyclic voltammograms (CVs) of the complexes show reversible oxidation waves at potentials slightly above 0 V vs. ferrocene/ferrocenium along with several reduction waves in the range from –2 to –3 V which are either partially reversible or irreversible (Figures 3-11 and 3-12).

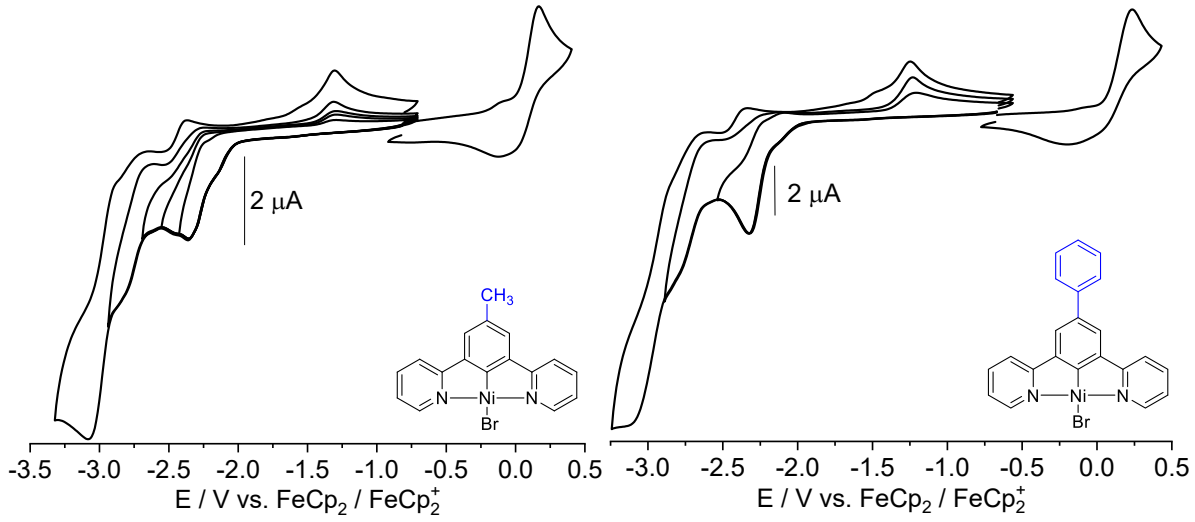

Figure 3-11 Cyclic voltammograms of [Ni(Py(5PhPh)Py)Br] (left) and [Ni(Py(5MePh)Py)Br] (right) measured in 0.1M solution of nBu$_4$PF$_6$ in THF at rt with a scan rate of 100 mV/s.

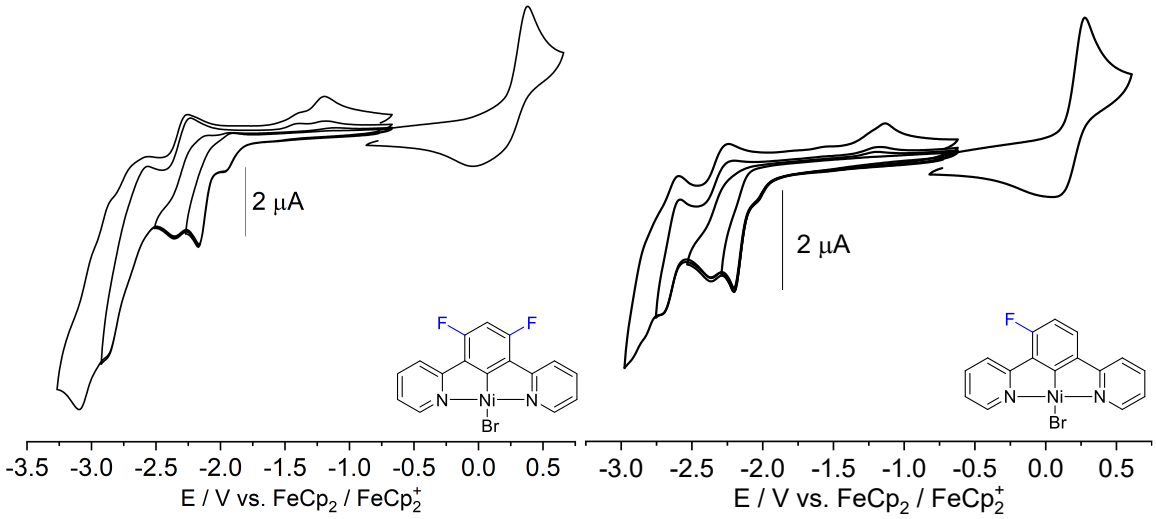

Figure 3-12 Cyclic voltammograms of [Ni(Py(4,6FPh)Py)Br] (left) and [Ni(Py(4FPh)Py)Br] (right), measured in 0.1M solution of nBu$_4$PF$_6$ in THF at rt with a scan rate of 100 mV/s.

The oxidation waves vary from 0.02 to 0.17 V (Table 3-7) and can be assigned to Ni(II)/Ni(III) redox pairs, based on the findings for the [Ni(Py(4,6MePh)Py)Cl] derivative[140] and the parent [Ni(PyPhPy)Br] complex.[92] When compared to the parent complex, the derivatives bearing substituents at position R_4 and R_6 show anodically shifted oxidations (0.10 to 0.16 V). This is in line with the finding that in [Ni(Py(4,6MePh)Py)Cl] and [Ni(PyPhPy)Br] the highest occupied molecular orbitals (HOMO) are not only localized on the metal, but also obtain contributions from the central phenide unit of the N^C^N ligand and the coligands.[92, 140] The first reductions are all essentially irreversible and show cathodic peak potentials ranging from –2.17 to –2.36 V. The irreversible character indicates an EC mechanism, in which the reduced species [Ni(N^C^N)Br]$^{\bullet-}$ undergoes a cleavage of the Br$^-$ coligand (Figure 3-13), as already found for similar compounds.[89, 91, 92, 99, 142]

EC means that the initial reduction in an electrochemical step (E) is followed by a chemical reaction (C) of which the products are detected in the continued scans. The speed of the reaction C depends on the coligand X^- and the electronic inventory of the reduced [Ni(N^C^N)]• species, which might as well contain a solvent molecule as fourth ligand: [Ni(N^C^N)(Solv)]•.

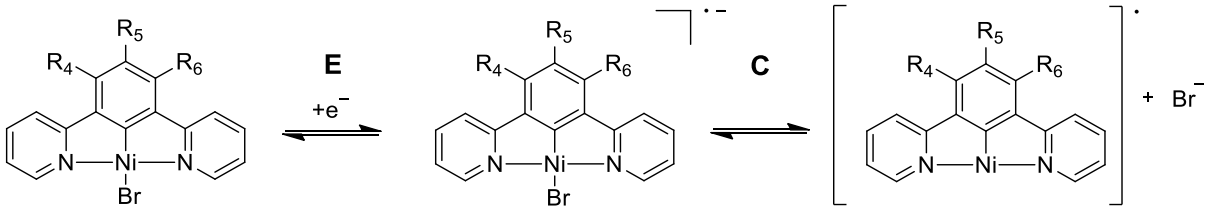

Figure 3-13 Proposed mechanism during the first reduction of [Ni(N^C^N)Br] adapted from *Klein et al.* from 2020.[92]

The reduction potentials are also markedly influenced by the substituents on the central C-ring. The highest (less negative) potentials are found for the 2,6-dimethyl-substituted complex, while a very low potential is found for the 5-*tert*-butyl-derivative. Remarkably, only the latter and the 5-Ph derivative show a lower potential than the parent [Ni(PyPhPy)Br] complex. Since the reduction is supposed to address the lowest unoccupied molecular orbital mainly localized on the two pyridyl units, as has been found for [Ni(Py(4,6MePh)Py)Cl] and Ni(PyPhPy)Br],[92, 140] the influence of the substituents cannot simply be rationalized. As the influence is even slightly larger (ΔE_{Red1} = 0.18 V) as for the oxidation (ΔE_{Ox1} = 0.15 V), the simple assignment of metal-centered oxidation and ligand-π* dominated reduction seems oversimplified. This calls for the calculation of HOMO and LUMO energies and character for each complex.

The electrochemical HOMO-LUMO gap ($\Delta E_{HOMO\text{-}LUMO}$) calculates as the difference between the first oxidation and first reduction potential (Table 3-7) and varies from 2.27 eV to 2.44 eV. The lowest values were found for the 5-CF_3-substituted complex, the highest for the trimethoxy derivative. This is in line with the above discussed impact of the central C-ring substitution on both HOMO and LUMO.

Table 3-7 Redox potentials of all central ring substituted Ni(II) complexes.

	***E* Ox$_1$ ($E_{1/2}$)**	***E* Red1 (E_{pc})**	***E* Red2**	***E* Red3**	***E* Red4 (E_{pc})**	**ΔE HOMO-LUMO**
[Ni(PyPhPy)Br][a]	0.07	–2.31	–2.75 (E_{pc})	–3.09 (E_{pc})	-	2.38 eV
[Ni(Py(5PhPh)Py)Br]	0.02	–2.33	–2.89 (E_{pc})	–3.18 (E_{pc})	-	2.35 eV
[Ni(Py(5MePh)Py)Br]	0.03	–2.35	–2.48 (E_{pc})	–2.65 (E_{pc})	–2.90	2.38 eV
[Ni(Py(5MeOPh)Py)Br]	0.05	–2.33	–2.73 ($E_{1/2}$)	–3.11 (E_{pc})	-	2.38 eV
[Ni(Py(5BuPh)Py)Br]	0.05	–2.34	–2.96 (E_{pc})	–3.18 (E_{pc})	-	2.39 eV
[Ni(Py(4,5,6MeOPh)Py)Br]	0.10	–2.34	–2.45 ($E_{1/2}$)	–2.87 ($E_{1/2}$)	-	2.44 eV

[Ni(Py(4,6MePh)Py)Cl]	0.11	–2.27	–2.37 ($E_{1/2}$)	–2.83 (E_{pc})	–3.11	2.38 eV
[Ni(Py(5CF_3Ph)Py)Br]	0.08	–2.19	–2.61 ($E_{1/2}$)	–3.23 (E_{pc})	-	2.27 eV
[Ni(Py(5FPh)Py)Br][b]	0.10	–2.27	–2.48 (E_{pc})	–2.60 ($E_{1/2}$)	–2.89 ($E_{1/2}$)	2.37 eV
[Ni(Py(4FPh)Py)Br]	0.16	–2.20	–2.38 (E_{pc})	–2.66 ($E_{1/2}$)	–3.00	2.36 eV
[Ni(Py(4,6FPh)Py)Br]	0.17	–2.17	–2.36 (E_{pc})	–2.74 ($E_{1/2}$)	–3.10	2.34 eV

measured in a 0.1M nBu$_4$NPF$_6$ solution in THF with a scan rate of 100 mV/s at rt. All potentials in V. E_{pc} = Cathodic Peak Potential, $E_{1/2}$ = Half-Step Potential. a = From ref.[92]. b = Red_5 at –3.08 V (E_{pc}).

UV/vis absorption spectra of the complexes in THF show intense absorptions in the UV/vis range from 230 to 300 nm (Figure 3-14, data in Table 3-8), almost identical to those observed for the protoligands (Chapter 3.1.1). Therefore, these bands can be assigned to π–π* transitions in the Ni(II) complexes.

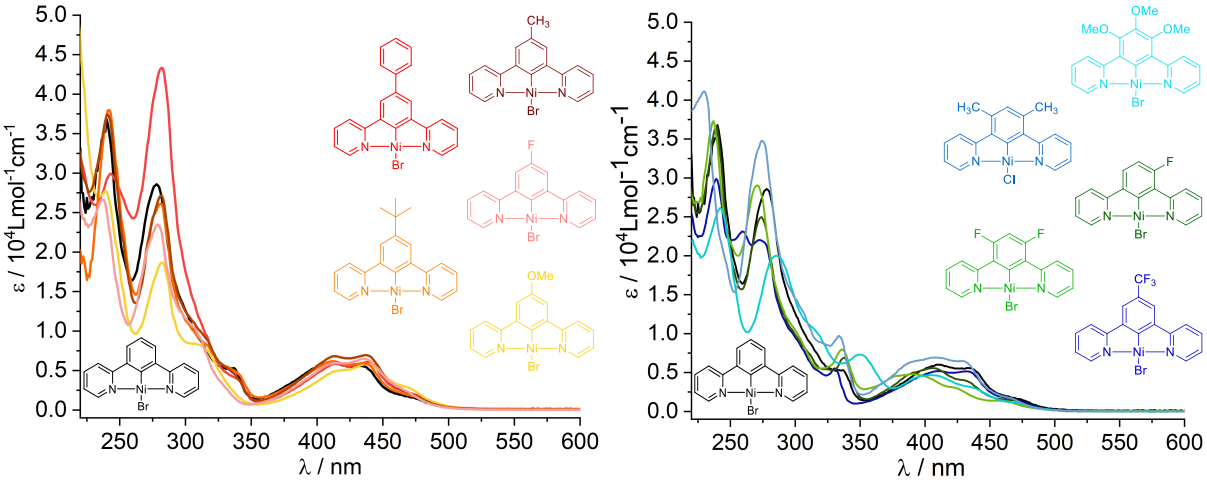

Figure 3-14 UV/vis absorption spectra of all central ring substituted [Ni(N^C^N)X] complex species measured in THF at rt. *Left:* All complexes showing a bathochromic shift of the charge transfer bands, correlating to EDGs. *Right:* All complexes showing a hypsochromic shift of the charge transfer bands, correlating to EWGs.

In the range 300 to 350 nm weak absorptions as shoulders on the intense π–π* bands are observed, followed by partially structured broad absorption bands in the range 350 to 500 nm. These long-wavelength absorption agree with the orange to red color of the complexes, as already proved for [Ni(Py(Ph)Py)X] by *Klein et al.* in 2020.[92]

Table 3-8 Absorption maxima and extinction coeff. of central ring substituted [Ni(N^C^N)X] complexes.

	Absorption Max. λ_x in nm (Ext. Coeff. ε in 1000 · Lmol^{-1}cm^{-1})					
	λ_1	**λ_2**	**λ_3**	**λ_5**	**λ_6**	**λ_8**
[Ni(PyPhPy)Br][a]	464 (1.8)	434 (5.6)	411 (6.0)	334 (5.3)	278 (28.8)	239 (36.4)
[Ni(Py(5MePh)Py)Br]	473 (2.0)	437 (6.9)	413 (6.9)	330 (5.4)	281 (27.3)	240 (37.5)
[Ni(Py(5FPh)Py)Br]	470 (2.3)	436 (6.5)	414 (6.0)	305 (10.8)^{sh}	279 (23.5)	236 (26.6)
[Ni(Py(5PhPh)Py)Br]	469 (2.2)	439 (6.1)	414 (5.9)	333 (4.5)	282 (43.3)	243 (29.9)

[Ni(Py(5BuPh)Py)Br]	468 (1.9)	435 (6.0)	412 (6.2)	331 (5.4)	280 (26.0)	242 (38.1)
[Ni(Py(5MeOPh)Py)Br]	465 (3.1)	438 (5.8)	416 (5.0)	306 (8.3)	282 (18.6)	239 (27.8)
[Ni(Py(4,6FPh)Py)Br][c]	459 (1.4)	418 (3.1)*sh*	391 (4.8)	336 (7.9)	271 (29.1)	237 (37.2)
[Ni(Py(4,6MePh)Py)Cl][b]	462 (1.7)	429 (6.5)	408 (6.9)	334 (9.7)	274 (34.9)	230 (41.1)
[Ni(Py(5CF_3Ph)Py)Br][d]	463 (1.8)*sh*	432 (5.1)	411 (5.2)	330 (5.6)	273 (22.1)	239 (29.8)
[Ni(Py(4FPh)Py)Br][b]	463 (1.5)	427 (4.1)	405(5.6)	337 (6.9)	274 (24.9)	239 (36.7)
[Ni(Py(4,5,6MeOPh)Py)Br]	464 (1.1)	434 (3.1)	405 (4.7)	350 (7.3)	285 (20.0)	242 (26.2)

Measured in THF at rt. *sh* = shoulder. a = From ref. [92] b = λ_4 at 391 nm (ε = 6400 $Lmol^{-1}cm^{-1}$). c = λ_4 at 377 nm (ε = 4500 $Lmol^{-1}cm^{-1}$). d = λ_7 at 260 nm (ε = 23200 $Lmol^{-1}cm^{-1}$).

Upon EDG-substitution of the central C-ring, the long-wavelength absorption maxima are slightly redshifted compared with the standard complex [Ni(PyPhPy)Br] (Table 3-8). Upon EWG-substitution, these band are blueshifted. Overall the variations are small, which is in line with the chromophoric unit being mainly localized in the di-pyridyl unit of the complex as outlined in detail through density functional theory (DFT) and time-dependent (TD-DFT) calculations on the [Ni(Py)(4,6MePh)Py)Cl] complex.[140] Because the influence of these do not change the optical properties of the complex, these positions can be used for changing secondary properties, e.g. solubility of these species. It is noteworthy, that substitutions at position R_4 and R_6 show a bigger effect on the optical properties of the complexes as position R_5, which also was proved in *Klein et al.* (see Chapter 3.1.3).[140]

3.1.3 Photoluminescence of Ni(II), Pd(II) and Pt(II) Complexes [M(Py(4,6dPh)PyCl] obtained from C–H Activation of 1,3-di(2-pyridyl)-4,6-dimethylbenzene Py(4,6MePhH)Py[140]

Luminescent transition metal complexes have gained enormous importance in the past decade with various potential applications.[150-163] Efficient intersystem crossing (ISC) and otherwise spin-forbidden phosphorescence is favored through large spin-orbit coupling (SOC) of the heavy metal centers, [154-160] such as d^6-configured Re(I), Ru(II), Os(II) and Ir(III) [152, 153, 157-161] and d^8-configured Pt(II) and Au(III) complexes.[152-156, 158-165] The latter ones are mostly coordinated in a square-planar moiety and therefore show axial vacancies, allowing metal–metal (M···M) and/or π···π stacking interactions in aggregates with red-shifted emissions from MMLCT states (metal–metal-to-ligand charge transfer character, eventually with excimer M···M shortening), along with metal-perturbed ligand-centered (π–π*) excited configurations of the monomeric species.[166-175] Whereas luminescent Pt(II) complexes are well established, the lighter but isoelectronic Pd(II)[108, 162, 172-180] and Ni(II) [127] are not as famous. This mainly results from a smaller ligand field splitting, which thermally allows metal-centered states with dissociative character enabling the way of a non-radiative decay to the

ground state *via* conical intersections. [125, 180-182] Cyclometalated tri- or tetradentate complexes appear to be auspicious candidates for providing a stronger ligand field and energetically increase the d-d* states and to overcome the triplet-emitting MLCT and π–π* states.[108, 127, 146, 154-156, 162, 165, 166, 175-179, 183-189] In 2020, *Yam et al*. published a groundbreaking study or [Ni(Py(Ph)Py)Carb], that was luminescent at 77 K in a frozen glassy matrix and at 298 K in the solid state.[127]

Since isoleptic d^{10} metal triades were investigated in the past for several ligands,[108, 179, 190, 191] the field of Py(HPh)Py complexes should be investigated. The base-assisted C–H activation method from *Klein et al.* [92, 101] allowed omitting highly toxic organomercury intermediates, as they were required for [Ni(Py(Ph)Py)Cl] until 2020.[127] The synthetic route for Pt(II) analogues by using a platinate salt with N^CH^N ligands in glacial acetic acid is a well-established and never changed story (Figure 3-15).[116, 117, 120, 121, 123, 184, 192]

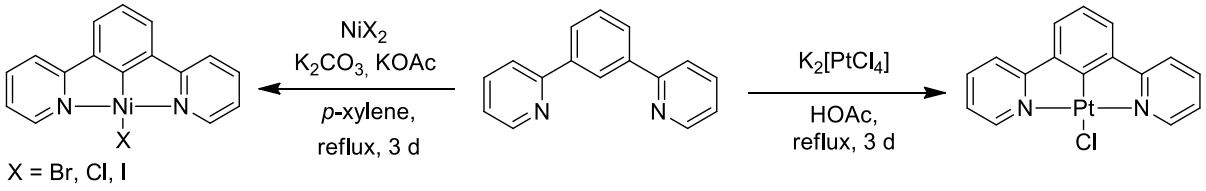

Figure 3-15 Cyclonickelation *via* base-assisted C-H activation (left) and cycloplatination in HOAc (right) of N^CH^N ligands. Adapted from [92, 116].

This method could not be adapted for [Pd(Py(Ph)Py)Cl], but led to unfavoured coordination by using $Li_2[PdCl_4]$ or $Pd(OAc)_2$, leading to a dimeric- or tetrameric structure (Figure 3-16).[116]

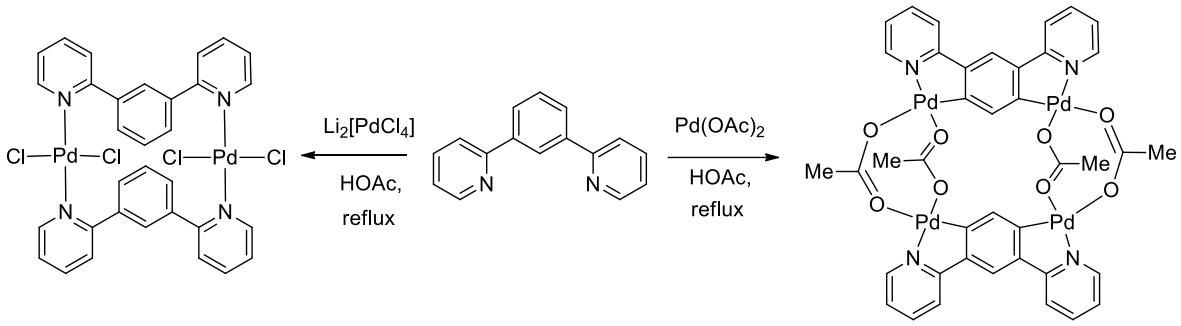

Figure 3-16 Cyclometalation reaction of Py(PhH)Py with $Li_2[PdCl_4]$ (left) and $Pd(OAc)_2$ (right). Adapted from [116].

Based on these results an alternative route was used for [Pd(Py(Ph)Py)X],[122] initially found for the C^N^N analogue,[103] in which the transmetalation from an organomercury precursor is the key-step. Later this group published a chiral derivative of [Pd(Py(Ph)Py)Cl], which was synthesized with a palladate salt and the N^CH^N protoligand.[123] In 2020, [Pd(Py(6'-(4MeO)Ph)$_2$Ph)Py)Cl] was synthesized with the use of $NaHCO_3$ in 42% yield,

whereas the connection of both MeO functions with an intramolecular ether-bridge gave 66% product.[193] By adopting the base-assisted cyclonickelation on palladium salts within this work, the tetranuclear and dinuclear species from Figure 3-16 were reproduced with a yield of 31% (Figure 3-17). Also, the use of potassium pivalate as a different base did not lead to a different result, but the pivalate bridged derivative (Yield: 28%).

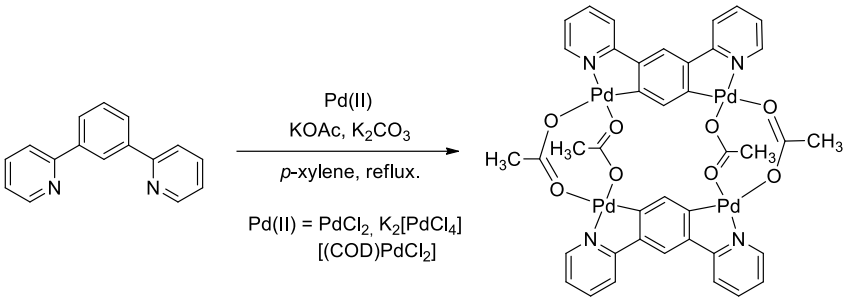

Figure 3-17 Cyclopalladation of PyPhHPy adapting the base-assisted cyclonickelation by *Klein et al.* 2020.[92]

Therefore, the 4,6-dimethylated ligand was chosen, which sterically block this preferred cyclopalladation from Figure 3-17. All three complexes with M =Ni, Pd, Pt, were synthesized using the base-assisted C–H activation method starting from the protoligand 1,3-di(2-pyridyl)-4,6-dimethylbenzene from *Klein et al*.[92], which allowed to study the homologous Ni, Pd, and Pt series of these complexes concerning their fundamental electronic properties and to investigate the influence of both methyl functions on the ligand system. For [Pt(Py(Ph)Py)X] derivatives, the influence of several substitution patterns were rigorously studied,[117, 119, 120, 123, 154, 165, 184, 194-199] in which [Pt(Py(4,6MePh)Py)Cl] was already synthesized in HOAc with 50% yield.[196] Our method increased the yield up to 70%, while heating for a way longer time, than the previously reported 1 h.[196] Using the base-assisted C–H activation method with KOAc and K_2CO_3 in *p*-xylene, the yield for the Pd derivative was increased from 6% to 68% by avoiding light. This procedure replaces the previously applied transmetalation using organomercury intermediates.[122] The yield could be further improved by using $Na_2[PdCl_4]$ and Py(4,6MePhH)Py in HOAc [123] up to 98%. The triade was completed by the successful isolation of the nickel derivative *via* base-assisted C–H activation in 94% yield.[92]

The crystal structure of the Pt(II) complex is already reported,[196] but this work could contribute the Ni(II) and Pd(II) analogue to proof the structure of these complexes. [Ni(Py(4,6MePh)Py)Cl] · CH_2Cl_2 was solved in the orthorhombic space group *P*bca, whereas the Pd(II) derivative crystallized in the monoclinic space group $P2_1/c$ (see Figure 3-18). These measurements were underpinned by DFT calculations (BP86/def-TZVP/D3/COSMO(THF)) by *Rose Jordan* and showed very good agreement with the experimental data.[140]

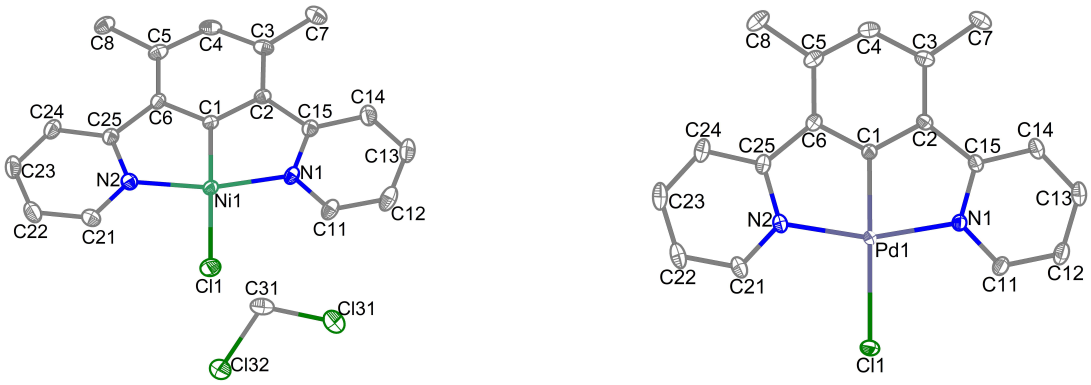

Figure 3-18 Asymmetric unit of [Ni(Py(4,6MePh)Py)Cl] · CH_2Cl_2 and [Pd(Py(4,6MePh)Py)Cl]. Hydrogen atoms are omitted for clarity. Ellipsoids are shown with a 50% probability.

Table 3-9 Crystal data and structure refinement for [M(Py(4,6MePh)Py)Cl].

Identification code	**[Ni(Py(4,6MePh)Py)Cl] CH_2Cl_2**	**[Pd(Py(4,6MePh)Py)Cl]**	**[Pt(Py(4,6MePh)Py)Cl] CH_2Cl_2[b]**
Empirical formula	$C_{18}H_{15}ClN_2Ni{\cdot}CH_2Cl_2$	$C_{18}H_{15}ClN_2Pd$	$C_{18}H_{15}ClN_2Pt{\cdot}CH_2Cl_2$ [b]
Temperature/K	100.0(2)	100.0(2)	100.0(2)
Crystal system	orthorhombic	monoclinic	triclinic
Space group	*P*bca	$P2_1/c$	$P\bar{1}$
a/Å	20.9923(9)	7.9526(4)	6.7959(3)
b/Å	7.9234(3)	10.3875(6)	16.0696(7)
c/Å	21.4048(9)	18.2198(1)	16.7798(8)
α/°	90	90	89.408(4)
β/°	90	101.889(2)	87.749(4)
γ/°	90	90	87.427(4)
Volume/Å^3	3560.3(3)	1472.81(1)	1829.15(1)
Z	8	4	4
ρ_{calc}g/cm^3	1.636	1.809	2.096
F(000)	1792.0	800.0	1096.0
Radiation	MoKα (λ = 0.71073)	MoKα (λ = 0.71073)	MoKα (λ = 0.71073)
2Θ range for data collection/°	3.806 to 78.912	5.234 to 84.208	5.62 to 55.58
Index ranges	–37 ≤ h ≤ 37, –8 ≤ k ≤ 14, –38 ≤ l ≤ 38	–15 ≤ h ≤ 14, –19 ≤ k ≤ 19, –34 ≤ l ≤ 34	–8 ≤ h ≤ 8, –20 ≤ k ≤ 21, 0 ≤ l ≤ 21
Reflections collected	163303	115130	7929
Independent reflections	10641 [R_{int} = 0.2423, R_{sigma} = 0.1213]	10323 [R_{int} = 0.0216, R_{sigma} = 0.0108]	7929 [R_{int} = 0.0450, R_{sigma} = 0.0310]
Data/restraints/parameters	10641/0/229	10323/0/202	7929/0/456
Goodness-of-fit on F^2	1.039	1.109	1.041
Final R indexes [I>=2σ (I)]	R_1 = 0.0876, wR_2 = 0.1316	R_1 = 0.0142, wR_2 = 0.0395	R_1 = 0.0227, wR_2 = 0.0515

Final R indexes [all data]	R_1 = 0.1794, wR_2 = 0.1616	R_1 = 0.0145, wR_2 = 0.0397	R_1 = 0.0264, wR_2 = 0.0527
Largest diff. peak/hole / e Å^{-3}	1.19/–1.30	0.65/–0.72	1.18/–0.93
CCDC	2093819	2095954	1448097

b = Data from Ref. [196]

Both structures show the typical square planar coordination by the tridentate N^C^N ligand and the halide coligand. The N_1–M–N_2 angle decreases with the size of the metal ion and the bond length C_1–M increases. Still the sum over all angles around the metal center is 360°. The crystal packing shows the aforementioned head-to-tail arrangement, weak intermolecular π-stackings between two phenyl-pyridyl units and no packing dimers.

Cyclic voltammetry shows that the first reduction appears to be at similar potentials around –2.3 V, regardless of the metal centre (Figure 3-19). But its reversibility changes from a reversible reduction for Pd, over a partial reversible reduction for Pt and an irreversible one for Ni. The irreversibility of [Ni(N^C^N)X] complexes was already studied for the unsubstituted parent complex.[92] It can be explained by an occurring EC mechanism, that was already known for [Ni(C^N^N)X] complexes (see Chapter 3.1.2).[99, 142] The reversibility of the first reduction for the Pd and Pt derivatives matches previously reported measurement for [Pt(Py(RPh)Py)Cl].[121, 196] The overall lower reduction potentials is in agreement with the superior accepting properties of the Phbpy ligand that contains a 2,2′-bipyridine unit, in contrast to the two phenyl-separated pyridyl units of the Py(PhH)Py ligand[92] and appears to be a ligand-based process. In addition, for the oxidation processes, the Ni derivative (reversible wave) differs markedly from the Pt and Pd (both irreversible) species.

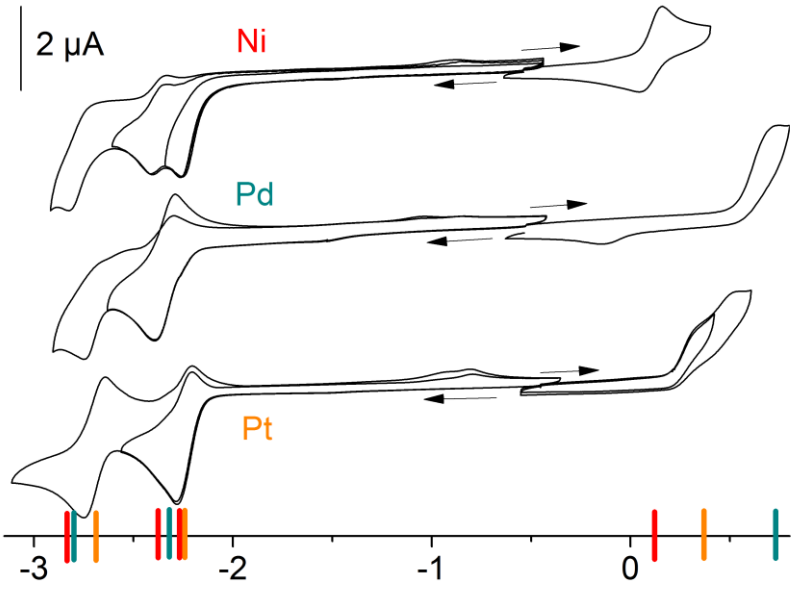

Figure 3-19 Cyclic voltammograms of [M(Py(4,6MePh)Py)Cl] in a 0.1M nBu$_4$NPF$_6$ solution in THF with a scan rate of 100 mV/s. Coloured bars represent half-wave potentials $E_{1/2}$ for reversible reductions and anodic peak potentials E_{pa} for irreversible oxidations. From Ref.[140].

The similarity in the LUMO potential underlines the low effect of a change of the metal centre on its energy level. However, the HOMO changes significantly and builds up the trend, that was observed within the optical measurements. It shows a series of increasing HOMO-LUMO gaps from Ni over Pt to Pd, which matches to previous results for Ni, Pd and Pt complex triades (Table 3-10).[108, 191]

Table 3-10 Redox potentials of Py(4,6MePhH)Py, complexes [M(Py(4,6MePh)Py)Cl] (M = Pt, Pd, Ni) and comparable complexes from cyclic voltammetry.

	***E* Red2**	***E* Red1**	***E* Ox1**	**ΔE HOMO-LUMO**	**solvent**
[Pt(Py(4,6MePh)Py)Cl][b]	-	–2.03 ($E_{1/2}$)	0.43 (E_{pa})	2.46 eV	CH_2Cl_2
[Ni(PyPhPy)Cl][c]	–2.57 (E_{pc})	–2.33 (E_{pc})	0.06 ($E_{1/2}$)	2.39 eV	THF
Py(4,6MePhH)Py	–2.52 (E_{pc})	–1.74 (E_{pc})	-	-	THF
[Ni(Py(4,6MePh)Py)Cl]	–2.37 ($E_{1/2}$)	–2.26 (E_{pc})	0.10 ($E_{1/2}$)	2.36 eV	THF
[Pd(Py(4,6MePh)Py)Cl]	–2.75 (E_{pc})	–2.34 ($E_{1/2}$)	0.74 (E_{pa})	3.07 eV	THF
[Pt(Py(4,6MePh)Py)Cl]	–2.69 (E_{pc})	–2.24 ($E_{1/2}$)	0.35 (E_{pa})[d]	2.59 eV	THF

Measured in a 0.1M nBu$_4$NPF$_6$ solution in THF with a scan rate of 100 mV/s at rt. All potentials in V. E_{pc} = Cathodic Peak Potential, E_{pa} = Anodic Peak Potential, $E_{1/2}$ = Half-Step Potential. b = Reduction measured in MeCN, oxidation in CH_2Cl_2, from ref.[196]. c = From ref. [92]. d = Ox2 at 0.52 V (E_{pa}).

Further *Rose Jordan* contributed DFT calculations of the frontier orbitals on geometry optimized structures using the hybrid functional TPSSh,[200] that delivered qualitative good data for organometallic Ni, Pd and Pt complexes.[92, 191, 201] The calculations show an essentially ligand-centred π*-type lowest unoccupied molecular orbital (LUMO) with very similar energies for all three complexes at around −2.3 eV, which agrees with the experimental data. The largest contribution mainly comes from both pyridyl units. These results agree with the reported Pt(II) complexes. A 4,6Me-substitution leads to slightly lower (more negative) potentials, while 5-Me substitution has no impact and anodic shifts for the reduction potentials of F- and CF_3-substituted complexes.[117, 121] The highest occupied molecular orbital (HOMO) gains essential contributions from phenyl C4, C2, C1, and C6, as well as metal d_{yz} and Cl p_z orbitals. Whereas their character does not change within the triade, the energies decrease from Ni > Pt > Pd, which confirms the measurements.

Further UV/vis absorption spectroscopy was performed to characterize the optical properties of this triade (Figure 3-20, Table 3-11). Since the free ligand Py(dMePhH)Py and all complexes show intense absorptions from 220 to 300 nm, they can be assigned to π−π* transitions from the tridentate ligand. Further, there are structured and less intense absorption bands up to 450 nm, that show a series of maxima redshifted from Pd (360 nm; cut-off at 402 nm) over Pt (380 nm; cut-off at 442 nm) to Ni (395 nm, an intense shoulder at 420 nm, a small component

at 465 nm; cut-off at 516 nm). This results in a series of increasing optical HOMO-LUMO gaps, i.e. Ni (2.40) < Pt (2.80) < Pd (3.08), that is already observed within the nickel group e.g. for [M(Phbpy)CN] complexes.[108]

The low energy bands of [Pt(Py(4,6MePh)Py)Cl] are assigned to spin-forbidden transitions into the triplet manifold, whose allowance increases with increasing spin-orbit coupling.[119, 121, 160, 184, 196] Differently substituted Pt(II) derivatives show shifts in the absorption maxima at around 380 nm. The 4,6F-substituted complex shows a small blueshift compared to the 4,6Me- or unsubstituted complex.[194] This 4,6-substitution shifts the absorption maxima around 400 nm in comparison to the parent complex, the 5-Me-, the 5-MeOOC- and the 4F-derivative.[121, 194] Remarkably, substitution with electronegative groups as in 3,4,5-F or 3,5-CF_3 seems to be detrimental for a blue-shift of the 380 nm band and the absorption maxima of these two complexes lie very close to the parent complex.[117]

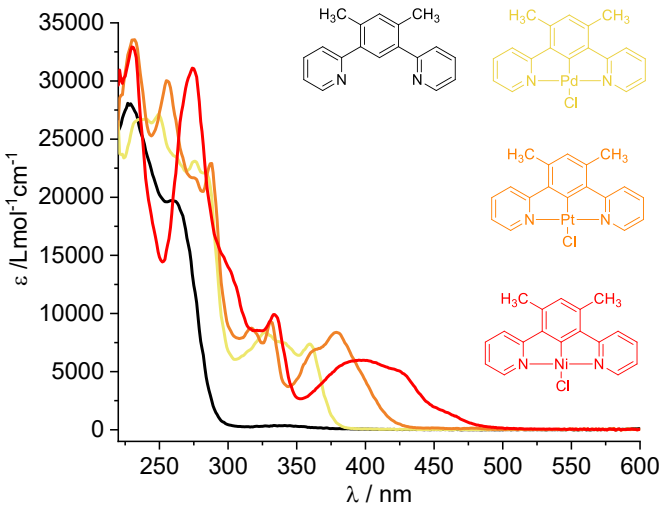

Figure 3-20 UV/vis absorption spectra of Py(4,6MePhH)Py and the complexes [M(Py(4,6MePh)Py)Cl] (M = Ni, Pd, Pt) in CH_2Cl_2 at rt. From Ref.[140].

Table 3-11 Selected UV/vis absorption maxima of Py(4,6MePhH)Py, the complexes [M(Py(4,6MePh)Py)Cl and related derivatives.

	Absorption Max. λ_x in nm (Ext. Coeff. ε in 1000 · $Lmol^{-1}cm^{-1}$)						
	λ_1	**λ_2**	**λ_3**	**λ_4**	**λ_5**	**λ_6**	**λ_7**
[Pt(PyPhPy)Cl][a,b,c]	-	255 (25.2)	289 (21.1)	332 (6.3)	379 (8.6)	402 (7.0)	485 (0.1)
[Ni(PyPhPy)Cl][d]	236 (35.5)	279 (26.8)	-	332 (5.7)	412 (6.3)	437 (6.7)	
Py(dMePhH)Py	227 (28.2)	260 (19.7)	340 (0.4)	636 (0.3)	-	-	-
[Pt(Py(dMePh)Py)Cl]	231 (33.7)	256 (30.0)	287 (22.9)	331 (9.2)	380 (8.3)	413 (1.5)	480 (0.1)

[Pd(Py(dMePh)Py)Cl]	239 (26.7)	275 (23.2)	283 (22.0)	327 (8.3)	360 (7.4)	375 (1.2)	-
[Ni(Py(dMePh)Py)Cl]	230 (33.0)	274 (31.2)	297 (14.7)	333 (9.0)	395 (6.1)	420 (5.3)^{sh}	465 (1.1)

Measured in CH_2Cl_2 at rt. sh = shoulder. a = From ref. [117]. b = From ref. [194]. c = From ref. [202]. d = From ref. [92].

Rose Jordan's TD-DFT calculations of the transitions generally agree qualitatively well with experimentally observed absorption maxima with the calculated low-energy transitions at 429 nm (Ni), 420 nm (Pt), and 394 nm (Pd), but slightly red-shifted if compared with the experimental maxima (395, 380, 360 nm).[140]

Further UV/vis spectroelectrochemical measurements were performed (Figure 3-21). Upon electrochemical reduction, all the three complexes [M(Py(4,6MePh)Py)Cl] exhibit long-wavelength absorptions at around 600 and 400 nm. We ascribe them to the radical anionic complexes $[M(Py(4,6MePh)Py)Cl]^{\bullet-}$ or $[M(Py(4,6MePh)Py)(THF)]^{\bullet}$ when assuming the cleavage of the Cl^- ligand after reduction. The bands can be assigned to transitions into π*–π* states within the reduced PyPhHPy ligand frame and they are very similar to those observed for [Ni(Py(Ph)Py)Cl].[92] The subtle red-shift of these two bands upon the second reduction for the Pt complex confirms this assignment. Upon oxidation, the long-wavelength MLCT bands vanish. As in all three cases, the oxidations are irreversible in the CV experiment and the species produced upon oxidation are not clear. However, in all three cases, very similar spectroscopic features are observed and pointing to comparable products from oxidation and subsequent decomposition.

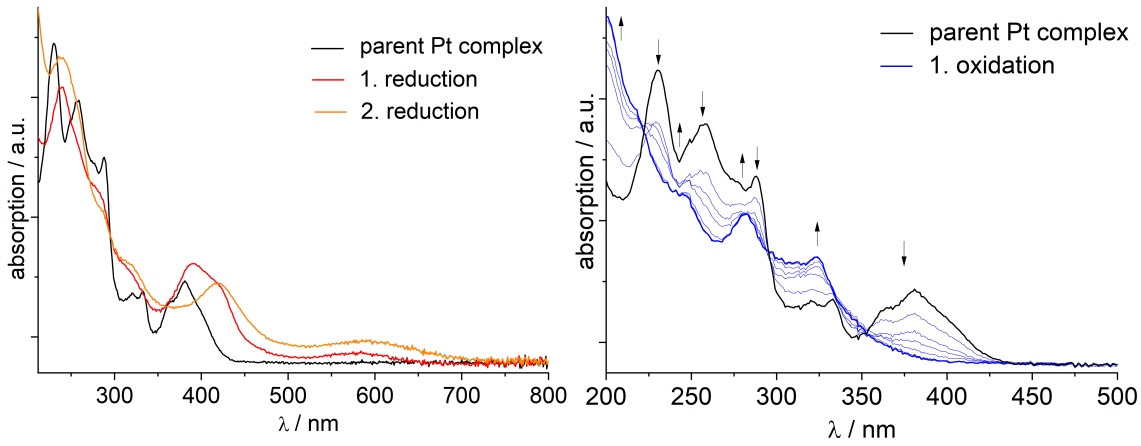

Figure 3-21 UV/vis absorption spectra of [Pt(Me_2dpb)Cl] in THF/$n$$Bu_4NPF_6$ recorded during cathodic reduction (left) and anodic oxidation (right).

The working group of *Strassert* contributed luminescence measurements for this triade.[140] The previously reported [Pt(Py(4,6MePh)Py)Cl] showed triplet luminescence at 495 nm in CH_2Cl_2 and at 498 nm in 2-MeTHF solution at 298 K, which shifted to 489 nm in a frozen glassy matrix at 77 K. This aligns with previous results.[117, 119, 121, 194, 196, 202] The Pd derivative showed a

structured emission band at 77 K peaking at 468 nm with a quantum yield of almost unity (as observed for the Pt derivative), joining the small list of equally performing isoleptical Pd and Pt complexes.[162, 173, 176, 177] Reports show a large number of Pt(II) complexes, that perform better than their Pd analogue.[108, 125, 172, 174, 175, 178-180, 187, 189] No emission was observed from the Ni complex at 77 K or at 298 K, not even in the solid state.

3.2 The Substitution of the Pyridylfunctions by other *N*-Heteroaromats

3.2.1 Synthesis and Characterization of the Ligands

The synthesis of the required N^C^N ligands bearing π-accepting units other than pyridine, turned out to be more challenging than for the central ring substituted ligands. For a central ring substitution under *Negishi* conditions,[5, 92] this reactive intermediate stays the same for each species, namely the easy to handle 2-pyridylzinc chloride. But changing the 2-pyridyl unit into a different *N*-heteroaromat, the reactivity and moreover the stability of these intermediates change as well. The therefore chosen *Negishi* (Figure 3-22, A) conditions are exactly the ones, that were successfully used for the ligand synthesis of central ring substituted N^CH^N protoligands.[92] Exept of the 2-pyrazylzinc chloride (used for the 1,3-di(2-pyrazyl)benzene ligand, PzPhHPz), all other zinc organyls at least partially decomposed. Therefore the use of *Suzuki-Miyaura* conditions was necessary to access these structures (Figure 3-22, B).[4, 203] By using 1,3-phenylene-diboronic acid, Bpin(PhH)Bpin or Bpin(4,6FPhH)Bpin (Bpin = 4,4,5,5-tetramethyl-1,3,2-dioxaborolanylide)[204], the reactive group is placed on the central phenide unit, which made the reaction less dependent of the varying peripheric π-acceptor.

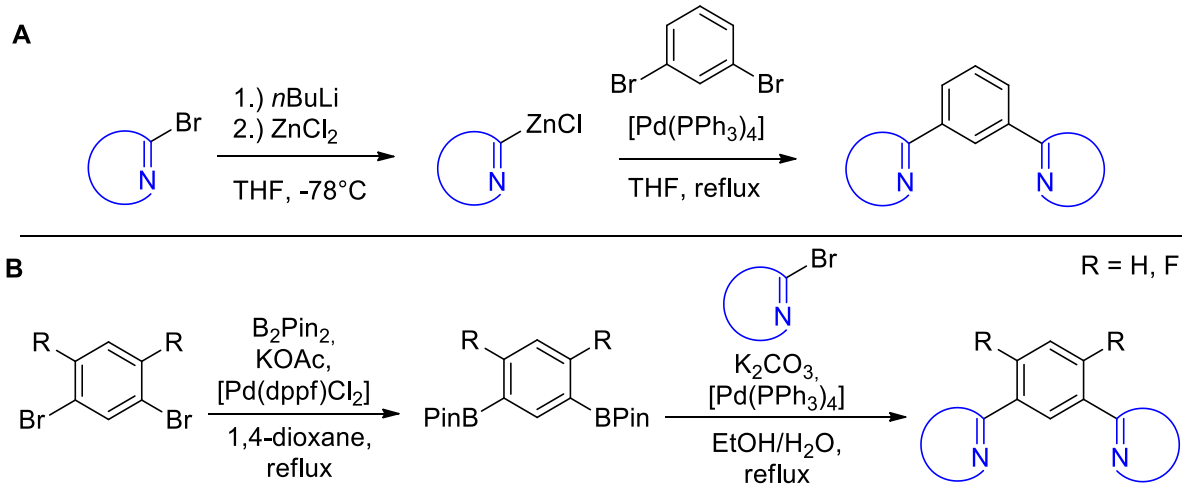

Figure 3-22 *Negishi* (A) vs. *Suzuki-Miyaura* (B) cross coupling used for the synthesis of peripheric ring substituted N^CH^N protoligands.[92, 203]

Both routes were combined to synthesize asymmetric N^CH^N' protoligands as well. Starting from 3-bromophenylene boronic acid, a *Suzuki-Miyaura* reaction [4, 203] giving HetAr(PhH)Br was performed, followed by a *Negishi* C–C cross coupling was performed giving a variety of HetAr(PhH)Py ligands (Figure 3-23).[5, 92]

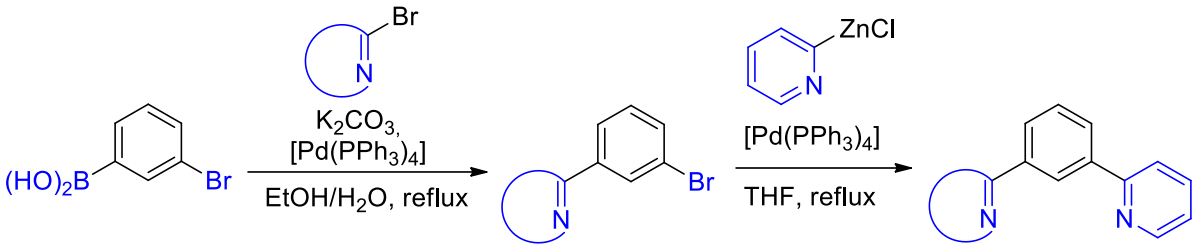

Figure 3-23 Synthetic route for asymmetric N^CH^N' protoligands of the type HetAr(PhH)Py.

Since the targeted base assisted C–H activation reaction turned out to be dependent on the geometry and sterics of the tridentate ligand (see Chapter 3.2.2), some ligands were synthesized bearing a chloride substituent at the to be coordinating carbon atom (Figure 3-24). These ligands were planned to be used in an oxidative addition reaction with a Ni(0) precursor. 1,3-dibromo-2-chloro benzene was transformed into the 1,3-BPin derivative,[204] which was then used under *Suzuki-Miyaura* conditions to form the protoligands.[4, 203]

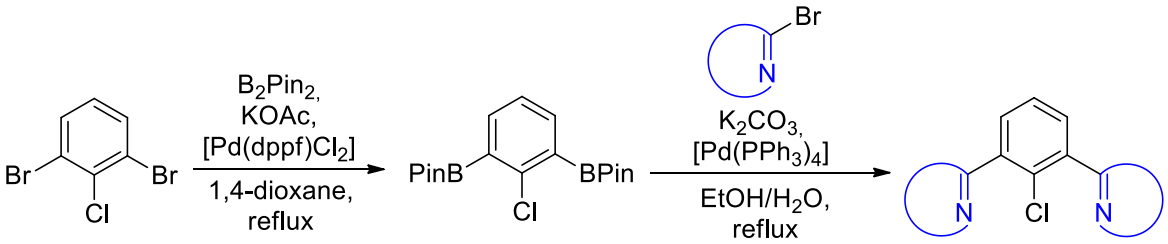

Figure 3-24 *Suzuki-Miyaura* conditions for the synthesis of chloro substituted ligands of the type N^CCl^N.

Using these routes 14 ligands were synthesized in yields ranging from 26 to 98% as off-white solids (Table 3-12). After purification *via* column chromatography or a selective precipitation, the products analyzed by ^{1}H NMR spectroscopy, mass spectrometry (MS) and elemental analysis (for details, see Experimental Section, Chapter 5.2.3).

Table 3-12 Synthesized N^CH^N, N^CH^N' and N^CCl^N ligands with substituted peripheric rings.

Compound Name	Structure	Synthetic Pathway	Yield
Pz(PhH)Pz	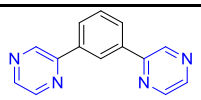	*Negishi* conditions	30%
Pym(PhH)Pym	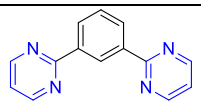	*Suzuki-Miyaura* conditions	78%
2^{i}Qu(PhH)2^{i}Qu	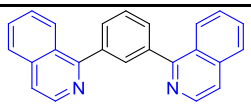	*Suzuki-Miyaura* conditions	98%
2^{i}Qu(4,6FPhH)2^{i}Qu	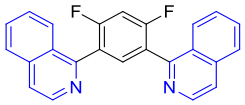	*Suzuki-Miyaura* conditions	94%
2Qu(PhCl)2Qu	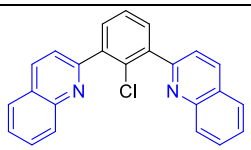	*Suzuki-Miyaura* conditions	87%
2Qu(PhH)Py	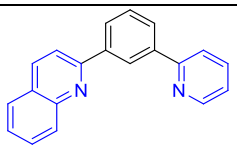	*Suzuki-Miyaura* + *Negishi* conditions	40%
2Tz(PhCl)2Tz	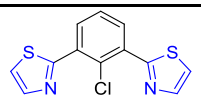	*Suzuki-Miyaura* conditions	93%
4Tz(PhCl)4Tz	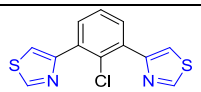	*Suzuki-Miyaura* conditions	62%
2Btz(PhCl)2Btz	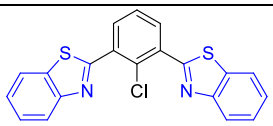	*Suzuki-Miyaura* conditions	61%
2Tz(PhH)Py	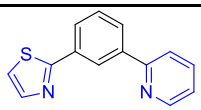	*Suzuki-Miyaura* + *Negishi* conditions	80%
4Tz(PhH)Py	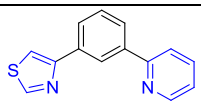	*Suzuki-Miyaura* + *Negishi* conditions	86%
2Btz(PhH)Py	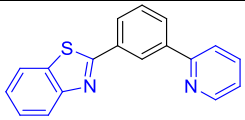	*Suzuki-Miyaura* + *Negishi* conditions	82%
3ClPy(PhH)3ClPy	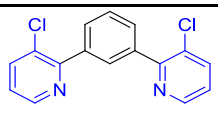	*Suzuki-Miyaura* conditions	55%
3FPy(4,6FPhH)3FPy	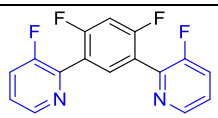	*Suzuki-Miyaura* conditions	26%

The synthesized N^C^N ligands can be divided into groups by their peripheric aromats. The ones bearing two-nitrogen atoms of which the 2-pyrimidine (2-Pym) derivative was firstly reported in 2010 as a product of a *Stille* cross coupling.[117] The synthesis of 1,3-di(2-pyrazyl) benzene was reported one year later using *Suzuki-Miyaura* conditions.[139] The second group is formed by quinoline containing ligands. The synthesis of 2^{i}Qu(PhH)2^{i}Qu was known since 1994,[205] followed by a publication using *Suzuki-Miyaura* conditions in 2010, which also gives the first report of the 4,6-difluoro-substituted derivative using same conditions.[117] Both 2-quinoline ligands, all symmetric thiazole N^CCl^N chloroligands, all asymmetric N^CH^N' protoligands, as well as both 3-halidopyridine containing ligands are literary unknown.

Cyclic voltammetry shows that the potentials of N^C^N ligands vary significantly depending on the type of the π-acceptor units with potentials for the first reduction going from –2.1 V to almost –3.0 V, followed by up to three more reductions (Figure 3-25).

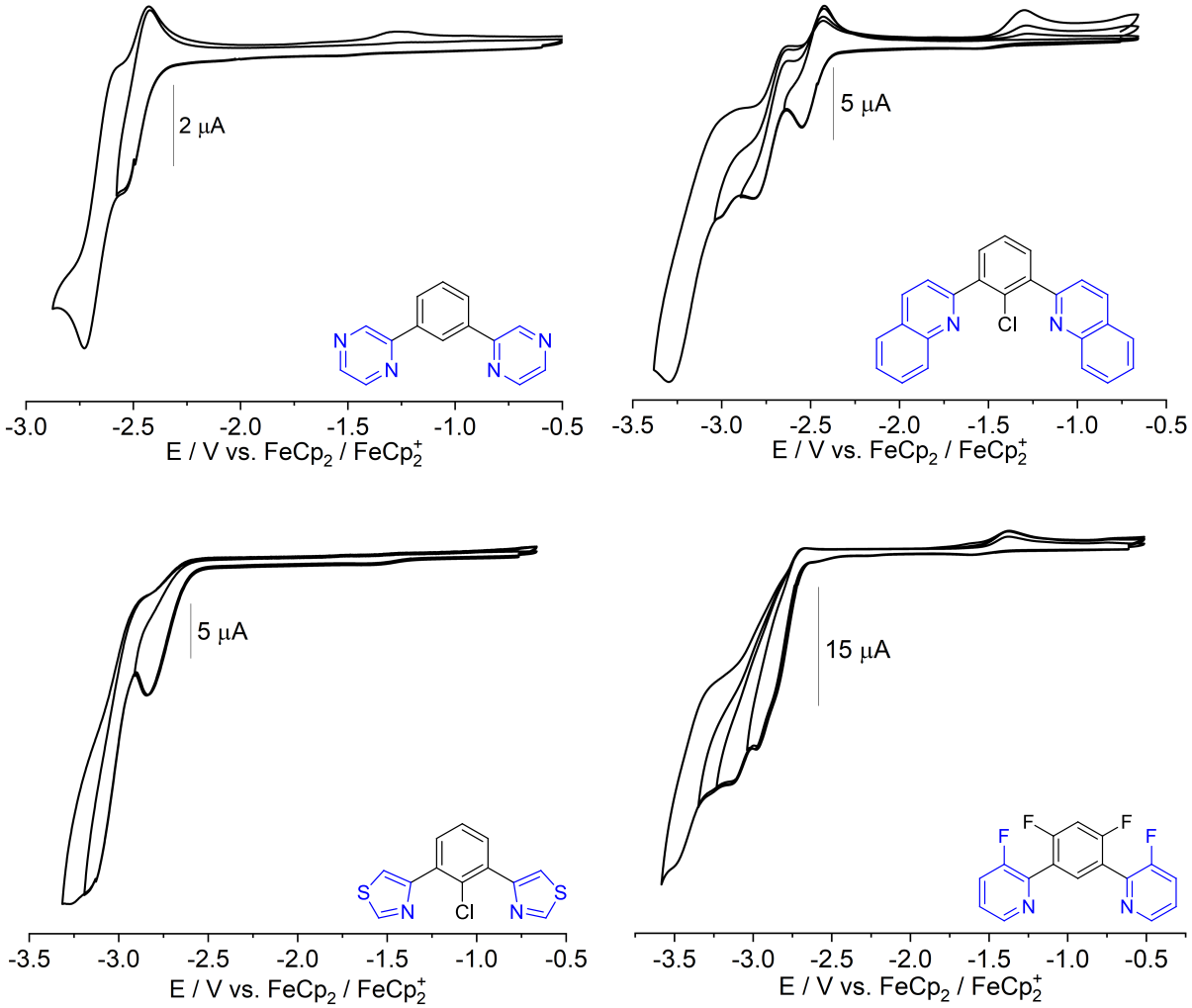

Figure 3-25 Cyclic voltammograms of Pz(PhH)Pz (*top left*), 2Qu(PhCl)2Qu (*top right*), 4Tz(PhCl)4Tz (*bottom left*) and 3FPy(4,6FPhH)3FPy (*bottom right*), measured in a 0.1M nBu$_4$NPF$_6$ solution in THF at a scan rate of 100 mV/s.

Both ligands bearing peripheric aromats with two nitrogen atoms show an anodic shift of both reductions in comparison to the standard PyPhHPy ligand to with a highest shift up to –2.50 V for Pz(PhH)Pz (Figure 3-25*, top left*). Same is true for the quinoline containing ligands. Surprisingly, both 2-isoquinoline derivatives show a first irreversible reduction at approx. –2.75 V, whereas the ligands bearing a 2-quinoline units show reversible first reductions at –2.48 V, indicating a stronger π-acceptor character for these ligands. 2Qu(PhCl)2Qu (Figure 3-25, *top right*) shows a reversible first reduction, although it is substituted by a halide and therefore indicating an EC mechanism, as it was observed by *Vogt* and *Sandleben* by investigating XC^N^N (X = F, Cl, Br, I) ligands.[91,89] However, in this case the LUMO is apparently not on the C–X position of the molecule, but more on the quinoline parts.

Thiazole containing ligands show a broad range of shifts within their group, as 4Tz(PhCl)4Tz (Figure 3-25, *bottom left*) shows a cathodic shift in comparison to the standard ligand with E_{Red1} = –2.84 V (E_{pc}), whereas 2Btz(PhCl)2Btz the largest anodic shift of the first reduction to peak potentials E_{Red1} = –2.15 V (E_{pc}). The highest cathodic shift of the reduction potentials and therefore gives 3FPy(4,6FPhH)3FPy with four irreversible reductions with E_{Red1} = –2.98 V(E_{pc}), (Figure 3-25, *bottom right*). For further cyclic voltammograms, see Chapter 7.4.

The large shifts of the reduction potentials by exchanging the π-accepting units aligns with previous calculations, showing that these units are responsible for uptaking an electron, as discussed in Chapter 3.1.1 (Table 3-13). [92, 117, 136, 138-140]

Table 3-13 Reduction potentials of all other than pyridine containing N^C^N and N^CCl^N ligands.

	***E* Red1**	***E* Red2 (E_{pc})**	***E* Red3 (E_{pc})**
PyPhHPy[a]	–2.83 ($E_{1/2}$)	–3.31	-
Pz(PhH)Pz	–2.50 ($E_{1/2}$)	–2.73	-
Pym(PhH)Pym	–2.63 ($E_{1/2}$)	–3.01	-
2^{i}Qu(PhH)2^{i}Qu	–2.79 (E_{pc})	–3.14	-
2^{i}Qu(4,6FPhH)2^{i}Qu	–2.75 (E_{pc})	–3.19	-
2Qu(PhCl)2Qu[b]	–2.49 ($E_{1/2}$)	–2.82	–3.02
2Qu(PhH)Py	–2.48 ($E_{1/2}$)	–2.96	–3.10
2Tz(PhCl)2Tz[c]	–2.34 (E_{pc})	–2.57 ($E_{1/2}$)	–3.05
4Tz(PhCl)4Tz	–2.84 (E_{pc})	–3.18	–3.27
2Btz(PhCl)2Btz[d]	–2.15 (E_{pc})	–2.31 ($E_{1/2}$)	–2.70
2Tz(PhH)Py	–2.64 ($E_{1/2}$)	–3.17	–3.35
4Tz(PhH)Py	–2.82 ($E_{1/2}$)	–3.20	–3.35
2Btz(PhH)Py	–2.43 ($E_{1/2}$)	–2.93	–3.22
3ClPy(PhH)3ClPy[e]	–2.73 (E_{pc})	–2.84 ($E_{1/2}$)	–3.30
3FPy(4,6FPhH)3FPy[f]	–2.98 (E_{pc})	–3.14	–3.30

Measured in a 0.1M *n*Bu_4NPF_6 solution in THF at rt with a scan rate of 100 mV/s. All potentials in V. E_{pc} = Cathodic Peak Potential, $E_{1/2}$ = Half-Step Potential. a = From ref. [92]. b = Red4 at –3.30 V (E_{pc}). c = Red4 at –3.36 V (E_{pc}). d = Red4 at –2.90 V ($E_{1/2}$). e = Red4 at –3.61 V (E_{pc}). f = Red4 at –3.53 V (E_{pc}).

These results could be supported by UV/vis absorption spectroscopy, recorded in dry THF, showing that the absorption bands of this ligand class change significantly by the character of the π-accepting unit with absorption maxima between 230 and 350 nm and extinction coefficients up to 61000 $Lmol^{-1}cm^{-1}$. These can be assigned to π–π* transitions based on previous work (see Chapter 3.1.1).[89, 91, 92, 117, 121, 134-139] 3ClPy(PhH)3ClPy and 3FPy(4,6FPhH)3FPy showed highly similar absorption properties and are therefore not discussed in detail (spectra, see Chapter 7.5).

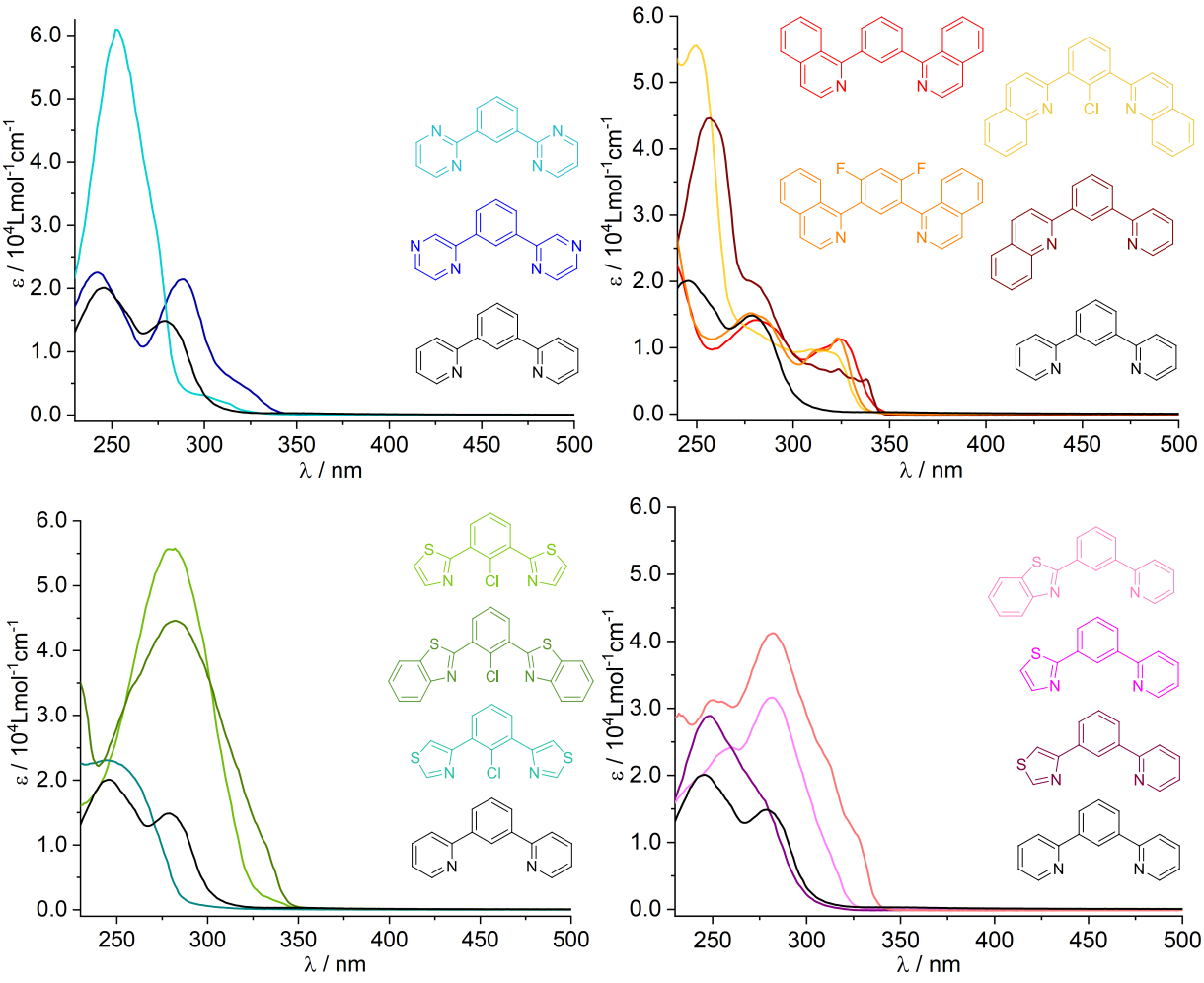

Figure 3-26 UV/vis spectra of N^C^N ligands bearing different π-acceptor units than pyridine in comparison to the standard ligand Py(PhH)Py, measured in THF at rt. *Top left:* Pyrimidine and Pyrazine ligands. *Top right:* Quinoline containing ligands. *Bottom left:* Symmetric thiazole containing ligands. *Bottom right:* Asymmetric thiazole containing ligands.

Starting from the pyrazine and pyrimidine derivative (Figure 3-26, *top left*) it is notable that the position of the second nitrogen atom plays a substantial role for the optical properties of the N^C^N ligands. Whereas Pz(PhH)Pz shows very similar absorption maxima to the standard ligand (242 and 288 nm), the pyrimidine derivative shows only one hypsochromically shifted absorption maximum at 253 nm with a much higher extinction coefficient (61000 $Lmol^{-1}cm^{-1}$). This might be the result of a new C_2 symmetry within the peripheric aromatic ring and its orbitals

by the setup of a 1,3-diheteroatom containing aromat on both sides of the ligand, leading to a combination of two transitions and therefore a higher intensity. This phenomenon is observed for the symmetric 2-thiazole (2Tz) and 2-benzothiazole (2Btz) containing ligands as well (Figure 3-26, *bottom left*). Besides the redshift of the absorption maximum of those, that on the one hand bases on the substitution of the ligand through a chloride function, leading to a lower electron density within the ligand, and on the second hand gets even stronger with an expansion of the π-system in the benzothiazole derivative, one can see that there is only one absorption maximum at 280 nm for each ligand with an much higher extinction coefficient, than the standard ligand or the 4-thiazole (4Tz) derivative. However, the 4-thiazole containing ligand shows an absorption maxima to 245 nm, which underlines the importance of the position of the second heteroatom within the chosen aromats. Comparing these properties to the asymmetric thiazole containing ligands (Figure 3-26, *bottom right*) shows that the described effects are still observable, but weaker than the ligands containing two thiazole functions. The quinoline containing ligands (Figure 3-26, *top right*) show that the 2-isoquinoline derivatives have a significant hypochromic redshift of both absorption maxima to 288 and 325 nm in comparison to the standard ligand, whereas the 2-quinoline derivatives show one absorption maximum at approx. 250 nm with higher extinction coefficients (44600 and 55500 $Lmol^{-1}cm^{-1}$) followed by lower absorption maxima at the energies 300 to 350 nm. The shoulder at 280 nm in the absorption spectrum of 2Qu(PhH)Py is a result of the asymmetric character of this ligand, due to the similarity of this band to the one from Py(PhH)Py at the same wavelength.

Table 3-14 Absorption max. and extinction coeff. of other than pyridine containing N^C^N and N^CCl^N ligands.

Ligand	Absorption Max. λ_x in nm (Ext. Coeff. ε in 1000 · $Lmol^{-1}cm^{-1}$)		
	λ_3	λ_2	λ_1
PyPhHPy[a]	-	279 (14.9)	245 (20.1)
Pz(PhH)Pz	311 (6.6)[sh]	289 (21.5)	241 (22.5)
Pym(PhH)Pym	-	293 (3.5)[sh]	253 (60.9)
2[i]Qu(PhH)2[i]Qu	324 (11.4)	317 (10.0)[sh]	280 (14.2)
2[i]Qu(4,6FPhH)2[i]Qu	323 (11.5)	314 (9.7)[sh]	278 (15.2)
2Qu(PhCl)2Qu	316 (9.7)	274 (13.5)[sh]	249 (55.5)
2Qu(PhH)Py[b]	324 (6.5)	277 (20.0)[sh]	257 (44.5)
2Tz(PhCl)2Tz	-	-	279 (55.7)
4Tz(PhCl)4Tz	-	-	245 (22.9)
2Btz(PhCl)2Btz	-	-	283 (44.6)
2Tz(PhH)Py	-	281 (31.6)	260 (24.2)
4Tz(PhH)Py	-	266 (20.8)[sh]	248 (28.9)
2Btz(PhH)Py[c]	306 (24.9)[sh]	282 (41.2)	251 (31.4)

3ClPy(PhH)3ClPy	-	280 (12.9)	239 (21.2)
3FPy(4,6FPhH)3FPy	-	274 (18.7)	233 (24.9)^{sh}

Measured in THF at rt. sh = shoulder. a = From ref. [92]. b = λ_4 at 338 nm (ε = 5200 Lmol^{-1}cm^{-1}). c = λ_4 at 320 nm (ε = 13500 Lmol^{-1}cm^{-1})^{sh}.

In general, the substitution of the peripheric rings leads to greater shifts, than a substitution of the central phenide unit (see Chapter 3.1.1). This again proofs, that the main chromophore of these ligands is localized in the peripheric units and not in the central C-ring.[92, 117, 136, 138, 140]

3.2.2 Synthesis and Characterization of the Ni(II) Complexes

Most N^C^N complexes carrying different *N*-heteroaromats as peripheric rings than pyridine were synthesized *via* base-assisted C–H activation, that could already be used for central ring substituted derivatives (see Chapter 3.1.2).[92] However, in this work new limitations of this synthetic route could be discovered. Whereas ligands, that are built up by three connected six-membered rings (e.g. Pz(PhH)Pz) showed a successful cyclometalation with yields from 26 to 62% (Figure 3-27, A), the ones that bear two five membered rings on a phenide unit (e.g. 2Tz(PhH)2Tz) lead to a reisolation of the protoligand (Figure 3-27, C). This indicates the relevant aspect of the N^C^N bite angle for this cyclonickelation method. Asymmetric ligands with a slightly smaller bite angle bearing with a five-membered ring on one side and a six-membered ring on the other side of the phenide unit (e.g. 4Tz(PhH)Py) are again able to perform this reaction (yields from 40 to 77%, Figure 3-27, B). Since Ni(II) C^N^N complexes with two 5-membered rings on the central aromat were investigated by *Vogt*,[91] it conclusively led to an adaption of the oxidative addition method from *Klein et al.* from 2014 onto Ni(II) N^C^N systems.[99] [Ni(COD)$_2$] was oxidatively added into the carbon-halide bond of the halidoligand N^CCl^N in THF, allowing the access to these cyclonickelated complexes (Figure 3-27, D) with very good yields (up to >99%).

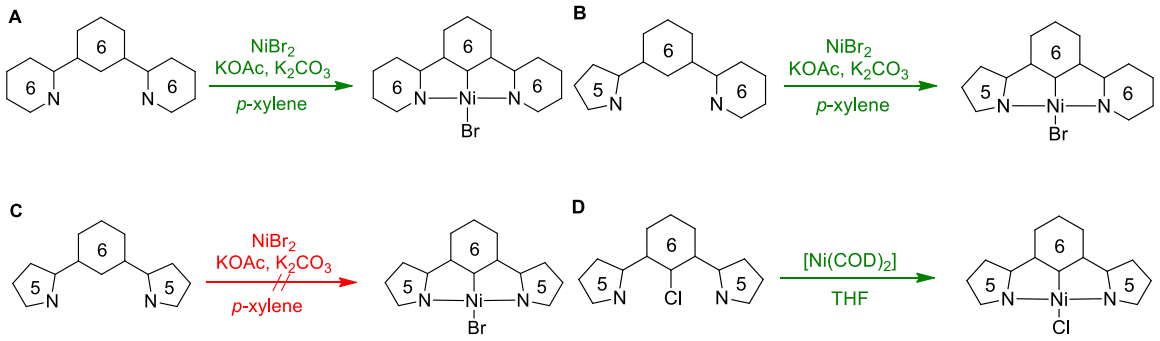

Figure 3-27 6ring-6ring-6ring (*A*) and 5ring-6ring-6-ring (*B*) N^CH^N' ligand systems were transformed into Ni(II) complexes *via* C–H activation. 5ring-6ring-5ring N^CH^N (*C*) ligand systems failed to produce the Ni(II) complex *via* C–H activation. Alternatively, the oxidative addition reaction using the chlorido-substituted ligand N^CCl^N and Ni(0) was successful (*D*).

The second limitation of the base assisted C–H activation occurred when using ligands with a blocked ortho-*N* position of the peripheric aromats (e.g. 2Qu(PhH)2Qu), where again the protoligands were quantitively isolated after each reaction. The problem might be the result of sterics, where the position to be cyclometalated is shielded too much. The strong driving force of an oxidative addition reaction was therefore used (Figure 3-28).

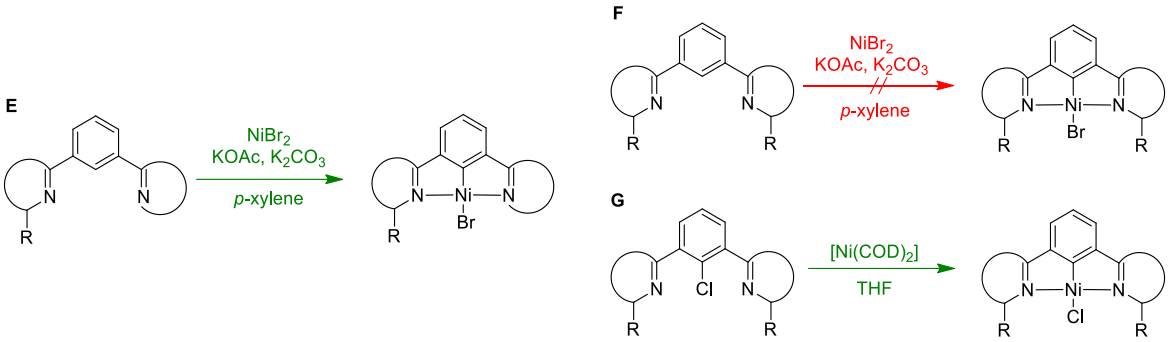

Figure 3-28 Asymmetric ortho-*N* substituted N^CH^N' ligands can successfully be transformed into the respective Ni(II) species (*E*), whereas symmetrically doubly ortho-*N* substituted ligands fail to produce the Ni(II) species (*F*). Alternatively, the oxidative addition reaction using the chlorido substituted ligand N^CCl^N and Ni(0) was successful (*G*).

The proof of all synthesized compounds is given by ^{1}H NMR spectroscopy and mass spectrometry and elemental analysis (see Chapter 5.4.2). Further most compounds could be crystalized using isothermal evaporation out of a concentrated THF solution at 3°C for a structure solution of [Ni(Pym(Ph)Pym)Br] in the triclinic spacegroup $P\bar{1}$ with two units per unit cell (Figure 3-29, Table 3-15).

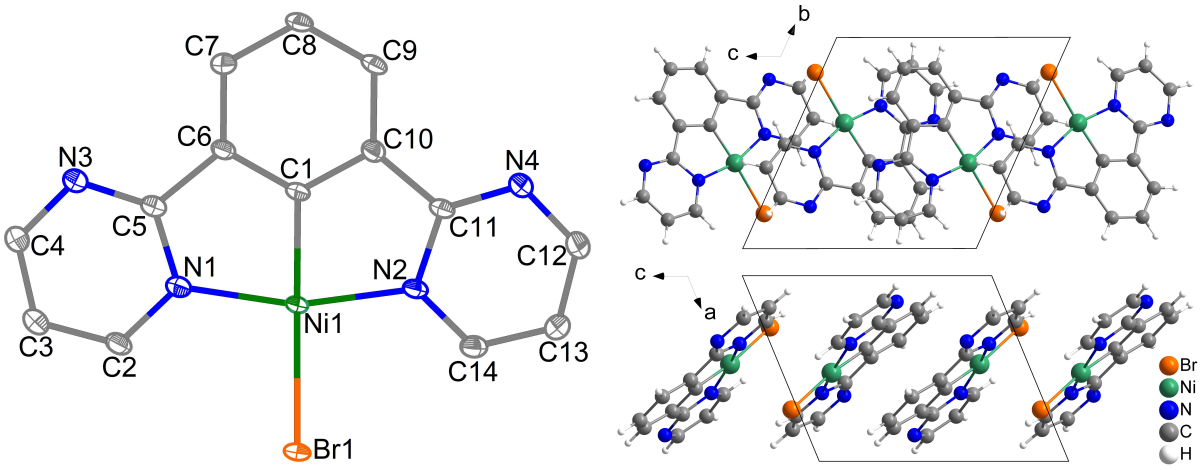

Figure 3-29 *Left:* Asymmetric unit of [Ni(Pym(Ph)Pym)Br]. Hydrogen atoms are omitted for clarity. Ellipsoids are shown with a 50% probability. *Right:* Crystal structure viewed along the crystallographic *a*- (top) and *b*-axis (bottom).

Table 3-15 Crystallographic data for [Ni(Pym(Ph)Pym)Br].

Identification code	**[Ni(Pym(Ph)Pym)Br]**
Empirical formula	$C_{14}H_9BrN_4Ni$
Temperature/K	100.00
Crystal system	triclinic
Space group	$P\bar{1}$
a/Å	7.7380(6)
b/Å	9.6145(7)
c/Å	9.8063(6)
α/°	108.190(3)
β/°	106.069(3)
γ/°	104.167(3)
Volume/Å^3	620.66(8)
Z	2
ρ_{calc}g/cm^3	1.990
F(000)	368.0
Radiation	MoKα (λ = 0.71073)
2Θ range for data collection/°	4.734 to 56.564
Index ranges	–10 ≤ h ≤ 10, –12 ≤ k ≤ 12, –13 ≤ l ≤ 13
Reflections collected	34963
Independent reflections	3074 [R_{int} = 0.0472, R_{sigma} = 0.0234]
Data/restraints/parameters	3074/0/181
Goodness-of-fit on F^2	1.087
Final R indexes [I>=2σ (I)]	R_1 = 0.0288, wR_2 = 0.0713
Final R indexes [all data]	R_1 = 0.0320, wR_2 = 0.0730
Largest diff. peak/hole / eÅ^{-3}	1.15/–0.49
CCDC	2343476

The nickel(II) center is surrounded by the tridentate N^C^N ligand and the halide coligand in a square-planar geometry, as expected.[92, 127, 140] The typical chelate bite angle of around 82° and N1–Ni–N2 angles of 163° are typical for similar structures. [89, 91, 92, 99, 100, 104, 108, 116, 117, 122, 123, 127, 140-147] All aromats of the tridentate ligand are coplanar with a maximum torsion angle of 2.7° (N3–C5–C6–C7). The nickel atom stays in this plane, whereas the coligand turns out by a value of 6.8°. In general, the bond lengths and -angles of the geometry around the coordinated metal are very similar to the standard complex (Table 3-16).[92] The crystal structure along the crystallographic *a*-axis shows the typical head-to-tail arrangement, that is caused by a weak intermolecular π-stacking of two Pym-Ph functions with a distance of 3.63 Å.[149] Crystal structures of three Pt(II) complexes bearing substituted Pym(Ph)Pym ligands were known since 2022 and showing comparable trends for the bond lengths and -angles around the metal centre, as they are observed for [M(Py(4,6MePh)Py)Cl], when comparing the Ni(II) to the Pt(II) compound (CCDC: 2126978, 2126979 and 2164618).[140, 206, 207]

Table 3-16 Angles and bond lengths of [Ni(Pym(Ph)Pym)Br].

	[Ni(PyPhPy)Br][a]	[Pt(Pym(5MeOPh)Pym)CCPh][b]	[Ni(Pym(Ph)Pym)Br]
Distances / Å			
M–C1	1.8298(2)	1.951(8)	1.832(2)
M–N1	1.9489(1)	2.030(6)	1.940(1)
M–N2	1.9536(1)	2.029(7)	1.9353(2)
M–Br1/C16[b]	2.3963(3)	2.125(8)	2.3850(4)
Angles / °			
C1–M–N1	81.94(7)	79.00(3)	81.88(9)
C1–M–N2	81.85(7)	80.30(3)	81.98(9)
N1–M–Br1/C16[b]	97.83(4)	102.50(3)	98.73(6)
N2–M–Br1/C16[b]	98.39(4)	98.10(3)	97.54(6)
Sum / °	360.0		360.1
C1–M–Br1/C16[b]	179.48(5)	176.80(4)	173.14(7)
N1–M–N2	163.78(6)	159.30(2)	163.73(8)

a = From ref. [92]. b = From ref. [206]

The quinoline containing complexes crystallized within a few days by overlaying a CH_2Cl_2 or THF solution of the complex with *n*-pentane in a *Schlenk* tube at rt. Using this method [Ni(2^{i}Qu(Ph)2^{i}Qu)Br], [Ni(2^{i}Qu(4,6FPh)2^{i}Qu)Br] and [Ni(2Qu(Ph)2Qu)Cl] could be crystallized.

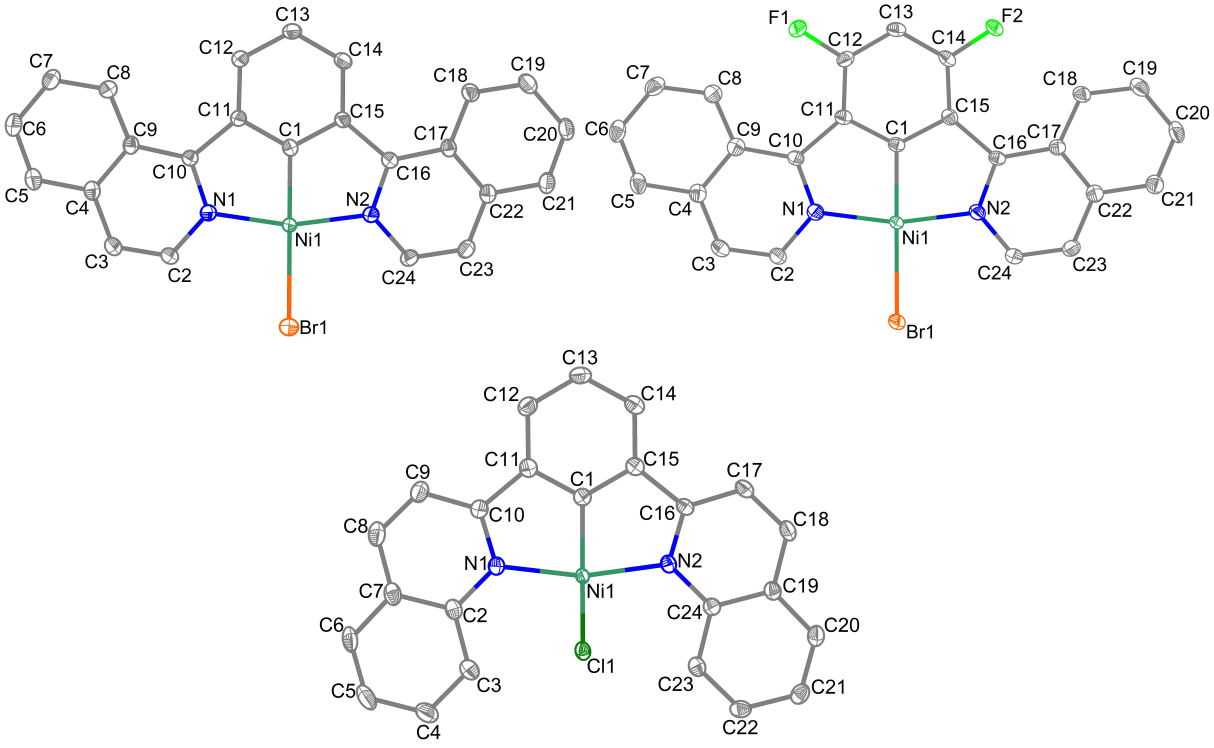

Figure 3-30 Asymmetric units of [Ni(2^{i}Qu(Ph)2^{i}Qu)Br] (*top left*), [Ni(2^{i}Qu(4,6FPh)2^{i}Qu)Br] (*top right*) and [Ni(2Qu(Ph)2Qu)Cl] (*bottom*). Hydrogen atoms are omitted for clarity. Ellipsoids are shown with a 50% probability.

Both 2-isoquinoline derivatives crystallized isostructurally in the triclinic spacegroup $P\bar{1}$ with two units per unit cell, whereas the 2-quinoline complex crystallized in the monoclinic spacegroup $P2_1/c$ with bearing four units per unit cell (Figure 3-30,Table 3-17).

Table 3-17 Crystallographic data of [Ni(2^{i}Qu(Ph)2^{i}Qu)Br], [Ni(2^{i}Qu(4,6FPh)2^{i}Qu)Br] and [Ni(2Qu(Ph)2Qu)Cl].

Identification code	**[Ni(2^{i}Qu(Ph)2^{i}Qu)Br]**	**[Ni(2^{i}Qu(4,6FPh)2^{i}Qu)Br]**	**[Ni(2Qu(Ph)2Qu)Cl]**
Empirical formula	$C_{24}H_{15}BrN_2Ni$	$C_{24}H_{13}BrF_2N_2Ni$	$C_{24}H_{15}ClN_2Ni$
Temperature/K	103.00	100.00	100.0
Crystal system	triclinic	triclinic	monoclinic
Space group	$P\bar{1}$	$P\bar{1}$	$P2_1/c$
a/Å	7.5676(4)	7.6925(5)	9.5913(4)
b/Å	10.8971(6)	10.8683(6)	12.4899(5)
c/Å	10.9976(6)	11.6319(7)	14.9938(6)
α/°	87.515(2)	87.772(2)	90
β/°	80.243(2)	72.098(2)	95.7960(1)
γ/°	76.359(2)	75.008(2)	90
Volume/Å^3	868.58(8)	893.02(9)	1786.99(1)
Z	2	2	4
ρ_{calc}g/cm^3	1.797	1.882	1.582
F(000)	472.0	504.0	872.0
Radiation	MoKα (λ = 0.71073)	MoKα (λ = 0.71073)	MoKα (λ = 0.71073)
2Θ range for data collection/°	5.368 to 61.026	3.884 to 56.72	4.254 to 56.558
Index ranges	–10 ≤ h ≤ 10, –15 ≤ k ≤ 15, 0 ≤ l ≤ 15	–10 ≤ h ≤ 10, –14 ≤ k ≤ 14, –15 ≤ l ≤ 15	–12 ≤ h ≤ 12, –16 ≤ k ≤ 16, –19 ≤ l ≤ 19
Reflections collected	9683	55139	63244
Independent reflections	9683 [R_{int} = 0.0428, R_{sigma} = 0.0277]	4457 [R_{int} = 0.0614, R_{sigma} = 0.0260]	4419 [R_{int} = 0.0656, R_{sigma} = 0.0245]
Data/restraints/parameters	9683/0/254	4457/0/271	4419/0/253
Goodness-of-fit on F^2	1.033	1.031	1.094
Final R indexes [I>=2σ (I)]	R_1 = 0.0362, wR_2 = 0.0857	R_1 = 0.0332, wR_2 = 0.0832	R_1 = 0.0364, wR_2 = 0.0809
Final R indexes [all data]	R_1 = 0.0470, wR_2 = 0.0916	R_1 = 0.0419, wR_2 = 0.0875	R_1 = 0.0438, wR_2 = 0.0855
Largest diff. peak/hole / eÅ^{-3}	0.97/–0.76	1.06/–0.47	0.70/–0.50
CCDC	2343470	2343473	2343468

All structures are set up with one complex molecule per asymmetric unit. The nickel center is surrounded in a square planar moiety, with sums of angles around the nickel center of 360.0 to 362.6° and bite angles of 82°, as typically reported for similar structures.[89, 91, 92, 99, 100, 104, 108, 116, 117, 122, 123, 127, 140-147] In general, the bond lengths and -angles around the nickel center are especially very similar to the reported standard complex.[92, 140] Through coordination, the ligands get slightly twisted with angles between the phenide and 2-quinoline units of up to 12.3°

for the 2-isoquinoline complex, which can be increased by a 4,6-phenide substitution up to 19.1°. This twist is way lower for the 2-quinoline derivative (6.3°), which can easily be explained by the difference in sterics of both 2-quinoline units and their correlation to the phenide unit. The structures for both 2-isoquinoline Pt(II) chlorido analogues were published in 2010 (4,6FPh, CCDC: 840430)[117] and 2022 (CCDC: 2164616),[207] of which only the difluoro-substituted complex shows this phenomenon. The type of quinoline also leads to different C1–Ni–X1 angles, in which the 2-quinoline derivative shows the largest difference from the ideal 180° with 149.3°, whereas both 2-isoquinoline derivatives show lower angles with 177.2° for [Ni(2*i*Qu(Ph)2*i*Qu)Br] and 168.2° for [Ni(2*i*Qu(4,6FPh)2*i*Qu)Br] (Figure 3-31).

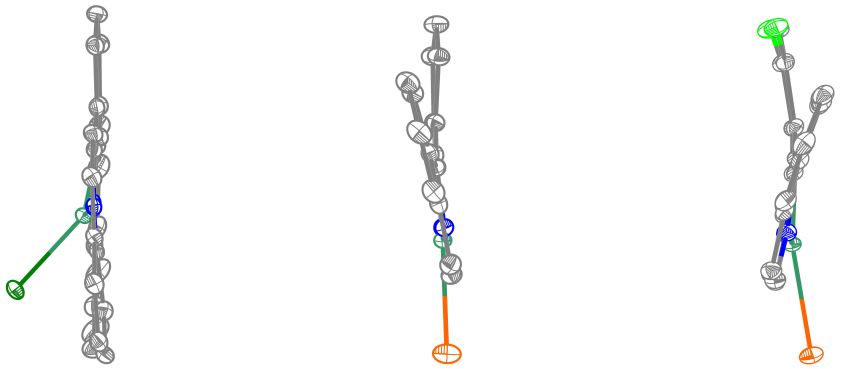

Figure 3-31 The structural influence on the geometry of [Ni(2Qu(Ph)2Qu)Cl] (*left*), [Ni(2^{i}Qu(Ph)2^{i}Qu)Br] (*middle*), [Ni(2^{i}Qu(4,6FPh)2^{i}Qu)Br] (*right*) on the C1–Ni–X1 angle and on the angle between quinolines and the phenide unit.

Both 2-isoquinoline complexes compared to each other show a very similar coordination around the nickel atom. The bond length around the Ni(II) centre are very similar to the parent complex.[92] Also the comparison of bond lengths and -angles to their Pt(II) analogues agrees with trends of other comparable isostructural Ni(II) and Pt(II) N^C^N complexes.[117, 140, 207] The 2-quinoline derivative also shows a similar Ni–C1 distance, but the bond ones to both nitrogen atoms gets larger and shows values around 1.98 Å. The bond to the coligand changes to a value of 2.28 Å. Interestingly, the chloride coligand is not placed in a centered position between both nitrogen atoms but shows an N1–Ni–Cl1 angle of 100.8° (Table 3-18).

Table 3-18 Angles and bond lengths of all synthesized quinoline containing complexes in comparison to the standard complexes [Ni(Py(Ph)Py)Cl] and [Ni(Py(Ph)Py)Br].

	[Ni(PyPhPy)Br][a]	[Ni(PyPhPy)Cl][a]	[Ni(2^{i}Qu(Ph)2^{i}Qu)Br]	[Ni(2^{i}Qu(4,6FPh)2^{i}Qu)Br]	[Ni(2Qu(Ph)2Qu)Cl]
Dist. / Å					
Ni–C1	1.8298(2)	1.836(7)	1.824(3)	1.829(2)	1.824(2)
Ni–N1	1.9489(1)	1.932(6)	1.937(2)	1.920(2)	1.9850(1)
Ni–N2	1.9536(1)	1.936(5)	1.939(2)	1.920(2)	1.9747(1)
Ni–X1	2.3963(3)	2.247(2)	2.4012(4)	2.3894(4)	2.2754(6)

Angles / °					
C1–Ni–N1	81.94(7)	81.6(3)	81.94(1)	82.65(1)	81.88(9)
C1–Ni–N2	81.85(7)	82.3(3)	82.16(1)	82.66(1)	81.48(9)
N1–Ni–X1	97.83(4)	98.23(2)	98.41(7)	97.97(7)	100.82(6)
N2–Ni–X1	98.39(4)	97.90(2)	97.58(7)	98.03(7)	98.37(5)
Sum / °	360.0	359.9	360.1	360.3	362.6
C1–Ni–X1	179.48(5)	179.7(2)	177.24(8)	168.21(8)	149.28(7)
N1–Ni–N2	163.78(6)	163.9(2)	163.91(9)	163.31(9)	160.80(8)

a = From ref. [92].

The crystal packing of [Ni(2^{i}Qu(4,6FPh)2^{i}Qu)Br] is very similar to the one of its non-fluorinated derivative (Figure 3-32). Again, the head-to-tail arrangement is observed, in which the orientation of a molecule alters with turns of 180°.[92, 99, 140, 148] The π-interaction between two single pyridyl units of 3.72 Å for the difluoro derivative is at the boarder of *Janiak's* definition and therefore a very weak stacking.[149] Same distance is 4.27 Å for the non-fluorinated derivative and therefore cannot be described as a π-interaction according to this definition. The 2-quinoline complex shows the aforementioned head-to-tail arrangement as well and stacks very similar to the standard complex, in which two pyridyl-phenyl units are involved, with a distance of 3.73 Å, which again indicates weak π-interactions according to *Janiak*.[149]

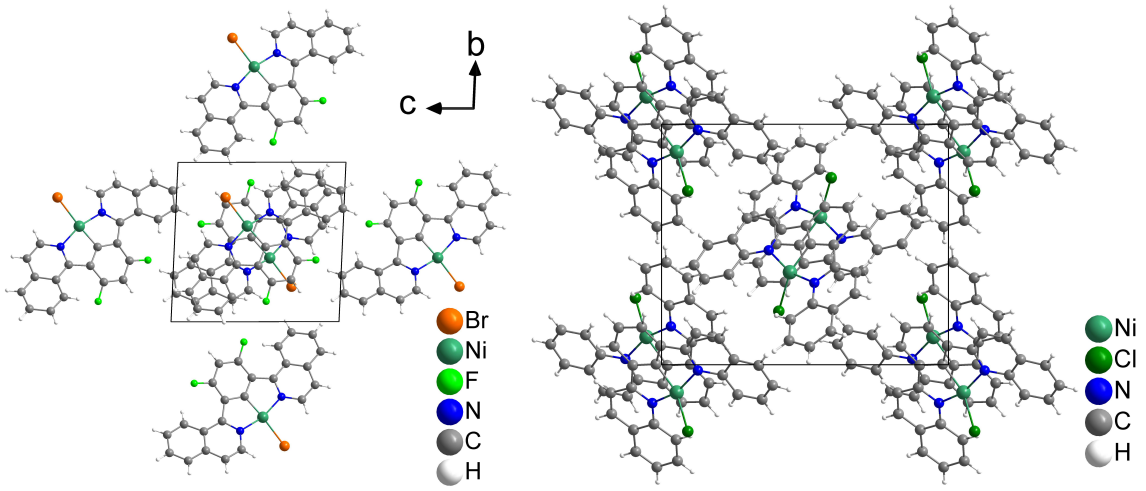

Figure 3-32 Crystal structures of [Ni(2^{i}Qu(4,6FPh)2^{i}Qu)Br] (*left*) and [Ni(2Qu(Ph)2Qu)Cl] (*right*) viewed along the crystallographic *a*-axis.

The symmetric thiazole containing complexes could be crystallized with the same method, as the quinoline containing species. Figure 3-33 shows the molecular structures of the derivatives (asymmetric units, see Chapter 7). The data of the solution and refinement are summarized in Table 3-19. Whereas [Ni(4Tz(Ph)4Tz)Cl] and [Ni(2Btz(Ph)2Btz)Cl] crystallized and could be solved in the monoclinic space groups $P2_1/n$ and $P2_1/c$, bearing four units per unit cell,

[Ni(2Tz(Ph)2Tz)Cl] crystallized in the monoclinic space group *C*2/c with eight units per unit cell. The number of molecules that builds the asymmetric unit varies from one half of a molecule for the 2-thiazole complex, over one full molecule for the 2-benzothiazole derivative, to five molecules for the 4-thiazole compound. Notable is that within this structure one molecule is disordered in two opposite directions with a relative occupancy of 14:86%.

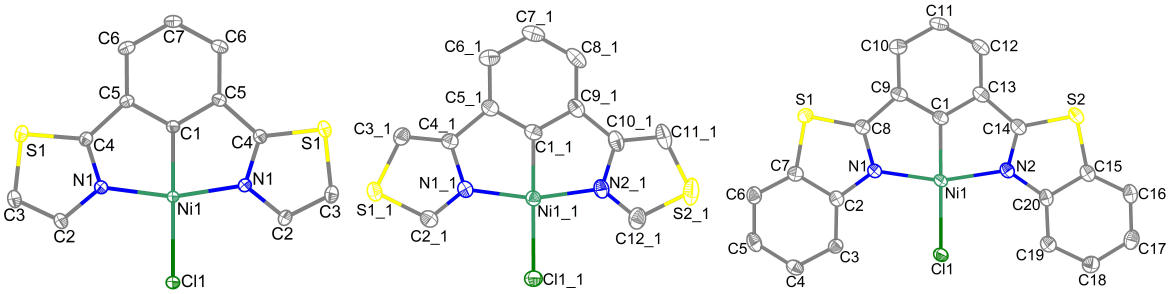

Figure 3-33 Molecular structures of [Ni(2Tz(Ph)2Tz)Cl] (*left*), [Ni(4Tz(Ph)4Tz)Cl] (*middle*) and [Ni(2Btz(Ph)2Btz)Cl] (*right*). Ellipsoids are shown with a 50% probability. Hydrogen atoms are omitted for clarity.

Table 3-19 Crystallographic data of [Ni(2Tz(Ph)2Tz)Cl], [Ni(4Tz(Ph)4Tz)Cl] and [Ni(2Btz(Ph)2Btz)Cl].

Identification code	**0.5[Ni(2Tz(Ph)2Tz)Cl]**	**5[Ni(4Tz(Ph)4Tz)Cl]**	**[Ni(2Btz(Ph)2Btz)Cl]**
Empirical formula	$C_6H_{3.5}Cl_{0.5}NNi_{0.5}S$	$C_{60}H_{35}Cl_5N_{10}Ni_5S_{10}$	$C_{20}H_{11}ClN_2NiS_2$
Temperature/K	100.0	100.0	101.0
Crystal system	monoclinic	monoclinic	monoclinic
Space group	*C*2/c	*P*2$_1$/n	*P*2$_1$/c
a/Å	9.6753(5)	12.4902(6)	8.8717(3)
b/Å	13.6967(7)	16.8148(7)	13.0581(5)
c/Å	9.1591(4)	30.0903(1)	14.6499(6)
β/°	97.015(2)	100.158(2)	95.0680(1)
Volume/Å^3	1204.68(1)	6220.5(5)	1690.52(1)
Z	8	4	4
ρ_{calc}g/cm^3	1.861	1.802	1.719
F(000)	680.0	3400.0	888.0
Radiation	MoKα (λ = 0.71073)	MoKα (λ = 0.71073)	MoKα (λ = 0.71073)
2Θ range for data collection/°	5.18 to 77.242	2.75 to 61.998	4.186 to 55.754
Index ranges	–16 ≤ h ≤ 16, –24 ≤ k ≤ 24, –16 ≤ l ≤ 16	–18 ≤ h ≤ 17, –24 ≤ k ≤ 24, –42 ≤ l ≤ 43	–11 ≤ h ≤ 10, –14 ≤ k ≤ 17, –19 ≤ l ≤ 18
Reflections collected	43123	265669	18296
Independent reflections	3397 [R_{int} = 0.0508, R_{sigma} = 0.0222]	19812 [R_{int} = 0.0786, R_{sigma} = 0.0395]	3971 [R_{int} = 0.0579, R_{sigma} = 0.0432]
Data/restraints/parameters	3397/0/85	19812/159/974	3971/0/235
Goodness-of-fit on F^2	1.098	1.214	1.039
Final R indexes [I>=2σ (I)]	R_1 = 0.0278, wR_2 = 0.0682	R_1 = 0.0484, wR_2 = 0.0944	R_1 = 0.0354, wR_2 = 0.0729
Final R indexes [all data]	R_1 = 0.0312, wR_2 = 0.0703	R_1 = 0.0710, wR_2 = 0.1042	R_1 = 0.0462, wR_2 = 0.0810

Largest diff. peak/hole / eÅ^{-3}	1.29/–0.66	0.57/–0.79	0.61/–0.35
CCDC	2277904	2277899	2277902

All structures show a square-planar coordination around the nickel center.[92, 127, 140] The 2- and 4-thiazole containing derivatives show a sum of angles of 360°, whereas the 2-benzothiazole species deviates by 1.0° with the nickel centre being slightly out of the ligand plane. Although binding gap of these ligands is bigger in comparison to the ones that are built up by three six-membered rings, the chelate bite angle of around 82° and N1–Ni–N2 angles of 163° are typical for similar structures.[89, 91, 92, 99, 100, 104, 108, 116, 117, 122, 123, 127, 140-147]

The torsion angles between a thiazole and the central phenide unit are up to 1.2° (N1–C4–C5–C6) for the 2-thiazole and 3.5° (N1–C4–C5–C6) for the 4-thiazole species (For full tables, see Chapter 7.3.12 to 6.3.14). This angle is 6.0° for one side of the benzothiazole derivative (N1–C8–C9–C10), which might be the result of the aforementioned steric situation of ortho-*N* substituted peripheric rings. Although binding gap of these ligands is bigger in comparison to the ones that are built up by three six-membered rings, the N1–Ni–N2 angle stays constant at angles of 161 to 164°. The thiazole units are bent towards the Ni(II) center with angles of 129.5° (4-Tz, N1–C4–C5), 131.0° (2-Btz, N1–C8–C9) and 131.9° (2-Tz, N1–C4–C5), deviating from the ideal trigonal angle of 120° due to the coordination to both nitrogen atoms to the nickel centre. The bond to the coligand gets slightly weakened for the 4- and 2-thiazole derivatives (2.26 and 2.25 Å), whereas the 2-benzothiazole species shows a shorter bond length of 2.23 Å in comparison to the standard chlorido complex (2.25 Å).

The coligand is mostly coplanar to the molecule except of the one from the benzothiazole species, which is another indication of the steric demand of an ortho-*N* substitution.

Literature reports first symmetric thiazole containing Pt(II) structures since 2006, bearing 2Btz units (CCDC: 611431 and 936036),[208, 209] and two Pd(II) complex structure published in 2012, with 4Tz units (CCDC: 862169 and 853770).[210] All these structures align with these new results and show the corresponding trend, comparing complexes within this triade.[117, 140]

Table 3-20 Angles and bond lengths of all synthesized symmetric thiazole containing complexes in comparison to the standard complex [Ni(Py(Ph)Py)Cl].

	[Ni(Py(Ph)Py)Cl]^{a}	**[Ni(2Tz(Ph)2Tz)Cl]^{b}**	**[Ni(4Tz(Ph)4Tz)Cl]^{c}**	**[Ni(2Btz(Ph)2Btz)Cl]**
Dist. / Å				
Ni–C1	1.836(7)	1.8414(1)	1.851(3)	1.837(2)
Ni–N1	1.932(6)	1.9097(9)	1.916(3)	1.972(2)
Ni–N2	1.936(5)	1.9097(9)	1.927(3)	1.968(2)
Ni–Cl1	2.247(2)	2.2529(4)	2.2580(9)	2.2328(7)

Angles / °				
C1–Ni–N1	81.6(3)	81.72(3)	82.44(1)	81.55(1)
C1–Ni–N2	82.3(3)	81.72(3)	82.02(1)	81.32(1)
N1–Ni–Cl1	98.23(2)	98.28(3)	97.77(9)	100.32(6)
N2–Ni–Cl1	97.90(2)	98.28(3)	97.46(9)	97.79(6)
Sum / °	359.9	360.0	359.7	361.0
C1–Ni–Cl1	179.7(2)	180.0	173.10(1)	164.89(8)
N1–Ni–N2	163.9(2)	163.43(5)	164.38(1)	161.84(9)

a = From ref. [92]. b = N2 equals N1 due to symmetry. c = all values for molecule 1.

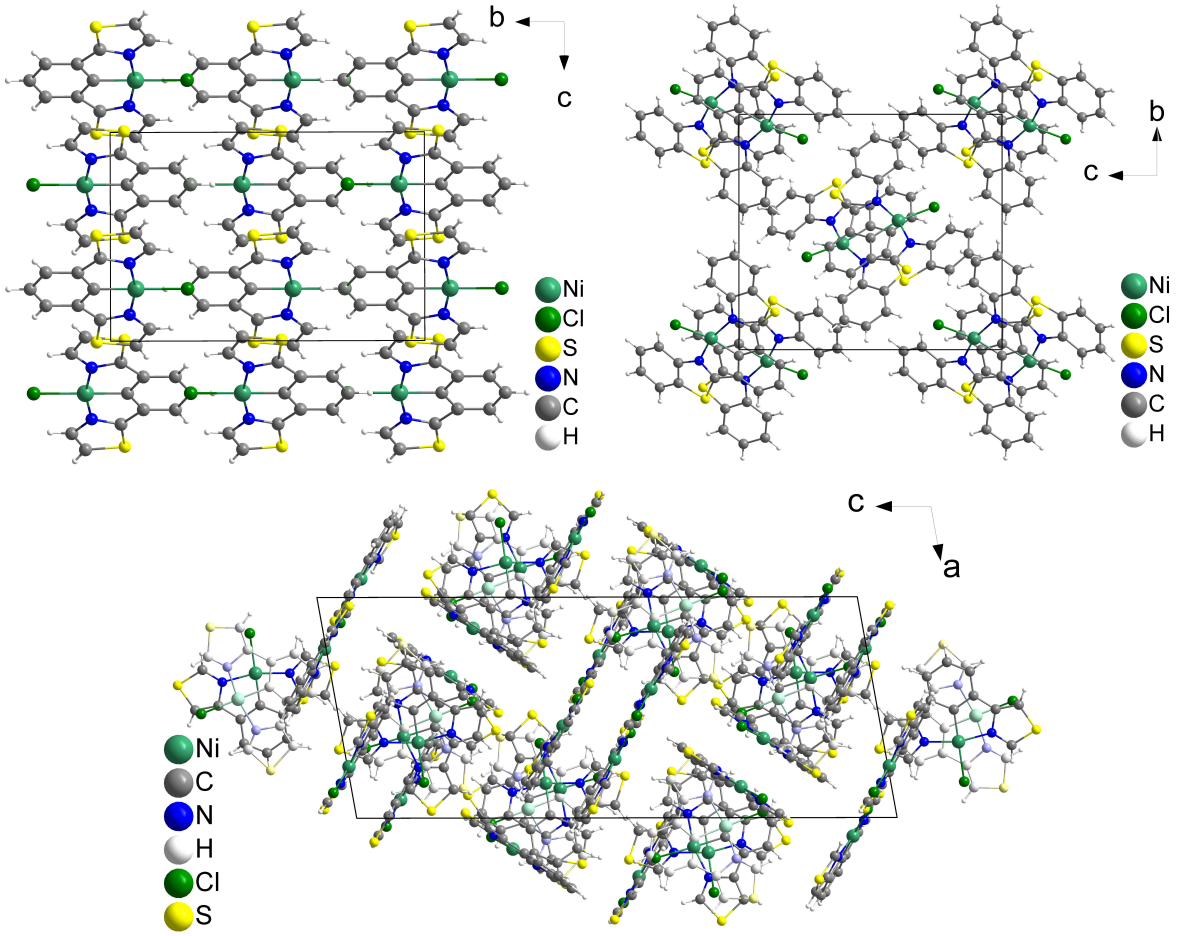

Figure 3-34 Crystal structure of [Ni(2Tz(Ph)2Tz)Cl] (*top left*) and [Ni(2Btz(Ph)2Btz)Cl] (*top right*) viewed along the crystallographic *a*-axis and of [Ni(4Tz(Ph)4Tz)Cl] (*bottom*) viewed along the crystallographic *b*-axis.

As shown in Figure 3-34, the crystal structure of [Ni(2Tz(Ph)2Tz)Cl] is very similar to the benzothiazole derivative, in which the classic head-to-tail arrangement is observable with no packing dimers.[92, 99, 140, 148] [Ni(2Tz(Ph)2Tz)Cl] shows a centered packing, in which the molecules are stacked orthogonally along the crystallographic *c*-axis with 2Tz-Ph distances of 3.71 Å. The structure of the benzothiazole containing complex shows a stacking of altering

central phenide rings and benzo-functions of a 2-benzothiazole unit with a distance of 3.66 Å, which ich much closer than for the quinoline derivatives, that show similar packings with distances starting from 3.72 Å. [Ni(4Tz(Ph)4Tz)Cl] shows a completely different structure in which two molecular stack pairwise with a distance of 3.60 Å.

The asymmetric thiazole and pyridine Ni(II) complexes were obtained by overlaying a concentrated THF solution of the complex with *n*-pentane at rt. The molecular structures are shown in Figure 3-35.

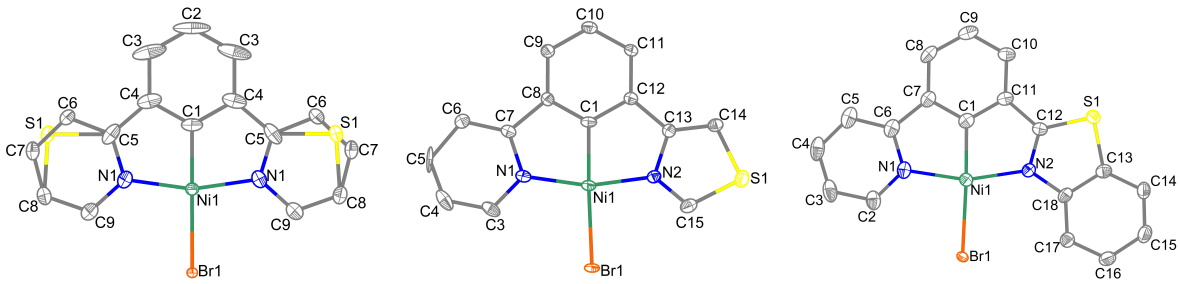

Figure 3-35 Molecular structures of [Ni(2Tz(Ph)Py)Br] (*left*), [Ni(4Tz(Ph)Py)Br] (*middle*) and [Ni(2Btz(Ph)Py)Br] (*right*). Ellipsoids are shown with a 50% probability. Hydrogen atoms are omitted for clarity.

[Ni(2Tz(Ph)Py)Br] and [Ni(2Btz(Ph)Py)Br] crystallize in the monoclinic space groups *C*2/c and $P2_1/c$, its 4Tz derivative could be crystallized in the triclinic space group $P\bar{1}$. The steric and electronic structure of a 2-thiazole function and a pyridine function is that similar, that even this asymmetric compound crystallized with an asymmetric unit of half a molecule (C_2 axis through the central phenide unit) and an overlapping 2-pyridine and -thiazole function. The crystal structure of the 4-thiazole compound bears two molecules within the asymmetric unit. The 2-benzothiazole derivative crystallizes with one molecule per asymmetric unit and contains 0.5 eq. of a two-directionally disordered THF molecule (Table 3-21).

Table 3-21 Crystallographic data of [Ni(2Tz(Ph)Py)Br], [Ni(4Tz(Ph)Py)Br] and [Ni(2Btz(Ph)Py)Br].

Identification code	**0.5[Ni(2Tz(Ph)Py)Br]**	**2[Ni(4Tz(Ph)Py)Br]**	**[Ni(2Btz(Ph)Py)Br]0.5THF**
Empirical formula	$C_7H_{4.5}Br_{0.5}NNi_{0.5}S_{0.5}$	$C_{28}H_{18}Br_2N_4Ni_2S_2$	$C_{20}H_{15}BrN_2NiO_{0.5}S$
Temperature/K	100.0	100.0	100.0
Crystal system	monoclinic	triclinic	monoclinic
Space group	*C*2/c	$P\bar{1}$	$P2_1/c$
a/Å	9.9854(4)	8.4248(4)	7.5738(2)
b/Å	14.0525(5)	9.5962(5)	15.2479(5)
c/Å	9.1400(3)	16.4753(7)	15.0726(5)
α/°	90	96.821(2)	90
β/°	98.9600(1)	101.248(2)	99.1900(1)
γ/°	90	104.386(2)	90
Volume/Å^3	1266.87(8)	1245.66(1)	1718.31(9)

Z	8	2	4
ρ_{calc}g/cm^3	1.971	2.004	1.786
F(000)	744.0	744.0	928.0
Radiation	MoKα (λ = 0.71073)	MoKα (λ = 0.71073)	MoKα (λ = 0.71073)
2Θ range for data collection/°	5.046 to 56.586	4.452 to 60.11	3.824 to 55.752
Index ranges	–13 ≤ h ≤ 13, –18 ≤ k ≤ 18, –12 ≤ l ≤ 11	–11 ≤ h ≤ 11, –13 ≤ k ≤ 13, –23 ≤ l ≤ 23	–9 ≤ h ≤ 9, –20 ≤ k ≤ 20, –19 ≤ l ≤ 19
Reflections collected	18230	54907	32525
Independent reflections	1576 [R_{int} = 0.0399, R_{sigma} = 0.0181]	7289 [R_{int} = 0.0672, R_{sigma} = 0.0400]	4087 [R_{int} = 0.0651, R_{sigma} = 0.0346]
Data/restraints/parameters	1576/0/102	7289/0/343	4087/103/244
Goodness-of-fit on F^2	1.129	1.077	1.040
Final R indexes [I>=2σ (I)]	R_1 = 0.0232, wR_2 = 0.0489	R_1 = 0.0527, wR_2 = 0.1148	R_1 = 0.0414, wR_2 = 0.1021
Final R indexes [all data]	R_1 = 0.0253, wR_2 = 0.0497	R_1 = 0.0637, wR_2 = 0.1204	R_1 = 0.0511, wR_2 = 0.1100
Largest diff. peak/hole / eÅ^{-3}	0.36/–0.64	4.94/–2.65	2.82/–0.52
CCDC	2277912	2277919	2277925

All shown structures show the expected square-planar coordination with a sum of all angles very close to 360°[92, 127, 140] with chelate bite angle of around 82° and N1–Ni–N2 angles of 163° are typical for comparable structures.[89, 91, 92, 99, 100, 104, 108, 116, 117, 122, 123, 127, 140-147] The torsion angles between the phenide and 2-pyridyl function are not higher than 1.9° and the ones between the phenide and a thiazole-unit of 3.35° for the 2-thiazole-, 5.46° for the 4-thiazole- and 2.89° for the 2-benzothiazole complex show the general planarity of these molecules (for full tables, see Chapter 7.3.15 to 6.3.17). Especially the comparably low torsion angle of the 2-Btz complex shows, that the steric hinderance of an ortho-*N* substituted peripheric ring does not affect the planarity in this case. The coligand is the only atom that is significantly out of the molecular plane for the 4-thiazole and 2-benzothiazole derivative with C1–Ni–Br1 angles of 171.4°. Although these molecules are asymmetric, the Ni–N1 and Ni–N2 bond lengths show very similar values and have a range of length of 1.92 to 1.99 Å. The Ni–C1 bond lengths, as well as the Ni–Br1 bond length are very similar to the ones from the standard complex (see Table 3-22).[92]

Table 3-22 Angles and bond lengths of all synthesized asymmetric thiazole containing complexes in comparison to [Ni(Py(Ph)Py)Br].

	[Ni(Py(Ph)Py)Br][a]	[Ni(2Tz(Ph)Py)Br][b]	[Ni(4Tz(Ph)Py)Br][c]	[Ni(2Btz(Ph)Py)Br]
Dist. / Å				
Ni–C1	1.8298(2)	1.834(3)	1.839(4)	1.840(3)
Ni–N1	1.9489(1)	1.9338(1)	1.920(4)	1.964(3)

Ni–N2	1.9536(1)	1.9338(1)	1.917(4)	1.986(3)
Ni–Br1	2.3963(3)	2.3875(4)	2.3981(7)	2.4007(5)
Angles / °				
C1–Ni–N1	81.94(7)	81.82(6)	81.92(1)	81.03(1)
C1–Ni–N2	81.85(7)	81.82(6)	82.46(1)	81.84(1)
N1–Ni–Br1	97.83(4)	98.18(5)	100.05(1)	95.66(9)
N2–Ni–Br1	98.39(4)	98.18(5)	95.70(1)	101.64(8)
Sum / °	360.0	360.0	360.1	360.2
C1–Ni–Br1	179.48(5)	180.0	171.43(1)	171.37(1)
N1–Ni–N2	163.78(6)	163.65(1)	164.25(1)	162.69(1)

a = From ref. [92]. b = N2 equals N1 due to symmetry. c = all values for molecule 1.

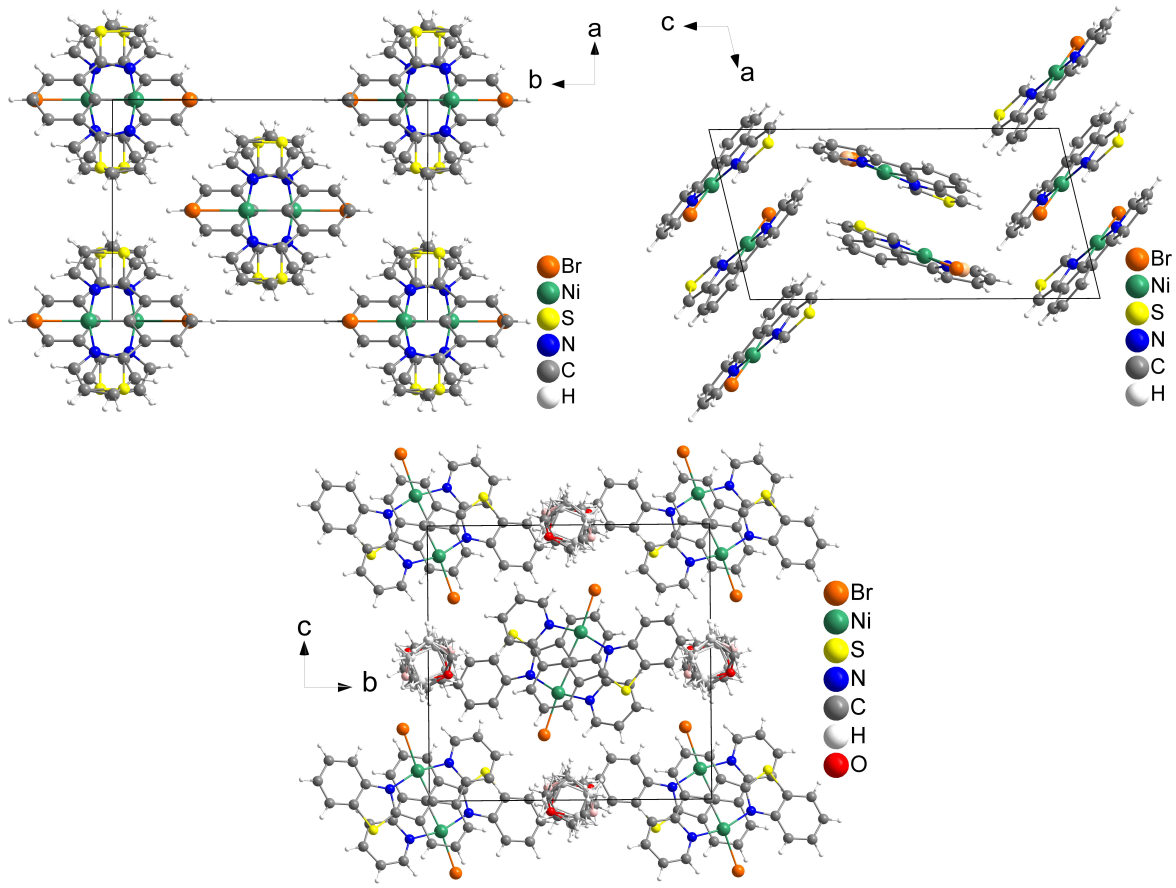

Figure 3-36 Crystal structure of [Ni(2Tz(Ph)Py)Br] viewed along the crystallographic *c*-axis (*top left*), of [Ni(4Tz(Ph)Py)Br] viewed along the crystallographic *b*-axis (*top right*) and of [Ni(2Btz(Ph)Py)Br] viewed along the crystallographic *a*-axis (*bottom*).

[Ni(2Tz(Ph)Py)Br] is isostructural to its symmetric 2-thiazole analogue and stacks perpendicularly to the crystallographic *a*-*b* plane in a head-to-tail arrangement with 2Tz/Py-Ph distances of 3.86 Å,[92, 99, 140, 148] which is bigger than in the case of [Ni(2Tz(Ph)2Tz)Cl], resulting from a larger ion radius of the coligand, as reported for [Ni(Py(Ph)Py)X] (X = Cl, Br).[92]

Analogously, the symmetric and asymmetric 2-benzothiazole containing complexes crystallized isostructurally with an increased stacking distance of the asymmetric structure of 3.93 Å, in comparison to the symmetric one.[92, 99, 140, 148] Interestingly, the aforementioned cocrystallized THF was required for the crystallization. It is positioned in the crystal structure on the edges of the crystallographic *b*-*c* plane due to a missing second aromatic ring in the asymmetric structure in comparison to the symmetric derivative. [Ni(4Tz(Ph)Py)Br] is also stacking by two 4Tz-Ph units in a distance of up to 4.03 Å. The pyridyl functions are not significantly involved in this stack and show a distance to the next phenide unit of 4.63 Å.

The complexes bearing a halide-substituted pyridyl unit were crystallized with the method of isothermal diffusion of cyclohexane into a concentrated THF solution. Figure 3-37 shows the molecular structures of both derivatives (asymmetric units, see Chapter 7.3.18 and 6.3.19).

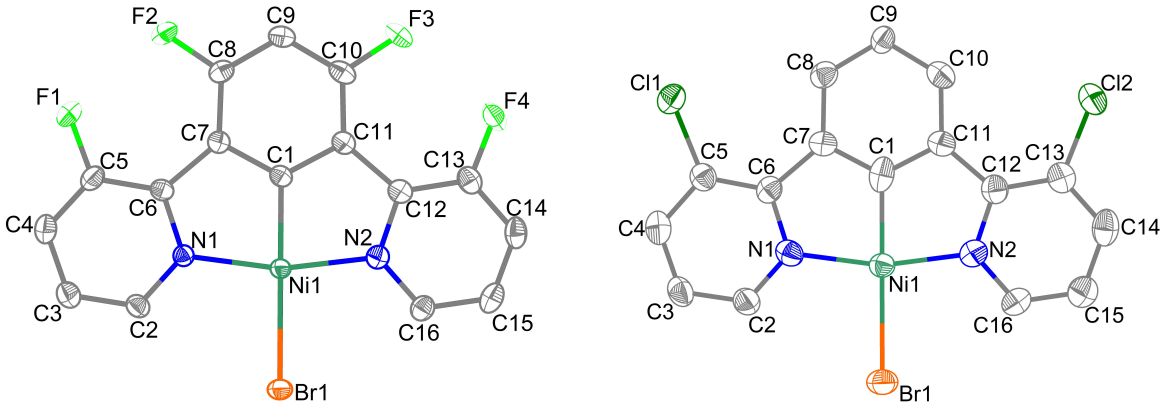

Figure 3-37 Molecular structures of [Ni(3FPy(4,6FPh)3FPy)Br] (*left*) and [Ni(3ClPy(Ph)3ClPy)Br] (*right*). Ellipsoids are shown with a 50% probability. Hydrogen atoms are omitted for clarity.

The structure of [Ni(3FPy(4,6FPh)3FPy)Br] was solved in the triclinic spacegroup $P\bar{1}$ and the one from [Ni(3ClPy(Ph)3ClPy)Br] in the monoclinic spacegroup $P2_1/c$. Both are bearing four units per unit cell. The asymmetric unit of the fluoro-containing species shows half of a cocrystallized cyclohexane molecule. It is exactly placed on one edge of the asymmetric unit. The 3-chloropyridyl species shows two molecules, that built the asymmetric unit (Table 3-23).

Table 3-23 Crystallographic data of [Ni(3ClPy(Ph)3ClPy)Br] and [Ni(3FPy(4,6FPh)3FPy)Br].

Identification code	**[Ni(3FPy(4,6FPh)3FPy)Br] 0.5 *c*Hex**	**2[Ni(3ClPy(Ph)3ClPy)Br]**
Empirical formula	$C_{19}H_{13}BrF_4N_2Ni$	$C_{16}H_9BrCl_2N_2Ni$
Temperature/K	103.00	293(2)
Crystal system	monoclinic	triclinic
Space group	$P2_1/c$	$P\bar{1}$
a/Å	12.1264(7)	8.0719(5)
b/Å	19.5518(1)	9.9861(6)
c/Å	6.7291(4)	18.2862(1)

α/°	90	91.040(5)
β/°	98.604(2)	97.112(5)
γ/°	90	98.510(5)
Volume/Å^3	1577.48(1)	1445.56(1)
Z	4	4
ρ_{calc}g/cm^3	2.038	2.016
F(000)	960.0	864.0
Radiation	MoKα (λ = 0.71073)	MoKα (λ = 0.71073)
2Θ range for data collection/°	3.984 to 56.584	4.126 to 58.386
Index ranges	–16 ≤ h ≤ 16, –26 ≤ k ≤ 26, –8 ≤ l ≤ 8	–11 ≤ h ≤ 11, –13 ≤ k ≤ 13, –23 ≤ l ≤ 25
Reflections collected	33002	15995
Independent reflections	3916 [R_{int} = 0.0504, R_{sigma} = 0.0286]	7450 [R_{int} = 0.0593, R_{sigma} = 0.0759]
Data/restraints/parameters	3916/0/244	7450/0/398
Goodness-of-fit on F^2	1.074	0.990
Final R indexes [I>=2σ (I)]	R_1 = 0.0356, wR_2 = 0.0891	R_1 = 0.0442, wR_2 = 0.1013
Final R indexes [all data]	R_1 = 0.0487, wR_2 = 0.0954	R_1 = 0.0947, wR_2 = 0.1326
Largest diff. peak/hole / eÅ^{-3}	0.70/–0.70	1.54/–1.04
CCDC	2343454	2343467

Both structures show a square-planar coordination similar sums of the angles around the metal center of 360.0°. The distances around the nickel(II) atom are not changing much in comparison to the standard complex,[92] with very typical bite and N–Ni–N angles (82 and 163°) for this complex class.[89, 91, 92, 99, 100, 104, 108, 116, 117, 122, 123, 127, 140-147] The planarity of these complexes gets supported by the torsion angles between the phenide- and the pyridyl units N1–C6–C7–C8 and N2–C12–C11–C10 of up to 4.2° for the chloro- and 2.2° for the fluoro substituted derivative. Especially for the last one it was counterintuitive, that the steric (or electronic) demand of the fluoro substituents do not affect the geometry of the ligand and therefore for the complex. Further, there could be an acid-base interaction between the chloro substituents Cl1 and Cl2 with the hydrogen atoms H8 and H10 of the central phenide unit. They show a constant Cl–H distances of 2.55 Å (Table 3-24).

Table 3-24 Angles and bond lengths of [Ni(3FPy(4,6FPh)3FPy)Br] and [Ni(3ClPy(Ph)3ClPy)Br] in comparison to the standard complex [Ni(Py(Ph)Py)Br].

	[Ni(Py(Ph)Py)Br]^a	**[Ni(3FPy(4,6FPh)3FPy)Br]^b**	**[Ni(3ClPy(Ph)3ClPy)Br]^b**
Dist. / Å			
Ni–C1	1.8298(2)	1.830(3)	1.863(6)
Ni–N1	1.9489(1)	1.931(3)	1.939(5)
Ni–N2	1.9536(1)	1.935(3)	1.925(5)
Ni–Br1	2.3963(3)	2.3898(5)	2.3908(8)

Angles / °			
C1–Ni–N1	81.94(7)	82.75(1)	82.3(2)
C1–Ni–N2	81.85(7)	82.89(1)	82.9(2)
N1–Ni–Br1	97.83(4)	97.35(8)	97.37(1)
N2–Ni–Br1	98.39(4)	97.01(9)	97.45(1)
Sum / °	360.0	360.0	360.0
C1–Ni–Br1	179.48(5)	179.37(1)	178.11(1)
N1–Ni–N2	163.78(6)	165.63(1)	165.16(1)

a = From ref. [92]. b = all values for molecule 1.

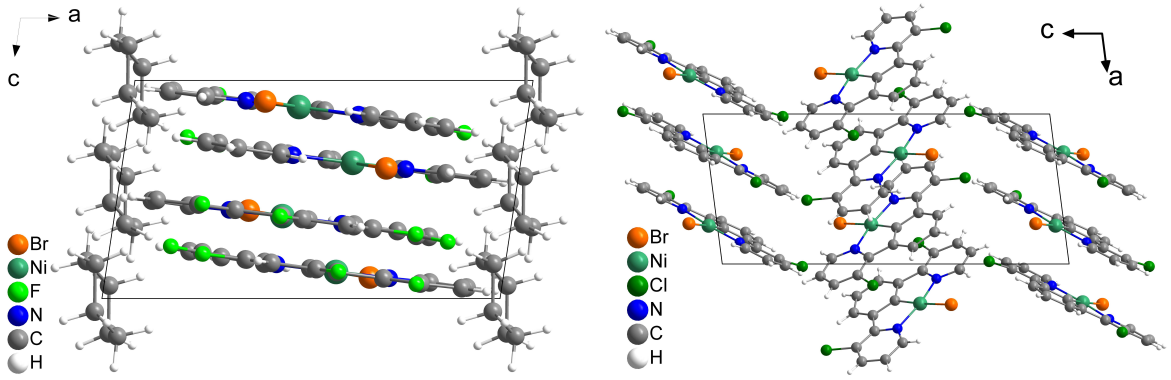

Figure 3-38 Crystal structure of [Ni(3FPy(4,6FPh)3FPy)Br] viewed along the crystallographic *b*-axis (*left*) and of [Ni(3ClPy(Ph)3ClPy)Br] viewed along the crystallographic *b*-axis (*right*).

The structure of [Ni(3ClPy(Ph)3ClPy)Br] shows the expected head-to-tail arrangement, steadily notable for related structures,[92, 99, 140, 148] and stack with two PyPh units with distances of 3.68 to 3.78 Å, which is defined as a very weak stacking according to *Janiak*.[149] The fluoro substituted derivative only stacks by two single pyridyl units with distances of 3.78 Å and therefore shows a similar strength of π-interaction. In this structure, the cocrystallized cyclohexane molecules is shown in Figure 3-38 and is defined on all four cell corners of the crystallographic *bc*-plane, shared by all surrounding eight unit cells, as well as one in its center, shared with the neighboring cell.

Cyclic voltammetry generally also shows one reversible oxidation with half-step potentials of 0.0 to 0.2 V, referenced to ferrocene/ferrocenium. The number of reduction waves varies from one up to six waves in a range from –1.7 to –3.0 V (Figure 3-39 to Figure 3-42).

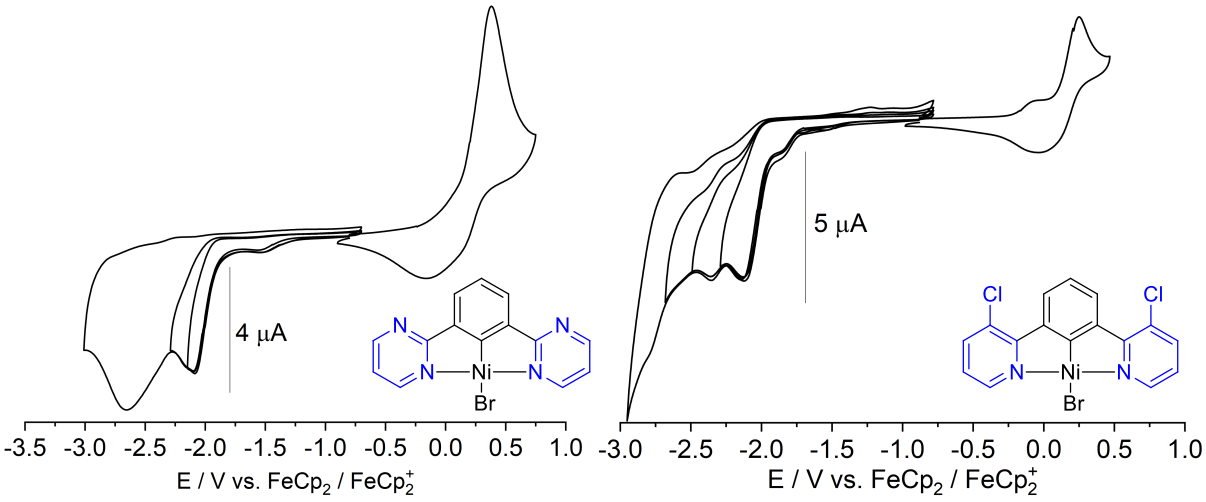

Figure 3-39 Cyclic voltammograms of [Ni(Pym(Ph)Pym)Br] (*left*) and [Ni(3ClPy(Ph)3ClPy)Br] (*right*), measured in a 0.1M *n*Bu$_4$NPF$_6$ solution in THF at rt with a scan rate of 100 mV/s.

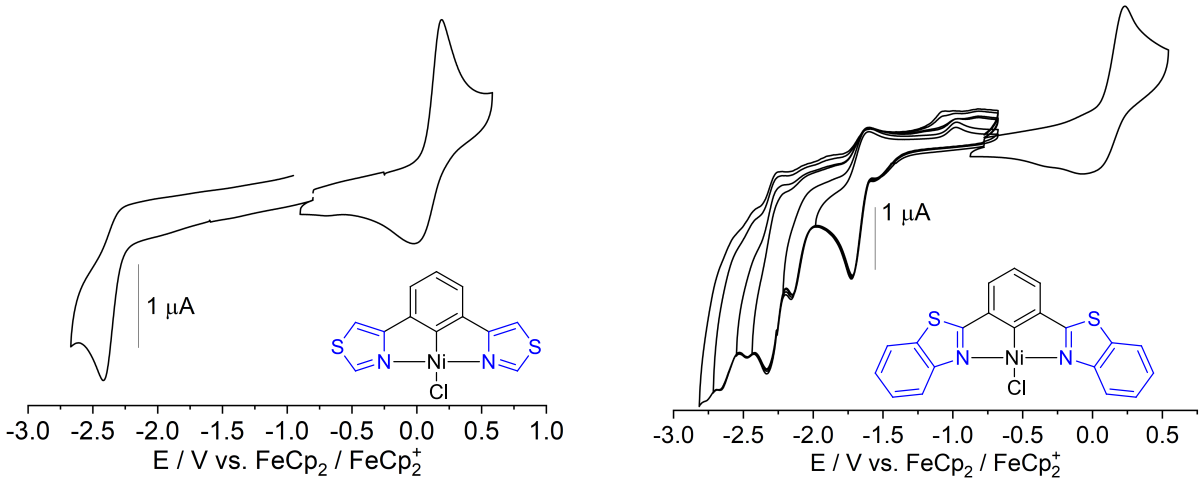

Figure 3-40 Cyclic voltammograms of [Ni(4Tz(Ph)4Tz)Cl] (*left*) and [Ni(2Btz(Ph)2Btz)Cl] (*right*), measured in a 0.1M *n*Bu$_4$NPF$_6$ solution in THF at rt with a scan rate of 100 mV/s.

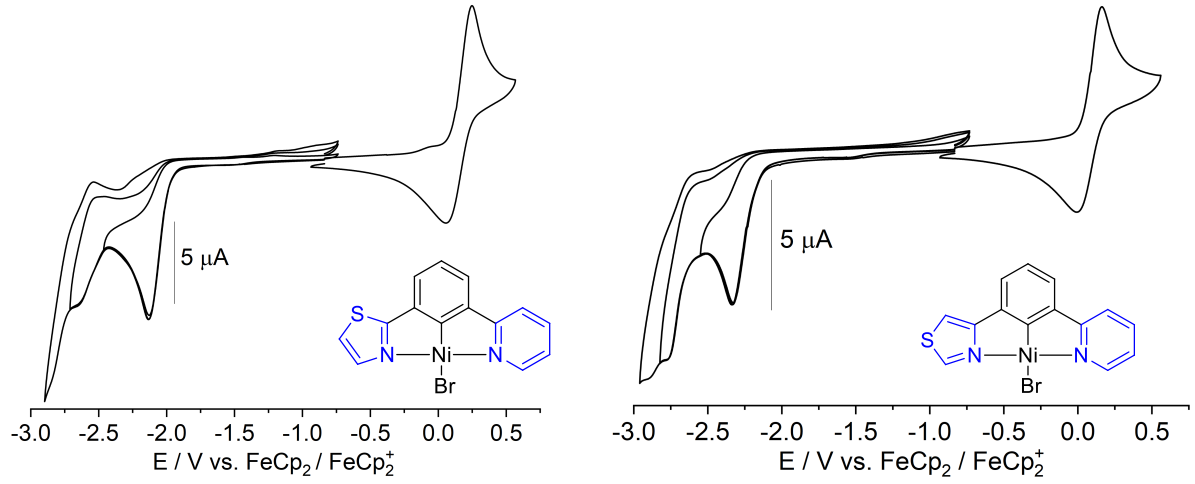

Figure 3-41 Cyclic voltammograms of [Ni(2Tz(Ph)Py)Br] (*left*) and [Ni(4Tz(Ph)Py)Br] (*right*), measured in a 0.1M *n*Bu$_4$NPF$_6$ solution in THF at rt with a scan rate of 100 mV/s.

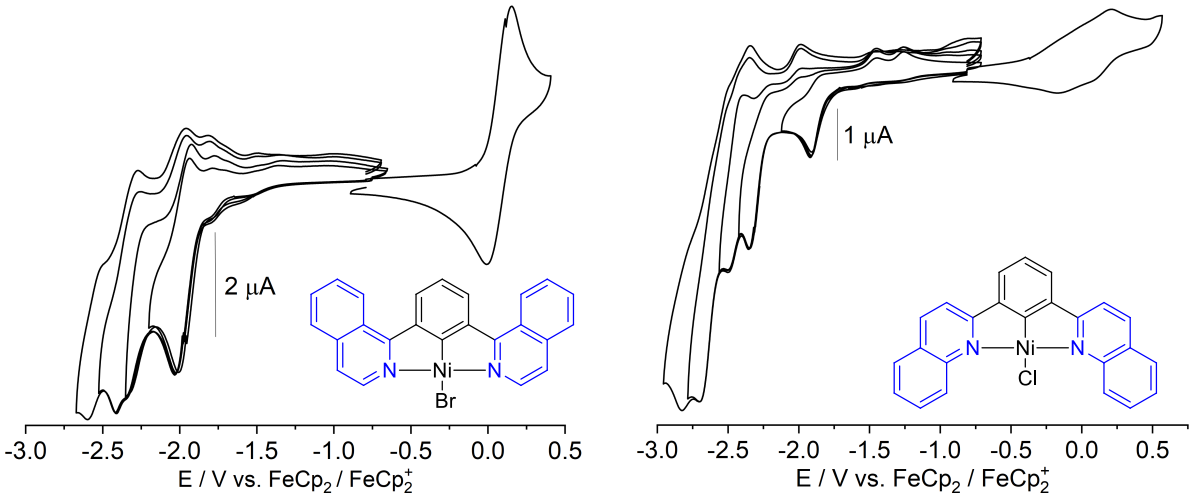

Figure 3-42 Cyclic voltammograms of [Ni(2^{i}Qu(Ph)2^{i}Qu)Br] (*left*) and [Ni(2Qu(Ph)2Qu)Cl] (*right*), measured in a 0.1M *n*Bu$_4$NPF$_6$ solution in THF at rt with a scan rate of 100 mV/s.

The reversible first oxidations at a small potential range again can be assigned to a position of the HOMO energy level on the metal center of [Ni(N^C^N)X] complexes, the Ni(II)/Ni(III) redox pair, as already calculated for the parent Ni(II) complex and reported Pt(II) analogues.[92, 117, 140, 206-210] All complexes bear a halido coligand, which leads to the assumption of an occurring EC mechanism for the first reduction.[89, 91, 92, 99, 142] This explains the dominating irreversible character of most first reductions. First reductions are reversible only for the 2-isoquinoline complexes, as well as for the symmetric 2-benzothiazole derivative. In general, this substitution pattern concerns exclusively the tridentate ligand backbone, which leads to the first observation, that mainly the LUMO energy level gets changed within this series of complexes (see Table 3-25 and further CVs in Chapter 7.4).

The 2-pyrimidine and 3-chloropyridine containing complexes (Figure 3-39 and Chapter 7.4) have a slightly smaller electrochemical HOMO-LUMO gap than the standard complex [Ni(Py(Ph)Py)Br] with values around 2.2 eV. Due to the substitution of the pyridine units with two chloro substituents, the electron density of these parts of the complexes gets decreased by these EWGs and their -I effect shifting all redox processes to higher (less negative) potentials in comparison to the standard complex. This is also observed for the 2-pyrimidine derivative, which shows reductions and oxidations at very similar potentials (Ox1 = 0.11 V and Red1 = –2.11 V). The pyrazine derivative (CV, see Chapter 7) shows the same potential for the first oxidation, but the first reduction is further anodically shifted to –1.78 V a smaller HOMO-LUMO gap, which supports the results from the UV/vis absorption spectrum (see below). Cyclic voltammetry of [Ni(3FPy(4,6FPh)3FPy)Br] shows that a substitution of the standard complex by four EWGs, leads to even stronger anodic shifts of the potentials

(Ox1 = 0.20 V and Red1 = –1.94 V), although the HOMO-LUMO gap only gets slightly decreased to a value of 2.14 eV.

The synthesized symmetric thiazole complexes (Figure 3-40 and Chapter 7.4) show the large impact of different thiazole units on the HOMO-LUMO gap of these complexes. The 4Tz derivative shows the highest value of 2.52 eV, whereas the 2Btz complex represents the lowest one of 1.77 eV. Again mainly the LUMO level gets affected by the substitution of both pyridine units by the corresponding thiazole derivative. The symmetric 2Tz compound shows an anodic shift of all waves with a half-step potential of the first oxidation of 0.17 V, whereas its electrochemical HOMO-LUMO gap stays at 2.28 eV, very similar to [Ni(Py(Ph)Py)Cl] (2.38 eV). The complexes, that were built up by only one thiazole unit generally show smaller shifts (Figure 3-41 and Chapter 7.4). However, the trend is still observed with a decreasing HOMO-LUMO gap going from a 4Tz (2.41 eV) over 2Tz (2.28 eV) to the 2Btz derivative (1.96 eV).

The quinoline containing complexes (Figure 3-42 and Chapter 7.4) show electrochemical HOMO-LUMO gaps of around 2.00 eV. Whereas the potential of the first oxidation of [Ni(2^{l}Qu(Ph)2^{l}Qu)Br] stays untouched at 0.07 V in comparison to the standard complex, the ones from its difluoro substituted derivative and the 2-quinoline derivative get anodically shifted to a values around 0.13 V. Regarding the first reductions, both 2-isoquinoline derivatives show reversible waves with half-step potentials of –1.90 and –1.98 V, whereas the quinoline derivatives show irreversible ones at –1.92 and –1.98 V, implying the dependence of the EC mechanism on the used quinoline and the sterical effects along with them.

Table 3-25 Redox potentials of all other than pyridine containing [Ni(N^C^N)X] complexes.

	***E* Ox1 ($E_{1/2}$)**	***E* Red1 (E_{pc})**	***E* Red2 (E_{pc})**	***E* Red3 (E_{pc})**	***E* Red4 (E_{pc})**	**Δ*E*$_{HOMO-LUMO}$**
[Ni(Py(Ph)Py)Cl][a]	0.06	–2.33	–2.57	–2.69	-	2.38 eV
[Ni(Py(Ph)Py)Br][a]	0.07	–2.30	–2.75	–3.09	-	2.37 eV
[Ni(Pz(Ph)Pz)Br][b]	0.11	–1.78	–1.92	–2.21 ($E_{1/2}$)	–2.65	1.89 eV
[Ni(Pym(Ph)Pym)Br]	0.10	–2.09	–2.17	–2.66	-	2.19 eV
[Ni(2^{l}Qu(Ph)2^{l}Qu)Br]	0.07	–1.98 ($E_{1/2}$)	–2.35	–2.36 ($E_{1/2}$)	–2.60	2.05 eV
[Ni(2^{l}Qu(4,6FPh)2^{l}Qu)Br]	0.14	–1.90 ($E_{1/2}$)	–2.32	–2.46	–2.60 ($E_{1/2}$)	2.04 eV
[Ni(2Qu(Ph)2Qu)Cl][c]	0.13	–1.92	–2.35	–2.44 ($E_{1/2}$)	–2.70	2.05 eV
[Ni(2Qu(Ph)Py)Br][d]	0.01	–1.98	–2.13	–2.47 ($E_{1/2}$)	–2.69	1.99 eV
[Ni(2Tz(Ph)2Tz)Cl]	0.17	–2.11	–2.45	–2.73	–3.16	2.28 eV
[Ni(4Tz(Ph)4Tz)Cl]	0.10	–2.42	-	-	-	2.52 eV
[Ni(2Btz(Ph)2Btz)Cl][e]	0.10	–1.67 ($E_{1/2}$)	–2.15	–2.33	–2.48	1.77 eV
[Ni(2Tz(Ph)Py)Br]	0.15	–2.13	–2.68	–2.87	-	2.28 eV
[Ni(4Tz(Ph)Py)Br]	0.08	–2.33	–2.78	–2.91	-	2.41 eV
[Ni(2Btz(Ph)Py)Br][f]	0.01	–1.95	–2.08	–2.49	–2.63	1.96 eV
[Ni(3ClPy(Ph)3ClPy)Br]	0.12	–2.12	–2.36	–2.66	–2.83	2.24 eV

[Ni(3FPy(4,6FPh)3FPy)Br][g]	0.20	–1.94	–2.13	–2.43	–2.60	2.14 eV

Measured in a 0.1M nBu$_4$NPF$_6$ solution in THF at rt with a scan rate of 100 mV/s. All potentials in V. E_{pc} =Cathodic Peak Potential, E_{pa} = Anodic Peak Potential, $E_{1/2}$ = Half-Step Potential. a = From ref. [92]. b = Ox2 at 0.41 V (E_{pa}). c = Red5 at –2.83 V (E_{pc}). d = Red5 at –2.85 V (E_{pc}) and Red6 at –3.00 V (E_{pc}). e = Red5 at –2.67 V (E_{pc}) and Red6 at –2.77 (E_{pc}). f = Red5 at –2.84 V (E_{pc}). g = Red5 at –2.93 V (E_{pc}).

UV/vis absorption spectra in THF of complexes with other peripheric *N*-heteroaromats than pyridine show intense absorptions in the UV/vis range from 230 to 300 nm, which are very similar to those observed for the protoligands (Chapter 3.2.1). Therefore, these bands can be assigned to π–π* transitions in the Ni(II) complexes. The weaker bands from 350 to 550 nm go in line with the color appearance of these complexes, as reported for the parent complexes.[92] The complexes show colors in a range from a light yellow color for [Ni(4Tz(Ph)4Tz)Cl] to a dark red solid [Ni(2^{i}Qu(Ph)2^{i}Qu)Br]. Four different groups of [Ni(N^C^N)X] complexes with other *N*-heteroaromats than pyridine were shown in comparison to the respective standard complex [Ni(Py(Ph)Py)X] (X = Cl, Br) (Figure 3-43, Table 3-26).

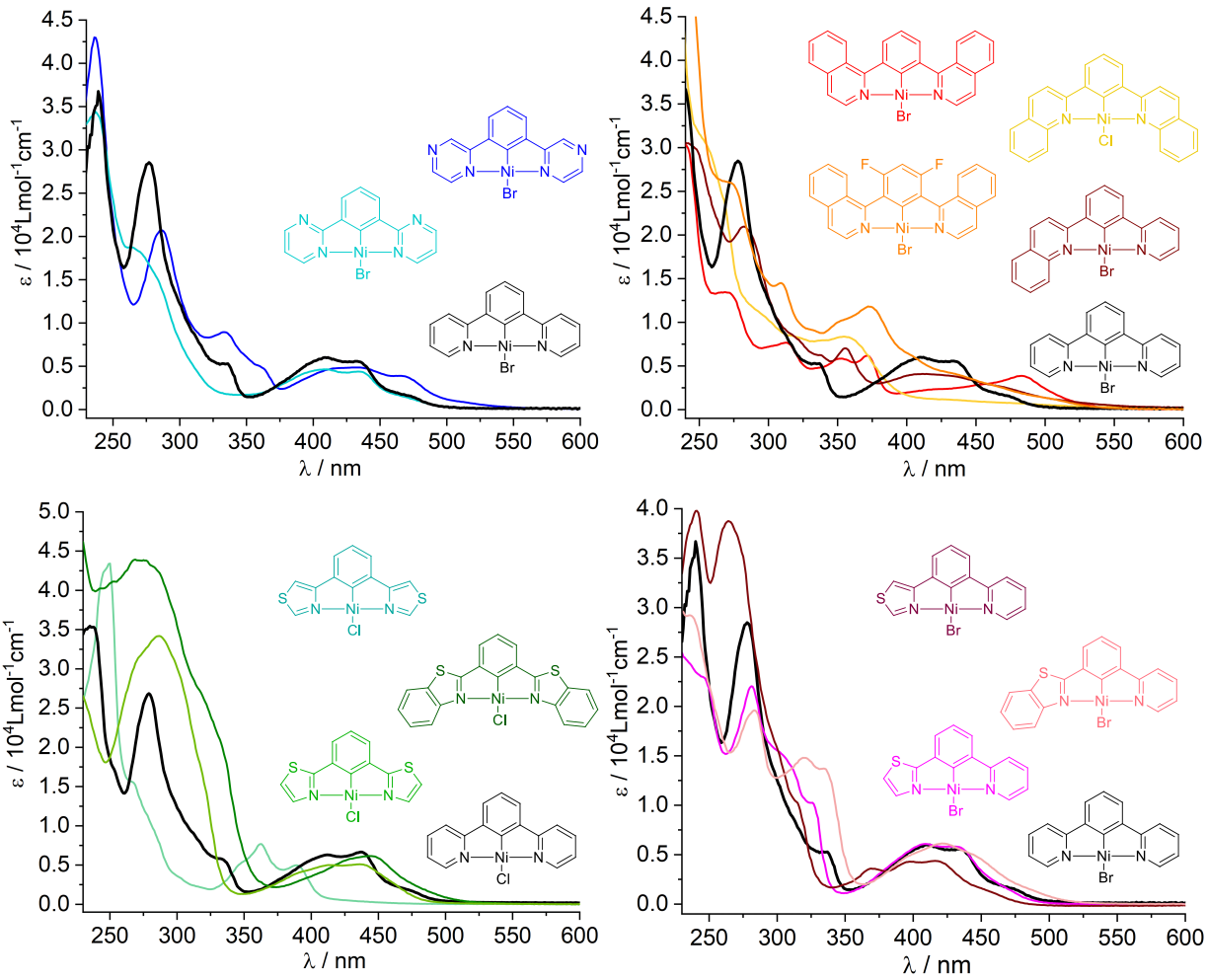

Figure 3-43 UV/vis spectra of Ni(II) N^C^N complexes bearing different π-acceptor units than pyridine in comparison to the standard complex [Ni(Py(Ph)Py)X] (X = Cl, Br), measured in THF at rt. *Top left:* Pyrimidine and Pyrazine containing complexes. *Top right:* Quinoline containing complexes. *Bottom left:* Symmetric thiazole containing complexes. *Bottom right:* Asymmetric thiazole containing complexes.

The last group of complexes within this studies, namely [Ni(3ClPy(Ph)3ClPy)Br] and [Ni(3FPy(4,6FPhH)3FPy)Br], showed highly similar optical properties and is therefore not discussed in detail (spectra: see Chapter 7.5). Complexes bearing pyrimidine and pyrazine as π-accepting units, one can see, that the change from 2Py to 2Pym does not lead to a significant change in the absorption spectra. The π–π* transitions with absorption maxima at 230 to 280 nm, as well as the CT bands from 350 to 500 nm show very similar maxima, which also explains the electrochemical similarity to the standard complex. The pyrazine containing derivative shows a slightly redshifted bands at 287 nm and redshifted CT bands with an additional shoulder starting at 508 nm (900 $Lmol^{-1}cm^{-1}$). The absorption band at around 350 nm increased in the extinction from 5000 to 8000 $Lmol^{-1}cm^{-1}$. In general, the difference between both absorption spectra needs to be explained by the position of the second nitrogen atom of the peripheric rings. It assumably takes influence on the acidity of the ortho-*N* protons and their acid-base interaction with the coligand and therefore on the LUMO energy level.

The quinoline containing complexes show large shifts of the absorption bands resulting in a different structure of the UV/vis spectra, showing absorption maxima with lower energies than 480 nm. However, comparing both 2-isoquinoline complexes, their similarity clearly can be observed by showing absorption maxima at the same energies at different extinction coefficients. In general, [Ni(2*i*Qu(4,6FPh)2*i*Qu)Br] shows higher extinctions for these absorption bands. Both, 2-quinoline complexes show similar UV/vis absorption spectra as well. [Ni(2Qu(Ph)Py)Br] underlines its mixed character by partially showing similar absorption bands similar to the standard complex, e.g. at 282, 339 and 464 nm, but also showing similar bands to [Ni(2Qu(Ph)2Qu)Cl] at 356 nm and the broad CT band >464 nm.

The UV/vis absorption spectra of all thiazole-containing complexes align with their electrochemical measurements as well by showing large shifts of the absorption maxima, especially in the CT bands. Whereas for the 2-thiazole derivatives close similarities to the one of the standard complex (around 350 to 500 nm), the one bearing 4-thiazole units shows a blue-shifted band (round 325 to 425 nm). The opposite effect can be achieved by expanding the π-system and using 2-benzothiazole as peripheric units (up to 525 nm). This can be explained by a stabilization of the LUMO level by an acid-base interaction of the chloride coligand with the acidic ortho-N proton from the 4Tz units, which is not applicable on the other thiazole isomers. Looking at the π-π* transitions, it generally can be noted, that introducing a thiazole unit, independent on its character, the absorption bands broaden significantly. The effect gets reduced, when only one pyridyl unit is substituted by a thiazole function, as well as the aforementioned shifts of the CT bands. In general it can be assumed, that all discussed changes of the absorption bands made by structural changes at the peripheric units of the ligand backbone, affect the LUMO levels of the complex, which is in line with the chromophoric

unit being mainly localized in these as reported in detail through density functional theory (DFT) and time-dependent (TD-DFT) calculations on the [Ni(Py(4,6MePh)Py)Cl] and [Ni(Py(Ph)Py)X] complexes and already reported Pt(II) N^C^N analogues.[92, 140, 206-208]

Table 3-26 Absorption maxima and extinction coeff. of other than pyridine containing N^C^N complexes in comparison to [Ni(Py(Ph)Py)Cl] and [Ni(Py(Ph)Py)Br].

Complex	Absorption Max. λ_x in nm (Ext. Coeff. ε in 1000 · $Lmol^{-1}cm^{-1}$)							
	λ_8	λ_7	λ_6	λ_5	λ_4	λ_3	λ_2	λ_1
[Ni(Py(Ph)Py)Cl][a]	-	-	463^{sh} (1.8)	437 (6.7)	412 (6.3)	332 (5.7)	279 (26.8)	236 (35.5)
[Ni(Py(Ph)Py)Br][a]	-	-	464^{sh} (1.8)	434 (5.6)	411 (6.0)	334 (5.3)	278 (28.8)	239 (36.4)
[Ni(Pz(Ph)Pz)Br]	-	508^{sh} (0.9)	467 (3.8)	432 (4.9)	360^{sh} (5.0)	334 (8.9)	287 (20.7)	236 (42.9)
[Ni(Pym(Ph)Pym)Br]	-	-	-	463^{sh} (1.6)	435 (4.5)	409 (4.6)	265 (18.8)	236 (34.3)
[Ni(2^{i}Qu(Ph)2^{i}Qu)Br]	-	484 (4.0)	419^{sh} (2.4)	372 (6.1)	352 (5.8)	315 (7.8)	270 (13.4)	239 (30.0)
[Ni(2^{i}Qu(4,6FPh)2^{i}Qu)Br]	434^{sh} (4.2)	401^{sh} (6.4)	374 (11.8)	353^{sh} (10.2)	330^{sh} (9.2)	309 (14.5)	271^{sh} (26.1)	<240 (62.4)
[Ni(2Qu(Ph)2Qu)Cl]	426^{sh} (1.4)	356 (8.3)	339 (8.0)	317^{sh} (8.6)	287^{sh} (11.9)	267^{sh} (24.4)	250^{sh} (31.7)	<240 (42.9)
[Ni(2Qu(Ph)Py)Br]	-	464^{sh} (2.7)	409 (4.1)	355 (7.1)	339 (6.2)	316^{sh} (8.6)	282 (21.0)	243 (30.3)
[Ni(2Tz(Ph)2Tz)Cl]	-	-	437 (5.0)	413 (5.1)	394^{sh} (4.2)	315^{sh} (18.6)	286 (34.2)	274^{sh} (32.4)
[Ni(4Tz(Ph)4Tz)Cl]	-	-	390 (5.0)	362 (7.8)	350^{sh} (5.6)	302^{sh} (3.4)	267^{sh} (15.6)	250 (43.3)
[Ni(2Btz(Ph)2Btz)Cl]	-	-	475^{sh} (2.7)	446 (6.3)	430^{sh} (5.9)	405^{sh} (4.1)	315^{sh} (27.7)	275 (44.0)
[Ni(2Tz(Ph)Py)Br]	-	464^{sh} (1.8)	433 (5.8)	408 (6.0)	324 (10.3)	300^{sh} (15.5)	281 (22.1)	245 (22.9)
[Ni(4Tz(Ph)Py)Br]	-	449^{sh} (1.6)	419 (4.4)	397 (4.3)	370 (3.7)	314^{sh} (10.5)	264 (38.7)	240 (39.8)
[Ni(2Btz(Ph)Py)Br]	483^{sh} (1.6)	445^{sh} (4.9)	421 (6.2)	399^{sh} (5.1)	334 (13.7)	320 (14.8)	283 (19.6)	236 (29.3)
[Ni(3ClPy(Ph)3ClPy)Br]	447 (2.9)	419 (3.5)	403 (3.5)	382 (3.2)	341^{sh} (5.0)	319^{sh} (7.5)	283 (18.1)	221^{sh} (31.9)
[Ni(3FPy(4,6FPh)3FPy)Br]	463^{sh} (1.8)	428^{sh} (3.4)	393 (5.9)	348 (11.9)	335^{sh} (9.1)	300^{sh} (10.5)	268 (25.2)	234 (41.0)

Measured in THF at rt. sh = shoulder. a = From ref. [92].

3.3 Exchange of the Coligand X for [Ni(Py(Ph)Py)X]

The synthesis of [Ni(N^C^N)R] species bearing different coligands other than halides needed to be investigated individually. Many failed attempts to synthesize these complexes resulted in a reisolation of the used halido precursor or a decomposition of the compound. Therefore, the exact conditions, especially the type of solvent and the reaction time and -temperature, needed to be found to succeed in the formation of the desired species.

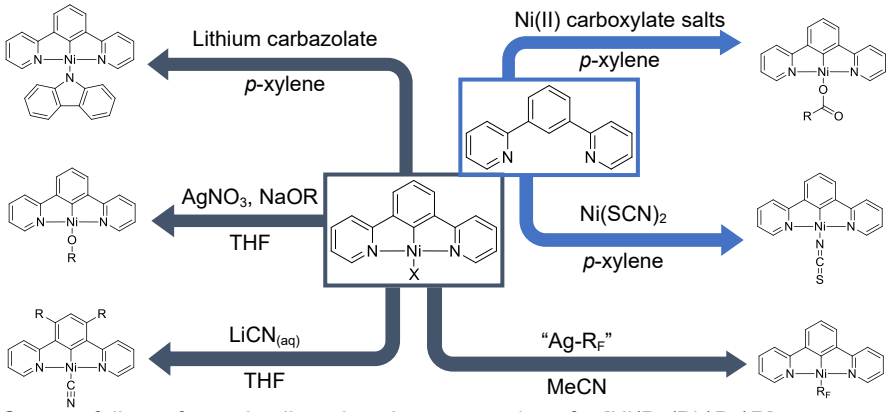

Figure 3-44 Successfully performed coligand exchange reactions for [Ni(Py(Ph)Py)R].

As Figure 3-44 shows, all successful synthetic approaches summarized in two main procedures – On the one hand the real coligand exchange reaction, starting with the halido species and exchanging it by an (in-)organic monodentate ligand (Chapter 3.3.1 to 3.3.5) and on the other hand the use of (in-)organic Ni(II) salts undergoing the base-assisted C–H activation reaction to give the cyclometalated Ni(II) species (Chapter 3.3.6 and 3.3.7).

3.3.1 Synthesis and Characterization of [Ni(Py(Ph)Py)F]

The first successful coligand exchange reaction was an interligand exchange from chloride to fluoride to generally prove the possibility of a change of the coligand after cyclometalation. The failure of the base-assisted C–H activation method of NiF_2 in *p*-xylene made a coligand exchange reaction necessary. [Ni(Py(Ph)Py)F] was isolated with 86% yield (Figure 3-45).

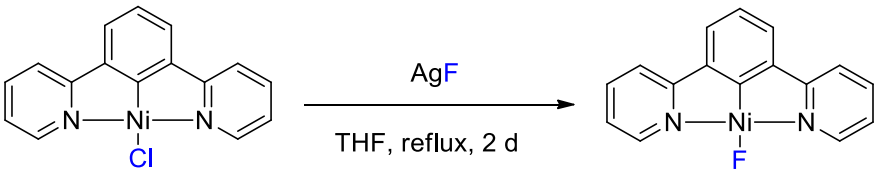

Figure 3-45 Reaction scheme of the coligand exchange reaction for [Ni(Py(Ph)Py)F].

The full conversion from [Ni(Py(Ph)Py)Cl] to [Ni(Py(Ph)Py)F] was proved by ^{1}H and ^{19}F NMR spectroscopy, mass spectrometry and elemental analysis (full data, see Chapter 5.4.3). The change of the size of the coligand and the resulting change of its acidity leads to a characteristic change of the shift of the ortho-*N* proton signal of the pyridyl units from 8.70 to 8.35 ppm in DMSO-d_6, as already reported for [Ni(Py(Ph)Py)X] with X = Cl, Br, I(Figure 3-46, *left*).[92]

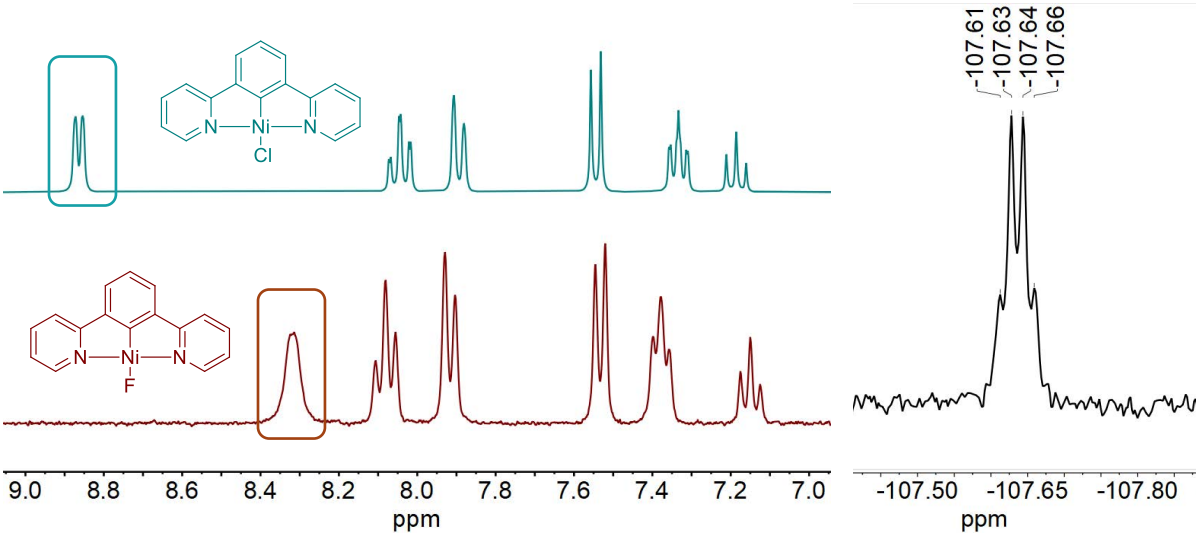

Figure 3-46 300 MHz ^{1}H NMR spectra of [Ni(Py(Ph)Py)Cl] (*top, left*) and [Ni(Py(Ph)Py)F] (*bottom, left*) and 282 MHz ^{19}F NMR spectrum of [Ni(Py(Ph)Py)F] (*right*), all measured in DMSO-d_6 at rt.

Further ^{19}F NMR spectroscopy was performed giving one quartet with a chemical shift of –108 ppm indicating the coupling of the fluoride nucleus with both nitrogen nuclei from the ligand backbone with a coupling constant of 4.3 Hz (Figure 3-46, *right*).

Figure 3-47 shows the UV/vis absorption spectrum of [Ni(Py(Ph)Py)F] in comparison to its halide analogues and its cyclic voltammogram. As already reported in 2020 by *Klein et al*.[92] the optical and electrochemical properties of complexes bearing different halide coligands do not change, which supports the measurements.

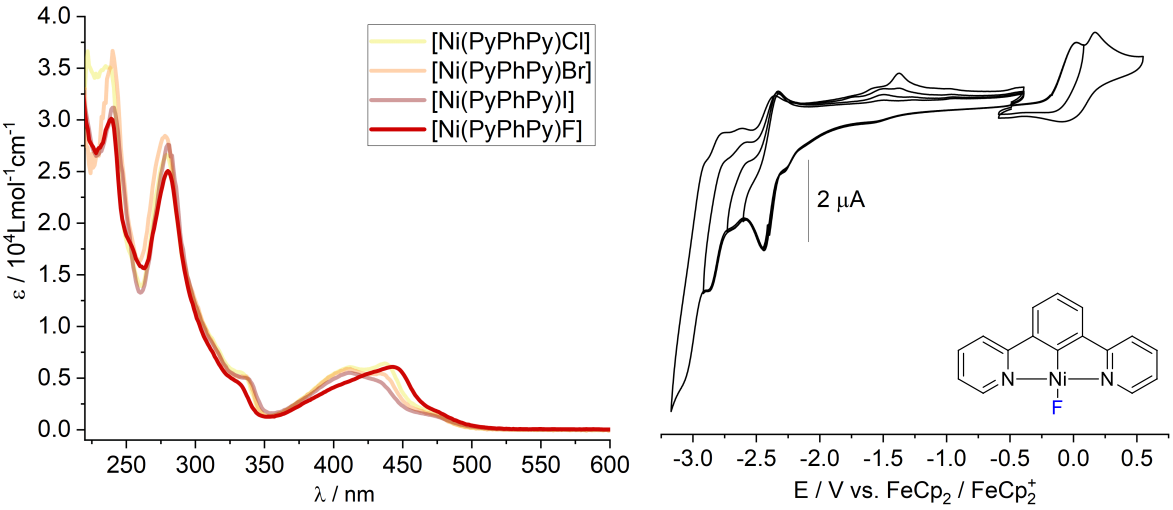

Figure 3-47 UV/vis spectrum of [Ni(Py(Ph)Py)F] in comparison to its halido analogues, all measured in THF at rt (*left*) and its cyclic voltammograms (*right*), measured in a 0.1M nBu$_4$PF$_6$ solution in THF with a scan rate of 100 mV/s.

Cyclic voltammetry gives a very similar value for the electrochemical HOMO–LUMO gap of 2.40 eV. However, all reduction waves are slightly shifted cathodically and a second oxidation could be measured. Therefore, it can be assumed, that the HOMO energy level is no longer located on the fluoride coligand, as it is the case for [Ni(Phbpy)F].[91] Calculations for this species showed, that the HOMO energy level is mainly located on the phenide unit of the complex (Figure 3-27).[92]

Table 3-27 Redox potentials of [Ni(Py(Ph)Py)F] in comparison to its chlorido derivative.

	***E* Ox2**	***E* Ox1**	***E* Red1**	***E* Red2**	***E* Red3**	**Δ*E* HOMO-LUMO**
[Ni(Py(Ph)Py)Cl][a]	-	0.06 ($E_{1/2}$)	–2.33 (E_{pc})	–2.57 (E_{pc})	–2.69 (E_{pc})	2.39 eV
[Ni(Phbpy)F][b]	-	0.01 (E_{pa})	–1.97 ($E_{1/2}$)	–2.67 ($E_{1/2}$)	-	1.98 eV
[Ni(Py(Ph)Py)F]	0.09 ($E_{1/2}$)	0.02 (E_{pa})	–2.38 ($E_{1/2}$)	–2.60 (E_{pc})	–2.87 (E_{pc})	2.40 eV

Measured in THF at rt with a scan rate of 100 mV/s. All potentials in V. E_{pc} = Cathodic Peak Potential, E_{pa} = Anodic Peak Potential, $E_{1/2}$ = Half-Step Potential. a = From ref. [92]. b = From ref. [91].

The UV/Vis absorption spectrum supports the aforementioned report, that the optical properties of [Ni(Py(Ph)Py)F] do not change significantly in comparison to the chlorido, bromido and iodido analogue.[92] The π–π* transitions show very similar maxima at 235 and 280 nm. Also, the first CT band at 332 nm is fitting into the series. The following CT bands merge into one maximum at 444 nm, which is slightly redshifted in comparison to the chlorido derivative. All in all, this do not lead to a change in the HOMO–LUMO gap.

Table 3-28 Absorption maxima of [Ni(Py(Ph)Py)F] in comparison to [Ni(Py(Ph)Py)Cl].

Complex	Absorption Max. λ_x in nm (Ext. Coeff. ε in 1000 · $Lmol^{-1}cm^{-1}$)					
	λ_6	λ_5	λ_4	λ_3	λ_2	λ_1
[Ni(Py(Ph)Py)Cl][a]	463[sh] (1.8)	437 (6.7)	412 (6.3)	332 (5.7)	279 (26.8)	236 (35.5)
[Ni(Py(Ph)Py)F]	472[sh] (1.9)	443 (6.1)	407[sh] (4.6)	330[sh] (4.6)	280 (24.9)	239 (30.0)

Measured in a 0.1M nBu$_4$PF$_6$ solution in THF with a scan rate of 100 mV/s. sh = shoulder. a = From ref. [92].

3.3.2 Synthesis and Characterization of [Ni(Py(Ph)Py)Carb]

In 2020 *Yam et al.* published a [Ni(N^C^N)R] complex containing carbazolate (Carb) as a coligand, that was luminescent at 77 K in a frozen glassy matrix and at 298 K in the solid state.[127] The application of this species for C–C cross coupling catalysis was nit investigated yet and therefore interesting for this topic. It was synthesized by firstly isolating lithium carbazolate out of toluene as a colorless salt and using it as a coligand exchange reagent in hot *p*-xylene for the target complex in 96% yield (Figure 3-48).

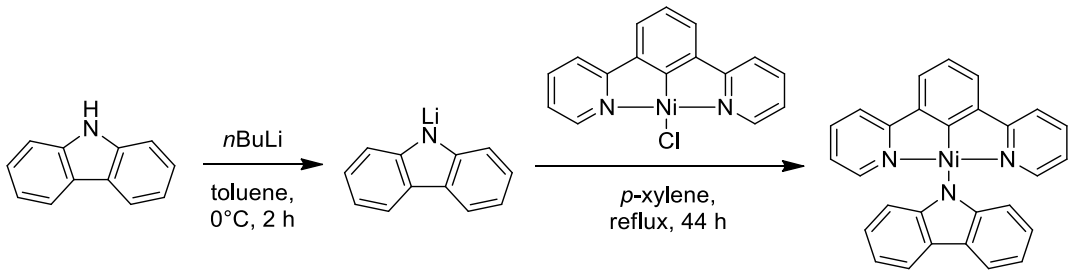

Figure 3-48 Synthetic route for [Ni(Py(Ph)Py)Carb].

The existence and pureness of this compound could be proved by ^{1}H NMR spectroscopy and EI(+) mass spectrometry, as well as an elemental analysis. Furthermore, it was possible to crystallize this species out of a concentrated *p*-xylene solution. The crystal structure was solved in the orthorhombic spacegroup $P2_12_12_1$ bearing four units per unit cell. Figure 3-49 shows one molecule of the asymmetric unit, as well as the crystal packing along the crystallographic *a*-axis. Table 3-29 summarizes the crystallographic data for the presented solution.

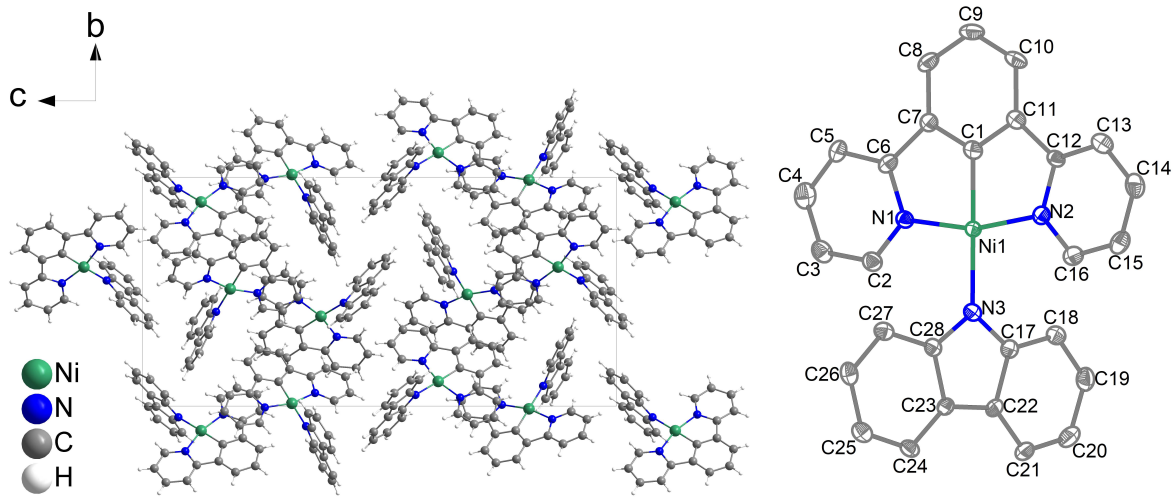

Figure 3-49 *Left:* Crystal structure of [Ni(Py(Ph)Py)Carb] viewed along the crystallographic *a*-axis. *Right*: Molecular structure of [Ni(Py(Ph)Py)Carb]. Hydrogen atoms are omitted for clarity. Ellipsoids are shown with a 50% probability.

Table 3-29 Crystallographic data for [Ni(Py(Ph)Py)Carb].

Identification code	**2 [Ni(Py(Ph)Py)Carb]**
Empirical formula	2 $C_{28}H_{19}N_3Ni$
Temperature/K	100.0
Crystal system	orthorhombic
Space group	$P2_12_12_1$
a/Å	9.0665(3)
b/Å	14.8314(5)
c/Å	30.7378(1)
Volume/Å^3	4133.3(2)
Z	4
ρ_{calc}g/cm^3	1.466
F(000)	1888.0
Radiation	MoKα (λ = 0.71073)
2Θ range for data collection/°	3.816 to 54.206
Index ranges	–11 ≤ h ≤ 10, –19 ≤ k ≤ 19, –35 ≤ l ≤ 39
Reflections collected	33940
Independent reflections	8961 [R_{int} = 0.0775, R_{sigma} = 0.0756]
Data/restraints/parameters	8961/0/577
Goodness-of-fit on F^2	1.031
Final R indexes [I>=2σ (I)]	R_1 = 0.0419, wR_2 = 0.0769
Final R indexes [all data]	R_1 = 0.0608, wR_2 = 0.0862
Largest diff. peak/hole / eÅ^{-3}	0.40/–0.34
Flack parameter	0.015(9)
CCDC	2248235

The crystal structure of [Ni(Py(Ph)Py)Carb] has not been literary known. This species shows a typical square-planar coordination around the nickel center with an overall sum of the angles of 360.0° with bite angles of around 82° and N_1–Ni–N_2 angles of 163°, as typically known for similar complexes.[89, 91, 92, 99, 100, 104, 108, 116, 117, 122, 123, 127, 140-147] The bond lengths and angles from the Ni(II) center to the tridentate ligand does not change in comparison to the parent complex, but the Ni–N3 shortens to 1.94 Å. The planar tridentate ligand is in the same plane as the nitrogen atom from the coligand, but the plane from the planar carbazolate is positioned almost perpendicularly to the N^C^N ligand backbone (see Table 3-30).

The crystal packing, as shown in Figure 3-49 also shows an assumable intermolecular π–π interaction between two PyPh units, but with the shortest distance of 5.09 Å. This is no longer defined as a π-stacking, according to *Janiak*.[149]

Table 3-30 Angles and bond lengths of [Ni(Py(Ph)Py)Carb] (*for molecule 1*) in comparison to the standard chlorido complex.

	[Ni(Py(Ph)Py)Cl][a]	**[Ni(Py(Ph)Py)Carb]**
Distances / Å		
Ni–C1	1.836(7)	1.838(5)
Ni–N1	1.932(6)	1.933(4)
Ni–N2	1.936(5)	1.940(4)
Ni–Cl1/N3	2.247(2)	1.941(4)
Angles / °		
C1–Ni–N1	81.6(3)	82.14(1)
C1–Ni–N2	82.3(3)	81.84(1)
N1–Ni–Cl1/N3	98.23(2)	97.42(1)
N2–Ni–Cl1/N3	97.90(2)	98.64(1)
Sum / °	359.9	360.0
C1–Ni–Cl1/N3	179.7(2)	179.5(2)
N1–Ni–N2	163.9(2)	163.96(1)

a = From ref. [92].

Cyclic voltammetry (Figure 3-50*, right*) were already studied in detail by *Yam et al.* in detail and align with the measured values.[127] They show, that the electrochemical properties of the carbazolato complex are very similar to the chloride compound by showing three reductions starting at –2.33 V and one reversible oxidation at 0.04 V referenced to ferrocene/ferrocenium (full potentials see Table 3-31).[92] Whereas the oxidation is mainly irreversible for the carbazolato species and its first reduction seems to be fully reversible, it is the other way around for the chlorido precursor. This implies, that the EC mechanism is no longer be applicable for complexes with carbazolate as a coligand.[89, 91, 92, 99, 142]

The observed changes align with the theory, that the highest occupied molecular orbitals (HOMO) are not only localized on the metal, but also obtain contributions from the central phenide unit of the N^C^N ligand and the coligands.[92, 140] The second and third reduction are cathodically shifted, which indicates a higher electrochemical stability of the reduced complex species.

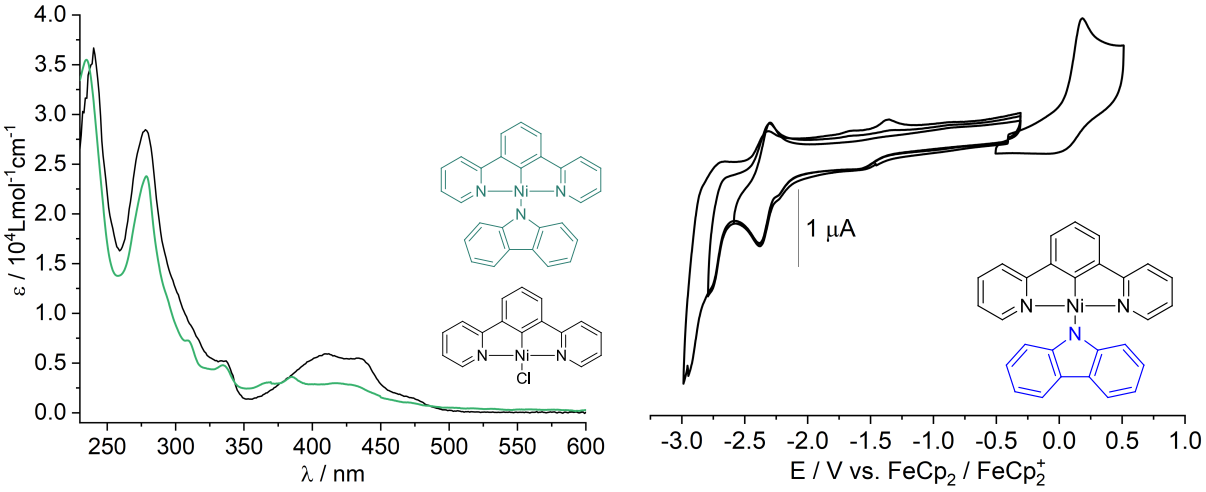

Figure 3-50 UV/vis spectrum of [Ni(Py(Ph)Py)Carb] in comparison to its chlorido analogue, measured in THF at rt (*left*) and its cyclic voltammograms (*right*), measured in a 0.1M nBu$_4$PF$_6$ solution in THF with a scan rate of 100 mV/s.

Table 3-31 Redox potentials of [Ni(Py(Ph)Py)Carb] in comparison to its chlorido derivative.

	***E* Ox1**	***E* Red1**	***E* Red2**	***E* Red3**	**Δ*E*$_{HOMO-LUMO}$**
[Ni(Py(Ph)Py)Cl][a]	0.06 ($E_{1/2}$)	–2.33 (E_{pc})	–2.57 (E_{pc})	–2.69 (E_{pc})	2.39 eV
[Ni(Py(Ph)Py)Carb]	0.04 ($E_{1/2}$)	–2.34 ($E_{1/2}$)	–2.78 (E_{pc})	–2.96 (E_{pc})	2.38 eV

Measured in a 0.1M nBu$_4$PF$_6$ solution in THF with a scan rate of 100 mV/s. All potentials in V. E_{pc} = Cathodic Peak Potential, E_{pa} = Anodic Peak Potential, $E_{1/2}$ = Half-Step Potential. a = From ref. [92].

Also UV/vis absorption spectroscopy was performed earlier by *Yam et al.* and fits to our measurements (Table 3-32).[127] It shows that the ligand centered absorption bands from π–π* transitions, do not change much with absorption maxima at 235 and 280 nm, whereas λ_3 from the chlorido complex changes into two absorption maxima at 309 and 335 nm. The absorption maxima at higher wavelengths are lower in extinction but spread over a range of 340 to 600 nm. Especially λ_8 is measured as a very broad shoulder starting at 500 nm and ending at 600 nm, which explains the orange color of this compound in THF solution, which appeared weaker than the intense yellow color from the chlorido precursor.

Table 3-32 Absorption maxima of [Ni(Py(Ph)Py)Carb] in comparison to [Ni(Py(Ph)Py)Cl].

Complex	Absorption Max. λ_x in nm (Ext. Coeff. ε in 1000 · $Lmol^{-1}cm^{-1}$)								
	λ_9	λ_8	λ_7	λ_6	λ_5	λ_4	λ_3	λ_2	λ_1
[Ni(Py(Ph)Py)Cl][a]	-	-	-	463[sh] (1.8)	437 (6.7)	412 (6.3)	332 (5.7)	279 (26.8)	236 (35.5)
[Ni(Py(Ph)Py)Carb]	500[sh] (0.5)	470[sh] (1.1)	417 (2.9)	385 (3.8)	367 (3.1)	335 (3.8)	309 (7.2)	278 (23.8)	235 (35.3)

Measured in THF at rt. sh = shoulder. a = From ref. [92].

3.3.3 Synthesis and Characterization of [M(Py(4,6dRPh)Py)CN] with M = Ni, Pd and Pt and R = H, Me and F

Another very interesting group of complexes are the cyanido complexes, as bearing one of the strongest monodentate ligands as a coligand with potential in yielding a luminescent Ni(II) compounds, as well as being potential catalysts.[127, 140] In 2021, it was found, that [M(C^N^N)CN] complexes showed very interesting electrochemical and optical properties.[108] Since there is still no synthetic route for a synthesis of the required precursor [Pd(Py(Ph)Py)Cl] without the use of highly toxic organomercury intermediates, this species was excluded (Table 3-33).

Table 3-33 Synthesized complexes bearing a cyanido coligand.

Metal center / Ligand	Py(Ph)Py	Py(4,6FPh)Py	Py(4,6MePh)Py
Ni	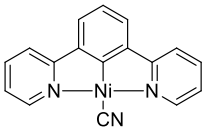 Yield: 20%	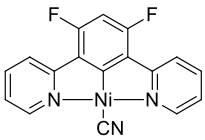 Yield: 26%	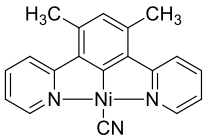 Yield: 25%
Pd	-	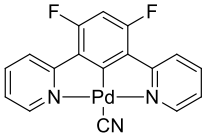 Yield: 50%	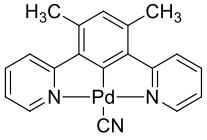 Yield: 73%
Pt	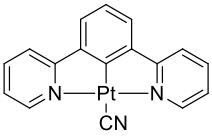 Yield: 38%	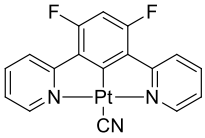 Yield: 55%	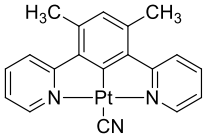 Yield: 65%

The synthesis of all halido complexes was performed by using the described procedures from the recently published triade [M(Py(4,6MePh)Py)Cl] by *Klein et al.*[140] The cyclopalladation and -platination reaction in acetic acid was adapted from *Cardenas et al.* and *Soro et al.* with yields between 70 and 85% for the Pt(II) compounds 55 to 99% for the Pd(II) compounds.[116, 122] The Ni(II) compounds were synthesized using the base assisted C–H activation from *Klein et al.* with yields of 71 to 94%.[92]

Having all eight halido species in hand, the coligand exchange reaction was performed by adapting the already published routes for the C^N^N derivatives. [108, 167] The desired Nickel species were synthesized using the chlorido or acetato precursor in THF at 0°C and adding a diluted aqueous solution of NaCN dropwise using a syringe pump over 6 h. Several other synthetic routes failed to synthesize [Ni(Py(Ph)Py)CN]. By using $Ni(CN)_2$ for the base-assisted C–H activation, the reaction yielded exclusively different tetracyanido nickelates. The use of AgCN as a coligand exchange reagent was not successful either, due to the poor solubility of this salt in organic solvents as THF. The slow addition of an extremely diluted solution of NaCN in combination with a low temperature allowed a direct precipitation of the less soluble cyanido complex in yields of 20 to 26%, preventing that more cyanide anions could attack the product and form the undesired but preferably formed tetracyanido nickelates. The corresponding palladium species could directly be converted to the cyanido complex by using NaCN in MeOH with yields of 50% for the difluoro-substituted complex and 73% for the dimethyl derivative. The Pt derivatives were synthesized using $AgNO_3$ in DMSO forming the nitrato complex, which then *in situ* undergoes a second coligand exchange reaction with NaCN (Figure 3-51) with yields between 38 and 65%.

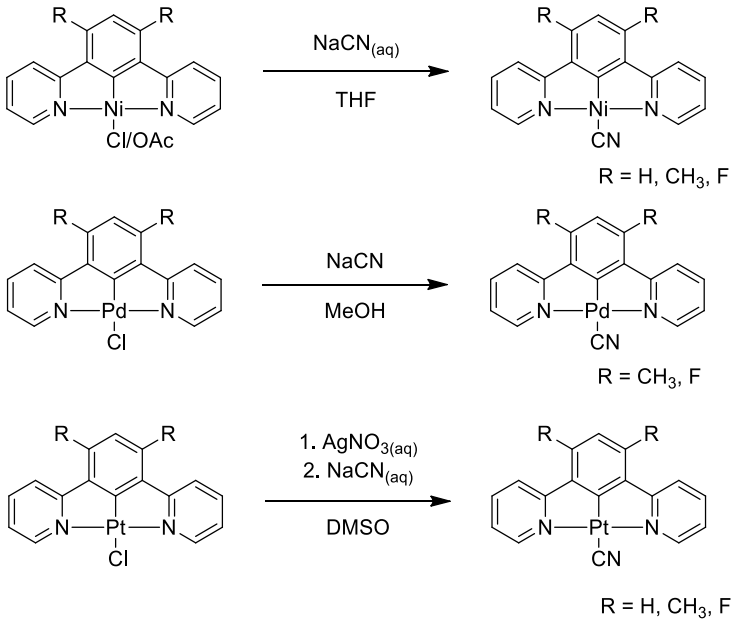

Figure 3-51 Synthetic procedures giving [M(N^C^N)CN] (M = Ni, Pd, Pt).

To proof the success of these coligand exchange reactions, firstly ^{1}H NMR spectroscopy, EI(+) mass spectrometry and elemental analysis was performed. Due to a poorer solubility of CN^- compounds, especially for the platinum derivatives, the resolution in NMR spectroscopy decreased. Nevertheless, the proton signal from the proton of the ortho-*N* carbon atom was indicating the conversion from a halido to a cyanido species, as exemplarily shown in Figure 3-52 to Figure 3-54.

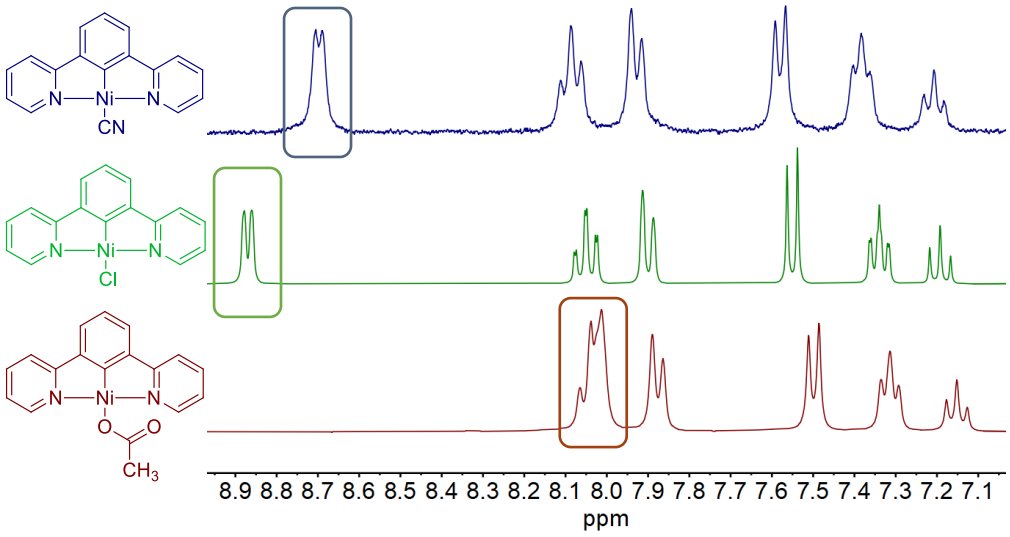

Figure 3-52 300 MHz ^{1}H NMR spectra of [Ni(Py(Ph)Py)CN] in DMSO-d_6 (*top, blue*) in comparison to its precursors [Ni(Py(Ph)Py)Cl] (*middle, green*) and [Ni(Py(Ph)Py)OAc] (*bottom, red*).

The acidity of the ortho-*N* proton changes with the coligand and is rather low for the acetato derivative (δ = 8.05 ppm) and relatively high for the chloride compound (δ = 8.87 ppm). The cyanido species shows a shift of 8.70 ppm, that lies in between of both species (Figure 3-52).

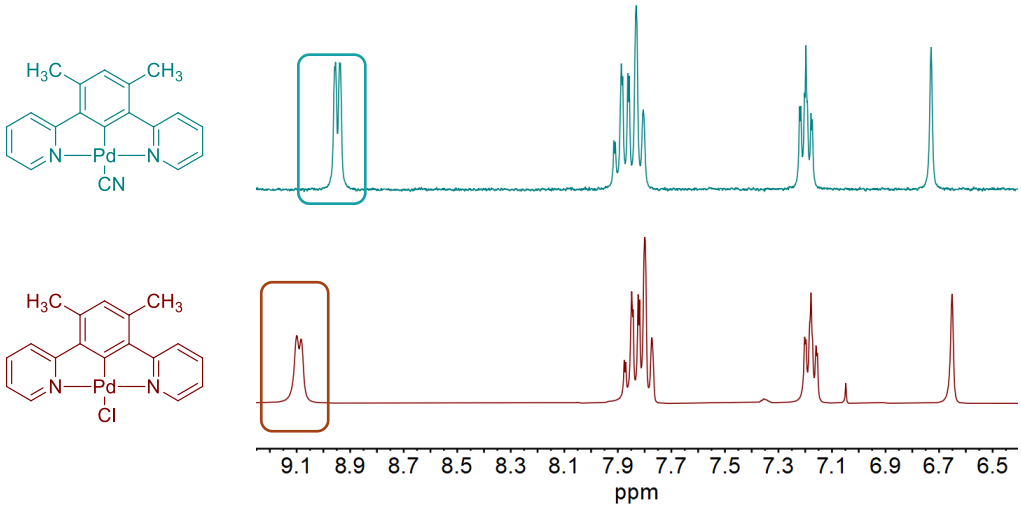

Figure 3-53 300 MHz ^{1}H NMR spectra of [Pd(Py(4,6MePh)Py)CN] in CD_2Cl_2 (*top, blue*) in comparison to its precursor [Pd(Py(4,6MePh)Py)Cl] (*bottom, red*).

Figure 3-53 shows spectra of the Pd(II) complexes from the ligand Py(4,6MePh)Py from the chlorido precursor (blue) and the one after a successful coligand exchange forming the cyanido species (red). One clearly can see the same trend as for the nickel analogues, in which the proton signal from the one ortho-nitrogen atom shifts from 9.1 to 9.0 ppm indicating a change of the surrounding of this proton.

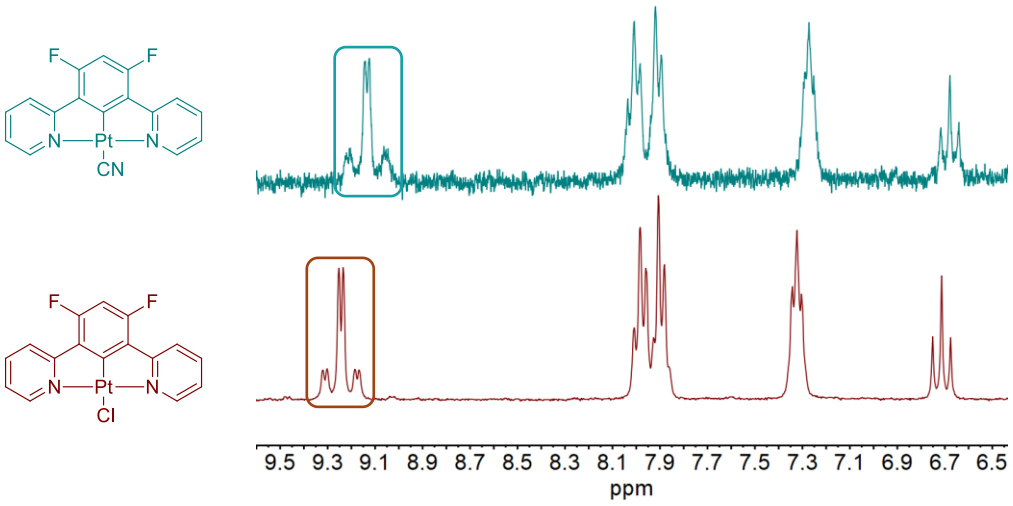

Figure 3-54 300 MHz ^{1}H NMR spectra of [Pt(Py(4,6FPh)Py)CN] in CD_2Cl_2 (*top, blue*) in comparison to its precursor [Pt(Py(4,6FPh)Py)Cl] (*bottom, red*).

The platinum complexes complete this series, showing the same shifts for the difluoro-substituted complexes, with the addition of platinum satellites for the highest shifted signals.

Crystallization approaches were successful for all three nickel compounds, as well as for the dimethyl-substituted Pd(II) derivative by overlaying a concentrated complex solution in THF with *n*-pentane. [Ni(Py(Ph)Py)CN] and [Ni(Py(4,6FPh)Py)CN] come in the monoclinic space group $P2_1/n$ with four units per unit cell, whereas [Ni(Py(4,6MePh)Py)CN] was solved in the monoclinic spacegroup $P2_1/c$, also bearing four units per unit cell.

The asymmetric unit of the difluoro-substituted species bears two independent complex units and one cocrystallized CH_2Cl_2 molecule. The only palladium complex crystallized in the monoclinic spacegroup $P2_1/c$ as well with four units per unit cell (Figure 3-55, Table 3-34).

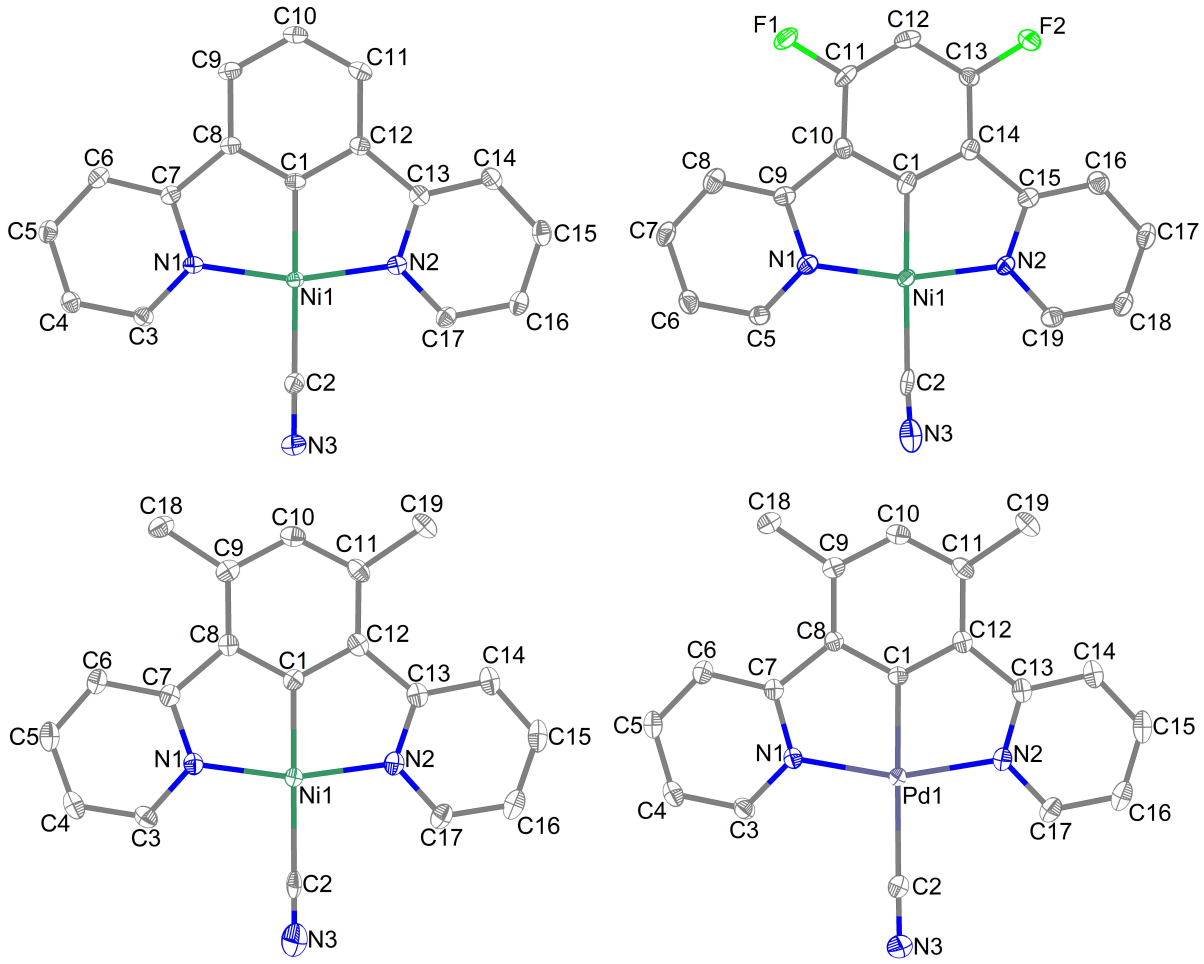

Figure 3-55 Molecular structures of [Ni(Py(Ph)Py)CN] (*top left*), [Ni(Py(4,6FPh)Py)CN] (*top right*), [Ni(Py(4,6MePh)Py)CN] (*bottom left*) and [Pd(Py(4,6MePh)Py)CN] (*bottom right*). Ellipsoids are shown with a 50% probability. Hydrogen atoms are omitted for clarity.

Table 3-34 Crystallographic data of [Ni(Py(Ph)Py)CN], [Ni(Py(4,6FPh)Py)CN], [Ni(Py(4,6MePh)Py)CN] and [Pd(Py(4,6MePh)Py)CN].

Identification code	**[Ni(Py(Ph)Py)CN]**	**[Ni(Py(dFPh)Py)CN]**	**[Ni(Py(dMePh)Py)CN]**	**[Pd(Py(dMePh)Py)CN]**
Empirical formula	$C_{17}H_{11}N_3Ni$	$C_{35}H_{20}Cl_2F_4N_6Ni_2$	$C_{19}H_{15}N_3Ni$	$C_{19}H_{15}N_3Pd$
T/K	100.0	100.0	100.0	100.0
Crystal system	monoclinic	monoclinic	monoclinic	monoclinic
Space group	$P2_1/n$	$P2_1/n$	$P2_1/c$	$P2_1/c$
a/Å	8.8536(6)	6.6847(5)	7.7996(5)	7.8883(3)
b/Å	16.4635(9)	36.052(3)	10.4099(7)	10.3760(4)
c/Å	8.8635(5)	12.3884(1)	18.1779(1)	18.4881(7)
β/°	92.670(2)	98.516(3)	101.199(2)	101.7700(1)
Volume/Å^3	1290.55(1)	2952.7(4)	1447.83(1)	1481.42(1)
Z	4	4	4	4
ρ_{calc}g/cm^3	1.626	1.775	1.578	1.756
F(000)	648.0	1592.0	712.0	784.0
Radiation	MoKα (λ = 0.71073)	MoKα (λ = 0.71073)	MoKα (λ = 0.71073)	MoKα (λ = 0.71073)

2Θ range for data collection/°	4.948 to 71.356	4.02 to 55.754	4.53 to 56.696	4.5 to 63.012
Index ranges	–14 ≤ h ≤ 14, –26 ≤ k ≤ 26, –14 ≤ l ≤ 14	–8 ≤ h ≤ 8, –47 ≤ k ≤ 47, –16 ≤ l ≤ 16	–10 ≤ h ≤ 9, –13 ≤ k ≤ 13, –24 ≤ l ≤ 24	–11 ≤ h ≤ 11, –15 ≤ k ≤ 15, –26 ≤ l ≤ 26
Reflections collected	103118	89016	42922	42103
Independent reflections	5974 [R_{int} = 0.0809, R_{sigma} = 0.0309]	7045 [R_{int} = 0.0901, R_{sigma} = 0.0433]	3607 [R_{int} = 0.0720, R_{sigma} = 0.0305]	4865 [R_{int} = 0.0249, R_{sigma} = 0.0146]
Data/restraints/ parameters	5974/0/190	7045/0/443	3607/0/210	4865/0/211
Goodness-of-fit on F^2	1.113	1.117	1.096	1.076
Final R indexes [I>=2σ (I)]	R_1 = 0.0370, wR_2 = 0.0756	R_1 = 0.0587, wR_2 = 0.1056	R_1 = 0.0344, wR_2 = 0.0730	R_1 = 0.0201, wR_2 = 0.0476
Final R indexes [all data]	R_1 = 0.0508, wR_2 = 0.0871	R_1 = 0.0778, wR_2 = 0.1135	R_1 = 0.0488, wR_2 = 0.0837	R_1 = 0.0235, wR_2 = 0.0499
Largest diff. peak/hole / eÅ^{-3}	0.59/–0.56	0.56/–0.58	0.65/–0.39	0.79/–0.72
CCDC	2248200	2343451	2343443	2343434

All complexes show a square planar coordination around the metal center. Since the coordination is slightly distorted along the N–M–N axis with angles around 164° for Ni(II) and 160° for Pd(II), having chelate bite-angles of 82° for all Ni(II) and 80° for the Pd(II) compound, which is already known from related complexes. [89, 91, 92, 99, 100, 104, 108, 116, 117, 122, 123, 127, 140-147]

The nickel complexes show a very similar coordination around the nickel center in comparison to the corresponding chlorido complex (Table 3-35).[92] However, it shows a significantly shorter bond length to the coligand in a range of 1.94 to 2.03 Å, instead of 2.24 to 2.25 Å for the chlorido species.[92, 140] The Pd(II) species shows a Pd–C2 bond of 2.11 Å, instead 2.45 Å for the Pd–Cl1 bond. It is noteworthy, that within the series of all three nickel cyanido complexes, the Ni–C2 bond length increases the least for the difluoro substituted complex in comparison to all other species, which is explainable by the -I effect of fluoride substituents and their impact on the electron density of the central phenide unit. The distance between C2 and N3 is 1.03 to 1.15 Å, which verifies the triple bond character of the cyanide coligand.[108]

Table 3-35 Angles and bond lengths of [Ni(Py(Ph)Py)CN], [Ni(Py(4,6FPh)Py)CN], [Ni(Py(4,6MePh)Py)CN] and [Pd(Py(4,6MePh)Py)CN] in comparison to their chloride precursors.

	[Ni(Py(Ph)Py)CN]	**[Ni(Py(4,6FPh)Py)CN]**[c]	**[Ni(Py(4,6MePh)Py)CN]**	**[Pd(Py(4,6MePh)Py)**CN**]**
Dist. / Å				
M–C1	1.8339(14)	1.837(4)	1.845(2)	1.935(13)
M–N1	1.9297(13)	1.917(3)	1.9134(19)	2.037(11)
M–N2	1.9317(13)	1.926(3)	1.9142(19)	2.038(11)
M–C2	1.9448(15)	1.999(5)	2.026(3)	2.107(15)

Angles / °				
C1–M–N1	81.88(6)	82.48(15)	82.40(9)	80.28(5)
C1–M–N2	81.79(6)	82.34(15)	82.15(9)	80.21(5)
N1–M–C2	97.99(6)	98.45(14)	97.80(8)	100.34(5)
N2–M–C2	98.34(6)	96.73(14)	97.67(8)	99.17(5)
Sum / °	360.0	360.0	360.0	360.0
C1–M–C2	179.52(7)	179.05(16)	178.08(9)	179.12(5)
N1–M–N2	163.67(5)	164.79(14)	164.54(8)	160.49(5)
	[Ni(Py(Ph)Py)Cl][a]		**[Ni(Py(4,6MePh)Py)Cl]**[b]	**[Pd(Py(4,6MePh)Py)Cl]**[b]
Dist. / Å				
M–C1	1.836(7)		1.827(5)	1.916(5)
M–N1	1.932(6)		1.920(4)	2.035(5)
M–N2	1.936(5)		1.916(4)	2.035(5)
M–Cl1	2.247(2)		2.243(15)	2.4512(18)
Angles / °				
C1–M–N1	81.6(3)		83.0(2)	80.72(2)
C1–M–N2	82.3(3)		82.7(2)	80.59(2)
N1–M–Cl1	98.23(2)		96.95(14)	99.76(15)
N2–M–Cl1	97.90(2)		97.36(14)	98.93(15)
Sum / °	359.9		360.0	360.0
C1–M–Cl1	179.7(2)		179.76(17)	178.27(16)
N1–M–N2	163.9(2)		165.65(19)	161.30(2)

a = From ref. [92]. b = From ref. [140]. c = all values for molecule 1.

The crystal structures of all cyanido species show the typical head-to-tail arrangement, [92, 99, 108, 140, 148] except of [Ni(Py(4,6FPh)Py)CN] (Figure 3-56). This structure bears CH_2Cl_2 molecules, that fill gaps on the edges of the unit cell along the crystallographic *a*-axis. All other systems are isostructural, also according to their chlorido precursors, which indicates a similar size for cyanide in comparison to chloride and therefore a same behavior in the packing of the crystal structure of the corresponding complex.[92, 108]

The stacking distance of two PyPh units for these three species is in a range of 3.71 Å (for the standard nickel cyanido species) to 3.79 Å (for the dimethyl substituted palladium species), which is very similar to the ones from the halido species (3.74 Å for [Ni(Py(Ph)Py)Cl])[92] and therefore at the boarder of *Janiak's* definition of a weak π-stacking.[149]

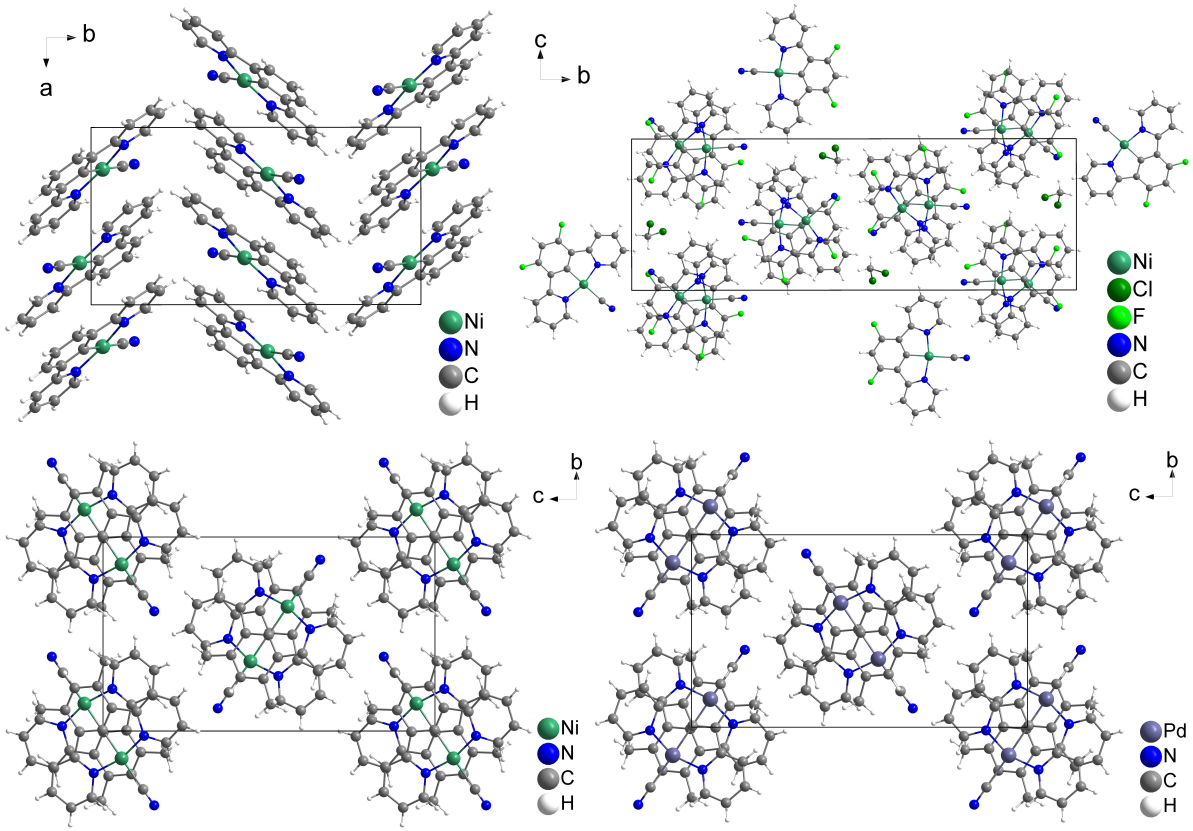

Figure 3-56 Crystal structure of [Ni(Py(Ph)Py)CN] along the crystallographic *c*-axis (*top left*), [Ni(Py(4,6FPh)Py)CN] along the crystallographic *a*-axis (*top, right*), [Ni(Py(4,6MePh)Py)CN] along the crystallographic *a*-axis (*bottom left*) and [Pd(Py(4,6MePh)Py)CN] along the crystallographic *a*-axis (*bottom right*).

Cyclic voltammetry allows the comparison of all three synthesized Ni(II) cyanido species, as well as a comparison of the three different d^{10} metal complexes bearing the same ligand system. All nickel species show an irreversible oxidation at 0.3 to 0.4 V and four to five reductions starting at –2.1 to –3.4 V (Figure 3-57).

By exchanging the coligand from chloride to cyanide, the reversibility of the first oxidation and reduction change. Whereas the first reduction followed the irreversible EC mechanism for the chlorido complexes,[89, 91, 92, 99, 142] this seems not to be the case for cyanido species. The first reduction appears at similar potentials but gets fully reversible, with half-step potentials of –2.14 V for the difluoro-, –2.27 V for the unsubstituted and –2.30 V for the dimethyl-substituted complex. The first oxidations get less reversible for these species and are anodically shifted with half-step potentials of 0.30 V for the dimethyl-, 0.39 V for the unsubstituted and 0.46 V for the difluoro compound, showing that the HOMO energy level is at least partially placed on the coligand, which aligns with published reports.[92, 108, 140] The stronger ligand field stabilizes the complex structure by an increased electrochemical HOMO-LUMO gap of up to 2.66 eV. As well the inverted reversibility of the first oxidation and reduction, as the higher electrochemical HOMO-LUMO gap align to the recently published results, dealing with [M(Phbpy)CN] (M = Ni,

Pd, Pt) complexes and their electrochemical measurements.[108] Within these measurements also mainly the potential of the first oxidation changes, whereas the reductions stay mostly at same potentials in comparison to their chlorido precursors. The difluoro substituted compound again shows an anodic shift of all waves in comparison to the unsubstituted and dimethyl substituted derivatives, which again can be explains by the -I effect, that impacts the electron density around the complex in general (see Chapter 3.1.2).

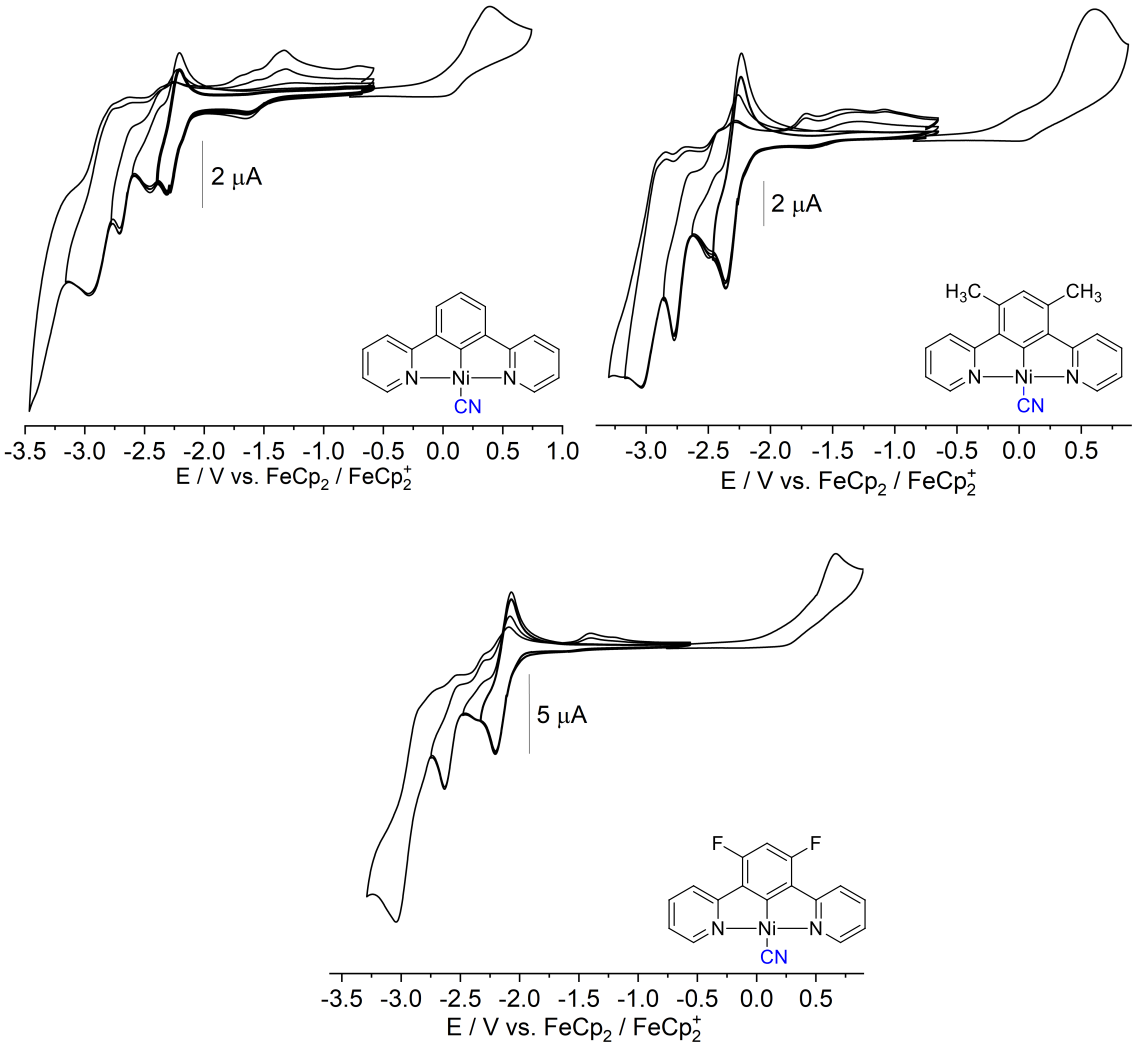

Figure 3-57 Cyclic voltammograms of [Ni(Py(Ph)Py)CN] (*top, left*), [Ni(Py(4,6MePh)Py)CN] (*top, right*) and [Ni(Py(4,6FPh)Py)CN] (*bottom*), measured in a 0.1M nBu$_4$PF$_6$ solution THF at rt with a scan rate of 100 mV/s.

Due to the fact, that the oxidation is metal centered for these complex species,[108, 140] it was assumable, that the oxidation waves shift anodically by substituting the metal ion from Ni (0.30 V) over Pt (0.43 V) to Pd (0.79 V) for the dimethyl substituted complexes (Figure 3-58). Same trends could be observed for the difluoro substituted complexes with further anodically shifted potentials (Cyclic voltammograms, see Chapter 7.4, Ox1: Ni = 0.46 V ($E_{1/2}$); Pt = 0.62 V (E_{pa}); Pd = 1.05 V (E_{pa})). These results fit perfectly into the already observed trends and

changes of the potentials in literature for [M(Py(4,6MePh)Py)Cl] and [M(Phbpy)CN] (M = Ni, Pd, Pt)[108, 140] as well as to the CT bands of UV/vis absorption spectroscopy (see below). The first reduction potentials are generally reversible (as they are for C^N^N analogues)[108] and do not shift significantly within a group of compounds in comparison to their chloride precursors. For the 4,6-dimethyl substituted complexes with M = Ni, Pd and Pt all six complexes show first reductions at around –2.30 V. It shows, that the LUMO is again not affected by the metal and the coligand (values for further complexes, see Table 3-36). The electrochemical HOMO-LUMO are therefore mainly changing with the change of the first oxidation potential and show increased values as their chlorido derivative, as well as the aforementioned trend within the d^{10} metal series. For the dimethyl compounds it is 2.60 eV for the Ni(II), 2.67 eV for the Pt(II) and 3.11 eV for the Pd(II) derivative.[108, 140,191]

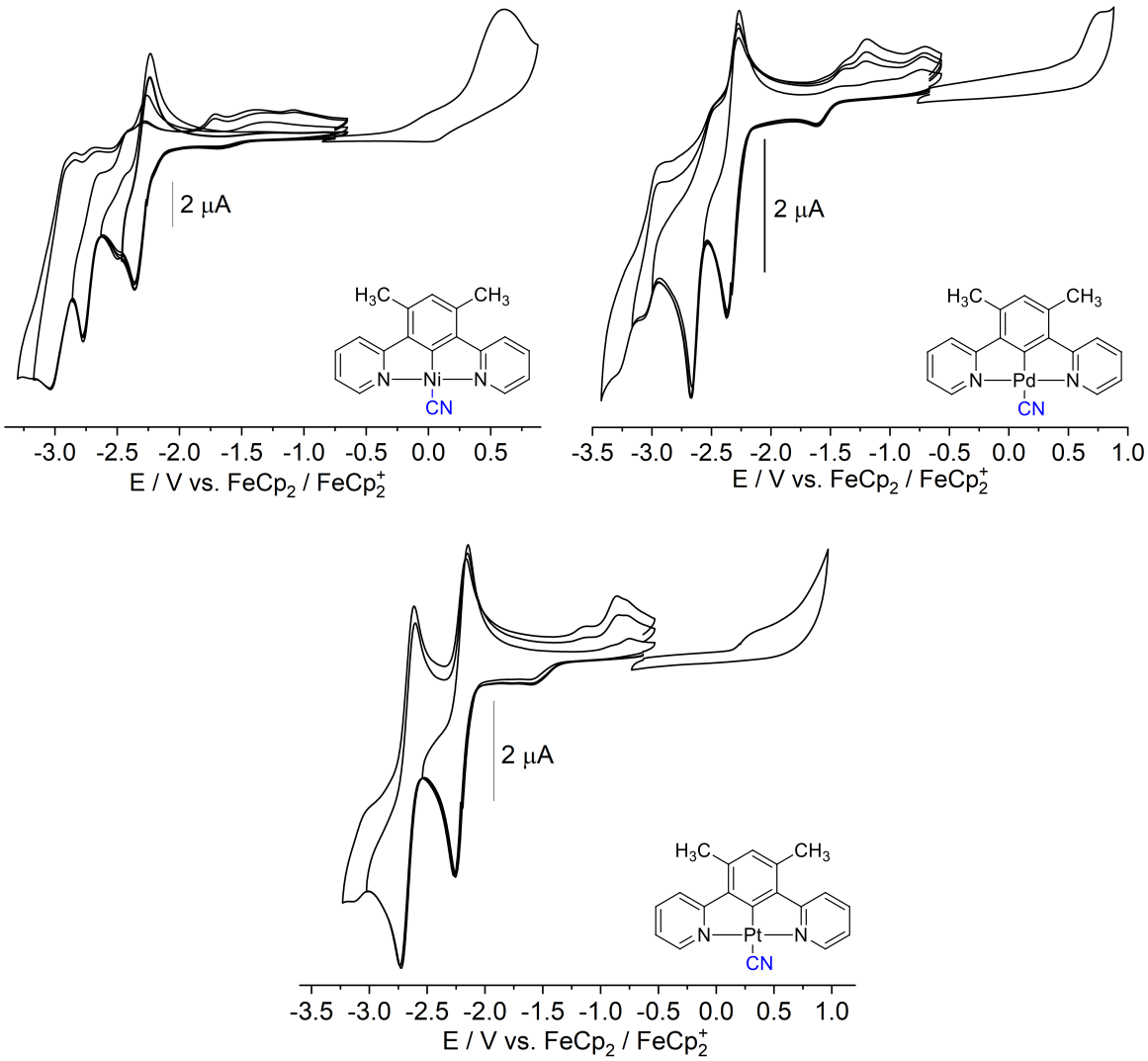

Figure 3-58 Cyclic voltammograms of [Ni(Py(4,6MePh)Py)CN] (*top, left*), [Pd(Py(4,6MePh)Py)CN] (*top, right*) and [Pt(Py(4,6MePh)Py)CN] (*bottom*), measured in a 0.1M nBu$_4$PF$_6$ solution THF at rt with a scan rate of 100 mV/s.

Table 3-36 Redox potentials of [M(Py(4,6RPh)Py)CN] in comparison to [M(Py(4,6RPh)Py)Cl] (M = Ni, Pd, Pt. R = H, Me, F).

	E **Ox1**	***E*** **Red1**	***E*** **Red2**	***E*** **Red3**	***E*** **Red4**	***E*** **Red5**	$\Delta E_{\text{HOMO-LUMO}}$
[Ni(Py(Ph)Py)Cl][a]	0.06 ($E_{1/2}$)	–2.33 (E_{pc})	–2.57 (E_{pc})	–2.69 (E_{pc})	-	-	2.39 eV
[Ni(Py(4,6MePh)Py)Cl][b]	0.10 ($E_{1/2}$)	–2.26 (E_{pc})	–2.37 ($E_{1/2}$)	-	-	-	2.36 V
[Ni(Py(4,6FPh)Py)Br]	0.17 ($E_{1/2}$)	–2.17 (E_{pc})	–2.36 (E_{pc})	–2.74 ($E_{1/2}$)	–3.10 (E_{pc})	-	2.34 eV
[Pd(Py(4,6MePh)Py)Cl][b]	0.74 (E_{pa})	–2.34 ($E_{1/2}$)	–2.75 (E_{pc})	-	-	-	3.07 V
[Pd(Py(4,6FPh)Py)Cl]	0.89 (E_{pa})	–2.15 (E_{pc})	–2.30 (E_{pc})	–2.78 (E_{pc})	–2.92 (E_{pc})	-	3.04 eV
[Pt(Py(Ph)Py)Cl][c,]	0.35 (E_{pa})	-2.18 ($E_{1/2}$)	-	-	-	-	2.59 eV
[Pt(Py(4,6MePh)Py)Cl][b]	0.35 (E_{pa})	–2.24 ($E_{1/2}$)	–2.69 (E_{pc})	-	-	-	2.59 V
[Pt(Py(4,6FPh)Py)Cl]	0.56 (E_{pa})	–2.07 ($E_{1/2}$)	–2.55 ($E_{1/2}$)	–2.89 (E_{pc})	–3.12 (E_{pc})	–3.46 (E_{pc})	2.63 eV
[Ni(Py(Ph)Py)CN]	0.39 (E_{pa})	–2.27 ($E_{1/2}$)	–2.46 (E_{pc})	–2.71 (E_{pc})	–2.97 (E_{pc})	–3.43 (E_{pc})	2.66 eV
[Ni(Py(4,6MePh)Py)CN]	0.30 ($E_{1/2}$)	–2.30 ($E_{1/2}$)	–2.50 (E_{pc})	–2.78 (E_{pc})	–2.94 ($E_{1/2}$)	–3.20 (E_{pc})	2.60 eV
[Ni(Py(4,6FPh)Py)CN]	0.46 ($E_{1/2}$)	–2.14 ($E_{1/2}$)	–2.36 (E_{pc})	–2.63 (E_{pc})	–3.05 (E_{pc})	-	2.60 eV
[Pd(Py(4,6MePh)Py)CN]	0.79 (E_{pa})	–2.32 ($E_{1/2}$)	–2.67 (E_{pc})	–3.10 (E_{pc})	–3.33 (E_{pc})	-	3.11 eV
[Pd(Py(4,6FPh)Py)CN][d]	1.05 (E_{pa})	–2.10 ($E_{1/2}$)	–2.34 ($E_{1/2}$)	–2.55 (E_{pc})	–2.72 (E_{pc})	–2.89 (E_{pc})	3.15 eV
[Pt(Py(Ph)Py)CN]	0.59 (E_{pa})	–2.22 (E_{pc})	–2.33 (E_{pc})	–2.70 (E_{pc})	–2.84 (E_{pc})	-	2.81 eV
[Pt(Py(4,6MePh)Py)CN]	0.43 (E_{pa})	–2.24 ($E_{1/2}$)	–2.67 ($E_{1/2}$)	–3.14 (E_{pc})	-	-	2.67 eV
[Pt(Py(4,6FPh)Py)CN]	0.62 (E_{pa})	–2.15 ($E_{1/2}$)	–2.65 ($E_{1/2}$)	-	-	-	2.77 eV

Measured in a 0.1M nBu$_4$PF$_6$ solution THF at rt with a scan rate of 100 mV/s. All potentials in V. E_{pc} = Cathodic Peak Potential, E_{pa} = Anodic Peak Potential, $E_{1/2}$ = Half-Step Potential. a = From ref. [92]. b = From ref. [140]. c = From ref. [117], measured in MeCN at rt. d = Red6 at –3.07 V (E_{pc}) and Red7 at –3.29 V (E_{pc}).

UV/vis spectroscopy shows intense bands at 230 to 300 nm, which are very similar to the absorption bands from the protoligands Py(4,6RPhH)Py, with R = H, Me, F. These were followed by broader and more structured bands with lower extinctions up to 500 nm, which are responsible for the yellow to red color of these compounds.[92, 108, 140] Figure 3-59 compares all

nickel complexes with different ligands to their chloride precursors and Figure 3-60 shows the d^{10} metal triade bearing the same tridentate ligand, exemplarily for Py(4,6FPh)Py complexes.

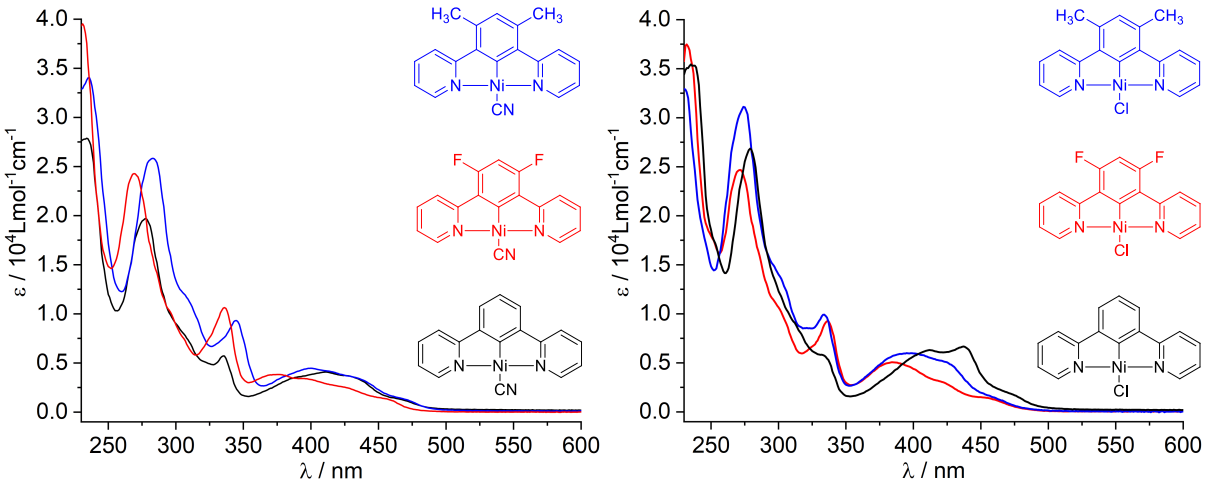

Figure 3-59 *Left*: UV/vis spectra of [Ni(Py(4,6dRPh)Py)CN] (R = H (*black*), Me (*blue*) and F (*red*)). *Right*: UV/vis spectra of [Ni(Py(4,6dRPh)Py)Cl] (R = H (*black*), Me (*blue*) and F (*red*)). All spectra were measured in THF at rt.

According to previously reported C^N^N analogues,[108] the strength of the ligand field was increased with the coligand exchange from chloride to cyanide. This led to an increase of the HOMO-LUMO gap by a stabilization through the ligand field, aligning with the results from cyclic voltammetry. The notable blue-shift of the CT-bands from a [Ni(Py(4,6RPh)Py)Cl] complex to the corresponding cyanido compound is observed for all the synthesized nickel species with constant extinction coefficients (Table 3-37).

The general absorption spectra do not show a significant shift by changing the ligand, which is in line with the chromophoric unit being mainly localized in the di-pyridyl unit of the complex as outlined in by DFT and TD-DFT calculations on the [M(Py)(4,6MePh)Py)Cl] complexes (see Chapter 3.1.2).[140]

Table 3-37 Absorption maxima of [Ni(Py(4,6RPh)Py)CN] in comparison to [Ni(Py(4,6RPh)Py)Cl] (R = H, Me, F).

Complex	Absorption Max. λ_x in nm (Ext. Coeff. ε in 1000 · Lmol^{-1}cm^{-1})							
	λ_8	λ_7	λ_6	λ_5	λ_4	λ_3	λ_2	λ_1
[Ni(Py(Ph)Py)Cl][a]	-	-	463^{sh} (1.8)	437 (6.7)	412 (6.3)	332 (5.7)	279 (26.8)	236 (35.5)
[Ni(Py(4,6MePh)Py)Cl][b]	-	453^{sh} (1.8)	424^{sh} (5.1)	396 (6.0)	334 (9.9)	295^{sh} (15.0)	274 (31.1)	231 (32.8)
[Ni(Py(4,6FPh)Py)Cl]	-	452^{sh} (1.5)	418^{sh} (3.1)	385 (5.2)	336 (9.3)	296^{sh} (11.3)	272 (24.7)	232 (37.5)

[Ni(Py(Ph)Py)CN]	461^{sh} (1.4)	428^{sh} (3.5)	411 (4.1)	390^{sh} (3.6)	336 (5.8)	301^{sh} (9.0)	278 (19.7)	234 (27.9)
[Ni(Py(4,6MePh)Py)CN]	462^{sh} (1.5)	431^{sh} (3.6)	412^{sh} (4.2)	399 (4.4)	345 (9.4)	304^{sh} (12.2)	283 (25.8)	235 (34.0)
[Ni(Py(4,6FPh)Py)CN]	450^{sh} (1.5)	420^{sh} (2.6)	393^{sh} (3.4)	377 (3.7)	336 (10.7)	294^{sh} (10.5)	269 (24.2)	231 (39.5)

Measured in THF at rt. sh = shoulder. a = From ref. [92]. b = From ref. [140]

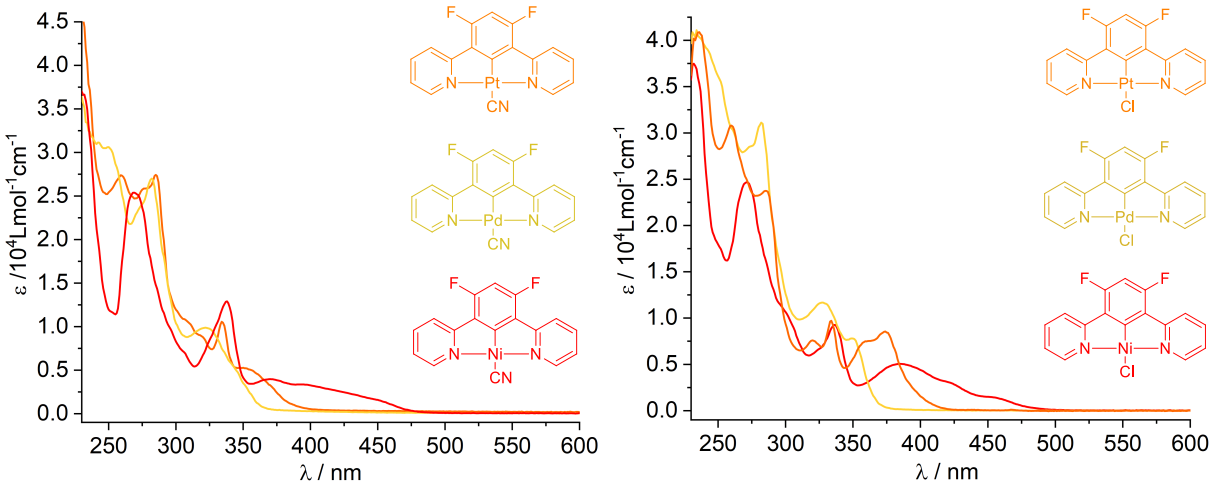

Figure 3-60 *Left*: UV/vis spectra of [M(Py(4,6FPh)Py)CN] (M = Ni (*red*), Pd (*yellow*) and Pt (*orange*)). *Right*: UV/vis spectra of [M(Py(4,6FPh)Py)Cl] (M = Ni (*red*), Pd (*yellow*) and Pt (*orange*)). All spectra were measured in CH_2Cl_2 at rt.

The series of [M(Py(4,6FPh)Py)CN] for M = Ni, Pd and Pt gets exemplary compared to their chlorido precursors (Figure 3-60, trends are the same for 4,6Me-substituted species. For full spectra see Chapter 7.5). The optical HOMO-LUMO gap increases in this case as well by exchanging the chlorido coligand with a cyanide anion and show energetically lowest transitions at 510 nm for Ni, 425 nm for Pt and 380 nm for Pd, the ones from the cyanido species increase in energy to values of 475 nm for Ni, 400 nm for Pt and 365 nm for Pd. Within the d^{10} metal triade, the trend of an increase of the HOMO-LUMO gap from Ni over Pt to Pd is special but not unusual for this metal complex series and already could be observed in all our new measurements and in numerous works in the literature, dealing with the series of similar chloride complexes.[108, 140, 141, 191]

These measurements also correlate with the observed color of these species in solution and as solids: Whereas the Ni(II) species is found as a deep orange solid, the Pt(II) species appears intensively yellow and the Pd(II) is almost colorless (light yellow) and DFT and TD-DFT calculations from former studies.[108, 140, 141, 191]

Table 3-38 Absorption maxima of [M(Py(4,6RPh)Py)CN] in comparison to [M(Py(4,6RPh)Py)Cl] (M = Ni, Pd, Pt. R = H, Me, F).

Complex	Absorption Max. λ_x in nm (Ext. Coeff. ε in 1000 · $Lmol^{-1}cm^{-1}$)							
	λ_8	λ_7	λ_6	λ_5	λ_4	λ_3	λ_2	λ_1
[Ni(Py(Ph)Py)Cl][a]	-	-	463^{sh} (1.8)	437 (6.7)	412 (6.3)	332 (5.7)	279 (26.8)	236 (35.5)
[Ni(Py(4,6MePh)Py)Cl][b]	-	453^{sh} (1.8)	424^{sh} (5.1)	396 (6.0)	334 (9.9)	295^{sh} (15.0)	274 (31.1)	231 (32.8)
[Ni(Py(4,6FPh)Py)Cl]	-	452^{sh} (1.5)	418^{sh} (3.1)	385 (5.2)	336 (9.3)	296^{sh} (11.3)	272 (24.7)	232 (37.5)
[Pd(Py(4,6MePh)Py)Cl][b]	-	-	375 (1.2)	360 (7.4)	327 (8.3)	283 (22.0)	275 (23.2)	239 (26.7)
[Pd(Py(4,6FPh)Py)Cl]	-	-	-	-	350 (7.8)	328 (11.7)	283 (31.1)	234 (40.7)
[Pt(Py(Ph)Py)Cl][c]	402 (4.5)	380 (5.5)	364^{sh} (3.6)	331^{sh} (4.6)	289 (19.1)	280 (18.8)	256 (19.9)	232 (34.4)
[Pt(Py(4,6MePh)Py)Cl][b]	-	-	413 (1.5)	380 (8.3)	331 (9.2)	287 (22.9)	256 (30.0)	231 (33.7)
[Pt(Py(4,6FPh)Py)Cl]	-	374 (8.6)	360 (7.5)	333 (9.7)	320 (7.7)	286 (23.8)	260 (30.8)	236 (40.8)
[Ni(Py(Ph)Py)CN]	-	-	451^{sh} (1.3)	403 (3.6)	334 (5.9)	297^{sh} (11.2)	277 (22.3)	230^{sh} (31.6)
[Ni(Py(4,6MePh)Py)CN]	-	455^{sh} (1.5)	422^{sh} (3.6)	392 (4.5)	345 (10.6)	303^{sh} (13.4)	282 (27.3)	235 (35.6)
[Ni(Py(4,6FPh)Py)CN]	-	-	446^{sh} (1.7)	397 (3.3)	369 (4.0)	338 (13.0)	269 (25.5)	231 (37.2)
[Pd(Py(4,6MePh)Py)CN]	-	-	363^{sh} (3.2)	338 (5.0)	295 (11.5)	285 (12.4)	259 (16.0)	<230 (<18.4)
[Pd(Py(4,6FPh)Py)CN]	-	-	343^{sh} (5.6)	322 (9.8)	282 (27.0)	275^{sh} (24.1)	250 (30.6)	<230 (<36.2)
[Pt(Py(Ph)Py)CN]	374 (3.3)	359 (3.3)	333 (5.3)	317^{sh} (5.7)	289 (13.3)	279 (12.7)	248^{sh} (17.8)	230 (34.0)
[Pt(Py(4,6MePh)Py)CN]	378^{sh} (8.5)	367 (9.0)	342 (16.2)	317 (16.6)	297 (30.6)	283^{sh} (30.6)	266 (40.7)	234 (44.1)
[Pt(Py(4,6FPh)Py)CN]	350^{sh} (5.2)	335 (10.5)	318^{sh} (9.2)	308^{sh} (10.8)	285 (27.5)	278^{sh} (25.9)	259 (27.4)	231^{sh} (45.0)

Measured in CH_2Cl_2 at rt. sh = shoulder. a = From ref. [92]. b = From ref. [140]. c = From ref. [116].

3.3.4 Synthesis and Characterization of [Ni(Py(Ph)Py)OR]

Although nickel alkoxide salts tend to be very unstable compounds. Ni(II) complexes, prepared in this work are air stable and storable as a solid over months. First attempts for the direct

coligand exchange using [Ni(Py(Ph)Py)Cl] and an alkali alkoxide did not work and the precursor complex could be either reisolated or decomposed over time in solution. Also the synthesis of a silver(I) alkoxide and the in situ use of it in a coligand exchange reaction was unsuccessful. A third attempt, synthesizing Ni(O*t*Bu)$_2$ from [Ni(TMEDA)(OAc)$_2$] and KO*t*Bu adapted from *Buslov et al.* from 2016[211] and using it in the base assisted C–H activation for the synthesis of [Ni(Py(Ph)Py)O*t*Bu] directly led to a thermal decomposition of the salt. The idea was born to isolate [Ni(Py(Ph)Py)NO$_3$] from a coligand exchange reaction first, adapted from the coligand exchange reaction for platinum(II) chlorido to cyanido complexes,[108] and use it then for further coligand exchange reactions. This coligand seems to be easily exchangeable by other ligands using the simple organic alkali metal salt. The reaction of AgNO$_3$ with [Ni(Py(Ph)Py)Cl] was carried out in CH_2Cl_2 at rt under exclusion of light with a yield of 81% (Figure 3-61).

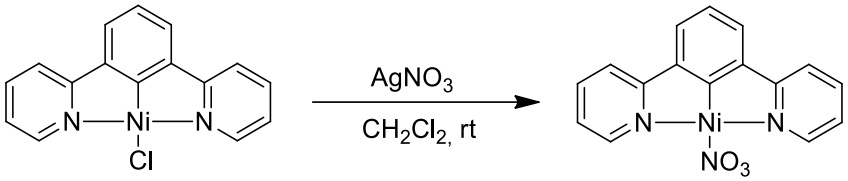

Figure 3-61 Synthesis of [Ni(Py(Ph)Py)NO$_3$] using AgNO$_3$ in CH_2Cl_2.

The new nitrato species was then used to perform further coligand exchange reaction to the corresponding alkoxido species using NaOPh and NaO*t*Bu in an equimolar suspension in dry THF giving two representatives of [Ni(Py(Ph)Py)OR] complexes in moderate to good yields (60% for R = *t*Bu and 68% for R = Ph, Figure 3-62).

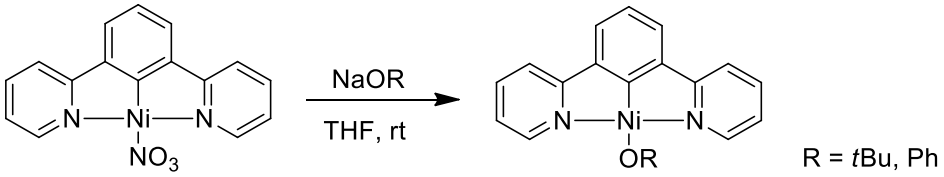

Figure 3-62 Synthesis of [Ni(Py(Ph)Py)OR] with R = *t*Bu and Ph.

The proof of the success for these reactions comes from mass spectrometry, elemental analysis and ^{1}H NMR spectroscopy. For the latter, the *tert.*-butoxido complex shows broad signals, because it was not very stable in solution. The structure of all three complexes could further be verified through SC-XRD analysis. The crystals were obtained by overlaying a concentrated complex solution in THF with *n*-pentane (Figure 3-63).

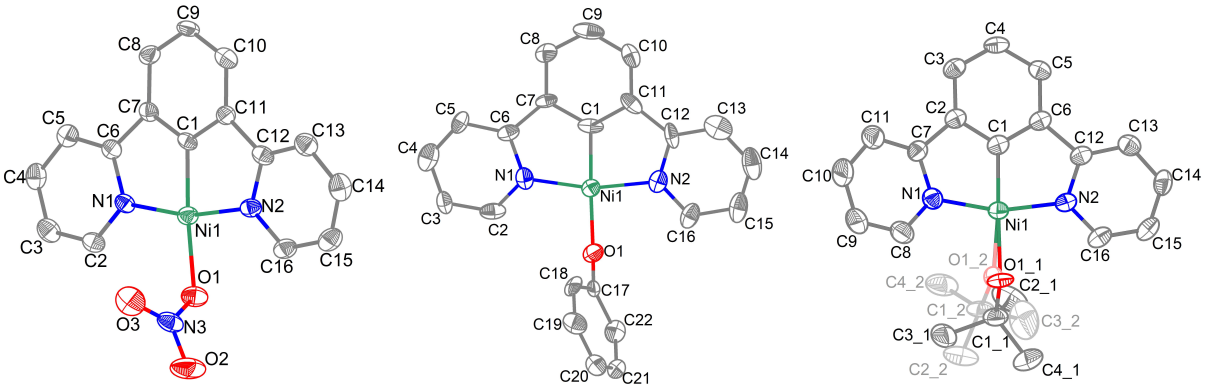

Figure 3-63 Molecular structures of [Ni(Py(Ph)Py)NO_3] (*left*), [Ni(Py(Ph)Py)OPh] (*middle*) and [Ni(Py(Ph)Py)O*t*Bu] (*right*). Ellipsoids are shown with a 50% probability. Hydrogen atoms are omitted for clarity.

[Ni(Py(Ph)Py)NO_3] crystallizes in the monoclinic space group $P2_1/c$ with four units per unit cell. The asymmetric unit is described by one single complex molecule. [Ni(Py(Ph)Py)OPh] crystallized in the triclinic space group $P\bar{1}$ bearing four units per unit cell, with an asymmetric unit containing two independent complex molecules. [Ni(Py(Ph)Py)O*t*Bu] crystallized in the monoclinic space group $P2_1/c$ with four units per unit cell, with a cocrystallized solvent, which could not be identified due to a poor quality of data and therefore was squeezed. The *tert*.-butyl function of the coligand is disordered in two directions (Table 3-39).

Table 3-39 Crystallographic data of [Ni(Py(Ph)Py)NO_3], [Ni(Py(Ph)Py)OPh] and [Ni(Py(Ph)Py)O^{t}Bu].

Identification code	**[Ni(Py(Ph)Py)NO_3]**	**[Ni(Py(Ph)Py)OPh]**	**[Ni(Py(Ph)Py)O^{t}Bu]**
Empirical formula	$C_{16}H_{11}N_3NiO_3$	$C_{22}H_{16}N_2NiO$	$C_{20}H_{20}N_2NiO$
Temperature/K	150.0	150.0	150(2)
Crystal system	monoclinic	triclinic	monoclinic
Space group	$P2_1/c$	$P\bar{1}$	$P2_1/c$
a/Å	9.4575(9)	11.7795(10)	14.9647(10)
b/Å	7.0258(7)	11.7960(11)	11.7733(8)
c/Å	20.911(2)	13.9308(12)	12.0344(8)
α/°	90	97.886(3)	90
β/°	99.352(3)	105.937(3)	107.280(2)
γ/°	90	110.959(3)	90
Volume/Å^3	1371.0(2)	1677.3(3)	2024.6(2)
Z	4	4	4
ρ_{calc}g/cm^3	1.705	1.517	1.191
F(000)	720.0	792.0	760.0
Radiation	MoKα (λ = 0.71073)	MoKα (λ = 0.71073)	MoKα (λ = 0.71073)
2Θ range for data collection/°	6.346 to 49.37	5.564 to 41.068	5.164 to 50.71
Index ranges	–8 ≤ h ≤ 9, –8 ≤ k ≤ 8, –16 ≤ l ≤ 24	–11 ≤ h ≤ 11, –11 ≤ k ≤ 11, –13 ≤ l ≤ 13	–18 ≤ h ≤ 18, –14 ≤ k ≤ 14, –14 ≤ l ≤ 14
Reflections collected	4426	16069	24164

Independent reflections	1995 [R_{int} = 0.0370, R_{sigma} = 0.0559]	3362 [R_{int} = 0.1002, R_{sigma} = 0.0964]	3702 [R_{int} = 0.0868, R_{sigma} = 0.0723]
Data/restraints/parameters	1995/0/208	3362/0/469	3702/154/263
Goodness-of-fit on F^2	1.001	1.095	1.122
Final R indexes [I>=2σ (I)]	R_1 = 0.0393, wR_2 = 0.0821	R_1 = 0.0574, wR_2 = 0.1237	R_1 = 0.0763, wR_2 = 0.1249
Final R indexes [all data]	R_1 = 0.0622, wR_2 = 0.0905	R_1 = 0.1003, wR_2 = 0.1365	R_1 = 0.1023, wR_2 = 0.1351
Largest diff. peak/hole / eÅ^{-3}	0.46/–0.38	0.57/–0.36	0.45/–0.35
CCDC	2343421	2343424	2343429

All three crystals show the expected square planar coordination around the nickel center with a sum of all angles of values very close to 360°. The nickel centers show a slightly stronger bond to C1 in comparison to the standard complex with Ni–C1 distances of 1.80 Å for the nitrato- and 1.81 Å for both alkoxido complexes.[92] The Ni–N1/N2 distances do not change and stay constantly at 1.90 to 1.93 Å. Also the bond to the nitrato and alkoxido coligands gets shorter with values of 1.98 Å for the nitrato complex and values around 1.90 Å for the alkoxido compounds. Compared with the previously reported complex [Ni(PyPhPy)Cl], the C_1–Ni–O1 angles, especially for the nitrato derivative, are markedly deviating from the ideal 180°.[92] Further, the typical chelate bite-angles of around 82° and N_1–Ni–N_2 angles of around 163° were found.[89, 91, 92, 99, 100, 104, 108, 116, 117, 122, 123, 127, 140-147] Interestingly, N1–Ni–O1 and N2–Ni–O1 are differing notably for these three new structures, indicating that the coligand is orientated towards one side of the C_2 axis through the centre of the molecule. This can be explained by the increased steric demand of these new coligands, that need to orientate into one specific direction for crystal packing.

Further the orientation of the coligands themselves in relation to the planar molecule is noteworthy. The nitrate and the phenoxy ligand, as planar multiatomic units are perpendicularly orientated to the N^C^N ligand plane with an Ni–O1–C/N3 angle of 113.6° for the nitrato and 120.2° for the phenoxido compound. The *tert*.-butyl unit ligand stands out of the plane as well in an angle of 127.4°.

Table 3-40 Angles and bond lengths of [Ni(Py(Ph)Py)NO_3], [Ni(Py(Ph)Py)OPh] (*molecule 1*) and [Ni(Py(Ph)Py)O*t*Bu] in comparison to the standard chlorido complex.

	[Ni(Py(Ph)Py)Cl]^a	**[Ni(Py(Ph)Py)NO_3]**	**[Ni(Py(Ph)Py)OPh]**	**[Ni(Py(Ph)Py)O^{t}Bu]**
Distances / Å				
Ni–C1	1.836(7)	1.812(4)	1.798(9)	1.807(5)
Ni–N1	1.932(6)	1.919(3)	1.896(7)	1.924(4)
Ni–N2	1.936(5)	1.918(3)	1.929(7)	1.916(4)
Ni–Cl1/O1	2.247(2)	1.975(3)	1.904(6)	1.934(18)

Angles / °				
C1–Ni–N1	81.6(3)	82.68(15)	83.8(4)	81.8(2)
C1–Ni–N2	82.3(3)	82.72(15)	82.2(4)	82.21(19)
N1–Ni–Cl1/O1	98.23(2)	100.67(13)	97.7(3)	99.0(7)
N2–Ni–Cl1/O1	97.90(2)	93.91(12)	96.4(3)	96.7(7)
Sum / °	359.9	360.0	360.1	359.7
C1–Ni–Cl1/O1	179.7(2)	175.57(14)	177.1(3)	177.4(5)
N1–Ni–N2	163.9(2)	165.39(14)	166.0(4)	162.64(17)

a = From ref. [92].

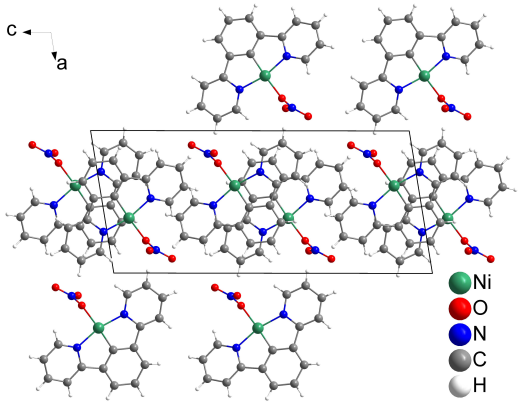

Figure 3-64 Crystal structure of [Ni(Py(Ph)Py)NO_3] viewed along the crystallographic *b*-axis.

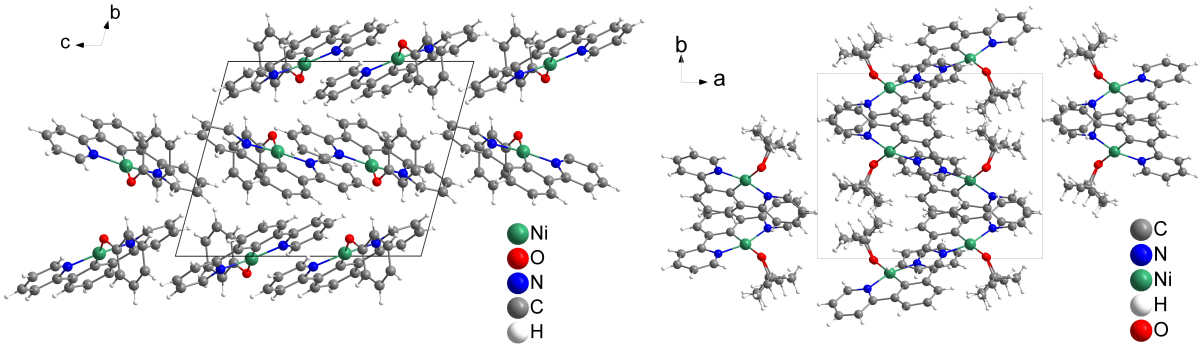

Figure 3-65 Crystal structure of [Ni(Py(Ph)Py)OPh] viewed along the crystallographic *a*-axis (*left*) and [Ni(Py(Ph)Py)O*t*Bu] viewed along the crystallographic *c*-axis (*right*).

All structures show the standard head-to-tail arrangement, that already was described for many structures of the type [Ni(N^C^N)X/R] (Figure 3-64 and 3-65). [92, 99, 140, 148] The angle and distance of the packing is depending on the sterics and the orientation of the coligand. This determines the intermolecular distance of two neighboring and almost coplanar PyPh units. The distance of two neighboring PyPh units of the nitrato complex is 3.86 Å, 3.66 Å for the phenoxido- and 3.77 Å for the *tert*.-butoxido derivative, which are at the border of *Janiak's*

definition of a weak π-interaction and slightly bigger than the same distance in the structure of the chlorido precursor.[149] The reason for the close packing of the phenoxido complex is the orientation of the phenoxide coligands, that are completely turned away from the complex molecule and allow the closest possible packing of two complex molecules, which is not applicable on the *tert*.-butoxido complex with a non-planar coligand and its larger steric demand. (Figure 3-65, for further pictures, see Chapter 7.3.25 to 6.3.27).

Cyclic voltammetry shows oxidations starting at potentials of slightly above 0 V vs. ferrocene/ferrocenium. Reductions were measured in a range of –2.3 V to –3.0 V (Figure 3-66 and Figure 3-67).

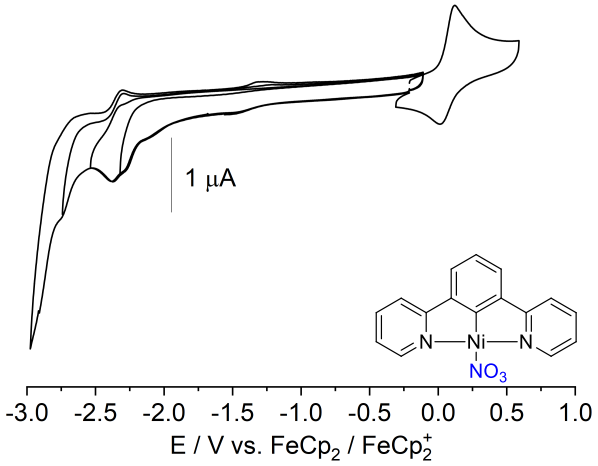

Figure 3-66 Cyclic voltammograms of [Ni(Py(Ph)Py)NO_3], measured in a 0.1M nBu$_4$PF_6 solution in THF at rt with a scan rate of 100 mV/s.

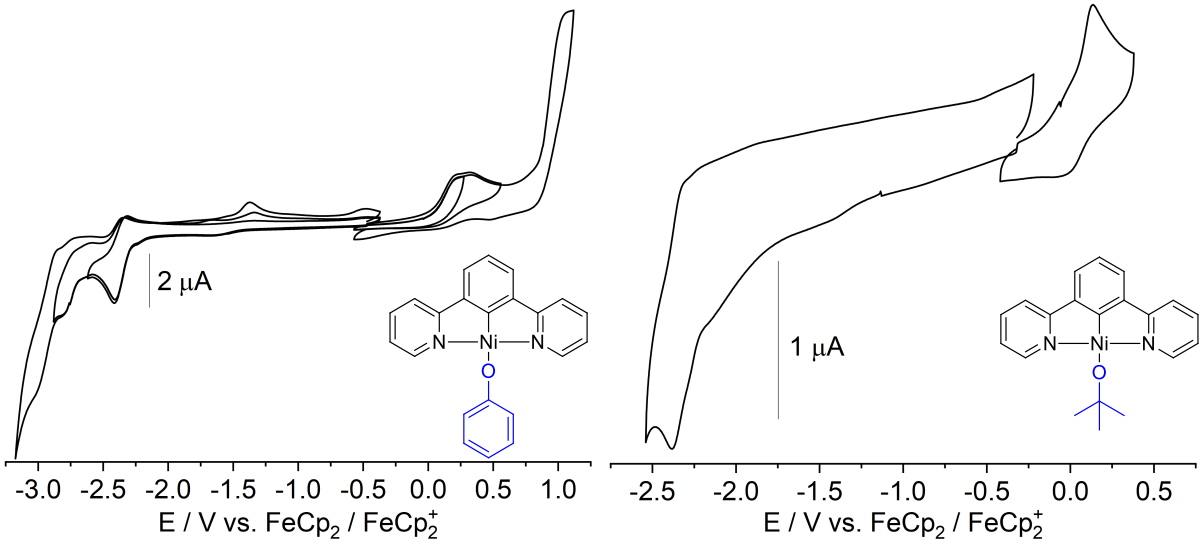

Figure 3-67 Cyclic voltammograms of [Ni(Py(Ph)Py)OPh] (*left*) and [Ni(Py(Ph)Py)O*t*Bu] (*right*), measured in a 0.1M nBu$_4$PF_6 solution in THF at rt with a scan rate of 100 mV/s.

The first oxidation of the nitrato and the phenoxido complex are anodically shifted to potentials of 0.33 V ($E_{1/2}$) and 0.20 V (E_{pa}), whereas the *tert*.-butoxido complex shows the same half-step potential in comparison to the chloride standard complex. These can again be assigned to the Ni(II)/Ni(III) redox pair.[92] The phenoxido complex shows two more oxidations, that assumingly result from the oxidation of the phenolate. The first reductions appear at similar potentials compared to the standard complex (NO_3: –2.29 V (E_{pa}), OPh: –2.38 V ($E_{1/2}$), O*t*Bu: –2.36 V (E_{pa})), indicating that the LUMO energy level does not get changed for these species. This fits to previous results, showing that the LUMO is ligand centered on both pyridyl functions for [Ni(Py(Ph)Py)X] complexes.[92, 140] Due to the bulkiness of a phenolate anion and a therefore suppressed diffusion, its first reduction gets reversible, whereas the other species probably undergo a mechanism, that is similar to the EC mechanism.[89, 91, 92, 99, 142] The electrochemically determined HOMO-LUMO gap of the nitrato complex is 2.62 eV (Cl: 2.39 eV), the alkoxido complexes show values of 2.58 eV (OPh) and 2.41 eV (O*t*Bu). Noteworthy is the low stability of the *tert*.-butoxido complex in solution. The potentials therefore need to be considered carefully (Table 3-41).

Table 3-41 Redox potentials of [Ni(Py(Ph)Py)NO_3] and [Ni(Py(Ph)Py)OR] (R = Ph, *t*Bu) in comparison to [Ni(Py(Ph)Py)Cl].

	***E* Ox3**	***E* Ox2**	***E* Ox1**	***E* Red1**	***E* Red2**	***E* Red3**	***E* Red4**	**ΔE HOMO-LUMO**
[Ni(Py(Ph)Py)Cl][a]	-	-	0.06 ($E_{1/2}$)	–2.33 (E_{pc})	–2.57 (E_{pc})	–2.69 (E_{pc})	-	2.39 eV
[Ni(Py(Ph)Py)NO_3]	-	-	0.33 ($E_{1/2}$)	–2.29 (E_{pc})	–2.38 (E_{pc})	–2.75 (E_{pc})	–2.95 (E_{pc})	2.62 eV
[Ni(Py(Ph)Py)OPh]	1.08 (E_{pa})	0.33 (E_{pa})	0.20 (E_{pa})	–2.38 ($E_{1/2}$)	–2.83 (E_{pc})	–3.07 (E_{pc})	-	2.58 eV
[Ni(Py(Ph)Py)O*t*Bu]	-	-	0.06 ($E_{1/2}$)	–2.36 (E_{pc})	-	-	-	2.41 eV

Measured in a 0.1M nBu$_4$PF$_6$ solution in THF at rt with a scan rate of 100 mV/s. All potentials in V. E_{pc} = Cathodic Peak Potential, E_{pa} = Anodic Peak Potential, $E_{1/2}$ = Half-Step Potential. a = From ref. [92].

UV/vis absorption spectroscopy was performed in THF (Figure 3-68) showing intense absorption bands from 230 to 300 nm, assigned to π–π* transitions followed by bands with a lower extinction coefficient in a range up to 550 nm, that are responsible for the orange to red color of these species, as already reported for the halido precursors.[92]

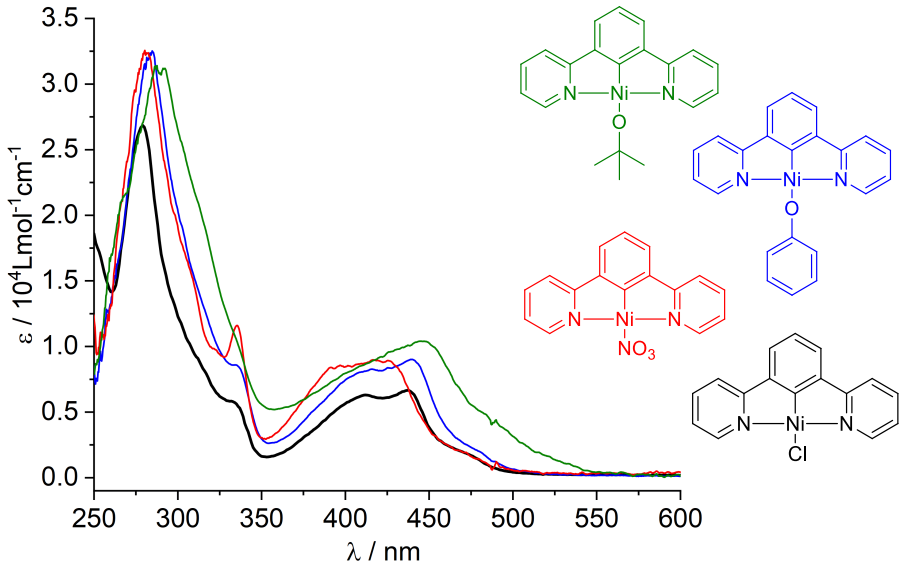

Figure 3-68 UV/vis spectra of [Ni(Py(Ph)Py)Cl] (*black*), [Ni(Py(Ph)Py)NO_3] (*red*), [Ni(Py(Ph)Py)OPh] (*blue*) and [Ni(Py(Ph)Py)O*t*Bu] (*green*). All spectra were measured in THF at rt.

The overall shapes of the absorption spectra are very similar to the standard chlorido complex, especially for the π–π* transitions at around 280 nm, that only are slightly redshifted. Whereas the nitrato complex (red) shows a blueshift of the absorption bands, both alkoxido complex show the opposite effect (green and blue). Especially the *tert*.-butoxido derivative shows a hash shift of the CT band absorption maxima into lower energies up to a shoulder maximum at 487 nm. Calculations for related compounds showed, that the HOMO energy level is partially located at the coligand,[92, 140] which underpins the main shifts in the area of CT bands. Theoretical studies could elucidate these results. Because these measurements were performed at a different UV/vis spectrometer, the UV cut-off was at 250 nm, which led to a lack of data for λ_1 (Table 3-42).

Table 3-42 Absorption maxima of [Ni(Py(Ph)Py)NO_3] and [Ni(Py(Ph)Py)OR] (R = Ph, *t*Bu) in comparison to [Ni(Py(Ph)Py)Cl].

Complex	Absorption Max. λ_x in nm (Ext. Coeff. ε in 1000 · $Lmol^{-1}cm^{-1}$)					
	λ_6	λ_5	λ_4	λ_3	λ_2	λ_1
[Ni(Py(Ph)Py)Cl][a]	463[sh] (1.8)	437 (6.7)	412 (6.3)	332 (5.7)	279 (26.8)	236 (35.5)
[Ni(Py(Ph)Py)NO_3]	462[sh] (2.5)	420 (8.9)	397 (8.6)	335 (11.7)	281 (32.3)	-
[Ni(Py(Ph)Py)OPh]	472[sh] (2.7)	440 (9.1)	415 (8.3)	334 (8.6)	285 (32.4)	-
[Ni(Py(Ph)Py)O*t*Bu]	487[sh] (4.5)	446 (10.4)	410[sh] (8.6)	331[sh] (11.9)	289 (31.4)	-

Measured in THF at rt. sh = shoulder. a = From ref. [92].

3.3.5 Synthesis and Characterization of [Ni(Py(Ph)Py)R_F] with R_F = C_2F_5, C_3F_7 and C_6F_5

The coligand exchange reaction for the introduction of perfluoroalkylide or -arylide coligands was performed by a different route, since perfluorinated their anions are not thermally stable. This route was adapted from famous route of *Vicic et al.* from 2013, that was firstly used for the synthesis of $[Ni(MeCN)_2(CF_3)_2]$[212] and then further investigated giving related catalytically active Ni(II) compounds.[213-215] By using the respective perfluoroalkyl or -aryl trimethylsilane (TMS-R_F) and silver(I) fluoride in MeCN, the Ag-R_F salt was successfully be prepared and in situ used with the chlorido standard complex, to perform the desired coligand exchange reaction (Figure 3-69). The reaction was performed successfully for C_2F_5, C_3F_7 and C_6F_5 as coligands with yields of 90%, 99% and 40%.

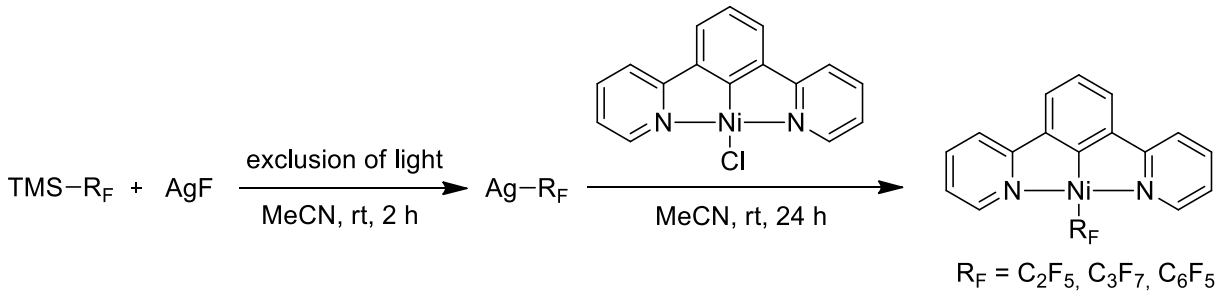

Figure 3-69 Synthesis of [Ni(Py(Ph)Py)R_F] *via* coligand exchange reaction using silver(I) salts.[212-215]

The success of this reaction and pureness of all products was proved by mass spectrometry, elemental analysis and ^{1}H and ^{19}F NMR spectroscopy (Figure 3-70 and for full measurements, see chapter 5.4.3). Again, the chemical shift of the ortho-*N* proton was significantly changing and therefore indicating a full conversion to the desired product.

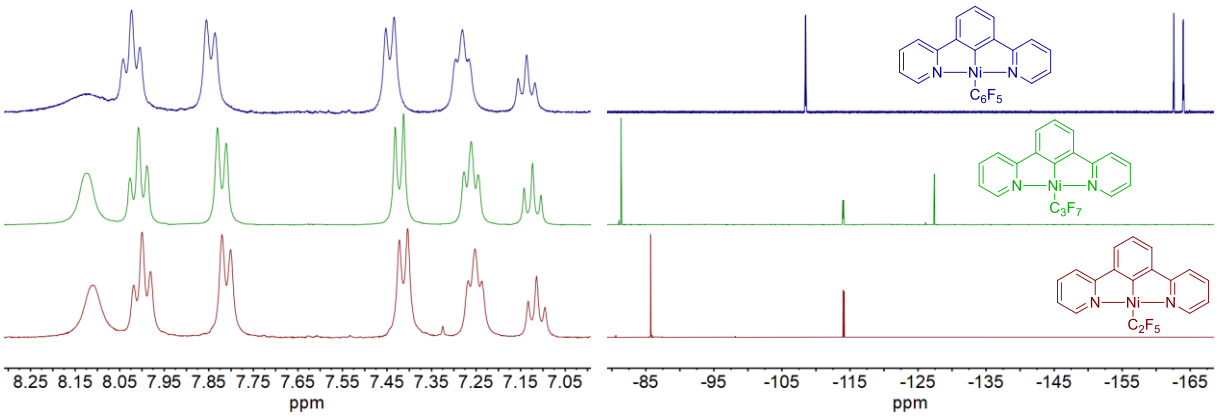

Figure 3-70 400 MHz ^{1}H NMR (*left, reference on the solvent*) and ^{19}F NMR (*right, referenced to TFT*) of [Ni(Py(Ph)Py)R_F] measured in DMSO-d_6. Blue: R_F = C_6F_5. Green: R_F = C_3F_7. Red: R_F = C_2F_5.

The signals from the ^{1}H NMR spectra integrate to a sum of eleven protons, which fits to all of the postulated structures. The ortho-*N* signal shifts from 8.7 ppm down to 8.1 ppm and fuses with the signal para-*N* proton signal of the pyridyl function. The other signals do not shift significantly in relation to the chlorido standard complex. ^{19}F NMR spectroscopy supports the existence of these species by the correct number and integrals of the signals in a range of –80 to –170 ppm, referenced to α,α,α-trifluoro toluene (TFT).

[Ni(Py(Ph)Py)C_2F_5] could be crystallized *via* isothermal evaporation from a THF solution and solved in the monoclinic space group *P*2$_1$/c bearing four units per unit cell (Figure 3-71, Table 3-43).

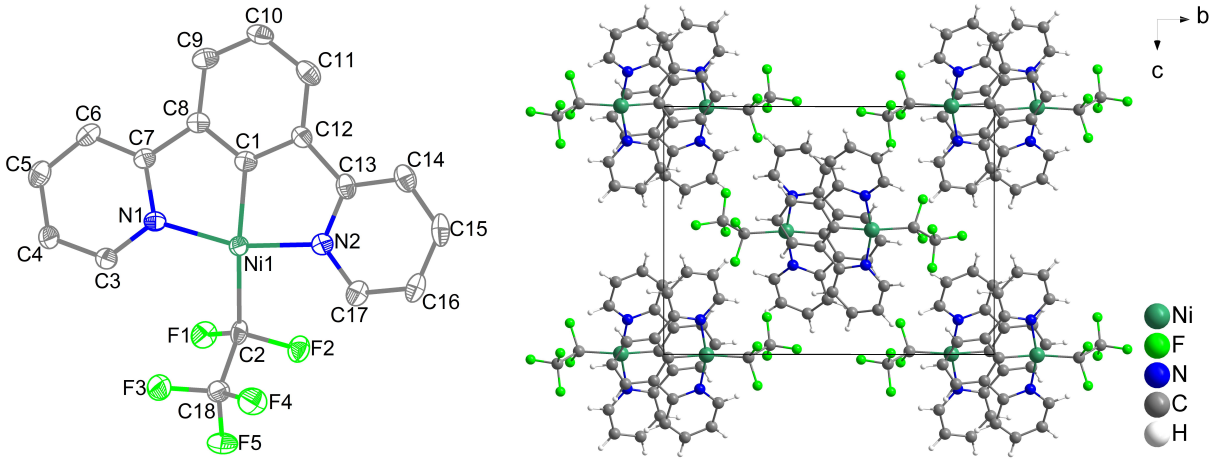

Figure 3-71 *Left:* Asymmetric unit of [Ni(Py(Ph)Py)C_2F_5]. Hydrogen atoms are omitted for clarity. Ellipsoids are shown with a 50% probability. *Right:* Crystal structure of [Ni(Py(Ph)Py)C_2F_5] viewed along the crystallographic *a*-axis.

Table 3-43 Crystallographic data for [Ni(Py(Ph)Py)C_2F_5].

Identification code	**[Ni(Py(Ph)Py)C_2F_5]**
Empirical formula	$C_{18}H_{11}F_5N_2Ni$
Temperature/K	150.0
Crystal system	monoclinic
Space group	*P*2$_1$/c
a/Å	8.1443(5)
b/Å	15.7664(10)
c/Å	12.3871(8)
β/°	107.846(2)
Volume/Å^3	1514.05(17)
Z	4
ρ_{calc}g/cm^3	1.794
F(000)	824.0
Radiation	MoKα (λ = 0.71073)
2Θ range for data collection/°	5.168 to 55.15

Index ranges	–10 ≤ h ≤ 10, –20 ≤ k ≤ 20, –16 ≤ l ≤ 16
Reflections collected	22760
Independent reflections	3493 [R_{int} = 0.0709, R_{sigma} = 0.0651]
Data/restraints/parameters	3493/0/235
Goodness-of-fit on F^2	1.030
Final R indexes [I>=2σ (I)]	R_1 = 0.0434, wR_2 = 0.0796
Final R indexes [all data]	R_1 = 0.0852, wR_2 = 0.0919
Largest diff. peak/hole / eÅ^{-3}	0.47/–0.35
CCDC	2343419

Figure 3-71 (*left*), shows the molecular structure of [Ni(Py(Ph)Py)C_2F_5] a square planar Ni(II) complex. Except of the bond to the coligand, which is at 2.01 Å, all bond lengths and angles around Ni1 are very similar to the ones previously reported for Ni(II) complexes of the tridentate ligands PyPhPy.[92] Again, the N1–Ni–N2 bond of 162° and the chelate bite-angle of 81° fit to the reported structure of related structures.[89, 91, 92, 99, 100, 104, 108, 116, 117, 122, 123, 127, 140-147] Noteworthy is the C1–Ni–C2 angle at 165°, that is way smaller than the one from the standard complex at 180°.[92] Whereas C18 is lying in the plane of the N^C^N ligand, and C2 is out of the plane. Whereas the bond length from the nickel center to C1, N1 and N2 do not significantly change, the one to the coligand does and decreases to a value of 2.01 Å. The crystal packing, (Figure 3-71*, right*) shows the classic head-to-tail arrangement along the crystallographic *a*-axis.[92, 99, 140, 148] The intermolecular distance of two PyPh units shows a constant value of 3.69 Å, which is slightly smaller than the estimated value for the chlorido precursor and is within the definition of *Janiak*, classified as a weak π-interaction.[149]

Table 3-44 Angles and bond lengths of [Ni(Py(Ph)Py)C_2F_5] in comparison to the standard chlorido complex.

	[Ni(Py(Ph)Py)Cl][a]	**[Ni(Py(Ph)Py)C_2F_5]**
Distances / Å		
Ni–C1	1.836(7)	1.847(3)
Ni–N1	1.932(6)	1.952(2)
Ni–N2	1.936(5)	1.951(2)
Ni–Cl1/C2	2.247(2)	2.014(3)
Angles / °		
C1–Ni–N1	81.6(3)	81.12(11)
C1–Ni–N2	82.3(3)	81.30(11)
N1–Ni–Cl1/C2	98.23(2)	98.84(11)
N2–Ni–Cl1/C2	97.90(2)	99.47(11)
Sum / °	359.9	360.7
C1–Ni–Cl1/C2	179.7(2)	164.92(11)
N1–Ni–N2	163.9(2)	161.68(10)

a = From ref. [92].

Further, cyclic voltammetry was performed, shown in Figure 3-72. The measurement for [Ni(Py(Ph)Py)C_2F_5] is attached in Chapter 7.4. All complexes show oxidations starting at 0 V and first reductions in a range of –2.3 V to –3.1 V referenced to ferrocene/ferrocenium. All redox processes are mostly irreversible. The first reduction is therefore assumingly explained by an EC mechanism.[89, 91, 92, 99, 142] The first oxidations of [Ni(Py(Ph)Py)R_F] complexes appear at potentials of 0.25 V for the C_2F_5, 0.22 V for the C_3F_7 and 0.01 V for the C_6F_5 complex and can be assigned to the Ni(II)/Ni(III) oxidation, due to reported investigations for [Ni(Py(Ph)Py)X].[92] The pentafluorophenide complex also shows a second oxidation at 0.25 V.

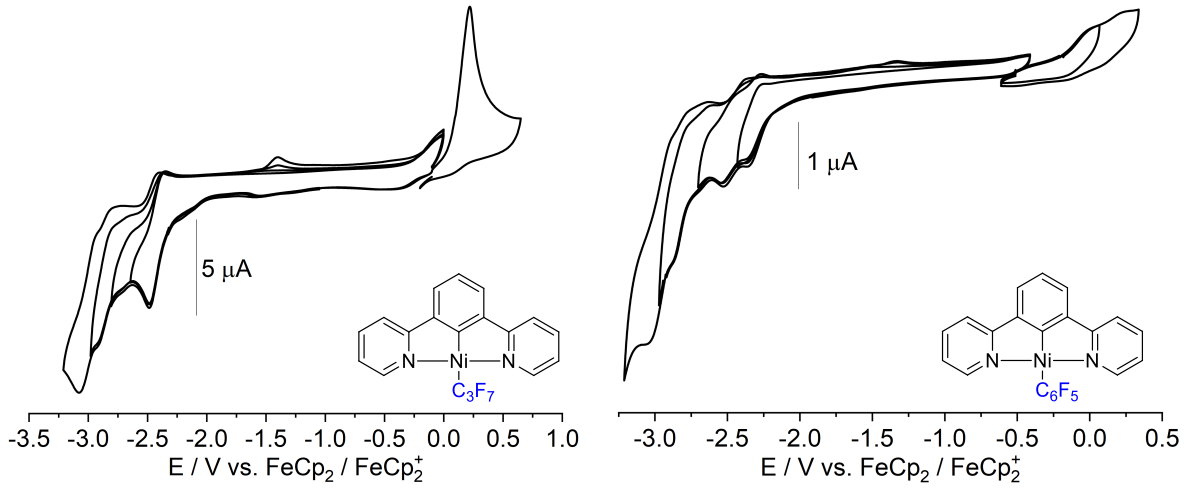

Figure 3-72 Cyclic voltammograms of [Ni(Py(Ph)Py)C_3F_7] (*left*) and [Ni(Py(Ph)Py)C_6F_5] (*right*), measured in a 0.1M *n*Bu_4PF_6 solution in THF at rt with a scan rate of 100 mV/s.

Not only the oxidation of this derivative differs from the perfluoroalkylide compounds, but also the first reduction appears already –2.3 V, which is more similar to the standard chloride complex (Red1: –2.38 V) than to the perfluoroalkylide derivatives (Red1, C_2F_5: –2.41 V; Red1 C_3F_7: –2.42 V). This affects the HOMO-LUMO gap and shows a significantly lower one for the pentafluorophenide complex of 2.31 eV, compared to the other species (C_2F_5: 2.66 eV and C_3F_7: 2.64 eV, see Table 3-45). This is also observed in UV/vis spectroscopy (see below).

Table 3-45 Redox potentials of [Ni(Py(Ph)Py)C_2F_5], [Ni(Py(Ph)Py)C_3F_7] and [Ni(Py(Ph)Py)C_6F_5] in comparison to [Ni(Py(Ph)Py)Cl].

	***E* Ox1**	***E* Red1**	***E* Red2**	***E* Red3**	***E* Red4**	**Δ*E*$_{HOMO-LUMO}$**
[Ni(Py(Ph)Py)Cl][a]	0.06 ($E_{1/2}$)	–2.33 (E_{pc})	–2.57 (E_{pc})	–2.69 (E_{pc})	-	2.39 eV
[Ni(Py(Ph)Py)C_2F_5]	0.25 (E_{pa})	–2.41 ($E_{1/2}$)	–3.03 (E_{pc})	-	-	2.66 eV
[Ni(Py(Ph)Py)C_3F_7]	0.22 (E_{pa})	–2.42 ($E_{1/2}$)	–2.76 (E_{pc})	–2.93 (E_{pc})	–3.08 (E_{pc})	2.64 eV
[Ni(Py(Ph)Py)C_6F_5][b]	0.01 (E_{pa})	–2.30 (E_{pc})	–2.53 (E_{pc})	–2.90 (E_{pc})	–3.06 (E_{pc})	2.31 eV

Measured in a 0.1M *n*Bu_4PF_6 solution in THF at rt with a scan rate of 100 mV/s. All potentials in V. E_{pc} = Cathodic Peak Potential, E_{pa} = Anodic Peak Potential, $E_{1/2}$ = Half-Step Potential. a = From ref. [92]. b = Ox2 at 0.25 V (E_{pa}).

UV/vis absorption spectra of all three synthesized perfluoroalkylide and -arylide complexes show absorption bands at similar energies as the standard chloride complex, namely intense absorption bands at 230 to 320 nm, assigned to ligand centered π–π*. These are followed by energetically lower bands up to 550 nm, assigned to CT bands from the metal and responsible for the orange to red color of these species (Figure 3-73).[92]

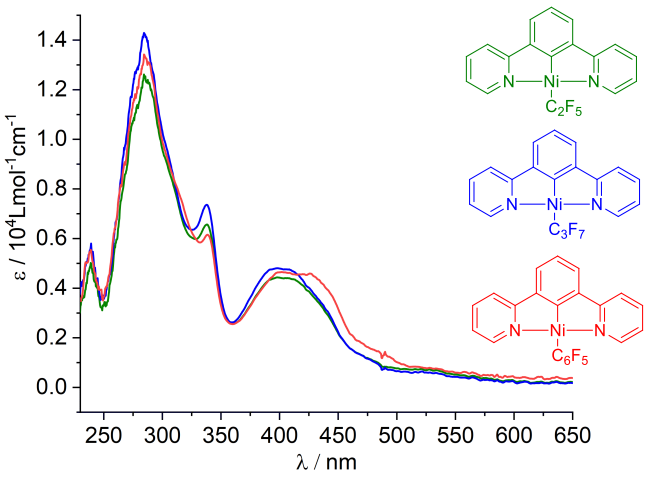

Figure 3-73 UV/vis absorption spectra of perfluoroalkylide and -arylide complexes [Ni(Py(Ph)Py)R_F] (R_F = C_2F_5, C_3F_7, C_6F_5), measured in THF at rt.

Especially the π-π* transitions in the area up to 320 nm are lower in the extinction coefficient with one lower absorption maximum at 239 nm and one more intensive band at 284 nm. The first CT band at a wavelength of 338 nm is constant for all three species. However, the ones in the range of 360 to 550 nm are differing with the coligand by shifting bathochromically from the C_2F_5 over the C_3F_7 to the C_6F_5 species (Table 3-46). The latter shows the biggest shift in comparison to the other spectra, which can be explained by the aromatic character of this one, which results in a smaller HOMO-LUMO gap, especially for this species, aligning with the results from electrochemical measurements. DFT and TD-DFT measurements for [Ni(Py(Ph)Py)X] show the coligand being partially located at the coligand, which supports these shifts,[92, 108] but should be performed for these derivatives specifically in the future.

Table 3-46 Absorption maxima of [Ni(Py(Ph)Py)C_2F_5], [Ni(Py(Ph)Py)C_3F_7] and [Ni(Py(Ph)Py)C_6F_5] in comparison to [Ni(Py(Ph)Py)Cl].

Complex	Absorption Max. λ_x in nm (Ext. Coeff. ε in 1000 · Lmol^{-1}cm^{-1})					
	λ_6	λ_5	λ_4	λ_3	λ_2	λ_1
[Ni(Py(Ph)Py)Cl][a]	463^{sh} (1.8)	437 (6.7)	412 (6.3)	332 (5.7)	279 (26.8)	236 (35.5)
[Ni(Py(Ph)Py)C_2F_5]	464^{sh} (1.6)	412 (4.4)	399 (4.4)	338 (6.6)	285 (12.5)	239 (5.0)

[Ni(Py(Ph)Py)C_3F_7]	466^{sh} (1.5)	409 (4.7)	395 (4.8)	338 (7.4)	284 (14.3)	239 (5.8)
[Ni(Py(Ph)Py)C_6F_5]	472^{sh} (1.8)	426 (4.6)	402 (4.7)	338 (6.2)	285 (13.4)	238 (5.6)

Measured in THF at rt. sh = shoulder. a = From ref. [92].

3.3.6 Synthesis and Characterization of [Ni(Py(Ph)Py)NCS]

The use of thermally stable carbon containing nickel(II) salts in a base-assisted C–H activation reaction led to a second successful route towards [Ni(N^C^N)R] complexes. By adapting *Klein's* base-assisted C–H activation reaction with anhydrous $Ni(SCN)_2$, a 1:1 ratio of KOAc and K_2CO_3 and the ligand in *p*-xylene gave the desired compound in an isolated yield of 26% (Figure 3-74).[92]

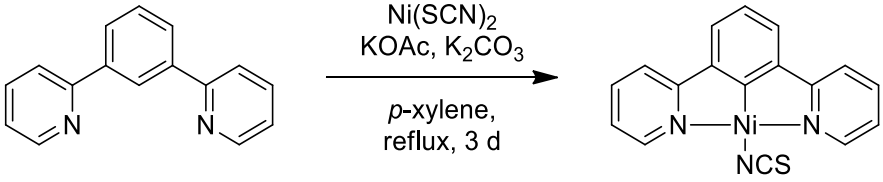

Figure 3-74 Reaction scheme towards [Ni(Py(Ph)Py)NCS] *via* base assisted C–H activation reaction.[92]

The success of this reaction could be verified by ^{1}H NMR spectroscopy, EI(+) mass spectrometry and elemental analysis (full data in the Experimental Section 5.4.3). This ambidentate coligand is only N-bound to the Ni(II) center, proven by ^{1}H NMR spectroscopy, which only shows one species and SC-XRD measurements. Figure 3-75 shows the asymmetric unit, as well as a picture of the crystal structure along the crystallographic face diagonal between the *a*- and *b*-axis.

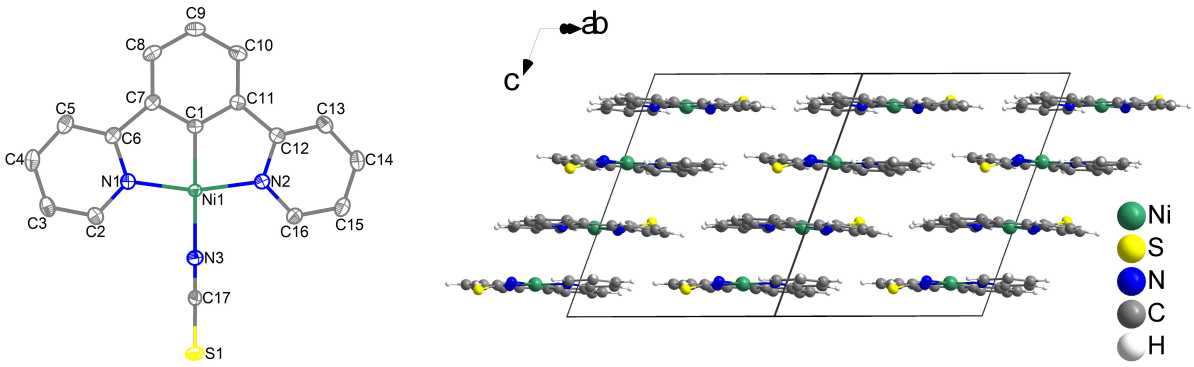

Figure 3-75 *Left:* Asymmetric unit of [Ni(Py(Ph)Py)NCS]. Hydrogen atoms are omitted for clarity. Ellipsoids are shown with a 50% probability. *Right*: Crystal structure of [Ni(Py(Ph)Py)NCS] viewed along the crystallographic face diagonal between the *a*- and *b*-axis.

Taking the HSAB principle into account,[12, 13] this outcome was expectable, due to the hard character of a Ni(II) ion should building a stronger bond to the harder nitrogen atom. The crystal structure of [Ni(Py(Ph)Py)NCS] crystallizes in the monoclinic space group *C*2/c with eight units per unit cell (Table 3-47).

Table 3-47 Crystallographic data for [Ni(Py(Ph)Py)NCS].

Identification code	**[Ni(Py(Ph)Py)NCS]**
Empirical formula	$C_{17}H_{11}N_3NiS$
Temperature/K	100.00
Crystal system	monoclinic
Space group	*C*2/c
a/Å	16.9632(7)
b/Å	13.5861(6)
c/Å	14.3464(5)
β/°	120.2810(1)
Volume/Å^3	2855.2(2)
Z	8
ρ_{calc}g/cm^3	1.619
F(000)	1424.0
Radiation	MoKα (λ = 0.71073)
2Θ range for data collection/°	4.088 to 56.606
Index ranges	–22 ≤ h ≤ 22, –18 ≤ k ≤ 18, –19 ≤ l ≤ 16
Reflections collected	27709
Independent reflections	3506 [R_{int} = 0.0385, R_{sigma} = 0.0210]
Data/restraints/parameters	3506/0/199
Goodness-of-fit on F^2	1.056
Final R indexes [I>=2σ (I)]	R_1 = 0.0239, wR_2 = 0.0631
Final R indexes [all data]	R_1 = 0.0269, wR_2 = 0.0648
Largest diff. peak/hole / eÅ^{-3}	0.35/–0.29
CCDC	2343418

Its structure does not vary significantly from the standard complex.[92] The bond length to the central carbon atom from the tridentate N^C^N ligand is slightly shorter than the one from the standard halido complex (Ni–C1 = 1.82 Å) , as well as the one to the coligand Ni–N3 (1.91 Å). The sum of all angles around the nickel atom of exactly 360.0° verifies the general square planar geometry around the nickel centre with bite angles of 82° and a N-Ni-N angle of 165°, typical to comparable compounds.[89, 91, 92, 99, 100, 104, 108, 116, 117, 122, 123, 127, 140-147] The coligand is placed in one plane together with the tridentate ligand and the nickel centre, which gets described by the C1–Ni–N3 angle of around 178.5°. The crystal packing shows a classic head-to-tail arrangement, which can be observed along the *a*–*b* face diagonal of the unit cell.[92, 99, 140, 148] The molecules are perfectly arranged in two opposite directions and show a π-stacking

by using two PyPh units with a distance of 3.93 Å, which is weaker by 0.21 Å, than for the structure of the chlorido derivative (Table 3-48).[149]

Table 3-48 Angles and bond lengths of [Ni(Py(Ph)Py)NCS] in comparison to the standard chlorido complex.

	[Ni(Py(Ph)Py)Cl][a]	[Ni(Py(Ph)Py)NCS]
Distances / Å		
Ni–C1	1.836(7)	1.8185(1)
Ni–N1	1.932(6)	1.9231(1)
Ni–N2	1.936(5)	1.9245(1)
Ni–Cl1/N3	2.247(2)	1.9115(1)
Angles / °		
C1–Ni–N1	81.6(3)	82.39(5)
C1–Ni–N2	82.3(3)	82.36(5)
N1–Ni–Cl1/N3	98.23(2)	97.58(5)
N2–Ni–Cl1/N3	97.90(2)	97.66(5)
Sum / °	359.9	360.0
C1–Ni–Cl1/N3	179.7(2)	178.47(5)
N1–Ni–N2	163.9(2)	164.75(5)

a = From ref. [92].

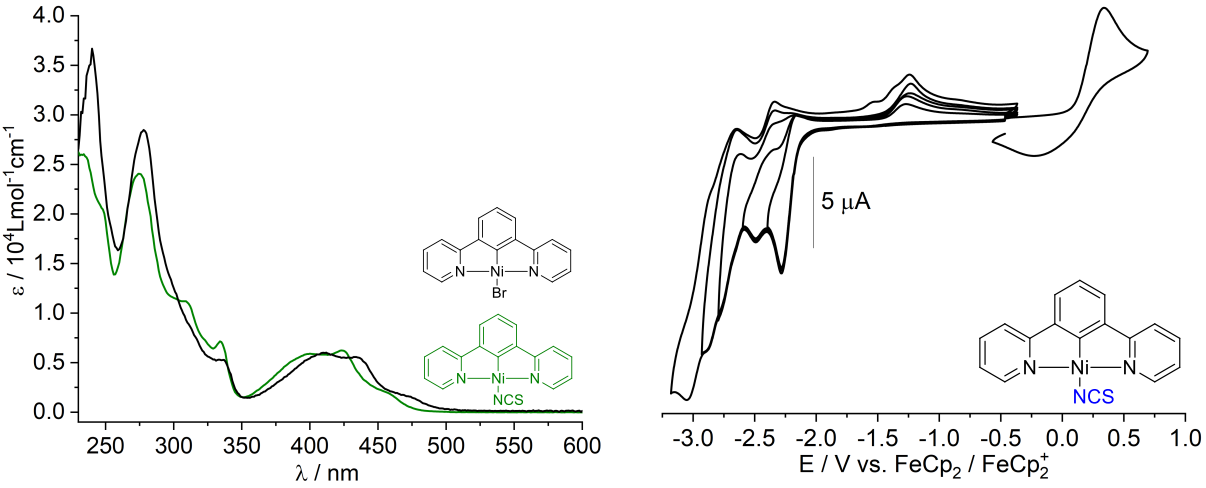

Figure 3-76 UV/vis absorption spectrum of [Ni(Py(Ph)Py)NCS] in comparison to its bromido analogue in THF at rt (*left*) and its cyclic voltammogram (*right*), measured in a 0.1M nBu$_4$PF$_6$ solution in THF with a scan rate of 100 mV/s.

Cyclic voltammetry shows one reversible oxidation at $E_{1/2}$ of 0.16 V and five reductions starting with an irreversible one at –2.28 V (Figure 3-76, *right* and Table 3-49). The oxidation is slightly anodically shifted in comparison to the standard complex and can be assigned to the Ni(II)/Ni(III) redox pair basing on calculations for the standard complex.[92] The first reduction

shows the ligand-centred EC mechanism, as typical for comparable compounds.[89, 91, 92, 99, 142] Except of the third reduction, all reductions are irreversible. The electrochemical HOMO-LUMO gap increases up to 2.44 eV, which supports the blue shifted absorption bands of the UV/vis measurements.

Table 3-49 Redox potentials of [Ni(Py(Ph)Py)NCS] in comparison to its bromido derivative.

	***E* Ox1**	***E* Red1**	***E* Red2**	***E* Red3**	***E* Red4**	***E* Red5**	**Δ*E* HOMO-LUMO**
[Ni(Py(Ph)Py)Br][a]	0.07 ($E_{1/2}$)	–2.31 (E_{pc})	–2.75 (E_{pc})	–3.09 (E_{pc})	-	-	2.38 eV
[Ni(Py(Ph)Py)NCS]	0.16 ($E_{1/2}$)	–2.28 (E_{pc})	–2.50 (E_{pc})	–2.70 ($E_{1/2}$)	–2.90 (E_{pc})	–3.05 (E_{pc})	2.44 eV

Measured in a 0.1M nBu$_4$PF$_6$ solution in THF with a scan rate of 100 mV/s. All potentials in V. E_{pc} = Cathodic Peak Potential, E_{pa} = Anodic Peak Potential, $E_{1/2}$ = Half-Step Potential. a = From ref. [92].

Further, UV/vis absorption spectroscopy was performed, showing that the absorption bands from 235 and 280 nm do not change much and therefore can again be assigned to π–π* transitions (Table 3-50). However, there is an additional shoulder, energetically between both, appearing at 244 nm. All CT bands of lower energies are blueshifted for the thiocyanato complex in comparison to the standard bromido complex. The CT band around 334 nm is not differing at all but is showing one more shoulder at 308 nm (11200 Lmol^{-1}cm^{-1}). The absorption maxima were measured at 399 and 424 nm, with a shoulder starting at 450 nm (Br: 411 and 434 nm, shoulder at 464 nm).

Table 3-50 Absorption maxima of [Ni(Py(Ph)Py)NCS] in comparison to [Ni(Py(Ph)Py)Br].

Complex	**Absorption Max. λ_x in nm (Ext. Coeff. ε in 1000 · Lmol^{-1}cm^{-1})**							
	λ_8	**λ_7**	**λ_6**	**λ_5**	**λ_4**	**λ_3**	**λ_2**	**λ_1**
[Ni(Py(Ph)Py)Br][a]	-	-	464 (1.8)	434 (5.6)	411 (6.0)	334 (5.3)	278 (28.8)	239 (36.4)
[Ni(Py(Ph)Py)NCS]	450^{sh} (2.5)	424 (6.3)	399 (5.9)	334 (7.2)	308 (11.2)	275 (24.1)	244^{sh} (21.3)	234 (26.0)

Measured in THF at rt. sh = shoulder. a = From ref. [92].

3.3.7 Synthesis and Characterization of [Ni(Py(Ph)Py)OAc] and other carboxylate derivatives

Nickel(II) acetate (tetrahydrate) is one of the only commercially available carboxylate salts of nickel, different carboxylate coligands first needed to be synthesized. Nickel(II) benzoate (Ni(OBz)$_2$) was synthesized by a procedure of *Lindoy et al.* from 2003,[216] using basic nickel carbonate with benzoic acid in methanol to give the dihydrate as a green salt. The pivalate

(OPiv) and trifluoroacetate (TFA) salts were synthesized by synthetic procedures from *Winpenny et al.* from 2004[217] and *Muzafarov et al.* from 2020[218] also starting from basic nickel carbonate and the use of the corresponding carboxylic acid as a reactant and solvent at the same time. The nickel(II) 9-anthracyl carboxylate (OOC-atc) salt was synthesized according to works from *Jiménez-Aparicio et al.* from 2015,[219] that start from basic nickel carbonate as well, but use beside of the anthracylcarboxylic acid, pyridine as a base in a H_2O/EtOH mixture giving a mixed salt, that also contains pyridine and water in its structure. These reactions gave polynuclear mixed solids (Figure 3-77).

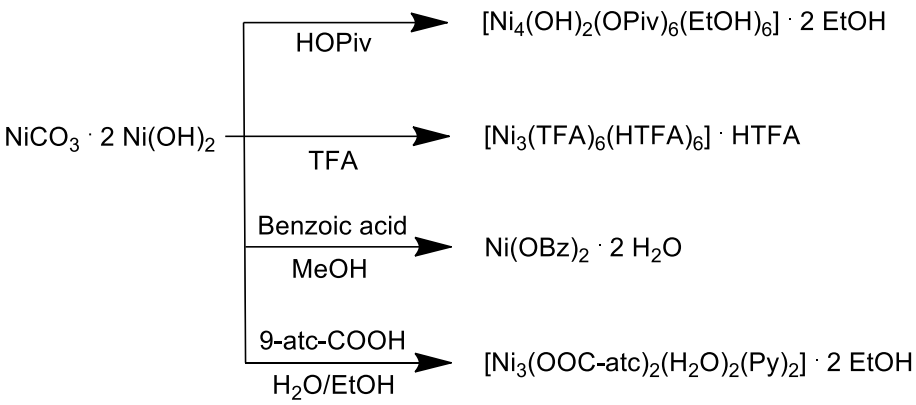

Figure 3-77 Synthetic procedures of carboxylate containing nickel(II) salts.[216-219]

All synthesized salts were not further analyzed, predried and directly used in a base-assisted C–H activation.[92] It could be proved, that the composition of the used nickel carboxylate salts did not play a substantial role for the success of the complex formation of carboxylate complexes of the tridentate Py(Ph)Py ligand.

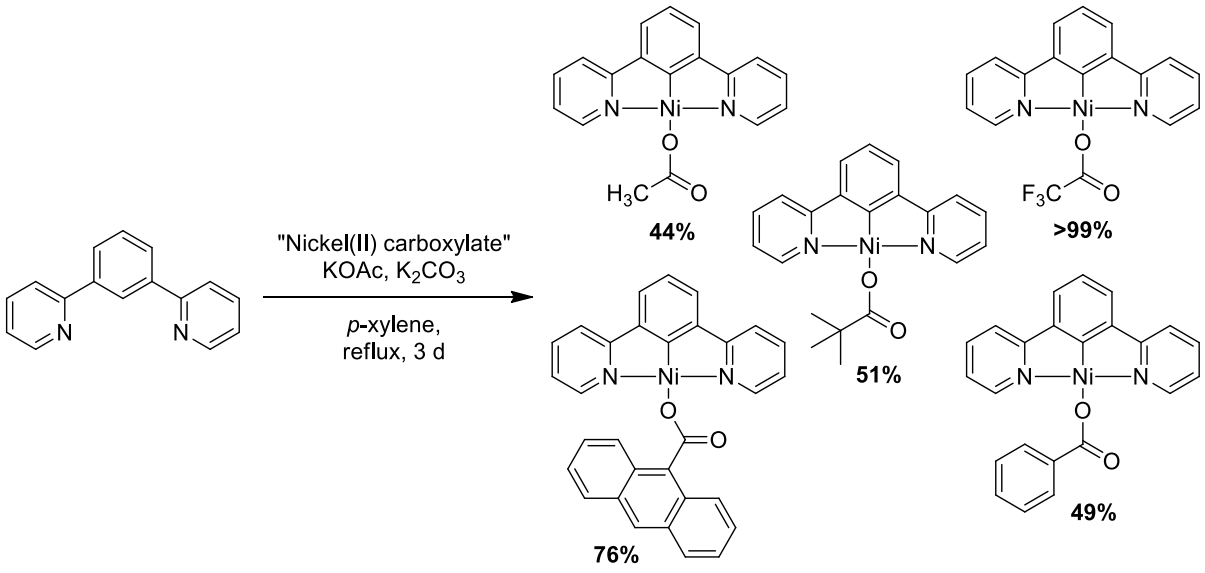

Figure 3-78 Synthesis of [Ni(Py(Ph)Py)OOC-R] (R = CH_3, CF_3, *t*Bu, OBz and 9-atc) *via* base-assisted C–H activation reaction.

All compounds were analyzed by ^{1}H NMR spectroscopy, mass spectrometry and elemental analysis (figure 3-78, for full data see Chapter 5.4.3). Further, SC-XRD delivered structures for the benzoato and trifluoroacetato species, (Figure 3-79), grown by a gas diffusion method of *n*-pentane into a concentrated solution of the complex in THF at rt. The structure of [Ni(Py(Ph)Py)OAc] · H_2O was already published by our working group in 2020.[92] Nevertheless, a specific route towards this species was not known yet and therefore was systematically synthesized and characterized.

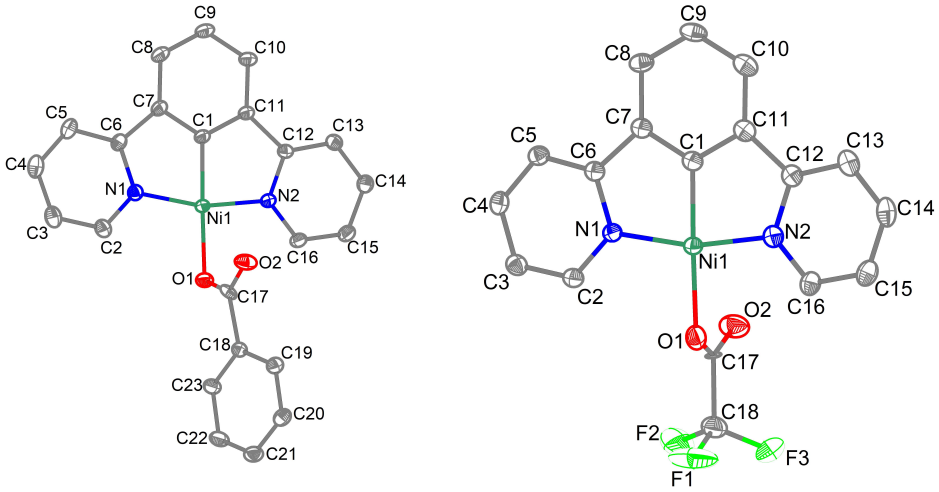

Figure 3-79 Asymmetric unit of [Ni(Py(Ph)Py)OBz] (*left*) and [Ni(Py(Ph)Py)TFA] (*right*). Hydrogen atoms are omitted for clarity. Ellipsoids are shown with a 50% probability.

Both crystal structures were solved in the monoclinic spacegroups $P2_1/n$ (benzoate complex) and $P2_1/c$ (trifluoracetato complex) and therefore are isostructural. Their unit cells bear four formal units (Table 3-51).

Table 3-51 Crystallographic data for [Ni(Py(Ph)Py)OBz] and [Ni(Py(Ph)Py)TFA].

Identification code	**[Ni(Py(Ph)Py)OBz]**	**[Ni(Py(Ph)Py)TFA]**
Empirical formula	$C_{23}H_{16}N_2NiO_2$	$C_{18}H_{11}F_3N_2NiO_2$
Temperature/K	100.00	100.00
Crystal system	monoclinic	monoclinic
Space group	$P2_1/n$	$P2_1/c$
a/Å	13.2713(5)	9.4616(3)
b/Å	9.1026(4)	19.6594(7)
c/Å	14.8552(7)	8.2274(2)
β/°	98.744(2)	91.2160(1)
Volume/Å^3	1773.70(1)	1530.03(8)
Z	4	4
ρ_{calc}g/cm^3	1.539	1.749
F(000)	848.0	816.0

Radiation	MoKα (λ = 0.71073)	MoKα (λ = 0.71073)
2Θ range for data collection/°	4.468 to 68.712	4.144 to 56.61
Index ranges	–21 ≤ h ≤ 18, –14 ≤ k ≤ 14, –23 ≤ l ≤ 23	–12 ≤ h ≤ 12, –26 ≤ k ≤ 26, –10 ≤ l ≤ 10
Reflections collected	75522	41961
Independent reflections	7366 [R_{int} = 0.0448, R_{sigma} = 0.0236]	3799 [R_{int} = 0.0843, R_{sigma} = 0.0350]
Data/restraints/parameters	7366/0/253	3799/0/235
Goodness-of-fit on F^2	1.059	1.061
Final R indexes [I>=2σ (I)]	R_1 = 0.0322, wR_2 = 0.0869	R_1 = 0.0453, wR_2 = 0.1114
Final R indexes [all data]	R_1 = 0.0340, wR_2 = 0.0879	R_1 = 0.0578, wR_2 = 0.1191
Largest diff. peak/hole / eÅ^{-3}	1.43/–0.50	1.50/–0.56
CCDC	2343408	2343412

Both compounds show the expected square planar coordination around the nickel atom with a sum of all four angled of perfectly 360.0°. Overall, the bond lengths and angles around Ni are very similar to those previously reported for [Ni(Py(Ph)Py)OAc].[92] The C1–Ni–N chelate-bite angles show values around 82° and N_1–Ni–N_2 angles of around 165° (Table 3-52). [89, 91, 92, 99, 100, 104, 108, 116, 117, 122, 123, 127, 140-147] All carboxylate complexes show a Ni–O1 distance, that is way shorter than the Ni–Cl1 bond for the standard chlorido complex (2.25 Å).[92] The acetato and trifluoracetato derivatives show similar distances of 1.94 Å, however the one from the benzoato complex is slightly longer (1.97 Å). As the coordinating oxygen atom O1 stays in line with the (Py(Ph-Ni)Py) unit, further parts of the coligands starting with the carbonyl carbon atom C17 does not. For instance, the phenyl function of the benzoate complex stays almost perpendicularly to the complex unit.

Table 3-52 Angles and bond lengths of [Ni(Py(Ph)Py)OBz] and [Ni(Py(Ph)Py)TFA] in comparison to the standard chlorido and acetato complex.

	[Ni(Py(Ph)Py)Cl][a]	[Ni(Py(Ph)Py)OAc][a]	[Ni(Py(Ph)Py)OBz]	[Ni(Py(Ph)Py)TFA]
Distances / Å				
Ni–C1	1.836(7)	1.8136(19)	1.8181(10)	1.817(3)
Ni–N1	1.932(6)	1.9203(17)	1.9180(9)	1.916(2)
Ni–N2	1.936(5)	1.9232(17)	1.9174(9)	1.921(2)
Ni–Cl1/O1	2.247(2)	1.9794(15)	1.9467(8)	1.977(2)
Angles / °				
C1–Ni–N1	81.6(3)	82.48(8)	82.47(4)	82.69(11)
C1–Ni–N2	82.3(3)	82.59(8)	82.49(4)	82.68(12)
N1–Ni–Cl1/O1	98.23(2)	96.61(7)	98.62(4)	97.03(9)
N2–Ni–Cl1/O1	97.90(2)	98.31(7)	96.45(4)	97.64(9)
Sum / °	359.9	360.0	360.0	360.0

C1–Ni–Cl1/O1	179.7(2)	178.99(8)	178.42(4)	176.09(11)
N1–Ni–N2	163.9(2)	165.00(7)	164.85(4)	165.33(10)

a = From ref. [92].

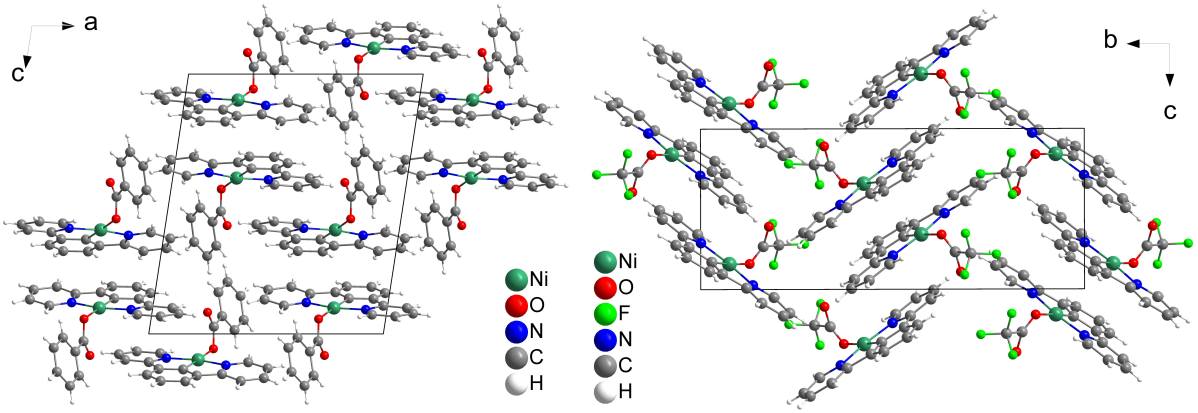

Figure 3-80 Crystal structure of [Ni(Py(Ph)Py)OBz] viewed along the crystallographic *b*-axis (*left*) and [Ni(Py(Ph)Py)TFA] viewed along the crystallographic *a*-axis (*right*).

The crystal structures show the classic head-to-tail arrangement along the crystallographic *c*-axis, or along the *a*-*c* face diagonal with shortest intermolecular PyPh distances of 3.74 Å for the benzoate and 3.60 Å for the trifluoracetato derivative,[92, 99, 140, 148] which are both still within the definition of a weak π-stacking interaction according to *Janiak*.[149]

The trifluoroacetate groups are turned away from the center of the crystal structure and all placed at the cell edges along the *c*-axis, whereas the phenyl groups from the benzoate derivative are included into the structure. The shortest distance between two phenyl functions is 5.13 Å, which is no longer in the range of π-stacking interactions, although these aromats are oriented into the same direction (Figure 3-80).

The cyclic voltammograms (Figure 3-81 and 3-82) show oxidations starting from 0.01 V and reductions in a range from –2.3 V to –3.2 V, all referenced to ferrocene/ferrocenium.

The oxidations appear at similar potentials as the standard bromido complex (from 0.01 V for the acetato- and 0.10 V for the 9-atc-COO complex), and therefore can be assigned to the Ni(II)/Ni(III) oxidation, regarding reported calculations.[92] Nevertheless, the small changes show, that the HOMO energy level is located not exclusively on the metal center, but also on the coligand and the functional groups of the acetate derivatives. The benzoato and 9-anthracylcarboxylato derivative show further oxidations up to 1.0 V, that necessarily need to result from the coligand.

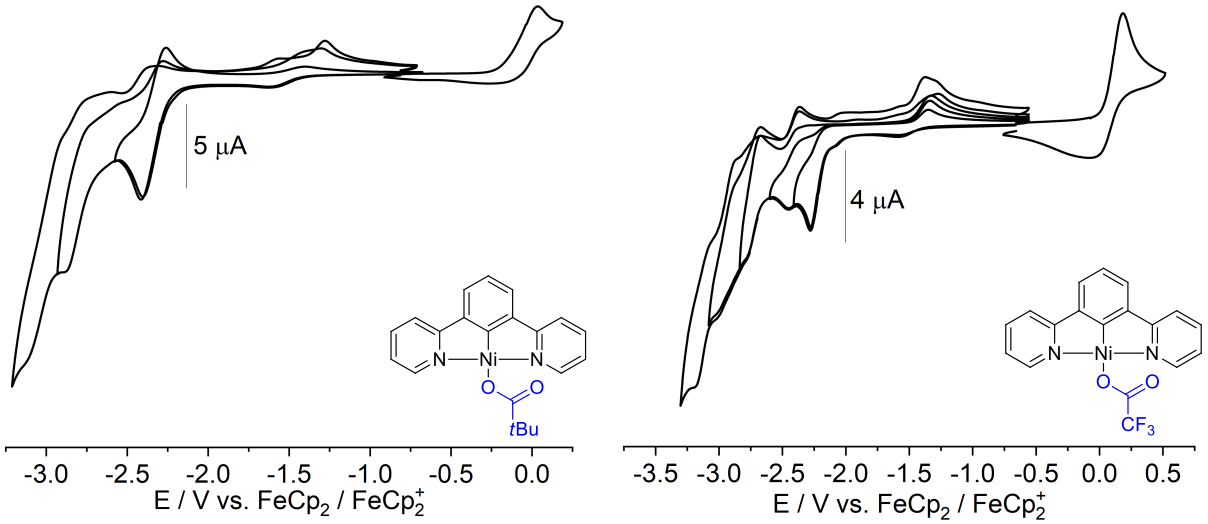

Figure 3-81 Cyclic voltammograms of [Ni(Py(Ph)Py)OPiv] (*left*), [Ni(Py(Ph)Py)TFA] (*right*), measured in a 0.1M nBu$_4$PF$_6$ solution THF at rt with a scan rate of 100 mV/s.

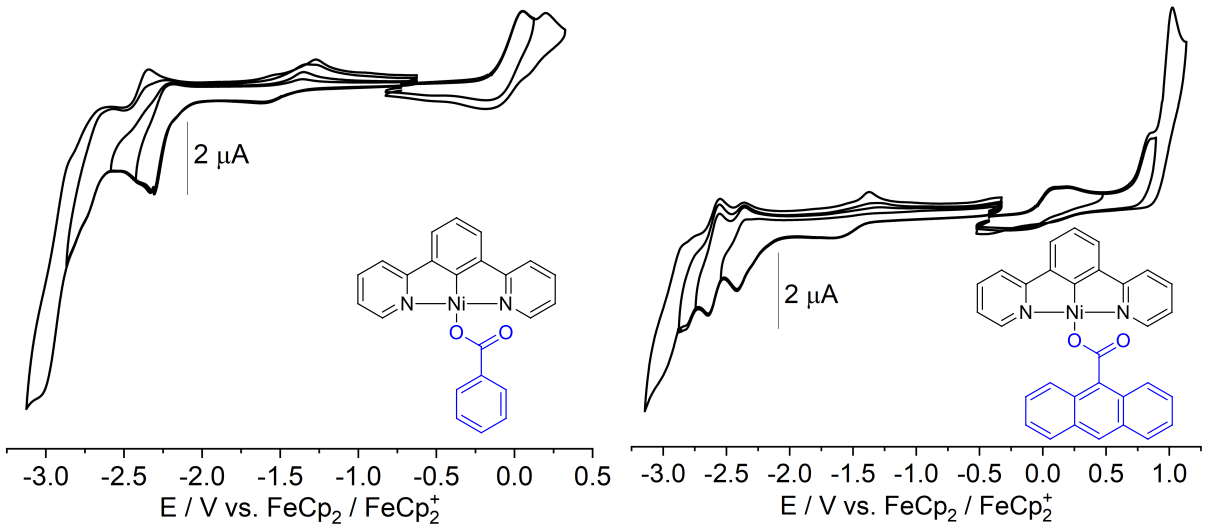

Figure 3-82 Cyclic voltammograms of [Ni(Py(Ph)Py)OBz] (*left*) and [Ni(Py(Ph)Py)OOC-atc] (*right*), measured in a 0.1M nBu$_4$PF$_6$ solution THF at rt with a scan rate of 100 mV/s.

All first reductions, except the ones from the 9-atc carboxylato species, appear at same potentials, indicating, that the LUMO energy level is located at the tridentate N^C^N ligands, based on studies on the standard halido species and therefore does not significantly change.[92] The electrochemical HOMO-LUMO gap for these derivatives are slightly changing in comparison to the bromide standard complex for the acetate (2.33 eV), pivalate (2.34 eV), benzoate (2.37 eV) and trifluoroacetate (2.40 EV) bearing complexes, which supports the measurements from UV/vis absorption spectroscopy (see below). The anthracene carboxylato complex shows the highest value with 2.52 eV (Table 3-53).

Table 3-53 Redox potentials of [Ni(Py(Ph)Py)OOC-R] (R = CH_3, *t*Bu, CF_3, Ph and 9-atc) in comparison to [Ni(Py(Ph)Py)Br].

	***E* Ox2**	***E* Ox1**	***E* Red1**	***E* Red2**	***E* Red3**	***E* Red4**	**Δ*E*$_{HOMO-LUMO}$**
[Ni(Py(Ph)Py)Br][a]	-	0.07 ($E_{1/2}$)	–2.31 (E_{pc})	–2.75 (E_{pc})	–3.09 (E_{pc})	-	2.38 eV
[Ni(Py(Ph)Py)OAc]	-	0.01 (E_{pa})	–2.32 ($E_{1/2}$)	–2.40 ($E_{1/2}$)	–3.05 (E_{pc})	-	2.33 eV
[Ni(Py(Ph)Py)OPiv]	-	0.02 (E_{pa})	–2.32 ($E_{1/2}$)	–2.87 (E_{pc})	–3.14 (E_{pc})	-	2.34 eV
[Ni(Py(Ph)Py)TFA][b]	-	0.08 ($E_{1/2}$)	–2.32 (E_{pc})	–2.46 (E_{pc})	–2.74 ($E_{1/2}$)	–3.04 (E_{pc})	2.40 eV
[Ni(Py(Ph)Py)OBz]	0.19 (E_{pa})	0.05 (E_{pa})	–2.33 (E_{pc})	–2.44 (E_{pc})	–2.83 (E_{pc})	–3.05 (E_{pc})	2.37 eV
[Ni(Py(Ph)Py)OOC-atc][c]	0.85 (E_{pa})	0.10 (E_{pa})	–2.42 (E_{pc})	–2.60 ($E_{1/2}$)	–2.84 (E_{pc})	–3.06 (E_{pc})	2.52 eV

Measured in a 0.1M nBu$_4$PF$_6$ solution THF at rt with a scan rate of 100 mV/s. All potentials in V. E_{pc} = Cathodic Peak Potential, E_{pa} = Anodic Peak Potential, $E_{1/2}$ = Half-Step Potential. a = From ref. [92]. b = Red5 at –3.20 V (E_{pc}). c = Ox3 at 1.02 V (E_{pa}).

UV/vis absorption spectroscopy was performed, as shown in Figure 3-83. All spectra show intense bands with two maxima two absorption maxima, one between 233 and 239 nm and the second one at 276 to 279 nm , which again can be assigned to π–π* transitions in the Ni(II) complexes, due to the high similarity of those from the standard ligand Py(PhH)Py.[92] Regarding the 9-anthracyl carboxylate derivative, these absorption maxima increase harshly with extinctions up to 161000 Lmol^{-1}cm^{-1}.

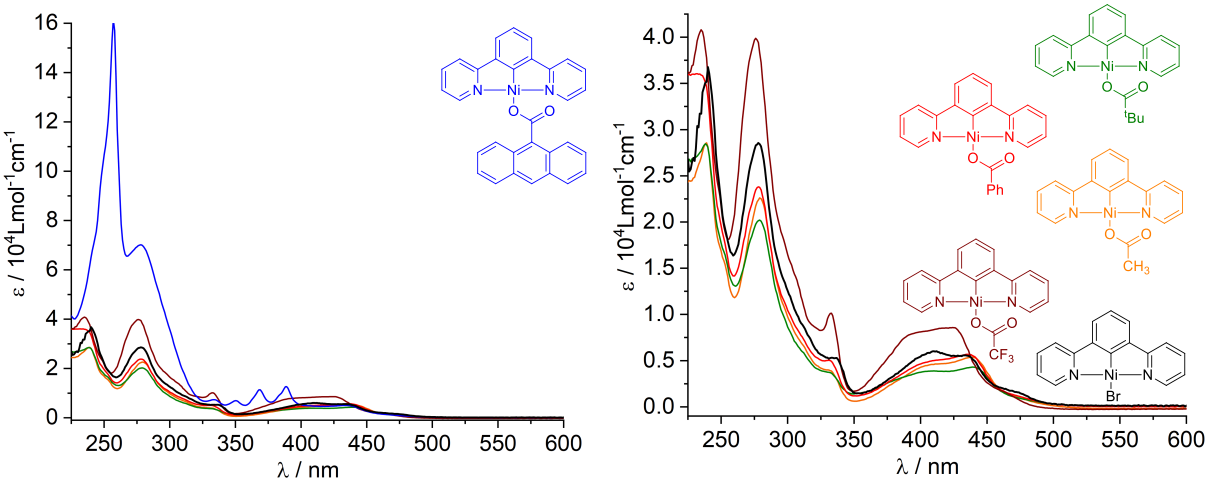

Figure 3-83 UV/vis spectra of carboxylate complexes [Ni(Py(Ph)Py)OOC-R] (R = CH_3, *t*Bu, CF_3, Ph and 9-atc), measured in THF at rt. *Left:* The full spectra. *Right:* A close-up, without the 9-atc carboxylato complex.

These two absorption maxima are followed by shoulders at a range of 300 to 350 nm and broad absorption bands up to 500 nm, assignable to CT bands based on former results on [Ni(Py(Ph)Py)X/R] compounds.[92] The 9-atc carboxylate complex shows more absorption

maxima in the range of CT bands (especially between 325 and 400 nm), besides the three maxima around 330 nm, between 390 and 415 nm and 430 to 440 nm, with an additional shoulder at 460 to 470 nm. The trifluoracetato derivative shows a slight blueshift of the absorption bands and appears with a higher extinction (8000 to 10000 $Lmol^{-1}cm^{-1}$), whereas the other species do not influence the CT bands significantly. Especially the similarity of the structure of the CT bands it can be assumed that these are built up with a similar electronically, including same transitions, as already calculated for the acetato complex in 2020.[92] The optical HOMO-LUMO gap therefore is very similar to the standard bromido complex, except of the one from [Ni(Py(Ph)Py)TFA], which is slightly bigger, which aligns with the results from cyclic voltammetry (Table 3-54, for all measurements see Chapter 7.4).

Table 3-54 Absorption maxima of [Ni(Py(Ph)Py)OOC-R] (R = CH_3, *t*Bu, CF_3, Ph and 9-atc) in comparison to [Ni(Py(Ph)Py)Br].

Complex	Absorption Max. λ_x in nm (Ext. Coeff. ε in 1000 · $Lmol^{-1}cm^{-1}$)							
	λ_8	λ_7	λ_6	λ_5	λ_4	λ_3	λ_2	λ_1
[Ni(Py(Ph)Py)Br][a]	-	-	464 (1.8)	434 (5.6)	411 (6.0)	334 (5.3)	278 (28.8)	239 (36.4)
[Ni(Py(Ph)Py)OAc]	-	468^{sh} (1.1)	439 (5.4)	410^{sh} (4.6)	326^{sh} (4.1)	279 (22.6)	249^{sh} (17.5)	238 (28.6)
[Ni(Py(Ph)Py)OPiv]	-	467^{sh} (1.0)	440 (4.3)	406 (3.8)	329^{sh} (3.7)	279 (20.2)	248^{sh} (18.7)	238 (28.6)
[Ni(Py(Ph)Py)TFA]	-	456^{sh} (2.0)	422 (8.5)	395^{sh} (8.0)	333 (10.1)	293^{sh} (19.5)	276 (39.9)	235 (40.8)
[Ni(Py(Ph)Py)OBz]	-	464^{sh} (1.4)	436 (5.7)	412^{sh} (5.0)	331 (5.1)	298^{sh} (11.4)	278 (23.8)	233 (36.1)
[Ni(Py(Ph)Py)OOC-atc]	467^{sh} (1.0)	435 (5.0)	389 (12.5)	360 (11.4)	350 (6.9)	334 (7.4)	278 (70.2)	257 (161.5)

Measured in THF at rt. sh = shoulder. a = From ref. [92].

3.4 Catalytic experiments with [Ni(N^C^N)X/R]

As one of the main applications of the [Ni(N^C^N)X/R] complexes, we studied them in C–C cross coupling catalysis of the *Negishi*-type. Starting from the terpyridine complexes [Ni(N^N^N)X/R] (N^N^N = derivatives of 2,2';6',6''-terpyridine; X = Cl or Br, R = Me) studied intensively from 2004 on by *Vicic et al.*[80-82, 84] the *Klein* and *Vicic* groups reported cyclometalated Ni(II) analogues for sp^2–sp^3 C atom cross coupling reactions under *Negishi* conditions in 2021 for the first time.[109] The [Ni(C^N^N)X] complexes (HC^N^N = derivatives of 6-phenyl-2,2'-bipyridine, X = I, Br, Cl, or F), showed moderate yields (up to 45%) for two different types of reactions, shown in Figure 3-84.

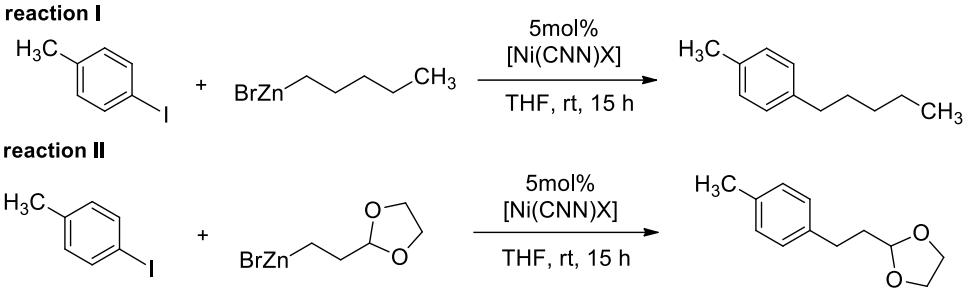

Figure 3-84 C–C cross coupling reactions catalyzed by [Ni(C^N^N)X] complexes by *Klein et al*. in 2021.[109]

The catalysts in this study differed in their halido coligands (X = F, Cl, Br, I) and in substitution on the phenide and the central pyridyl unit of the tridentate C^N^N ligand, to probe for their influence on yields and selectivity.

A research stay at the *Vicic Lab* at Lehigh University, PA, USA, allowed to perform the same *Negishi*-type coupling experiments to using the [Ni(N^C^N)X] catalysts (5 mol% catalyst, THF, rt, 15 h; response factor for reaction I = 0.985; for reaction II = 0.794, GC-MS separation, hexamethylbenzene as standard).[109, 220] Table 3-55 shows all potential outcomes of reaction I and II with their m/z value and retention time t_R in THF, which is used in the following tables. A first catalyst screening was carried out to get a general overview of the potentially best performing species, Figure 3-85 shows selected results, Table 3-56 (reaction I) and Table 3-57 (reaction II) provide all data.

Table 3-55 Expected products from the cross coupling catalysis using [Ni(N^C^N)X/R] catalysts.

	Reaction I	**Reaction II**
Starting Materials		**A** m/z: 217.96 t_R = 5.81 min
	B_1 m/z: 72.09 t_R = 2.79 min	**B_2** m/z: 102.07 t_R = 2.56 min
Hetero-coupling Products	**C_1** m/z: 162.14 t_R = 6.49 min	**C_2** m/z: 192.12 t_R = 8.16 min
Homo-coupling Products	**D** m/z: 182.11 t_R = 8.62 min	
	E_1 m/z: 156.19 t_R = ?	**E_2** m/z: 202.12 t_R = 8.10 min

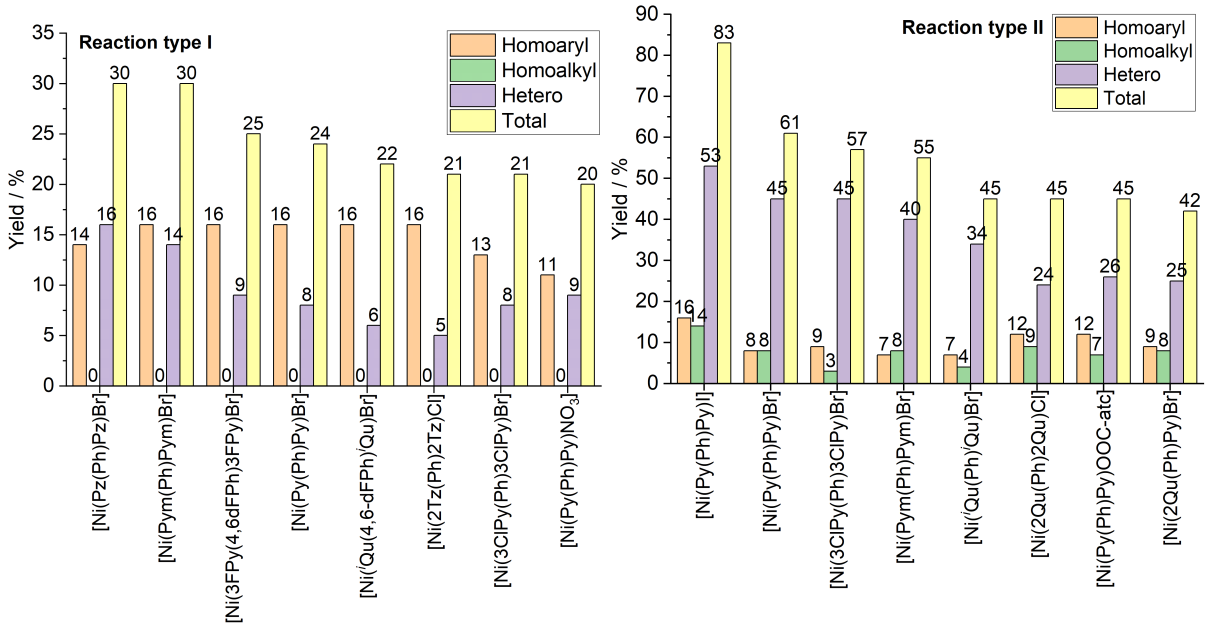

Figure 3-85 Yields and selectivity of [Ni(N^C^N)X/R] catalysts for reaction I (*left*) and reaction II (*right*). Conditions: 5 mol% catalyst, THF, rt, 15 h; no additives; response factor for reaction I = 0.985; for reaction II = 0.794, GC-MS separation, hexamethylbenzene as standard.

Table 3-56 Results of the cross coupling catalysis for reaction I.[a]

Catalyst	A	B_1	C_1	D	E_1	Total Yield $C_1 + D + E_1$
[Ni(Pz(Ph)Pz)Br]	8.13	16.17	16.47	13.90	0.00	30.37
[Ni(Pym(Ph)Pym)Br]	0.50	21.54	13.83	15.70	0.00	29.53
[Ni(3FPy(4,6FPh)3FPy)Br]	3.25	23.09	9.05	15.82	0.00	24.87
[Ni(Py(Py)Py)Br]	5.04	19.74	7.41	16.41	0.00	23.82
[Ni(2^{i}Qu(4,6FPh)2^{i}Qu)Br]	2.47	21.74	6.25	15.69	0.00	21.95
[Ni(2Tz(Ph)2Tz)Cl]	11.44	19.91	5.42	15.55	0.00	20.97
[Ni(3ClPy(Ph)3ClPy)Br]	3.55	21.65	8.02	12.69	0.00	20.70
[Ni(Py(5NO_2Ph)Py)Br]	8.58	17.64	4.64	16.01	0.00	20.65
[Ni(2Qu(Ph)Py)Br]	5.44	21.44	6.88	13.48	0.00	20.36
[Ni(Py(Ph)Py)I]	8.58	27.02	5.19	14.79	0.00	19.98
[Ni(Py(Ph)Py)NO_3]	15.96	18.11	9.05	10.83	0.00	19.87
[Ni(Py(Ph)Py)Br]	7.97	27.68	4.98	14.36	0.00	19.34
[Ni(2Qu(Ph)2Qu)Cl]	4.14	23.30	4.11	14.76	0.00	18.87
[Ni(Py(4,6FPh)Py)Br]	7.57	23.67	4.91	13.88	0.00	18.79
[Ni(2BTz(Ph)2BTz)Cl]	11.97	20.76	5.80	12.96	0.00	18.76
[Ni(Py(Ph)Py)OAc]	7.99	24.31	5.10	13.52	0.00	18.63
[Ni(Py(5MePh)Py)Br]	5.53	23.70	4.53	13.94	0.00	18.47

[Ni(Py(Ph)Py)OOC-atc]	3.38	24.58	4.33	14.01	0.00	18.34
[Ni(Py(5FPh)Py)Br]	6.10	23.96	4.53	13.67	0.00	18.20
[Ni(2^{i}Qu(Ph)2^{i}Qu)Br]	4.64	23.38	4.56	13.52	0.00	18.08
[Ni(Py(Ph)Py)C_3F_7]	10.70	20.80	5.96	11.83	0.00	17.79
[Ni(Py(5BuPh)Py)Br]	6.69	24.81	4.40	13.33	0.00	17.73
[Ni(Py(5MeOPh)Py)Br]	4.95	23.28	3.93	13.71	0.00	17.63
[Ni(Py(4,6MePh)Py)Cl]	3.92	24.85	4.43	13.07	0.00	17.50
[Ni(Py(4,5,6MeOPh)Py)Br]	6.85	25.06	4.51	12.70	0.00	17.21
[Ni(Py(4,6FPh)Py)Cl]	7.11	23.33	4.57	12.10	0.00	16.67
[Ni(Py(Ph)Py)CN]	0.00	27.29	6.54	10.11	0.00	16.65
[Ni(Py(Ph)Py)Cl]	5.53	25.05	3.91	12.54	0.00	16.46
[Ni(Py(4FPh)Py)Br]	8.64	23.56	4.11	12.25	0.00	16.36
[Ni(Py(Ph)Py)OPh]	5.04	25.53	3.86	12.50	0.00	16.35
[Ni(Py(Ph)Py)TFA]	9.90	24.14	4.11	12.20	0.00	16.31
[Ni(Py(Ph)Py)OBz]	11.00	24.16	4.07	11.99	0.00	16.06
[Ni(Py(Ph)Py)Carb]	9.91	23.63	4.27	11.69	0.00	15.96
[Ni(Py(5CF_3Ph)Py)Br]	12.12	21.32	4.56	11.22	0.00	15.79
[Ni(2Btz(Ph)Py)Br]	18.57	20.81	7.46	8.29	0.00	15.75
[Ni(Py(Ph)Py)OPiv]	8.50	24.11	3.60	12.02	0.00	15.63
[Ni(Py(Ph)Py)C_2F_5]	20.75	16.91	5.65	9.76	0.00	15.41
[Ni(Py(Ph)Py)O*t*Bu]	14.80	21.28	4.46	10.80	0.00	15.26
[Ni(Py(Ph)Py)C_6F_5]	9.68	21.60	5.18	9.73	0.00	14.91
[Ni(Py(5PhPh)Py)Br]	10.49	21.37	3.80	10.58	0.00	14.38
[Ni(Py(4,6FPh)Py)CN]	6.55	25.76	5.19	7.51	0.00	12.70
[Ni(2Tz(Ph)Py)Br]	17.96	22.86	3.52	8.68	0.00	12.20
[Ni(4Tz(Ph)4Tz)Cl]	42.33	8.41	7.66	2.40	0.00	10.06
[Ni(Py(4,6MePh)Py)CN]	28.28	14.89	2.90	4.74	0.00	7.64
[Ni(4Tz(Ph)Py)Br]	27.47	17.41	3.27	3.54	0.00	6.80
[Ni(Py(Ph)Py)NCS]	38.88	11.80	2.02	1.92	0.00	3.94

[a] Conditions: 5 mol% catalyst, THF, rt, 15 h; no additives; response factor = 0.985, GC-MS separation, hexamethylbenzene as standard.

Table 3-57 Results of the cross coupling catalysis for reaction II.[a]

Catalyst	A	B_2	C_2	D	E_2	Total Yield C_2 + D + E_2
[Ni(Py(Ph)Py)I]	45.79	27.48	53.40	15.77	13.53	82.70
[Ni(Py(Ph)Py)Br]	60.39	21.37	44.19	8.16	8.15	60.50
[Ni(3ClPy(Ph)3ClPy)Br]	6.40	3.50	45.30	8.73	2.64	56.67
[Ni(Pym(Ph)Pym)Br]	44.21	9.22	40.10	7.33	7.66	55.09
[Ni(2^{i}Qu(Ph)2^{i}Qu)Br]	11.46	2.45	34.23	6.52	4.40	45.14
[Ni(2Qu(Ph)2Qu)Cl]	6.43	1.54	23.54	12.24	9.22	45.00
[Ni(Py(Ph)Py)OOC-atc]	10.54	2.35	26.40	11.77	6.78	44.95
[Ni(2Qu(Ph)Py)Br]	11.68	2.32	24.75	9.47	7.96	42.18
[Ni(3FPy(4,6FPh)3FPy)Br]	15.87	3.33	28.07	10.43	3.47	41.98
[Ni(Py(4,6FPh)Py)Br]	18.60	8.31	29.16	5.25	4.98	39.38
[Ni(Py(Py)Py)Br]	14.40	2.05	22.67	7.95	5.96	36.59
[Ni(Py(Ph)Py)OPiv]	19.36	6.28	22.44	7.18	5.49	35.11
[Ni(Py(5NO_2Ph)Py)Br]	16.33	2.26	25.13	3.78	6.05	34.95
[Ni(Py(Ph)Py)NO_3]	18.46	2.60	24.35	4.51	5.59	34.46
[Ni(Py(5CF_3Ph)Py)Br]	20.08	7.63	19.93	8.03	5.21	33.17
[Ni(Pz(Ph)Pz)Br]	17.40	2.77	19.10	7.72	4.70	31.52
[Ni(Py(4,6FPh)Py)Cl]	21.93	9.15	21.49	3.19	2.79	27.47
[Ni(2^{i}Qu(4,6FPh)2^{i}Qu)Br]	25.30	10.00	16.74	5.14	4.29	26.16
[Ni(Py(5PhPh)Py)Br]	24.88	10.53	19.07	3.81	3.25	26.13
[Ni(Py(Ph)Py)OAc]	29.46	9.13	16.82	6.11	3.15	26.08
[Ni(Py(Ph)Py)TFA]	30.77	11.09	21.49	3.27	0.85	25.61
[Ni(Py(5MeOPh)Py)Br]	26.31	10.99	18.24	3.36	2.96	24.57
[Ni(Py(5FPh)Py)Br]	24.03	10.35	15.73	4.82	3.92	24.47
[Ni(Py(4,6FPh)Py)CN]	20.99	5.27	20.24	1.35	2.17	23.76
[Ni(Py(Ph)Py)C_2F_5]	28.67	11.05	15.75	3.89	3.53	23.17
[Ni(Py(4FPh)Py)Br]	26.65	12.26	17.06	2.68	2.31	22.06
[Ni(Py(5MePh)Py)Br]	30.14	12.46	16.75	2.54	2.41	21.70
[Ni(Py(5BuPh)Py)Br]	26.07	12.16	15.19	3.55	2.80	21.54
[Ni(2Btz(Ph)Py)Br]	22.77	7.12	10.24	6.41	3.49	20.14
[Ni(Py(Ph)Py)Cl]	27.21	14.10	14.79	2.49	2.52	19.80
[Ni(Py(4,5,6MeOPh)Py)Br]	31.53	14.10	14.69	1.51	1.88	18.08
[Ni(2Tz(Ph)2Tz)Cl]	27.17	9.42	10.42	6.35	1.08	17.85

[Ni(2BTz(Ph)2BTz)Cl]	18.36	14.17	5.00	11.42	0.52	16.95
[Ni(Py(Ph)Py)O*t*Bu]	35.52	14.69	12.75	1.92	2.15	16.83
[Ni(4Tz(Ph)4Tz)Cl]	37.98	14.35	12.35	2.35	0.68	15.37
[Ni(Py(Ph)Py)OPh]	33.72	16.49	11.60	0.93	0.75	13.28
[Ni(Py(Ph)Py)C_6F_5]	34.04	10.78	9.74	0.75	1.35	11.84
[Ni(Py(Ph)Py)C_3F_7]	35.73	11.41	9.36	0.73	1.71	11.80
[Ni(Py(4,6MePh)Py)Cl]	38.07	17.90	7.36	0.62	0.95	8.93
[Ni(Py(Ph)Py)OBz]	44.68	15.97	7.02	0.25	0.65	7.92
[Ni(2Tz(Ph)Py)Br]	42.79	16.30	3.27	0.35	0.57	4.20
[Ni(Py(Ph)Py)NCS]	47.13	16.42	2.18	0.00	0.20	2.38
[Ni(4Tz(Ph)Py)Br]	47.41	17.28	1.11	0.00	0.38	1.49
[Ni(Py(Ph)Py)Carb]	48.49	16.55	1.10	0.00	0.12	1.22
[Ni(Py(Ph)Py)CN]	47.30	22.13	0.00	0.00	0.00	0.00
[Ni(Py(4,6MePh)Py)CN]	49.82	22.43	0.00	0.00	0.00	0.00

[a] Conditions: 5 mol% catalyst, THF, rt, 15 h; no additives; response factor = 0.794, GC-MS separation, hexamethylbenzene as standard.

Generally, the yields were higher yield for reaction II (up to 83%) than for reaction I (up to 30%). Reaction I worked out best for systems, that bear EWGs or π-acceptor substitutions at the peripheric rings. Other coligands than halides led to rather lower yields, with the exception of carboxylates. We assume that the coligands are markedly governing the solubility and thus the efficiency. At the same time their leaving-group character is important, as the activation step in the catalysis is assumed to be a reduction, followed by X^- cleavage (see Chapter 3.3.3). This is supported by the very low activity of the CN complexes, as CN^- is a poor leaving group.

For reaction II, the highest yields were found for the standard iodido and bromido complexes [Ni(Py(Ph)Py)X]. Generally, the trend is the same as for reaction as high yields were found for catalysts bearing either very good π-acceptors as peripheric rings or an electron-poor central phenide unit. Reaction II also confirms that solubility plays a crucial role, as very good performance for carboxylates as co-ligands and poor performance of the cyanido complexes was found. Very generally, those complexes, that showed the lowest HOMO-LUMO gaps or showed the highest anodic shifts of all measured potentials in cyclic voltammetry were the best catalysts in this first round of catalysis.

The second round was performed to optimize the solvent. Therefore, three well performing catalysts were used for a solvent screening in four (reaction I) or five (reaction II) different solvents. Figure 3-86 shows the selected results for reaction I and II and Table 3-58 and Table 3-59 summarize the data.

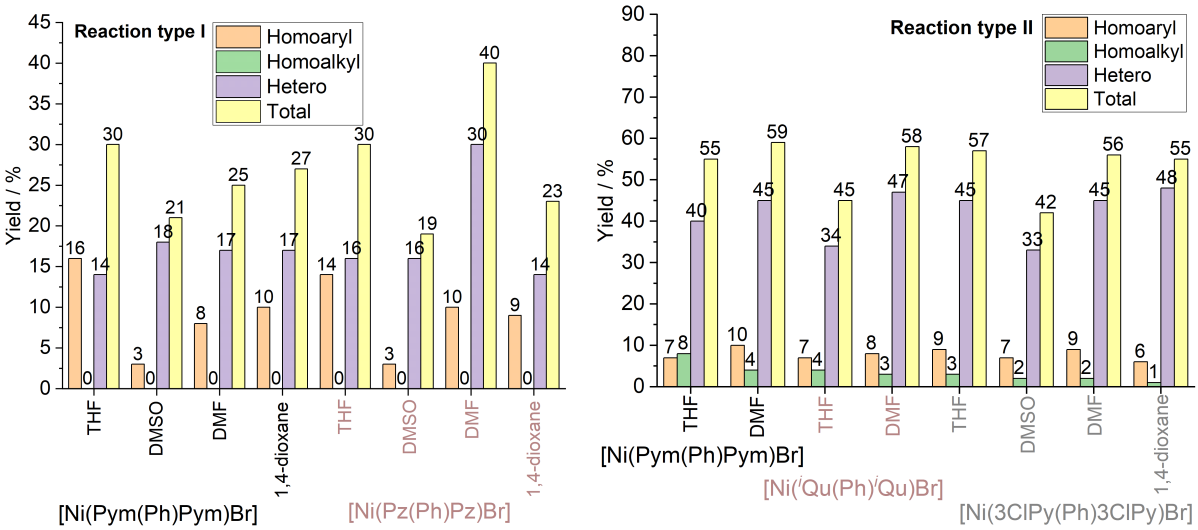

Figure 3-86 Selected results from the solvent screening for reaction I (*left*) and reaction II (*right*). Conditions: 5 mol% catalyst, THF, rt, 15 h; no additives; response factor for reaction I = 0.985; for reaction II = 0.794, GC-MS separation, hexamethylbenzene as standard.

Table 3-58 Yields from the solvent screening for reaction I.[a]

Catalyst	Solvent	A	B_1	C_1	D	E_1	Total Yield C_1 + D + E_1
[Ni(Pym(Ph)Pym)Br]	THF	0.50	21.54	13.83	15.70	0.00	29.53
	DMSO	50.58	8.29	17.85	2.67	0.00	20.52
	DMF	15.69	21.79	16.93	8.43	0.00	25.36
	MeCN	43.31	8.40	15.08	8.01	0.00	23.09
	1,4-dioxane	13.00	12.00	16.60	9.79	0.00	26.39
[Ni(Py(Ph)Py)NO_3]	THF	15.96	18.11	9.05	10.83	0.00	19.87
	DMSO	49.87	4.94	4.50	0.98	0.00	5.49
	DMF	19.52	18.33	9.12	5.31	0.00	14.43
	MeCN	50.27	7.59	9.49	2.95	0.00	12.45
	1,4-dioxane	45.67	3.22	10.15	2.44	0.00	12.60
[Ni(Pz(Ph)Pz)Br]	THF	8.13	16.17	16.47	13.90	0.00	30.37
	DMSO	40.44	7.76	15.83	2.91	0.00	18.75
	DMF	12.42	16.01	29.68	9.67	0.00	39.34
	MeCN	53.06	6.49	6.15	1.85	0.00	7.99
	1,4-dioxane	21.78	10.44	13.56	8.69	0.00	22.25

[a] Conditions: 5 mol% catalyst, THF, rt, 15 h; no additives; response factor = 0.985, GC-MS separation, hexamethylbenzene as standard.

Table 3-59 Yields from the solvent screening for reaction II.[a]

Catalyst	Solvent	A	B_2	C_2	D	E_2	Total Yield C_2 + D + E_2
[Ni(Pym(Ph)Pym)Br]	THF	44.21	9.22	40.10	7.33	7.66	55.09
	DMSO	39.03	13.84	17.99	0.84	1.11	19.94
	DMF	15.25	5.48	44.65	10.26	4.21	59.12
	MeCN	49.63	5.21	2.14	0.22	1.09	3.44
	1,4-dioxane	37.44	10.95	7.29	2.63	2.92	12.84
	DMI	44.48	15.22	3.49	0.28	1.16	4.93
[Ni(2^{i}Qu(Ph)2^{i}Qu)Br]	THF	11.46	2.45	34.23	6.52	4.40	45.14
	DMSO	37.08	12.32	21.51	1.38	1.19	24.08
	DMF	11.05	2.32	46.18	8.23	3.30	57.71
	MeCN	46.76	5.15	2.52	0.00	1.49	4.01
	1,4-dioxane	31.92	6.69	11.39	3.82	4.01	19.23
	DMI	44.59	14.32	3.66	0.32	1.05	5.04
[Ni(3ClPy(Ph)3ClPy)Br]	THF	6.40	3.50	45.30	8.73	2.64	56.67
	DMSO	28.83	10.20	33.08	6.90	1.88	41.85
	DMF	6.25	2.68	45.27	8.57	2.01	55.85
	MeCN	42.00	5.80	9.01	2.75	0.52	12.27
	1,4-dioxane	10.82	4.70	48.38	5.77	1.00	55.15
	DMI	44.25	14.17	5.27	0.00	0.55	5.82

[a] Conditions: 5 mol% catalyst, THF, rt, 15 h; no additives; response factor = 0.794, GC-MS separation, hexamethylbenzene as standard.

In the third round of catalytic experiments, we focusing on additives to obtain higher yields, based on previous studies,[221-224] and added to two well performing catalytic systems [Ni(Pym(Ph)Pym)Br] and [Ni(Pz(Ph)Pz)Br]. While LiBr, NaI, *n*Bu_4Br and $ZnCl_2$ additives should form more reactive tetrahalido zincates $RZnX_2^-$ or $RZnX_3^-$,[221-223] styrene was added to form π-complexes with the catalyst to activate the Ni–X/R bond, as reported by *Yamamoto et al*.[224] Figure 3-87 shows selected results, whereas Table 3-60 and Table 3-61 provide the data.

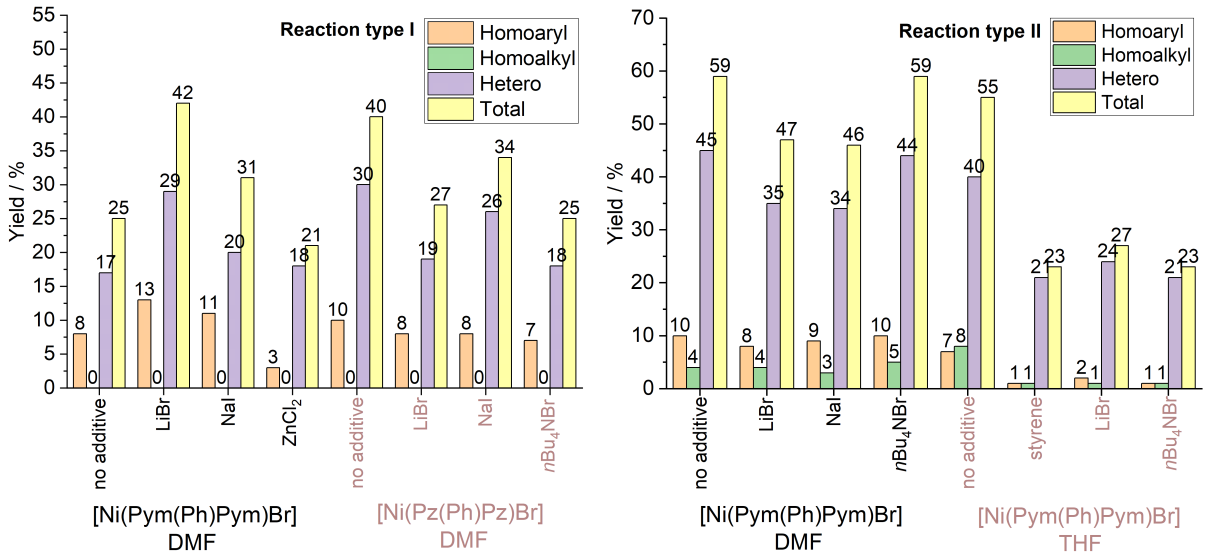

Figure 3-87 Chosen results from the additive screening for reaction I (*left*) and reaction II (*right*). Conditions: 5 mol% catalyst, THF, rt, 15 h; response factor for reaction I = 0.985; for reaction II = 0.794, GC-MS separation, hexamethylbenzene as standard.

An increase in yield for reaction I was observed for [Ni(Pym(Ph)Pym)Br] in DMF, when using NaI (from 16 to 21%) or LiBr (16 to 28%). In other cases, the yield remained constant upon addition of additives. Remarkably, most additives decreased the yields significantly. This is especially true for reaction II.

Table 3-60 Yields from the screening for additives for reaction I.[a]

Catalyst	Solvent	Additive	A	B_1	C_1	D	E_1	Total Yield $C_1 + D + E_1$
[Ni(Pym(Ph)Pym)Br]	DMF	-	15.69	21.79	16.93	8.43	0.00	25.36
		styrene	4.33	17.98	13.15	8.09	0.00	21.24
		LiBr	0.00	11.23	28.30	13.19	0.00	41.49
		NaI	5.28	13.32	20.14	11.24	0.00	31.38
		*n*Bu$_4$NBr	12.11	8.04	12.34	0.00	0.00	12.34
		$ZnCl_2$	30.58	3.42	18.10	3.21	0.00	21.31
[Ni(Pz(Ph)Pz)Br]	DMF	-	12.42	16.01	29.68	9.67	0.00	39.34
		styrene	15.65	7.98	12.35	0.22	0.00	12.57
		LiBr	2.18	15.76	19.22	8.25	0.00	27.47
		NaI	4.97	14.44	25.33	8.27	0.00	33.60
		*n*Bu$_4$NBr	6.23	17.75	17.88	7.19	0.00	25.07
		$ZnCl_2$	45.04	5.74	3.89	0.59	0.00	4.48

[a] Conditions: 5 mol% catalyst, THF, rt, 15 h; no additives; response factor = 0.985, GC-MS separation, hexamethylbenzene as standard.

Table 3-61 Yields from the screening for additives for reaction II.[a]

Catalyst	Solvent	Additive	A	B_2	C_2	D	E_2	Total Yield C_2 + D + E_2
[Ni(Pym(Ph)Pym)Br]	DMF	-	15.25	5.48	44.65	10.26	4.21	59.12
		styrene	28.71	8.37	31.33	2.31	1.02	34.66
		LiBr	17.99	5.17	35.10	7.53	4.26	46.89
		NaI	16.44	4.92	32.96	9.27	3.44	45.67
		nBu_4NBr	26.25	7.16	44.25	10.18	4.90	59.33
		$ZnCl_2$	49.99	15.47	5.69	1.15	0.72	7.56
[Ni(Pym(Ph)Pym)Br]	THF	-	44.21	9.22	40.10	7.33	7.66	55.09
		styrene	8.10	8.10	21.30	0.91	0.99	23.20
		LiBr	29.32	6.88	24.55	1.48	1.04	27.07
		NaI	39.31	7.18	12.16	1.38	0.61	14.15
		nBu_4NBr	32.82	8.24	21.31	0.98	0.95	23.25
		$ZnCl_2$	47.56	13.89	4.38	0.00	0.23	4.61

[a] Conditions: 5 mol% catalyst, THF, rt, 15 h; no additives; response factor = 0.794, GC-MS separation, hexamethylbenzene as standard.

4 Summary of the Results

In this study, organometallic Ni(II) complexes [Ni(N^C^N)X] containing tridentate cyclometalating ligands N^C$^-$^N and various ancillary ligands (coligands) X or R were synthesized and studied. The main focus was set to the impact of the variation of the central C-ring of the tridentate ligand, the peripheral N moieties and the coligands on the electronic structure of these square planar complexes (Figure 4-1). The electronic structure was studied by a combination of UV/vis absorptions and emission spectroscopy and detailed electrochemical investigations, including cyclic voltammetry and spectroelectro chemistry. The latter is a combination of electrolysis and in situ spectroscopy of the thus generated species. The ultimate motivation lies in attempts to produce photoluminescent, triplet emitting, Ni(II) complexes based on this scaffold. The specific main motivation for this study comes from *Negishi*-type C–C cross coupling reactions, for which these complexes should be suitable (pre)catalysts. While the triplet emitting complexes remain a future goad, requiring more studies to find the optimum combination of donor and acceptor-moieties and chromophores in such complexes, first *Negishi*-coupling experiments were successful.

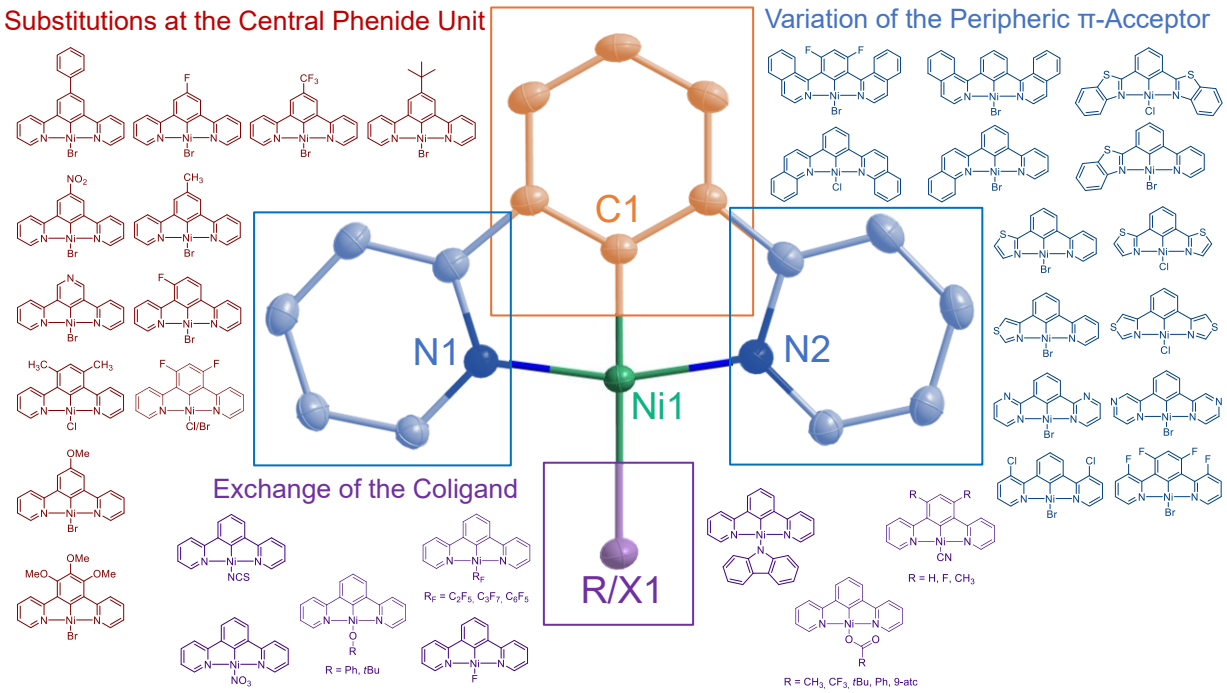

Figure 4-1 Summary of investigated [Ni(N^C^N)X/R] complexes, sorted by their group of substitution.

The substitution of the central phenide unit (Figure 4-1, marked in red) was achieved by synthesizing the corresponding N^C^N protoligand using *Negishi* conditions, followed by the cyclonickelation using the base-assisted C–H activation reaction with yields ranging from 50 to 97%. The substitution of the 4 and 6 positions (*meta* to the nickel-bound carbon atom) had

a larger impact on the optical and electrochemical properties of the [Ni(N^C^N)X] complex, than a substitution at position 5 (in *para* position to the nickel-bound carbon atom). Although the overall impact on these properties is rather low, electron-withdrawing groups (EWGs) (e.g. -F, -CF_3, -NO_2) lead to an increase of the optical gap, as defined by the lowest-energy absorption (Figure 4-2, *right*), as well as the electrochemical gap, as defined by the difference between the first oxidation and first reduction potentials (Figure 4-2, *left*). Electron-donating groups (EDGs) (e.g. -OMe, -Me, -Ph) show either the opposite effect or have no influence at all. The HOMO–LUMO which is well represented by the electrochemical gap range from 2.39 eV for [Ni(Py(4,5,6MeOPh)Py)Br] to 2.34 eV for [Ni(Py(4,6FPh)Py)Br]. Moreover, the positions 4, 5 and 6 can selectively be used for changing secondary properties of these systems such as solubility or for placing marker atoms for desired applications without changing the properties of the complex. [Ni(Py(5BuPhPy)Br] is the perfect example of a complex with a significantly higher solubility in organic solvents compared with its unsubstituted (standard) complex [Ni(Py(Ph)Py)Br], without a significant variation in the optoelectronic properties.

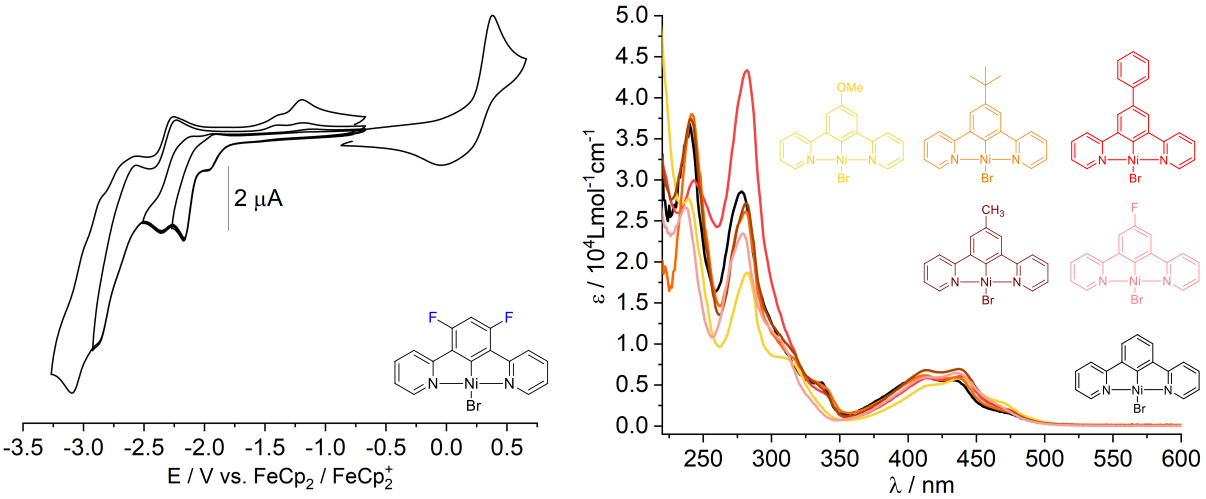

Figure 4-2 *Left*: Cyclic voltammograms of [Ni(Py(4,6FPh)Py)Br], measured in 0.1M solution of *n*Bu_4PF_6 in THF at rt with a scan rate of 100 mV/s. *Right*: UV/vis spectra of the shown complexes, measured in THF at rt.

Overall, the pretty small response of the electrochemical potentials and the UV/Vis absorption spectra upon variation of the central phenide unit, is in line with relatively small contributions of this moiety to the, mainly N-heteroaromatic-centered lowest unoccupied molecular orbital (LUMO) and the highest occupied molecular orbital (HOMO) which receives main contributions from the metal d orbitals and the coligand p-orbitals, in addition to the central phenide unit, as has been worked out in detail for the 4,6-dimethyl-substituted complex [Ni(Py(4,6MePh)Py)Cl].

Most N^C^N ligands with varied peripheric *N*-heteroaromatic units (Figure 4-1, marked in blue) were synthesized using *Suzuki-Miyaura* conditions with yields ranging from 26% to 98% with

a clear trend for high yields for electron-rich *N*-heteroaromats. The success of the base-assisted C–H activation reaction for the synthesis of the Ni(II) complexes appears to be dependent on the ring-size of the C and N components the tridentate ligand. The C–H activation was successful for ligands that are built up from three six-membered rings, while ligands bearing two five-membered peripheric rings or having both ortho-*N* positions blocked by substituents needed to be synthesized using the oxidative addition method starting from the Ni(0) precursor [Ni(COD)$_2$] (COD = 2,5-cyclooctadiene) and the chloro-substituted ligand precursors N^C(Cl)^N. We assume that five-membered peripheric rings fail to bring the pre-coordinated nickel atom in suitable proximity to the C–H function for cyclometalation. In future theoretical studies using density functional theory methods, this might be further elucidated.

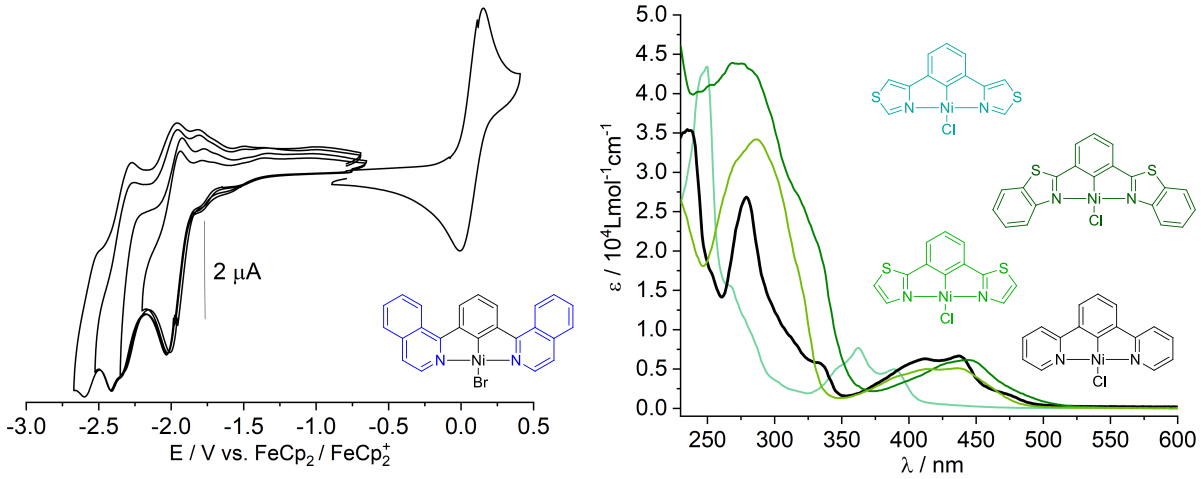

Figure 4-3 *Left*: Cyclic voltammograms of [Ni(2^{i}Qu(Ph)2^{i}Qu)Br], measured in 0.1M solution of *n*Bu$_4$PF$_6$ in THF at rt with a scan rate of 100 mV/s. *Right*: UV/vis absorption spectra of symmetric thiazole containing complexes, measured in THF at rt.

Cyclic voltammetry of the N-varied complexes (Figure 4-3, *left*) shows almost constant values for the reversible oxidations, involving the metal, the coligand and the central phenide unit, as discussed above. The reduction potentials, especially for the first reductions, vary massively, with values ranging from –1.67 V (for [Ni(2Btz(Ph)2Btz)Cl]) to –2.42 V (for [Ni(4Tz(Ph)4Tz)Cl]). This is in line with the LUMO localized in the N-heterocyclic units. Increasing the number of N-atoms in the peripheric rings from pyridine (Py) to pyrazine (Pz) or pyrimidine (Pym) lead to lower solubility of the complexes but markedly decreased the reduction potentials and thus the HOMO–LUMO gap with 1.89 eV for the pyrazine- and 2.19 eV for pyrimidine-derivatives, compared with the 2.37 eV of the standard Py complex [Ni(Py(Ph)Py)Br]. The quinoline containing complexes show relatively low HOMO–LUMO gaps, ranging from varying around 2.00 eV. Generally, the doubly (benzo)thiazole-containing complexes show varying gaps, depending on the used thiazole unit, of 2.28 eV for the 2-thiazole, 2.52 eV for the 4-thiazole

and 1.77 eV for the benzothiazole complex, than their counterparts bearing one thiazole and one pyridine function (2.28 eV, 2.41 eV, and 1.96 eV, respectively).

Synthetically, the variation of the anionic coligand (X or R) turned out to be the most challenging part within this project and two general routes turned out to be successful. The introduction of the coligand during the base assisted C–H activation using a Ni(II) salt containing the target coligand such as $Ni(SCN)_2$ or $Ni(OAc)_2 \cdot 4\ H_2O$, which were dried before use and gave the aimed complexes in yields from 44 to 99% (Figure 4-4, marked in blue). The spectrum of different carboxylate complexes was extended by synthesizing organic Ni(II) salts bearing the desired carboxylate anion out of basic nickel(II) carbonate.

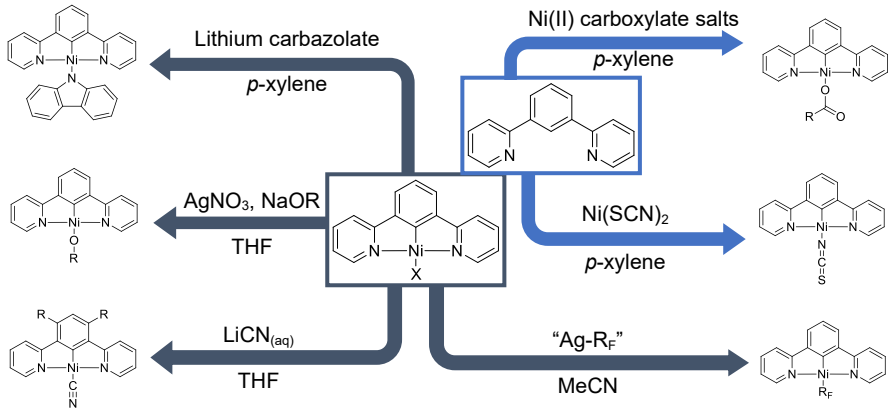

Figure 4-4 Examples for successfully performed coligand exchange reactions.

Alternatively, halide-containing complexes [Ni(N^C^N)X] with X = Cl or Br were transformed into the target complexes using Li(I) or Ag(I) salt to de-halogenate the complex and addition of the new coligand in form of the anion of this salt or another soluble form of the anionic coligand (Figure 4-4, marked in dark blue). Using lithium carbazolate, the carbazolato complex can be synthesized in *p*-xylene in quantitative yields and reacting a diluted aqueous solution of LiCN and the acetato or chlorido complex is successful in synthesizing the cyanido derivative in THF with yields up to 26%. Ag(I) salts can be used for a conversion of the bromido complex to the fluorido species in 86% yield, which is not accessible *via* C–H activation out of NiF_2. They further were used to convert the chlorido complex to one bearing a perfluoroalkylide or -arylide coligands, such as $C_2F_5^-$ or $C_6F_5^-$ in yields from 40 to 99%. Silver nitrate was used to perform the coligand exchange reaction from chloride to nitrate in CH_2Cl_2, which turns out to be the most interesting precursor species for further coligand exchange reaction, as nitrate is a perfect leaving group and can be easily exchanged by stronger ligands. The proof of concept was exemplarily done by using the isolated [Ni(Py(Ph)Py)NO_3] and sodium(I) alkoxide salts in THF to give two alkoxido (-OR) complexes in yields of 60% for R = *t*Bu and 68% for R = Ph.

The exchange of the coligand mainly affects the HOMO energy level of the respective Ni(II) N^C^N complex, which gets determined in cyclic voltammetry (Figure 4-5, *left*). The range of first oxidation potentials varies from 0.01 V for [Ni(Py(Ph)Py)OAc] up to 0.46 V for [Ni(Py(4,6FPh)Py)CN], which is in line with the localization of the HOMO level on the metal center and the coligand, A change of the latter is also affecting the reversibility of the first redox steps. A more irreversible character of the first reduction, supports the thesis of an occurring EC mechanism and a less reversible oxidations allows assumptions about a stronger localization of the HOMO on the coligand. With the characterization of the fluoride complex, the dataset on all halido Py(Ph)Py complexes was completed, showing similar electrochemical properties the standard halido analogues with a HOMO-LUMO gap of 2.40 eV. Same is generally true for the carbazolato- (2.38 eV), the thiocyanato- (2.44 eV) and most carboxylato (OOC-R) complexes (R = CH_3: 2.33 eV, CF_3: 2.40 eV, *t*Bu: 2.34 eV, Ph: 2.37 eV and 9-atc: 2.52 eV). The cyanido complexes represent the group with the highest HOMO-LUMO gaps of 2.60 eV for [Ni(Py(Ph)Py)CN] and [Ni(Py(4,6MePh)Py)CN] and 2.66 eV for [Ni(Py(4,6FPh)Py)CN]. The nitrato complex has a HOMO-LUMO gap of 2.62 eV and by coligand exchange reaction for alkoxido complexes the gap gets lowered to 2.41 eV for the O*t*Bu and 2.58 eV for the OPh derivative. The perfluoroalkylide complexes show 2.66 eV (C_2F_5) and 2.64 eV (C_3F_7) and [Ni(Py(Ph)Py)C_6F_5] gives 2.41 eV as the electrochemical HOMO-LUMO gap. Stronger ligands than halides increase the HOMO-LUMO gap, which got visible by a general blueshift of the energetically low transitions of the UV/vis absorption spectrum (down to 446 nm for [Ni(Py(4,6FPh)Py)CN], Figure 4-5, *right*), supported by a bigger gap between the first oxidation and first reduction in cyclic voltammetry (up to 2.66 eV for [Ni(Py(Ph)Py)CN]) and the Ni–R bond from SC-XRD measurements (shortest Ni1–R1 distance: 1.90 Å for [Ni(Py(Ph)Py)OPh]).

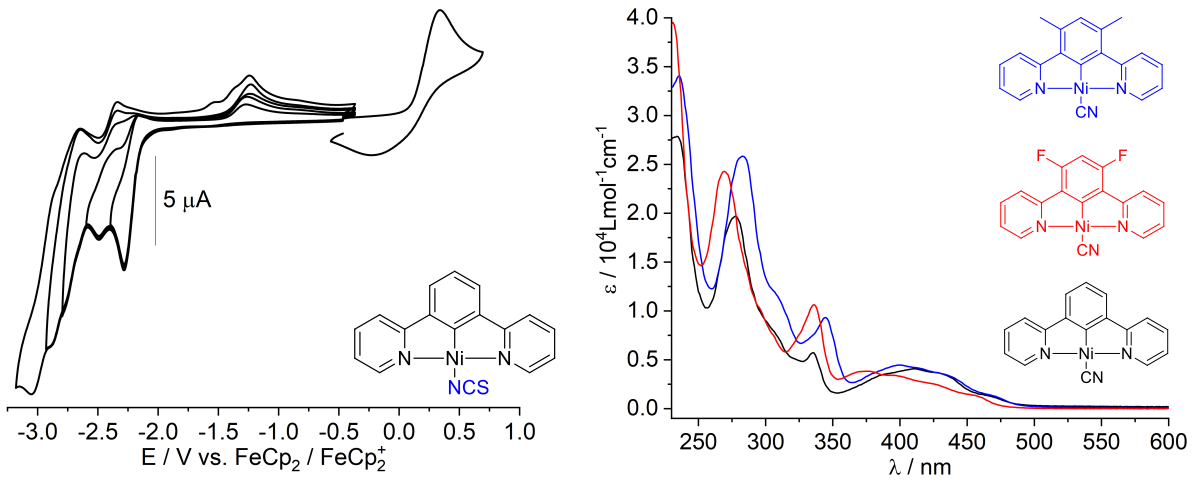

Figure 4-5 *Left:* Cyclic voltammograms of [Ni(Py(Ph)Py)NCS], measured in 0.1M solution of *n*Bu$_4$PF$_6$ in THF at rt with a scan rate of 100 mV/s. *Right*: UV/vis absorption spectra of the cyanido complexes, measured in THF at rt.

All synthesized complexes were tested in three rounds of catalysis for two types of reactions (Figure 4-6). With this first round, the best three catalysts for each reaction were chosen to be used in further tests. Influenced by the availability and the performance, [Ni(Pym(Ph)Pym)Br], [Ni(2^{i}Qu(Ph)2^{i}Qu)Br] and [Ni(3ClPy(Ph)3ClPy)Br] should then further be investigated.

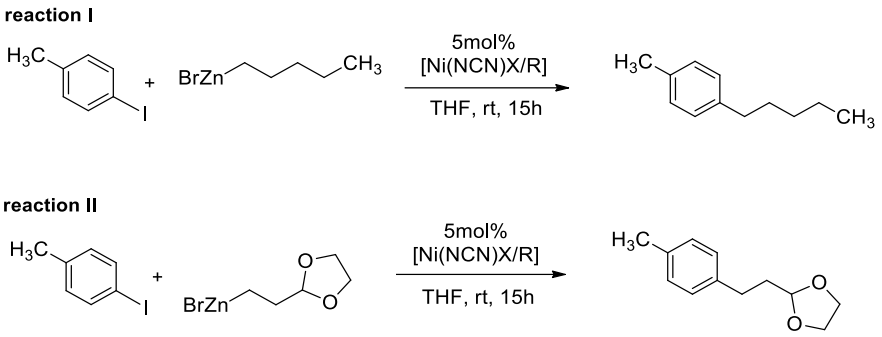

Figure 4-6 Performed *Negishi*-typed C–C cross coupling reactions using [Ni(N^C^N)X/R] complexes.

In the second round of catalysis, in which the best solvent for these systems should be pointed out. With the best combinations of catalyst and solvent in hand, the third round was performed to see, if additives could further improve the yield of these reactions (Figure 4-7). All species show a high selectivity for the desired hetero cross coupling product. However, the yields for reaction type II were significantly higher (48% selective yield) than for reaction type I (30% selective yield).

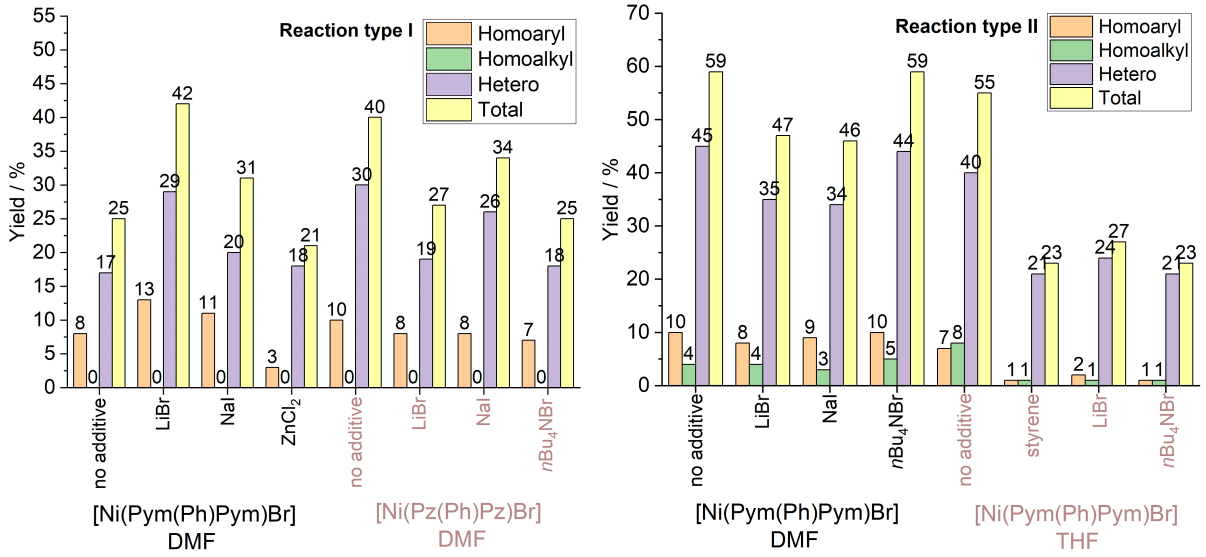

Figure 4-7 Selected results of the catalyst screening: Left: The screening for additives led to a slight increase of two systems for reaction I. Right: Solvent screening for the top three catalysts for reaction II.

Within the three substitution classes of [Ni(N^C^N)X/R] complexes, trends were figured out, that resulted from these tests. In general, central ring substituted complexes, that bear EWGs

performed best at these reactions within their substance class. The electron poorer the central ring, the better is the conversion, e.g. [Ni(Py(4,6FPh)Py)Cl]. The class of catalysts with other *N*-heteroaromats than pyridine show, that the better the introduced π-acceptor, the better the performance in the tested Negishi-typed C–C cross coupling catalysis. This relation gets further underlined through electrochemical measurements, that show the trend of a better conversion for complexes with the lowest potential for the first reduction (e.g. [Ni(2*i*Qu(Ph)2*i*Qu)Br], reaction II). The trend within the coligand exchanges species is not determined, since the best performing C–C cross coupling synthesis was catalyzed by halido species. The effect of the other two substitution classes (changes at the central phenide unit and the different coligands) are suppressed by the influence of the π-accepting peripheric rings by far. In comparison to [Ni(C^N^N)X] systems, the selectivity and the overall yields could be improved, which gives hope for further investigations, which could include other than the tested catalyst systems or could investigate a combination of all three substitution patterns: The one at the central phenide unit, the exchange of the peripheric π-acceptors and the coligand.

5 Experimental Section

5.1 Materials and Methods

Commercially available chemicals were purchased from *ACROS, ABCR, Sigma Aldrich, Carbolution, BLDPharm, TCI* and *Alfa Aesar* and used without any further purification. Oxygen- and water sensitive reactions were carried out under argon atmosphere supplied by *Linde* (99.998%), using *Schlenk*-techniques.

Dry tetrahydrofuran (THF) was freshly distilled over a Na/K alloy (3:7), *p*-xylene was freshly stilled over sodium and further solvents were dried using the solvent cleaning system *MBRAUN* MB SPS-800.

NMR spectroscopy (^{1}H, ^{13}C, ^{19}F, ^{195}Pt and correlation spectra) was performed on a *Bruker* Avance II 300 MHz spectrometer (^{1}H: 300 MHz, ^{13}C: 75 MHz, ^{19}F: 282 MHz, ^{195}Pt: 64 MHz) equipped with a L.T. BBO ATM 5 mm probe head with *z*-gradient coil (*Bruker*, Rheinhausen, Germany), on a *Bruker* Avance III HD 400 MHz spectrometer (^{1}H: 400 MHz, ^{19}F: 376 MHz) equipped with a BBI and BB ATM 5 mm probe head with z-gradient coil (*Bruker*, Rheinhausen, Germany) or on a *Bruker* Avance III 500 MHz (^{1}H: 500 MHz, ^{13}C: 126 MHz) equipped with a TCI prodigy 5 mm probe head with z-gradient coil (*Bruker*, Rheinhausen, Germany). Chemical shifts were referenced to tetramethylsilane (TMS) for ^{1}H and ^{13}C spectra (δ = 0.00 ppm) or to the respective solvent shift for ^{1}H and ^{13}C spectra using residual ^{1}H and ^{13}C solvent signals and to *α*,*α*,*α*-trifluorotoluene (TFT, δ = –63.7 ppm) for ^{19}F spectra.

UV/vis absorption spectra were recorded on a Cary 50, a Cary 60 spectrophotometer by *Varian* (*Varian Medical Systems*, Darmstadt, Germany) or on an *Ocean Insight* diode array spectrometer (*Ocean Insight*, Orlando, FL, USA) at ambient temperature using quartz glass cuvettes with an optical path length of 1 cm. All spectra are baseline corrected.

EI(+) MS spectra were measured using either a *Thermo Scientific* Exactive GC Orbitrap Analyser mass spectrometer (*Thermo Fisher Scientific GmbH*, Dreieich, Germany) or a *Finnigan* MAT 95 spectrometer (*Finnigan Instrument Corporation*, Bremen, Germany) with an ionisation energy of 70 eV. The spectra were simulated using ISOPRO 3.0.

Electrochemical measurements (Cyclic Voltammetry) were carried out in 0.1M nBu$_4$NPF$_6$ solution in THF (tetrahydrofuran) with a scan rate of 100 mV/s using a three-electrode configuration (glassy carbon working electrode, Pt counter electrode, Ag/AgCl reference) and an Autolab PGSTAT30 or µStat400 potentiostat by *Metrohm* (*Metrohm*, Filderstadt, Germany). The potentials were referenced against the ferrocene/ferrocenium redox couple as internal standard. UV/vis-spectroelectrochemical measurements (in 0.1M nBu$_4$NPF$_6$ solution in THF)

were performed using an optically transparent thin-layer electrode (OTTLE) cell[225] at room temperature.

Single crystal structure analysis by X-ray diffractometry (SC-XRD): The measurements were performed using a *Bruker* D8 Venture, including a *Bruker* Photon 100 CMOS detector, a *Bruker* **D8 Quest** (*Bruker*, Rheinhausen, Germany) or an IPDS II T diffractometer (*STOE & Cie.*, Darmstadt, Germany) at 293 K,170(2) K or 100 K using Mo-K_α radiation (λ = 0.71073 Å). The crystal data were collected and the multi-scan absorption correction was performed using APEX3 v2015.5-2, *SAINT* and *SADABS.*[226-228] The structures were solved in OLEX2 v1.3 and v1.5[229] by intrinsic phasing methods using SHELXT (*Sheldrick 2015*)[230] and the structural refinement was carried out with SHELXL 2015[231] employing full-matrix least-squares methods on $F_0^2 \geq 2\sigma(F_0^2)$. Non-hydrogen atoms were refined with anisotropic displacement parameters without any constraints. The hydrogen atoms were included by riding models. The illustration of crystal structures was performed using Diamonds v4.2.[232] The data of the structural solutions and refinements are available at https://summary.ccdc.cam.ac.uk/ structures of the Cambridge Crystallographic Data Centre (CCDC).

Elemental analyses were either obtained using a *HEKAtech* CHNS EuroEA 3000 analyzer (*HEKAtech*, Wegberg, Germany) or externally performed by *Micro-Analysis Inc.*, (*Micro-Analysis Inc.*, Wilmington, DE, USA).

GC-MS analysis was performed with a *SHIMADZU QP2010 Ultra* device and evaluated using *GCMS Postrun Analysis software by SHIMADZU* (*SHIMADZU USA*, Columbia, MA, USA).

5.2 Synthesis of the Ligands

5.2.1 Synthesis of the Ligands Precursors

5.2.1.1 Bromination of 1,2,3-trimethoxybenzene for 1,3-dibromo-4,5,6-trimethoxybenzene (Br(4,5,6MeOPhH)Br)[133]

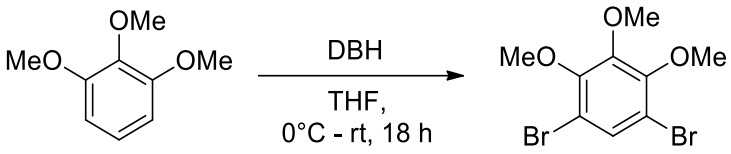

10.1 g (59.6 mmol, 1.00 eq.) 1,2,3-trimethoxybenzene was dissolved in THF (70 mL) and cooled to 0°C. In a separate flask, 25.6 g (89.2 mmol, 1.50 eq.) 1,3-dibromo-5,5-dimethylhydantoin (DBH) was dissolved in THF (80 mL) and slowly added to the reaction mixture. It was warmed up to rt and stirred for 18 h. The reaction was quenched with a saturated aqueous solution of sodium thiosulfate until the reaction mixture turned yellow and the solvent was removed. The product mixture was then extracted with CH_2Cl_2 (3 x 200 mL) and washed with water (3 x 50 mL). The combined organic fractions were dried over anhydrous $MgSO_4$ and the product was purified using column chromatography (SiO_2, *c*Hex:EtOAc 19:1, R_f = 0.51) and 13.0 g (40.0 mmol, 67%) of a colorless liquid was obtained.

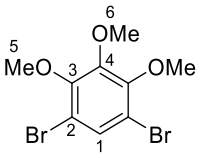

^{1}H NMR (300 MHz, $CDCl_3$) δ / ppm = 7.48 (s, 1H, H-1), 3.93 (s, 3H, H-6), 3.89 (s, 6H, H-5).

^{13}C NMR (75 MHz, $CDCl_3$) δ / ppm = 151.5 (C-2), 148.9 (C-4), 130.4 (C-1), 112.9 (C-3), 61.9 (C-6), 61.6 (C-5).

5.2.1.2 Synthesis of 2,2'-(2-Chloro-1,3-phenylene)bis(4,4,5,5-tetramethyl-1,3,2-dioxaborolane) (BPin(PhCl)BPin) [204]

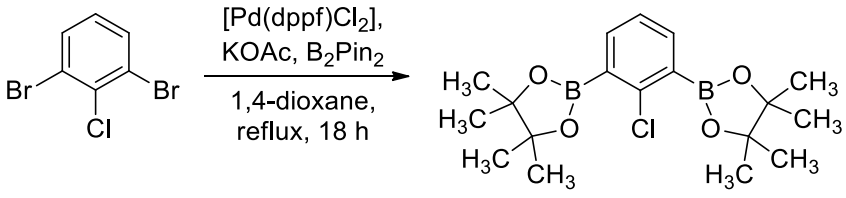

A stirred suspension of 10.0 g (37.0 mmol, 1.00 eq.) 1,3-dibromo-2-chlorobenzene, 18.2 g (185 mmol, 5.00 eq.) KOAc and 18.8 g (74.0 mmol, 2.00 eq.) B_2Pin_2 in dry 1,4-dioxane (120 mL) was degassed with argon for 30 min. 1.00 g (1.37 mmol, 0.04 eq.) [Pd(dppf)Cl_2] was added and the suspension was heated to reflux overnight. After removal of the solvent under reduced pressure, the residue was re-dissolved in EtOAc (300 mL) and washed with water

(3 x 300 mL). The organic phase was dried over anhydrous $MgSO_4$, and the solvent removed under reduced pressure. The crude product was filtered over a silica plug with CH_2Cl_2 (R_f = 0.71) and removal of the solvent gave 7.58 g (20.8 mmol, 56%) of a colorless solid.

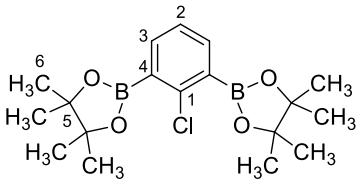

^{1}H NMR (300 MHz, $CDCl_3$) δ / ppm = 7.66 (d, *J* = 7.4 Hz, 2H, H-3), 7.22 (t, *J* = 7.4 Hz, 1H, H-2), 1.38 (s, 24H, H-6).

^{13}C NMR (75 MHz, $CDCl_3$) δ / ppm = 143.2 (C-4), 138.1 (C-3), 130.1 (C-1), 125.2 (C-2), 84.2 (C-5), 24.9 (C-6).

5.2.1.3 Synthesis of 2,2'-(4,6-difluoro-1,3-phenylene)bis(4,4,5,5-tetramethyl-1,3,2-dioxaborolane) (BPin(4,6FPhCl)BPin)[204]

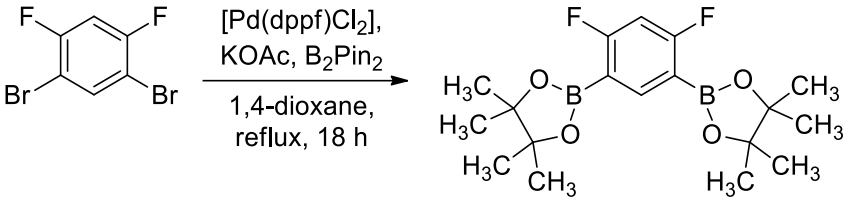

A stirred suspension of 2.50 g (9.20 mmol, 1.00 eq.) 1,3-dibromo-4,6-difluorobenzene, 4.51 g (46.0 mmol, 5.00 eq.) KOAc and 6.54 g (25.8 mmol, 2.80 eq.) B_2Pin_2 in dry 1,4-dioxane (60 mL) was degassed with argon for 30 min. 0.39 g (0.55 mmol, 0.06 eq.) $[Pd(PPh_3)_2Cl_2]$ was added and the suspension was heated to reflux overnight. After removal of the solvent under reduced pressure, the residue was re-dissolved in EtOAc (100 mL) and washed with brine (3 x 100 mL). The organic phase was dried over anhydrous Na_2SO_4, and the solvent removed under reduced pressure. The product was purified by column chromatography (SiO_2, cHex:EtOAc 25:1, R_f = 0.01) and removal of the solvent gave 1.28 g (3.50 mmol, 42%) of a colorless solid.

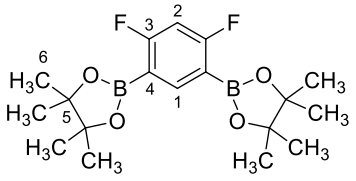

^{1}H NMR (300 MHz, $CDCl_3$) δ / ppm = 8.13 (t, *J* = 7.6 Hz, 1H, H-1), 6.73 (t, *J* = 9.7 Hz, 1H, H-6), 1.35 (s, 24H, H-6).

5.2.1.4 Syntheses of 3-Bromo-1-(N-heteroaromat) benzene (HetArPhBr) – *General Procedures*

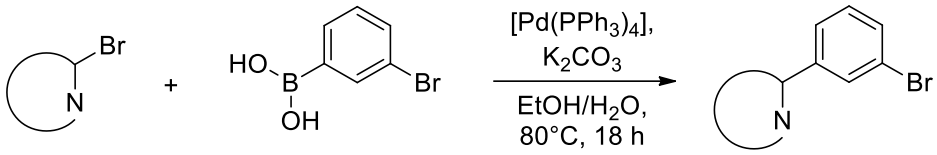

General Procedure A.[203] A mixture of EtOH/H_2O (100 mL, 4:1) was degassed with constant argon flow for 2 h. Under argon 2.01 g (10.0 mmol, 1.00 eq.) 3-bromophenylene boronic acid, a brominated heteroaromat (11.0 mmol, 1.10 eq.), 4.15 g (30.0 mmol, 3.00 eq.) K_2CO_3 and 0.58 g (0.50 mmol, 0.05 eq.) [$Pd(PPh_3)_4$] were added. The mixture was heated to reflux overnight and after 18 h cooled to room temperature. Removal of the solvent under reduced pressure yielded a crude product, which was re-dissolved in EtOAc (50 mL) and H_2O (50 mL) was added. After the phases were separated, the aqueous phase was extracted with EtOAc (3 x 50 mL). The organic phase was dried over anhydrous $MgSO_4$ and the solvent was removed under reduced pressure.

2Tz(PhH)Br. Following *General Procedure A* and using 1.80 g (11.0 mmol, 1.10 eq.) 2-bromothiazole. After purification of the crude product by column chromatography (SiO_2, *c*Hex:EtOAc 4:1, R_f = 0.65) the product was isolated as 2.25 g (9.37 mmol, 94%) colorless oil.

^{1}H NMR (500 MHz, $CDCl_3$): δ / ppm = 8.14 (t, *J* = 1.8 Hz, 1H, H-1), 7.90 – 7.84 (m, 2H, H-3, H-9), 7.54 (ddd, *J* = 8.0, 1.9, 1.0 Hz, 1H, H-5), 7.36 (d, *J* = 3.2 Hz, 1H, H-8), 7.31 (t, *J* = 7.9 Hz, 1H, H-4).

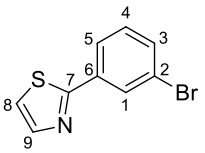

^{13}C NMR (75 MHz, $CDCl_3$): δ / ppm = 166.7 (C-7), 143.7 (C-3), 135.5 (C-2), 132.5 (C-5), 130.5 (C-4), 129.0 (C-1), 125.0 (C-9), 123.0 (C-6), 119.4 (C-8).

4Tz(PhH)Br. Following *General Procedure A* and using 1.80 g (11.0 mmol, 1.10 eq.) 4-bromothiazole. After purification of the crude product by column chromatography (SiO_2, *c*Hex:EtOAc 9:1, R_f = 0.43) the product was isolated as 1.10 g (4.58 mmol, 46%) colorless oil.

^{1}H NMR (500 MHz, $CDCl_3$): δ / ppm = 8.87 (d, *J* = 1.9 Hz, 1H, H-9), 8.10 (t, *J* = 1.8 Hz, 1H, H-1), 7.85 (dt, *J* = 7.8, 1.2 Hz, 1H, H-3), 7.56 (d, *J* = 2.0 Hz, 1H, H-8), 7.47 (ddd, *J* = 8.0, 1.8, 0.9 Hz, 1H, H-5), 7.30 (s, 1H, H-4).

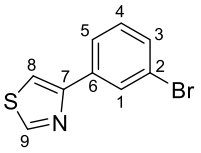

^{13}C NMR (75 MHz, $CDCl_3$): δ / ppm = 153.4 (C-9), 152.6 (C-6), 134.5 (C-2), 131.2 (C-5), 130.3 (C-4), 129.5 (C-1), 128.8 (C-8), 125.0 (C-3), 123.0 (C-7).

2Btz(PhH)Br. Following *General Procedure A* and using 2.35 g (11.0 mmol, 1.10 eq.) 2-bromobenzothiazole. After purification of the crude product by column chromatography (SiO_2, *c*Hex:EtOAc 9:1) the product was isolated as 2.90 g (10.0 mmol, >99%, R_f = 0.71) colorless solid.

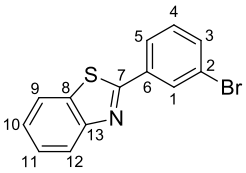

^{1}H NMR (500 MHz, $CDCl_3$): δ / ppm = 8.28 (t, *J* = 1.7 Hz, 1H, H-1), 8.08 (d, *J* = 8.2 Hz, 1H, H-12), 7.98 (dt, *J* = 7.8, 1.2 Hz, 1H, H-3), 7.91 (d, *J* = 8.0 Hz, 1H, H-9), 7.61 (ddd, *J* = 8.0, 1.8, 0.9 Hz, 1H, H-5), 7.51 (ddd, *J* = 8.3, 7.2, 1.1 Hz, 1H, H-11), 7.41 (ddd, *J* = 8.1, 7.1, 1.0 Hz, 1H, H-10), 7.36 (t, *J* = 7.9 Hz, 1H, H-4).

^{13}C NMR (75 MHz, $CDCl_3$): δ / ppm = 166.2 (C-6), 154.0 (C-13), 135.5 (C-8), 133.8 (C-5), 130.5 (C-4), 130.3 (C-1), 126.6 (C-11), 126.2 (C-3), 125.6 (C-10), 123.5 (C-12), 123.2 (C-2, C-7), 121.7 (C-9).

2Qu(PhH)Br. Following *General Procedure A* and using 2.29 g (11.0 mmol, 1.10 eq.) 2-bromoquinoline. After purification of the crude product by column chromatography (SiO_2, *c*Hex:EtOAc 19:1, R_f = 0.52) the product was isolated as 1.65 g (5.81 mmol, 58%) colorless solid.

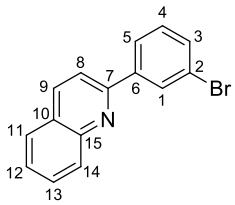

^{1}H NMR (500 MHz, $CDCl_3$): δ / ppm = 8.21 (d, *J* = 8.6 Hz, 1H. H-9), 8.19 – 8.16 (m, 2H, H-1, H-14), 7.87 (d, *J* = 8.6 Hz, 1H, H-8), 7.82 (d, *J* = 8.1 Hz, 1H, H-11), 7.72 (ddd, *J* = 8.4, 6.9, 1.3 Hz, 1H, H-13), 7.52 (dtd, *J* = 6.9, 3.7, 1.8 Hz, 3H, H-3, H-5, H-12), 7.46 (t, *J* = 7.3 Hz, 1H, H-4).

^{13}C NMR (75 MHz, $CDCl_3$): δ / ppm = 157.4 (C-7), 148.3 (C-15), 139.7 (C-10), 136.8 (C-9), 129.7 (C-13), 129.3 (C-1), 128.9 (C-3 C-4, C-5), 127.6 (C-11), 127.47 (C-14), 127.2 (C-2, C-6), 126.3 (C-12), 119.0 (C-8).

5.2.2 Synthesis of Central Ring Substituted N^C^N Protoligands – *General Procedures*

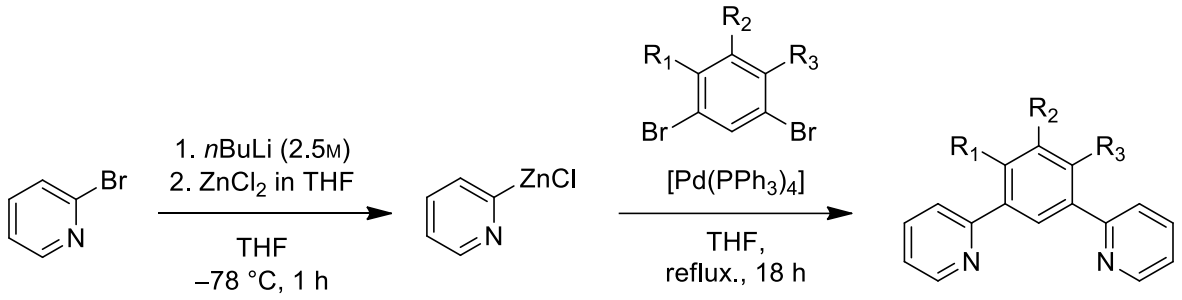

General procedure B.[92] 10.9 g $ZnCl_2$ (80.0 mmol, 4.00 eq.) was dried overnight at 140 °C under vacuum. Under inert conditions, a second flask was equipped with 25.4 mL (64.0 mmol, 3.20 eq.) of a 2.5M solution of *n*BuLi in hexanes, diluted with THF (140 mL) and cooled down to –78 °C. A solution of 5.85 mL (60.0 mmol, 3.00 eq.) 2-bromopyridine in THF (20 mL) was slowly added dropwise and stirred for 1 h. Afterwards, a suspension of the dried $ZnCl_2$ in THF (60 mL) was added to the reaction mixture and the reaction warmed up to rt. Lastly, 1.16 g (1.00 mmol, 0.05 eq.) $[Pd(PPh_3)_4]$ and a substituted 1,3-dibromobenzene (20.0 mmol, 1.00 eq.) were added to the solution, which was then refluxed for 17 h. The reaction was terminated through addition of 3.21 g (60.0 mmol, 3.00 eq.) ammonium chloride in water (10 mL). The solution was extracted three times with dichloromethane (3 x 100 mL), washed three times with water (3 x 100 mL) and dried over anhydrous $MgSO_4$. The combined organic layers were evaporated to isolate the crude product.

PyHPhPy. Following *General Procedure B* and using 4.72 g (20.0 mmol, 1.00 eq.) Br(PhH)Br. The product was purified by column chromatography (SiO_2, *c*Hex:EtOAc 4:1, R_f = 0.22) and obtained as 4.03 g (17.3 mmol, 87%) yellow oil.

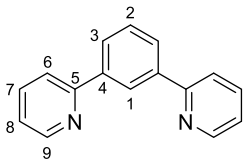

^{1}H NMR (300 MHz, DMSO-d_6) δ / ppm = 8.82 (t, *J* = 1.8 Hz, 1H, H-1), 8.72 (ddd, *J* = 4.8 Hz, 1.9 Hz, 1.0 Hz, 2H, H-9), 8.17 (dd, *J* = 7.8 Hz, 1.9 Hz, 2H, H-6), 8.08 (dt, *J* = 7.9 Hz, 1.1 Hz, 2H, H-3), 7.93 (td, *J* = 7.7 Hz, 1.8 Hz, 2H, H-7), 7.63 (t, *J* = 7.8 Hz, 1H, H-2), 7.40 (ddd, *J* = 7.5 Hz, 4.8 Hz, 1.1 Hz, 2H, H-8).

^{13}C NMR (75 MHz, DMSO-d_6) δ / ppm = 155.8 (C-5), 149.6 (C-9), 139.2 (C-4), 137.3 (C-7), 129.3 (C-2), 127.1 (C-6), 124.7 (C-1), 122.8 (H-8), 120.4 (C-3).

EI(+) MS (70 eV) m/z = 232 $[M]^+$ (100%), 204 $[M\text{-}NCH]^+$ (20%), 154 $[M\text{-}Py]^+$ (10%), 78 $[Py]^+$ (5%).

EA (CHNS) Meas. / % (Calc. for $C_{16}H_{12}N_2$ / %): C, 81.21 (82.73); H, 4.86 (5.21); N, 11.52 (12.06).

Py(5MeOPhH)Py. Following *General Procedure B* and using 5.32 g (20.0 mmol, 1.00 eq.) Br(5MeOPhH)Br. The product was purified by column chromatography (SiO_2, *c*Hex:EtOAc 3:1, R_f = 0.14) and obtained as 5.03 g (19.2 mmol, 96%) yellow solid.

^{1}H NMR (300 MHz, DMSO-d_6) δ / ppm = 8.72 (ddd, *J* = 4.8, 1.8, 0.9 Hz, 2H, H-9), 8.40 (t, *J* = 1.5 Hz, 1H, H-1), 8.11 (dt, *J* = 8.1, 1.1 Hz, 2H, H-6), 7.92 (td, *J* = 7.8, 1.9 Hz, 2H, H-7), 7.74 (d, *J* = 1.5 Hz, 2H, H-3), 7.40 (ddd, *J* = 7.5, 4.8, 1.1 Hz, 2H, H-8), 3.94 (s, 3H, H-10).

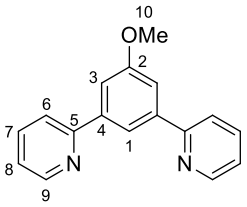

^{13}C NMR (75 MHz, DMSO-d_6) δ / ppm = 160.2 (C-5), 155.6 (C-2), 149.5 (C-9), 140.5 (C-4), 137.3 (C-7), 123.3 (C-8), 120.6 (C-6), 117.2 (C-1), 112.6 (C-3), 56.5 (C-10).

EI(+) MS (70 eV) m/z = 262 $[M]^+$ (100%), 232 $[M\text{-}MeO]^+$ (40%), 204 $[M\text{-}NCH\text{-}MeO]^+$ (5%), 154 $[PhPy]^+$ (20%), 78 $[Py]^+$ (5%).

EA (CHNS) Meas. / % (Calc. for $C_{17}H_{14}N_2O$ / %): C, 80.00 (77.84); H, 5.60 (5.38); N, 10.65 (10.68).

Py(5BuPhH)Py. Following *General Procedure B* and using 5.84 g (20.0 mmol, 1.00 eq.) Br(5BuPhH)Br. The product was purified by column chromatography (SiO_2, *c*Hex:EtOAc 4:1, R_f = 0.30) and obtained as 5.25 g (18.2 mmol, 91%) yellow solid.

^{1}H NMR (300 MHz, DMSO-d_6) δ / ppm = 8.72 (ddd, *J* = 4.9, 1.9, 0.9 Hz, 2H, H-9), 8.56 (t, *J* = 1.7 Hz, 1H, H-1), 8.19 (d, *J* = 1.6 Hz, 2H, H-3), 8.10 (dt, *J* = 8.0, 1.1 Hz, 2H, H-6), 7.92 (td, *J* = 7.7, 1.9 Hz, 2H, H-7), 7.39 (ddd, *J* = 7.5, 4.8, 1.1 Hz, 2H, H-8), 1.42 (s, 9H, H-11).

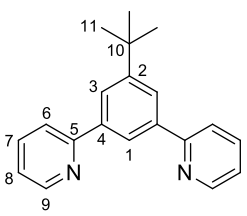

^{13}C NMR (75 MHz, DMSO-d_6) δ / ppm = 156.7 (C-5), 152.2 (C-2), 150.0 (C-9), 139.5 (C-4), 137.7 (C-7), 124.6 (C-3), 123.1 (C-8), 122.7 (C-1), 121.09 (C-6), 35.3 (C-10), 31.7 (C-11).

EI(+) MS (70 eV) m/z = 288 $[M]^+$ (95%), 273 $[M\text{-}CH_3]^+$ (100%), 257 $[M\text{-}2CH_3]^+$ (20%), 232 [M-*t*Bu] (20%), 204 [M-NCH-*t*Bu]$^+$ (5%), 195 $[M\text{-}CH_3\text{-}Py]^+$ (5%), 180 $[M\text{-}2CH_3\text{-}Py]^+$ (5%), 154 $[PhPy]^+$ (20%), 78 $[Py]^+$ (5%).

EA (CHNS) Meas. / % (Calc. for $C_{20}H_{20}N_2$ / %): C, 83.33 (83.30); H, 7.05 (6.99); N, 8.85 (9.71).

Py(5MePhH)Py.[135] Following *General Procedure B* and using 5.00 g (20.0 mmol, 1.00 eq.) Br(5MePhH)Br. The product was purified by column chromatography (SiO_2, *c*Hex:EtOAc 4:1, R_f = 0.25) and obtained as 4.60 g (18.7 mmol, 93%) yellow solid.

^{1}H NMR (300 MHz, DMSO-d_6) δ / ppm = 8.71 (dt, *J* = 3.8, 1.0 Hz, 2H, H-9), 8.61 (d, *J* = 1.8 Hz, 1H, H-1), 8.06 (dt, *J* = 8.0, 1.1 Hz, 2H, H-6), 7.99 (d, *J* = 1.7 Hz, 2H, H-3), 7.91 (td, *J* = 7.7, 1.9 Hz, 2H, H-7), 7.39 (ddd, *J* = 7.4, 4.8, 1.1 Hz, 2H, H-8), 2.49 (s, 3H, H-10).

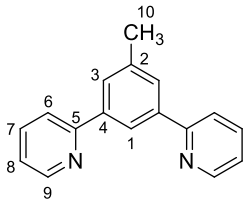

^{13}C NMR (75 MHz, DMSO-d_6) δ / ppm = 156.4 (C-5), 150.0 (C-9), 139.6 (C-2), 138.9 (C-4), 137.7 (C-7), 128.3 (C-3), 123.2 (C-8), 122.5 (C-1), 120.9 (C-6), 21.7 (C-10).

EI(+) MS (70 eV) m/z = 246 $[M]^+$ (100%), 231 $[M\text{-}CH_3]^+$ (5%), 219 [M-NCH]$^+$ (10%), 168 $[M\text{-}Py]^+$ (10%), 139 [M-Py-NCH]$^+$ (5%).

EA (CHNS) Meas. / % (Calc. for $C_{17}H_{14}N_2$ / %): C, 82.80 (82.90); H, 5.76 (5.74); N, 10.31 (11.37).

Py(5PhPhH)Py. Following *General Procedure B* and using 6.24 g (20.0 mmol, 1.00 eq.) Br(5PhPhH)Br. The product was purified by column chromatography (SiO_2, *c*Hex:EtOAc 4:1, R_f = 0.19) and obtained as 5.36 g (17.4 mmol, 87%) yellow solid.

^{1}H NMR (300 MHz, DMSO-d_6) δ / ppm = 8.81 (t, *J* = 1.6 Hz, 1H, H-1), 8.75 (ddd, *J* = 4.8, 1.9, 0.9 Hz, 2H, H-9), 8.41 (d, *J* = 1.7 Hz, 2H, H-3), 8.22 (dt, *J* = 8.0, 1.1 Hz, 2H, H-6), 7.95 (td, *J* = 7.7, 1.9 Hz, 2H, H-7),

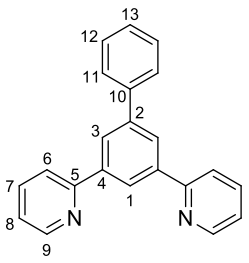

7.87 (d, *J* = 7.0 Hz, 2H, H-11), 7.55 (t, *J* = 7.4 Hz, 2H, H-12), 7.47 – 7.40 (m, 3H, H-8 and H-13).

^{13}C NMR (75 MHz, DMSO-d_6) δ / ppm = 156.0 (C-5), 149.4 (C-9), 141.7 (C-2), 140.3 (C-10), 140.3 (C-4), 137.7 (C-7), 129.4 (C-12), 128.2 (C-13), 127.4 (C-11), 125.8 (C-3), 124.2 (C-1), 123.3 (C-8), 121.1 (C-6).

EI(+) MS (70 eV) m/z = 308 $[M]^+$ (100%), 292 $[M\text{-}CH]^+$ (5%), 280 $[M\text{-}(CH)_2]^+$ (10%), 231 $[M\text{-}Ph]^+$ (10%), 204 $[M\text{-}Ph\text{-}NCH]^+$ (5%), 154 $[PyPh]^+$ (10%), 78 $[Py]^+$ (5%).

EA (CHNS) Meas. / % (Calc. for $C_{22}H_{16}N_2$ / %): C, 84.48 (85.69); H, 5.33 (5.26); N, 8.26 (9.08).

Py(5NO$_2$PhH)Py. Following *General Procedure B* and using 5.62 g (20.0 mmol, 1.00 eq.) Br(5NO$_2$PhH)Br. The product was purified by column chromatography (SiO_2, *c*Hex:EtOAc 3:1, R_f = 0.28) and obtained as 2.24 g (8.08 mmol, 41%) colorless solid.

^{1}H NMR (300 MHz, DMSO-d_6) δ / ppm = 9.20 (t, *J* = 1.5 Hz, 1H, H-1), 8.96 (d, *J* = 1.5 Hz, 2H, H-3), 8.79 (ddd, *J* = 4.7, 1.9, 0.9 Hz, 2H, H-9), 8.32 (d, *J* = 8.0 Hz, 2H, H-6), 8.01 (td, *J* = 7.8, 1.8 Hz, 2H, H-7), 7.50 (ddd, *J* = 7.5, 4.8, 0.8 Hz, 2H, H-8).

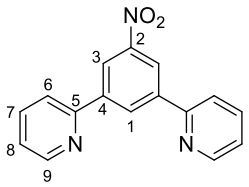

^{13}C NMR (75 MHz, DMSO-d_6) δ / ppm = 153.8 (C-5), 150.3 (C-9), 149.7 (C-2), 141.3 (C-4), 138.2 (C-7), 130.5 (C-1), 124.4 (C-8), 121.7 (C-6), 121.6 (C-3).

EI(+) MS (70 eV) m/z = 277 $[M]^+$ (55%), 247 $[M\text{-}2O]^+$ (10%), 231 $[M\text{-}NO_2]^+$ (100%), 204 $[M\text{-}NO_2\text{-}NCH]^+$ (10%), 152 $[PhPy]^+$ (5%), 115 $[M\text{-}Py\text{-}2O\text{-}(CH)_4]^+$ (10%), 78 $[Py]^+$ (10%).

EA (CHNS) Meas. / % (Calc. for $C_{16}H_{11}N_3O_2$ / %): C, 68.93 (69.31); H, 4.02 (4.00); N, 15.45 (15.15).

Py(5CF$_3$PhH)Py. Following *General Procedure B* and using 6.08 g (20.0 mmol, 1.00 eq.) Br(5CF$_3$PhH)Br. The product was purified by column chromatography (SiO_2, *c*Hex:EtOAc 4:1, R_f = 0.31) and obtained as 5.83 g (19.4 mmol, 97%) yellow solid.

^{1}H NMR (300 MHz, DMSO-d_6) δ / ppm = 9.04 (d, *J* = 1.7 Hz, 1H, H-1), 8.74 (dt, *J* = 4.6, 1.5 Hz, 2H, H-9), 8.47 (d, *J* = 1.6 Hz, 2H, H-3), 8.23 (d, *J* = 8.0 Hz, 2H, H-6), 7.96 (td, *J* = 7.7, 1.8 Hz, 2H, H-7), 7.45 (ddd, *J* = 7.5, 4.8, 1.0 Hz, 2H, H-8).

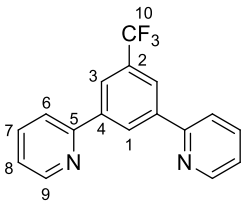

^{19}F NMR (282 MHz, DMSO-d_6) δ / ppm = –61.2 (s, F-10).

^{13}C NMR (75 MHz, DMSO-d_6) δ / ppm = 154.5 (C-5), 150.2 (C-9), 140.8 (C-4), 138.0 (C-7), 130.8 (q, *J* = 31.81 Hz, C-10), 128.5 (C-1), 124.0 (C-8), 123.8 (q, *J* = 3.8 Hz, C-3), 121.4 (C-6).

EI(+) MS (70 eV) m/z = 300 $[M]^+$ (100%), 280 $[M\text{-}F]^+$ (10%), 272 $[M\text{-}NCH]^+$ (10%), 260 $[M\text{-}2F]^+$ (5%), 231 $[M\text{-}CF_3]^+$ (10%), 222 $[M\text{-}Py]^+$ (10%), 202 $[M\text{-}CF_3\text{-}NCH$ and $M\text{-}F\text{-}Py]^+$ (10%), 150 $[M\text{-}CF_3\text{-}Py]^+$ (5%), 78 $[Py]^+$ (10%).

EA (CHNS) Meas. / % (Calc. for $C_{17}H_{11}N_2F_3$ / %): C, 67.97 (68.00); H, 3.74 (3.69); N, 9.38 (9.33).

Py(5FPhH)Py. Following *General Procedure B* and using 5.08 g (20.0 mmol, 1.00 eq.) Br(5FPhH)Br. The product was purified by column chromatography (SiO_2, *c*Hex:EtOAc 4:1, R_f = 0.19) and obtained as 4.03 g (16.1 mmol, 80%) yellow solid.

^{1}H NMR (300 MHz, DMSO-d_6) δ / ppm = 8.74 (ddd, *J* = 4.8, 1.8, 0.9 Hz, 2H, H-9), 8.71 (t, *J* = 1.6 Hz, 1H, H-1), 8.16 (dt, *J* = 8.1, 1.1 Hz, 2H, H-6), 8.01 – 7.91 (m, 4H, H-3 and H-7), 7.44 (ddd, *J* = 7.5, 4.8, 1.1 Hz, 2H, H-8).

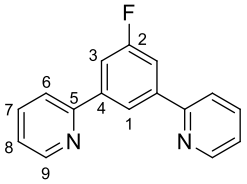

^{19}F NMR (282 MHz, DMSO-d_6) δ / ppm = –112.6 (t, *J* = 10.1 Hz, F-2).

^{13}C NMR (75 MHz, DMSO-d_6) δ / ppm = 163.7 (d, *J* = 242.6 Hz, C-2), 154.9 (d, *J* = 3.0 Hz, C-5), 150.1 (C-9), 142.0 (d, *J* = 8.1 Hz, C-4), 137.9 (C-7), 123.9 (C-8), 121.2 (C-6), 121.0 (d, *J* = 2.4 Hz, C-1), 114.1 (d, *J* = 23.3 Hz, C-3).

EI(+) MS (70 eV) m/z = 250 $[M]^+$ (100%), 229 $[M\text{-}F]^+$ (5%), 222 $[M\text{-}NCH]^+$ (20%), 202 $[M\text{-}F\text{-}NCH]^+$ (5%), 172 $[M\text{-}Py]^+$ (10%), 145 $[M\text{-}Py\text{-}NCH]^+$ (5%), 125 $[M\text{-}F\text{-}Py\text{-}NCH]^+$ (5%), 93 $[PhF]^+$ (5%), 78 $[Py]^+$ (5%), 18 $[F]^+$ (20%).

EA (CHNS) Meas. / % (Calc. for $C_{16}H_{11}N_2F$ / %): C, 75.87 (76.69); H, 4.69 (4.43); N, 10.97 (11.17).

Py(4FPhH)Py. Following *General Procedure B* and using 5.08 g (20.0 mmol, 1.00 eq.) Br(4FPhH)Br. The product was purified by column chromatography (SiO_2, *c*Hex:EtOAc 3:1, R_f = 0.20) and obtained as 4.30 g (17.2 mmol, 86%) yellow solid.

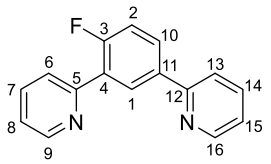

^{1}H NMR (500 MHz, DMSO-d_6) δ / ppm = 8.79 (d, *J* = 4.1 Hz, 1H, H-16), 8.75 – 8.70 (m, 2H, H-1 and H-9), 8.20 (ddd, *J* = 8.5, 4.7, 2.5 Hz, 1H, H-10), 8.03 (dt, *J* = 8.1, 1.2 Hz, 1H, H-6), 7.96 (td, *J* = 7.7, 1.8 Hz, 1H, H-14), 7.91 (td, *J* = 7.8, 1.9 Hz, 1H, H-7), 7.90 – 7.86 (m, 1H, H-13), 7.50 – 7.45 (m, 2H, H-2 and H-15), 7.39 (ddd, *J* = 7.5, 4.7, 1.1 Hz, 1H, H-8).

^{19}F NMR (282 MHz, DMSO-d_6) δ / ppm = –117.3 (s, F-3).

^{13}C NMR (126 MHz, DMSO-d_6) δ / ppm = 160.9 (d, *J* = 252.8 Hz, C-3), 155.2 (C-5), 152.7 (d, *J* = 2.5 Hz, C-12), 150.3 (C-16), 150.1 (C-9), 137.8 (C-7), 137.4 (C-14), 135.8 (d, *J* = 3.3 Hz, C-4), 129.7 (d, *J* = 3.4 Hz, C-1), 129.3 (d, *J* = 9.0 Hz, C-10), 127.6 (d, *J* = 12.1 Hz, C-11), 124.7 (d, *J* = 9.1 Hz, C-13), 123.6 (C-15), 123.2 (C-8), 120.6 (C-6), 117.3 (d, *J* = 23.29 Hz, C-2).

EI(+) MS (70 eV) m/z = 250 $[M]^+$ (100%), 229 $[M\text{-}F]^+$ (10%), 222 $[M\text{-}NCH]^+$ (20%), 202 $[M\text{-}F\text{-}NCH]^+$ (5%), 172 $[M\text{-}Py]^+$ (15%), 145 $[M\text{-}Py\text{-}NCH]^+$ (5%), 125 $[M\text{-}F\text{-}Py\text{-}NCH]^+$ (5%), 78 $[Py]^+$ (10%).

EA (CHNS) Meas. / % (Calc. for $C_{16}H_{11}N_2F$ / %): C, 76.27 (76.69); H, 4.47 (4.43); N, 10.29 (11.17).

Py(4,6FPhH)Py. Following *General Procedure B* and using 5.44 g (20.0 mmol, 1.00 eq.) Br(4,6FPhH)Br. The product was purified by column chromatography (SiO_2, *c*Hex:EtOAc 4:1, R_f = 0.37) and obtained as 3.80 g (14.2 mmol, 71%) yellow solid.

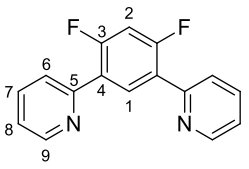

^{1}H NMR (300 MHz, DMSO-d_6) δ / ppm = 8.76 (ddd, *J* = 4.8, 1.9, 1.0 Hz, 2H, H-9), 8.63 (t, *J* = 9.1 Hz, 1H, H-1), 7.95 (td, *J* = 7.7, 1.9 Hz, 2H, H-7), 7.85 (dt, *J* = 8.0, 1.2 Hz, 2H, H-6), 7.56 (t, *J* = 11.2 Hz, 1H, H-2), 7.45 (ddd, *J* = 7.4, 4.8, 1.2 Hz, 2H, H-8).

^{19}F NMR (282 MHz, DMSO-d_6) δ / ppm = –112.4 (t, *J* = 10.4 Hz, F-3).

^{13}C NMR (75 MHz, DMSO-d_6) δ / ppm = 162.1 (d, *J* = 254.5 Hz, C-3), 158.7 (d, *J* = 254.5 Hz, C-5), 151.8 (t, *J* = 1.9 Hz, C-4), 150.4 (C-9), 137.6 (C-7), 133.4 (t, *J* = 4.5 Hz, C-1), 124.5 (t, *J* = 4.8 Hz, C-6), 123.6 (C-8), 106.0 (t, *J* = 27.7 Hz, C-2).

EI(+) MS (70 eV) m/z = 268 $[M]^+$ (100%), 247 $[M-F]^+$ (10%), 240 $[M-NCH]^+$ (20%), 220 $[M-F-NCH]^+$ (5%), 203 $[M-2F-NCH]^+$ (5%), $[M-Py]^+$ (10%), 163 $[M-Py-NCH]^+$ (5%), 78 $[Py]^+$ (10%).

EA (CHNS) Meas. / % (Calc. for $C_{16}H_{10}N_2F_2$ / %): C, 71.27 (71.64); H, 3.88 (3.76); 10.13 (10.44).

Py(4,6MePhH)Py.[140] Following *General Procedure B* and using 5.28 g (20.0 mmol, 1.00 eq.) Br(4,6MePhH)Br. The product was purified by column chromatography (SiO_2, *c*Hex:EtOAc 5:1, R_f = 0.14) and obtained as 4.14 g (15.9 mmol, 84%) yellow solid.

^{1}H NMR (300 MHz, DMSO-d_6) δ / ppm = 8.67 (ddd, *J* = 4.8, 1.9, 1.0 Hz, 2H, H-9), 7.87 (td, *J* = 7.7, 1.9 Hz, 2H, H-7), 7.57 (dt, *J* = 7.9, 1.1 Hz, 2H, H-6), 7.46 (s, 1H, H-1), 7.36 (ddd, *J* = 7.6, 4.8, 1.1 Hz, 2H, H-8), 7.26 (s, 1H, H-2), 2.38 (s, 6H, H-10).

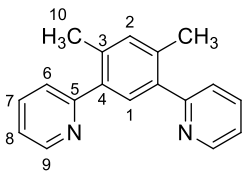

^{13}C NMR (75 MHz, DMSO-d_6) δ / ppm = 158.7 (C-5), 149.0 (C-9), 137.7 (C-4), 136.5 (C-7), 135.2 (C-3), 133.1 (C-2), 131.0 (C-1), 123.9 (C-6), 121.88 (C-8), 19.8 (C-10).

EI(+) MS (70 eV) m/z = 259 (100%) $[M]^+$, 245 (95%) $[M-CH_3]^+$, 182 (10%) $[M-Py]^+$, 167 (10%) $[M-Py-CH_3]^+$, 129 (20%) $[PyPh-NCH]^+$, 102 (5%) $[(CH_3)_2Ph]^+$, 78 (5%) $[Py]^+$.

EA (CHNS) Meas. / % (Calc. for $C_{18}H_{16}N_2$ / %): C, 83.07 (83.04); H, 6.13 (6.19); N, 10.66 (10.76).

Py(4,5,6MeOPhH)Py. Following *General Procedure B* and using 6.52 g (20.0 mmol, 1.00 eq.) Br(4,5,6MeOPhH)Br. The product was purified by column chromatography (SiO_2, *c*Hex:EtOAc 1:4, R_f = 0.38) and obtained as 1.97 g (6.11 mmol, 30%) yellow solid.

^{1}H NMR (300 MHz, DMSO-d_6) δ / ppm = 8.69 (dt, J = 4.8, 1.5 Hz, 2H, H-9), 7.96 (s, 1H, H-1), 7.86 (m, 4H, H-7 and H-6), 7.36 (ddd, J = 6.7, 4.9, 2.3 Hz, 2H, H-8), 3.94 (s, 3H, H-10), 3.81 (s, 6H, H-11).

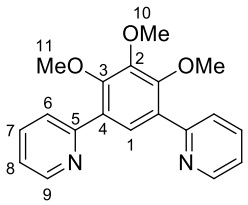

^{13}C NMR (75 MHz, DMSO-d_6) δ / ppm = 155.1 (C-5), 152.6 (C-3), 149.9 (C-9), 146.9 (C-2), 136.9 (C-7), 129.6 (C-4), 127.0 (C-1), 124.5 (C-6), 122.7 (C-8), 61.5 (C-11), 61.3 (C-10).

EI(+) MS (70 eV) m/z = 322 $[M]^+$ (10%), 307 $[M\text{-}CH_3]^+$ (100%), 293 $[M\text{-}MeO]^+$ (10%), 279 $[M\text{-}3CH_3]^+$ (15%), 273 $[M\text{-}MeO\text{-}CH_3]^+$ (20%), 264 $[M\text{-}MeO\text{-}NCH]^+$ (40%), 231 $[M\text{-}3MeO]^+$ (5%), 207 $[M\text{-}2NCH\text{-}2MeO]^+$ (15%), 166 $[M\text{-}2Py]^+$ (5%).

EA (CHNS) Meas. / % (Calc. for $C_{19}H_{18}N_2O_3$ / %): C, 69.44 (70.79); H, 5.81 (5.63); N, 7.79 (8.69).

Py(PyH)Py.[141] Following *General Procedure B* and using 4.74 g (20.0 mmol, 1.00 eq.) Br(PyH)Br. The product was purified by column chromatography (SiO_2, EtOAc, R_f = 0.20) and obtained as 3.31 g (14.2 mmol, 71%) colorless solid.

^{1}H NMR (300 MHz, DMSO-d_6) δ / ppm = 9.34 (d, J = 2.2 Hz, 2H, H-2), 9.09 (t, J = 2.2 Hz, 1H, H-1), 8.77 (dd, J = 4.8, 0.9 Hz, 2H, H-8), 8.20 (d, J = 7.9 Hz, 2H, H-5), 7.98 (td, J = 7.8, 1.9 Hz, 2H, H-7), 7.47 (ddd, J = 7.5, 4.8, 1.1 Hz, 2H, H-6).

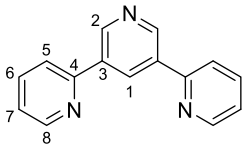

^{13}C NMR (75 MHz, DMSO-d_6) δ / ppm = 154.0 (C-4), 150.4 (C-8), 148.4 (C-2), 138.0 (C-7), 135.0 (C-3), 132.1 (C-1), 123.5 (C-6), 121.4 (C-5).

EI(+) MS (70 eV) m/z = 233 $[M]^+$ (100%), 205 $[M\text{-}NCH]^+$ (15%), 155 $[M\text{-}Py]^+$ (45%), 128 $[M\text{-}Py\text{-}NCH]^+$ (5%), 78 $[Py]^+$ (10%).

EA (CHNS) Meas. / % (Calc. for $C_{15}H_{11}N_3$ / %): C, 76.83 (77.23); H, 4.97 (4.75); N, 16.83 (18.01).

5.2.3 Synthesis of N^C^N Ligands with a Variation of the π-Acceptor Unit

5.2.3.1 Synthesis of 1-Chlorosubstituted Ligands *via Suzuki* conditions – *General Procedures*

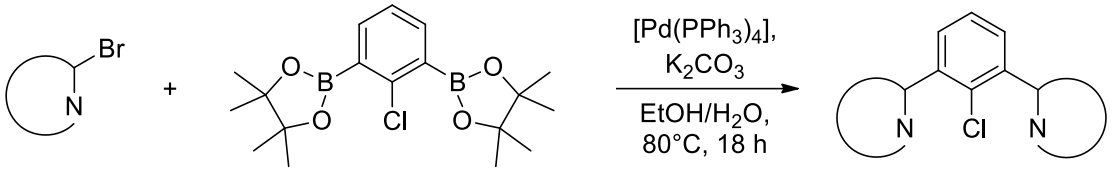

General Procedure C.[203] 1.82 g (5.00 mmol, 1.00 eq.) Bpin(2ClPh)Bpin**,** equivalent amounts 2-bromo heteroaromat (11.5 mmol, 2.30 eq.), 2.07 g (15.0 mmol, 3.00 eq.) K_2CO_3 and 0.35 g (0.30 mmol, 0.06 eq.) $[Pd(PPh_3)_4]$ were added into a degassed mixture of EtOH/H_2O (60 mL, 4:1), heated to reflux overnight and cooled to room temperature. Removal of the solvent under reduced pressure gave a crude product, which was dissolved in EtOAc (100 mL) and H_2O (100 mL) was added. After the phases were separated, the aqueous phase was extracted with EtOAc (3 x 100 mL). The organic phase was dried over anhydrous $MgSO_4$, and the solvent was removed under reduced pressure.

2Tz(ClPh)2Tz. Following *General Procedure C* and using 1.89 g (11.5 mmol, 2.30 eq.) 2-bromothiazole. The crude product was purified by column chromatography (SiO_2*,* *c*Hex:EtOAc 4:1, R_f = 0.43) and yielded 1.30 g (4.66 mmol, 93%) colorless solid.

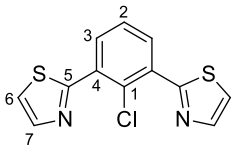

^{1}H NMR (500 MHz, DMSO-d_6, mixture of rotamers) δ / ppm = 8.19 (d, *J* = 7.8 Hz, 2H, H-3), 8.08 (d, *J* = 3.2 Hz, 1.7 H, H-7), 8.03 (d, *J* = 3.2 Hz, 1.7 H, H-6), 8.00 (d, *J* = 3.1 Hz, 0.3 H, H-6), 7.94 (d, *J* = 3.1 Hz, 0.3 H, H-7), 7.65 (t, *J* = 7.8 Hz, 1H, H-2).

^{13}C NMR (75 MHz, DMSO-d_6) δ / ppm = 162.8 (C-5), 144.6 (C-7), 143.4 (C-7), 133.7 (C-1, C-4), 132.7 (C-3), 128.2 (C-2), 123.2 (C-6), 123.1 (C-6).

EI(+) MS (70eV) m/z = 278 $[M]^+$ (100%), 243 $[M\text{-}Cl]^+$ (25%), 221 $[M\text{-}(CH)_2S]^+$ (40%), 58 $[(CH)_2S]^+$ (20%).

EA (CHNS) Meas. / % (Calc. for $C_{12}H_7ClN_2S_2$ / %): C, 51.29 (51.70); H, 2.82 (2.53); N, 9.07 (10.05); S, 21.13 (23.00).

4Tz(ClPh)4Tz. Following *General Procedure C* and using 1.89 g (11.5 mmol, 2.30 eq.) 4-bromothiazole. The crude product was purified by column chromatography (SiO_2, *c*Hex:EtOAc 4:1, R_f = 0.31) and gave 0.86 g (3.08 mmol, 62%) pale-yellow solid.

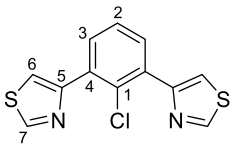

^{1}H NMR (300 MHz, DMSO-d_6) δ / ppm = 9.24 (d, *J* = 1.9 Hz, 1.83H, H-7), 9.20 (d, *J* = 2.0 Hz, 0.13H, H-7), 8.15 (d, *J* = 1.8 Hz, 0.13H, H-6), 8.11 (d, *J* = 1.9 Hz, 1.74H, H-6), 8.07 (d, *J* = 2.0 Hz, 0.13H, H-6), 7.79 (d, *J* = 7.7 Hz, 2H, H-3), 7.53 (t, *J* = 7.7 Hz, 1H, H-2).

^{13}C NMR (75 MHz, DMSO-d_6) δ / ppm = 154.1 (C-7), 152.7 (C-5), 135.2 (C-1, C-4), 131.9 (C-3), 127.5 (C-2), 119.7 (C-6).

EI(+) MS (70eV) m/z = 278 $[M]^+$ (100%), 251 $[M\text{-}NCH]^+$ (30%), 243 $[M\text{-}Cl]^+$ (60%), 224 $[M\text{-}2NCH]^+$ (25%), 216 $[M\text{-}Cl\text{-}NCH]^+$ (25%), 189 $[M\text{-}Cl\text{-}2NCH]^+$ (25%).

EA (CHNS) Meas. / % (Calc. for $C_{12}H_7ClN_2S_2$ / %): C, 51.59 (51.70); H, 2.74 (2.53); N, 9.34 (10.05); S, 22.32 (23.00).

2Btz(ClPh)2Btz. Following *General Procedure C* and using 2.46 g (11.5 mmol, 2.30 eq.) 2-bromobenzothiazole. The crude product was purified by column chromatography (SiO_2, *c*Hex:EtOAc 4:1, R_f = 0.31) and gave 1.16 g (3.07 mmol, 61%) yellow solid.

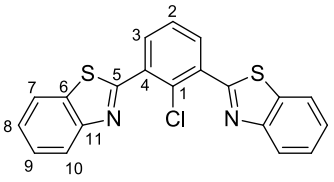

^{1}H NMR (300 MHz, CD_2Cl_2) δ / ppm = 8.23 (d, *J* = 7.8 Hz, 2H, H-10), 8.14 (d, *J* = 8.1 Hz, 2H, H-3), 8.01 (d, *J* = 8.0 Hz, 2H, H-7), 7.63 – 7.53 (m, 3H, H-2, H-9), 7.48 (t, *J* = 7.2 Hz, 2H, H-8). Sample barely soluble in DMSO-d_6.

^{13}C NMR (75 MHz, CD_2Cl_2) δ / ppm = 162.9 (C-5), 151.9 (C-11), 136.7 (C-4), 134.2 (C-10), 133.5 (C-6), 127.2 (C-2), 126.4 (C-9), 125.7 (C-8), 125.6 (C-1), 123.5 (C-3), 121.5 (C-7).

EI(+) MS (70eV) m/z = 378 $[M]^+$ (100%), 343 $[M\text{-}Cl]^+$ (20%), 311 $[M\text{-}Cl\text{-}S]^+$ (20%), 189 $[M\text{-}Cl\text{-}PhNS]^+$ (15%), 108 $[PhS]^+$ (20%).

EA (CHNS) Meas. / % (Calc for $C_{20}H_{11}ClN_2S_2$ / %): C, 62.64 (63.40); H, 2.86 (2.93); N, 7.04 (7.39); S, 16.53 (16.92).

2Qu(ClPh)2Qu. Following *General Procedure C* and using 2.39 g (11.5 mmol, 2.30 eq.) 2-bromoquinoline. The crude product was purified by precipitation from *c*Hex and gave 1.60 g (4.36 mmol, 87%) yellow solid.

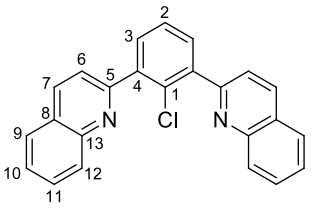

^{1}H NMR (500 MHz, CD_2Cl_2) δ / ppm = 8.26 (d, *J* = 8.5 Hz, 2H, H-12), 8.15 (d, *J* = 8.4 Hz, 2H, H-7), 7.92 (d, *J* = 8.1 Hz, 2H, H-9), 7.77 (dt, *J* = 8.3, 3.3 Hz, 4H, H-6, H-11), 7.73 (d, *J* = 7.6 Hz, 2H, H-3), 7.61 (t, *J* = 7.1 Hz, 2H, H-10), 7.57 (t, *J* = 7.6 Hz, 1H, H-2). Sample barely soluble in DMSO-d_6.

^{13}C NMR (75 MHz, CD_2Cl_2) δ / ppm = 157.7 (C-5), 148.1 (C-13), 140.9 (C-4), 135.6 (C-12), 131.7 (C-3), 130.4 (C-1), 129.6 (C-11), 129.6 (C-7), 127.6 (C-9), 127.2 (C-8), 127.0 (C-2), 126.8 (C-10), 122.9 (C-6).

EI(+) MS (70eV) m/z = 366 $[M]^+$ (70%), 331 $[M\text{-}Cl]^+$ (100%), 304 $[M\text{-}Cl\text{-}NCH]^+$ (5%), 277 (1%) $[M\text{-}PhCH]^+$, 238 (5%) $[M\text{-}Qu]^+$, 204 (5%) $[M\text{-}Cl\text{-}Qu]^+$, 164 (5%) $[Qu+0.5Ph]^+$, 152 (5%) $[Qu+CCH]^+$, 128 (10%) $[Qu]^+$, 75 (5%) $[Ph]^+$.

EA (CHNS) Meas. / % (Calc. for $C_{24}H_{15}ClN_2$ / %): C, 78.42 (78.58); H, 4.13 (4.12); N, 7.55 (7.64).

5.2.3.2 Synthesis of the 4,6-Difluorophenyl-containing Ligands *via Suzuki* conditions – *General Procedures*

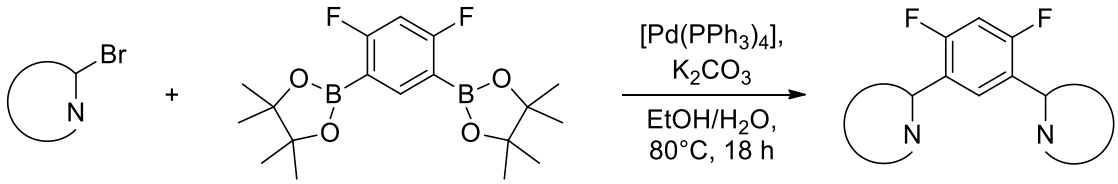

*General Procedur*e D.[203] 1.28 g (3.50 mmol, 1.00 eq.) Bpin(4,6FPhH)Bpin**,** a brominated heteroaromat (8.05 mmol, 2.30 eq.), 1.45 g (10.5 mmol, 3.00 eq.) K_2CO_3 and 0.20 g (0.21 mmol, 0.06 eq.) $[Pd(PPh_3)_4]$ were added into a degassed mixture of EtOH/H_2O (40 mL, 4:1), heated to reflux overnight and cooled to room temperature. Removal of the solvent under reduced pressure a crude product was obtained, which was re-dissolved in EtOAc (50 mL) and H_2O (50 mL) was added. After the phases were separated, the aqueous phase was extracted with EtOAc (3 x 50 mL). The organic phase was dried over anhydrous $MgSO_4$, and the solvent was removed under reduced pressure.

3FPy(4,6FPhH)3FPy. Following *General Procedure D* and using 1.43 g (8.05 mmol, 2.30 eq.) 2-bromo-3-fluoropyridine. The product was purified by column chromatography (SiO_2, *c*Hex:EtOAc 8:1, R_f = 0.09) and obtained as 0.28 g (0.92 mmol, 26%) brown solid.

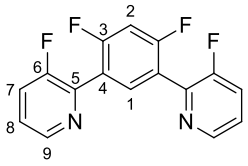

^{1}H NMR (500 MHz, DMSO-d_6) δ / ppm = 8.60 (dt, *J* = 4.5, 1.5 Hz, 2H, H-9), 7.96 – 7.85 (m, 3H, H-1 and H-7), 7.66 – 7.59 (m, 3H, H-2 and H-8).

^{19}F NMR (282 MHz, DMSO-d_6) δ / ppm = –109.2 (m, F-6), –121.6 (m, F-3).

^{13}C NMR (75 MHz, DMSO-d_6) δ / ppm = 162.3 (C-3), 155.6 (C-6), 146.6 (d, *J* = 5.07 Hz, C-9), 140.9 (C-5), 134.9 (C-1), 126.2 (d, *J* = 4.3 Hz, C-8), 124.8 (d, *J* = 19.5 Hz, C-6), 120.5 (C-4), 105.5 (C-2).

EI(+) MS (70 eV) m/z = 304 $[M]^+$ (100%), 285 $[M-F]^+$ (45%), 276 $[M-NCH]^+$ (10%), 265 $[M-2F]^+$ (10%), 258 $[M-CHN-F]^+$ (25%), 245 $[M-3F]^+$ (5%), 152 $[PhPy]^+$ (10%).

EA (CHNS) Meas. / % (Calc. for $C_{16}H_8N_2F_4$ / %): C, 62.04 (63.16); H, 3.11 (2.65); N, 7.21 (9.21).

2^{i}Qu(4,6FPhH)2^{i}Qu. Following *General Procedure D* and using 1.69 g (8.05 mmol, 2.30 eq.) 2-bromoisoquinoline. The product was purified by column chromatography (SiO_2, *c*Hex:EtOAc 2:1, R_f = 0.29) and obtained as 1.21 g (3.28 mmol, 94%) colorless solid.

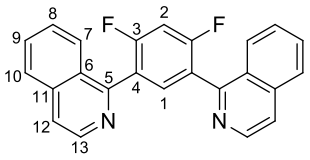

^{1}H NMR (500 MHz, $CDCl_3$) δ / ppm = 8.62 (d, *J* = 5.7 Hz, 2H, H-13), 7.93 (d, *J* = 8.5 Hz, 2H, H-7), 7.90 (d, *J* = 8.2 Hz, 2H, H-10), 7.85 (t, *J* = 8.0 Hz, 1H, H-1), 7.75 – 7.69 (m, 4H, H-9 and H-12), 7.60 (ddd, *J* = 8.2, 6.8, 1.0 Hz, 2H, H-8), 7.19 (t, *J* = 9.4 Hz, 1H, H-2).

^{19}F NMR (282 MHz, $CDCl_3$) δ / ppm = –109.0 (t, *J* = 8.6 Hz, F-3).

^{13}C NMR (126 MHz, $CDCl_3$) δ / ppm = 161.5 (d, *J* = 12.5 Hz, C-3), 159.5 (d, *J* = 12.5 Hz, C-4), 154.7 (C-5), 142.3 (C-13), 136.4 (C-11), 135.2 (t, *J* = 4.8 Hz, C-1), 130.4 (C-9), 127.7 (C-8), 127.5 (C-6), 127.2 (C-7), 127.0 (C-10), 121.0 (C-12), 104.5 (t, *J* = 26.3 Hz, C-2).

EI(+) MS (70 eV) m/z = 368 $[M]^+$ (100%), 347 $[M-F]^+$ (40%), 326 $[M-2F]^+$ (10%), 299 $[M-CHN-2F]^+$ (5%), 277 [M-2F-C4H4 and M-2F-2NCH]$^+$ (10%), 240

[M-^{i}Qu]$^{+}$ (65%), 220 [M-^{i}Qu-F]$^{+}$ (10%), 183 [M-^{i}Qu-C_4H_4]$^{+}$ (30%), 173 [M-2F-^{i}Qu-NCH]$^{+}$ (10%), 128 [^{i}Qu]$^{+}$ (30%).

EA (CHNS) Meas. / % (Calc. for $C_{24}H_{14}N_2F_2$ / %): C, 77.07 (78.25); H, 4.50 (3.83); N, 6.65 (7.60).

5.2.3.3 Synthesis of Central Ring unsubstituted Ligands *via Suzuki* conditions – *General Procedures*

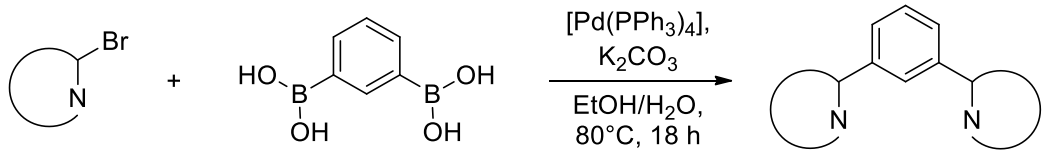

General Procedure E.[203] 0.83 g (5.00 mmol, 1.00 eq.) Phenylene-1,3-diboronic acid**,** a brominated heteroaromat (11.5 mmol, 2.30 eq.), 2.07 g (15.0 mmol, 3.0 eq.) K_2CO_3 and 0.35 g (0.30 mmol, 0.06 eq.) [$Pd(PPh_3)_4$] were added into a degassed mixture of EtOH/H_2O (60 mL, 4:1), heated to reflux overnight and cooled to room temperature. By removal of the solvent under reduced pressure a crude product was obtained, which was re-dissolved in EtOAc (50 mL) and H_2O (50 mL) was added. After the phases were separated, the aqueous phase was extracted with EtOAc (3 x 50 mL). The organic phase was dried over anhydrous $MgSO_4$ and the solvent was removed under reduced pressure.

Pym(PhH)Pym. Following *General Procedure E* and using 1.83 g (11.5 mmol, 2.30 eq.) 2-bromopyrimidine. The crude product was purified by column chromatography (SiO_2, *c*Hex:EtOAc 2:1, R_f = 0.31) to obtain the product as 0.92 g (3.93 mmol, 78%) colorless solid.

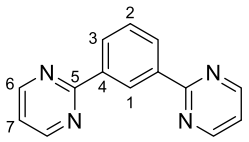

^{1}H NMR (500 MHz, DMSO-d_6) δ / ppm = 9.55 (s, 1H, H-1), 8.99 (d, *J* = 4.8 Hz, 4H, H-6), 8.58 (dd, *J* = 7.8, 1.7 Hz, 2H, H-3), 7.71 (t, *J* = 7.8 Hz, 1H, H-2), 7.52 (t, *J* = 4.8 Hz, 2H, H-7).

^{13}C NMR (126 MHz, DMSO-d_6) δ / ppm = 163.4 (C-5), 158.3 (C-6), 138.2 (C-4), 130.3 (C-3), 139.7 (C-2), 127.7 (C-1), 120.6 (C-7).

EI(+) MS (70eV) m/z = 234 [M]$^{+}$ (100%), 206 [M-NCH]$^{+}$ (15%), 181 [M-2(NCH)]$^{+}$ (45%), 155 [M-Pym]$^{+}$ (5%), 128 [M-Pym-NCH]$^{+}$ (30%).

EA (CHNS) Meas. / % (Calc. for $C_{14}H_{10}N_4$ / %): C, 72.24 (71.78); H, 4.47 (4.30); N, 23.35 (23.92).

2^{i}Qu(PhH)2^{i}Qu. Following *General Procedure E* and using 2.39 g (11.5 mmol, 2.30 eq.) 2-bromoisoquinoline. The crude product was purified by column chromatography (SiO_2, *c*Hex:EtOAc 1:1, R_f = 0.34) to obtain the product as 1.63 g (4.90 mmol, 98%) colorless solid.

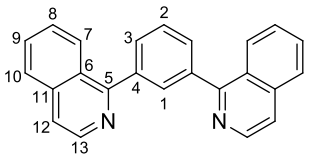

^{1}H NMR (500 MHz, $CDCl_3$) δ / ppm =8.64 (d, *J* = 5.8 Hz, 2H, H-13), 8.24 (d, *J* = 8.5 Hz, 2H, H-7), 8.06 (t, *J* = 1.4 Hz, 1H, H-1), 7.95 – 7.87 (m, 4H, H-3 and H-10), 7.76 (t, *J* = 7.6 Hz, 1H, H-2), 7.74 – 7.69 (m, 4H, H-9 and H-12), 7.59 (ddd, *J* = 8.4, 6.9, 1.4 Hz, 2H, H-8).

^{13}C NMR (75 MHz, $CDCl_3$) δ / ppm = 160.4 (C-5), 142.3 (C-13), 139.7 (C-4), 137.6 (C-6), 136.9 (C-11), 131.5 (C-1), 130.2 (C-9), 130.1 (C-3), 128.6 (C-2), 127.6 (C-7), 127.3 (C-8), 127.0 (C-10), 120.1 (C-12).

EI(+) MS (70eV) m/z = 331 $[M]^+$ (100%), 304 $[M\text{-}NCH]^+$ (5%), 277 $[M\text{-}2(NCH)]^+$ (10%), 229 $[M\text{-}2(NCH)\text{-}C_4H_4]^+$ (5%), 204 $[M\text{-}^{i}Qu]^+$ (40%), 176 $[M\text{-}^{i}Qu\text{-}NCH]^+$ (5%), 165 $[0.5M]^+$ (25%), 151 $[M\text{-}^{i}Qu\text{-}C_4H_4]^+$ (10%), 128 $[^{i}Qu]^+$ (15%).

EA (CHNS) Meas. / % (Calc. for $C_{24}H_{16}N_2$ / %): C, 80.96 (86.72); H, 5.14 (4.85); N, 7.31 (8.43).

3ClPy(PhH)3ClPy. Following *General Procedure E* and using 2.21 g (11.5 mmol, 2.30 eq.) 2-bromo-3-chloropyridine. The crude product was purified by column chromatography (SiO_2, *c*Hex:EtOAc 9:1, R_f = 0.11) to obtain the product as 0.82 g (2.72 mmol, 55%) colorless solid.

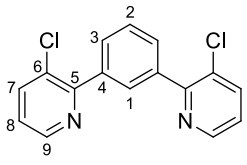

^{1}H NMR (300 MHz, DMSO-d_6) δ / ppm = 8.66 (dd, *J* = 4.6, 1.4 Hz, 2H, H-9), 8.08 (dd, *J* = 8.1, 1.4 Hz, 2H, H-7), 7.99 (t, *J* = 1.6 Hz, 1H, H-1), 7.80 (dd, *J* = 7.8, 1.5 Hz, 2H, H-3), 7.64 (t, *J* = 7.8 Hz, 1H, H-2), 7.47 (dd, *J* = 8.1, 4.6 Hz, 2H, H-8).

^{13}C NMR (75 MHz, DMSO-d_6) δ / ppm = 155.4 (C-5), 148.6 (C-9), 138.9 (C-7), 138.1 (C-6), 130.5 (C-1), 130.1 (C-3), 129.7 (C-4), 128.3 (C-2), 124.7 (C-8).

EI(+) MS (70eV) m/z = 300 $[M]^+$ (45%), 273 $[M\text{-}NCH]^+$ (10%), 265 $[M\text{-}Cl]^+$ (100%), 238 $[M\text{-}Cl\text{-}NCH]^+$ (5%), 229 $[M\text{-}2Cl]^+$ (25%), 201 $[M\text{-}2Cl\text{-}NCH]^+$ (10%), 188 $[M\text{-}ClPy]^+$ (5%), 175 $[M\text{-}2Cl\text{-}2NCH]^+$ (5%), 153 $[M\text{-}ClPy\text{-}N(CH)_2]^+$ (5%).

EA (CHNS) Meas. / % (Calc. for $C_{16}H_{10}N_2Cl_2$ / %): C, 57.15 (57.26); H, 2.81 (2.70); N, 7.64 (8.35).

5.2.3.4 Synthesis of Central Ring Unsubstituted Protoligands using *Negishi* conditions[92]

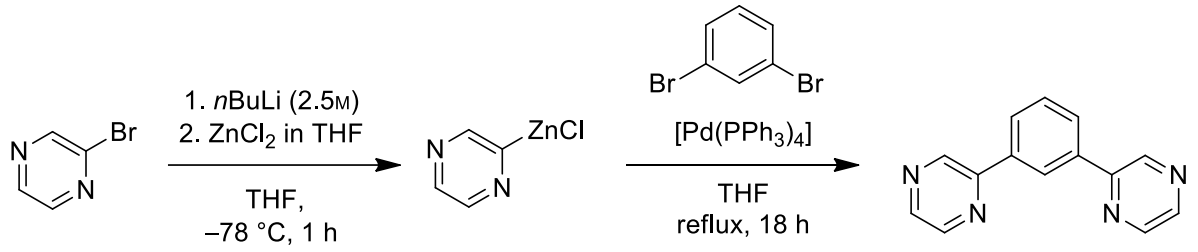

Pz(PhH)Pz. 10.9 g (80.0 mmol, 4.00 eq.) $ZnCl_2$ was dried overnight at 140 °C under vacuum. Under inert conditions, a second flask was equipped with 25.4 mL (64.0 mmol, 3.20 eq.) of a 2.5M solution of *n*BuLi in hexanes, diluted with THF (140 mL) and cooled down to –78 °C. A solution of 9.54 g (60.0 mmol, 3.00 eq.) 2-bromopyrazine in THF (20 mL) was slowly added dropwise and stirred for 1 h. Afterwards, a suspension of the dried $ZnCl_2$ in THF (60 mL) was added to the reaction mixture and the reaction warmed up to rt. Lastly, 1.16 g (1.00 mmol, 0.05 eq.) $[Pd(PPh_3)_4]$ and 2.42 mL (20.0 mmol, 1.00 eq.) 1,3-dibromo-benzene were added to the solution, which was then refluxed for 17 h. The reaction was terminated through addition of 3.21 g (60.0 mmol, 3.00 eq.) ammonium chloride in water (10 mL). The solution was extracted three times with chloroform (3 x 100 mL), washed three times with water (3 x 100 mL) and dried over anhydrous $MgSO_4$. The combined organic layers were evaporated to isolate the crude product. The product was purified by column chromatography (SiO_2, EtOAc, R_f = 0.37) and obtained as 1.42 g (6.07 mmol, 30%) colorless solid.

^{1}H NMR (300 MHz, DMSO-d_6) δ / ppm = 9.42 (d, *J* = 1.4 Hz, 2H, H-8), 8.90 (t, *J* = 1.6 Hz, 1H, H-1), 8.78 (dd, *J* = 2.4, 1.6 Hz, 2H, H-6), 8.68 (d, *J* = 2.5 Hz, 2H, H-7), 8.29 (dd, *J* = 7.8, 1.8 Hz, 2H, H-3), 7.73 (t, *J* = 7.8 Hz, 1H, H-2).

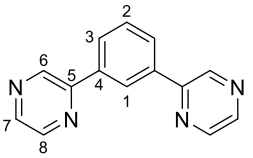

^{13}C NMR (75 MHz, DMSO-d_6) δ / ppm = 151.5 (C-5), 144.8 (C-6), 144.3 (C-7), 142.8 (C-8), 137.2 (C-4), 130.3 (C-2), 128.6 (C-3), 125.5 (C-1).

EI(+) MS (70 eV) m/z = 234 $[M]^+$ (100%), 206 $[M\text{-}NCH]^+$ (10%), 181 $[M\text{-}2NCH]^+$ (25%), 154 $[M\text{-}Pz]^+$ (10%), 128 $[M\text{-}Pz\text{-}NCH]^+$ (30%), 81 $[Pz]^+$ (5%).

EA (CHNS) Meas. / % (Calc. for $C_{14}H_{10}N_4$ / %): C, 71.41 (71.78); H, 4.21 (4.30); N, 24.00 (23.92).

5.2.3.5 Synthesis of Asymmetric N^C^N' Protoligands using *Negishi* conditions – *General Procedure*

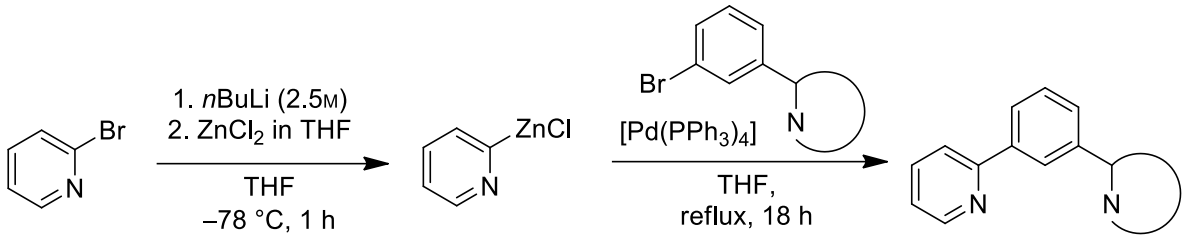

General Procedure F.[92] 1.26 g (9.00 mmol, 2.00 eq.) $ZnCl_2$ was dried overnight at 140 °C under vacuum. Under inert conditions, a second flask was equipped with 3.06 mL (7.65 mmol, 1.70 eq.) of a 2.5M solution of *n*BuLi in hexanes, diluted with THF (40 mL) and cooled down to –78 °C. A solution of 1.07 g (6.75 mmol, 1.50 eq.) 2-bromopyridine in THF (5 mL) was slowly added dropwise and stirred for 30 min. Afterwards, a suspension of the dried $ZnCl_2$ in THF (60 mL) was added to the reaction mixture and the reaction warmed up to rt. Lastly, 0.26 g (0.23 mmol, 0.05 eq.) $[Pd(PPh_3)_4]$ and equivalent amounts (4.50 mmol, 1.00 eq.) of HetAr(PhH)Br were added to the solution, which was then refluxed for 17 h. The reaction was terminated through addition of 0.72 g (13.5 mmol, 3.00 eq.) ammonium chloride in water (10 mL). The solution was extracted three times with EtOAc (3 x 50 mL), washed three times with water (3 x 50 mL) and dried over anhydrous $MgSO_4$. The combined organic layers were evaporated to isolate the crude product.

2Tz(PhH)Py. Following *General Procedure F* and using 1.08 g (4.50 mmol, 1.00 eq.) 2Tz(PhH)Br. Purification of the crude product by column chromatography (SiO_2, *c*Hex:EtOAc 4:1, R_f = 0.36) gave 0.85 g (3.57 mmol, 80%) yellow oil.

^{1}H NMR (500 MHz, DMSO-d_6) δ / ppm = 8.74 (d, *J* = 4.0 Hz, 1H, H-14), 8.70 (t, *J* = 1.7 Hz, 1H, H-1), 8.19 (dt, *J* = 7.8, 1.2 Hz, 1H, H-8), 8.08 (dt, *J* = 8.1, 1.2 Hz, 1H, H-11), 8.04 (dt, *J* = 7.7, 1.2 Hz, 1H, H-3), 7.99 (d, *J* = 3.2 Hz, 1H, H-7), 7.94 (td, *J* = 7.7, 1.8 Hz, 1H, H-12), 7.85 (d, *J* = 3.2 Hz, 1H, H-6), 7.64 (t, *J* = 7.8 Hz, 1H, H-2), 7.42 (ddd, *J* = 7.4, 4.8, 0.8 Hz, 1H, H-13).

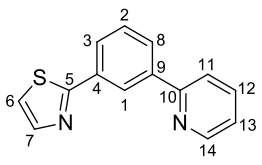

^{13}C NMR (75 MHz, DMSO-d_6) δ / ppm = 167.4 (C-5), 155.5 (C-10), 150.2 (C-14), 144.4 (C-7), 140.0 (C-9), 137.5 (C-12), 134.1 (C-6), 130.3 (C-2), 128.6 (C-8), 127.7 (C-3), 124.6 (C-1), 123.6 (C-13), 121.2 (C-6), 121.0 (C-11).

EI(+) MS (70 eV) m/z = 238 $[M]^+$ (100%), 205 $[M\text{-}S]^+$ (10%), 181 $[M\text{-}S(CH)_2]^+$ (55%), 152 $[M\text{-}Tz]^+$ (5%), 78 $[Py]^+$ (5%).

EA (CHNS) Meas. / % (Calc. for $C_{14}H_{10}N_2S$ / %): C, 70.59 (70.56); H, 4.29 (4.23); N, 11.74 (11.76); S, 13.38 (13.45).

4Tz(PhH)Py. Following *General Procedure F* and using 1.08 g (4.50 mmol, 1.00 eq.) 4Tz(PhH)Br. Purification of the crude product by column chromatography (SiO_2, *c*Hex:EtOAc 4:1, R_f = 0.31) gave 0.92 g (3.86 mmol, 86%) yellow oil.

^{1}H NMR (500 MHz, DMSO-d_6) δ / ppm = 9.26 (d, *J* = 1.8 Hz, 1H, H-7), 8.76 (t, *J* = 1.5 Hz, 1H, H-1), 8.73 (ddd, *J* = 4.9, 1.8, 1.0 Hz, 1H, H-14), 8.32 (d, *J* = 1.9 Hz, 1H, H-6), 8.10 – 8.04 (m, 3H, H-3, H-8, H-11), 7.93 (td, *J* = 7.8, 1.8 Hz, 1H, H-12), 7.60 (t, *J* = 7.7 Hz, 1H, H-2), 7.40 (dd, *J* = 6.4, 4.7 Hz, 1H, H-13).

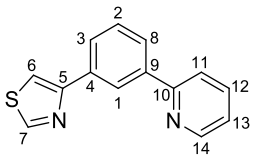

^{13}C NMR (75 MHz, DMSO-d_6) δ / ppm = 156.2 (C-10), 155.4 (C-5), 154.6 (C-7), 150.0 (C-14), 139.0 (C-9), 137.7 (C-12), 135.0 (C-4), 129.8 (C-2), 127.2 (C-8), 126.7 (C-3), 124.8 (C-1), 123.3 (C-13), 120.5 (C-11), 115.2 (C-6).

EI(+) MS (70 eV) m/z = 238 $[M]^+$ (100%), 210 $[M\text{-}NCH]^+$ (45%), 166 $[PyPh+C]^+$ (15%), 139 $[PyPh\text{-}C]^+$ (10%), 105 $[Py+C_2H]^+$ (5%), 83 $[Tz]^+$ (10%).

EA (CHNS) Meas. / % (Calc. / %): C, 70.54 (70.56); H, 4.43 (4.23); N, 11.63 (11.76); S, 13.40 (13.45). Calc. for $C_{14}H_{10}N_2S$.

2Btz(PhH)Py. Following *General Procedure F* and using 1.31 g (4.50 mmol, 1.00 eq.) 2Btz(PhH)Br. Purification of the crude product by column chromatography (SiO_2, *c*Hex:EtOAc 4:1, R_f = 0.31) gave 1.07 g (3.71 mmol, 82%) yellow oil.

^{1}H NMR (500 MHz, DMSO-d_6) δ / ppm = 8.86 (t, *J* = 1.7 Hz, 1H, H-1), 8.76 (d, *J* = 3.9 Hz, 1H, H-18), 8.28 (dt, *J* = 7.9, 1.4 Hz, 1H, H-12), 8.19 (d, *J* = 7.9 Hz, 1H, H-10), 8.16 (dt, *J* = 7.8, 1.3 Hz, 1H, H-3), 8.16 – 8.09 (m, 2H, H-7, H-15), 7.96 (td, *J* = 7.7,

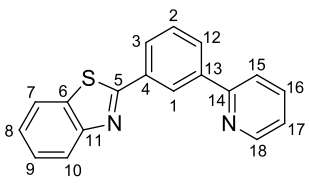

1.8 Hz, 1H, H-16), 7.72 (t, *J* = 7.8 Hz, 1H, H-2), 7.59 (ddd, *J* = 8.3, 7.1, 1.2 Hz, 1H, H-8), 7.50 (t, *J* = 7.1 Hz, 1H, H-9), 7.45 (dd, *J* = 6.7, 4.8 Hz, 1H, H-17).

^{13}C NMR (75 MHz, DMSO-d_6) δ / ppm = 167.6 (C-5), 155.3 (C-14), 154.0 (C-6), 150.2 (C-18), 140.1 (C-13), 138.0 (C-16), 135.0 (C-11), 133.9 (C-4), 130.5 (C-2), 129.7 (C-12), 128.3 (C-3), 127.2 (C-8), 126.1 (C-9), 125.5 (C-1), 123.7 (C-17), 123.5 (C-7), 122.3 (C-10), 121.0 (C-15).

EI(+) MS (70 eV) m/z = 288 $[M]^+$ (100%), 260 $[M\text{-}NCH]^+$ (5%), 255 $[M\text{-}S]^+$ (10%), 211 $[M\text{-}Ph]^+$ (5%), 210 $[M\text{-}Py]^+$ (5%), 179 $[PyPh+CN]^+$ (5%), 154 $[M\text{-}BzTz]^+$ (5%), 130 $[PyPh\text{-}C_2H]^+$ (5%).

EA (CHNS) Meas. / % (Calc. for $C_{18}H_{12}N_2S$ / %): C, 74.88 (74.97); H, 4.09 (4.19); N, 9.76 (9.71); S, 11.27 (11.12).

2Qu(PhH)Py. Following *General Procedure F* and using 1.28 g (4.50 mmol, 1.00 eq.) 2Qu(PhH)Br. Purification of the crude product by column chromatography (SiO_2, *c*Hex:EtOAc 2:1, R_f = 0.61) gave 0.50 g (1.77 mmol, 40%) yellow oil.

^{1}H NMR (500 MHz, DMSO-d_6) δ / ppm = 8.98 (t, *J* = 1.6 Hz, 1H, H-1), 8.75 (d, *J* = 3.9 Hz, 1H, H-20), 8.51 (d, *J* = 8.6 Hz, 1H, H-6), 8.35 (dt, *J* = 7.8, 1.5 Hz, 1H, H-3), 8.28 (d, *J* = 8.6 Hz, 1H, H-7), 8.22 (dt, *J* = 7.8, 1.4 Hz, 1H, H-14), 8.14 (d, *J* = 8.1 Hz, 2H, H-9, H-17), 8.04 (d, *J* = 7.6 Hz, 1H, H-12), 7.96 (td, *J* = 7.8, 1.8 Hz, 1H, H-18), 7.81 (ddd, *J* = 8.3, 6.9, 1.4 Hz, 1H, H-10), 7.70 (t, *J* = 7.7 Hz, 1H, H-2), 7.63 (ddd, *J* = 8.0, 6.7, 1.0 Hz, 1H, H-11), 7.42 (ddd, *J* = 7.4, 4.8, 0.8 Hz, 1H, H-19).

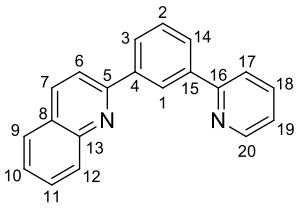

^{13}C NMR (75 MHz, DMSO-d_6) δ / ppm = 156.8 (C-5), 156.3 (C-16), 150.1 (C-20), 148.1 (C-8), 139.8 (C-15), 139.7 (C-4), 137.8 (C-18), 137.7 (C-6), 130.4 (C-10), 129.8 (C-2), 129.6 (C-9), 128.4 (C-3), 128.3 (C-12), 128.1 (C-14), 127.6 (C-13), 127.0 (C-11), 125.8 (C-1), 123.3 (C-19), 121.0 (C-17), 119.4 (C-7).

EI(+) MS (70 eV) m/z = 282 $[M]^+$ (100%), 254 $[M\text{-}CHN]^+$ (10%), 230 $[PyPhPy]^+$ (5%), 204 $[M\text{-}Py]^+$ (25%), 154 $[M\text{-}Qu]^+$ (5%), 141 $[PyPh\text{-}C]^+$ (10%), 127 $[Qu]^+$ (10%), 113 $[Py+C_3H_2]^+$ (5%).

EA (CHNS) Meas. / % (Calc. for $C_{20}H_{14}N_2$ / %): C, 84.84 (85.08); H, 5.11 (5.00); N, 10.05 (9.92).

5.3 Synthesis of the Complex Precursors

5.3.1 Synthesis of *bis*(cycloocta-1,5-diene) nickel(0)[233]

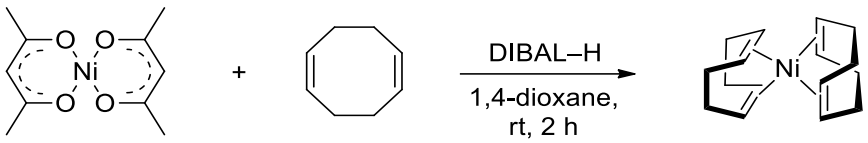

3.92 g (15.0 mmol, 1.00 eq.) $Ni(acac)_2$ was vacuum dried and suspended in THF (60 mL) under an inert atmosphere. 8.00 mL (64.5 mmol, 4.30 eq.) cycloocta-1,5-diene and 50.0 mL (48.0 mmol, 3.20 eq.) of a 0.95M DIBAL-H solution in hexanes were added and stirred for 2 h at room temperature. To this mixture Et_2O (100 mL) was added and the biphasic system was stored at –18°C overnight. The next day, the liquid phase was removed and the remaining solid was washed with acetone (50 mL) and twice with *n*-heptane (50 mL). After drying under reduced pressure, the product was obtained as 0.82 g (2.98 mmol, 20%) yellow crystals, which were used for following syntheses without further characterization.

5.3.2 Synthesis of nickel carboxylates

5.3.2.1 Synthesis of nickel benzoate dihydrate[216]

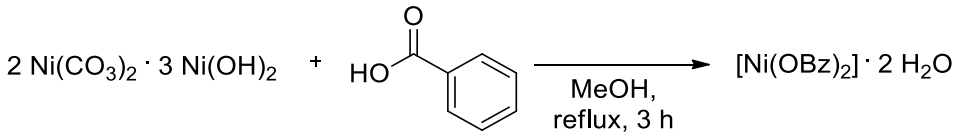

6.18 g (49.4 mmol, 3.80 eq.) benzoic acid was dissolved in MeOH (130 mL) and 5.01 g (13.0 mmol, 1.00 eq.) basic nickel carbonate was added. The reaction mixture was heated to reflux for 3 h and cooled down to rt. The bright green precipitate was filtered off and washed with MeOH. Remaining carboxylic acid was removed *via* sublimation at 180°C and $3 \cdot 10^{-2}$ mbar. The product was obtained as 1.16 g (3.27 mmol, 25%) green solid.

EA (CHNS) Meas. / % (Calc. for $C_{14}H_{14}NiO_6$ / %): C, 50.44 (49.90); H, 4.57 (4.19).

5.3.2.2 Synthesis of nickel pivalate and nickel trifluoroacetate salts – *General Procedures*

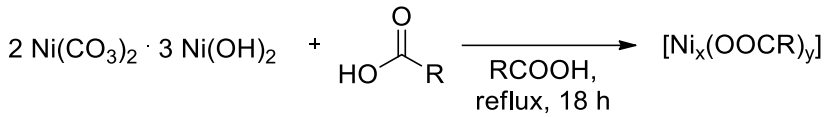

General procedure G.[217,218] 3.00 g (8.50 mmol, 1.00 eq.) Basic nickel carbonate was suspended in a carboxylic acid derivative (153 mmol, 18.0 eq.). The solution was heated to reflux. After 18 h, the mixture was cooled down to rt and the remaining carboxylic acid was removed (distilled / sublimed). The resulting solid was recrystallized from EtOH.

$[Ni_4(\mu_3\text{-}OH_2)(OPiv)_6(EtOH)_6] \cdot 2\ H_2O$. Following *General Procedure G* and using 15.3 g (153 mmol, 18.0 eq.) pivalic acid. The product was obtained as 4.18 g (3.32 mmol, 40%) green solid.

EA (CHNS) Meas. / % (Calc. for $C_{42}H_{96}Ni_4O_{22}$ / %): C, 42.46 (40.05); H, 8.14 (5.60).

$[Ni_3(TFA)_6(HTFA)_6] \cdot HTFA$. Following *General Procedure G* and using 17.1 g (153 mmol, 18.0 eq.) trifluoroacetic acid. The product was obtained as 6.27 g (3.84 mmol, 45%) green solid.

EA (CHNS) Meas. / % (Calc. for $C_{26}H_7Ni_3O_{22}F_{39}$ / %): C, 14.79 (18.90); H, 1.81 (0.43).

5.3.2.3 Synthesis of nickel-9-anthracyl carboxylate salt[219]

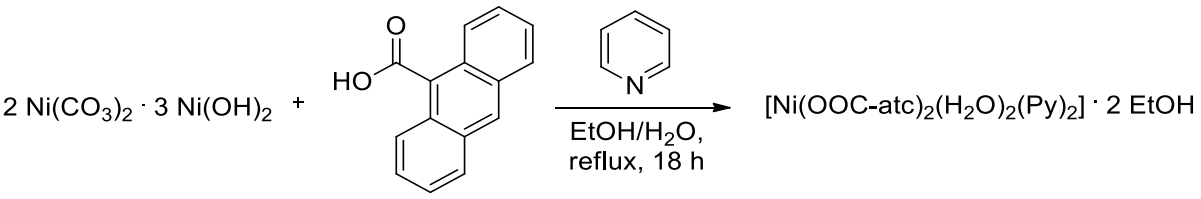

0.31 g (1.00 mmol, 1.00 eq.) Basic nickel carbonate and 1.29 g (5.80 mmol, 5.80 eq.) 9-atc-COOH were suspended in a mixture of water and ethanol (1:4, 200 mL). The solution was heated to reflux and after 18 h the mixture cooled down to rt. Then 1.00 mL (1.20 mmol, 1.20 eq.) pyridine was added and the reaction mixture was cooled down to 4°C. The resulting solid was filtered. 0.79 g (1.00 mmol, >99%) $[Ni(OOC\text{-}atc)_2(H_2O)_2(Py)_2] \cdot 2\ EtOH$ was obtained as a cyan solid and used without further analytics.

5.4 Synthesis of Nickel N^C^N Complexes

5.4.1 Synthesis of Central Ring Substituted Nickel N^C^N Complexes *via* C–H Activation – *General Procedures*

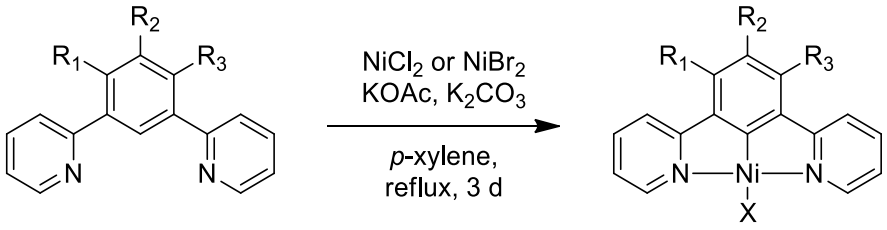

General procedure H.[92] A *Dean-Stark* apparatus was equipped with 0.17 g (1.30 mmol, 1.30 eq.) $NiCl_2$ or 0.28 g (1.30 mmol, 1.30 eq.) $NiBr_2$, 0.100 g (1.00 mmol, 1.00 eq.) potassium acetate and 0.140 g (1.00 mmol, 1.00 eq.) potassium carbonate and dried under vacuum and 140°C for 1 h. Then the central ring substituted N^C^N protoligand (1.00 mmol, 1.00 eq.) and *p*-xylene (200 mL) were added, the reaction mixture was refluxed for 3 d and cooled to rt.

[Ni(Py(5MeOPh)Py)Br]. Following *General Procedure H* and using 0.26 g (1.00 mmol, 1.00 eq.) Py(5MeOPhH)Py. The solid was separated by filtration, washed once with *p*-xylene (50 mL) and then extracted using THF until the filtrate turned colorless. The product was obtained as 0.29 g (0.72 mmol, 72%) brown solid.

^{1}H NMR (300 MHz, DMSO-d_6) δ / ppm = 8.75 (d, *J* = 5.7 Hz, 2H, H-9), 8.01 (td, *J* = 7.7, 1.6 Hz, 2H, H-7), 7.88 (d, *J* = 7.8 Hz, 2H, H-6), 7.27 (ddd, *J* = 7.4, 5.7, 1.5 Hz, 2H, H-8), 7.22 (s, 2H, H-3), 3.83 (s, 3H, H-10).

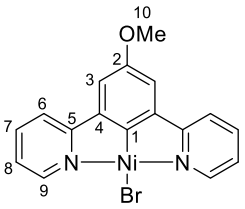

EI(+) MS (70 eV) m/z = 400 $[M]^+$ (30%), 319 $[M\text{-}Br]^+$ (100%), 304 $[M\text{-}CH_3Br]^+$ (40%), 276 $[M\text{-}Br\text{-}CH_3\text{-}NCH]^+$ (30%), 262 $[M\text{-}NiBr]^+$ (5%), 232 $[M\text{-}NiBr\text{-}MeO]^+$ (5%), 218 $[M\text{-}NiBr\text{-}CH_3\text{-}NCH]^+$ (20%), 191 $[M\text{-}NiBr\text{-}CH_3\text{-}2(NCH)]^+$ (10%), 138 $[NiBr]^+$ (10%), 78 $[Py]^+$ (5%).

EA (CHNS) Meas. / % (Calc. for $C_{17}H_{13}BrN_2NiO$ / %): C, 52.59 (51.06); H, 3.60 (3.24); N, 6.40 (7.01).

[Ni(Py(5BuPh)Py)Br]. Following *General Procedure H* and using 0.29 g (1.00 mmol, 1.00 eq.) Py(5BuPhH)Py. The solid was purified through filtration and extraction using *p*-xylene and isolating the product as 0.39 g (0.92 mmol, 92%) yellow solid by removing the solvent.

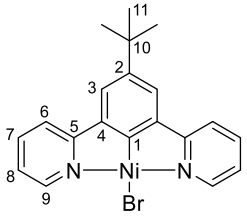

^{1}H NMR (300 MHz, DMSO-d_6) δ / ppm = 8.92 (d, *J* = 5.7 Hz, 2H, H-9), 8.08 – 7.97 (m, 4H, H-6 and H-7), 7.63 (s, 2H, H-3), 7.31 (td, *J* = 6.2, 2.5 Hz, 2H, H-8), 1.37 (s, 9H, H-11).

EI(+) MS (70 eV) m/z = 426 $[M]^+$ (30%), 345 $[M\text{-}Br]^+$ (100%), 329 $[M\text{-}Br\text{-}CH_3]^+$ (50%), 315 $[M\text{-}Br\text{-}2CH_3]^+$ (10%), 288 $[M\text{-}NiBr]^+$ (10%), 273 $[M\text{-}NiBr\text{-}CH_3]^+$ (10%), 257 $[M\text{-}NiBr\text{-}2CH_3]^+$ (5%), 229 [M-NiBr-*t*Bu]$^+$ (5%), 204 [M-NiBr-*t*Bu-NCH]$^+$ (15%), 151 $[PyPh]^+$ (10%).

EA (CHNS) Meas. / % (Calc. for $C_{20}H_{19}BrN_2Ni$ / %): C, 57.12 (56.39); H, 4.90 (4.50); N, 5.32 (5.72).

[Ni(Py(5MePh)Py)Br]. Following *General Procedure H* and using 0.25 g (1.00 mmol, 1.00 eq.) Py(5MePhH)Py. The solid was separated by filtration, washed once with *p*-xylene (50 mL) and then extracted using THF until the filtrate turned colorless. The product was obtained as 0.29 g (0.76 mmol, 76%) brown solid.

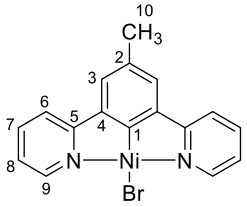

^{1}H NMR (300 MHz, DMSO-d_6) δ / ppm = 8.37 (d, *J* = 5.7 Hz, 2H, H-9), 7.87 (dt, *J* = 7.7, 4.5 Hz, 2H, H-7), 7.62 (d, *J* = 7.9 Hz, 2H, H-6), 7.20 – 7.07 (m, 4H, H-3 and H-8), 2.30 (s, 3H, H-10).

EI(+) MS (70 eV) m/z = 384 $[M]^+$ (10%), 303 $[M\text{-}Br]^+$ (100%), 246 $[M\text{-}NiBr]^+$ (30%), 229 $[M\text{-}NiBr\text{-}CH_3]^+$ (5%), 218 $[M\text{-}NiBr\text{-}NCH]^+$ (10%), 167 $[PyPhCH_3]^+$ (10%), 78 $[Py]^+$ (5%).

EA (CHNS) Meas. / % (Calc. for $C_{17}H_{13}BrN_2Ni$ / %): C, 55.33 (53.19); H, 3.72 (3.41); N, 6.77 (7.30).

[Ni(Py(5PhPh)Py)Br]. Following *General Procedure H* and using 0.31 g (1.00 mmol, 1.00 eq.) Py(5PhPhH)Py. The solid was separated by filtration, washed once with *p*-xylene (50 mL) and then extracted using THF until the filtrate turned colorless. The product was obtained as 0.30 g (0.67 mmol, 67%) yellow solid.

^{1}H NMR (300 MHz, DMSO-d_6) δ / ppm = 8.70 (s, 2H, H-9), 8.03 – 7.96 (m, 4H, H-6 and H-7), 7.77 (s, 2H, H-3), 7.72 (d, *J* = 7.5 Hz, 2H, H-11), 7.45 (dd, *J* = 8.2, 6.3 Hz, 2H, H-12), 7.38 (t, *J* = 7.1 Hz, H-13), 7.24 (td, *J* = 6.1, 2.5 Hz, 2H, H-8).

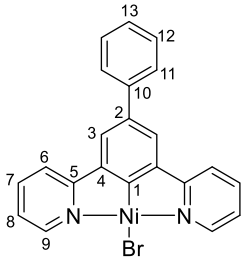

EI(+) MS (70 eV) m/z = 446 $[M]^+$ (20%), 365 $[M\text{-}Br]^+$ (100%), 305 $[M\text{-}NiBr]^+$ (10%), 280 $[M\text{-}NiBr\text{-}NCH]^+$ (10%), 254 $[M\text{-}NiBr\text{-}2NCH]^+$ (5%), 228 $[M\text{-}NiBr\text{-}Py]^+$ (10%), 202 $[PhPhPy\text{-}NCH]^+$ (5%), 182 $[M\text{-}Br\text{-}Ph\text{-}NCH]^+$ (10%), 78 $[Py]^+$ (5%).

EA (CHNS) Meas. / % (Calc. for $C_{22}H_{15}BrN_2Ni$ / %): C, 60.61 (59.25); H, 3.73 (3.29); N, 5.77 (6.28).

[Ni(Py(5NO$_2$Ph)Py)Br]. Following *General Procedure H* and using 0.28 g (1.00 mmol, 1.00 eq.) Py(5NO$_2$PhH)Py. The solid was separated by filtration, washed once with *p*-xylene (50 mL) and then extracted using THF until the filtrate turned colorless. The product was obtained as 0.21 g (0.51 mmol, 51%) brown solid.

^{1}H NMR (300 MHz, DMSO-d_6) δ / ppm = 8.64 (d, *J* = 3.9 Hz, 2H, H-9), 8.45 (s, 2H, H-3), 8.24 (d, *J* = 7.4 Hz, 2H, H-6), 8.13 (t, *J* = 7.5 Hz, 2H, H-7), 7.42 (t, *J* = 6.2 Hz, 2H, H-8).

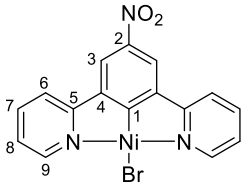

EI(+) MS (70 eV) m/z = 414 $[M]^+$ (15%), 368 $[M\text{-}NO_2]^+$ (20%), 334 $[M\text{-}Br]^+$ (100%), 304 $[M\text{-}Br\text{-}2O]^+$ (10%), 288 $[M\text{-}Br\text{-}NO_2]^+$ (70%), 277 $[M\text{-}NiBr]^+$ (10%), 247 $[M\text{-}NiBr\text{-}2O]^+$ (10%), 229 $[M\text{-}NiBr\text{-}NO_2]^+$ (35%), 204 $[M\text{-}NiBr\text{-}NO_2\text{-}NCH]^+$ (20%), 176 $[M\text{-}NiBr\text{-}NO_2\text{-}2NCH]^+$ (5%).

EA (CHNS) Meas. / % (Calc. for $C_{16}H_{10}BrN_3NiO_2$ / %): C, 49.80 (46.32); H, 3.44 (2.43); 8.81 (10.13).

[Ni(Py(5CF$_3$Ph)Py)Br]. Following *General Procedure H* and using 0.30 g (1.00 mmol, 1.00 eq.) Py(5CF$_3$PhH)Py. The solid was separated by filtration, washed once with *p*-xylene (50 mL) and then extracted using THF until the filtrate turned colorless. The product was obtained as 0.37 g (0.85 mmol, 85%) yellow solid.

^{1}H NMR (300 MHz, DMSO-d_6) δ / ppm = 8.55 (d, J = 5.4 Hz, 2H, H-9), 7.99 (d, J = 6.4 Hz, 4H, H-6 and H-7), 7.77 (s, 2H, H-3), 7.26 (td, J = 6.1, 2.5 Hz, 2H, H-8).

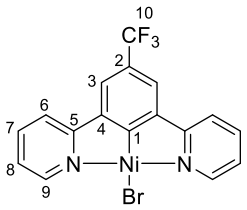

^{19}F NMR (282 MHz, DMSO-d_6) δ / ppm = –60.1 (F-10).

EI(+) MS (70 eV) m/z = 438 $[M]^+$ (25%), 392 $[M\text{-}2F]^+$ (5%), 357 $[M\text{-}Br]^+$ (25%), 300 $[M\text{-}NiBr]^+$ (5%), 279 $[M\text{-}NiBr\text{-}F]^+$ (5%), 241 $[M\text{-}NiBr\text{-}3F]^+$ (5%), 202 $[M\text{-}NiBr\text{-}F\text{-}Py]^+$ (10%), 179 $[PyPh\text{-}NCH\text{-}F]^+$ (5%), 78 $[Py]^+$ (5%).

EA (CHNS) Meas. / % (Calc. / for $C_{17}H_{10}BrF_3N_2Ni$ %): C, 49.11 (46.63); H, 2.93 (2.30); N, 6.56 (6.40).

[Ni(Py(5FPh)Py)Br]. Following *General Procedure H* and using 0.25 g (1.00 mmol, 1.00 eq.) Py(5FPhH)Py. The solid was separated by filtration, washed once with *p*-xylene (50 mL) and then extracted using THF until the filtrate turned colorless. The product was obtained as 0.32 g (0.83 mmol, 83%) yellow solid.

^{1}H NMR (300 MHz, DMSO-d_6) δ / ppm = 8.42 (s, 2H, H-9), 7.98 (td, J = 7.7, 1.6 Hz, 2H, H-7), 7.81 (d, J = 7.9 Hz, 2H, H-6), 7.40 (d, J = 10.1 Hz, 2H, H-3), 7.22 (t, J = 6.4 Hz, 2H, H-8).

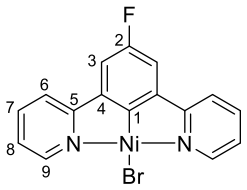

^{19}F NMR (282 MHz, DMSO-d_6) δ / ppm = –117.0 (t, J = 9.9 Hz, F-2).

EI(+) MS (70 eV) m/z = 388 $[M]^+$ (20%), 307 $[M\text{-}Br]^+$ (100%), 250 $[M\text{-}NiBr]^+$ (25%), 222 $[M\text{-}NiBr\text{-}NCH]^+$ (20%), 202 $[M\text{-}NiBr\text{-}NCH\text{-}F]^+$ (5%), 152 $[PhPy]^+$ (10%), 125 $[PhPy\text{-}NCH]^+$ (5%), 78 $[Py]^+$ (5%).

EA (CHNS) Meas. / % (Calc. / %): C, 55.94 (49.55); H, 4.01 (2.60); N, 7.12 (7.22). Calc. for $C_{16}H_{10}BrFN_2Ni$.

[Ni(Py(4FPh)Py)Br]. Following *General Procedure H* and using 0.25 g (1.00 mmol, 1.00 eq.) Py(4FPhH)Py. The solid was purified through filtration and extraction using *p*-xylene and isolating the product as 0.31 g (0.81 mmol, 81%) yellow solid.

^{1}H NMR (300 MHz, DMSO-d_6) δ / ppm = 8.93 (dd, J = 5.9, 1.5 Hz, 1H, H-16), 8.83 (d, J = 5.6 Hz, 1H, H-9), 8.05 (td, J = 7.1, 6.4, 1.0 Hz, 1H, H-14), 8.00 (td, J = 7.6, 1.3 Hz, 1H, H-7), 7.81 (dd, J = 8.0, 1.4 Hz, 1H, H-6), 7.70 (dd,

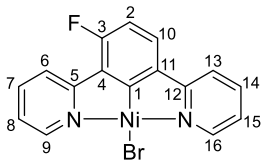

J = 8.0, 1.4 Hz, 1H, H-13), 7.53 (dd, *J* = 8.4, 4.1 Hz, 1H, H-2), 7.35 (td, *J* = 5.9, 2.9 Hz, 1H, H-15), 7.28 (ddd, *J* = 7.4, 5.7, 1.5 Hz, 1H, H-8), 6.98 (dd, *J* = 11.4, 8.4 Hz, 1H, H-10).

^{19}F NMR (282 MHz, DMSO-d_6) δ / ppm = –114.9 (dd, *J* = 11.4, 4.2 Hz, F-3).

EI(+) MS (70 eV) m/z = 388 $[M]^+$ (25%), 307 $[M\text{-}Br]^+$ (100%), 286 $[M\text{-}Br\text{-}F]^+$ (5%), 250 $[M\text{-}NiBr]^+$ (20%), 229 $[M\text{-}NiBr\text{-}F]^+$ (5%), 222 $[M\text{-}NiBr\text{-}NCH]^+$ (10%), 202 $[M\text{-}NiBr\text{-}NCH\text{-}F]^+$ (5%), 153 $[PhPy]^+$ (10%), 78 $[Py]^+$ (5%).

EA (CHNS) Meas. / % (Calc. for $C_{16}H_{10}BrFN_2Ni$ / %): C, 51.61 (49.55); H, 2.58 (2.60); N, 7.17 (7.22).

[Ni(Py(4,6FPh)Py)Br]. Following *General Procedure H* and using 0.27 g (1.00 mmol, 1.00 eq.) Py(4,6FPhH)Py. The solid was separated by filtration, washed once with *p*-xylene (50 mL) and then extracted using THF until the filtrate turned colorless. The product was obtained as 0.29 g solid (0.71 mmol, 71%) orange solid.

^{1}H NMR (300 MHz, DMSO-d_6) δ / ppm = 8.22 (d, *J* = 5.7 Hz, 2H, H-9), 7.93 (td, *J* = 7.8, 1.6 Hz, 2H, H-7), 7.47 (d, *J* = 7.9 Hz, 2H, H-6), 7.16 (ddd, *J* = 7.3, 5.7, 1.4 Hz, 2H, H-8), 6.94 (t, *J* = 11.0 Hz, 1H, H-2).

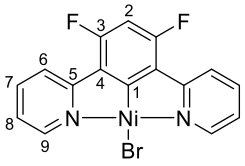

^{19}F NMR (282 MHz, DMSO-d_6) δ / ppm = – 111.1 (d, *J* = 11.0 Hz, F-3).

EI(+) MS (70 eV) m/z = 406 $[M]^+$ (25%), 325 $[M\text{-}Br]^+$ (100%), 304 $[M\text{-}Br\text{-}F]^+$ (5%), 267 $[M\text{-}NiBr]^+$ (10%), 247 $[M\text{-}NiBr\text{-}F]^+$ (10%), 240 $[M\text{-}NiBr\text{-}NCH]^+$ (10%), 220 $[M\text{-}NiBr\text{-}F\text{-}NCH]^+$ (5%), 163 $[M\text{-}NiBr\text{-}2F\text{-}NCH\text{-}N(CH)_2]^+$ (5%), 78 $[Py]^+$ (5%).

EA (CHNS) Meas. / % (Calc. for $C_{16}H_9BrF_2N_2Ni$ / %): C, 49.22 (47.35); H, 2.61 (2.24); N, 6.30 (6.90).

[Ni(Py(4,6FPh)Py)Cl]. Following *General Procedure H* and using 0.27 g (1.00 mmol, 1.00 eq.) Py(4,6FPhH)Py. The solid was separated by filtration, washed once with *p*-xylene (50 mL) and then extracted using THF until the filtrate turned colorless. The product was obtained as 0.34 g (0.93 mmol, 93%) orange solid.

^{1}H NMR (300 MHz, CD_2Cl_2) δ / ppm = 9.04 (d, *J* = 4.6 Hz, 2H, H-9), 7.82 (d, *J* = 7.3 Hz, 2H, H-7), 7.68 (d, *J* = 8.0 Hz, 2H, H-6), 7.13 (t, *J* = 6.1 Hz, 2H, H-8), 6.62 (t, *J* = 10.7 Hz, 1H, H-2).

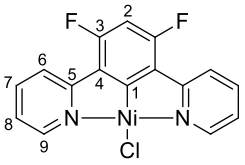

(300 MHz, DMSO-d_6) δ / ppm = 8.62 (s, 2H, H-9), 8.07 (td, *J* = 7.9, 1.5 Hz, 2H, H-7), 7.68 (d, *J* = 7.8 Hz, 2H, H-6), 7.36 (t, *J* = 6.6 Hz, 2H, H-8), 7.05 (t, *J* = 11.1 Hz, 1H, H-2).

^{19}F NMR (282 MHz, CD_2Cl_2) δ / ppm = –111.8 (d, *J* = 10.4 Hz, F-3).

(282 MHz, DMSO-d_6) δ / ppm = –111.2 (d, *J* = 11.0 Hz, F-3).

EI(+) MS (70 eV) m/z = 360 $[M]^+$ (40%), 325 $[M\text{-}Cl]^+$ (100%), 267 $[M\text{-}NiCl]^+$ (10%), 247 $[M\text{-}NiCl\text{-}F]^+$ (20%), 240 $[M\text{-}NiCl\text{-}NCH]^+$ (20%), 162 $[M\text{-}NiCl\text{-}2F\text{-}NCH\text{-}N(CH)_2]^+$ (10%), 78 $[Py]^+$ (5%).

EA (CHNS) Meas. / % (Calc. for $C_{16}H_9ClF_2N_2Ni$ / %): C, 50.21 (53.18); H, 2.42 (2.51); N, 7.45 (7.75).

[Ni(Py(4,6MePh)Py)Cl].[140] Following *General Procedure H* and using 0.26 g (1.00 mmol, 1.00 eq.) Py(4,6MePhH)Py. The solid was separated by filtration, washed once with *p*-xylene (50 mL) and then extracted using THF until the filtrate turned colorless. The product was obtained as 0.32 g (0.94 mmol, 94%) dark orange solid.

^{1}H NMR (300 MHz, CD_2Cl_2) δ / ppm = 8.84 (s, 2H, H-9), 7.81 (td, 2H, *J* = 7.8, 1.7 Hz, H-7), 7.65 (d, 2H, *J* = 8.1 Hz, H-6), 7.09 (ddd, 2H, *J* = 7.3, 5.8, 1.4 Hz, H-8), 6.71 (s, 1H, H-2), 2.55 (s, 6H, H-10).

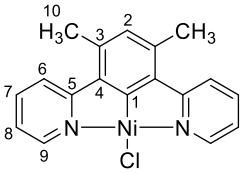

(300 MHz, DMSO-d_6) δ / ppm = 8.61 (s, 2H, H-9), 7.92 (t, *J* = 7.2 Hz, 2H, H-7), 7.63 (d, *J* = 8.1 Hz, 2H, H-6), 7.17 (t, *J* = 6.5 Hz, 2H, H-8), 6.65 (s, 1H, H-2), 2.43 (s, 6H, H-10).

EI(+) MS (70 eV) m/z = 352 $[M]^+$ (25%), 317 $[M–Cl]^+$ (100%), 259 $[M–NiCl]^+$ (25%), 245 $[M–NiCl–CH_3]^+$ (25%), 229 $[PyPhPy]^+$ (5%), 180 $[M–NiCl–Py]^+$ (5%), 167 $[PyPhCH_3]^+$ (5%), 151 $[PhPy]^+$ (5%), 129 $[M–L+Cl]^+$ (5%).

EA (CHNS) Meas. / % (Calc. for $C_{18}H_{15}N_2NiCl$ / %): C, 61.20 (61.16); H, 4.36 (4.28); N, 7.96 (7.93).

[Ni(Py(4,5,6MeOPh)Py)Br]. Following *General Procedure H* and using 0.32 g (1.00 mmol, 1.00 eq.) Py(4,5,6MeOPhH)Py. The solid was separated by filtration, washed once with *p*-xylene (50 mL) and then extracted using THF until the filtrate turned colorless. The product was obtained as 0.45 g (0.97 mmol, 97%) red solid.

^{1}H NMR (300 MHz, DMSO-d_6) δ / ppm = 8.09 (s, 2H, H-9), 7.83 (t, *J* = 7.4 Hz, 2H, H-7), 7.66 (d, *J* = 7.8 Hz, 2H, H-6), 7.01 (t, *J* = 6.1 Hz, 2H, H-8), 3.93 (s, 6H, H-11), 3.80 (s, 3H, H-10).

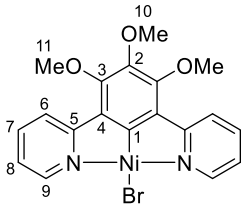

EI(+) MS (70 eV) m/z = 459 $[M]^+$ (30%), 414 $[M\text{-}NCH\text{-}CH_3]^+$ (15%), 379 $[M\text{-}Br]^+$ (100%), 349 $[M\text{-}Br\text{-}MeO]^+$ (45%), 318 $[M\text{-}NiBr]^+$ (25%), 278 $[M\text{-}NiBr\text{-}3CH_3]^+$ (25%), 250 $[M\text{-}NiBr\text{-}NCH\text{-}3CH_3]^+$ (10%).

EA (CHNS) Meas. / % (Calc. for $C_{19}H_{17}BrN_2NiO_3$ / %): C, 54.43 (49.62); H, 4.65 (3.73); N, 5.70 (6.09).

[Ni(PyPyPy)Br].[141] Following *General Procedure H* and using 0.23 g (1.00 mmol, 1.00 eq.) Py(PyH)Py. The solid was separated by filtration, washed once with *p*-xylene (50 mL) and then extracted using THF until the filtrate turned colorless. The product was obtained as 0.15 g (0.38 mmol, 38%) yellow solid.

^{1}H NMR (300 MHz, DMSO-d_6) δ / ppm = 8.44 (s, 2H, H-8), 8.15 (s, 2H, H-2), 8.00 (t, *J* = 7.2 Hz, 2H, H-6), 7.88 (d, *J* = 7.5 Hz, 2H, H-5), 7.23 (t, *J* = 6.3 Hz, 2H, H-7).

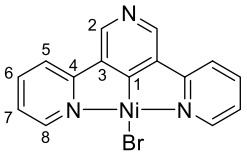

EI(+) MS (70 eV) m/z = 371 $[M]^+$ (15%), 290 $[M\text{-}Br]^+$ (100%), 246 $[M\text{-}Br\text{-}N\text{-}NCH]^+$ (10%), 233 $[M\text{-}NiBr]^+$ (40%), 205 $[M\text{-}NiBr\text{-}NCH]^+$ (15%), 178 $[M\text{-}NiBr\text{-}2NCH]^+$ (5%), 155 $[PhPy]^+$ (20%), 78 $[Py]^+$ (10%).

EA (CHNS) Meas. / % (Calc. for $C_{15}H_{10}BrN_3Ni$ / %): C, 51.25 (48.58); H, 3.41 (2.72); N, 10.17 (11.33).

5.4.2 Synthesis of Nickel N^C^N Complexes with a Variation of the π-Acceptor Unit

5.4.2.1 Synthesis of Complexes *via* Oxidative Addition – *General Procedures*

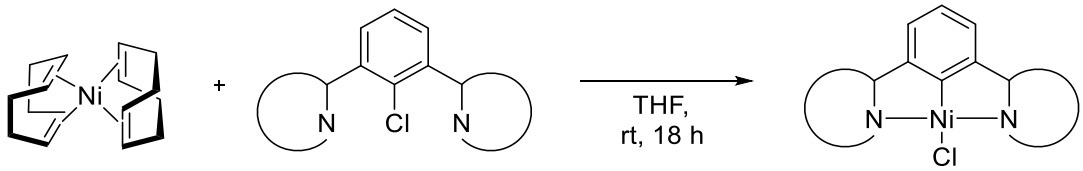

General procedure I.[99] Under inert conditions, 0.28 g (1.00 mmol, 1.00 eq.) [Ni(COD)$_2$] was suspended in THF (10 mL) and equivalent amounts (1.20 mmol, 1.20 eq.) HetAr(ClPh)HetAr was added. The reaction was stirred overnight and then treated with *n*-pentane (20 mL). After removal of the solvent, the remaining solid was washed with additional *n*-pentane (2 × 20 mL). The solvent was removed and the solid subsequently dried under reduced pressure.

[Ni(2Tz(Ph)2Tz)Cl]. Following *General Procedure I* and using 0.34 g (1.20 mmol, 1.20 eq.) 2Tz(PhCl)2Tz. The product was obtained as 0.28 g (0.82 mmol, 82%) yellow solid.

^{1}H NMR (300 MHz, DMSO-d$_6$) δ / ppm = 7.76 (s, 4H, H-6, H-7), 7.52 (d, *J* = 7.6 Hz, 2H, H-3), 7.19 (t, *J* = 7.6 Hz, 1H, H-2).

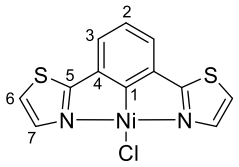

EI(+) MS (70eV) m/z = 336 [M]$^+$ (40%), 301 [M-Cl]$^+$ (100%), 244 [M-NiCl]$^+$ (40%), 216 [M-NiCl-2CH]$^+$ (5%), 211 [M-NiCl-S]$^+$ (25%), 187 [M-NiCl-2NCH]$^+$ (15%), 159 [PhTz]$^+$ (15%).

EA (CHNS) Meas. / % (Calc. for $C_{12}H_7ClN_2NiS_2$ / %): C, 42.36 (42.71); H, 2.21 (2.09); N, 7.88 (8.30); S, 18.81 (19.00).

[Ni(4Tz(Ph)4Tz)Cl]. Following *General Procedure I* and using 0.34 g (1.20 mmol, 1.20 eq.) 4Tz(PhCl)4Tz. The product was quantitively obtained as 0.33 g (1.00 mmol, >99%) yellow solid.

^{1}H NMR (300 MHz, DMSO-d$_6$) δ / ppm = 9.10 (d, *J* = 1.3 Hz, 2H, H-7), 8.00 (d, *J* = 1.00 Hz, 2H, H-6), 7.34 (d, *J* = 7.6 Hz, 2H, H-3), 7.16 (t, *J* = 7.5 Hz, 1H, H-2).

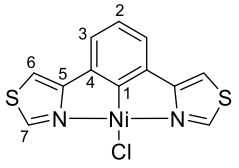

EI(+) MS (70eV) m/z = 336 $[M]^+$ (50%), 301 $[M\text{-}Cl]^+$ (100%), 274 $[M\text{-}Cl\text{-}2CH]^+$ (15%), 244 $[M\text{-}NiCl]^+$ (20%), 216 $[M\text{-}NiCl\text{-}2CH]^+$ (10%), 189 $[M\text{-}NiCl\text{-}2NCH]^+$ (5%), 159 $[PhTz]^+$ (20%), 144 $[PhTz\text{-}N]^+$ (15%).

EA (CHNS) Meas. / % (Calc. for $C_{12}H_7ClN_2NiS_2$ / %): C, 41.12 (42.71); H, 2.20 (2.09); N, 7.73 (8.30); S, 17.96 (19.00).

[Ni(2Btz(Ph)2Btz)Cl]. Following *General Procedure I* and using 0.45 g (1.20 mmol, 1.20 eq.) 2Btz(PhCl)2Btz. The product was quantitively obtained as 0.43 g (1.00 mmol, >99%) orange solid.

^{1}H NMR (300 MHz, DMSO-d_6) δ / ppm = 8.31 – 8.22 (m, 4H, H-3, H-10), 8.18 (d, *J* = 8.2 Hz, 1H, H-7), 7.77 (t, *J* = 7.8 Hz, 1H, H-2), 7.63 (t, *J* = 7.99 Hz, 2H, H-8), 7.56 (t, *J* = 7.5 Hz, 2H, H-9).

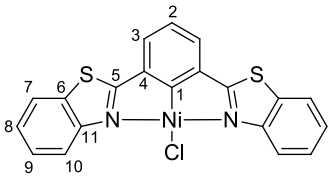

EI(+) MS (70 eV) m/z = 435 $[M]^+$ (5%), 401 $[M\text{-}Cl]^+$ (5%), 378 $[M\text{-}Ni]^+$ (100%), 344 $[M\text{-}Ni\text{-}S]^+$ (80%), 311 $[M\text{-}NiCl\text{-}S]^+$ (20%), 267 $[M\text{-}Cl\text{-}BzTz]^+$ (5%), 235 $[M\text{-}Cl\text{-}BzTz\text{-}S]^+$ (5%), 209 $[BzTzPh]^+$ (10%), 189 $[M\text{-}NiCl\text{-}PhNS]^+$ (20%), 108 $[PhS]^+$ (30%).

EA (CHNS) Meas. / % (Calc. for $C_{20}H_{11}ClN_2NiS_2$ / %): C, 55.55 (54.90); H, 2.54 (2.53); N, 6.13 (6.40); S, 13.81 (14.85).

[Ni(2Qu(Ph)2Qu)Cl]. Following *General Procedure I* and using 0.44 g (1.20 mmol, 1.20 eq.) 2Qu(PhCl)2Qu. The product was quantitively obtained as 0.42 g (1.00 mmol, >99%) red solid.

^{1}H NMR (300 MHz, DMSO-d_6) δ / ppm = 8.50 (d, *J* = 8.4 Hz, 2H), 8.08 (t, *J* = 7.8 Hz, 6H), 7.84 (d, *J* = 8.4 Hz, 3H), 7.76 (d, *J* = 6.9 Hz, 2H), 7.68 (t, *J* = 7.0 Hz, 2H).

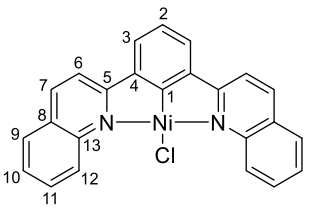

EI(+) MS (70eV) m/z = 424 $[M]^+$ (5%), 389 $[M\text{-}Cl]^+$ (5%), 366 $[M\text{-}Ni]^+$ (15%), 348 $[M\text{-}Ph]^+$ (100%), 331 $[M\text{-}NiCl]^+$ (30%), 304 $[M\text{-}NiCl\text{-}NCH]^+$ (5%), 220 $[PhNiCl+2(CN)]^+$ (20%), 204 $[M\text{-}NiCl\text{-}Qu]^+$ (10%), 174 $[M\text{-}NiCl\text{-}Qu\text{-}NCH]^+$ (30%), 166 $[Qu+0.5Ph]^+$ (15%), 151 $[Qu+CCH]^+$ (5%), 128 $[Qu]^+$ (10%).

EA (CHNS) Meas. / % (Calc. for $C_{24}H_{15}ClN_2Ni$ / %): C, 67.70 (67.74); H, 3.55 (3.55); N, 6.43 (6.58).

5.4.2.2 Synthesis of Complexes *via* C–H Activation – *General Procedures*

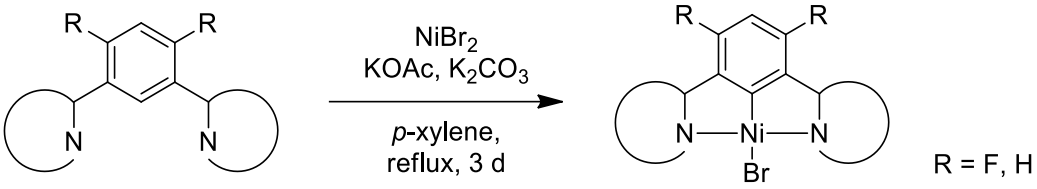

General procedure J.[92] A *Dean-Stark* apparatus was equipped with 0.28 g (1.30 mmol, 1.30 eq.) $NiBr_2$, 0.10 g (1.00 mmol, 1.00 eq.) potassium acetate and 0.14 g (1.00 mmol, 1.00 eq.) potassium carbonate and dried under vacuum at 140°C for 1 h. Then the N^C^N protoligand (1.00 mmol, 1.00 eq.) and *p*-xylene (200 mL) were added, the reaction mixture was refluxed for 3 d and cooled down to rt.

[Ni(3FPy(4,6FPh)3FPy)Br]. Following *General Procedure J* and using 0.30 g (1.00 mmol, 1.00 eq.) 3FPy(4,6FPhH)3FPy. The solid was separated by filtration, washed once with *p*-xylene (50 mL) and then extracted using THF until the filtrate turned colorless. The product was obtained as 0.19 g (0.43 mmol, 43%) intense orange solid.

^{1}H NMR (300 MHz, DMSO-d_6) δ / ppm = 8.69 (s, 2H, H-9), 8.06 (t, *J* = 9.6 Hz, 2H, H-8), 7.44 (dt, *J* = 8.2, 5.2 Hz, 2H, H-7), 6.99 (t, *J* = 11.4 Hz, 1H, H-2).

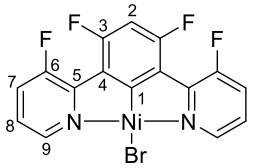

^{19}F NMR (282 MHz, DMSO-d_6) δ / ppm = –96.5 (d, *J* = 122.9 Hz, F-3), –113.1 (d, *J* = 125.4 Hz, F-6).

EI(+) MS (70 eV) m/z = 440 $[M]^+$ (5%), 420 $[M\text{-}F]^+$ (5%), 401 $[M\text{-}2F]^+$ (5%), 382 $[M\text{-}3F]^+$ (10%), 338 $[M\text{-}4F\text{-}NCH]^+$ (15%), 303 $[M\text{-}NiBr]^+$ (100%), 284 $[M\text{-}NiBr\text{-}F]^+$ (30%), 277 $[M\text{-}NiBr\text{-}NCH]^+$ (20%), 236 $[M\text{-}NiBr\text{-}2F\text{-}NCH]^+$ (5%), 207 $[M\text{-}NiBr\text{-}FPy]^+$ (10%), 158 $[FPyF_2Ph\text{-}NCH\text{-}F]^+$ (10%), 143 $[FPyF_2Ph\text{-}NCH\text{-}2F]^+$ (10%).

EA (CHNS) Meas. / % (Calc. for $C_{16}H_7BrF_4N_2Ni$ / %): C, 44.82 (43.49); H, 1.94 (1.60); N, 5.87 (6.34).

[Ni(2^{i}Qu(4,6FPh)2^{i}Qu)Br]. Following *General Procedure J* and using 0.37 g (1.00 mmol, 1.00 eq.) 2^{i}Qu(4,6FPhH)2^{i}Qu. The solid was separated by filtration, washed once with *p*-xylene (50 mL) and then extracted using THF until the filtrate turned colorless. The product was obtained as 0.28 g (0.55 mmol, 55%) red solid.

^{1}H NMR (300 MHz, $CDCl_3$) δ / ppm = 8.64 (d, *J* = 5.7 Hz, 2H), 7.94 (t, *J* = 8.6 Hz, 4H), 7.75 (t, *J* = 6.2 Hz, 4H), 7.66 – 7.58 (m, 2H), 7.21 (t, *J* = 9.4 Hz, 1H).

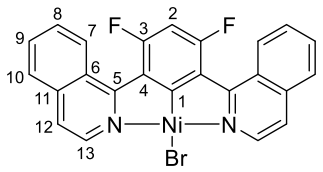

^{19}F NMR (282 MHz, $CDCl_3$) δ / ppm = –94.3 (s, 2F, F-3).

EI(+) MS (70 eV) m/z = 504 $[M]^+$ (5%), 438 $[M\text{-}C_5H_4]^+$ (10%), 408 [M-F-Ph]$^+$ (5%), 393 $[M\text{-}F\text{-}C_7H_4]^+$ (25%), 381 $[M\text{-}F\text{-}2(C_4H_4)]^+$ (100%), 367 [M-NiBr]$^+$ (70%), 347 [M-NiBr-F]$^+$ (35%), 326 [M-NiBr-2F]$^+$ (10%), 253 [M-NiBr-^{i}Qu+C]$^+$ (45%), 240 [M-NiBr-^{i}Qu]$^+$ (50%), 233 [PyPhPy]$^+$ (5%), 189 $[F_2Ph^iQu\text{-}C_4H_4]^+$ (30%).

EA (CHNS) Meas. / % (Calc. for $C_{24}H_{13}N_2F_2NiBr$ / %): C, 62.82 (56.97); H, 4.07 (2.59); N, 5.01 (5.54).

[Ni(Pym(Ph)Pym)Br]. Following *General Procedure J* and using 0.23 g (1.00 mmol, 1.00 eq.) Pym(PhH)Pym. The solid was separated by filtration, washed once with *p*-xylene (50 mL) and then extracted using THF until the filtrate turned colorless. The product was obtained as 0.10 g (0.28 mmol, 28%) yellow solid.

^{1}H NMR (500 MHz, DMSO-d_6) δ / ppm = 8.92 (dd, *J* = 4.8, 2.0 Hz, 2H, H-6), 8.69 (d, *J* = 4.1 Hz, 2H, H-8), 7.56 (d, *J* = 7.5 Hz, 2H, H-3), 7.40 (t, *J* = 5.3 Hz, 2H, H-7), 7.28 (t, *J* = 7.5 Hz, 1H, H-2).

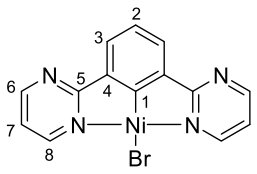

EI(+) MS (70 eV) m/z = 372 $[M]^+$ (20%), 291 [M-Br]$^+$ (100%), 234 [M-NiBr]$^+$ (20%), 206 [M-NiBr-NCH]$^+$ (30%), 180 [M-NiBr-2NCH]$^+$ (10%), 154 [PymPh]$^+$ (10%), 128 [PymPh-NCH]$^+$ (5%).

EA (CHNS) Meas. / % (Calc. for $C_{14}H_9BrN_4Ni$ / %): C, 47.71 (45.22); N, 14.11 (15.07); H, 2.02 (2.44).

[Ni(2^{i}Qu(Ph)2^{i}Qu)Br]. Following *General Procedure J* and using 0.33 g (1.00 mmol, 1.00 eq.) 2^{i}Qu(PhH)2^{i}Qu. The solid was separated by filtration, washed once with *p*-xylene (50 mL) and then extracted using THF until the filtrate turned colorless. The product was obtained as 0.29 g (0.62 mmol, 62%) red solid.

^{1}H NMR (300 MHz, CD_2Cl_2) δ / ppm = 9.31 (s, 2H), 8.89 (d, *J* = 8.5 Hz, 2H), 8.11 (d, *J* = 7.8 Hz, 2H), 7.91 (d, *J* = 8.3 Hz, 2H), 7.82 (t, *J* = 7.3 Hz, 2H), 7.74 (t, *J* = 7.8 Hz, 2H), 7.55 (d, *J* = 6.4 Hz, 2H), 7.39 (t, *J* = 7.7 Hz, 1H).

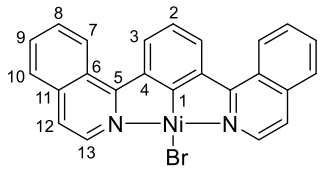

EI(+) MS (70 eV) m/z = 470 $[M]^+$ (10%), 426 $[M\text{-}N(CH)_2]^+$ (20%), 389 $[M\text{-}Br]^+$ (80%), 345 $[M\text{-}Br\text{-}N(CH)_2]^+$ (10%), 331 $[M\text{-}NiBr]^+$ (100%), 304 $[M\text{-}NiBr\text{-}NCH]^+$ (10%), 229 $[PyPhPy]^+$ (5%), 204 $[PyPhPy\text{-}NCH]^+$ (30%), 165 $[Ph^iQu\text{-}N(CH)_2]^+$ (25%), 128 $[^iQu]^+$ (20%).

EA (CHNS) Meas. / % (Calc. for $C_{24}H_{15}N_2NiBr$ / %): C, 63.97 (61.33); H, 4.03 (3.22); N, 5.85 (5.96).

[Ni(3ClPy(Ph)3ClPy)Br]. Following *General Procedure J* and using 0.30 g (1.00 mmol, 1.00 eq.) 3ClPy(PhH)3ClPy. The solid was purified through filtration and extraction using *p*-xylene and isolating the product as 0.11 g (0.26 mmol, 26%) orange solid.

^{1}H NMR (300 MHz, DMSO-d_6) δ / ppm = 8.18 (s, 2H, H-9), 8.04 (d, *J* = 8.1 Hz, 2H, H-7), 7.83 (d, *J* = 8.3 Hz, 2H, H-3), 7.17 – 7.02 (m, 3H, H-2 and H-8).

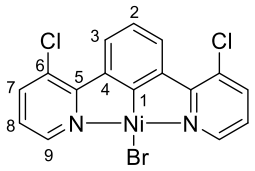

EI(+) MS (70 eV) m/z = 438 $[M]^+$ (15%), 393 $[M\text{-}N(CH)_2]^+$ (20%), 357 $[M\text{-}Br]^+$ (100%), 289 $[M\text{-}Br\text{-}2Cl]^+$ (25%), 263 $[M\text{-}NiBr\text{-}Cl]^+$ (30%), 228 $[M\text{-}NiBr\text{-}2Cl]^+$ (25%).

EA (CHNS) Meas. / % (Calc. for $C_{16}H_9N_2Cl_2NiBr$ / %): C, 43.70 (43.80); H, 2.33 (2.07); N, 5.68 (6.38).

[Ni(Pz(Ph)Pz)Br]. Following *General Procedure J* and using 0.23 g (1.00 mmol, 1.00 eq.) Pz(PhH)Pz. The solid was separated by filtration, washed once with *p*-xylene (50 mL) and then extracted using THF until the filtrate turned colorless. The product was obtained as 0.18 g (0.48 mmol, 48%) red solid.

^{1}H NMR (500 MHz, DMSO-d_6) δ / ppm = 9.24 (s, 2H, H-6), 8.61 (s, 2H, H-7), 8.15 (s, 2H, H-8), 7.70 (d, *J* = 7.6 Hz, 2H, H-3), 7.25 (t, *J* = 7.7 Hz, 1H, H-2).

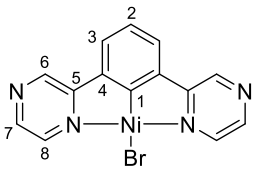

EI(+) MS (70 eV) m/z = 372 $[M]^+$ (10%), 325 $[M\text{-}N(CH)_2]^+$ (15%), 291 $[M\text{-}Br]^+$ (100%), 234 $[M\text{-}NiBr]^+$ (45%), 206 $[M\text{-}NiBr\text{-}NCH]^+$ (15%), 182 $[M\text{-}NiBr\text{-}2NCH]^+$ (10%).

EA (CHNS) Meas. / % (Calc. for $C_{14}H_9BrN_4Ni$ / %): C, 54.63 (45.22); N, 13.93 (15.07); H, 4.51 (2.44).

[Ni(2Tz(Ph)Py)Br]. Following *General Procedure J* and using 0.24 g (1.00 mmol, 1.00 eq.) 2Tz(PhH)Py. The solid was separated by filtration, washed once with *p*-xylene (50 mL) and then extracted using THF until the filtrate turned colorless. The product was obtained as 0.24 g (0.64 mmol, 64%) orange solid.

^{1}H NMR (300 MHz, DMSO-d_6) δ / ppm = 8.69 (d, *J* = 4.5 Hz, 1H, H-14), 8.05 (t, *J* = 7.5 Hz, 1H, H-12), 7.89 (d, *J* = 7.6 Hz, 1H, H-11), 7.80 (d, *J* = 3.4 Hz, 1H, H-7), 7.69 (d, *J* = 3.2 Hz, 1H, H-6), 7.52 (d, *J* = 7.3 Hz, 1H, H-3), 7.43 (d, *J* = 7.5 Hz, 1H, H-8), 7.30 (t, *J* = 6.4 Hz, 1H, H-13), 7.17 (t, *J* = 7.6 Hz, 1H, H-2).

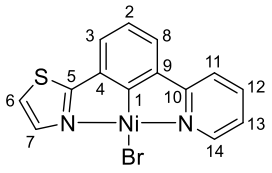

EI(+) MS (70 eV) m/z = 370 $[M]^+$ (50%), 320 $[M\text{-}S(CH)_2]^+$ (15%), 289 $[M\text{-}Tz]^+$ (25%), 253 $[NiBrPy+C_3H]^+$ (100%), 225 $[M\text{-}NiBr\text{-}N]^+$ (20%), 204 $[M\text{-}NiBr\text{-}S]^+$ (20%), 195 $[M\text{-}NiBr\text{-}CHS]^+$ (25%), 185 $[M\text{-}Ni\text{-}Br\text{-}(SCH)_2]^+$ (15%).

EA (CHNS) Meas. / % (Calc. for $C_{14}H_9BrN_2NiS$ / %): C, 45.35 (44.73); H, 2.50 (2.41); N, 7.33 (7.45); S, 7.63 (8.53).

[Ni(4Tz(Ph)Py)Br]. Following *General Procedure J* and using 0.24 g (1.00 mmol, 1.00 eq.) 4Tz(PhH)Py. The solid was separated by filtration, washed once with *p*-xylene (50 mL) and then extracted using THF until the filtrate turned colorless. The product was obtained as 0.29 g (0.77 mmol, 77%) orange solid.

^{1}H NMR (300 MHz, DMSO-d_6) δ / ppm = 9.27 (d, *J* = 1.9 Hz, 1H, H-7), 8.82 (d, *J* = 5.5 Hz, 1H, H-14), 8.01 (t, *J* = 7.6 Hz, 2H, H-12, H-6), 7.87 (d, *J* = 7.4 Hz, 1H, H-11), 7.46 (d, *J* = 7.5 Hz, 1H, H-3), 7.39 (d, *J* = 7.5 Hz, 1H, H-8), 7.30 (t, *J* = 6.9 Hz, 1H, H-13), 7.18 (t, *J* = 7.5 Hz, 1H, H-2).

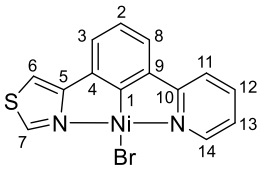

EI(+) MS (70 eV) m/z = 375 $[M]^+$ (5%), 366 $[M\text{-}N]^+$ (20%), 331 $[M\text{-}SCH]^+$ (40%), 314 $[M\text{-}S(CH)_2]^+$ (40%), 294 $[M\text{-}Br]^+$ (10%), 277 $[M\text{-}Tz\text{-}C]^+$ (25%), 254 $[M\text{-}Br\text{-}C_3H_3]^+$ (100%), 238 $[M\text{-}NiBr]^+$ (40%), 210 $[TzPhPy\text{-}NCH]^+$ (25%).

EA (CHNS) Meas. / % (Calc. for $C_{14}H_9BrN_2NiS$ / %): C, 45.25 (44.73); H, 2.44 (2.41); N, 7.40 (7.45); S, 7.72 (8.53).

[Ni(2Btz(Ph)Py)Br]. Following *General Procedure J* and using 0.29 g (1.00 mmol, 1.00 eq.) 2Btz(PhH)Py. The solid was separated by filtration, washed once with *p*-xylene (50 mL) and then extracted using THF until the filtrate turned colorless. The product was obtained as 0.20 g (0.47 mmol, 47%) intense orange solid.

^{1}H NMR (300 MHz, CD_2Cl_2) δ / ppm = 9.20 (s, 1H, H-18), 9.03 (s, 1H, H-10), 7.77 – 7.60 (m, 2H, H-7, H-15), 7.38 (t, *J* = 7.2 Hz, 2H, H-9, H-17), 7.28 (t, *J* = 7.0 Hz, 1H, H-16), 7.22 – 7.12 (m, 2H, H-3, H-12), 7.03 – 6.94 (m, 2H, H-8, H-2).

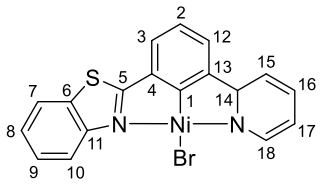

EI(+) MS (70 eV) m/z = 424 $[M]^+$ (5%), 395 $[M\text{-}S]^+$ (5%), 366 $[M\text{-}S(CH)_2]^+$ (10%), 347 $[M\text{-}Ph]^+$ (10%), 331 $[M\text{-}Br\text{-}CH]^+$ (25%), 301 $[NiBrPyPh+C]^+$ (100%), 288 $[M\text{-}NiBr]^+$ (45%), 255 $[M\text{-}NiBr\text{-}S]^+$ (5%), 238 $[PhBzTz+CN]^+$ (5%), 209 $[PhBzTz]^+$ (10%), 195 $[PhBzTz\text{-}C]^+$ (15%), 166 $[PyPh+C]^+$ (10%).

EA (CHNS) Meas. / % (Calc. for $C_{18}H_{11}BrN_2NiS$ / %): C, 49.41 (50.76); H, 2.51 (2.60); N, 6.51 (6.58); S, 7.33 (7.53).

[Ni(2Qu(Ph)Py)Br]. Following *General Procedure J* and using 0.28 g (1.00 mmol, 1.00 eq.) 2Qu(PhH)Py. The solid was separated by filtration, washed once with *p*-xylene (50 mL) and then extracted using THF until the filtrate turned colorless. The product was obtained as 0.17 g (0.40 mmol, 40%) brown solid.

EI(+) MS (70 eV) m/z = 420 $[M]^+$ (5%), 374 $[M\text{-}C_3H_3]^+$ (5%), 339 $[M\text{-}Br]^+$ (55%), 295 $[M\text{-}Qu]^+$ (5%), 282 $[M\text{-}NiBr]^+$ (100%), 254 $[M\text{-}NiBr\text{-}CHN]^+$ (10%), 229 $[PyPhPy]^+$ (5%), 204 $[PhQu]^+$ (25%), 178 $[QuPh\text{-}C_2H]^+$ (5%), 141 $[PyPh\text{-}C]^+$ (10%).

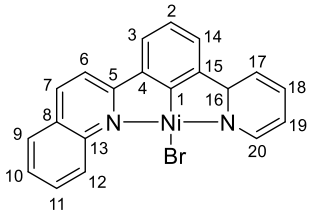

EA (CHNS) Meas. / % (Calc. for $C_{20}H_{13}BrN_2Ni$ / %): C, 55.85 (57.20); H, 3.42 (3.12); N, 6.46 (6.67).

5.4.3 Synthesis of the Complexes varying the Coligand

5.4.3.1 Synthesis of [Ni(Py(Ph)Py)X/R] *via* base-assisted C–H Activation – *General Procedures*

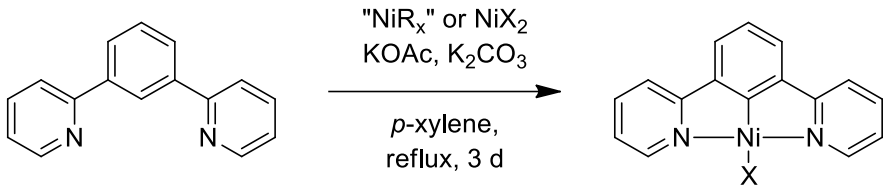

General procedure K.[92] A *Dean-Stark* apparatus was equipped with an (in-)organic nickel(II) salt (1.30 mmol, 1.30 eq.), 0.10 g (1.00 mmol, 1.00 eq.) potassium acetate and 0.14 g (1.00 mmol, 1.00 eq.) potassium carbonate and dried under vacuum at 140°C for 1 h. Then 0.23 g (1.00 mmol, 1.00 eq.) Py(HPh)Py and *p*-xylene (200 mL) were added, the reaction mixture was refluxed for 3 d and cooled down to rt.

[Ni(PyPhPy)Cl].[92] Following *General Procedure K* and using 0.17 g (1.30 mmol, 1.30 eq.) $NiCl_2$. The solid was separated by filtration, washed once with *p*-xylene (50 mL) and then extracted using THF until the filtrate turned colorless. The product was obtained as 0.25 g (0.76 mmol, 76%) orange solid.

^{1}H NMR (300 MHz, DMSO-d_6) δ / ppm = 8.87 (d, *J* = 5.5 Hz, 2H, H-9), 8.05 (td, *J* = 7.7, 1.4 Hz, 2H, H-7), 7.90 (d, *J* = 7.8 Hz, 2H, H-6), 7.55 (d, *J* = 7.6 Hz, 2H, H-3), 7.34 (ddd, *J* = 7.2, 5.5, 1.2 Hz, 2H, H-8), 7.19 (t, *J* = 7.6 Hz, 1H, H-2).

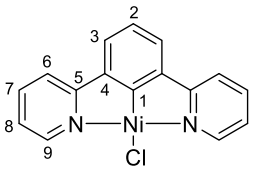

EI(+) MS (70 eV) m/z = 324 $[M]^+$ (65%), 289 $[M\text{-}Cl]^+$ (100%), 232 $[M\text{-}NiCl]^+$ (50%), 154 $[PyPh]^+$ (5%), 78 $[Py]^+$ (5%).

EA (CHNS) Meas. / % (Calc. for $C_{16}H_{11}N_2NiCl$ / %): C, 59.21 (59.05); H, 3.56 (3.41); N, 8.56 (8.61).

[Ni(PyPhPy)Br].[92] Following *General Procedure K* and using 0.29 g (1.30 mmol, 1.30 eq.) $NiBr_2$. The solid was separated by filtration, washed once with *p*-xylene (50 mL) and then extracted using THF until the filtrate turned colorless. The product was obtained as 0.23 g (0.63 mmol, 63%) orange solid.

^{1}H NMR (300 MHz, DMSO-d_6) δ / ppm = 8.91 (dd, *J* = 5.8, 1.6 Hz, 2H), 8.06 (td, *J* = 7.7, 1.6 Hz, 2H), 7.92 (dt, *J* = 7.9, 1.3 Hz, 2H), 7.56 (d, *J* = 7.6 Hz, 2H), 7.34 (ddd, *J* = 7.4, 5.8, 1.5 Hz, 2H), 7.22 (t, *J* = 7.6 Hz, 1H).

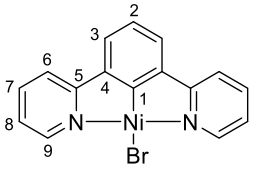

EI(+) MS (70 eV) m/z = 370 $[M]^+$ (25%), 289 $[M\text{-}Br]^+$ (100%), 232 $[M\text{-}NiBr]^+$ (40%), 154 $[PyPh]^+$ (5%), 78 $[Py]^+$ (5%).

EA (CHNS) Meas. / % (Calc. for $C_{16}H_{11}N_2NiBr$ / %): C, 51.92 (51.96); H, 3.08 (3.00); N, 7.71 (7.57).

[Ni(PyPhPy)I].[92] Following *General Procedure K* and using 0.41 g (1.30 mmol, 1.30 eq.) NiI_2. The solid was separated by filtration, washed once with *p*-xylene (50 mL) and then extracted using THF until the filtrate turned colorless. The product was obtained as 0.27 g (0.65 mmol, 65%) red solid.

^{1}H NMR (300 MHz, DMSO-d_6) δ / ppm = 8.17 (d, *J* = 5.6 Hz, 2H, H-9), 8.07 (td, *J* = 7.6, 1.5 Hz, 2H, H-7), 7.89 (d, *J* = 7.9 Hz, 2H, H-6), 7.49 (d, *J* = 7.6 Hz, 2H, H-3), 7.32 (t, *J* = 6.7 Hz, 2H, H-8), 7.18 (t, *J* = 7.6 Hz, 1H, H-2).

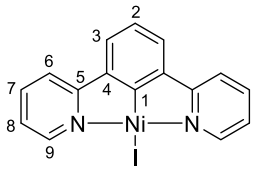

EI(+) MS (70 eV) m/z = 416 $[M]^+$ (5%), 289 $[M\text{-}I]^+$ (100%), 232 $[M\text{-}NiI]^+$ (20%), 154 $[PyPh]^+$ (5%), 78 $[Py]^+$ (5%).

EA (CHNS) Meas. / % (Calc. for $C_{16}H_{11}N_2NiI$ / %): C, 48.34 (46.10); H, 2.82 (2.66); N, 6.84 (6.72).

[Ni(PyPhPy)OAc]. Following *General Procedure K* and using 0.33 g (1.30 mmol, 1.30 eq.) $Ni(OAc)_2 \cdot 4\ H_2O$. The solid was purified through filtration and extraction using *p*-xylene and isolating the product as 0.15 g (0.44 mmol, 44%) orange solid by removing the solvent.

^{1}H NMR (500 MHz, DMSO-d_6) δ / ppm = 7.99 (m, 4H, H-7 and H-9), 7.80 (d, *J* = 7.7 Hz, 2H, H-6), 7.42 (d, *J* = 7.5 Hz, 2H, H-3), 7.26 (t, *J* = 6.3 Hz, 2H, H-8), 7.09 (t, *J* = 7.5 Hz, 1H, H-2), 2.04 (s, 3H, H-11).

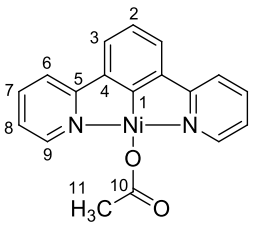

EI(+) MS (70 eV) m/z = 348 $[M]^+$ (5%), 323 $[M\text{-}NCH]^+$ (30%), 289 $[M\text{-}OAc]^+$ (100%), 231 $[M\text{-}NiOAc]^+$ (25%), 204 $[M\text{-}NiOAc\text{-}NCH]^+$ (20%), 153 $[PyPh]^+$ (10%), 78 $[Py]^+$ (5%).

EA (CHNS) Meas. / % (Calc. for $C_{18}H_{14}N_2NiO_2$ / %): C, 60.23 (61.95); H, 4.54 (4.04); N, 8.06 (8.03).

[Ni(PyPhPy)NCS]. Following *General Procedure K* and using 0.23 g (1.30 mmol, 1.30 eq.) $Ni(NCS)_2$. The solid was purified through filtration and extraction using *p*-xylene and isolating the product as 0.10 g (0.26 mmol, 26%) yellow solid by removing the solvent.

^{1}H NMR (500 MHz, DMSO-d_6) δ / ppm = 8.14 (d, *J* = 4.6 Hz, 2H, H-9), 8.07 (td, *J* = 7.7, 1.5 Hz, 2H, H-7), 7.86 (d, *J* = 7.7 Hz, 2H, H-6), 7.46 (d, *J* = 7.6 Hz, 2H, H-3), 7.39 (td, *J* = 6.5, 5.8, 1.2 Hz, 2H, H-8), 7.13 (t, *J* = 7.6 Hz, 1H, H-2).

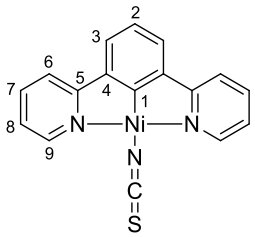

EI(+) MS (70 eV) m/z = 347 $[M]^+$ (15%), 323 $[M\text{-}NCH]^+$ (5%), 289 $[M\text{-}NCS]^+$ (100%), 231 $[M\text{-}NiNCS]^+$ (15%), 204 $[M\text{-}NiNCS\text{-}NCH]^+$ (15%), 153 $[PyPh]^+$ (10%).

EA (CHNS) Meas. / % (Calc. for $C_{17}H_{11}N_3NiS$ / %): C, 59.13 (58.67); H, 3.18 (3.19); N, 12.16 (12.07); S, 8.83 (9.21).

[Ni(PyPhPy)OBz]. Following *General Procedure K* and using 0.34 g (1.30 mmol, 1.30 eq.) $Ni(OBz)_2 \cdot 2\ H_2O$. The solid was purified through filtration and extraction using *p*-xylene and isolating the product as 0.20 g (0.49 mmol, 49%) red solid by removing the solvent.

^{1}H NMR (500 MHz, DMSO-d_6) δ / ppm = 8.09 (d, *J* = 7.1 Hz, 2H, H-12), 8.01 (t, *J* = 7.7 Hz, 2H, H-7), 7.96 (s, 2H, H-9), 7.88 (d, *J* = 7.8 Hz, 2H, H-6), 7.51 (m, 3H, H-3 and H-14), 7.46 (t, *J* = 7.3 Hz, 2H, H-13), 7.25 (t, *J* = 6.4 Hz, 2H, H-8), 7.17 (t, *J* = 7.6 Hz, 1H, H-2).

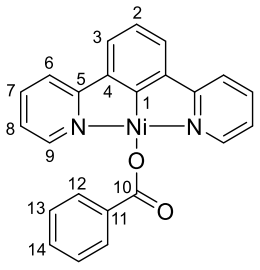

EI(+) MS (70 eV) m/z = 410 $[M]^+$ (5%), 369 $[M\text{-}N(CH)_2]^+$ (10%), 289 $[M\text{-}OBz]^+$ (100%), 231 $[M\text{-}NiOBz]^+$ (55%), 204 $[M\text{-}NiOBz\text{-}NCH]^+$ (35%), 176 $[M\text{-}NiOBz\text{-}2NCH]^+$ (10%), 154 $[PyPh]^+$ (15%), 122 $[OBz]^+$ (35%), 105 $[OBz\text{-}O]^+$ (40%), 78 $[Py]^+$ (20%).

EA (CHNS) Meas. / % (Calc. / %): C, 64.49 (67.20); H, 3.82 (3.92); N, 6.58 (6.81). Calc. for $C_{23}H_{16}N_2NiO_2$.

[Ni(PyPhPy)OPiv]. Following *General Procedure K* and using 1.61 g (1.30 mmol, 1.30 eq.) $[Ni_4(\mu_3\text{-}OH)_2(OPiv)_6(EtOH)_6] \cdot 2$ EtOH. The solid was purified through filtration and extraction using *p*-xylene and isolating the product as 0.20 g (0.51 mmol, 51%) orange solid by removing the solvent.

^{1}H NMR (500 MHz, DMSO-d_6) δ / ppm = 8.07 (t, *J* = 7.7 Hz, 2H, H-7), 7.93 (d, *J* = 7.5 Hz, 4H, H-6 and H-9), 7.56 (d, *J* = 7.5 Hz, 2H, H-3), 7.37 (t, *J* = 6.5 Hz, 2H, H-8), 7.18 (t, *J* = 7.5 Hz, 1H, H-2), 1.20 (s, 9H, H-12).

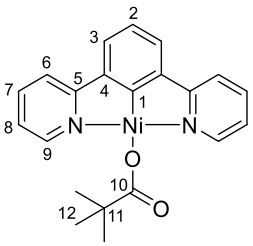

EI(+) MS (70 eV) m/z = 390 $[M]^+$ (5%), 289 $[M\text{-}OPiv]^+$ (100%), 277 $[M\text{-}Piv\text{-}NCH]^+$ (75%), 232 $[M\text{-}NiOPiv]^+$ (55%), 204 $[M\text{-}NiOPiv\text{-}NCH]^+$ (30%), 154 $[PyPh]^+$ (20%).

EA (CHNS) Meas. / % (Calc. for $C_{21}H_{20}N_2NiO_2$ / %): C, 60.60 (64.49); H, 5.53 (5.15); N, 7.23 (7.16).

[Ni(PyPhPy)TFA]. Following *General Procedure K* and using 2.15 g (1.30 mmol, 1.30 eq.) $[Ni_3(TFA)_6(HTFA)_6] \cdot$ HTFA. The solid was purified through filtration and extraction using *p*-xylene and isolating the product as 0.40 g (1.00 mmol, >99%) yellow solid by removing the solvent.

^{1}H NMR (500 MHz, DMSO-d_6) δ / ppm = 8.09 (td, *J* = 7.7, 1.4 Hz, 2H, H-7), 8.05 (d, *J* = 4.9 Hz, 2H, H-9), 7.93 (d, *J* = 7.8 Hz, 2H, H-6), 7.53 (d, *J* = 7.6 Hz, 2H, H-3), 7.37 (ddd, *J* = 7.2, 5.5, 1.2 Hz, 2H, H-8), 7.19 (t, *J* = 7.6 Hz, H-2).

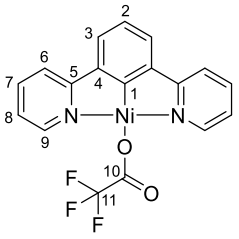

^{19}F NMR (282 MHz, DMSO-d_6) δ / ppm = –73.7 (F-11).

EI(+) MS (70 eV) m/z = 402 $[M]^+$ (5%), 383 $[M\text{-}F]^+$ (5%), 308 $[M\text{-}TFA+O]^+$ (30%), 277 $[M\text{-}CF_3CO\text{-}NCH]^+$ (10%), 245 $[M\text{-}2Py]^+$ (100%), 232 $[M\text{-}NiTFA]^+$ (5%), 167 $[NiTFA]^+$ (15%), 78 $[Py]^+$ (10%).

EA (CHNS) Meas. / % (Calc. / %): C, 53.44 (53.65); H, 2.85 (2.75); N, 6.58 (6.95). Calc. for $C_{18}H_{11}F_3N_2NiO_2$.

[Ni(PyPhPy)OOC-atc]. Following *General Procedure K* and using 0.79 g (1.30 mmol, 1.30 eq.) $[Ni(OOC\text{-}atc)_2(H_2O)_2(Py)_2]\cdot 2\,EtOH$**.** The solid was purified through filtration and extraction using *p*-xylene and isolating the product as 0.39 g (0.76 mmol, 76%) yellow solid by removing the solvent.

^{1}H NMR (500 MHz, DMSO-d_6) δ / ppm = 8.55 (s, 1H, H-18), 8.35 (s, 2H, H-9), 8.28 – 8.19 (m, 2H, H-16), 8.14 – 8.06 (m, 4H, H-7 and H-14), 7.98 (d, *J* = 7.8 Hz, 2H, H-6), 7.60 (d, *J* = 7.6 Hz, 2H, H-3), 7.56 – 7.48 (m, 4H, H-13 and H-15), 7.31 (t, *J* = 6.2 Hz, 2H, H-8), 7.24 (t, *J* = 7.6 Hz, 1H, H-2).

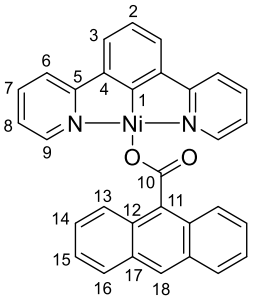

EI(+) MS (70 eV) m/z = 510 $[M]^+$ (5%), 289 $[M\text{-}OOCatc]^+$ (100%), 232 $[M\text{-}NiOOCatc]^+$ (80%), 221 $[OOCatc]^+$ (30%), 204 $[M\text{-}NiOOCatc\text{-}NCH]^+$ (25%), 178 $[M\text{-}NiOOCatc\text{-}2NCH]^+$ (25%), 154 $[PyPh]^+$ (15%).

EA (CHNS) Meas. / % (Calc. for $C_{31}H_{20}N_2NiO_2$ / %): C, 74.32 (72.84); H, 3.42 (3.94); N, 5.33 (5.48).

5.4.3.2 Synthesis of [Ni(Py(4,6RPh)Py)CN] *via* Coligand Exchange Reactions – *General Procedures*

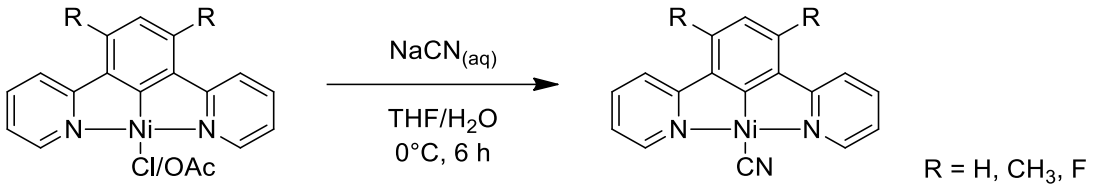

General procedure L.[108] Under inert conditions, [Ni(N^C^N)Cl/OAc] (1.00 mmol, 1.00 eq.) was dissolved in degassed THF (30 mL). A solution of 0.05 g (1.10 mmol, 1.10 eq.) NaCN in degassed H_2O (10 mL) was added *via* syringe pump (rate 1.66 mL/h) at 0°C. The mixture was warmed to room temperature and stirred for additional 30 minutes.

[Ni(PyPhPy)CN]. Following *General Procedure L* and using 0.33 g (1.00 mmol, 1.00 eq.) [Ni(PyPhPy)Cl] or 0.35 g (1.00 mmol, 1.00 eq.) [Ni(PyPhPy)OAc]. For work-up, *n*-pentane

(50mL) was added and the formed precipitate was filtrated and washed once with CH_2Cl_2. The aqueous phase was extracted with CH_2Cl_2 (150 mL) and THF (100 mL). The solvent of the combined organic layers was removed under reduced pressure. Recrystallization by layer diffusion in CH_2Cl_2 and *n*-pentane at room temperature afforded 0.06 g (0.20 mmol, 20%) deep orange crystals.

^{1}H NMR (300 MHz, DMSO-d_6) δ / ppm = 8.70 (d, *J* = 5.0 Hz, 2H, H-9), 8.09 (td, *J* = 7.9, 1.6 Hz, 2H, H-7), 7.94 (d, *J* = 8.1 Hz, 2H, H-6), 7.59 (d, *J* = 7.6 Hz, 2H, H-3), 7.39 (ddd, *J* = 7.1, 5.4, 1.4 Hz, 2H, H-8), 7.22 (t, *J* = 7.6 Hz, 1H, H-2).

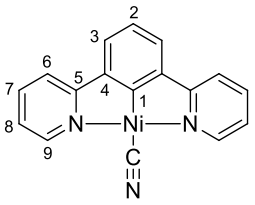

EI(+) MS (70eV) m/z = 315 $[M]^+$ (20%), 289 $[M\text{-}CN]^+$ (30%), 256 $[M\text{-}2NCH]^+$ (10%), 232 $[M\text{-}NiCN]^+$ (100%), 204 $[M\text{-}NiCN\text{-}NCH]^+$ (30%), 176 $[M\text{-}NiCN\text{-}2NCH]^+$ (10%), 154 $[PyPh]^+$ (25%).

EA (CHNS) Meas. / % (Calc. for $C_{17}H_{11}N_3Ni$ / %): C, 62.95 (64.62); H, 3.27 (3.51); N, 13.16 (13.30).

[Ni(Py(4,6FPh)Py)CN]. Following *General Procedure L* and using 0.36 g (1.00 mmol, 1.00 eq.) [Ni(Py(4,6FPhPy)Cl]. Afterwards, the solvent was removed under reduced pressure and CH_2Cl_2 (100 mL) was added. After precipitation overnight at ambient temperature, the precipitate filtered off and washed with CH_2Cl_2 (100 mL). The solvent was removed under reduced pressure. Recrystallization by layer diffusion in CH_2Cl_2 and *n*-pentane at room temperature afforded 0.09 g (0.26 mmol, 26%) yellow solid.

^{1}H NMR (300 MHz, DMSO-d_6) δ / ppm = 8.66 (d, *J* = 5.6 Hz, 2H, H-9), 8.11 (t, *J* = 7.5 Hz, 2H, H-7), 7.71 (d, *J* = 8.1 Hz, 2H, H-6), 7.42 (t, *J* = 6.7 Hz, 2H, H-8), 7.07 (t, *J* = 11.1 Hz, 1H, H-2).

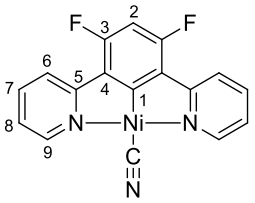

^{19}F NMR (282 MHz, DMSO-d_6) δ / ppm = –110.8 (d, *J* = 10.9 Hz, F-3).

EI(+) MS (70eV) m/z = 351 $[M]^+$ (50%), 325 $[M\text{-}CN]^+$ (100%), 280 $[M\text{-}CN\text{-}NCH\text{-}F]^+$ (20%), 267 $[M\text{-}NiCN]^+$ (50%), 240 $[M\text{-}NiCN\text{-}NCH]^+$ (25%), 220 $[M\text{-}NiCN\text{-}NCH\text{-}F]^+$ (10%), 170 $[PyPhF]^+$ (10%), 78 $[Py]^+$ (10%).

EA (CHNS) Meas. / % (Calc. for $C_{17}H_9F_2N_3Ni$ / %): C, 54.08 (58.01); H, 2.47 (2.58); N 10.76 (11.94).

[Ni(Py(4,6MePh)Py)CN]. Following *General Procedure L* and using 0.35 g (1.00 mmol, 1.00 eq.) [Ni(Py(4,6MePh)Py)Cl]. Afterwards, the solvent was removed under reduced pressure and CH_2Cl_2 (100 mL) was added. After precipitation overnight at ambient temperature, the precipitate filtered off and washed with CH_2Cl_2 (100 mL). The solvent was removed under reduced pressure. Recrystallization by layer diffusion in CH_2Cl_2 and *n*-pentane at room temperature afforded 0.09 g (0.25 mmol, 25%) yellow solid.

^{1}H NMR (300 MHz, CD_2Cl_2) δ / ppm = 8.91 (d, *J* = 4.3 Hz, 2H, H-9), 7.79 (td, *J* = 7.8, 1.5 Hz, 2H, H-7), 7.62 (d, *J* = 8.0 Hz, 2H, H-6), 7.05 (t, *J* = 6.2 Hz, 2H, H-8), 6.64 (s, 1H, H-2), 2.50 (s, 6H, H-10).

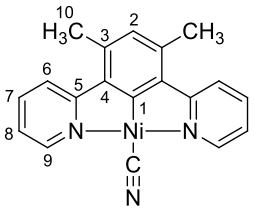

(300 MHz, DMSO-d_6) δ / ppm = 8.81 (d, *J* = 5.7 Hz, 2H, H-9), 8.04 (t, *J* = 7.7 Hz, 2H, H-7), 7.78 (d, *J* = 7.8 Hz, 2H, H-6), 7.33 (t, *J* = 6.4 Hz, 2H, H-8), 6.79 (s, 1H, H-2), 3.31 (s, 6H, H-10).

EI(+) MS (70eV) m/z = 343 $[M]^+$ (25%), 317 $[M\text{-}CN]^+$ (35%), 272 $[M\text{-}CN\text{-}CH_3\text{-}NCH]^+$ (15%), 259 $[M\text{-}NiCN]^+$ (75%), 245 $[M\text{-}NiCN\text{-}CH_3]^+$ (100%), 207 $[M\text{-}NiCN\text{-}2CH_3\text{-}NCH]^+$ (15%), 180 $[PyMe_2Ph]^+$ (25%).

EA (CHNS) Meas. / % (Calc. for $C_{19}H_{15}N_3Ni$ / %): C, 65.55 (66.33); H, 4.39 (4.39); N, 11.34 (12.21).

5.4.3.3 Synthesis of [Ni(Py(Ph)Py)Carb] *via C*oligand Exchange Reaction

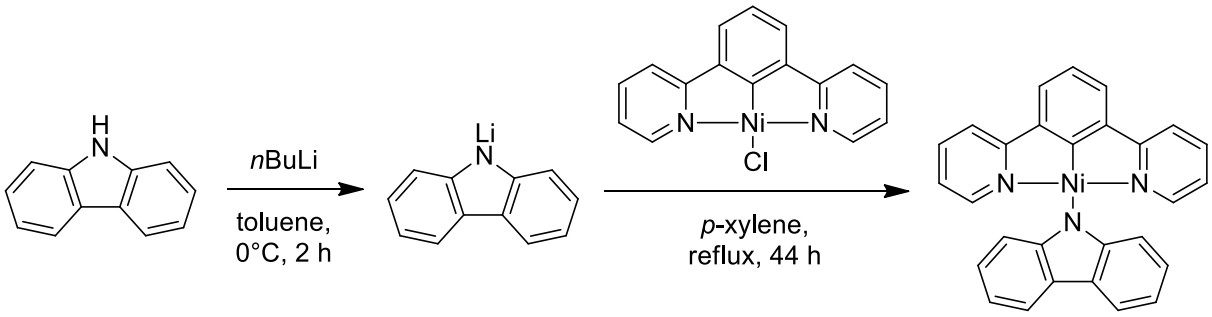

Lithium carbazolate.[234] 2.09 g (13.0 mmol, 1.00 eq.) 9*H*-carbazole was dried *in vacuo* and suspended in toluene (60 mL). The suspension was cooled to –78°C and 5.60 mL (14.0 mmol, 1.1 eq.) of a 2.5M solution of *n*BuLi in hexanes was added dropwise. The reaction mixture was warmed up to rt and stirred for 2 h. The formed precipitate was filtered under inert conditions, washed with warm toluene (20 mL) and then dissolved in dry THF (200 mL). The solid was then recrystallized using *n*-pentane at 4°C overnight yielding 1.11 g (6.64 mmol, 51%) colorless crystals.

^{1}H NMR (300 MHz, DMSO-d_6) δ / ppm = 7.96 (d, *J* = 7.7 Hz, 2H, H-2), 7.42 (d, *J* = 8.1 Hz, 2H, H-5), 7.16 (t, *J* = 7.5 Hz, 2H, H-4), 6.86 (t, *J* = 7.6 Hz, 2H, H-3).

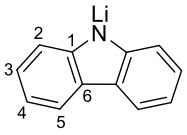

[Ni(PyPhPy)Carb].[127] Under inert conditions 0.33 g (1.00 mmol, 1.00 eq.) [Ni(PyPhPy)Cl] and 0.26 g (1.50 mmol, 1.50 eq.) lithium carbazolate were suspended in dry *p*-xylene (60 mL). The solution was degassed *via* freeze pump thaw thrice and refluxed for 44 h. The reaction mixture was cooled down to rt and the formed precipitate was filtered off and recrystallized from a mixture of THF and *n*-pentane giving 0.44 g (0.96 mmol, 96%) dark orange crystals.

^{1}H NMR (300 MHz, CD_2Cl_2) δ / ppm = 8.20 (d, *J* = 8.1 Hz, 2H, H-11), 8.14 (d, *J* = 7.7 Hz, 2H, H-14), 7.73 (td, *J* = 7.7, 1.6 Hz, 2H, H-8), 7.59 (d, *J* = 7.5 Hz, 2H, H-9), 7.43 (d, *J* = 7.5 Hz, 2H, H-3), 7.33 – 7.22 (m, 3H, H-2 and H-12), 7.02 (ddd, *J* = 7.8, 6.9, 1.0 Hz, 2H, H-13), 6.95 (d, *J* = 4.9 Hz, 2H, H-6), 6.70 (ddd, *J* = 7.2, 5.6, 1.4 Hz, 2H, H-7).

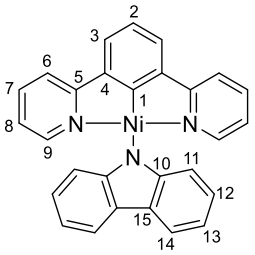

EI(+) MS (70eV) m/z = 455 $[M]^+$ (5%), 289 $[M\text{-}Carb]^+$ (20%), 231 $[M\text{-}NiCarb]^+$ (10%), 167 $[Carb]^+$ (100%), 139 $[Carb\text{-}2CH]^+$ (20%).

EA (CHNS) Meas. / % (Calc. for $C_{28}H_{19}N_3Ni$ / %): C, 69.64 (73.72); H, 4.17 (4.20); N, 9.37 (9.21).

5.4.3.4 Synthesis of [Ni(Py(Ph)Py)NO_3] *via* Coligand Exchange Reaction

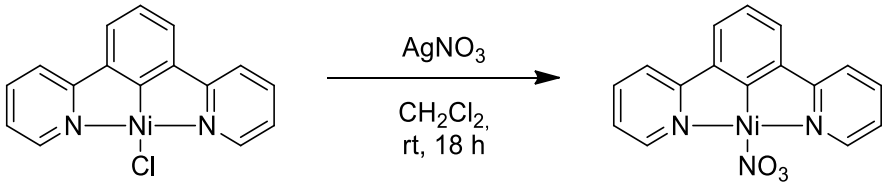

[Ni(PyPhPy)NO_3]. Under inert conditions 0.33 g (1.00 mmol, 1.00 eq.) [Ni(PyPhPy)Cl] was dissolved in CH_2Cl_2 (80 mL) and the flask was covered with tin foil. 0.19 g (1.10 mmol, 1.10 eq.) silver nitrate was added and the reaction mixture was stirred for 18 h. Then the reaction mixture was filtered over dry *Celite*®, the solvent was removed and the product was recrystallized from a mixture of CH_2Cl_2 and *n*-pentane giving 0.28 g (0.80 mmol, 80%) yellow solid.

^{1}H NMR (400 MHz, DMSO-d_6) δ / ppm = 8.18 – 8.07 (m, 4H, H-7 and H-9), 7.95 (d, J = 7.8 Hz, 2H, H-6), 7.54 (d, J = 7.5 Hz, 2H, H-3), 7.39 (t, J = 7.0 Hz, 2H, H-8), 7.21 (t, J = 7.5 Hz, 1H, H-2).

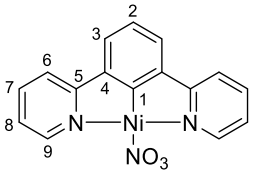

EI(+) MS (70eV) m/z = 351 $[M]^+$ (30%), 305 $[M\text{-}NO_2]^+$ (30%), 289 $[M\text{-}NO_3]^+$ (100%), 277 $[M\text{-}NO_2\text{-}NCH]^+$ (30%), 231 $[M\text{-}NiNO_3]^+$ (65%), 204 $[M\text{-}NiNO_3\text{-}NCH]^+$ (30%), 154 $[PyPh]^+$ (15%), 78 $[Py]^+$ (5%).

EA (CHNS) Meas. / % (Calc. for $C_{16}H_{11}N_3NiO_3$ / %): C, 53.66 (54.60); H, 2.81 (3.15); N, 11.65 (11.94).

5.4.3.5 Synthesis of [Ni(Py(Ph)Py)OR] *via* Coligand Exchange Reaction – *General Procedures*

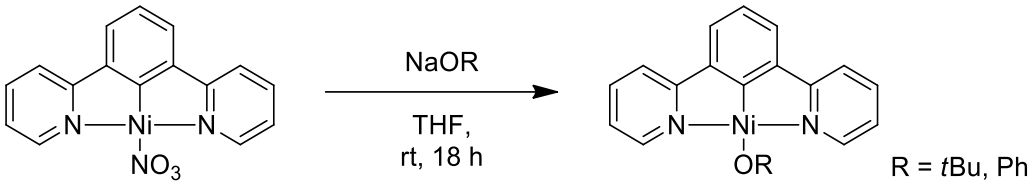

General procedure M. Under inert conditions, 0.08 g (0.20 mmol, 1.00 eq.) [Ni(PyPhPy)NO_3] was dissolved in THF (20 mL). A sodium alkoxide (0.22 mmol, 1.10 eq.) was added and the reaction mixture was stirred for 18 h. The solvent was removed and the crude product was redissolved in CH_2Cl_2 and filtered.

[Ni(PyPhPy)OPh]. Following *General Procedure M* and using 0.02 g (0.20 mmol, 1.0 eq.) NaOPh. After removal of the solvent, the product was recrystallized from a mixture of THF and *n*-pentane. The product was obtained as 0.06 g (0.15 mmol, 68%) orange solid.

^{1}H NMR (400 MHz, DMSO-d_6) δ / ppm = 8.05 (m, 4H, H-9 and H-7), 7.93 (d, J = 7.8 Hz, 2H, H-6), 7.57 (d, J = 7.6 Hz, 2H, H-3), 7.29 (t, J = 6.3 Hz, 2H, H-8), 7.20 (t, J = 7.6 Hz, 1H, H-2), 7.07 (d, J = 7.1 Hz, 2H, H-11), 6.94 (t, J = 6.9 Hz, 2H, H-12), 6.32 (t, J = 6.5 Hz, 1H, H-13).

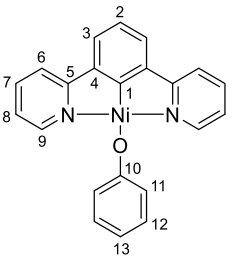

EI(+) MS (70eV) m/z = 382 $[M]^+$ (5%), 324 $[M\text{-}2NCH]^+$ (25%), 289 $[M\text{-}OPh]^+$ (100%), 232 $[M\text{-}NiOPh]^+$ (90%), 204 $[M\text{-}NiOPh\text{-}NCH]^+$ (35%), 154 $[PyPh]^+$ (20%).

EA (CHNS) Meas. / % (Calc. for $C_{22}H_{16}N_2NiO$ / %): C, 68.77 (68.98); H, 3.92 (4.21); N, 7.17 (7.35).

[Ni(PyPhPy)O*t*Bu]. Following *General Procedure M* and using 0.02 g (0.2 mmol, 1.0 eq.) NaO*t*Bu. The product was obtained as 0.05 g (0.12 mmol, 60%) orange-brown solid.

^{1}H NMR (400 MHz, CD_2Cl_2) δ / ppm = 8.78 (s, 2H, H-9), 7.85 (t, *J* = 7.4 Hz, 2H, H-7), 7.56 (d, *J* = 8.1 Hz, 2H, H-6), 7.34 (d, *J* = 7.3 Hz, 2H, H-3), 7.21 – 7.10 (m, 3H, H-2 and H-8), 1.26 (s, 6H, H-11), 1.23 (s, 3H, H-12).

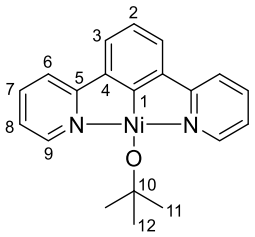

EI(+) MS (70eV) m/z = 362 $[M]^+$ (5%), 289 $[M\text{-}O\mathit{t}Bu]^+$ (100%), 232 $[M\text{-}NiO\mathit{t}Bu]^+$ (90%), 204 $[M\text{-}NiO\mathit{t}Bu\text{-}NCH]^+$ (35%), 154 $[PyPh]^+$ (20%), 78 $[Py]^+$ (5%).

EA (CHNS) Meas. / % (Calc. for $C_{20}H_{20}N_2NiO$ / %): C, 65.32 (66.16); H, 4.32 (5.55); N, 6.82 (7.72).

5.4.3.6 Synthesis of [Ni(Py(Ph)Py)F] *via* Coligand Exchange Reaction

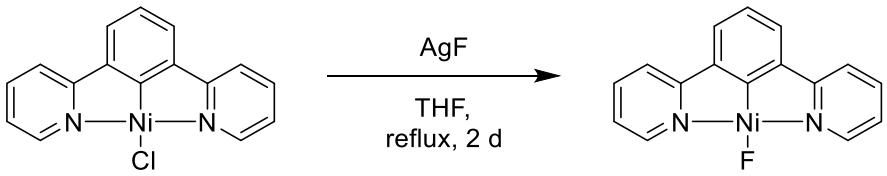

[Ni(PyPhPy)F]. Under inert conditions, 0.33 g (1.00 mmol, 1.00 eq.) [Ni(PyPhPy)Cl] was dissolved in THF (100 mL) and 0.25 g (2.00 mmol, 2.00 eq.) silver(I) fluoride was added. The reaction mixture was refluxed with exclusion of light for 48 h. The reaction mixture was filtered and the solvent was removed yielding 0.27 g (0.86 mmol, 86%) brown solid.

^{1}H NMR (300 MHz, DMSO-d_6) δ / ppm = 8.31 (d, *J* = 4.9 Hz, 2H, H-9), 8.08 (t, *J* = 7.6 Hz, 2H, H-7), 7.92 (d, *J* = 7.8 Hz, 2H, H-6), 7.53 (d, *J* = 7.5 Hz, 2H, H-3), 7.38 (t, *J* = 6.2 Hz, 2H, H-8), 7.15 (t, *J* = 7.6 Hz, 1H, H-2).

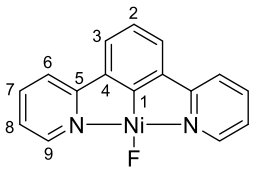

^{19}F NMR (282 MHz, DMSO-d_6) δ / ppm = –107.6 (q, *J* = 4.3 Hz, Ni-F).

EI(+) MS (70eV) m/z = 308 $[M]^+$ (5%), 289 $[M\text{-}F]^+$ (100%), 232 $[M\text{-}NiF]^+$ (35%), 204 $[M\text{-}NiF\text{-}NCH]^+$ (20%), 78 $[Py]^+$ (10%).

EA (CHNS) Meas. / % (Calc. for $C_{16}H_{11}N_2NiF$ / %): C, 58.79 (62.20); H, 4.12 (3.59); N, 7.95 (9.07).

5.4.3.7 Synthesis of [Ni(Py(Ph)Py)R_F] *via* Coligand Exchange Reaction – *General Procedures*

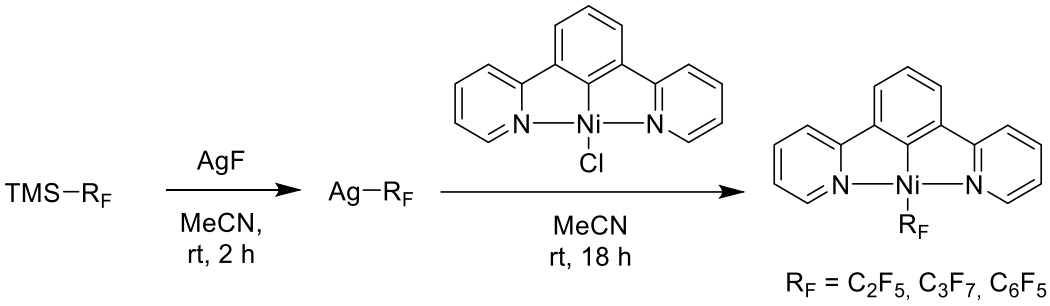

General procedure N.[86] Under inert conditions, 0.15 g (1.20 mmol, 2.00 eq.) silver(I) fluoride was suspended in dry MeCN (20 mL), a trimethylsilyl perfluoroalkylide or -aryilde (0.90 mmol, 1.50 eq.) was added. The reaction mixture was stirred in the glovebox for 2 h at rt under absence of light. 0.20 g (0.60 mmol, 1.00 eq.) [Ni(PyPhPy)Cl] was added and the reaction mixture was stirred overnight. The reaction mixture was centrifuged, and the red solution was freed of the solvent. The crude product was recrystallized from a THF / *n*-pentane mixture.

[Ni(PyPhPy)C_2F_5]. Following *General Procedure N* and using 0.17 g (0.90 mmol, 1.50 eq.) TMS-C_2F_5. The pure product was obtained as 0.22 g (0.54 mmol, 90%) red-brown solid.

^{1}H NMR (400 MHz, DMSO-d_6): δ / ppm = 8.15 (s, 2H, H-9), 8.04 (t, *J* = 7.6 Hz, 2H, H-7), 7.85 (d, *J* = 7.8 Hz, 2H, H-6), 7.45 (d, *J* = 7.2 Hz, 2H, H-3), 7.29 (t, *J* = 6.2 Hz, 2H, H-8), 7.15 (t, *J* = 7.5 Hz, 1H, H-2).

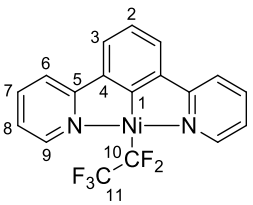

^{19}F NMR (376 MHz, DMSO-d_6): δ / ppm = –85.7 (d, *J* = 7.1 Hz, 3F, F-11), –114.1 (dt, *J* = 47.0, 2.6 Hz, 2F, F-10).

EI(+) MS (70 eV) m/z = 408 $[M]^+$ (5%), 289 $[M\text{-}C_2F_5]^+$ (25%), 232 $[M\text{-}NiC_2F_5]^+$ (100%), 204 $[M\text{-}NiC_2F_5\text{-}NCH]^+$ (25%), 154 $[PyPh]^+$ (20%).

EA (CHNS) Meas. / % (Calc. for $C_{18}H_{11}F_5N_2Ni$ / %): C, 53.36 (52.86); H, 2.81 (2.71); 6.23 (6.85).

[Ni(PyPhPy)C_3F_7]. Following *General Procedure N* and using 0.22 g (0.90 mmol, 1.50 eq.) TMS-C_3F_7. The pure product was obtained as 0.28 g (0.61 mmol, 99%) red solid.

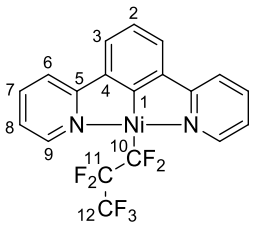

^{1}H NMR (400 MHz, DMSO-d_6): δ / ppm = 8.16 (s, 2H, H-9), 8.05 (t, *J* = 7.4 Hz, 2H, H-7), 7.86 (d, *J* = 7.7 Hz, 2H, H-6), 7.46 (d, *J* = 7.5 Hz, 2H, H-3), 7.30 (t, *J* = 6.3 Hz, 2H, H-8), 7.16 (t, *J* = 7.5 Hz, 1H, H-2).

^{19}F NMR (376 MHz, DMSO-d_6): δ / ppm = –78.8 (t, *J* = 9.0 Hz, 3F, F-12), –111.5 (dq, *J* = 44.3, 9.8 Hz, 2F, F-11), –124.9 (dt, *J* = 13.1, 7.2 Hz, 2F, F-10).

EI(+) MS (70 eV) m/z = 458 $[M]^+$ (10%), 289 $[M\text{-}C_3F_7]^+$ (100%), 231 $[M\text{-}NiC_3F_7]^+$ (40%), 204 $[M\text{-}NiC_3F_7\text{-}NCH]^+$ (15%).

EA (CHNS) Meas. / % (Calc. for $C_{19}H_{11}F_7N_2Ni$ / %): C, 49.58 (49.72); H, 2.66 (2.42); N, 6.09 (6.10).

[Ni(PyPhPy)C_6F_5]. Following *General Procedure N* and using 0.22 g (0.90 mmol, 1.50 eq.) TMS-C_6F_5. The pure product was obtained as 0.11 g (0.24 mmol, 40%) red solid.

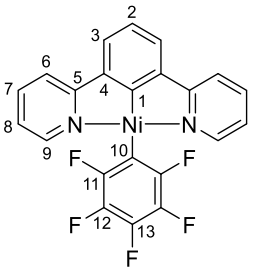

^{1}H NMR (400 MHz, DMSO-d_6): δ / ppm = 8.16 (s, 2H, H-9), 8.06 (t, *J* = 7.4 Hz, 2H, H-7), 7.88 (d, *J* = 7.7 Hz, 2H, H-6), 7.48 (d, *J* = 7.3 Hz, 2H, H-3), 7.32 (t, *J* = 6.0 Hz, 2H, H-8), 7.17 (t, *J* = 7.5 Hz, 1H, H-2).

^{19}F NMR (376 MHz, DMSO-d_6): δ / ppm = –108.5 (d, *J* = 25.3 Hz, 2F, F-11), –162.6 (t, *J* = 21.0 Hz, 1F, F-13), –164.0 (dd, *J* = 25.2, 21.1 Hz, 2F, F-12).

EI(+) MS (70 eV) m/z = 456 $[M]^+$ (5%), 398 $[M\text{-}3F]^+$ (5%), 325 $[M\text{-}5F\text{-}3C]^+$ (30%), 289 $[M\text{-}C_6F_5]^+$ (80%), 232 $[M\text{-}NiC_6F_5]^+$ (90%), 204 $[M\text{-}NiC_6F_5\text{-}NCH]^+$ (25%), 154 $[PyPh]^+$ (20%).

EA (CHNS) Meas. / % (Calc. for $C_{22}H_{11}F_5N_2Ni$ / %): C, 57.63 (57.82); H, 2.69 (2.43); N, 6.10 (6.13).

5.5 Synthesis of Pd N^C^N Complexes

5.5.1 Synthesis of [Pd(Py(4,6RPh)Py)Cl] *via* C–H Activation – *General Procedures*

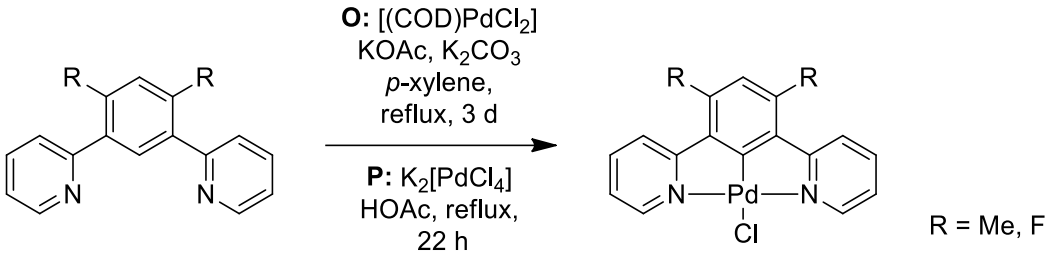

General procedure O.[92] In an inert flask with a water trap filled with molecular sieve (3 Å), 0.19 g (0.65 mmol, 1.30 eq.) [(COD)$PdCl_2$], 0.49 g (0.50 mmol, 1.00 eq.) KOAc and 0.69 g (0.50 mmol, 1.00 eq.) K_2CO_3 were prepared and a substituted N^C^N protoligand (0.50 mmol, 1.00 eq.) as well as dry *p*-xylene (120 mL) were added. The reaction was refluxed for 72 h under the strict exclusion of light. After cooling to ambient temperature, the precipitate was filtered off, washed once with *p*-xylene and the product was extracted using CH_2Cl_2. The solvent was subsequently removed.

General procedure P.[122, 123] A substituted N^C^N protoligand (0.40 mmol, 1.00 eq.) and 0.14 g (0.40 mmol, 1.00 eq.) $K_2[PdCl_4]$ were suspended in HOAc (30 mL) and heated under reflux for 22 h. The precipitated solid was filtered, washed with HOAc, MeOH and Et_2O (20 mL each) and dried under vacuum.

[Pd(Py(4,6MePh)Py)Cl]. Following *General Procedure O* and using 0.13 g (0.50 mmol, 1.00 eq.) Py(4,6MePhH)Py. 0.14 g (0.35 mmol, 68%) of the pale orange solid was dried in vacuum and isolated.

[Pd(Py(4,6MePh)Py)Cl]. Following *General Procedure P* and using 0.11 g (0.40 mmol, 1.00 eq.) Py(4,6MePhH)Py. 0.16 g (0.40 mmol, >99%) of the pale orange solid was dried in vacuum and isolated.

^{1}H NMR (300 MHz, CD_2Cl_2): δ / ppm = 9.01 (d, 2H, *J* = 4.8 Hz, H-9), 7.77 (td, 2H, *J* = 7.8, 7.3, 1.7 Hz, H-7), 7.70 (d, 2H *J* = 7.8 Hz, H-6), 7.10 (ddd, 2H, *J* = 7.1, 5.4, 1.4 Hz, H-8), 6.57 (s, 1H, H-2), 2.47 (s, 6H, H-10).

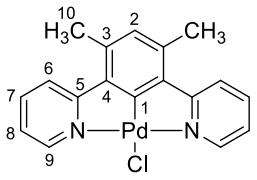

EI(+) MS (70 eV) m/z = 400 $[M]^+$ (20%), 365 $[M\text{-}Cl]^+$ (100%), 259 $[M\text{-}PdCl]^+$ (100%), 245 $[M\text{-}PdCl\text{-}CH_3]^+$ (40%), 229 $[PyPhPy]^+$ (5%), 180 $[M\text{-}PdCl\text{-}Py]^+$ (10%), 167 $[PyPhCH_3]^+$ (10%), 151 $[PhPy]^+$ (5%), 78 $[Py]^+$ (5%).

EA (CHNS) Meas. / % (Calc. for $C_{18}H_{15}N_2PdCl$ / %): C, 53.82 (53.89); H, 4.27 (4.28); N, 6.94 (6.98).

[Pd(Py(4,6FPh)Py)Cl]. Following *General Procedure O* and using 0.14 g (0.50 mmol, 1.00 eq.) Py(4,6FPhH)Py. 0.09 g (0.22 mmol, 55%) of the yellow solid was dried in vacuum and isolated.

[Pd(Py(4,6FPh)Py)Cl]. Following *General Procedure P* and using 0.11 g (0.40 mmol, 1.00 eq.) Py(4,6FPhH)Py. 0.16 g (0.39 mmol, 98%) of the pale orange solid was dried in vacuum and isolated.

^{1}H NMR (300 MHz, CD_2Cl_2): δ / ppm = 9.06 (d, *J* = 5.7 Hz, 2H, H-9), 7.97 – 7.87 (m, 4H, H-6 and H-7), 7.32 (ddd, *J* = 7.3, 5.5, 1.8 Hz, 2H, H-8), 6.69 (t, *J* = 11.3 Hz, 1H, H-1).

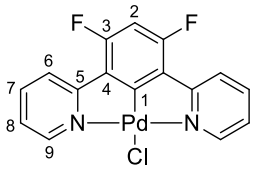

^{19}F NMR (282 MHz, CD_2Cl_2): δ / ppm = –108.6 (d, *J* = 11.4 Hz, F-3).

EI(+) MS (70 eV) m/z = 407 $[M]^+$ (10%), 372 $[M\text{-}Cl]^+$ (100%), 325 $[M\text{-}F\text{-}Cl\text{-}NCH]^+$ (5%), 267 [M-PdCl] (20%), 247 $[M\text{-}PdCl\text{-}F]^+$ (20%), 240 $[M\text{-}PdCl\text{-}NCH]^+$ (20%), 234 $[M\text{-}PdCl\text{-}2F]^+$ (10%), 187 $[PyF_2Ph]^+$ (10%).

EA (CHNS) Meas. / % (Calc. / %): C, 46.29 (46.97); H, 2.10 (2.22); N, 6.39 (6.85). Calc. for $C_{16}H_9ClF_2N_2Pd$.

5.5.2 Synthesis of [Pd(Py(4,6RPh)Py)CN] *via* Coligand Exchange Reaction – *General Procedures*

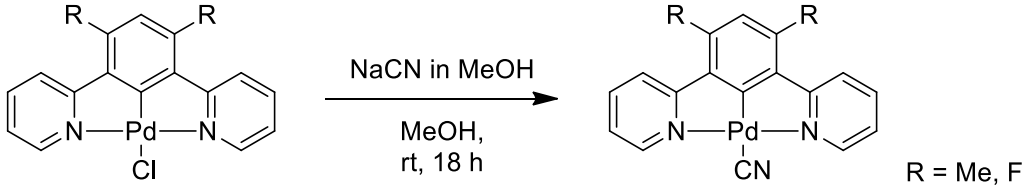

General procedure Q.[108, 167] Under inert atmosphere, of a Pd(II) complex of the type [Pd(N^C^N)Cl] (0.30 mmol, 1.00 eq.) was dissolved in MeOH (6 mL). 0.02 g (0.30 mmol, 1.00 eq.) NaCN was added as a solution in MeOH (6 mL) and the reaction mixture was stirred

at rt for 18 h. Then, the precipitate was filtered off and washed with MeOH and Et_2O (3 x 5 mL each).

[Pd(Py(4,6FPh)Py)CN]. Following *General Procedure Q* and using 0.12 g (0.30 mmol, 1.00 eq.) [Pd(Py(4,6FPh)Py)Cl]. The pure product was obtained as 0.08 g (0.22 mmol, 73%) colorless solid.

^{1}H NMR (300 MHz, CD_2Cl_2): δ / ppm = 8.94 (ddd, *J* = 5.6, 1.8, 0.9 Hz, 2H, H-9), 7.88 (td, *J* = 7.8, 7.3, 1.7 Hz, 2H, H-7), 7.81 (d, *J* = 7.8 Hz, 2H, H-6), 7.19 (ddd, *J* = 7.2, 5.5, 1.6 Hz, 2H, H-8), 6.72 (s, 1H, H-2), 2.57 (s, 6H, H-10).

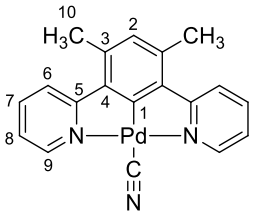

EI(+) MS (70 eV) m/z = 391 $[M]^+$ (5%), 365 $[M\text{-}CN]^+$ (10%), 284 $[M\text{-}CN\text{-}2CH_3\text{-}2NCH]^+$ (25%), 259 $[M\text{-}PdCN]^+$ (60%), 245 $[M\text{-}PdCN\text{-}CH_3]^+$ (100%), 207 $[M\text{-}PdCN\text{-}2NCH]^+$ (20%).

[Pd(Py(4,6MePh)Py)CN]. Following *General Procedure Q* and using 0.12 g (0.30 mmol, 1.00 eq.) [Pd(Py(4,6MePh)Py)Cl]. The pure product was obtained as 0.06 g (0.15 mmol, 50%) colorless solid.

^{1}H NMR (300 MHz, CD_2Cl_2): δ / ppm = 8.94 (d, *J* = 5.5 Hz, 2H, H-9), 7.99 (td, *J* = 7.8, 1.7 Hz, 2H, H-7), 7.92 (d, *J* = 7.1 Hz, 2H, H-6), 7.33 (ddd, *J* = 7.3, 5.6, 1.7 Hz, 2H, H-8), 6.69 (t, *J* = 11.2 Hz, 1H, H-2).

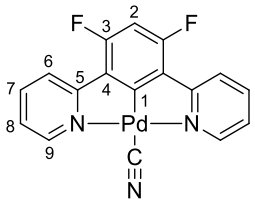

^{19}F NMR (282 MHz, CD_2Cl_2): δ / ppm = –108.4 (d, *J* = 11.2 Hz, F-3).

EI(+) MS (70 eV) m/z = 399 $[M]^+$ (5%), 372 $[M\text{-}CN]^+$ (20%), 267 $[M\text{-}PdCN]^+$ (100%), 247 $[M\text{-}PdCN\text{-}F]^+$ (25%), 240 $[M\text{-}PdCN\text{-}NCH]^+$ (35%), 220 $[M\text{-}PdCN\text{-}F\text{-}NCH]^+$ (10%), 134 $[PdCN]^+$ (5%), 78 $[Py]^+$ (10%).

5.6 Synthesis of Pt N^C^N Complexes

5.6.1 Synthesis of [Pt(Py(4,6RPh)Py)Cl] *via* C–H Activation – *General Procedures*

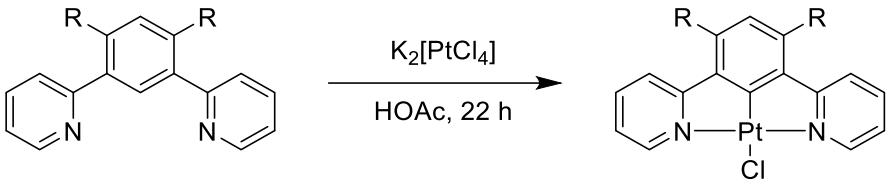

R = H, Me, F

General procedure R.[141] 0.13 g (0.30 mmol, 1.00 eq.) $K_2[PtCl_4]$ and a N^C^N protoligand (0.30 mmol, 1.00 eq.) were suspended in glacial acetic acid (10 mL) and refluxed for 3 d. The reaction mixture was cooled down to room temperature and the precipitated bright orange solid was filtered off, washed with MeOH, H_2O, EtOH and Et_2O and dried over phosphorous(V) oxide under reduced pressure.

[Pt(PyPhPy)Cl]. Following *General Procedure R* and using 0.07 g (0.30 mmol, 1.00 eq.) PyPhHPy. The product was isolated as 0.12 g (0.26 mmol, 85%) yellow solid.

^{1}H NMR (300 MHz, CD_2Cl_2): δ / ppm = 9.26 (td, J = 5.5 Hz, J_{PtH} = 41 Hz, 2H, H-9), 7.98 (td, J = 7.8, 1.6 Hz, 2H, H-7), 7.74 (q, J = 6.7 Hz, 2H, H-6), 7.51 (d, J = 7.7 Hz, 2H, H-3), 7.38 – 7.22 (m, 3H, H-2 and H-8).

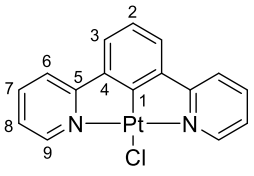

[Pt(Py(4,6MePh)Py)Cl]. Following *General Procedure R* and using 0.08 g (0.30 mmol, 1.00 eq.) Py(4,6MePhH)Py. The product was isolated as 0.11 g (0.23 mmol, 75%) orange solid.

^{1}H NMR (300 MHz, CD_2Cl_2): δ / ppm = 9.39 (td, 2H, J = 5.7, J_{PtH} = 42 Hz, H-9), 7.93 (ddd, 2H, J = 7.8, 7.3, 1.8 Hz, H-7), 7.85 (d, 2H J = 7.7 Hz, H-6), 7.24 (ddd, 2H, J = 7.4, 5.7, 1.6 Hz, H-8), 6.79 (s, 1H, H-2), 2.64 (s, 6H, H-10).

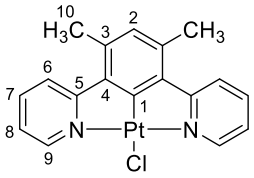

^{195}Pt NMR (64 MHz, CD_2Cl_2): δ / ppm = –3609.

EI(+)-MS(+) m/z = 489 $[M]^+$ (60%), 454 $[M\text{-}Cl]^+$ (100%), 438 $[M\text{-}Cl\text{-}CH_3]^+$ (20%), 424 $[M\text{-}Cl\text{-}2CH_3]^+$ (10%), 259 $[M\text{-}PtCl]^+$ (60%), 245 $[M\text{-}PtCl\text{-}CH_3]^+$ (60%), 229

[PyPhPy]$^+$ (5%), 180 [M-PtCl-Py]$^+$ (10%), 167 [PyPhCH$_3$]$^+$ (10%), 151 [PhPy]$^+$ (5%), 78 [Py]$^+$ (5%).

EA (CHNS) Meas. / % (Calc. for $C_{18}H_{15}N_2PtCl$ / %): C, 43.14 (44.13); H, 3.06 (3.09); N, 5.75 (5.72).

[Pt(Py(4,6FPh)Py)Cl]. Following *General Procedure R* and using 0.08 g (0.30 mmol, 1.00 eq.) Py(4,6FPhH)Py. The product was isolated as 0.10 g (0.21 mmol, 70%) yellow solid.

^{1}H NMR (300 MHz, CD_2Cl_2): δ / ppm = 9.25 (td, J = 5.7 Hz, J_{PtH} = 41 Hz, 2H, H-9), 7.99 (td, J = 7.9, 1.6 Hz, 2H, H-7), 7.90 (d, J = 7.1 Hz, 2H, H-6), 7.33 (ddd, J = 7.4, 5.7, 1.6 Hz, 2H, H-8), 6.72 (t, J = 11.3 Hz, 1H, H-2).

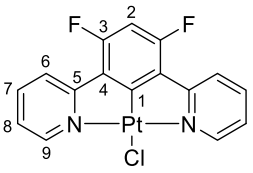

^{19}F NMR (282 MHz, CD_2Cl_2): δ / ppm = –108.8 (d, J = 11.3 Hz, J_{PtF} = 54 Hz, F-3).

EI(+)-MS(+) m/z = 497 [M]$^+$ (35%), 462 [M-Cl]$^+$ (100%), 409 [M-Cl-2NCH]$^+$ (10%), 265 [M-PtCl]$^+$ (10%), 240 [M-PtCl-NCH]$^+$ (25%), 165 [PyF$_2$Ph-NCH]$^+$ (5%).

EA (CHNS) Meas. / % (Calc. for $C_{16}H_9ClF_2N_2Pt$ / %): C, 37.16 (38.61); H, 1.67 (1.82); N, 5.57 (5.63).

5.6.2 Synthesis of [Pt(Py(4,6RPh)Py)CN] *via* Coligand Exchange Reaction – *General Procedures*

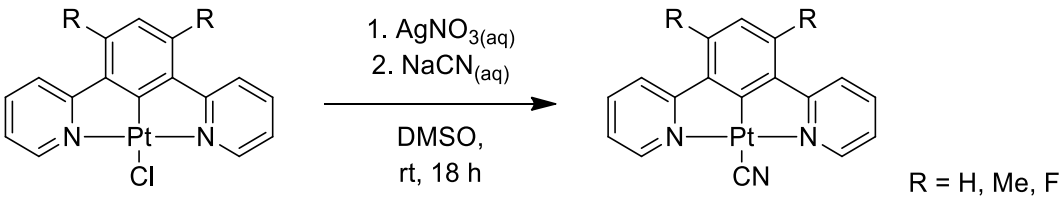

R = H, Me, F

General procedure S.[108, 167] Under exclusion of light, [Pt(N^C^N)Cl] (0.20 mmol, 1.00 eq.) was suspended in DMSO (1.50 mL) and 0.04 g (0.20 mmol, 1.00 eq.) $AgNO_3$ was added as a solution in water (0.50 mL). Then 0.01 g (0.20 mmol, 1.00 eq.) NaCN was added, and the reaction mixture was stirred for 18 h at rt. Water (10 mL) was added to the reaction mixture and the flask was stored at 3°C overnight for full crystallization. The precipitate was filtered over *Celite*® and washed with CH_2Cl_2 and MeOH.

[Pt(PyPhPy)CN]. Following *General Procedure S* and using 0.09 g (0.20 mmol, 1.00 eq.) [Pt(PyPhPy)Cl]. The pure product was obtained as 0.04 g (0.08 mmol, 38%) brown solid.

^{1}H NMR (300 MHz, CD_2Cl_2): δ / ppm = 9.20 (d, J = 8.2 Hz, J_{PtH} = 47 Hz, 2H, H-9), 8.04 (s, 2H, H-7), 7.77 (d, J = 7.9 Hz, 2H, H-6), 7.58 (d, J = 3.0 Hz, 2H, H-3), 7.37 – 7.21 (m, 3H, H-2 and H-8).

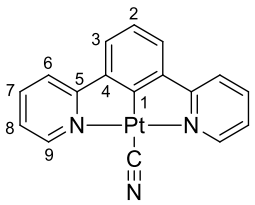

EI(+) MS (70 eV) m/z = 452 $[M]^+$ (5%), 426 $[M\text{-}CN]^+$ (5%), 435 $[M\text{-}NCH]^+$ (5%), 400 $[M\text{-}CN\text{-}NCH]^+$ (5%), 269 $[PhPtCN]^+$, 232 $[M\text{-}PtCN]^+$ (60%), 207 $[M\text{-}PtCN\text{-}NCH]^+$ (100%), 129 $[PyPh\text{-}NCH]^+$ (30%).

EA (CHNS) Meas. / % (Calc. for $C_{17}H_{11}N_3Pt$ / %): C, 43.56 (45.14); H, 2.03 (2.45); N, 9.08 (9.29).

[Pt(Py(4,6MePh)Py)CN]. Following *General Procedure S* and using 0.10 g (0.20 mmol, 1.00 eq.) [Pt(Py(4,6MePh)Py)Cl]. The pure product was obtained as 0.06 g (0.13 mmol, 65%) orange solid.

^{1}H NMR (300 MHz, CD_2Cl_2): δ / ppm = (td, J = 5.0 Hz, J_{PtH} = 48 Hz, 2H, H-9), 7.93 (t, J = 7.1 Hz, 2H, H-7), 7.81 (d, J = 7.8 Hz, 2H, H-6), 7.15 (t, J = 5.9 Hz, 2H, H-8), 6.73 (s, 1H, H-2), 2.58 (s, 6H, H-10).

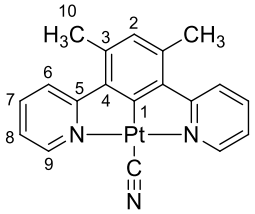

EI(+) MS (70 eV) m/z = 480 $[M]^+$ (20%), 454 $[M\text{-}CN]^+$ (20%), 375 $[M\text{-}NCH\text{-}Py]^+$ (10%), 259 $[M\text{-}PtCN]^+$ (50%), 245 $[M\text{-}PtCN\text{-}CH_3]^+$ (100%), 232 $[M\text{-}PtCN\text{-}2CH_3]^+$ (45%), 204 $[M\text{-}PtCN\text{-}2CH_3\text{-}NCH]^+$ (35%), 129 $[PyPh\text{-}NCH]^+$ (15%).

EA (CHNS) Meas. / % (Calc. for $C_{19}H_{15}N_3Pt$ / %): C, 45.87 (47.50); H, 2.94 (3.15); N, 8.53 (8.75).

[Pt(Py(4,6FPh)Py)CN]. Following *General Procedure S* and using 0.10 g (0.20 mmol, 1.00 eq.) [Pt(Py(4,6FPh)Py)Cl]. The pure product was obtained as 0.05 g (0.11 mmol, 55%) orange solid.

^{1}H NMR (300 MHz, CD_2Cl_2): δ / ppm = 9.13 (td, J = 5.0 Hz, J_{PtH} = 48 Hz, 2H, H-9), 8.01 (t, J = 6.3 Hz, 2H, H-7), 7.91 (d, J = 7.5 Hz, 2H, H-6), 7.27 (t, J = 6.0 Hz, 2H, H-8), 6.68 (t, J = 11.3 Hz, 1H, H-2).

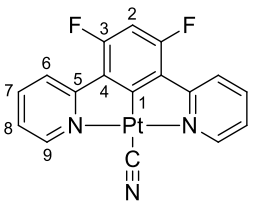

^{19}F NMR (282 MHz, CD_2Cl_2): δ / ppm = –108.6 (q, J = 11.4 Hz, J_{PtF} = 46 Hz, F-3).

EI(+) MS (70 eV) m/z = 488 $[M]^+$ (70%), 462 $[M\text{-}CN]^+$ (90%), 461 $[M\text{-}NCH]^+$ (100%), 409 $[M\text{-}CN\text{-}2NCH]^+$ (10%), 268 $[M\text{-}PtCN]^+$ (40%), 240 $[M\text{-}PtCN\text{-}NCH]^+$ (40%), 207 $[M\text{-}PtCN\text{-}2F\text{-}NCH]^+$ (20%), 129 $[PyPh]^+$ (10%).

EA (CHNS) Meas. / % (Calc. for $C_{17}H_9F_2N_3Pt$ / %): C, 39.77 (41.81); H, 1.56 (1.86); N, 8.33 (8.60).

5.7 Catalytic Experiments

Reaction type I

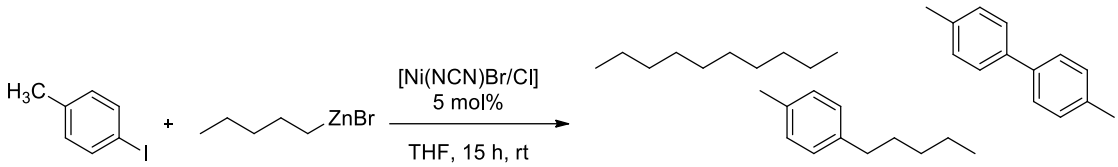

Reaction type II

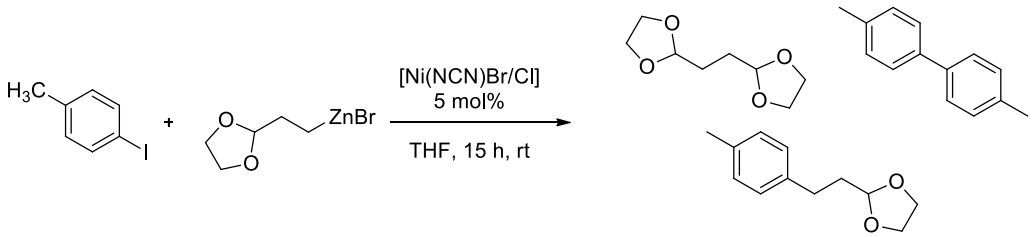

0.11 g (0.50 mmol, 1.00 eq.) 4-iodotoluene was dissolved in THF (5.00 mL) and 0.08 g (0.50 mmol, 1.00 eq. for 100% conversion) hexamethylbenzene was added as the internal standard. Then 1.00 mL (0.50 mmol, 1.00 eq.) of a 0.50M solution of a zinc reagent in THF was added into the solution. Response factor for 1-methyl-4-pentylbenzene is 0.985 and for 2-(4-methylphenethyl)-1,3-dioxane is 0.794. Then the Ni(II) catalyst (0.03 mmol, 0.05 eq.) was added into the solution while stirring. The stirring was stopped after 15 h by addition of H_2O (2.00 mL) and sit for 2 h. 1.00 mL of the organic layer was filtered through an alumina plug and washed with 10.0 mL of MeOH to reach a conc. of 1.00 mg/mL for the GC-MS analysis.

6 References

[1] J. K. Stille, *Angew. Chem. Int. Ed.* **1986**, *25* (6), 508–524.

[2] K. Tamao, K. Sumitani, M. Kumada, *J. Am. Chem. Soc.* **1972**, *94* (12), 4374–4376.

[3] Y. Hatanaka, T. Hiyama, *J. Org. Chem.* **1988**, *53* (4), 918–920.

[4] N. Miyaura, A. Suzuki, *Chem. Rev.* **1995**, *95* (7), 2457–2483.

[5] E.-i. Negishi, *Acc. Chem. Res.* **1982**, *15* (11), 340–348.

[6] R. F. Heck, J. P. Nolley, *J. Org. Chem.* **1972**, *37* (14), 2320–2322.

[7] X. F. Wu, P. Anbarasan, H. Neumann, M. Beller, *Angew. Chem. Int. Ed.* **2010**, *49* (48), 9047–9050.

[8] A. O. King, N. Okukado, E.-i. Negishi, *J. Chem. Soc., Chem. Commun.* **1977**, (19), 683–684.

[9] N. Miyaura, A. Suzuki, *J. Chem. Soc., Chem. Commun.* **1979**, (19), 866–867.

[10] C. Liu, H. Zhang, W. Shi, A. Lei, *Chem. Rev.* **2011**, *111* (3), 1780–1824.

[11] P. Ruiz-Castillo, S. L. Buchwald, *Chem. Rev.* **2016**, *116* (19), 12564–12649.

[12] A. F. Hollemann, E. Wiberg, N. Wiberg, *Lehrbuch der Anorganischen Chemie*; de Groyter, **2007**.

[13] C. Janiak, D. Gudat, R. Alsfasser, *RIEDEL Moderne Anorganische Chemie*; de Groyter, **2012**.

[14] J. Reinhard, *Angew. Chem.* **2009**, *121* (48), 9196–9199.

[15] H. Lindlar, *Helv. Chim. Acta* **1952**, *35* (2), 446–450.

[16] K. W. Rosenmund, *Ber. Dtsch. Chem. Ges.* **1918**, *51* (1), 585–593.

[17] I. Mejía-Centeno, S. Castillo, G. A. Fuentes, *Appl. Cat. B: Env.* **2012**, *119–120*, 234–240.

[18] C. Hageluken, *METALL-BERLIN* **2006**, *60* (1), 31.

[19] T. Hatakeyama, S. Hashimoto, K. Ishizuka, M. Nakamura, *J. Am. Chem. Soc.* **2009**, *131* (33), 11949–11963.

[20] A. Yamamoto, *J. Organomet. Chem.* **2002**, *653* (1–2), 5–10.

[21] V. P. W. Böhm, T. Weskamp, C. W. K. Gstöttmayr, W. A. Herrmann, *Angew. Chem. Int. Ed.* **2000**, *39* (9), 1602–1604.

[22] S. Katagiri, R. Sakamoto, H. Maeda, Y. Nishimori, T. Kurita, H. Nishihara, *Chem. Eur. J.* **2013**, *19* (16), 5088–5096.

[23] A. Fürstner, A. Leitner, M. Méndez, H. Krause, *J. Am. Chem. Soc.* **2002**, *124* (46), 13856–13863.

[24] M. Nakamura, K. Matsuo, S. Ito, E. Nakamura, *J. Am. Chem. Soc.* **2004**, *126* (12), 3686–3687.

[25] B. D. Sherry, A. Fürstner, *Acc. Chem. Res.* **2008**, *41* (11), 1500–1511.

[26] G. Cahiez, A. Moyeux, *Chem. Rev.* **2010**, *110* (3), 1435–1462.

[27] M. Moselage, J. Li, L. Ackermann, *ACS Catal.* **2016**, *6* (2), 498–525.

[28] A. M. Trzeciak, J. J. Ziółkowski, *Organometallics* **2002**, *21* (1), 132–137.

[29] C. Amatore, L. El Kaïm, L. Grimaud, A. Jutand, A. Meignié, G. Romanov, *Eur. J. Org. Chem.* **2014**, *2014* (22), 4709–4713.

[30] J. K. Pierce, L. D. Hiatt, J. R. Howard, H. Hu, F. Qu, K. H. Shaughnessy, *Organometallics* **2022**, *41* (24), 3861–3871.

[31] V. V. Grushin, H. Alper, *Organometallics* **1993**, *12* (5), 1890–1901.

[32] F. Ozawa, A. Kubo, T. Hayashi, *Chem. Lett.* **2006**, *21* (11), 2177–2180.

[33] C. Amatore, A. Jutand, M. A. M'Barki, *Organometallics* **1992**, *11* (9), 3009–3013.

[34] C. Amatore, E. Carre, A. Jutand, M. A. M'Barki, *Organometallics* **1995**, *14* (4), 1818–1826.

[35] L. Malatesia, M. Angoletta, *J. Chem. Soc. (Res.)* **1957**, (0), 1186–1188.

[36] T. Hayashi, M. Konishi, Y. Kobori, M. Kumada, T. Higuchi, K. Hirotsu, *J. Am. Chem. Soc.* **1984**, *106* (1), 158–163.

[37] G. A. Bowmaker, P. D. W. Boyd, G. K. Campbell, J. M. Hope, R. L. Martin, *Inorg. Chem.* **1982**, *21* (3), 1152–1159.

[38] C. J. Campbell, J. F. Rusling, C. Brückner, *J. Am. Chem. Soc.* **2000**, *122* (28), 6679–6685.

[39] L. Gomes, E. Pereira, B. de Castro, *J. Chem. Soc., Dalton Trans.* **2000**, (8), 1373–1379.

[40] M. Martelli, G. Pilloni, G. Zotti, S. Daolio, *Inorg. Chim. Acta* **1974**, *11*, 155–158.

[41] P. Sehnal, R. J. K. Taylor, I. J. S. Fairlamb, *Chem. Rev.* **2010**, *110* (2), 824–889.

[42] K. L. Vikse, G. N. Khairallah, A. Ariafard, A. J. Canty, R. A. O'Hair, *J. Am. Chem. Soc.* **2015**, *137* (42), 13588–13593.

[43] D. M. Grove, G. v. Koten, P. Mul, R. Zoet, J. G. M. v. d. Linden, J. Legters, J. E. J. Schmitz, N. W. Murrall, A. J. Welch, *Inorg. Chem.* **1988**, *27*, 2466–2473.

[44] E. P. Broering, S. Dillon, E. M. Gale, R. A. Steiner, J. Telser, T. C. Brunold, T. C. Harrop, *Inorg. Chem.* **2015**, *54* (8), 3815–3828.

[45] A. Klein, Y. H. Budnikova, O. G. Sinyashin, *J. Organomet. Chem.* **2007**, *692* (15), 3156–3166.

[46] B. Zheng, F. Tang, J. Luo, J. W. Schultz, N. P. Rath, L. M. Mirica, *J. Am. Chem. Soc.* **2014**, *136* (17), 6499–6504.

[47] W. Zhou, N. P. Rath, L. M. Mirica, *Dalton Trans.* **2016**, *45* (21), 8693–8695.

[48] W. Zhou, S. Zheng, J. W. Schultz, N. P. Rath, L. M. Mirica, *J. Am. Chem. Soc.* **2016**, *138* (18), 5777–5780.

[49] D. C. Powers, E. Lee, A. Ariafard, M. S. Sanford, B. F. Yates, A. J. Canty, T. Ritter, *J. Am. Chem. Soc.* **2012**, *134* (29), 12002–12009.

[50] T. Gryaznova, Y. Dudkina, M. Khrizanforov, O. Sinyashin, O. Kataeva, Y. Budnikova, *J. Solid State Electr.* **2015**, *19* (9), 2665–2672.

[51] S. R. Whitfield, M. S. Sanford, *J. Am. Chem. Soc.* **2007**, *129* (49), 15142–15143.

[52] D. J. Cárdenas, B. Martín-Matute, A. M. Echavarren, *J. Am. Chem. Soc.* **2006**, *128* (15), 5033–5040.

[53] Y. Ye, N. D. Ball, J. W. Kampf, M. S. Sanford, *J. Am. Chem. Soc.* **2010**, *132* (41), 14682–14687.

[54] F. Tang, F. Qu, J. R. Khusnutdinova, N. P. Rath, L. M. Mirica, *Dalton Trans.* **2012**, *41* (46), 14046–14050.

[55] G. Maestri, M. Malacria, E. Derat, *Chem. Commun.* **2013**, *49* (88), 10424–10426.

[56] F. Tang, Y. Zhang, N. P. Rath, L. M. Mirica, *Organometallics* **2012**, *31* (18), 6690–6696.

[57] L. M. Mirica, J. R. Khusnutdinova, *Coordin. Chem. Rev.* **2013**, *257* (2), 299–314.

[58] J. R. Khusnutdinova, N. P. Rath, L. M. Mirica, *J. Am. Chem. Soc.* **2010**, *132* (21), 7303–7305.

[59] J. R. Bour, N. M. Camasso, M. S. Sanford, *J. Am. Chem. Soc.* **2015**, *137* (25), 8034–8037.

[60] M. B. Watson, N. P. Rath, L. M. Mirica, *J. Am. Chem. Soc.* **2017**, *139* (1), 35–38.

[61] H.-F. Klein, A. Bickelhaupt, T. Jung, G. Cordier, *Organometallics* **1994**, *13* (7), 2557–2559.

[62] V. F. Plyusnin, V. P. Grivin, S. V. Larionov, *Coordin. Chem. Rev.* **1997**, *159*, 121–133.

[63] G. E. Martinez, C. Ocampo, Y. J. Park, A. R. Fout, *J. Am. Chem. Soc.* **2016**, *138* (13), 4290–4293.

[64] N. M. Camasso, M. S. Sanford, *Science* **2015**, *347* (6227), 1218–1220.

[65] W. Zhou, J. W. Schultz, N. P. Rath, L. M. Mirica, *J. Am. Chem. Soc.* **2015**, *137* (24), 7604–7607.

[66] M. S. Kharasch, *Grignard Reaktions of Nonmetallic Substances*; Prentice Hall, **1954**.

[67] A. Jutand, *Chem. Rev.* **2008**, *108* (7), 2300–2347.

[68] C. Hamacher, N. Hurkes, A. Kaiser, A. Klein *Z. Anorg. Allg. Chem.* **2007**, *633* (15), 2711–2718.

[69] Y. Budnikova, Y. Kargin, J.-Y. Nedelec, J. Perichon, *J. Organomet. Chem.* **1999**, *575*, 63–66.

[70] C. Kaes, A. Katz, M. W. Hosseini, *Chem. Rev.* **2000**, *100* (10), 3553–3590.

[71] E. C. Constable, *Chem. Soc. Rev.* **2007**, *36* (2), 246–253.

[72] A. Winter, G. R. Newkome, U. S. Schubert, *ChemCatChem* **2011**, *3* (9), 1384–1406.

[73] G. T. Morgan, F. H. Burstall, *J. Chem. Soc. (Res.)* **1932**, (0), 20–30.

[74] G. T. Morgan, F. H. Burstall, *J. Chem. Soc. (Res.)* **1937**, (0), 1649–1655.

[75] Z.-X. Wang, N. Liu, *Eur. J. Inorg. Chem.* **2012**, *2012* (6), 901–911.

[76] B. M. Rosen, K. W. Quasdorf, D. A. Wilson, N. Zhang, A. M. Resmerita, N. K. Garg, V. Percec, *Chem. Rev.* **2011**, *111* (3), 1346–1416.

[77] R. Jana, T. P. Pathak, M. S. Sigman, *Chem. Rev.* **2011**, *111* (3), 1417–1492.

[78] N. D. Schley, G. C. Fu, *J. Am. Chem. Soc.* **2014**, *136* (47), 16588–16593.

[79] P. T. Kaplan, L. Xu, B. Chen, K. R. McGarry, S. Yu, H. Wang, D. A. Vicic, *Organometallics* **2013**, *32* (24), 7552–7558.

[80] G. D. Jones, J. L. Martin, C. McFarland, O. R. Allen, R. E. Hall, A. D. Haley, R. J. Brandon, T. Konovalova, P. J. Desrochers, P. Pulay, D. A. Vicic, *J. Am. Chem. Soc.* **2006**, *128* (40), 13175–13183.

[81] T. J. Anderson, G. D. Jones, D. A. Vicic, *J. Am. Chem. Soc.* **2004**, *126*, 8100–8101.

[82] J. T. Ciszewski, D. Y. Mikhaylov, K. V. Holin, M. K. Kadirov, Y. H. Budnikova, O. Sinyashin, D. A. Vicic, *Inorg. Chem.* **2011**, *50* (17), 8630–8635.

[83] Y. H. Budnikova, D. A. Vicic, A. Klein, *Inorganics* **2018**, *6* (1), 1–18.

[84] G. D. Jones, C. McFarland, T. J. Anderson, D. A. Vicic, *Chem. Commun. (Camb)* **2005**, (33), 4211–4213.

[85] X. Lin, D. L. Phillips, *J. Org. Chem.* **2008**, *73* (10), 3680–3688.

[86] C.-P. Zhang, H. Wang, A. Klein, C. Biewer, K. Stirnat, Y. Yamaguchi, L. Xu, V. Gomez-Benitez, D. A. Vicic, *J. Am. Chem. Soc.* **2013**, *135* (22), 8141–8144.

[87] C. Hamacher, N. Hurkes, A. Kaiser, A. Klein, A. Schuren, *Inorg. Chem.* **2009**, *48* (20), 9947–9951.

[88] A. Klein, *Z. Anorg. Allg. Chem.* **2001**, *627*, 645–650.

[89] A. Sandleben, Neue Derivate des cyclometallierten Nickelkomplexes [Ni(Phbpy)Br]. *Dissertation*, Universität zu Köln, **2018**.

[90] A. Kaiser, Untersuchungen an Organonickel-Komplexen im Hinblick auf Nickel-katalysierte C-C Kupplungsreaktionen. *Dissertation*, Universität zu Köln, **2011**.

[91] N. Vogt, Neuartige Cyclometallierte Komplexe des Nickels mit Carbanionischen Konjugierten Triaren-CNN-Liganden. *Dissertation*, Universität zu Köln, **2018**.

[92] L. Kletsch, G. Hörner, A. Klein, *Organometallics* **2020**, *39* (15), 2820–2829.

[93] P. M. Feth, A. Klein, H. Bertagnolli, *Eur. J. Inorg. Chem* **2003**, (5), 839–852.

[94] Y. H. Budnikova, J. Perichon, D. G. Yakhvarov, Y. Kargin, O. G. Sinyashin, *J. Organomet. Chem.* **2001**, *630*, 185–192.

[95] C. Amatore, A. Jutand, J. Périchon, Y. Rollin, *Monatsh. Chem. / Chem. Mon.* **2000**, *131* (12), 1293–1304.

[96] V. Courtois, R. Barhdadi, M. Troupel, J. Périchon, *Tetrahedron* **1997**, *53* (34), 11569–11576.

[97] D. G. Yakhvarov, D. I. Tazeev, O. G. Sinyashin, G. Giambastiani, C. Bianchini, A. M. Segarra, P. Lönnecke, E. Hey-Hawkins, *Polyhedron* **2006**, *25* (7), 1607–1612.

[98] I. F. Sakhapov, Z. N. Gafurov, V. M. Babaev, V. A. Kurmaz, R. R. Mukhametbareev, I. K. Rizvanov, O. G. Sinyashin, D. G. Yakhvarov, *Russ. J. Electrochem.* **2015**, *51* (11), 1061–1068.

[99] A. Klein, B. Rausch, A. Kaiser, N. Vogt, A. Krest, *J. Organomet. Chem.* **2014**, *774*, 86–93.

[100] A. Klein, A. Sandleben, N. Vogt, *P. Natl. a. Sci. India. A* **2016**, *86* (4), 533–549.

[101] N. Vogt, V. Sivchik, A. Sandleben, G. Hörner, A. Klein, *Molecules* **2020**, *25*, 997.

[102] R. F. Knott, J. G.Breckenridge, *Can. J. Chem.* **1954**, *32* (5), 512–521.

[103] E. C. Constable, R. P. G. Henney, T. A. Leese, D. A. Tocher, *J. Chem. Soc., Dalton Trans.* **1990**, (2), 443–449.

[104] E. C. Constable, R. P. G. Henney, T. A. Leese, D. A. Tocher, *J. Chem. Soc., Chem. Commun.* **1990**, (6), 513–515.

[105] A. Sandleben, Darstellung und Charakterisierung von Nickel(II)-Komplexen mit tridentaten Liganden des Typs 6-(Phen-2-yl)-2,2‘-bipyridin. *Masterarbeit*, Universität zu Köln, Köln, **2014**.

[106] M. Petrick, Cyclometallierte Nickel-Komplexe. *Diplomarbeit*, Universität zu Köln, **2014**.

[107] J. Wencel-Delord, T. Droge, F. Liu, F. Glorius, *Chem. Soc. Rev.* **2011**, *40* (9), 4740–4761.

[108] T. Eskelinen, S. Buss, S. K. Petrovskii, E. V. Grachova, M. Krause, L. Kletsch, A. Klein, C. A. Strassert, I. O. Koshevoy, P. Hirva, *Inorg. Chem.* **2021**, *60* (12), 8777–8789.

[109] N. Vogt, A. Sandleben, L. Kletsch, S. Schäfer, M. T. Chin, D. A. Vicic, G. Hörner, A. Klein, *Organometallics* **2021**, *40* (11), 1776–1785.

[110] D. M. Grove, G. v. Koten, H. J. C. Ubbels, R. Zoet, *Organometallics* **1984**, *3*, 1003–1009.

[111] J.-P. Cloutier, L. Rechignat, Y. Canac, D. H. Ess, D. Zargarian, *Inorg. Chem.* **2019**, *58* (6), 3861–3874.

[112] J.-P. Cloutier, D. Zargarian, *Organometallics* **2018**, *37* (9), 1446–1455.

[113] J. P. Cloutier, B. Vabre, B. Moungang-Soume, D. Zargarian, *Organometallics* **2015**, *34* (1), 133–145.

[114] M. Beley, J. P. Collin, R. Louis, B. Metz, J. P. Sauvage, *J. Am. Chem. Soc.* **1991**, *113* (22), 8521–8522.

[115] H. Bönnemann, *Angew. Chem. Int. Ed.* **1978**, *17* (7), 505–515.

[116] D. J. Cardenas, A. M. Echavarren, M. C. R. de Arellano, *Organometallics* **1999**, *18* (17), 3337–3341.

[117] Z. Wang, E. Turner, V. Mahoney, S. Madakuni, T. Groy, J. Li, *Inorg. Chem.* **2010**, *49* (24), 11276–11286.

[118] W. Sotoyama, T. Satoh, H. Sato, A. Matsuura, N. Sawatari, *J. Phys. Chem. A* **2005**, *109* (43), 9760–9766.

[119] A. F. Rausch, L. Murphy, J. A. G. Williams, H. Yersin, *Inorg. Chem.* **2009**, *48* (23), 11407–11414.

[120] T. Abe, T. Itakura, N. Ikeda, K. Shinozaki, *Dalton Trans.* **2009**, (4), 711–715.

[121] J. A. G. Williams, A. Beeby, E. S. Davies, J. A. Weinstein, C. Wilson, *Inorg. Chem.* **2003**, *42* (26), 8609–8611.

[122] B. Soro, G. Minghetti, A. Zucca, M. A. Cinellu, S. Gladiali, M. Manassero, M. Sansoni, *Organometallics* **2005**, *24*, 53–61.

[123] B. Soro, S. Stoccoro, G. Minghetti, A. Zucca, M. A. Cinellu, M. Manassero, S. Gladiali, *Inorg. Chim. Acta* **2006**, *359* (6), 1879–1888.

[124] Y.-D. Wang, J.-K. Liu, X.-J. Yang, J.-F. Gong, M.-P. Song, *Organometallics* **2022**, *41* (8), 984–996.

[125] Y.-T. Liu, Y.-R. Li, X. Wang, F.-Q. Bai, *Dyes Pigments* **2017**, *142*, 55–61.

[126] K. Ogata, D. Sasano, T. Yokoi, K. Isozaki, R. Yoshida, T. Takenaka, H. Seike, T. Ogawa, H. Kurata, N. Yasuda, *et al. Chem. Eur. J.* **2013**, *19*, 12356–12375.

[127] Y.-S. Wong, M.-C. Tang, M. Ng, V. W.-W. Yam, *J. Am. Chem. Soc.* **2020**, *142* (16), 7638–7646.

[128] A. H. Mousa, K. Chakrabarti, G. Isapour, J. Bendix, O. F. Wendt, *E. J. Inorg. Chem.* **2020**, *2020* (45), 4270–4277.

[129] T. Ogawa, O. S. Wenger, *Angew. Chem. Int. Ed.* **2023**, *62* (46), e202312851.

[130] L. Xi, L. Du, Z. Shi, *Chin. Chem. Lett.* **2022**, *33* (9), 4287–4292.

[131] D. Moreth, G. Hörner, V. V. L. Müller, L. Geyer, U. Schatzschneider, *Inorg. Chem.* **2023**, *62* (39), 16000–16012.

[132] L. Kletsch, L. Payen, A. Fiorentino, B. Blom, D. Romano, G. Hörner, A. Klein, *Organometallics* **2023**, *42* (16), 2206–2215.

[133] A. K. J. Matsumoto, M. Munetaka, M. Yoshizawa, *Chemistry - An Asian Journal* **2017**, *12*, 2889–2893.

[134] X. Yang, Z. Wang, S. Madakuni, J. Li, G. E. Jabbour, *Adv. Mat.* **2008**, *20* (12), 2405–2409.

[135] M. Chavarot, Z. Pikramenou, *Tetrahedron Lett.* **1999**, *40* (37), 6865–6868.

[136] B. D. Koivisto, K. C. D. Robson, C. P. Berlinguette, *Inorg. Chem.* **2009**, *48* (20), 9644–9652.

[137] Y. Chen, K. Li, W. Lu, S. S. Chui, C. W. Ma, C. M. Che, *Angew. Chem. Int. Ed.* **2009**, *48* (52), 9909–9913.

[138] B. Tong, H.-Y. Ku, I. J. Chen, Y. Chi, H.-C. Kao, C.-C. Yeh, C.-H. Chang, S.-H. Liu, G.-H. Lee, P.-T. Chou, *J. Mater. Chem. C* **2015**, *3* (14), 3460-3471.

[139] B. Avitia, E. MacIntosh, S. Muhia, E. Kelson, *Tetrahedron Lett.* **2011**, *52* (14), 1631–1634.

[140] L. Kletsch, R. Jordan, A. S. Köcher, S. Buss, C. A. Strassert, A. Klein, *Molecules* **2021**, *26* (16), 5051.

[141] L. Payen, L. Kletsch, T. Lapić, M. Wickleder, A. Klein, *Inorganics* **2023**, *11* (4), 174.

[142] A. Sandleben, N. Vogt, G. Hörner, A. Klein, *Organometallics* **2018**, *37* (19), 3332–3341.

[143] E. C. Constable, R. P. G. Henney, T. A. Leese, D. A. Tocher, *J. Chem. Soc., Dalton Trans.* **1990**, 443.

[144] S.-W. Lai, T.-C. Cheung, M. C. W. Chan, K.-K. Cheung, S.-M. Peng, C.-M. Che, *Inorg. Chem.* **2000**, *39* (2), 255–262.

[145] G. Cheng, P.-K. Chow, S. C. F. Kui, C.-C. Kwok, C.-M. Che, *Adv. Mat.* **2013**, *25* (46), 6765–6770.

[146] S. Garbe, M. Krause, A. Klimpel, I. Neundorf, P. Lippmann, I. Ott, D. Brünink, C. A. Strassert, N. L. Doltsinis, A. Klein, *Organometallics* **2020**, *39* (5), 746–756.

[147] R. v. d. Stück, Synthese und Charakterisierung neuartiger, cyclometallierter Palladium(II)-Komplexe mit tridentaten CNN-Liganden. *Dissertation*, Universität zu Köln, **2020**.

[148] J. D. Cope, J. A. Denny, R. W. Lamb, L. E. McNamara, N. I. Hammer, C. E. Webster, T. K. Hollis, *J. Organomet. Chem.* **2017**, *845*, 258–265.

[149] C. A. Janiak, *J. Chem. Soc., Dalton Trans.* **2000**, (21), 3885–3896.

[150] K. Mori, H. Yamashita, *Chemistry – A European Journal* **2016**, *22* (32), 11122–11137.

[151] M. Parasram, V. Gevorgyan, *Chem. Soc. Rev.* **2017**, *46* (20), 6227–6240.

[152] V. Guerchais, J.-L. Fillaut, *Coordin. Chem. Rev.* **2011**, *255* (21), 2448–2457.

[153] Q. Zhao, F. Li, C. Huang, *Chem. Soc. Rev.* **2010**, *39* (8), 3007–3030.

[154] J. Kalinowski, V. Fattori, M. Cocchi, J. A. G. Williams, *Coordin. Chem. Rev.* **2011**, *255* (21), 2401–2425.

[155] K. Li, G. S. Ming Tong, Q. Wan, G. Cheng, W.-Y. Tong, W.-H. Ang, W.-L. Kwong C.-M. Che, *Chem. Science* **2016**, *7* (3), 1653–1673.

[156] V. W.-W. Yam, A. S.-Y. Law, *Coordin. Chem. Rev.* **2020**, *414*, 213298.

[157] S. Fantacci, F. A De Angelis, *Coordin. Chem. Rev.* **2011**, *255* (21), 2704–2726.

[158] C. E. Housecroft, E. C. Constable, *Coordin. Chem. Rev.* **2017**, *350*, 155–177.

[159] Y. Zhang, Y. Wang, J. Song, J. Qu, B. Li, W. Zhu, W.-Y. Wong, *Adv. Opt. Mat.* **2018**, *6* (18), 1800466.

[160] H. Yersin, A. F. Rausch, R. Czerwieniec, T. Hofbeck, T. Fischer, *Coordin. Chem. Rev.* **2011**, *255* (21), 2622–2652.

[161] C. Bizzarri, E. Spuling, D. M. Knoll, D. Volz, S. Bräse, *Coordin. Chem. Rev.* **2018**, *373*, 49–82.

[162] T. Fleetham, G. Li, J. Li, *Adv. Mat.* **2017**, *29* (5), 1601861.

[163] S. Archer, J. A. Weinstein, *Coordin. Chem. Rev.* **2012**, *256* (21), 2530–2561.

[164] T. Strassner, *Acc. Chem. Res.* **2016**, *49* (12), 2680–2689.

[165] C. Cebrián, M. Mauro, *Beilstein J. Org. Chem.* **2018**, *14*, 1459–1481.

[166] I. O. Koshevoy, M. Krause, A. Klein, *Coordin. Chem. Rev.* **2020**, *405*, 213094.

[167] V. Sivchik, A. Kochetov, T. Eskelinen, K. S. Kisel, A. I. Solomatina, E. V. Grachova, S. P. Tunik, P. Hirva, I. O. Koshevoy, *Chemistry – A European Journal* **2021**, *27* (5), 1787–1794.

[168] L. Ravotto, P. Ceroni, *Coordin. Chem. Rev.* **2017**, *346*, 62–76.

[169] H. B. Gray, S. Záliš, A. Vlček, *Coordin. Chem. Rev.* **2017**, *345*, 297–317.

[170] P. Ganesan, W.-Y. Hung, J.-Y. Tso, C.-L. Ko, T.-H. Wang, P.-T. Chen, H.-F. Hsu, S.-H. Liu, G.-H. Lee, P.-T. Chou, *et al. Adv. Funct. Mat.* **2019**, *29* (26), 1900923.

[171] L. M. Cinninger, L. D. Bastatas, Y. Shen, B. J. Holliday, J. D. Slinker, *Dalton Trans.* **2019**, *48* (26), 9684–9691.

[172] V. W. Yam, V. K. Au, S. Y. Leung, *Chem. Rev.* **2015**, *115* (15), 7589–7728.

[173] C. Zou, J. Lin, S. Suo, M. Xie, X. Chang, W. Lu, *Chem. Commun.* **2018**, *54*, 5319.

[174] M. D. Santana, L. López-Banet, G. Sánchez, J. Pérez, E. Pérez, L. García, J. L. Serrano, A. Espinosa, *Dalton Trans.* **2016**, *45* (20), 8601–8613.

[175] L. Liu, X. Wang, F. Hussain, C. Zeng, B. Wang, Z. Li, I. Kozin, S. Wang, *ACS Appl. Mat. and Interfaces* **2019**, *11* (13), 12666–12674.

[176] P. K. Chow, G. Cheng, G. S. M. Tong, C. S. Ma, W. M. Kwok, W. H. Ang, C. Y. S. Chung, C. Yang, F. Wang, C. M. Che, *Chemical Science* **2016**, *7* (9), 6083–6098.

[177] T. Fleetham, Y. Ji, L. Huang, T. S. Fleetham, J. Li, *Chemical Science* **2017**, *8* (12), 7983–7990.

[178] J. Lin, C. Zou, X. Zhang, Q. Gao, S. Suo, Q. Zhuo, X. Chang, M. Xie, W. Lu, *Dalton Trans.* **2019**, *48*, 10417.

[179] M. Krause, R. v. d. Stück, D. Brünink, S. Buss, N. L. Doltsinis, C. A. Strassert, A. Klein, *Inorg. Chim. Acta* **2021**, *518*, 120093.

[180] J. Föller, D. H. Friese, S. Riese, J. M. Kaminski, S. Metz, D. Schmidt, F. Würthner, C. Lambert, C. M. Marian, *Phys. Chem. Chem. Physics* **2020**, *22* (6), 3217–3233.

[181] P.-T. Chou, Y. Chi, M.-W. Chung, C.-C. Lin, *Coordin. Chem. Rev.* **2011**, *255* (21), 2653–2665.

[182] G. S.-M. Tong, C.-M. Che, *Chemistry – A European Journal* **2009**, *15* (29), 7225–7237.

[183] A. Haque, L. Xu, R. A. Al-Balushi, M. K. Al-Suti, R. Ilmi, Z. Guo, M. S. Khan, W.-Y. Wong, P. R. Raithby, *Chem. Soc. Rev.* **2019**, *48* (23), 5547–5563.

[184] J. A. Williams, *Chem. Soc. Rev.* **2009**, *38* (6), 1783–1801.

[185] M. Hebenbrock, L. Stegemann, J. Kösters, N. L. Doltsinis, J. Müller, C. A. Strassert, *Dalton Trans.* **2017**, *46* (10), 3160–3169.

[186] M. Cnudde, D. Brünink, N. L. Doltsinis, C. A. Strassert, *Inorg. Chim. Acta* **2021**, *518*, 120090.

[187] S. W. Lai, T. C. Cheung, M. C. W. Chan, K. K. Cheung, S. M. Peng, C. M. Che, *Inorg. Chem.* **2000**, *39* (2), 255–262.

[188] S. Cheung, K.-K. Cheung, S.-M. Peng, C.-M. Che, *Dalton Trans.* **1996**, *8*.

[189] T. Karlen, A. Ludi, H. U. Güdel, *Inorg. Chem. Commun.* **1991**, *30* (10), 2250–2251.

[190] M. Niazi, A. Klein, *Inorganics* **2021**, *9* (6), 47.

[191] A. Haseloer, R. Jordan, L. M. Denkler, M. Reimer, S. Olthof, I. Schmidt, K. Meerholz, G. Hörner, A. Klein, *Dalton Trans.* **2021**, *50*, 4311.

[192] A. Hofmann, L. Dahlenburg, R. v. Eldik, *Inorg. Chem.* **2003**, *42*, 6528–6538.

[193] K. Yamamoto, K. Higuchi, M. Ogawa, H. Sogawa, S. Kuwata, Y. Hayashi, S. Kawauchi, T. Takata, *Chemistry – An Asian Journal* **2020**, *15* (3), 356–359.

[194] A. Iwakiri, Y. Konno, K. Shinozaki, *J. Lumin.* **2019**, *207*, 482–490.

[195] E. Garoni, J. Boixel, V. Dorcet, T. Roisnel, D. Roberto, D. Jacquemin, V. Guerchais, *Dalton Trans.* **2018**, *47* (1), 224–232.

[196] B. Schulze, C. Friebe, M. Jäger, H. Görls, E. Birckner, A. Winter, U. S. Schubert, *Organometallics* **2018**, *37* (1), 145–155.

[197] A. Rodrigue-Witchel, D. L. Rochester, S.-B. Zhao, K. B. Lavelle, J. A. G. Williams, S. Wang, W. B. Connick, C. Reber, *Polyhedron* **2016**, *108*, 151–155.

[198] A. F. Rausch, L. Murphy, J. A. G. Williams, H. Yersin, *Inorg. Chem.* **2012**, *51* (1), 312–319.

[199] S. J. Farley, D. L. Rochester, A. L. Thompson, J. A. K. Howard, J. A. G. Williams, *Inorg. Chem.* **2005**, *44* (26), 9690–9703.

[200] K. P. Jensen, *Inorg. Chem.* **2008**, *47* (22), 10357–10365.

[201] R. Alrefai, G. Hörner, H. Schubert, A. Berkefeld, *Organometallics* **2021**, *40* (8), 1163–1177.

[202] S.-W. Lai, M. C.-W. Chan, T.-C. Cheung, S.-M. Peng, C.-M. Che, *Inorg. Chem.* **1999**, *38*, 4046–4055.

[203] I. Hoffmann, B. Blumenröder, S. Onodi neé Thumann, S. Dommer, J. Schatz, *Green Chem.* **2015**, *17* (7), 3844–3857.

[204] V. C. Wakchaure, K. C. Ranjeesh, Goudappagouda; T. Das, K. Vanka, R. Gonnade, S. S. Babu, *Chem. Commun.* **2018**, *54* (47), 6028–6031.

[205] G. Dyker, M. Gabler, M. Nouroozian, P. Schulz, *Tetrahedron Lett.* **1994**, *35* (52), 9697–9700.

[206] M. Hruzd, N. le Poul, M. Cordier, S. Kahlal, J.-Y. Saillard, S. Achelle, S. Gauthier, F. Robin-le Guen, *Dalton Trans.* **2022**, *51* (14), 5546–5560.

[207] P. Pander, A. Sil, R. J. Salthouse, C. W. Harris, M. T. Walden, D. S. Yufit, J. A. G. Williams, F. B. Dias, *J. Mater. Chem. C* **2022**, *10* (40), 15084–15095.

[208] A. K.-W. Chan, E. S.-H. Lam, A. Y.-Y. Tam, D. P.-K. Tsang, W. H. Lam, M.-Y. Chan, W.-T. Wong, V. W.-W. Yam, *Chemistry – A European Journal* **2013**, *19* (41), 13910-13924.

[209] K. Okamoto, T. Kanbara, T. Yamamoto, A. Wada, *Organometallics* **2006**, *25* (16), 4026–4029.

[210] Q.-L. Luo, J.-P. Tan, Z.-F. Li, W.-H. Nan, D.-R. Xiao, *J. Org. Chem.* **2012**, *77* (18), 8332–8337.

[211] I. Buslov, F. Song, X. Hu, *Angew. Chem. Int. Ed.* **2016**, *55* (40), 12295–12299.

[212] S. T. Shreiber, I. M. DiMucci, M. N. Khrizanforov, C. J. Titus, D. Nordlund, Y. Dudkina, R. E.Cramer, Y. Budnikova, K. M. Lancaster, D. A. Vicic, *Inorg. Chem.* **2020**, *59* (13), 9143–9151.

[213] S. T. Shreiber, D. A. Vicic, *Angew. Chem. Int. Ed.* **2021**, *60* (33), 18162–18167.

[214] S. T. Shreiber, G. I. Puchall, D. A. Vicic, *Tetrahedron Lett.* **2022**, *97*, 153795.

[215] L. F. Lindoy, M. S. Mahinay, B. W. Skelton, A. H. White, *J. Coordin. Chem.* **2003**, *56* (14), 1203–1213.

[216] G. Chaboussant, R. Basler, H.-U. Güdel, S. Ochsenbein, A. Parkin, S. Parsons, G. Rajaraman, A. Sieber, A. A. Smith, G. A. Timco, R. E. P. Winpenny, *Dalton Trans.* **2004**, (17), 2758–2766.

[217] F. V. Drozdov, T. Y. Glazunova, N. L. Shikut, N. V. Demchenko, E. A. Kurzina, P. Kalle, A. M. Muzafarov, *Mendeleev Commun.* **2020**, *30* (1), 43–45.

[218] M. Cortijo, P. Delgado-Martínez, R. González-Prieto, S. Herrero, R. Jiménez-Aparicio, J. Perles, J. L. Priego, M. R. Torres, *Inorg. Chim. Acta* **2015**, *424*, 176–185.

[219] C. Biewer, C. Hamacher, A. Kaiser, N. Vogt, A. Sandleben, M. T. Chin, S. Yu, D. A. Vicic, A. Klein, *Inorg. Chem.* **2016**, *55* (24), 12716–12727.

[220] G. T. Achonduh, N. Hadei, C. Valente, S. Avola, C. J. O'Brien, M. G. Organ, *Chem. Commun.* **2010**, *46*, 4109.

[221] L. C. McCann, H. N. Hunter, J. A. C. Clyburne, M. G. Organ, *Angew. Chem. Int. Ed.* **2012**, *51* (28), 7024–7027.

[222] P. Eckert, S. Sharif, M. G. Organ, *Angew. Chem. Int. Ed.* **2021**, *60*, 12224.

[223] T. Yamamoto, A. Yamamoto, S. Ikeda, *J. Am. Chem. Soc.* **1971**, *93* (14), 3350–3359.

[224] W. Kaim, J. Fiedler, *Chem. Soc. Rev.* **2009**, *38* (12), 3373–3382.

[225] *APEX4, BrukerAXS Inc., Madison, Wisconsin, USA.*, **2022**.

[226] *SAINT, V8.40B, Bruker AXS Inc., Madison, Wisconsin, USA.*, **2022**.

[227] L. Krause, R. Herbst-Irmer, G. M. Sheldrick, D. Stalke, *J. Appl. Crystallogr.* **2015**, *48* (1), 3–10.

[228] O. V. Dolomanov, L. J. Bourhis, R. J. Gildea, J. A. K. Howard, H. Puschmann, *J. Appl. Crystallogr.* **2009**, *42* (2), 339–341.

[229] G. Sheldrick, *Acta Cryst. Sect. A* **2015**, *71* (1), 3–8.

[230] G.Sheldrick, *Acta Cryst. Sect. C* **2015**, *71* (1), 3–8.

[231] K. Brandenburg, *Crystal Impact GbR, Bonn, Germany*, **1997-2020**.

[232] D. J. Krysan, P. B. A Mackenzie, *J. Org. Chem.* **1990**, *55*, 4229–4230.

[233] R. Dinnebier, H. Esbak, F. Olbrich, U. Behrens, *Organometallics* **2007**, *26* (10), 2604–2608.

7 Appendix

7.1 NMR spectra

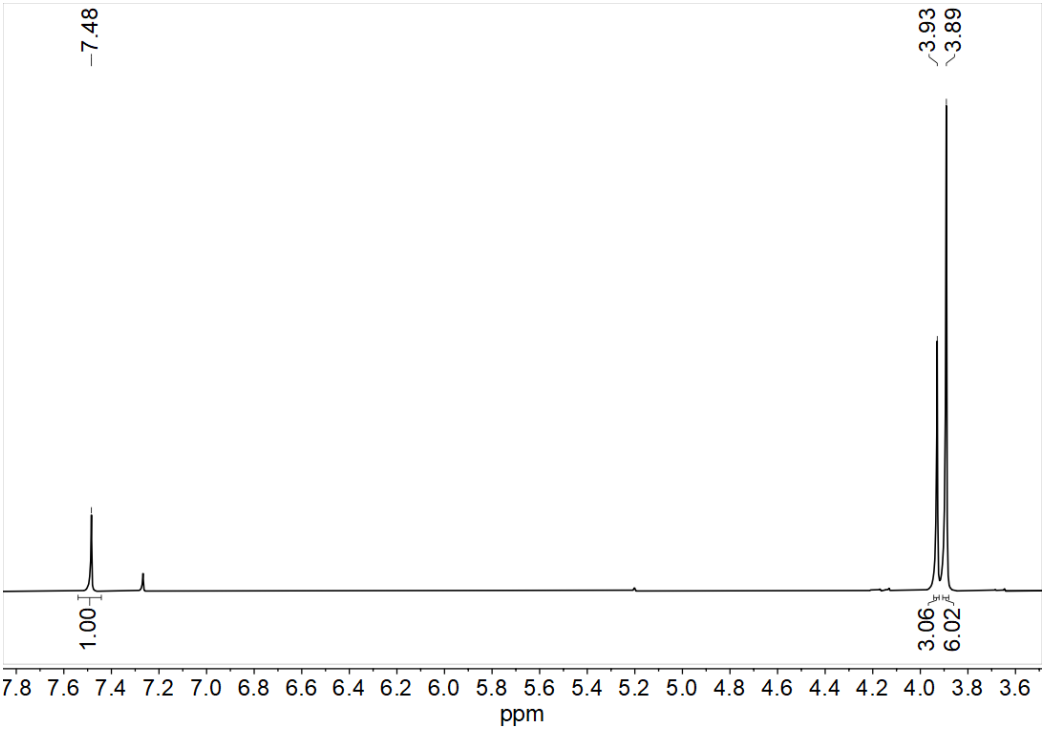

Figure 7-1 300MHz ^{1}H NMR spectrum of 1,2,3-Trimethoxy-4,6-dibromobenzene in $CDCl_3$.

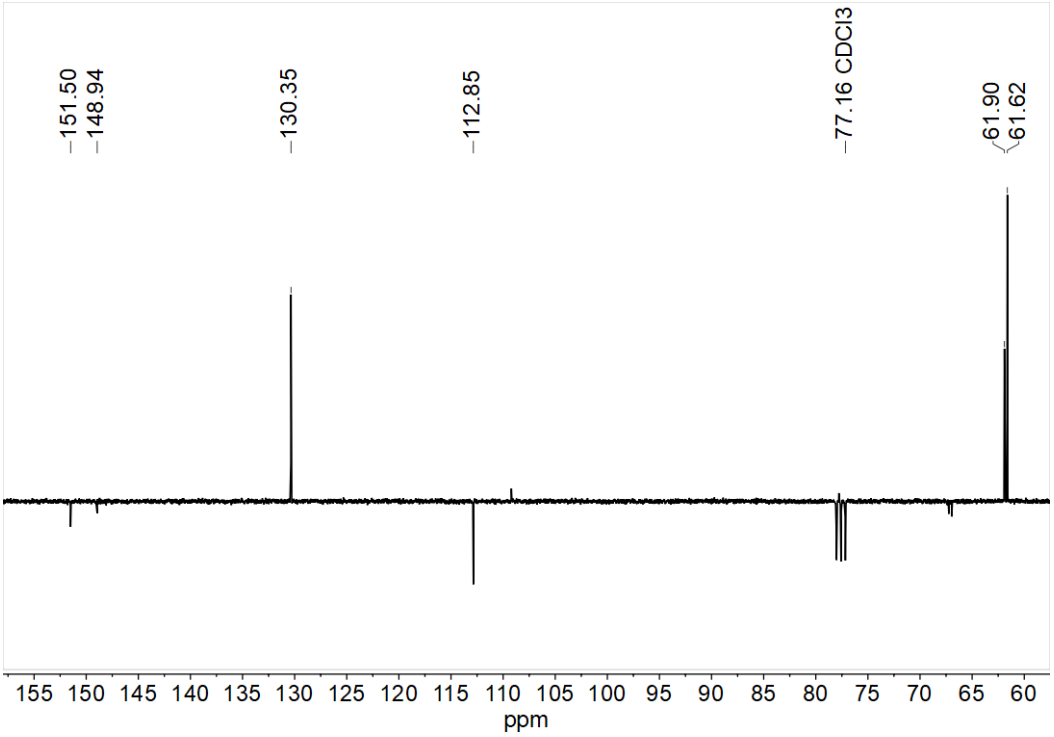

Figure 7-2 75 MHz ^{13}C NMR spectrum of 1,2,3-Trimethoxy-4,6-dibromobenzene in $CDCl_3$.

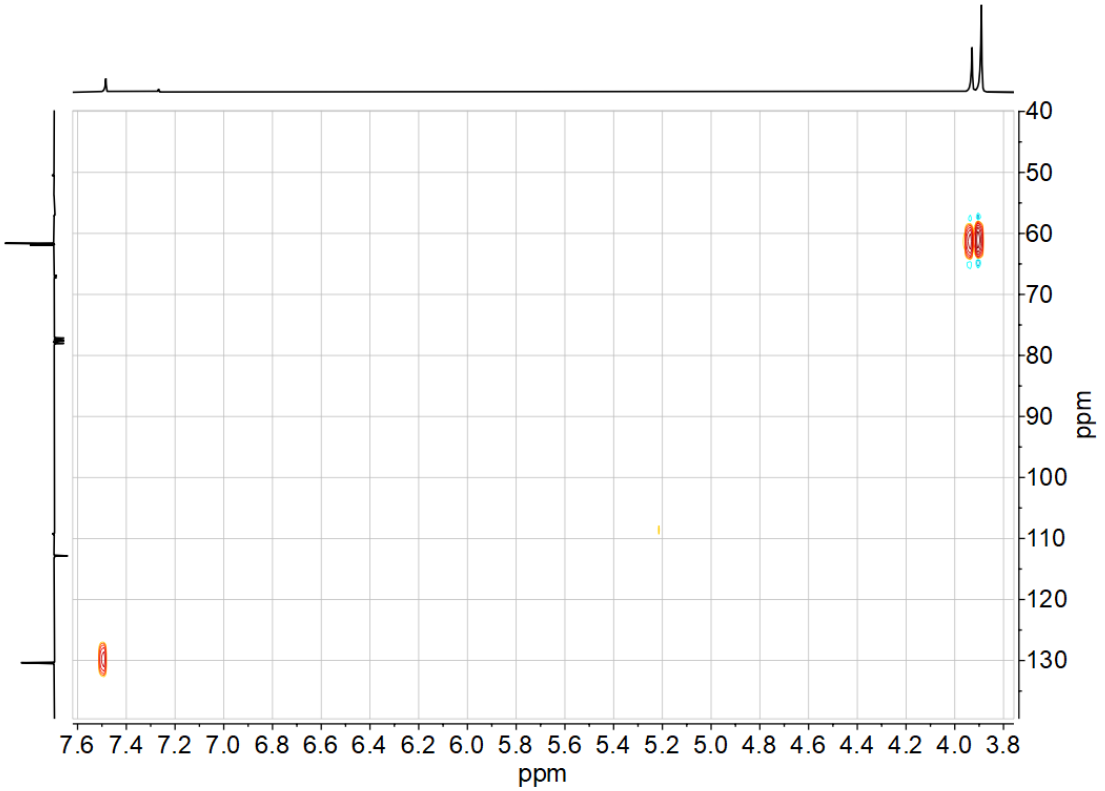

Figure 7-3 $^{1}H,^{13}C$ HSQC correlation spectrum of 1,2,3-Trimethoxy-4,6-dibromobenzene in $CDCl_3$.

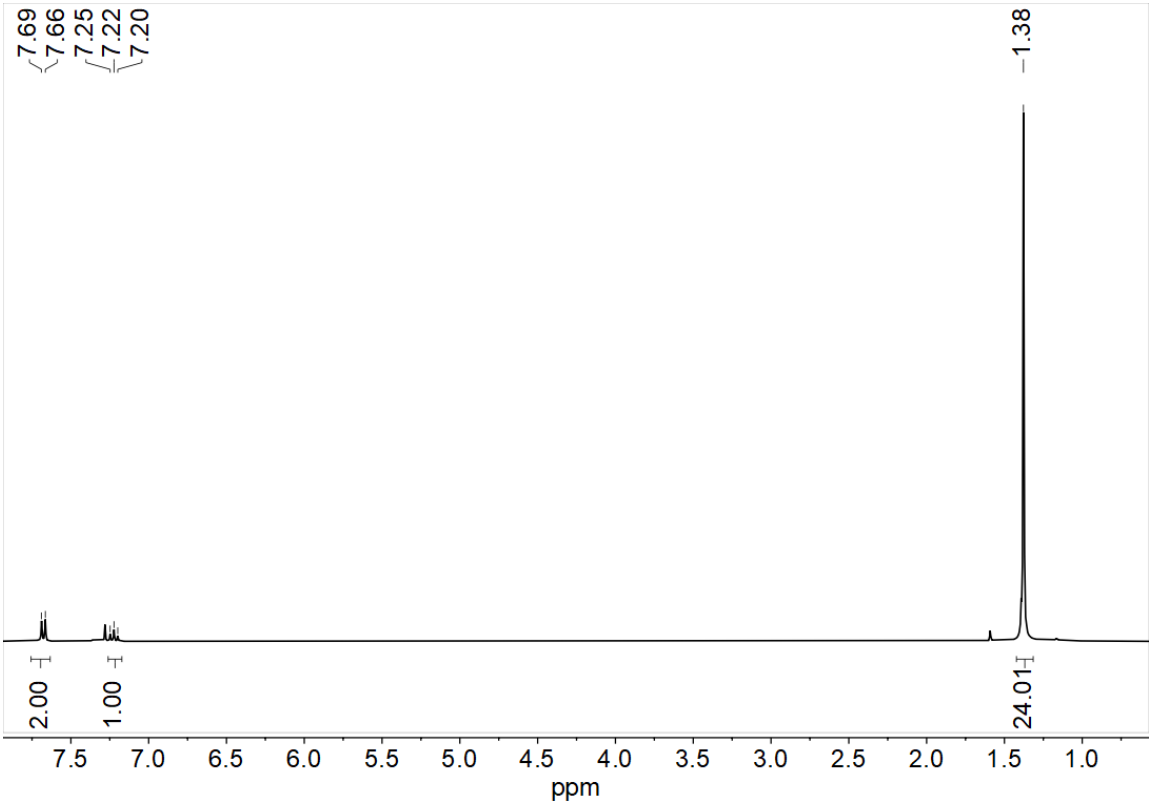

Figure 7-4 300 MHz ^{1}H NMR spectrum of Synthesis of 2,2'-(2-Chloro-1,3-phenylene)bis(4,4,5,5-tetramethyl-1,3,2-dioxaborolane) in $CDCl_3$.

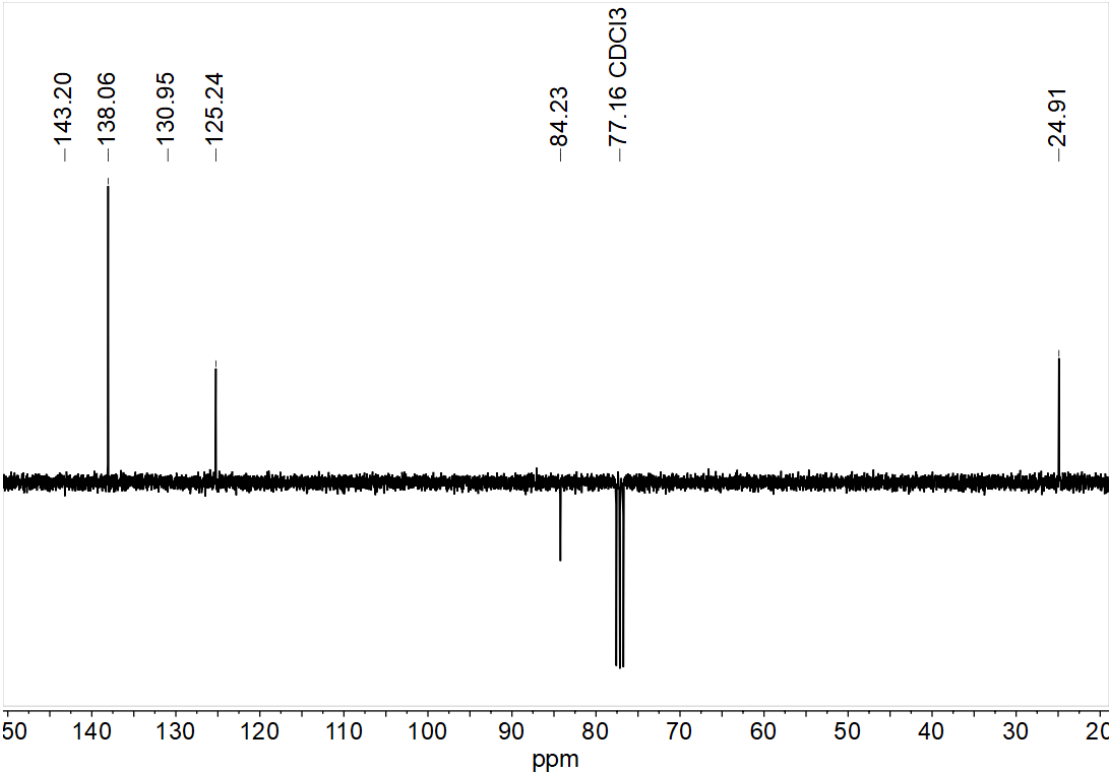

Figure 7-5 75 MHz ^{13}C NMR spectrum of 2,2'-(2-Chloro-1,3-phenylene)bis(4,4,5,5-tetramethyl-1,3,2-dioxaborolane) in $CDCl_3$.

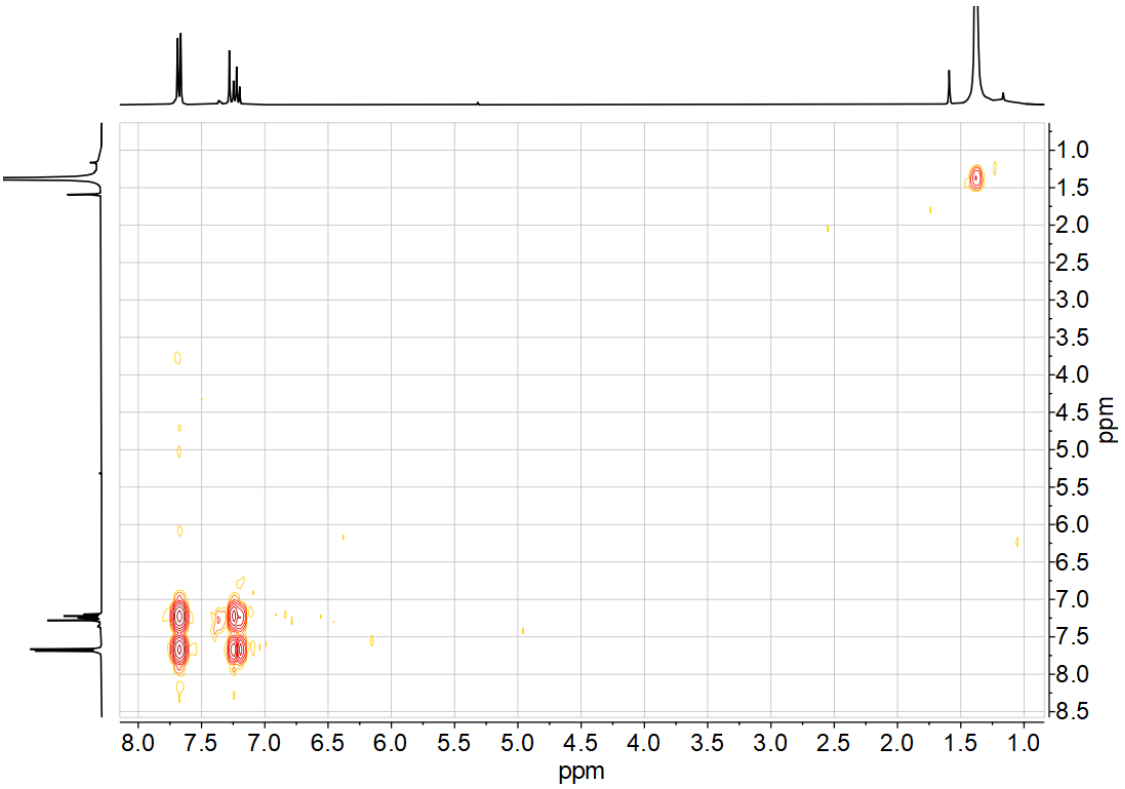

Figure 7-6 $^{1}H,^{1}H$ COSY correlation spectrum of 2,2'-(2-Chloro-1,3-phenylene)bis(4,4,5,5-tetramethyl-1,3,2-dioxaborolane) in $CDCl_3$.

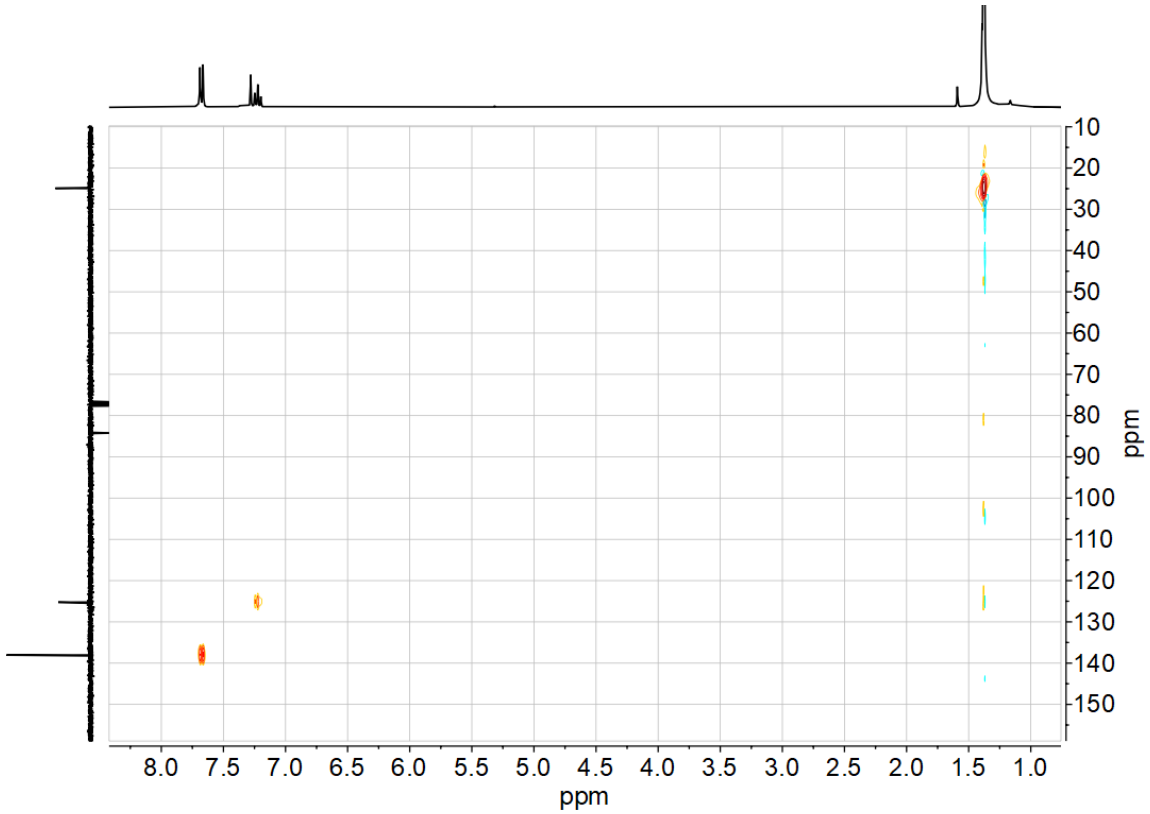

Figure 7-7 $^{1}H,^{13}C$ HSQC correlation spectrum of 2,2'-(2-Chloro-1,3-phenylene)bis(4,4,5,5-tetramethyl-1,3,2-dioxaborolane) in $CDCl_3$.

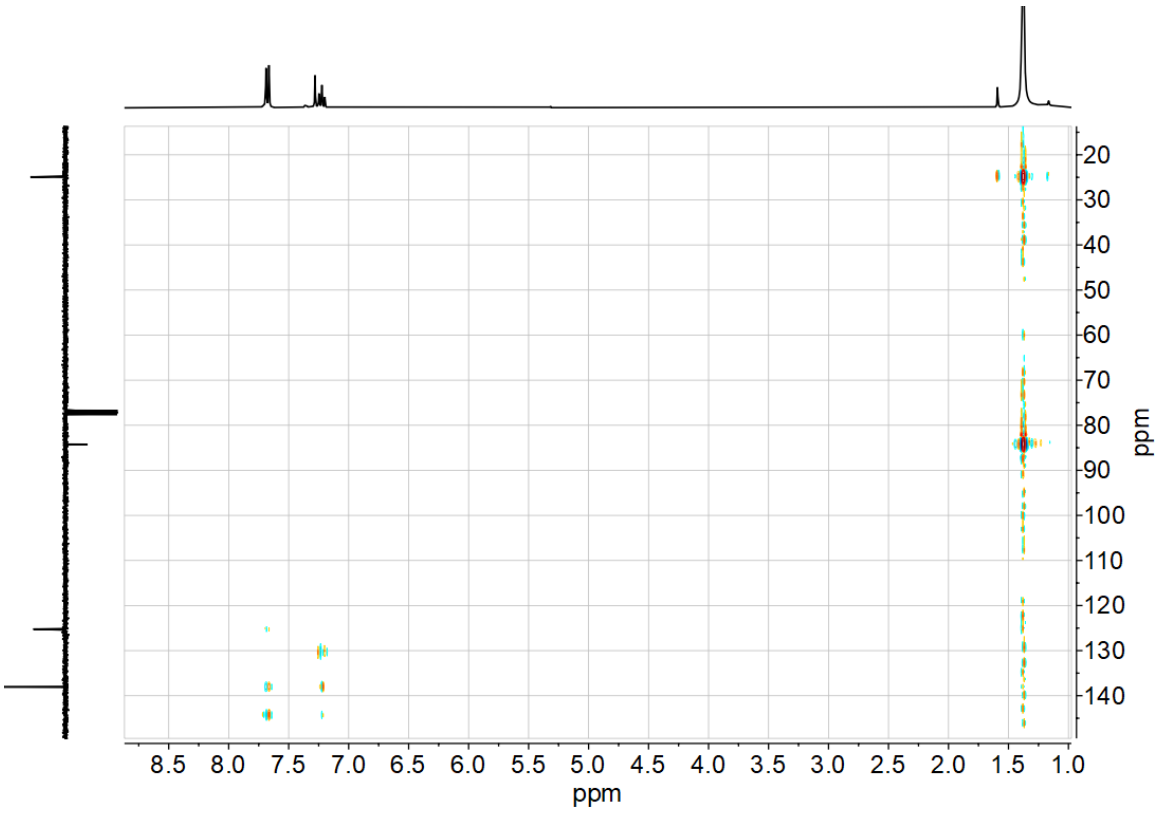

Figure 7-8 $^{1}H,^{13}C$ HMBC correlation spectrum of 2,2'-(2-Chloro-1,3-phenylene)bis(4,4,5,5-tetramethyl-1,3,2-dioxaborolane) in $CDCl_3$.

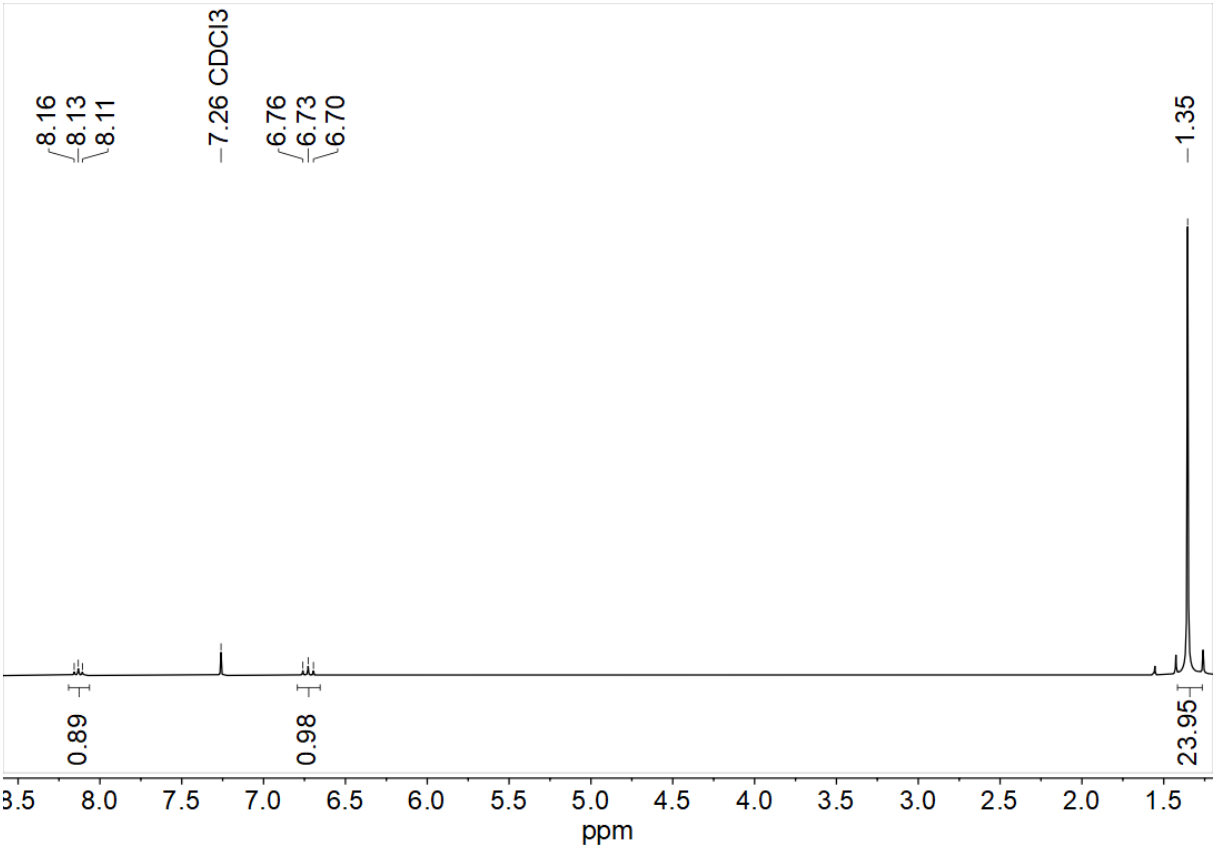

Figure 7-9 300MHz ^{1}H NMR spectrum of 2,2'-(4,6-difluoro-1,3-phenylene)bis(4,4,5,5-tetramethyl-1,3,2-dioxaborolane in $CDCl_3$.

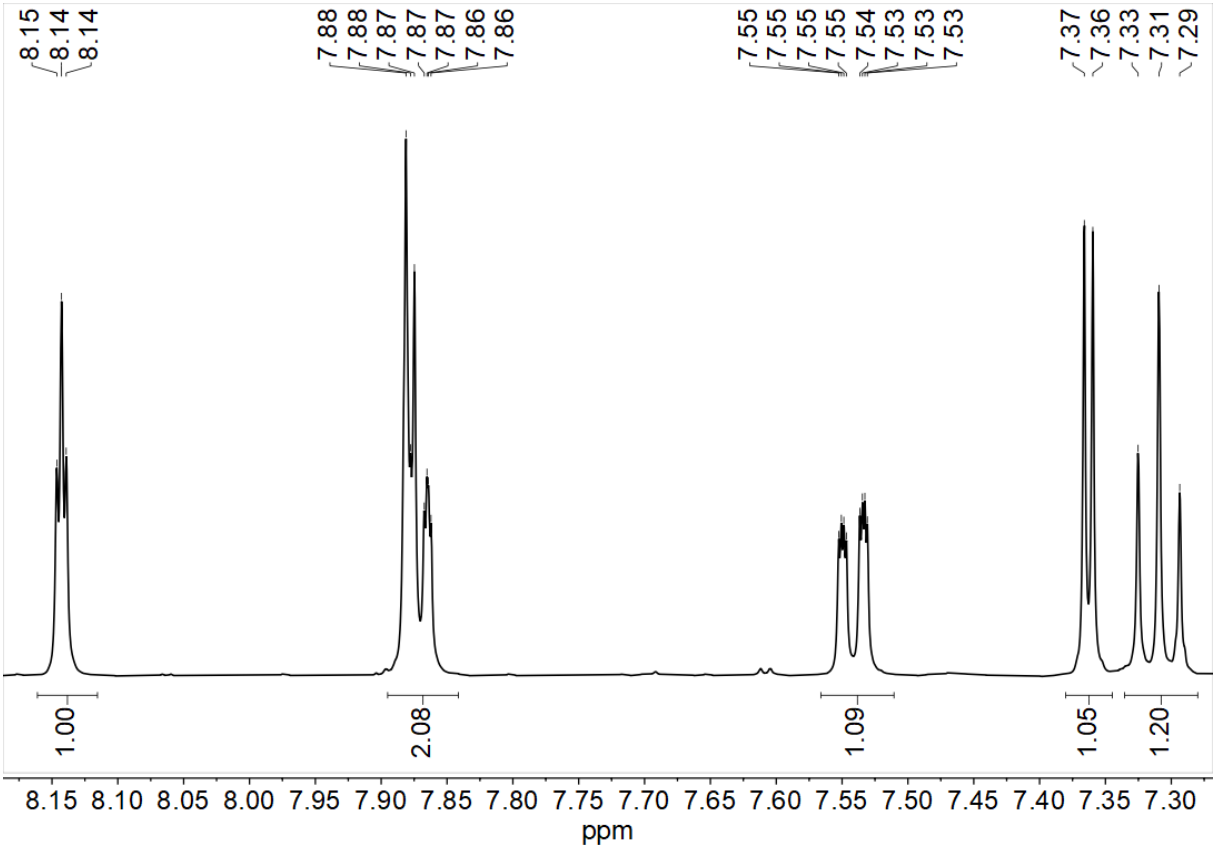

Figure 7-10 500 MHz ^{1}H NMR spectrum of 2Tz(PhH)Br in $CDCl_3$.

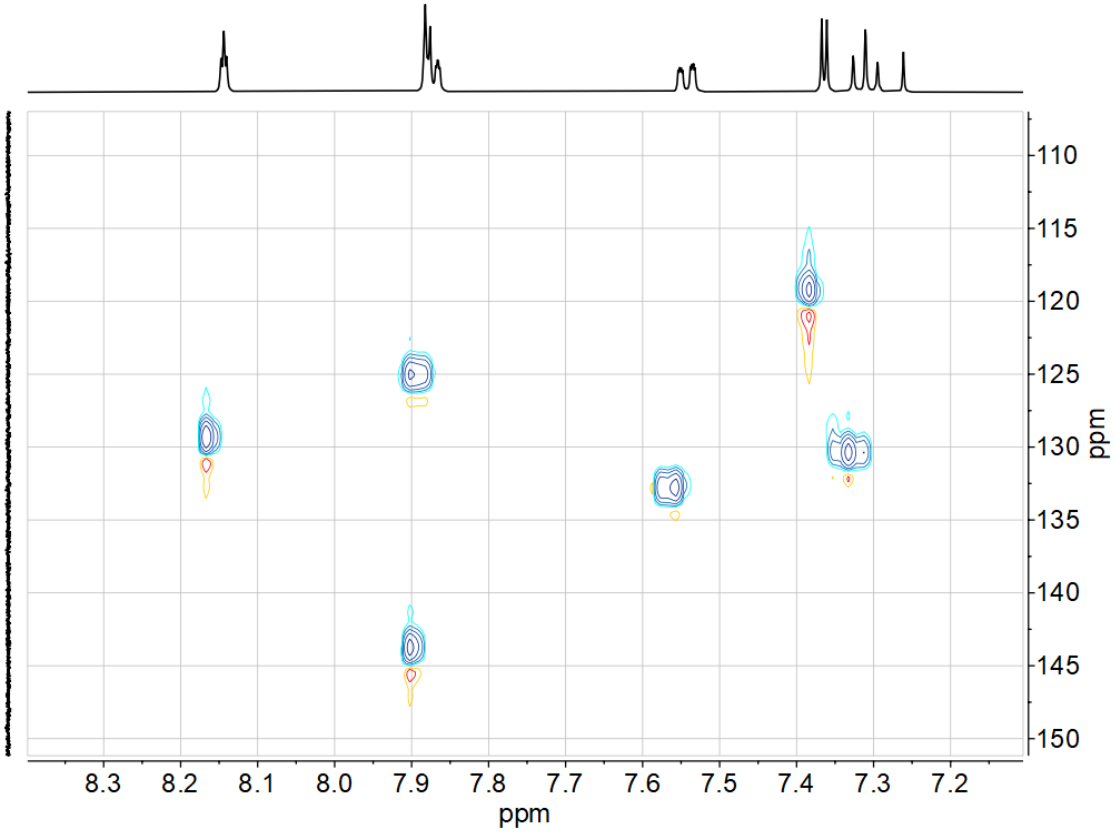

Figure 7-11 $^{1}H,^{13}C$ HSQC correlation spectrum of 2Tz(PhH)Br in $CDCl_3$.

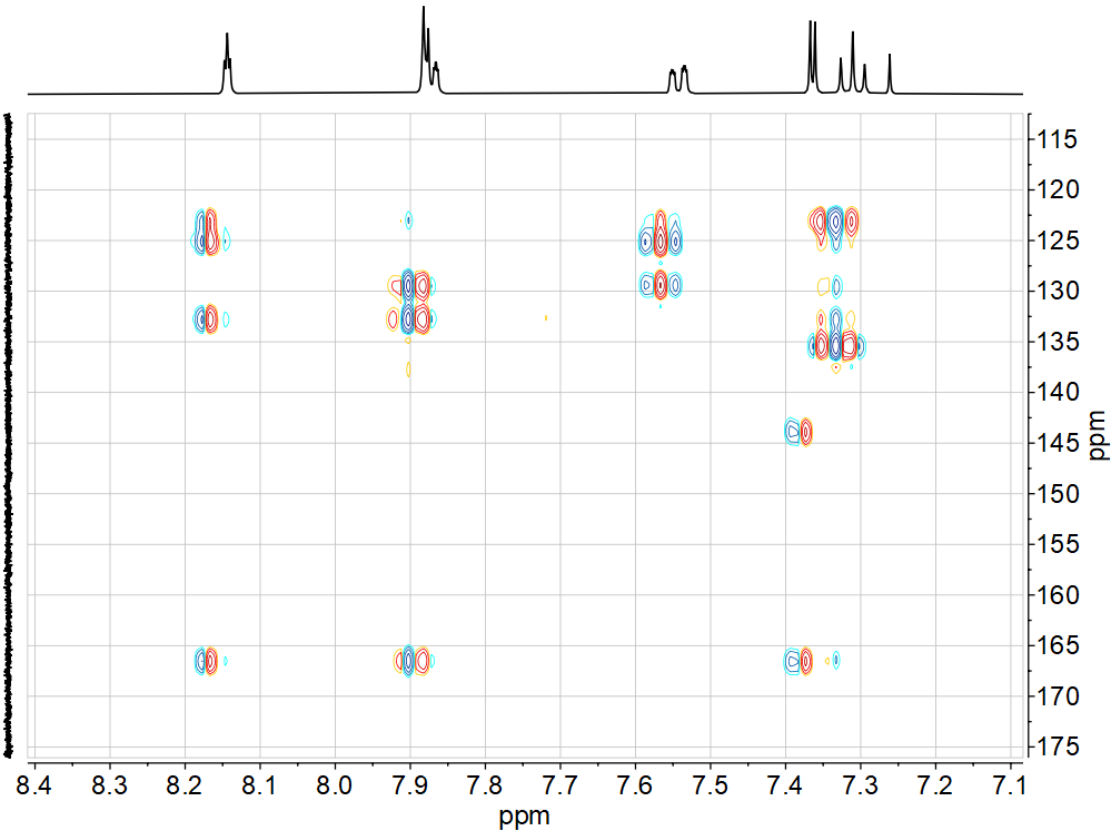

Figure 7-12 $^{1}H,^{13}C$ HMBC correlation spectrum of 2Tz(PhH)Br in $CDCl_3$.

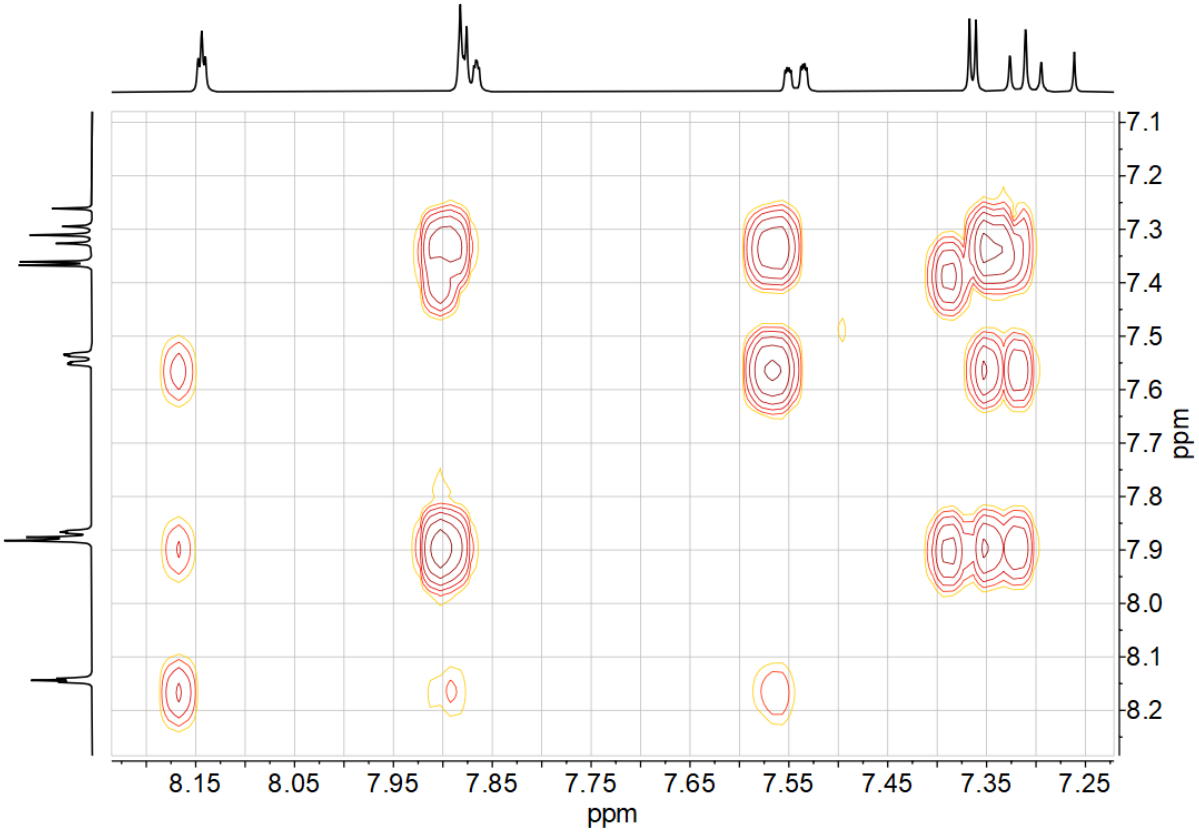

Figure 7-13 $^{1}H,^{1}H$ COSY correlation spectrum of 2Tz(PhH)Br in $CDCl_3$.

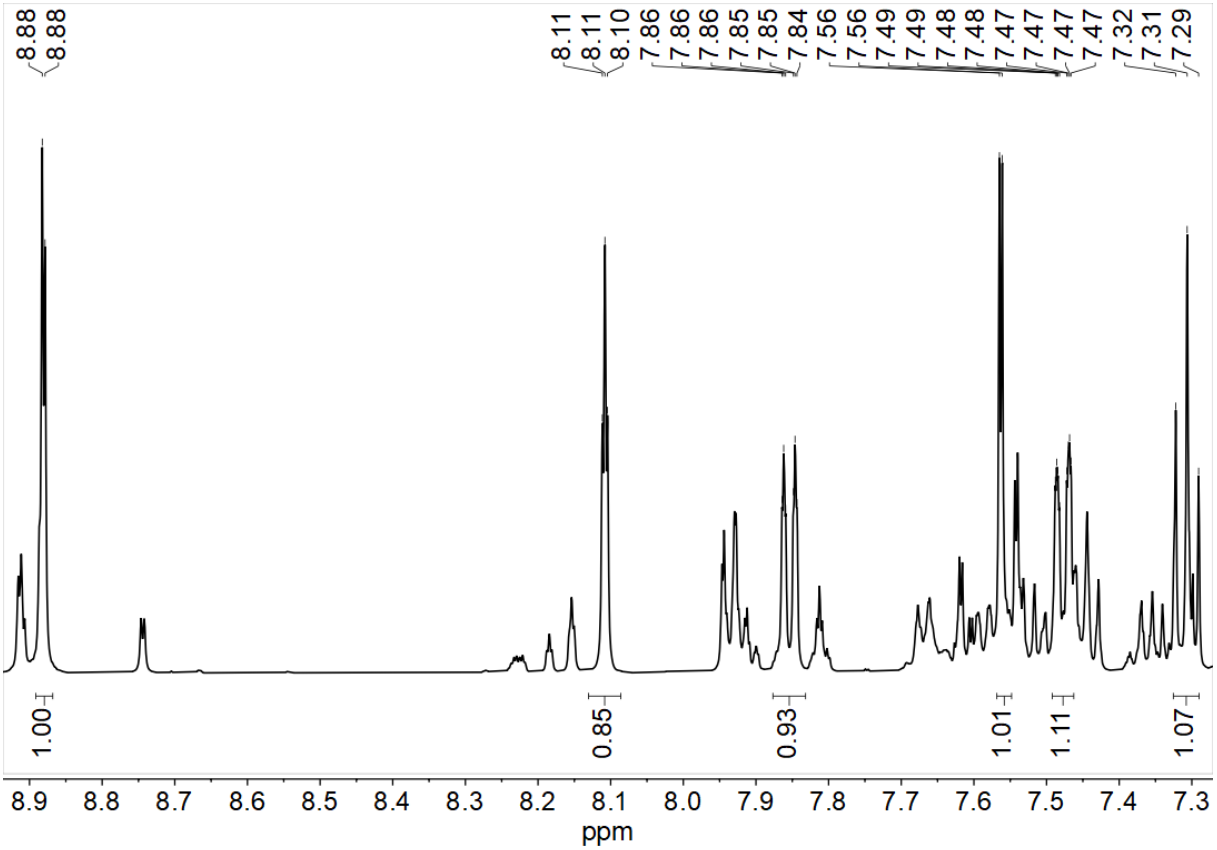

Figure 7-14 500 MHz ^{1}H NMR spectrum of 4Tz(PhH)Br in $CDCl_3$.

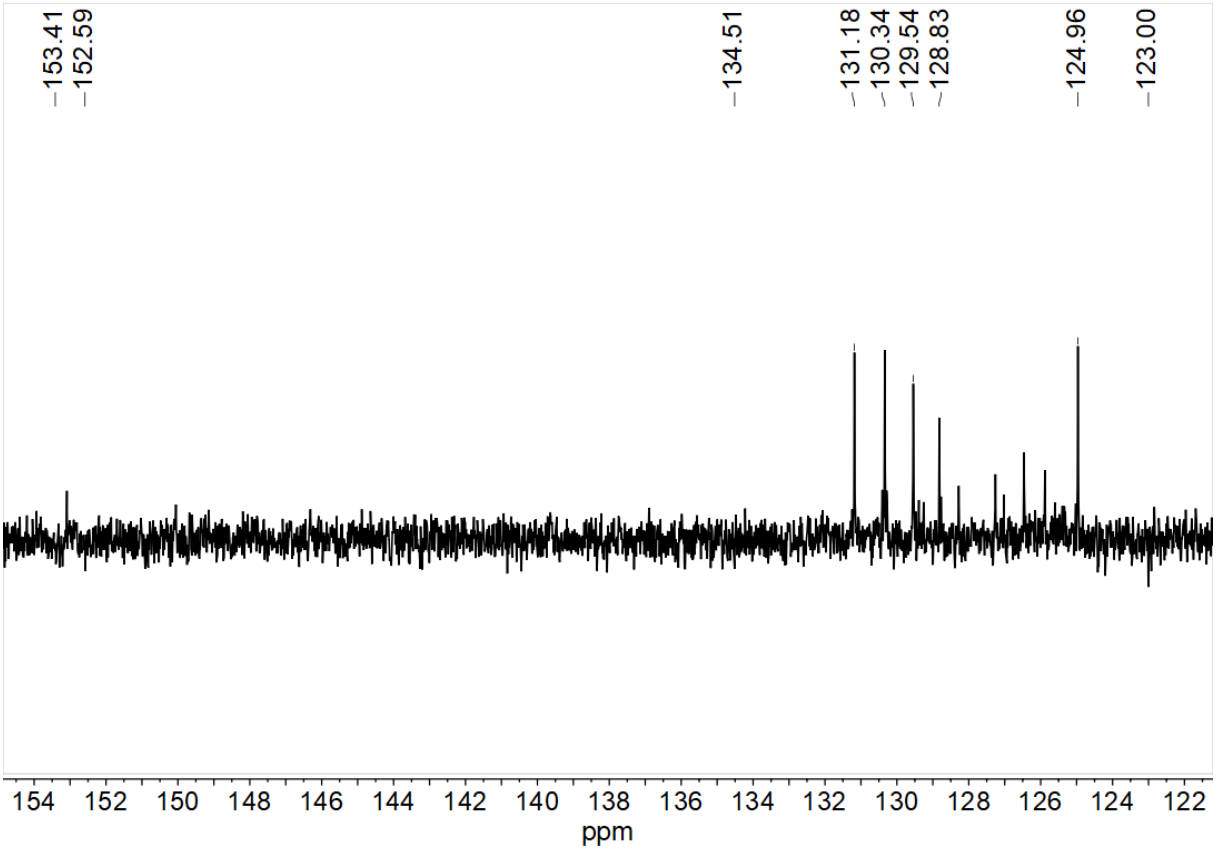

Figure 7-15 75 MHz ^{13}C NMR spectrum of 4Tz(PhH)Br in $CDCl_3$.

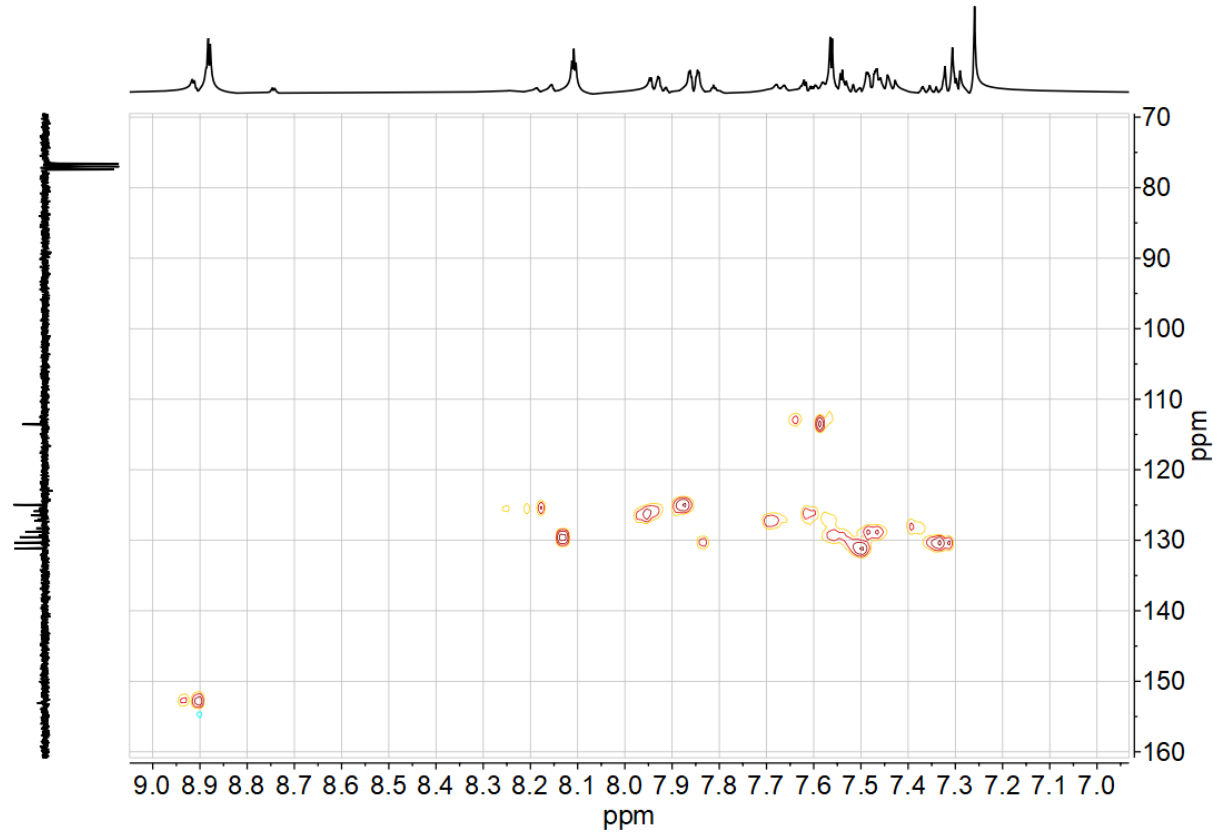

Figure 7-16 $^{1}H,^{13}C$ HSQC correlation spectrum of 4Tz(PhH)Br in $CDCl_3$.

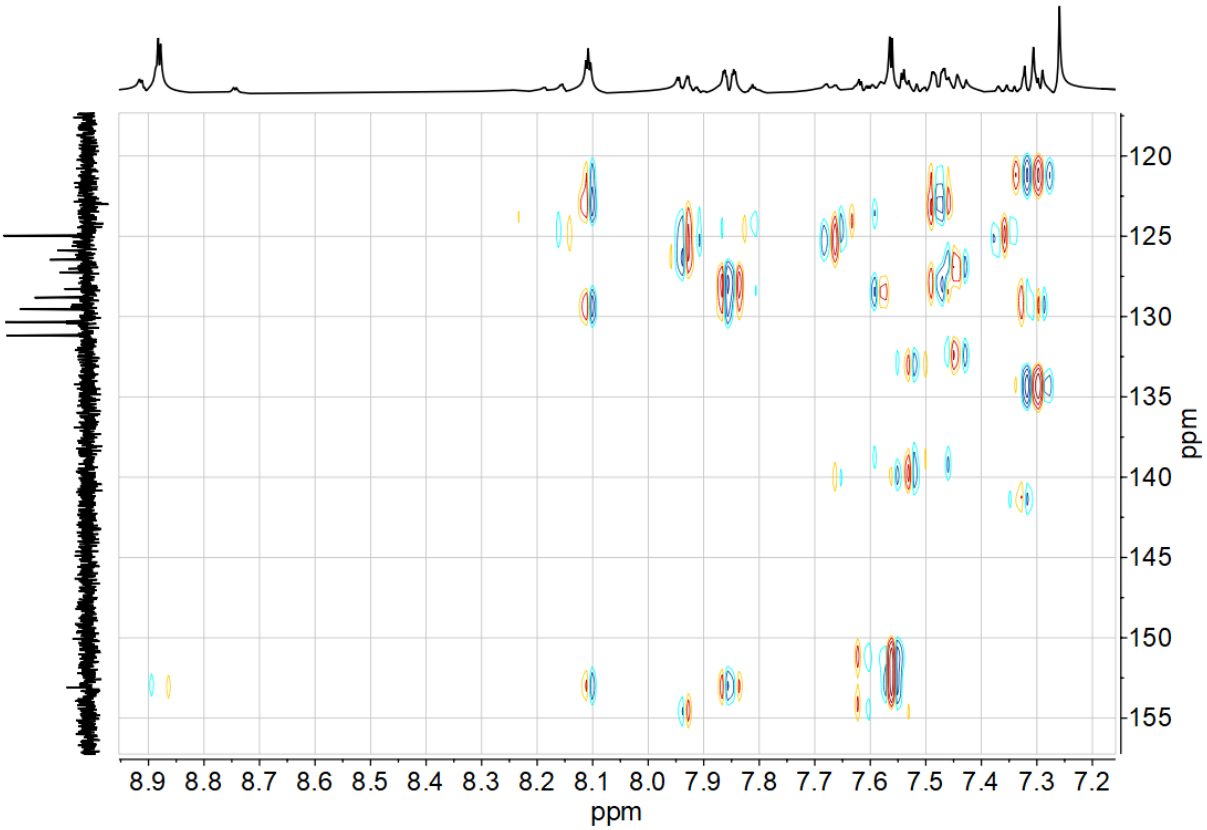

Figure 7-17 $^{1}H,^{13}C$ HMBC correlation spectrum of 4Tz(PhH)Br in $CDCl_3$.

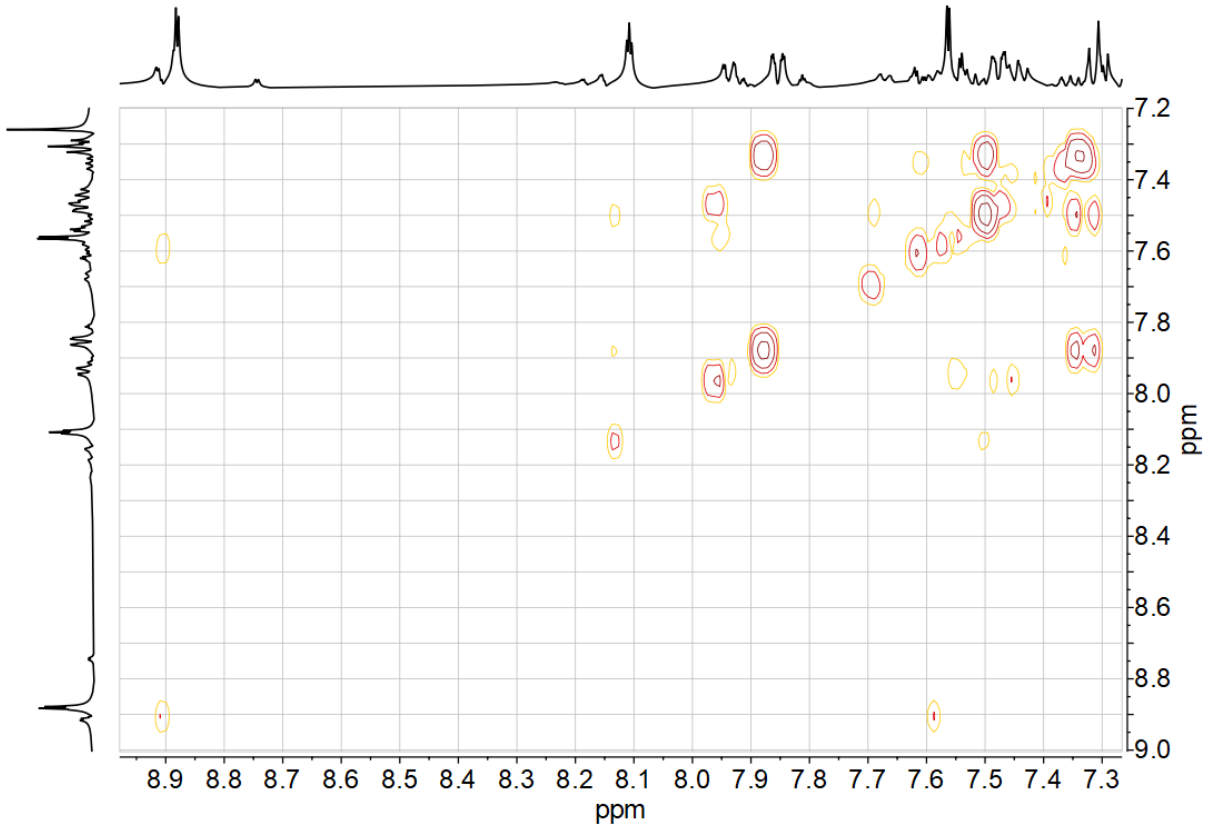

Figure 7-18 $^{1}H,^{1}H$ COSY correlation spectrum of 4Tz(PhH)Br in $CDCl_3$.

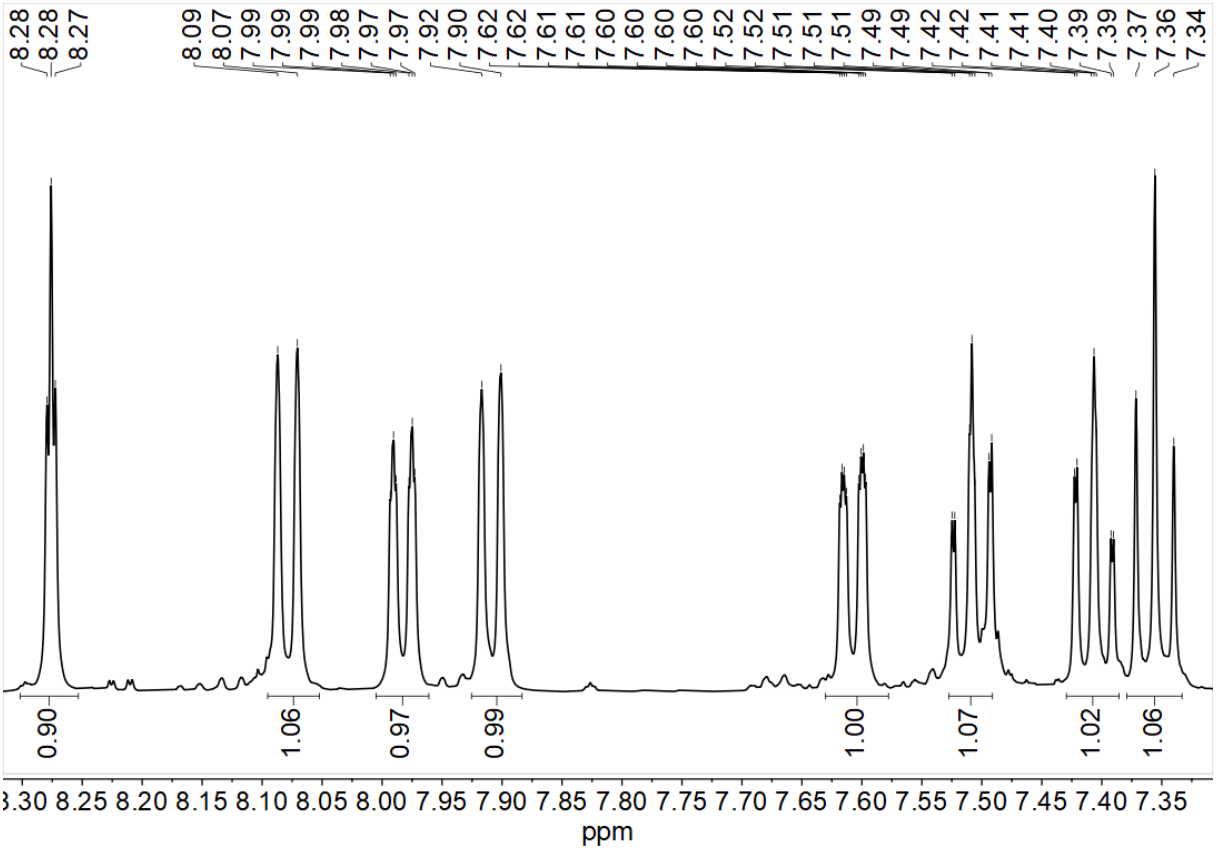

Figure 7-19 500 MHz ^{1}H NMR spectrum of 2Btz(PhH)Br in $CDCl_3$.

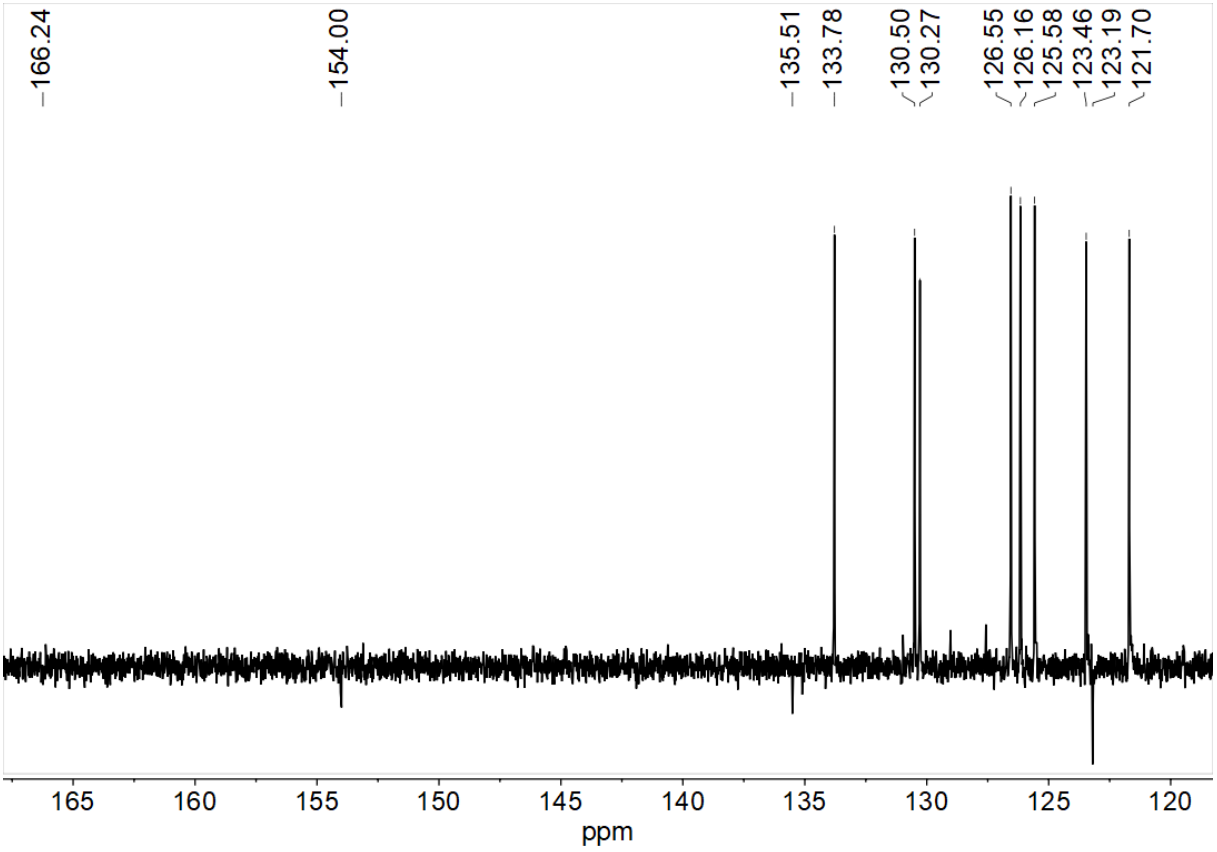

Figure 7-20 75 MHz ^{13}C NMR spectrum of 2Btz(PhH)Br in $CDCl_3$.

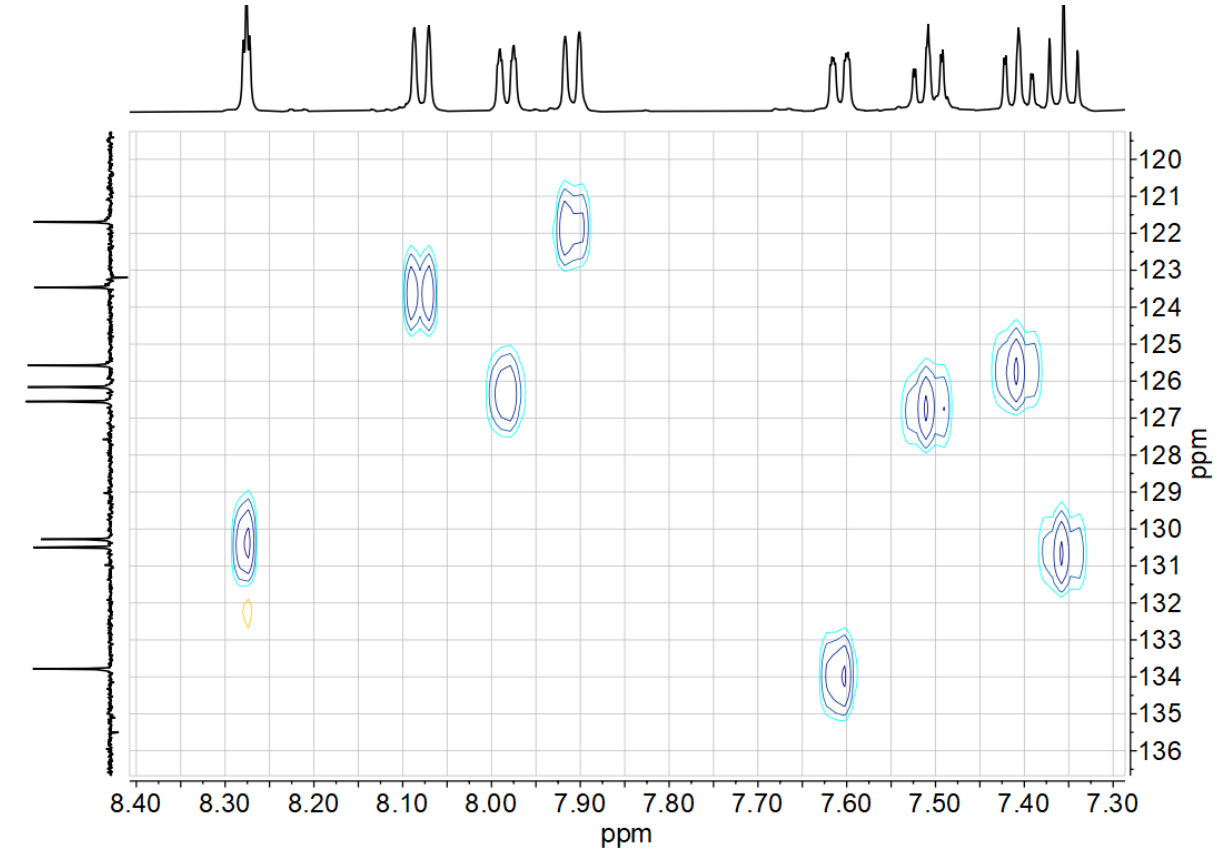

Figure 7-21 $^{1}H,^{13}C$ HSQC correlation spectrum of 2Btz(PhH)Br in $CDCl_3$.

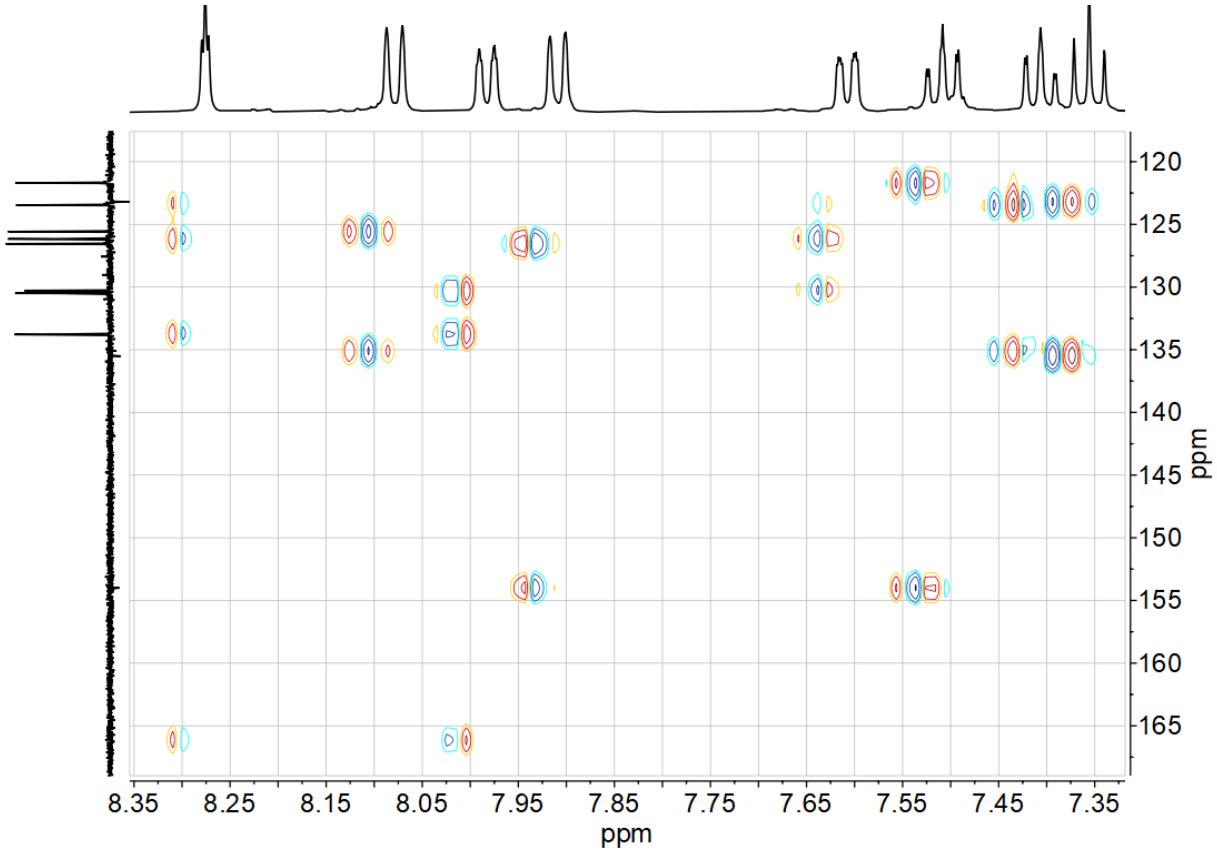

Figure 7-22 $^{1}H,^{13}C$ HMBC correlation spectrum of 2Btz(PhH)Br in $CDCl_3$.

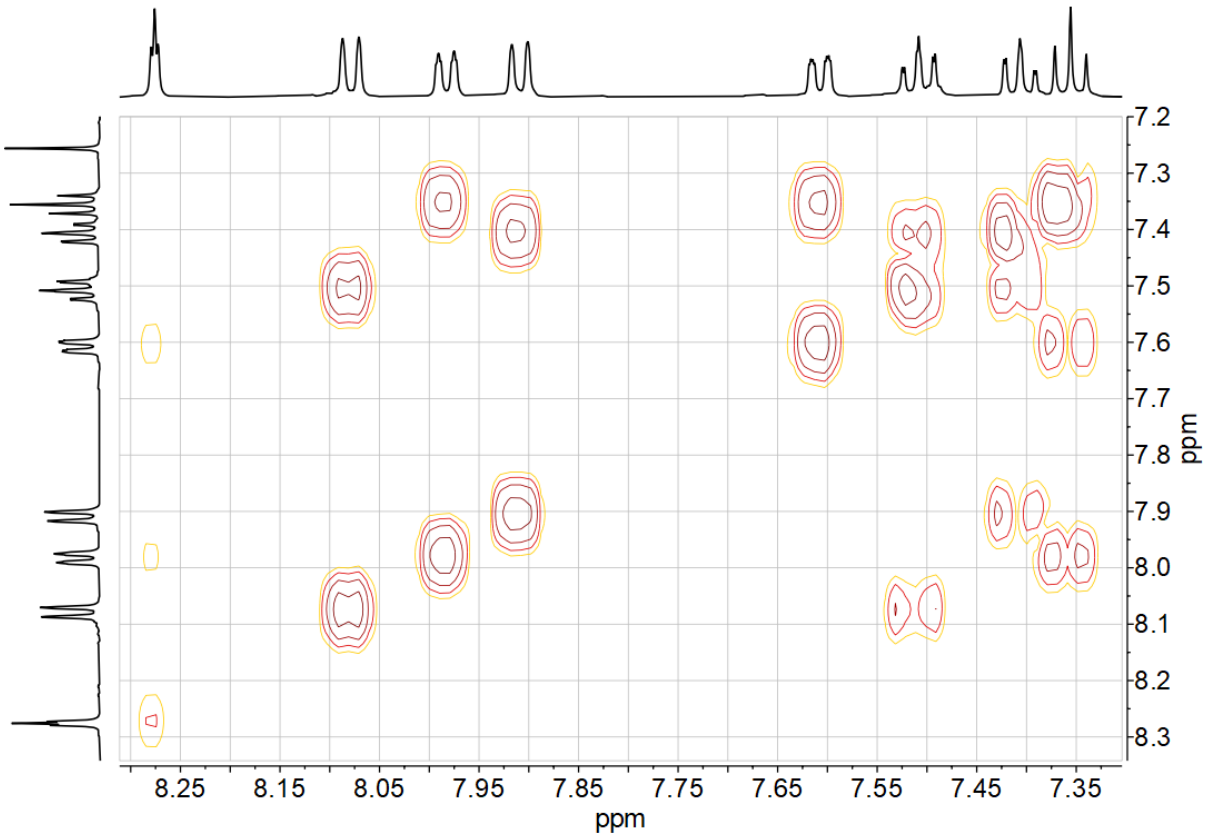

Figure 7-23 $^{1}H,^{1}H$ COSY correlation spectrum of 2Btz(PhH)Br in $CDCl_3$.

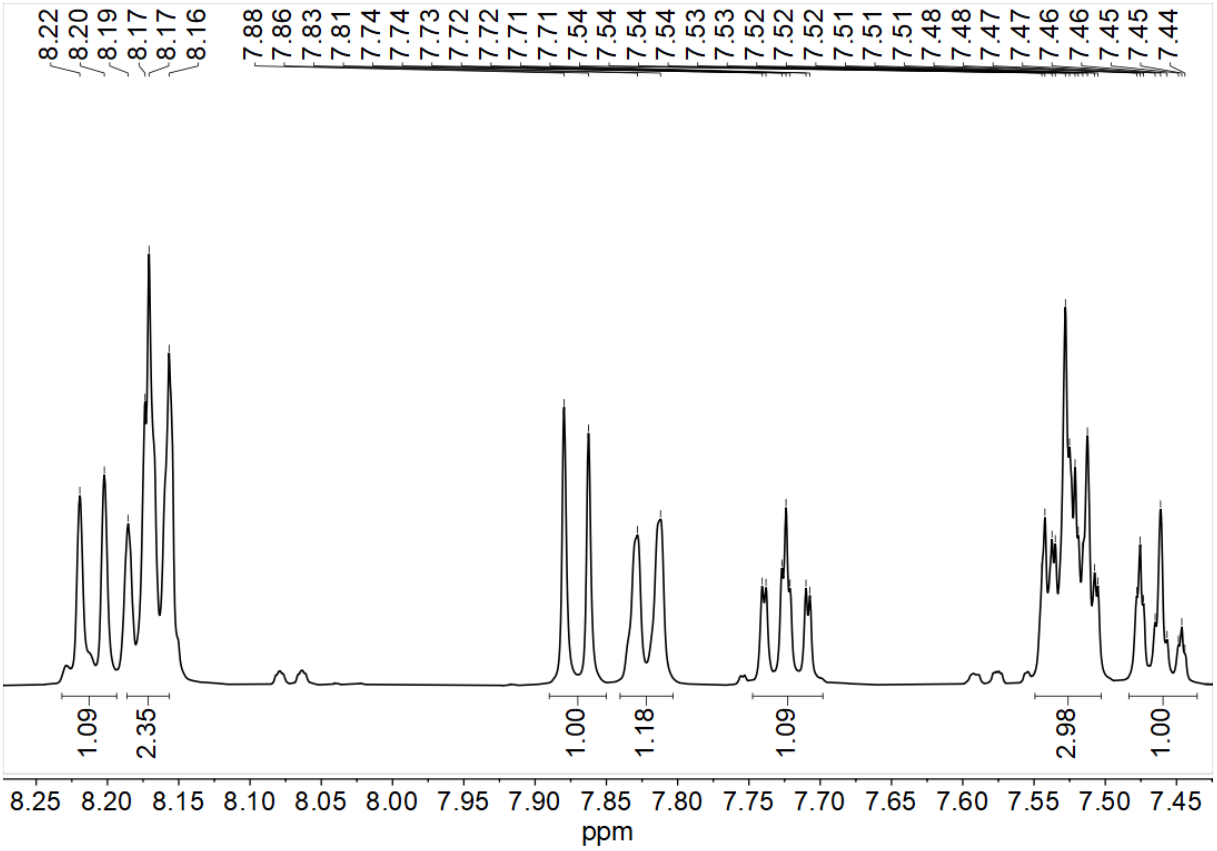

Figure 7-24 500 MHz ^{1}H NMR spectrum of 2Qu(PhH)Br in $CDCl_3$.

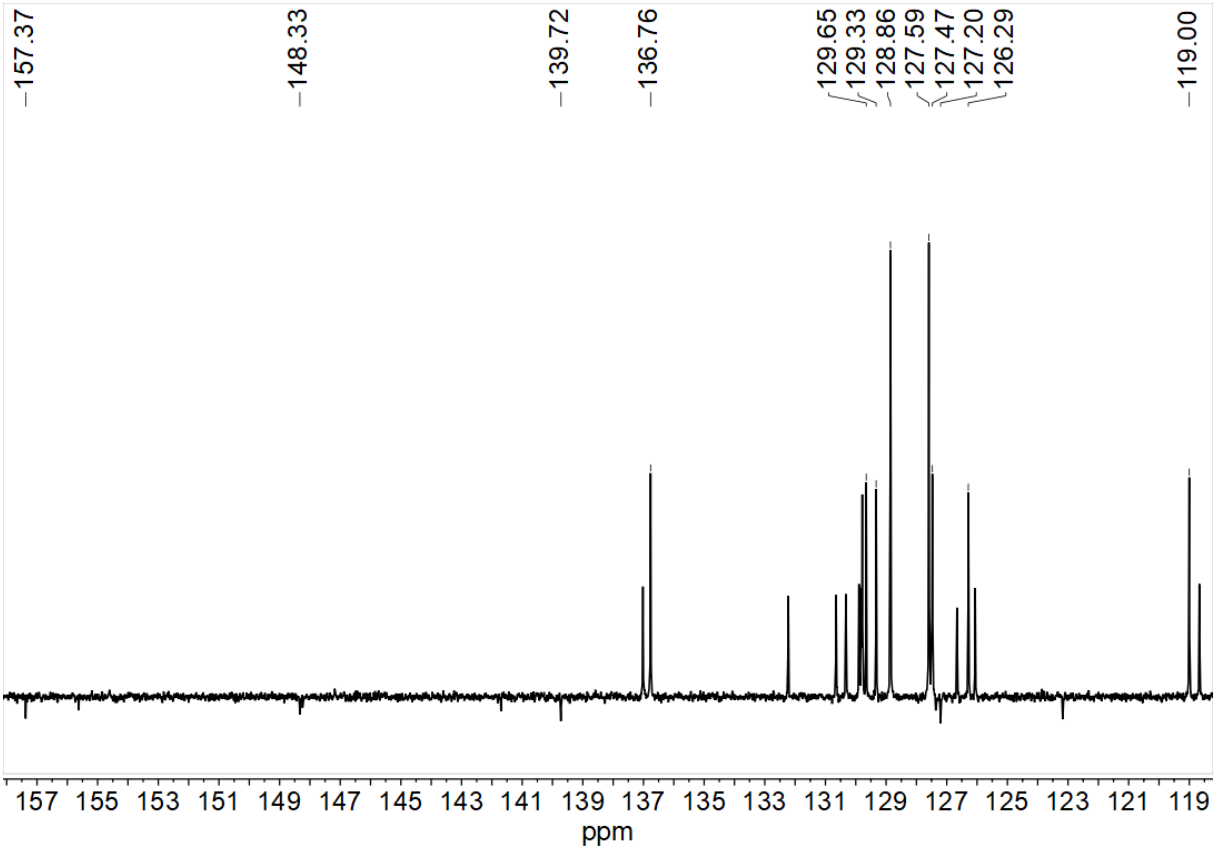

Figure 7-25 75 MHz ^{13}C NMR spectrum of 2Qu(PhH)Br in $CDCl_3$.

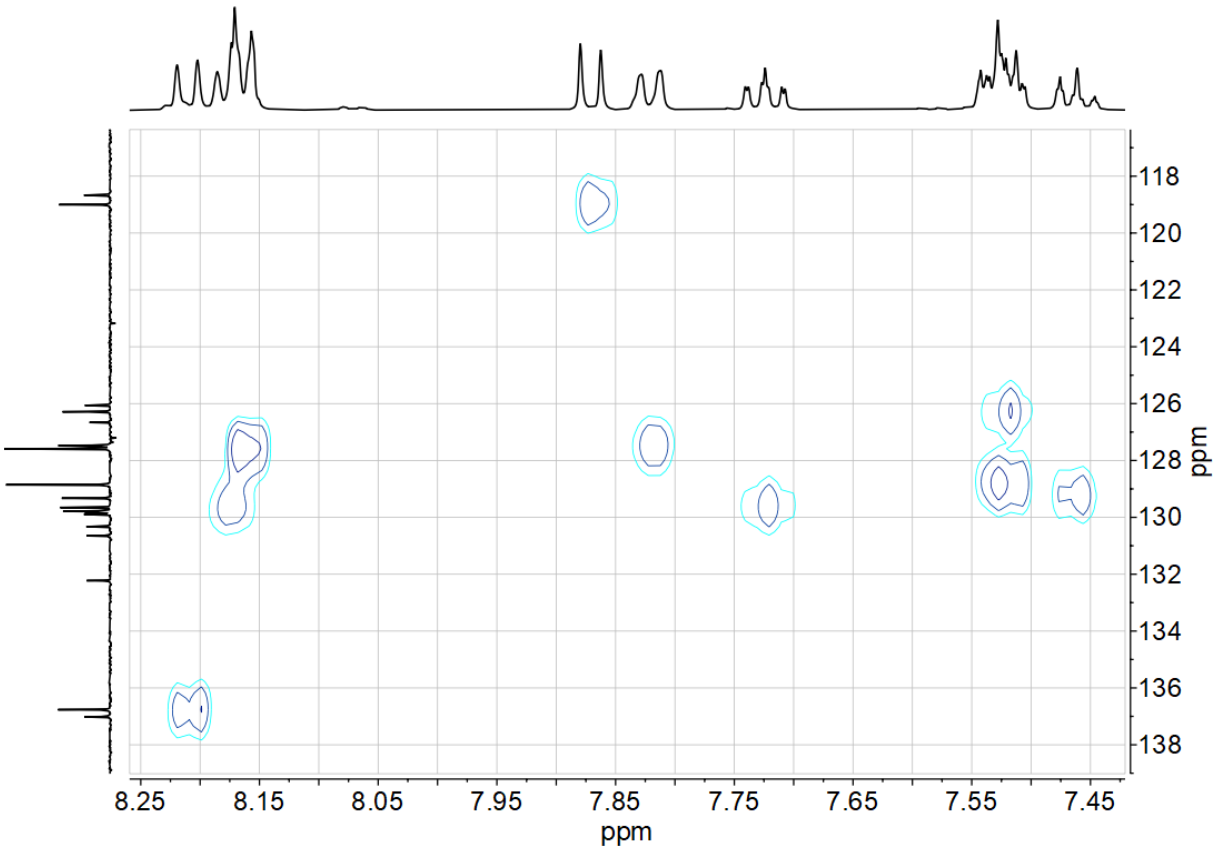

Figure 7-26 $^{1}H,^{13}C$ HSQC correlation spectrum of 2Qu(PhH)Br in $CDCl_3$.

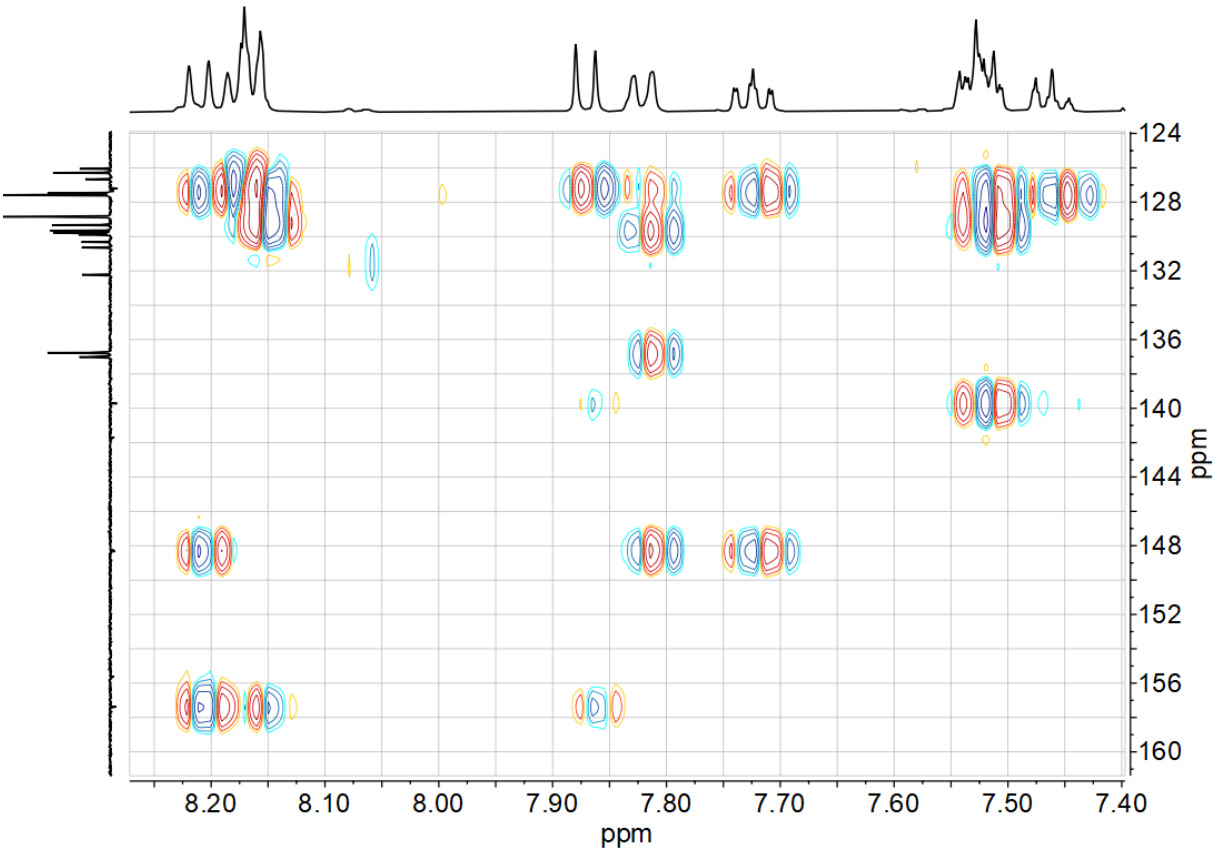

Figure 7-27 $^{1}H,^{13}C$ HMBC correlation spectrum of 2Qu(PhH)Br in $CDCl_3$.

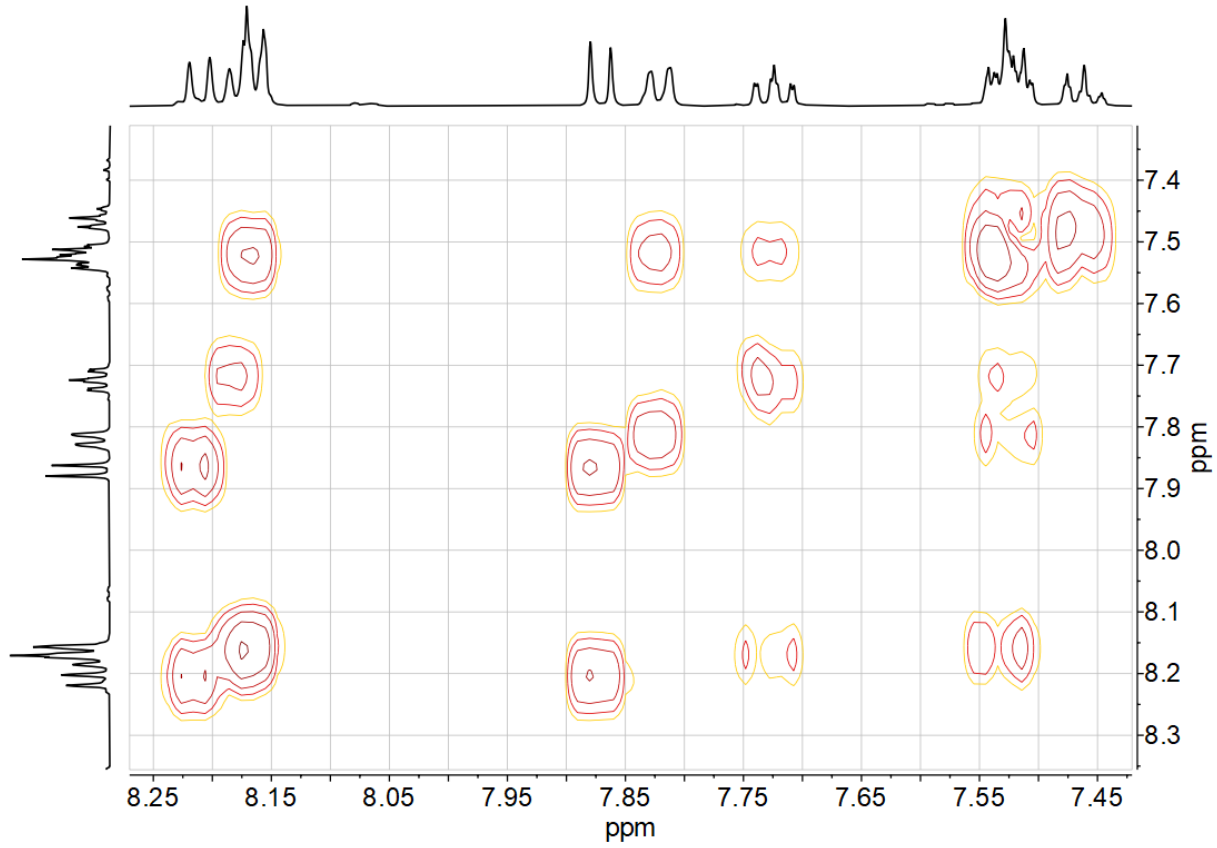

Figure 7-28 $^{1}H,^{1}H$ COSY correlation spectrum of 2Qu(PhH)Br in $CDCl_3$.

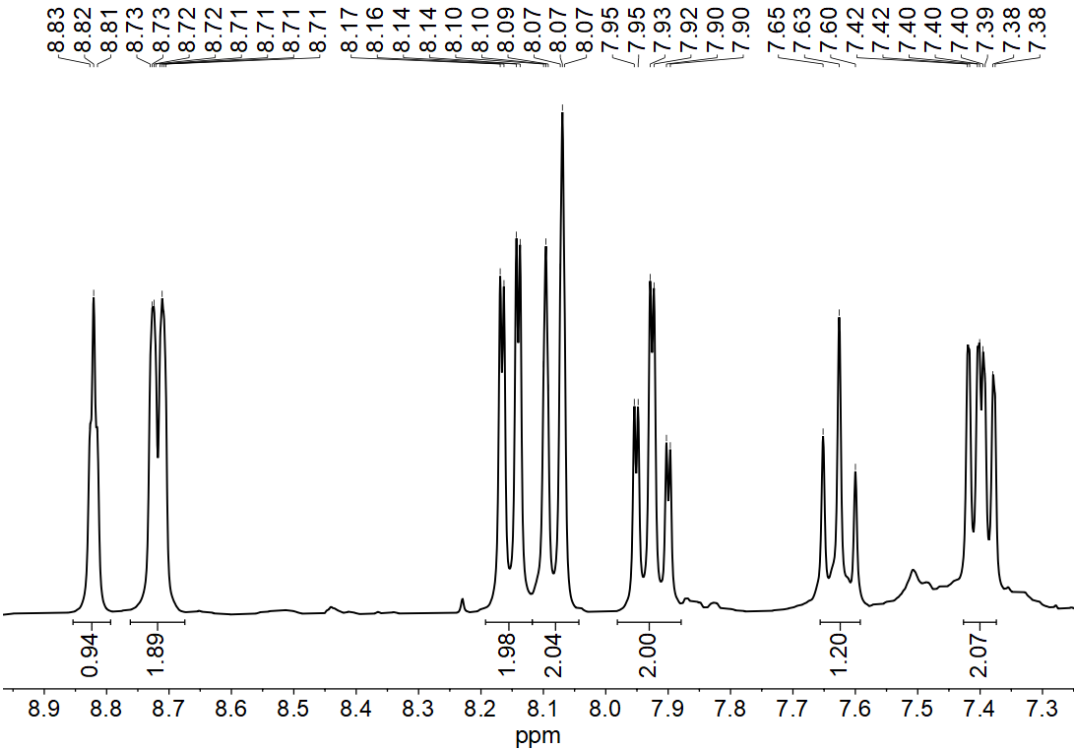

Figure 7-29 300 MHz ^{1}H NMR spectrum of Py(PhH)Py in DMSO-d_6.

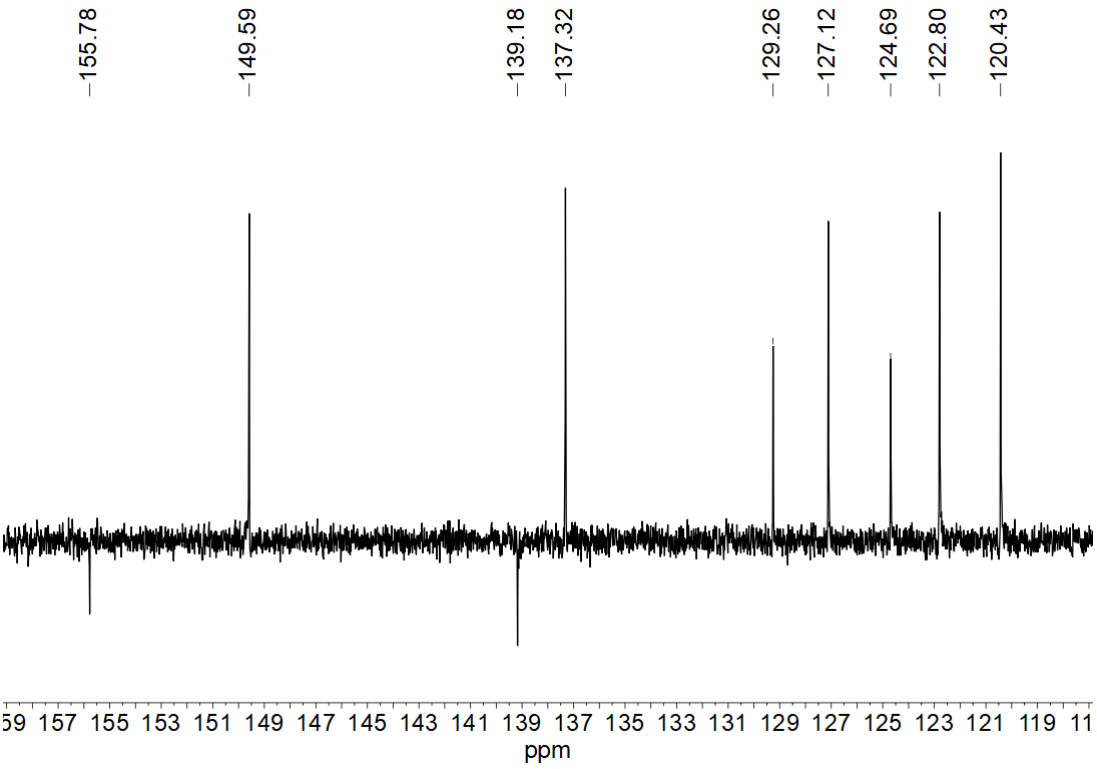

Figure 7-30 75MHz ^{13}C NMR spectrum of Py(PhH)Py in DMSO-d_6.

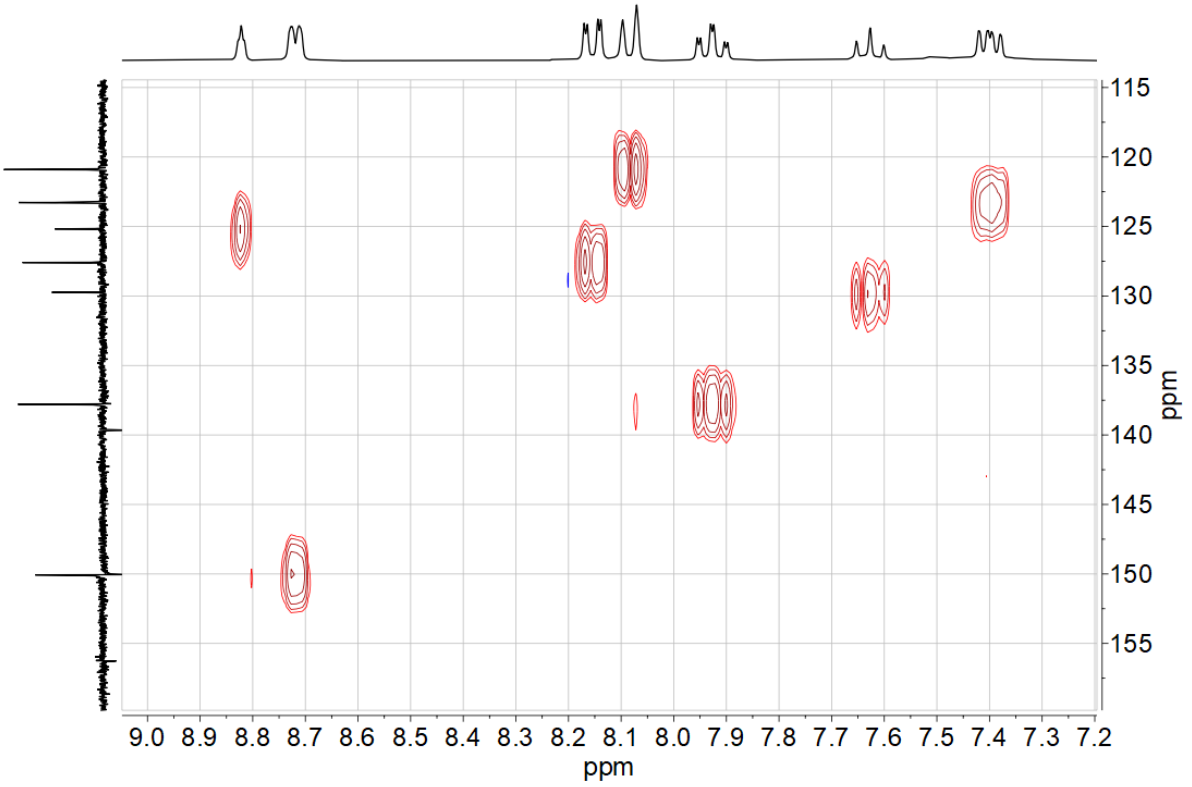

Figure 7-31 $^{1}H,^{13}C$ HSQC correlation spectrum of Py(PhH)Py in DMSO-d_6.

Figure 7-32 $^{1}H,^{1}H$ COSY correlation spectrum of Py(PhH)Py in DMSO-d_6.

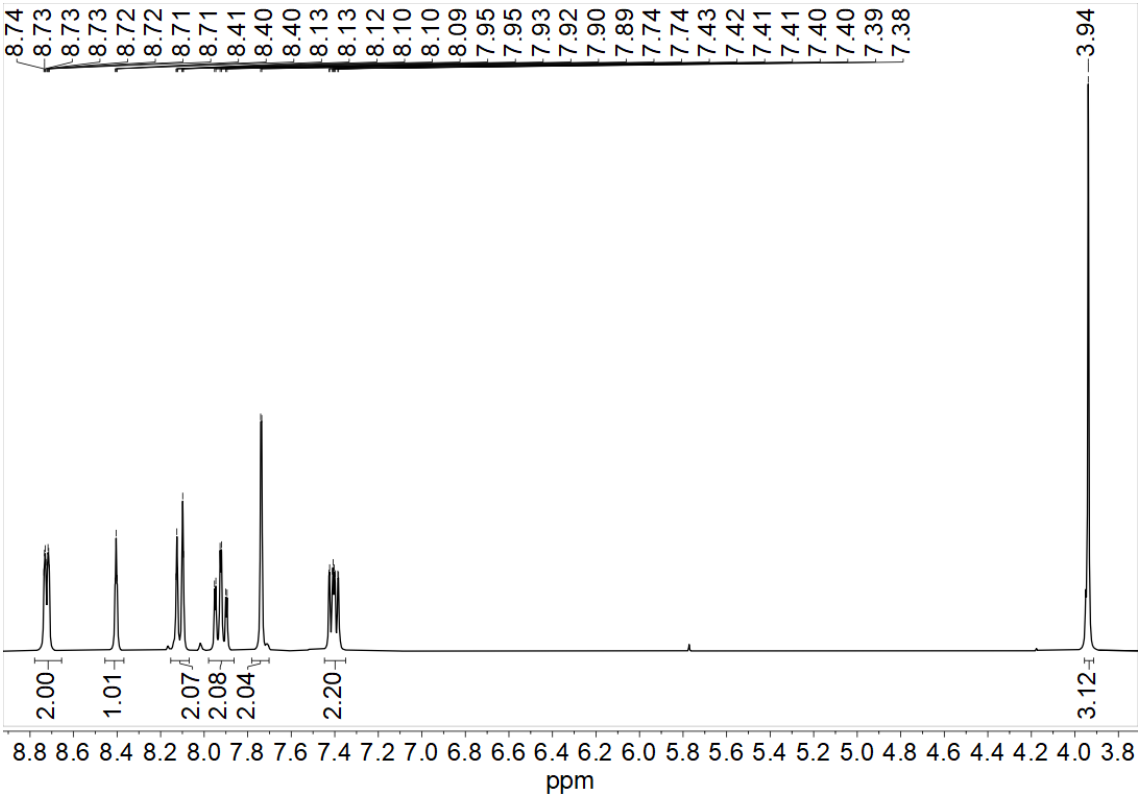

Figure 7-33 300 MHz ^{1}H NMR spectrum of Py(5MeOPhH)Py in DMSO-d_6.

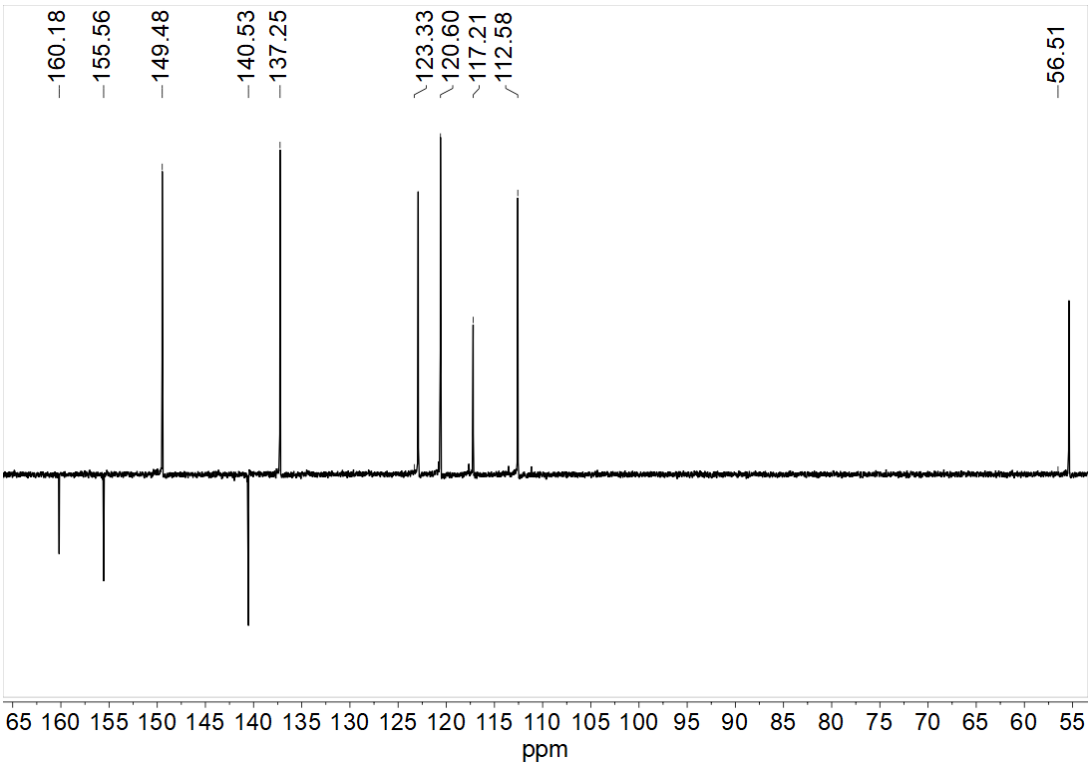

Figure 7-34 75 MHz ^{13}C NMR spectrum of Py(5MeOPhH)Py in DMSO-d_6.

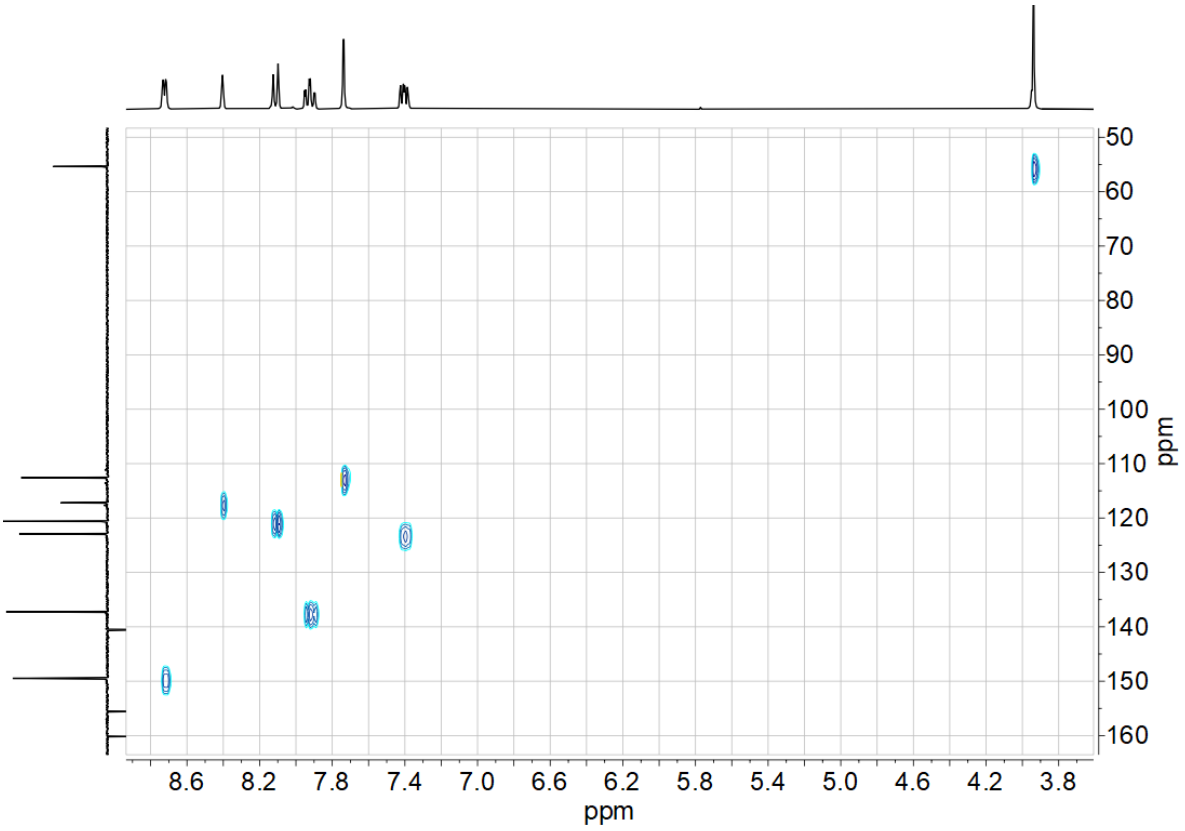

Figure 7-35 $^{1}H,^{13}C$ HSQC correlation spectrum of Py(5MeOPhH)Py in DMSO-d_6.

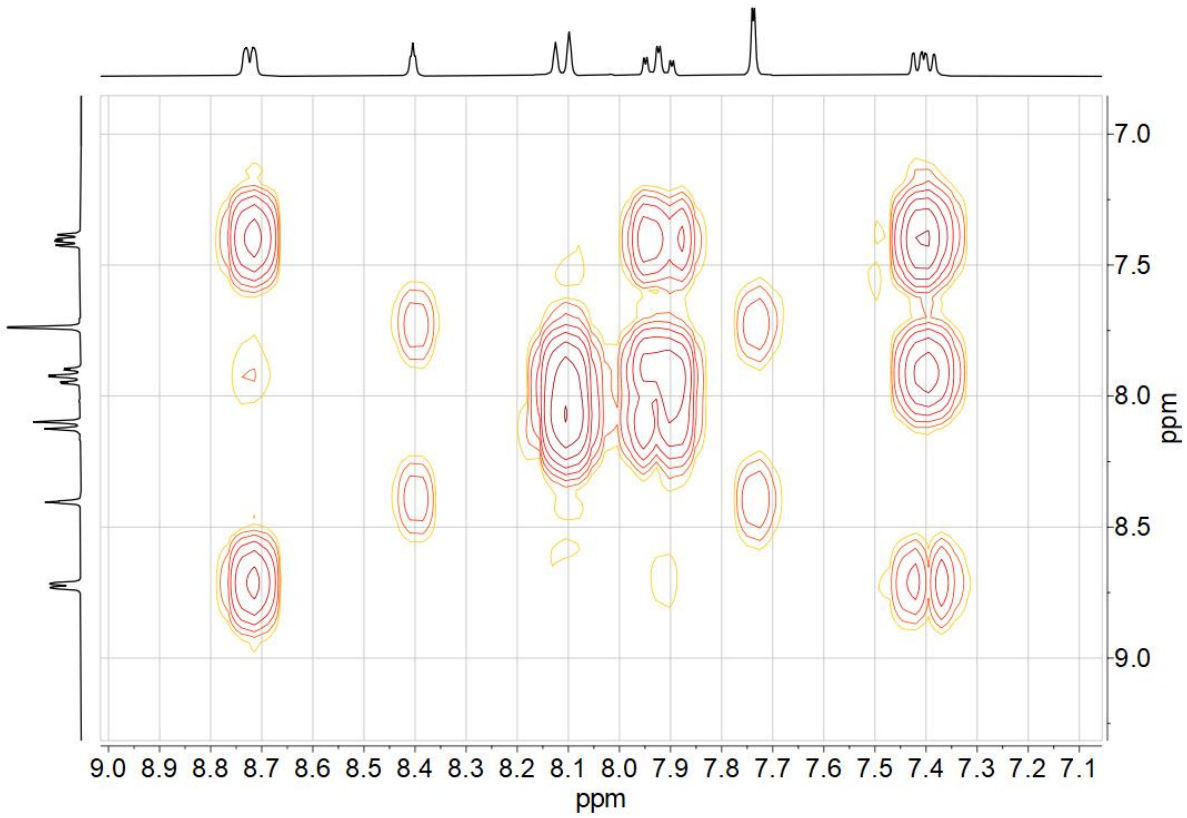

Figure 7-36 $^{1}H,^{1}H$ COSY correlation spectrum of Py(5MeOPhH)Py in DMSO-d_6.

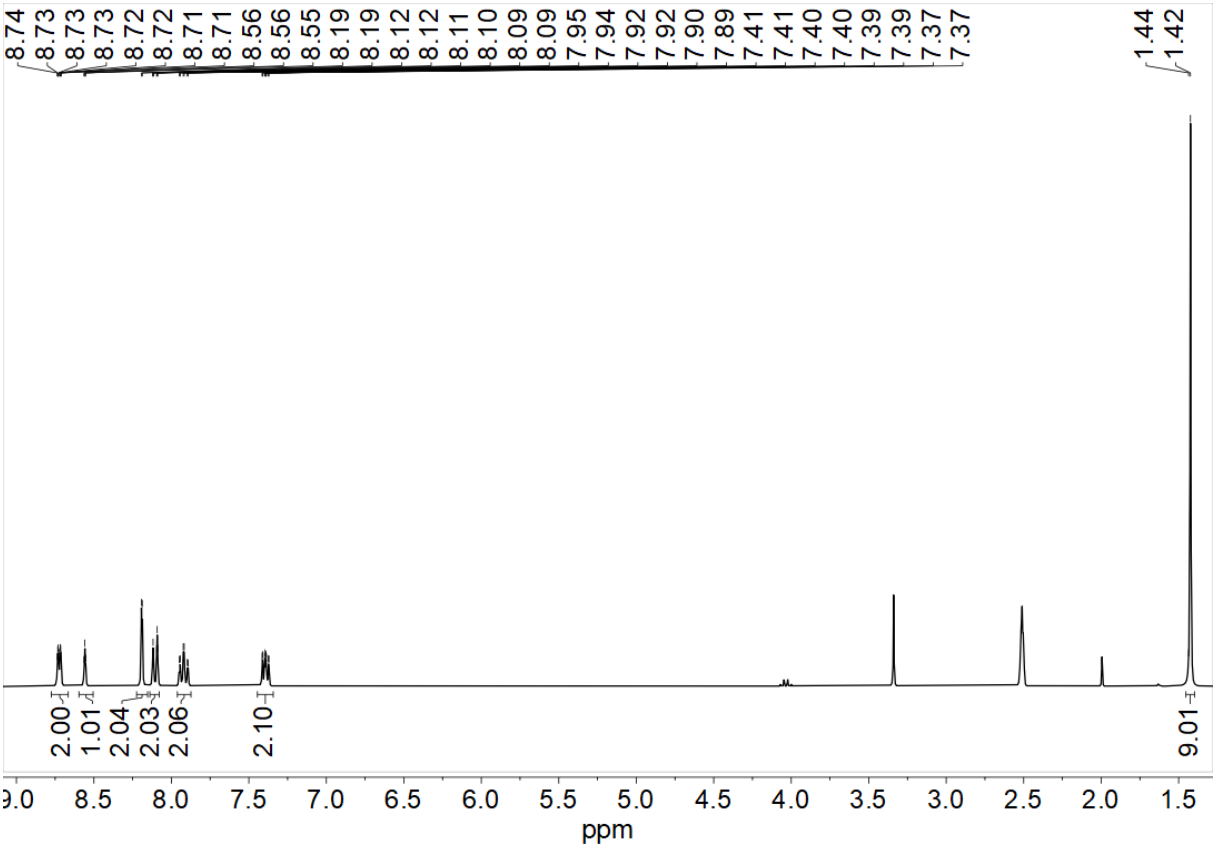

Figure 7-37 300 MHz ^{1}H NMR spectrum of Py(5BuPhH)Py in DMSO-d_6.

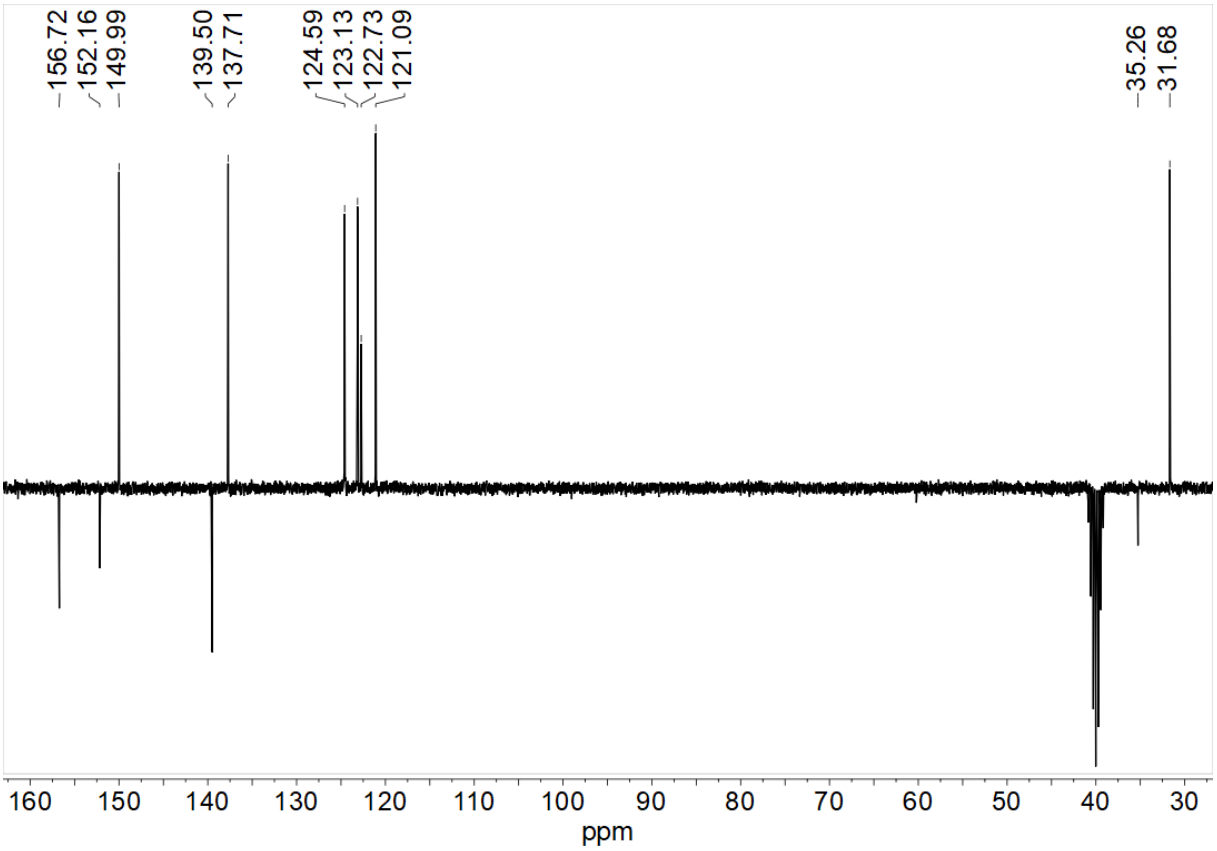

Figure 7-38 75 MHz ^{13}C NMR spectrum of Py(5BuPhH)Py in DMSO-d_6.

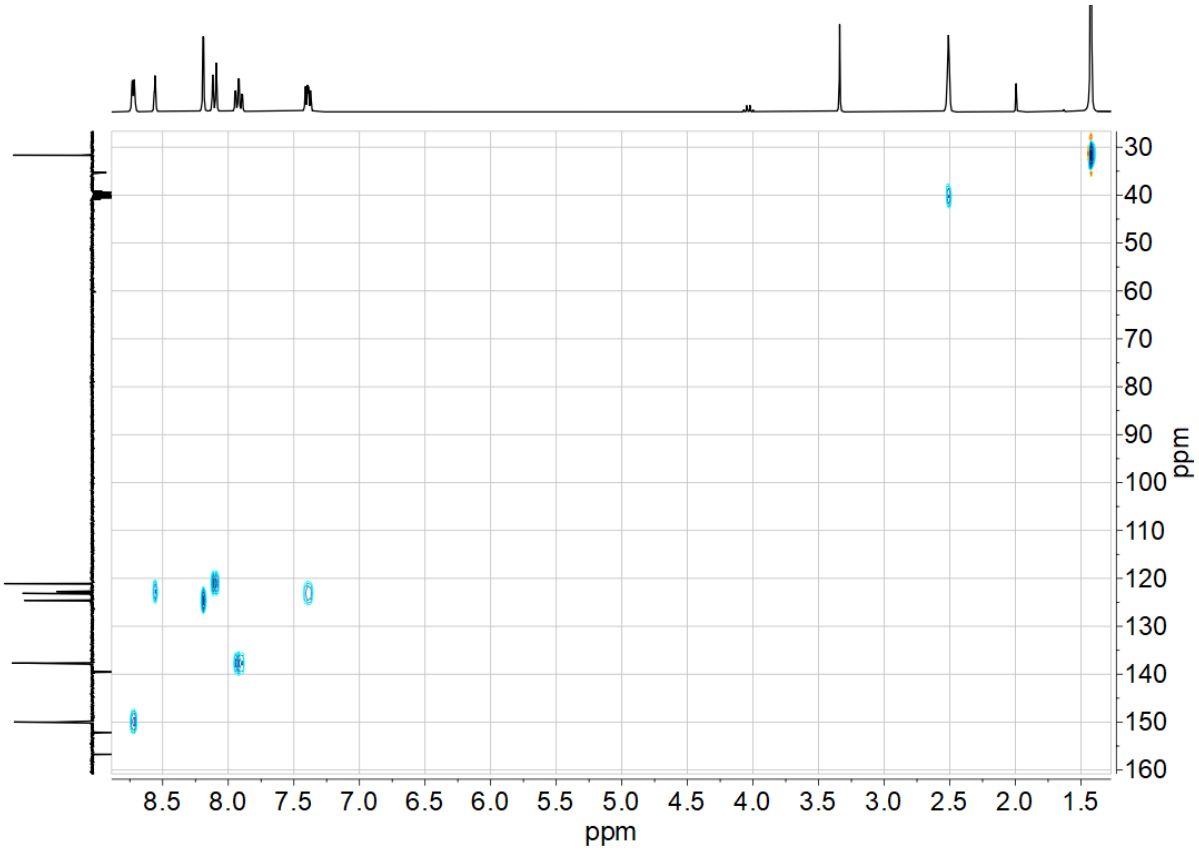

Figure 7-39 $^{1}H,^{13}C$ HSQC correlation spectrum of Py(5BuPhH)Py in DMSO-d_6.

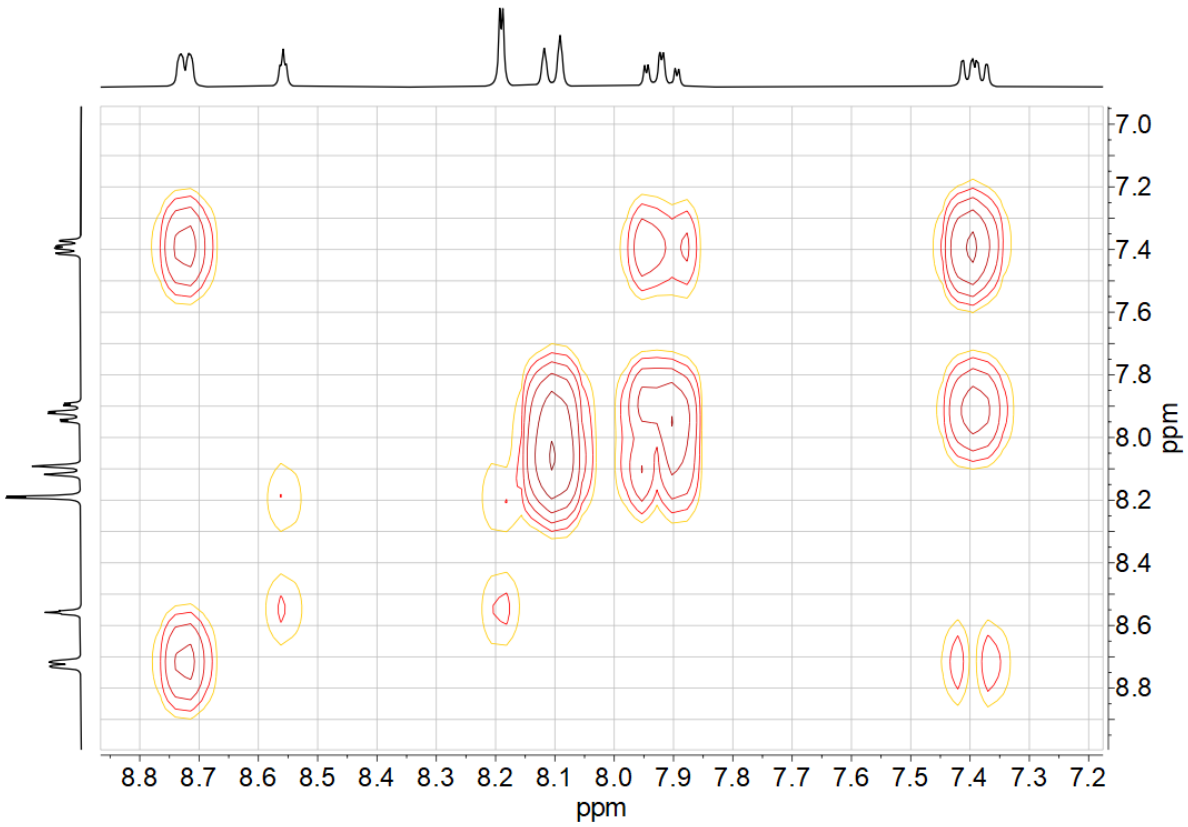

Figure 7-40 $^{1}H,^{1}H$ COSY correlation spectrum of Py(5BuPhH)Py in DMSO-d_6.

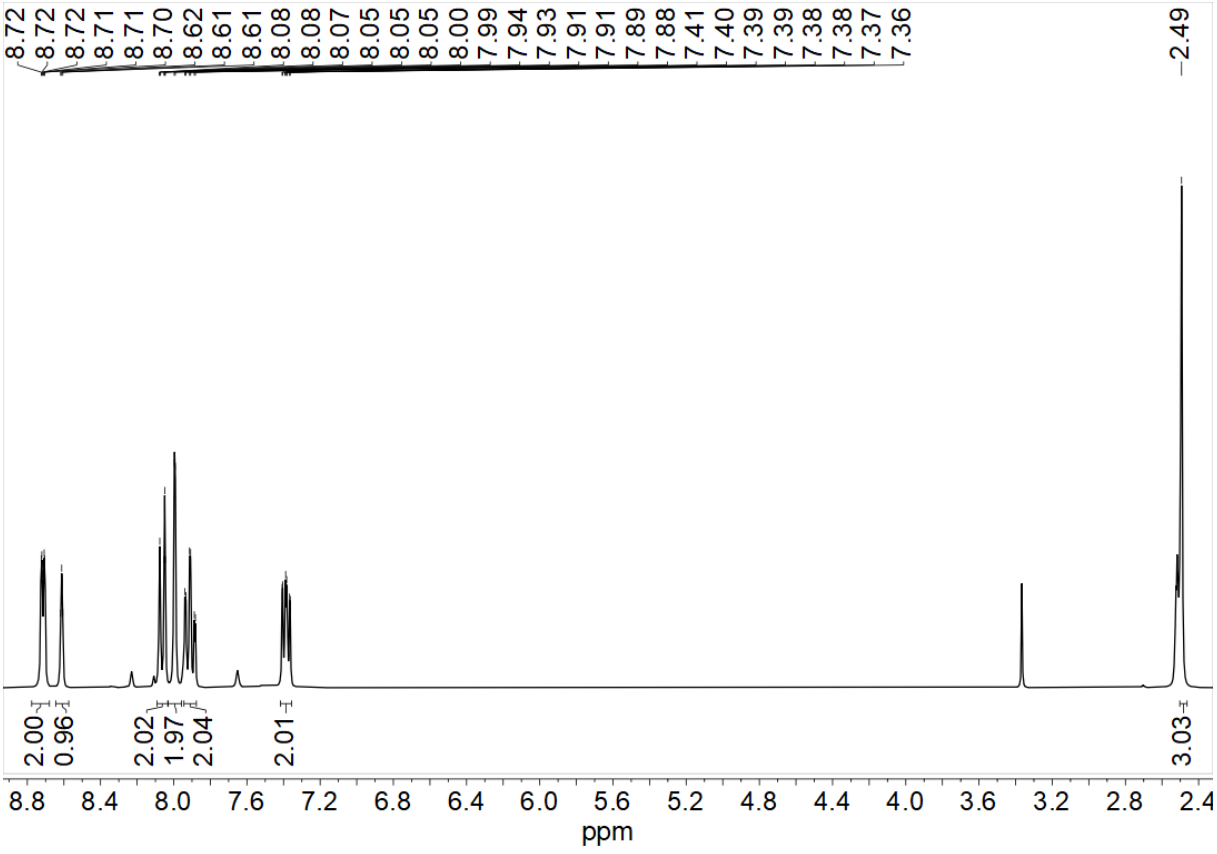

Figure 7-41 300 MHz ^{1}H NMR spectrum of Py(5MePhH)Py in DMSO-d_6.

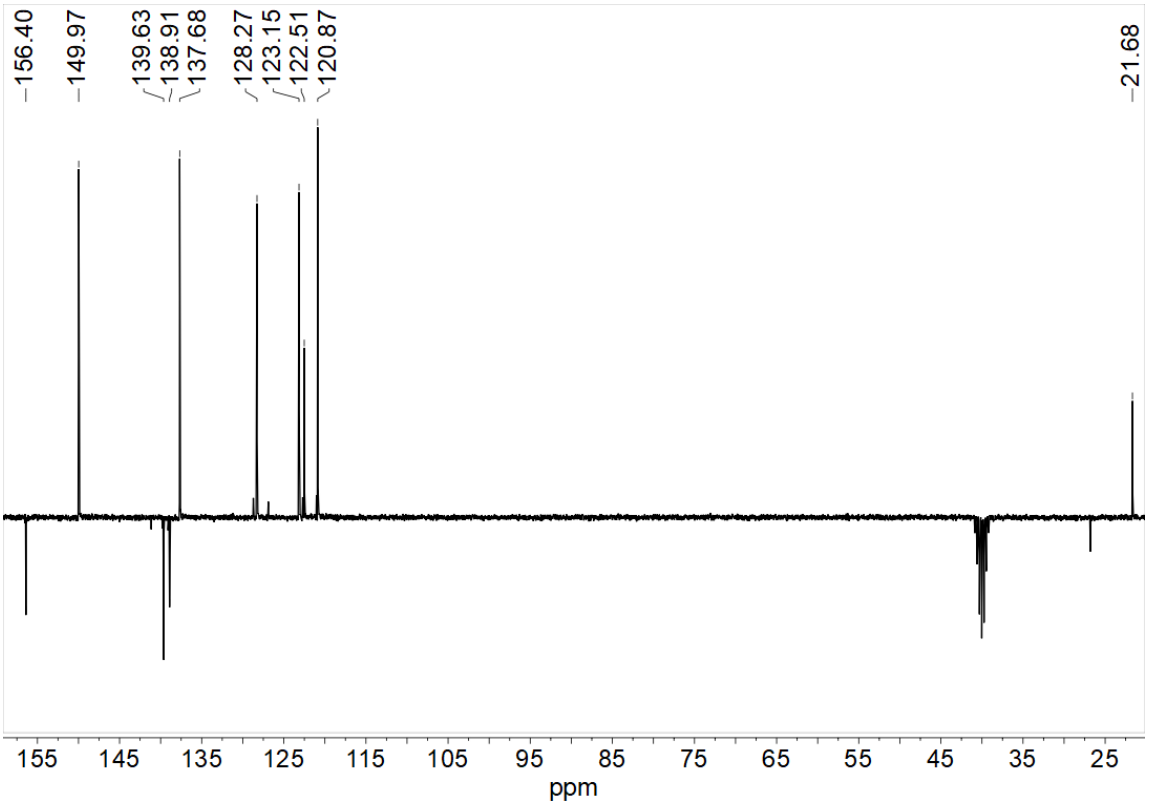

Figure 7-42 75 MHz ^{13}C NMR spectrum of Py(5MePhH)Py in DMSO-d_6.

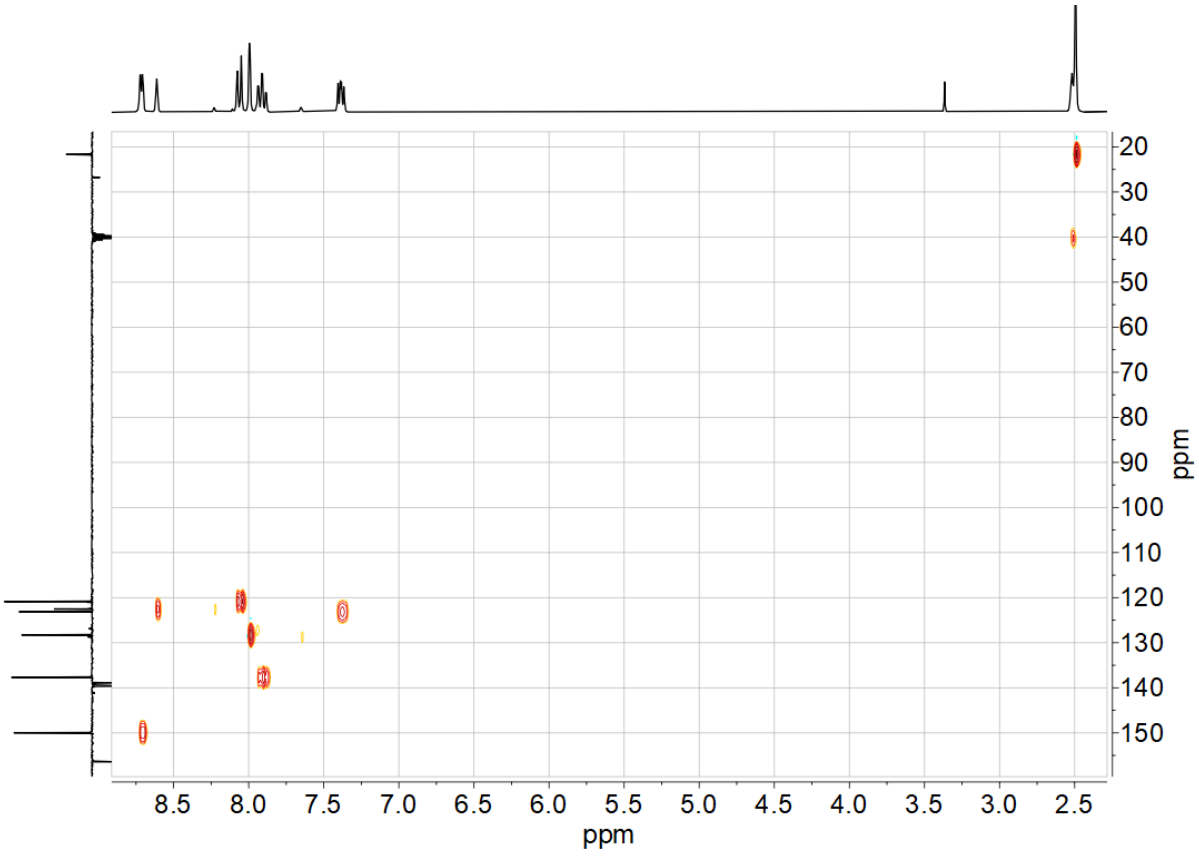

Figure 7-43 $^{1}H,^{13}C$ HSQC correlation spectrum of Py(5MePhH)Py in DMSO-d_6.

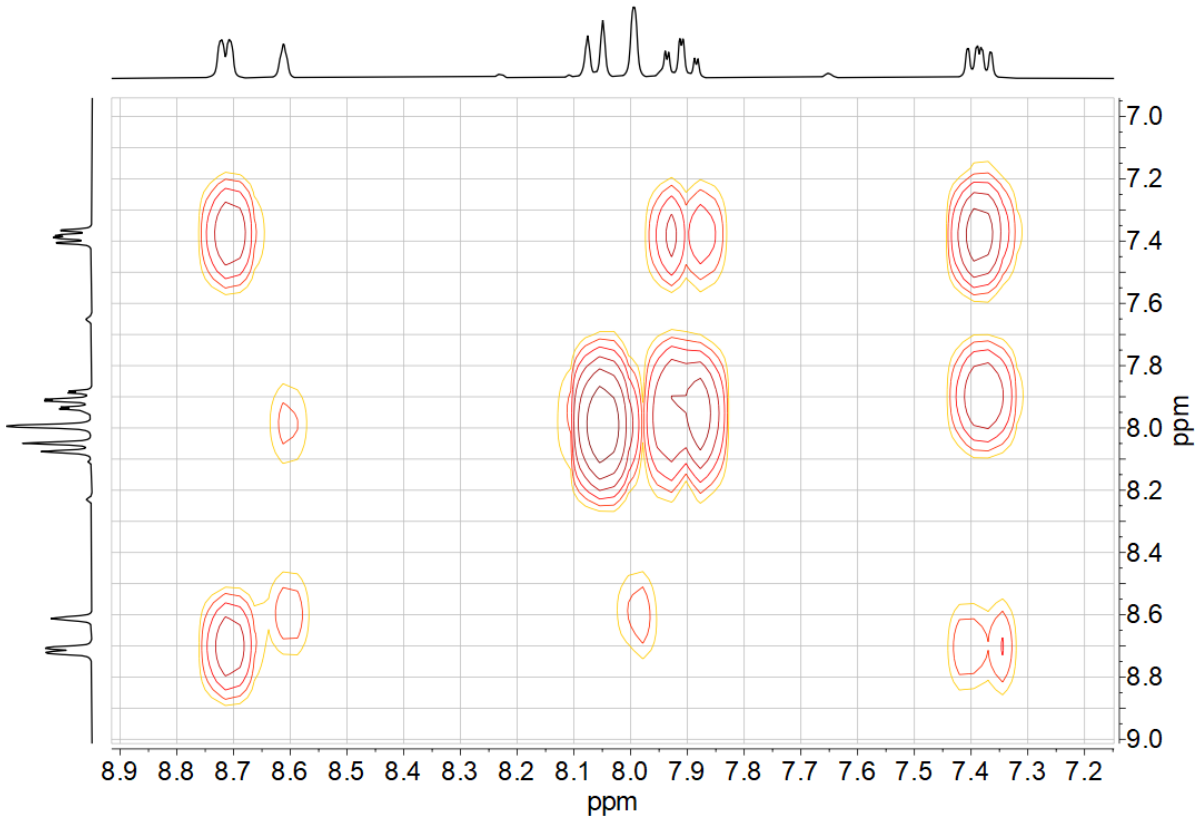

Figure 7-44 $^{1}H,^{1}H$ COSY correlation spectrum of Py(5MePhH)Py in DMSO-d_6.

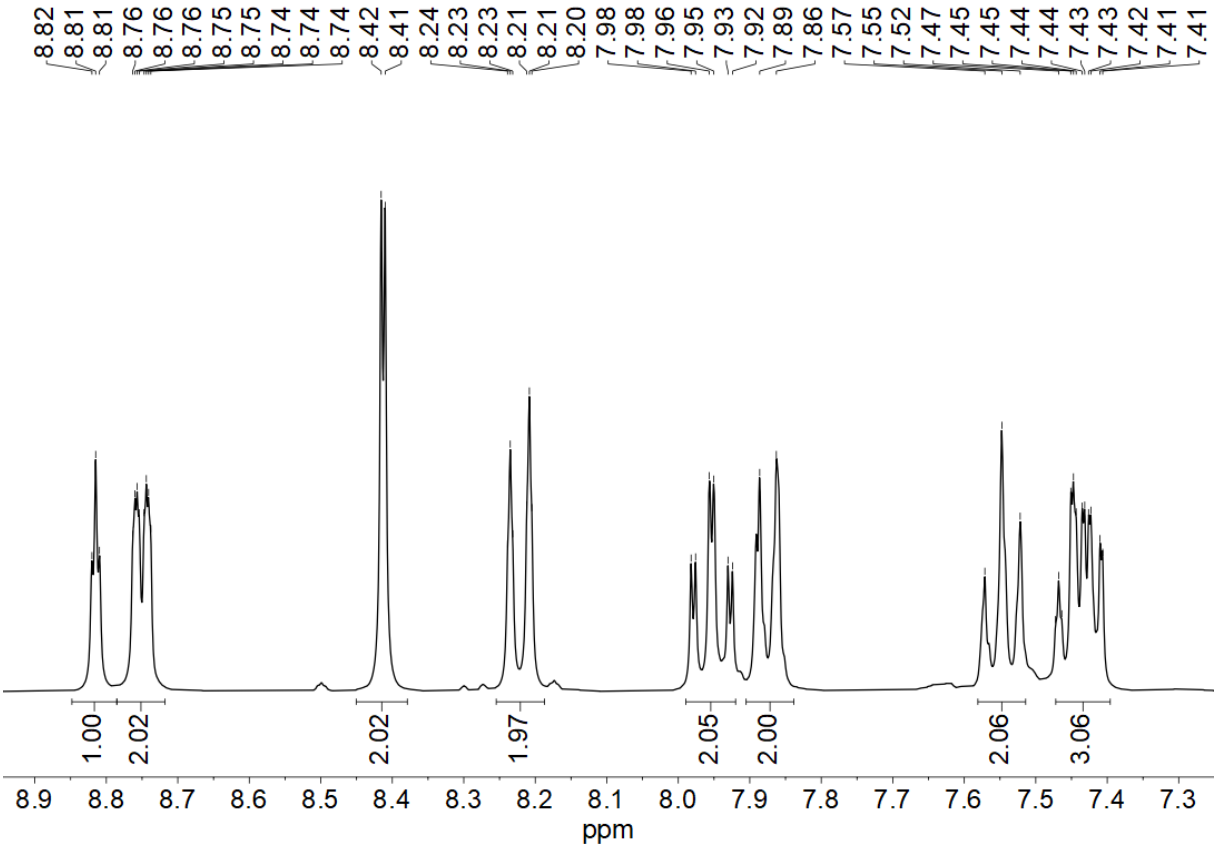

Figure 7-45 300 MHz ^{1}H NMR spectrum of Py(5PhPhH)Py in DMSO-d_6.

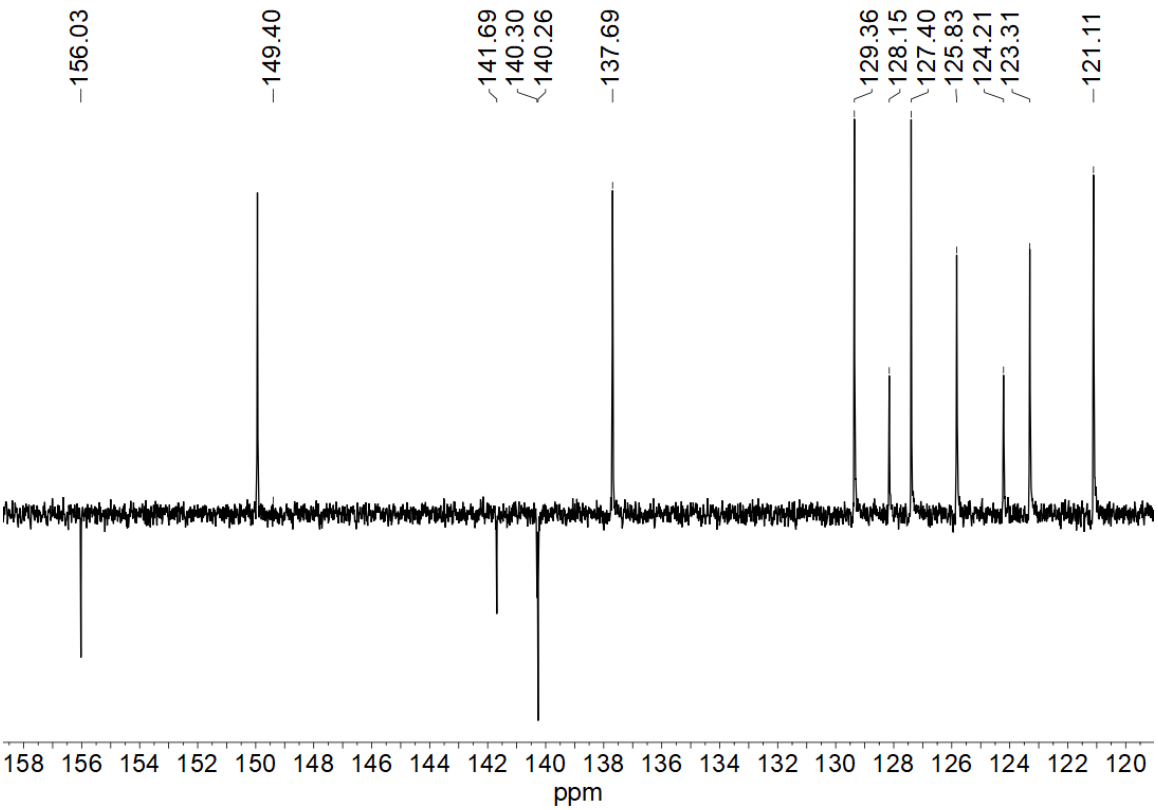

Figure 7-46 75 MHz ^{13}C NMR spectrum of Py(5PhPhH)Py in DMSO-d_6.

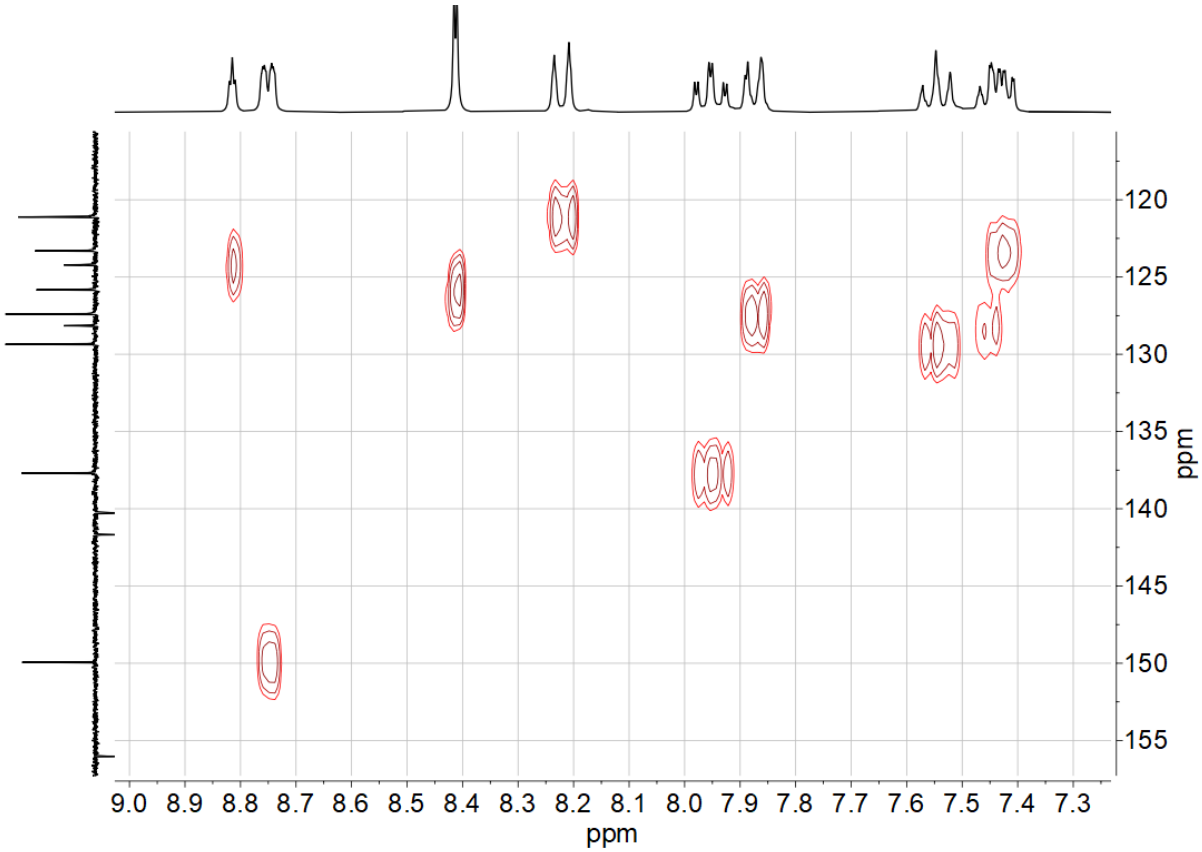

Figure 7-47 $^{1}H,^{13}C$ HSQC correlation spectrum of Py(5PhPhH)Py in DMSO-d_6.

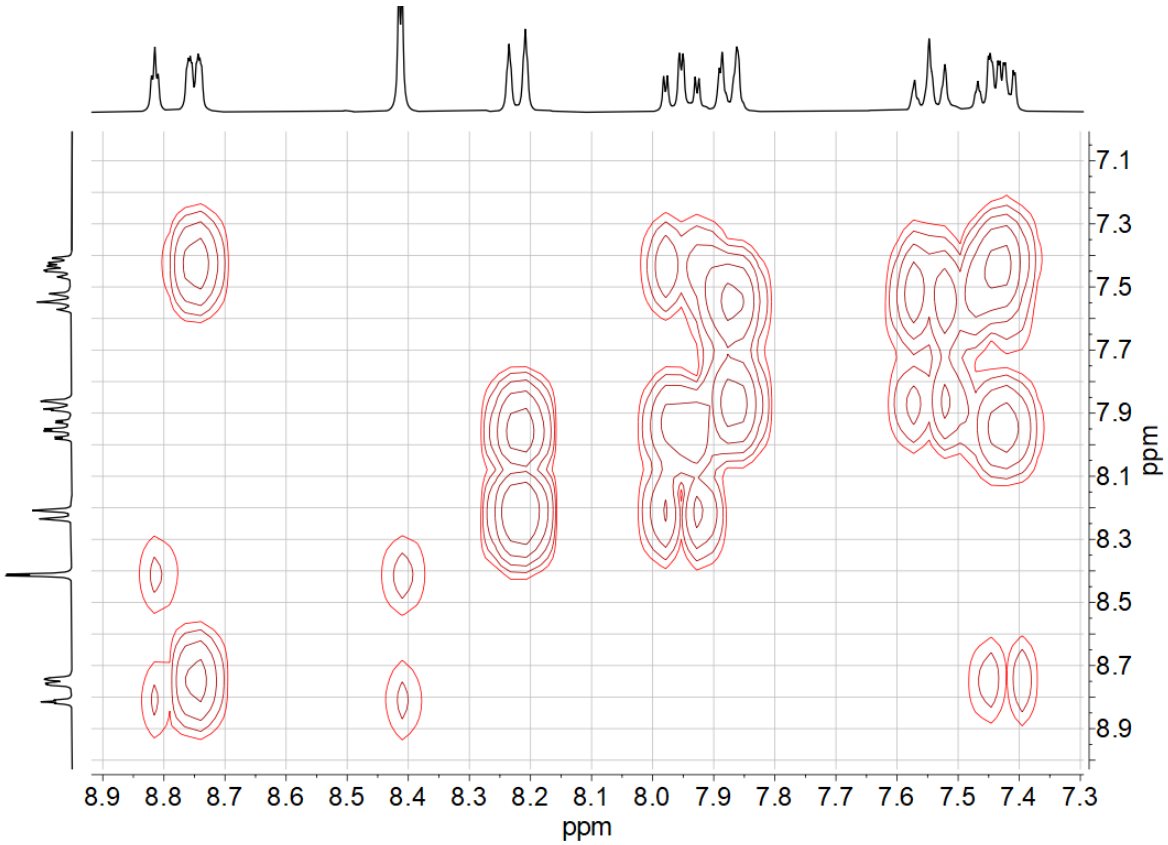

Figure 7-48 $^{1}H,^{1}H$ COSY correlation spectrum of Py(5PhPhH)Py in DMSO-d_6.

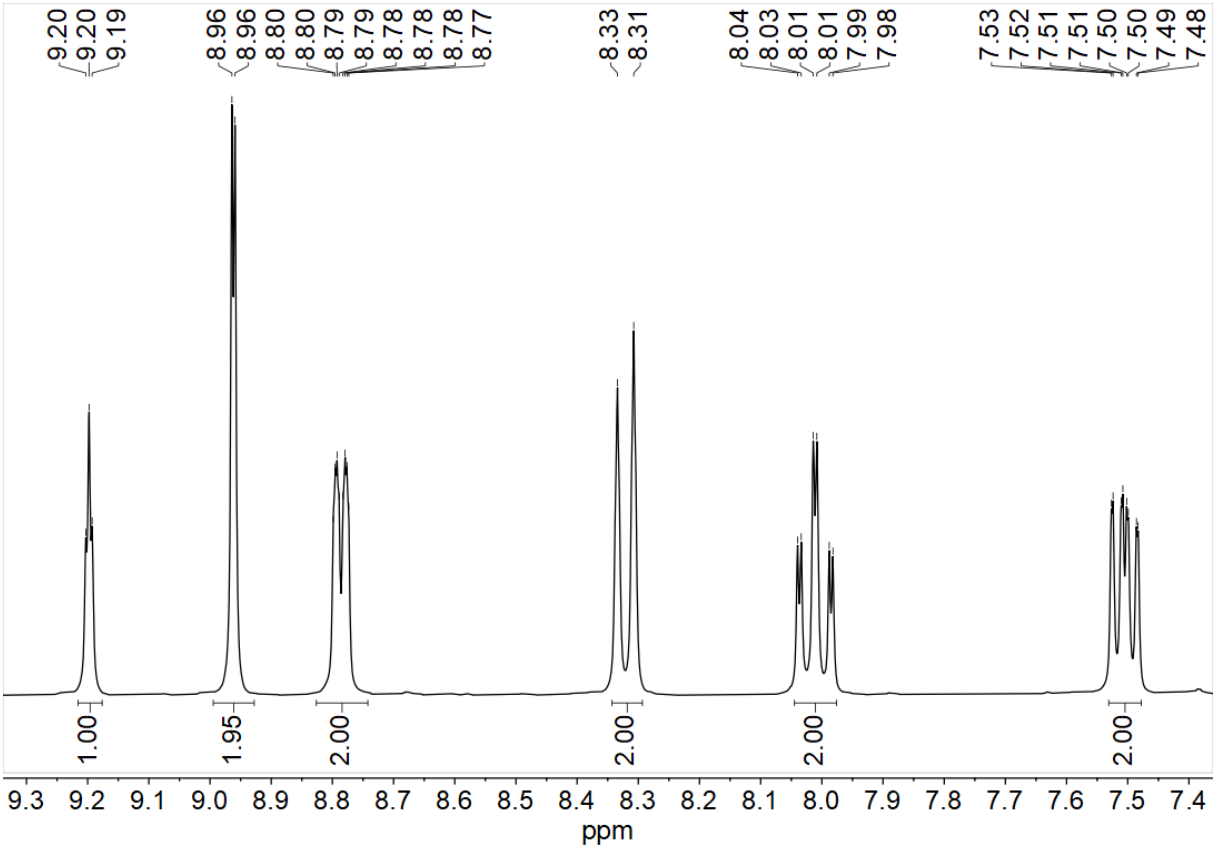

Figure 7-49 300 MHz ^{1}H NMR spectrum of Py(5NO$_2$PhH)Py in DMSO-d_6.

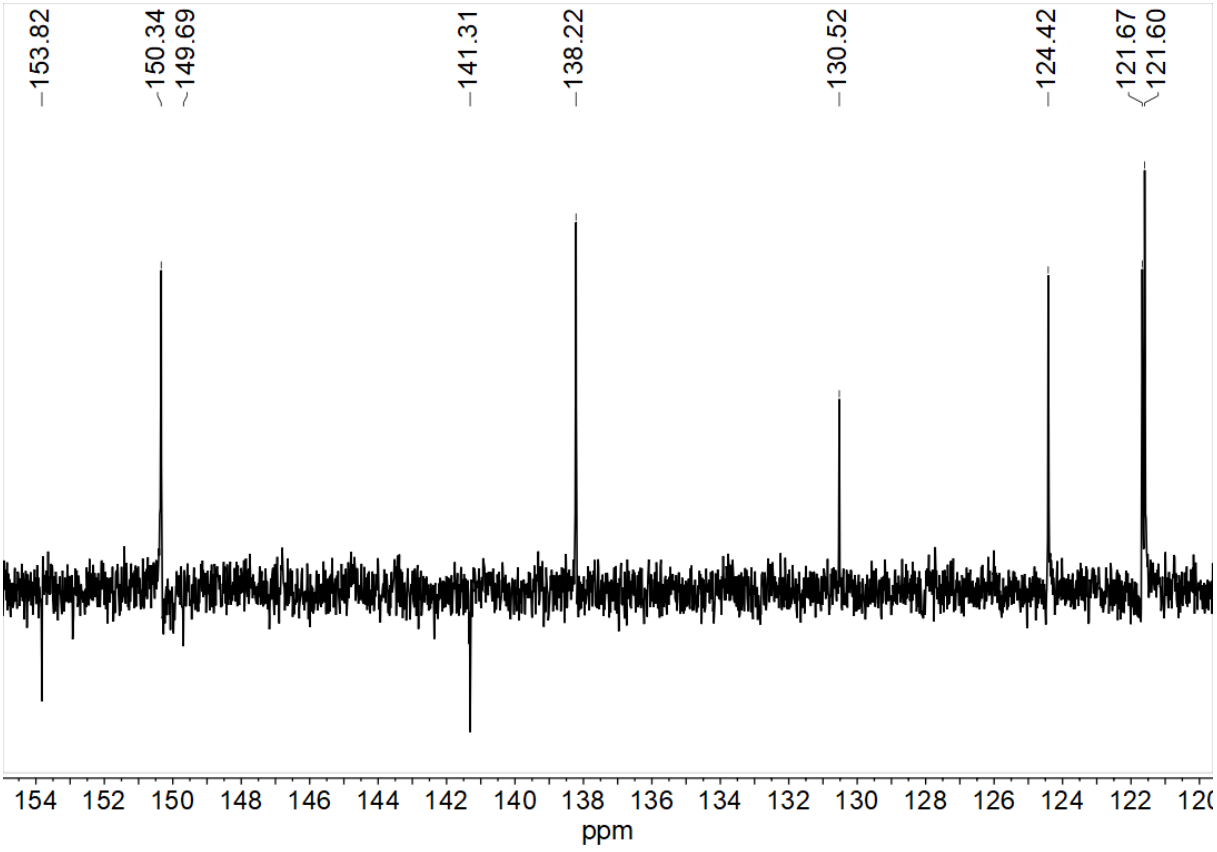

Figure 7-50 75 MHz ^{13}C NMR spectrum of Py(5NO$_2$PhH)Py in DMSO-d_6.

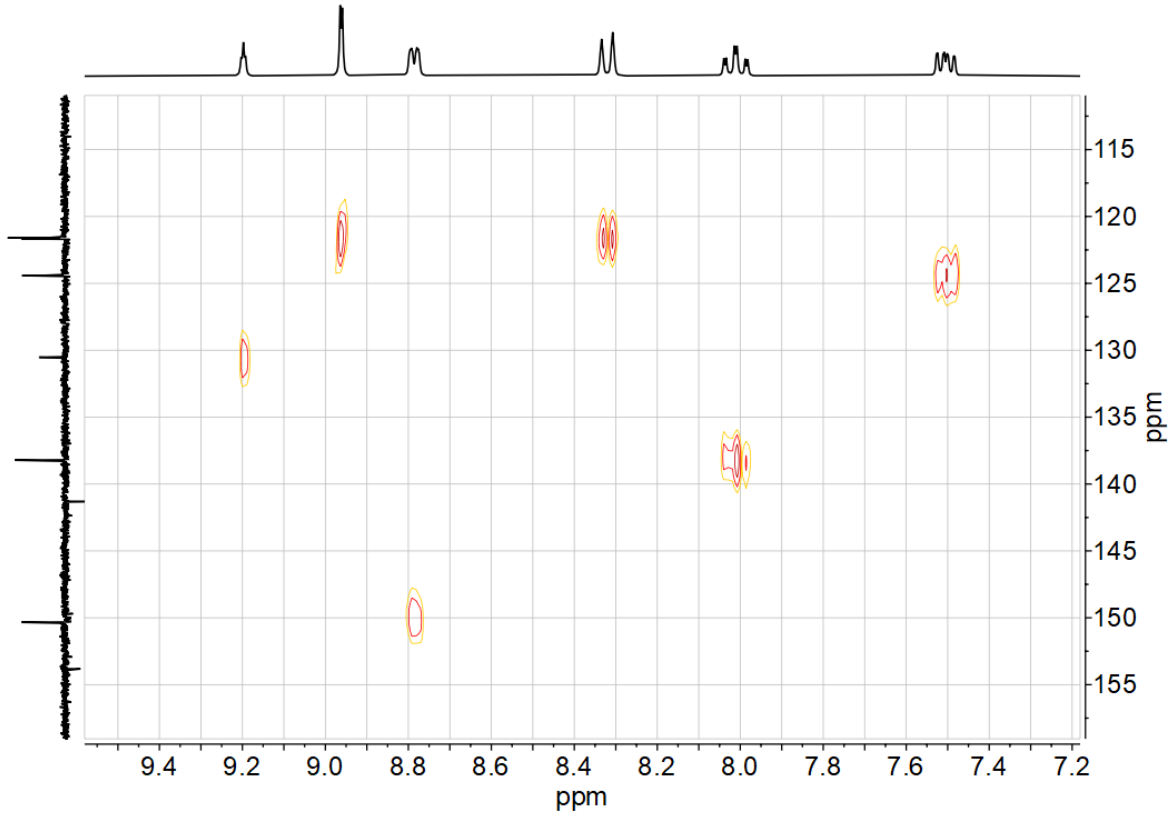

Figure 7-51 $^{1}H,^{13}C$ HSQC correlation spectrum of Py(5NO_2PhH)Py in DMSO-d_6.

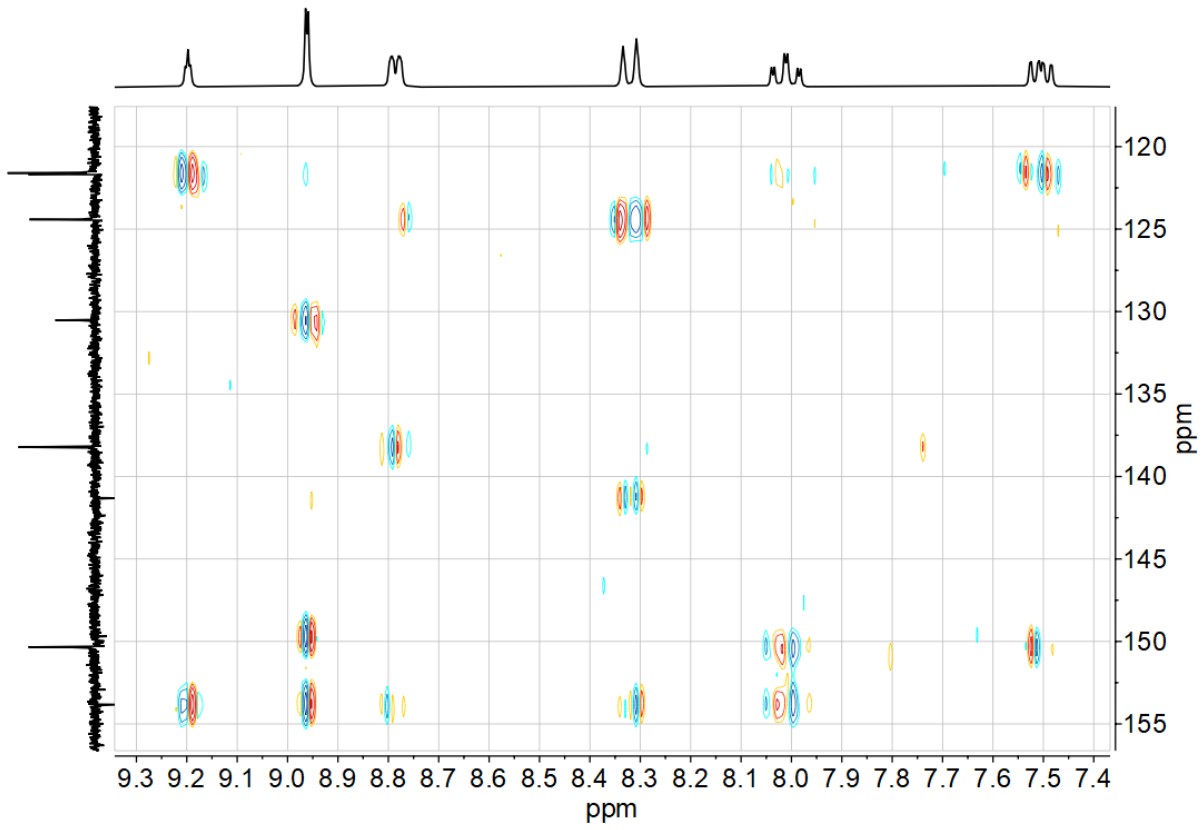

Figure 7-52 $^{1}H,^{13}C$ HMBC correlation spectrum of Py(5NO_2PhH)Py in DMSO-d_6.

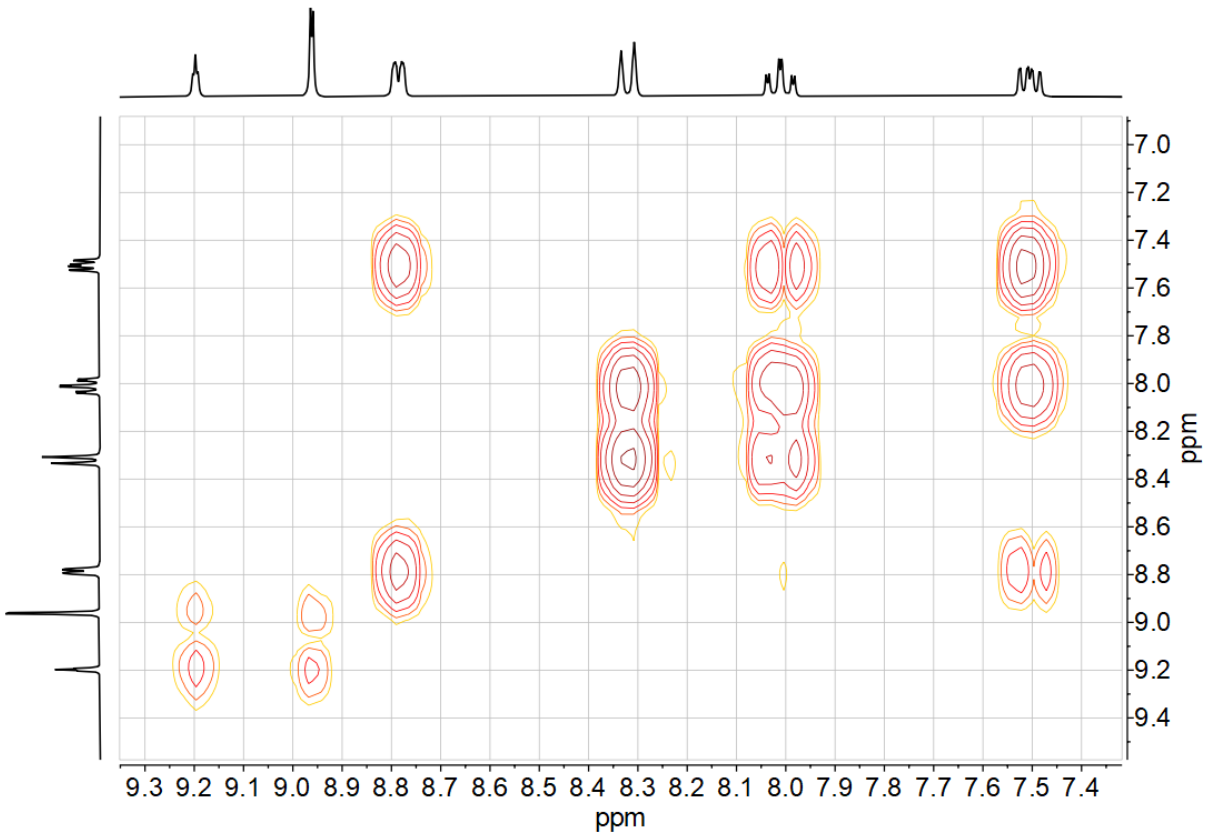

Figure 7-53 ^{1}H,^{1}H COSY correlation spectrum of Py(5NO_2PhH)Py in DMSO-d_6.

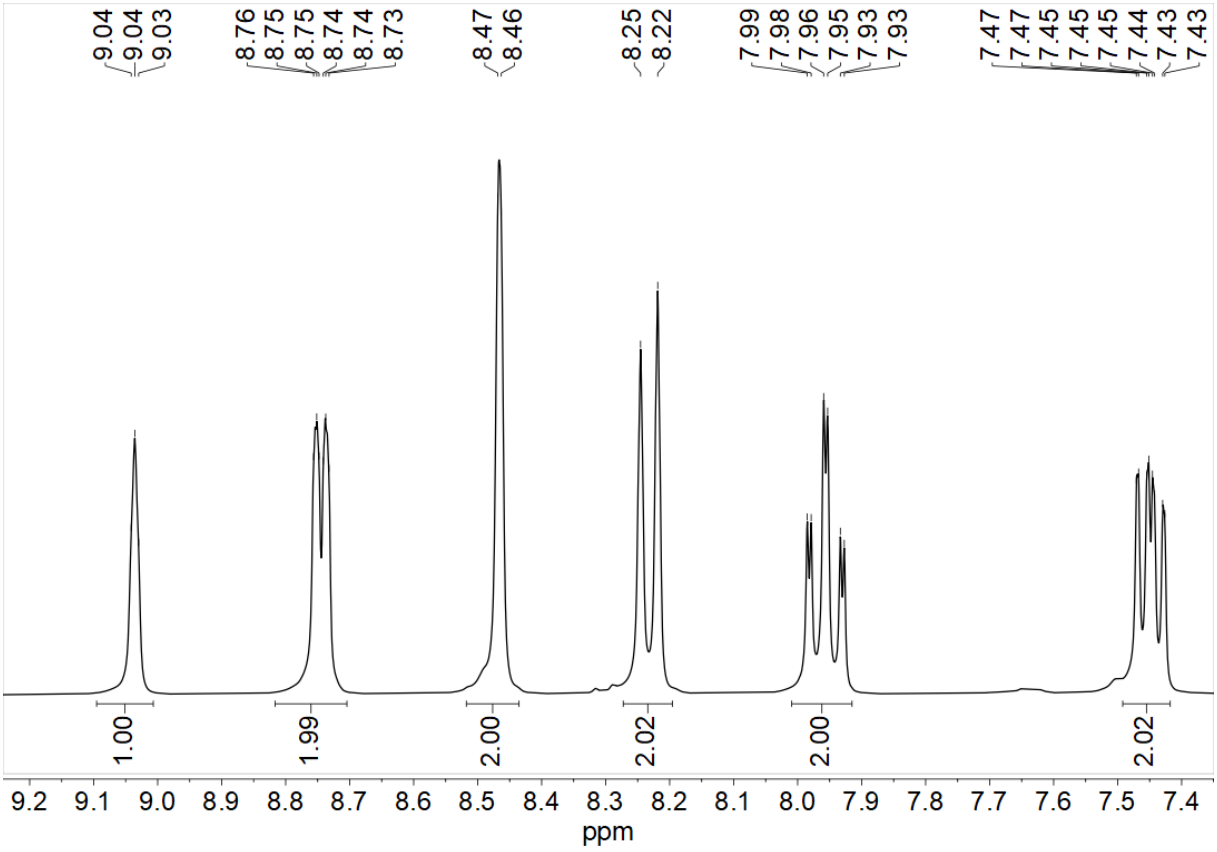

Figure 7-54 300 MHz ^{1}H NMR spectrum of Py(5CF_3PhH)Py in DMSO-d_6.

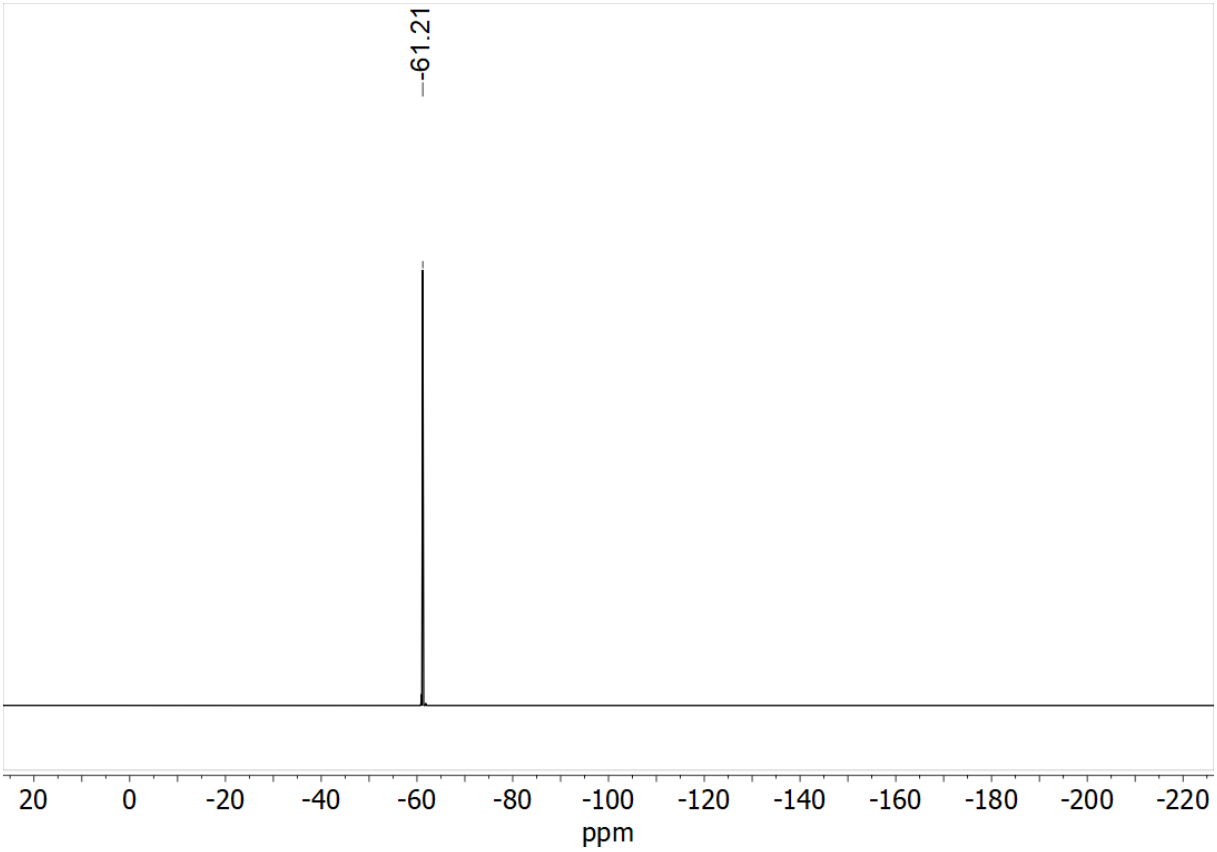

Figure 7-55 282 MHz ^{19}F NMR spectrum of Py(5CF$_3$PhH)Py in DMSO-d_6.

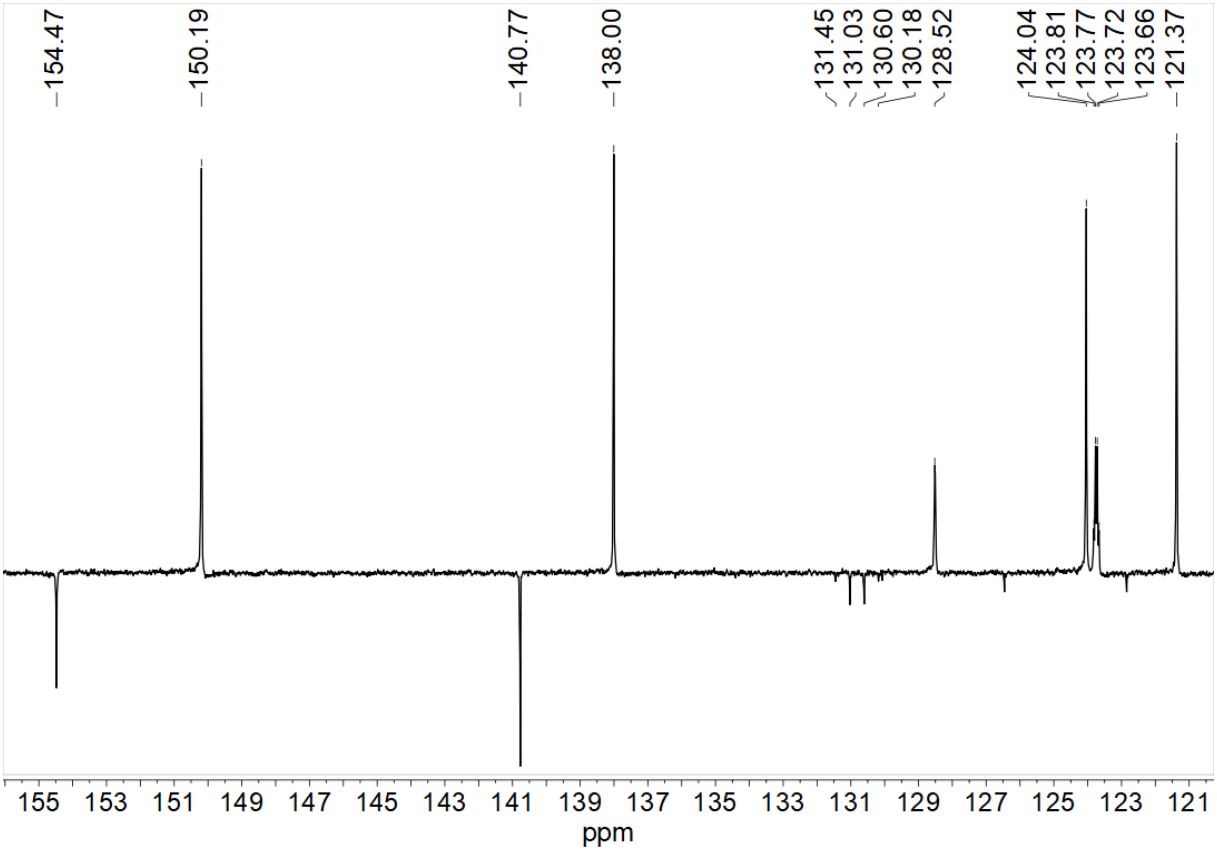

Figure 7-56 75 MHz ^{13}C NMR spectrum of Py(5CF$_3$PhH)Py in DMSO-d_6.

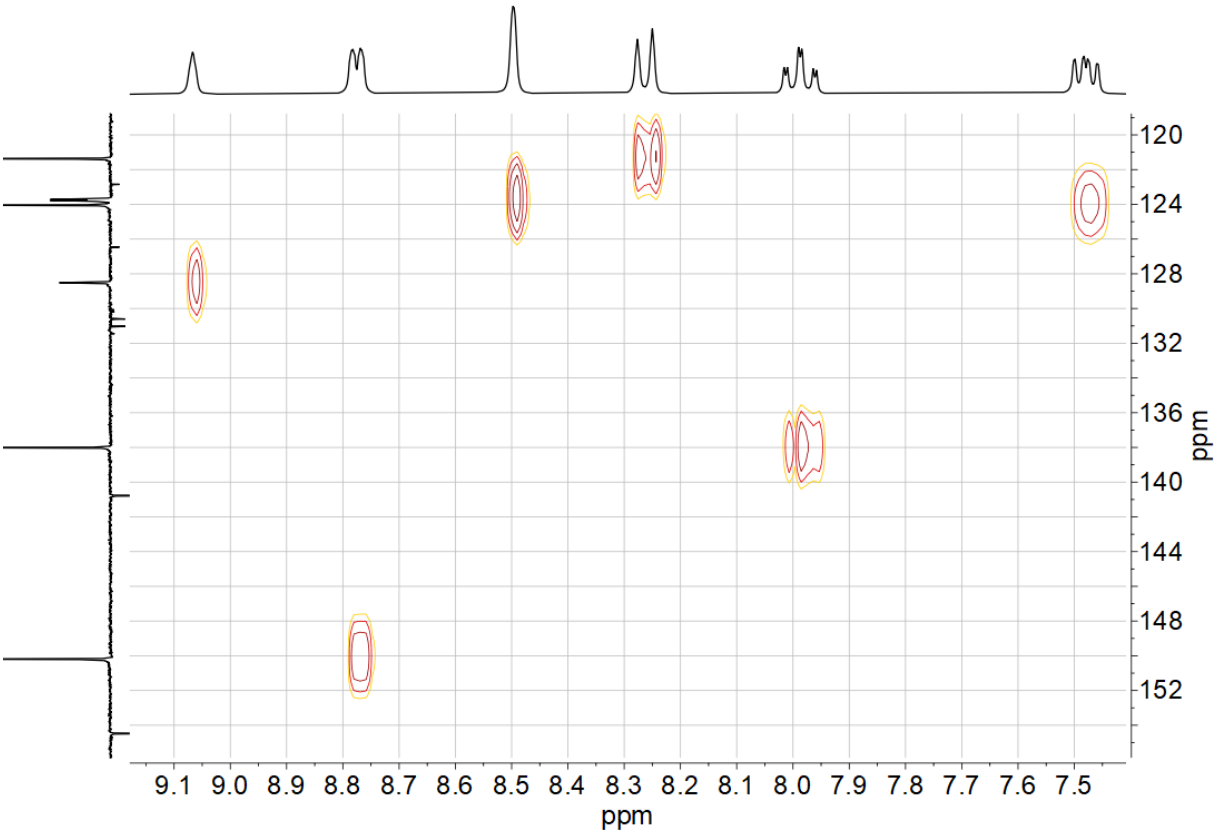

Figure 7-57 $^{1}H,^{13}C$ HSQC correlation spectrum of Py(5CF_3PhH)Py in DMSO-d_6.

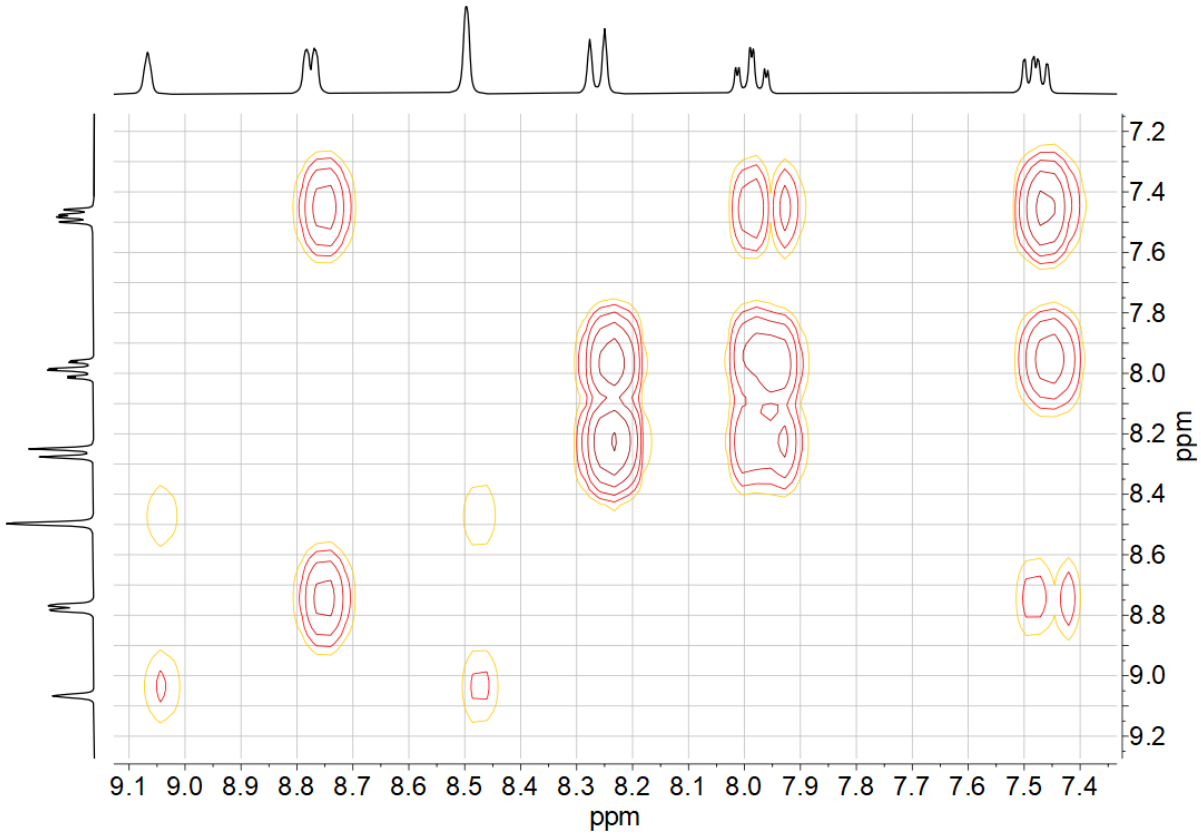

Figure 7-58 $^{1}H,H^{1}$ COSY correlation spectrum of Py(5CF_3PhH)Py in DMSO-d_6.

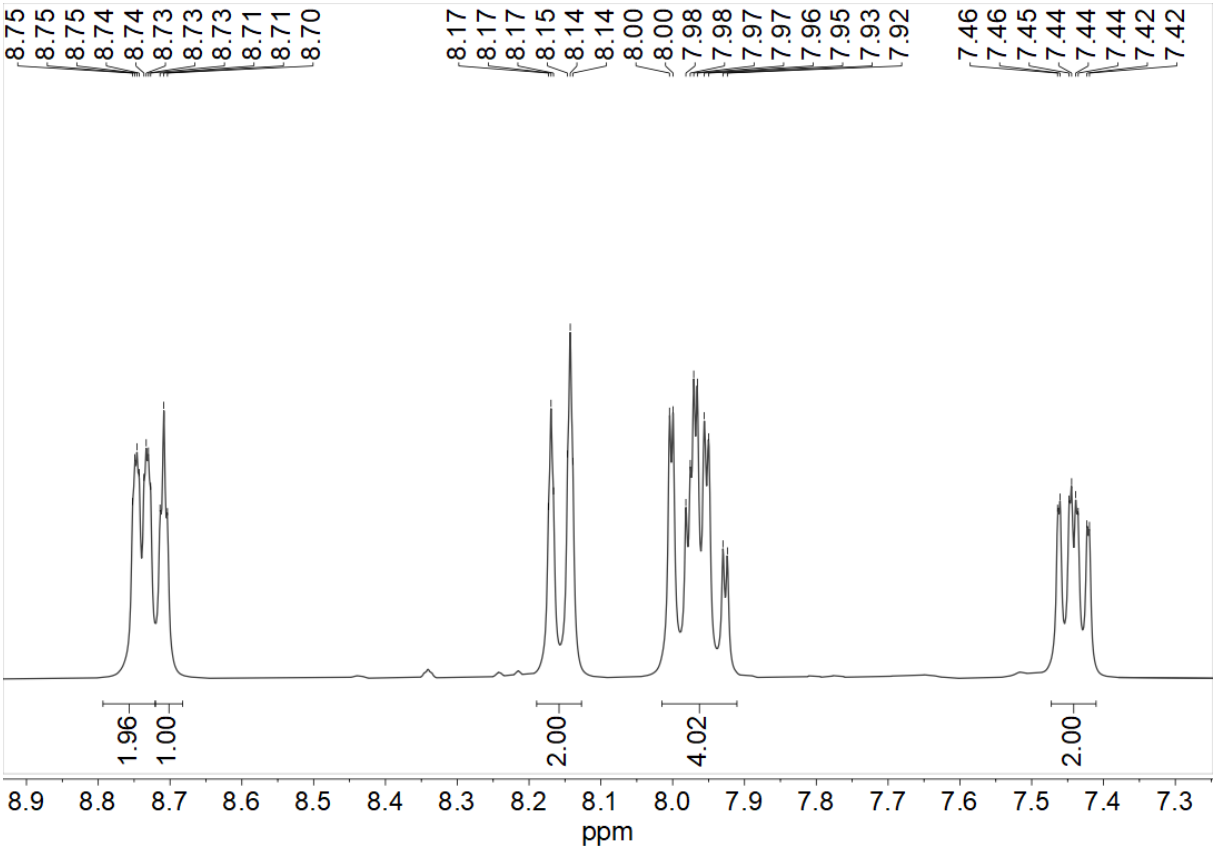

Figure 7-59 300 MHz ^{1}H NMR spectrum of Py(5FPhH)Py in DMSO-d_6.

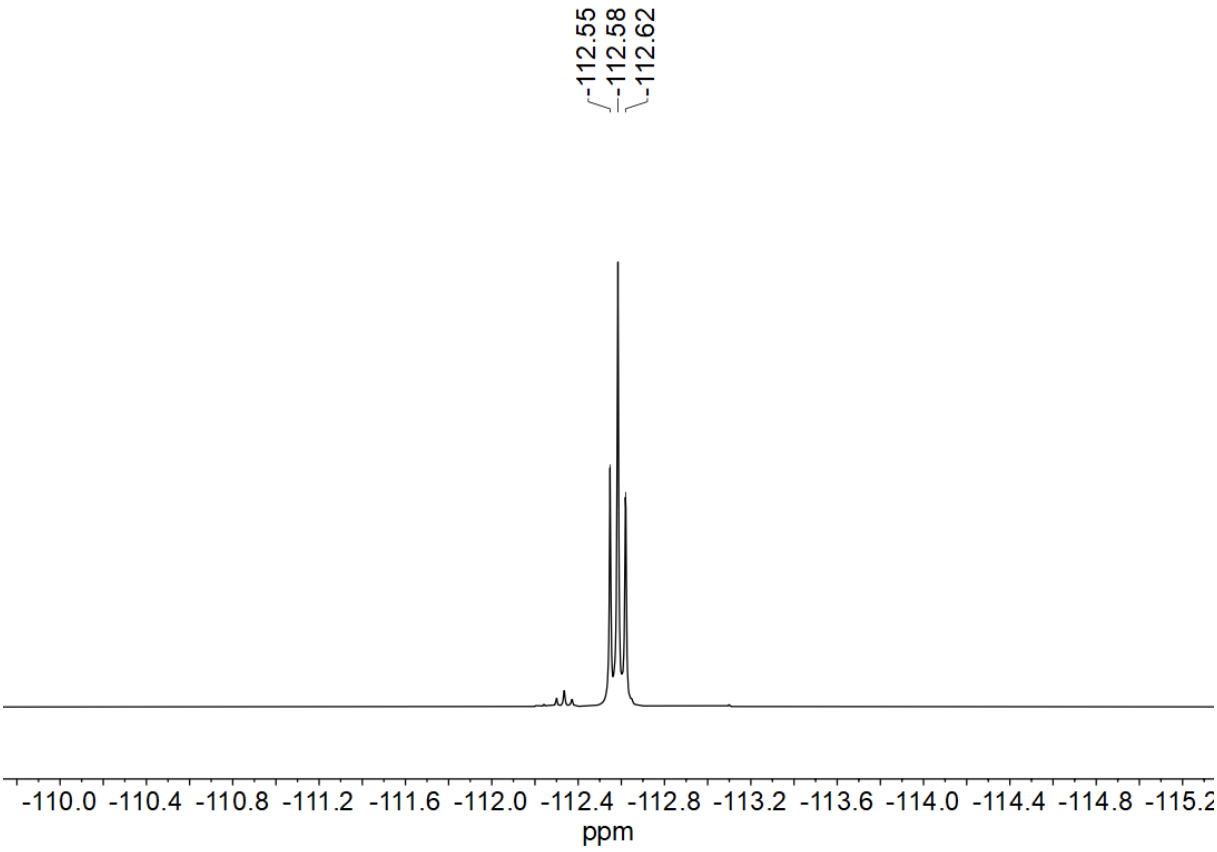

Figure 7-60 282 MHz ^{19}F NMR spectrum of Py(5FPhH)Py in DMSO-d_6.

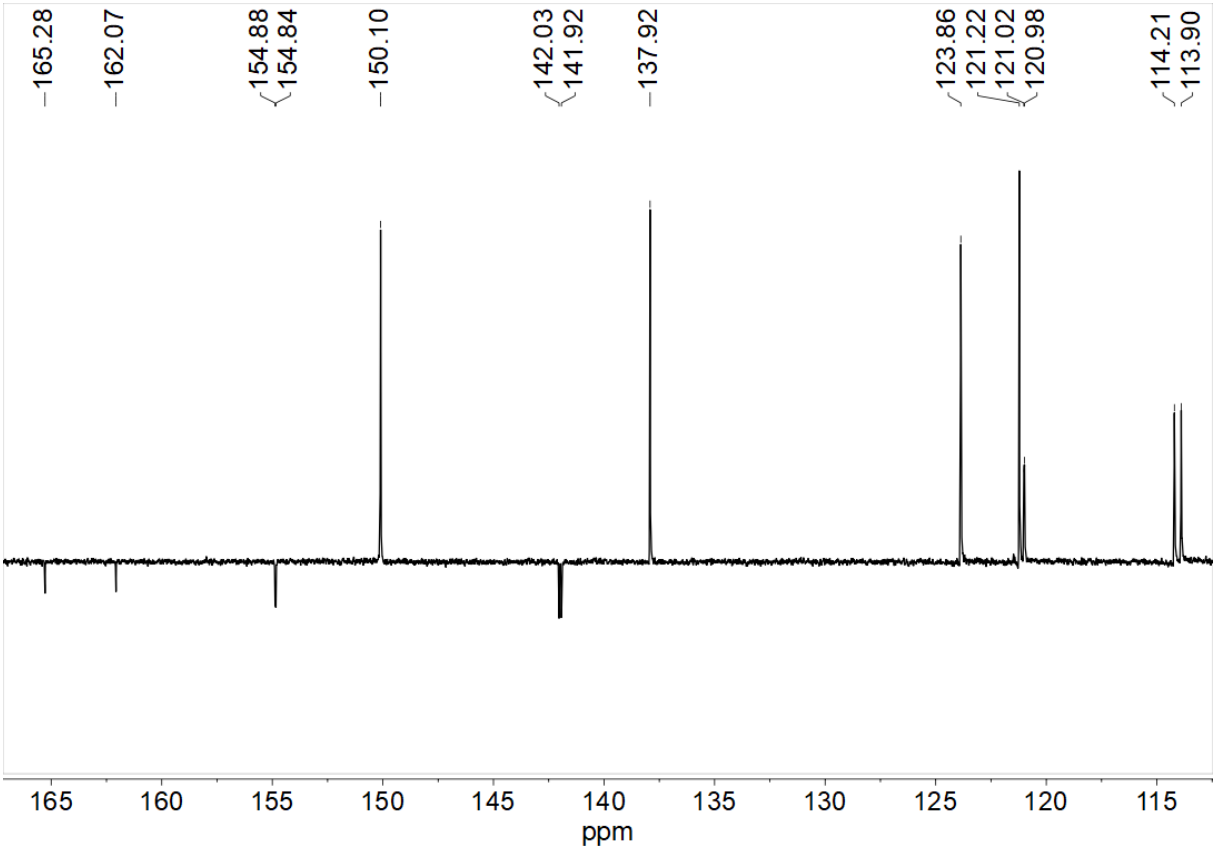

Figure 7-61 75 MHz ^{13}C NMR spectrum of Py(5FPhH)Py in DMSO-d_6.

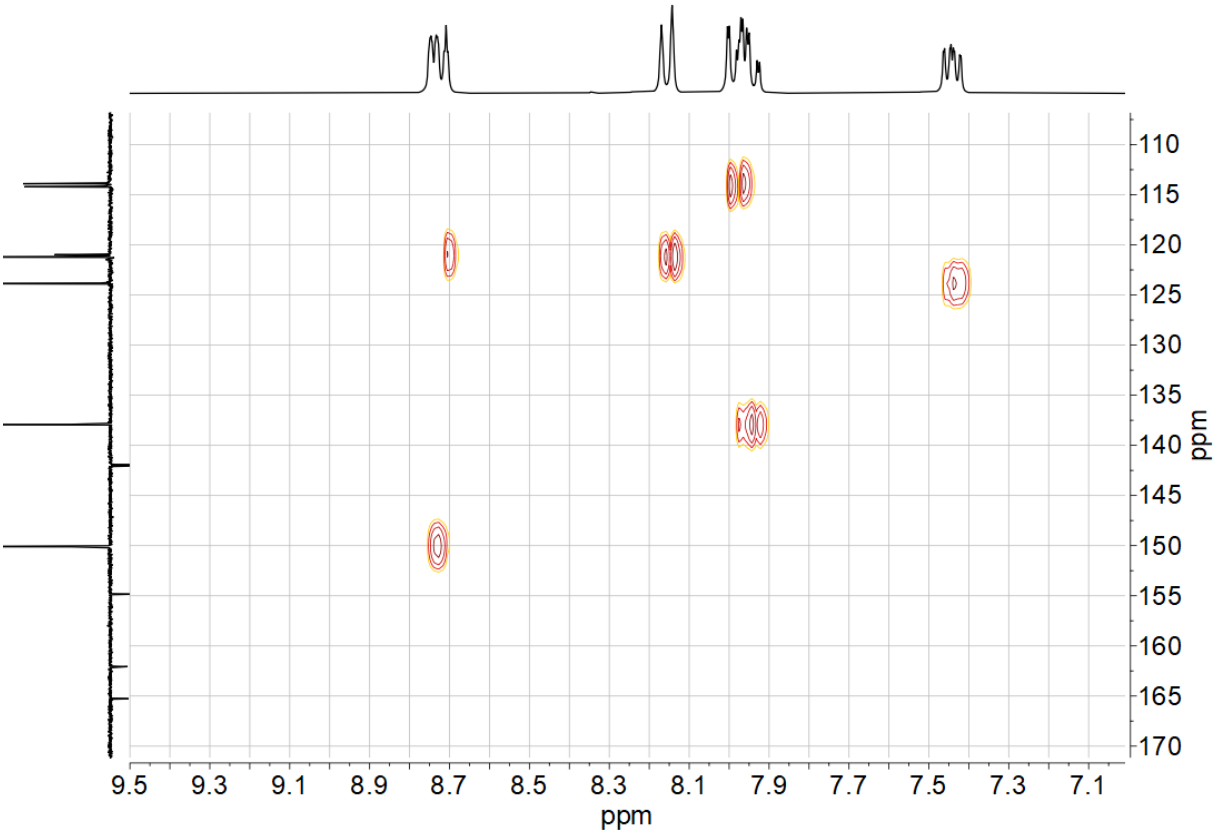

Figure 7-62 ^{1}H,^{13}C HSQC correlation spectrum of Py(5FPhH)Py in DMSO-d_6.

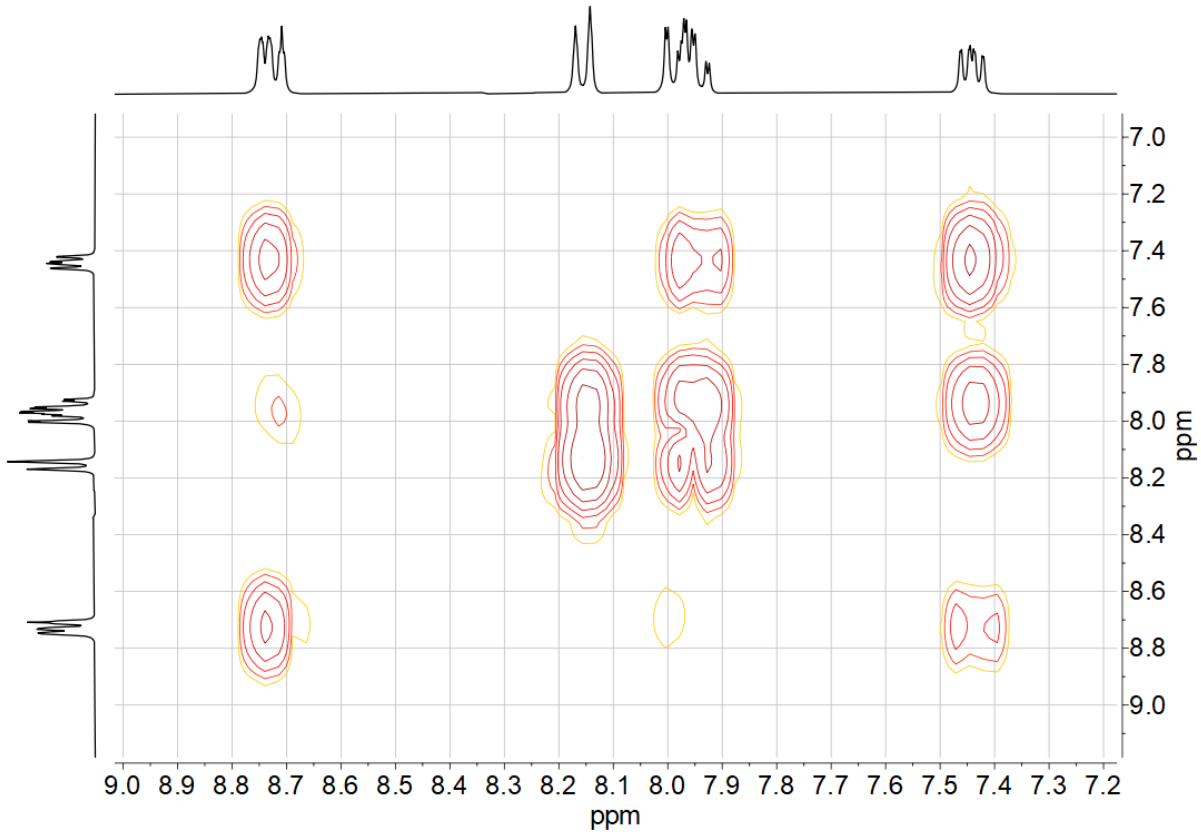

Figure 7-63 $^{1}H,H^{1}$ COSY correlation spectrum of Py(5FPhH)Py in DMSO-d_6.

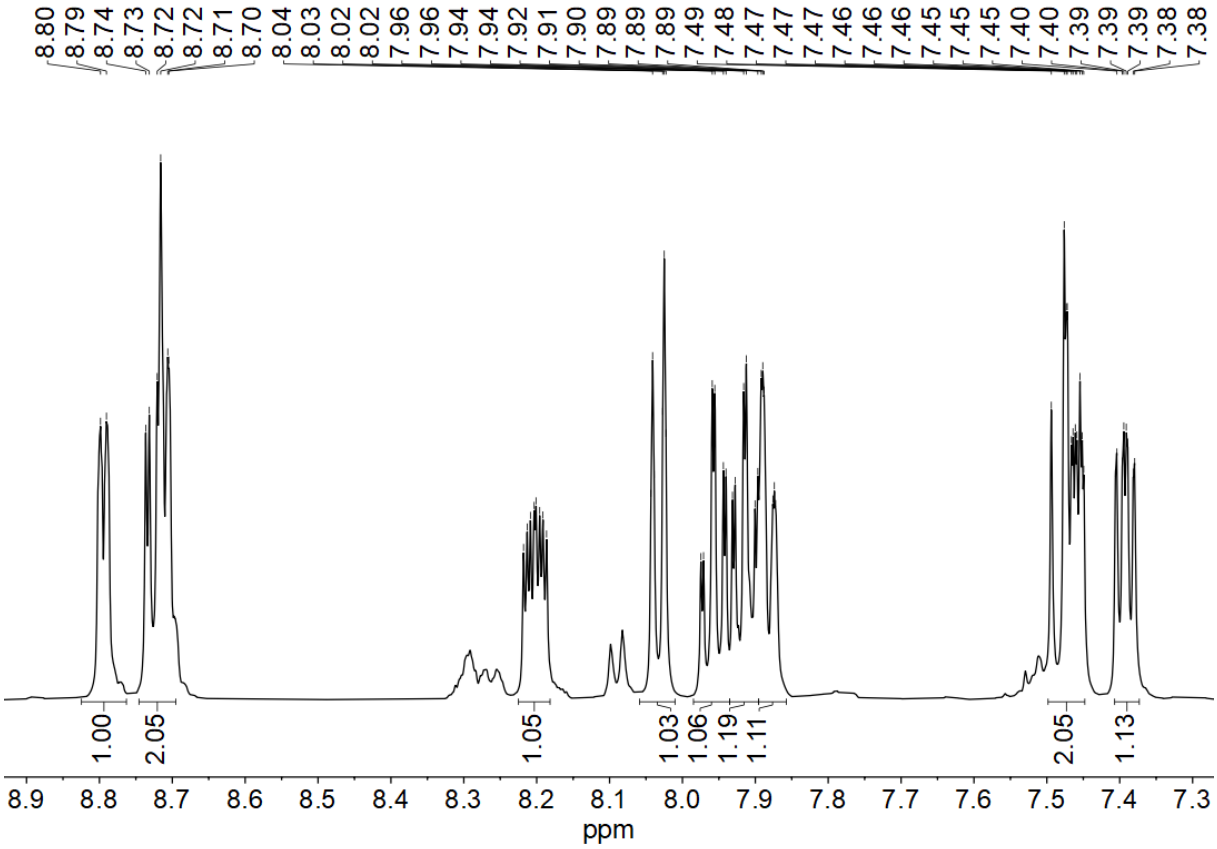

Figure 7-64 500 MHz ^{1}H NMR spectrum of Py(4FPhH)Py in DMSO-d_6.

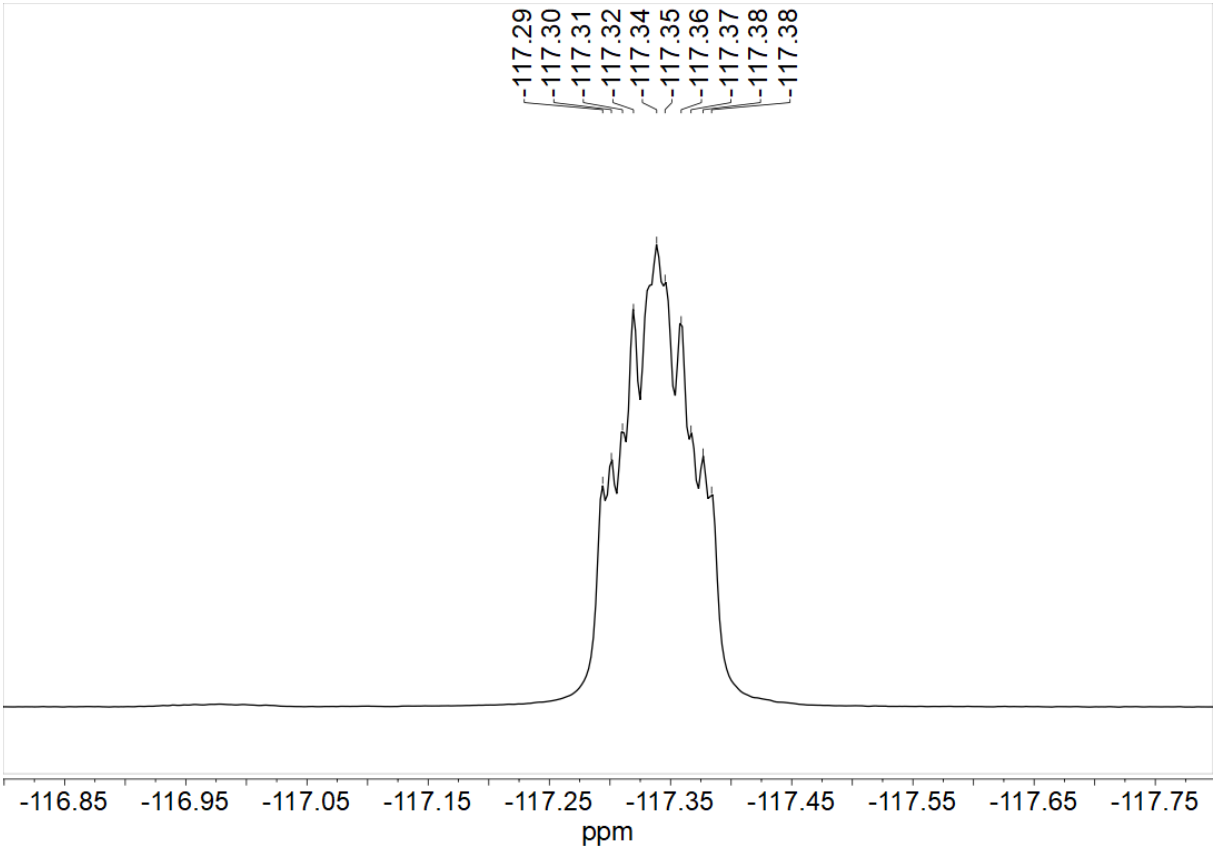

Figure 7-65 282 MHz ^{19}F NMR spectrum of Py(4FPhH)Py in DMSO-d_6.

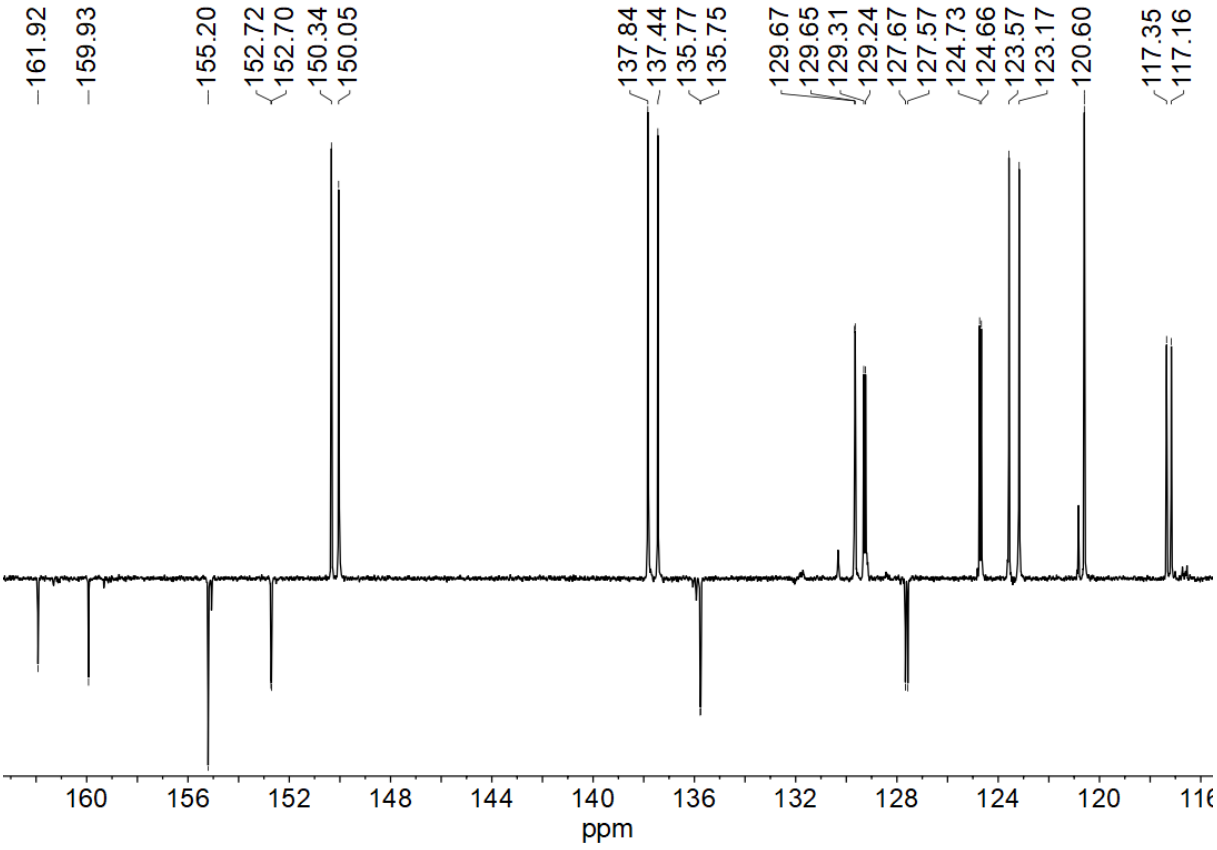

Figure 7-66 126 MHz ^{19}C NMR spectrum of Py(4FPhH)Py in DMSO-d_6.

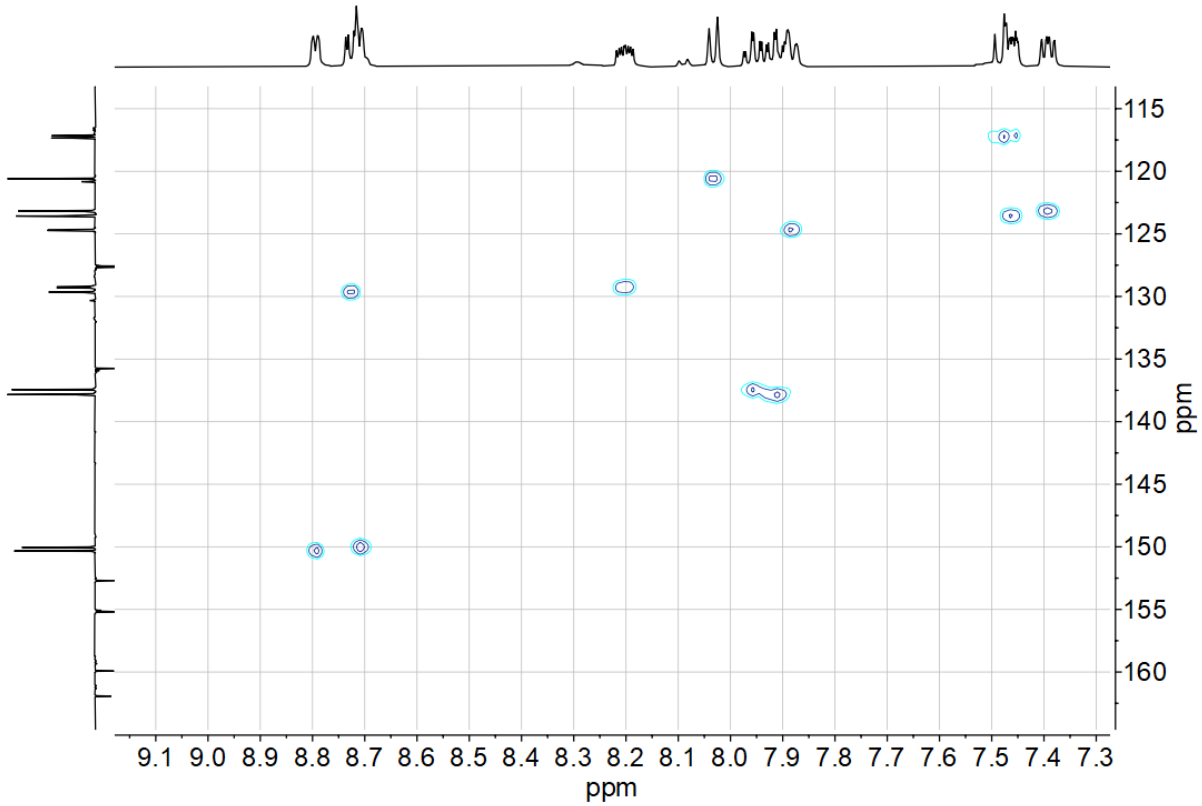

Figure 7-67 $^{1}H,^{13}C$ HSQC correlation spectrum of Py(4FPhH)Py in DMSO-d_6.

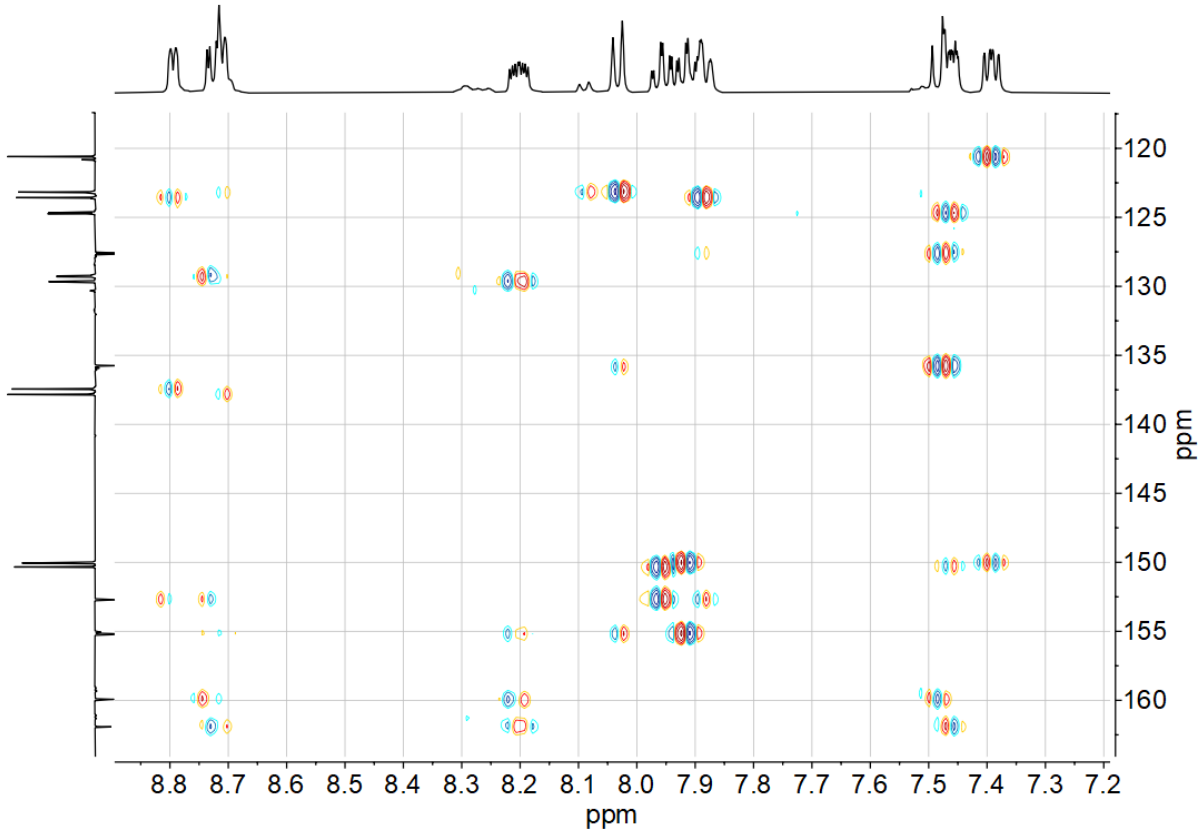

Figure 7-68 $^{1}H,^{13}C$ HMBC correlation spectrum of Py(4FPhH)Py in DMSO-d_6.

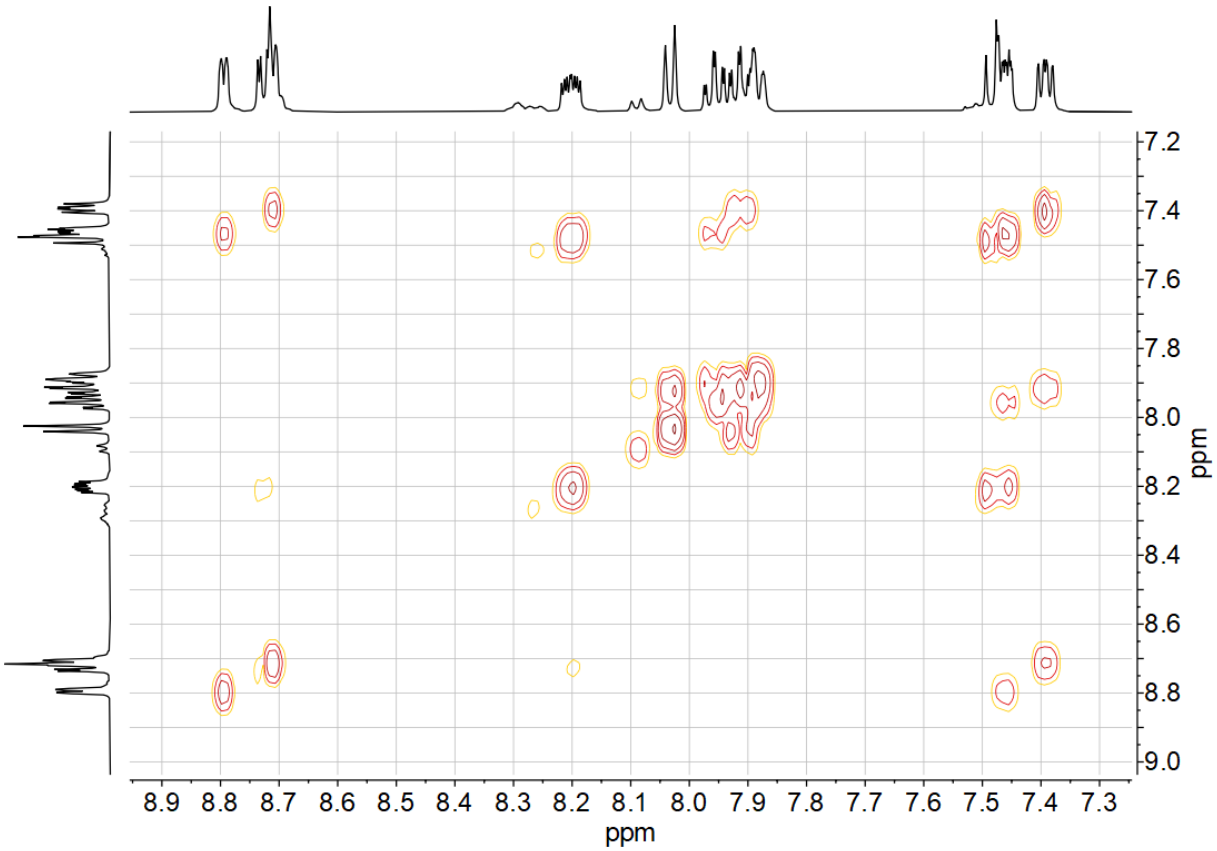

Figure 7-69 $^{1}H,H^{1}$ COSY correlation spectrum of Py(4FPhH)Py in DMSO-d_6.

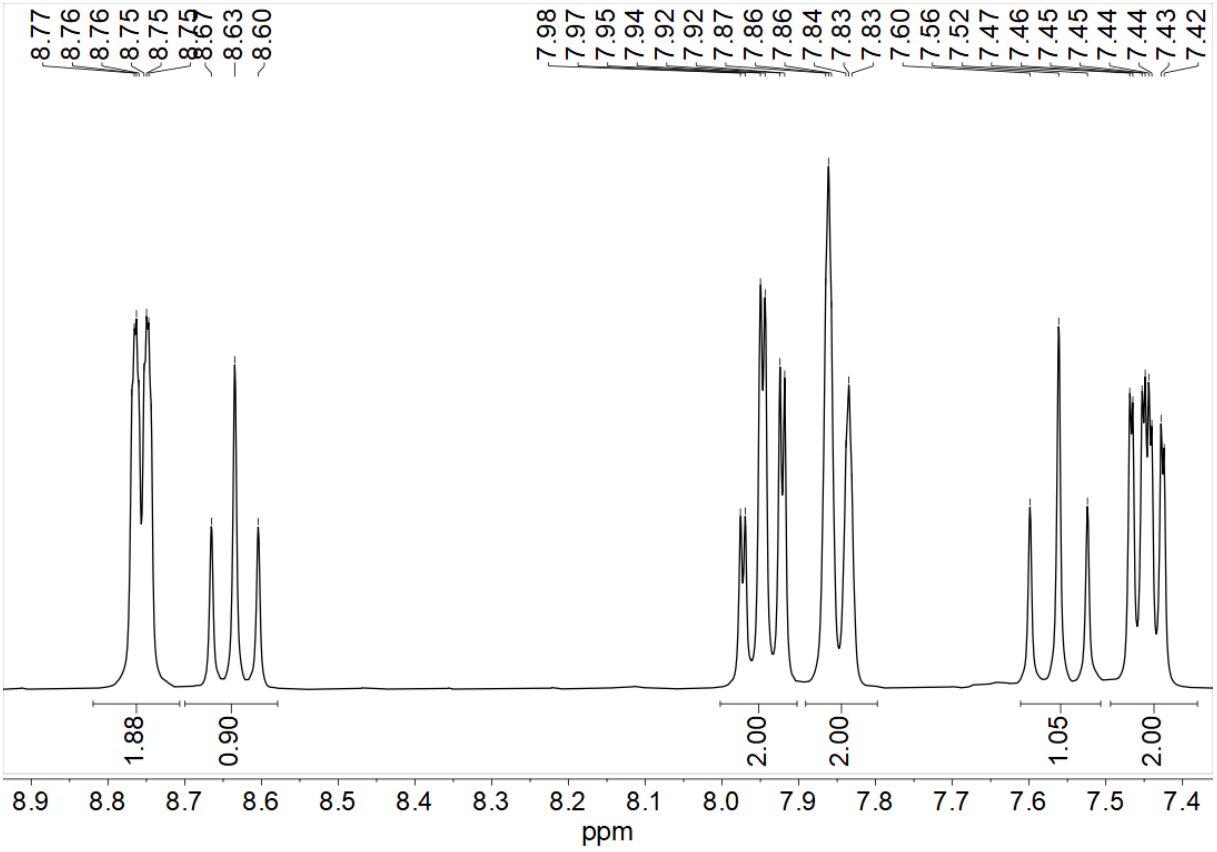

Figure 7-70 300 MHz ^{1}H NMR spectrum of Py(4,6FPhH)Py in DMSO-d_6.

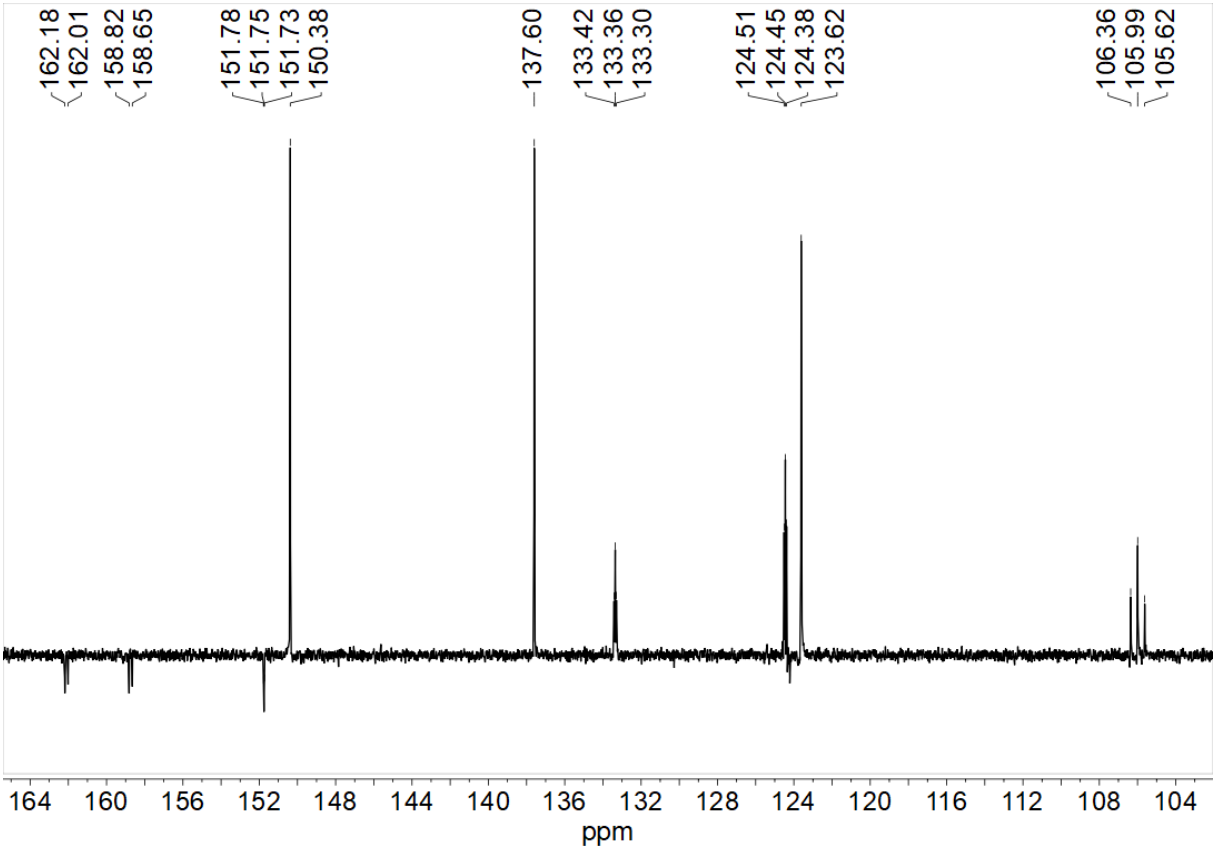

Figure 7-71 75 MHz ^{13}C NMR spectrum of Py(4,6FPhH)Py in DMSO-d_6.

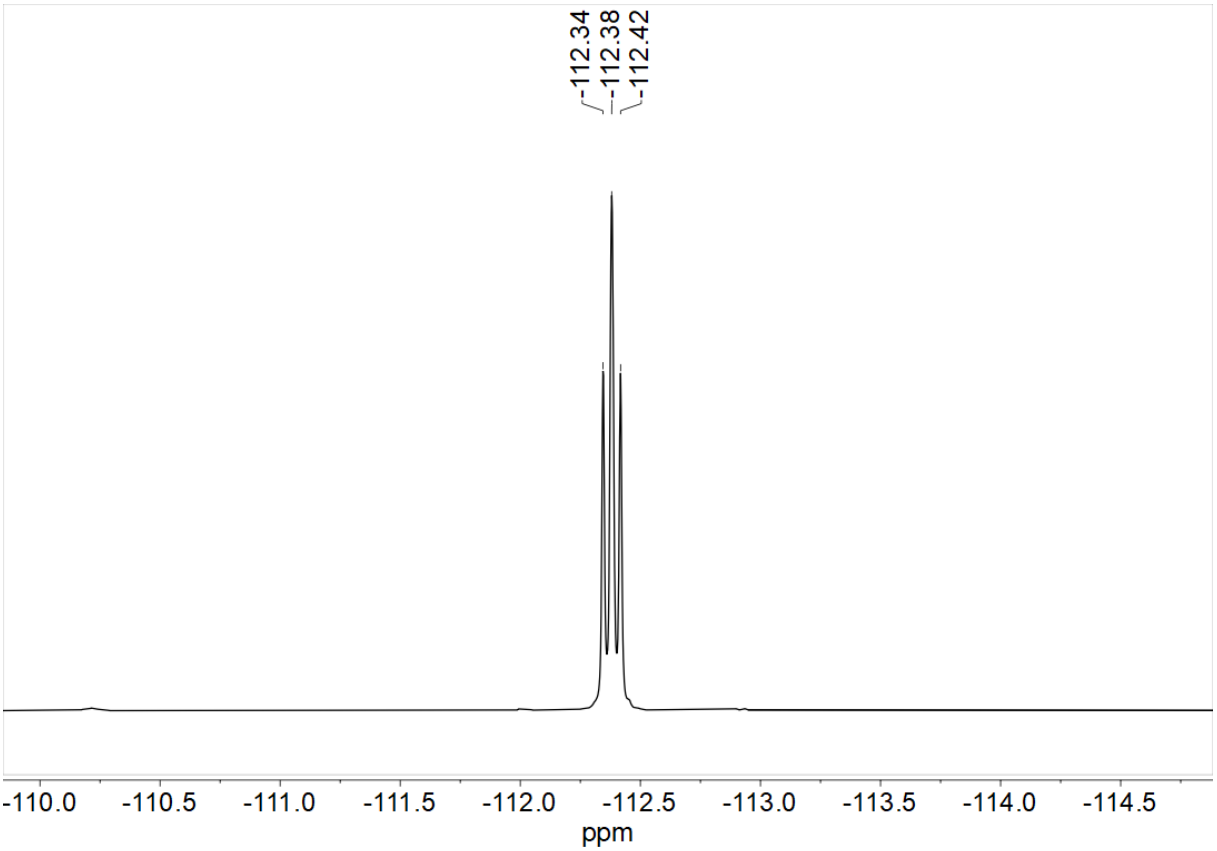

Figure 7-72 282 MHz ^{19}F NMR spectrum of Py(4,6FPhH)Py in DMSO-d_6.

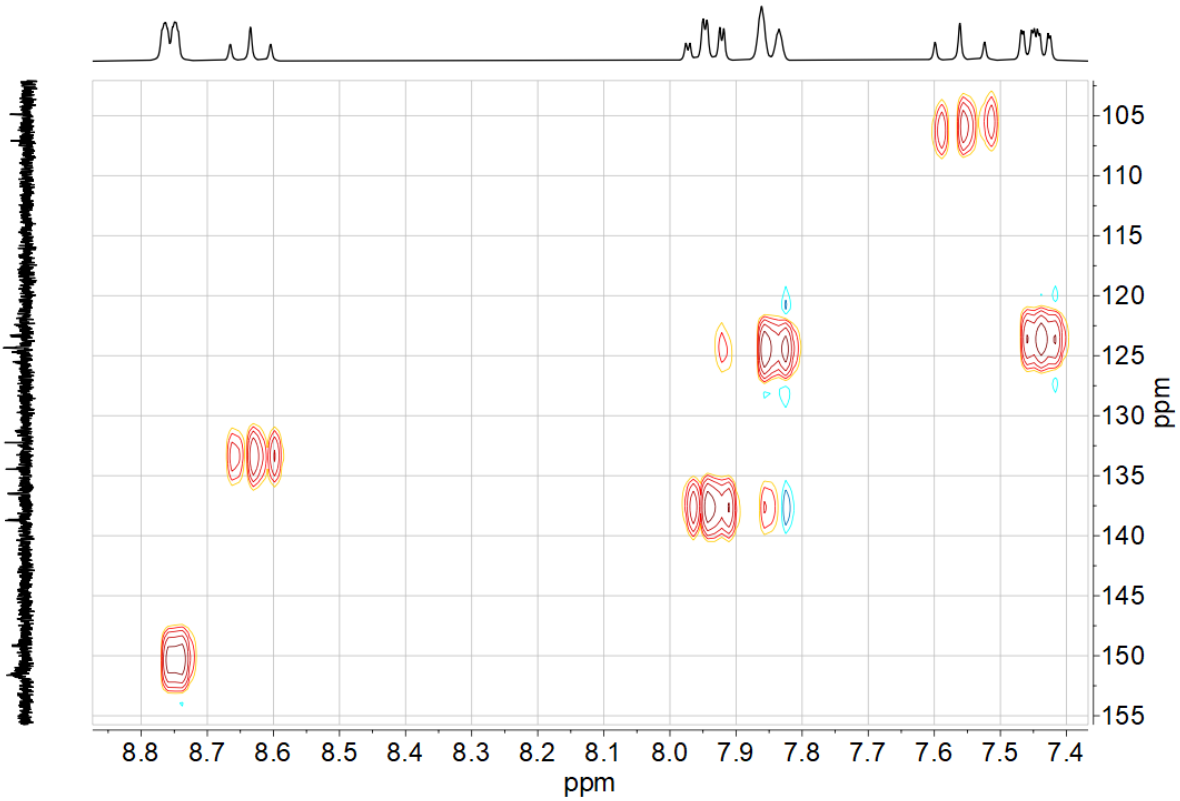

Figure 7-73 $^{1}H,^{13}C$ HSQC correlation spectrum of Py(4,6FPhH)Py in DMSO-d_6.

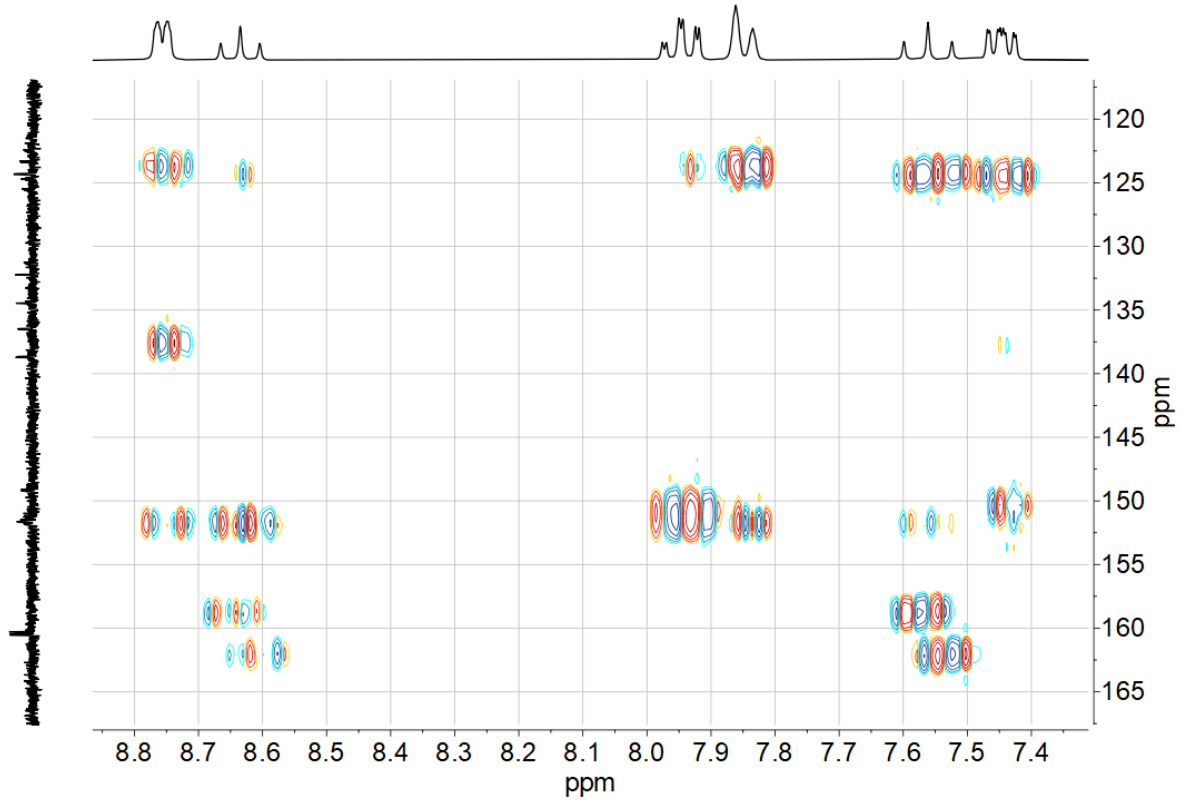

Figure 7-74 $^{1}H,^{13}C$ HMBC correlation spectrum of Py(4,6FPhH)Py in DMSO-d_6.

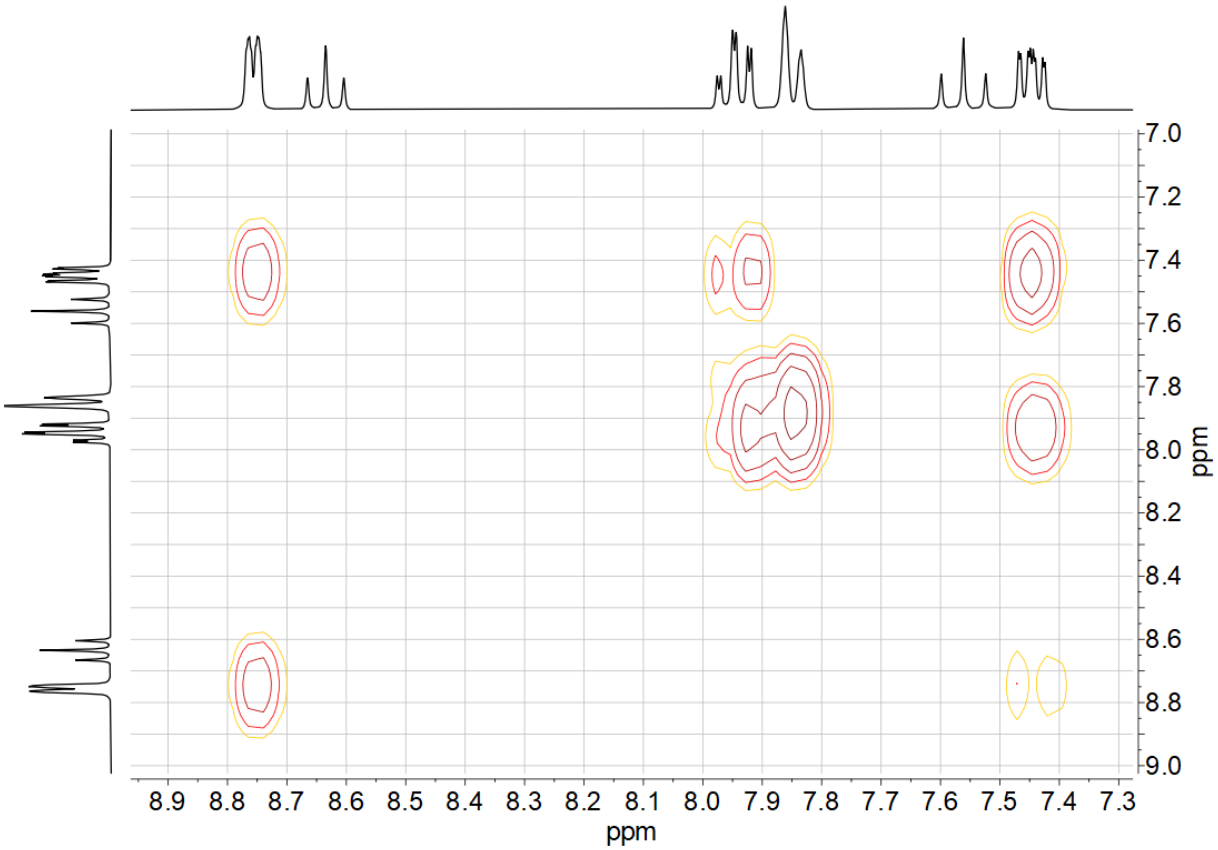

Figure 7-75 $^{1}H,H^{1}$ COSY correlation spectrum of Py(4,6FPhH)Py in DMSO-d_6.

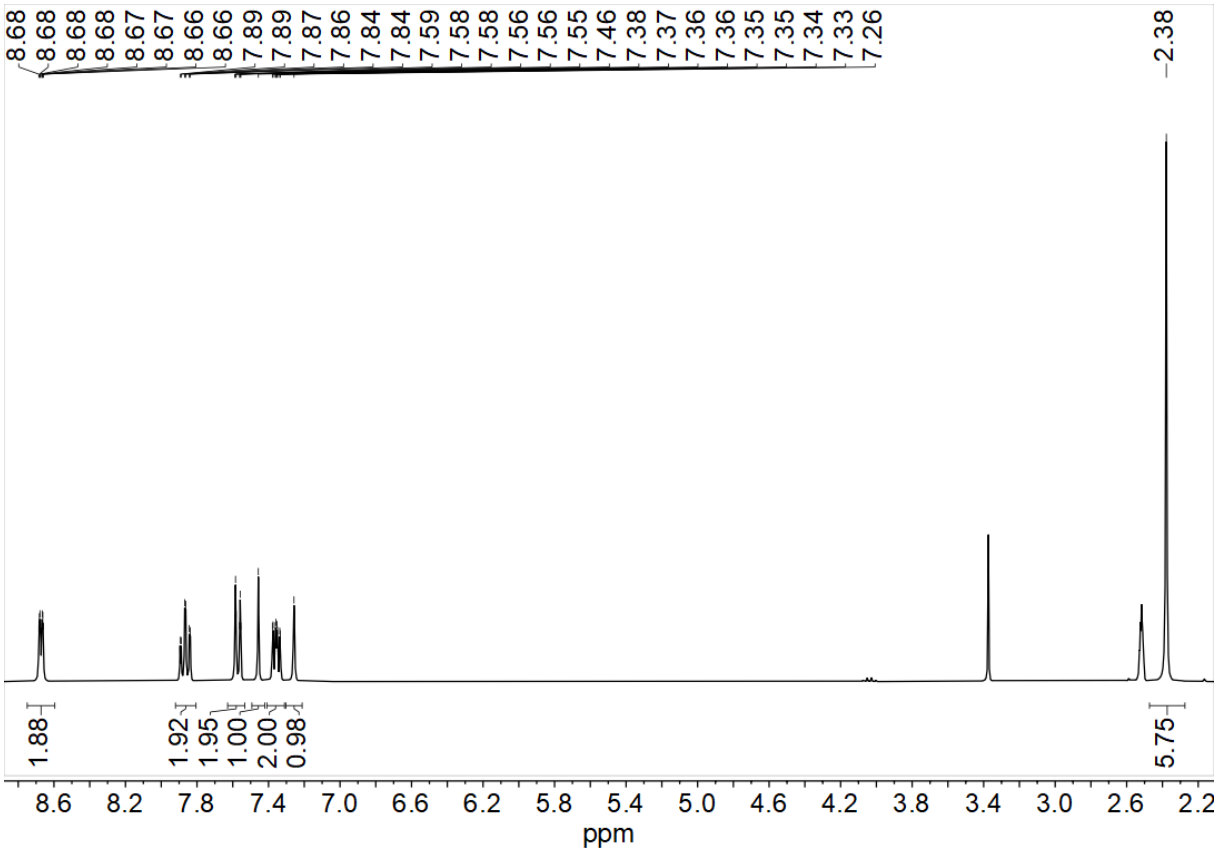

Figure 7-76 300 MHz ^{1}H NMR spectrum of Py(4,6MePhH)Py in DMSO-d_6.

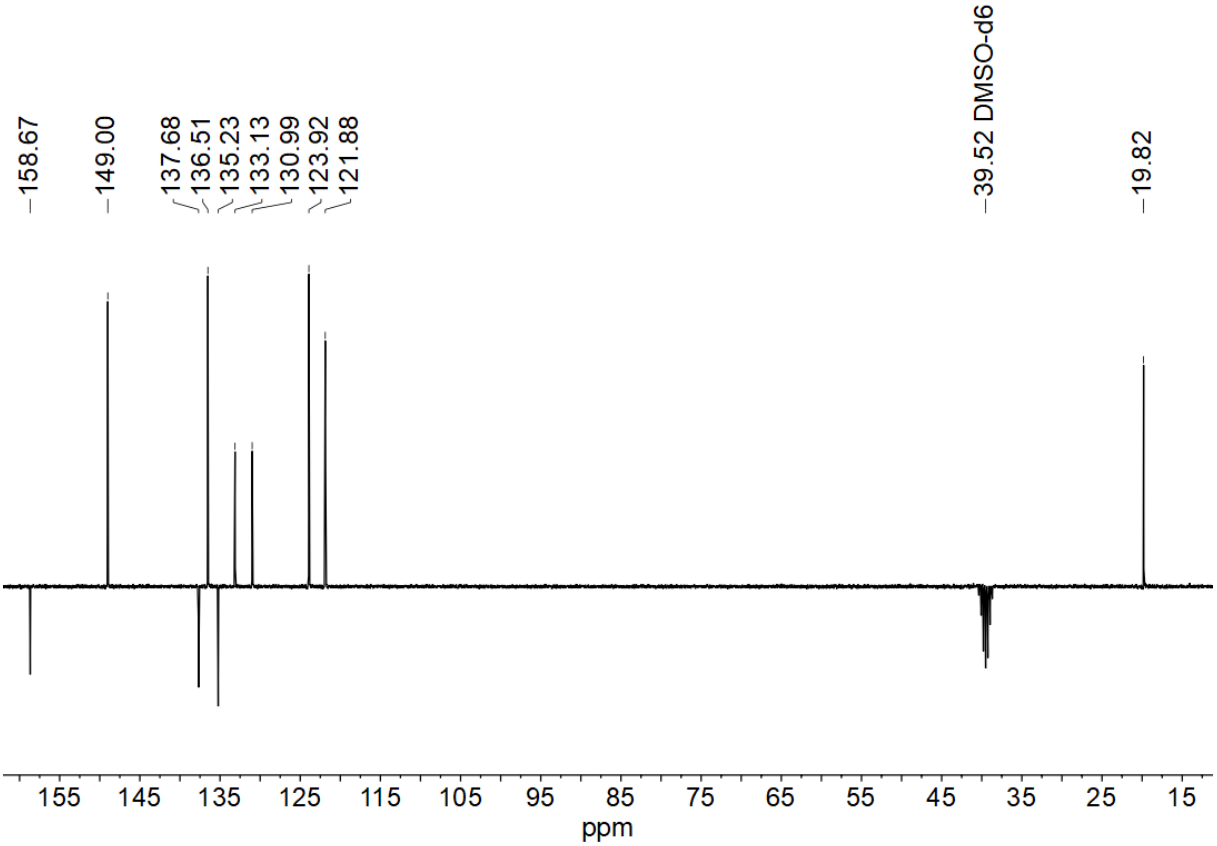

Figure 7-77 75 MHz ^{13}C NMR spectrum of Py(4,6MePhH)Py in DMSO-d_6.

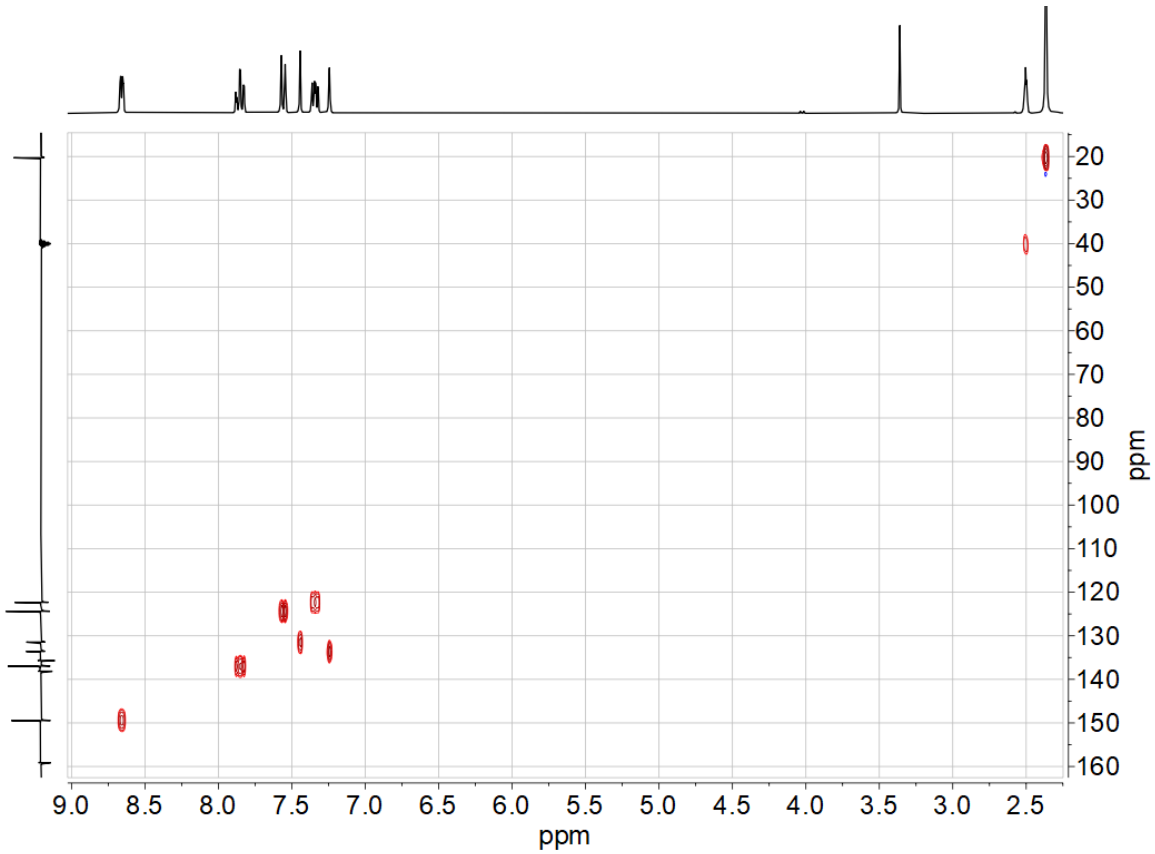

Figure 7-78 ^{1}H,^{13}C HSQC correlation spectrum of Py(4,6MePhH)Py in DMSO-d_6.

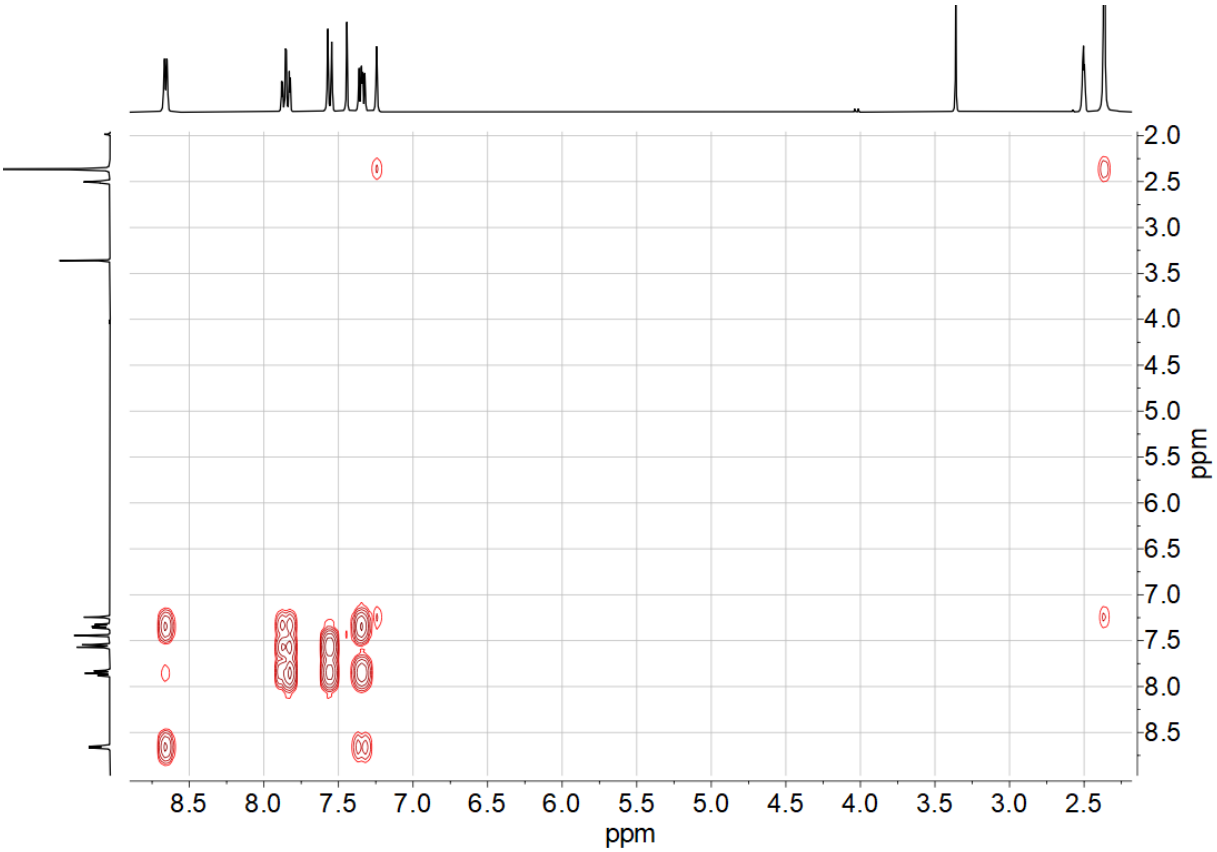

Figure 7-79 ^{1}H, ^{1}H COSY correlation spectrum of Py(4,6MePhH)Py in DMSO-d_6.

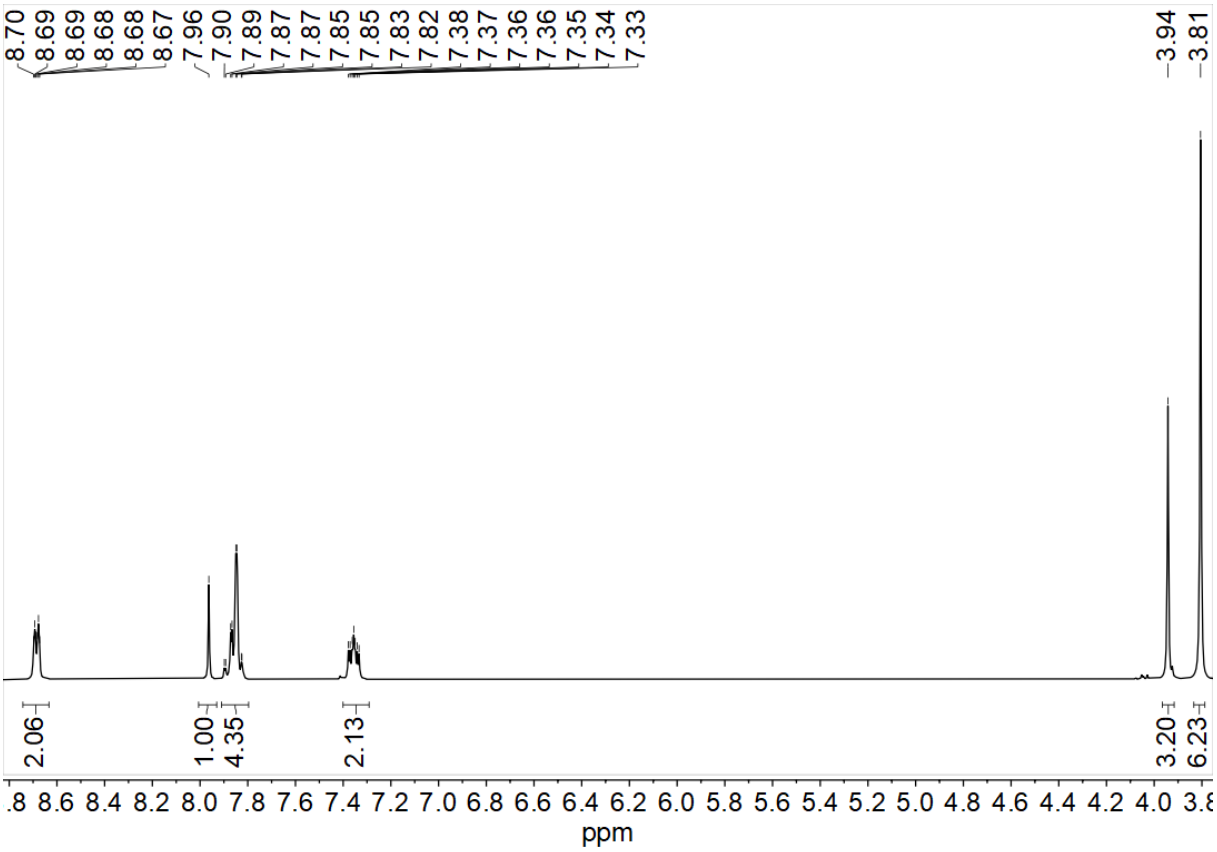

Figure 7-80 300 MHz ^{1}H NMR spectrum of Py(4,5,6MeOPhH)Py in DMSO-d_6.

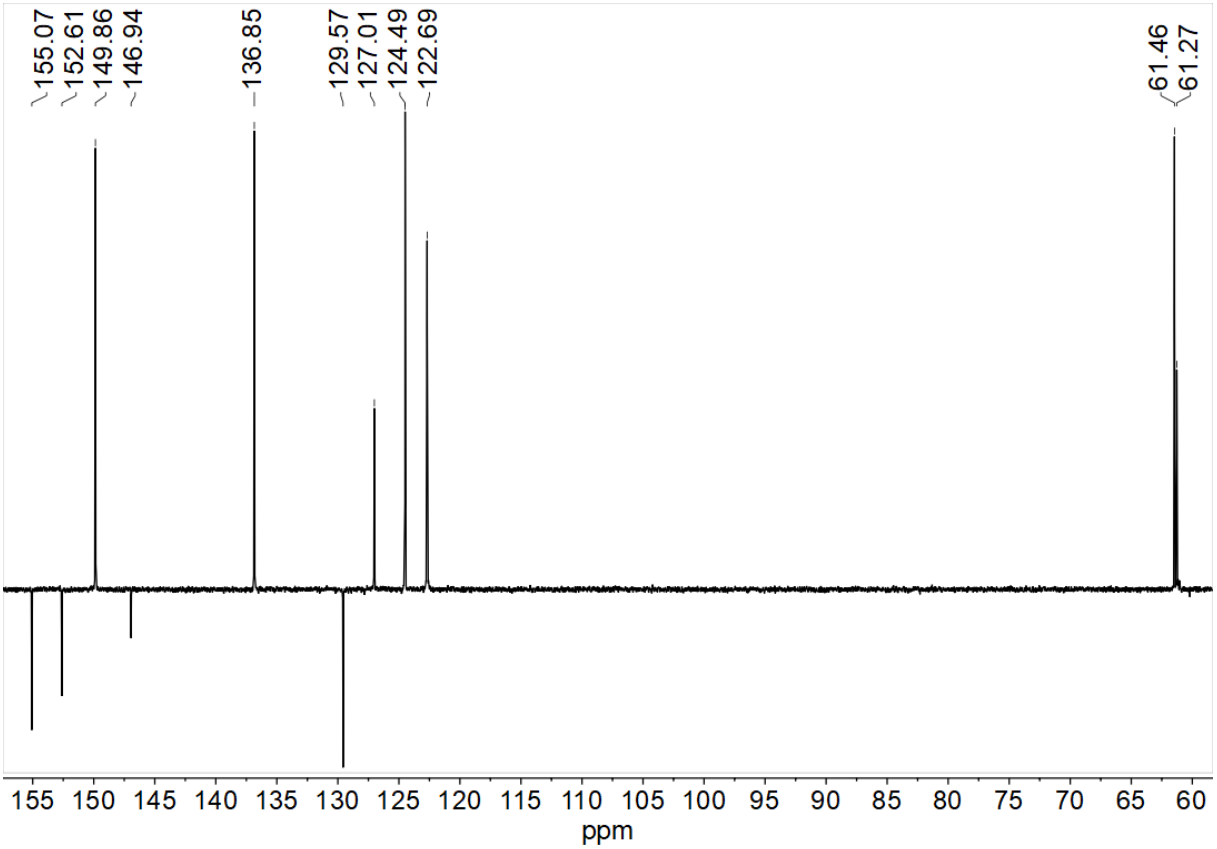

Figure 7-81 75 MHz ^{13}C NMR spectrum of Py(4,5,6MeOPhH)Py in DMSO-d_6.

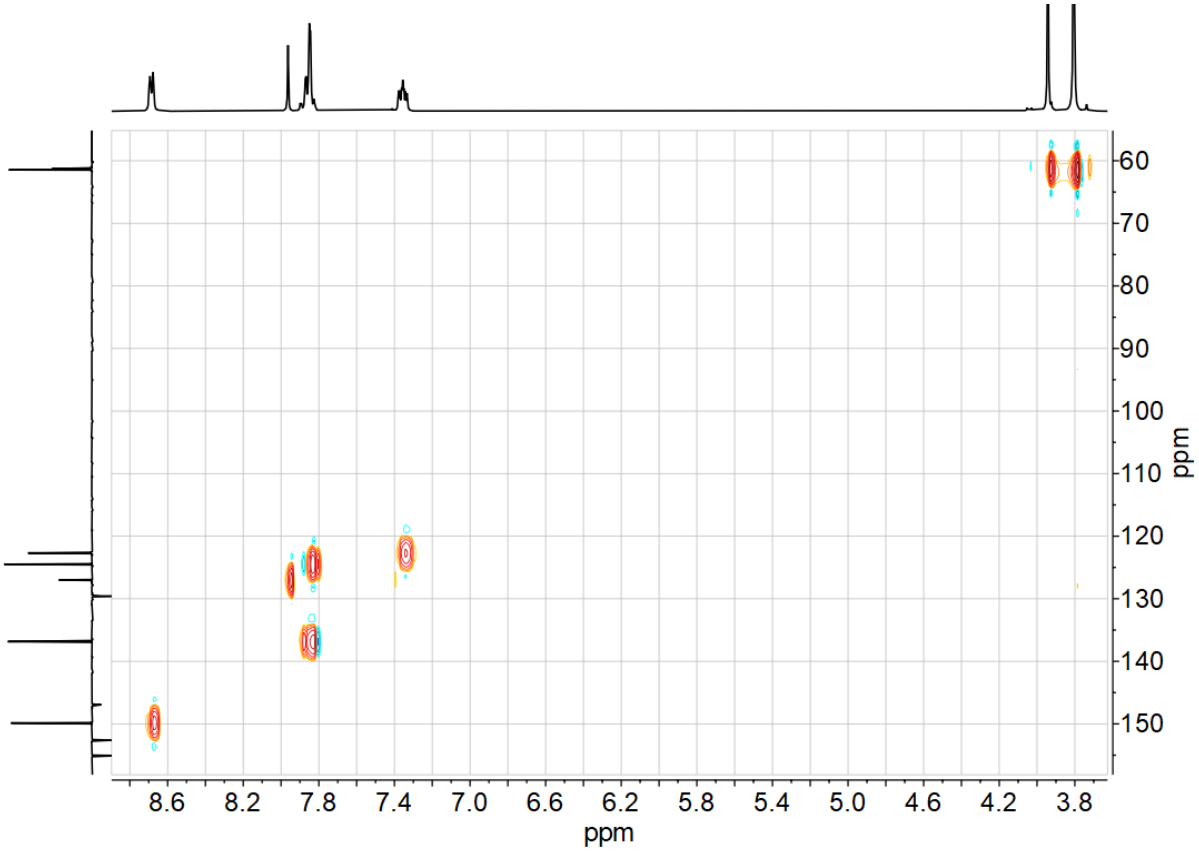

Figure 7-82 ^{1}H,^{13}C HSQC correlation spectrum of Py(4,5,6MeOPhH)Py in DMSO-d_6.

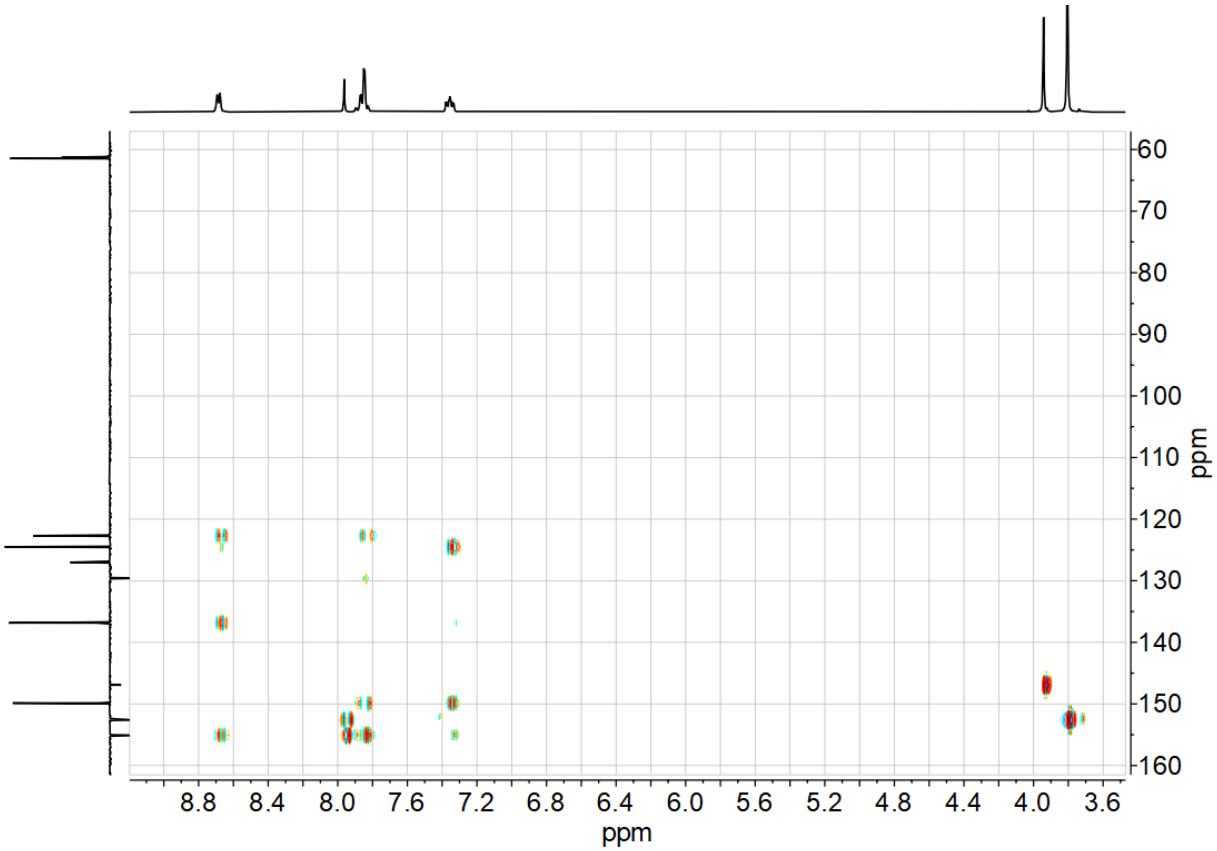

Figure 7-83 $^{1}H,^{13}C$ HMBC correlation spectrum of Py(4,5,6MeOPhH)Py in DMSO-d_6.

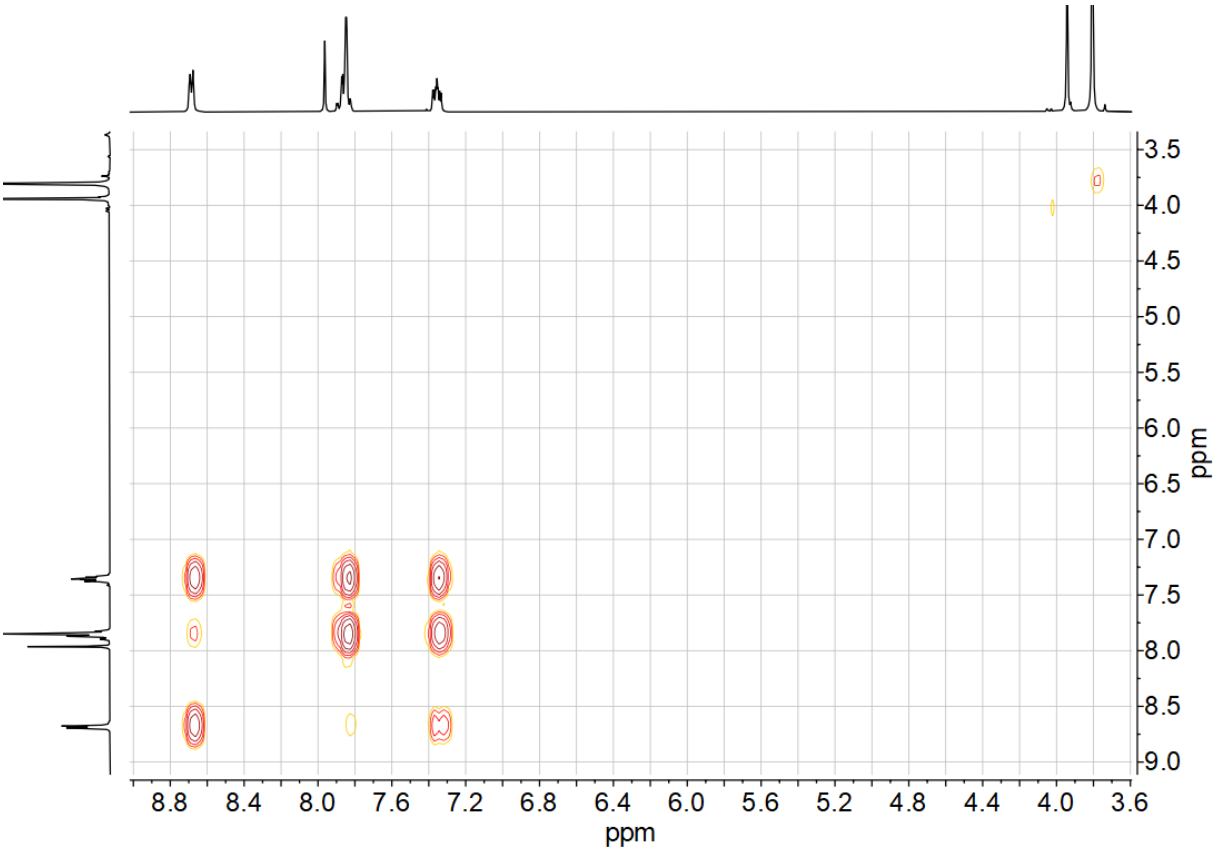

Figure 7-84 $^{1}H,^{1}H$ COSY correlation spectrum of Py(4,5,6MeOPhH)Py in DMSO-d_6.

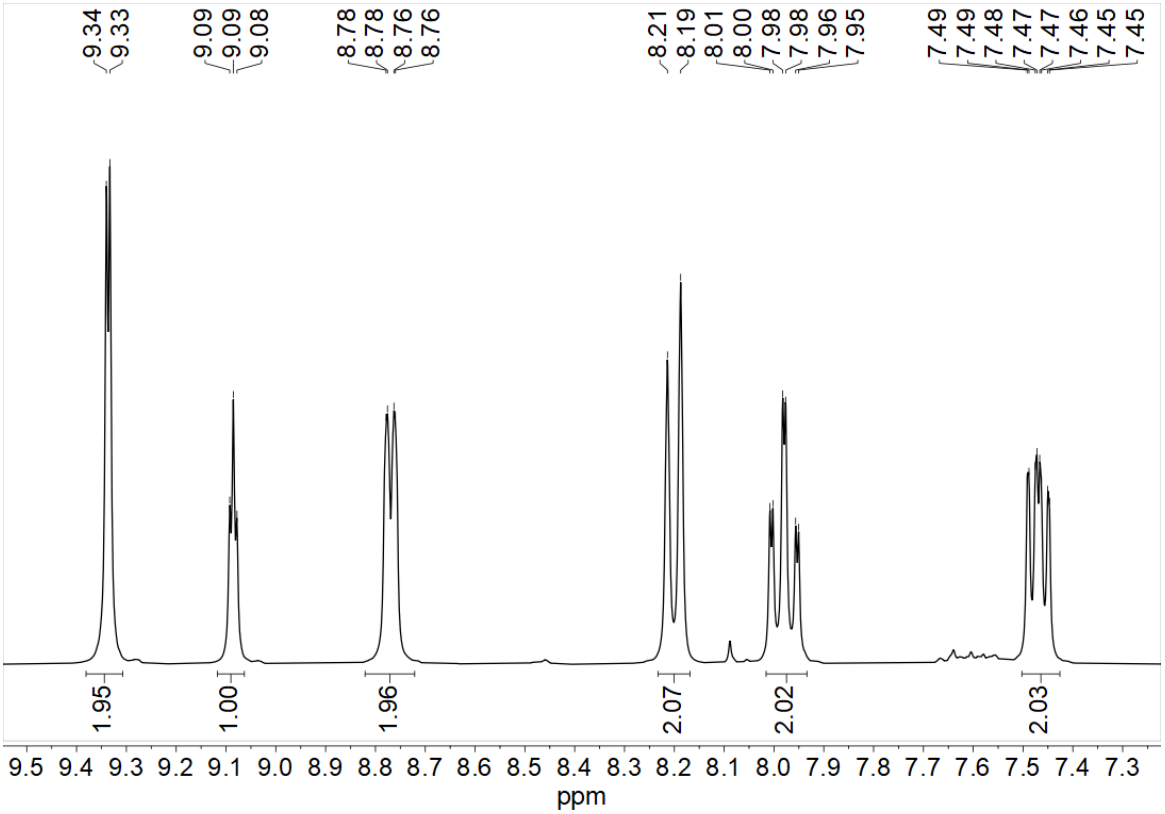

Figure 7-85 300 MHz ^{1}H NMR spectrum of Py(PyH)Py in DMSO-d_6.

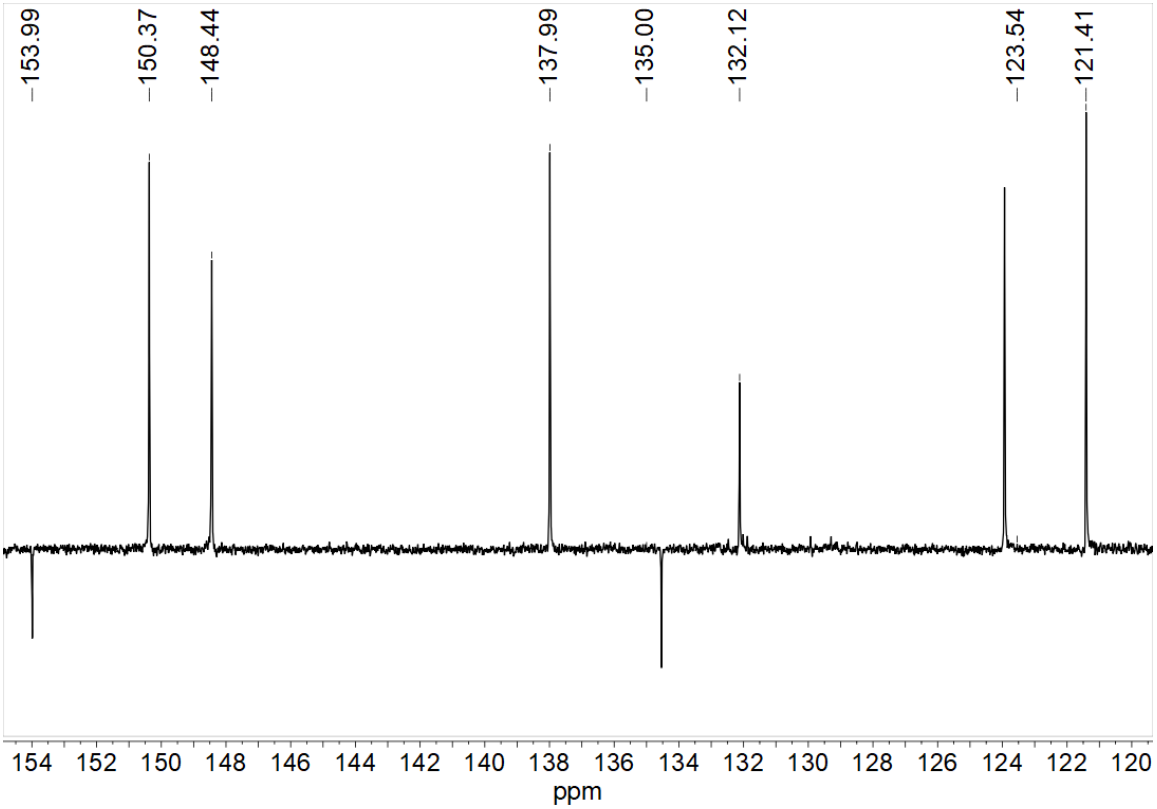

Figure 7-86 75 MHz ^{13}C NMR spectrum of Py(PyH)Py in DMSO-d_6.

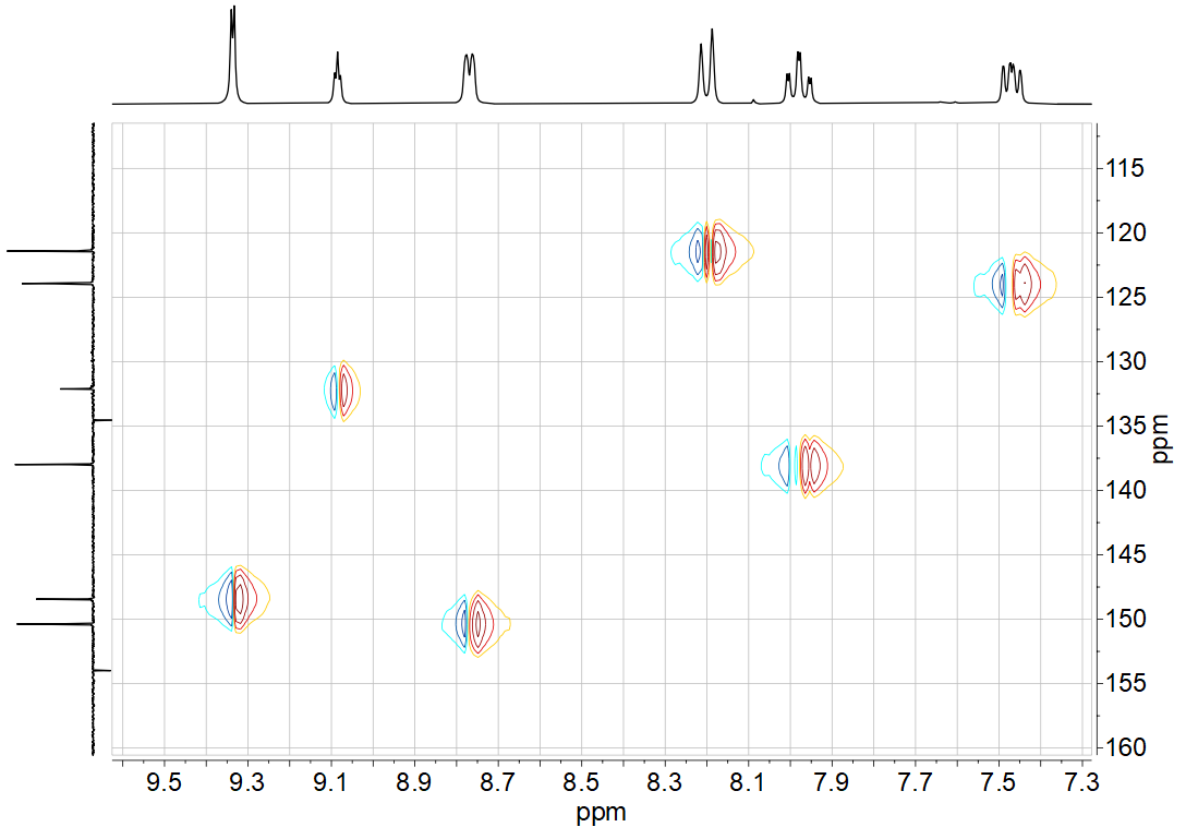

Figure 7-87 $^{1}H,^{13}C$ HSQC correlation spectrum of Py(PyH)Py in DMSO-d_6.

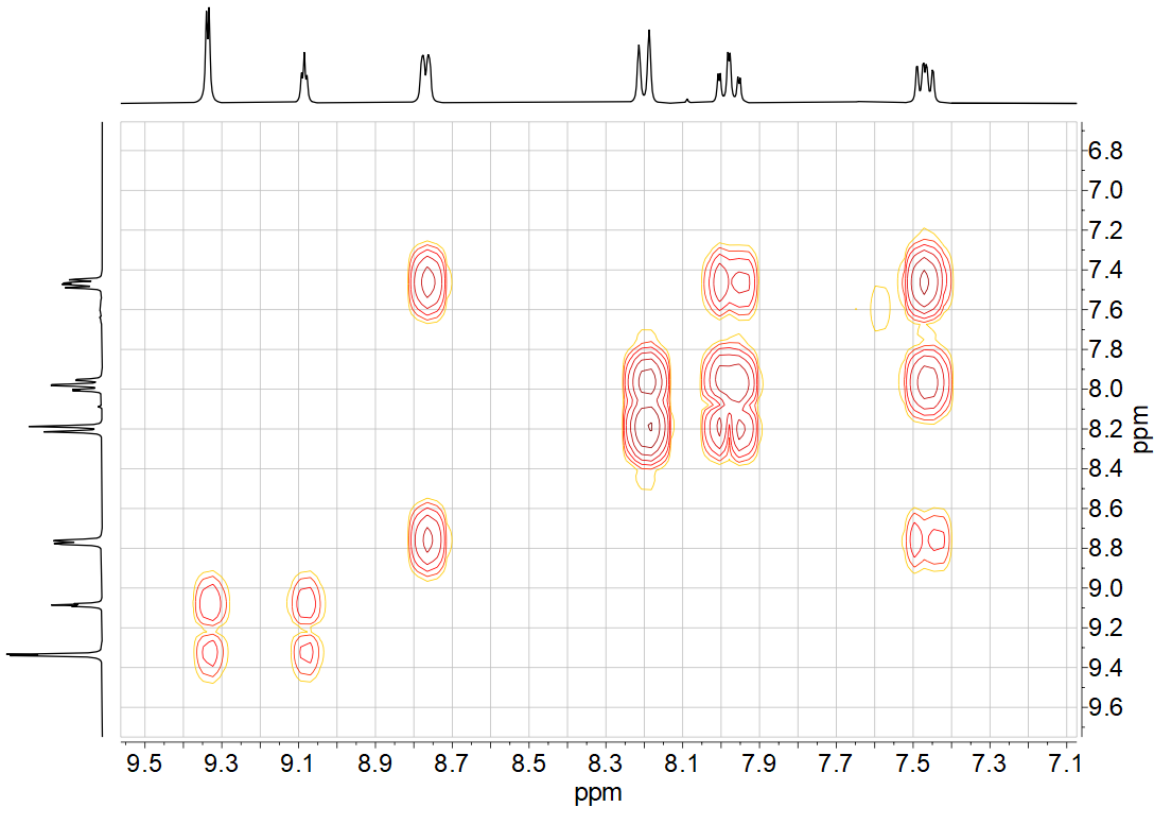

Figure 7-88 $^{1}H,^{1}H$ COSY correlation spectrum of Py(PyH)Py in DMSO-d_6.

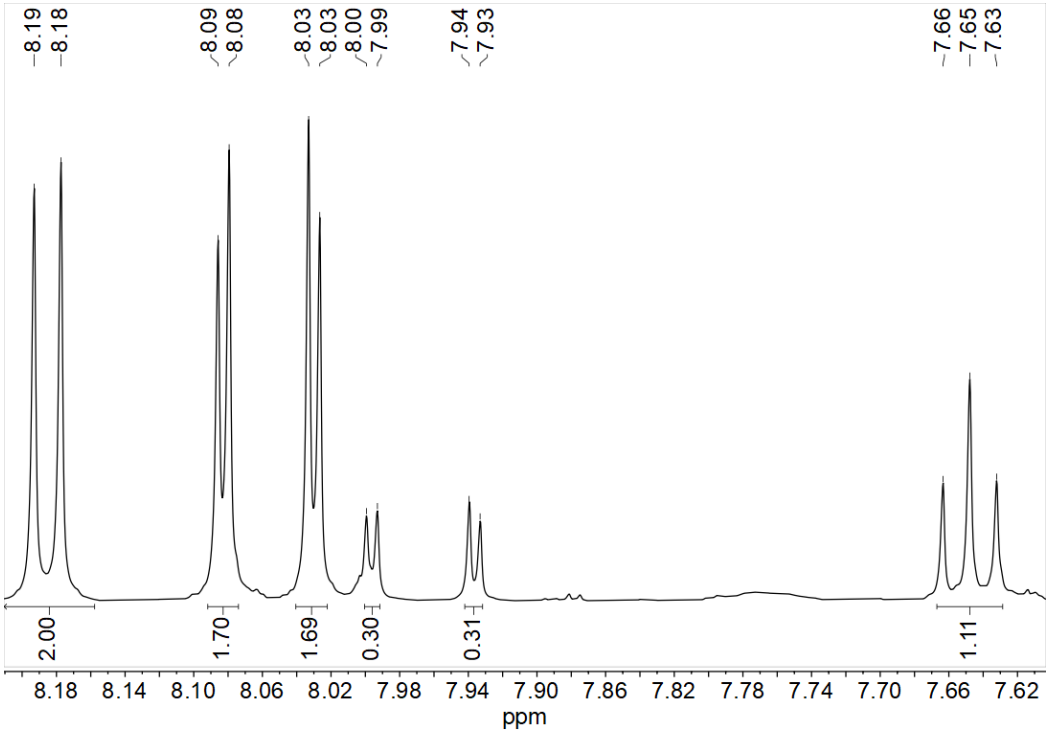

Figure 7-89 500 MHz ^{1}H NMR spectrum of 2Tz(PhCl)2Tz in DMSO-d_6.

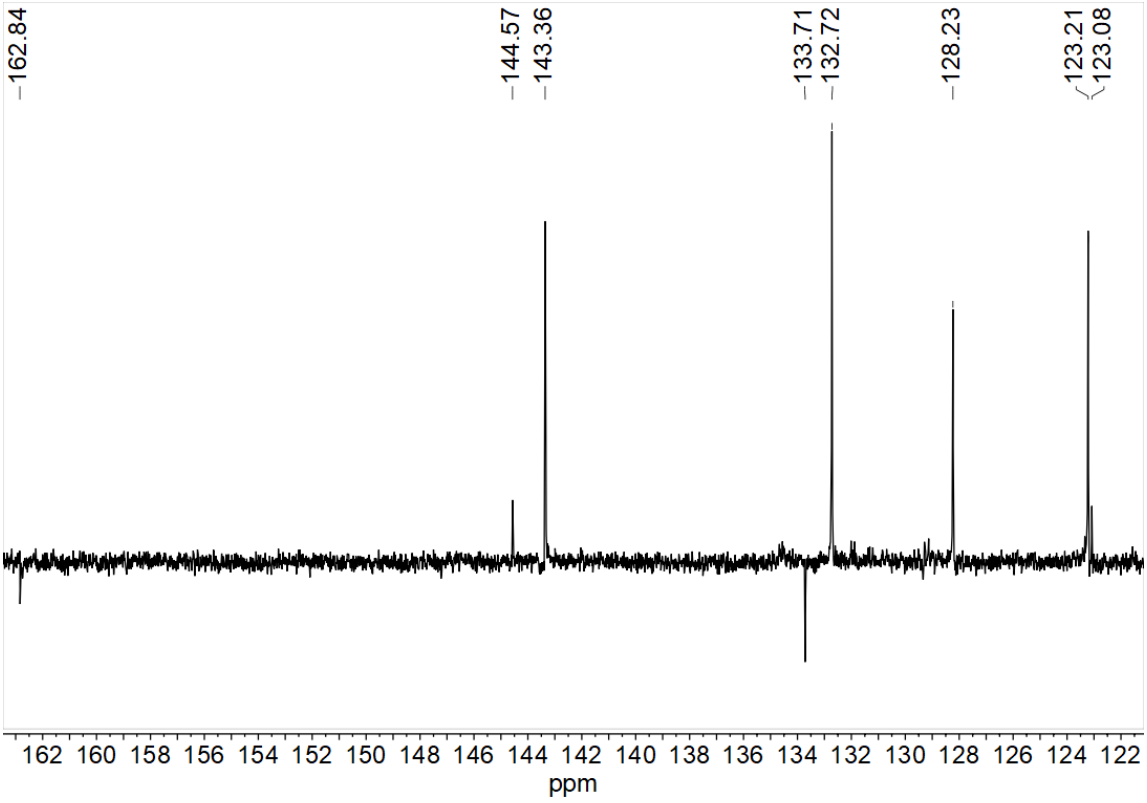

Figure 7-90 75 MHz ^{13}C NMR spectrum of 2Tz(PhCl)2Tz in DMSO-d_6.

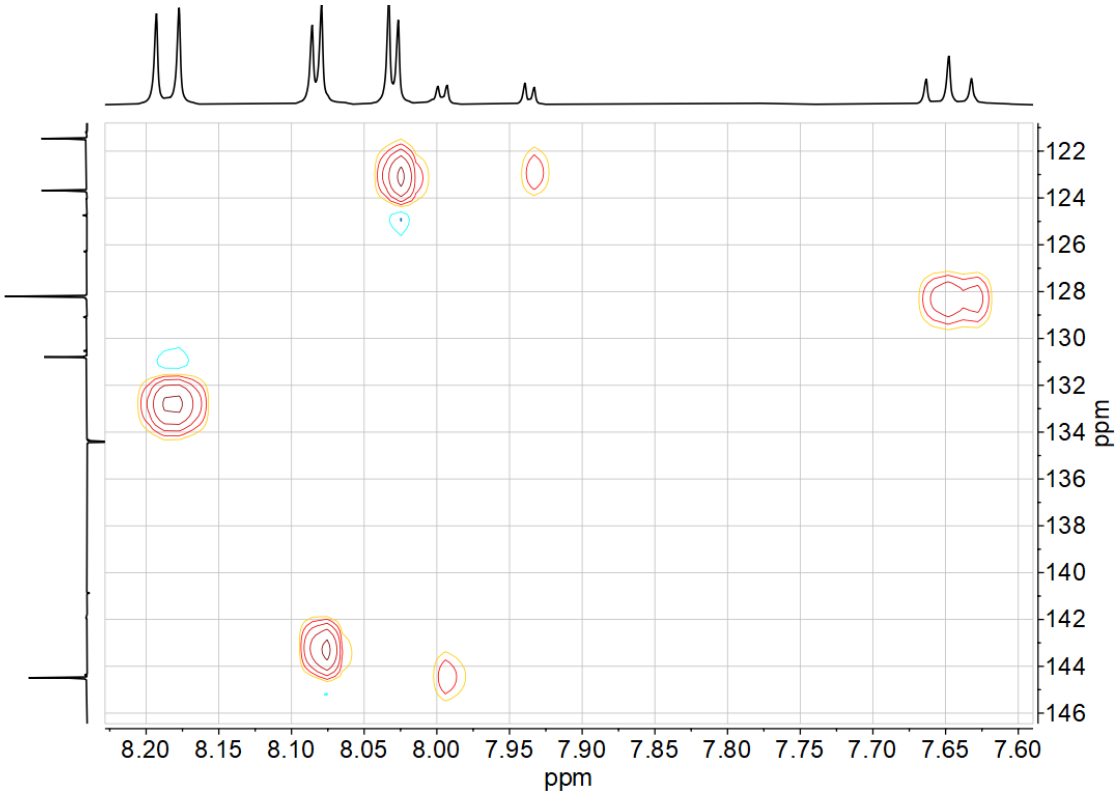

Figure 7-91 $^{1}H,^{13}C$ HSQC correlation spectrum of 2Tz(PhCl)2Tz in DMSO-d_6.

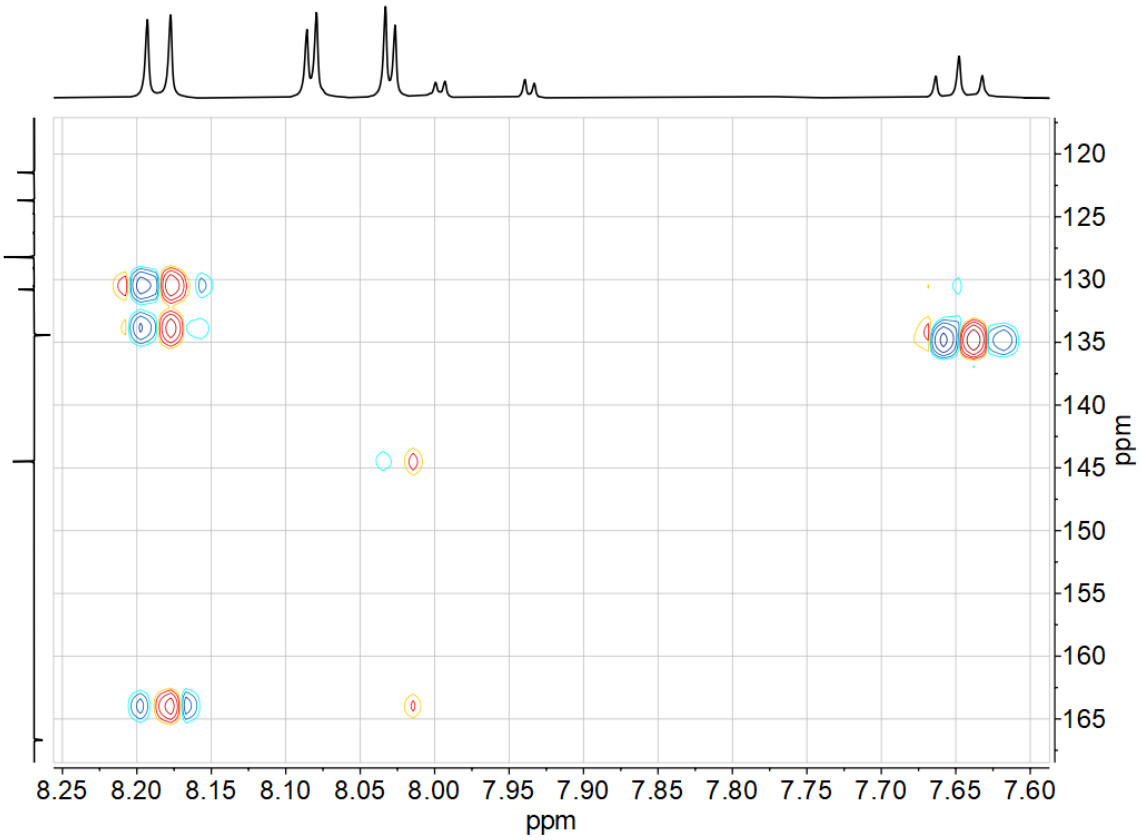

Figure 7-92 $^{1}H,^{13}C$ HMBC correlation spectrum of 2Tz(PhCl)2Tz in DMSO-d_6.

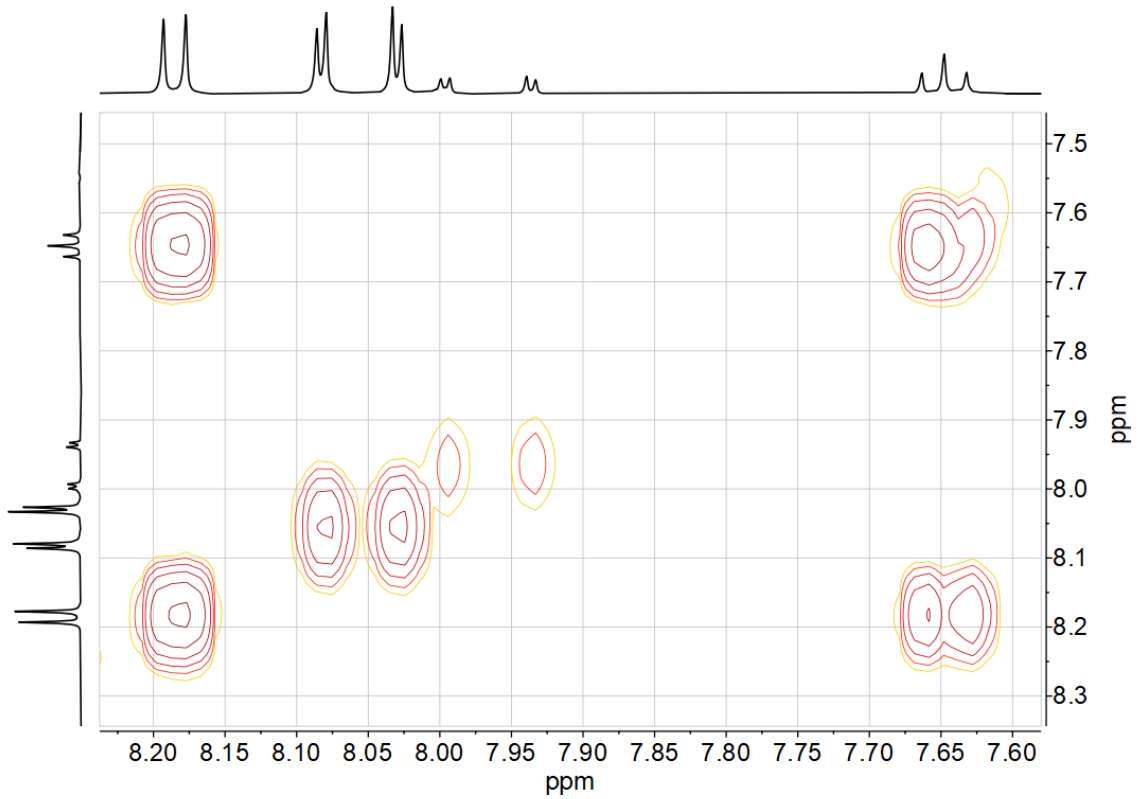

Figure 7-93 ^{1}H,^{1}H COSY correlation spectrum of 2Tz(PhCl)2Tz in DMSO-d_6.

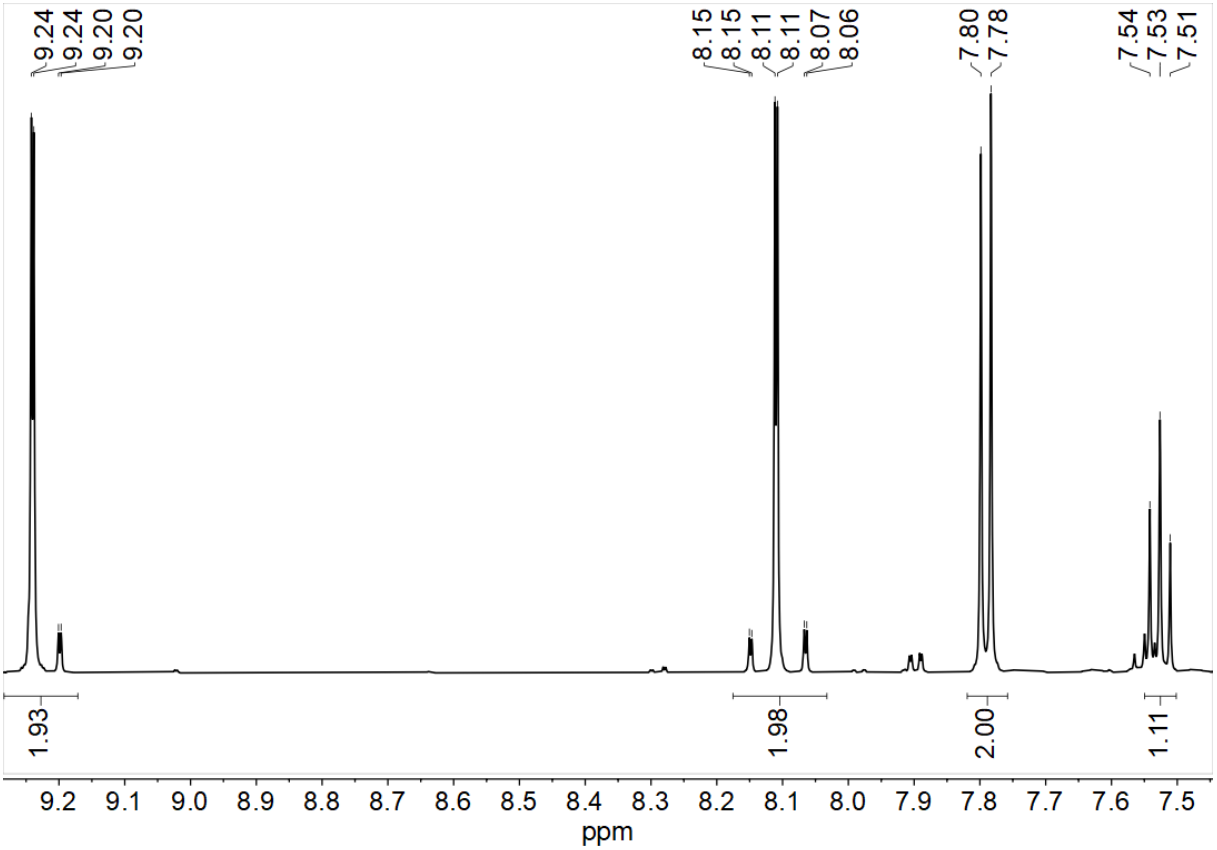

Figure 7-94 500 MHz ^{1}H NMR spectrum of 4Tz(PhCl)4Tz in DMSO-d_6.

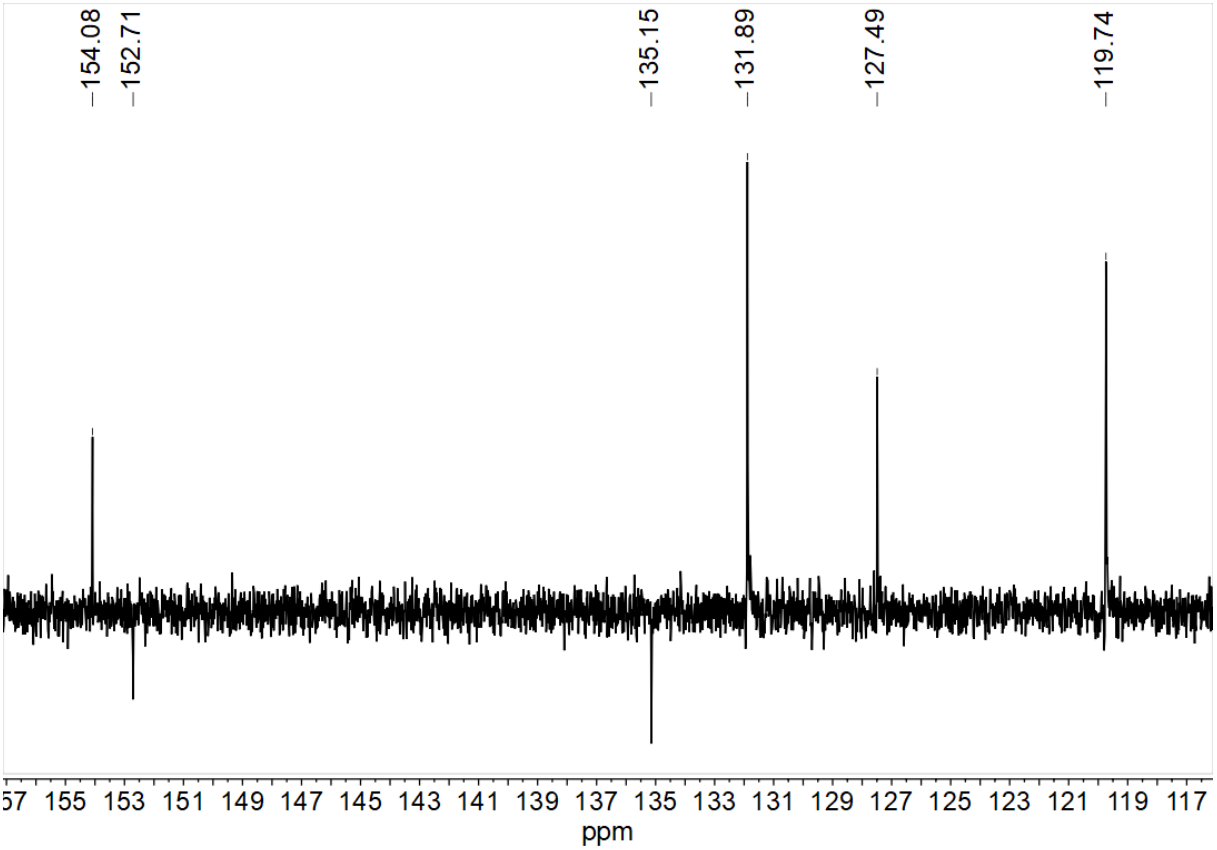

Figure 7-95 75 MHz ^{13}C NMR spectrum of 4Tz(PhCl)4Tz in DMSO-d_6.

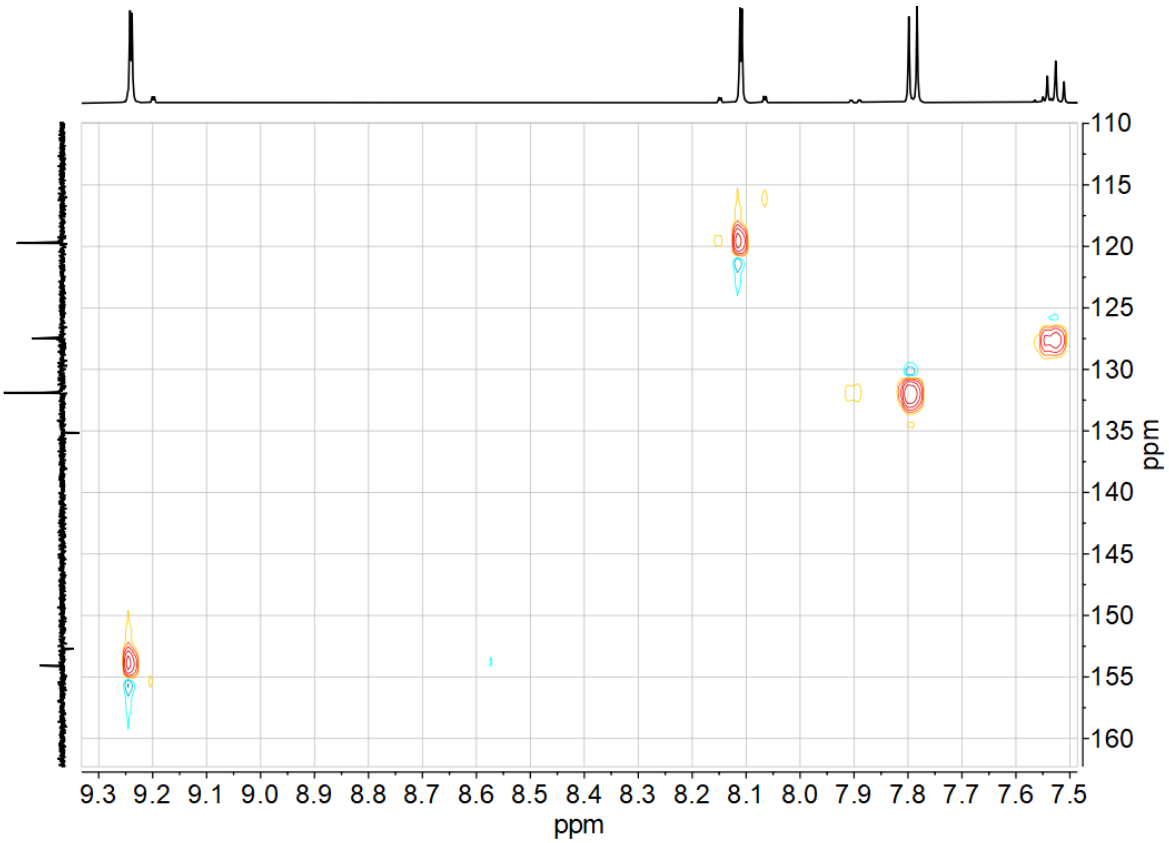

Figure 7-96 ^{1}H,^{13}C HSQC correlation spectrum of 4Tz(PhCl)4Tz in DMSO-d_6.

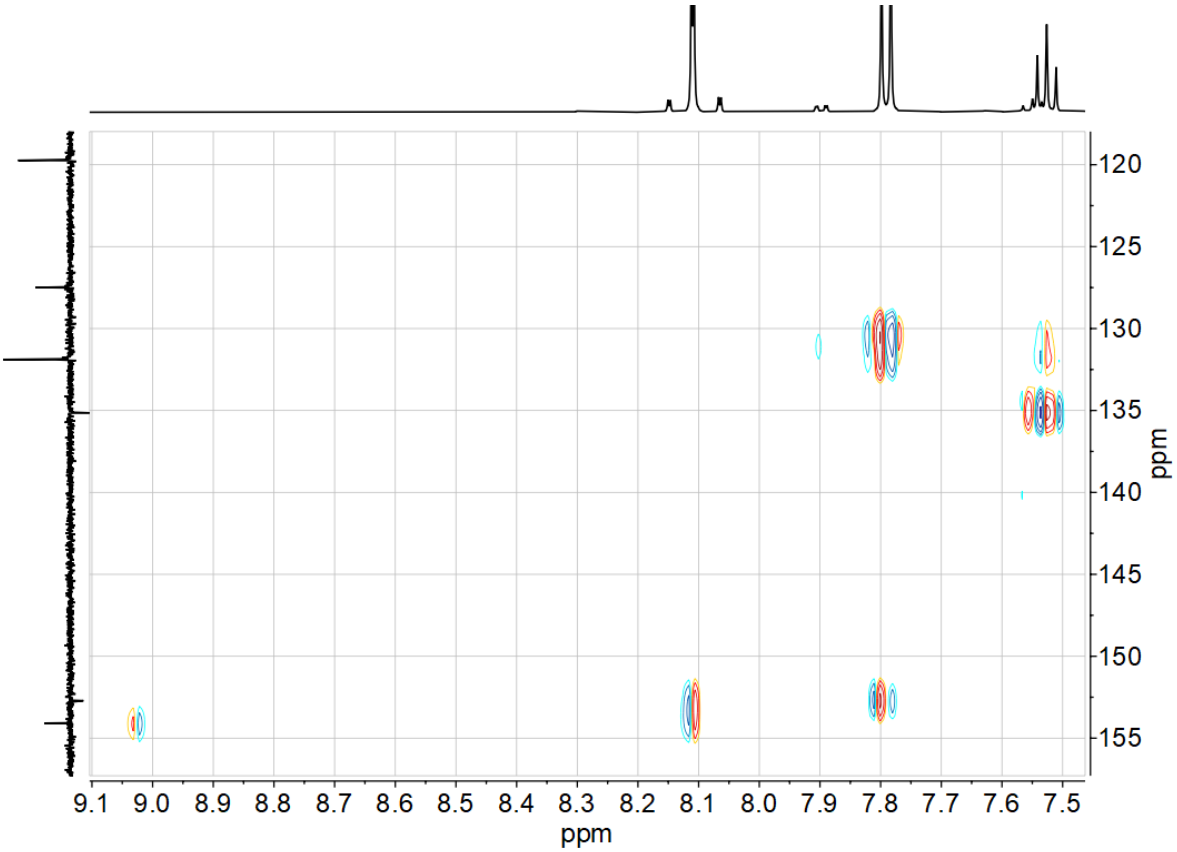

Figure 7-97 $^{1}H,^{13}C$ HMBC correlation spectrum of 4Tz(PhCl)4Tz in DMSO-d_6.

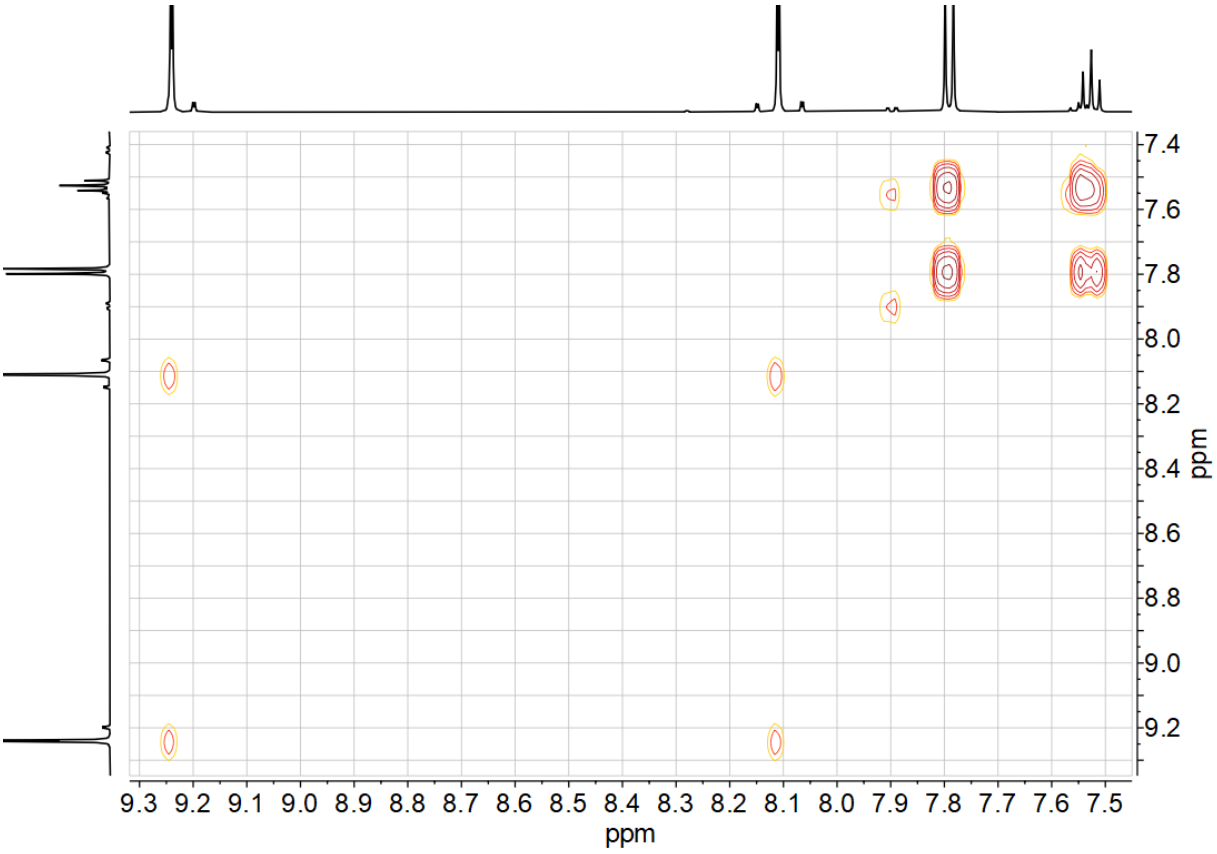

Figure 7-98 $^{1}H,^{1}H$ COSY correlation spectrum of 4Tz(PhCl)4Tz in DMSO-d_6.

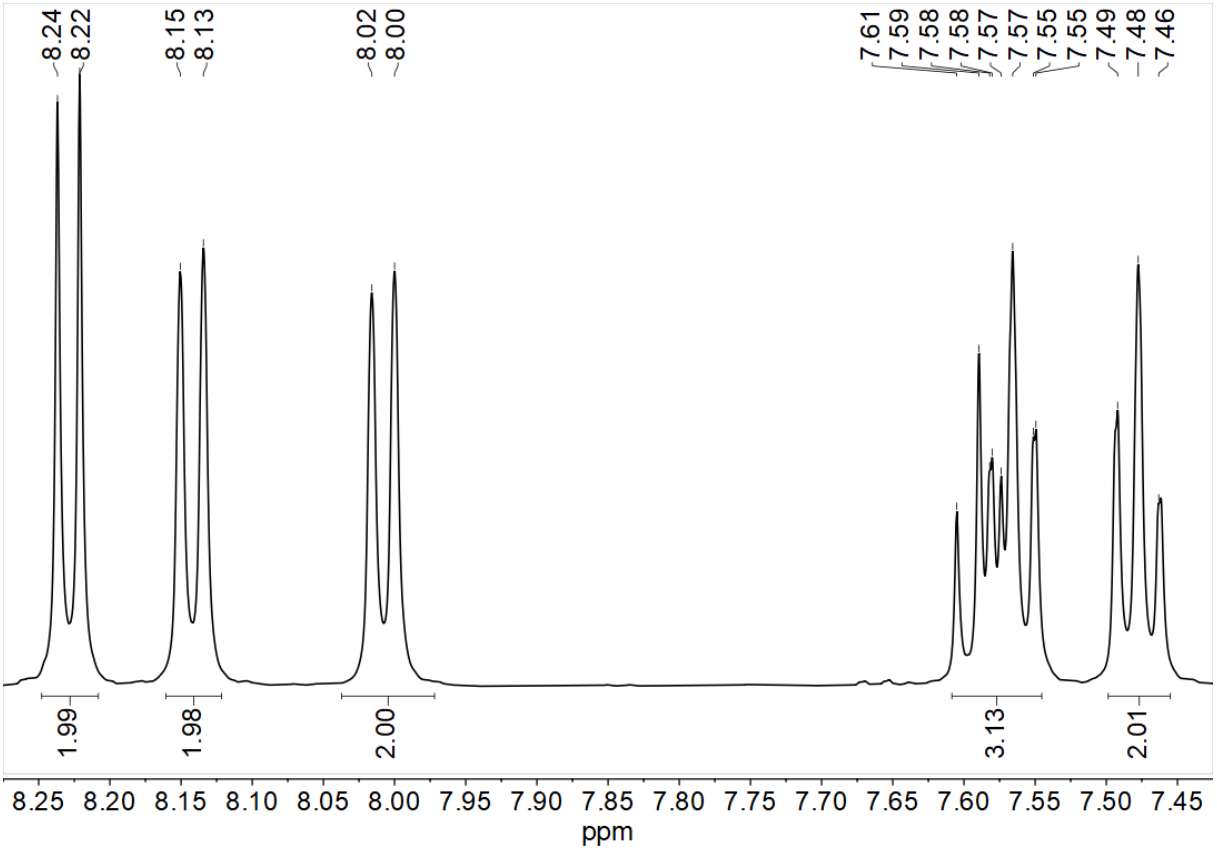

Figure 7-99 500 MHz ^{1}H NMR spectrum of 2Btz(PhCl)2Btz in CD_2Cl_2.

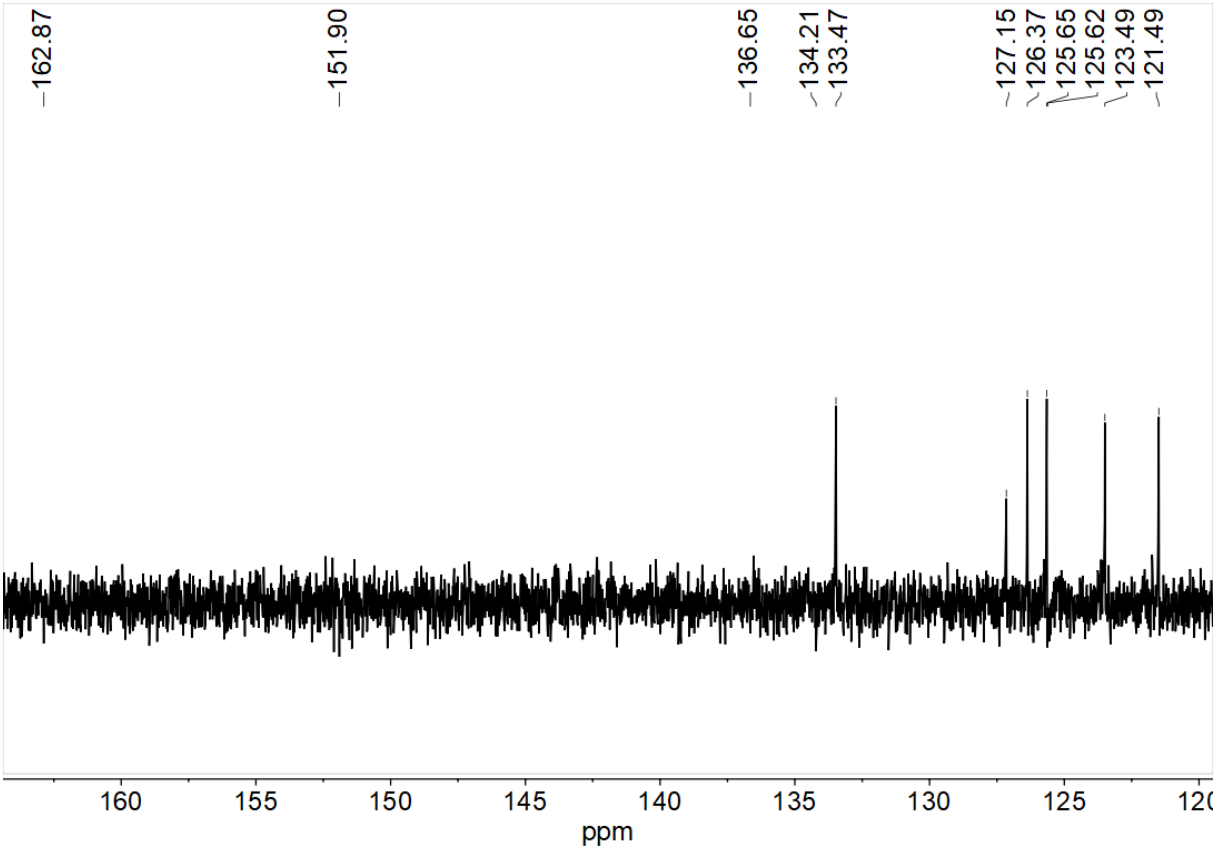

Figure 7-100 75 MHz ^{13}C NMR spectrum of 2Btz(PhCl)2Btz in CD_2Cl_2.

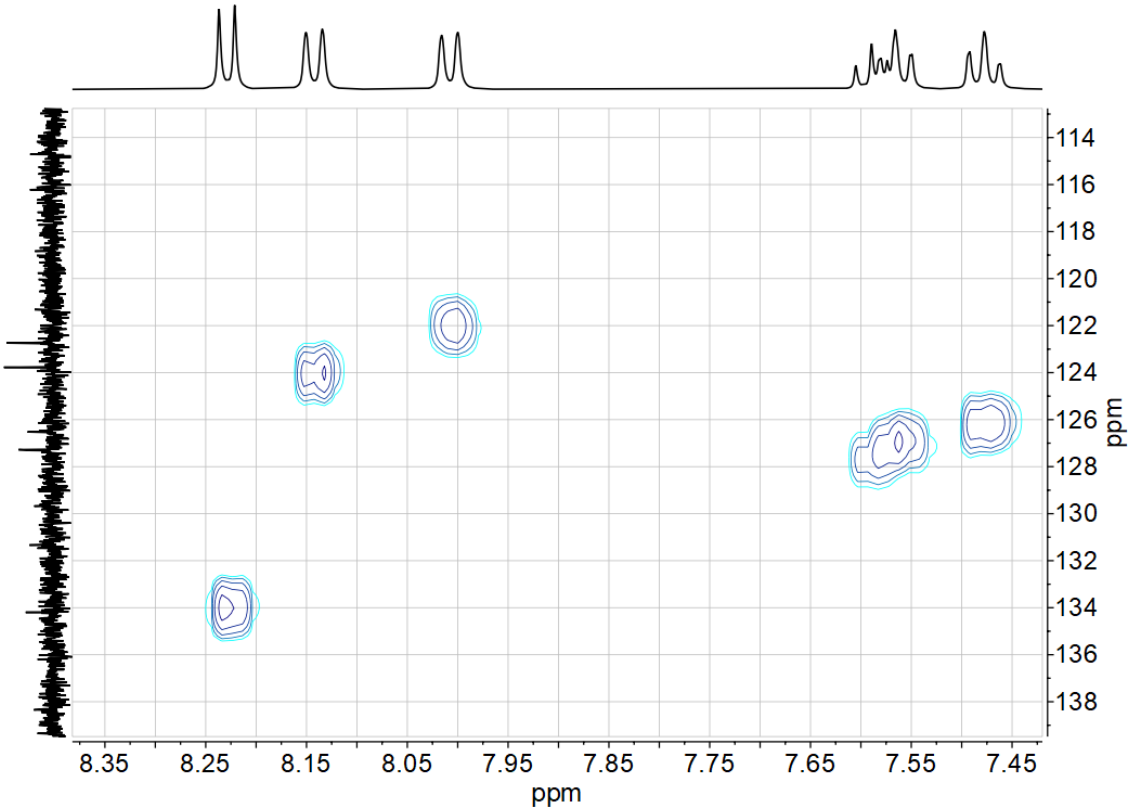

Figure 7-101 $^{1}H,^{13}C$ HSQC correlation spectrum of 2Btz(PhCl)2Btz in CD_2Cl_2.

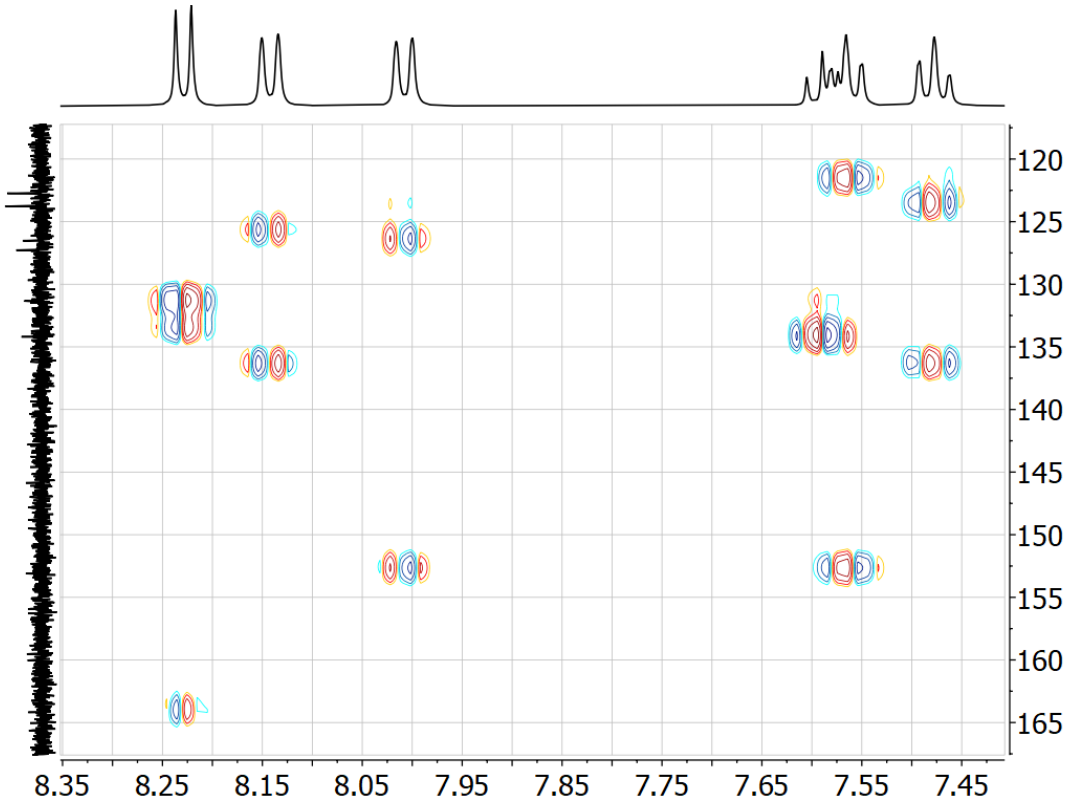

Figure 7-102 $^{1}H,^{13}C$ HMBC correlation spectrum of 2Btz(PhCl)2Btz in CD_2Cl_2.

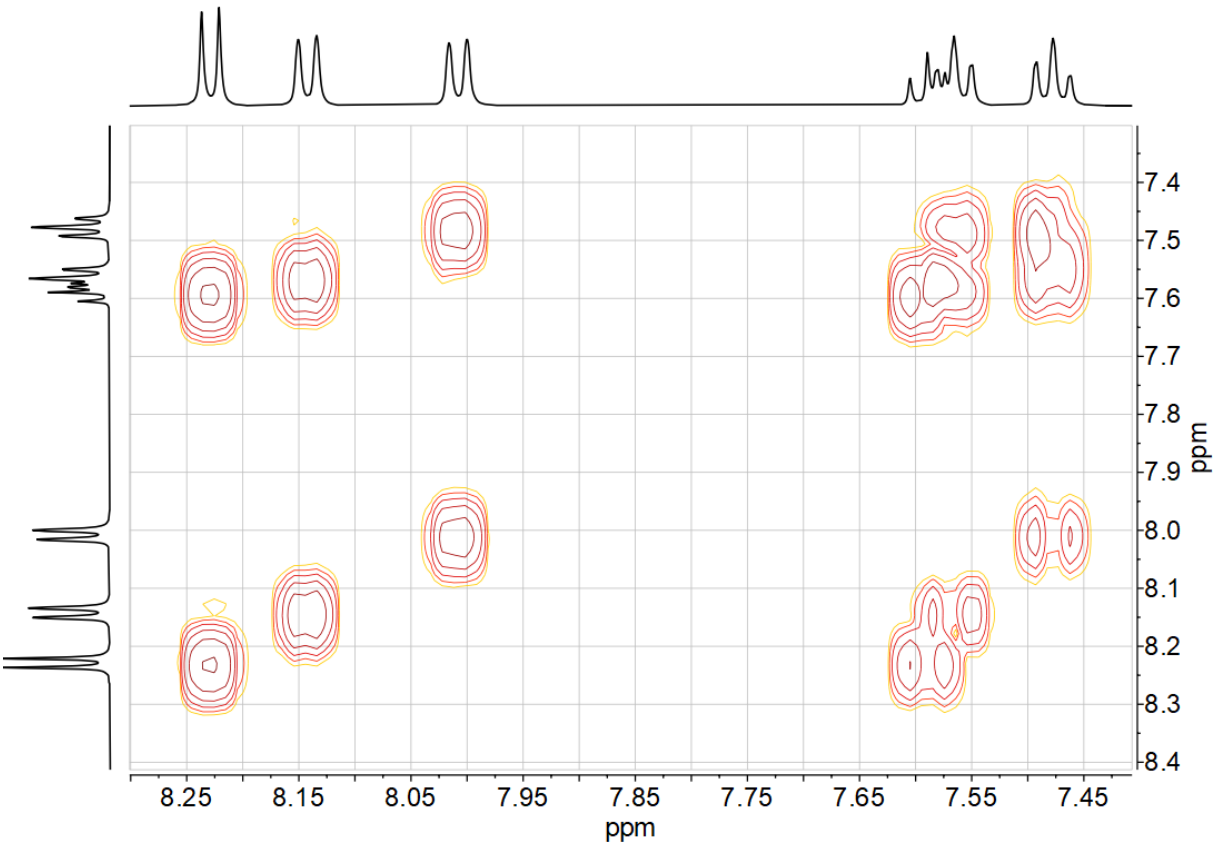

Figure 7-103 $^{1}H,^{1}H$ COSY correlation spectrum of 2Btz(PhCl)2Btz in CD_2Cl_2.

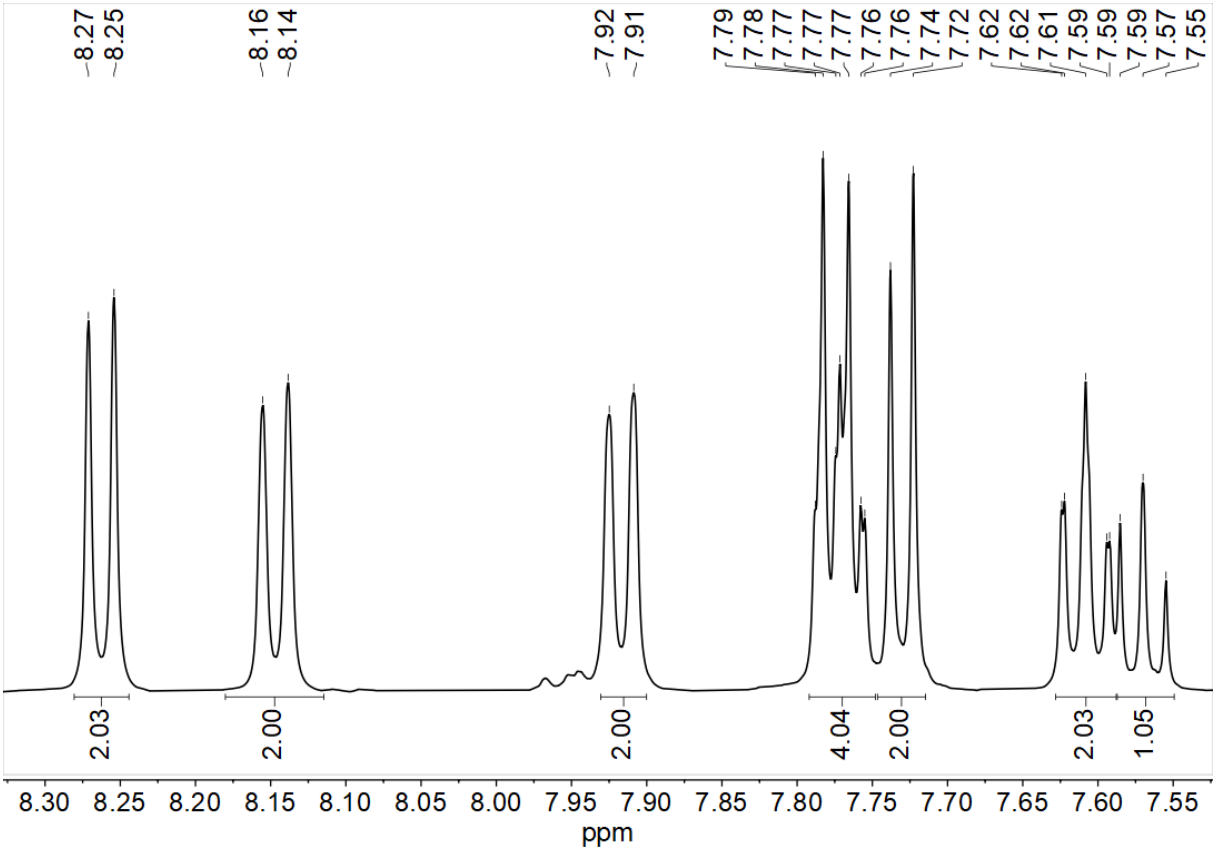

Figure 7-104 500 MHz ^{1}H NMR spectrum of 2Qu(PhCl)2Qu in CD_2Cl_2.

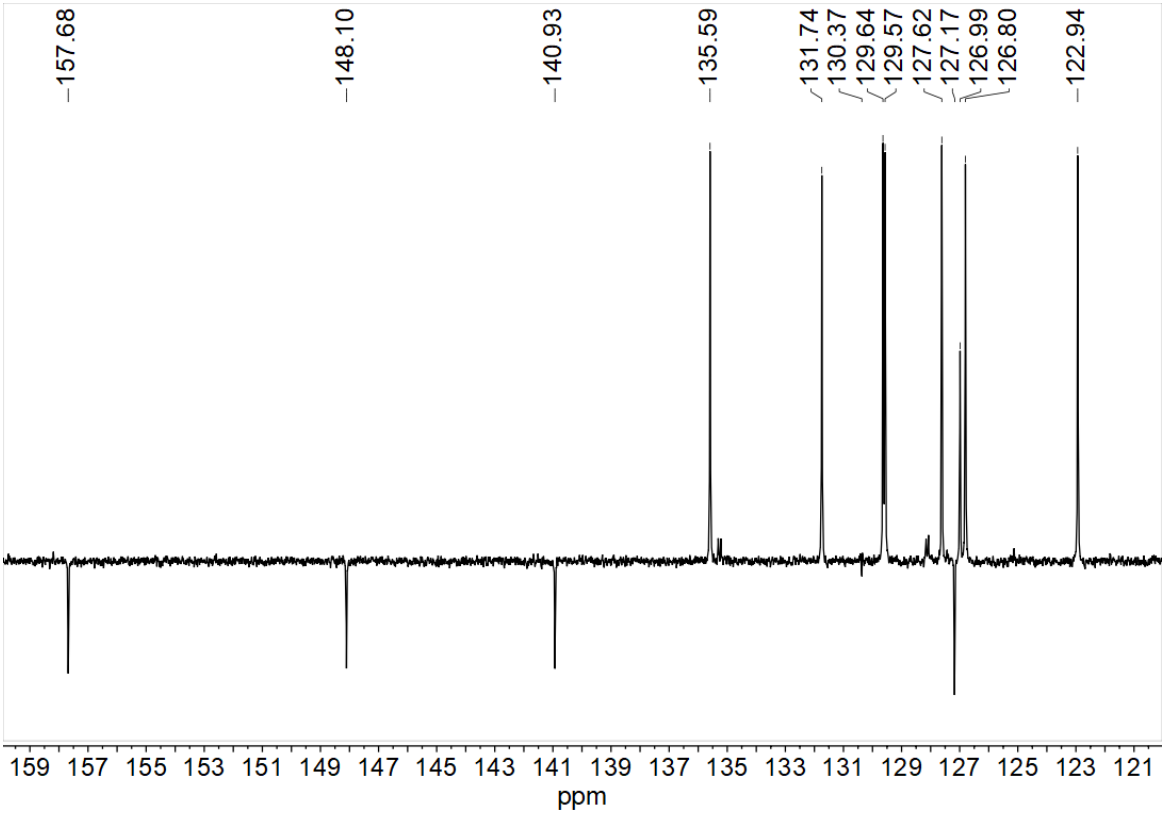

Figure 7-105 75 MHz ^{13}C NMR spectrum of 2Qu(PhCl)2Qu in CD_2Cl_2.

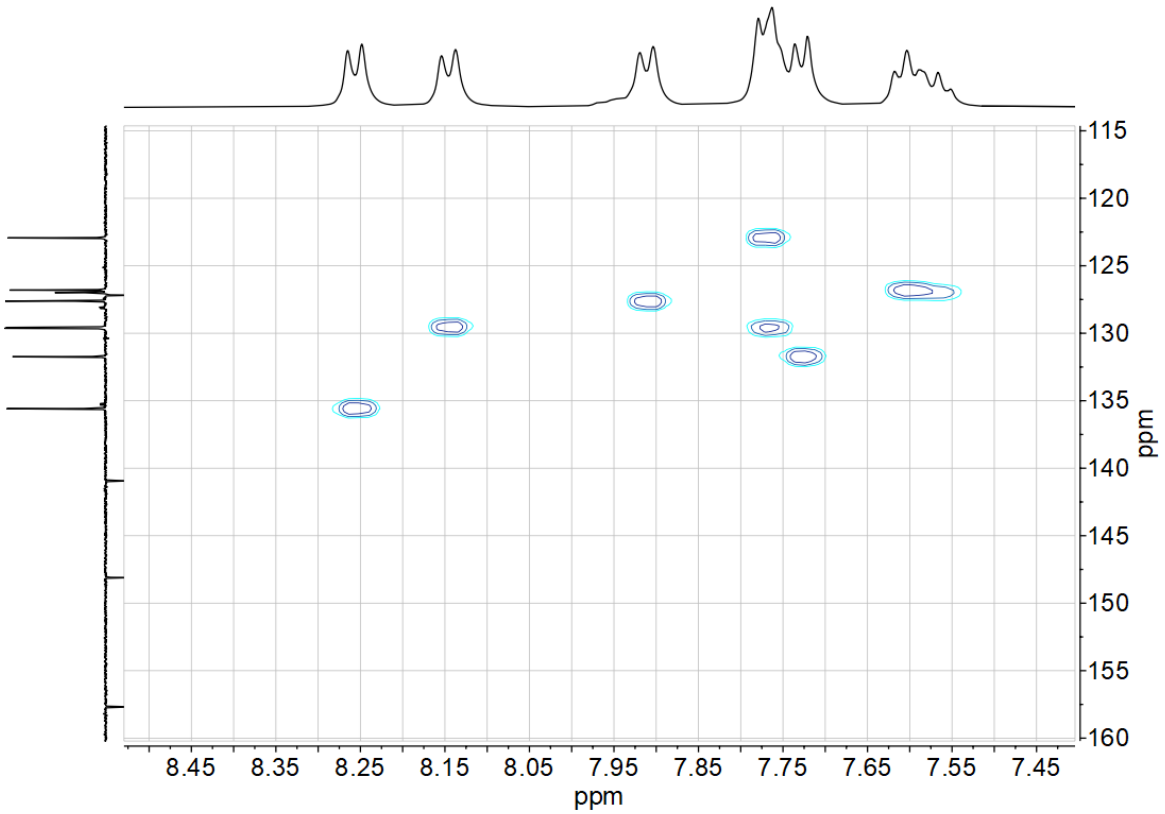

Figure 7-106 $^{1}H,^{13}C$ HSQC correlation spectrum of 2Qu(PhCl)2Qu in CD_2Cl_2.

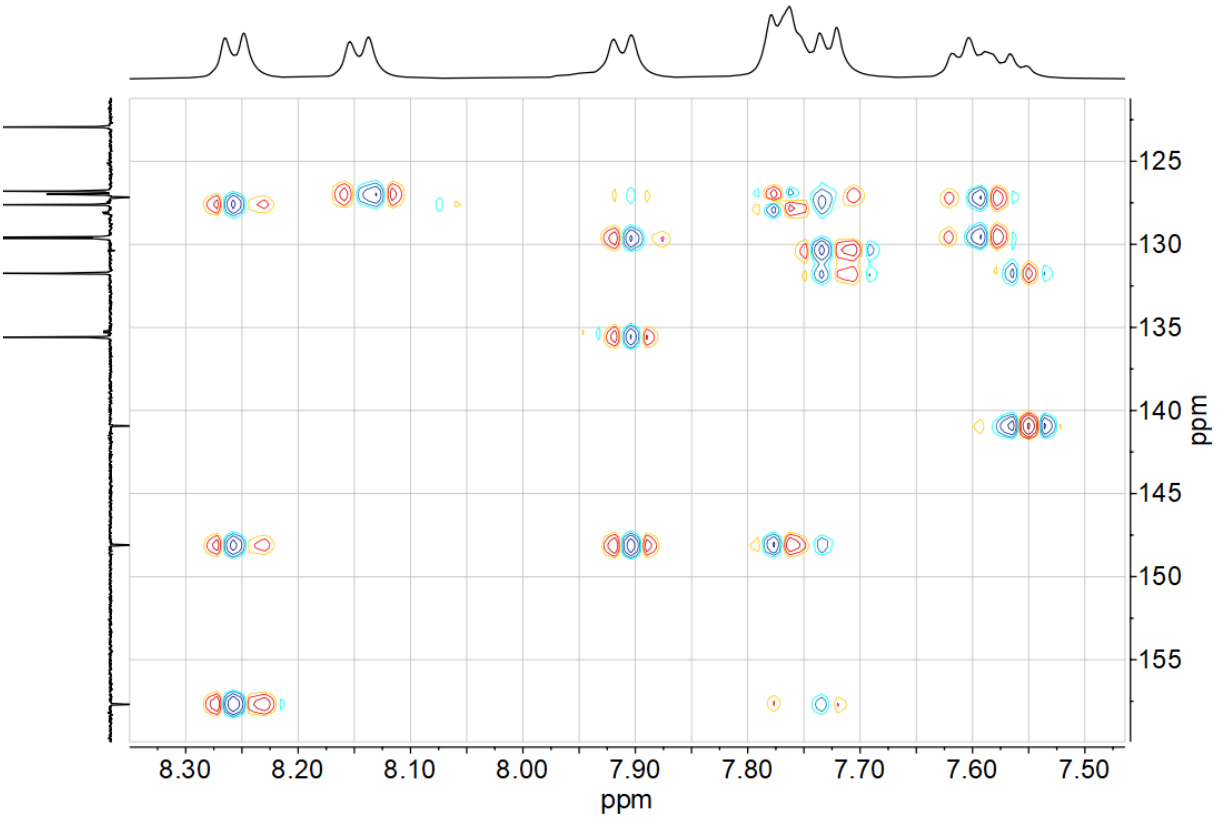

Figure 7-107 $^{1}H,^{13}C$ HMBC correlation spectrum of 2Qu(PhCl)2Qu in CD_2Cl_2.

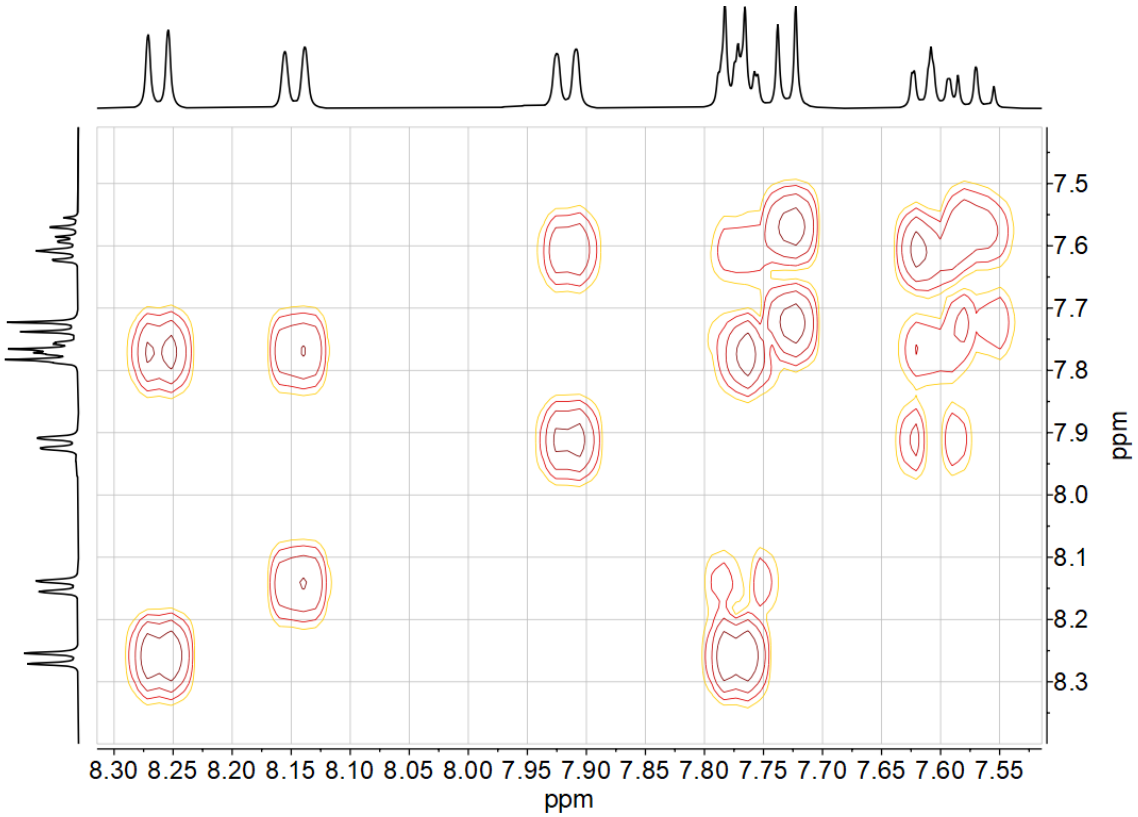

Figure 7-108 $^{1}H,^{1}H$ COSY correlation spectrum of 2Qu(PhCl)2Qu in CD_2Cl_2.

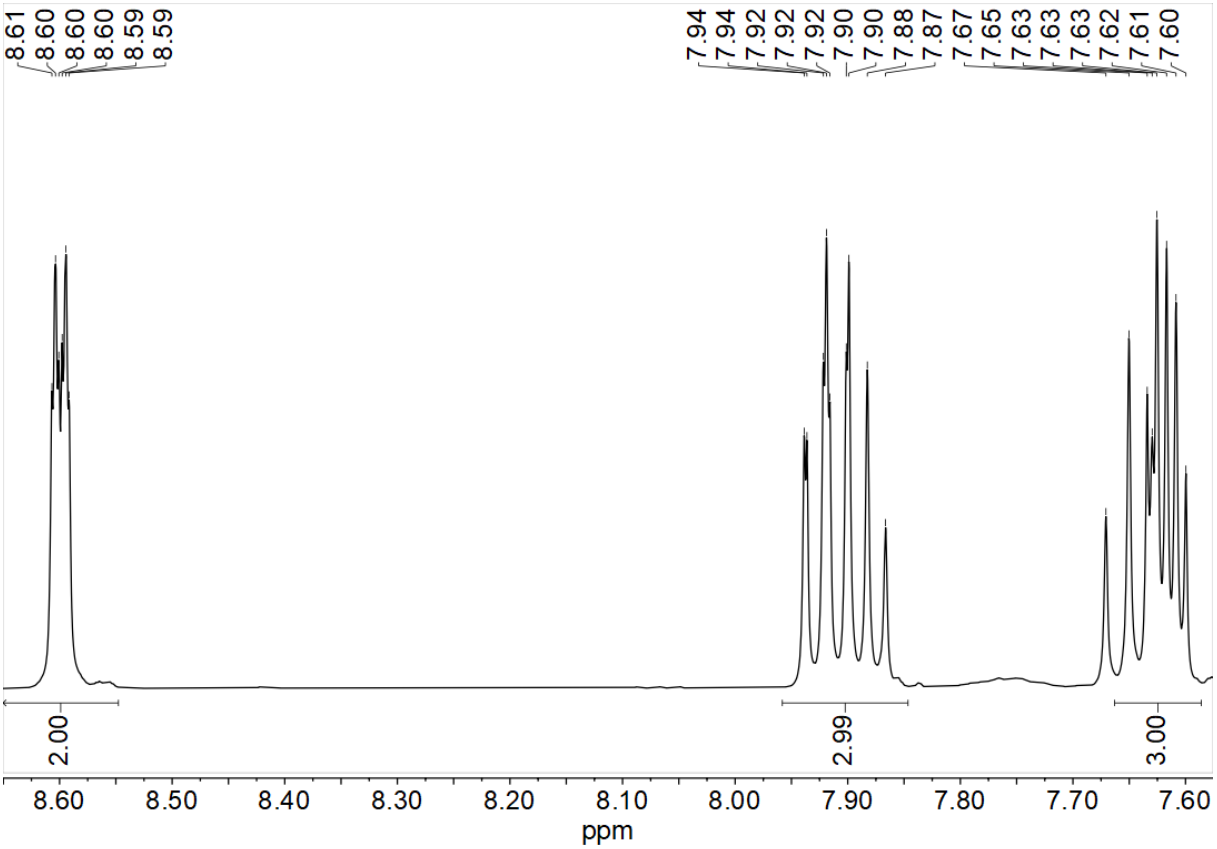

Figure 7-109 500 MHz ^{1}H NMR spectrum of 3FPy(4,6FPhH)3FPy in DMSO-d_6.

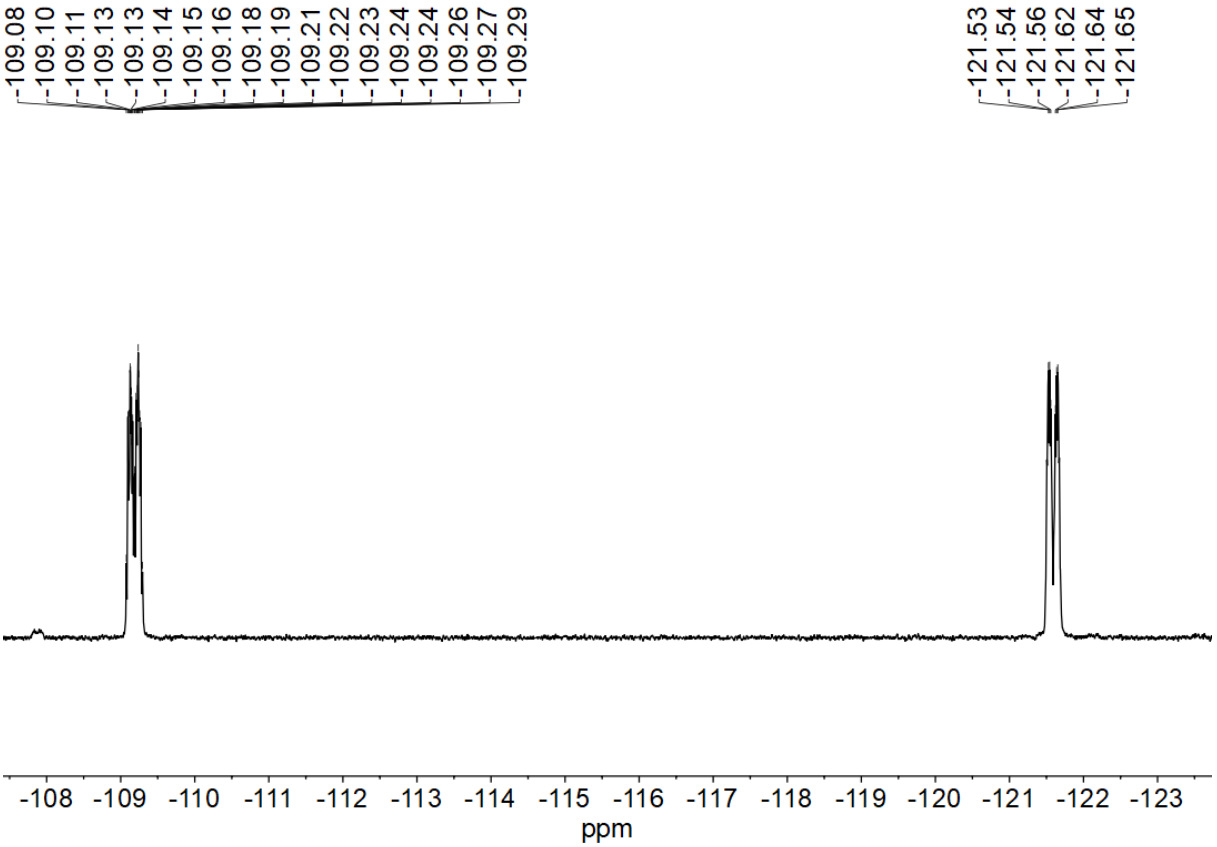

Figure 7-110 282 MHz ^{19}F NMR spectrum of 3FPy(4,6FPhH)3FPy in DMSO-d_6.

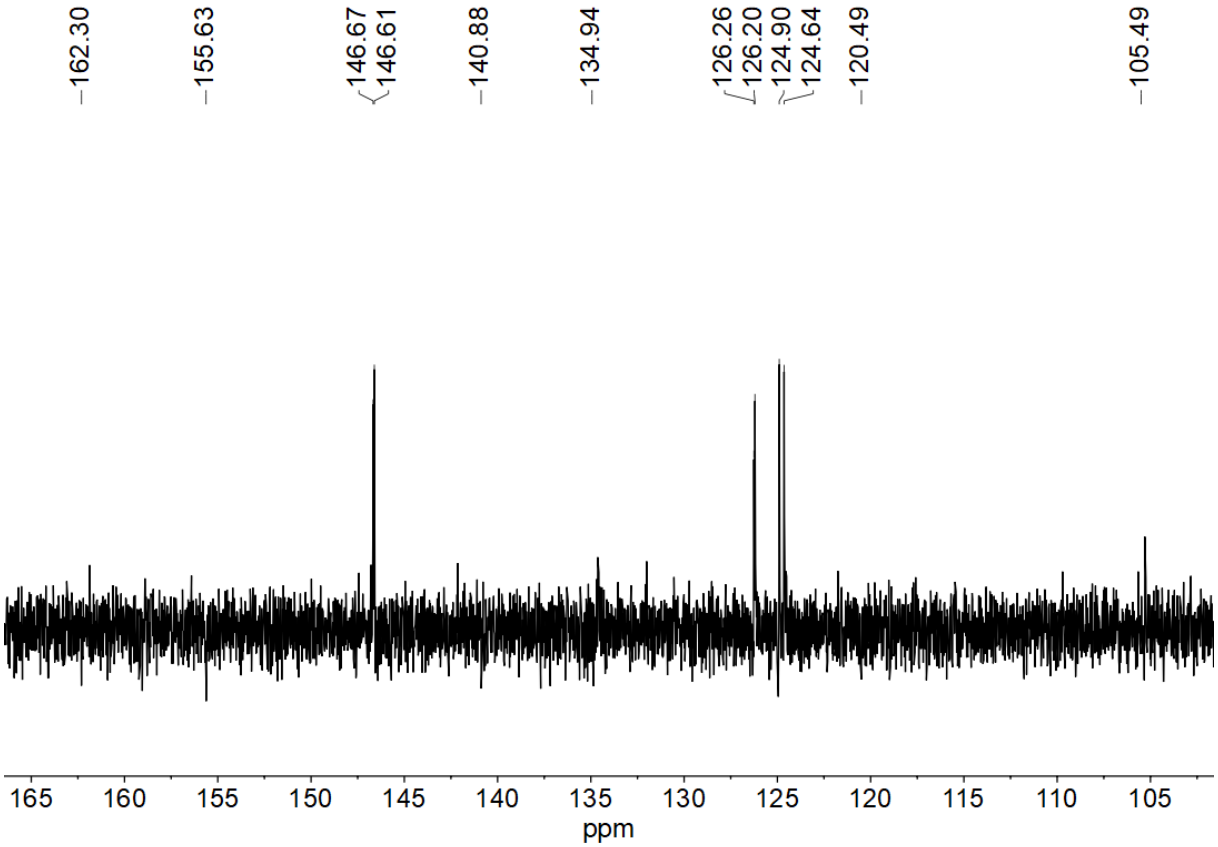

Figure 7-111 75 MHz ^{13}C NMR spectrum of 3FPy(4,6FPhH)3FPy in DMSO-d_6.

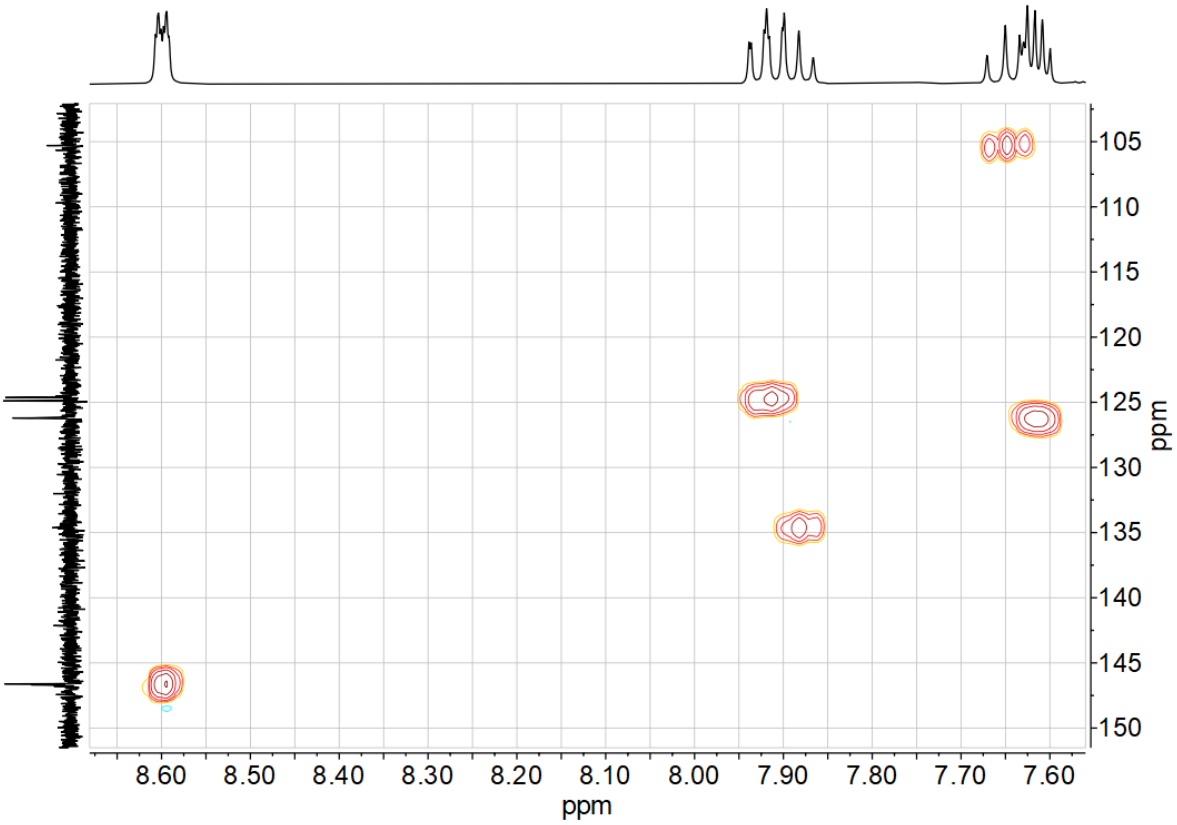

Figure 7-112 ^{1}H,^{13}C HSQC correlation spectrum of 3FPy(4,6FPhH)3FPy in DMSO-d_6.

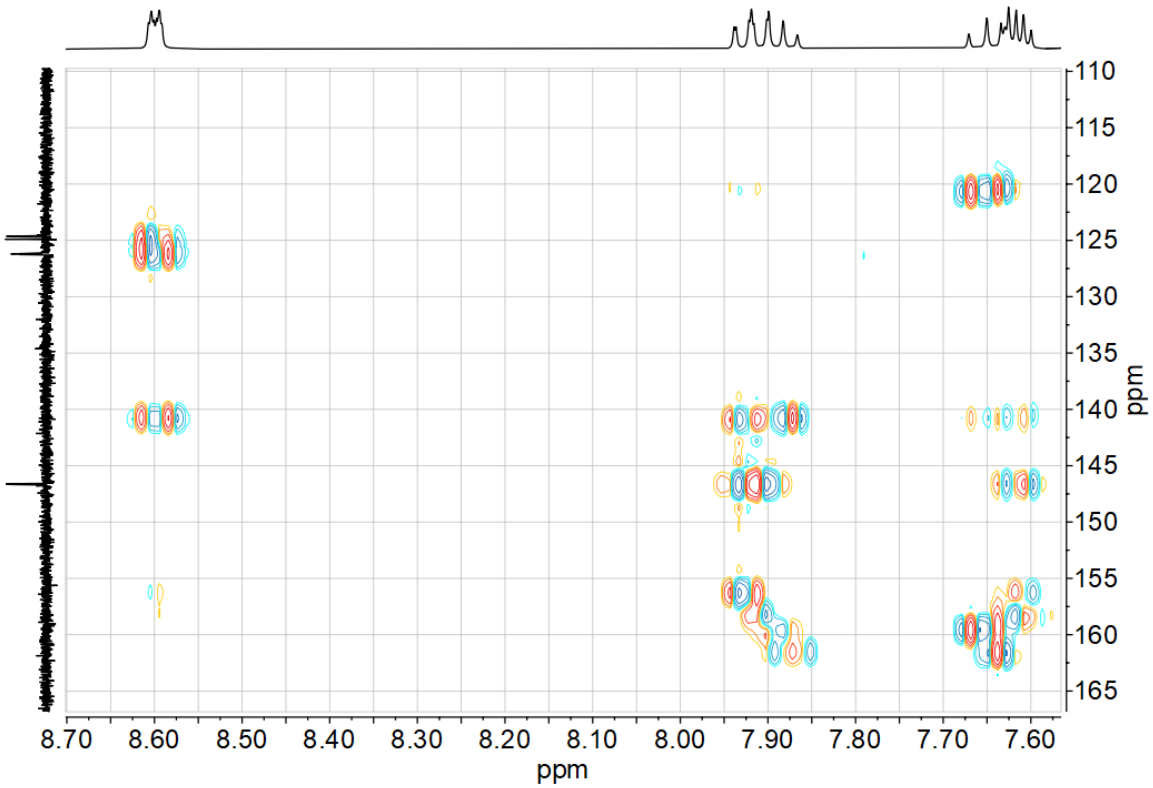

Figure 7-113 $^{1}H,^{13}C$ HMBC correlation spectrum of 3FPy(4,6FPhH)3FPy in DMSO-d_6.

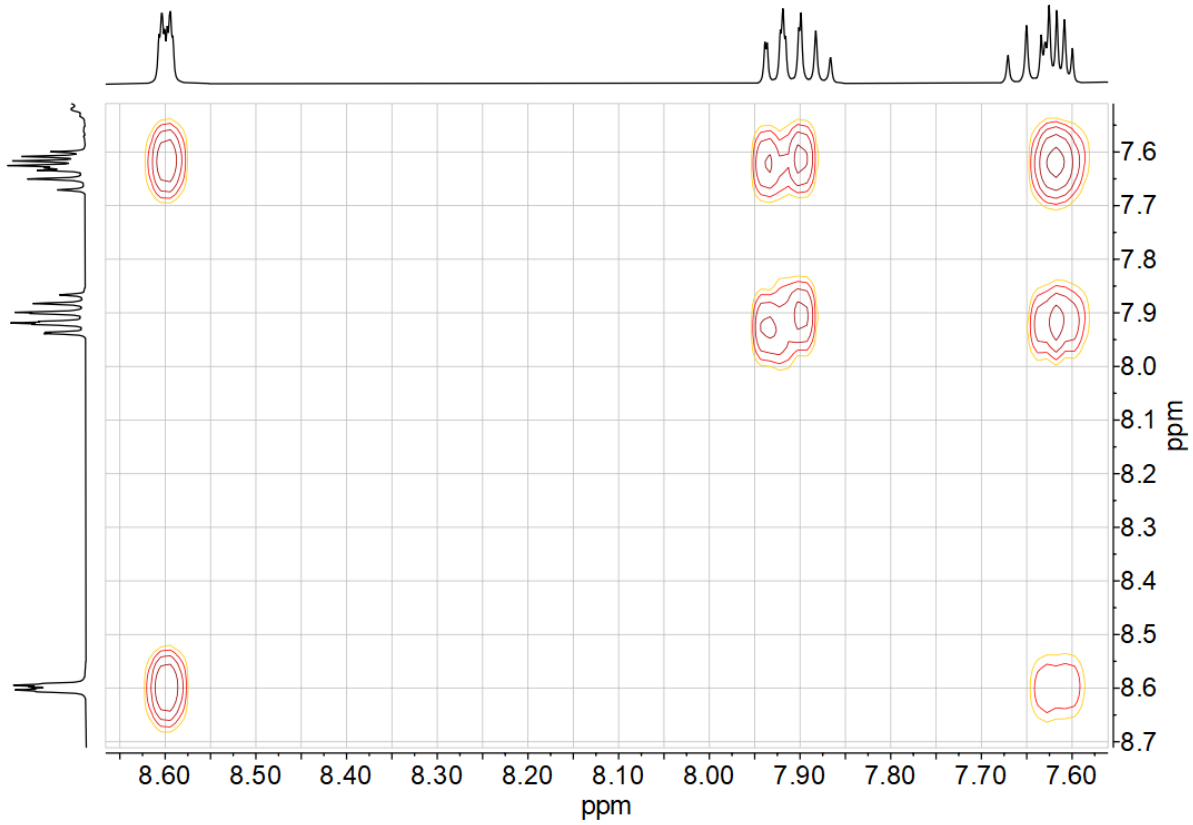

Figure 7-114 $^{1}H,^{1}H$ COSY correlation spectrum of 3FPy(4,6FPhH)3FPy in DMSO-d_6.

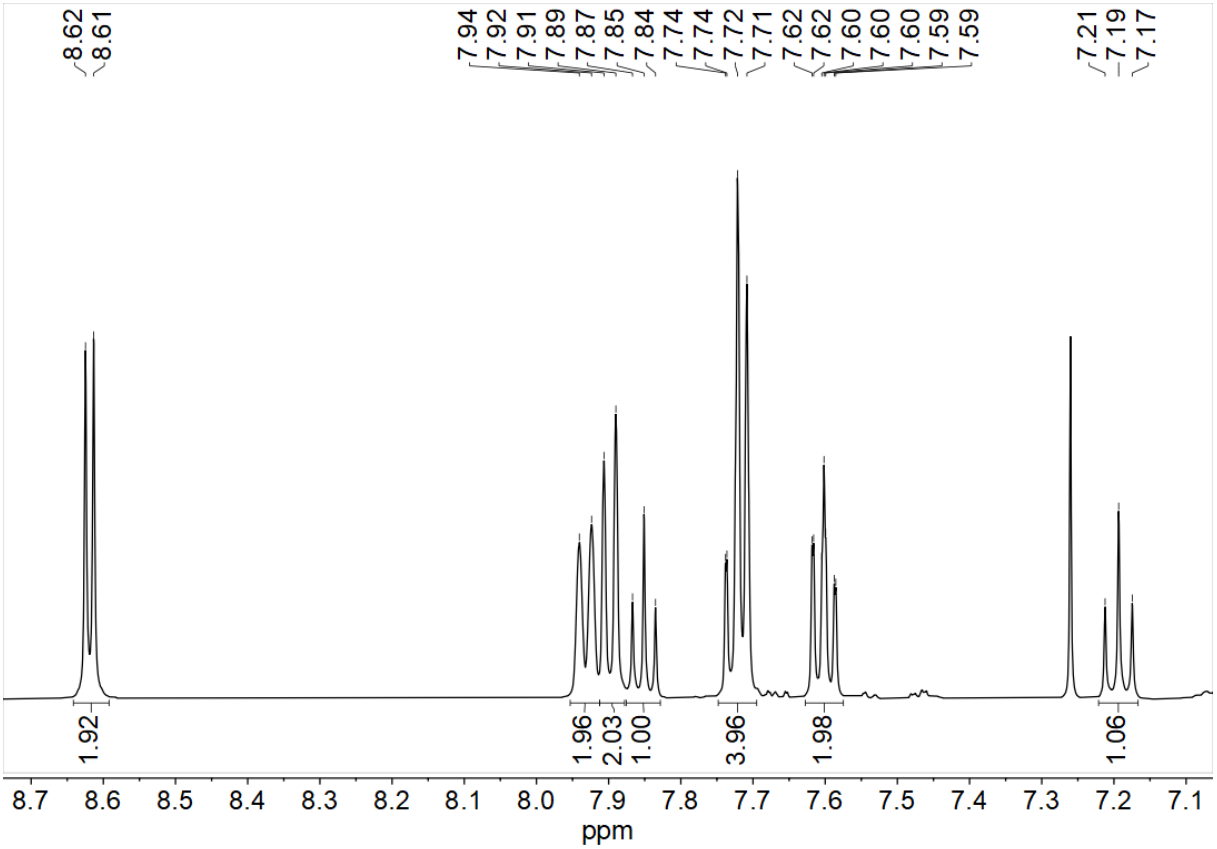

Figure 7-115 500 MHz ^{1}H NMR spectrum of 2^{i}Qu(4,6FPhH)2^{i}Qu in $CDCl_3$.

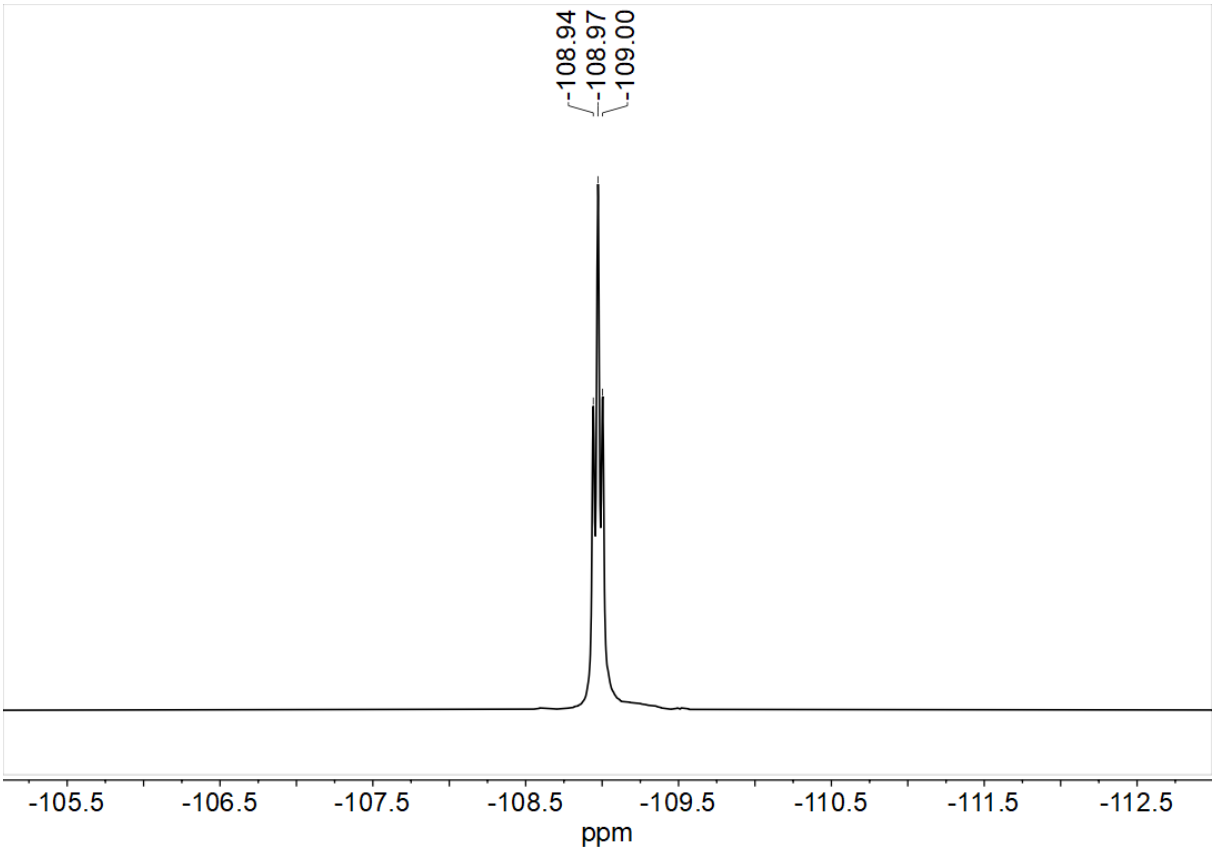

Figure 7-116 282 MHz ^{19}F NMR spectrum of 2^{i}Qu(4,6FPhH)2^{i}Qu in $CDCl_3$.

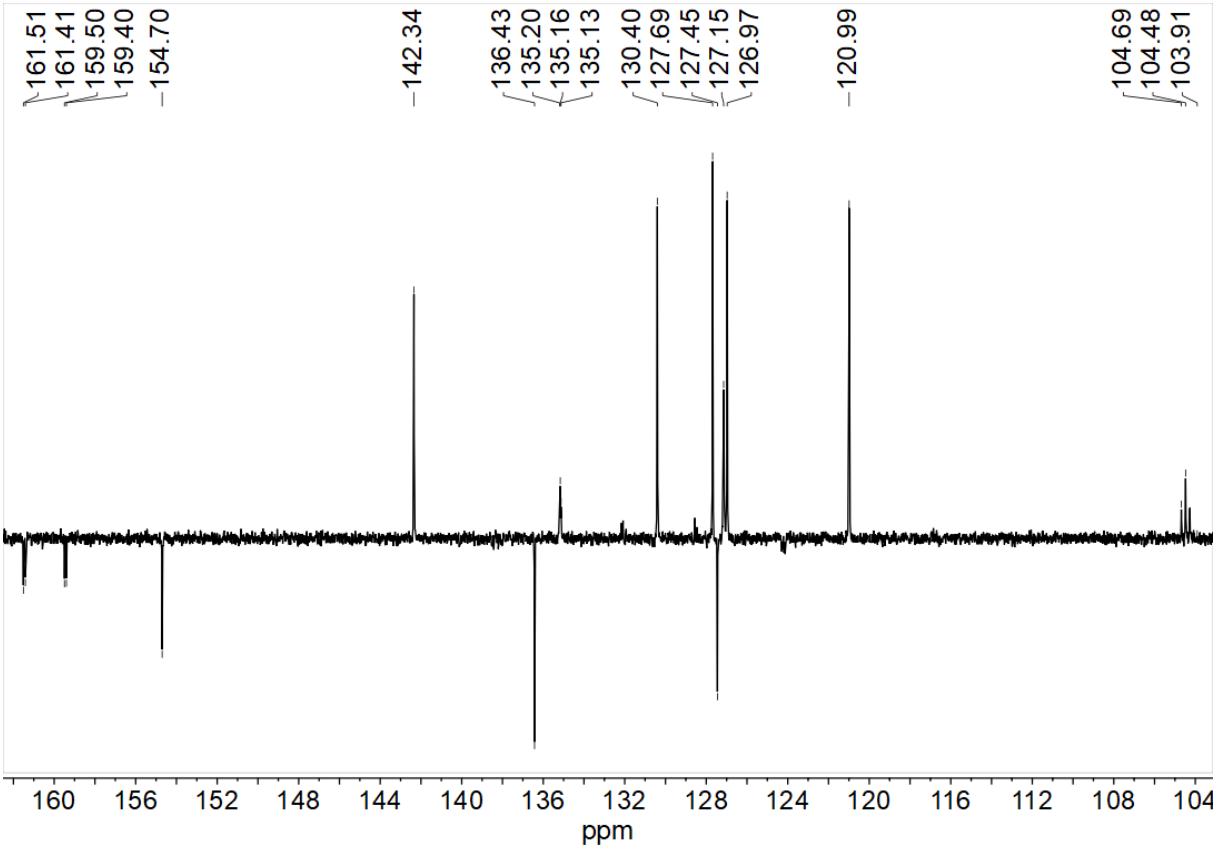

Figure 7-117 126 MHz ^{13}C NMR spectrum of 2^{i}Qu(4,6FPhH)2^{i}Qu in $CDCl_3$.

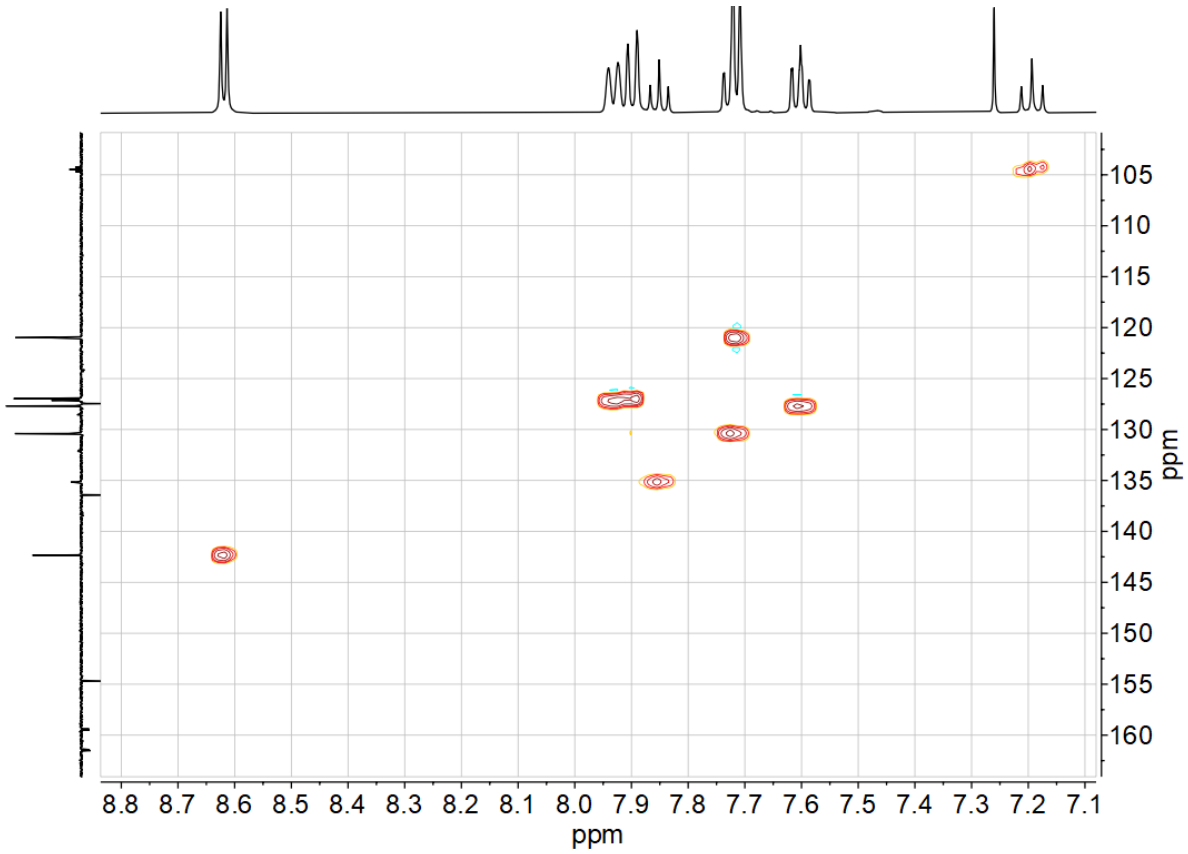

Figure 7-118 $^{1}H,^{13}C$ HSQC correlation spectrum of 2^{i}Qu(4,6FPhH)2^{i}Qu in $CDCl_3$.

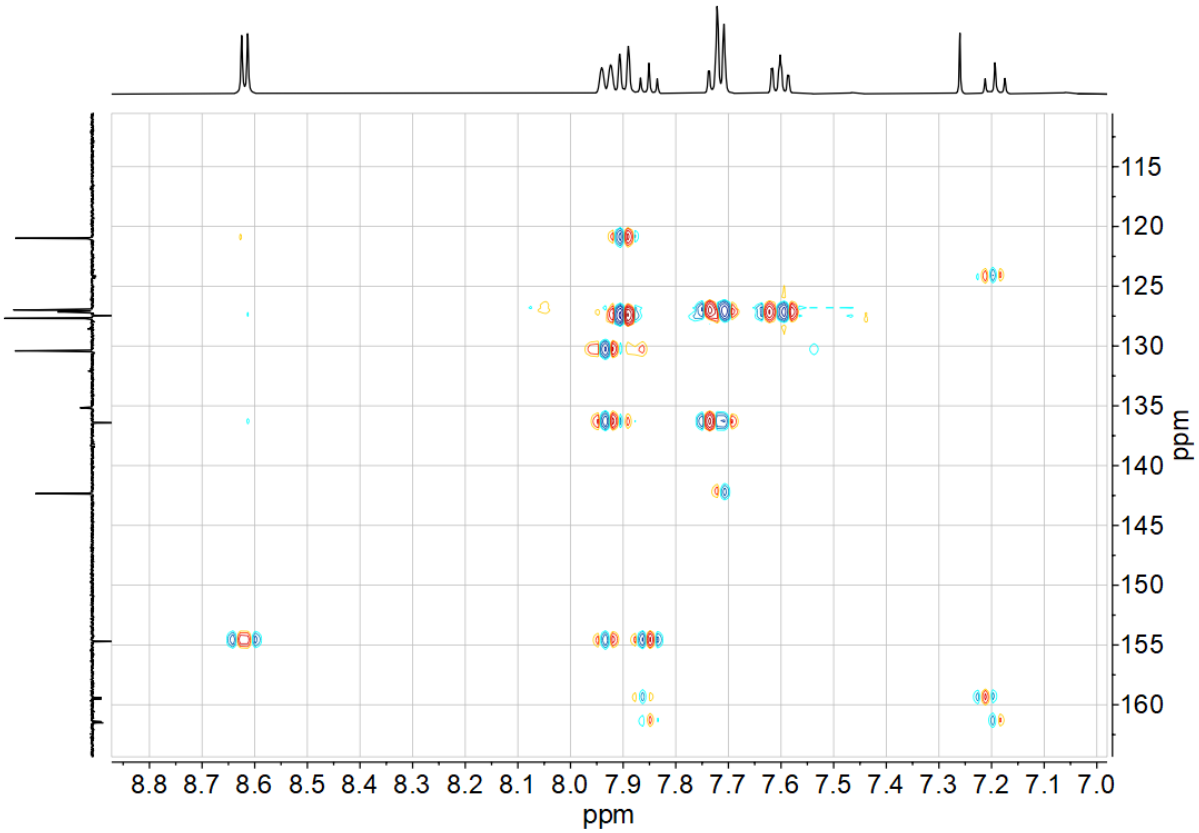

Figure 7-119 $^{1}H,^{13}C$ HMBC correlation spectrum of 2^{i}Qu(4,6FPhH)2^{i}Qu in $CDCl_3$.

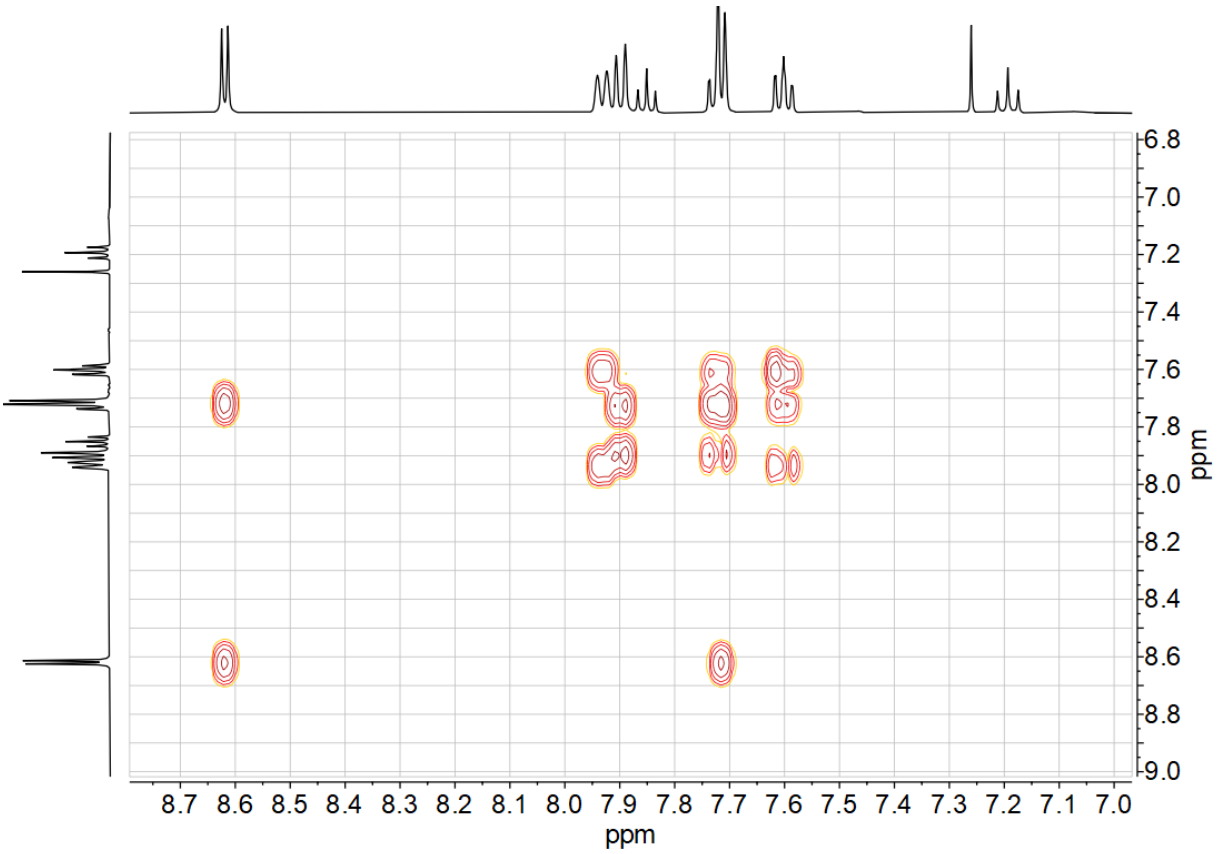

Figure 7-120 $^{1}H,^{1}H$ COSY correlation spectrum of 2^{i}Qu(4,6FPhH)2^{i}Qu in $CDCl_3$.

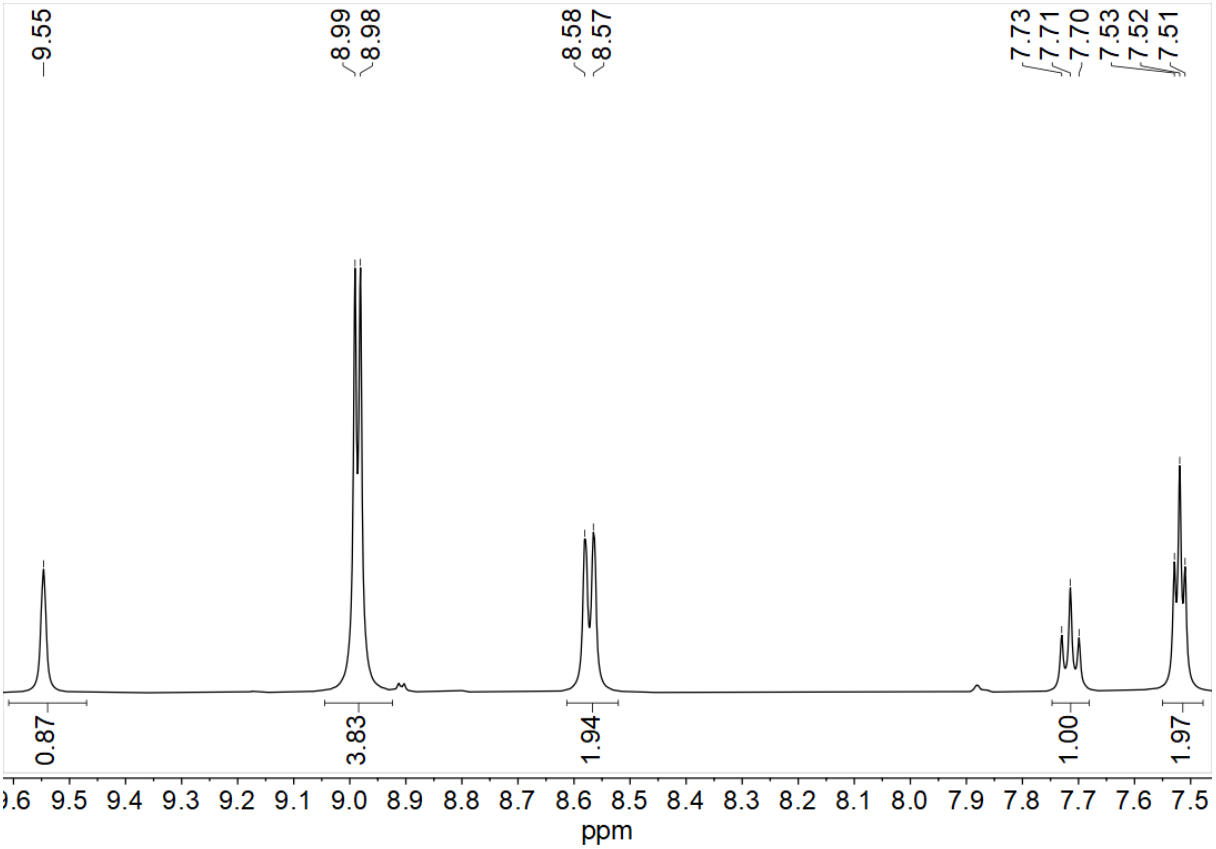

Figure 7-121 300 MHz ^{1}H NMR spectrum of Pym(PhH)Pym in DMSO-d_6.

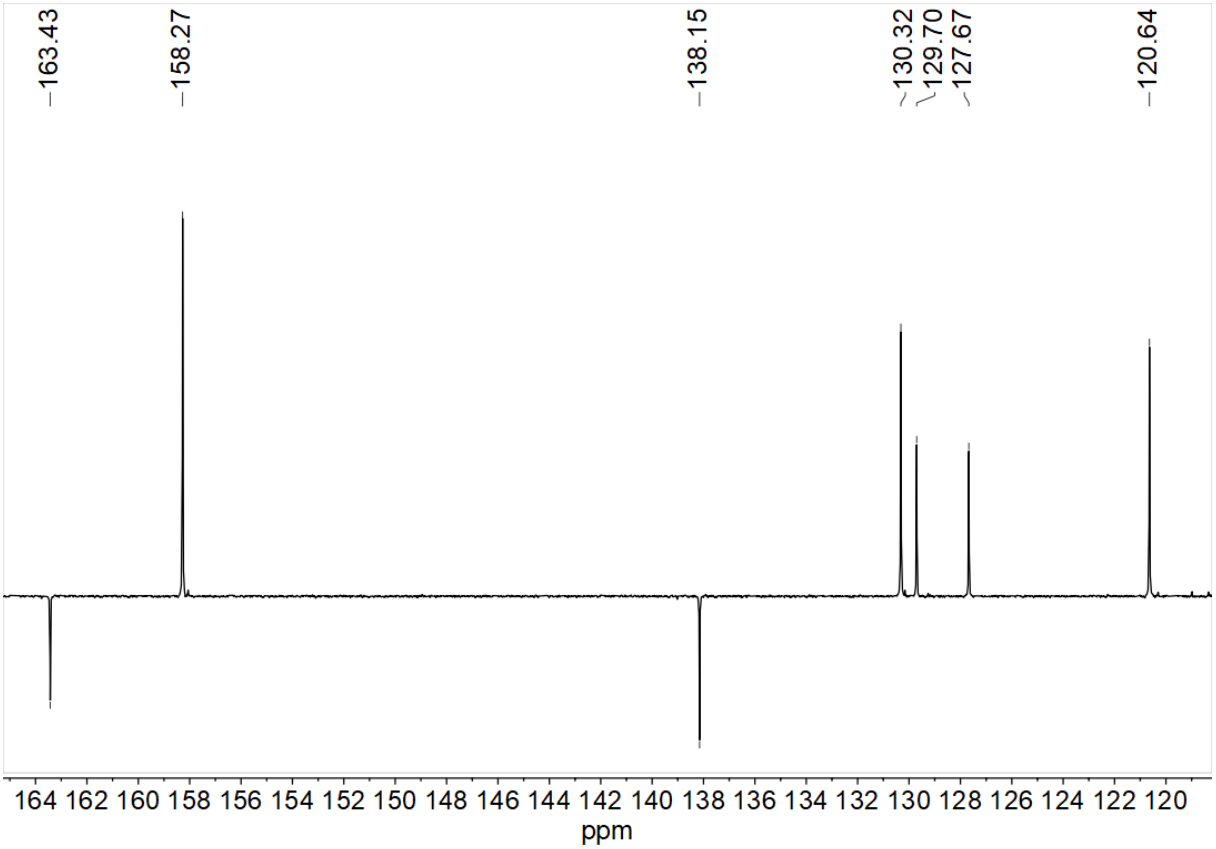

Figure 7-122 75 MHz ^{13}C NMR spectrum of Pym(PhH)Pym in DMSO-d_6.

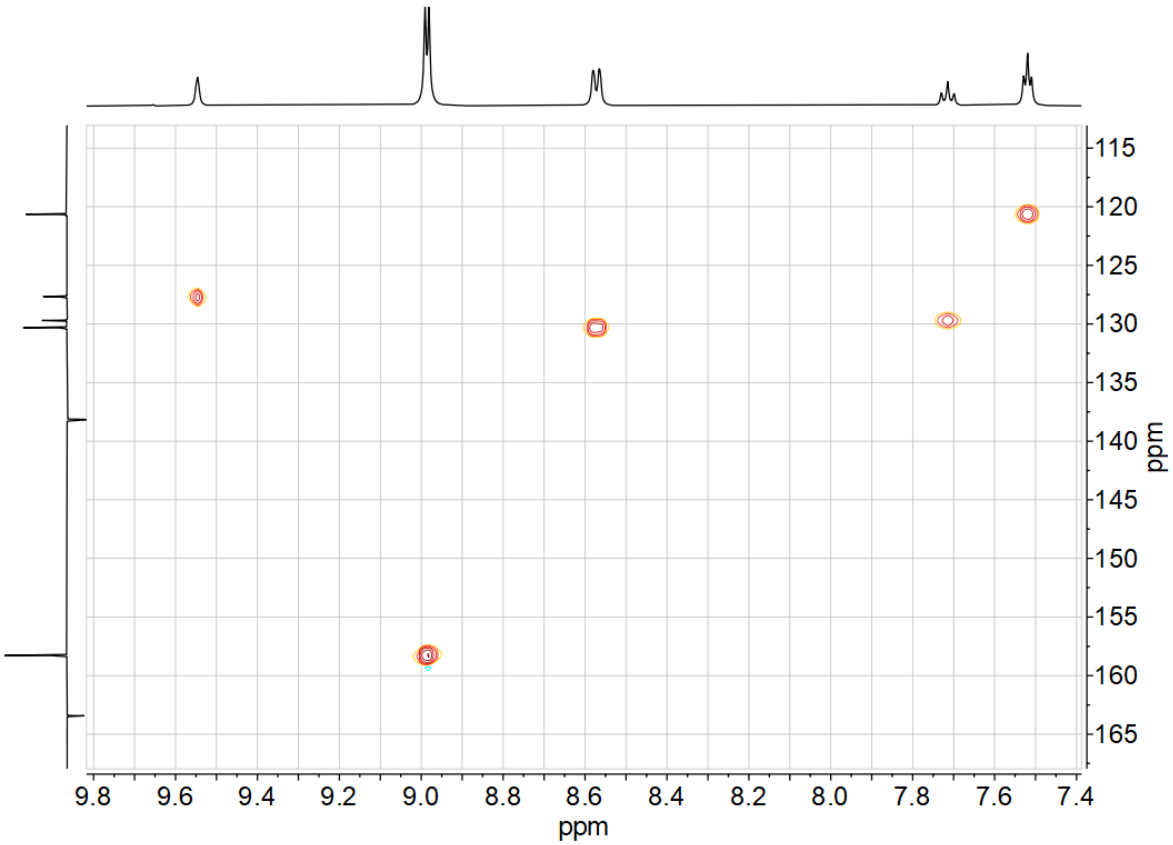

Figure 7-123 $^{1}H,^{13}C$ HSQC correlation spectrum of Pym(PhH)Pym in DMSO-d_6.

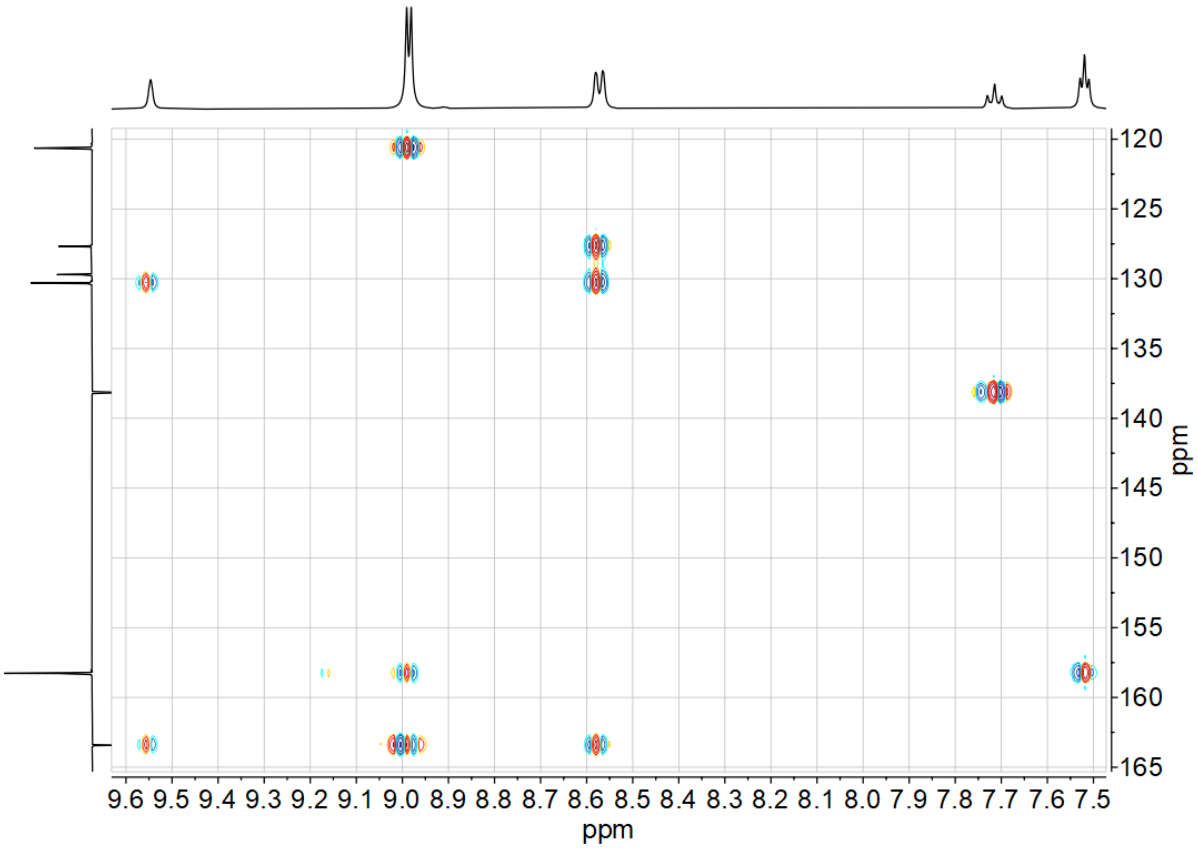

Figure 7-124 $^{1}H,^{13}C$ HMBC correlation spectrum of Pym(PhH)Pym in DMSO-d_6.

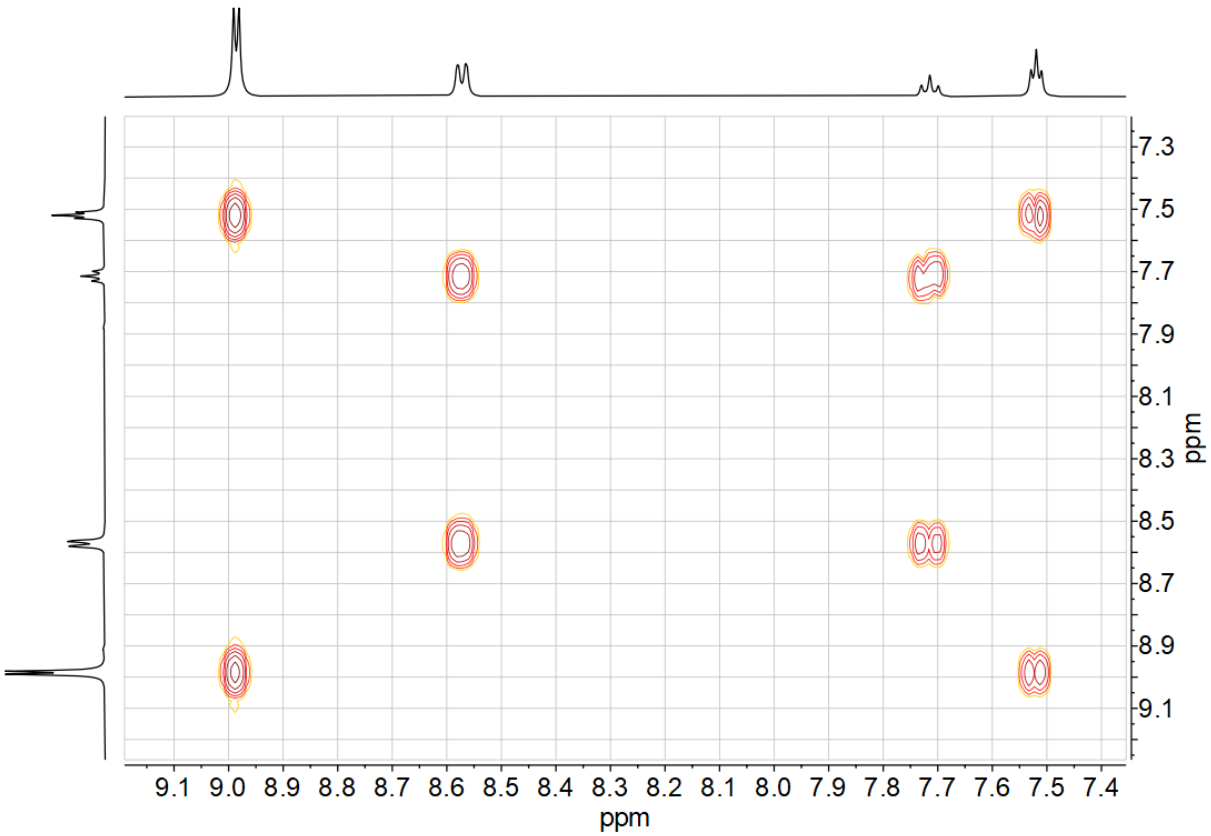

Figure 7-125 ^{1}H,^{1}H COSY correlation spectrum of Pym(PhH)Pym in DMSO-d_6.

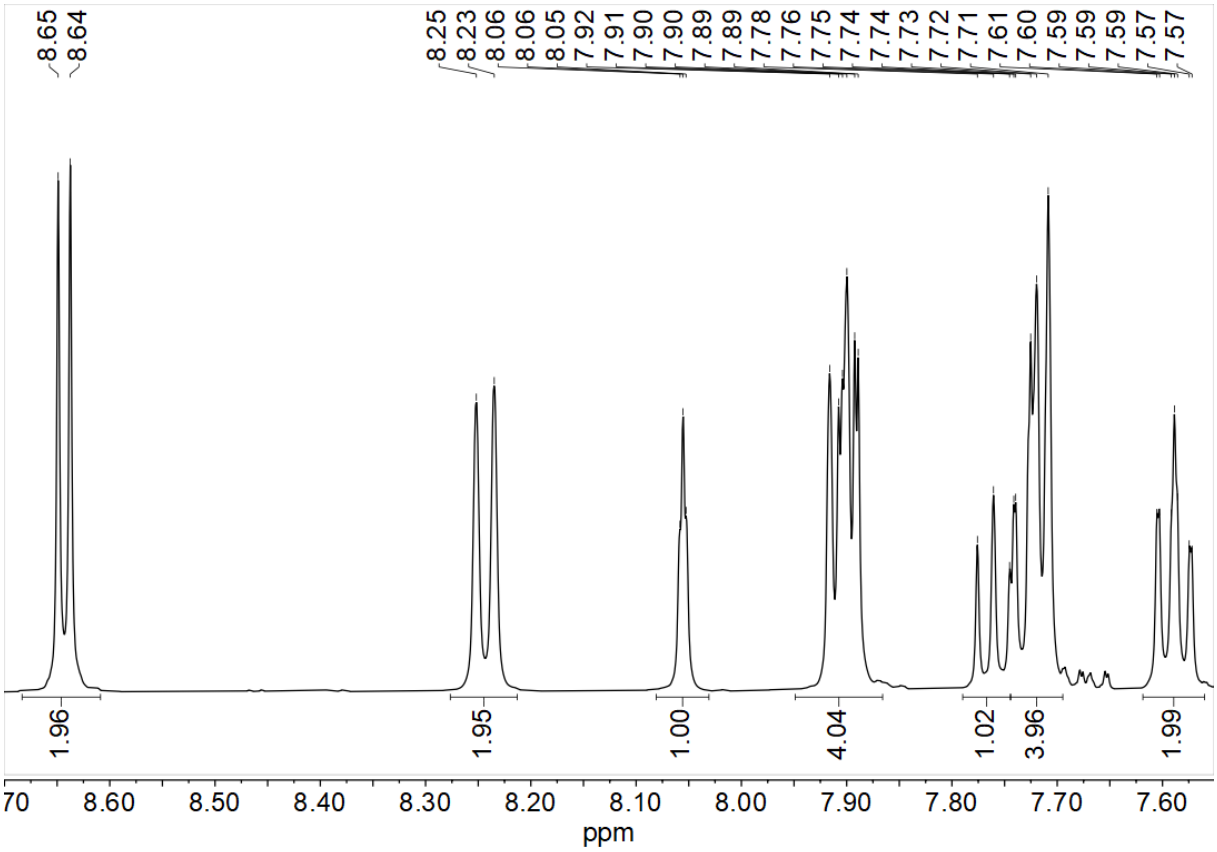

Figure 7-126 500 MHz ^{1}H NMR spectrum of 2^{i}Qu(PhH)2^{i}Qu in $CDCl_3$.

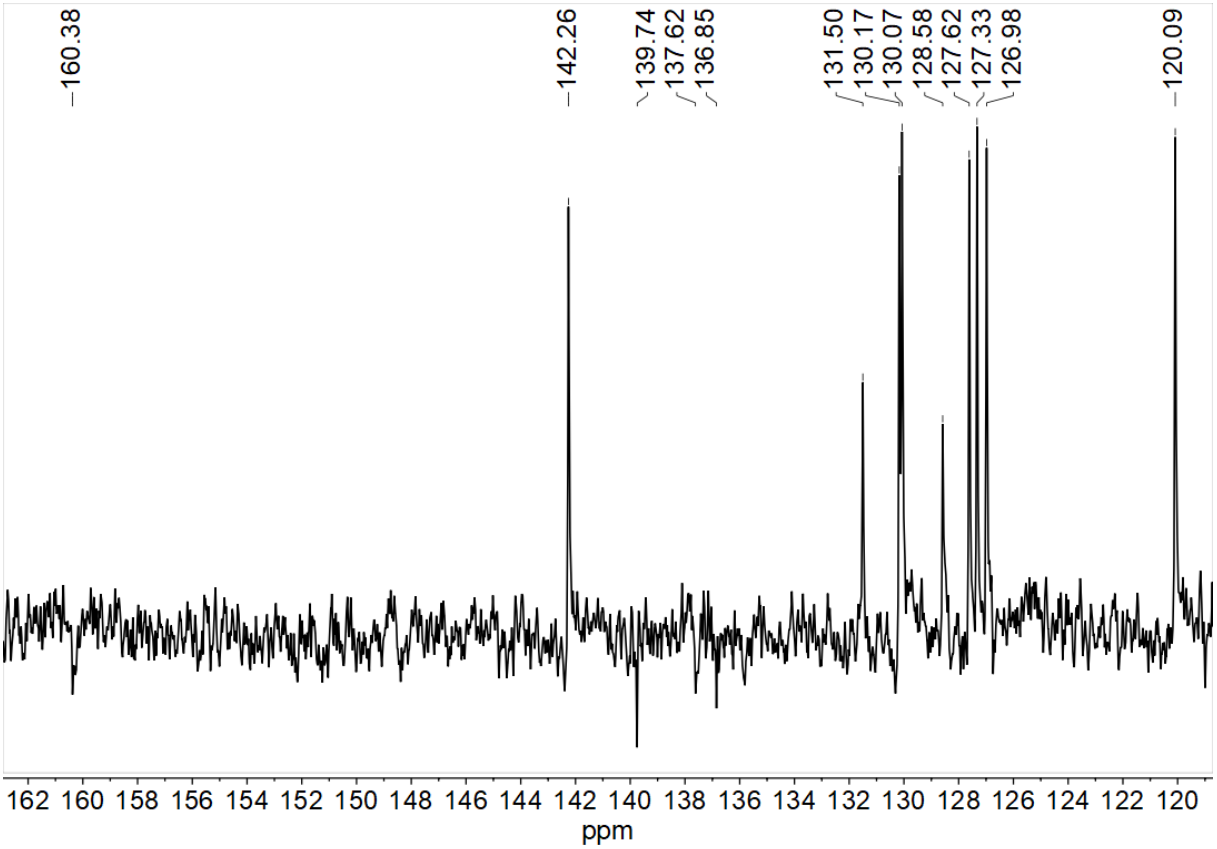

Figure 7-127 75 MHz ^{13}C NMR spectrum of 2^{i}Qu(PhH)2^{i}Qu in $CDCl_3$.

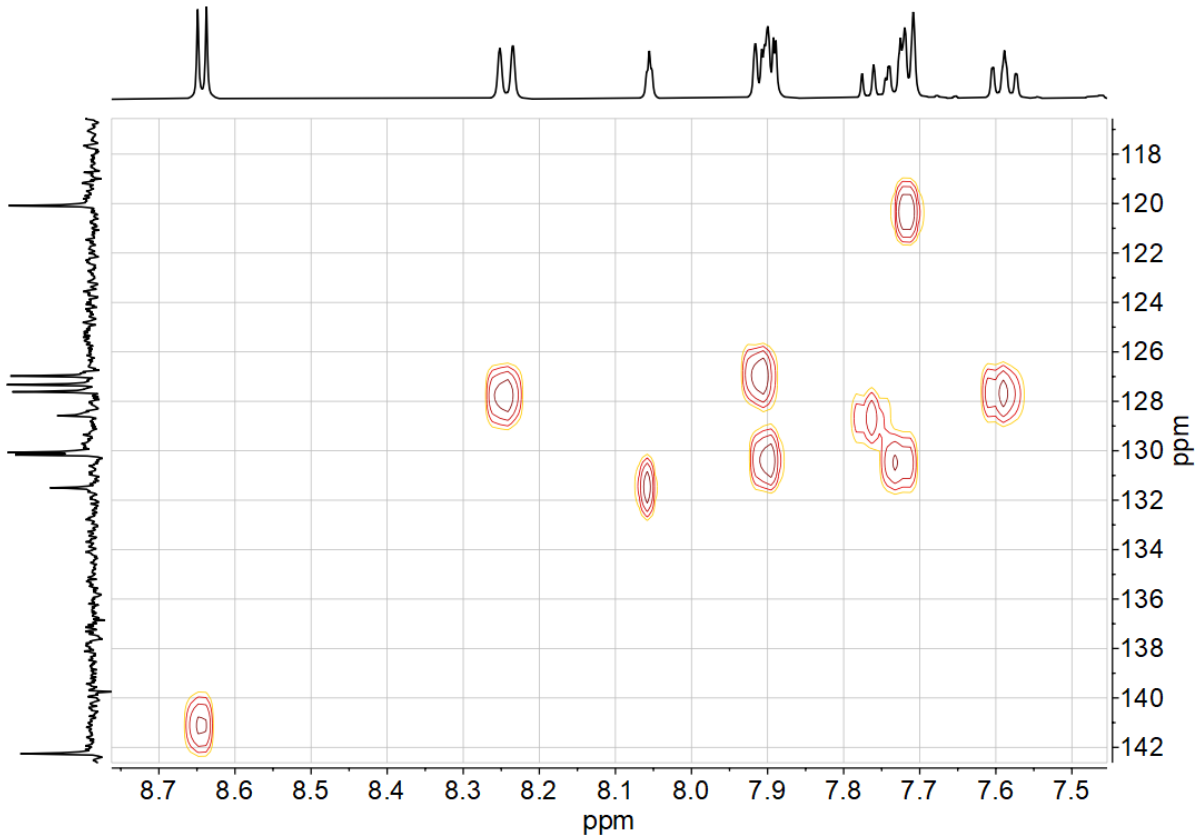

Figure 7-128 ^{1}H,^{13}C HSQC correlation spectrum of 2^{i}Qu(PhH)2^{i}Qu in $CDCl_3$.

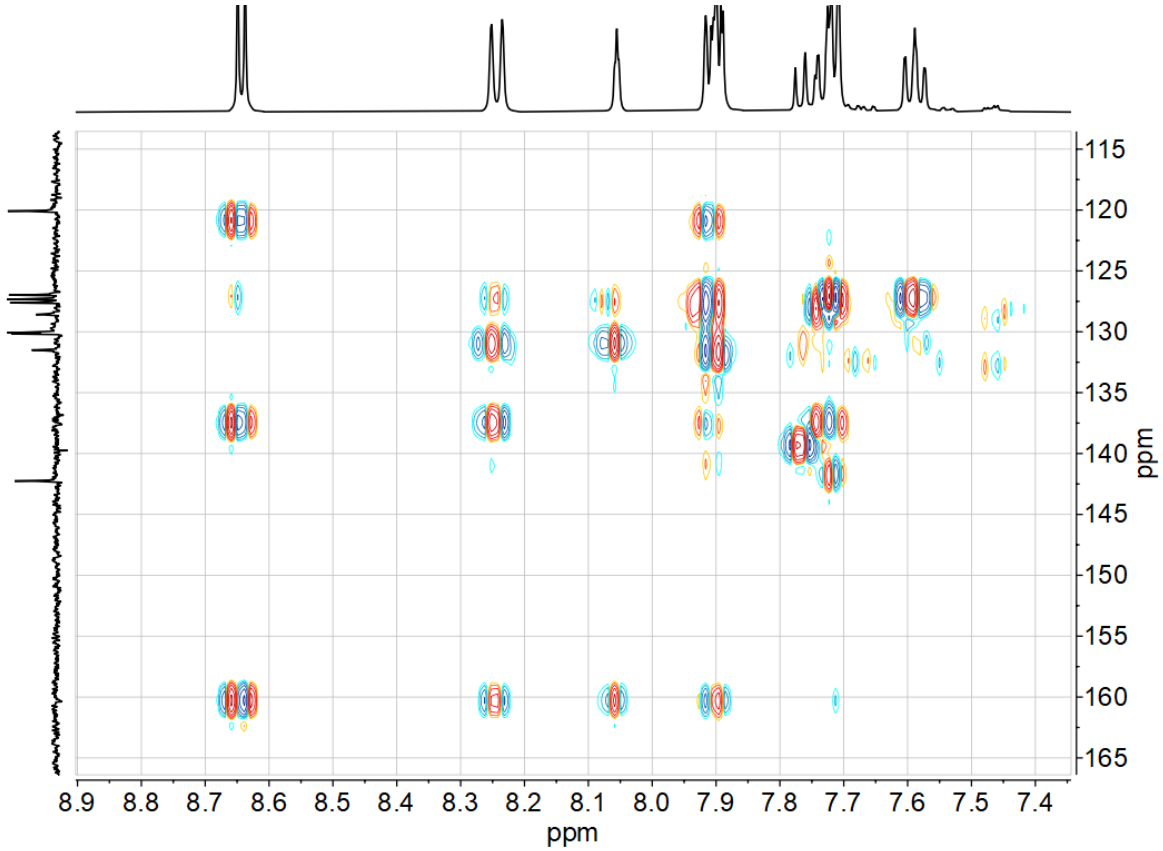

Figure 7-129 $^{1}H,^{13}C$ HMBC correlation spectrum of 2^{i}Qu(PhH)2^{i}Qu in $CDCl_3$.

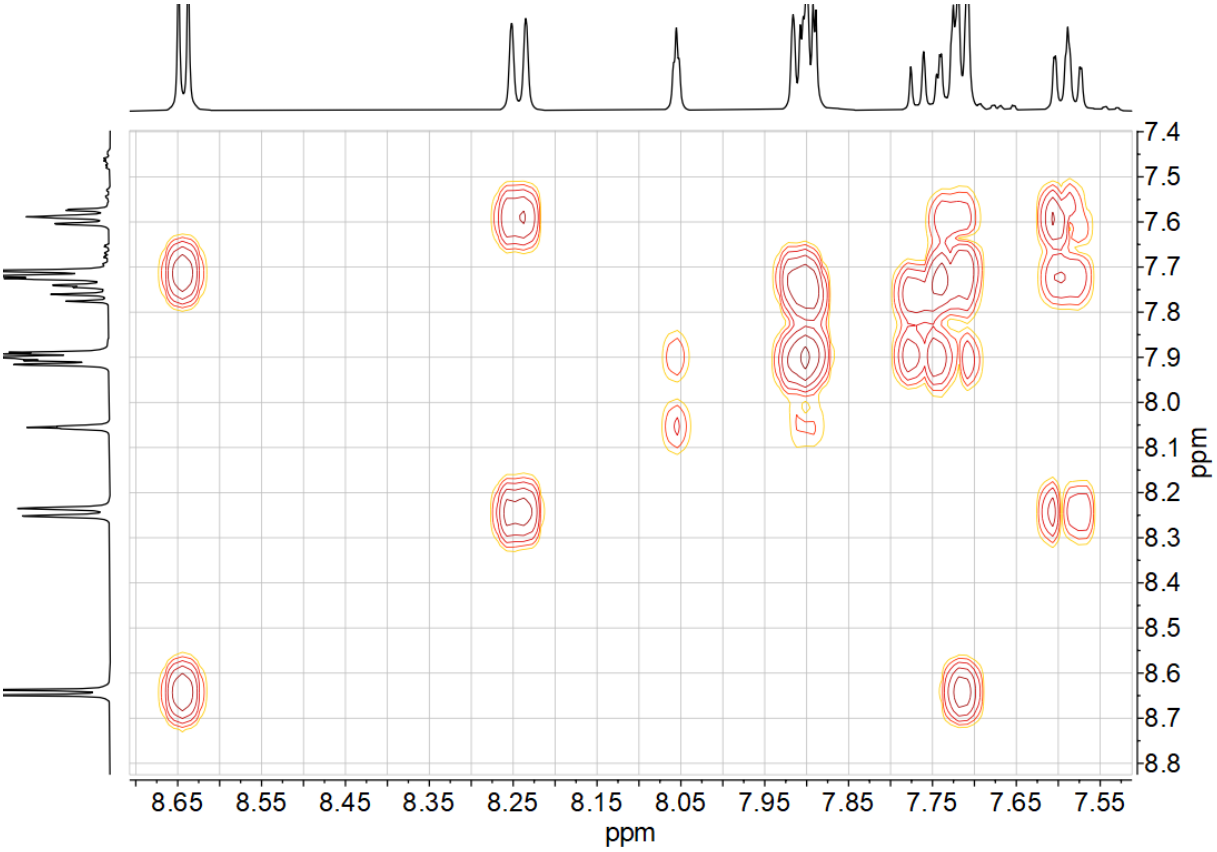

Figure 7-130 $^{1}H,^{1}H$ COSY correlation spectrum of 2^{i}Qu(PhH)2^{i}Qu in $CDCl_3$.

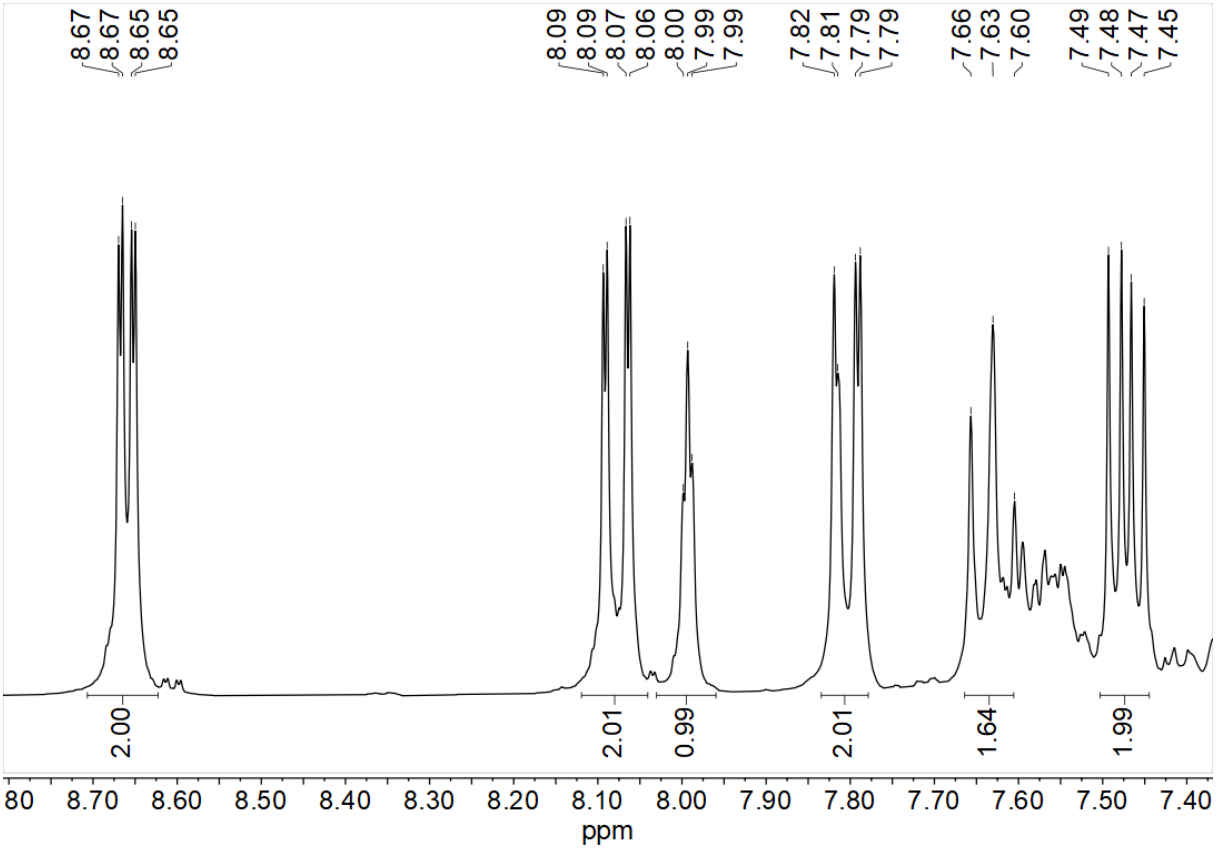

Figure 7-131 300 MHz ^{1}H NMR spectrum of 3ClPy(PhH)3ClPy in DMSO-d_6.

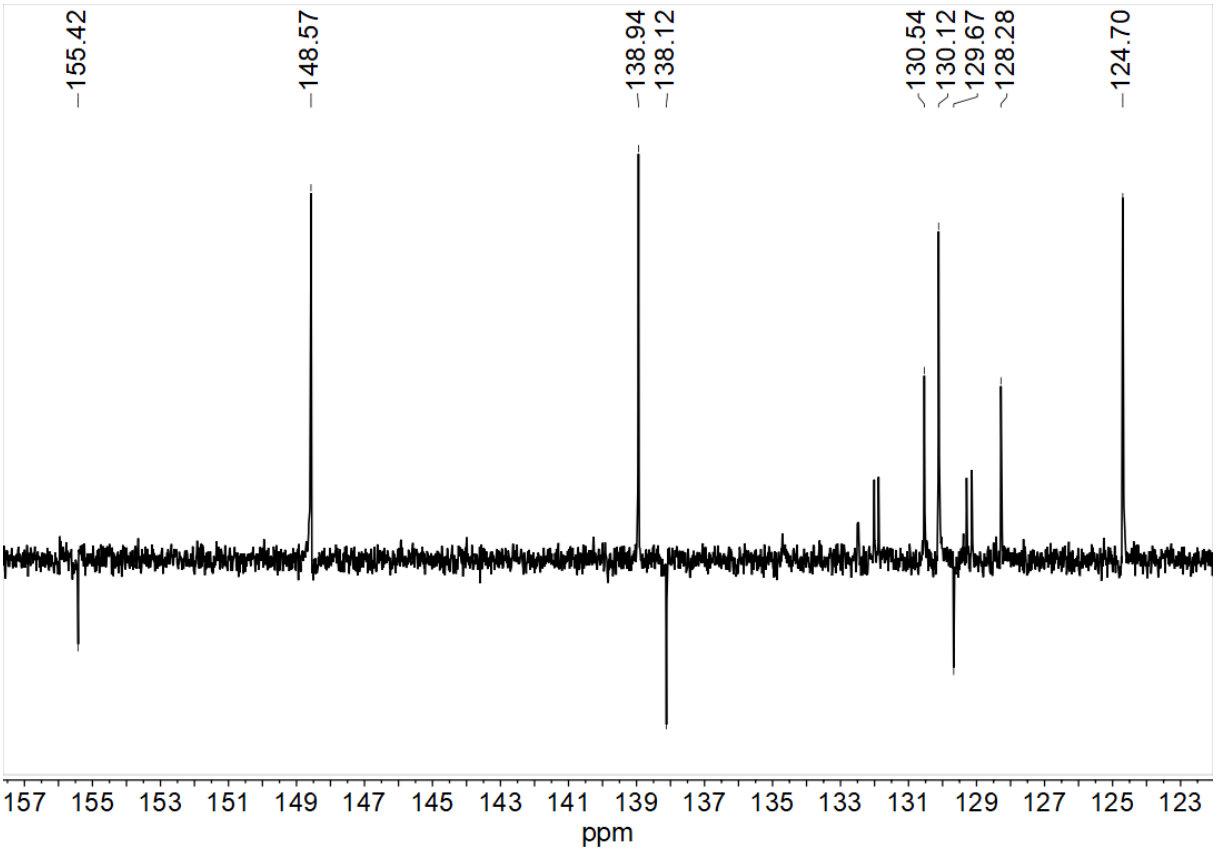

Figure 7-132 75 MHz ^{13}C NMR spectrum of 3ClPy(PhH)3ClPy in DMSO-d_6.

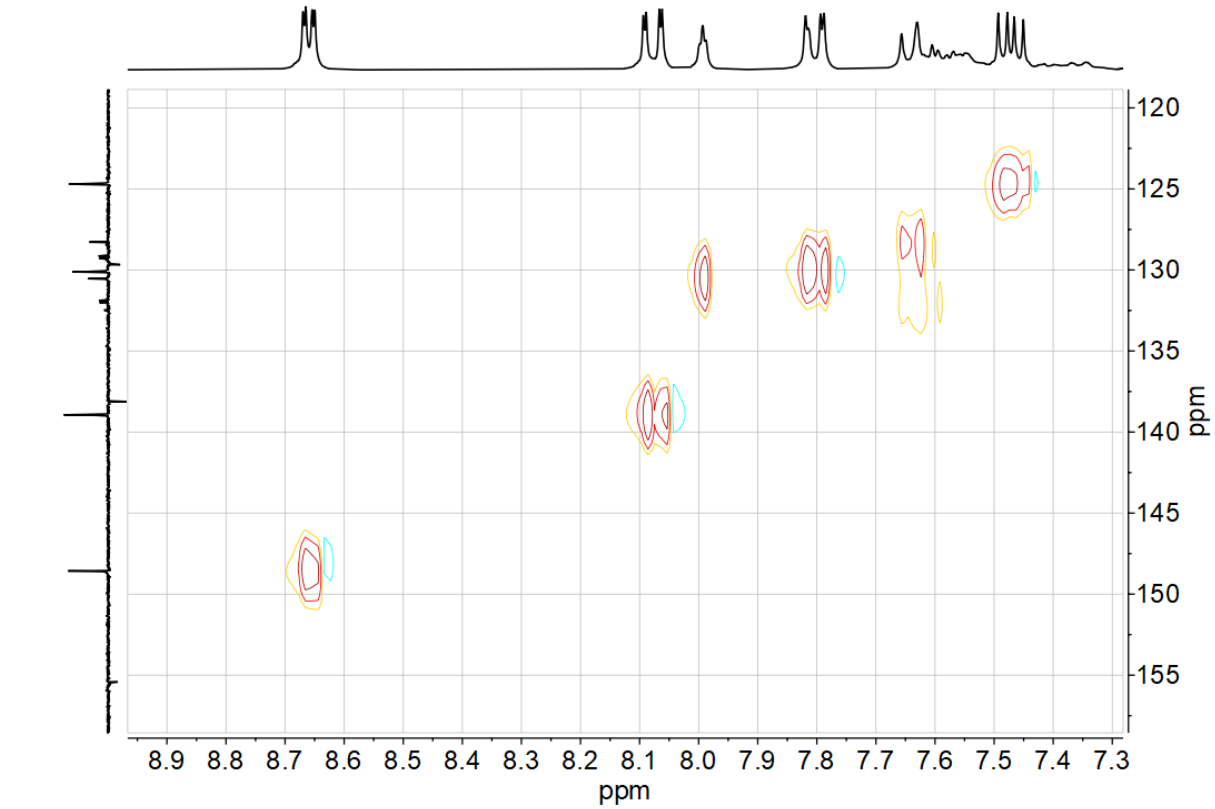

Figure 7-133 $^{1}H,^{13}C$ HSQC correlation spectrum of 3ClPy(PhH)3ClPy in DMSO-d_6.

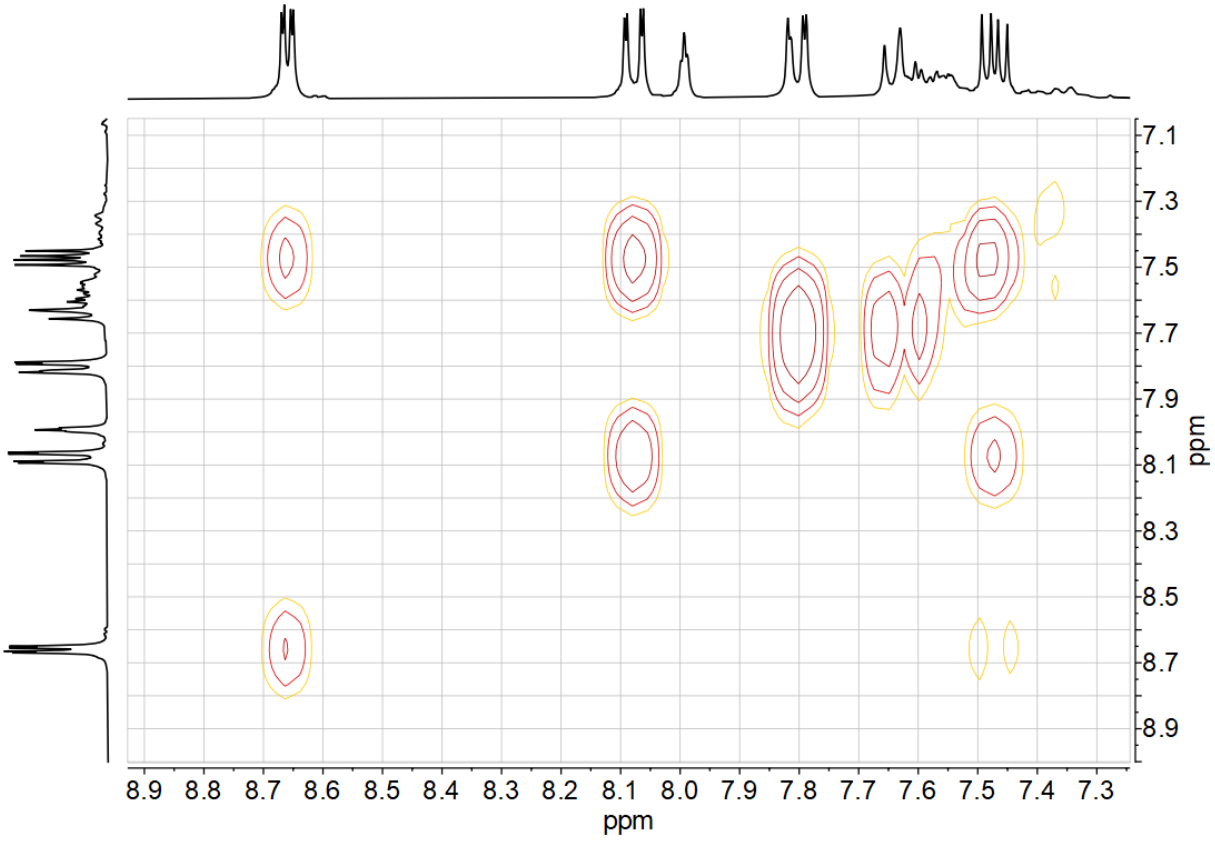

Figure 7-134 $^{1}H,^{1}H$ COSY correlation spectrum of 3ClPy(PhH)3ClPy in DMSO-d_6.

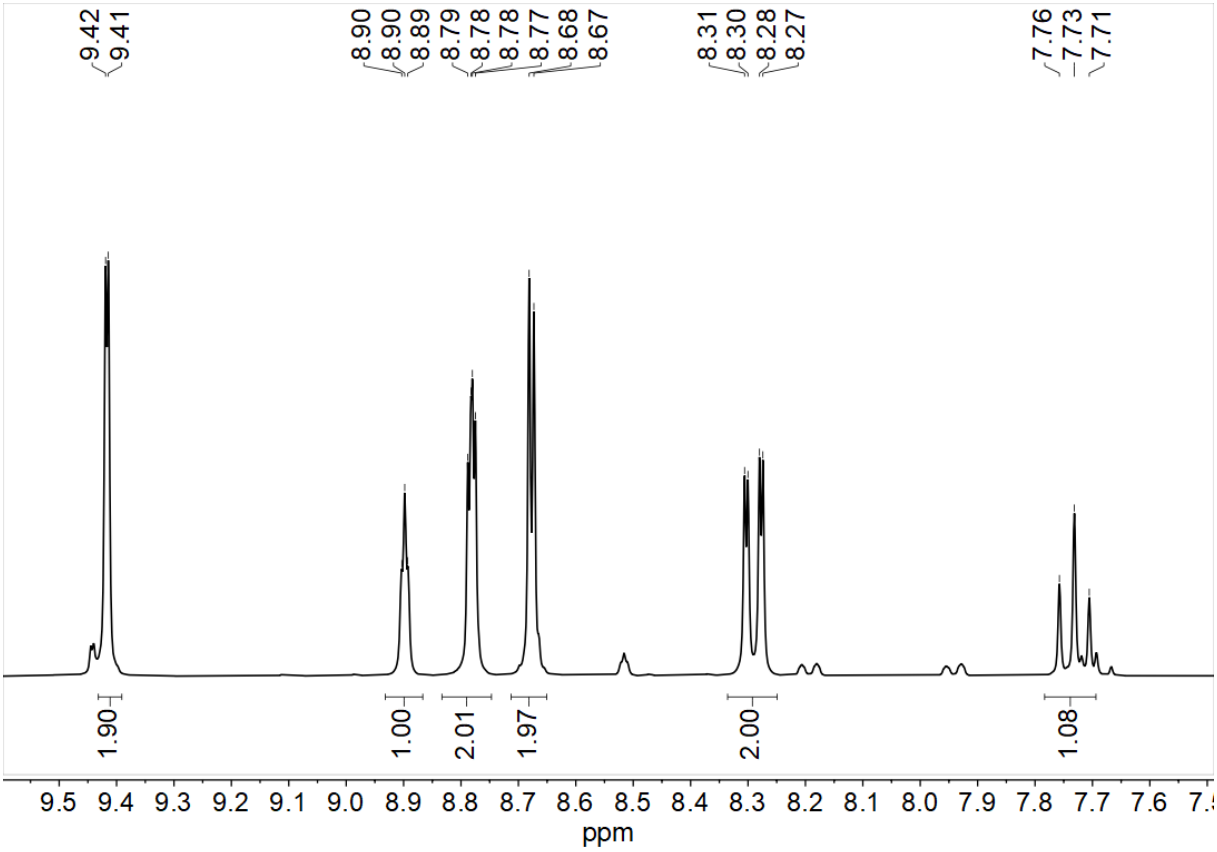

Figure 7-135 300 MHz ^{1}H NMR spectrum of Pz(PhH)Pz in DMSO-d_6.

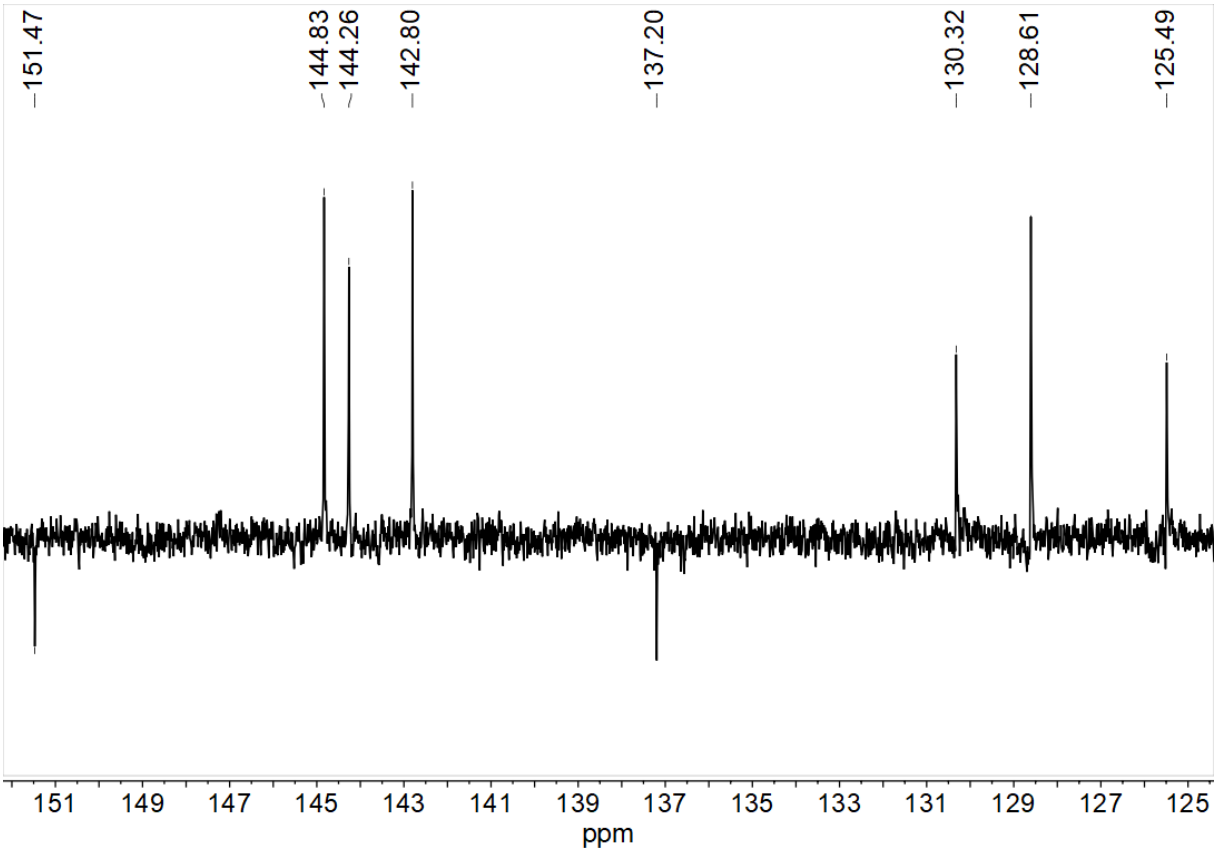

Figure 7-136 75 MHz ^{13}C NMR spectrum of Pz(PhH)Pz in DMSO-d_6.

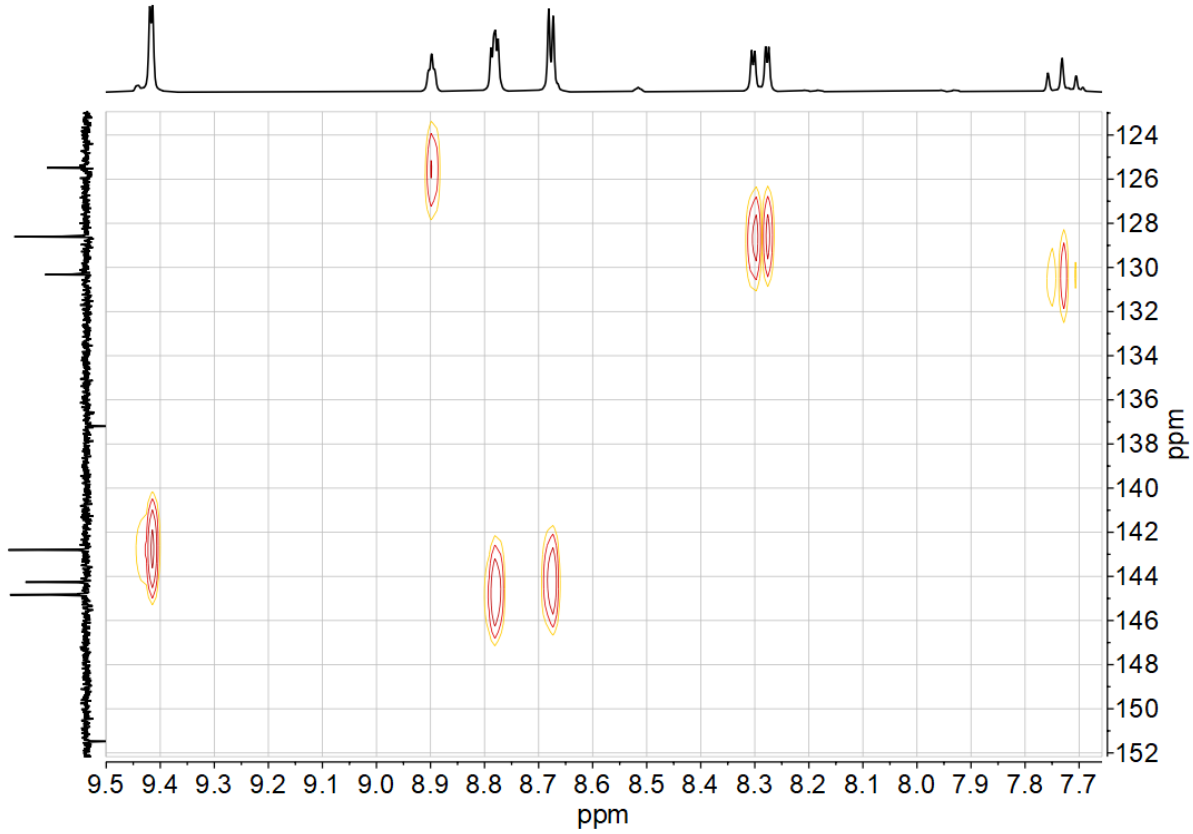

Figure 7-137 $^{1}H,^{13}C$ HSQC correlation spectrum of Pz(PhH)Pz in DMSO-d_6.

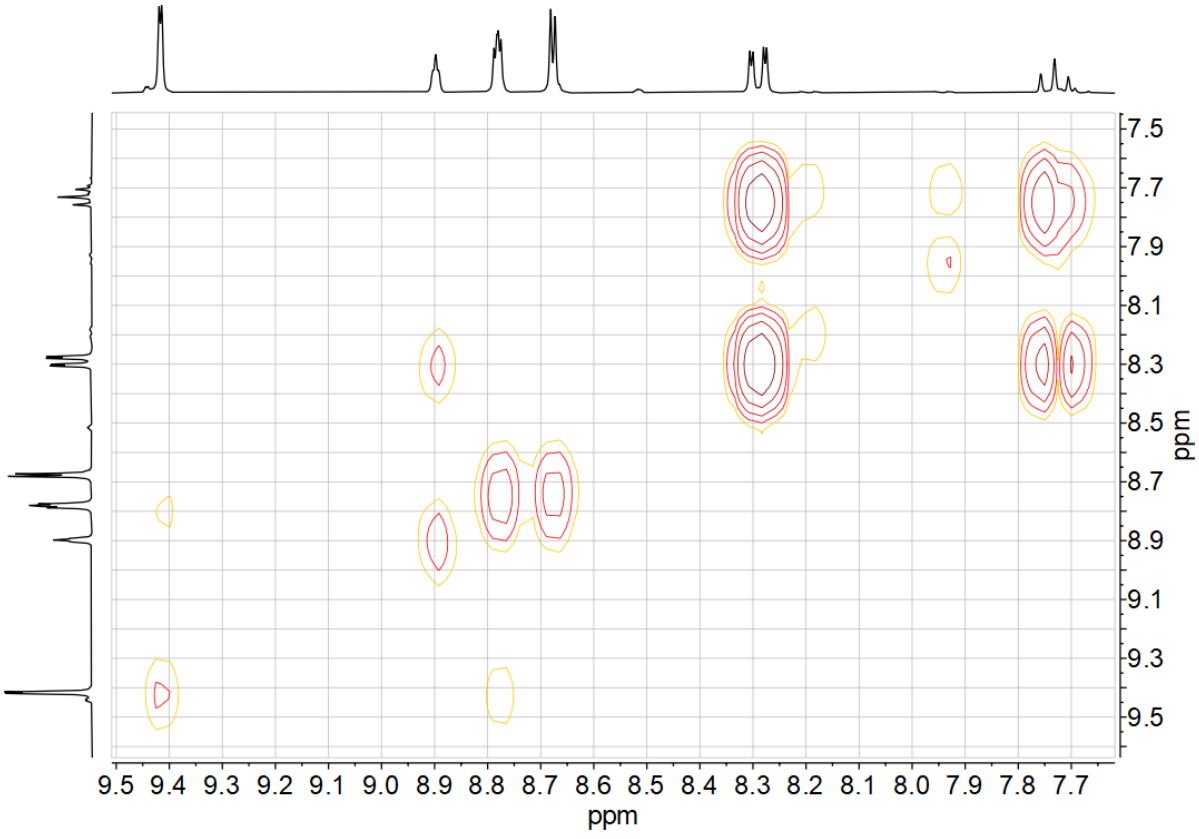

Figure 7-138 $^{1}H,^{1}H$ COSY correlation spectrum of Pz(PhH)Pz in DMSO-d_6.

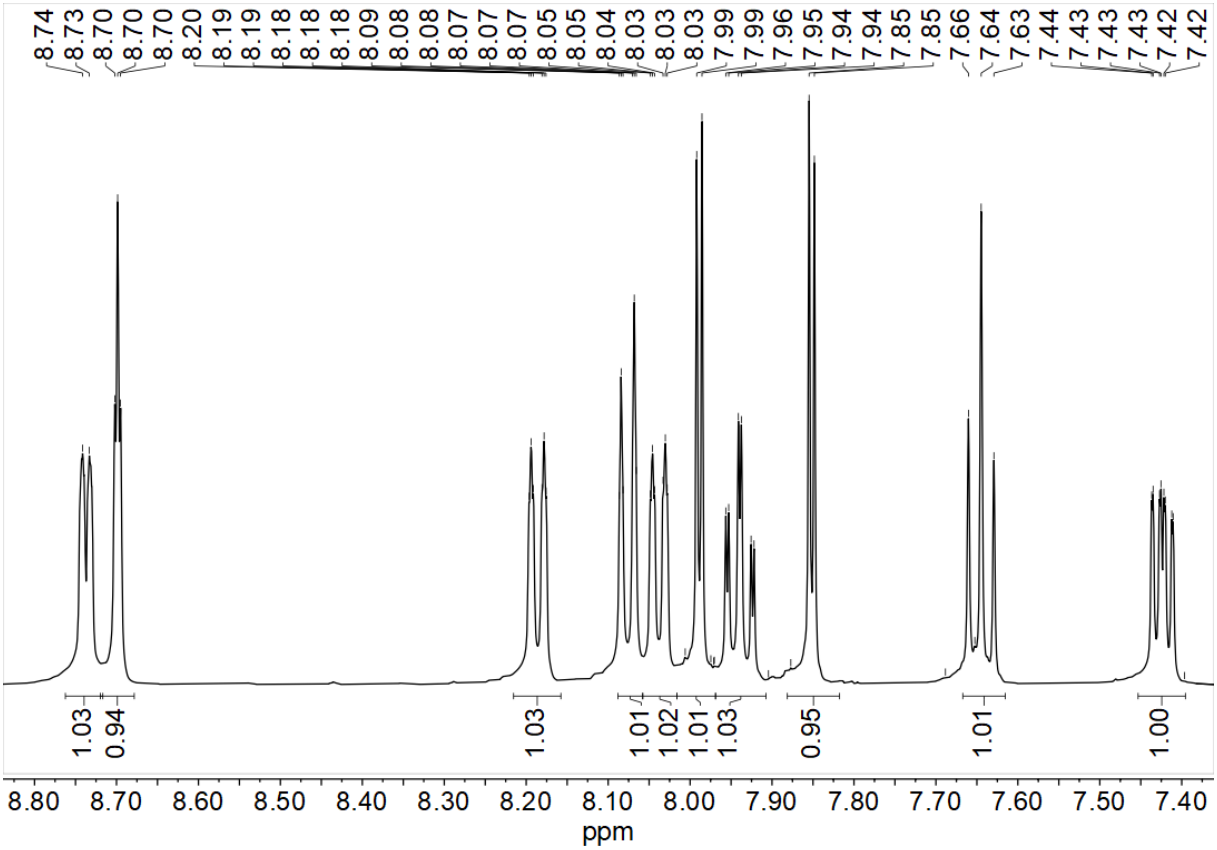

Figure 7-139 500 MHz ^{1}H NMR spectrum of 2Tz(PhH)Py in DMSO-d_6.

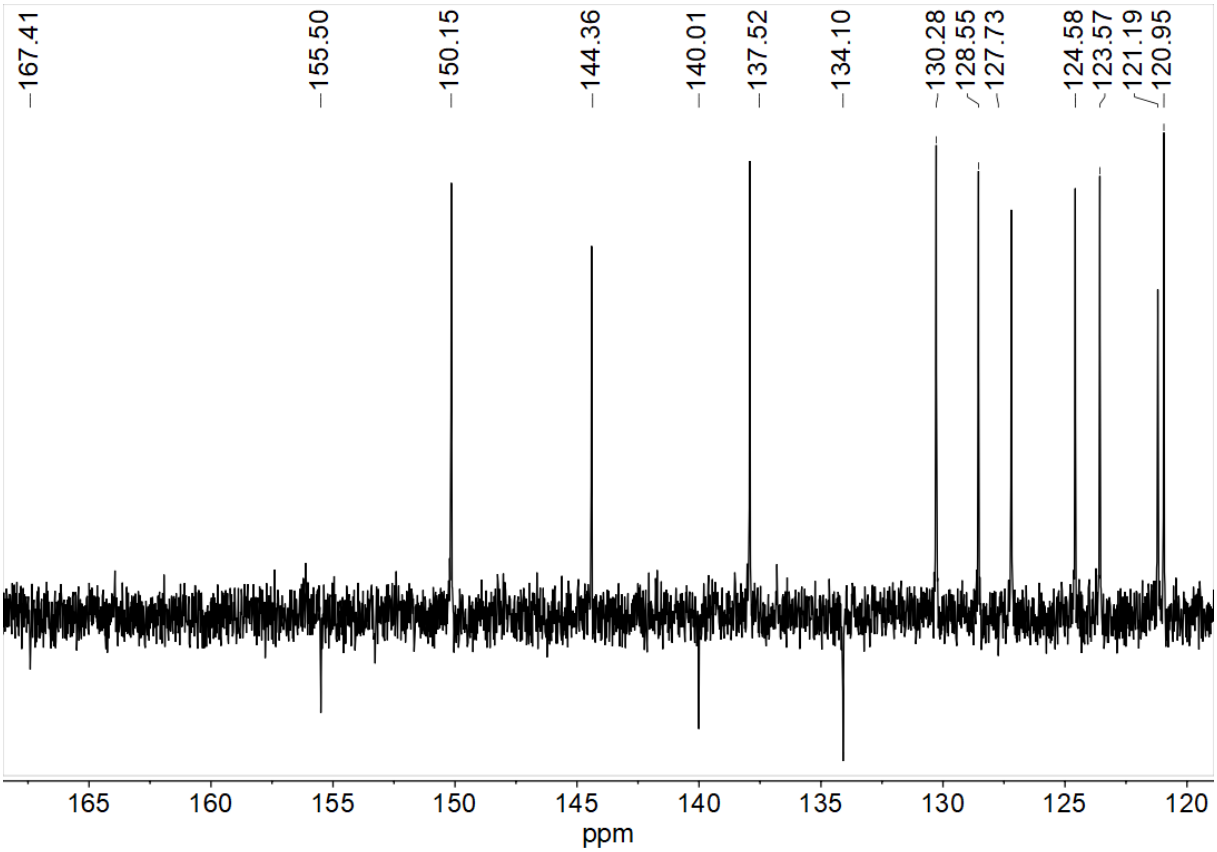

Figure 7-140 75 MHz ^{13}C NMR spectrum of 2Tz(PhH)Py in DMSO-d_6.

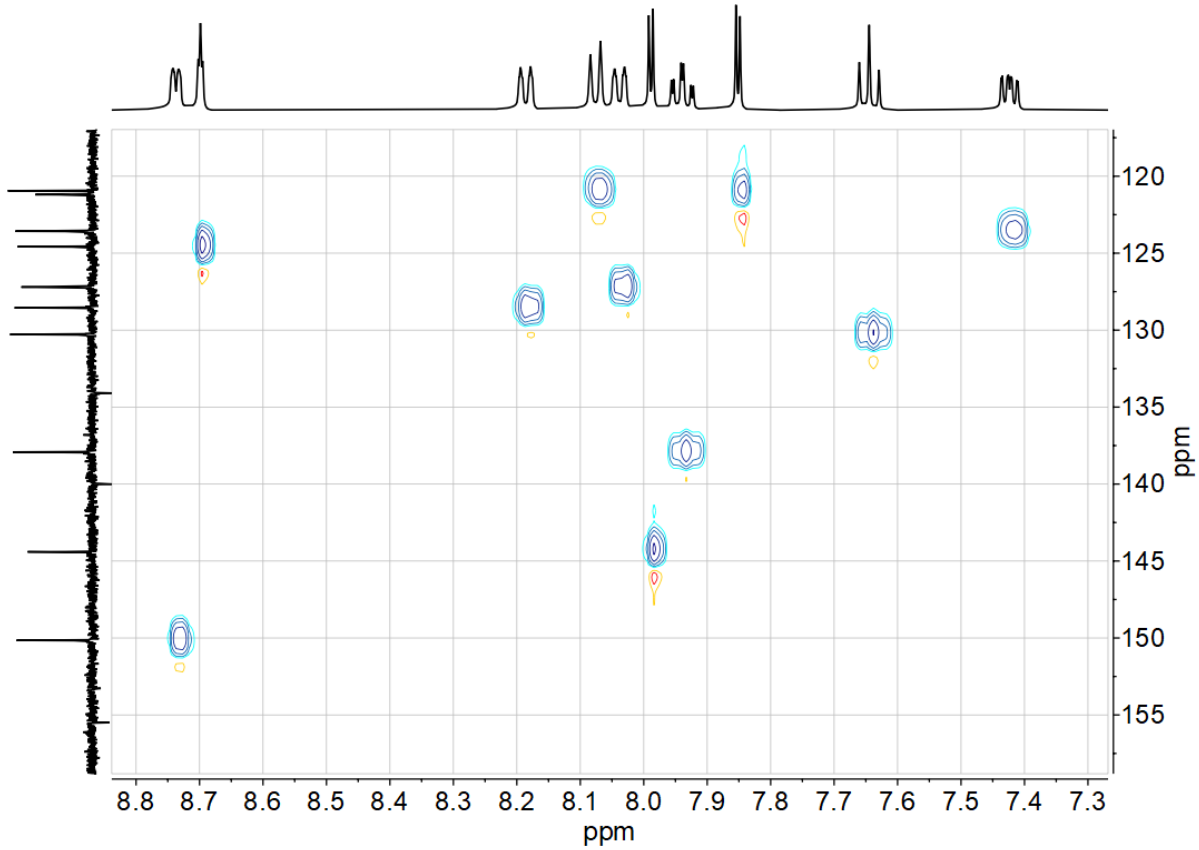

Figure 7-141 $^{1}H,^{13}C$ HSQC correlation spectrum of 2Tz(PhH)Py in DMSO-d_6.

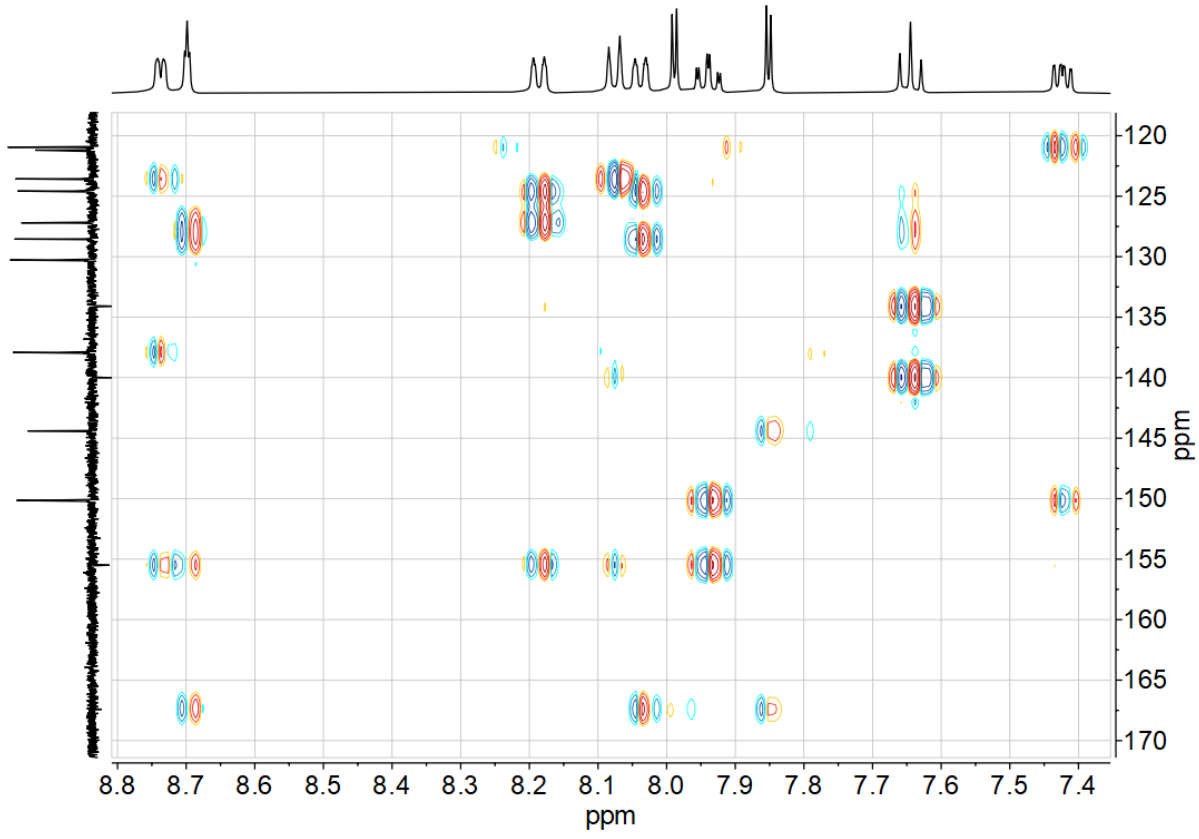

Figure 7-142 $^{1}H,^{13}C$ HMBC correlation spectrum of 2Tz(PhH)Py in DMSO-d_6.

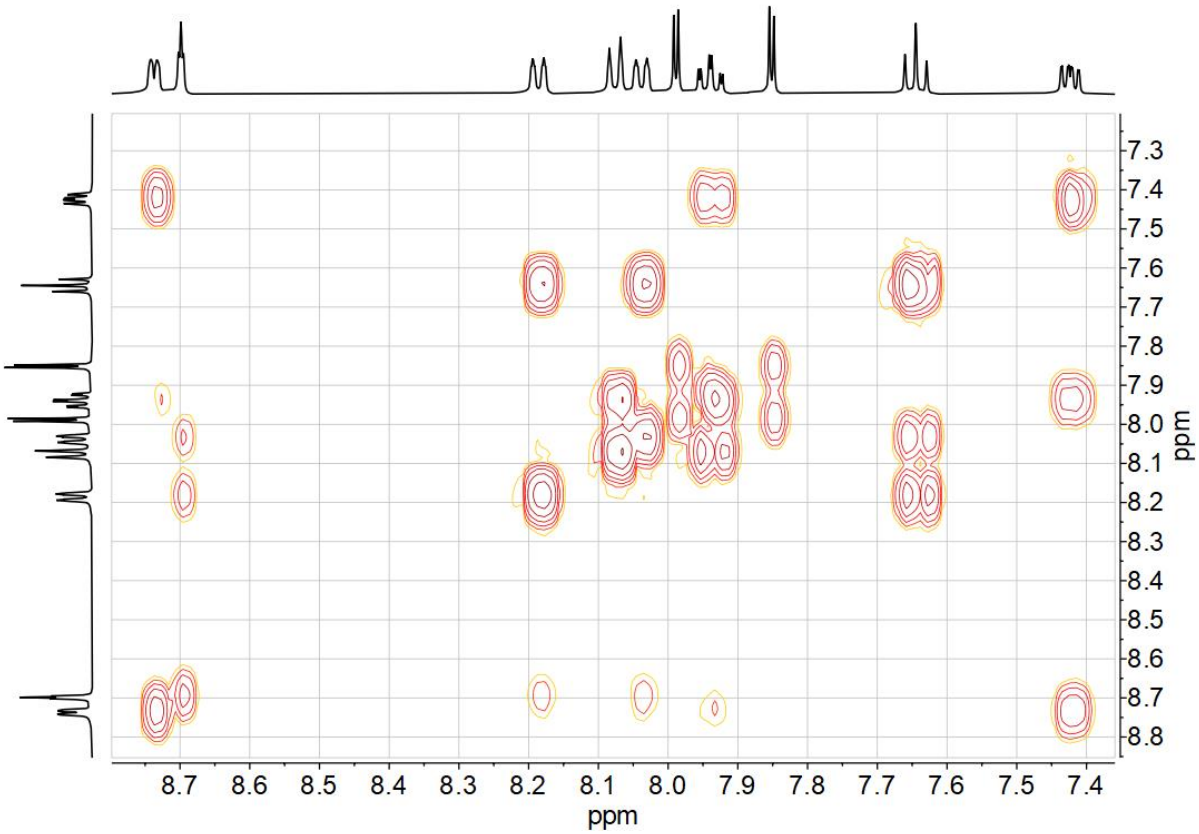

Figure 7-143 ^{1}H,^{1}H COSY correlation spectrum of 2Tz(PhH)Py in DMSO-d_6.

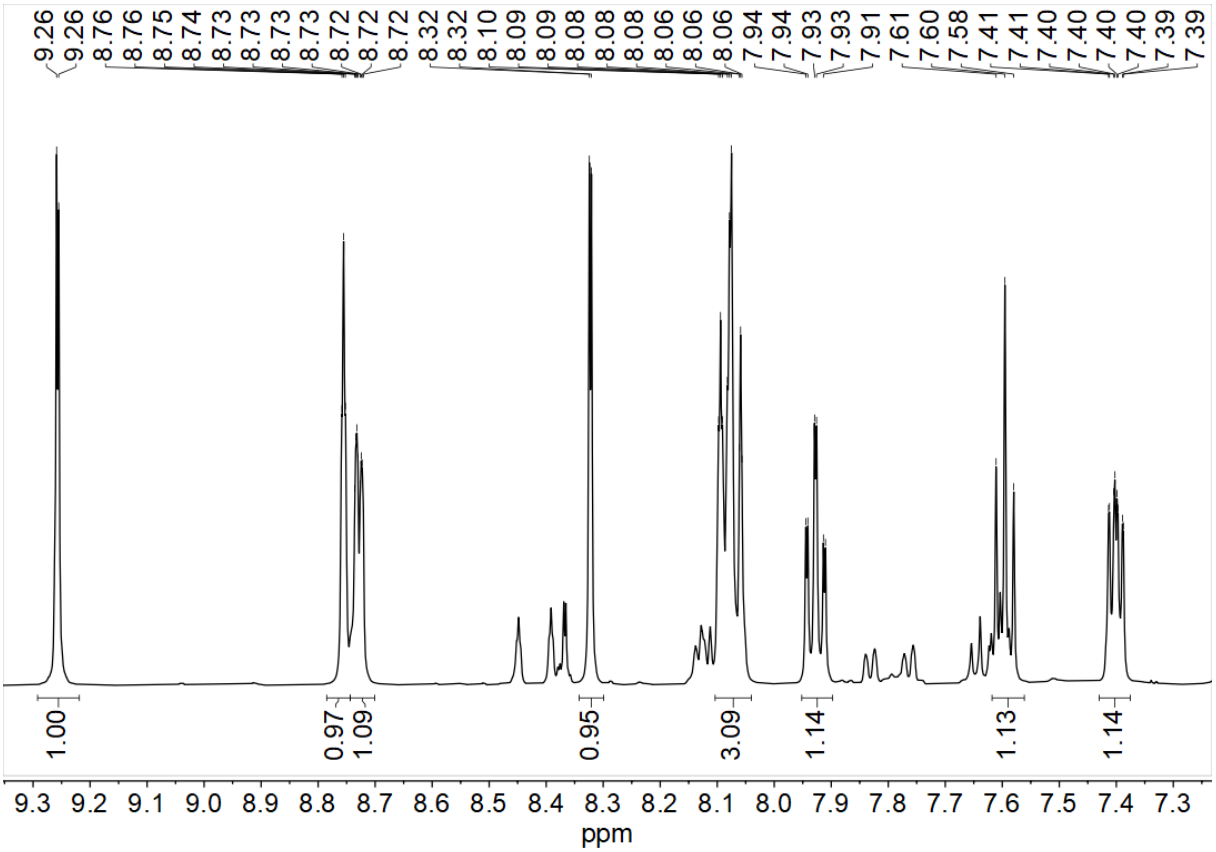

Figure 7-144 500 MHz ^{1}H NMR spectrum of 4Tz(PhH)Py in DMSO-d_6.

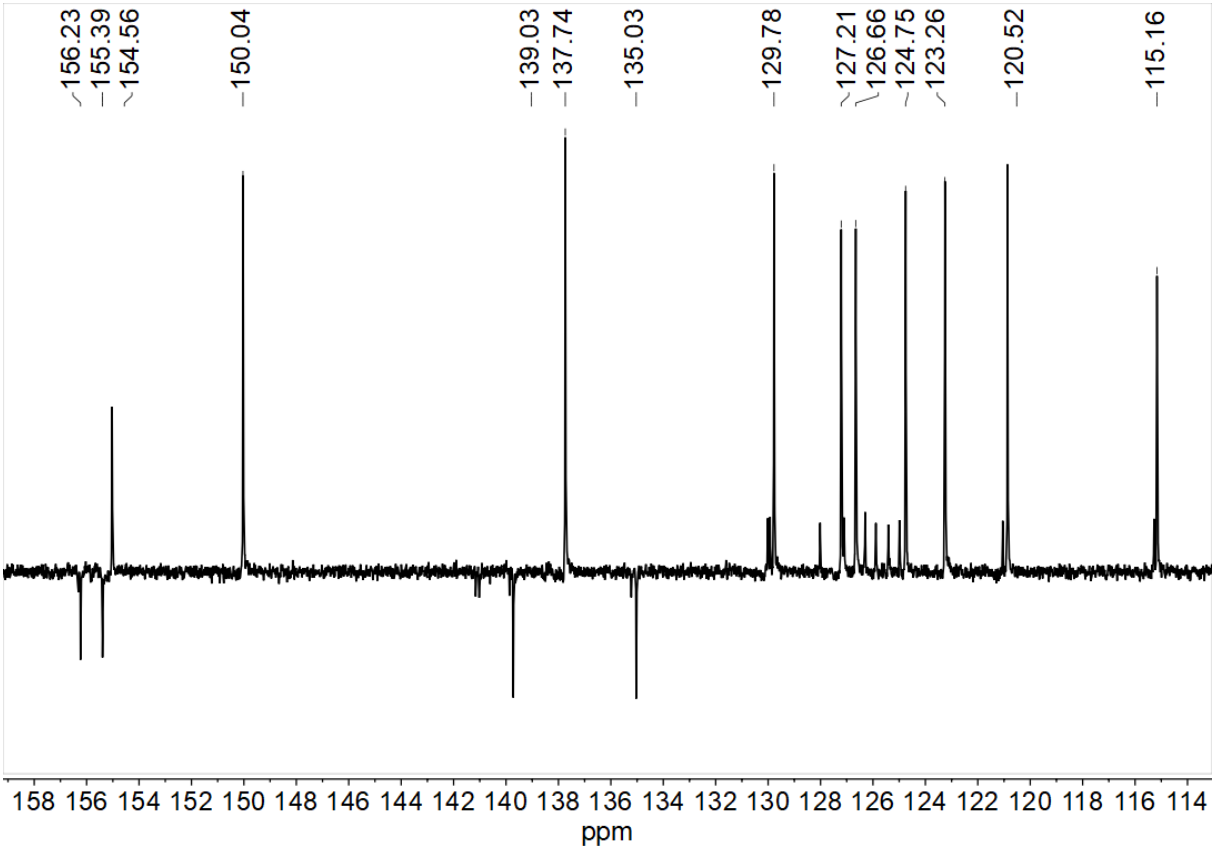

Figure 7-145 75 MHz ^{13}C NMR spectrum of 4Tz(PhH)Py in DMSO-d_6.

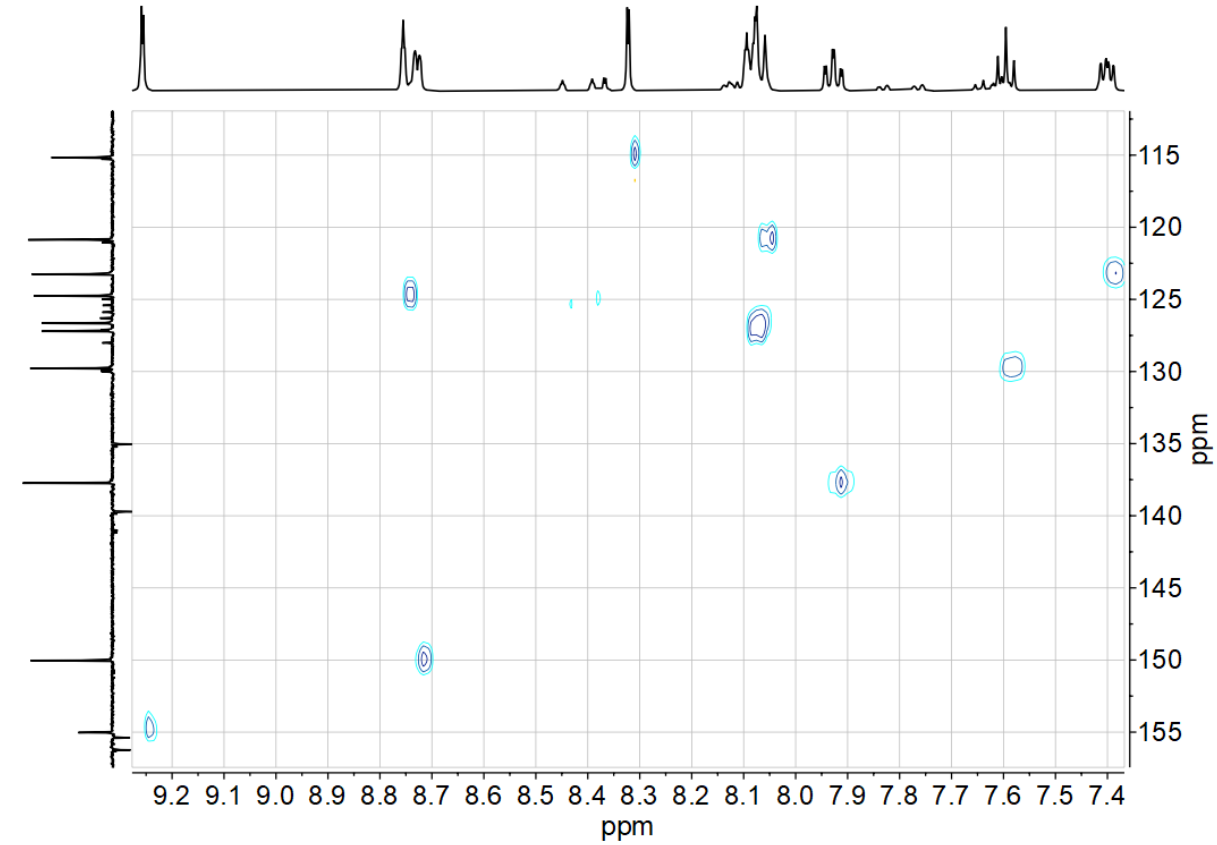

Figure 7-146 ^{1}H,^{13}C HSQC correlation spectrum of 4Tz(PhH)Py in DMSO-d_6.

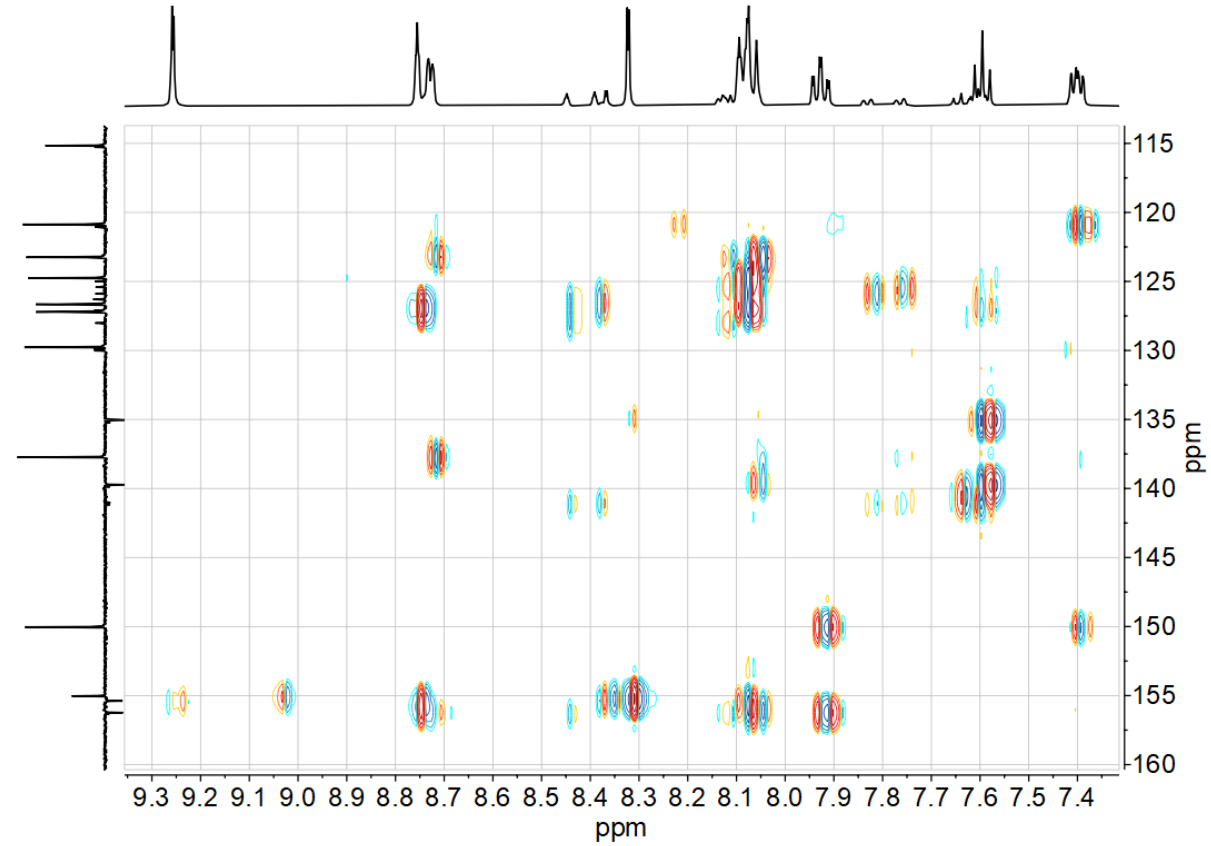

Figure 7-147 $^{1}H,^{13}C$ HMBC correlation spectrum of 4Tz(PhH)Py in DMSO-d_6.

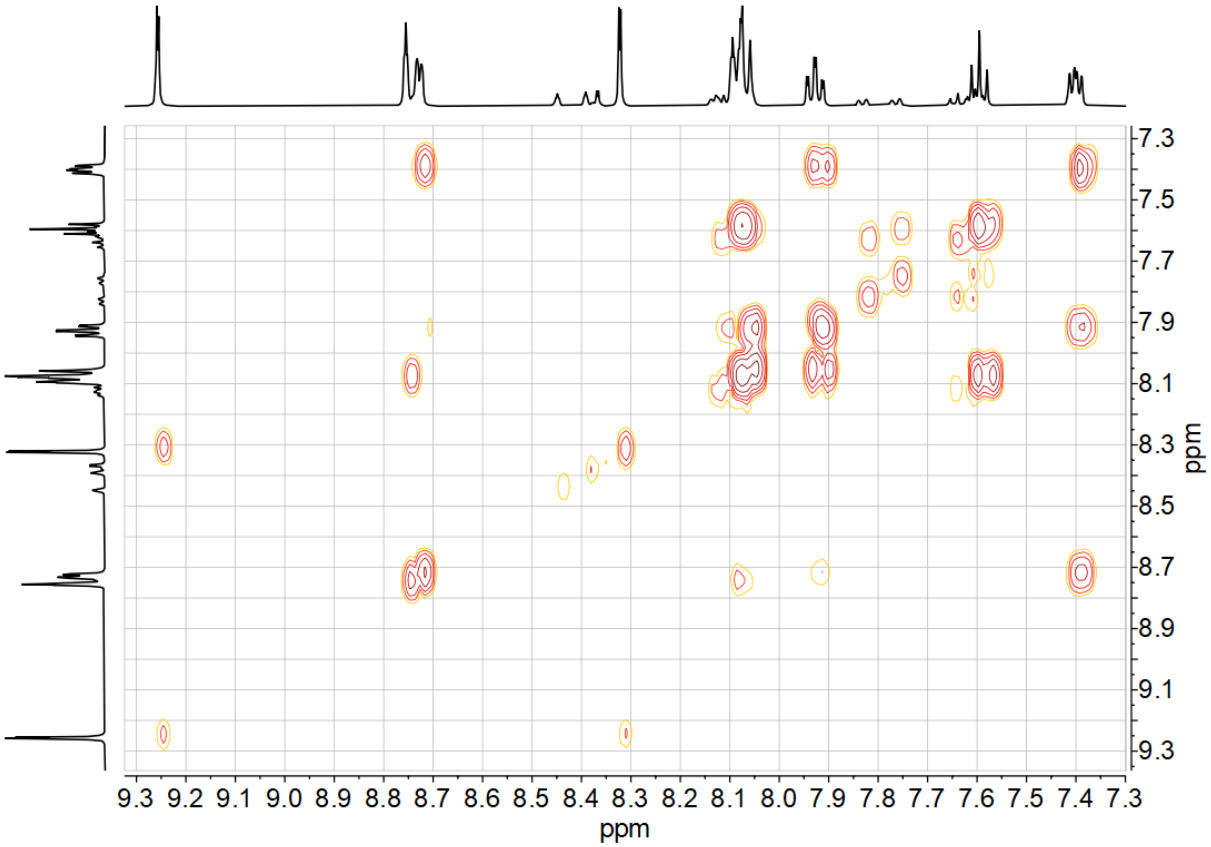

Figure 7-148 $^{1}H,^{1}H$ COSY correlation spectrum of 4Tz(PhH)Py in DMSO-d_6.

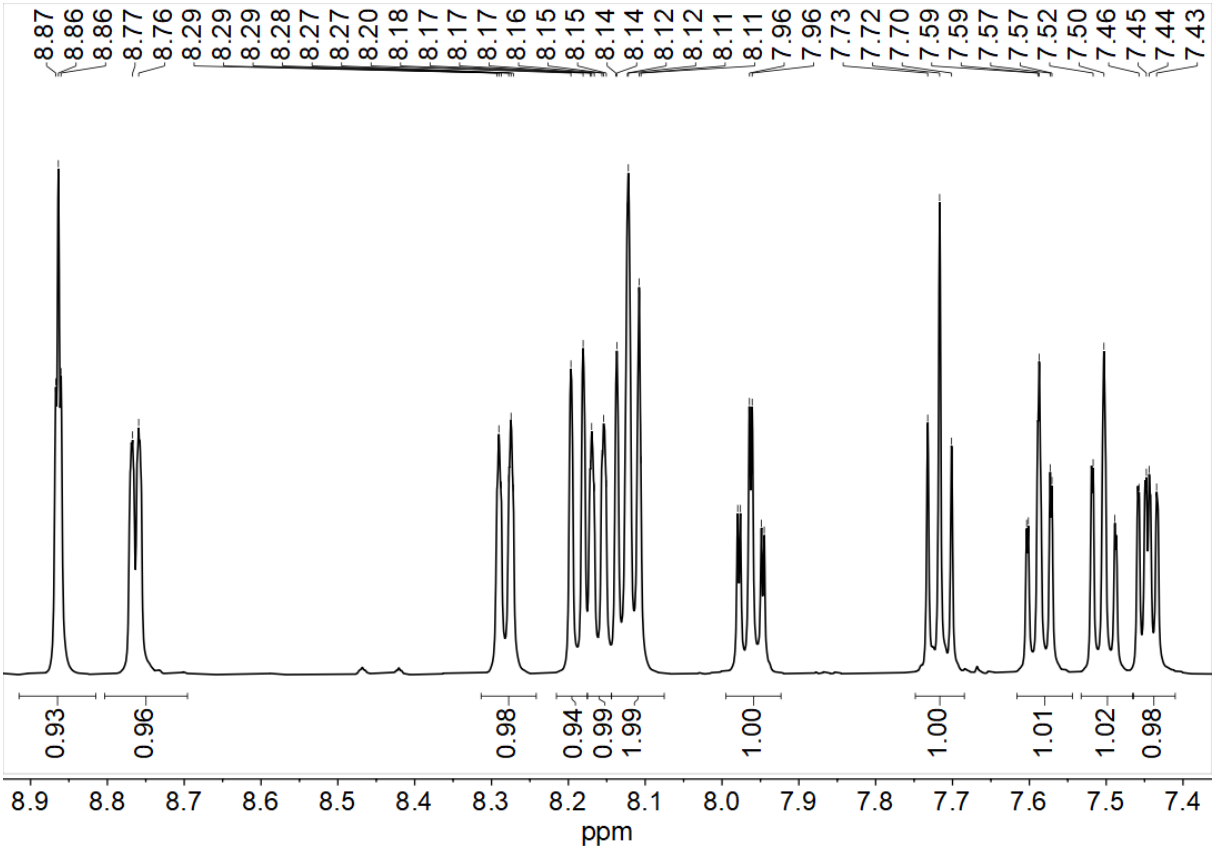

Figure 7-149 500 MHz ^{1}H NMR spectrum of 2Btz(PhH)Py in DMSO-d_6.

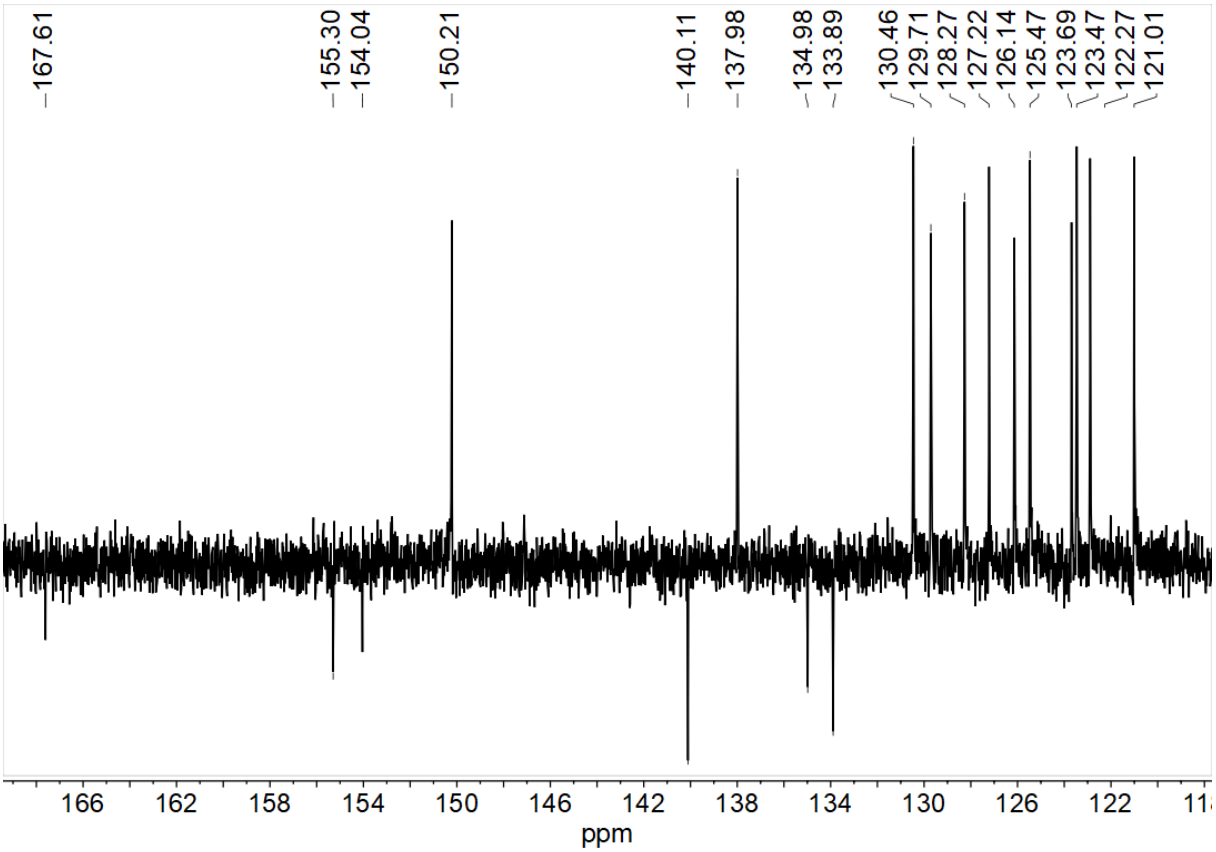

Figure 7-150 75 MHz ^{13}C NMR spectrum of 2Btz(PhH)Py in DMSO-d_6.

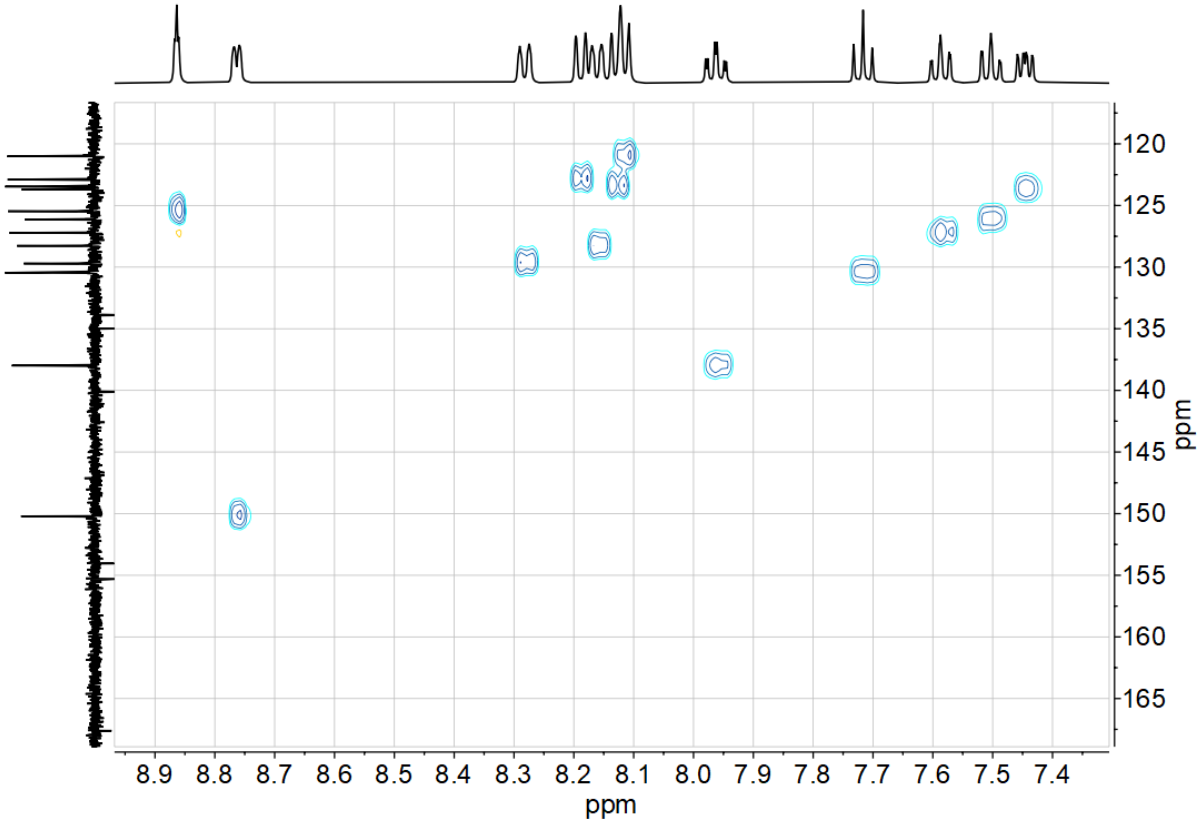

Figure 7-151 $^{1}H,^{13}C$ HSQC correlation spectrum of 2Btz(PhH)Py in DMSO-d_6.

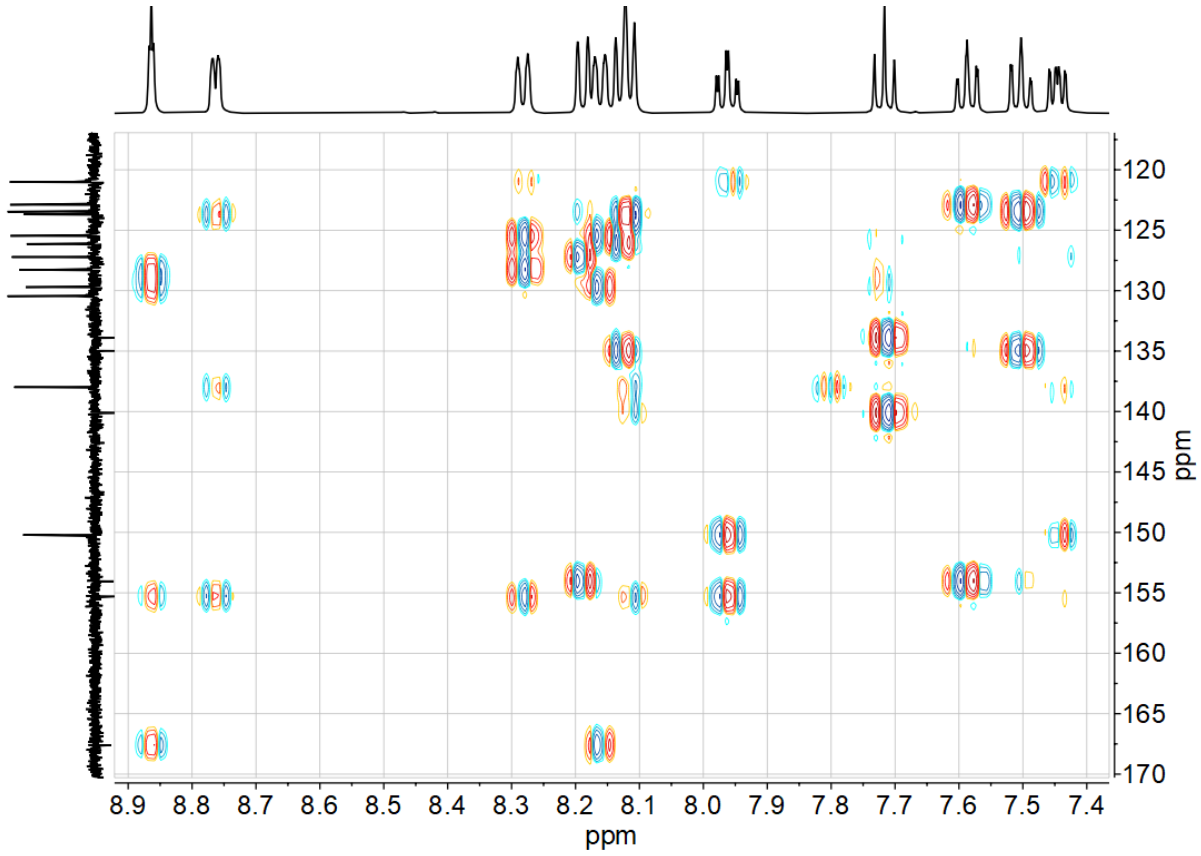

Figure 7-152 $^{1}H,^{13}C$ HMBC correlation spectrum of 2Btz(PhH)Py in DMSO-d_6.

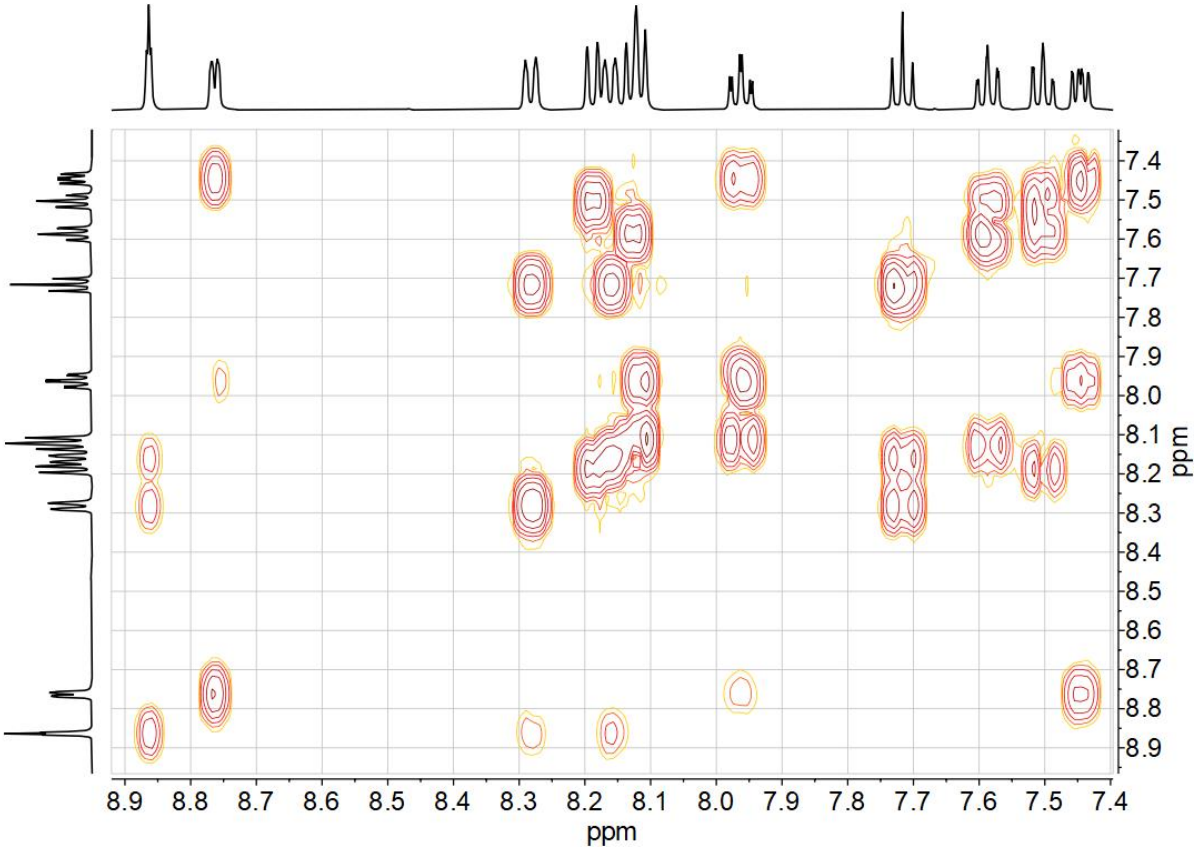

Figure 7-153 ^{1}H,^{1}H COSY correlation spectrum of 2Btz(PhH)Py in DMSO-d_6.

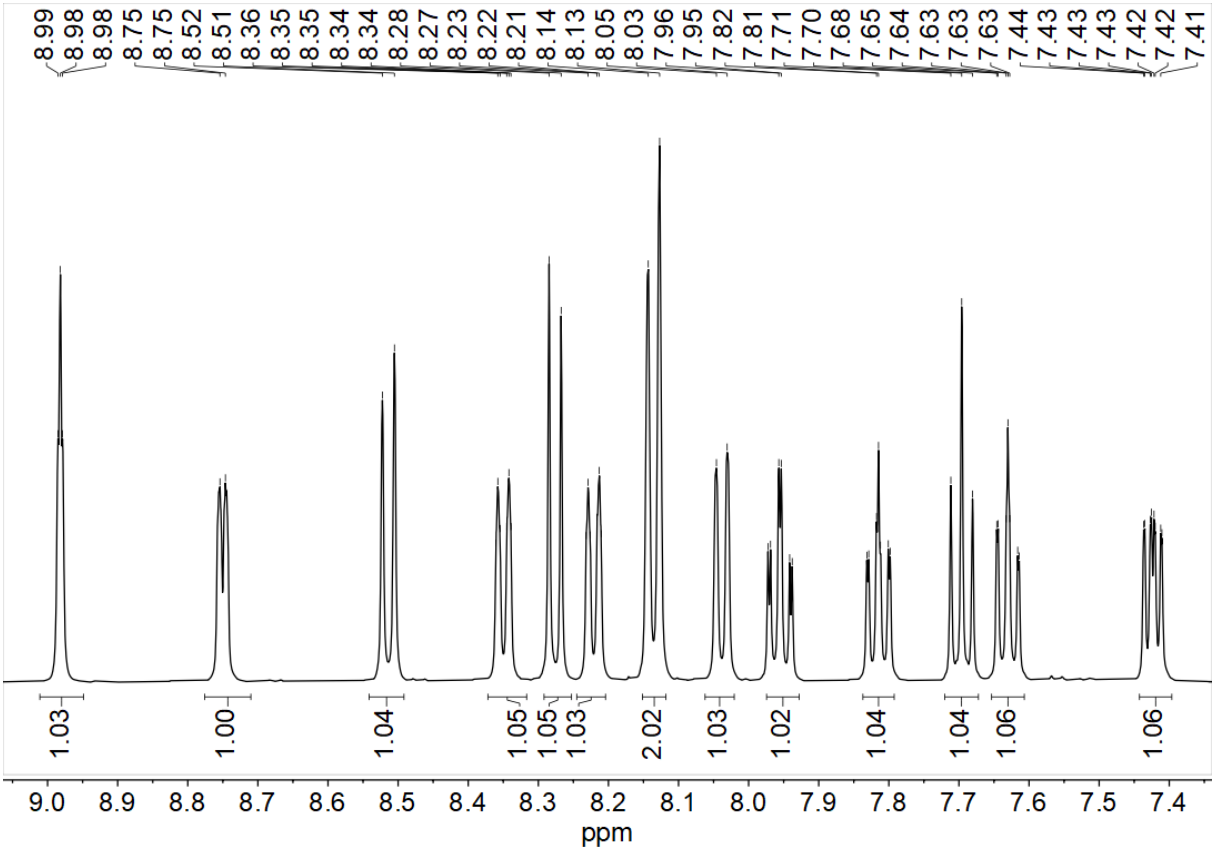

Figure 7-154 500 MHz ^{1}H NMR spectrum of 2Qu(PhH)Py in DMSO-d_6.

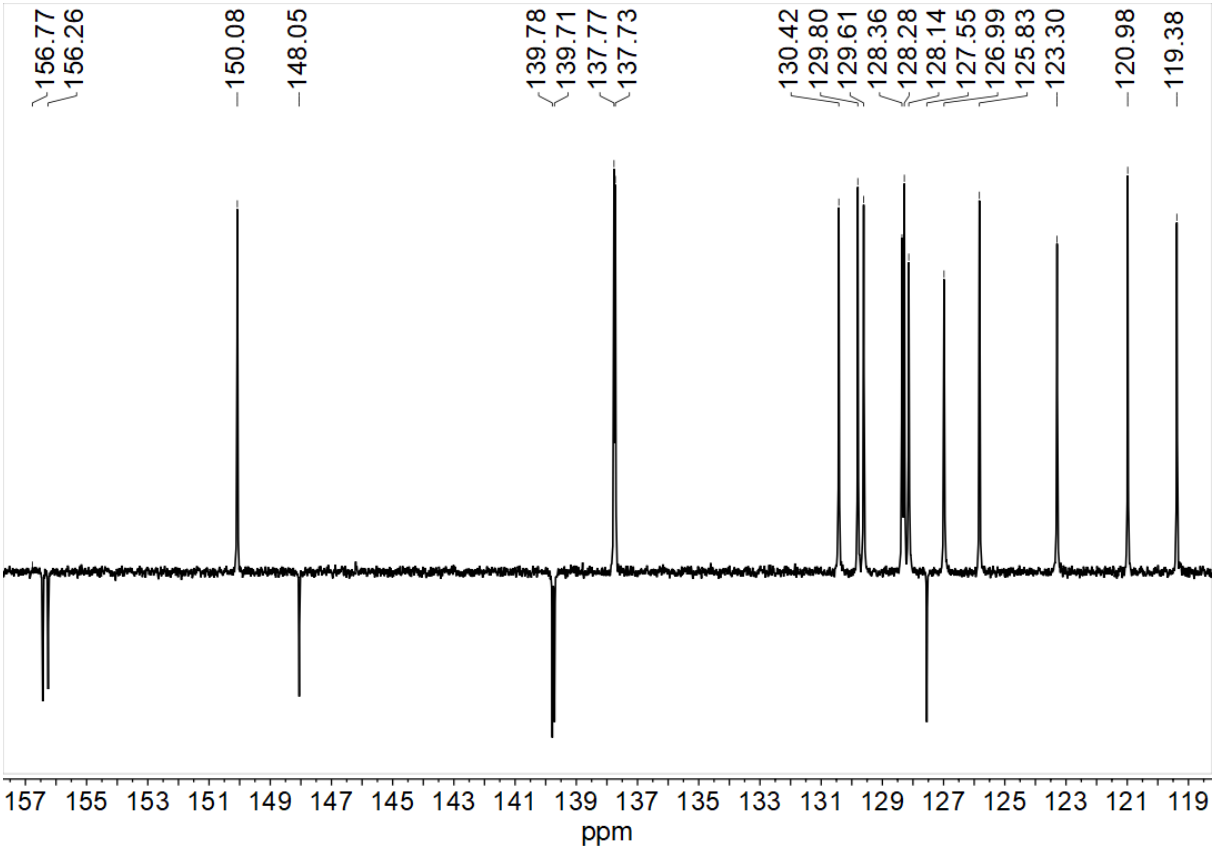

Figure 7-155 75 MHz ^{13}C NMR spectrum of 2Qu(PhH)Py in DMSO-d_6.

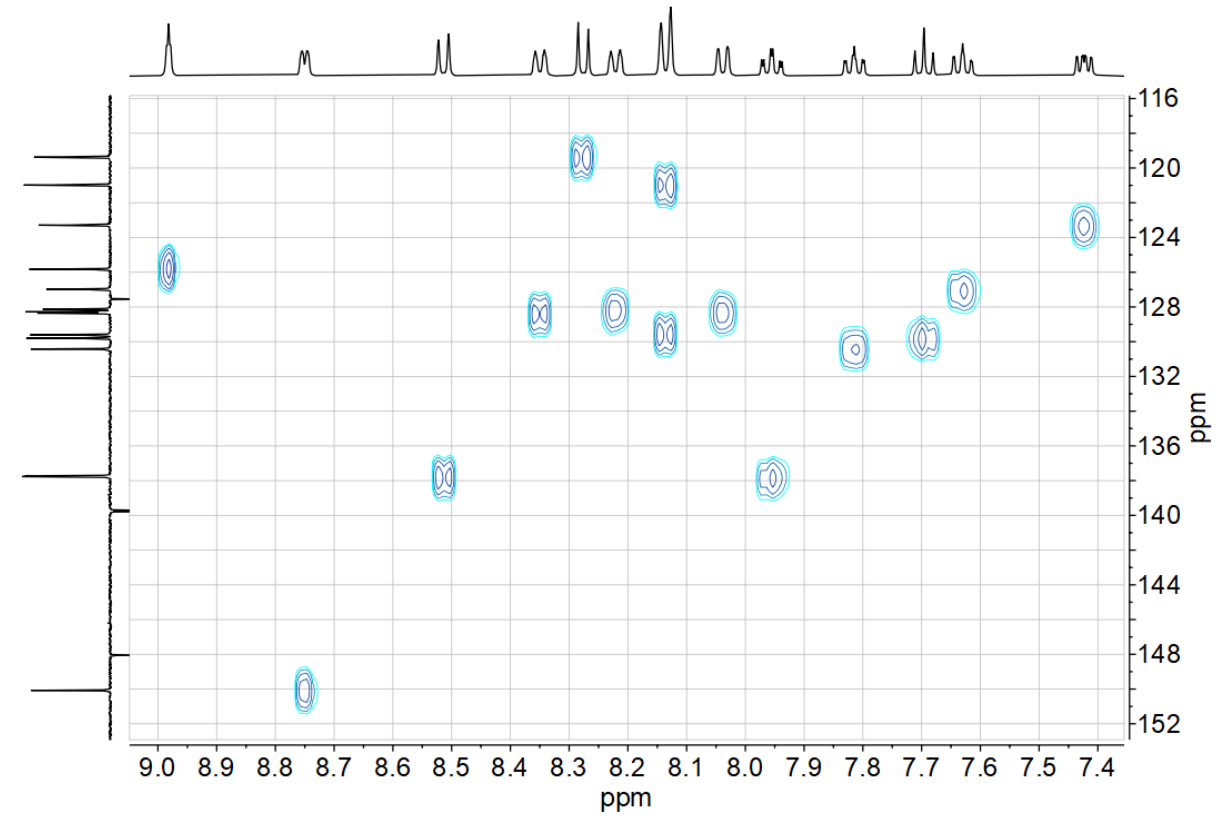

Figure 7-156 ^{1}H,^{13}C HSQC correlation spectrum of 2Qu(PhH)Py in DMSO-d_6.

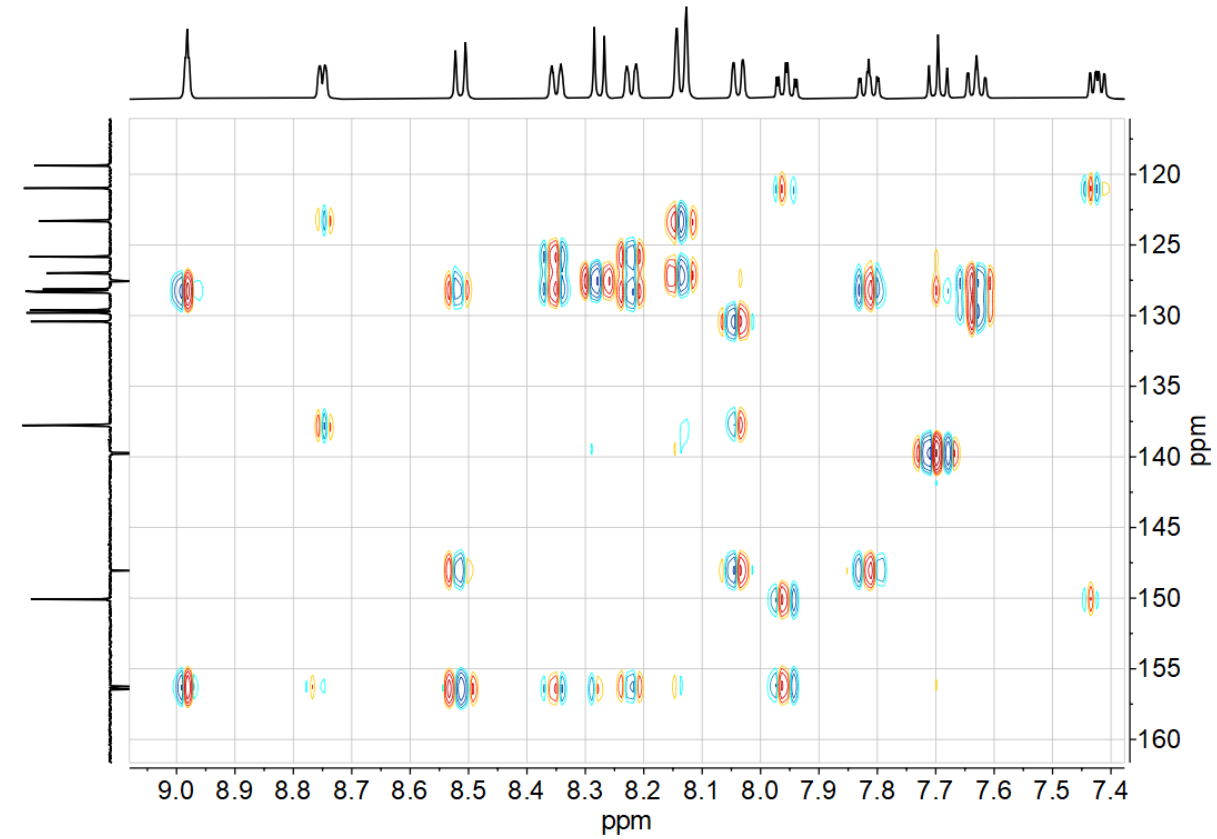

Figure 7-157 $^{1}H,^{13}C$ HMBC correlation spectrum of 2Qu(PhH)Py in DMSO-d_6.

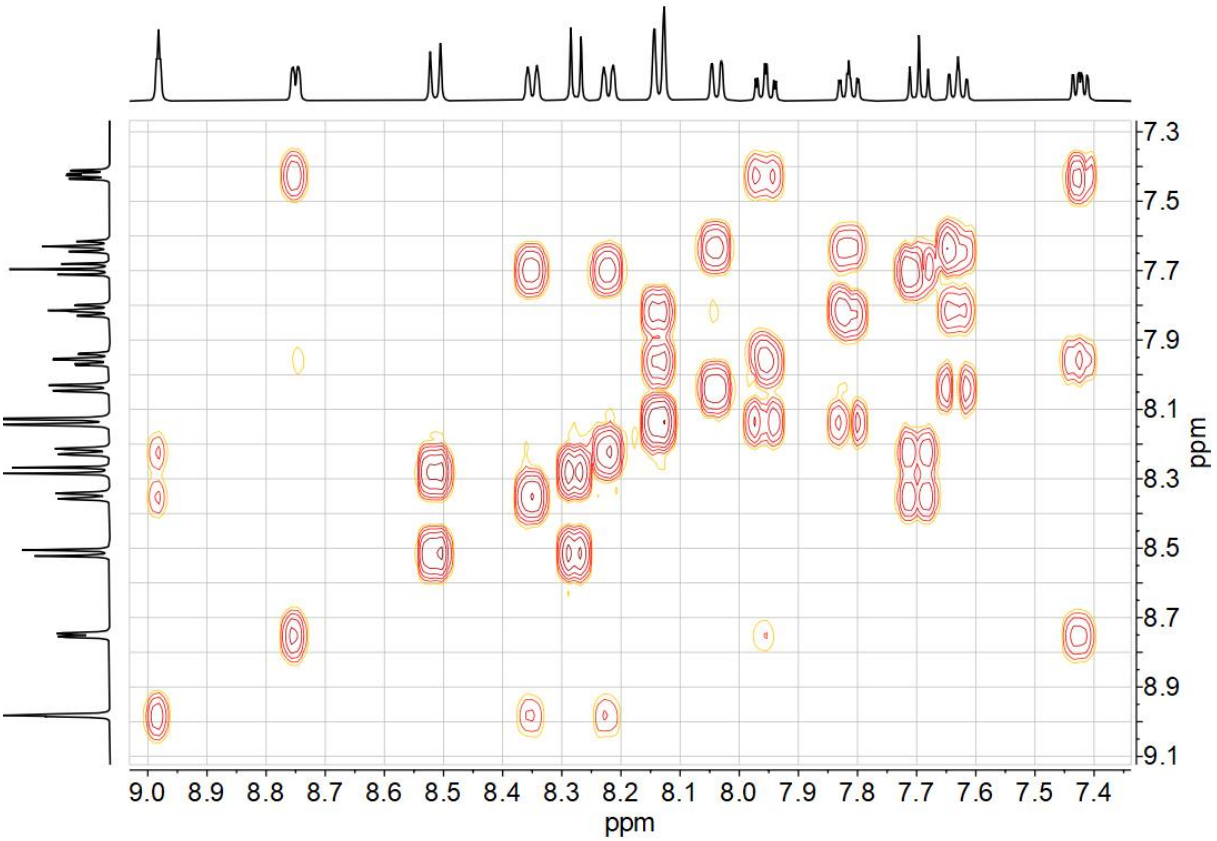

Figure 7-158 $^{1}H,^{1}H$ COSY correlation spectrum of 2Qu(PhH)Py in DMSO-d_6.

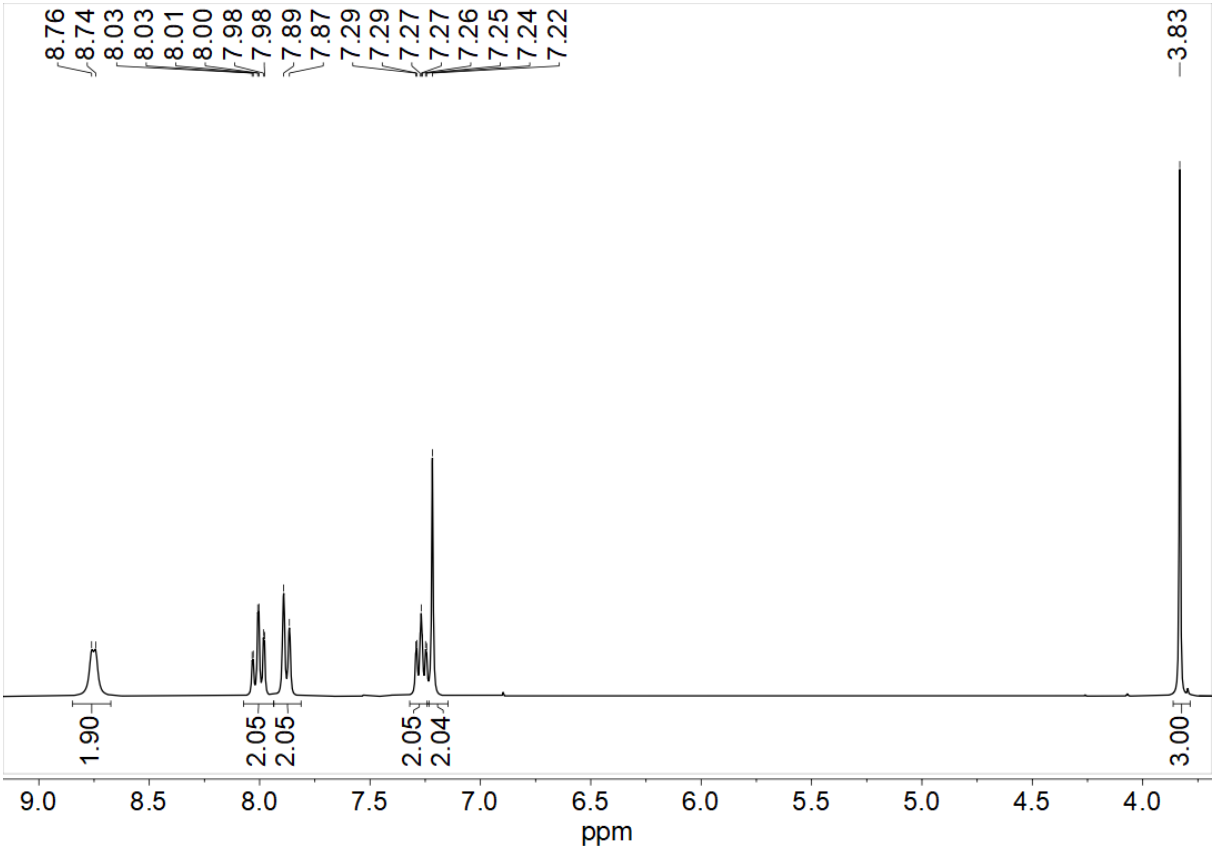

Figure 7-159 300 MHz ^{1}H NMR spectrum of [Ni(Py(5MeOPh)Py)Br] in DMSO-d_6.

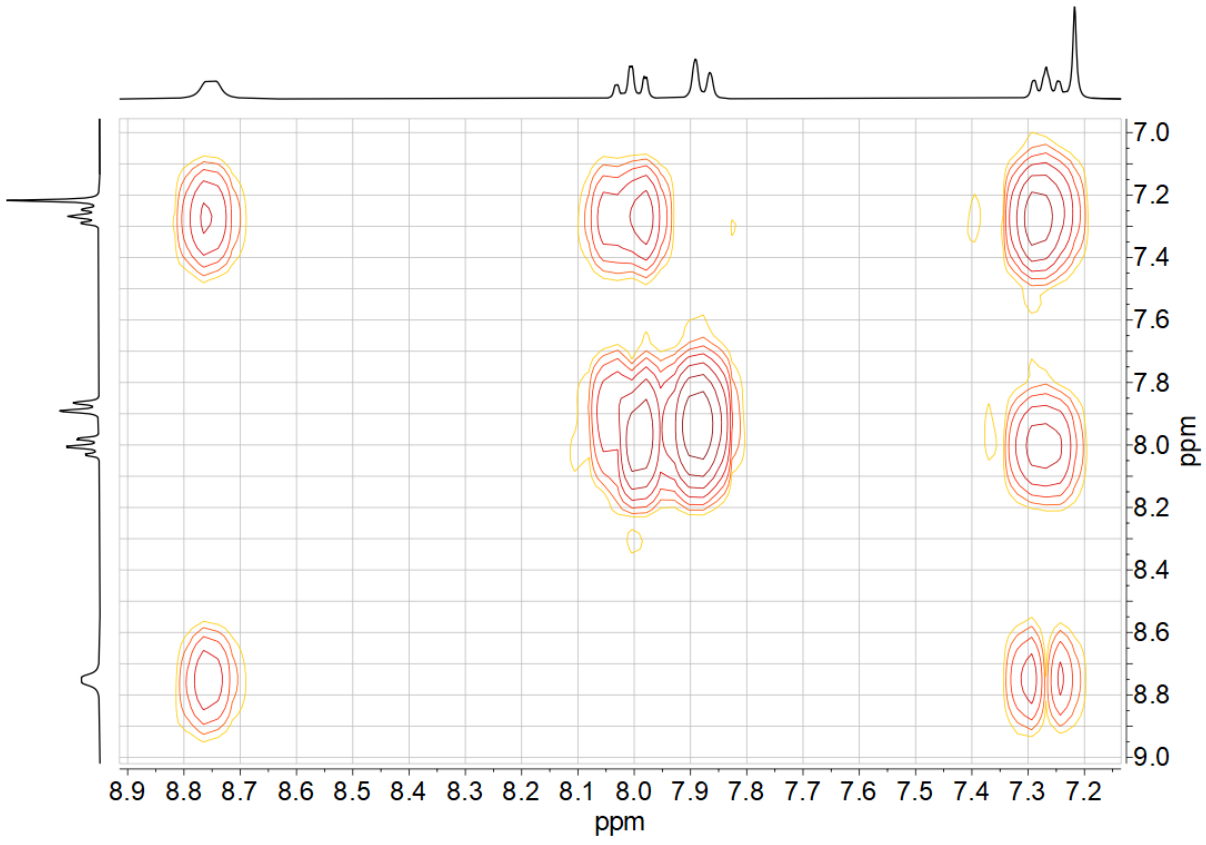

Figure 7-160 ^{1}H,^{1}H COSY correlation spectrum of [Ni(Py(5MeOPh)Py)Br] in DMSO-d_6.

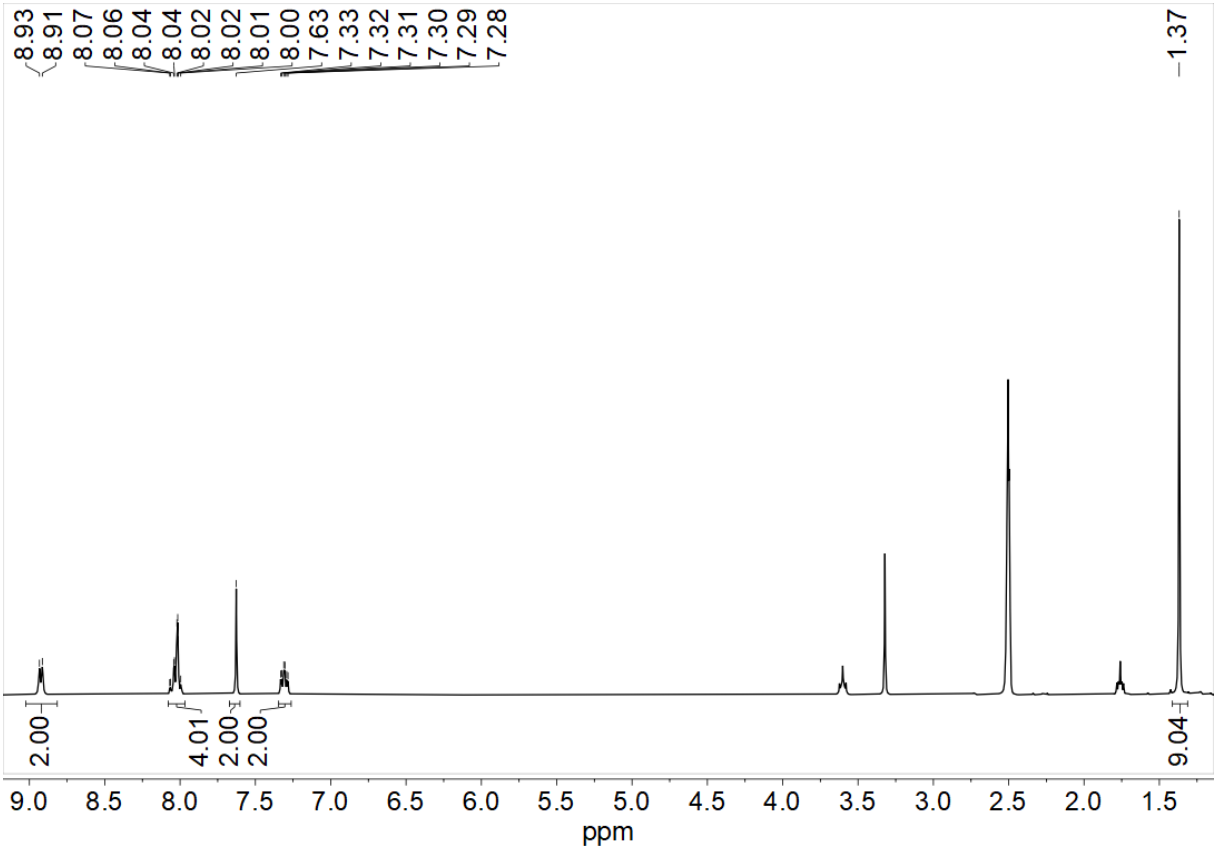

Figure 7-161 300 MHz ^{1}H NMR spectrum of [Ni(Py(5BuPh)Py)Br] in DMSO-d_6.

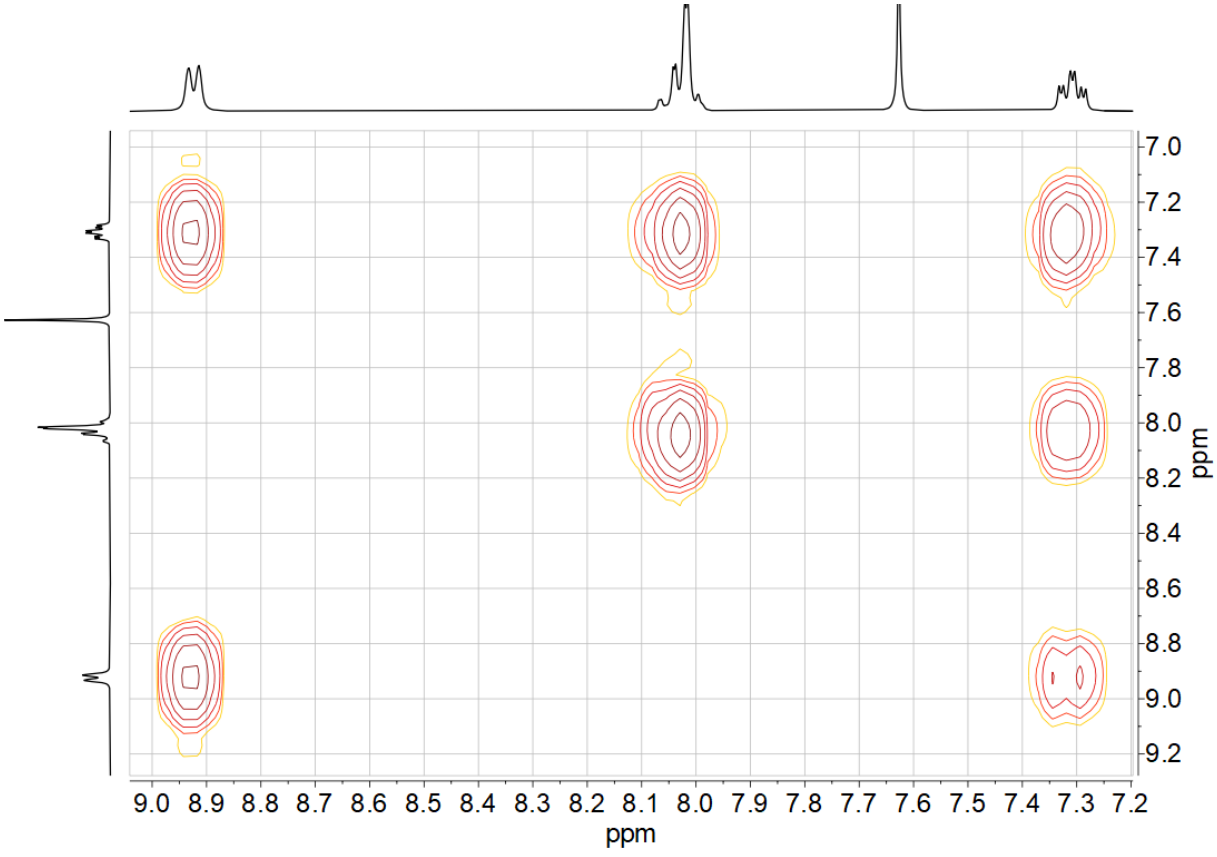

Figure 7-162 ^{1}H,^{1}H COSY correlation spectrum of [Ni(Py(5BuPh)Py)Br] in DMSO-d_6.

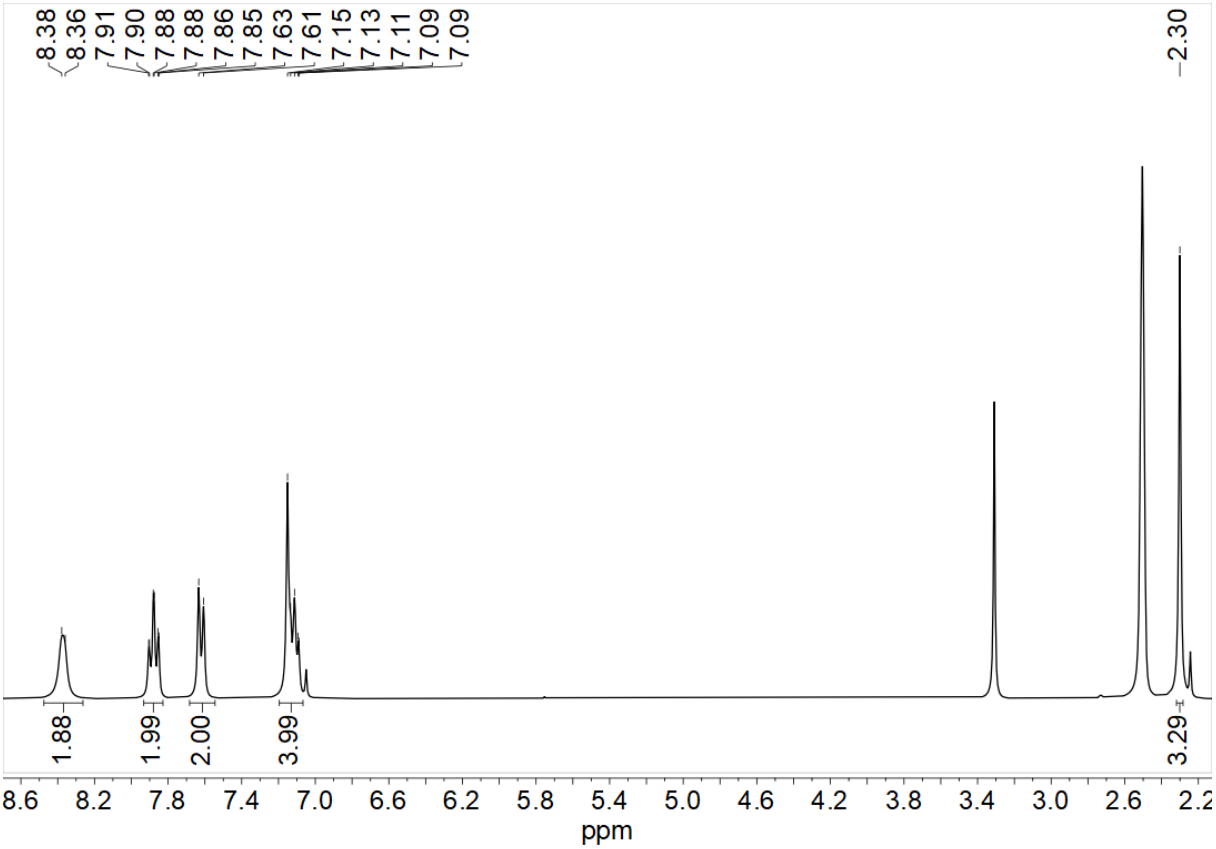

Figure 7-163 300 MHz ^{1}H NMR spectrum of [Ni(Py(5MePh)Py)Br] in DMSO-d_6.

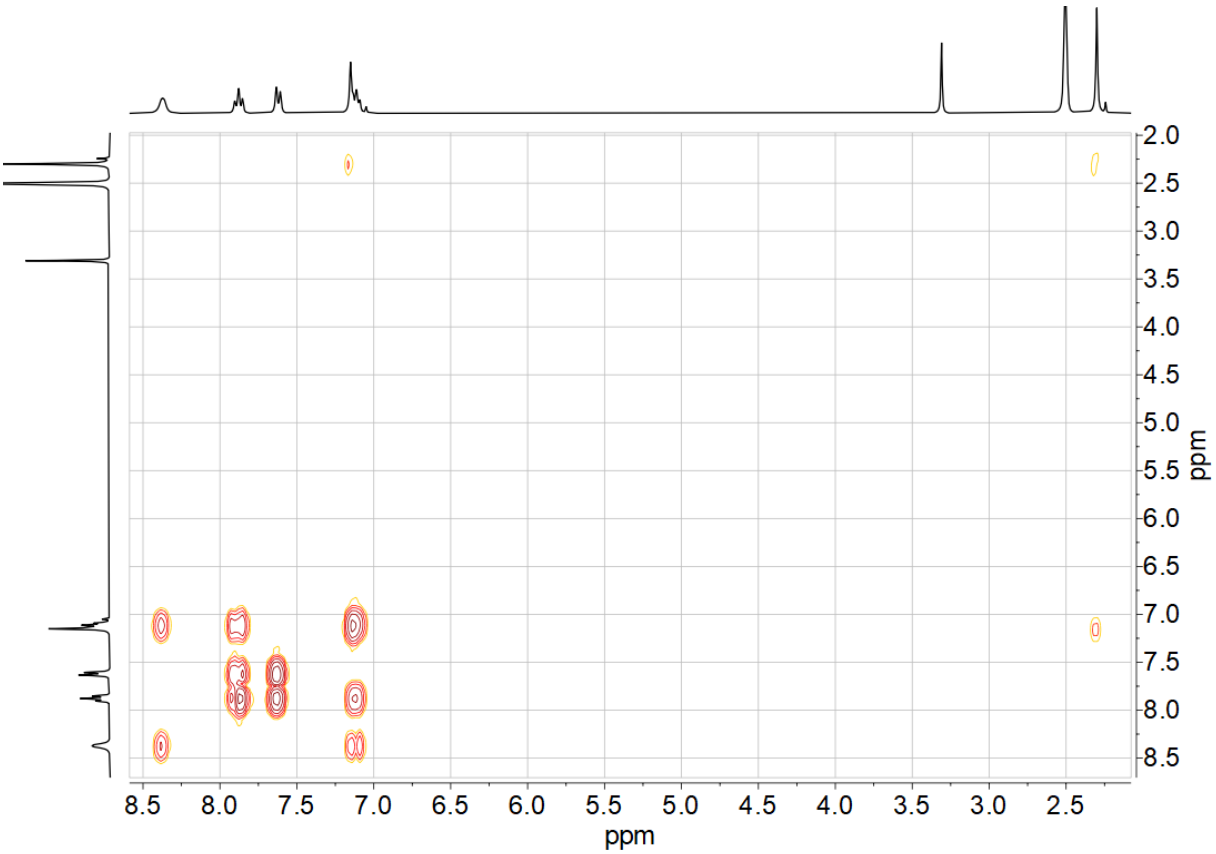

Figure 7-164 ^{1}H,^{1}H COSY correlation spectrum of [Ni(Py(5MePh)Py)Br] in DMSO-d_6.

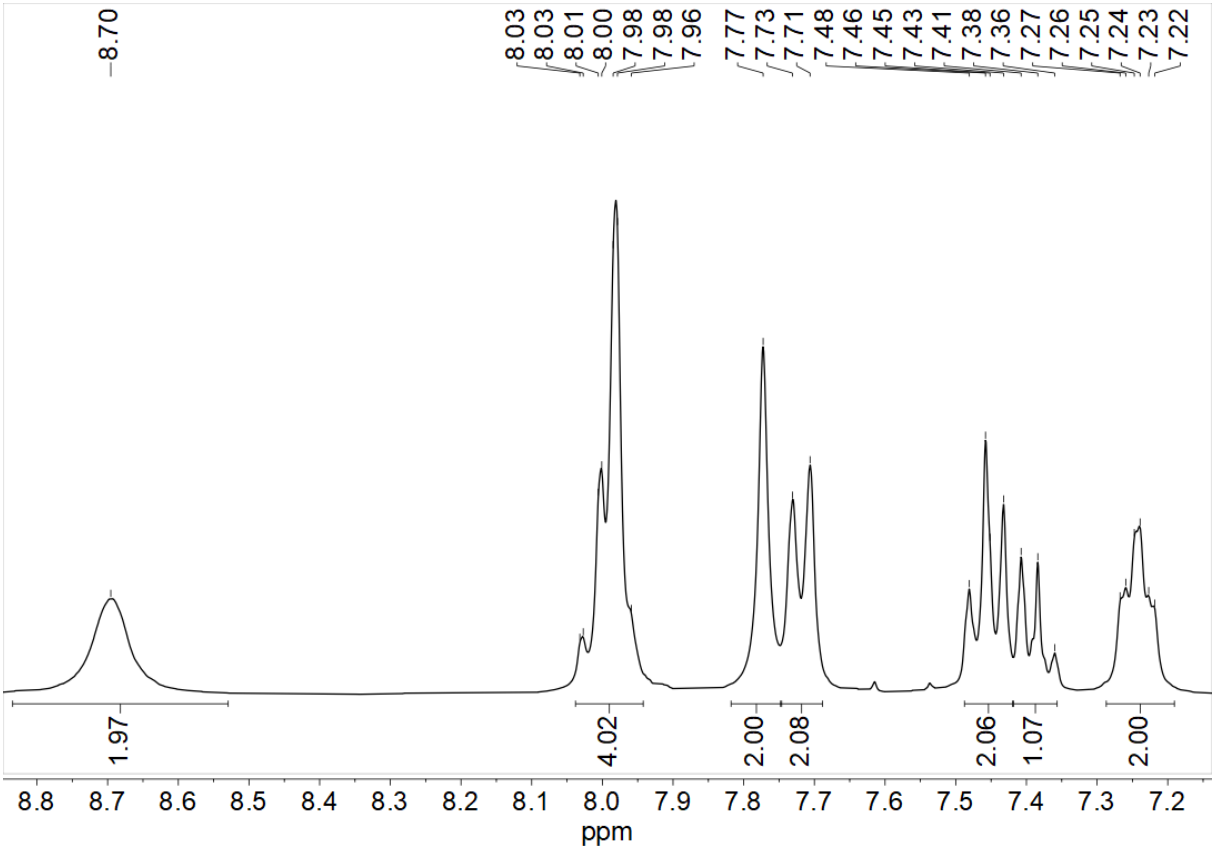

Figure 7-165 300 MHz ^{1}H NMR spectrum of [Ni(Py(5PhPh)Py)Br] in DMSO-d_6.

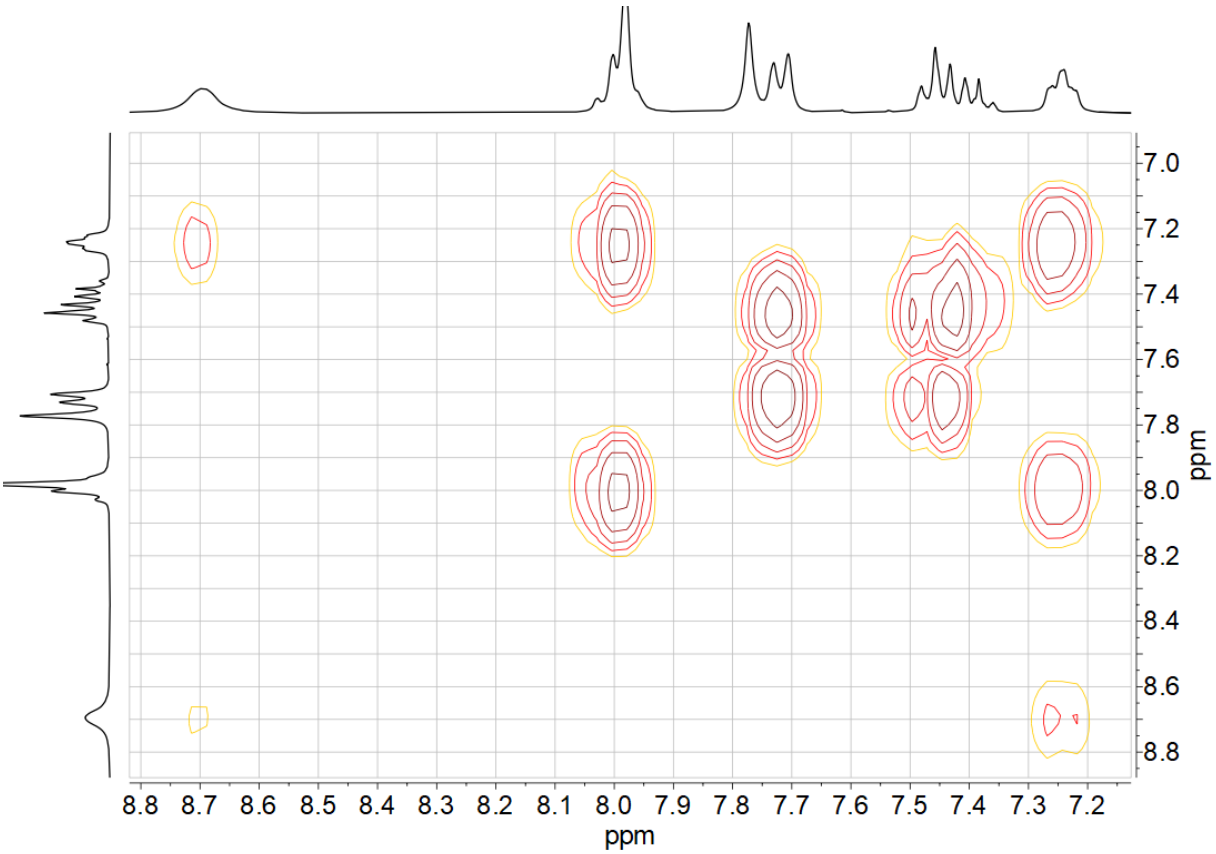

Figure 7-166 ^{1}H,^{1}H COSY correlation spectrum of [Ni(Py(5PhPh)Py)Br] in DMSO-d_6.

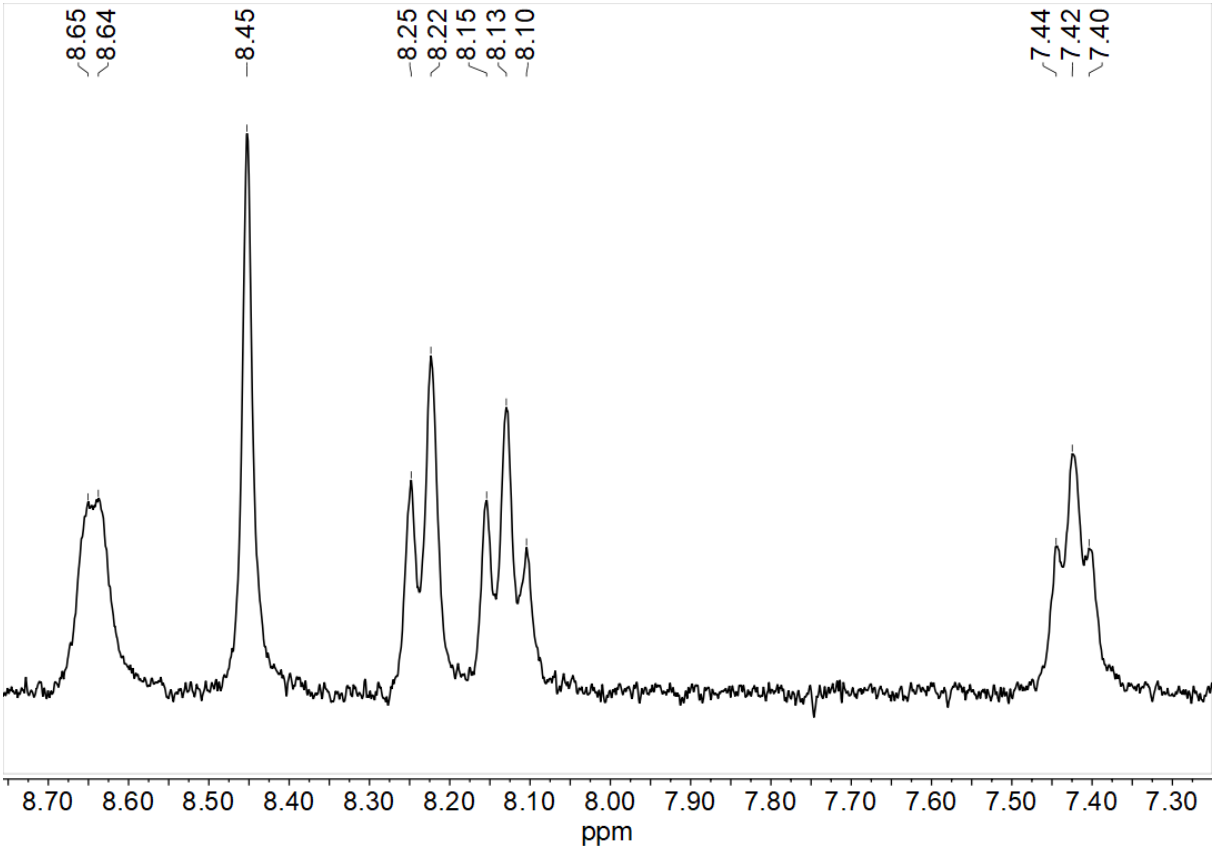

Figure 7-167 300 MHz ^{1}H NMR spectrum of [Ni(Py(5NO$_2$Ph)Py)Br] in DMSO-d_6.

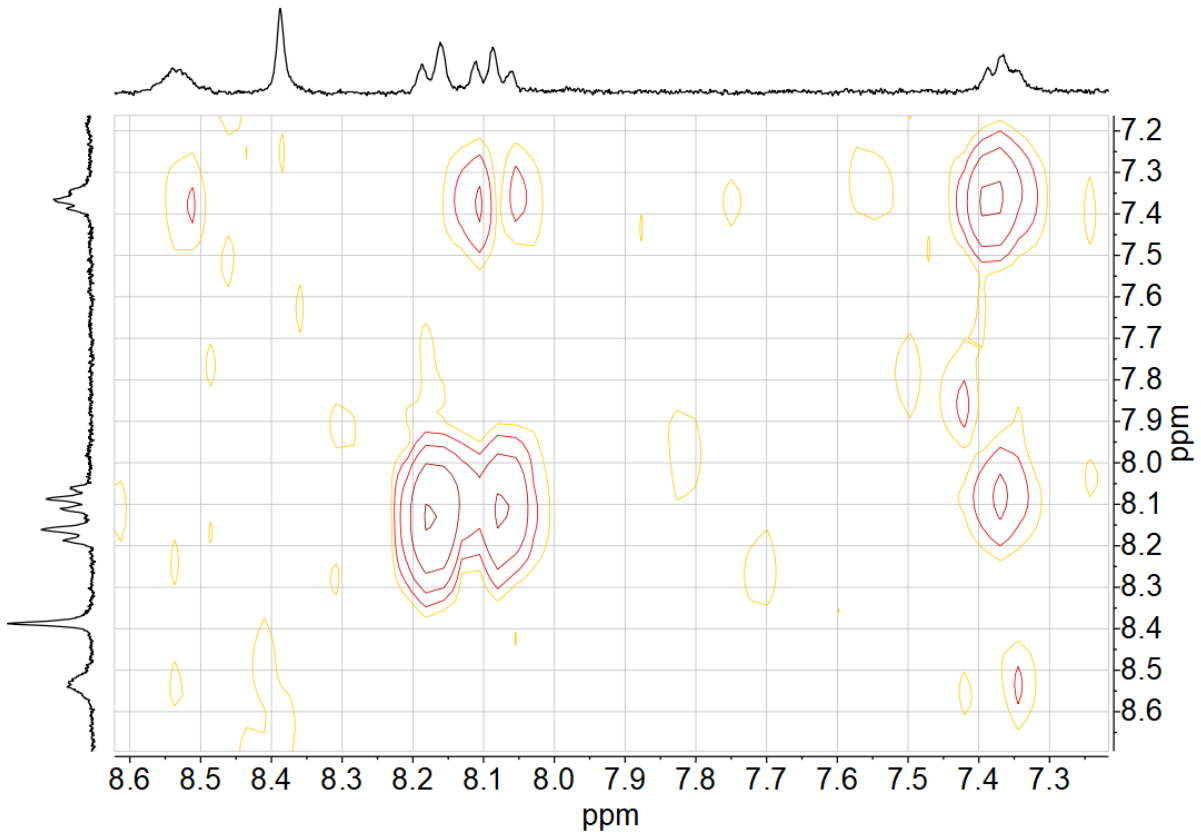

Figure 7-168 ^{1}H,^{1}H COSY correlation spectrum of [Ni(Py(5NO$_2$Ph)Py)Br] in DMSO-d_6.

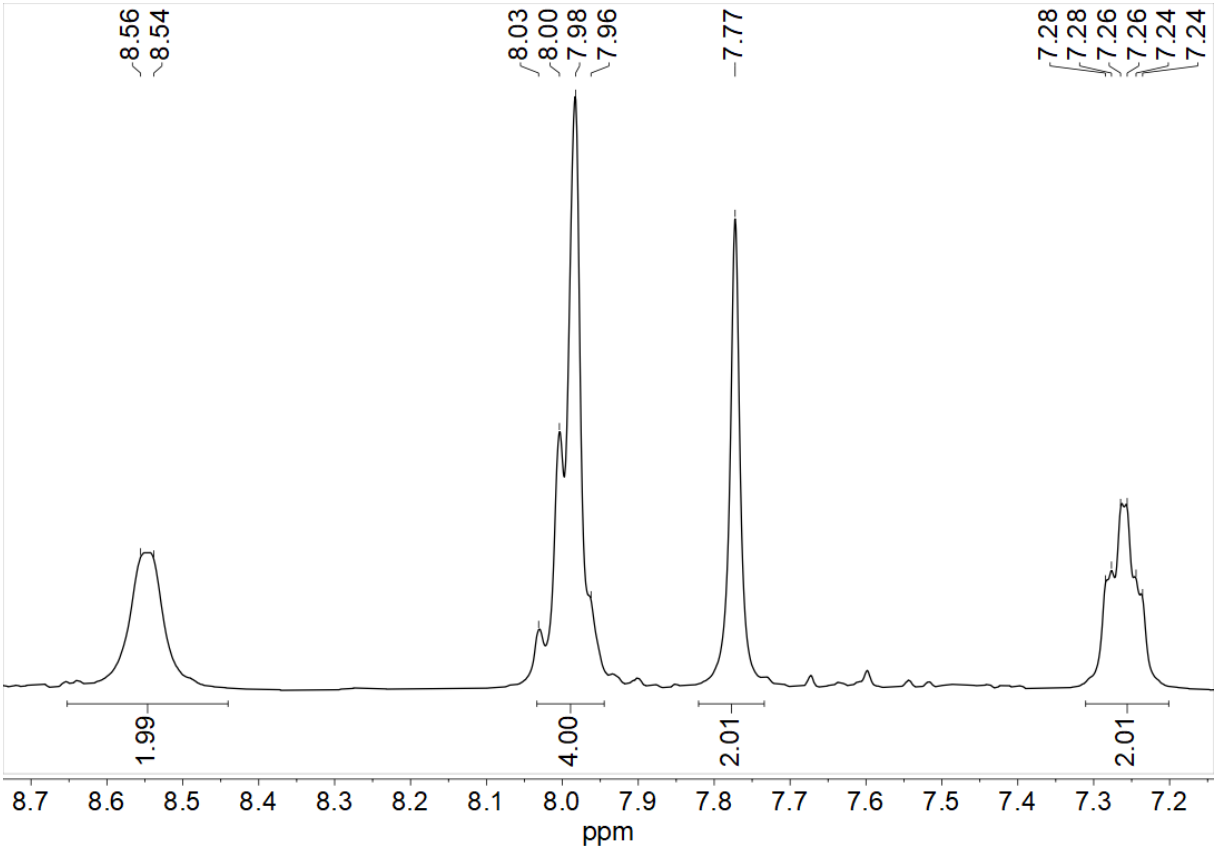

Figure 7-169 300 MHz ^{1}H NMR spectrum of [Ni(Py(5CF$_3$Ph)Py)Br] in DMSO-d_6.

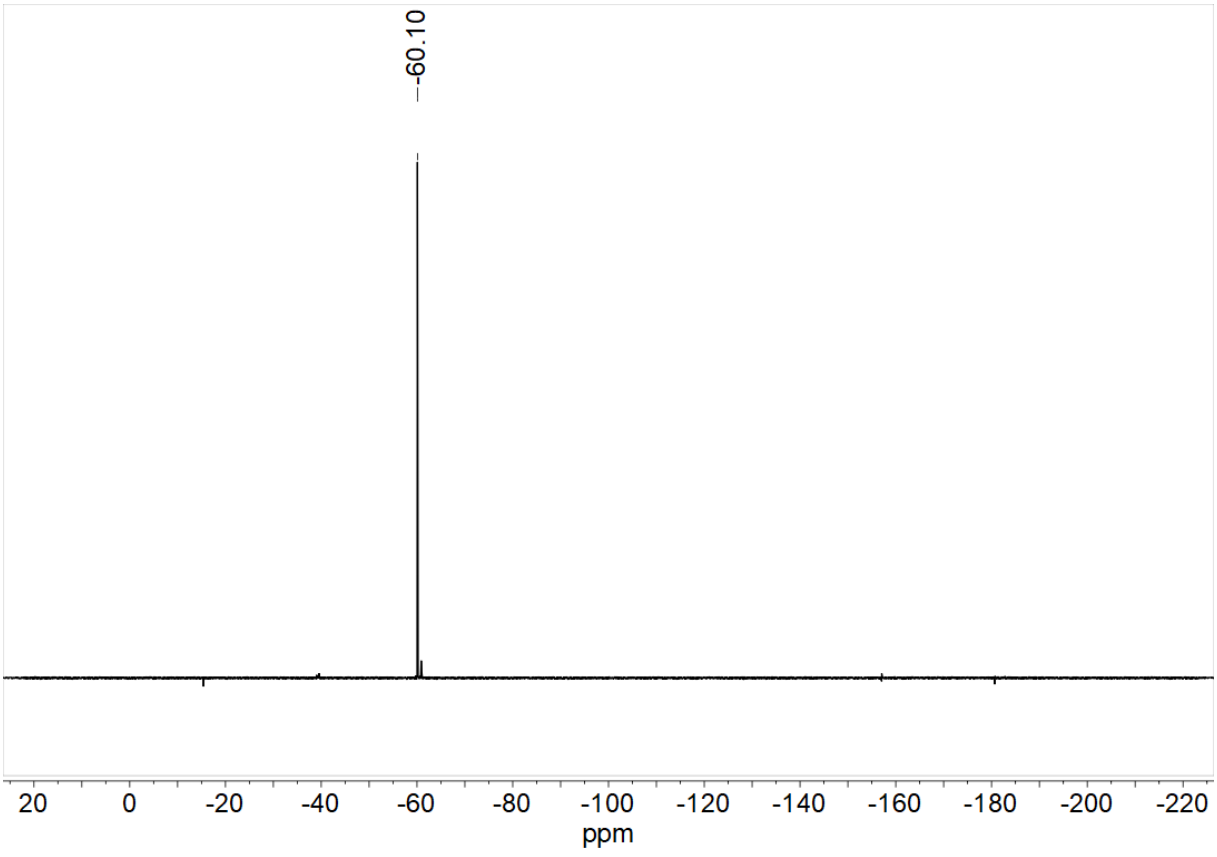

Figure 7-170 282 MHz ^{19}F NMR spectrum of [Ni(Py(5CF$_3$Ph)Py)Br] in DMSO-d_6.

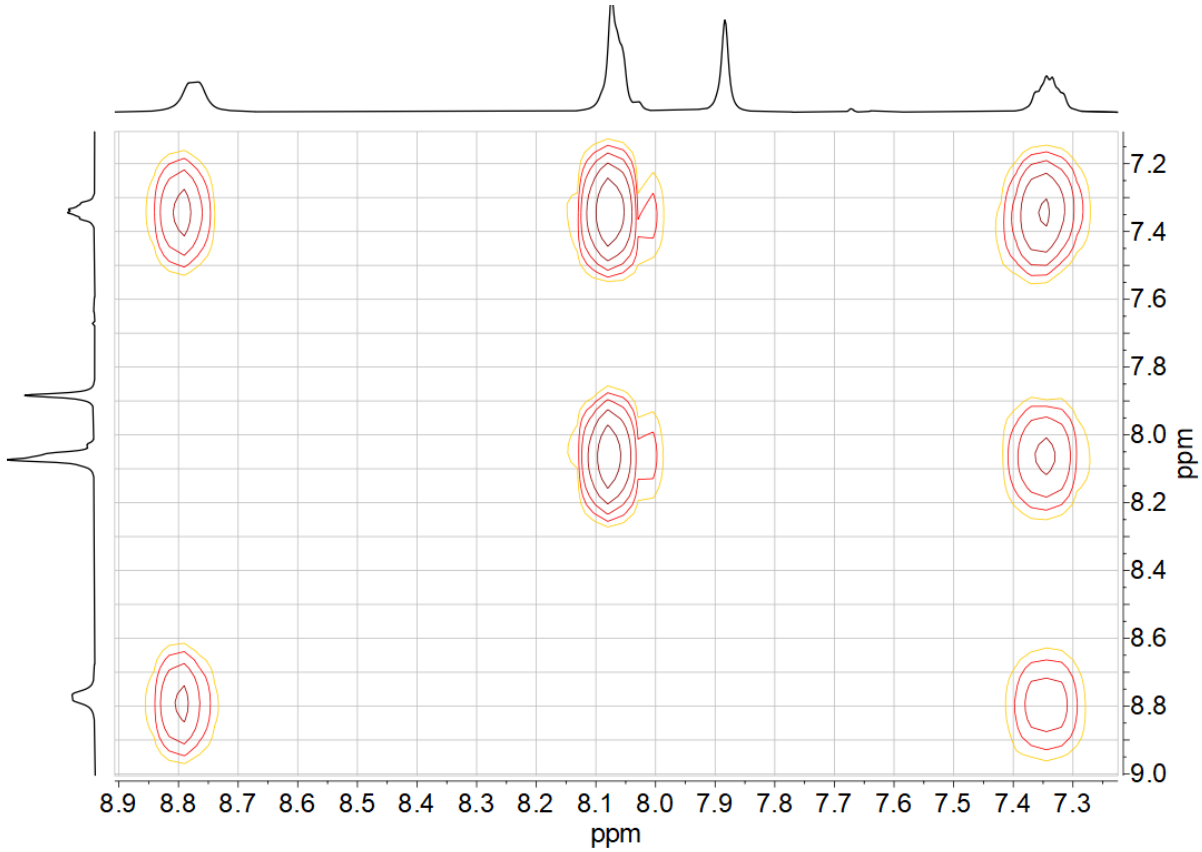

Figure 7-171 ^{1}H,^{1}H COSY correlation spectrum of [Ni(Py(5CF$_3$Ph)Py)Br] in DMSO-d_6.

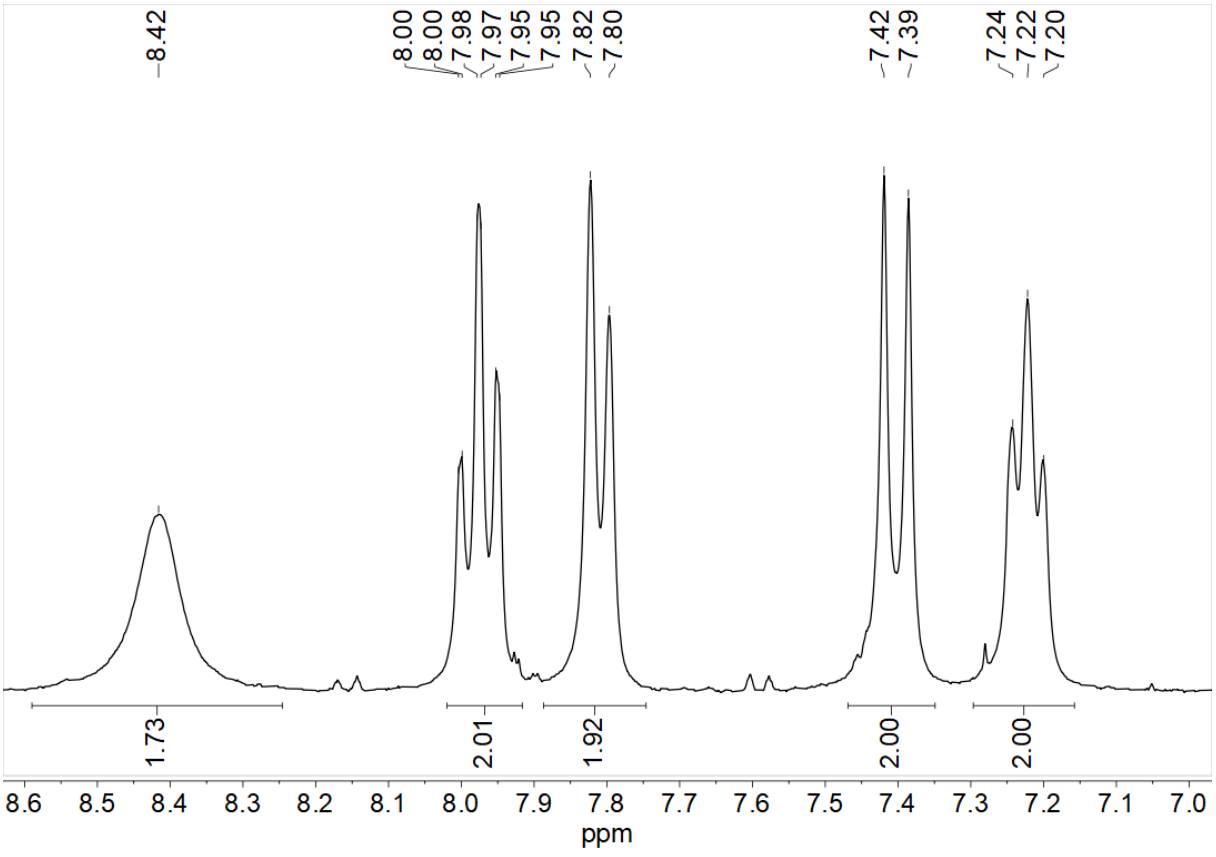

Figure 7-172 300 MHz ^{1}H NMR spectrum of [Ni(Py(5FPh)Py)Br] in DMSO-d_6.

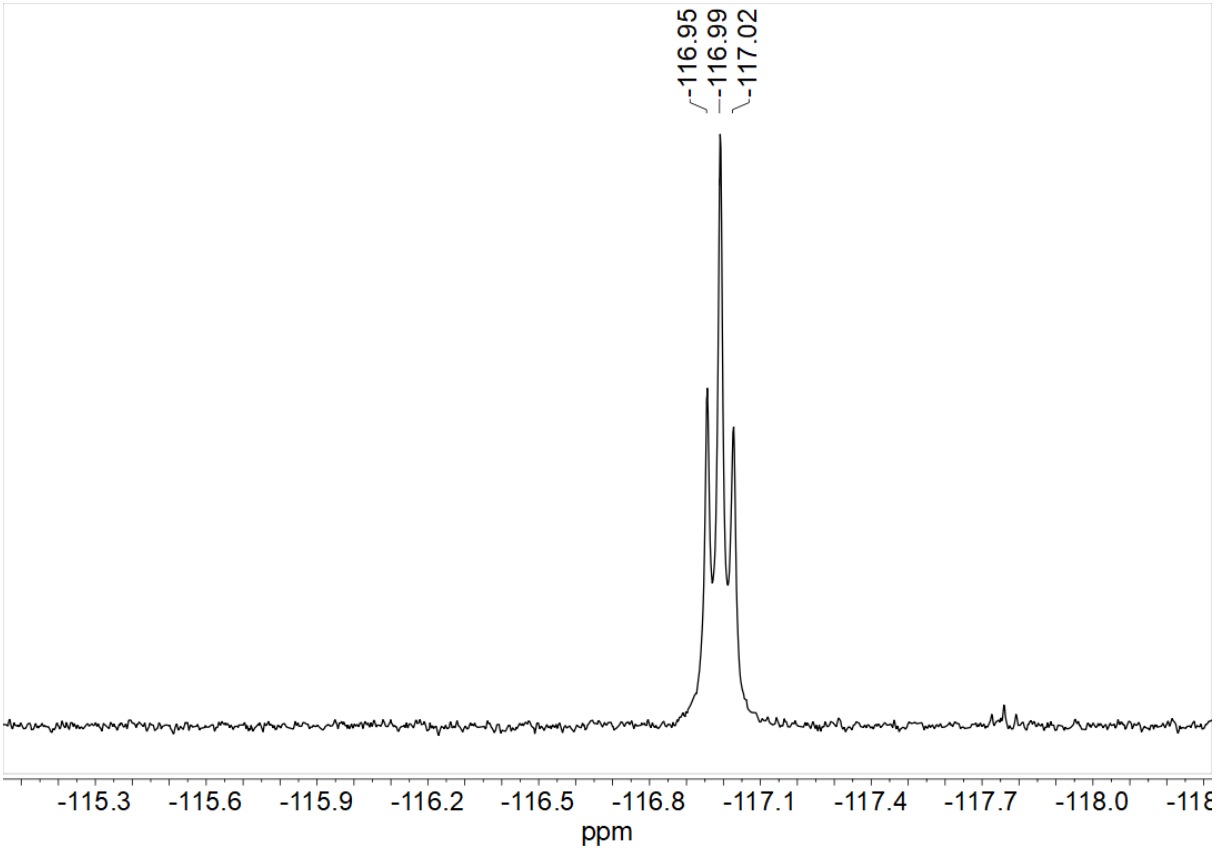

Figure 7-173 282 MHz ^{19}F NMR spectrum of [Ni(Py(5FPh)Py)Br] in DMSO-d_6.

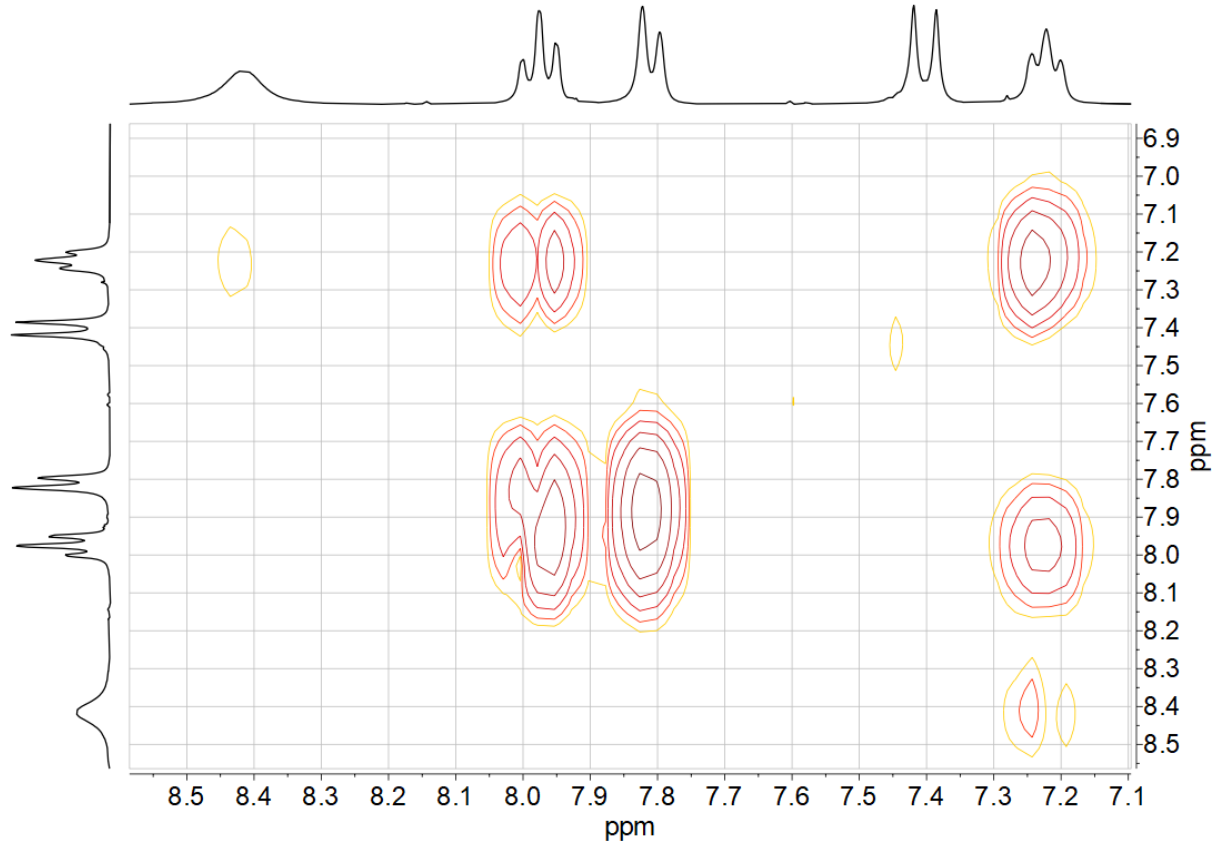

Figure 7-174 ^{1}H,^{1}H COSY correlation spectrum of [Ni(Py(5FPh)Py)Br] in DMSO-d_6.

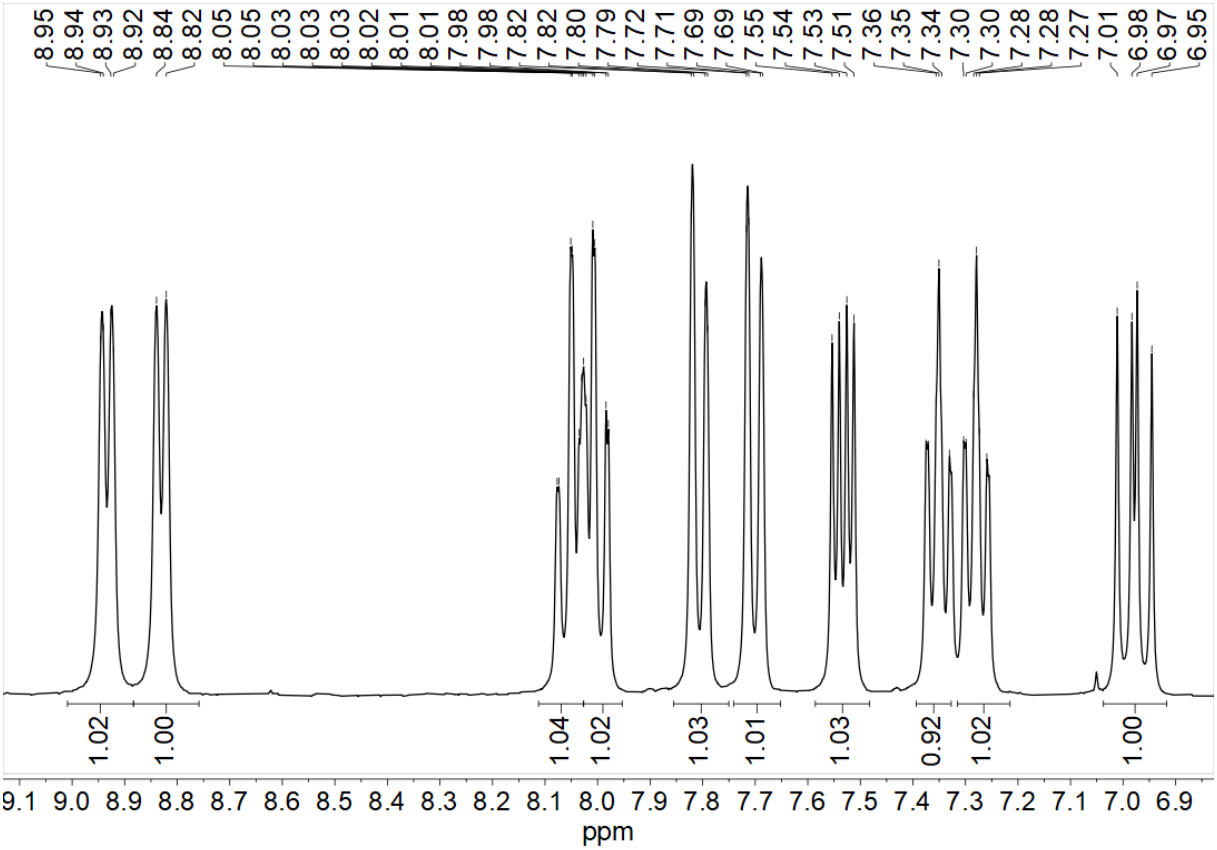

Figure 7-175 300 MHz ^{1}H NMR spectrum of [Ni(Py(4FPh)Py)Br] in DMSO-d_6.

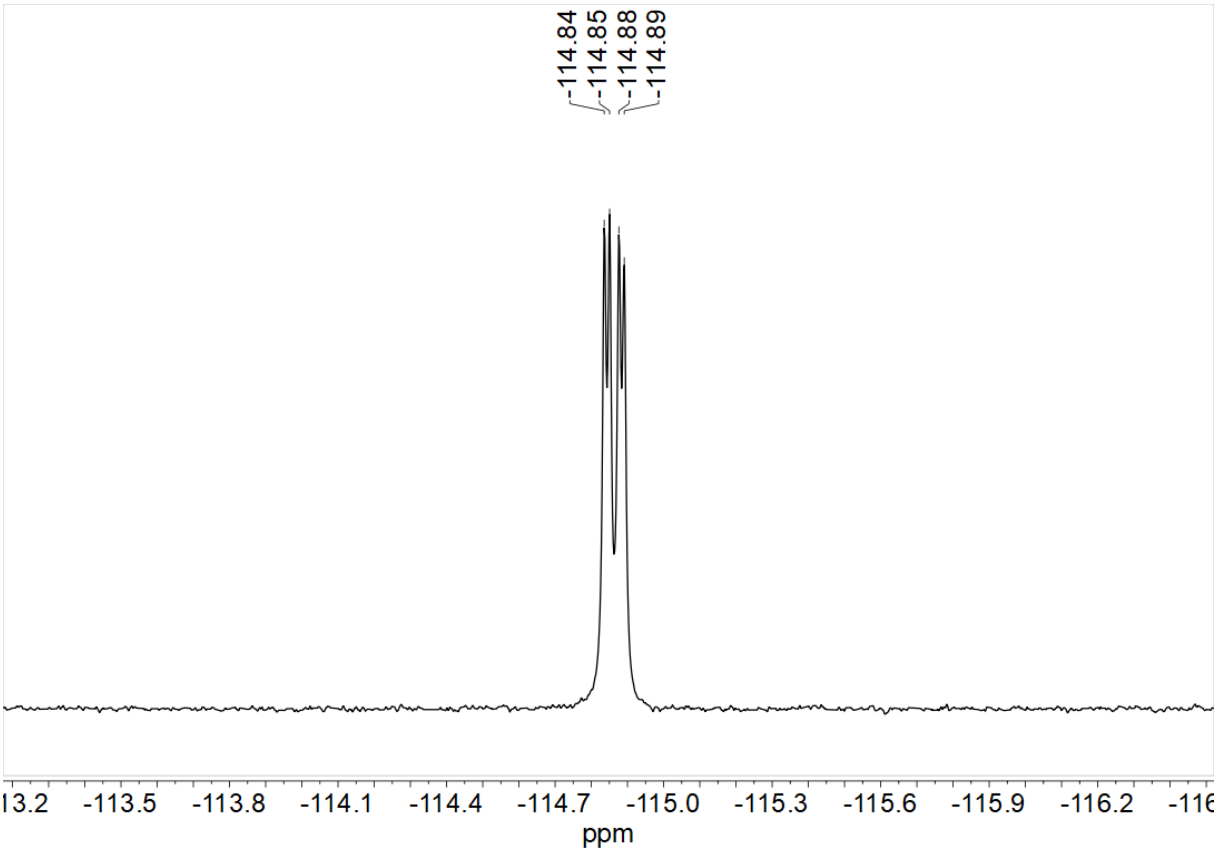

Figure 7-176 282 MHz ^{19}F NMR spectrum of [Ni(Py(4FPh)Py)Br] in DMSO-d_6.

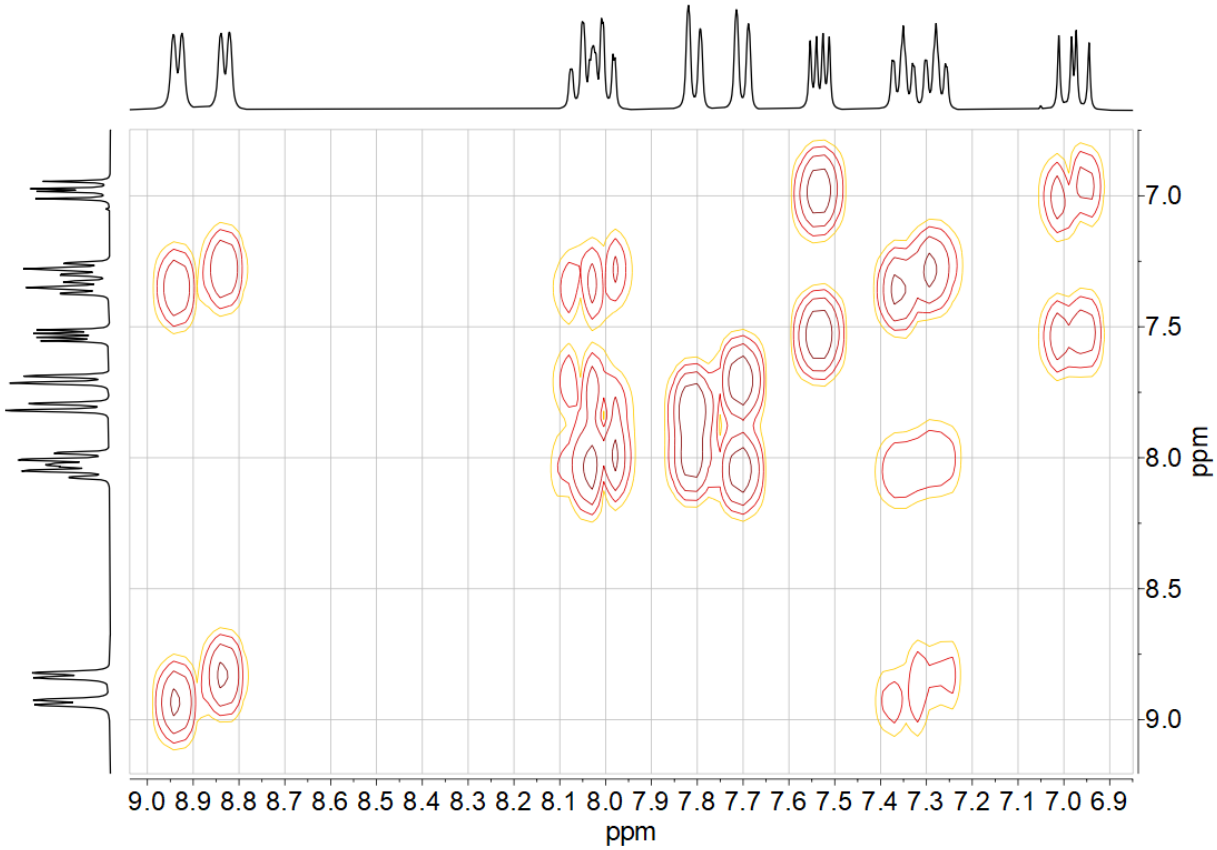

Figure 7-177 ^{1}H,^{1}H COSY correlation spectrum of [Ni(Py(4FPh)Py)Br] in DMSO-d_6.

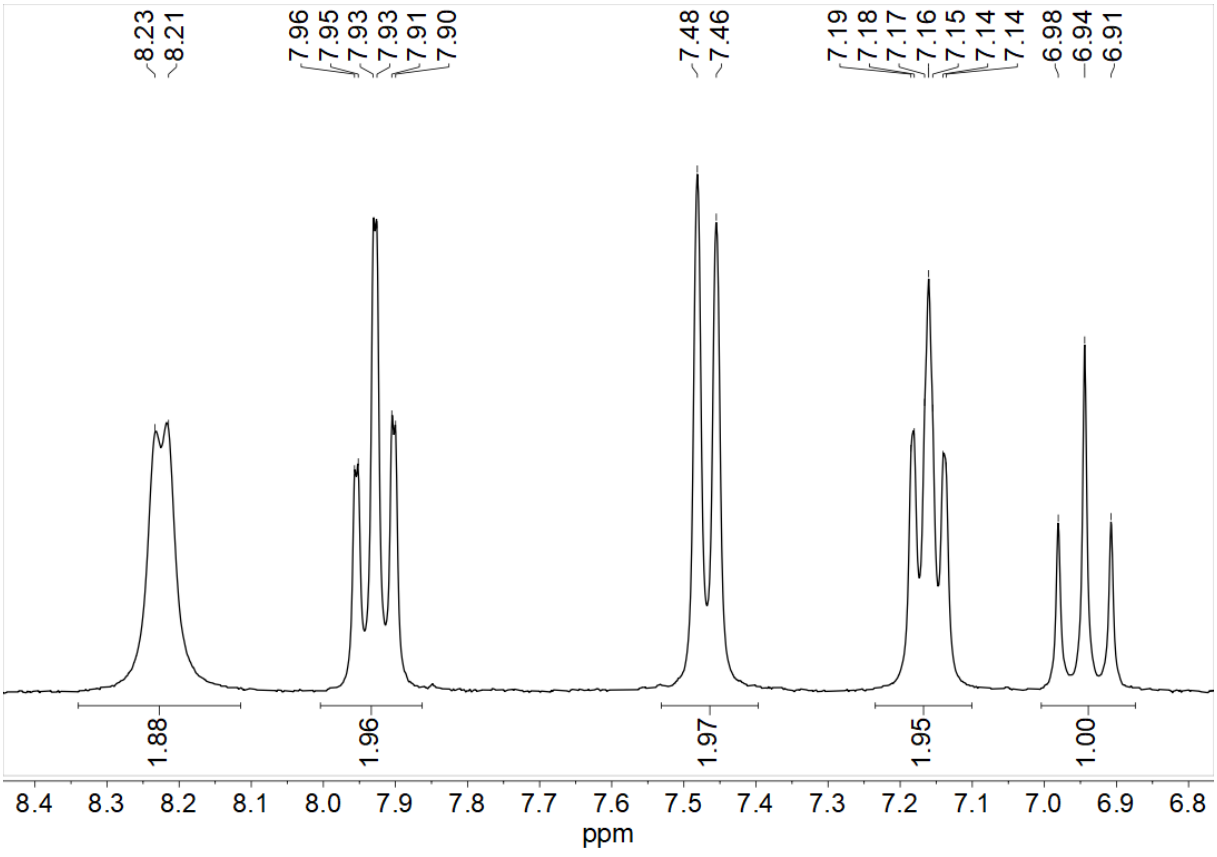

Figure 7-178 300 MHz ^{1}H NMR spectrum of [Ni(Py(4,6FPh)Py)Br] in DMSO-d_6.

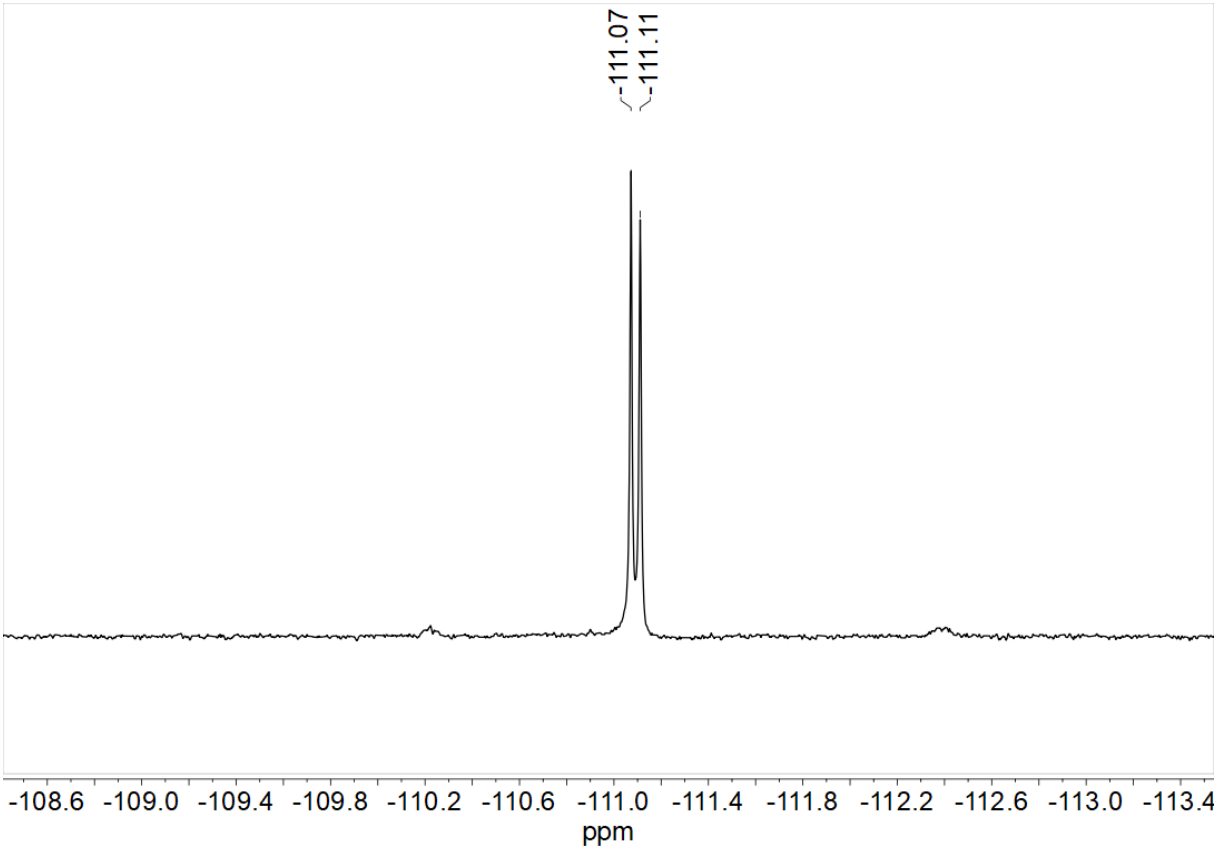

Figure 7-179 282 MHz ^{19}F NMR spectrum of [Ni(Py(4,6FPh)Py)Br] in DMSO-d_6.

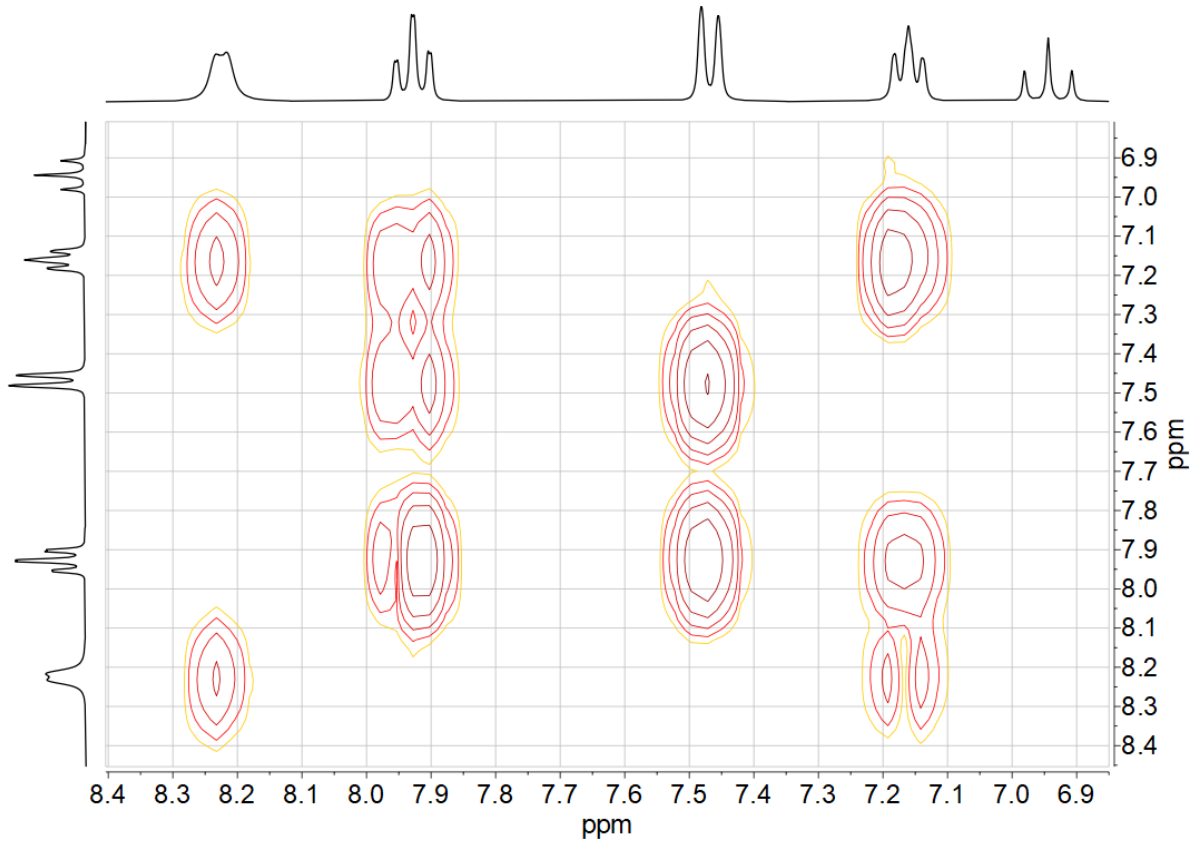

Figure 7-180 ^{1}H,^{1}H COSY correlation spectrum of [Ni(Py(4,6FPh)Py)Br] in DMSO-d_6.

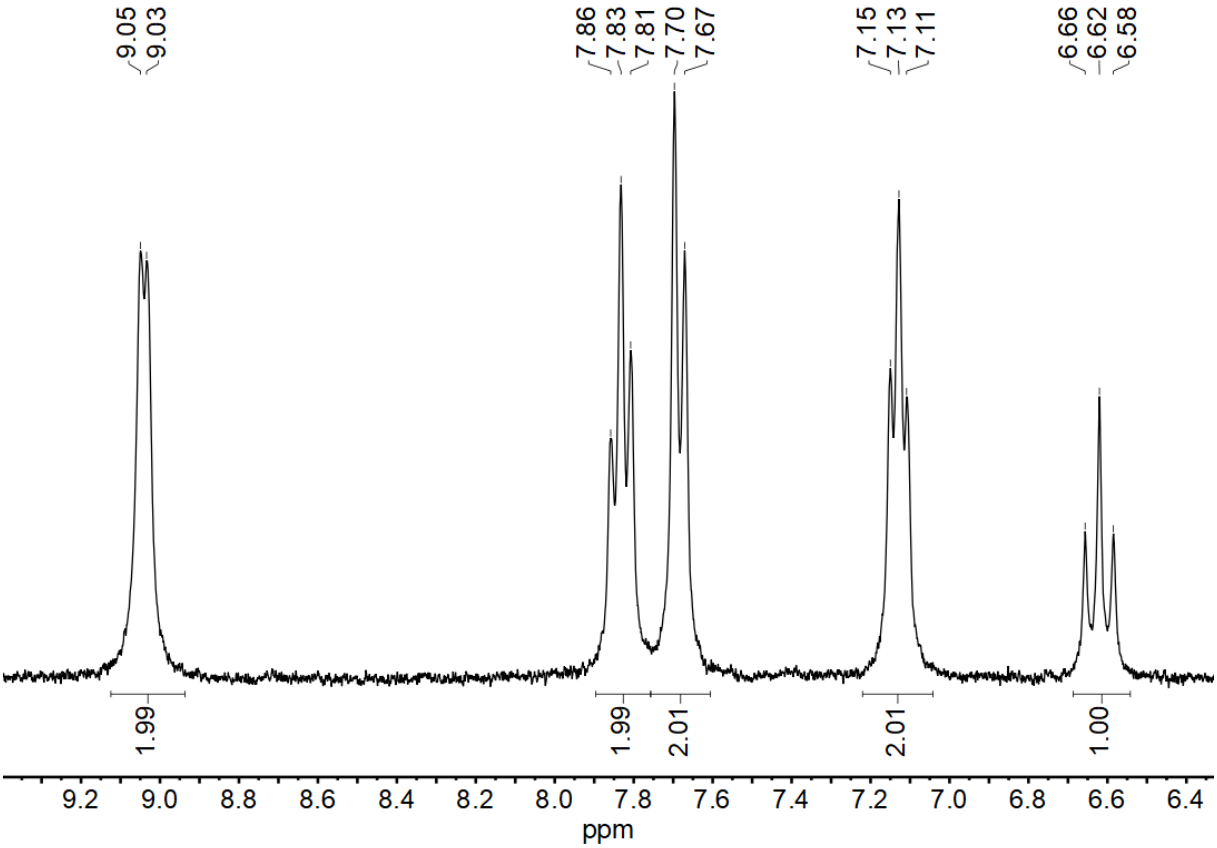

Figure 7-181 300 MHz ^{1}H NMR spectrum of [Ni(Py(4,6FPh)Py)Cl] in CD_2Cl_2.

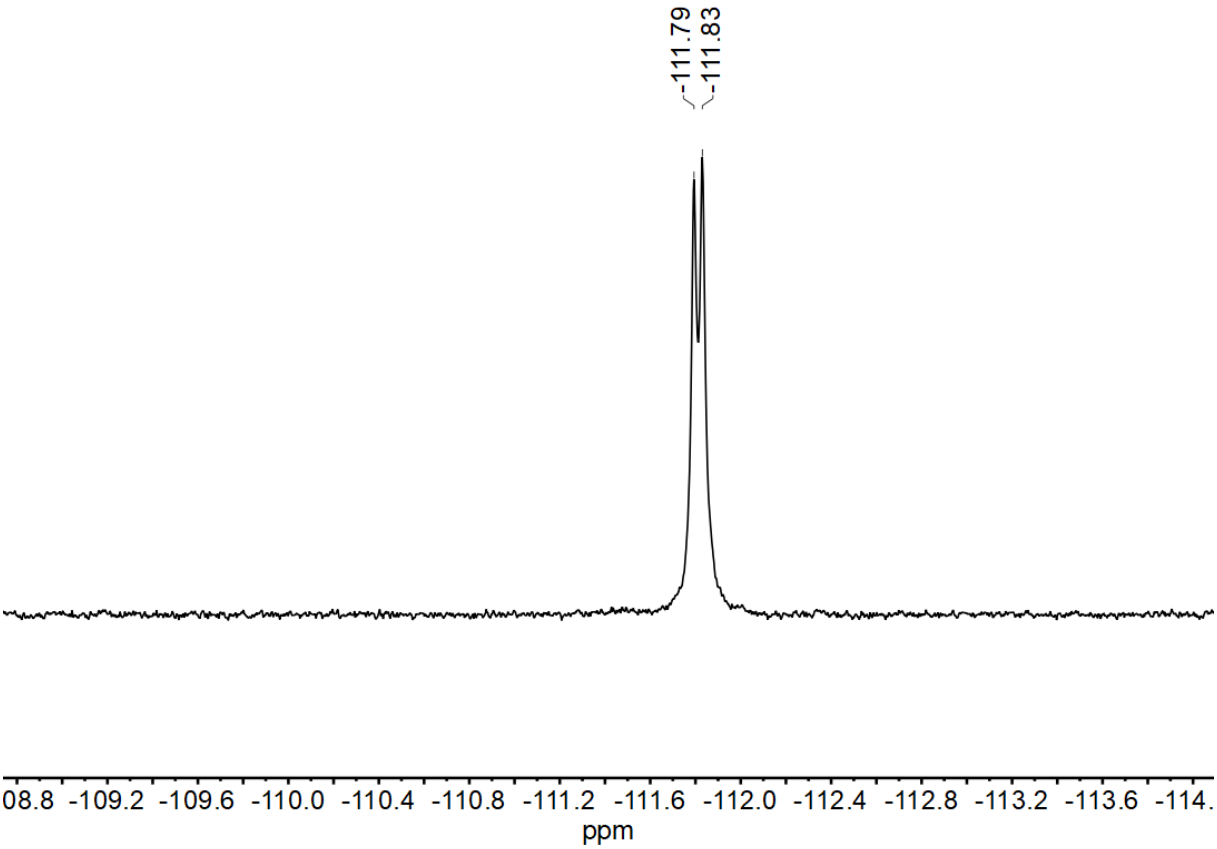

Figure 7-182 282 MHz ^{19}F NMR spectrum of [Ni(Py(4,6FPh)Py)Cl] in CD_2Cl_2.

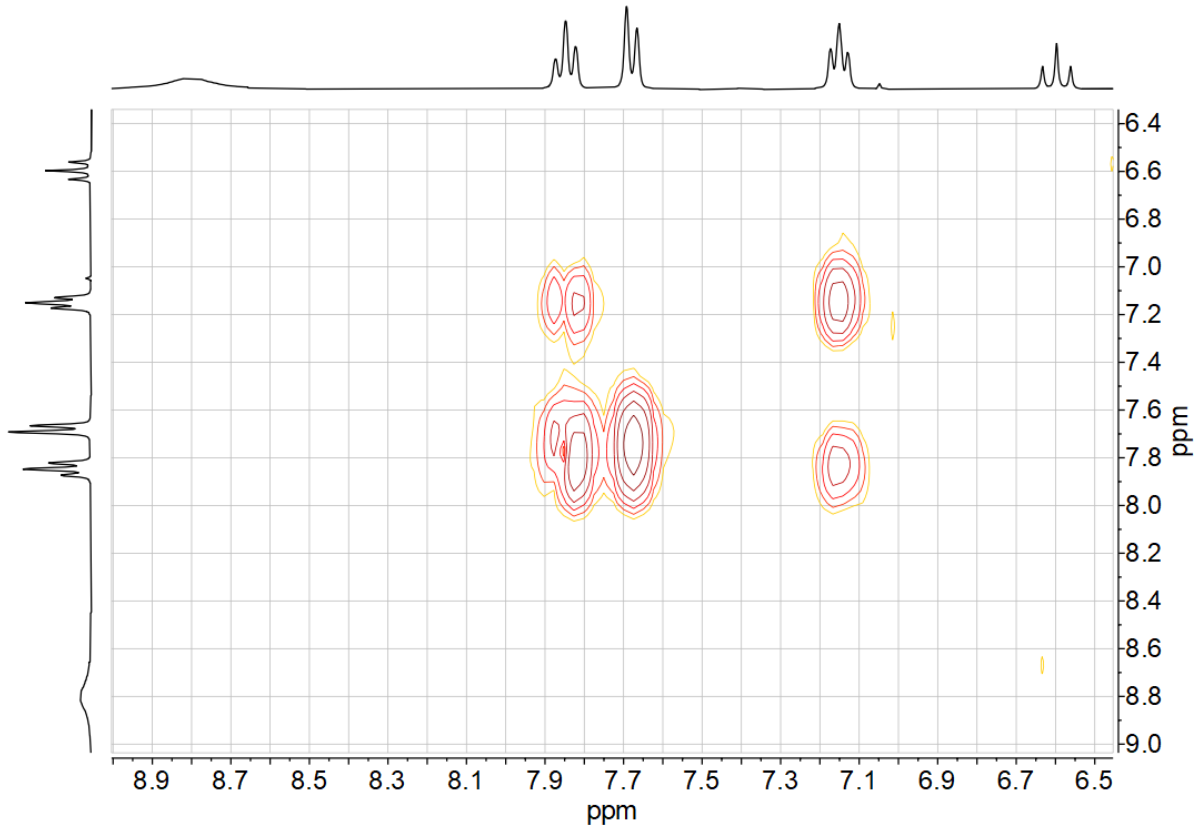

Figure 7-183 $^{1}H,^{1}H$ COSY correlation spectrum of [Ni(Py(4,6FPh)Py)Cl] in CD_2Cl_2.

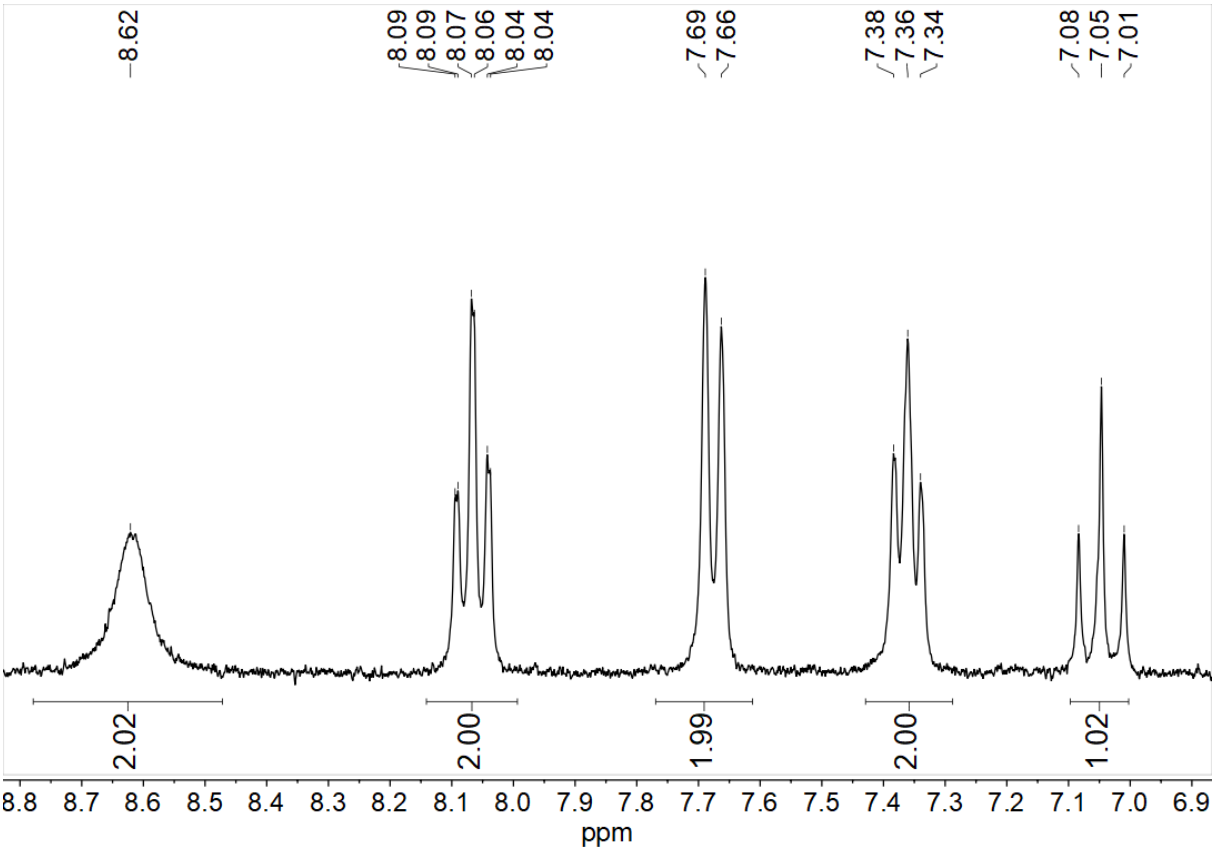

Figure 7-184 300 MHz ^{1}H NMR spectrum of [Ni(Py(4,6FPh)Py)Cl] in DMSO-d_6.

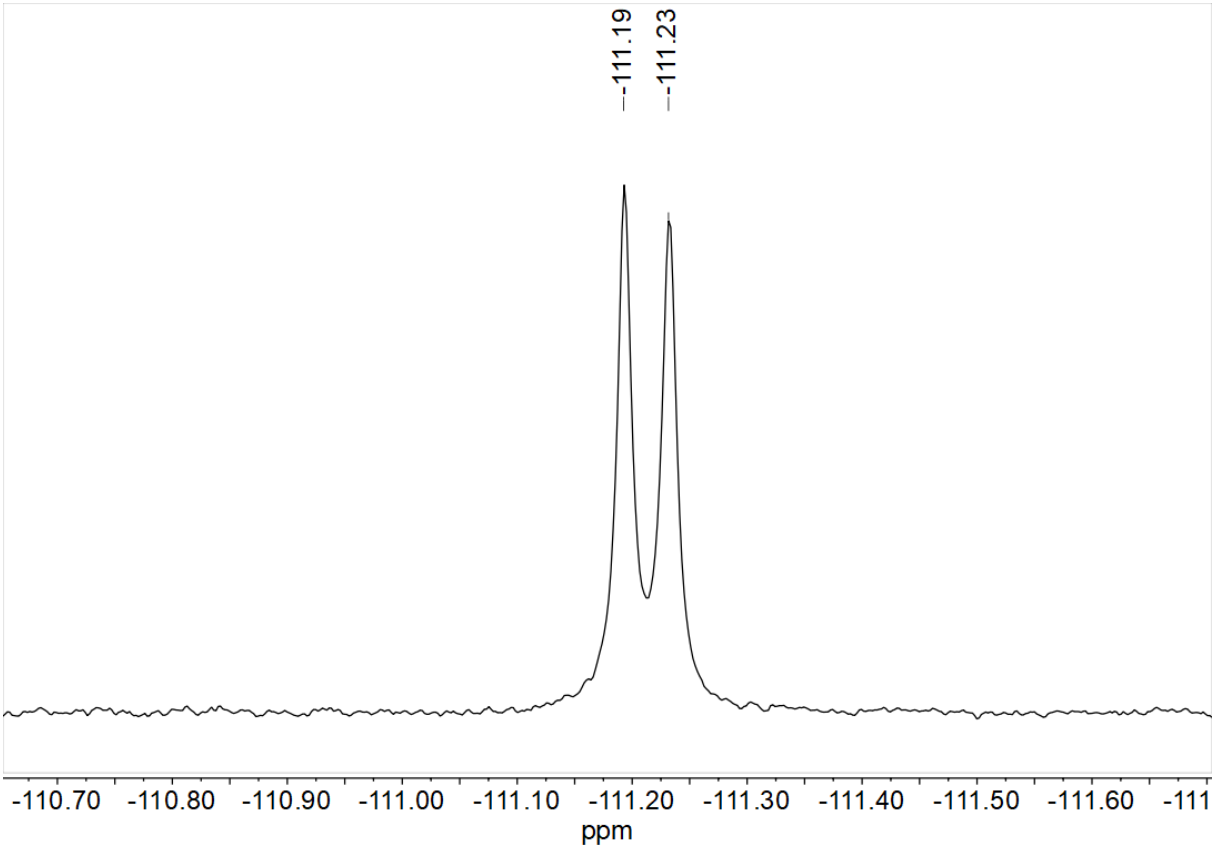

Figure 7-185 300 MHz ^{19}F NMR spectrum of [Ni(Py(4,6FPh)Py)Cl] in DMSO-d_6.

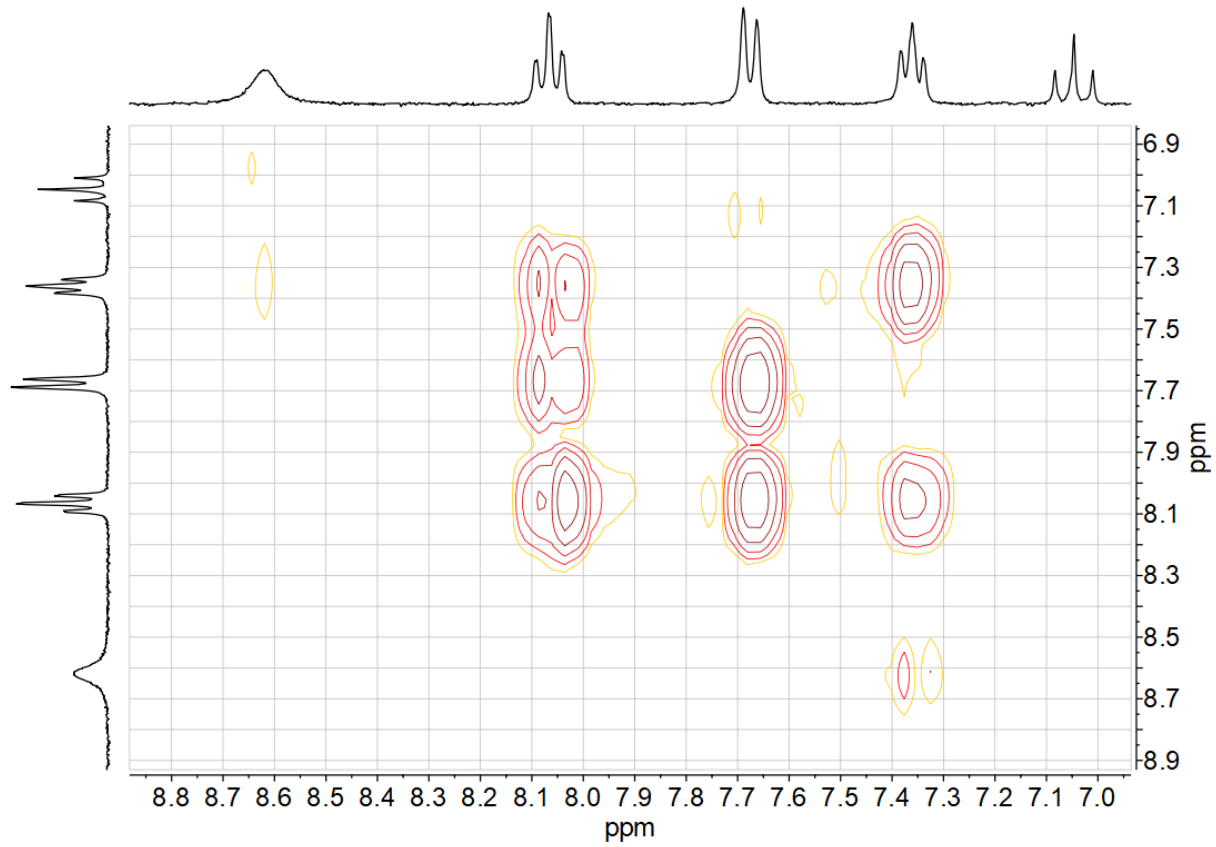

Figure 7-186 ^{1}H,^{1}H COSY correlation spectrum of [Ni(Py(4,6FPh)Py)Cl] in DMSO-d_6.

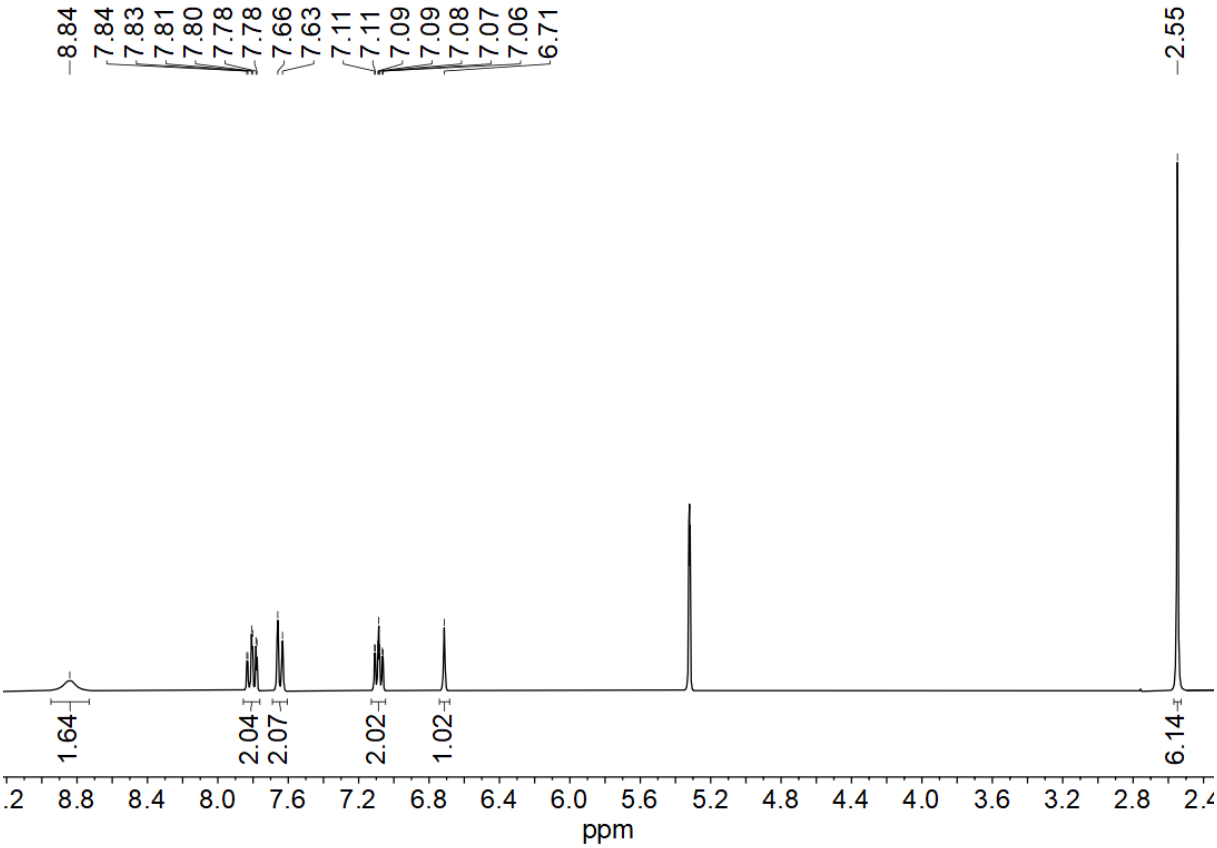

Figure 7-187 300 MHz ^{1}H NMR spectrum of [Ni(Py(4,6MePh)Py)Cl] in CD_2Cl_2.

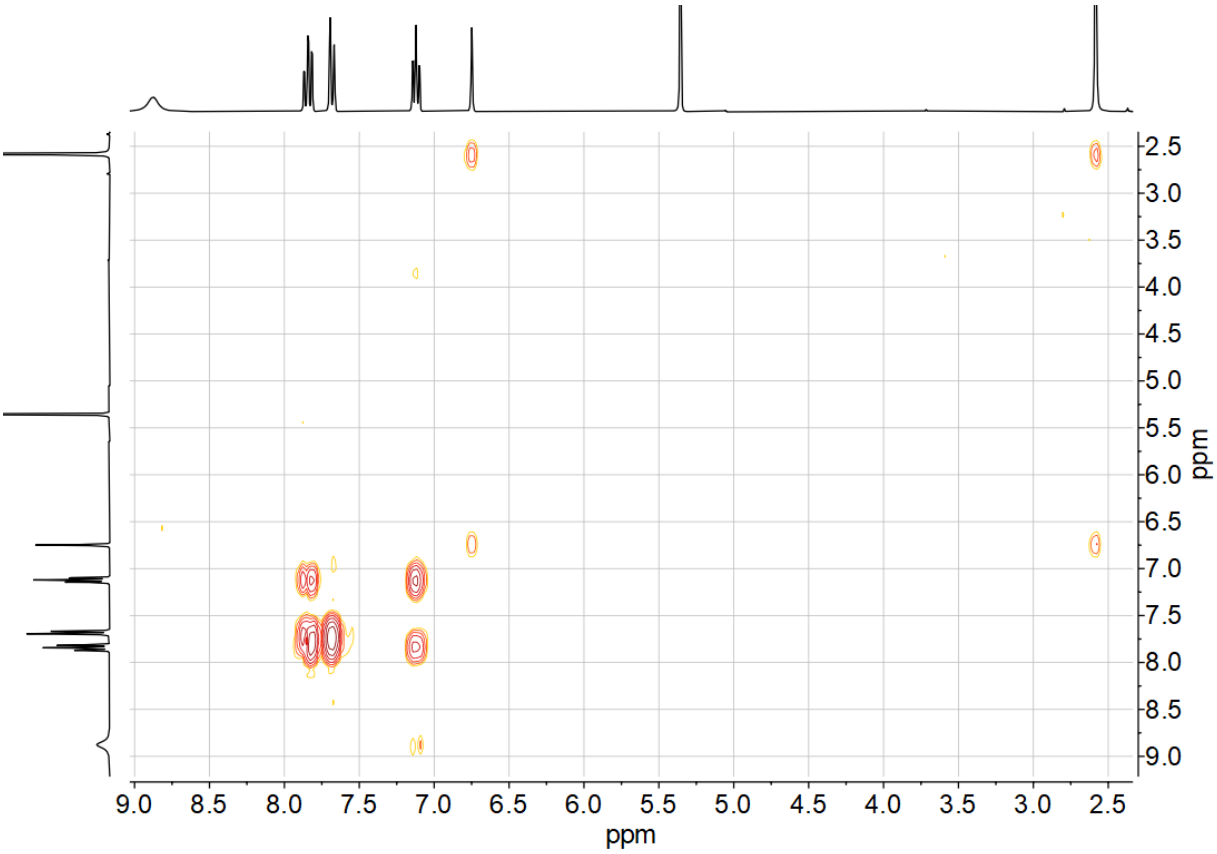

Figure 7-188 $^{1}H,^{1}H$ COSY correlation spectrum of [Ni(Py(4,6MePh)Py)Cl] in CD_2Cl_2.

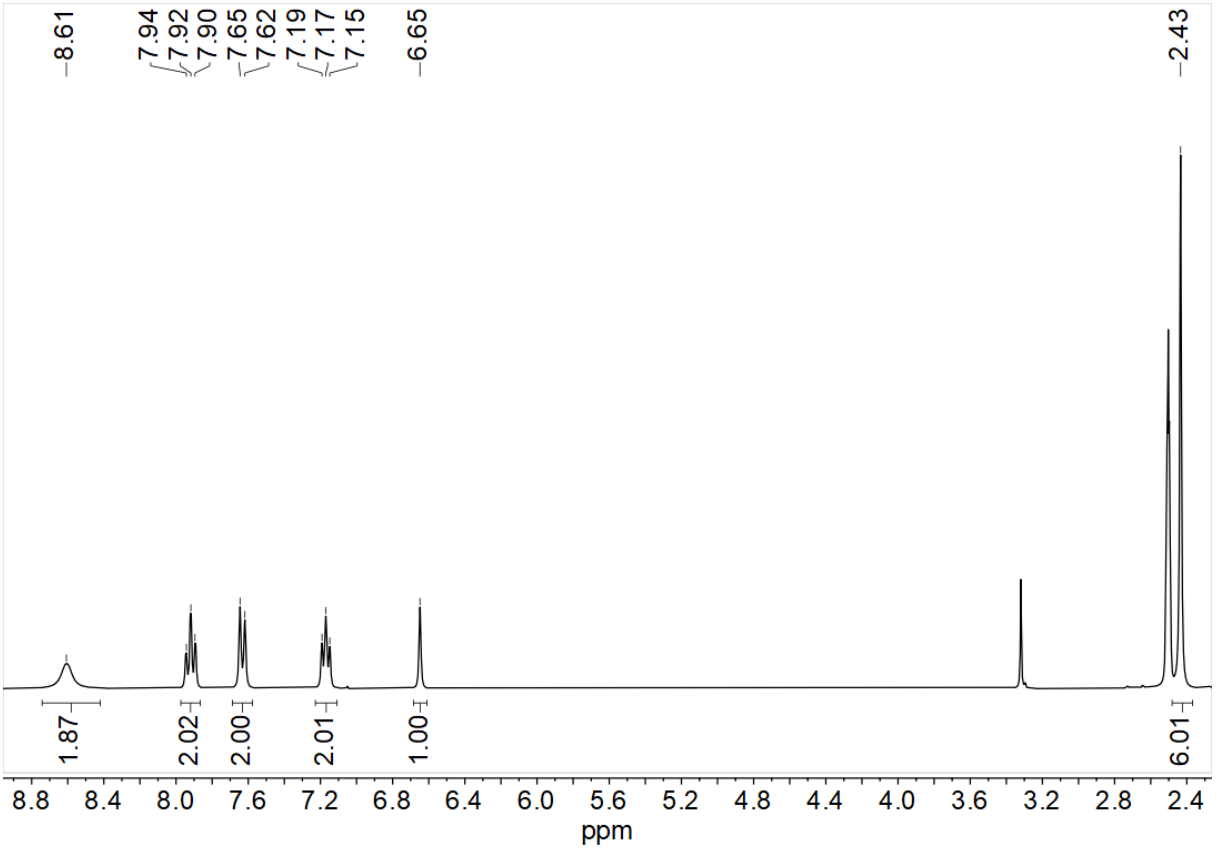

Figure 7-189 300 MHz ^{1}H NMR spectrum of [Ni(Py(4,6MePh)Py)Cl] in DMSO-d_6.

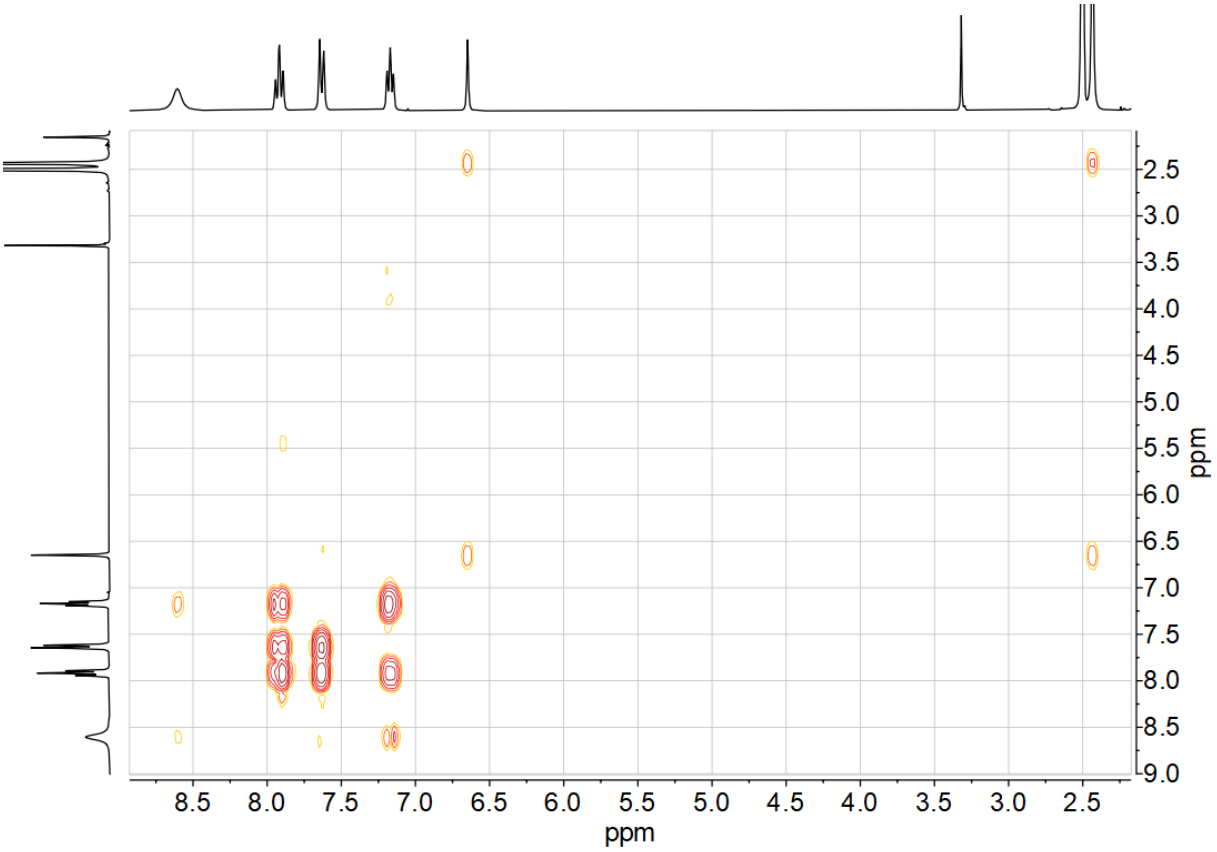

Figure 7-190 ^{1}H,^{1}H COSY correlation spectrum of [Ni(Py(4,6MePh)Py)Cl] in DMSO-d_6.

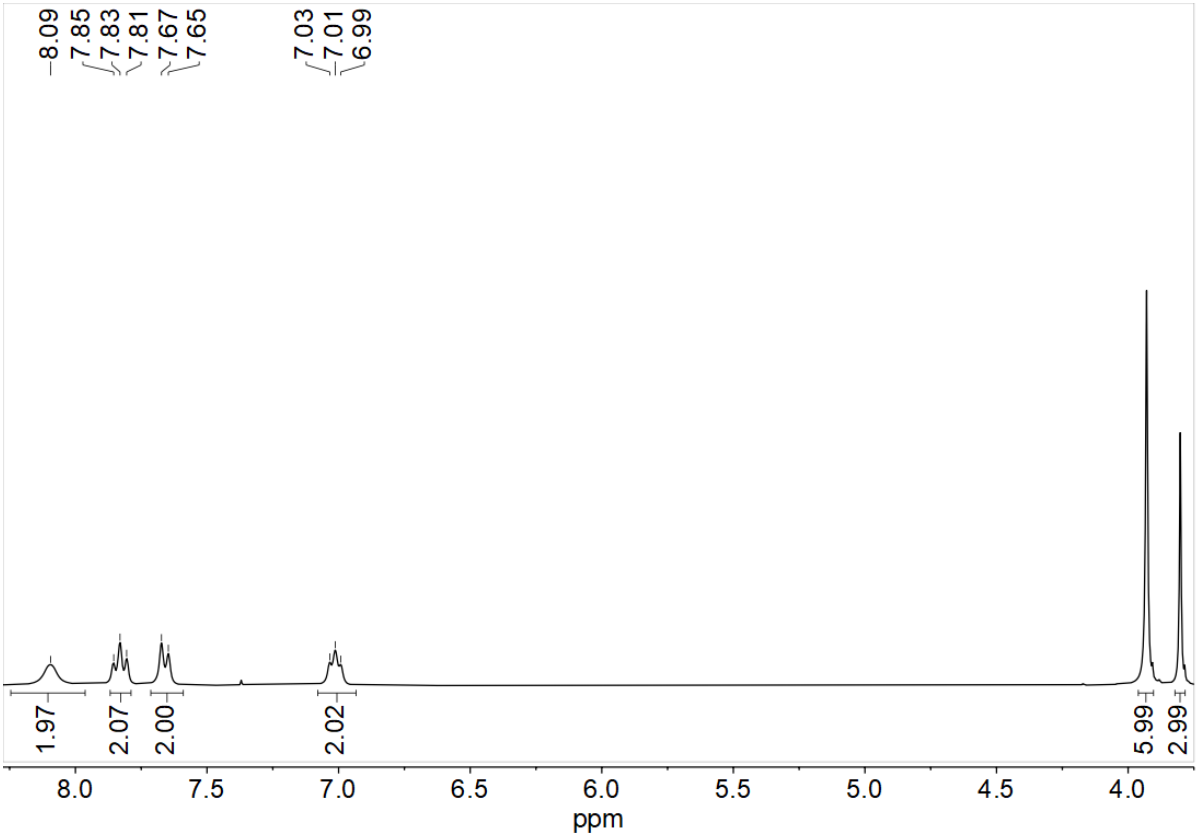

Figure 7-191 300 MHz ^{1}H NMR spectrum of [Ni(Py(4,5,6MeOPh)Py)Br] in DMSO-d_6.

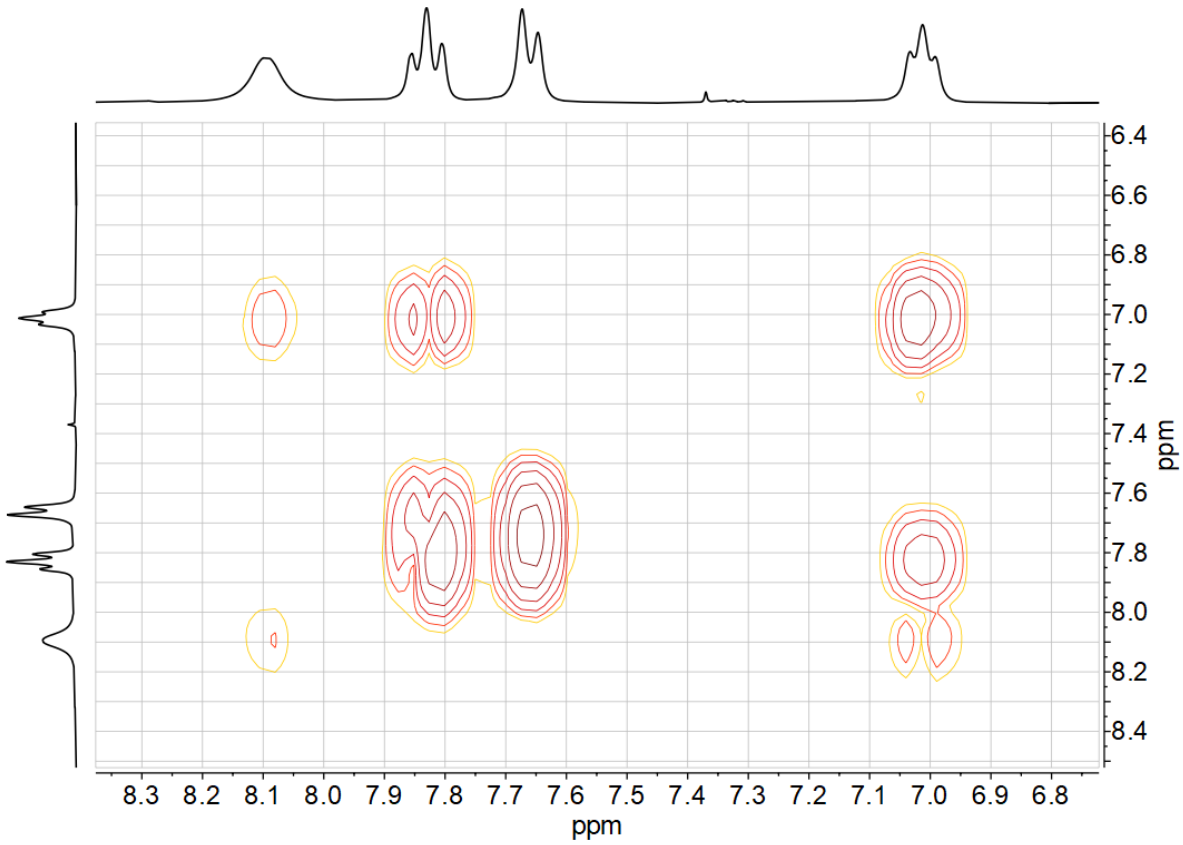

Figure 7-192 ^{1}H,^{1}H COSY correlation spectrum of [Ni(Py(4,5,6MeOPh)Py)Br] in DMSO-d_6.

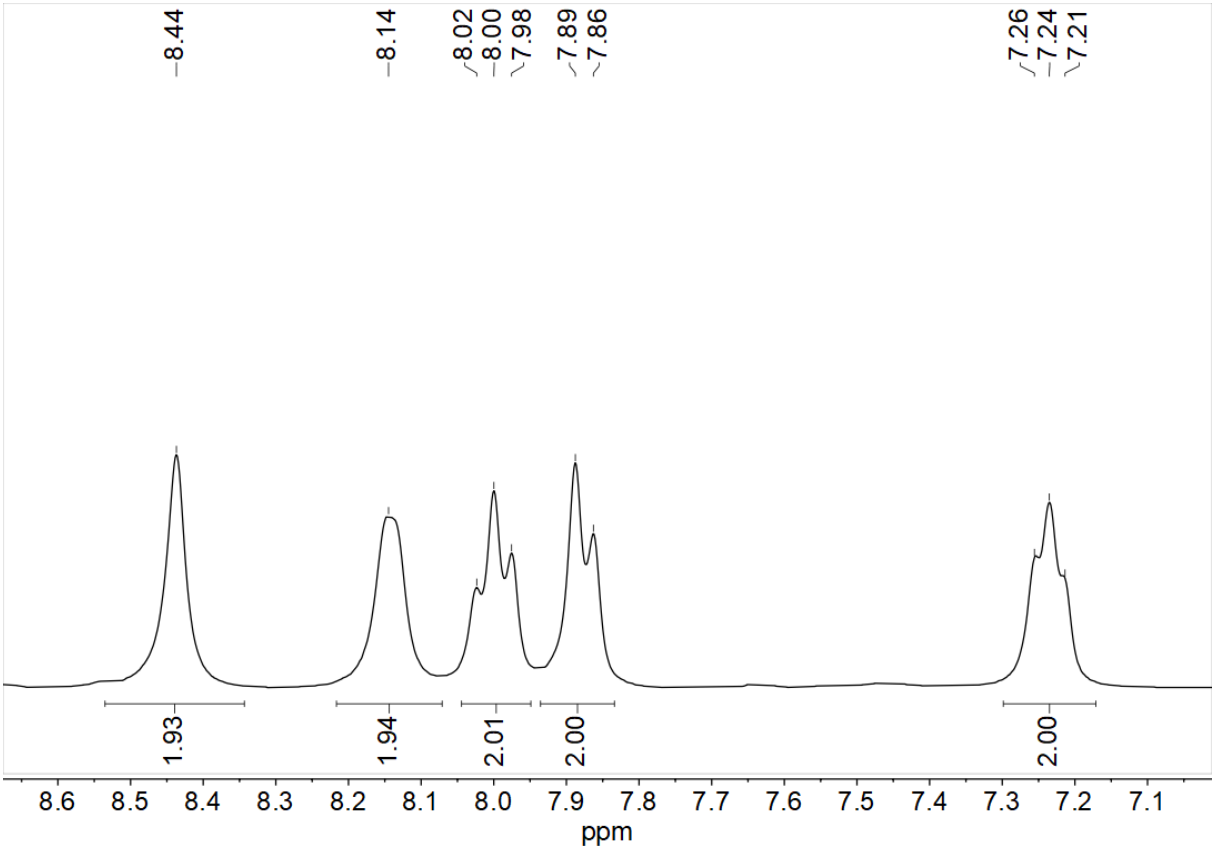

Figure 7-193 300 MHz ^{1}H NMR spectrum of [Ni(Py(Py)Py)Br] in DMSO-d_6.

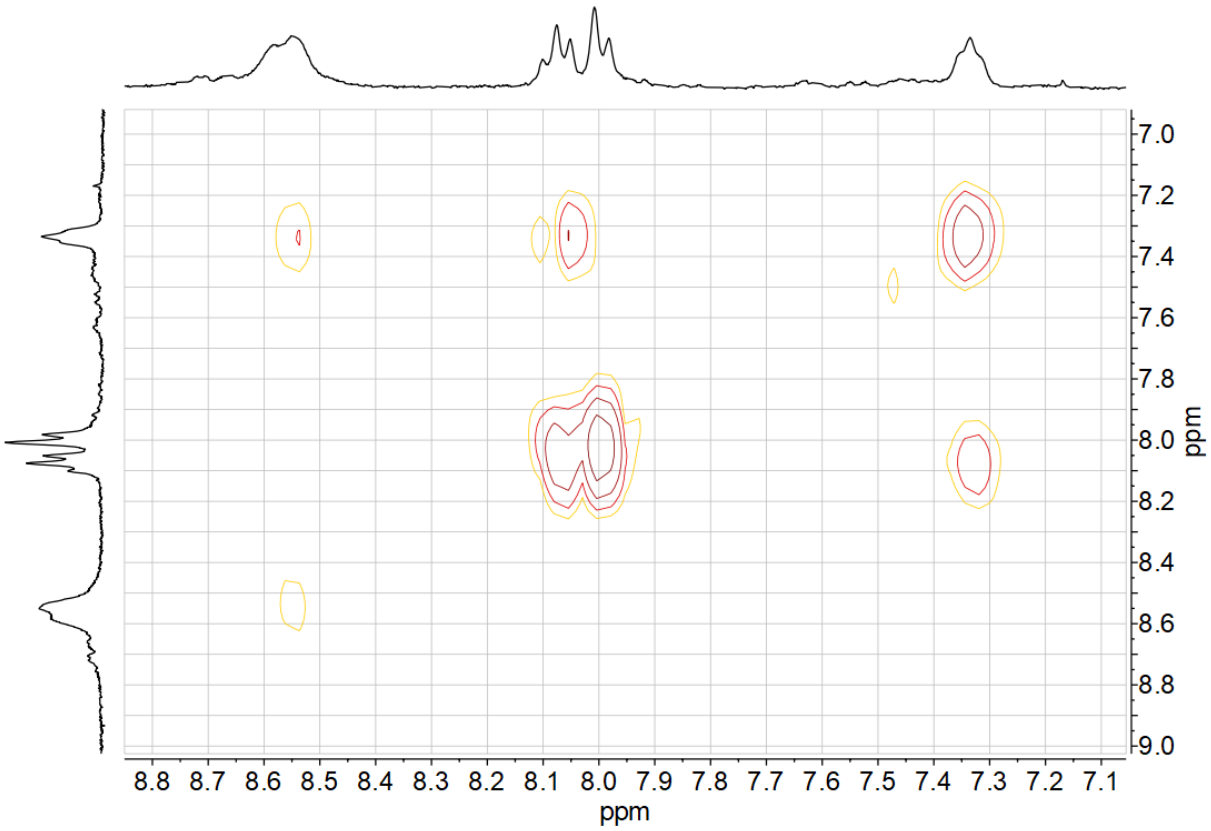

Figure 7-194 ^{1}H,^{1}H COSY correlation spectrum of [Ni(Py(Py)Py)Br] in DMSO-d_6.

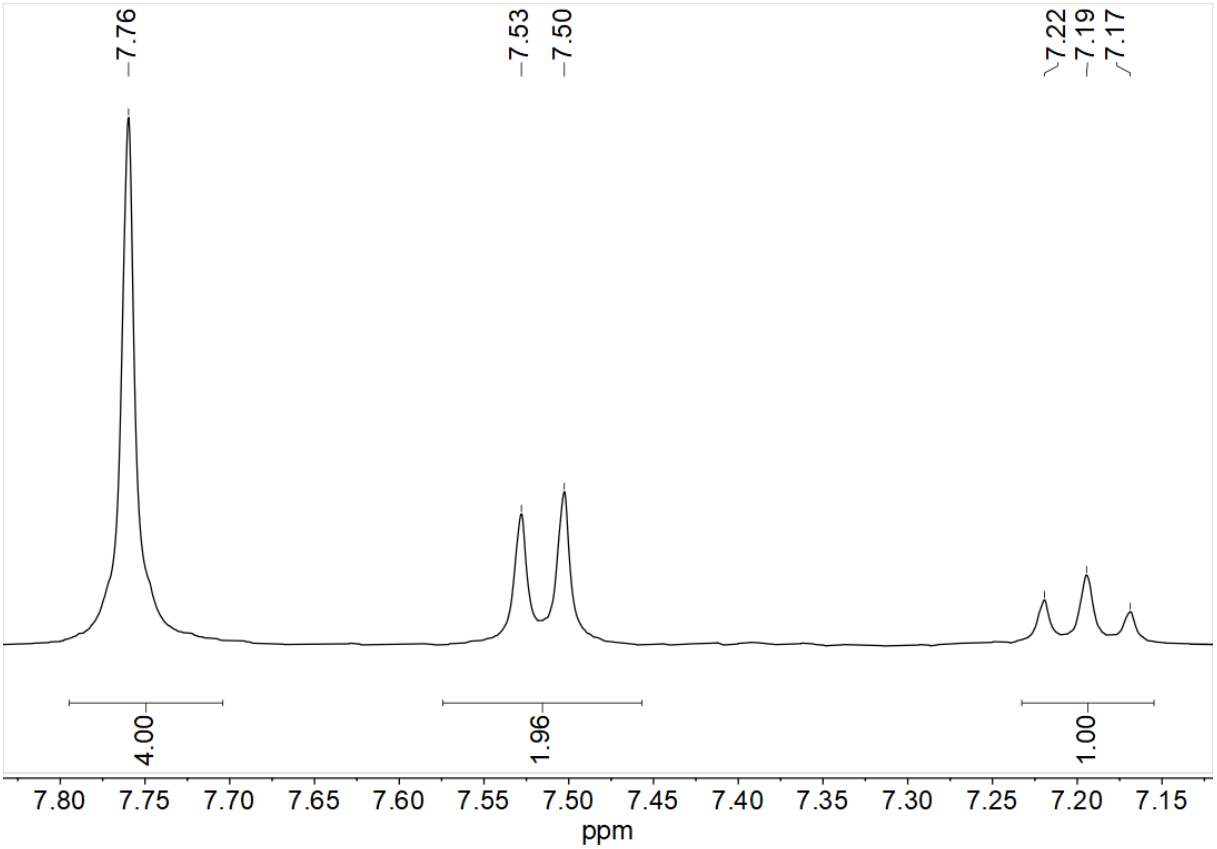

Figure 7-195 300 MHz ^{1}H NMR spectrum of [Ni(2Tz(Ph)2Tz)Cl] in DMSO-d_6.

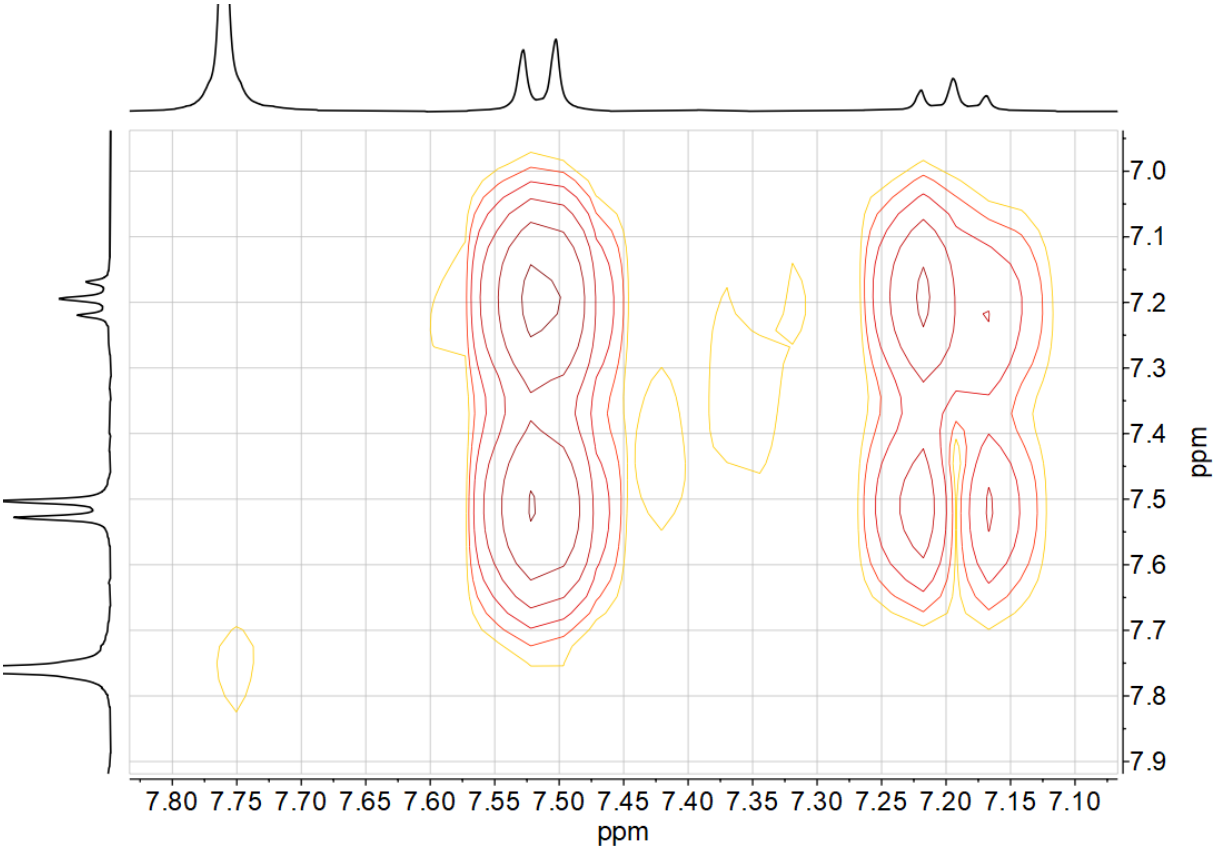

Figure 7-196 ^{1}H,^{1}H COSY correlation spectrum of [Ni(2Tz(Ph)2Tz)Cl] in DMSO-d_6.

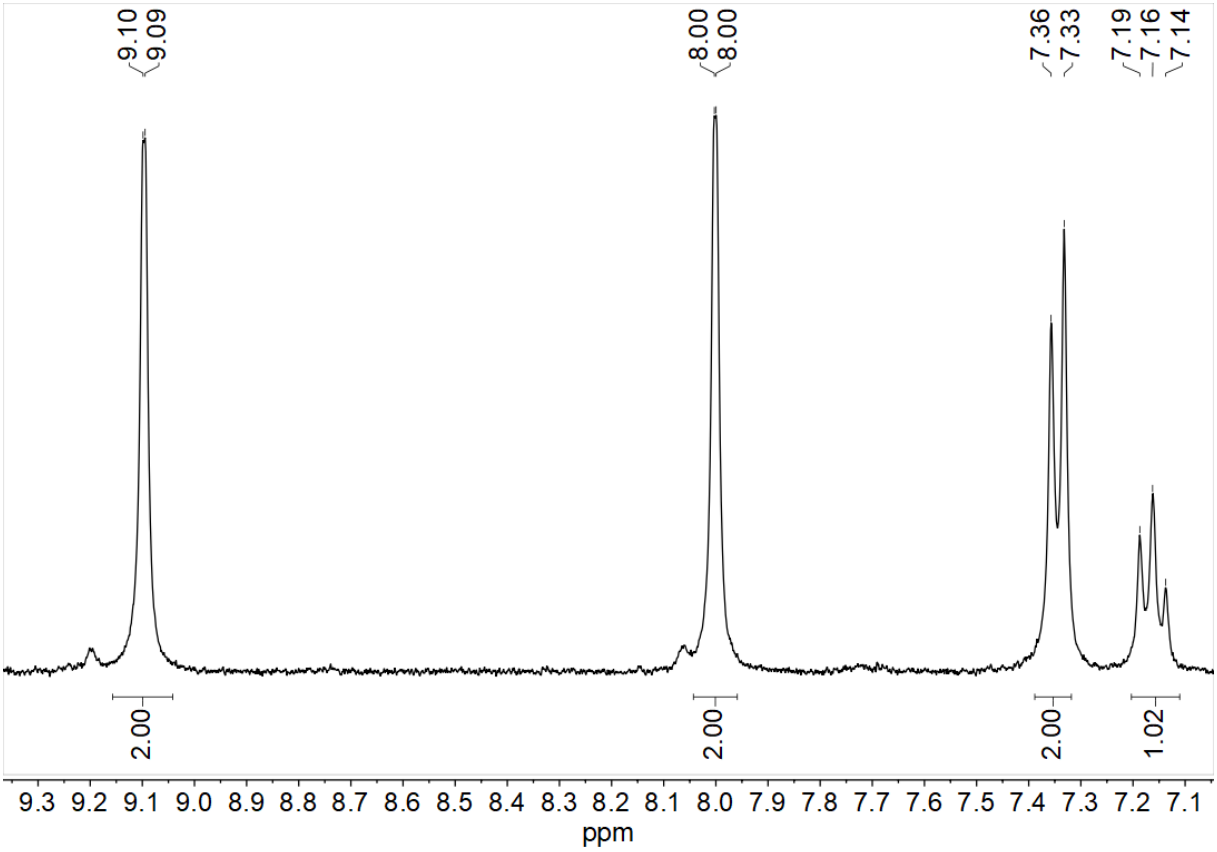

Figure 7-197 300 MHz ^{1}H NMR spectrum of [Ni(4Tz(Ph)4Tz)Cl] in DMSO-d_6.

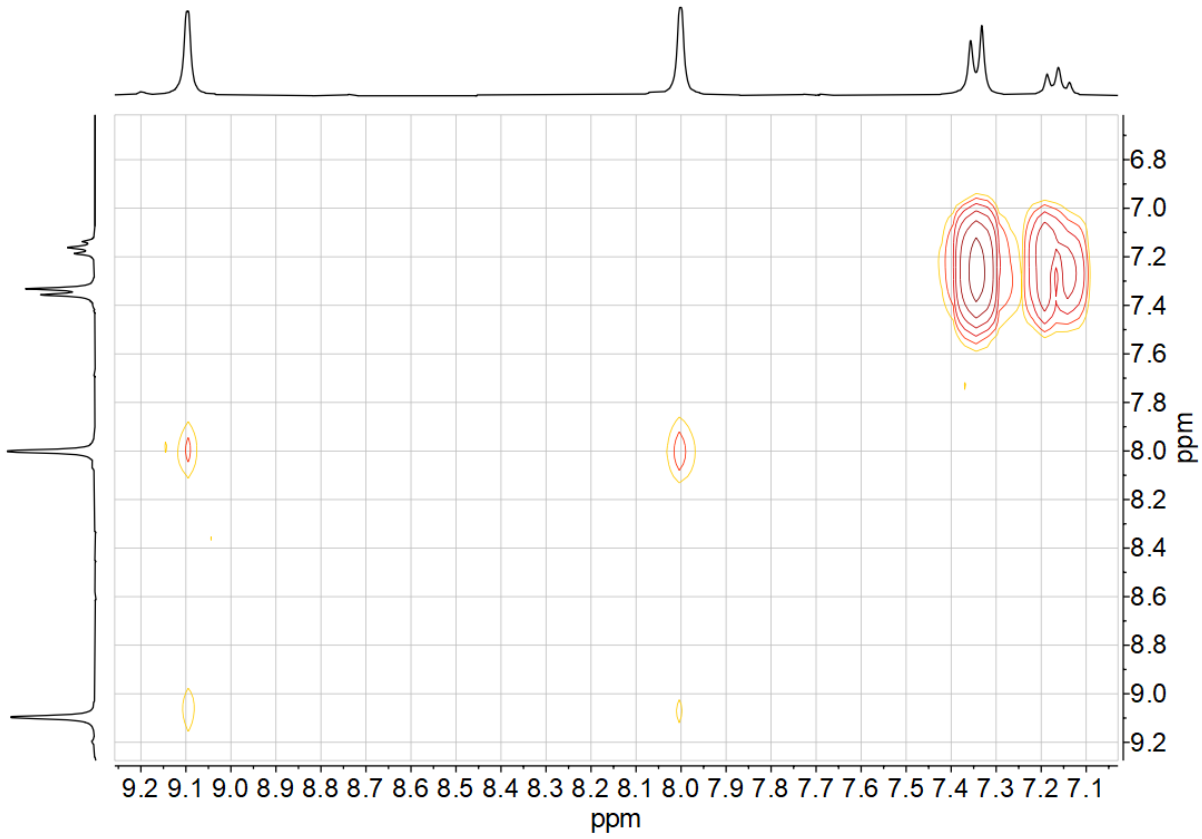

Figure 7-198 ^{1}H,^{1}H COSY correlation spectrum of [Ni(4Tz(Ph)4Tz)Cl] in DMSO-d_6.

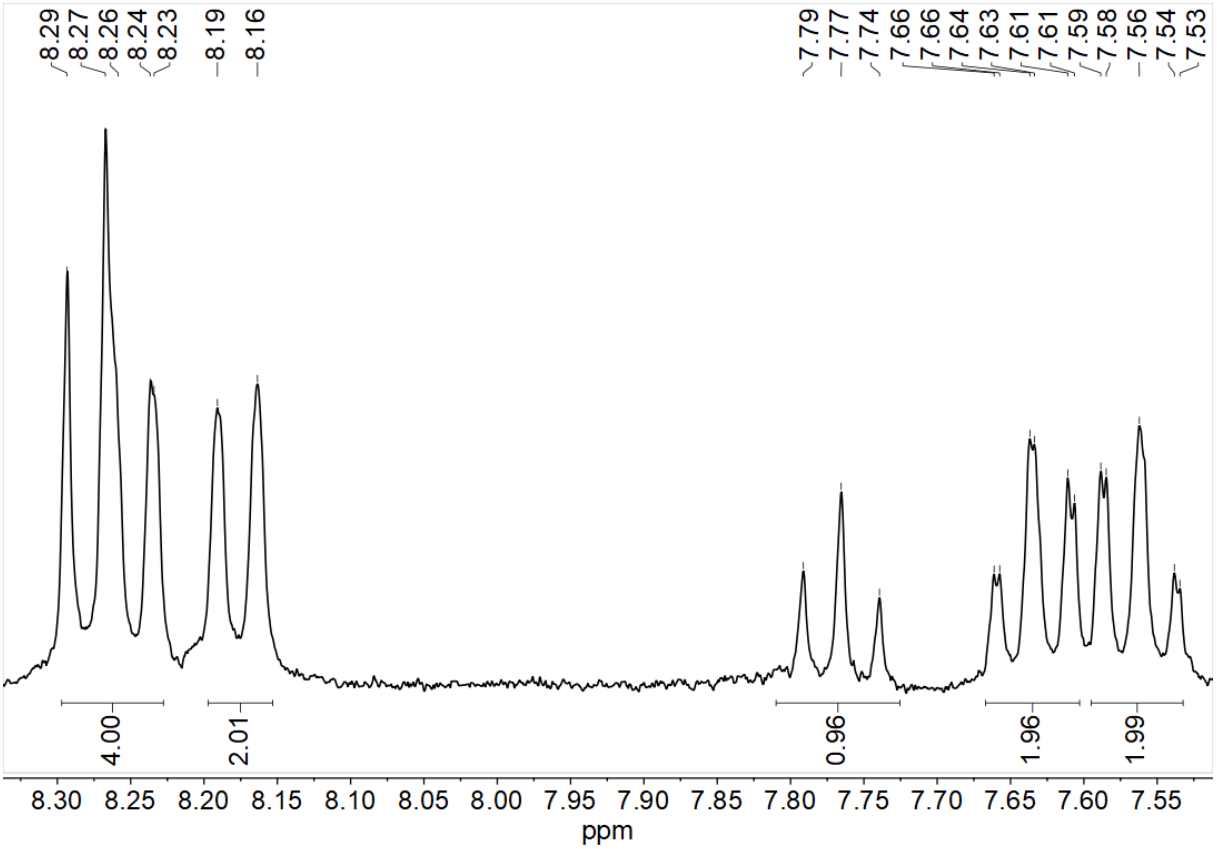

Figure 7-199 300 MHz ^{1}H NMR spectrum of [Ni(2Btz(Ph)2Btz)Cl] in DMSO-d_6.

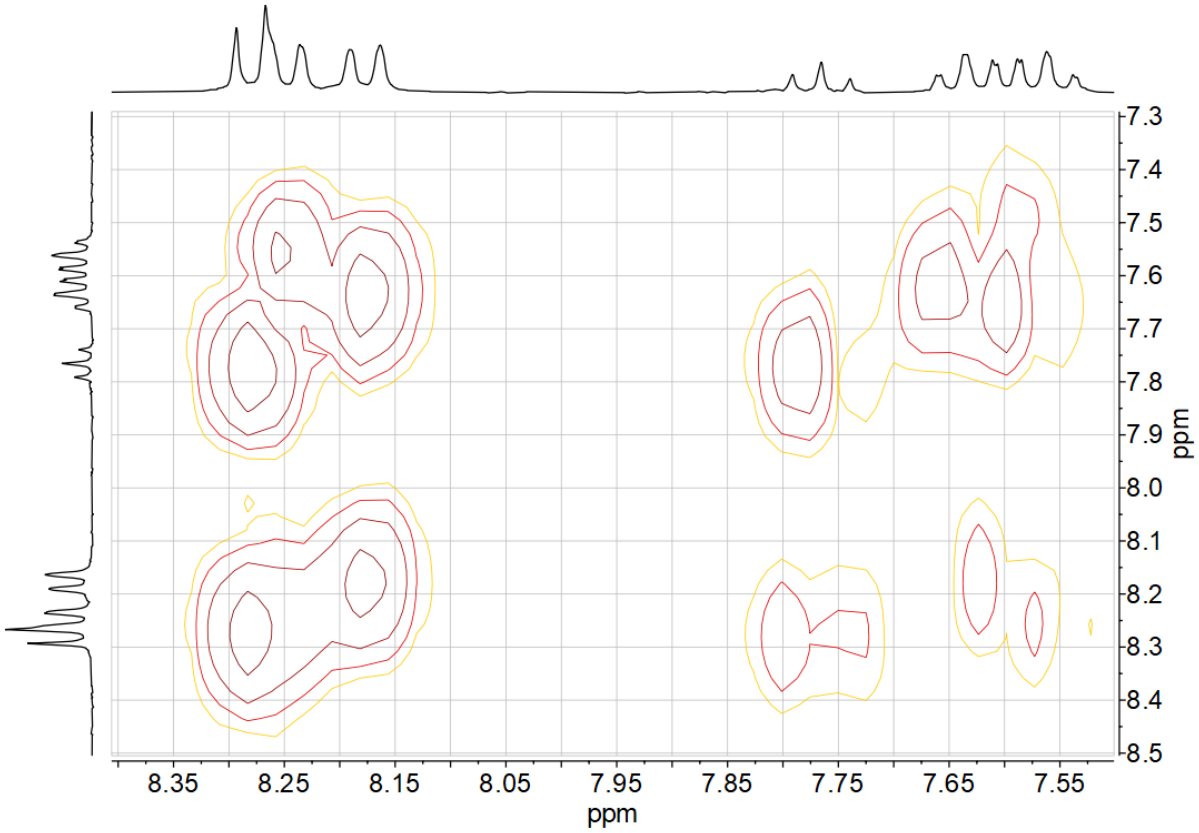

Figure 7-200 ^{1}H,^{1}H COSY correlation spectrum of [Ni(2Btz(Ph)2Btz)Cl] in DMSO-d_6.

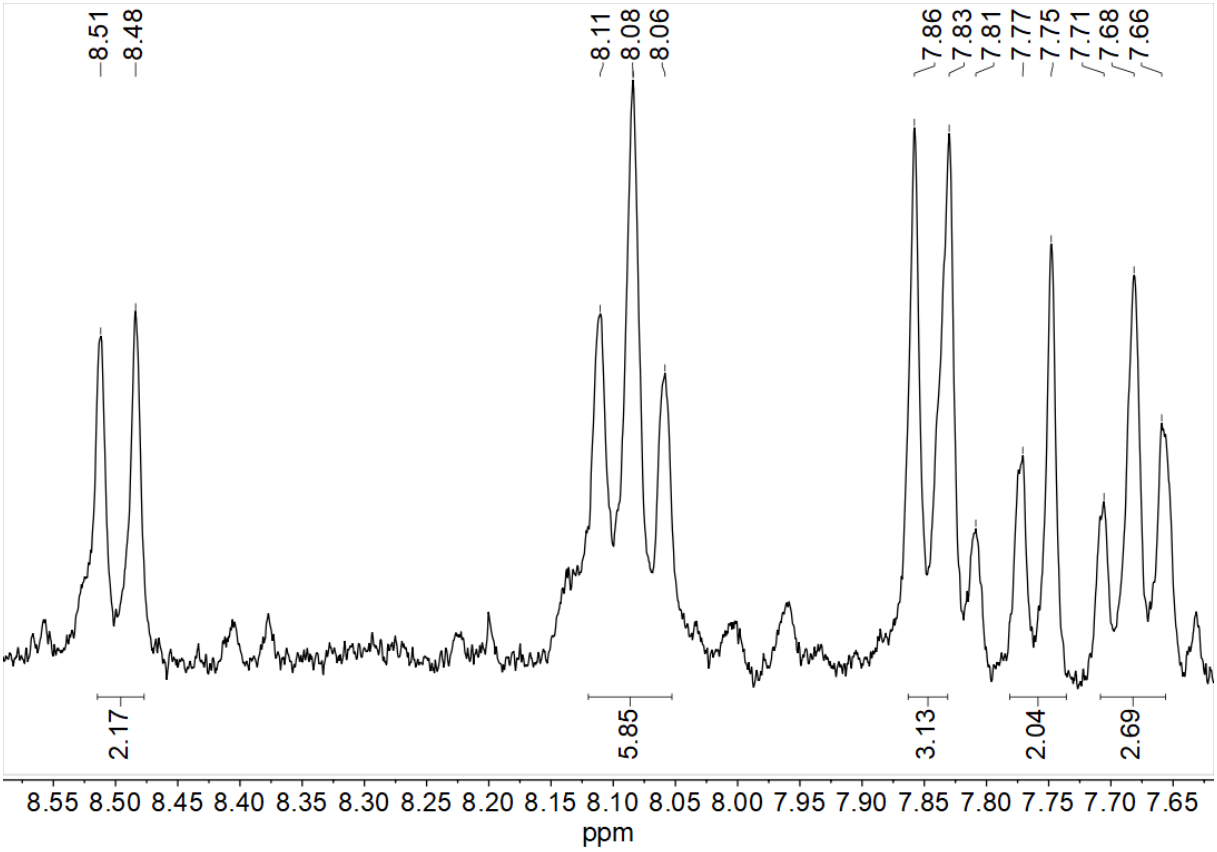

Figure 7-201 300 MHz ^{1}H-NMR spectrum of [Ni(2Qu(Ph)2Qu)Cl] in DMSO-d_6.

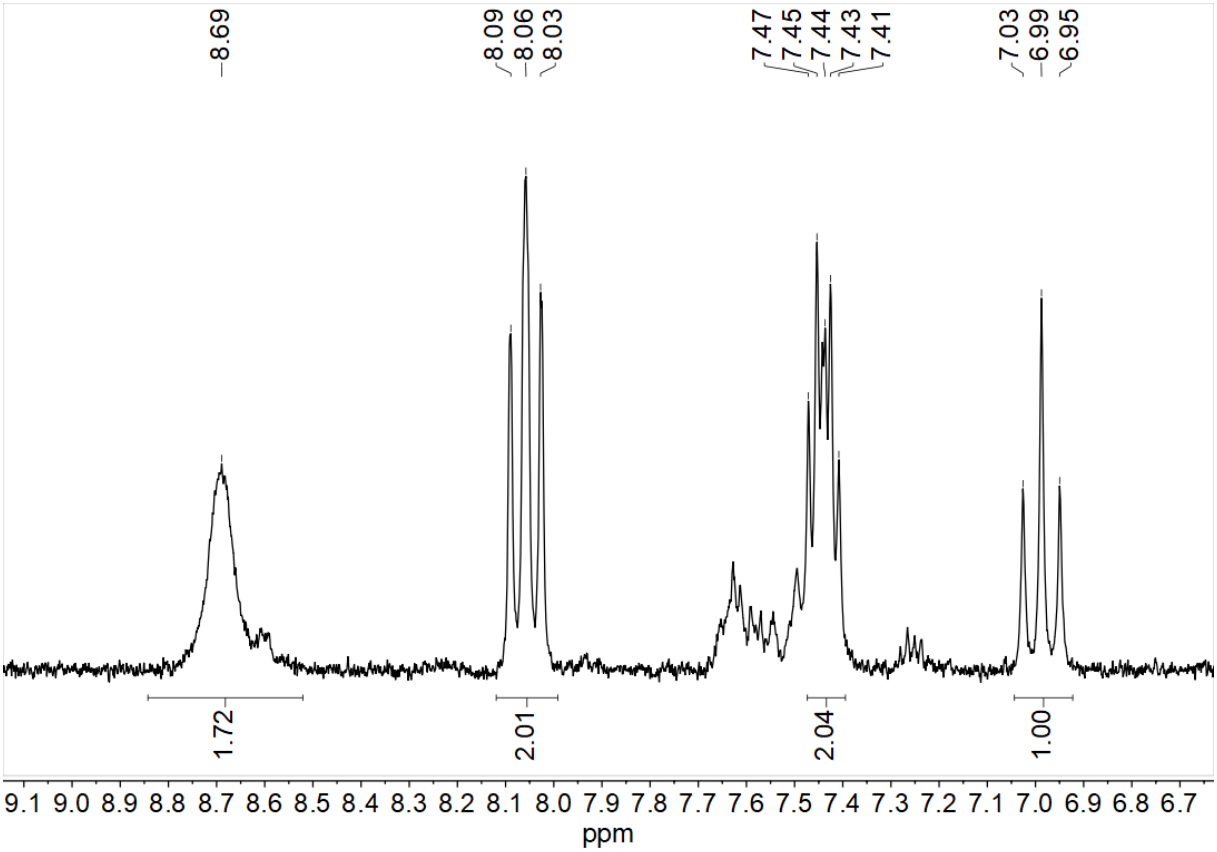

Figure 7-202 300 MHz ^{1}H NMR spectrum of [Ni(3FPy(4,6FPh)3FPy)Br] in DMSO-d_6.

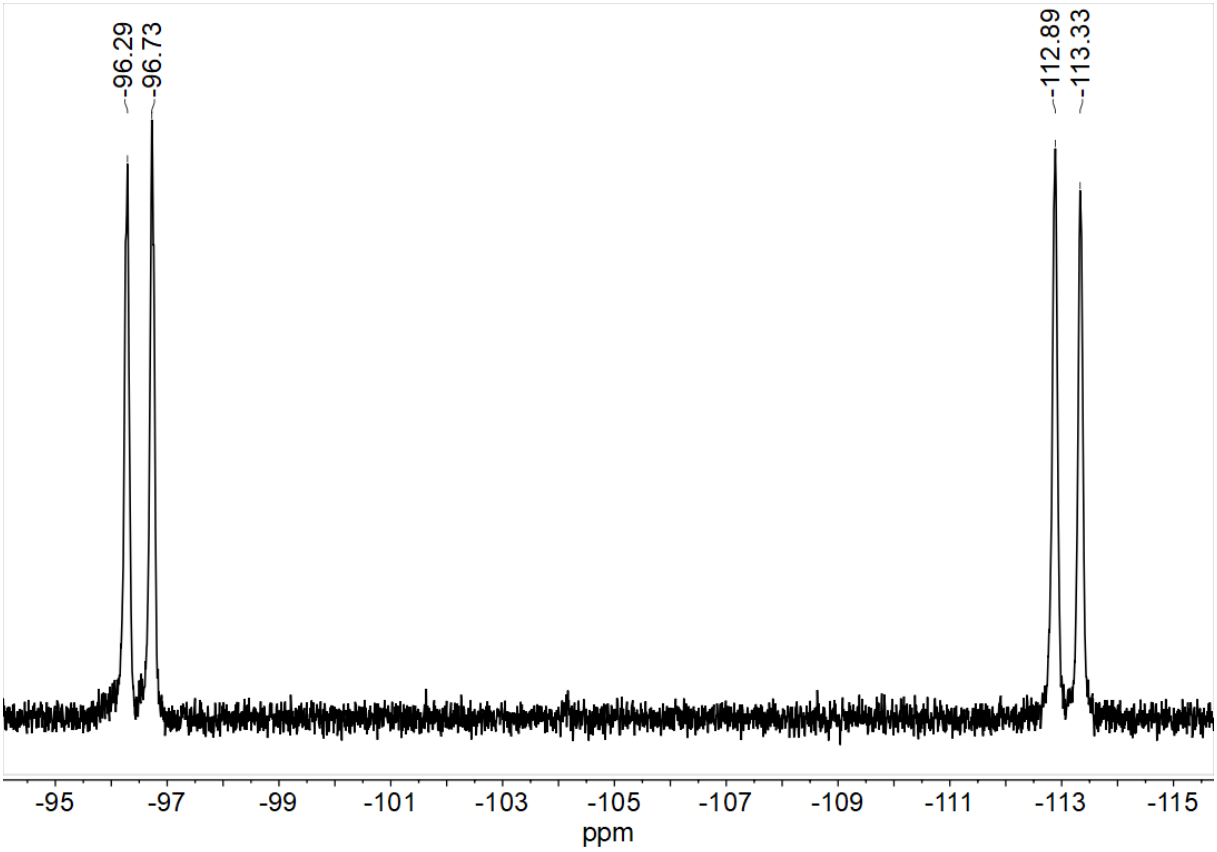

Figure 7-203 282 MHz ^{19}F NMR spectrum of [Ni(3FPy(4,6FPh)3FPy)Br] in DMSO-d_6.

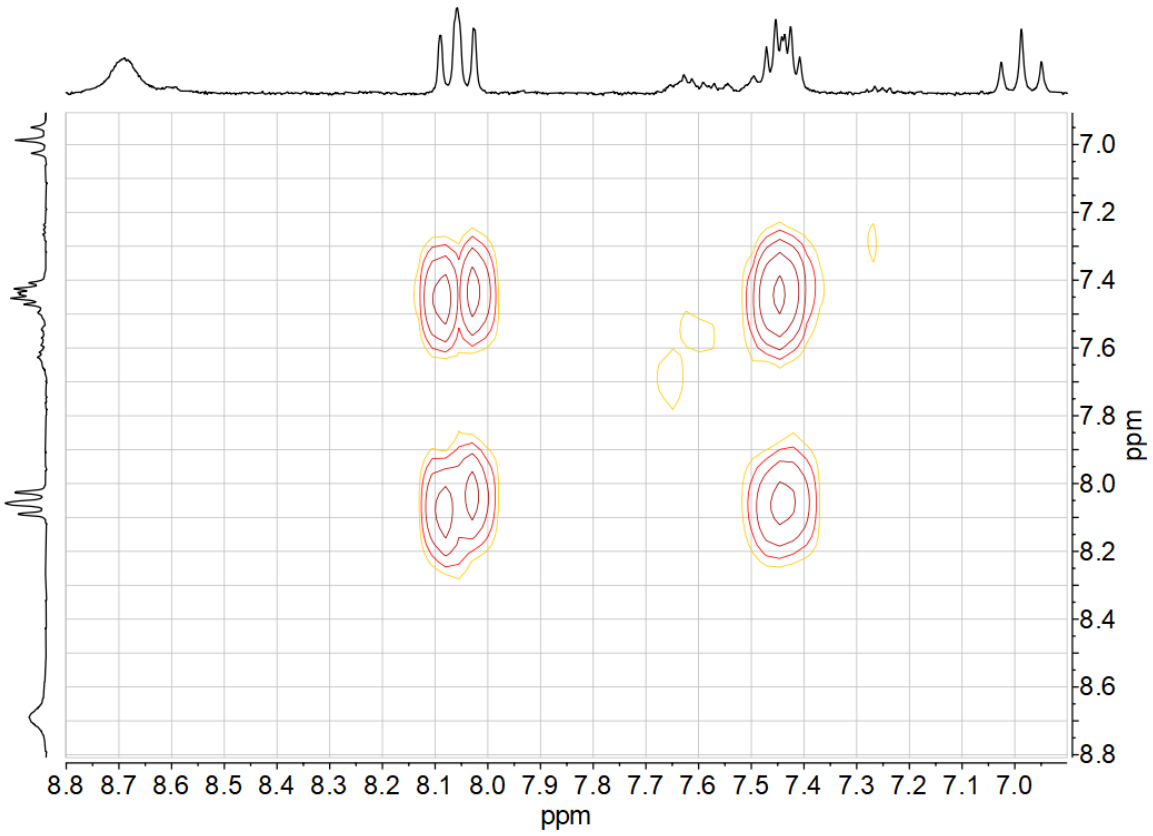

Figure 7-204 ^{1}H,^{1}H COSY correlation spectrum of [Ni(3FPy(4,6FPh)3FPy)Br] in DMSO-d_6.

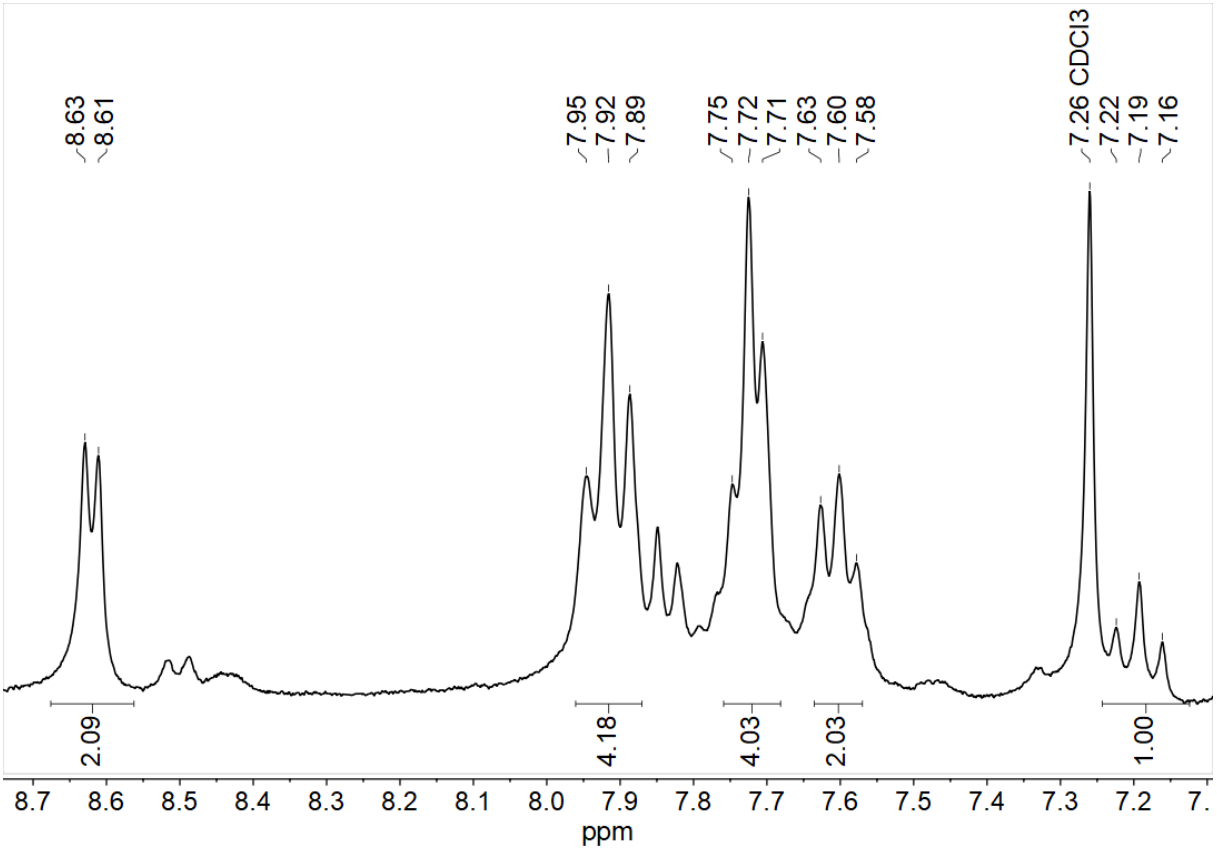

Figure 7-205 300 MHz ^{1}H NMR spectrum of [Ni(2^{i}Qu(4,6FPh)2^{i}Qu)Br] in $CDCl_3$.

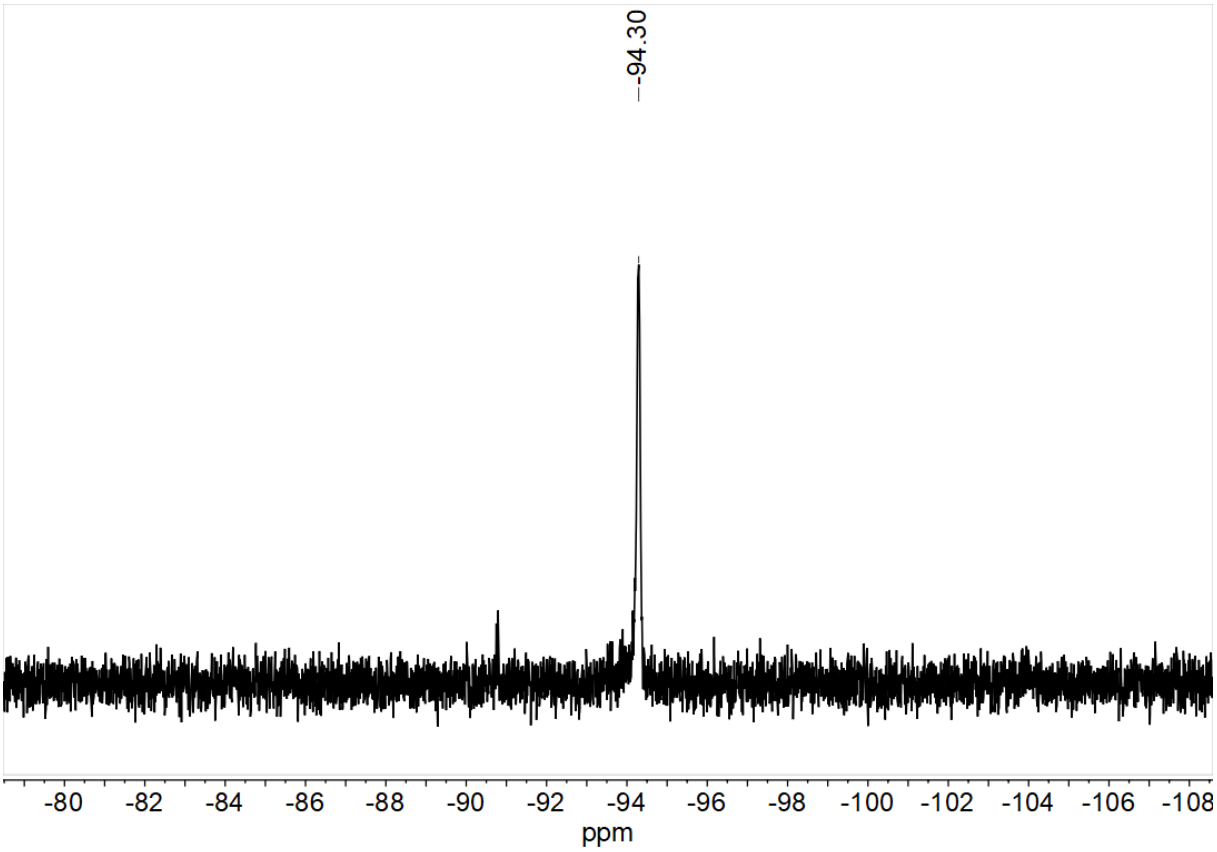

Figure 7-206 282 MHz ^{19}F NMR spectrum of [Ni(2^{i}Qu(4,6FPh)2^{i}Qu)Br] in $CDCl_3$.

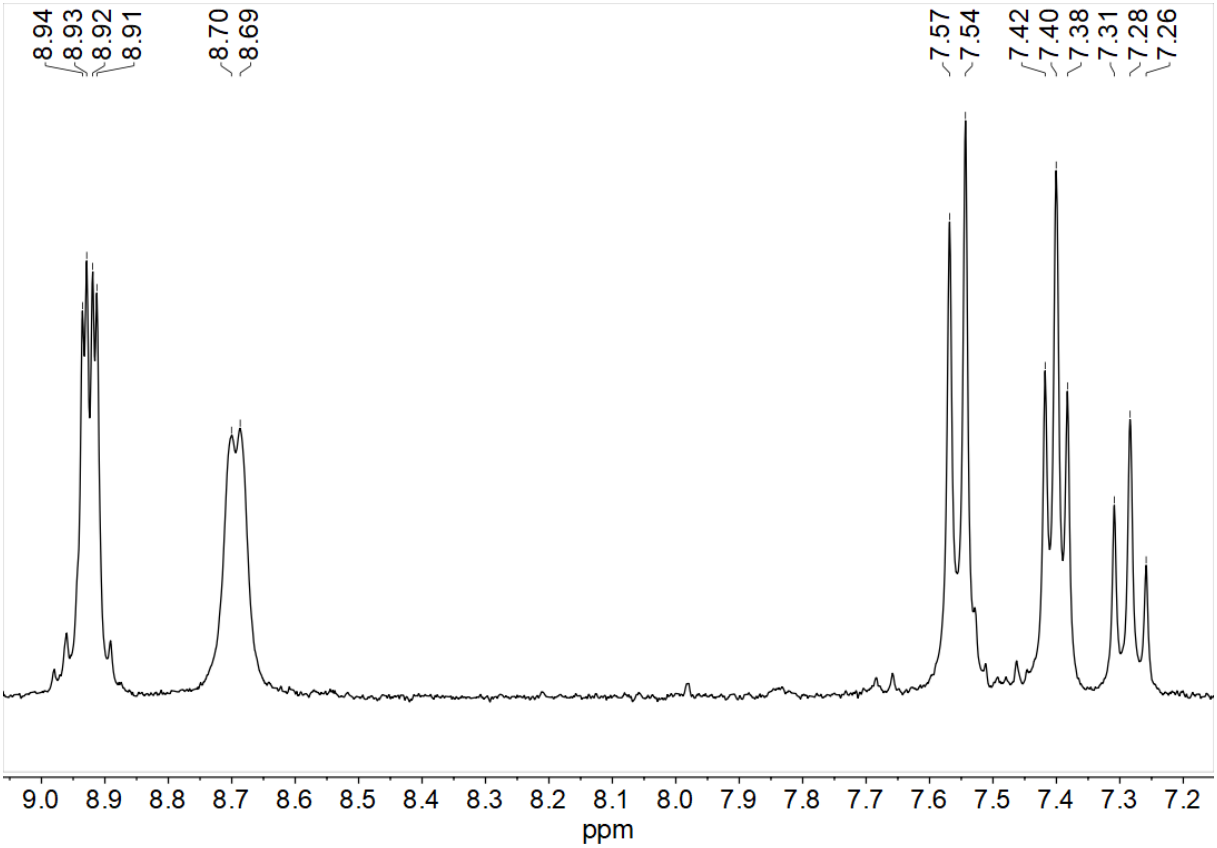

Figure 7-207 500 MHz ^{1}H NMR spectrum of [Ni(Pym(Ph)Pym)Br] in DMSO-d_6.

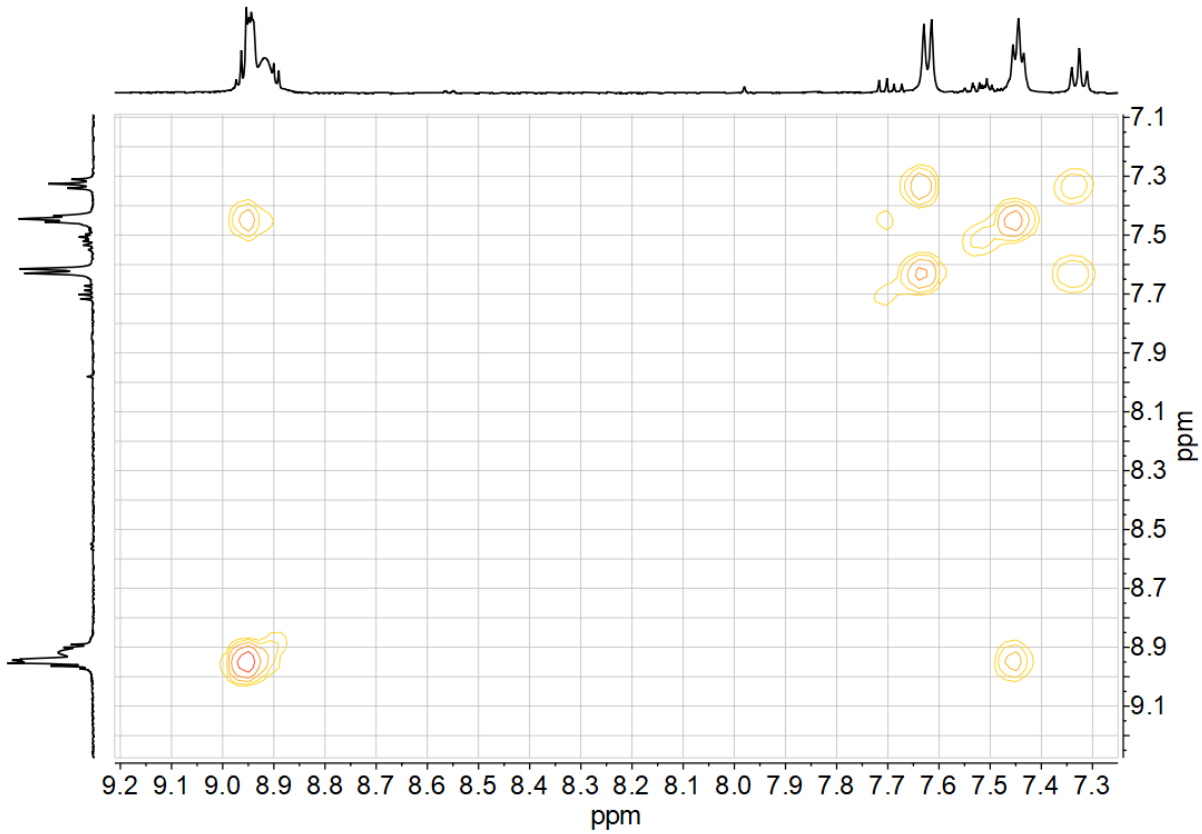

Figure 7-208 ^{1}H,^{1}H COSY correlation spectrum of [Ni(Pym(Ph)Pym)Br] in DMSO-d_6.

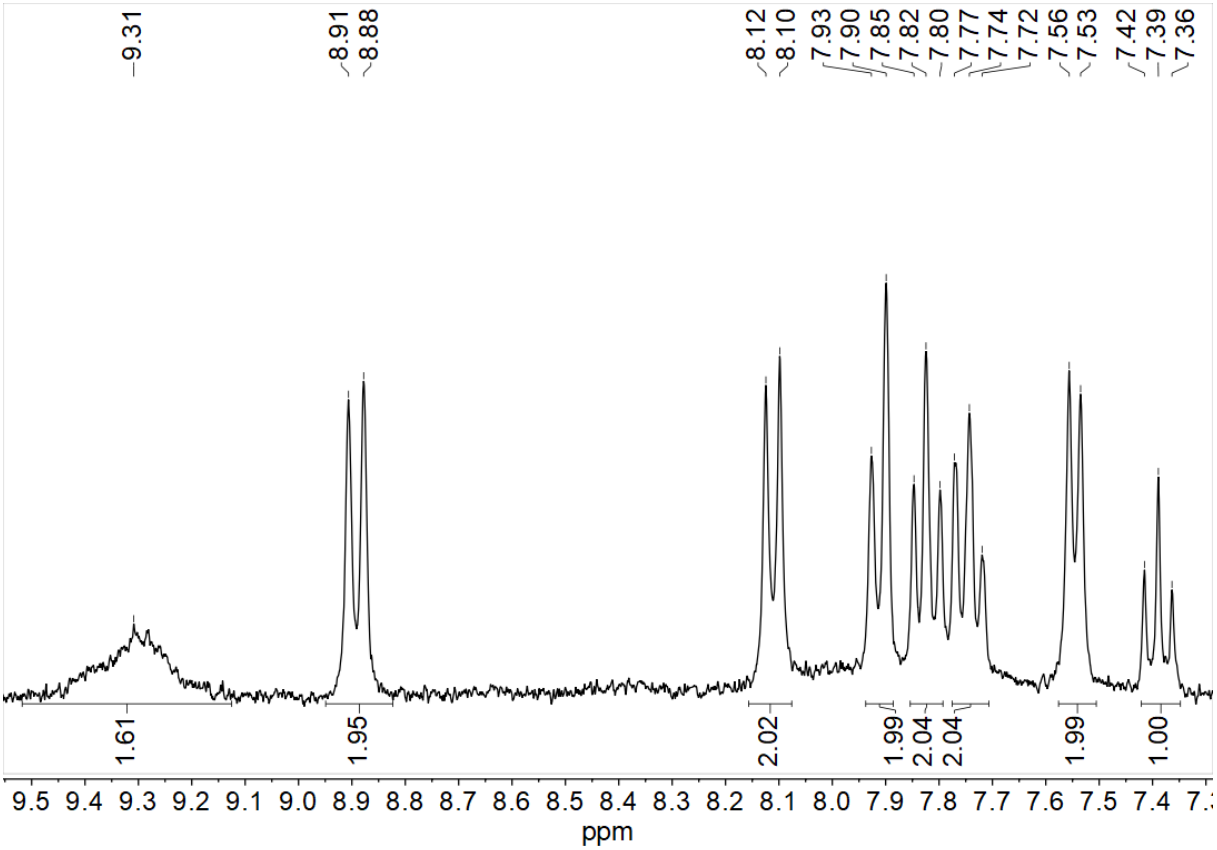

Figure 7-209 300 MHz ^{1}H NMR spectrum of [Ni(2^{i}Qu(Ph)2^{i}Qu)Br] in CD_2Cl_2.

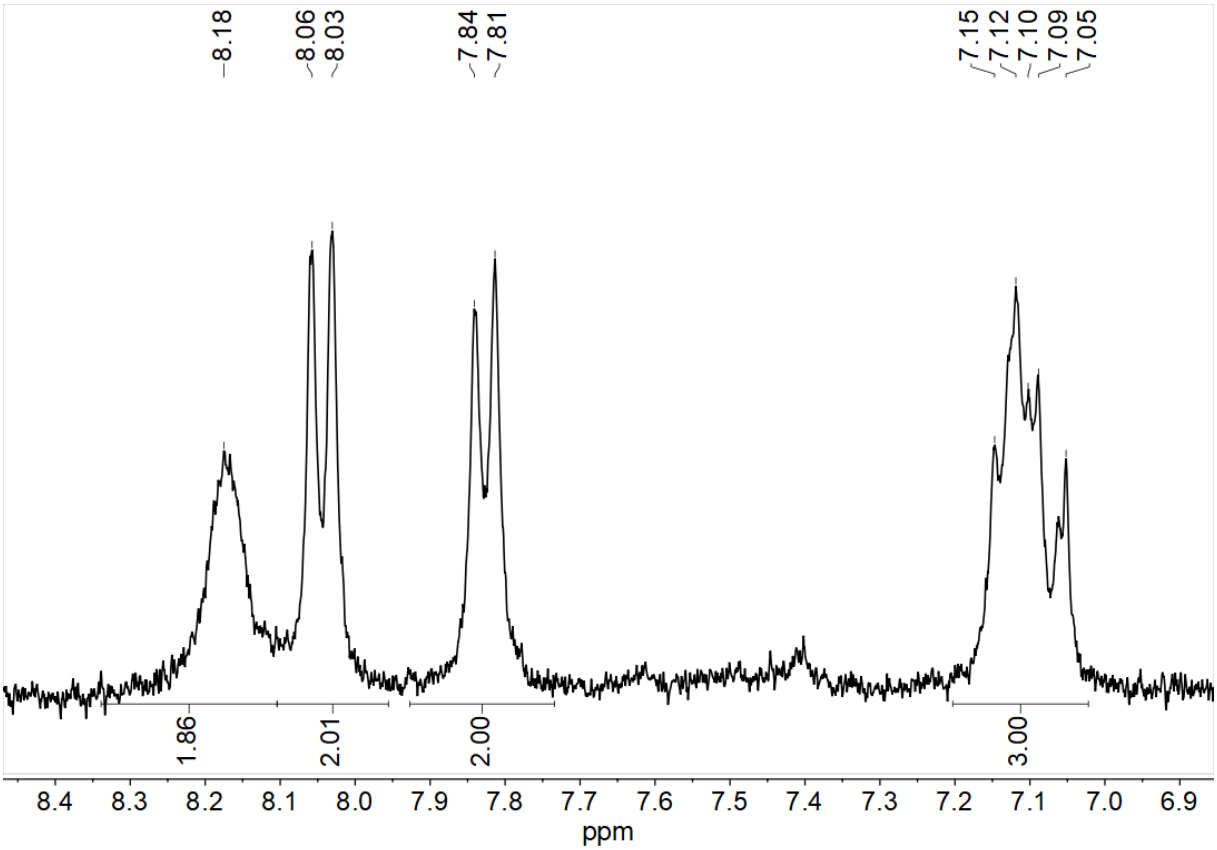

Figure 7-210 300 MHz ^{1}H NMR spectrum of [Ni(3ClPy(Ph)3ClPy)Br] in DMSO-d_6.

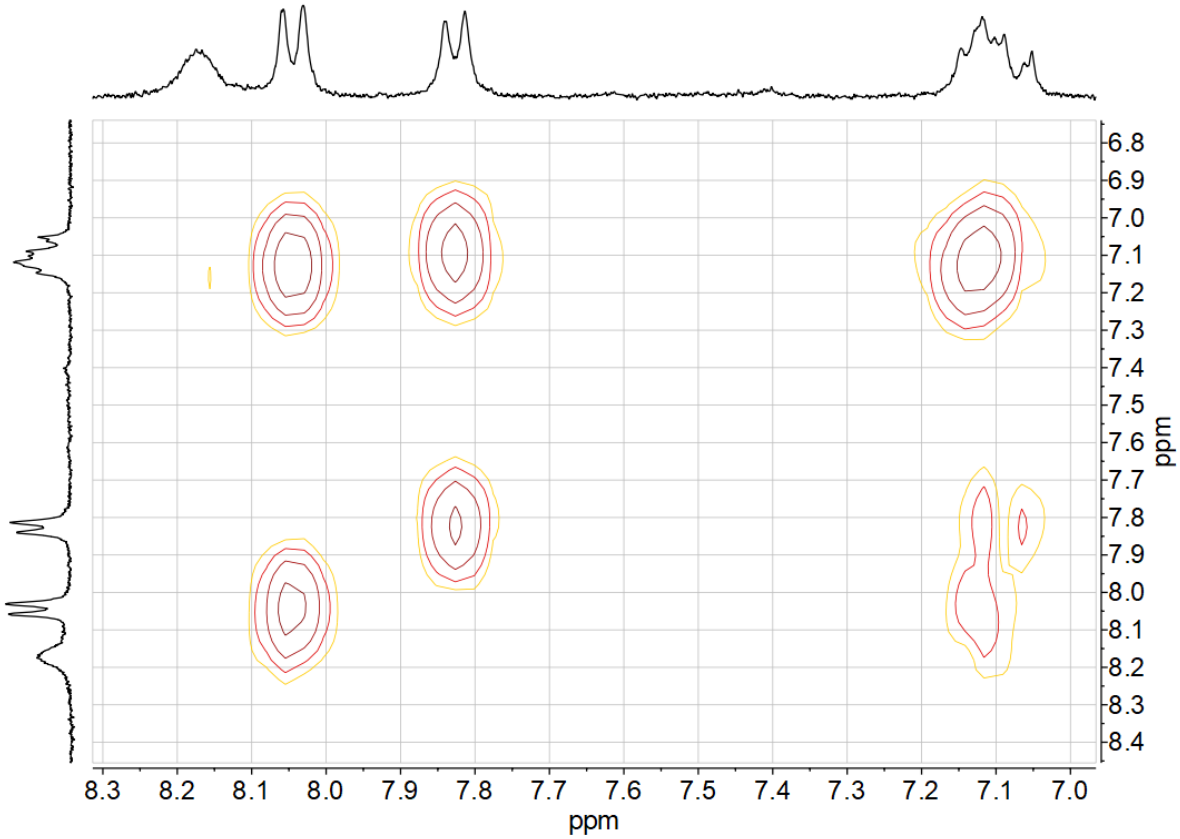

Figure 7-211 ^{1}H,^{1}H COSY correlation spectrum of [Ni(3ClPy(Ph)3ClPy)Br] in DMSO-d_6.

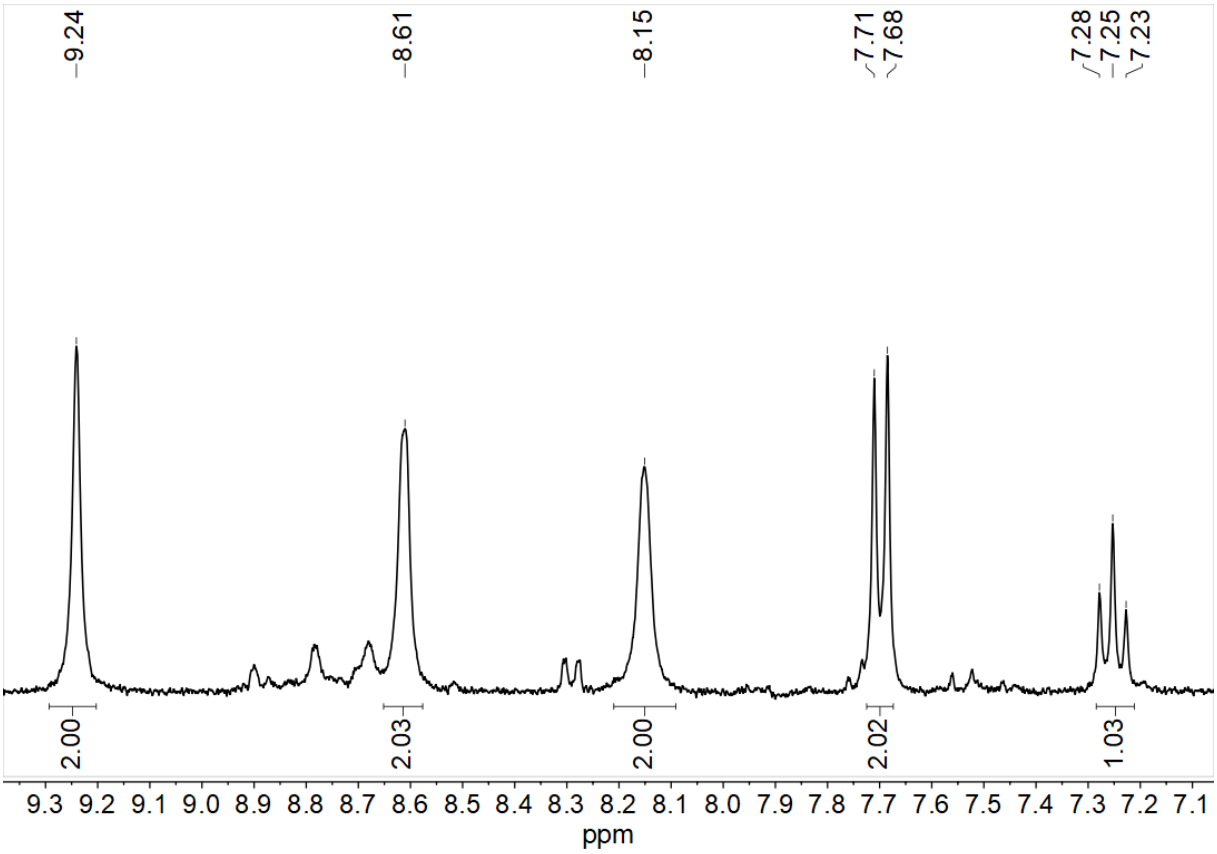

Figure 7-212 300 MHz ^{1}H NMR spectrum of [Ni(Pz(Ph)Pz)Br] in DMSO-d_6.

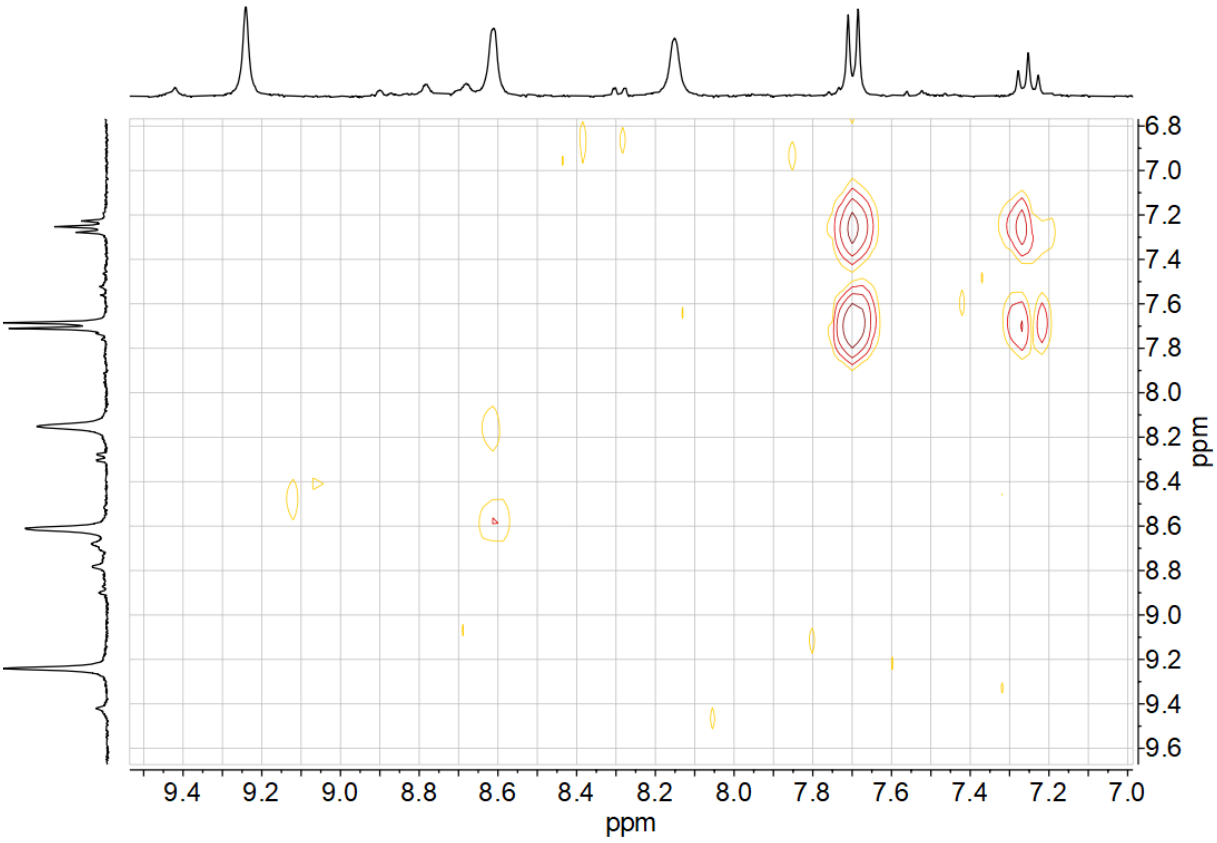

Figure 7-213 ^{1}H,^{1}H COSY correlation spectrum of [Ni(Pz(Ph)Pz)Br] in DMSO-d_6.

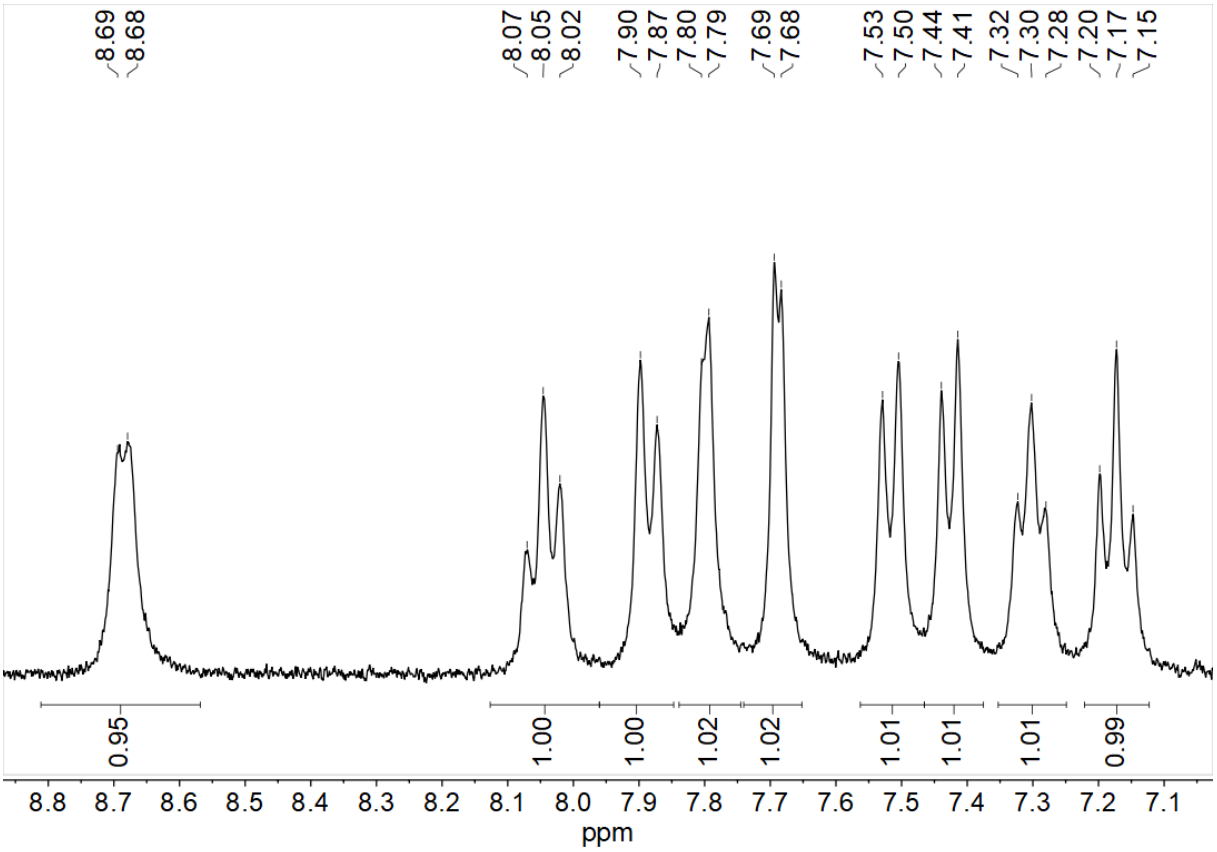

Figure 7-214 300 MHz ^{1}H NMR spectrum of [Ni(2Tz(Ph)Py)Br] in DMSO-d_6.

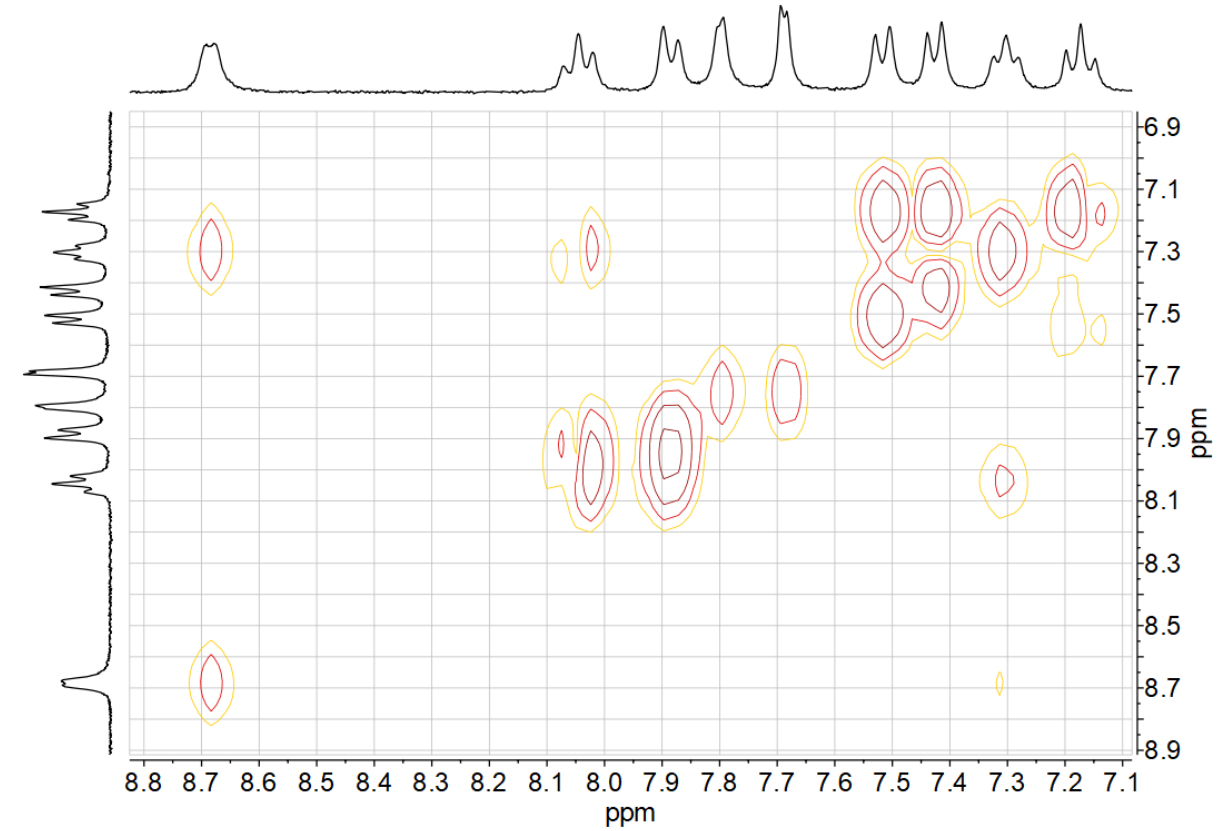

Figure 7-215 ^{1}H,^{1}H COSY correlation spectrum of [Ni(2Tz(Ph)Py)Br] in DMSO-d_6.

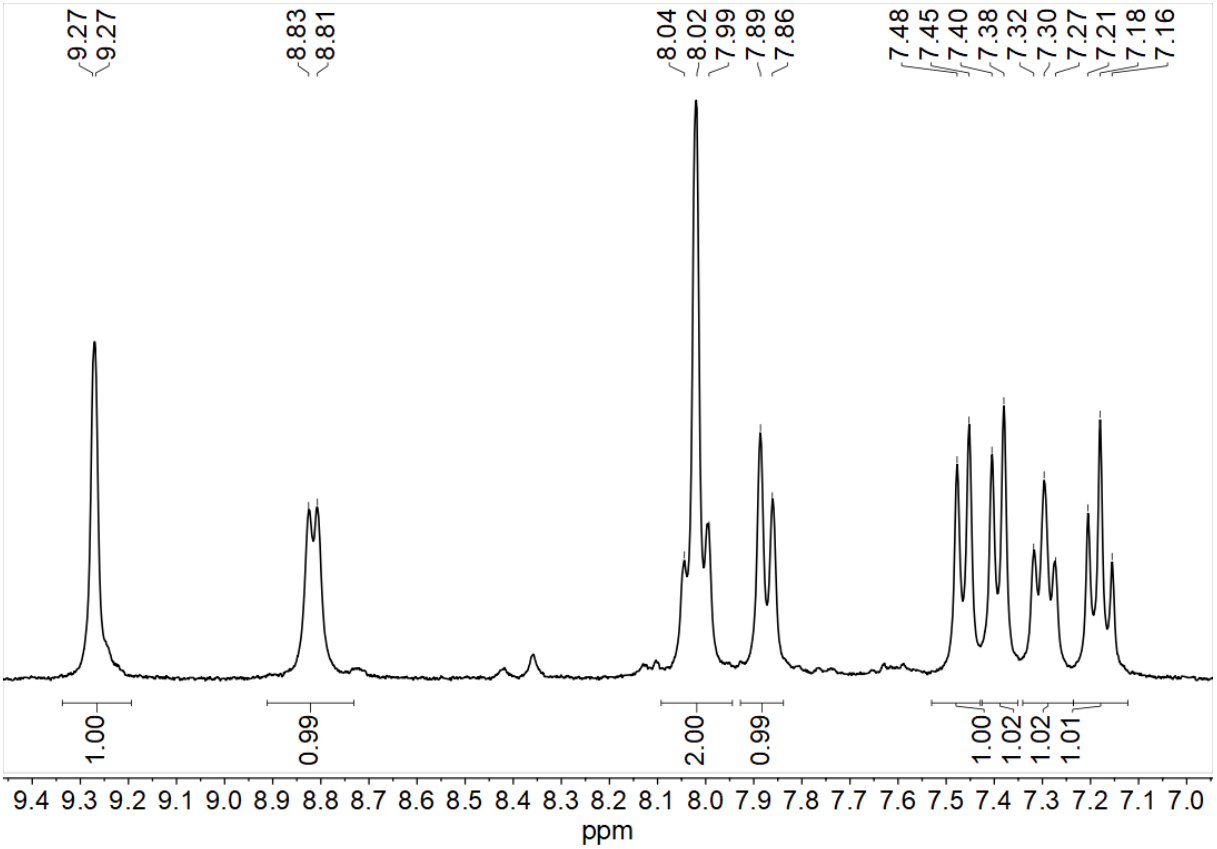

Figure 7-216 300 MHz ^{1}H NMR spectrum of [Ni(4Tz(Ph)Py)Br] in DMSO-d_6.

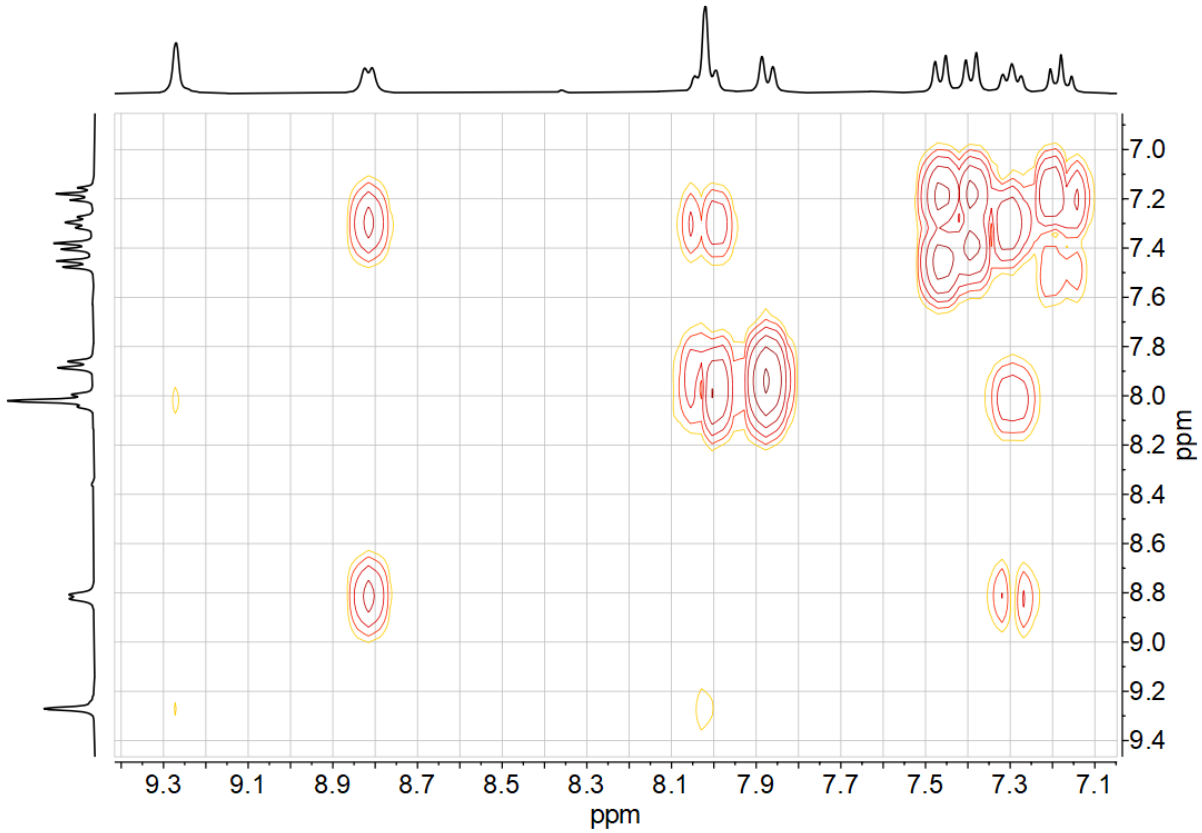

Figure 7-217 ^{1}H,^{1}H COSY correlation spectrum of [Ni(4Tz(Ph)Py)Br] in DMSO-d_6.

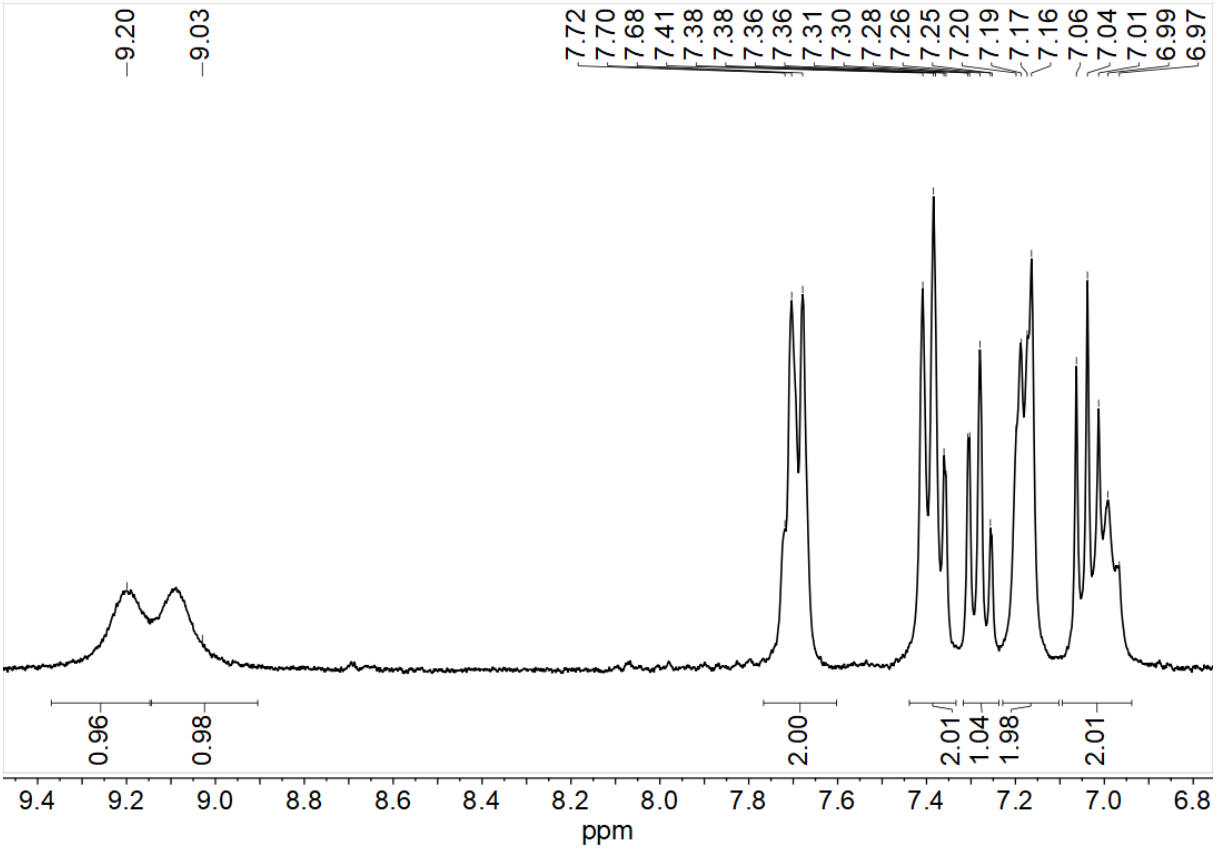

Figure 7-218 300 MHz ^{1}H NMR spectrum of [Ni(2Btz(Ph)Py)Br] in CD_2Cl_2.

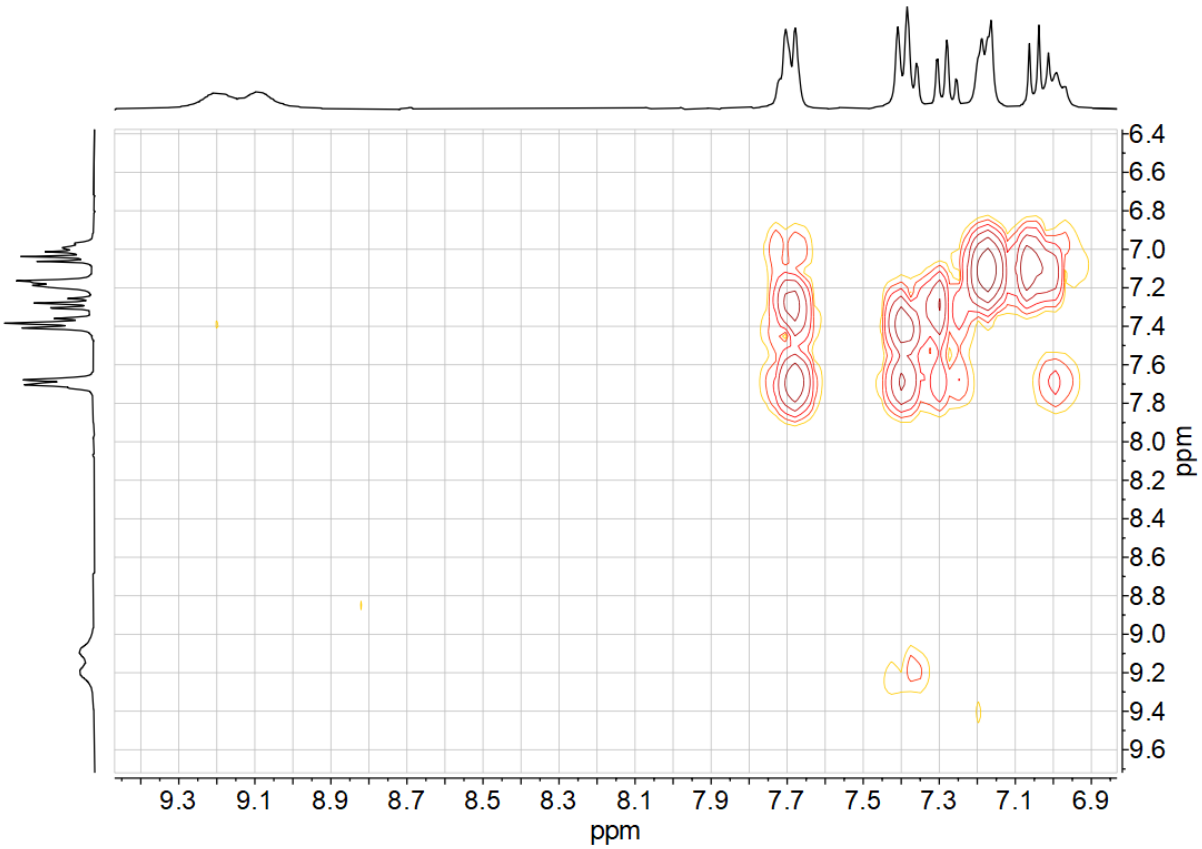

Figure 7-219 $^{1}H,^{1}H$ COSY correlation spectrum of [Ni(2Btz(Ph)Py)Br] in CD_2Cl_2.

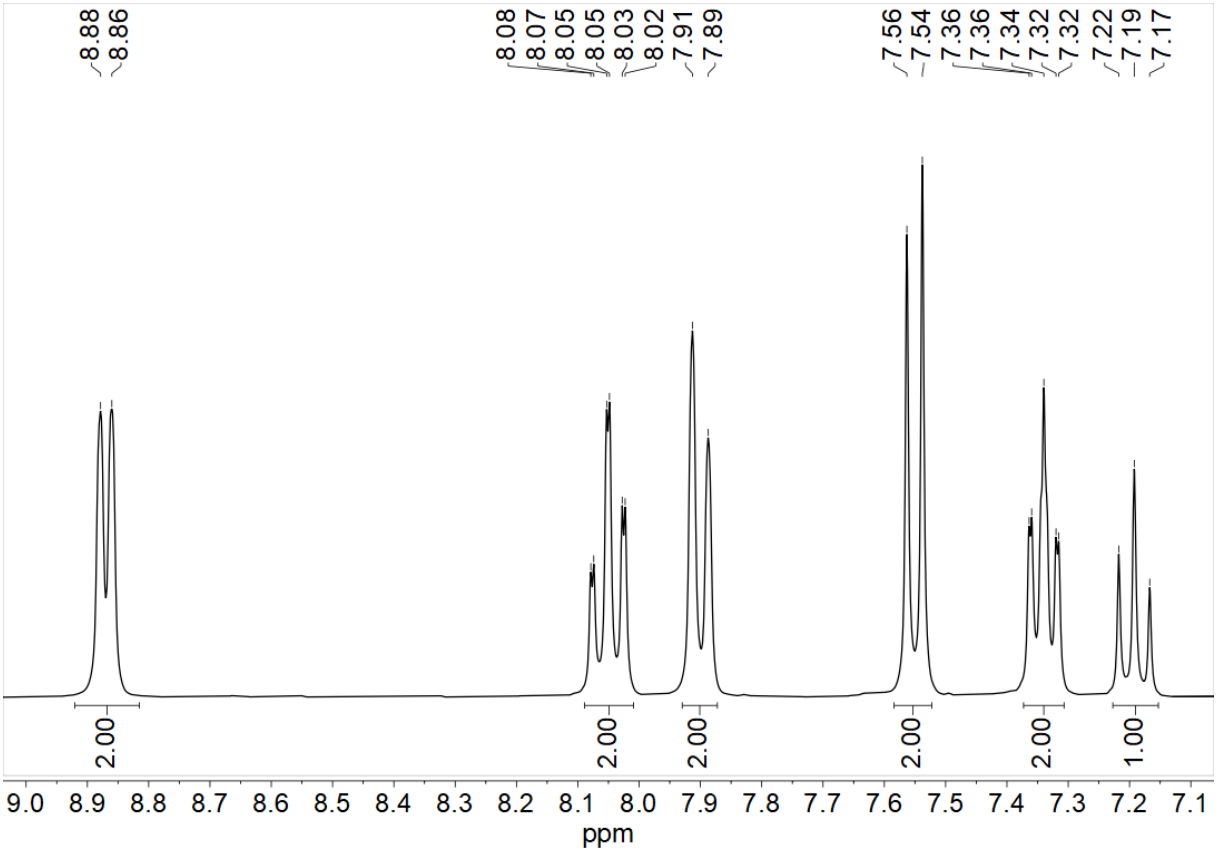

Figure 7-220 300 MHz ^{1}H NMR spectrum of [Ni(Py(Ph)Py)Cl] in DMSO-d_6.

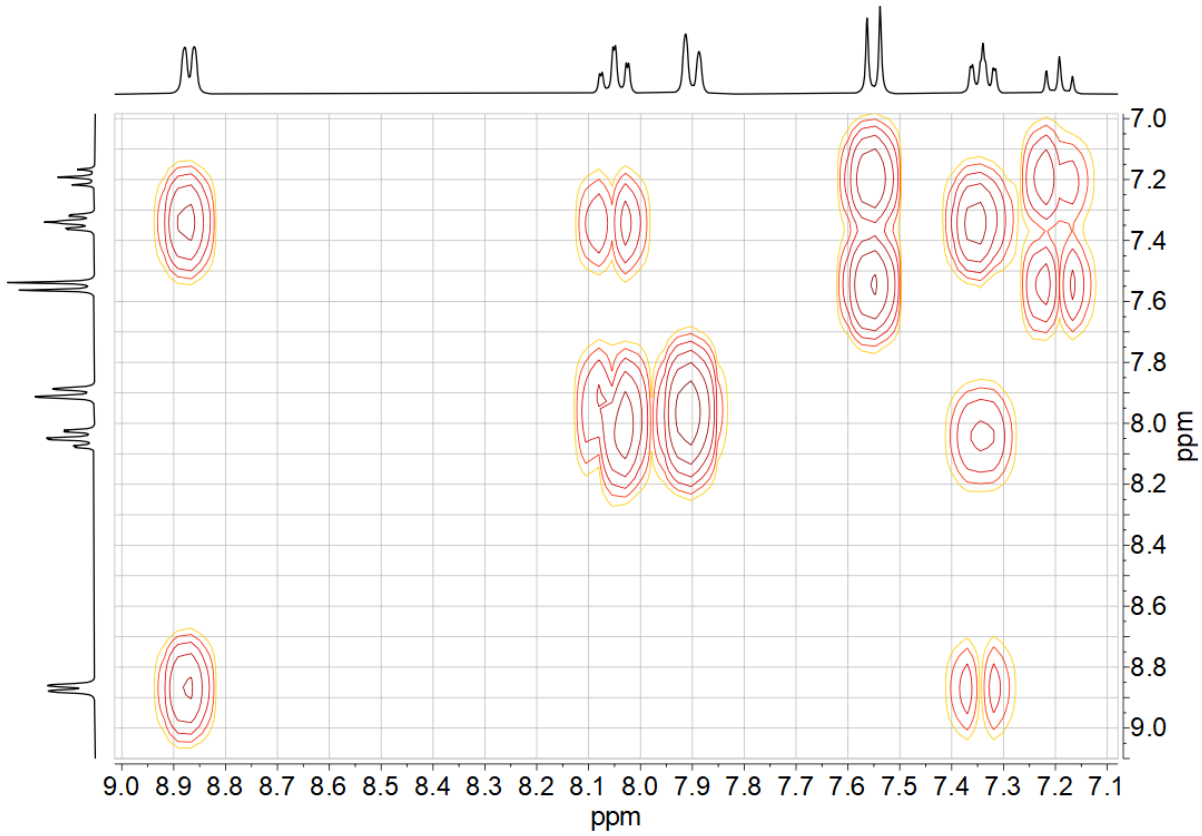

Figure 7-221 ^{1}H,^{1}H COSY correlation spectrum of [Ni(Py(Ph)Py)Cl] in DMSO-d_6.

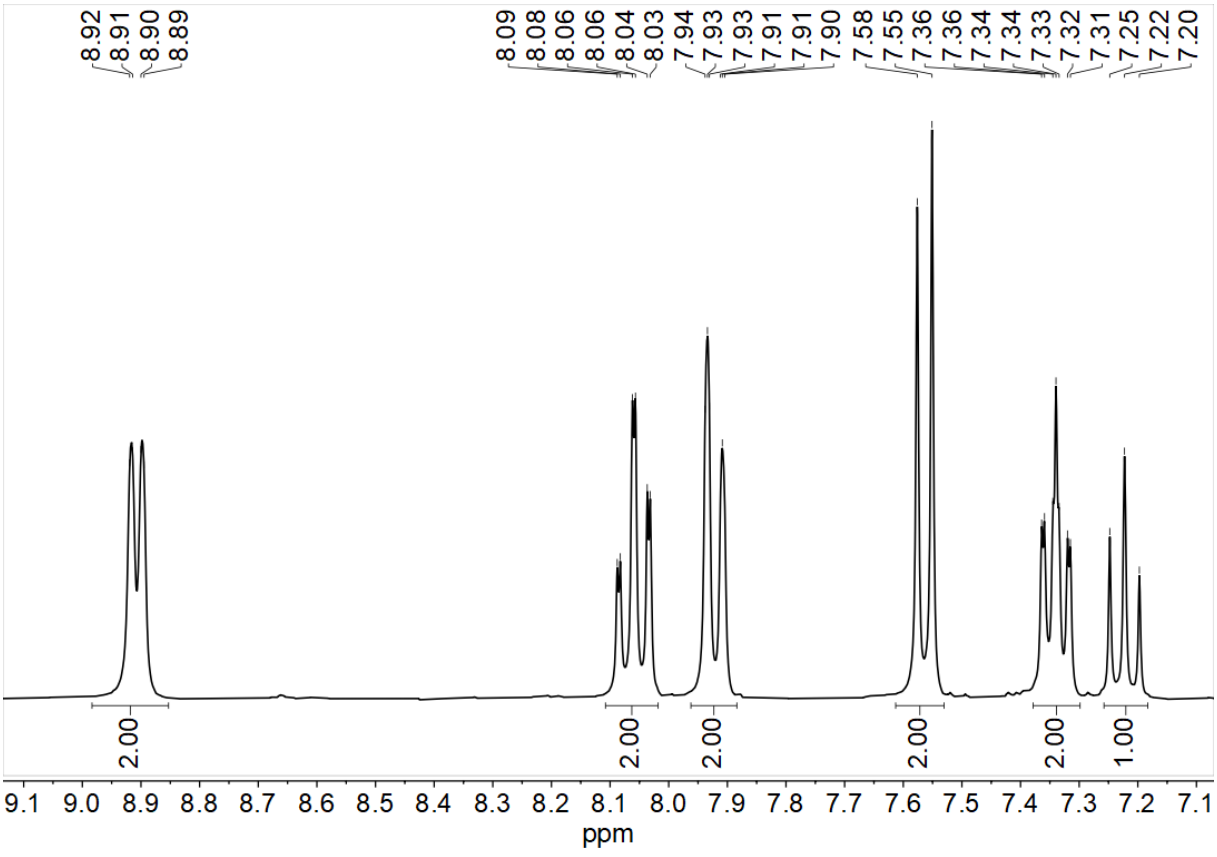

Figure 7-222 300 MHz ^{1}H NMR spectrum of [Ni(Py(Ph)Py)Br] in DMSO-d_6.

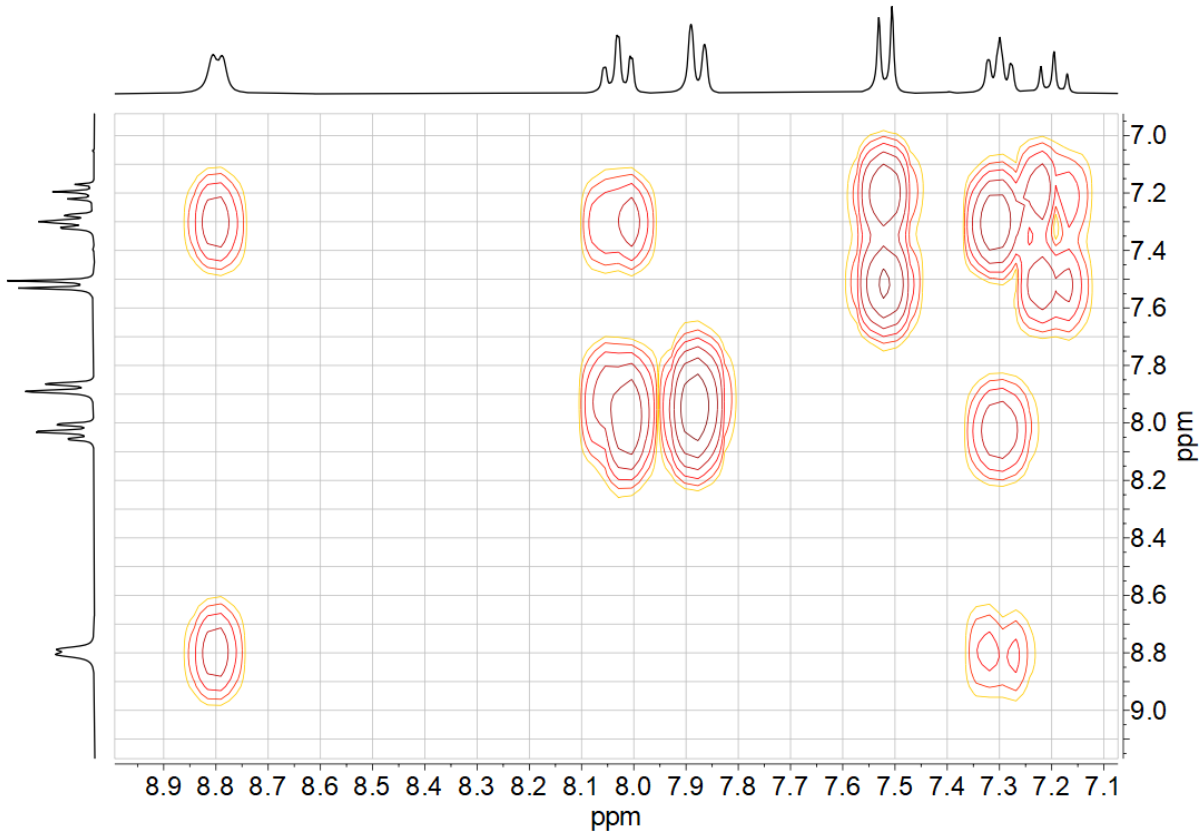

Figure 7-223 ^{1}H,^{1}H COSY correlation spectrum of [Ni(Py(Ph)Py)Br] in DMSO-d_6.

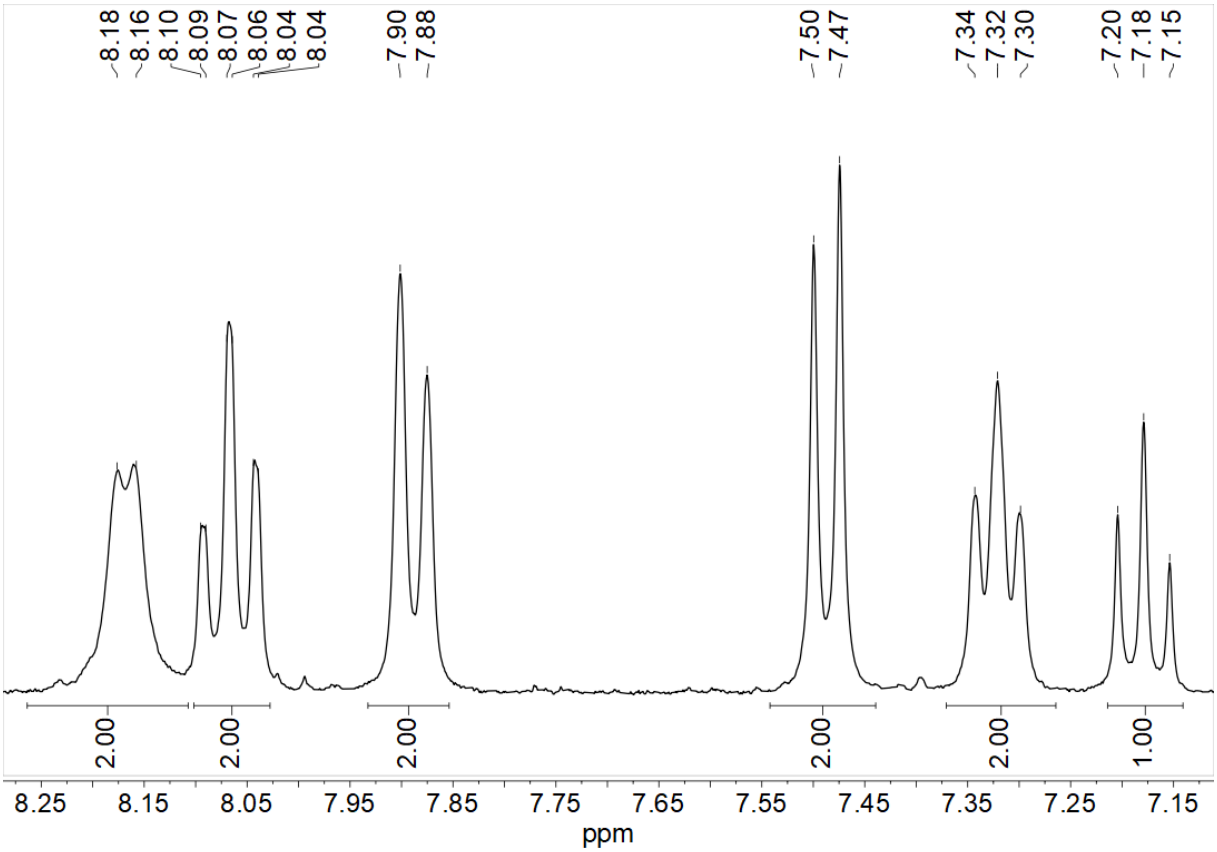

Figure 7-224 300 MHz ^{1}H NMR spectrum of [Ni(Py(Ph)Py)I] in DMSO-d_6.

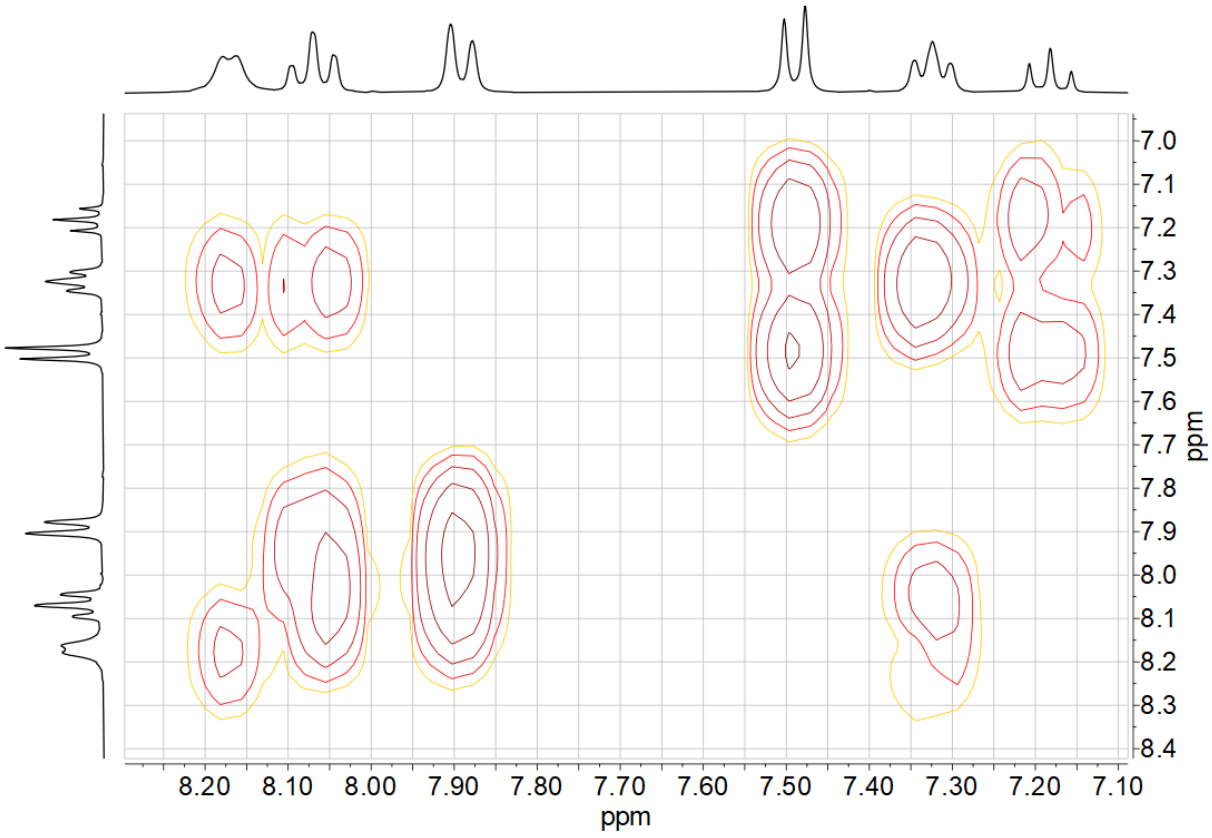

Figure 7-225 ^{1}H,^{1}H COSY correlation spectrum of [Ni(Py(Ph)Py)I] in DMSO-d_6.

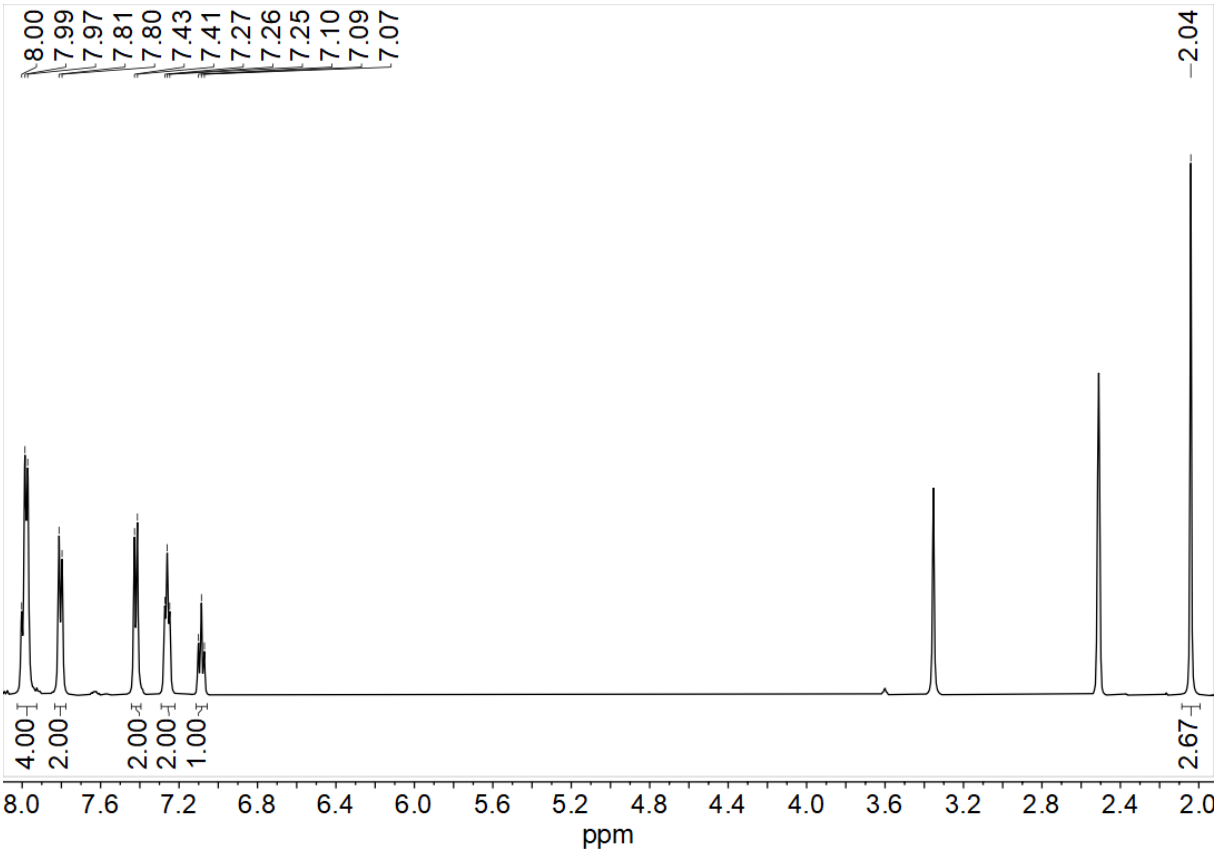

Figure 7-226 500 MHz ^{1}H NMR spectrum of [Ni(Py(Ph)Py)OAc] in DMSO-d_6.

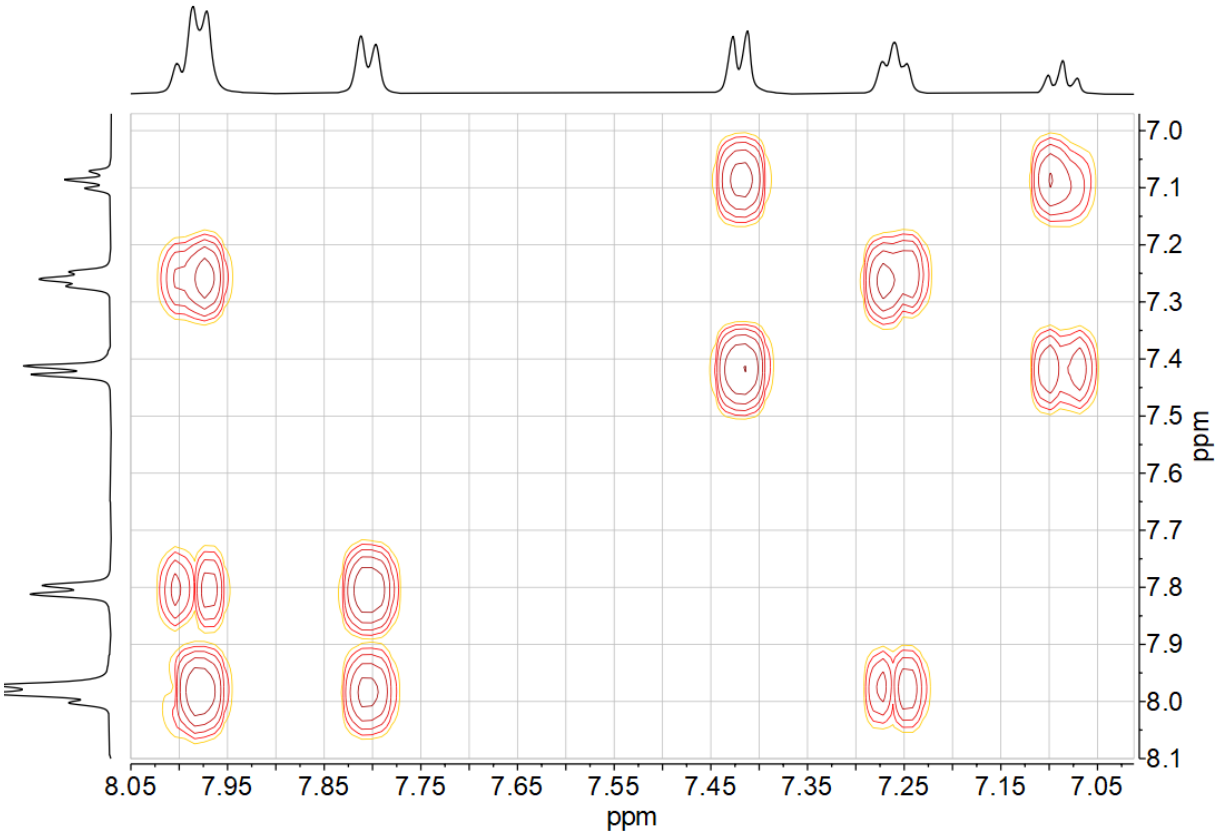

Figure 7-227 ^{1}H,^{1}H COSY correlation spectrum of [Ni(Py(Ph)Py)OAc] in DMSO-d_6.

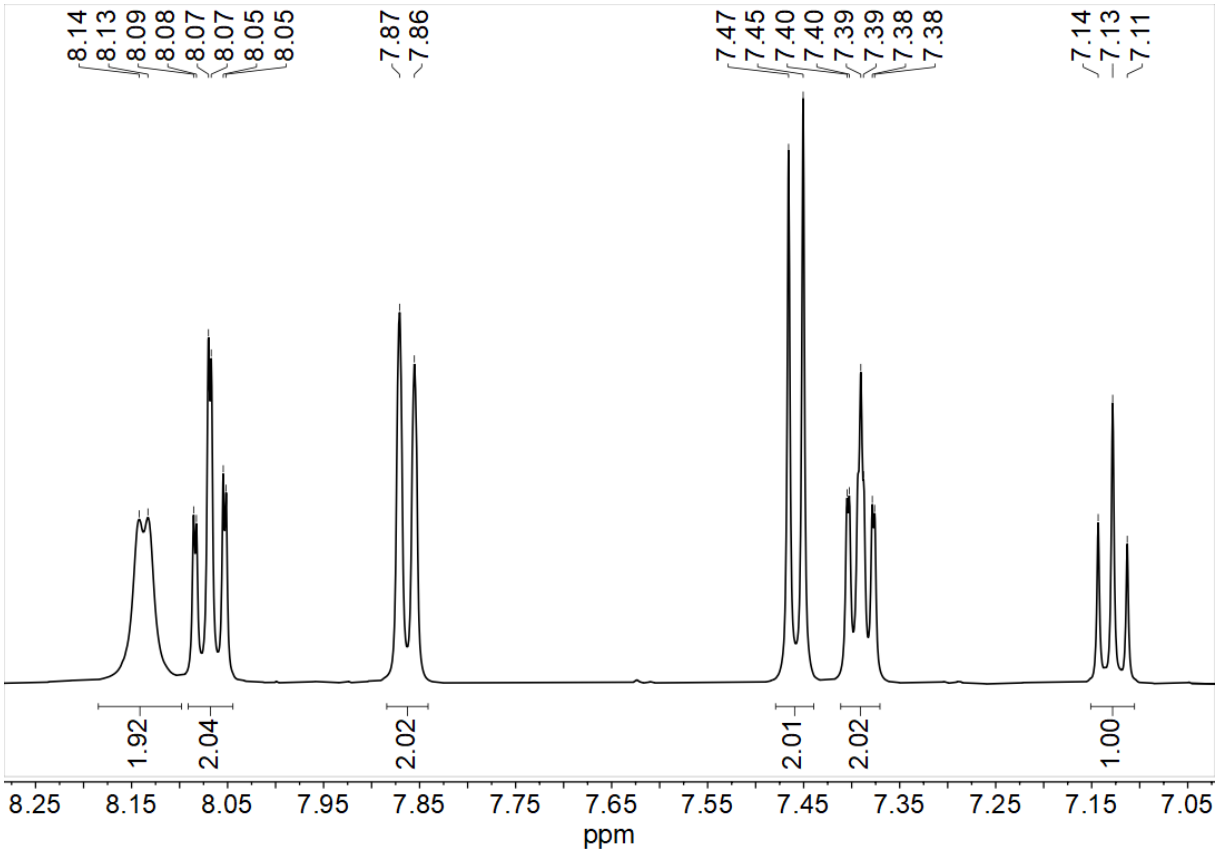

Figure 7-228 500 MHz ^{1}H NMR spectrum of [Ni(Py(Ph)Py)NCS] in DMSO-d_6.

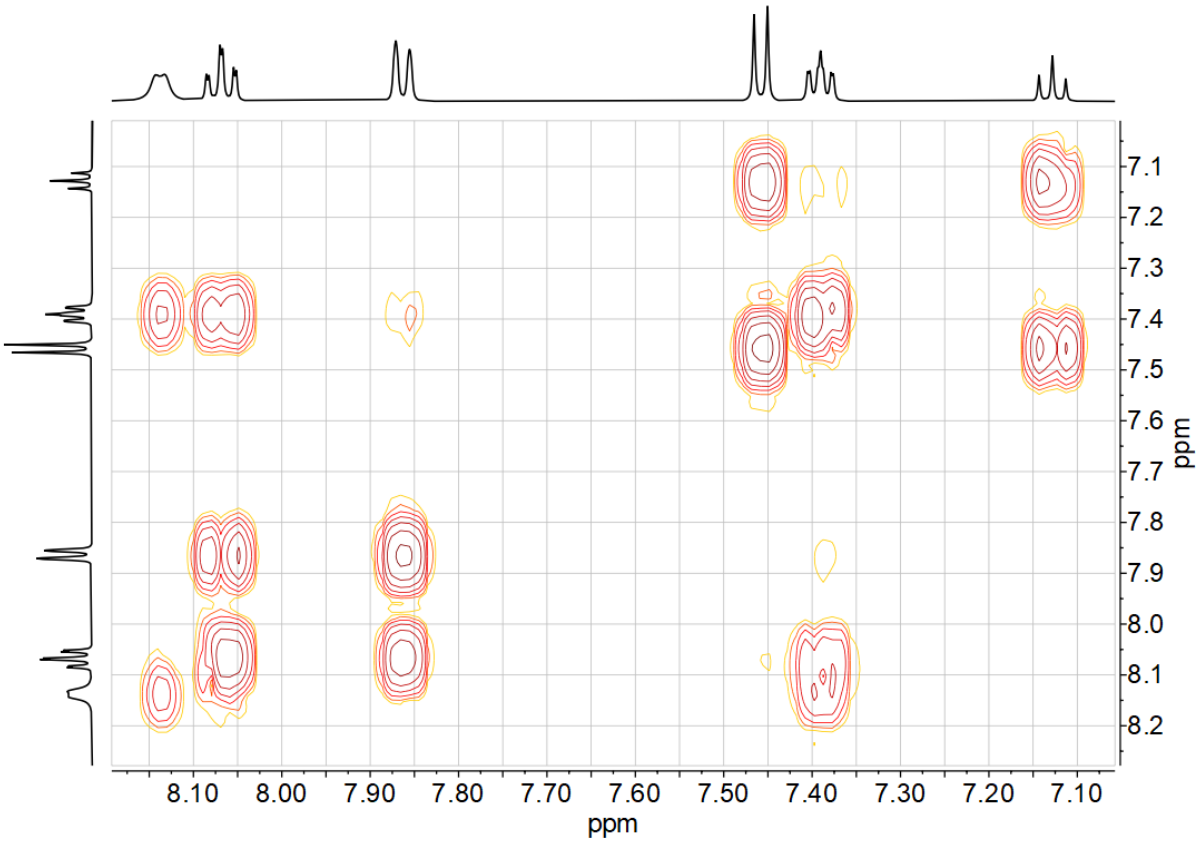

Figure 7-229 ^{1}H,^{1}H COSY correlation spectrum of [Ni(Py(Ph)Py)NCS] in DMSO-d_6.

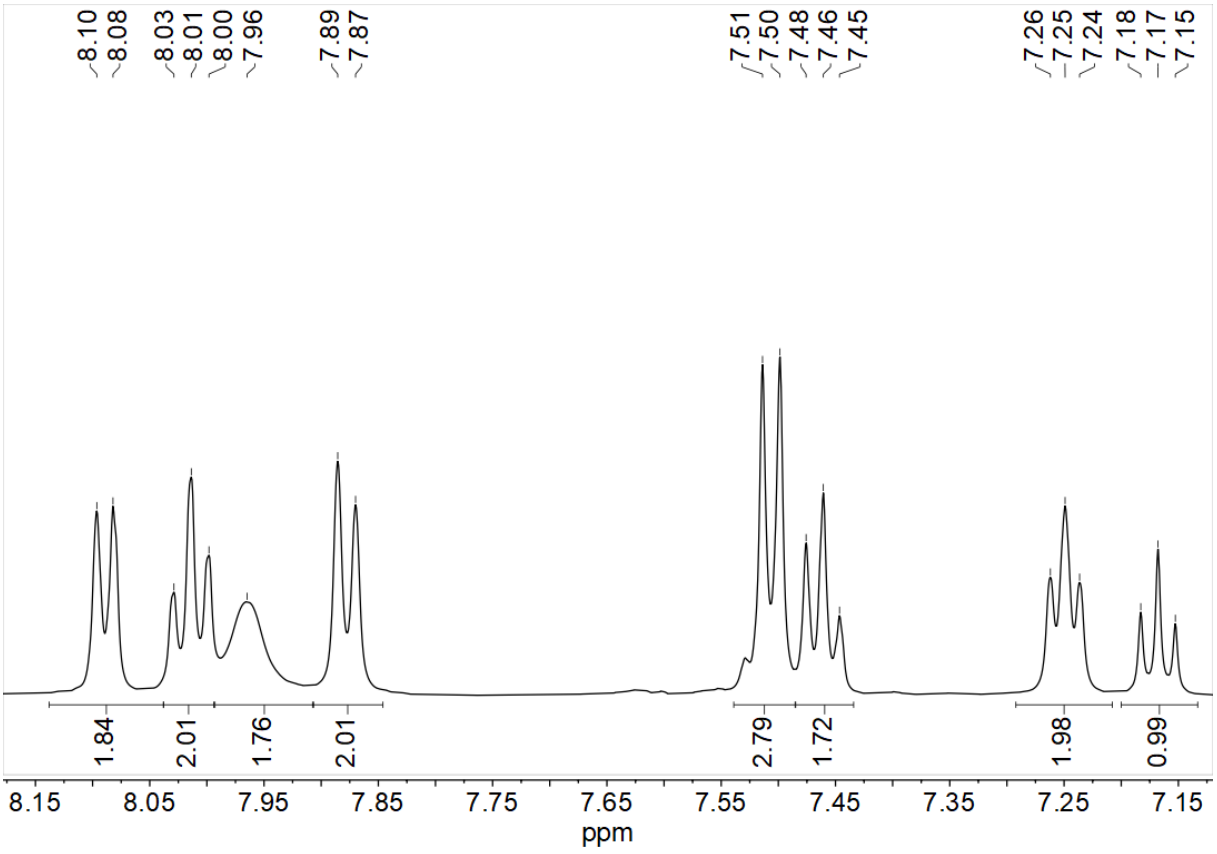

Figure 7-230 500 MHz ^{1}H NMR spectrum of [Ni(Py(Ph)Py)OBz] in DMSO-d_6.

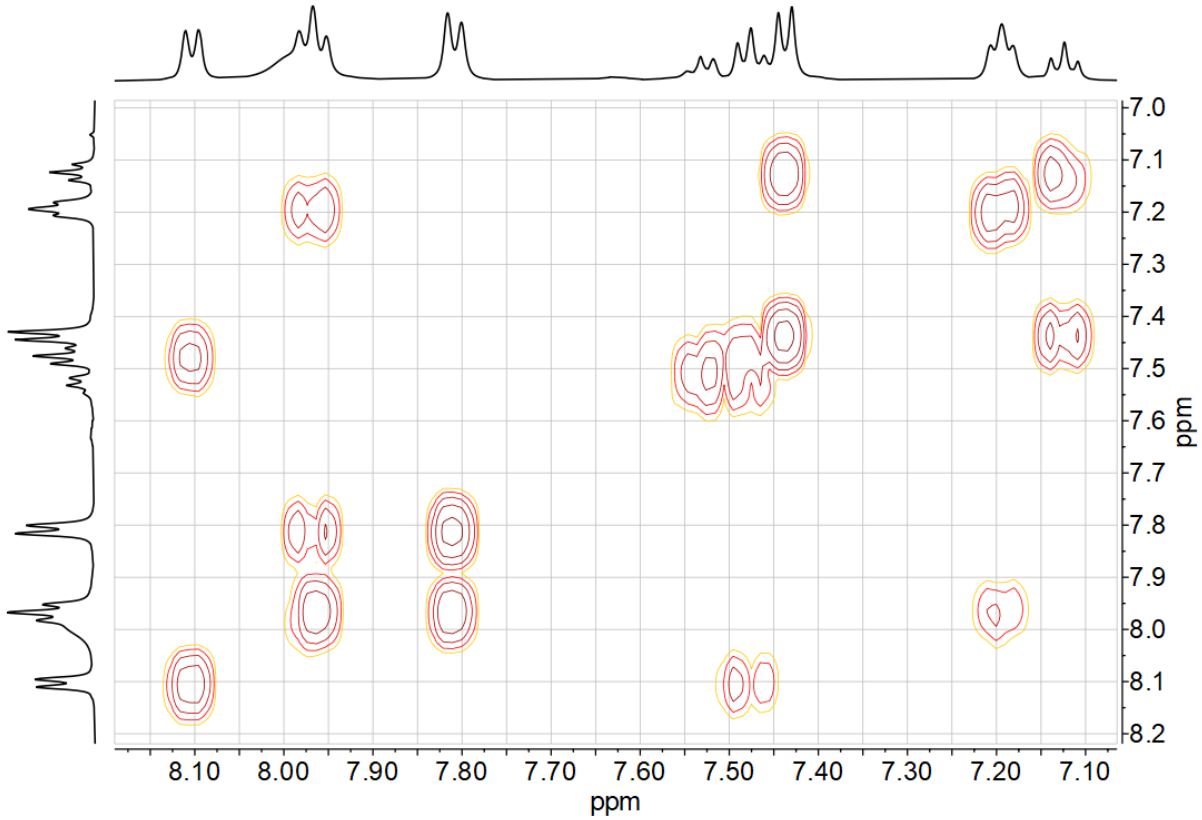

Figure 7-231 ^{1}H,^{1}H COSY correlation spectrum of [Ni(Py(Ph)Py)OBz] in DMSO-d_6.

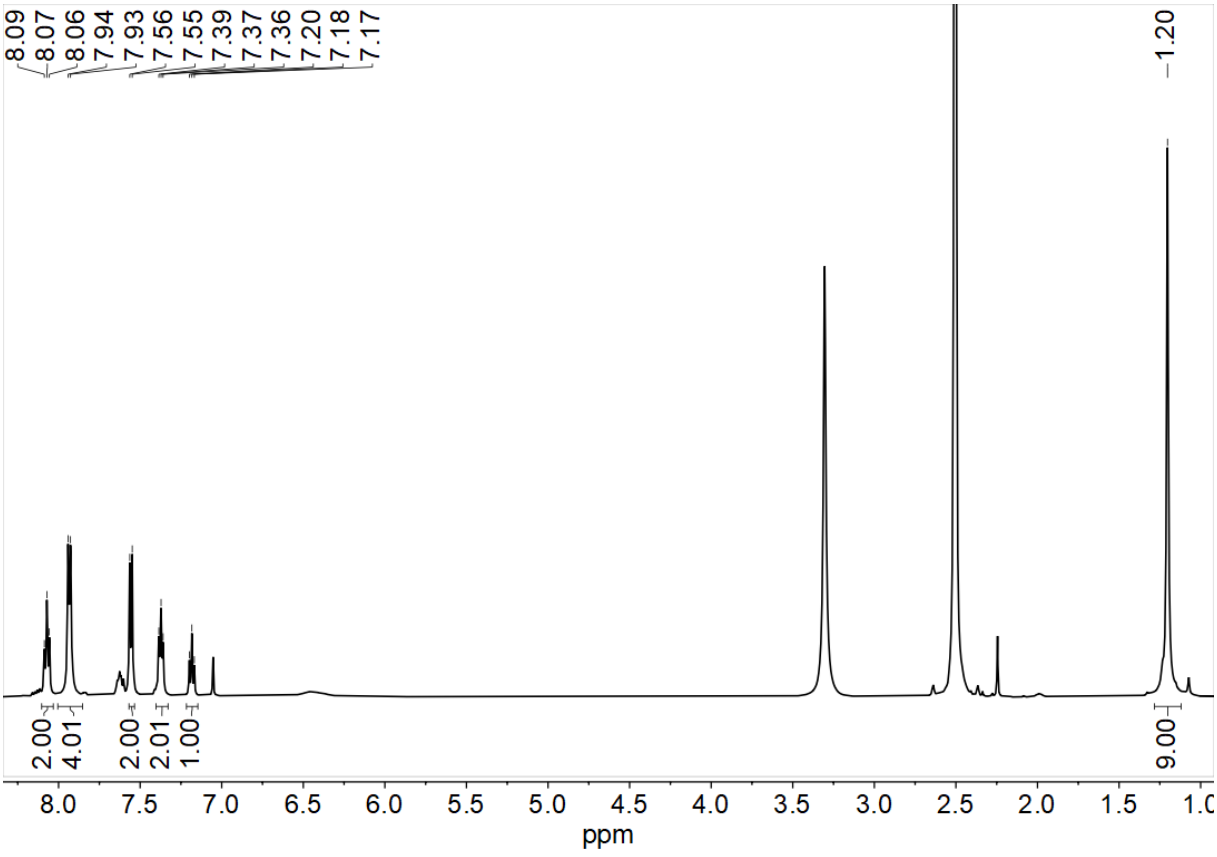

Figure 7-232 500 MHz ^{1}H NMR spectrum of [Ni(Py(Ph)Py)OPiv] in DMSO-d_6.

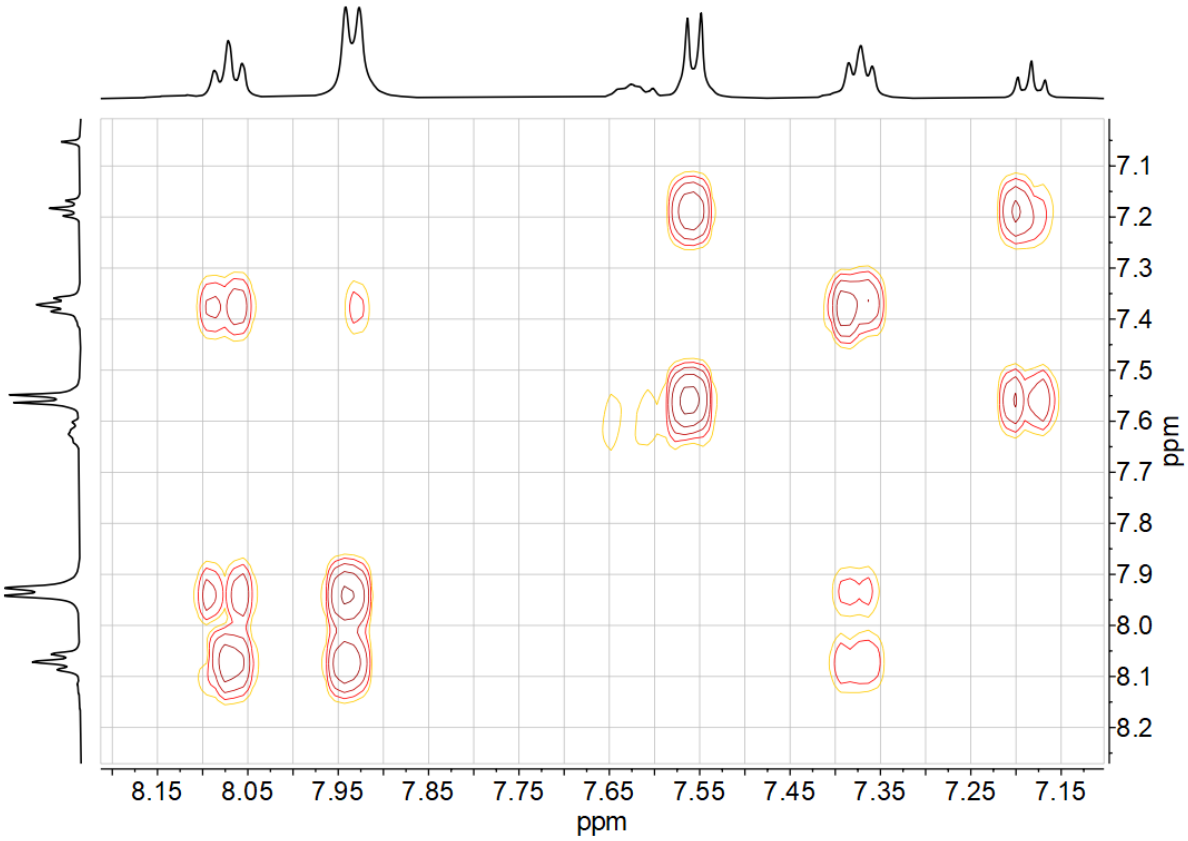

Figure 7-233 ^{1}H,^{1}H COSY correlation spectrum of [Ni(Py(Ph)Py)OPiv] in DMSO-d_6.

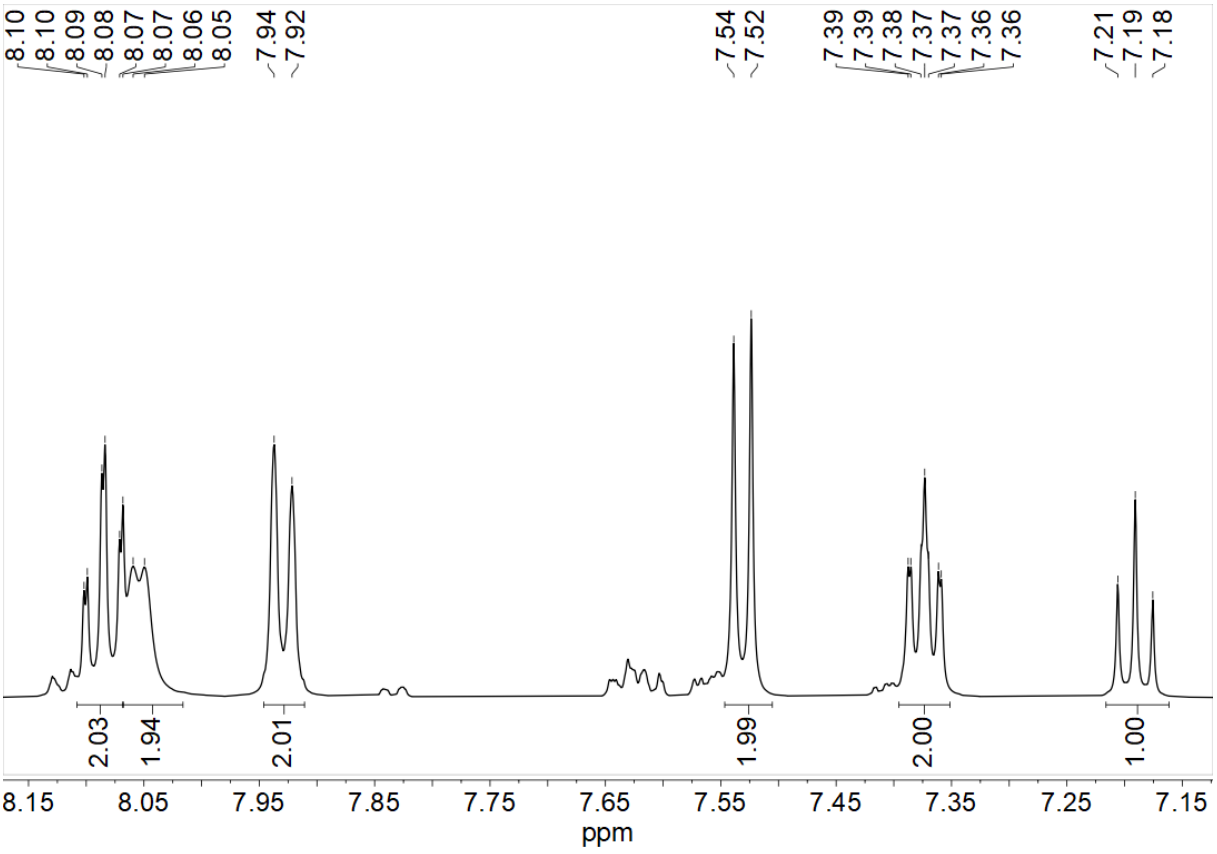

Figure 7-234 500 MHz ^{1}H NMR spectrum of [Ni(Py(Ph)Py)TFA] in DMSO-d_6.

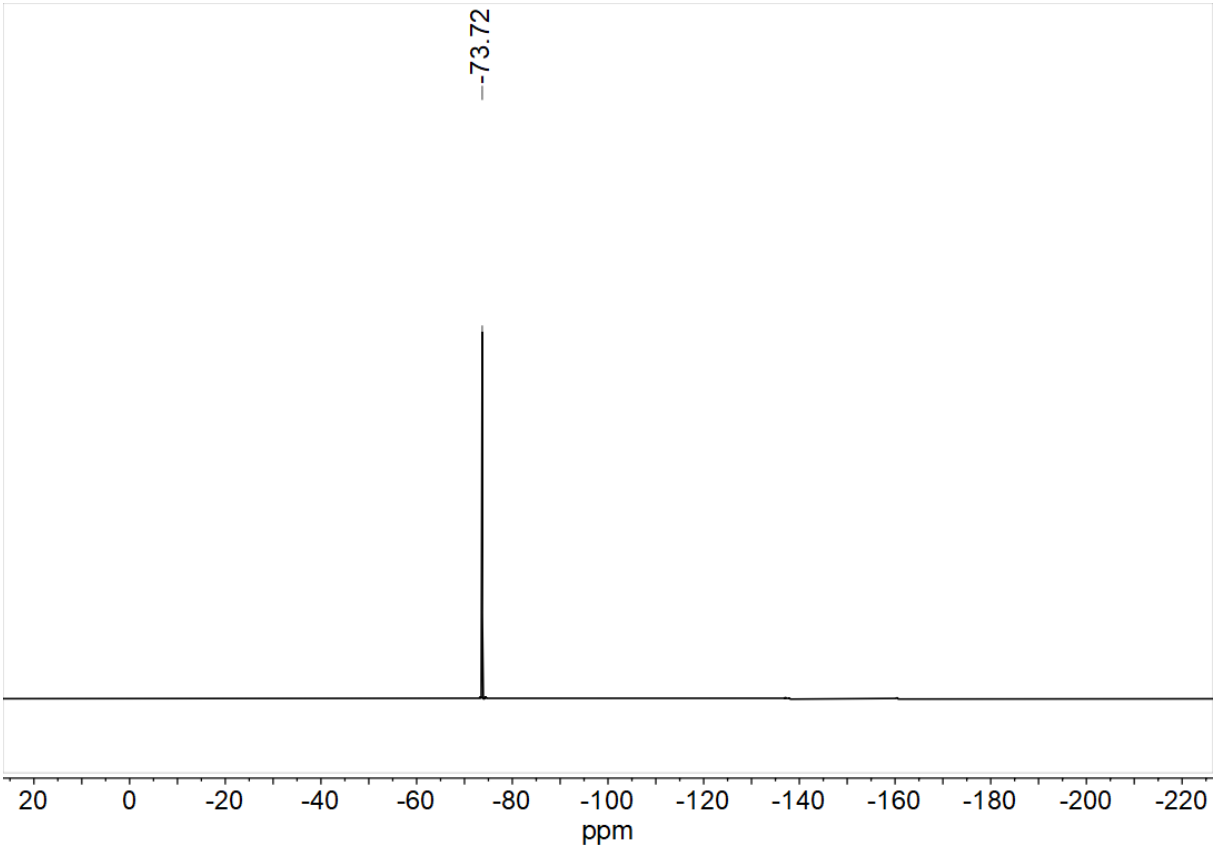

Figure 7-235 282 MHz ^{19}F NMR spectrum of [Ni(Py(Ph)Py)TFA] in DMSO-d_6.

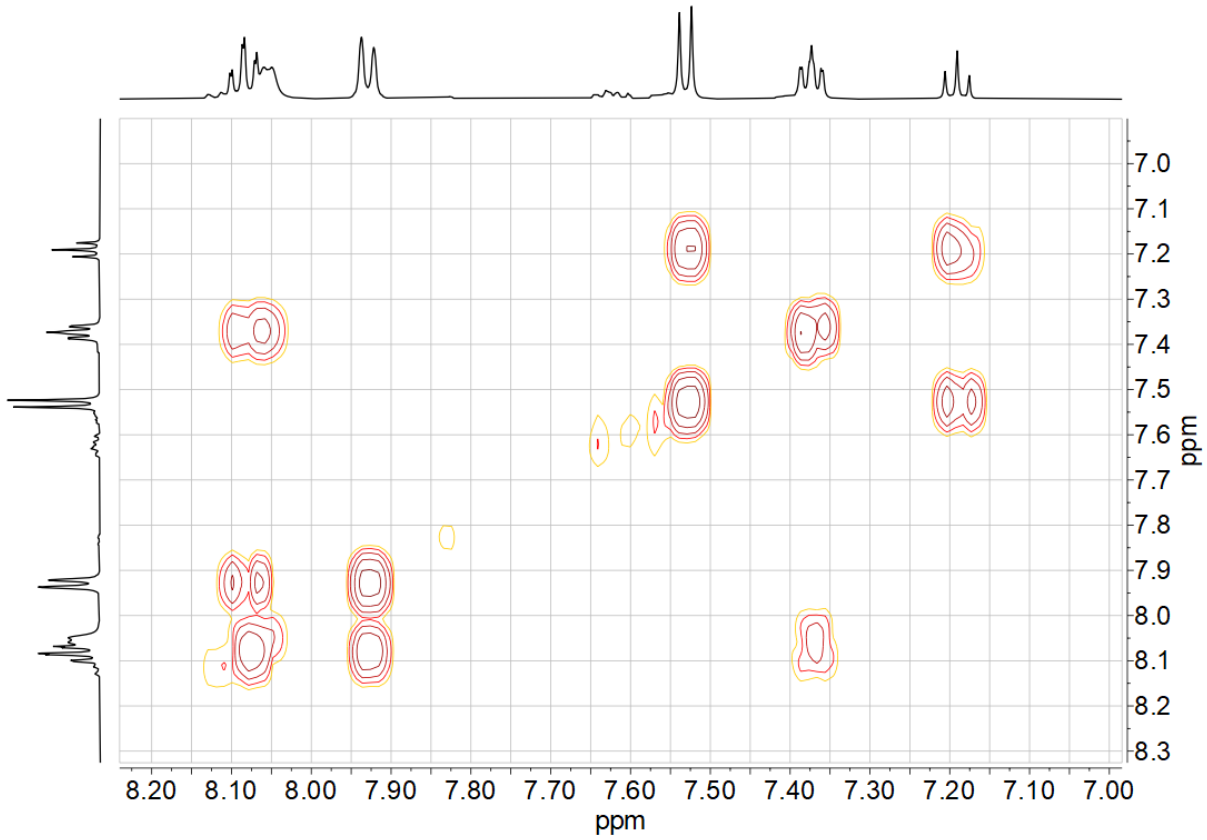

Figure 7-236 ^{1}H,^{1}H COSY correlation spectrum of [Ni(Py(Ph)Py)TFA] in DMSO-d_6.

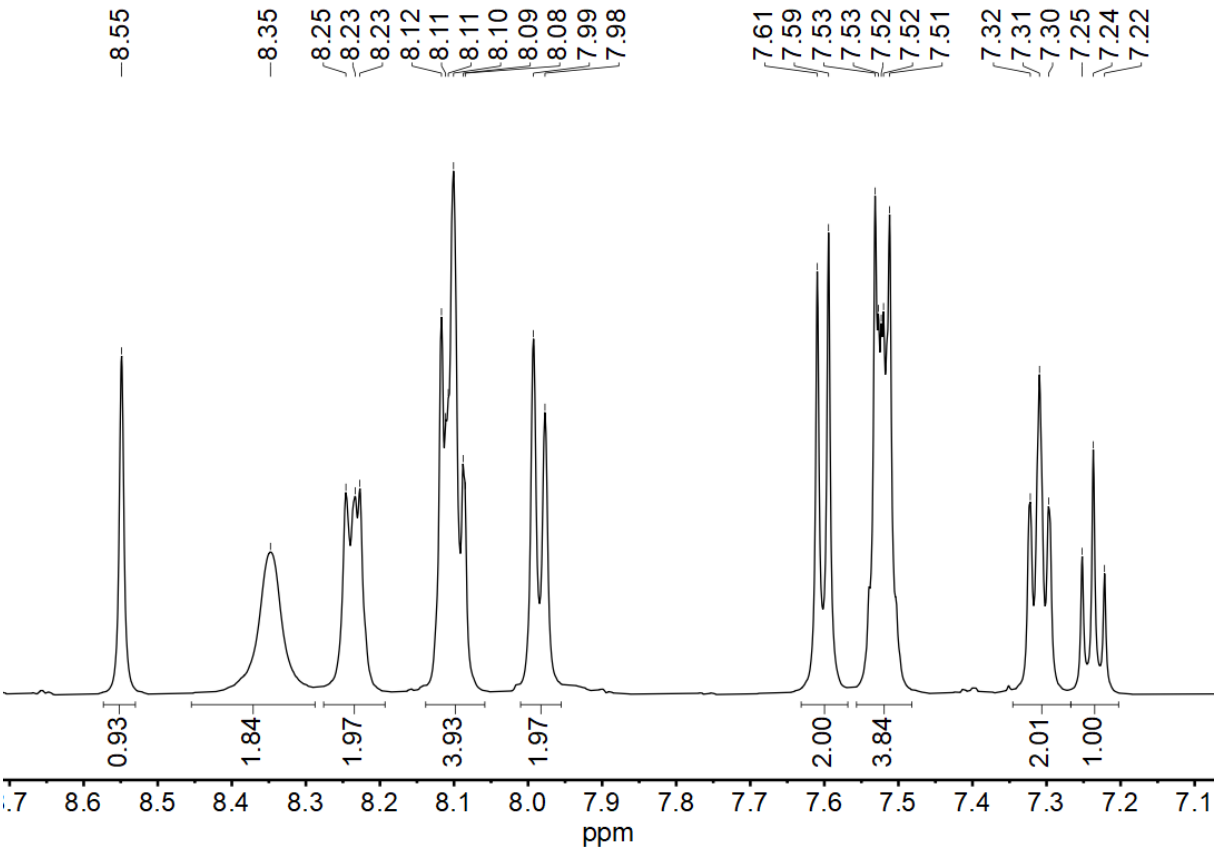

Figure 7-237 500 MHz ^{1}H NMR spectrum of [Ni(Py(Ph)Py)OOC-atc] in DMSO-d_6.

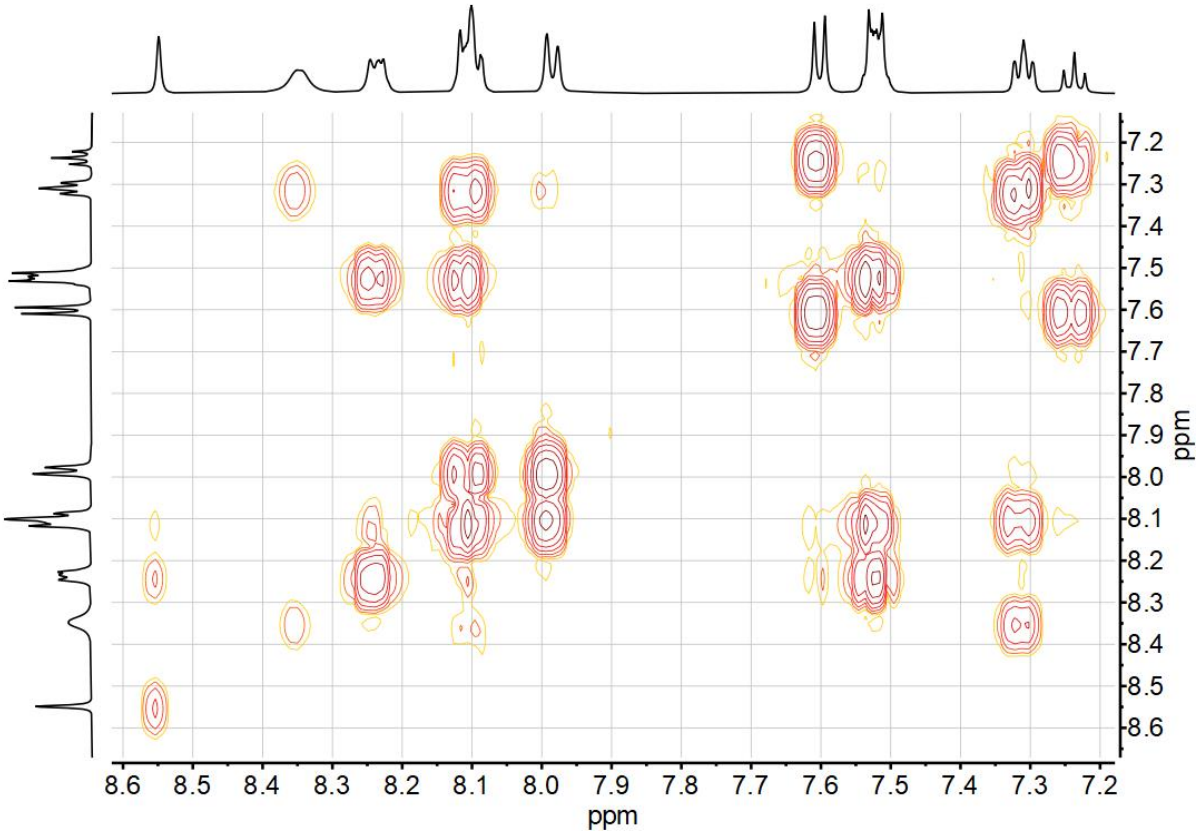

Figure 7-238 ^{1}H,^{1}H COSY correlation spectrum of [Ni(Py(Ph)Py)OOC-atc] in DMSO-d_6.

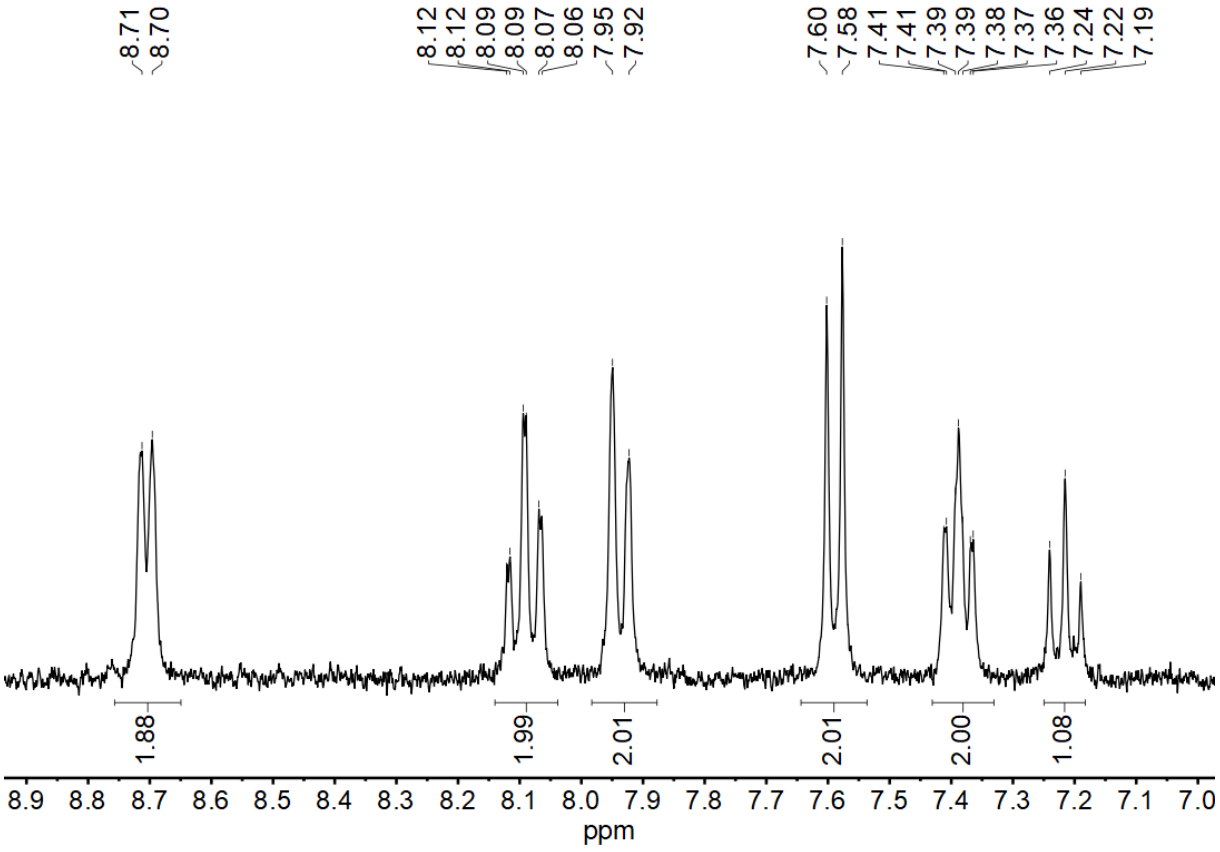

Figure 7-239 300 MHz ^{1}H NMR spectrum of [Ni(Py(Ph)Py)CN] in DMSO-d_6.

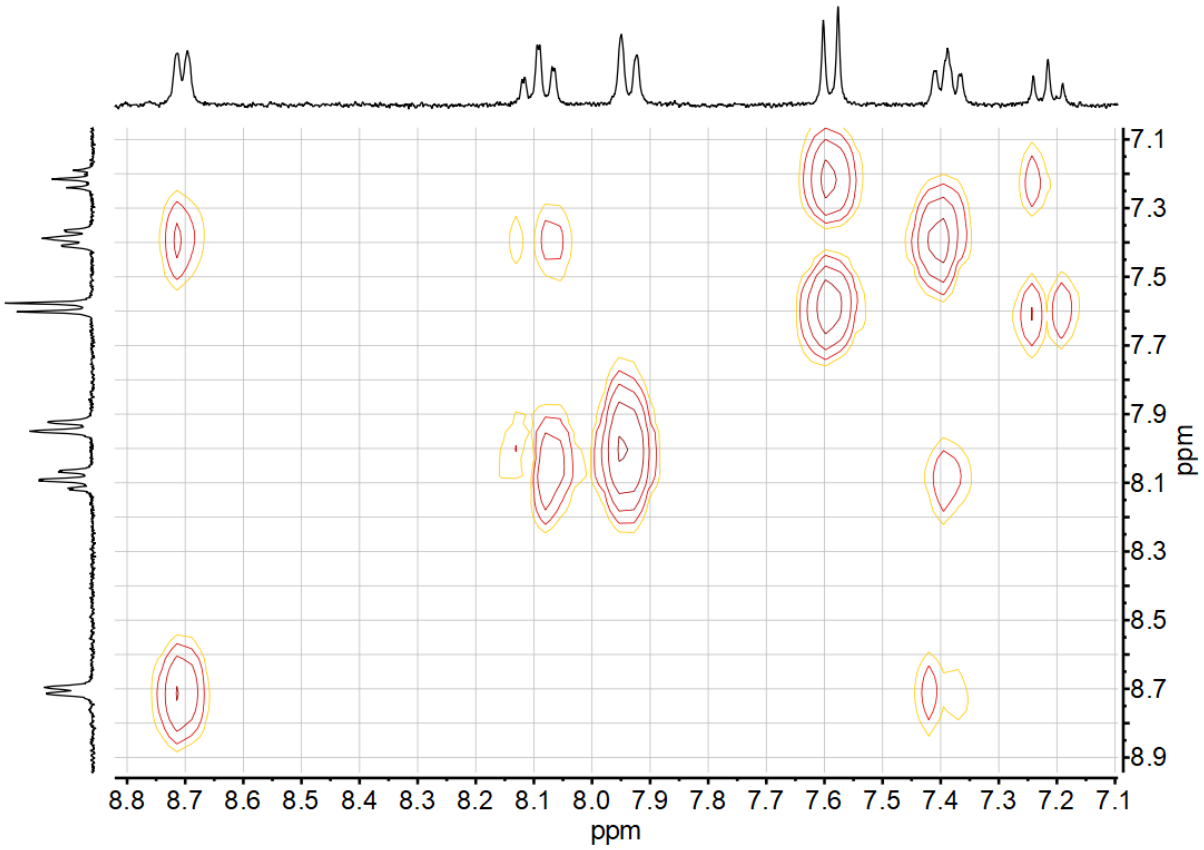

Figure 7-240 ^{1}H,^{1}H COSY correlation spectrum of [Ni(Py(Ph)Py)CN] in DMSO-d_6.

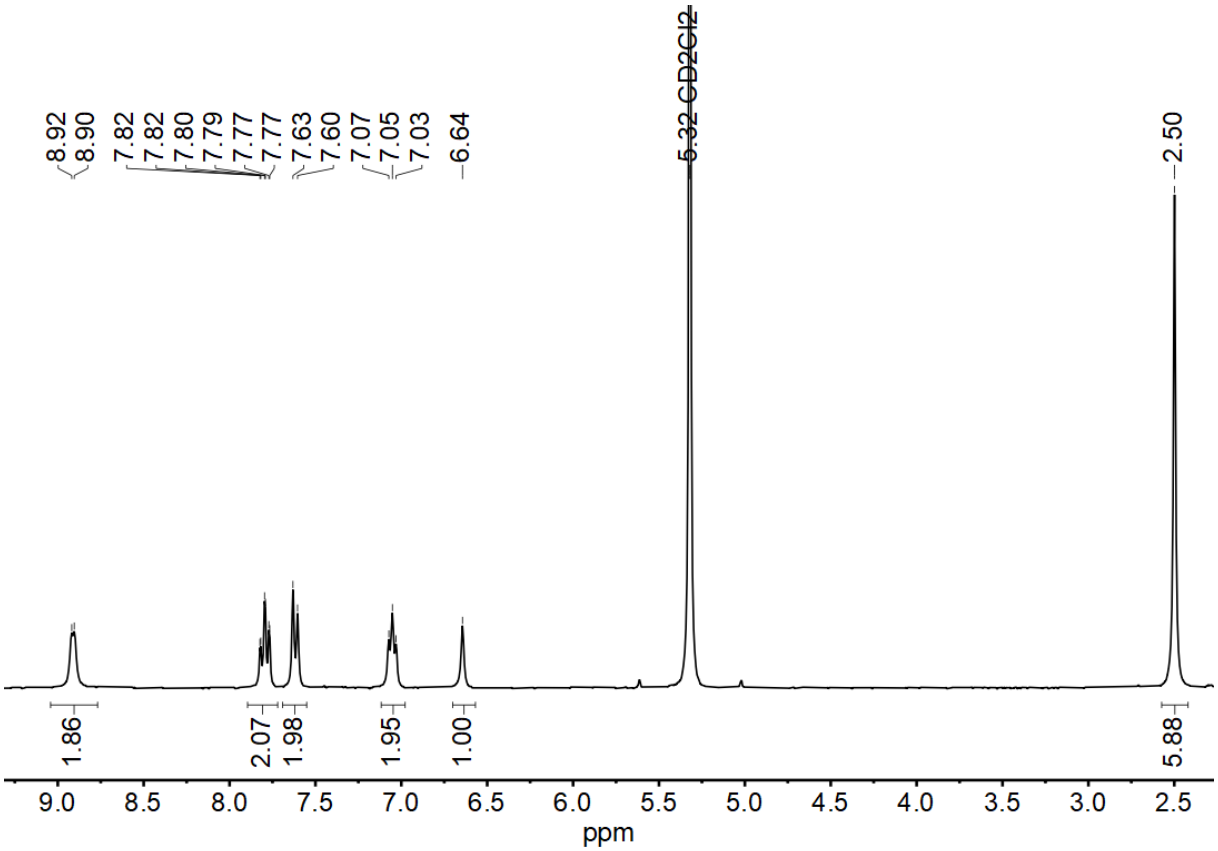

Figure 7-241 300 MHz ^{1}H NMR spectrum of [Ni(Py(4,6MePh)Py)CN] in CD_2Cl_2.

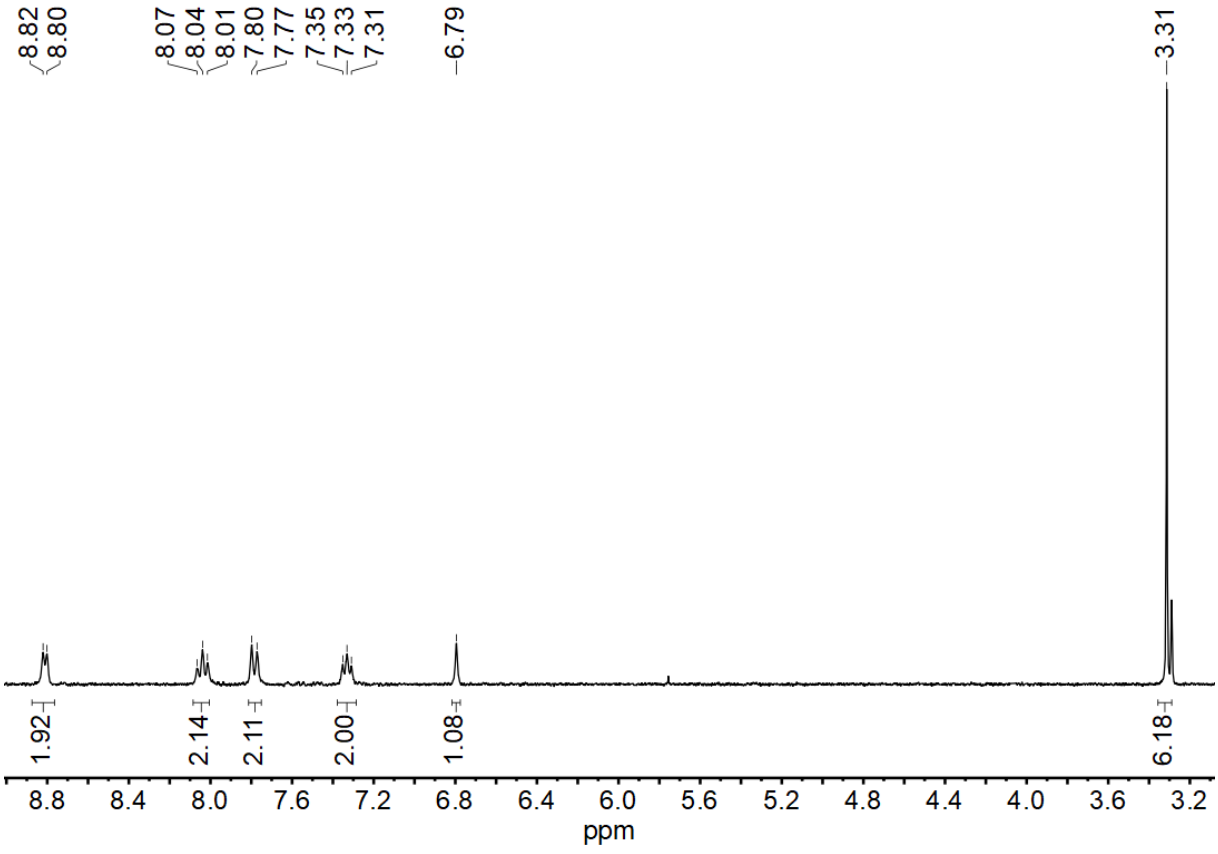

Figure 7-242 300 MHz ^{1}H NMR spectrum of [Ni(Py(4,6MePh)Py)CN] in DMSO-d_6.

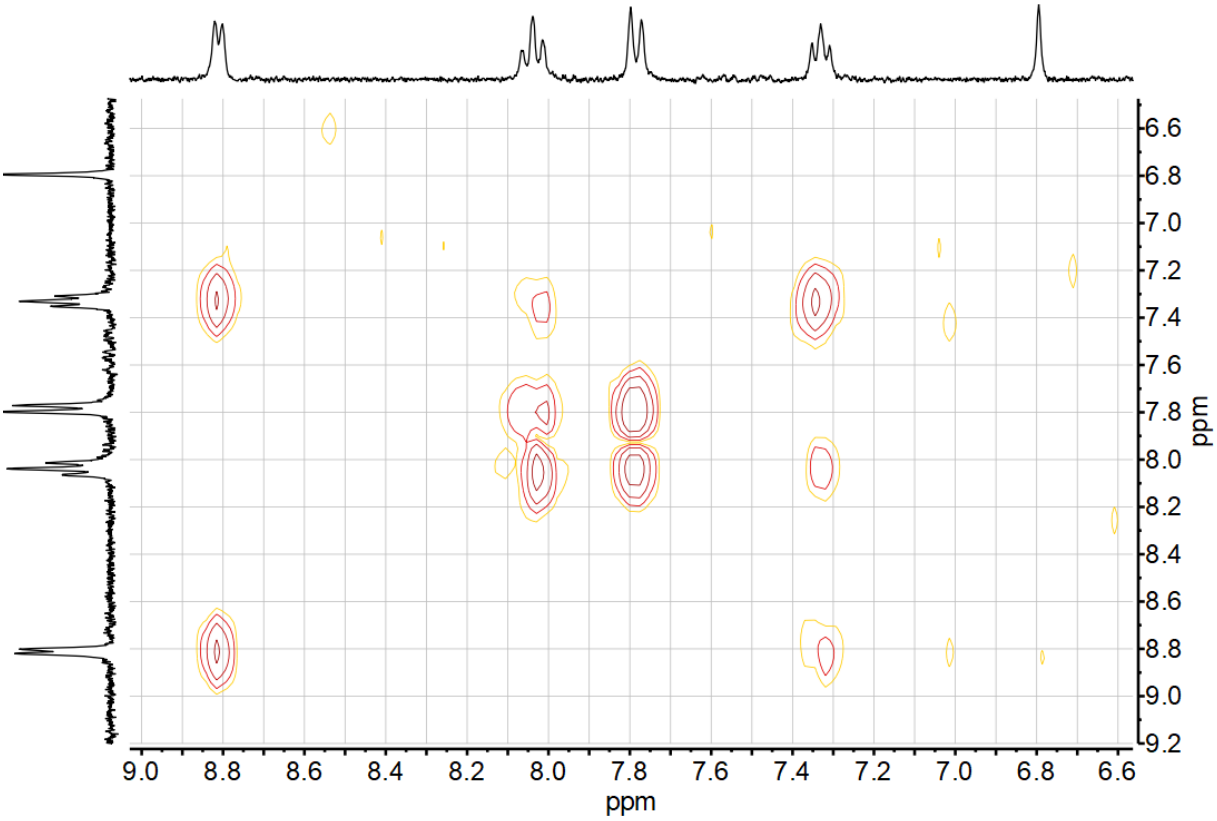

Figure 7-243 ^{1}H,^{1}H COSY correlation spectrum of [Ni(Py(4,6MePh)Py)CN] in DMSO-d_6.

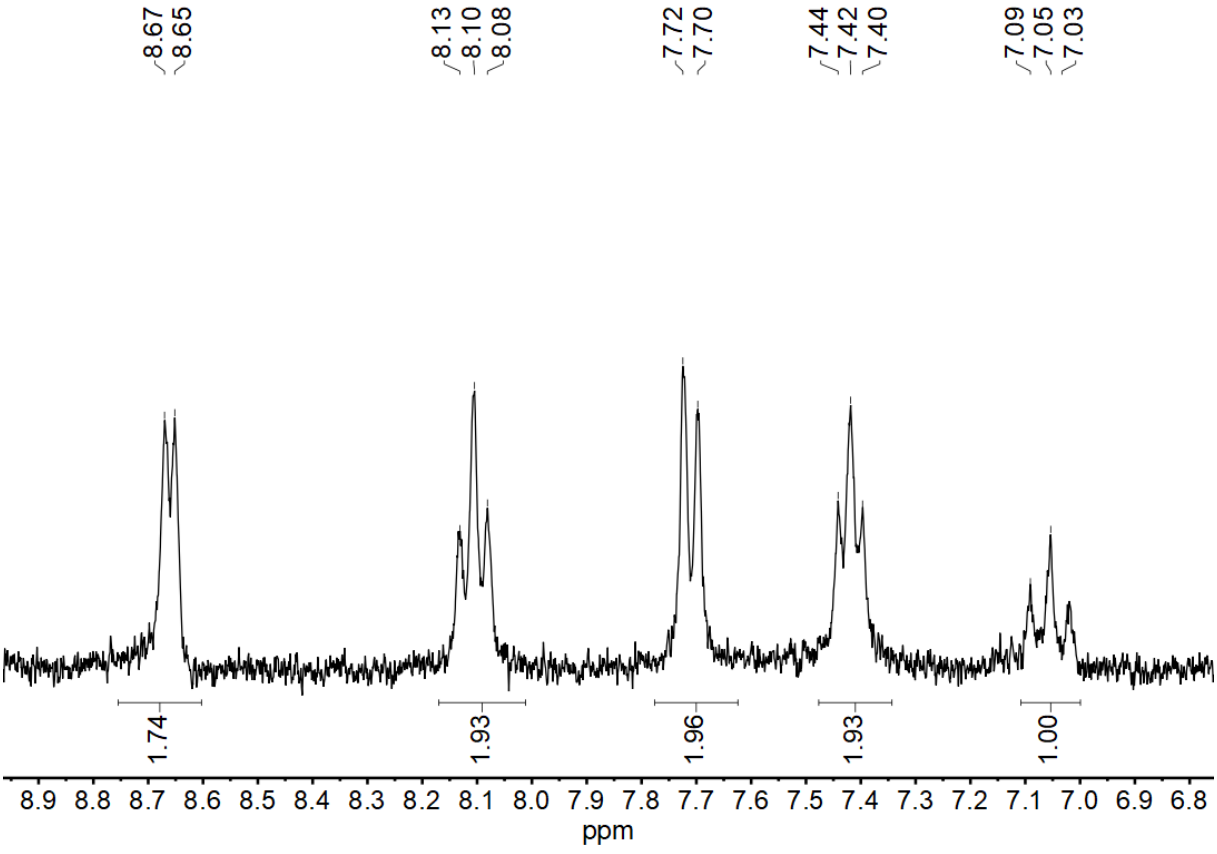

Figure 7-244 300 MHz ^{1}H NMR spectrum of [Ni(Py(4,6FPh)Py)CN] in DMSO-d_6.

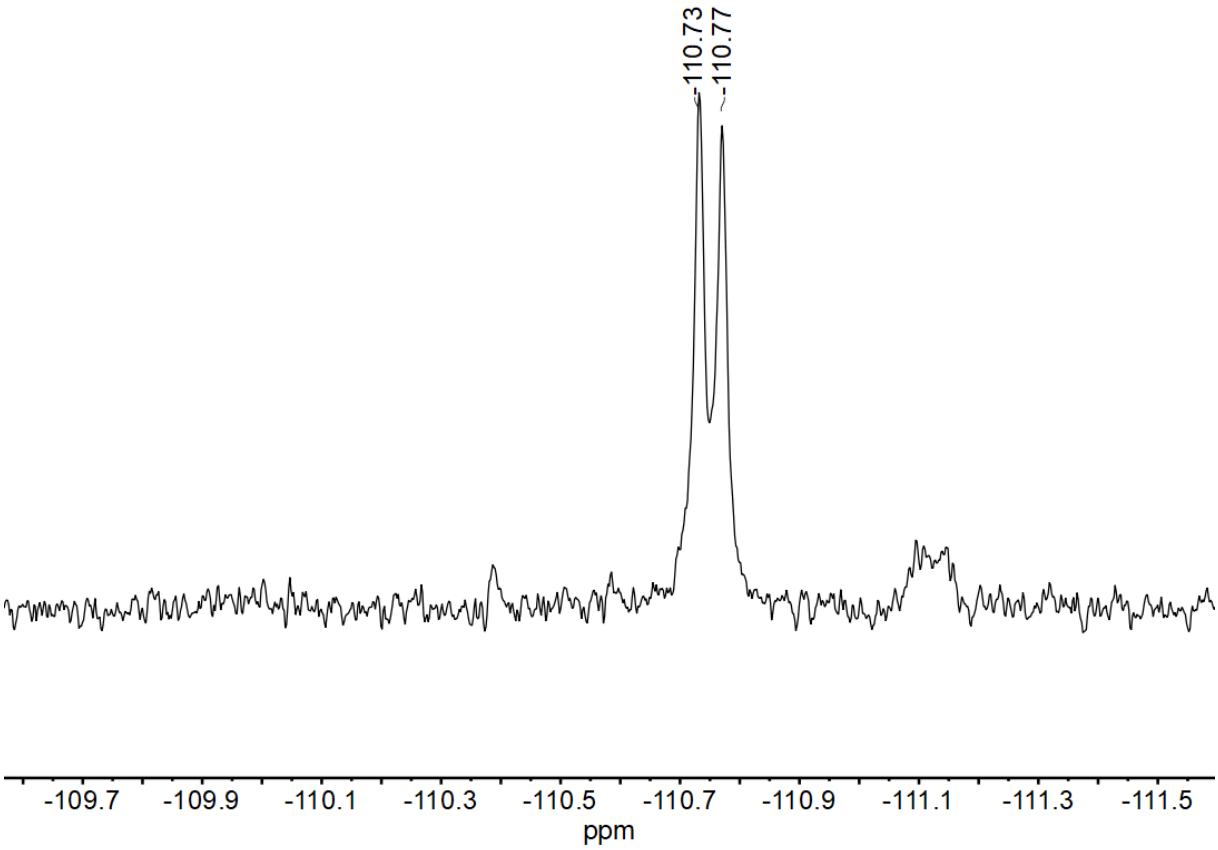

Figure 7-245 282 MHz ^{19}F NMR spectrum of [Ni(Py(4,6FPh)Py)CN] in DMSO-d_6.

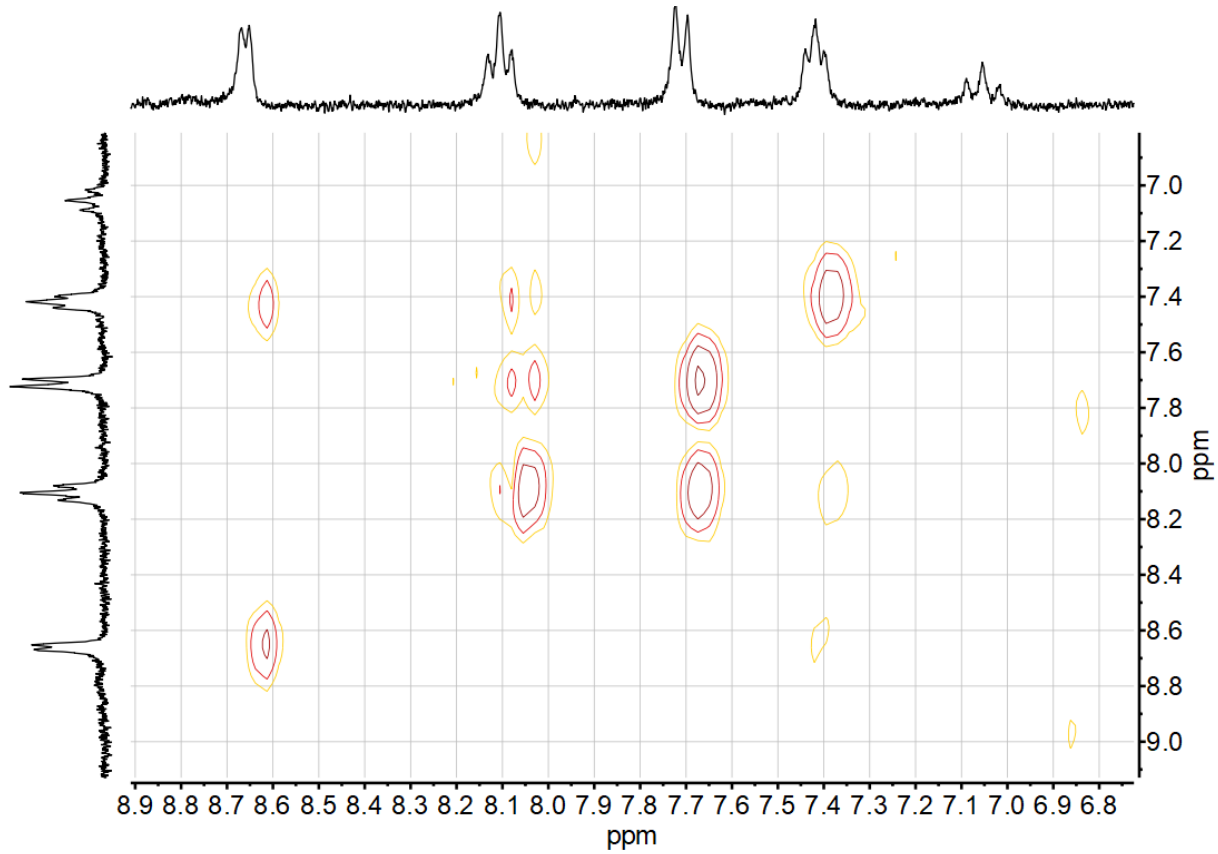

Figure 7-246 ^{1}H,^{1}H COSY correlation spectrum of [Ni(Py(4,6FPh)Py)CN] in DMSO-d_6.

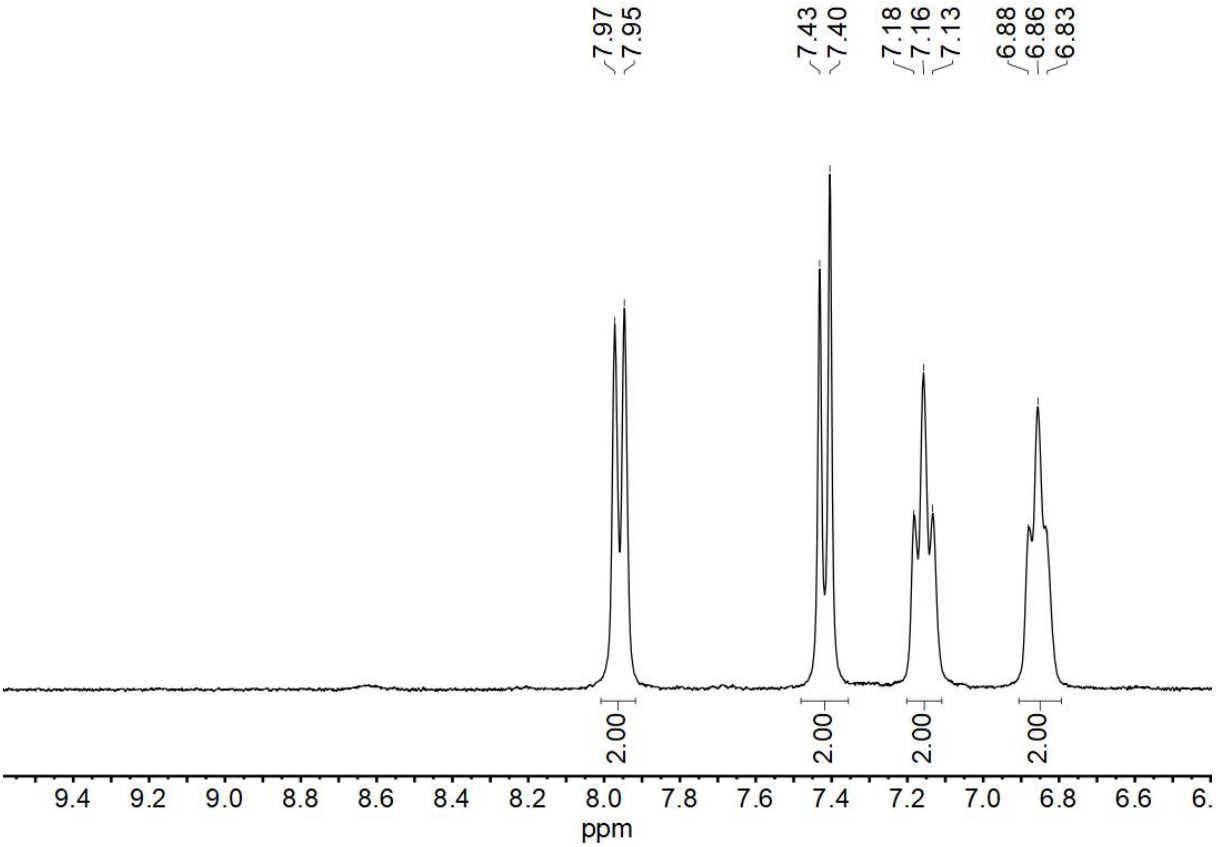

Figure 7-247 300 MHz ^{1}H NMR spectrum of lithium carbazolate in DMSO-d_6.

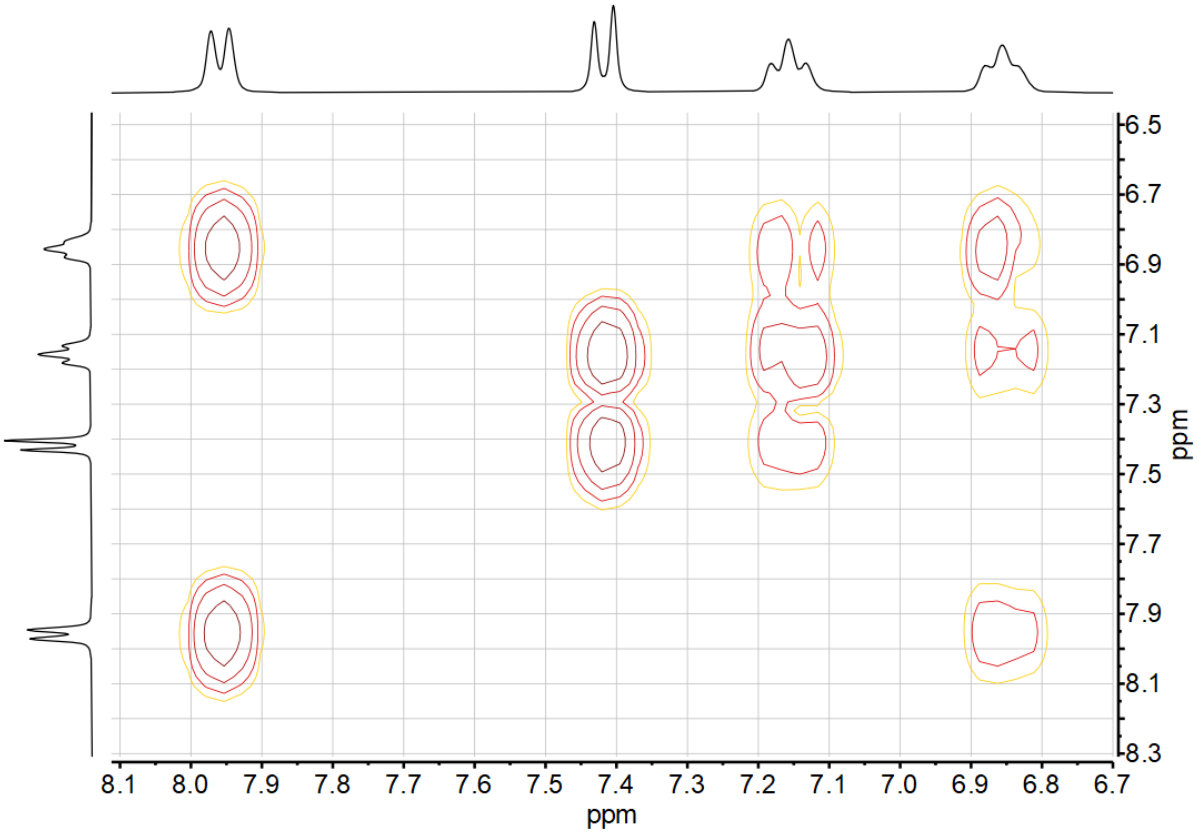

Figure 7-248 ^{1}H,^{1}H COSY correlation spectrum of lithium carbazolate in DMSO-d_6.

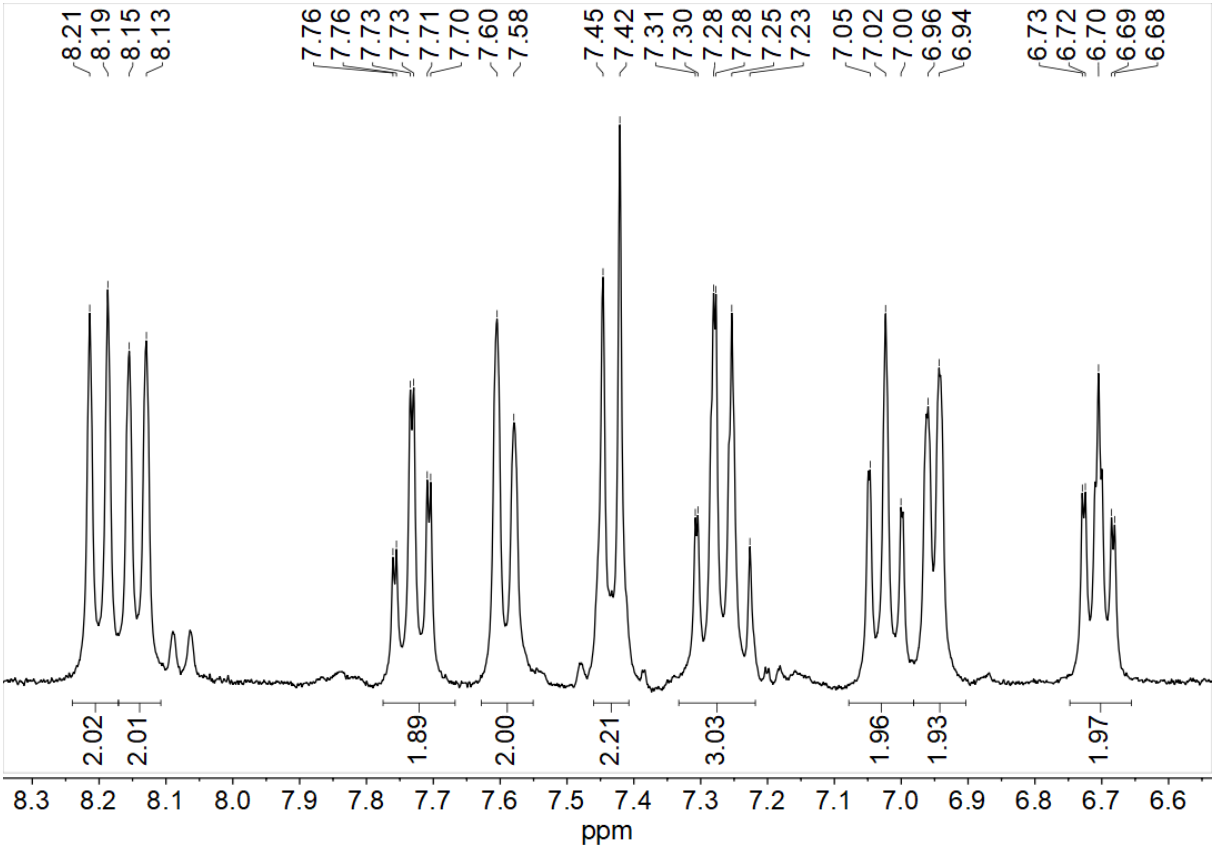

Figure 7-249 300 MHz ^{1}H NMR spectrum of [Ni(Py(Ph)Py)Carb] in CD_2Cl_2.

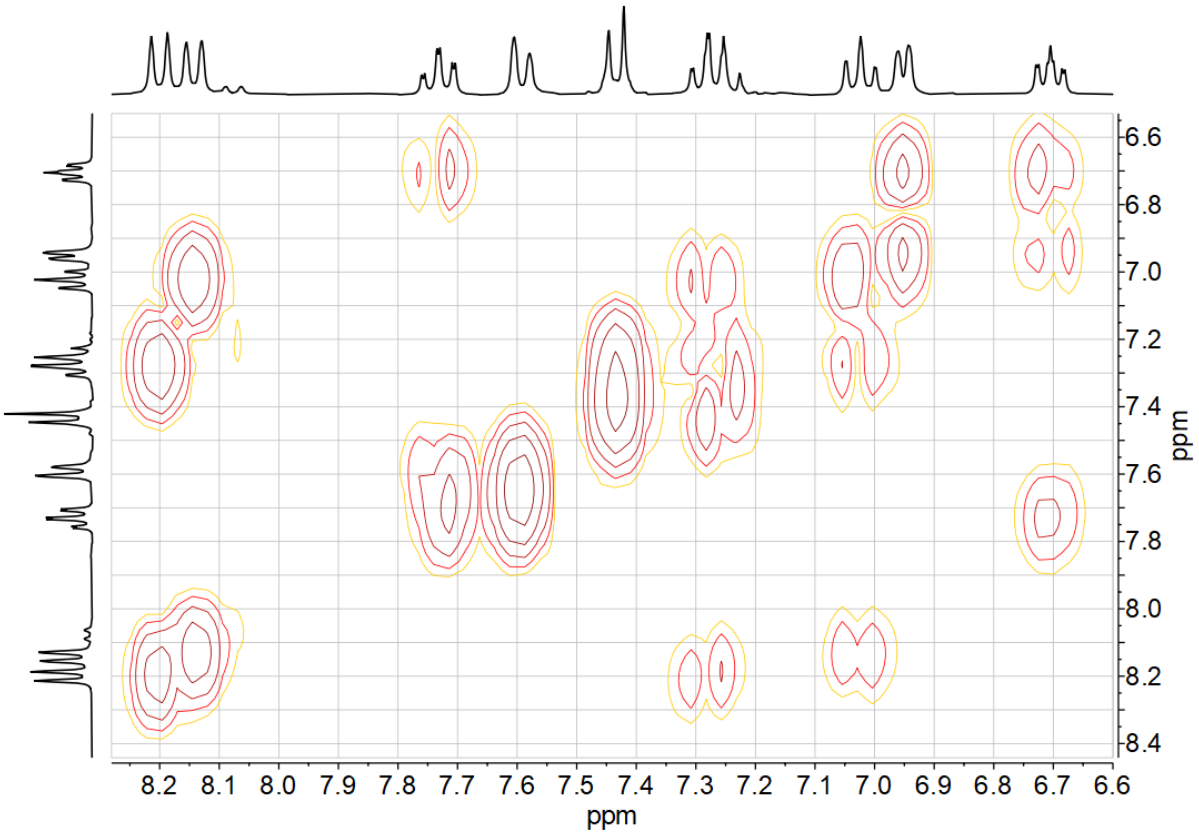

Figure 7-250 $^{1}H,^{1}H$ COSY correlation spectrum of [Ni(Py(Ph)Py)Carb] in CD_2Cl_2.

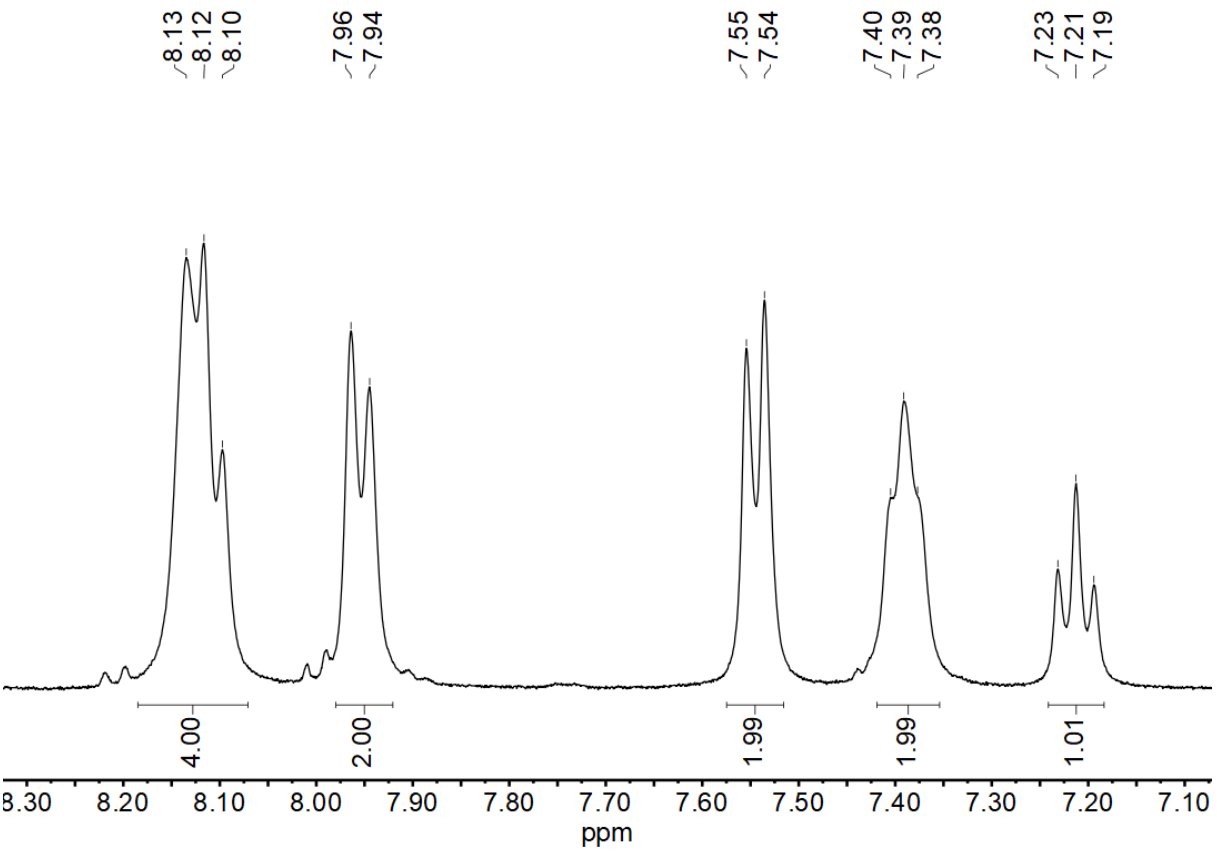

Figure 7-251 400 MHz ^{1}H NMR spectrum of [Ni(Py(Ph)Py)NO$_3$] in DMSO-*d*$_6$.

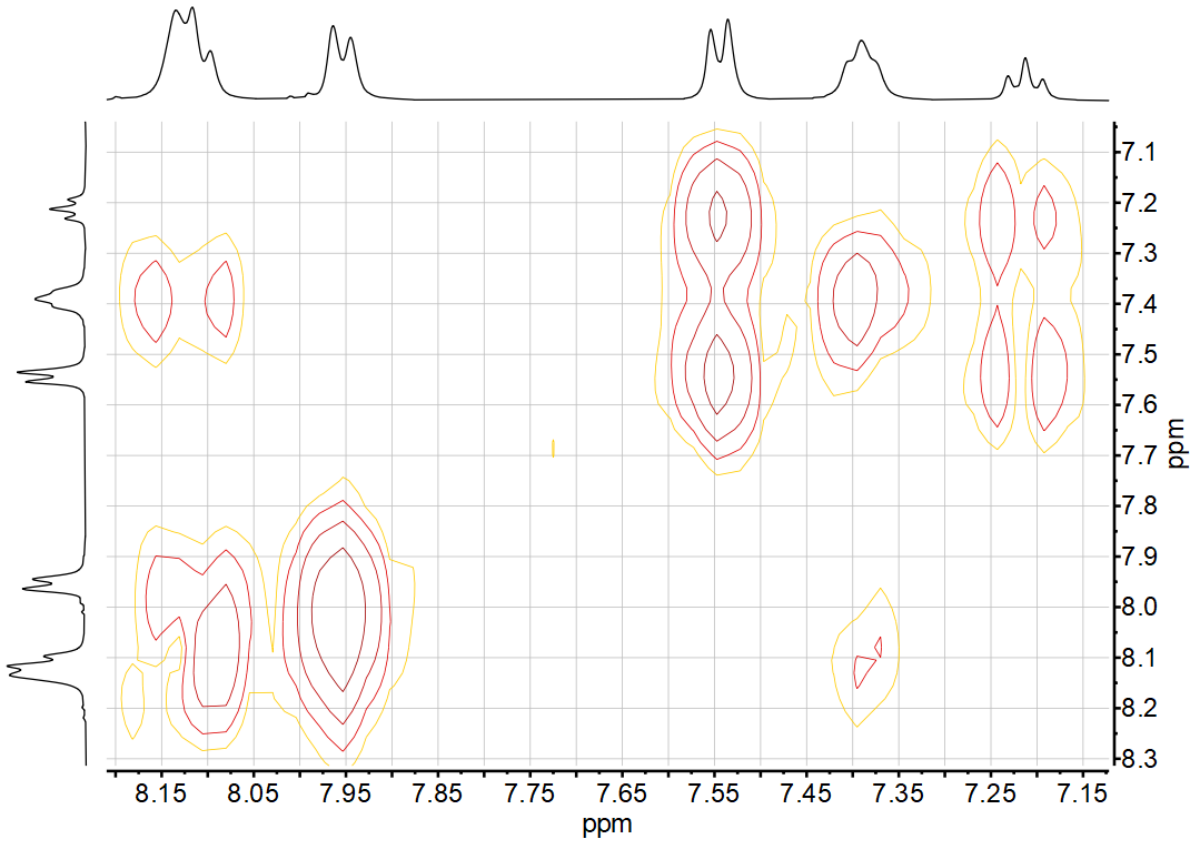

Figure 7-252 ^{1}H,^{1}H COSY correlation spectrum of [Ni(Py(Ph)Py)NO$_3$] in DMSO-*d*$_6$.

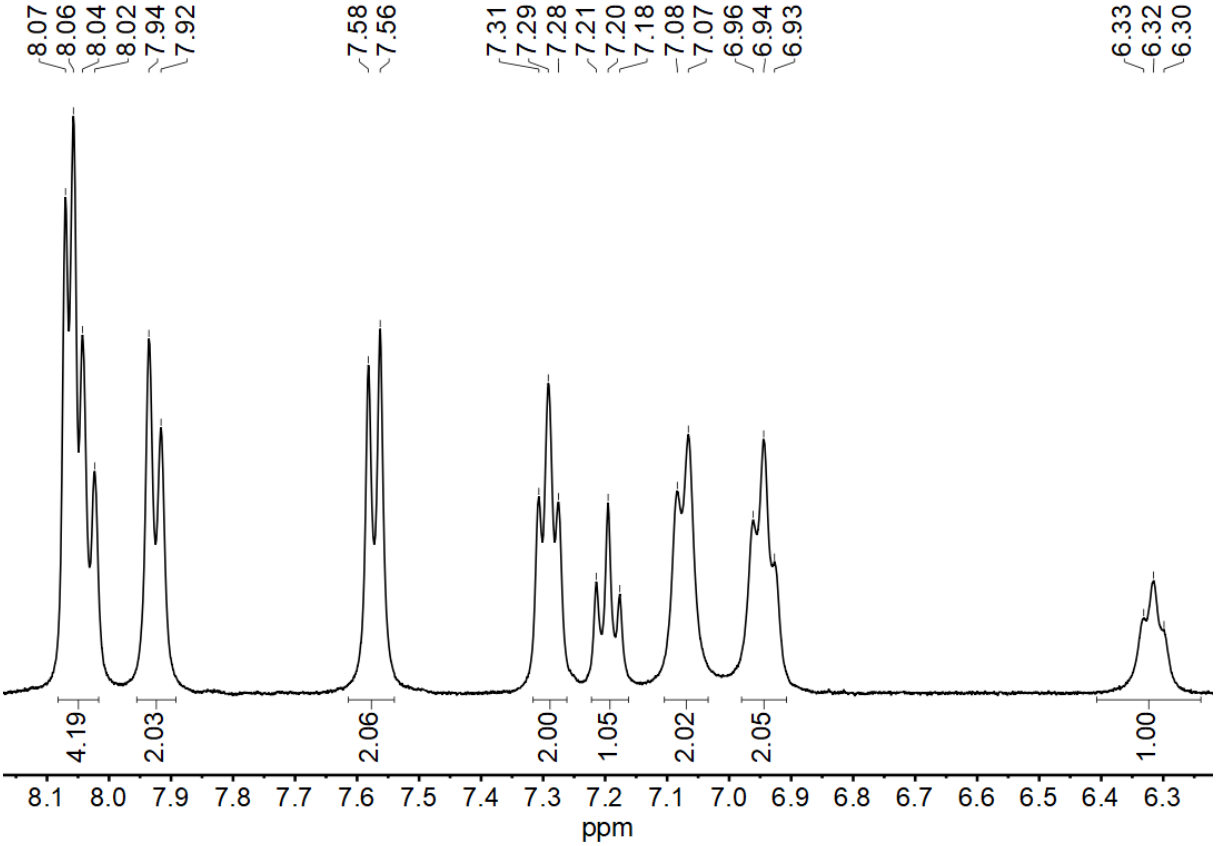

Figure 7-253 400 MHz ^{1}H NMR spectrum of [Ni(Py(Ph)Py)OPh] in DMSO-d_6.

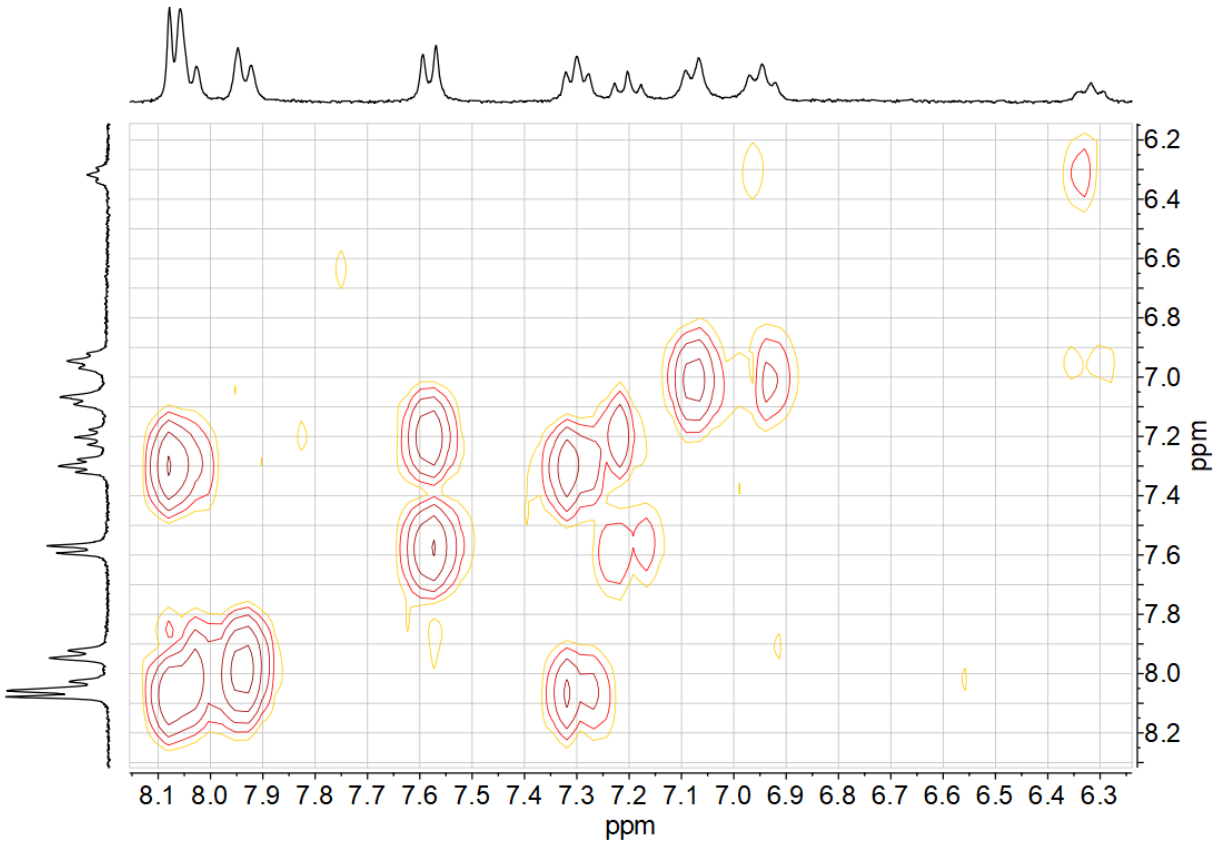

Figure 7-254 ^{1}H,^{1}H COSY correlation spectrum of [Ni(Py(Ph)Py)OPh] in DMSO-d_6.

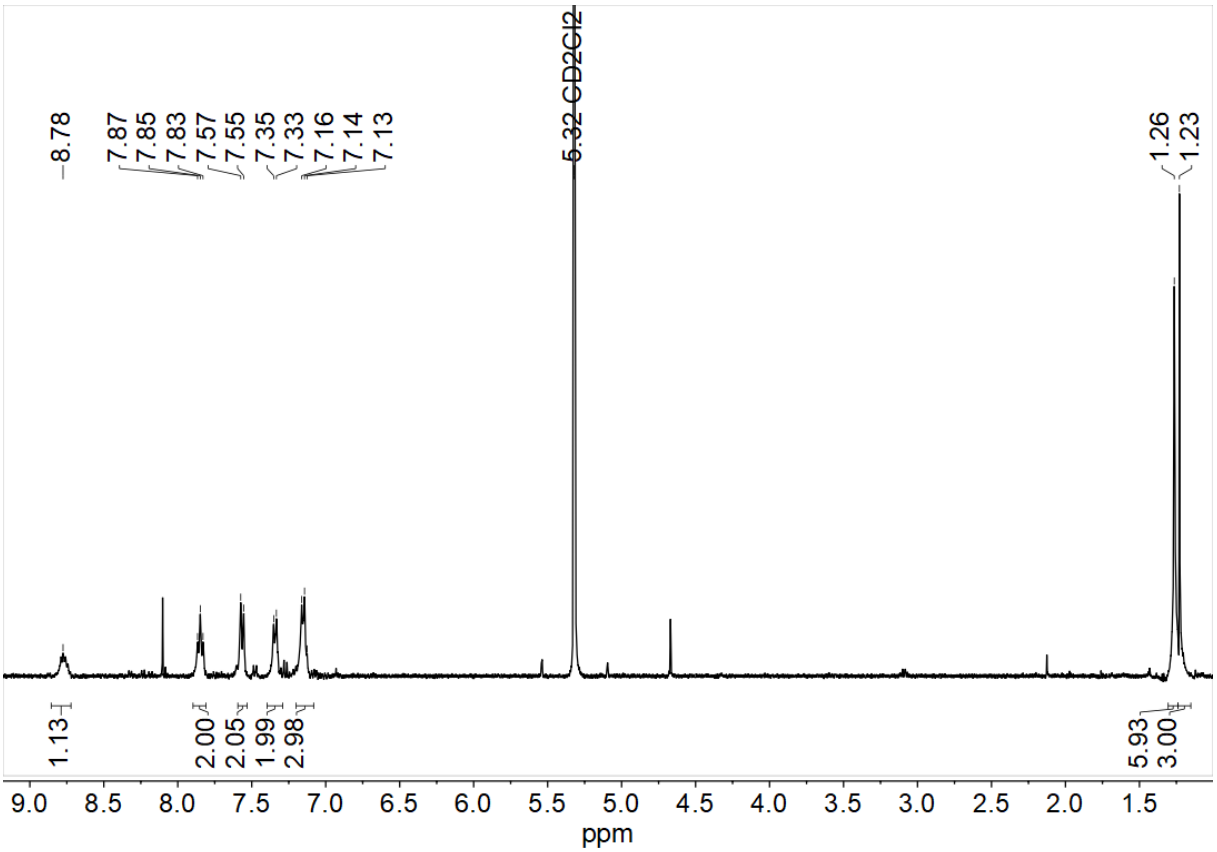

Figure 7-255 400 MHz ^{1}H NMR spectrum of [Ni(Py(Ph)Py)O*t*Bu] in CD_2Cl_2.

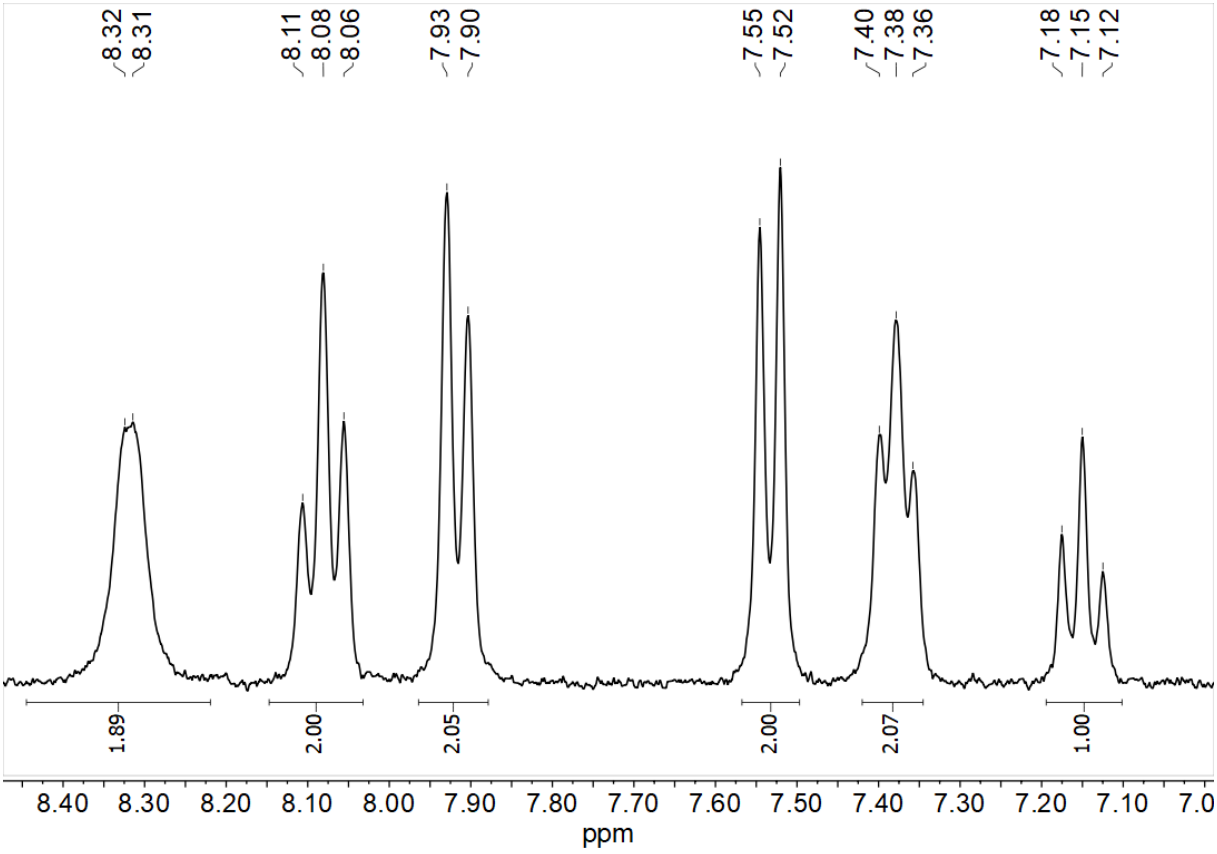

Figure 7-256 300 MHz ^{1}H NMR spectrum of [Ni(Py(Ph)Py)F] in DMSO-d_6.

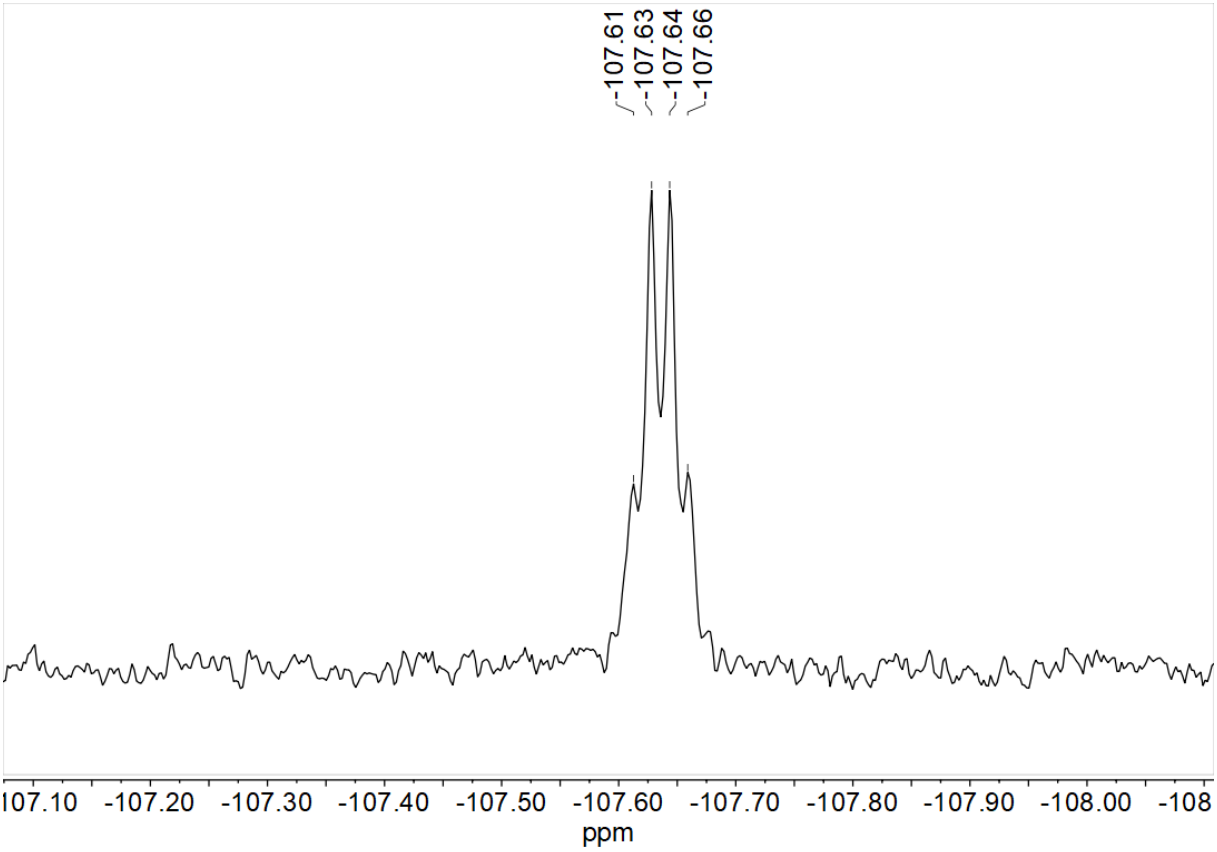

Figure 7-257 282 MHz ^{19}F NMR spectrum of [Ni(Py(Ph)Py)F] in DMSO-d_6.

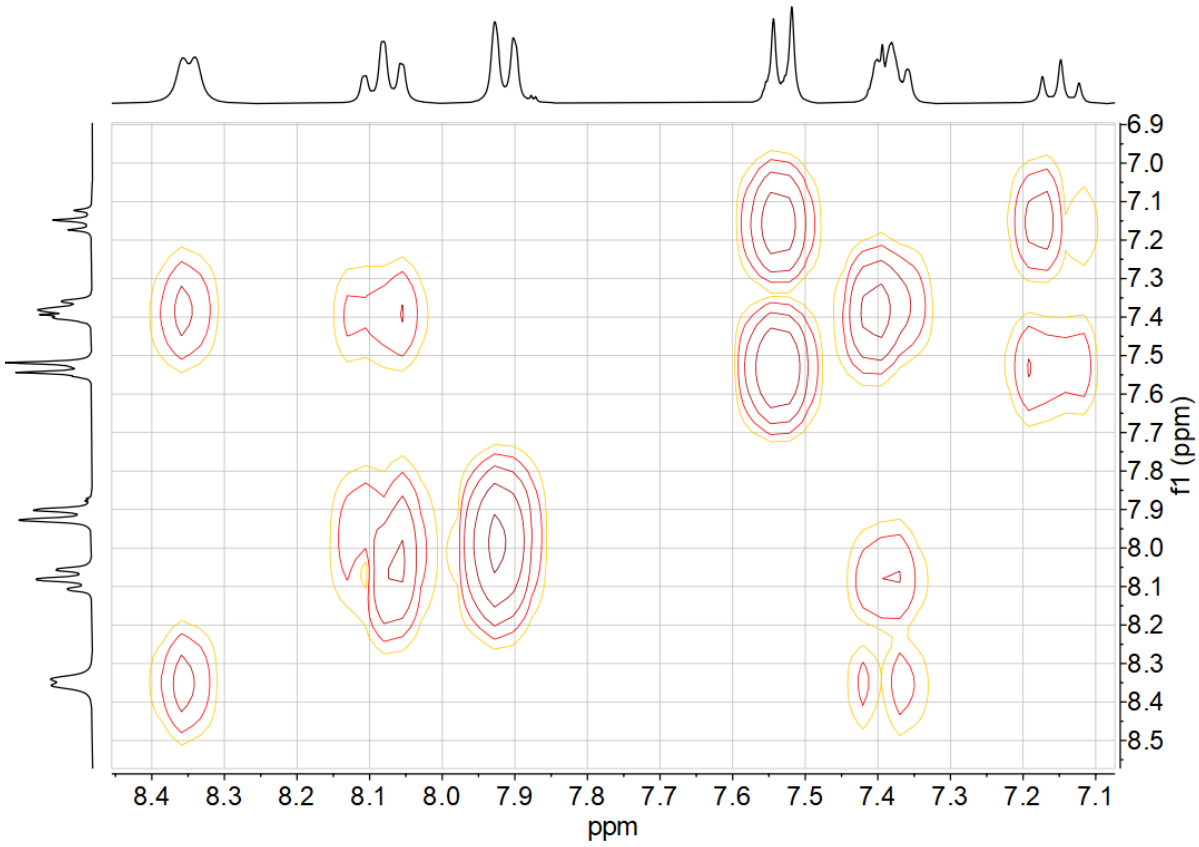

Figure 7-258 ^{1}H,^{1}H COSY correlation spectrum of [Ni(Py(Ph)Py)F] in DMSO-d_6.

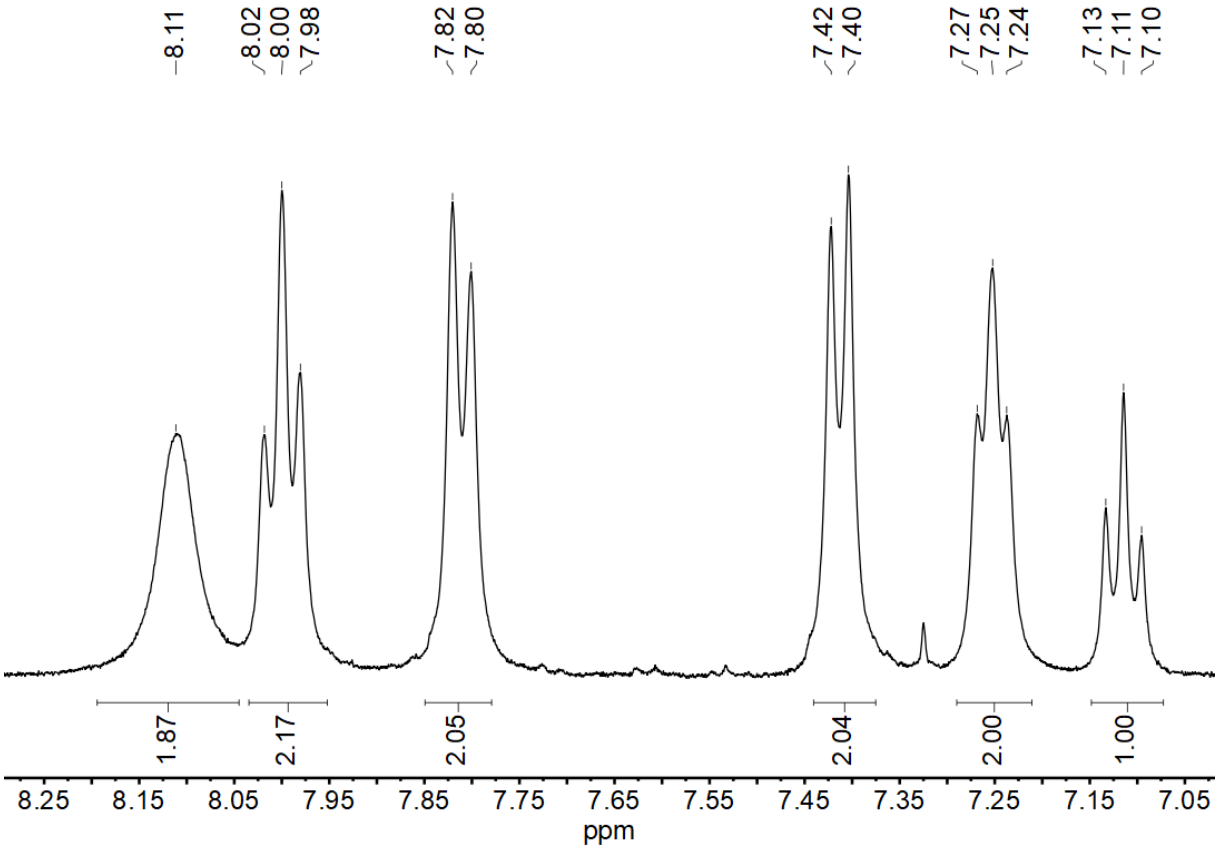

Figure 7-259 400 MHz ^{1}H NMR spectrum of [Ni(Py(Ph)Py)C_2F_5] in DMSO-d_6.

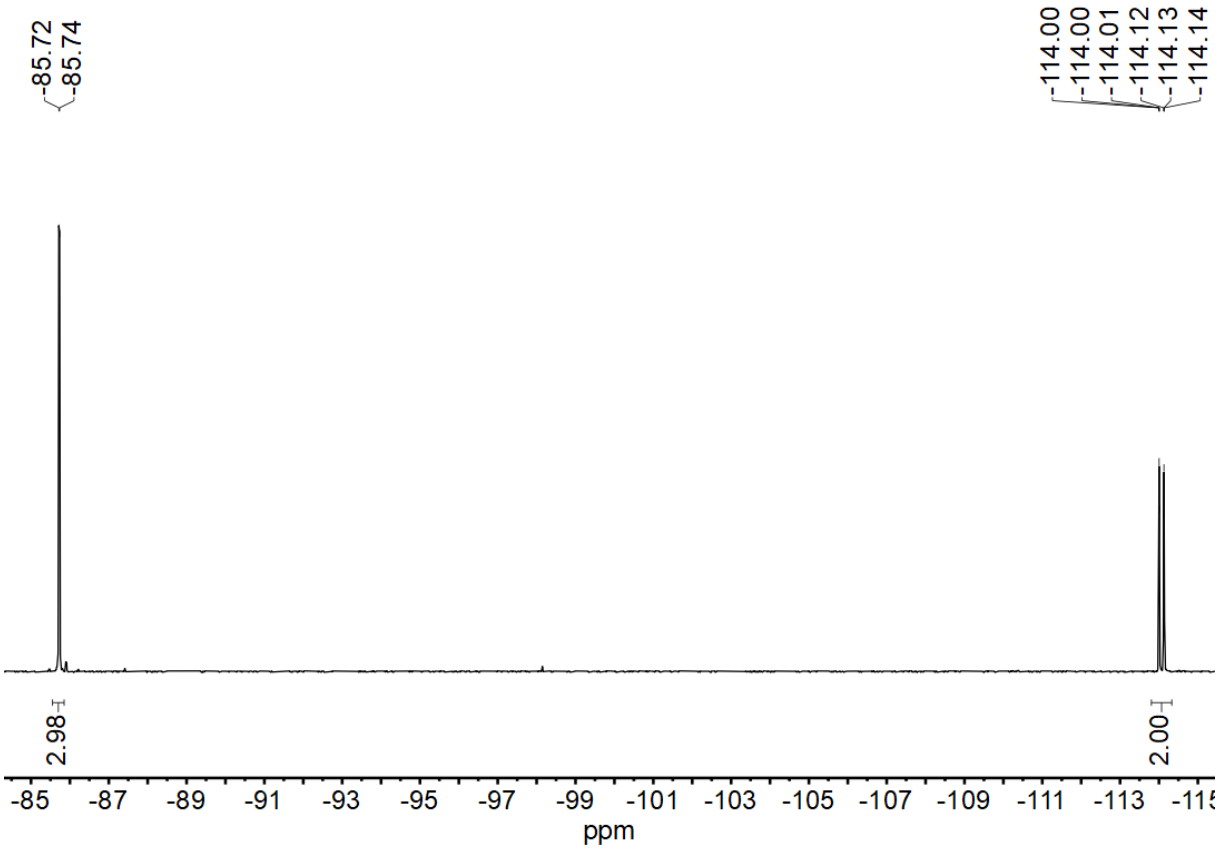

Figure 7-260 376 MHz ^{19}F NMR spectrum of [Ni(Py(Ph)Py)C_2F_5] in DMSO-d_6.

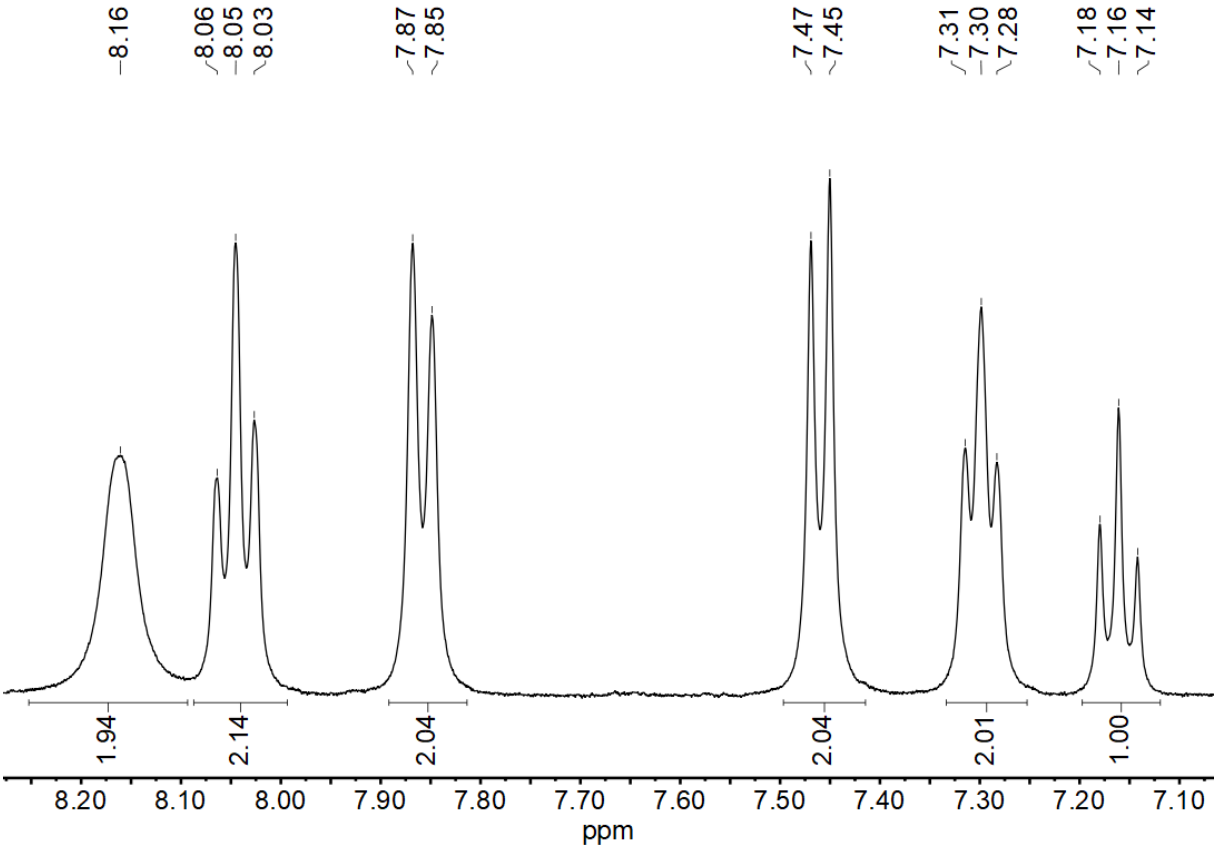

Figure 7-261 400 MHz ^{1}H NMR spectrum of [Ni(Py(Ph)Py)C_3F_7] in DMSO-d_6.

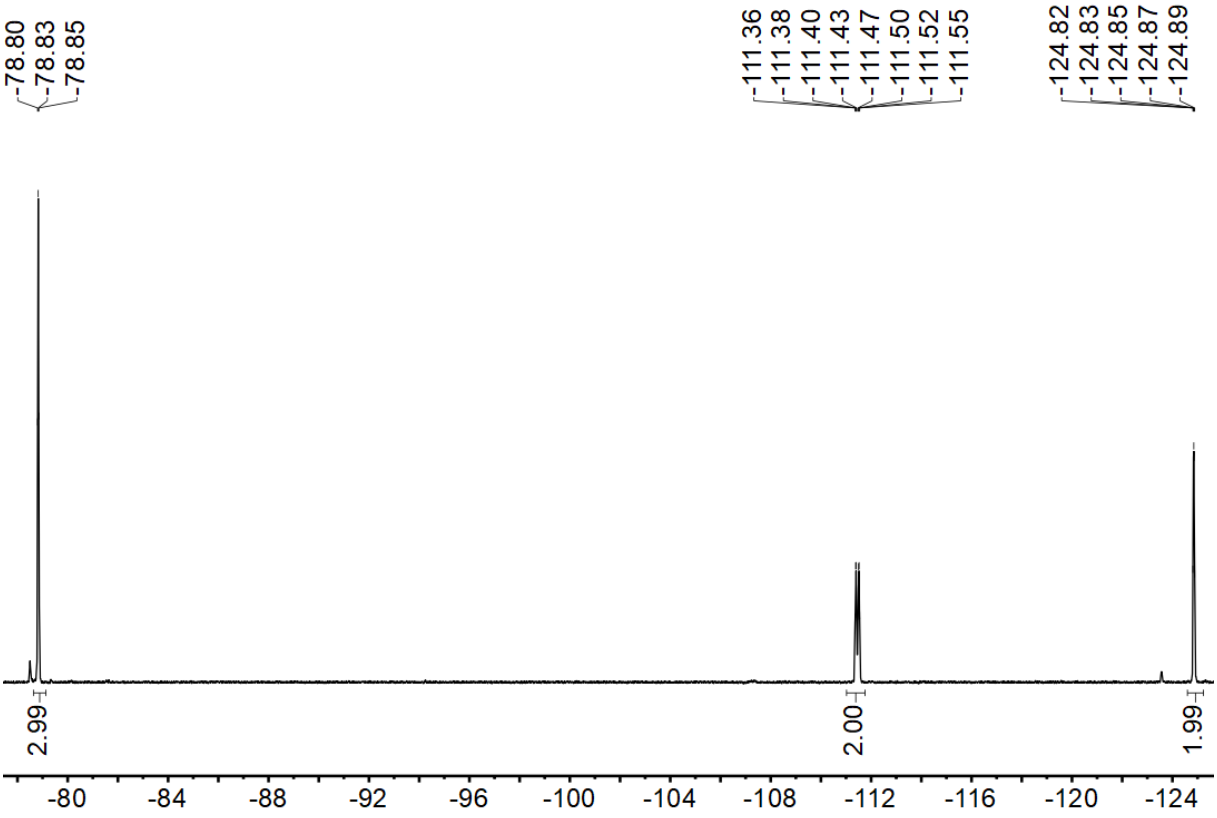

Figure 7-262 376 MHz ^{19}F NMR spectrum of [Ni(Py(Ph)Py)C_3F_7] in DMSO-d_6.

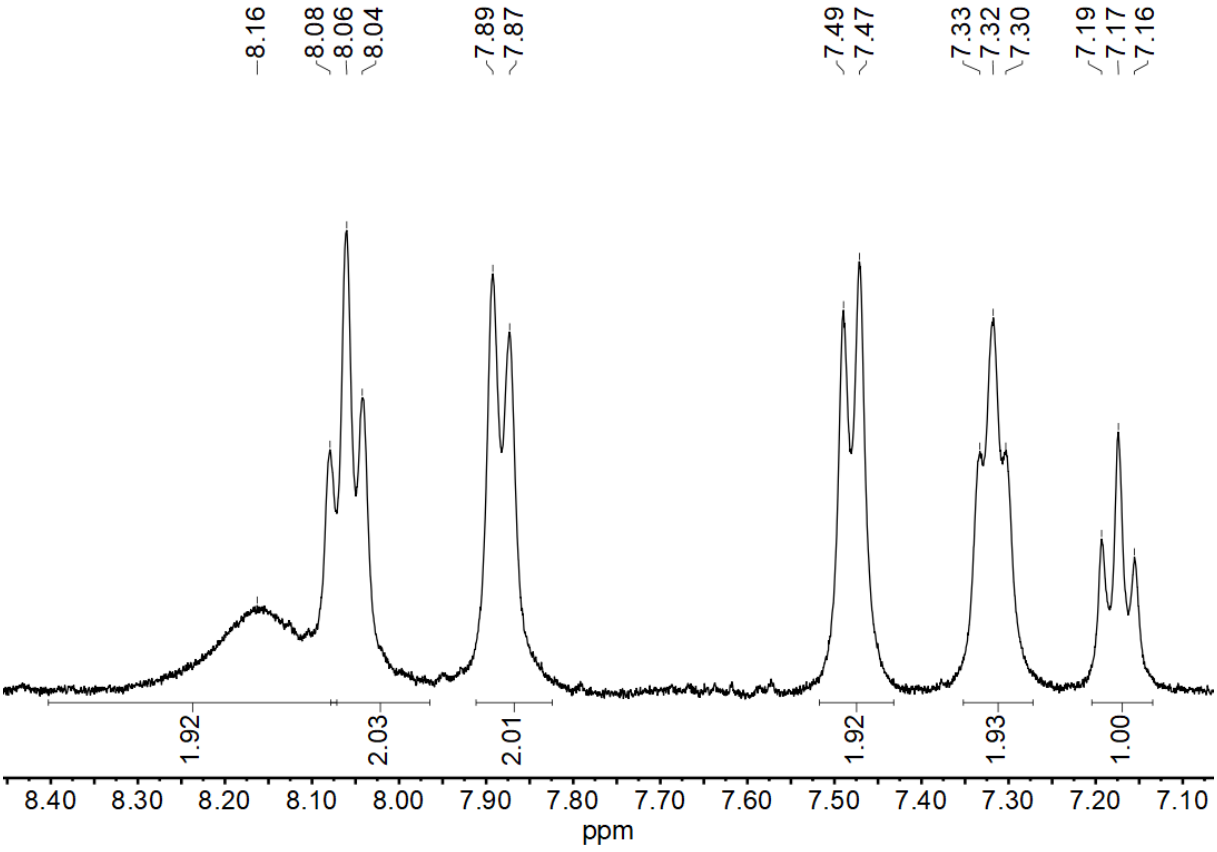

Figure 7-263 400 MHz ^{1}H NMR spectrum of [Ni(Py(Ph)Py)C_6F_5] in DMSO-d_6.

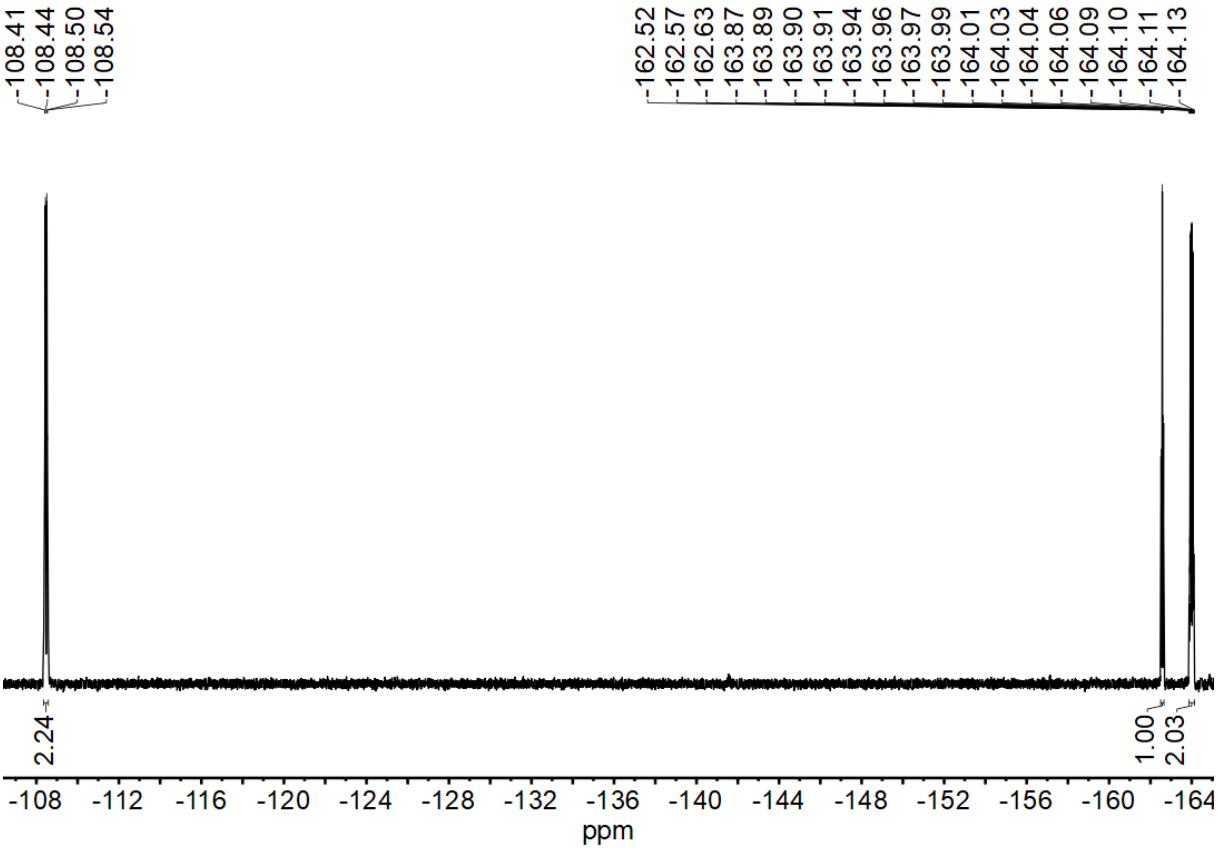

Figure 7-264 376 MHz ^{19}F NMR spectrum of [Ni(Py(Ph)Py)C_6F_5] in DMSO-d_6.

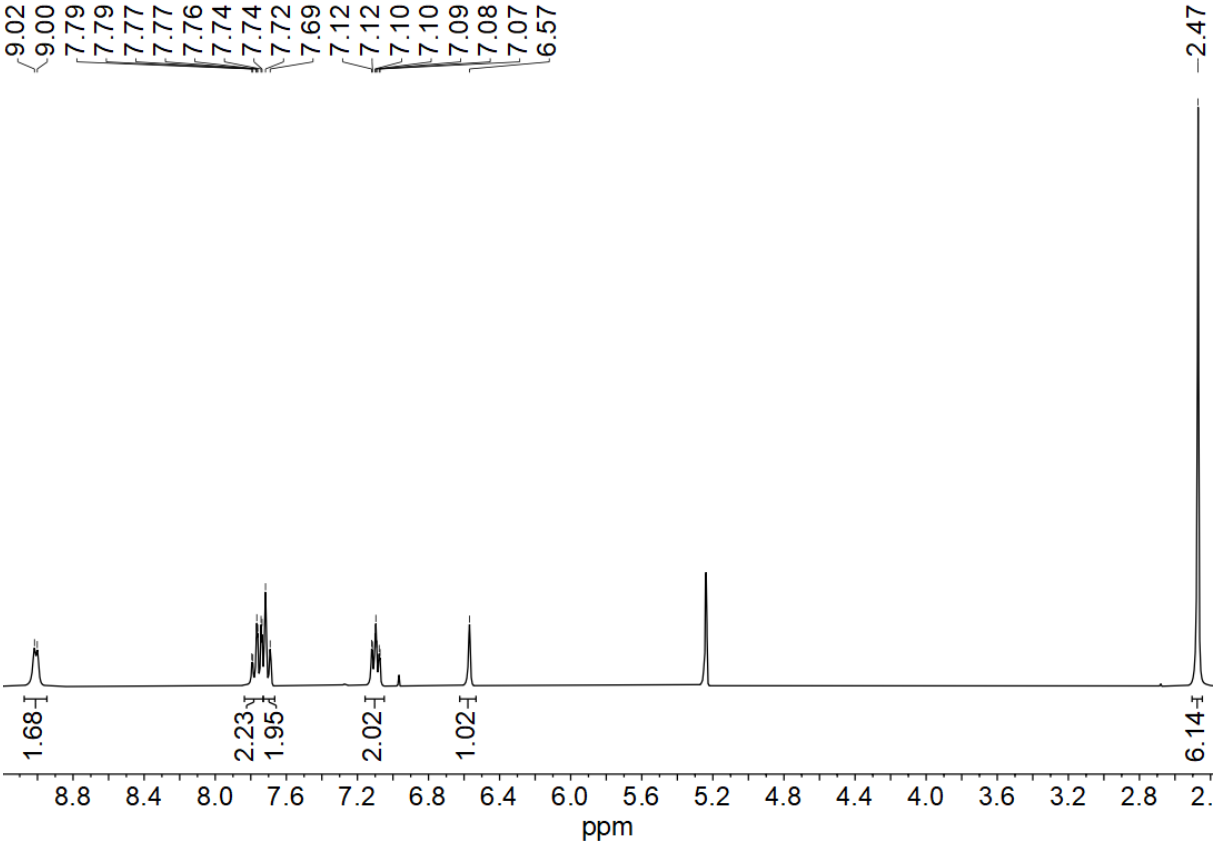

Figure 7-265 300 MHz ^{1}H NMR spectrum of [Pd(Py(4,6MePh)Py)Cl] in CD_2Cl_2.

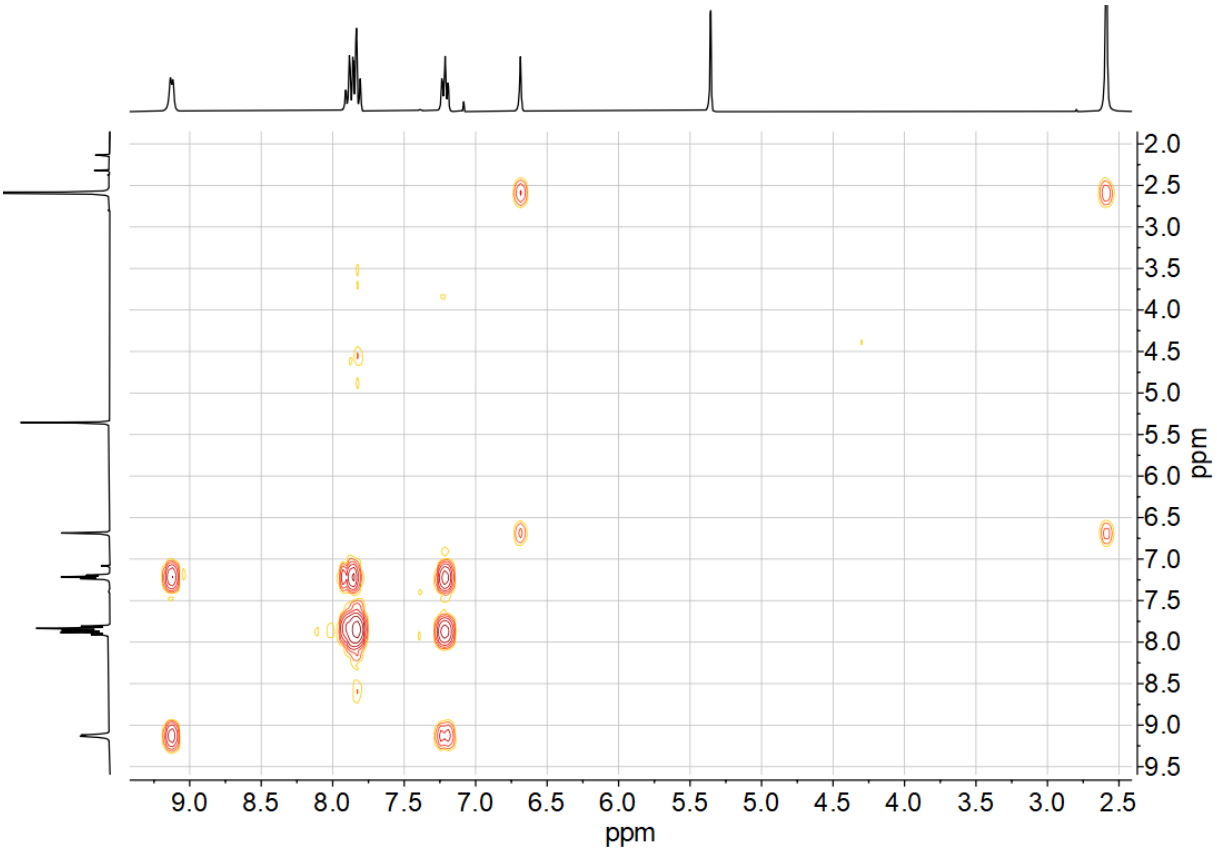

Figure 7-266 $^{1}H,^{1}H$ COSY correlation spectrum of [Pd(Py(4,6MePh)Py)Cl] in CD_2Cl_2.

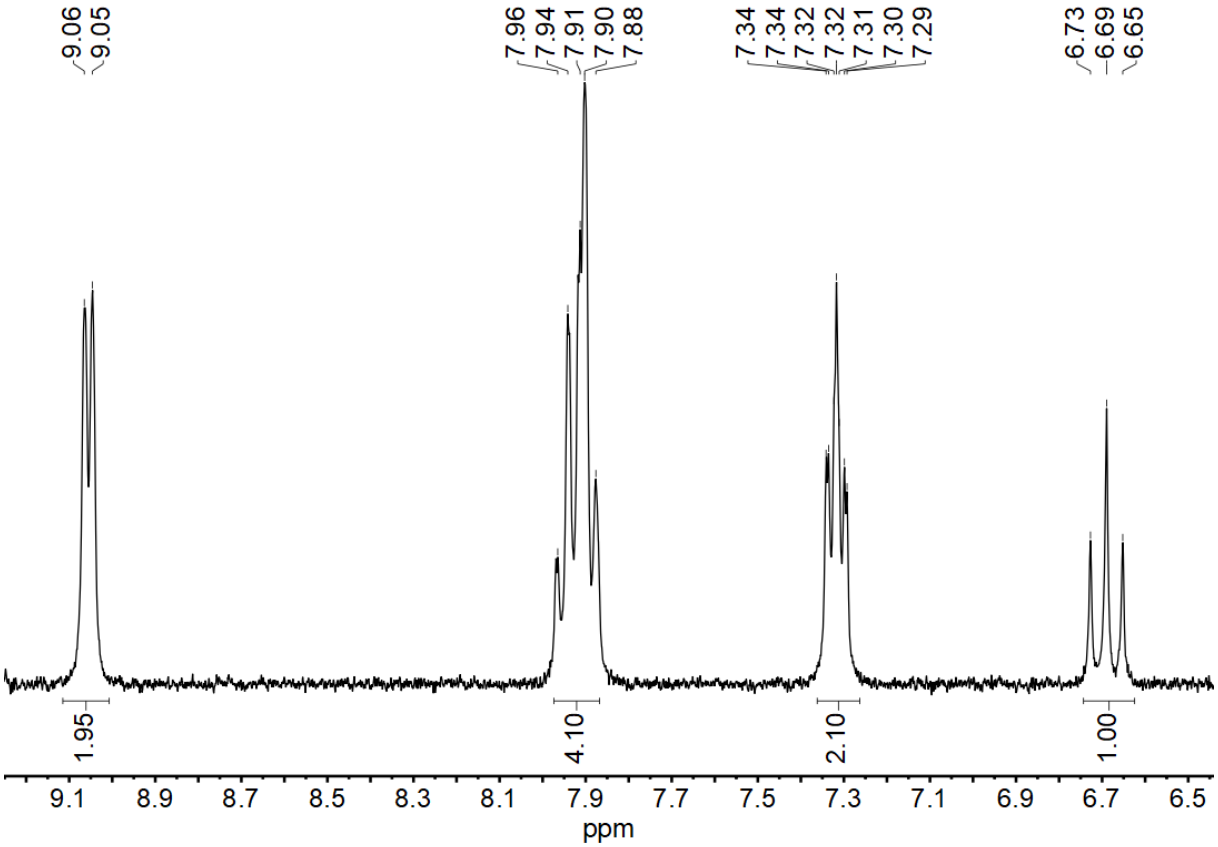

Figure 7-267 300 MHz ^{1}H NMR spectrum of [Pd(Py(4,6FPh)Py)Cl] in CD_2Cl_2.

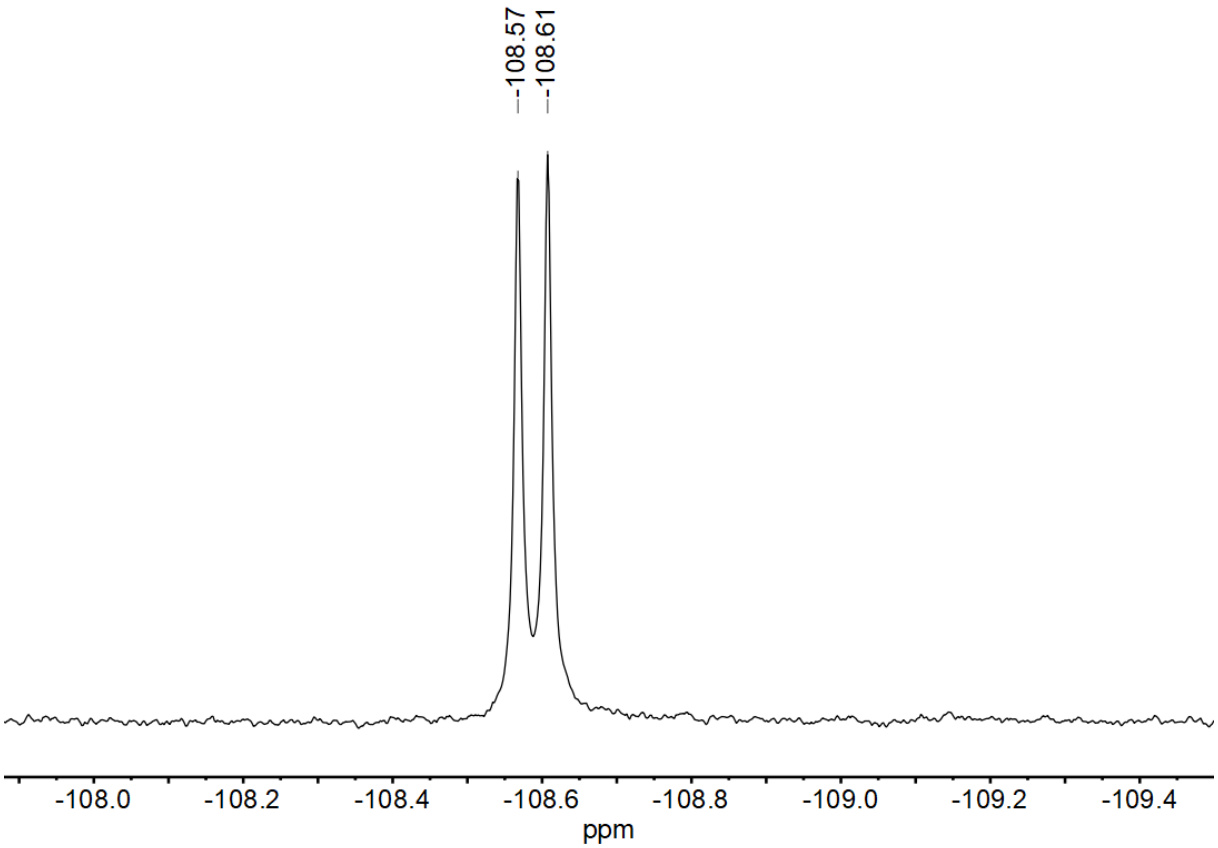

Figure 7-268 282 MHz ^{19}F NMR spectrum of [Pd(Py(4,6FPh)Py)Cl] in CD_2Cl_2.

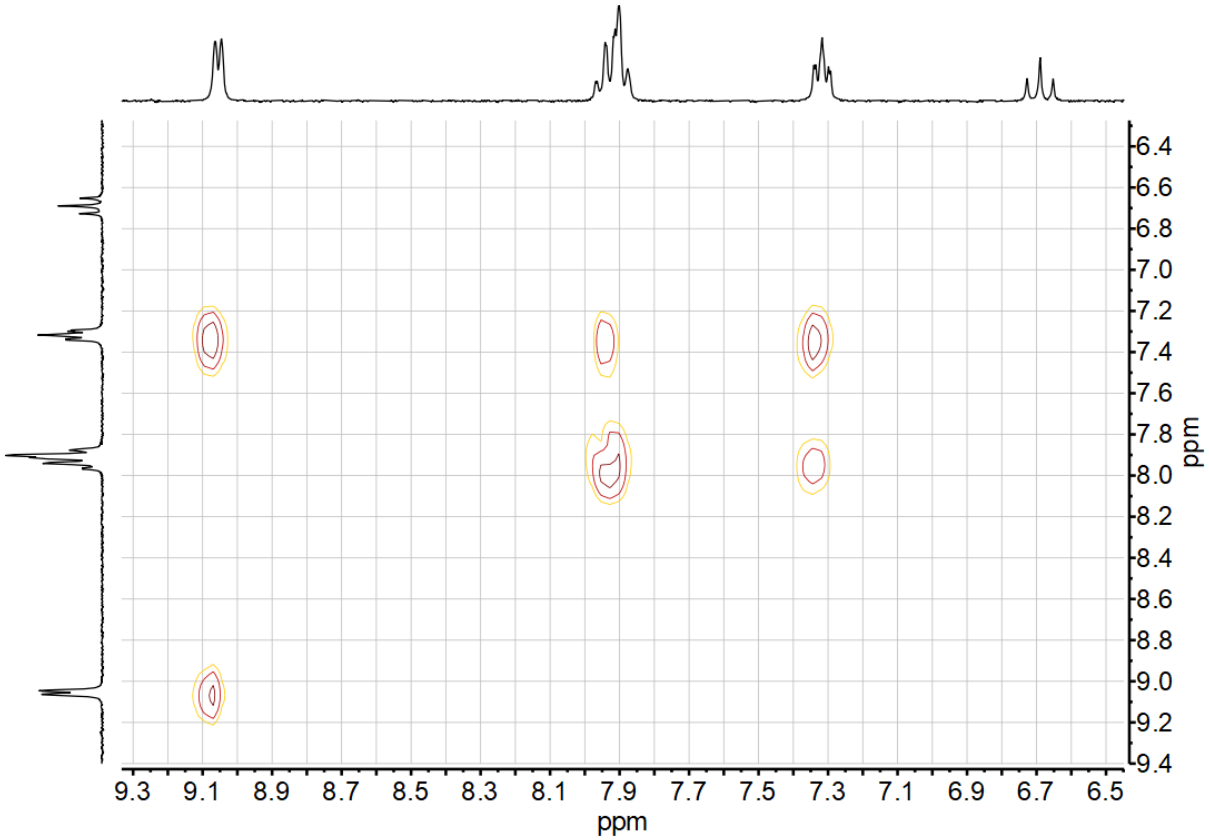

Figure 7-269 $^{1}H,^{1}H$ COSY correlation spectrum of [Pd(Py(4,6FPh)Py)Cl] in CD_2Cl_2.

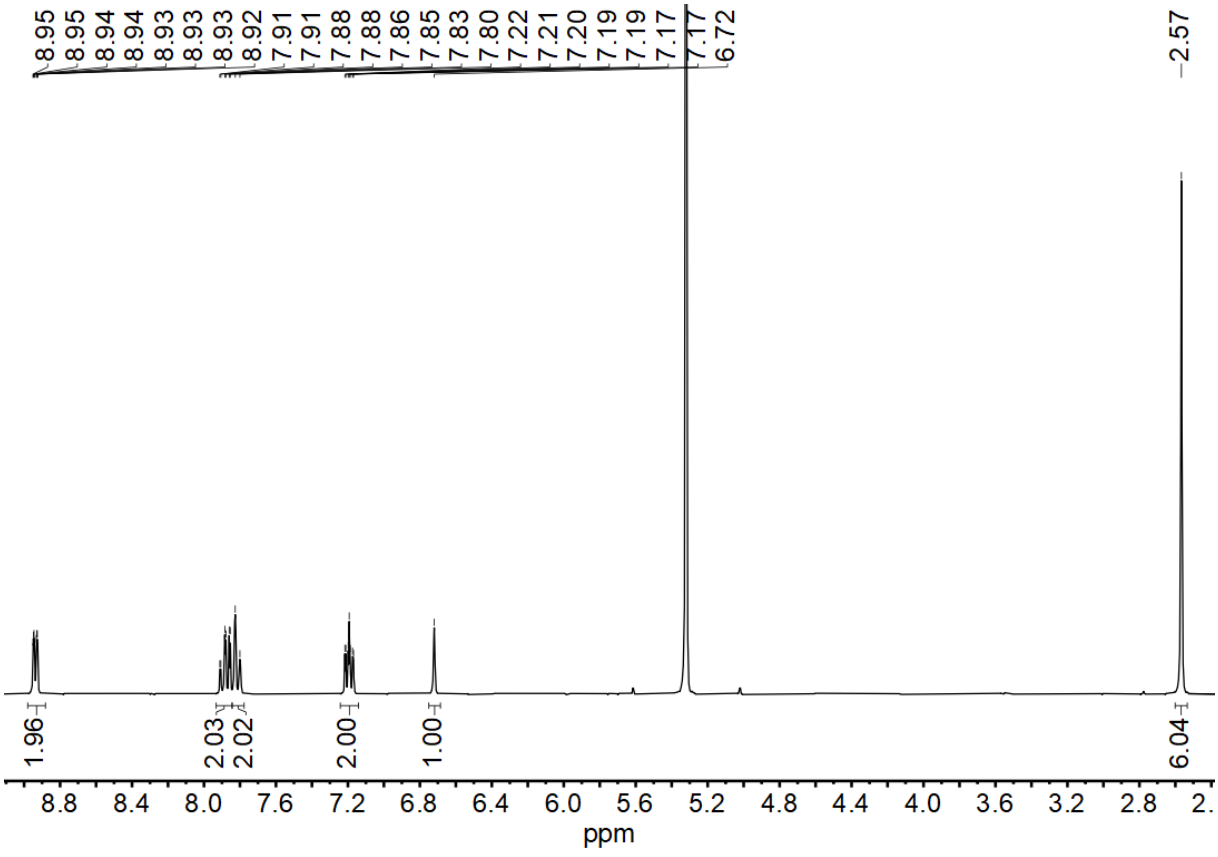

Figure 7-270 300 MHz ^{1}H NMR spectrum of [Pd(Py(4,6MePh)Py)CN] in CD_2Cl_2.

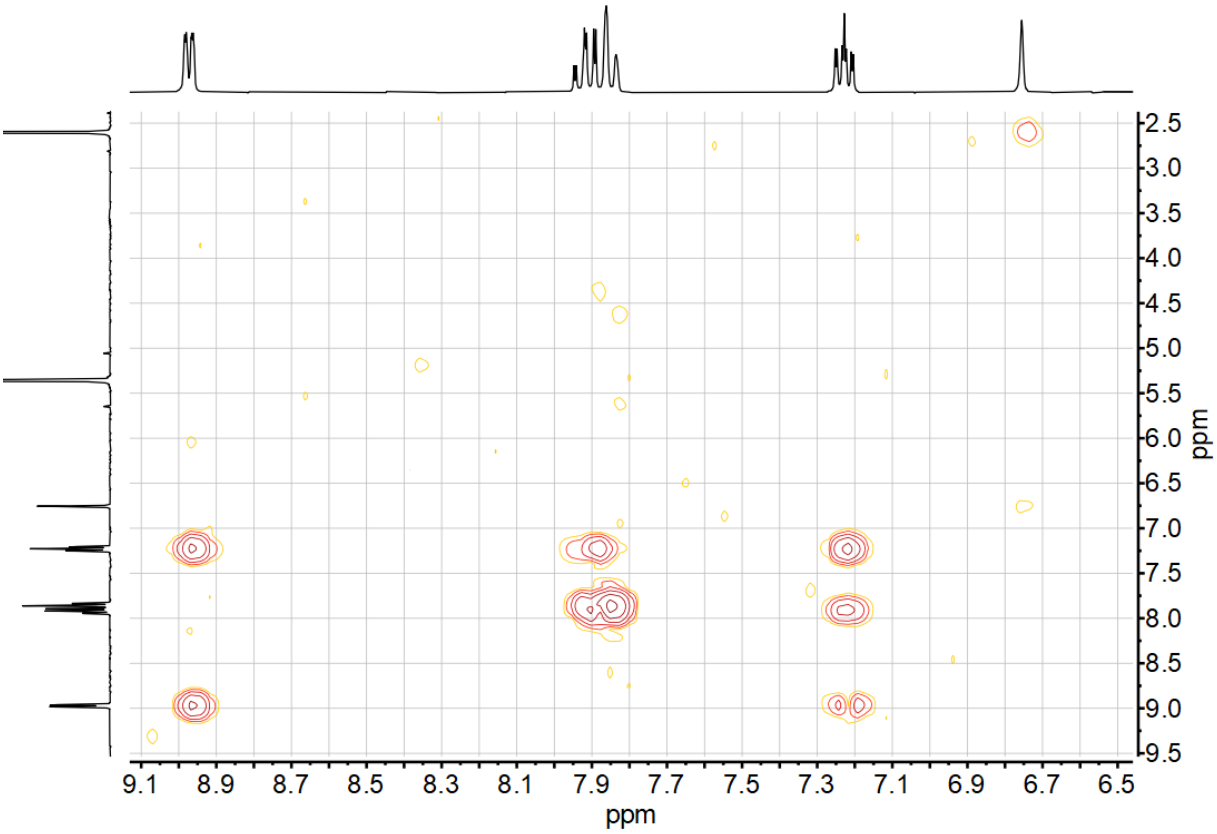

Figure 7-271 $^{1}H,^{1}H$ COSY correlation spectrum of [Pd(Py(4,6MePh)Py)CN] in CD_2Cl_2.

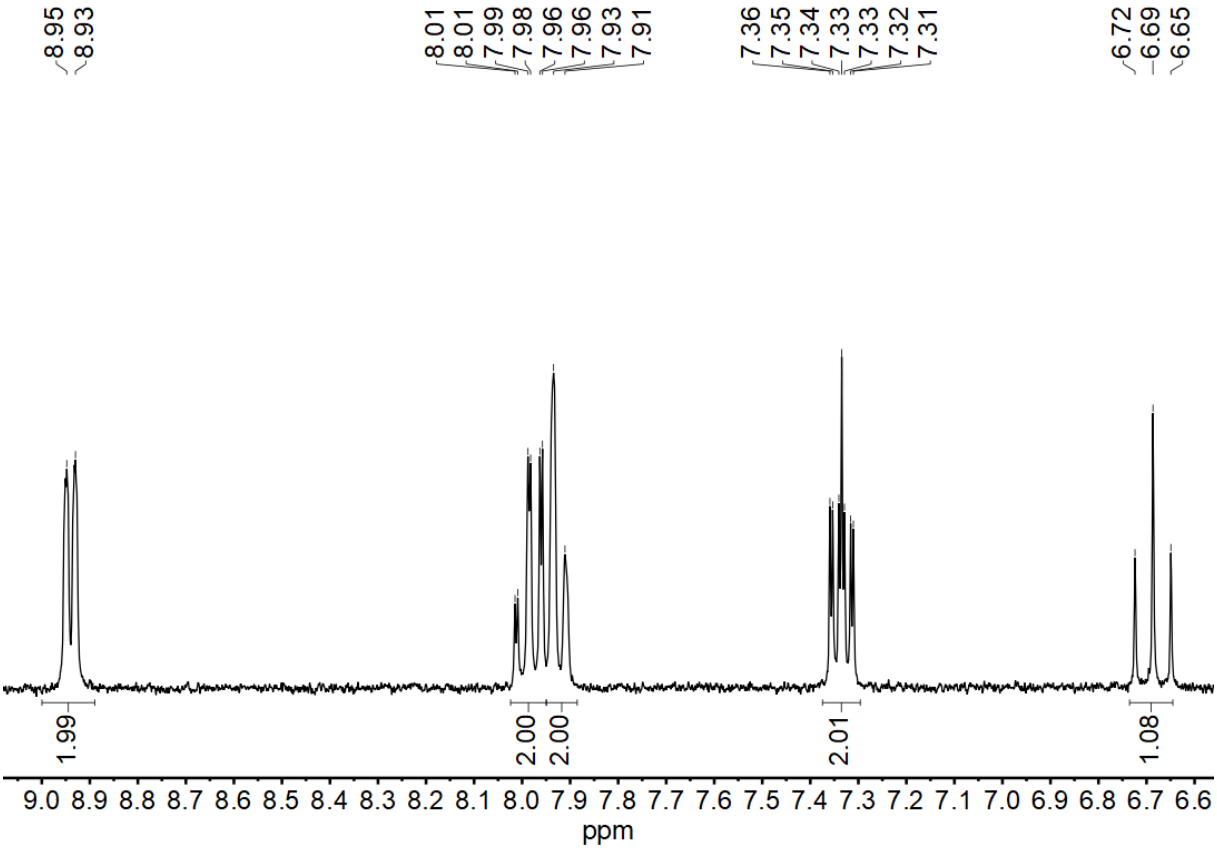

Figure 7-272 300 MHz ^{1}H NMR spectrum of [Pd(Py(4,6FPh)Py)CN] in CD_2Cl_2.

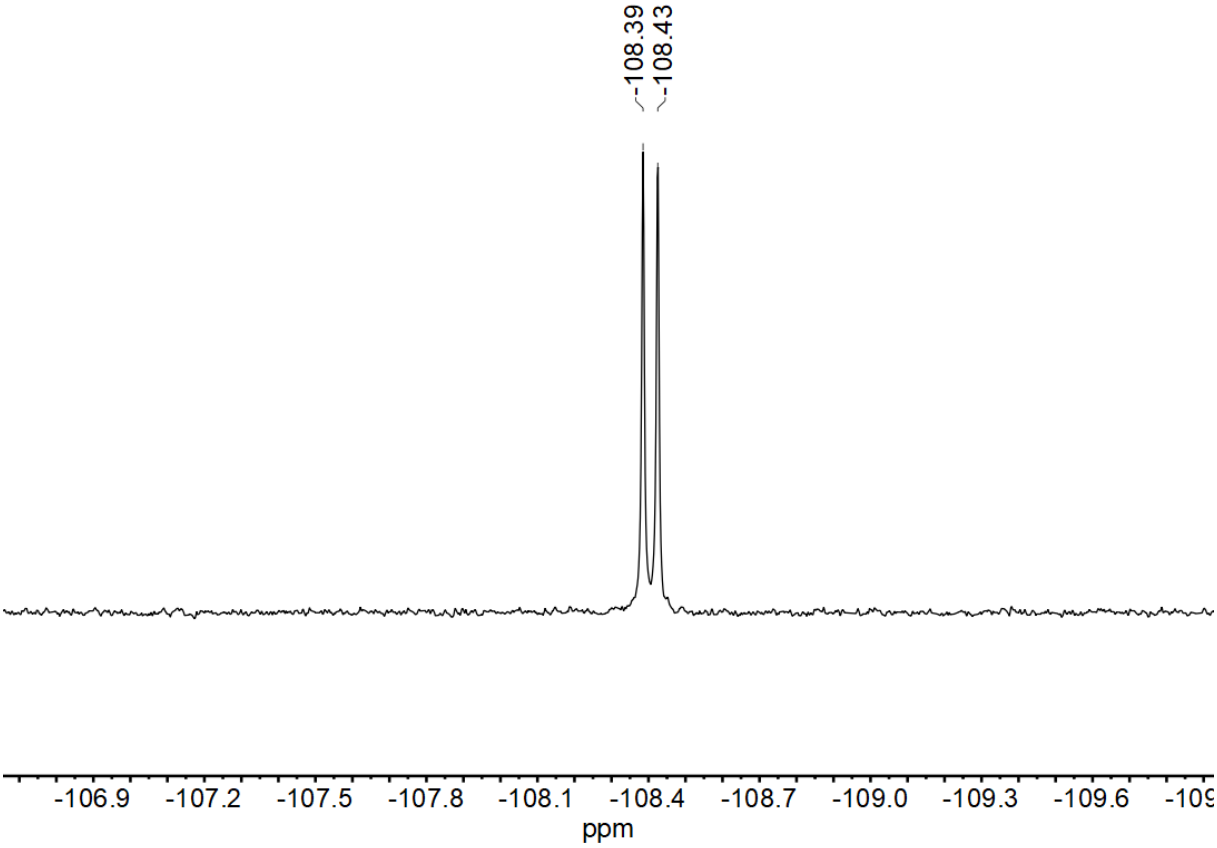

Figure 7-273 282 MHz ^{19}F NMR spectrum of [Pd(Py(4,6FPh)Py)CN] in CD_2Cl_2.

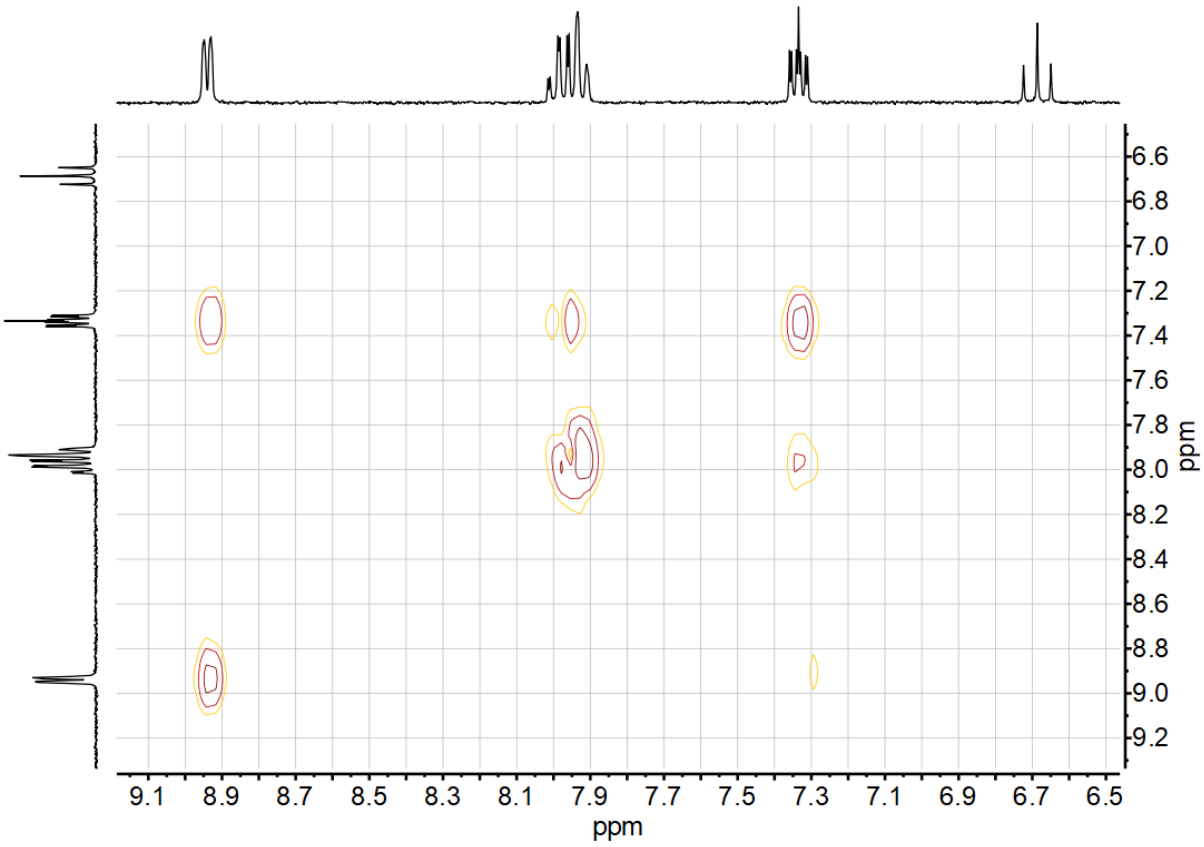

Figure 7-274 $^{1}H,^{1}H$ COSY correlation spectrum of [Pd(Py(4,6FPh)Py)CN] in CD_2Cl_2.

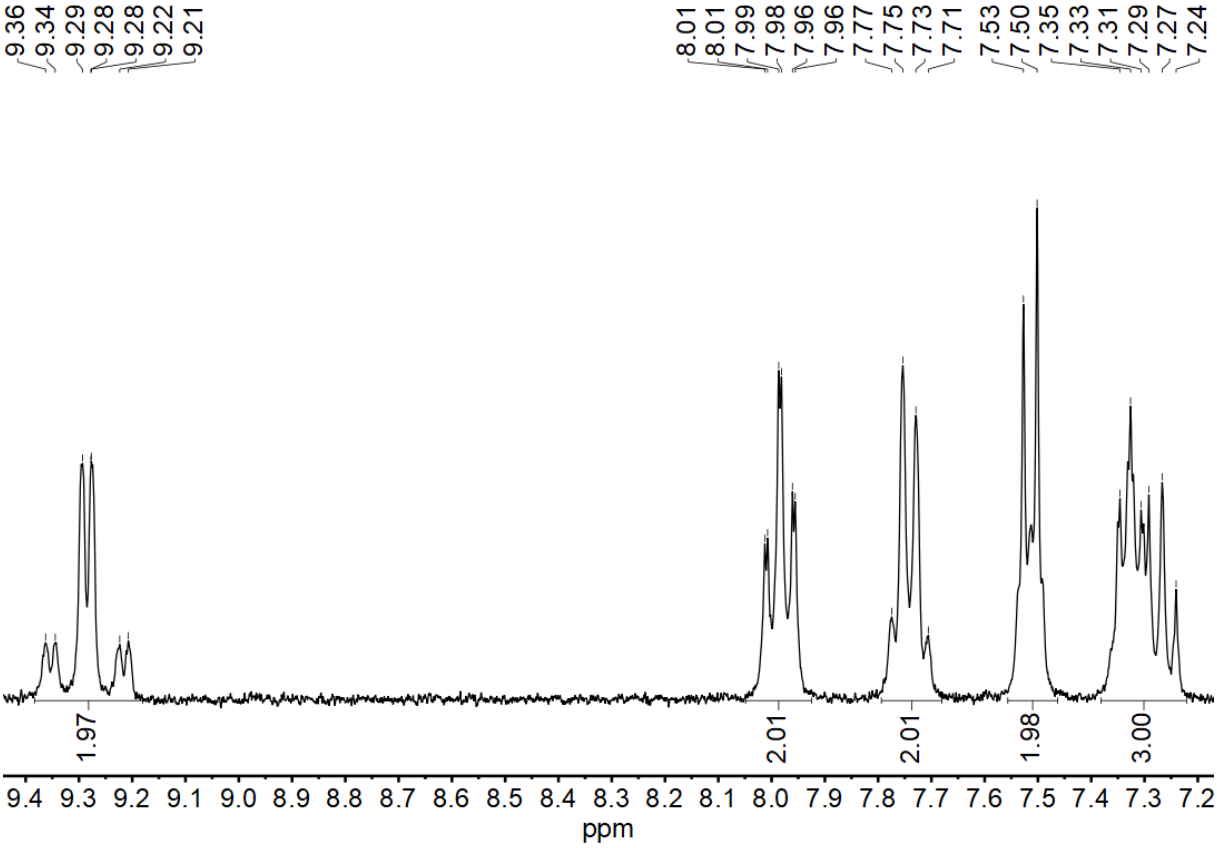

Figure 7-275 300 MHz ^{1}H NMR spectrum of [Pt(Py(Ph)Py)Cl] in CD_2Cl_2.

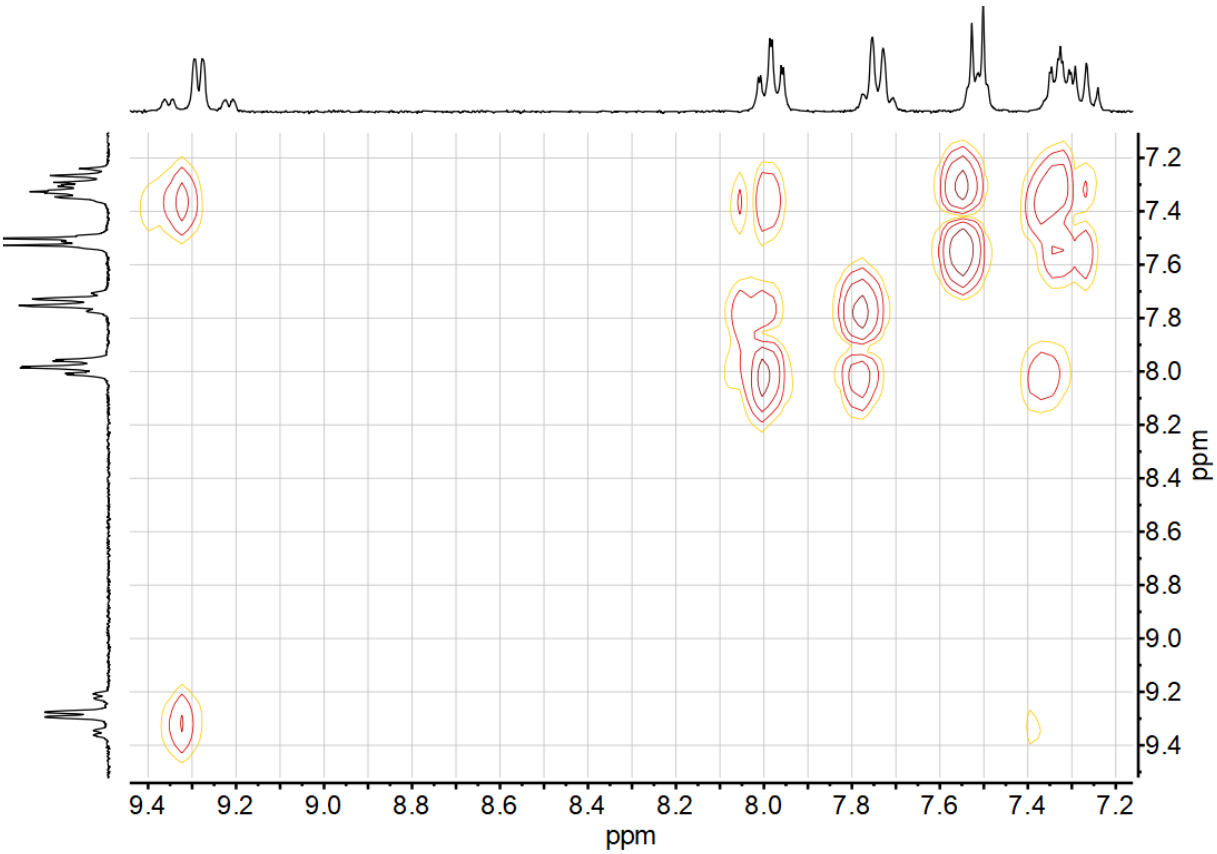

Figure 7-276 $^{1}H,^{1}H$ COSY correlation spectrum of [Pt(Py(Ph)Py)Cl] in CD_2Cl_2.

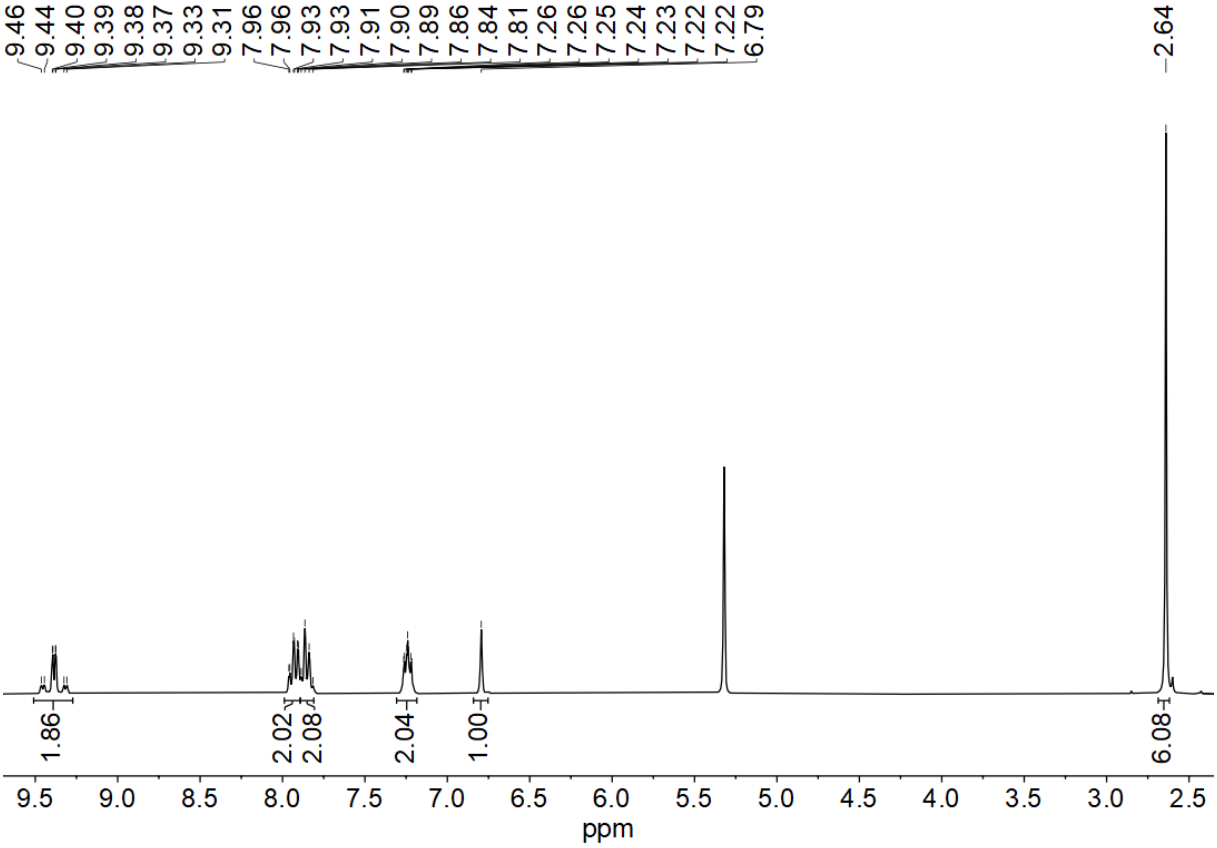

Figure 7-277 300 MHz ^{1}H NMR spectrum of [Pt(Py(4,6MePh)Py)Cl] in CD_2Cl_2.

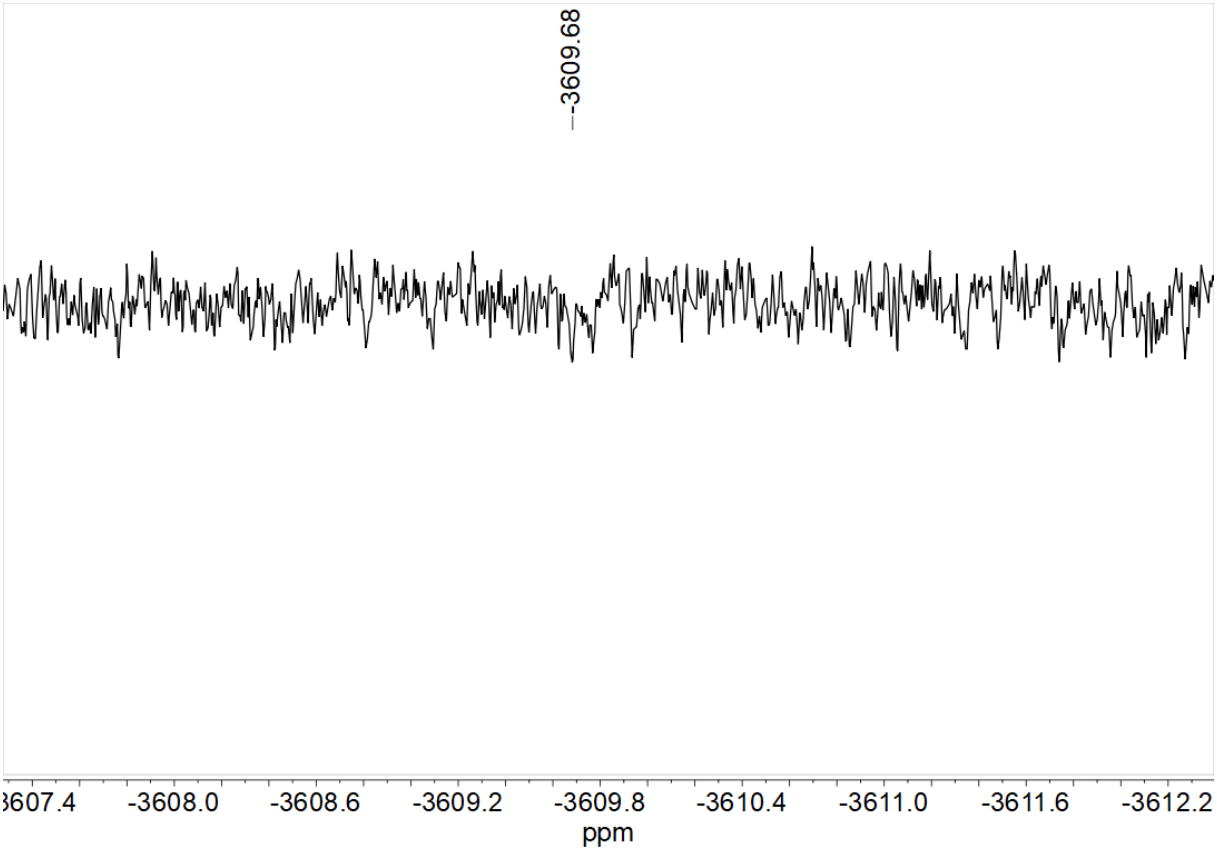

Figure 7-278 64 MHz ^{195}Pt NMR spectrum of [Pt(Py(4,6MePh)Py)Cl] in CD_2Cl_2.

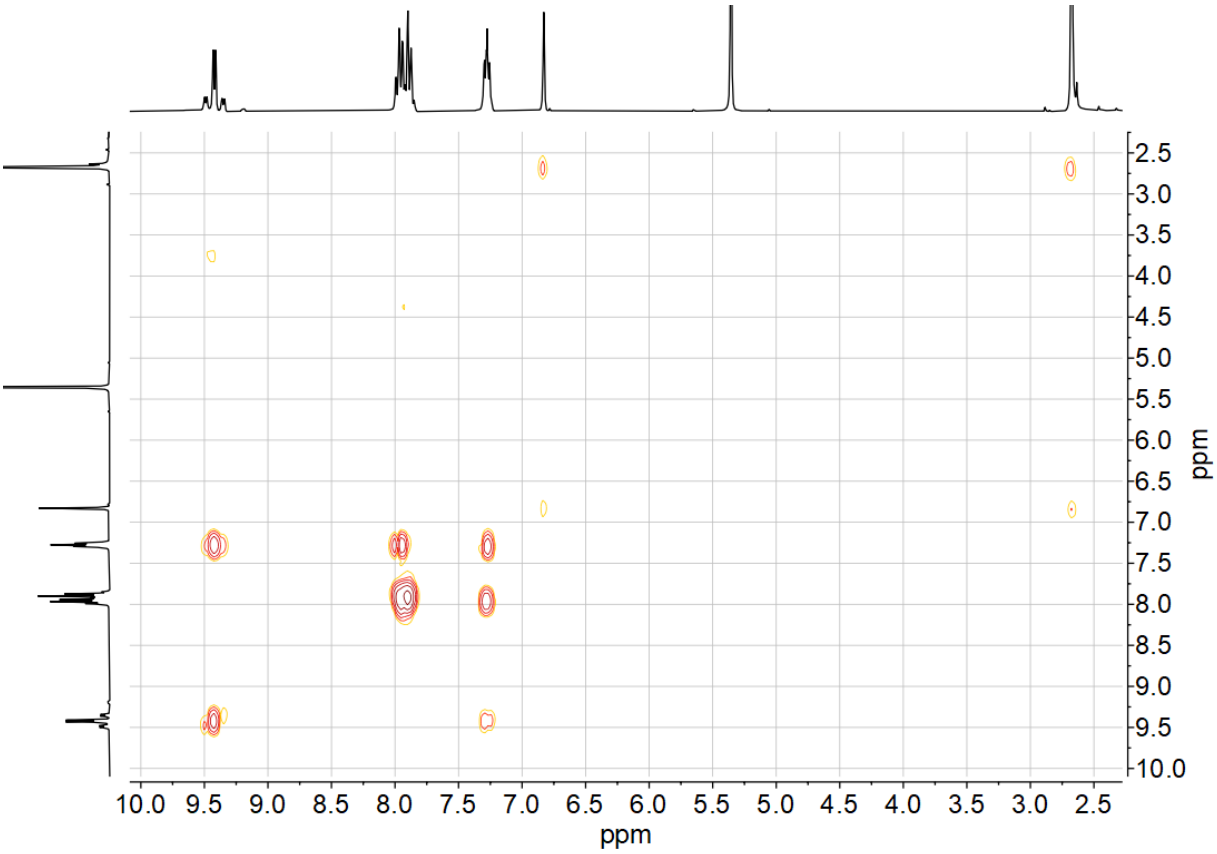

Figure 7-279 $^{1}H,^{1}H$ COSY correlation spectrum of [Pt(Py(4,6MePh)Py)Cl] in CD_2Cl_2.

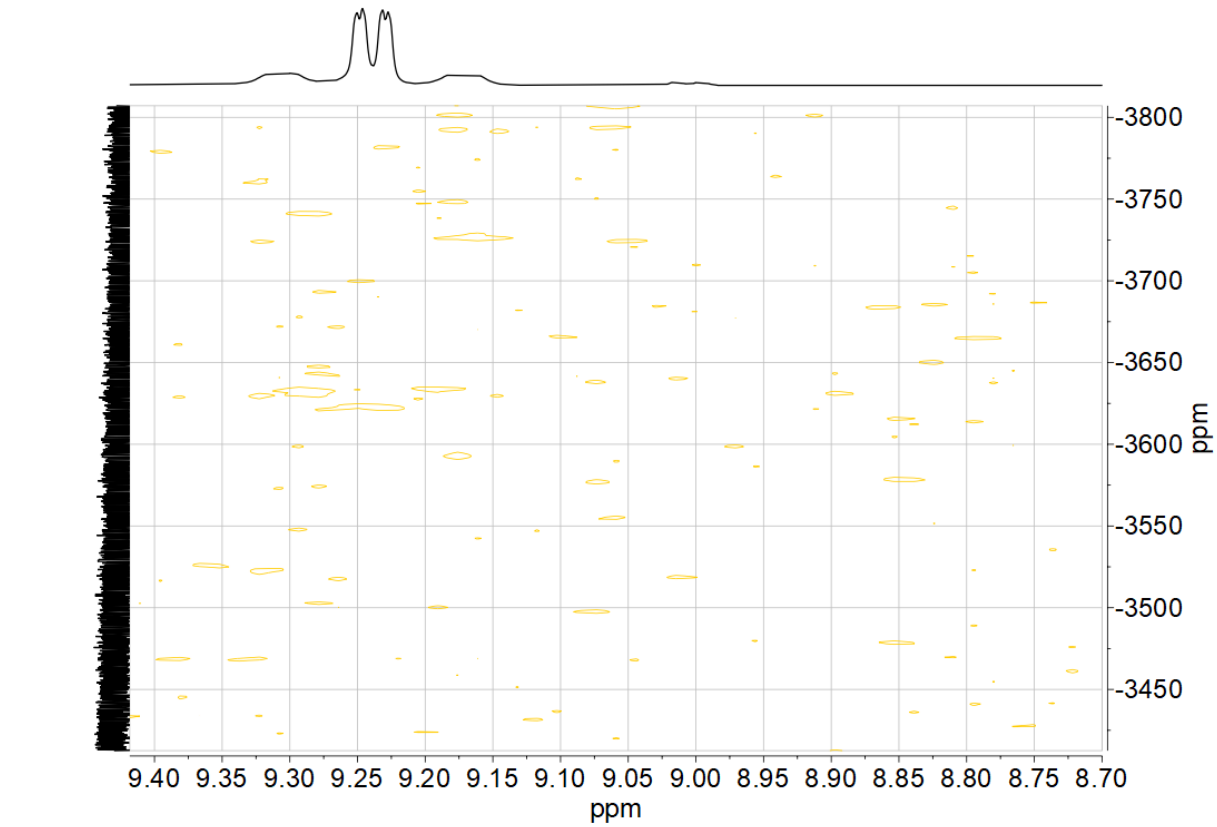

Figure 7-280 $^{1}H,^{195}Pt$ HMBC correlation spectrum of [Pt(Py(4,6MePh)Py)Cl] in CD_2Cl_2.

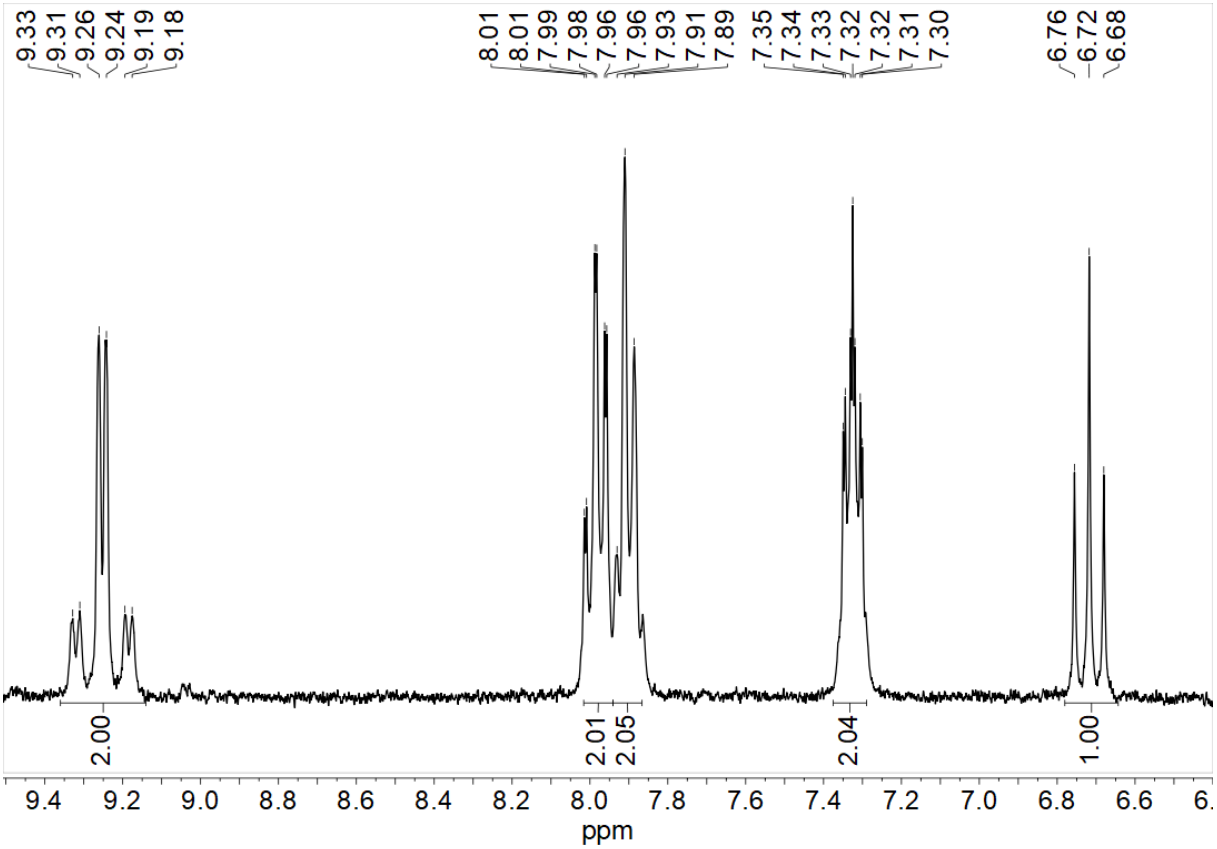

Figure 7-281 300 MHz ^{1}H NMR spectrum of [Pt(Py(4,6FPh)Py)Cl] in CD_2Cl_2.

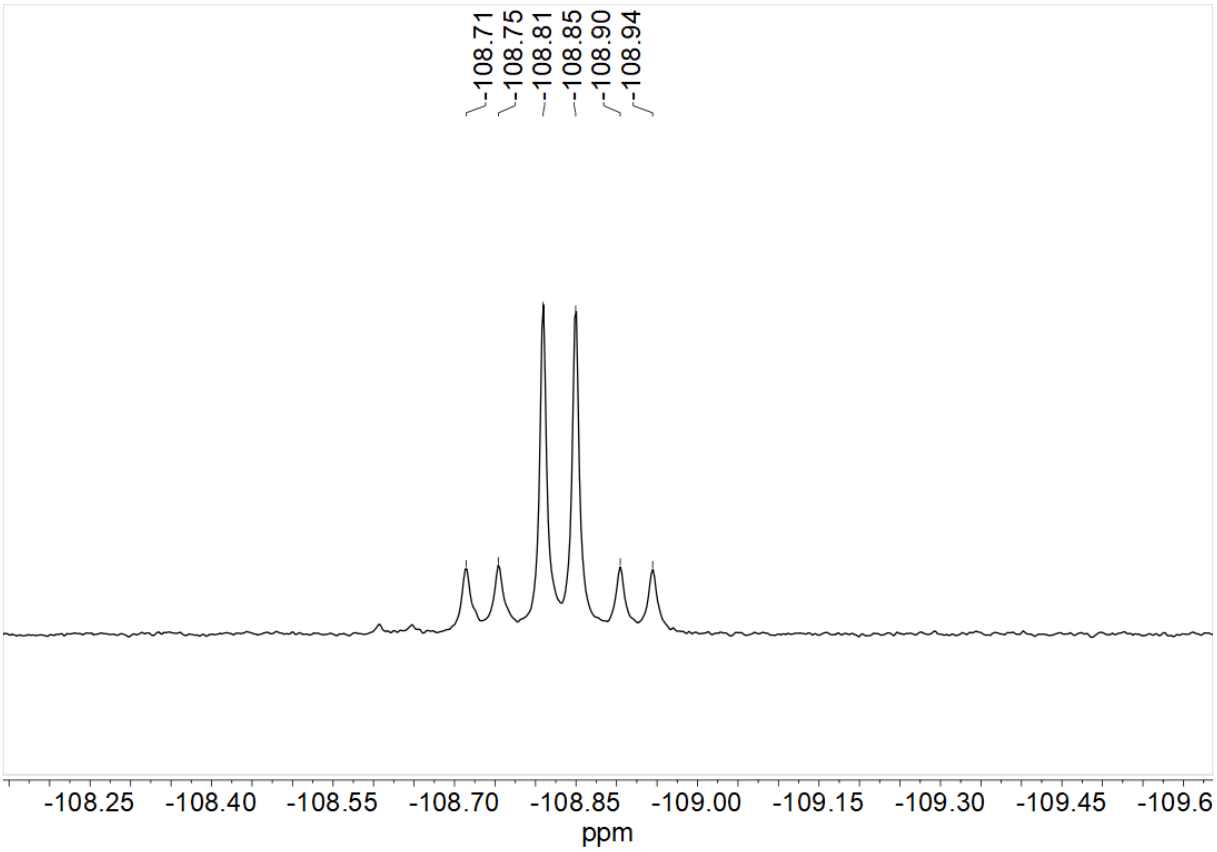

Figure 7-282 282 MHz ^{19}F NMR spectrum of [Pt(Py(4,6FPh)Py)Cl] in CD_2Cl_2.

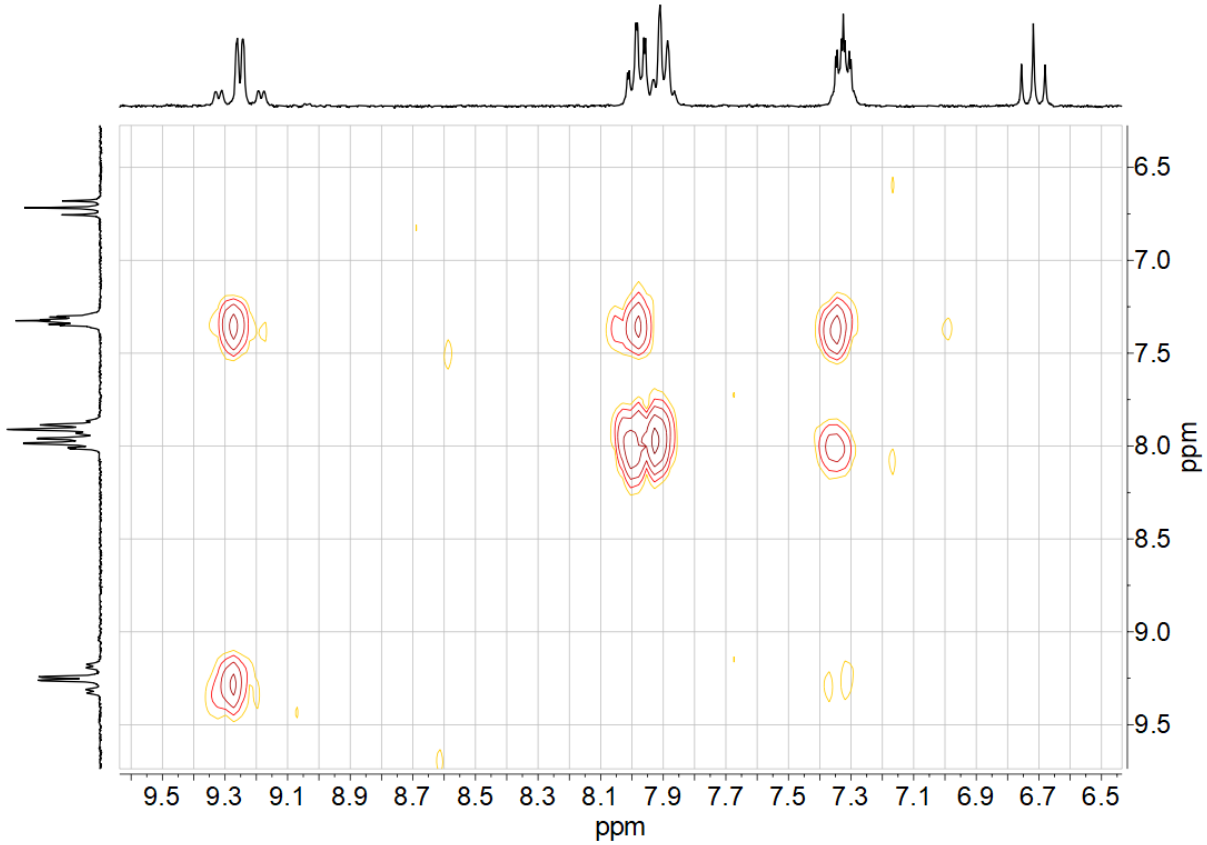

Figure 7-283 $^{1}H,^{1}H$ COSY correlation spectrum of [Pt(Py(4,6FPh)Py)Cl] in CD_2Cl_2.

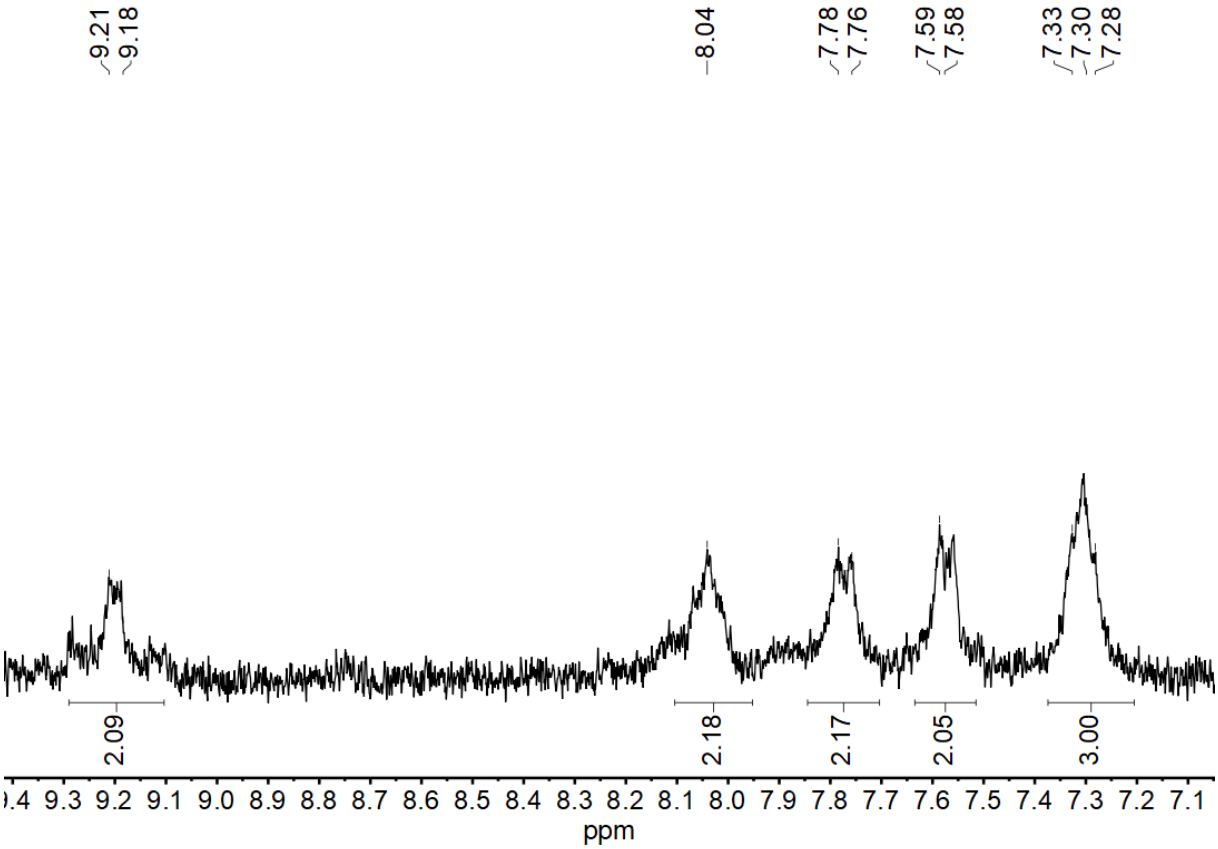

Figure 7-284 300 MHz ^{1}H NMR spectrum of [Pt(Py(Ph)Py)CN] in CD_2Cl_2.

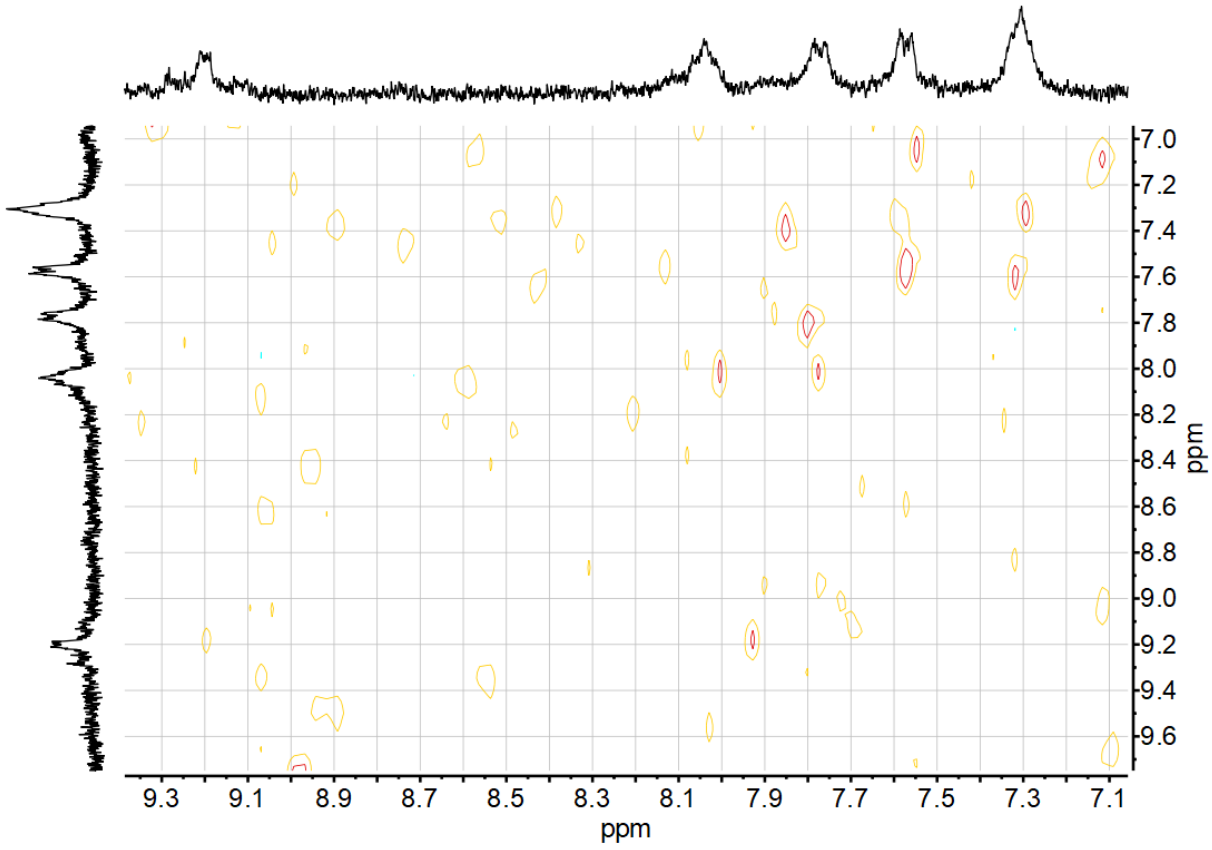

Figure 7-285 $^{1}H,^{1}H$ COSY correlation spectrum of [Pt(Py(Ph)Py)CN] in CD_2Cl_2.

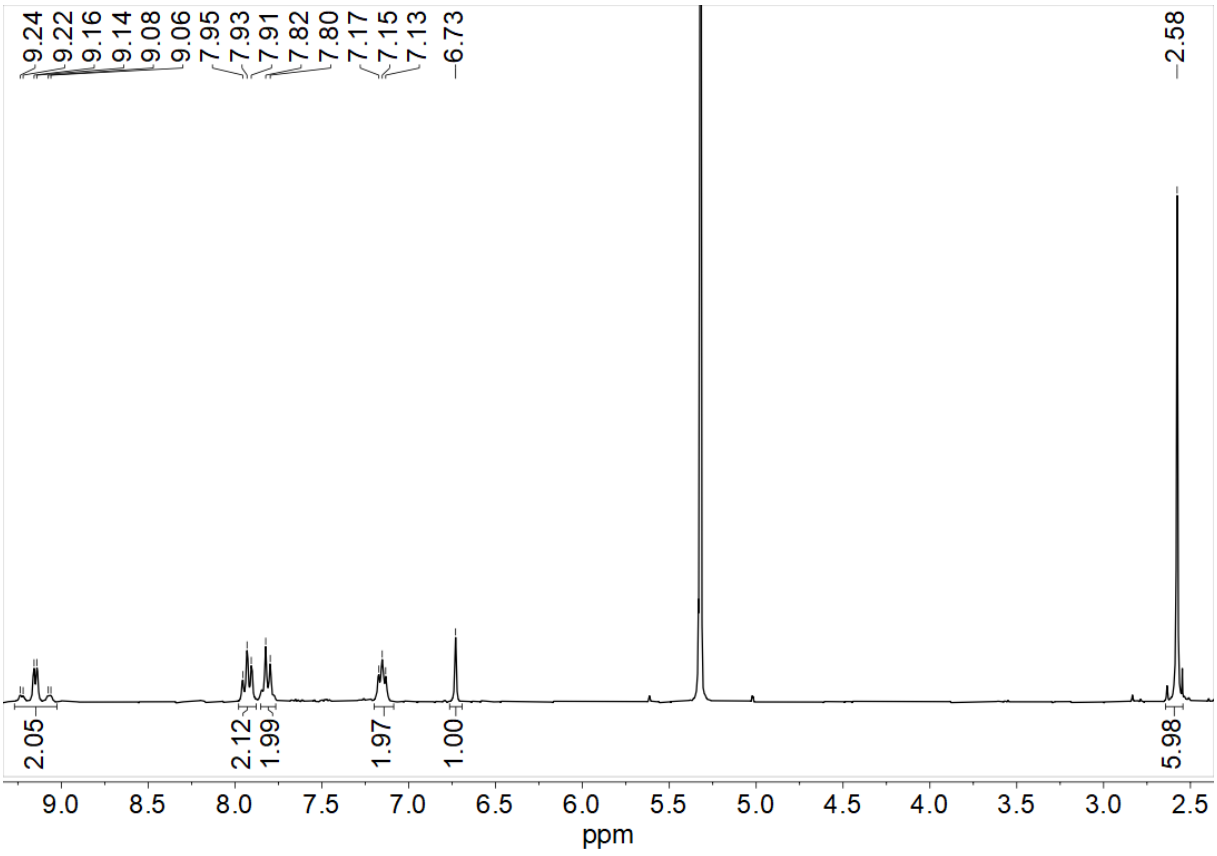

Figure 7-286 300 MHz ^{1}H NMR spectrum of [Pt(Py(4,6MePh)Py)CN] in CD_2Cl_2.

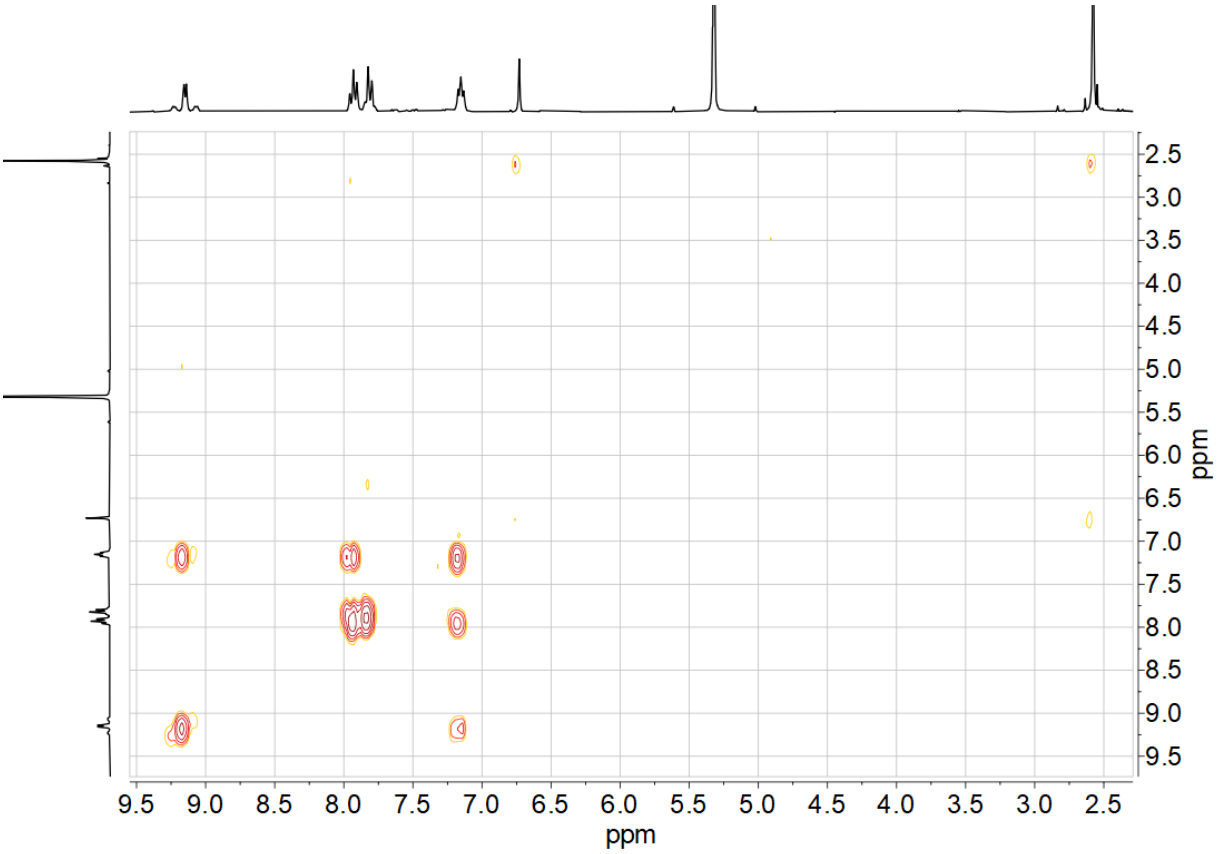

Figure 7-287 $^{1}H,^{1}H$ COSY correlation spectrum of [Pt(Py(4,6MePh)Py)CN] in CD_2Cl_2.

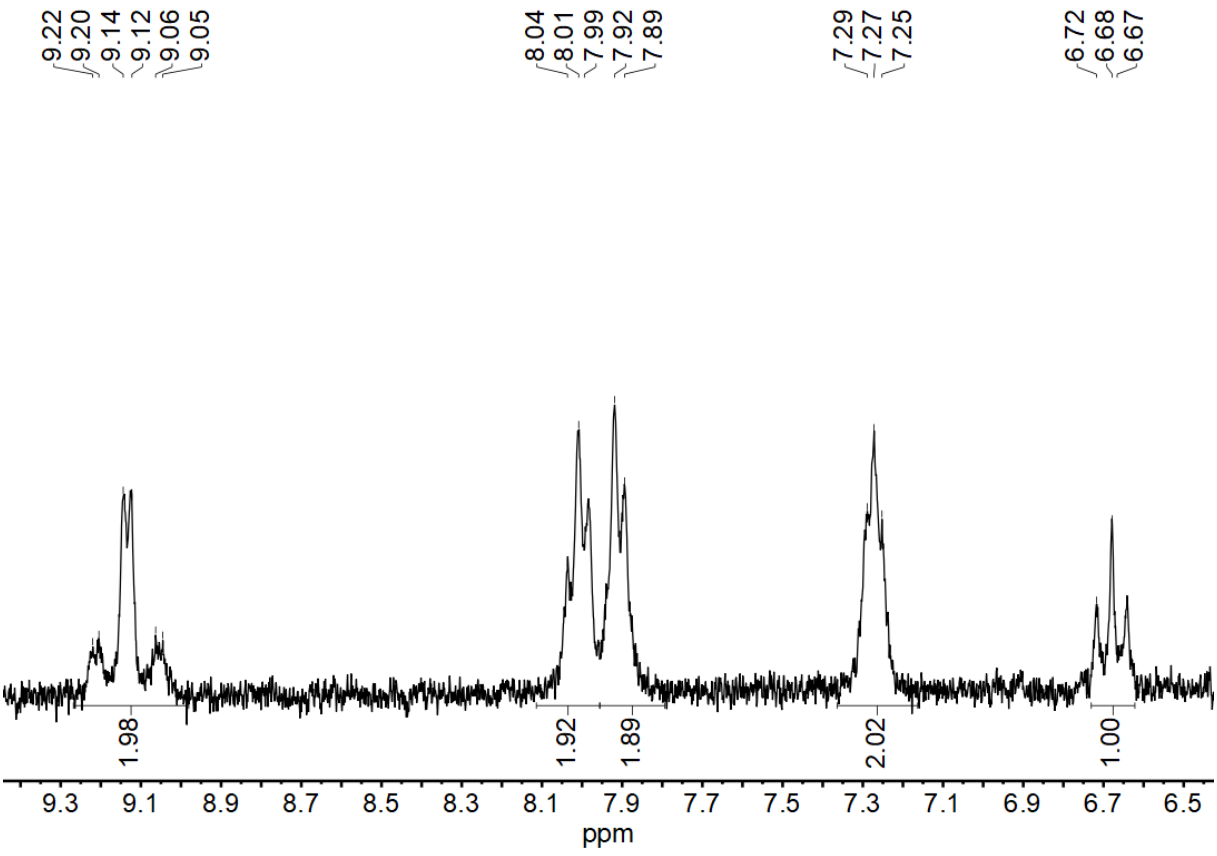

Figure 7-288 300 MHz ^{1}H NMR spectrum of [Pt(Py(4,6FPh)Py)CN] in CD_2Cl_2.

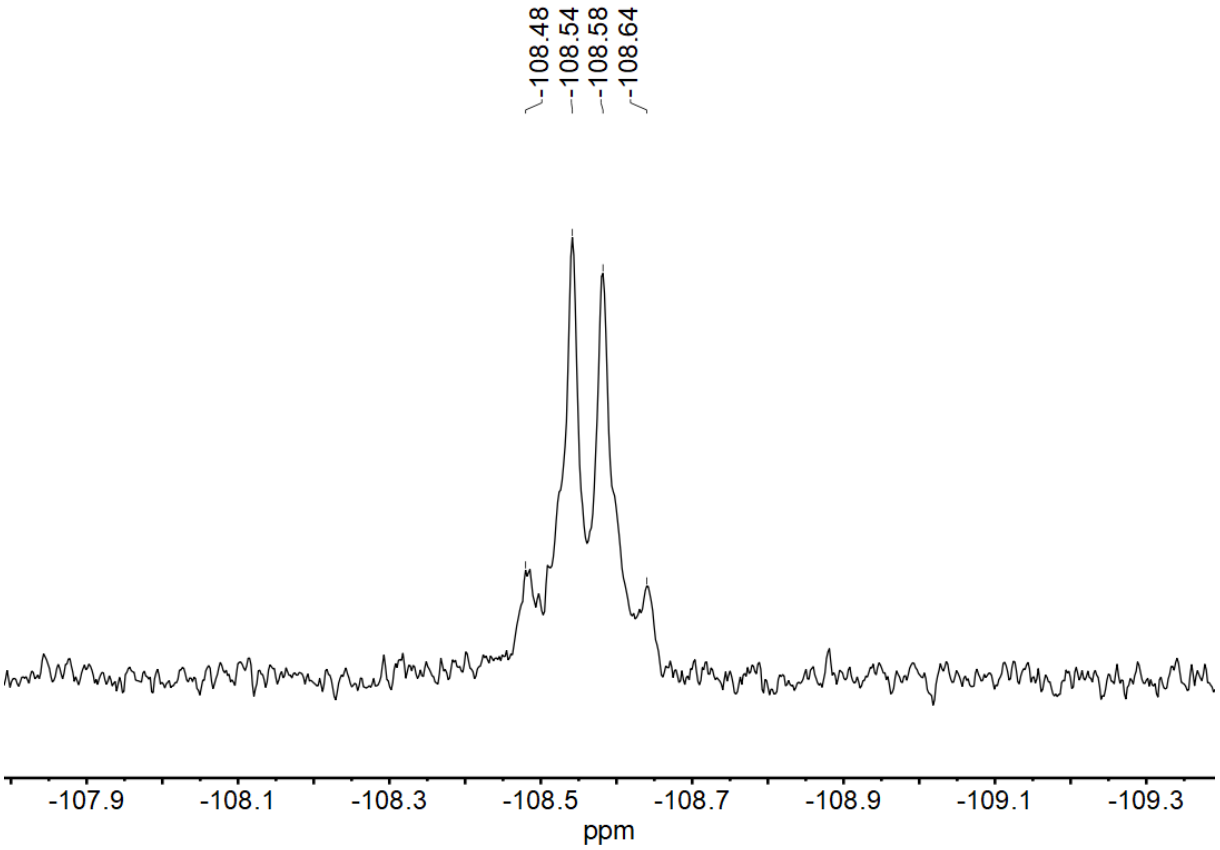

Figure 7-289 282 MHz ^{19}F NMR spectrum of [Pt(Py(4,6FPh)Py)CN] in CD_2Cl_2.

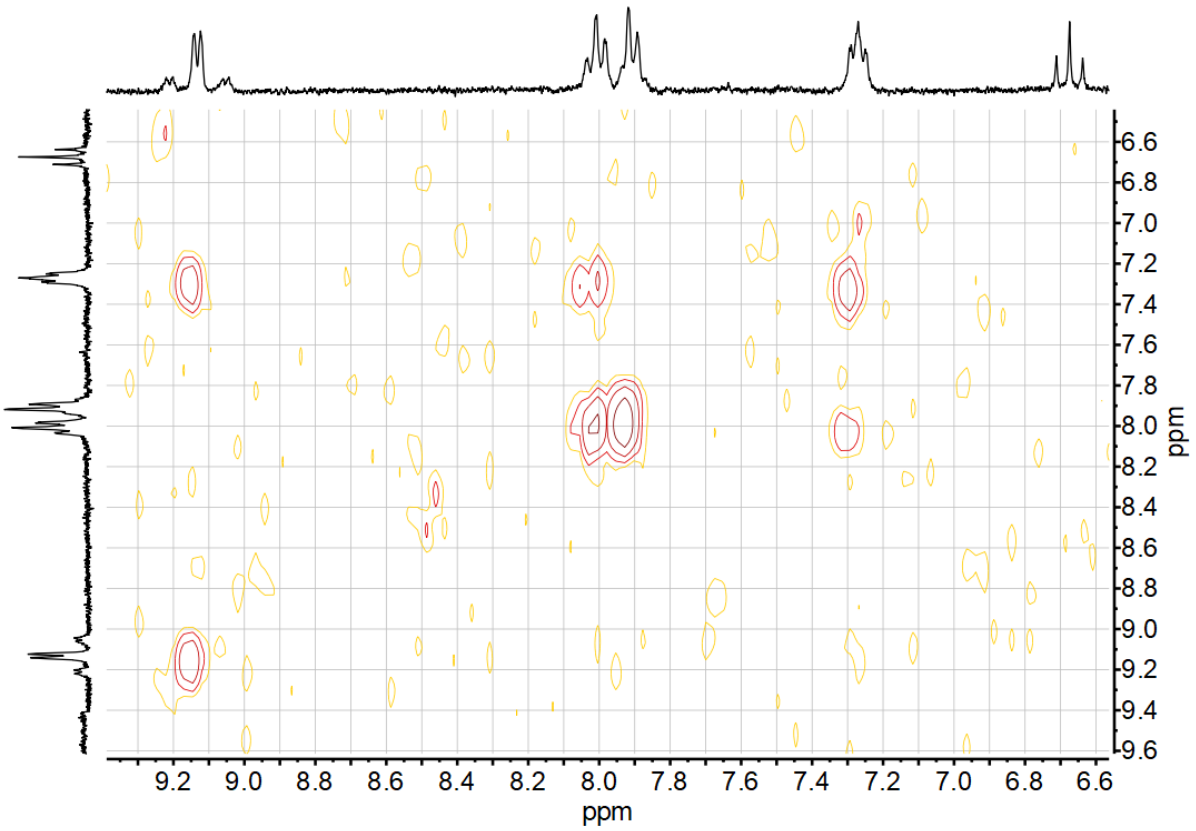

Figure 7-290 $^{1}H,^{1}H$ COSY correlation spectrum of [Pt(Py(4,6FPh)Py)CN] in CD_2Cl_2.

7.2 Mass spectra

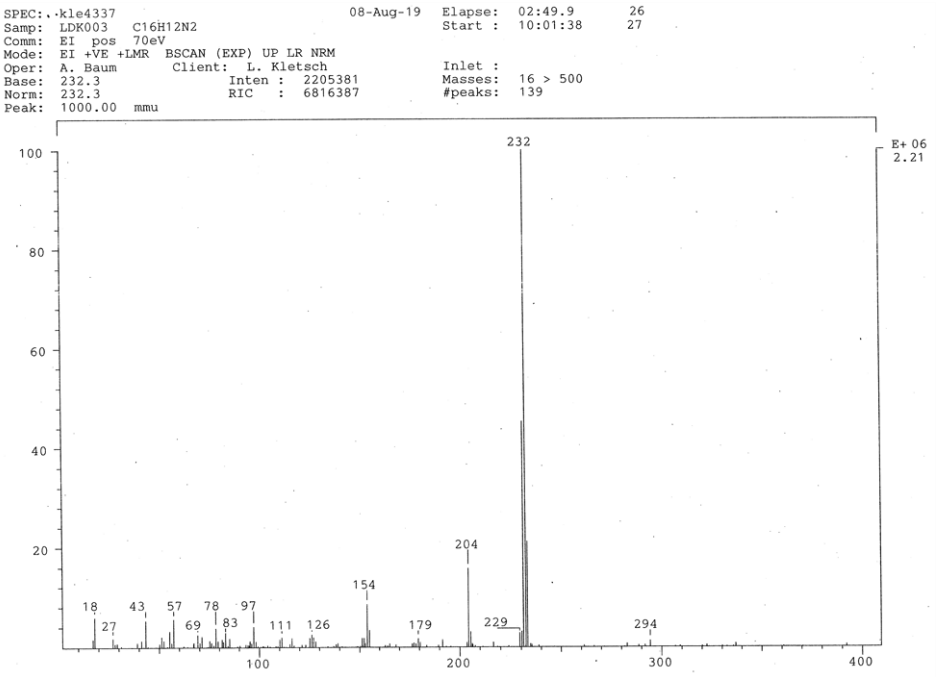

Figure 7-291 EI(+) mass spectrum (70eV) of Py(PhH)Py.

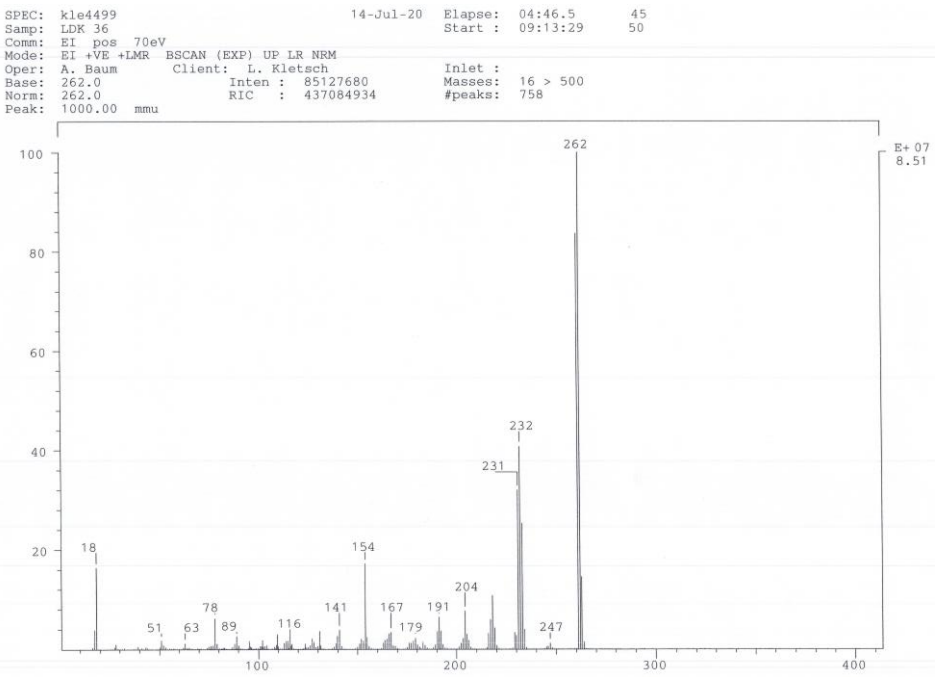

Figure 7-292 EI(+) mass spectrum (70eV) of Py(5MeOPhH)Py.

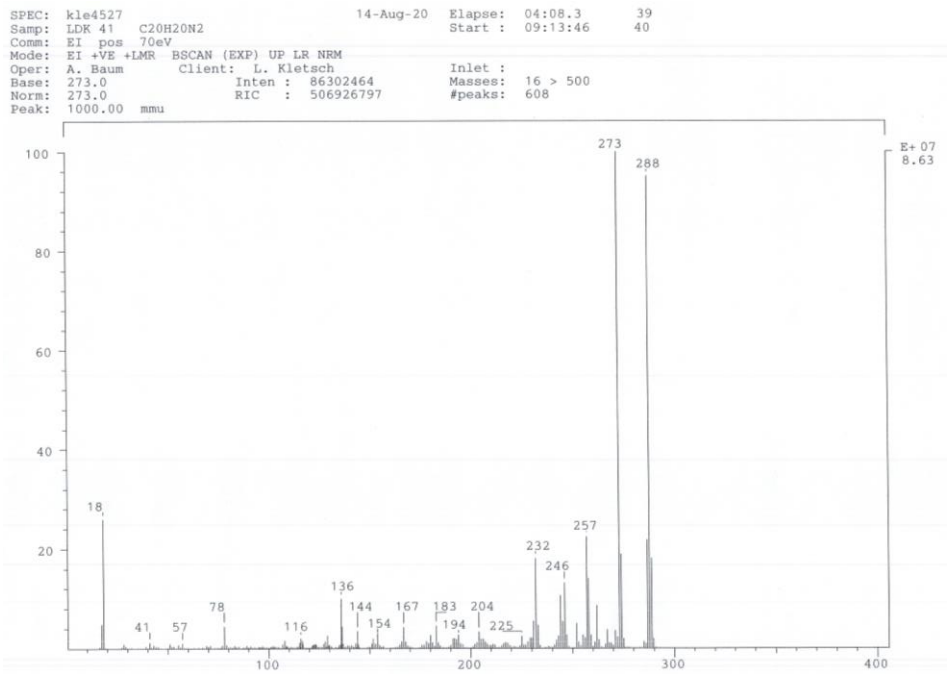

Figure 7-293 EI(+) mass spectrum (70eV) of Py(5BuPhH)Py.

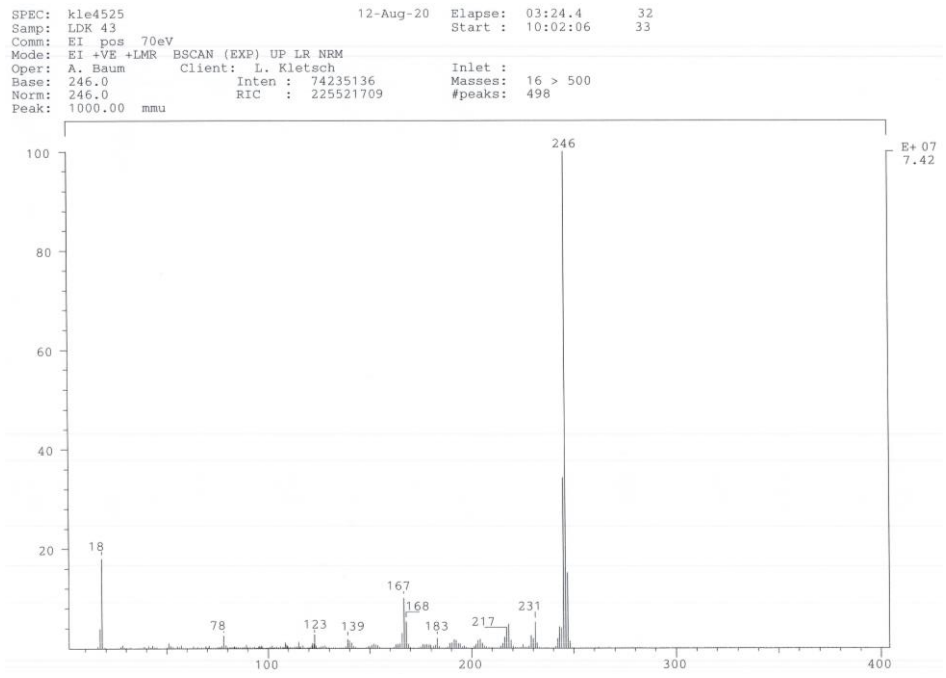

Figure 7-294 EI(+) mass spectrum (70eV) of Py(5MePhH)Py.

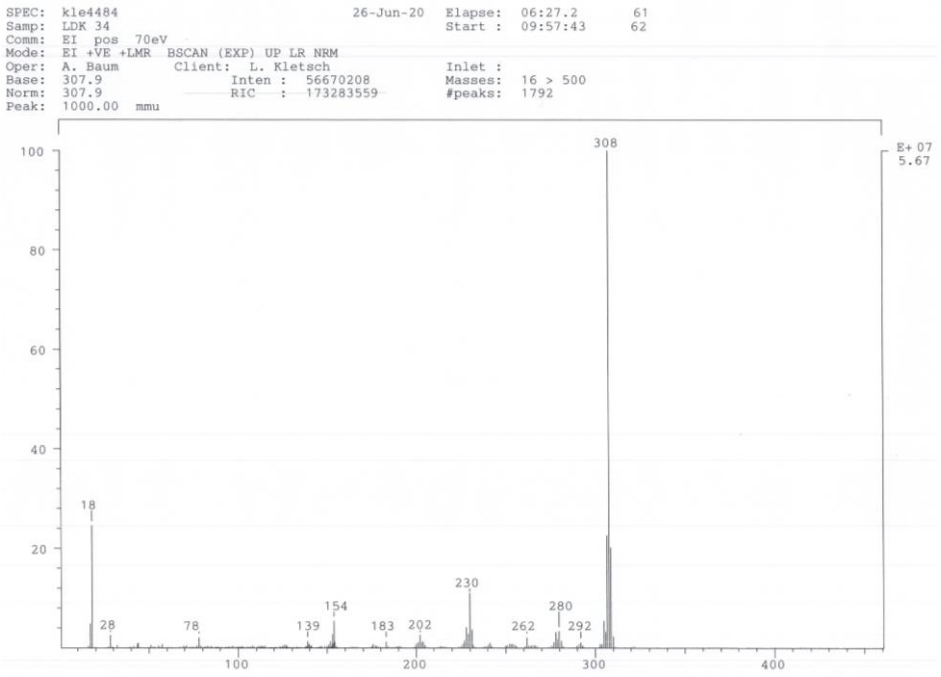

Figure 7-295 EI(+) mass spectrum (70eV) of Py(5PhPhH)Py.

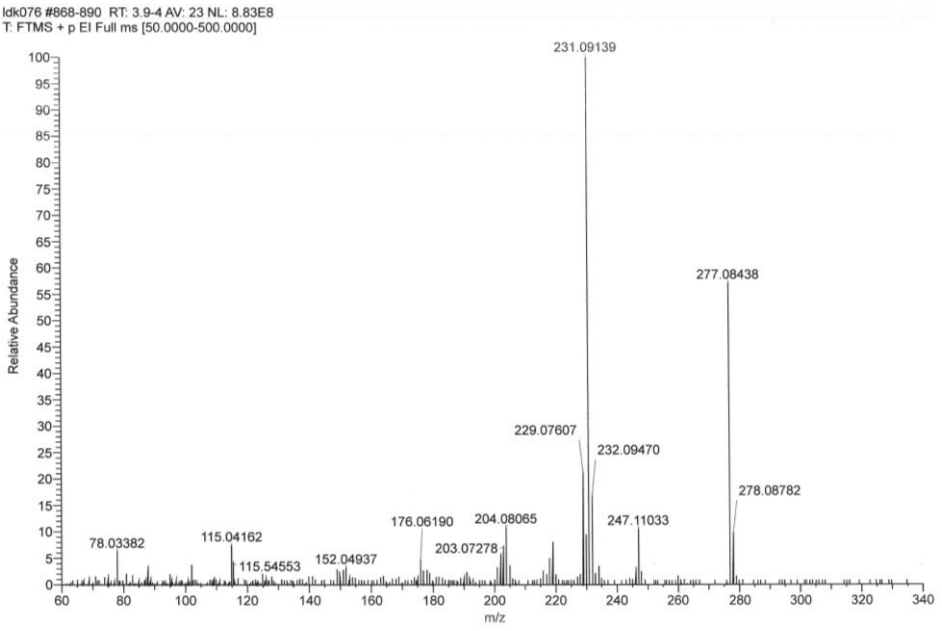

Figure 7-296 EI(+) mass spectrum (70eV) of Py(5NO_2PhH)Py.

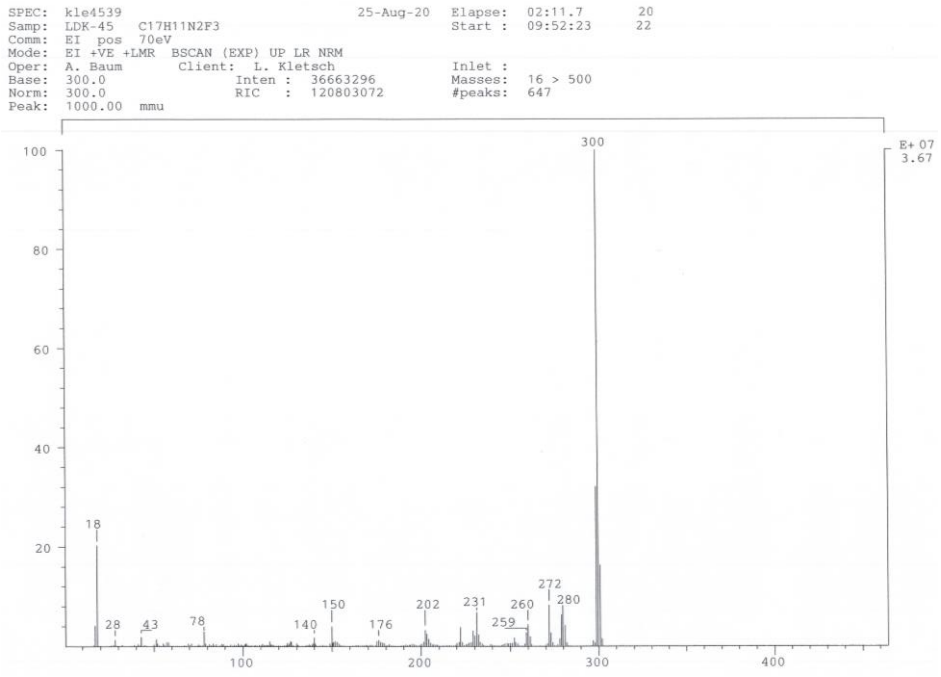

Figure 7-297 EI(+) mass spectrum (70eV) of Py(5CF_3PhH)Py.

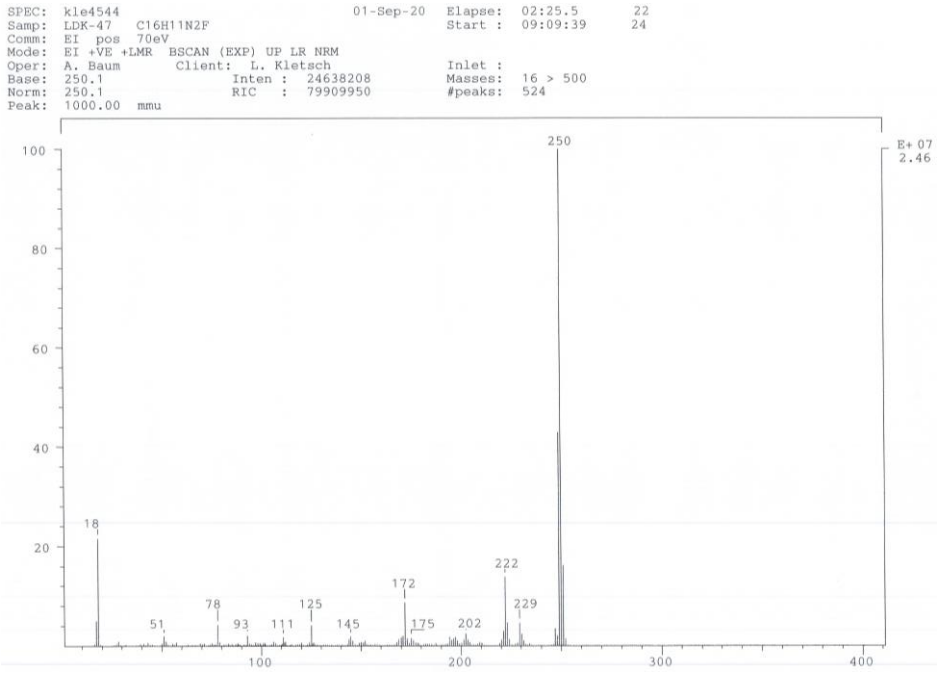

Figure 7-298 EI(+) mass spectrum (70eV) of Py(5FPhH)Py.

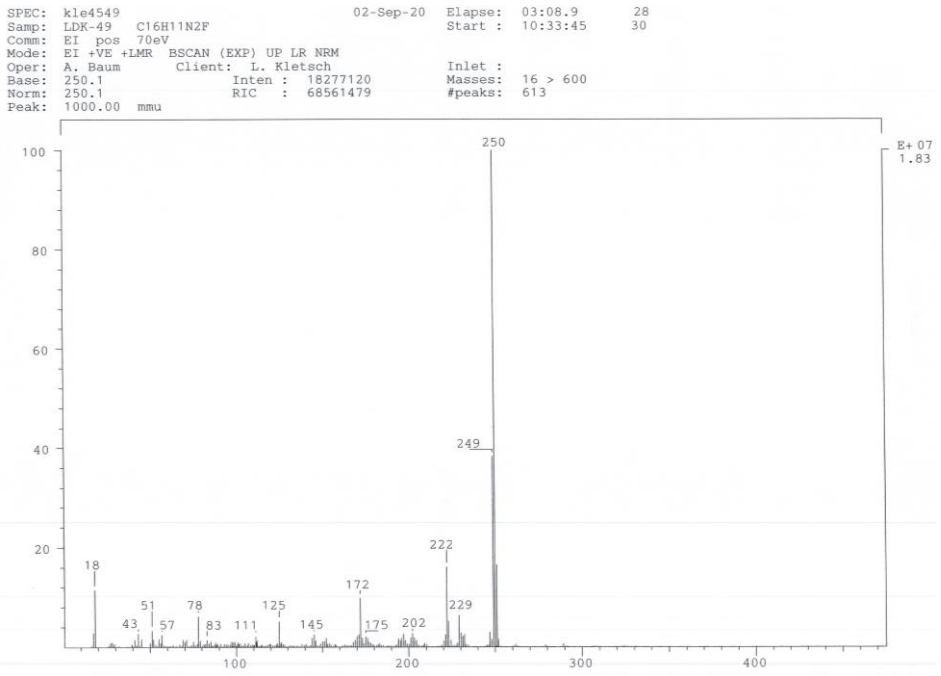

Figure 7-299 EI(+) mass spectrum (70eV) of Py(4FPhH)Py.

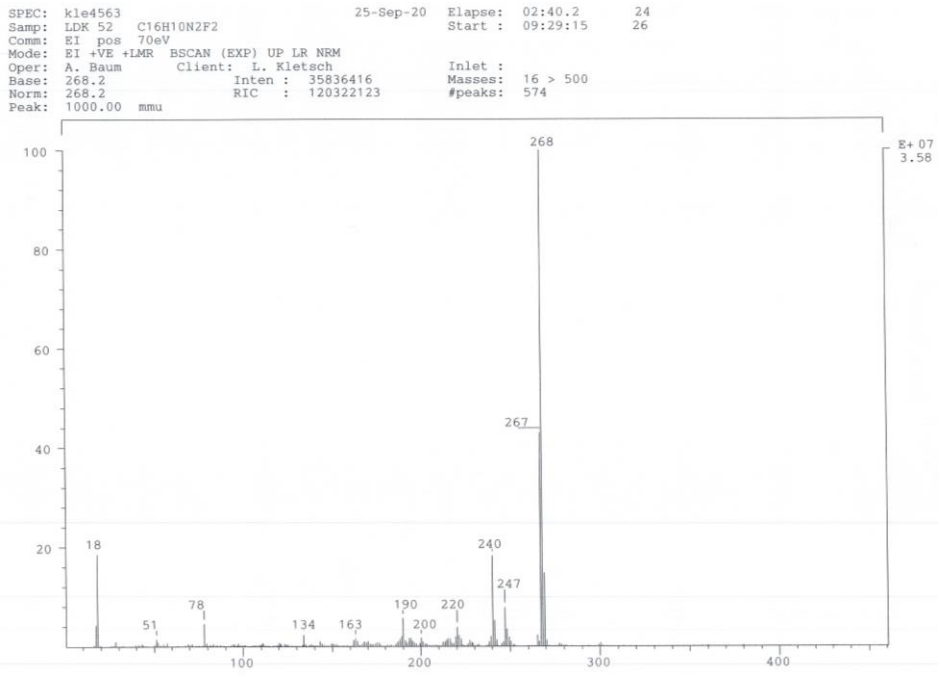

Figure 7-300 EI(+) mass spectrum (70eV) of Py(4,6FPhH)Py.

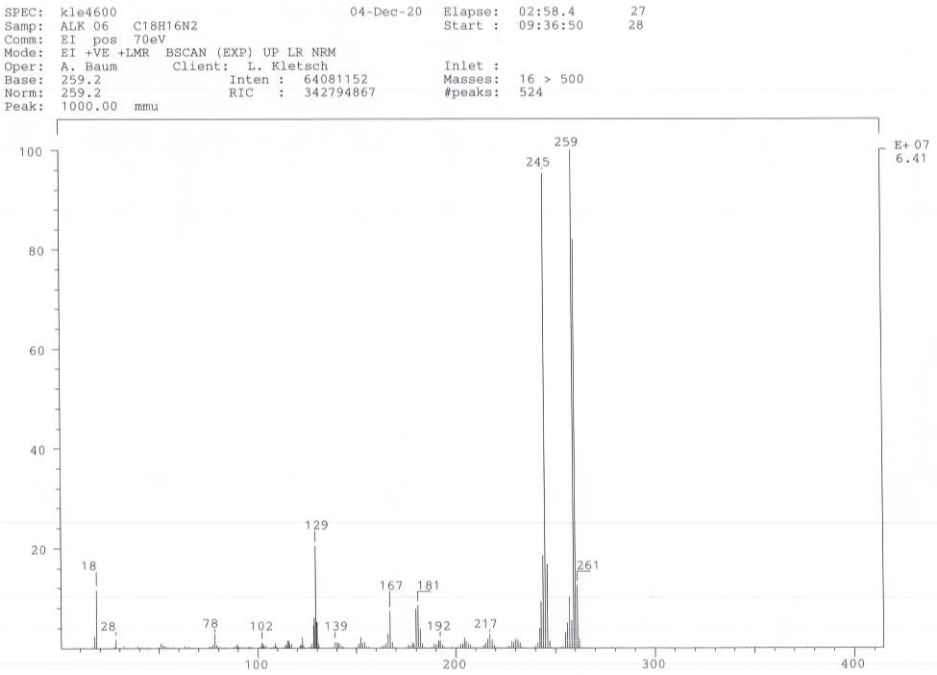

Figure 7-301 EI(+) mass spectrum (70eV) of Py(4,6MePhH)Py.

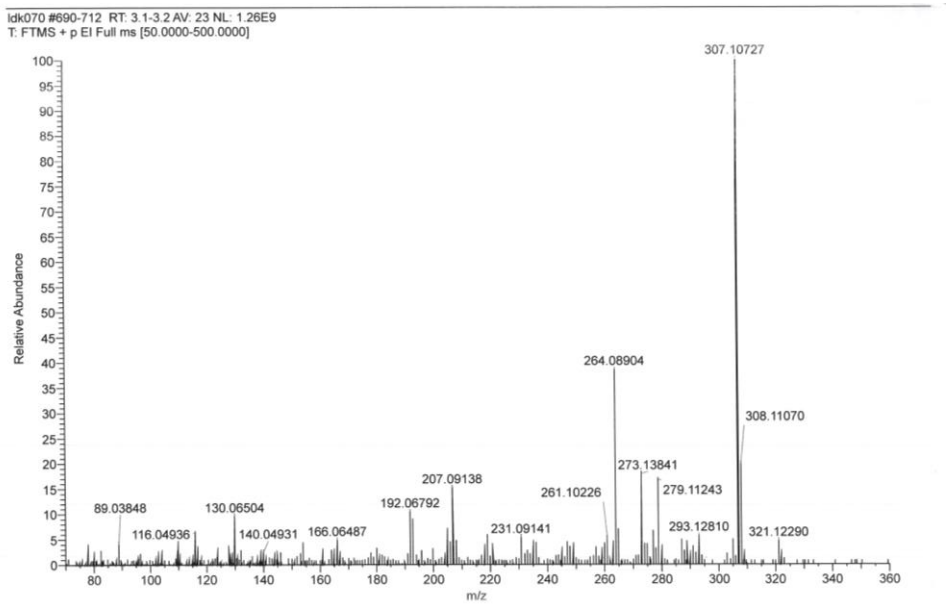

Figure 7-302 EI(+) mass spectrum (70eV) of Py(4,5,6MeOPhH)Py.

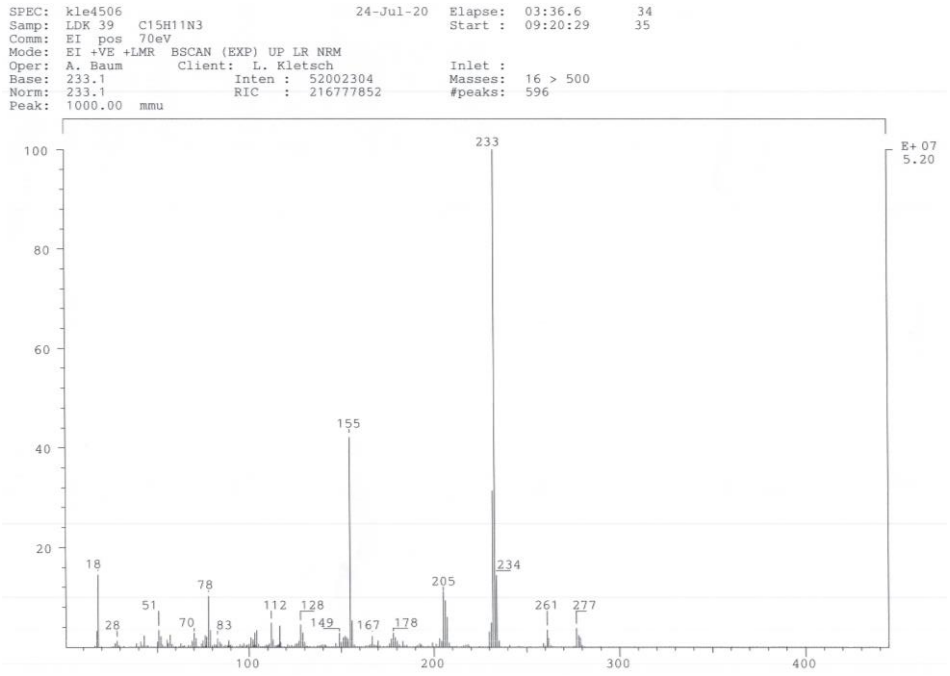

Figure 7-303 EI(+) mass spectrum (70eV) of Py(PyH)Py.

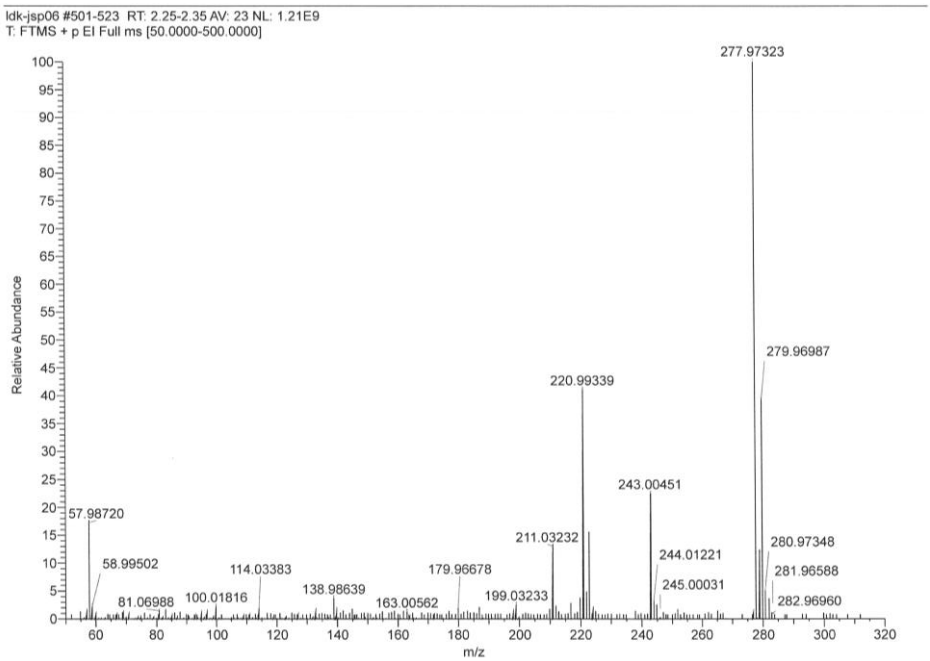

Figure 7-304 EI(+) mass spectrum (70eV) of 2Tz(PhCl)2Tz.

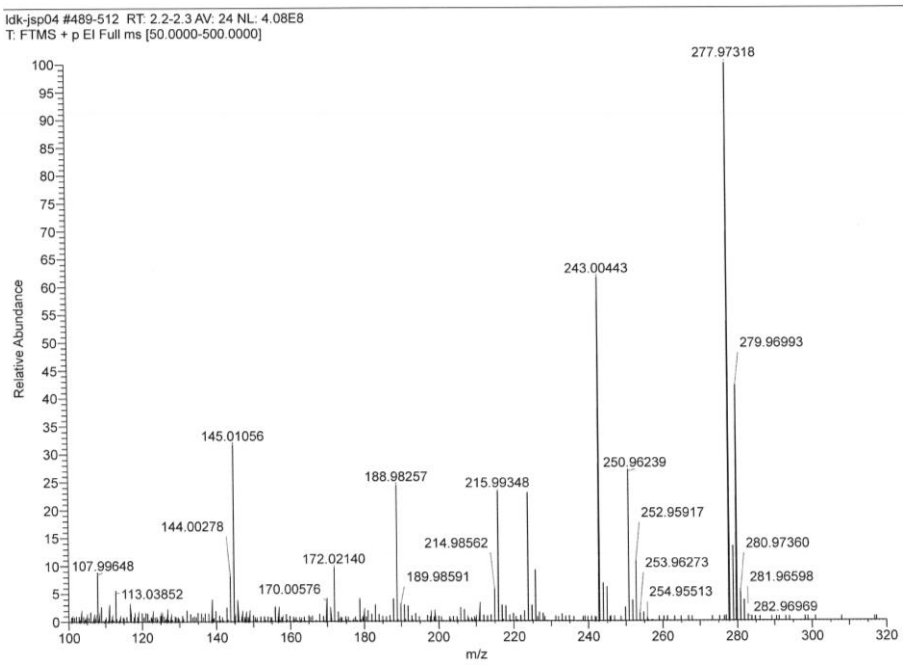

Figure 7-305 EI(+) mass spectrum (70eV) of 4Tz(PhCl)4Tz.

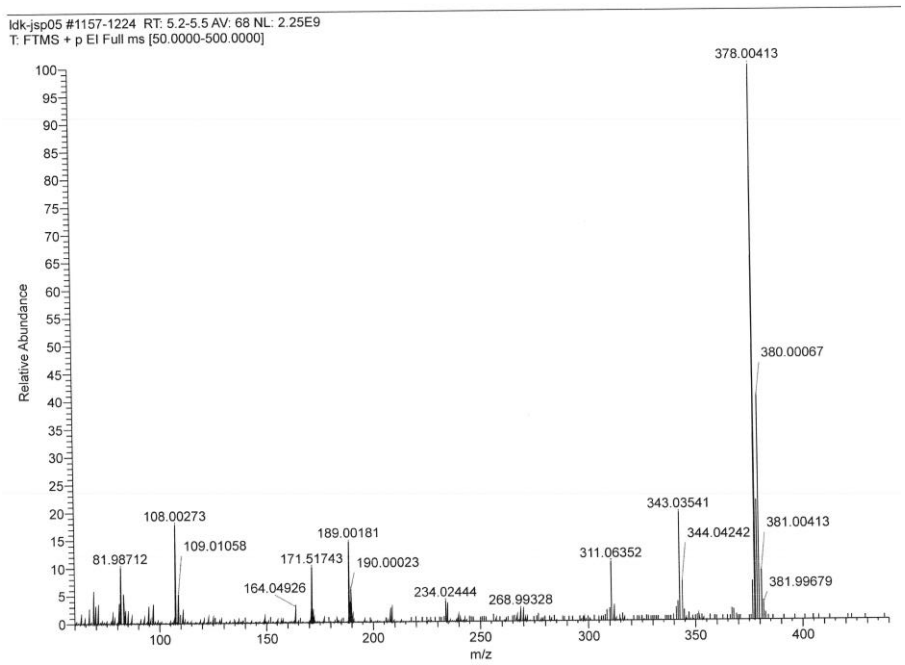

Figure 7-306 EI(+) mass spectrum (70eV) of 2Btz(PhCl)2Btz.

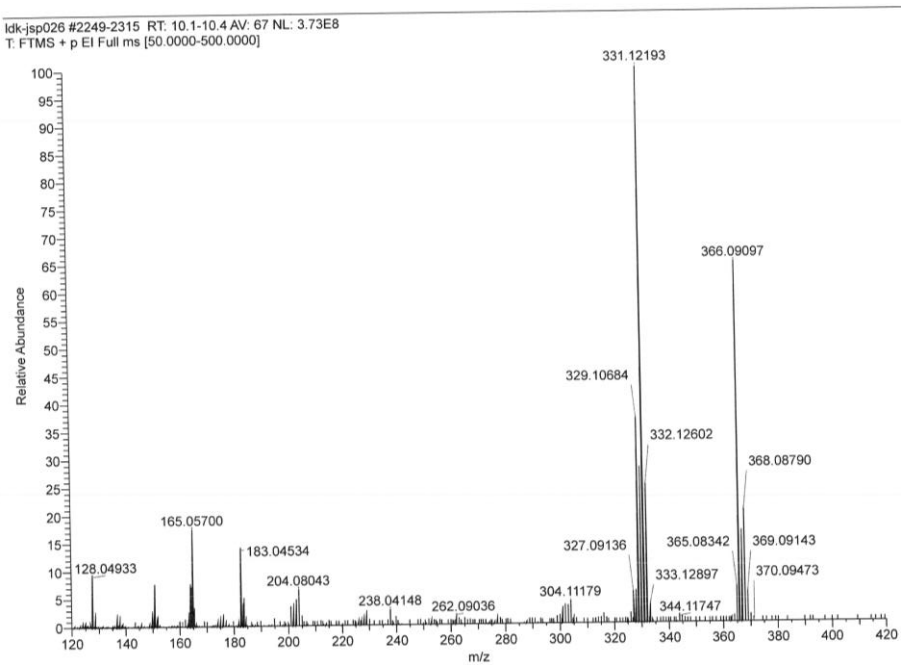

Figure 7-307 EI(+) mass spectrum (70eV) of 2Qu(PhCl)2Qu.

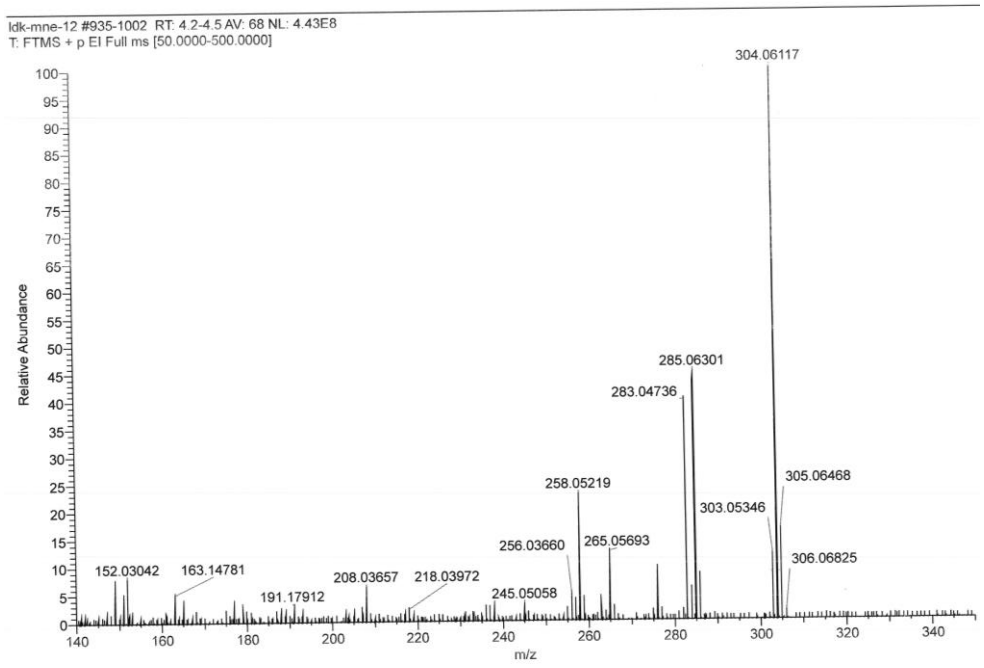

Figure 7-308 EI(+) mass spectrum (70eV) of 3FPy(4,6FPhH)3FPy.

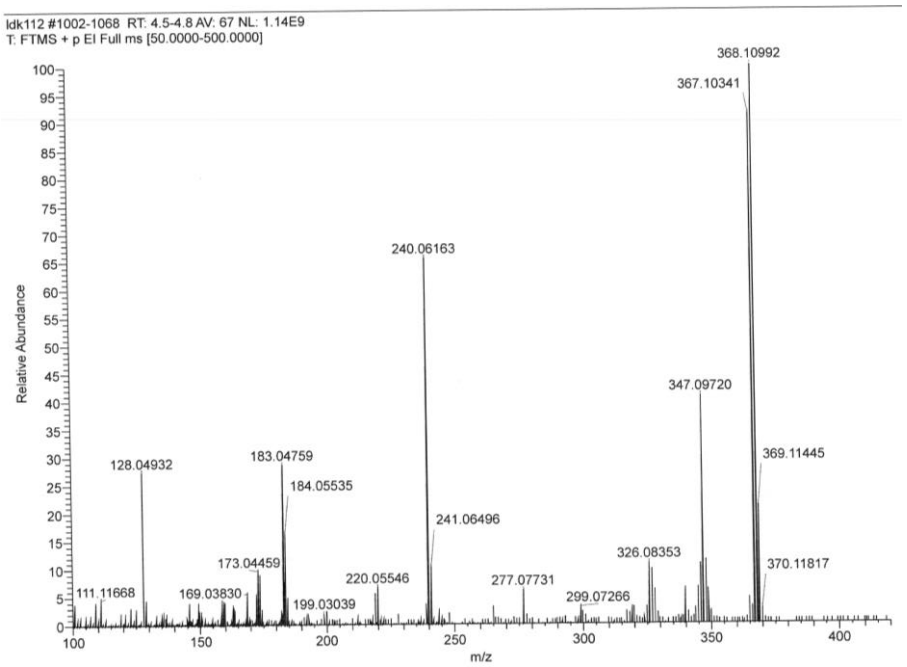

Figure 7-309 EI(+) mass spectrum (70eV) of 2*i*Qu(4,6FPhH)2*i*Qu.

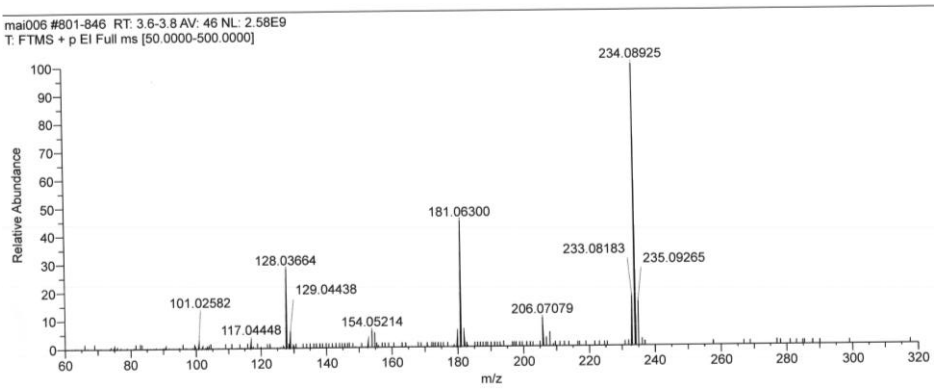

Figure 7-310 EI(+) mass spectrum (70eV) of Pym(PhH)Pym.

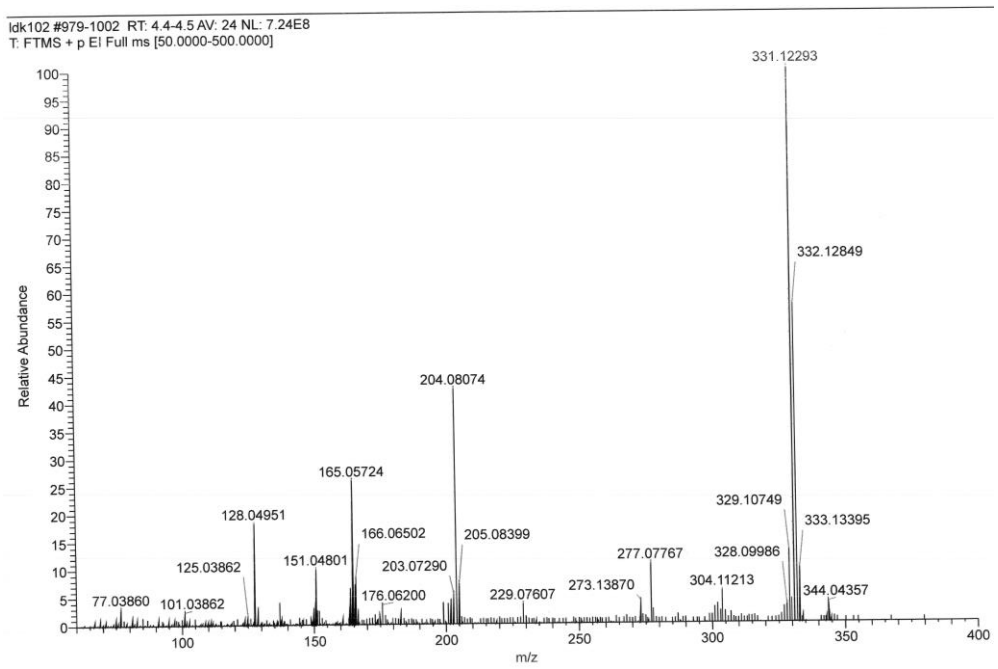

Figure 7-311 EI(+) mass spectrum (70eV) of 2*i*Qu(PhH)2*i*Qu.

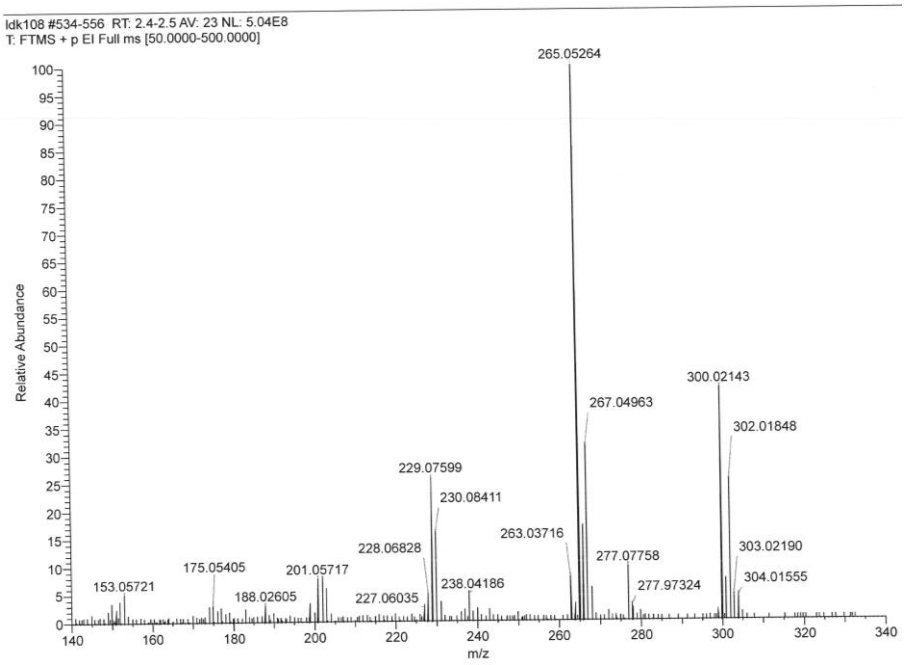

Figure 7-312 EI(+) mass spectrum (70eV) of 3ClPy(PhH)3ClPy.

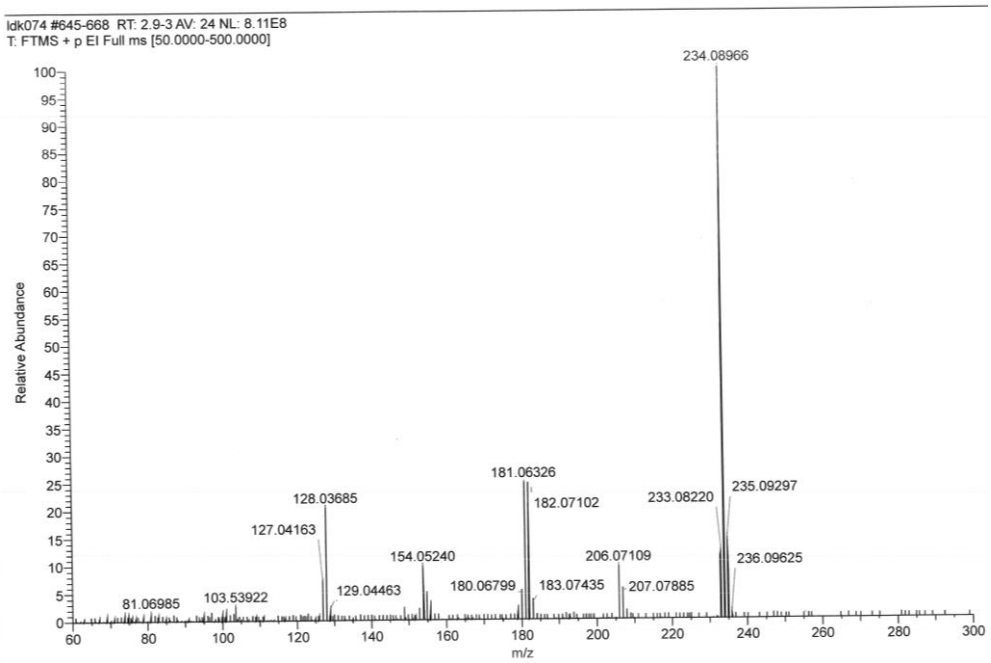

Figure 7-313 EI(+) mass spectrum (70eV) of Pz(PhH)Pz.

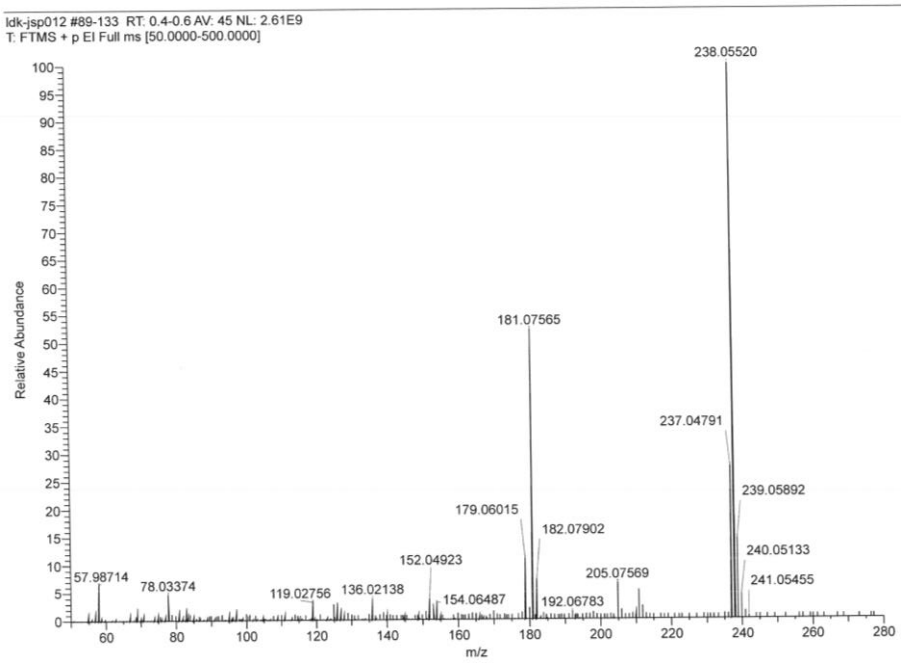

Figure 7-314 EI(+) mass spectrum (70eV) of 2Tz(PhH)Py.

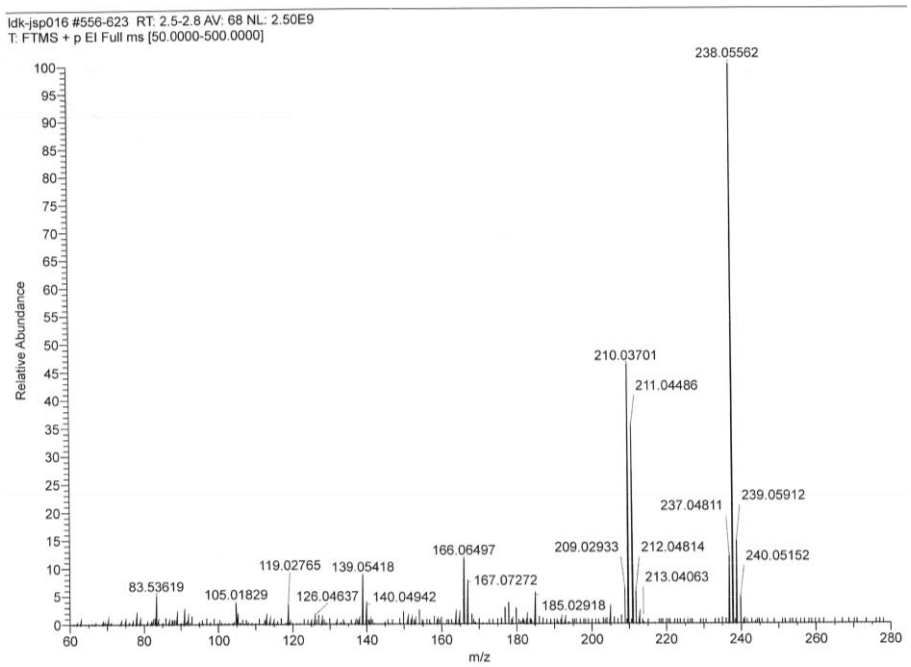

Figure 7-315 EI(+) mass spectrum (70eV) of 4Tz(PhH)Py.

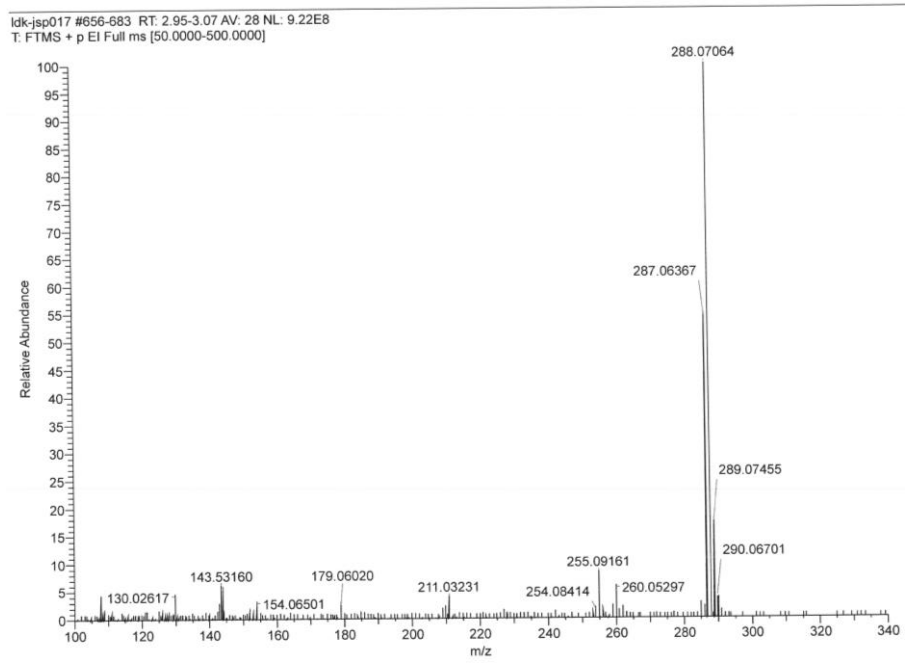

Figure 7-316 EI(+) mass spectrum (70eV) of 2Btz(PhH)Py.

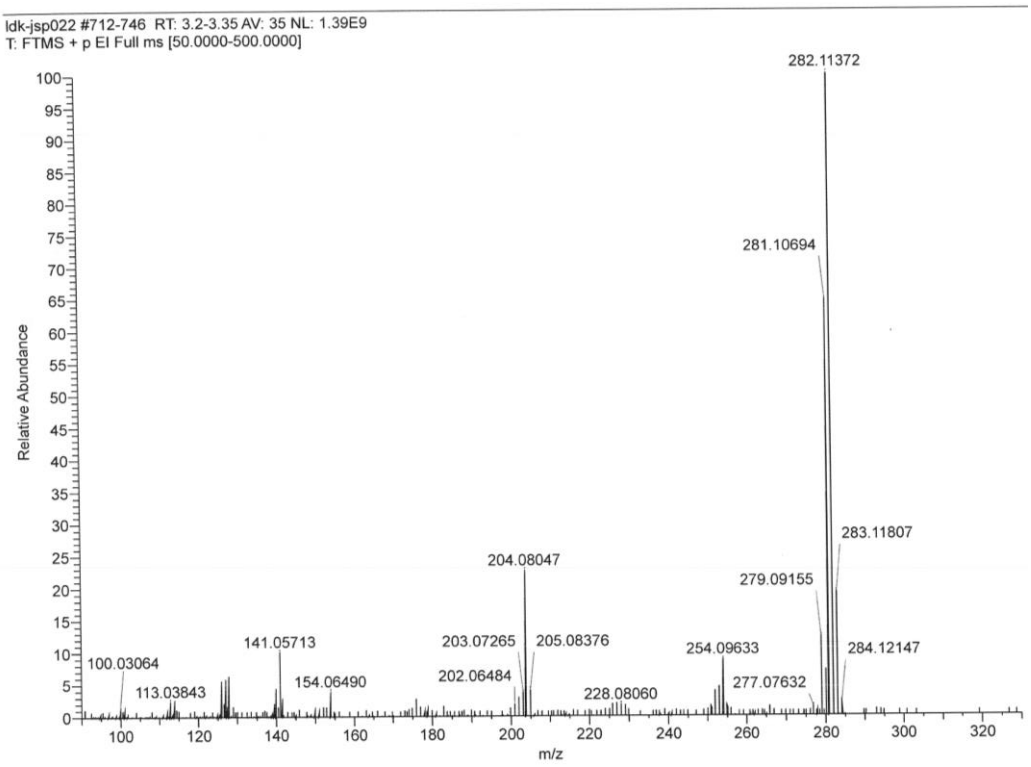

Figure 7-317 EI(+) mass spectrum (70eV) of 2Qu(PhH)Py.

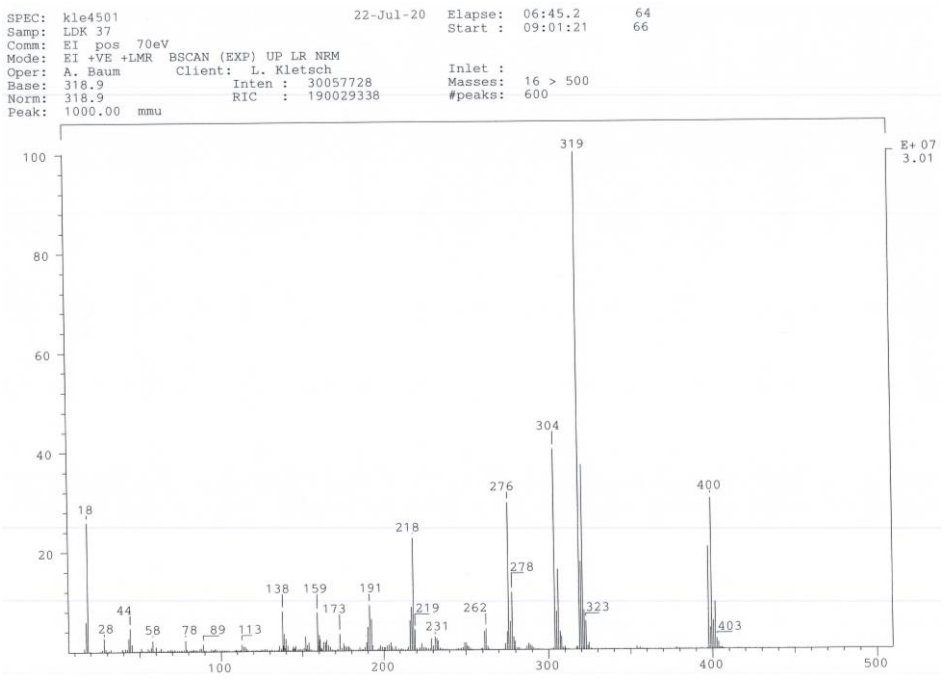

Figure 7-318 EI(+) mass spectrum (70eV) of [Ni(Py(5MeOPh)Py)Br].

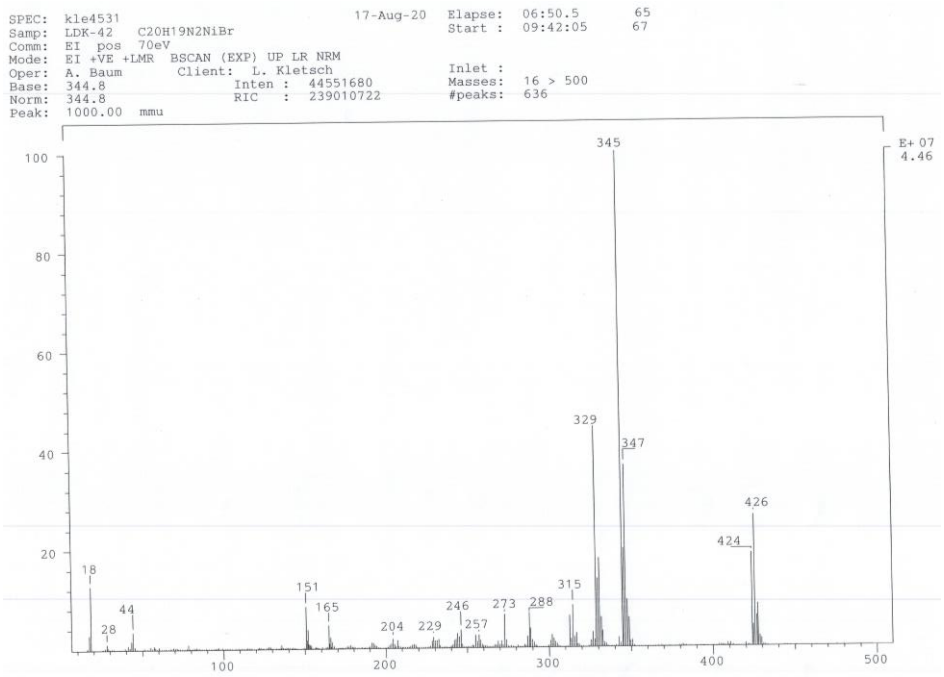

Figure 7-319 EI(+) mass spectrum (70eV) of [Ni(Py(5BuPh)Py)Br].

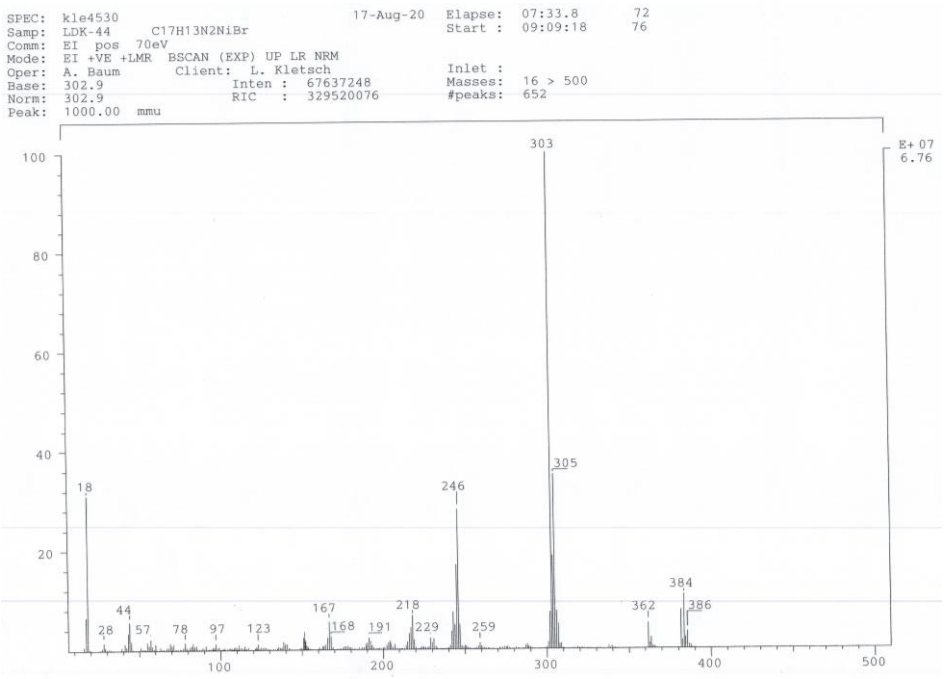

Figure 7-320 EI(+) mass spectrum (70eV) of [Ni(Py(5MePh)Py)Br].

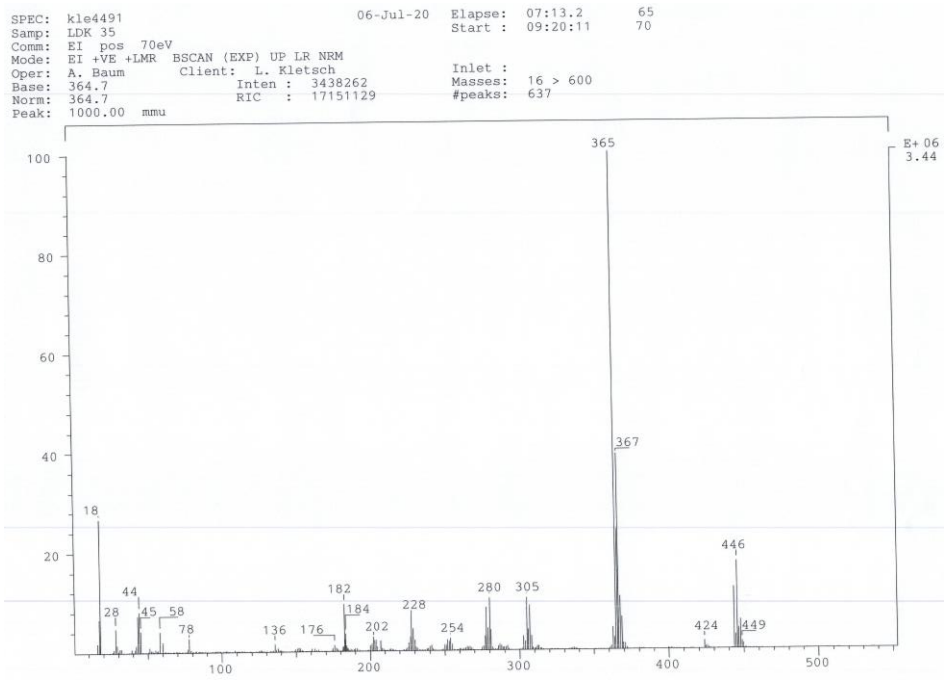

Figure 7-321 EI(+) mass spectrum (70eV) of [Ni(Py(5PhPh)Py)Br].

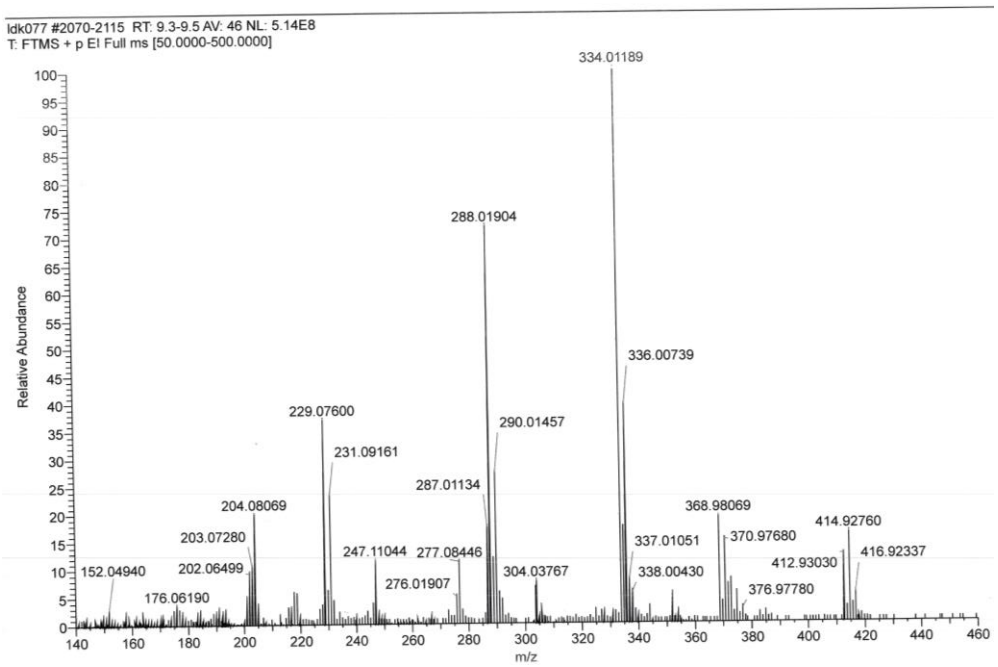

Figure 7-322 EI(+) mass spectrum (70eV) of [Ni(Py(5NO_2Ph)Py)Br].

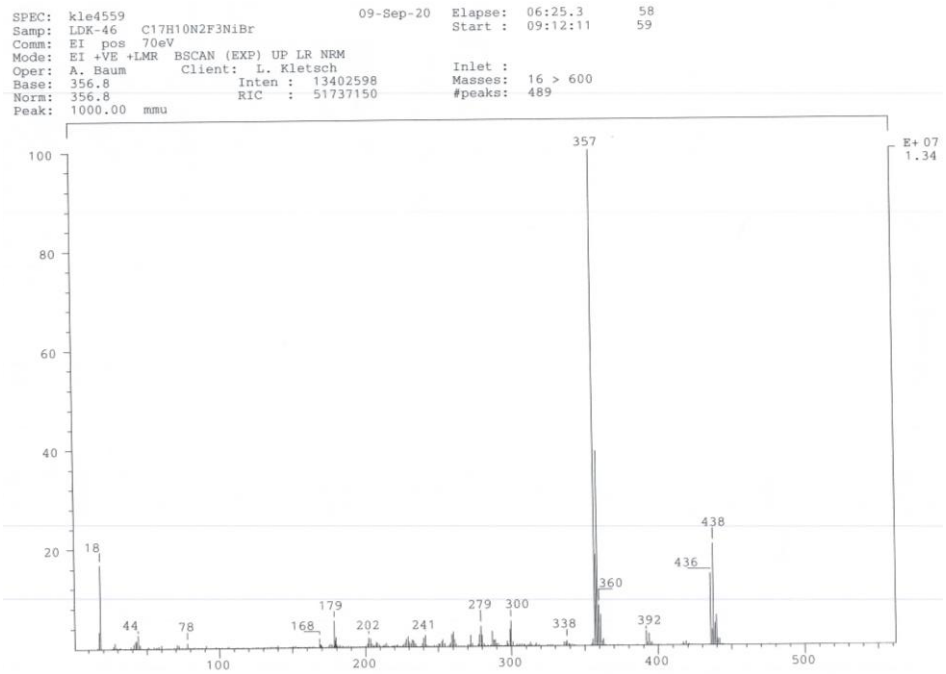

Figure 7-323 EI(+) mass spectrum (70eV) of [Ni(Py(5CF$_3$Ph)Py)Br].

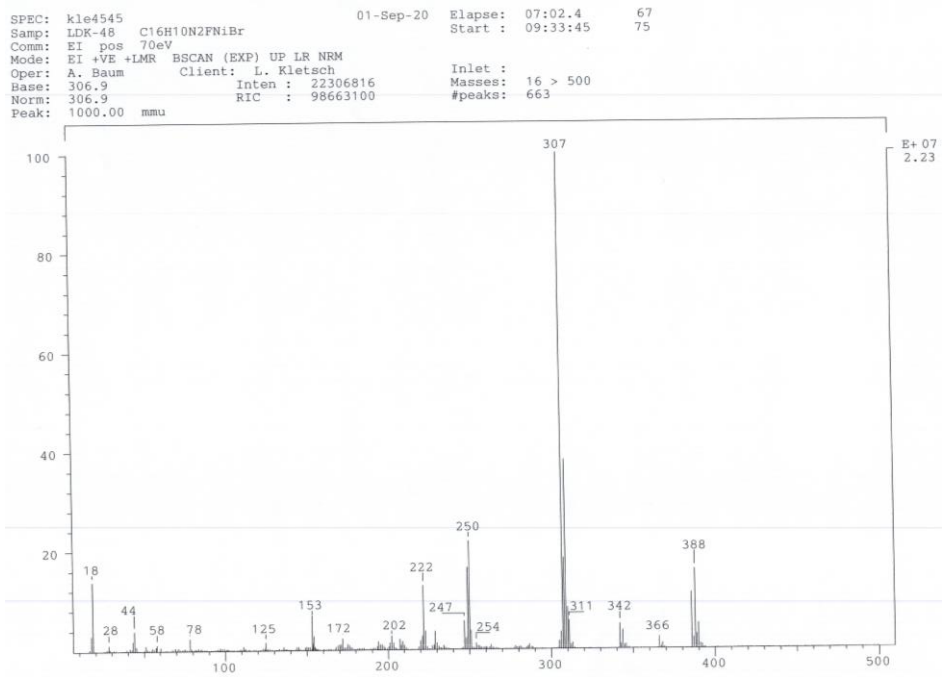

Figure 7-324 EI(+) mass spectrum (70eV) of [Ni(Py(5FPh)Py)Br].

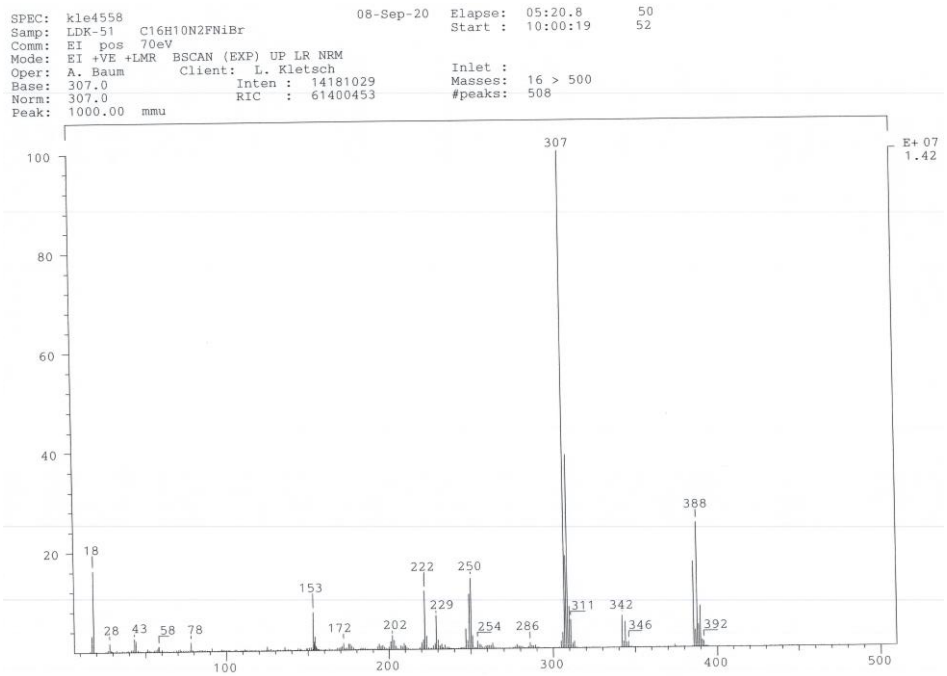

Figure 7-325 EI(+) mass spectrum (70eV) of [Ni(Py(4FPh)Py)Br].

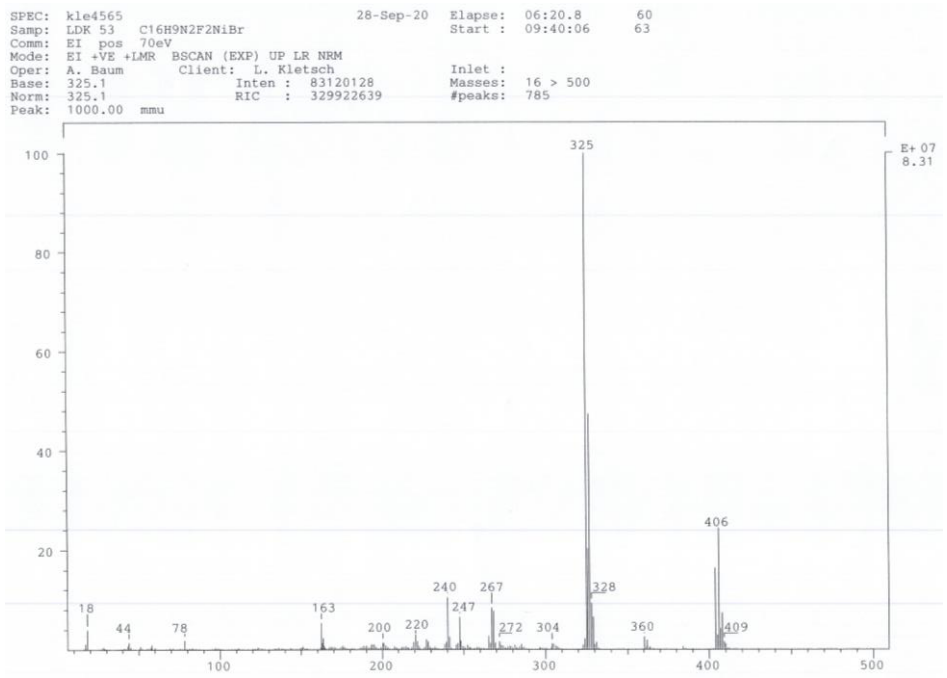

Figure 7-326 EI(+) mass spectrum (70eV) of [Ni(Py(4,6FPh)Py)Br].

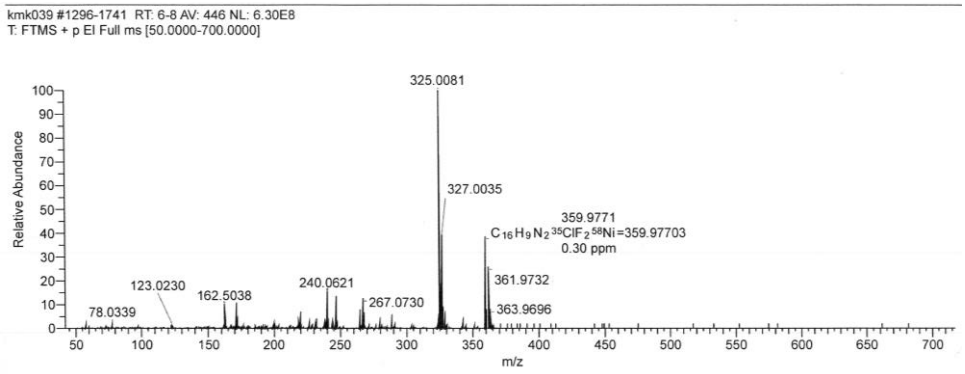

Figure 7-327 EI(+) mass spectrum (70eV) of [Ni(Py(4,6FPh)Py)Cl].

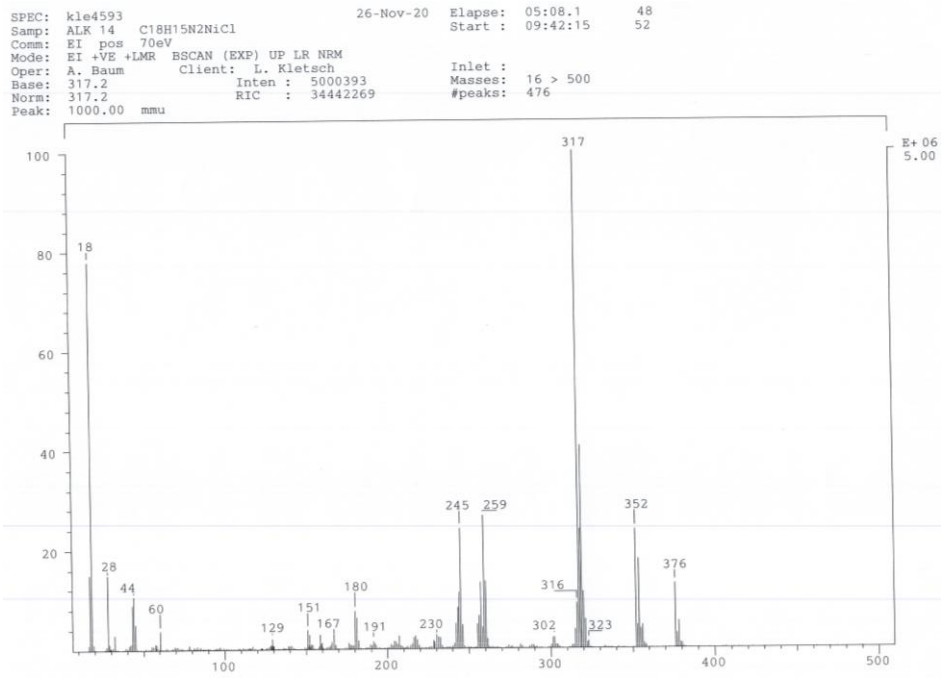

Figure 7-328 EI(+) mass spectrum (70eV) of [Ni(Py(4,6MePh)Py)Br].

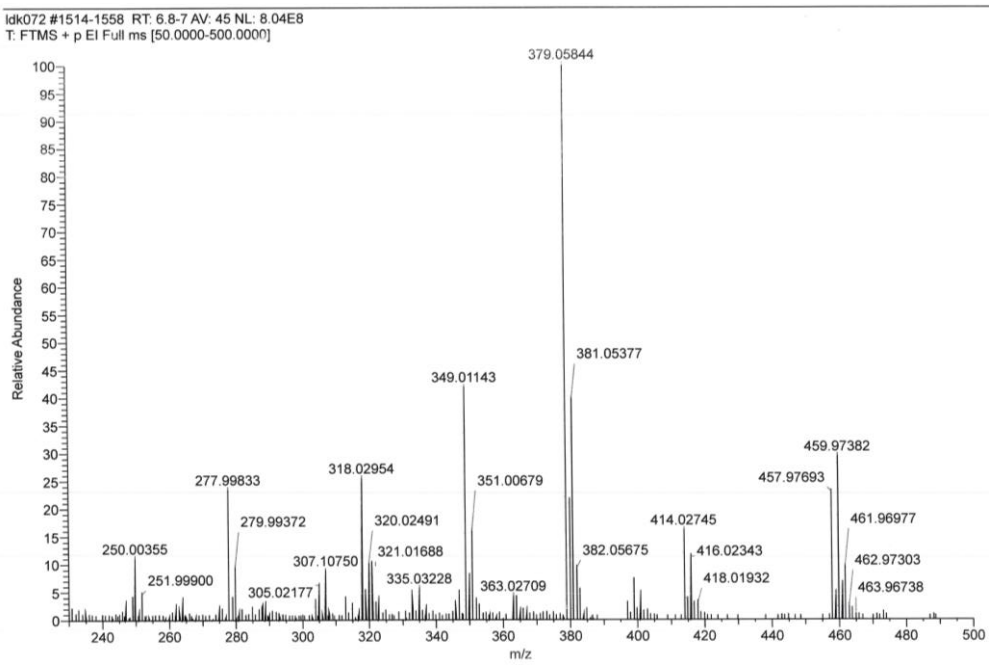

Figure 7-329 EI(+) mass spectrum (70eV) of [Ni(Py(4,5,6MeOPh)Py)Br].

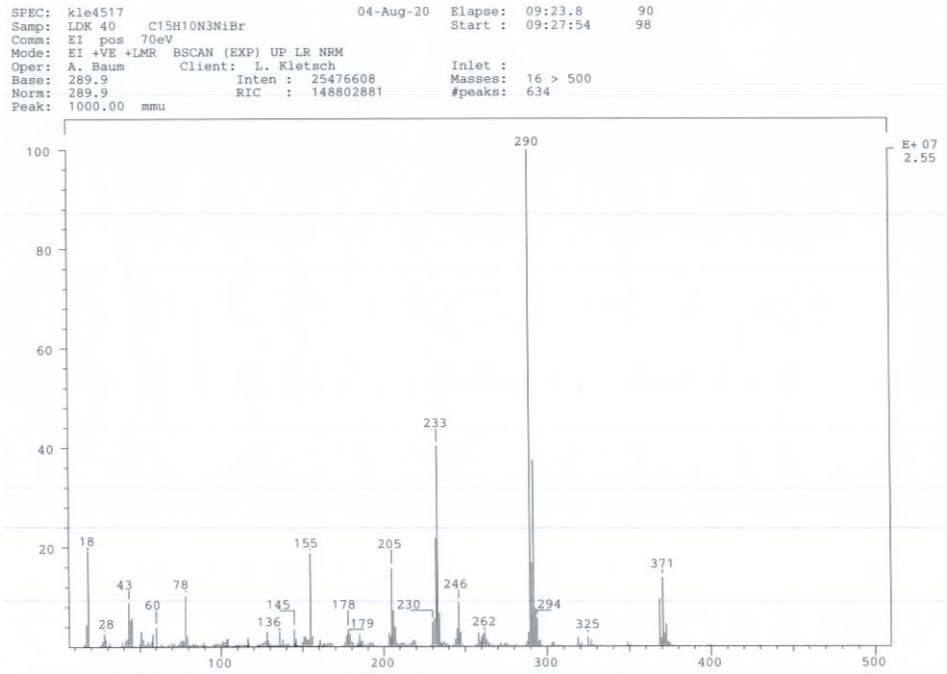

Figure 7-330 EI(+) mass spectrum (70eV) of [Ni(Py(Py)Py)Br].

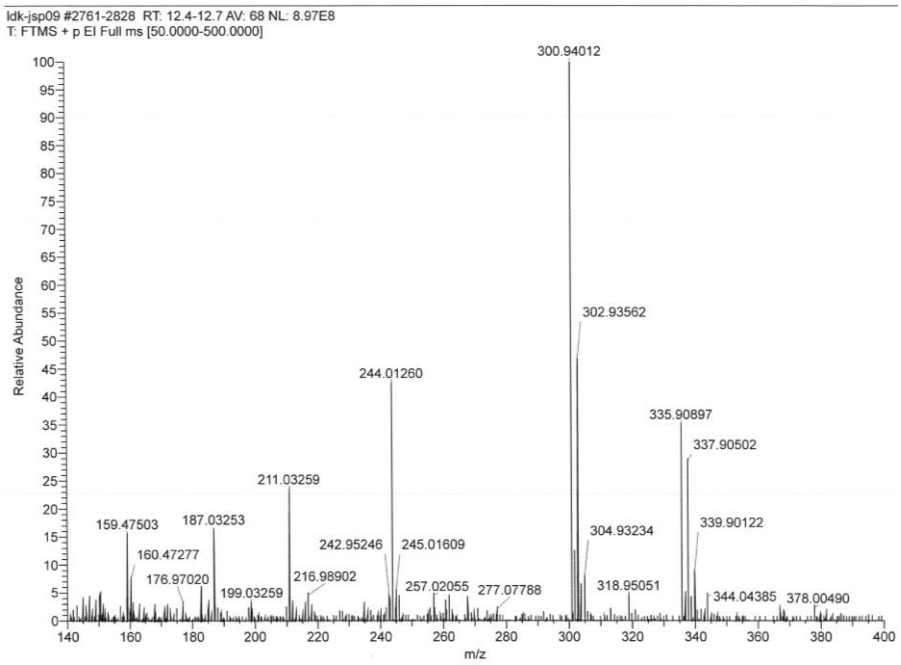

Figure 7-331 EI(+) mass spectrum (70eV) of [Ni(2Tz(Ph)2Tz)Cl].

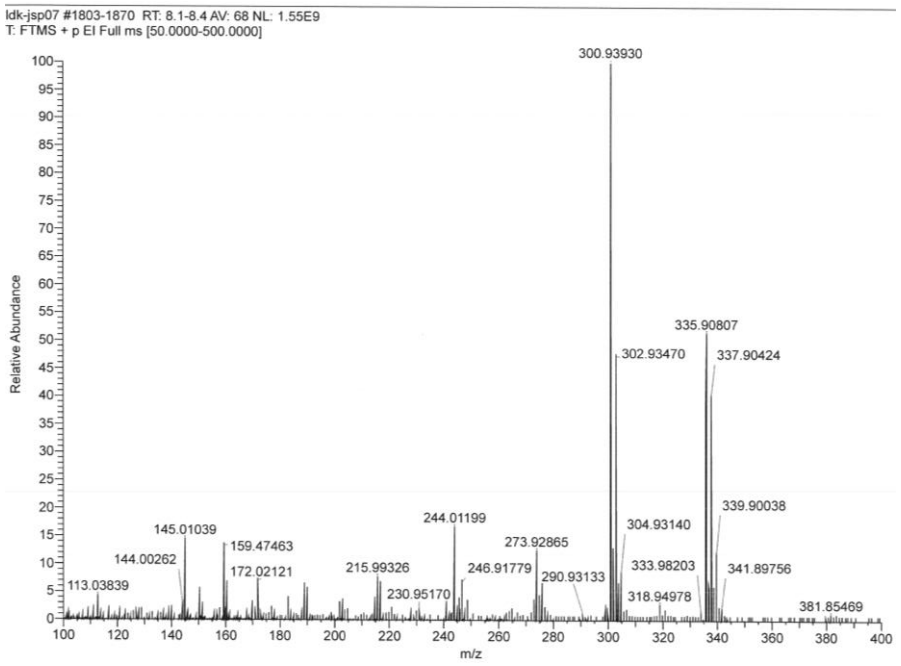

Figure 7-332 EI(+) mass spectrum (70eV) of [Ni(4Tz(Ph)4Tz)Cl].

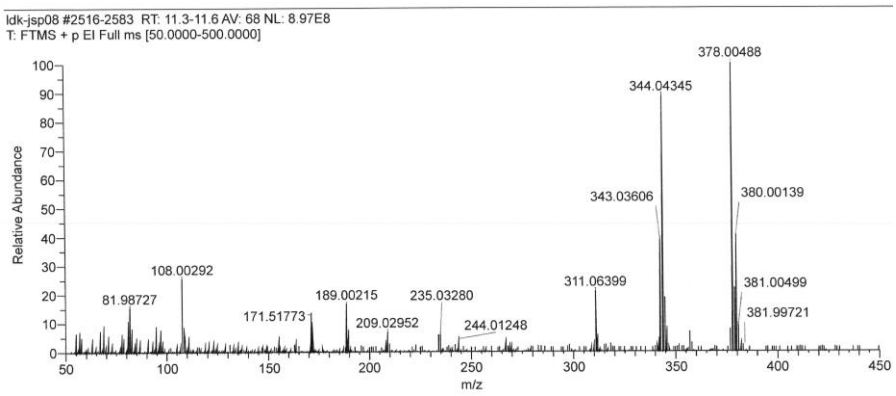

Figure 7-333 EI(+) mass spectrum (70eV) of [Ni(2Btz(Ph)2Btz)Cl].

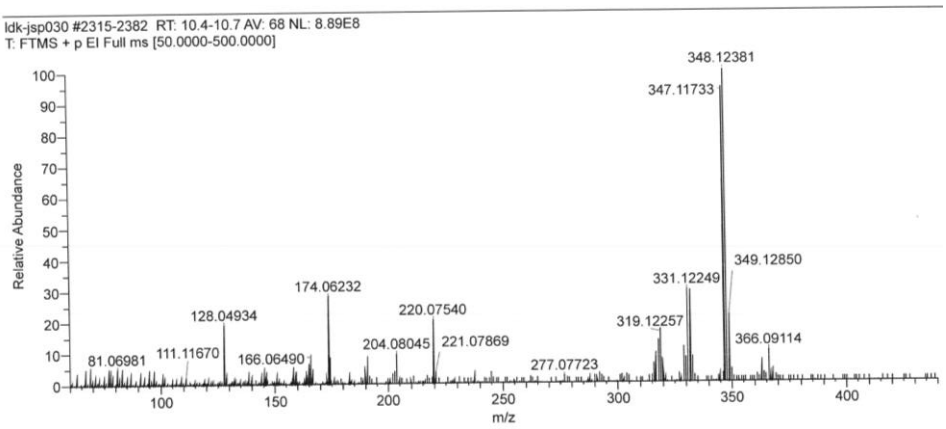

Figure 7-334 EI(+) mass spectrum (70eV) of [Ni(2Qu(Ph)2Qu)Cl].

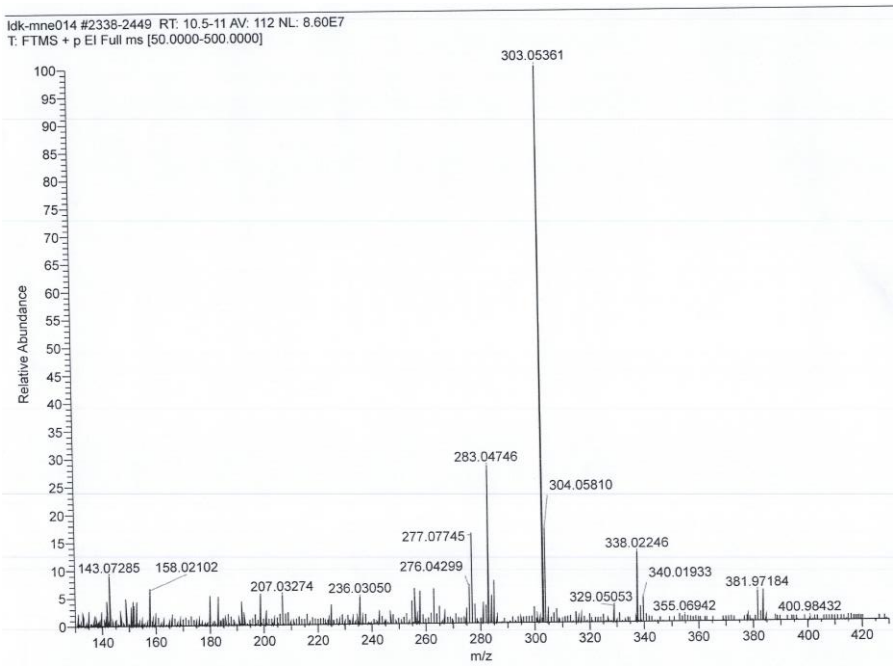

Figure 7-335 EI(+) mass spectrum (70eV) of [Ni(3FPy(4,6FPh)3FPy)Br].

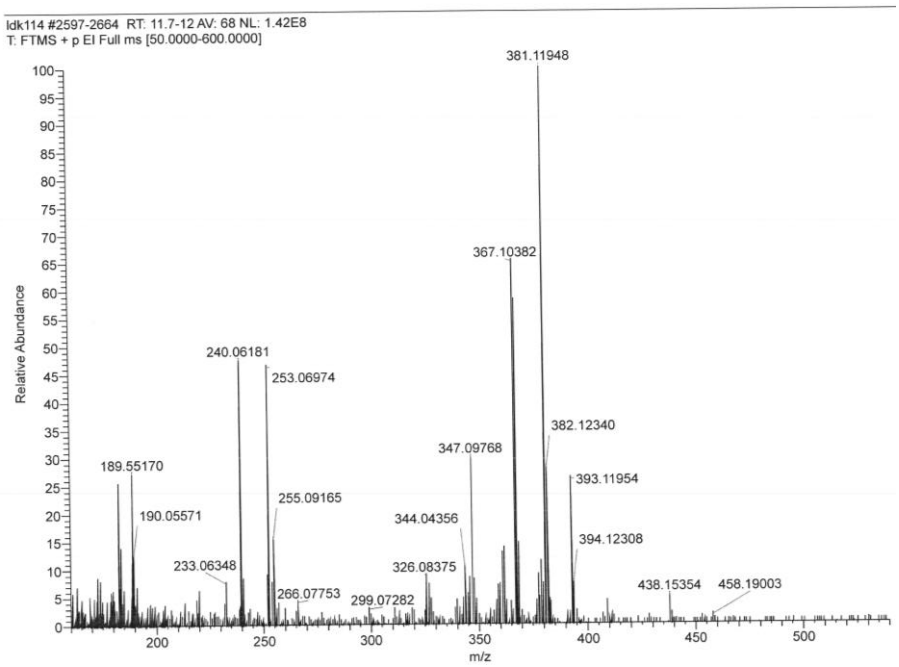

Figure 7-336 EI(+) mass spectrum (70eV) of [Ni(2^{i}Qu(4,6FPh)2^{i}Qu)Br].

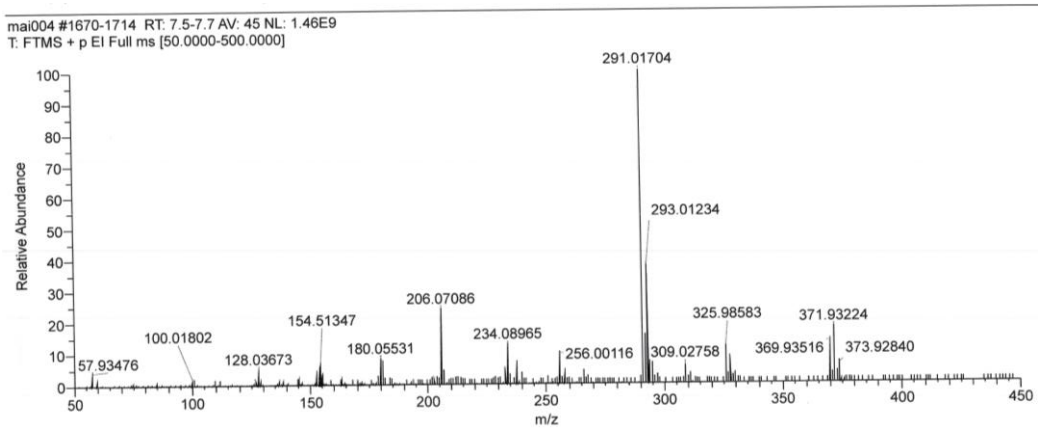

Figure 7-337 EI(+) mass spectrum (70eV) of [Ni(Pym(Ph)Pym)Br].

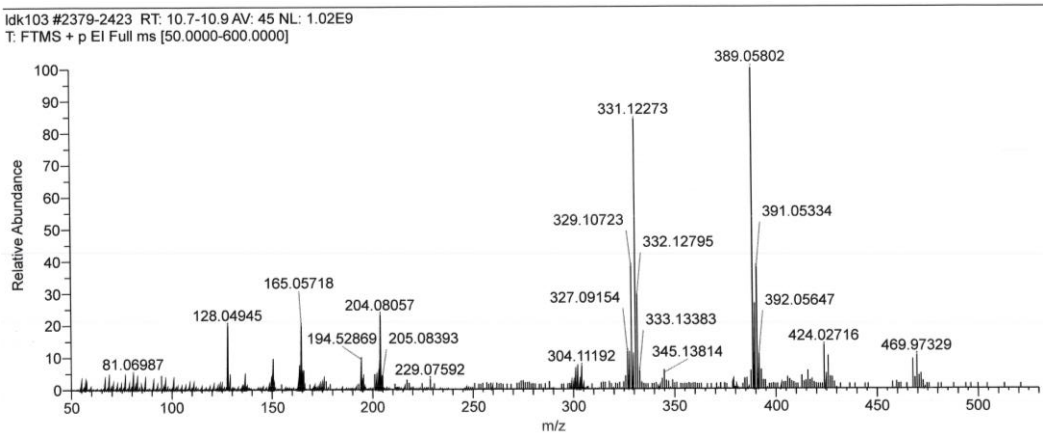

Figure 7-338 EI(+) mass spectrum (70eV) of [Ni(2^{i}Qu(Ph)2^{i}Qu)Br].

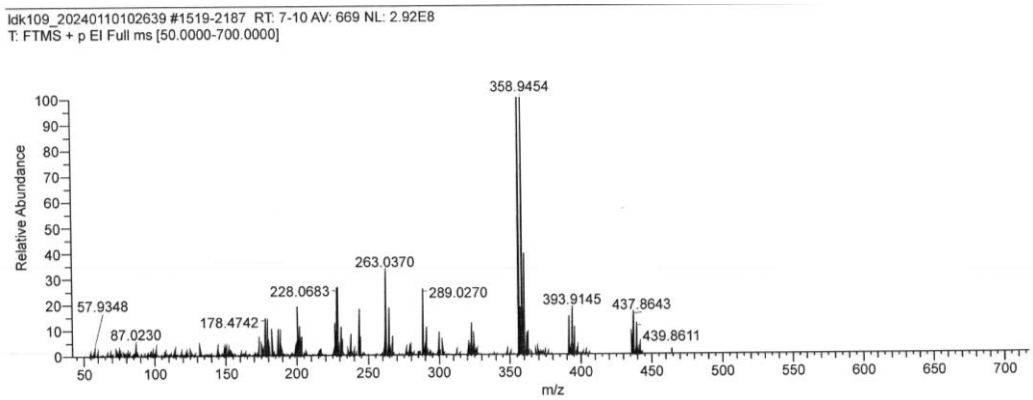

Figure 7-339 EI(+) mass spectrum (70eV) of [Ni(3ClPy(Ph)3ClPy)Br].

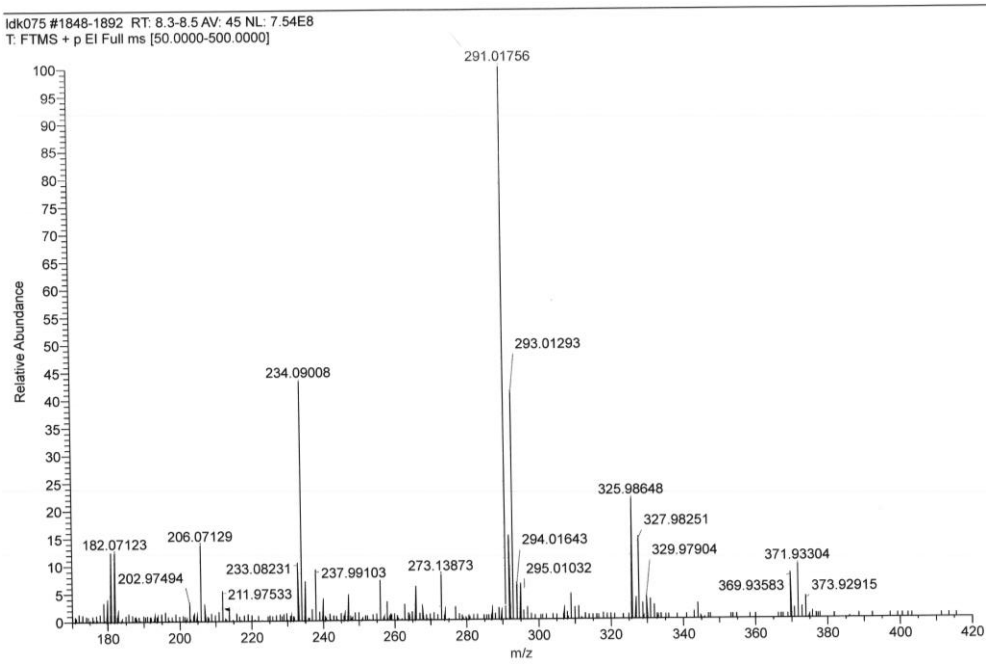

Figure 7-340 EI(+) mass spectrum (70eV) of [Ni(Pz(Ph)Pz)Br].

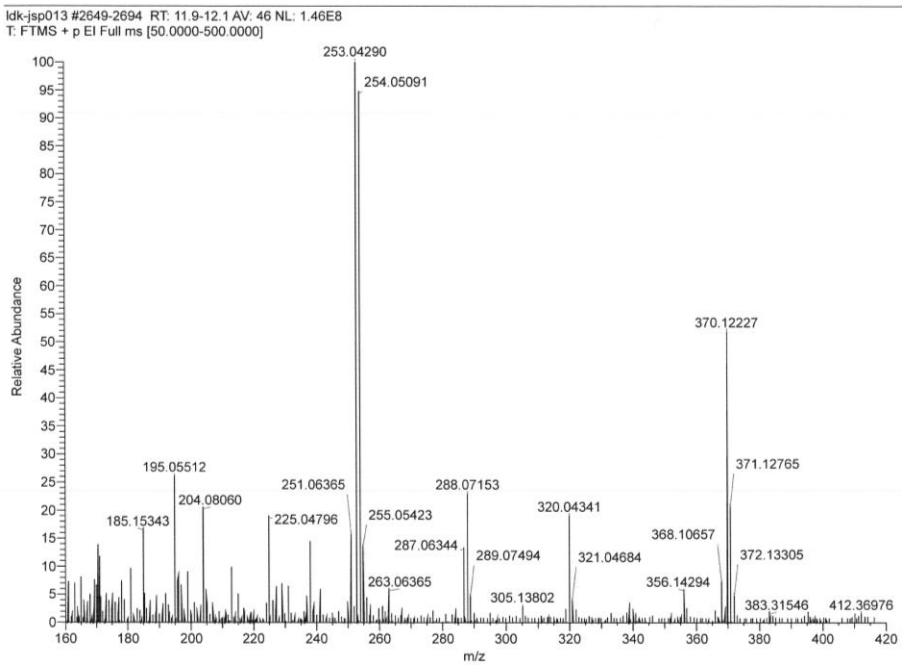

Figure 7-341 EI(+) mass spectrum (70eV) of [Ni(2Tz(Ph)Py)Br].

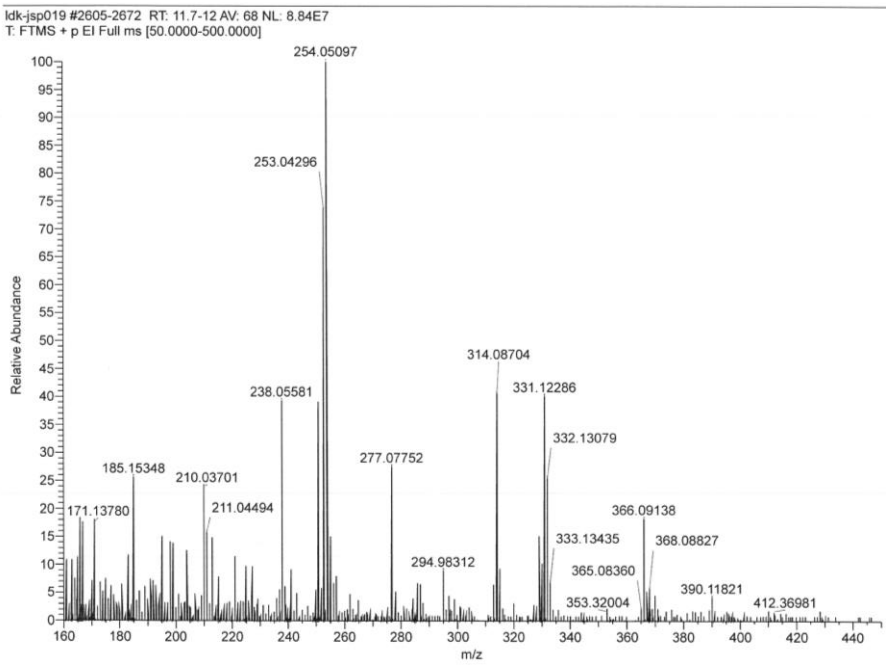

Figure 7-342 EI(+) mass spectrum (70eV) of [Ni(4Tz(Ph)Py)Br].

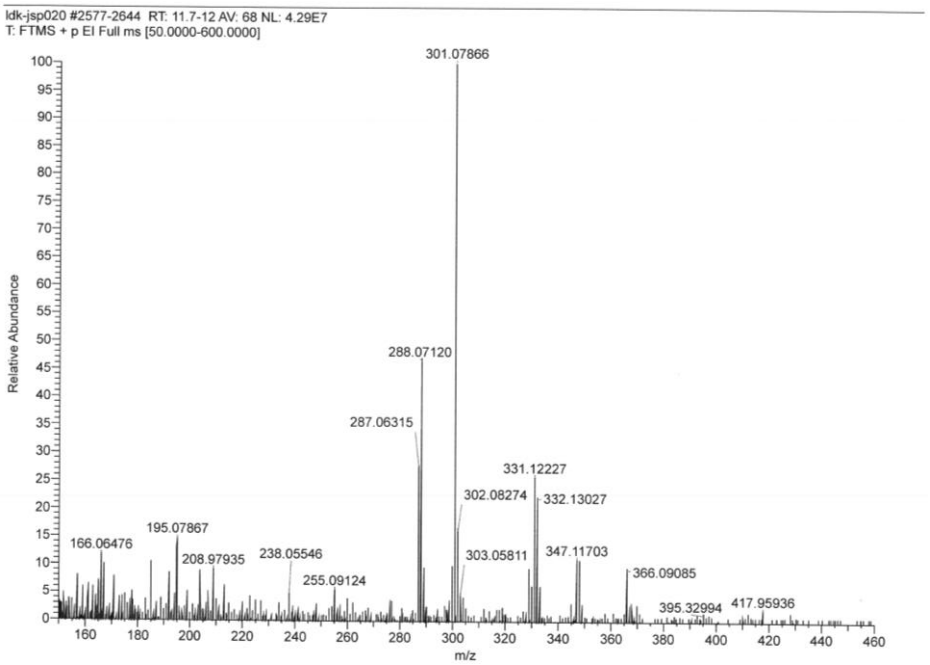

Figure 7-343 EI(+) mass spectrum (70eV) of [Ni(2Btz(Ph)Py)Br].

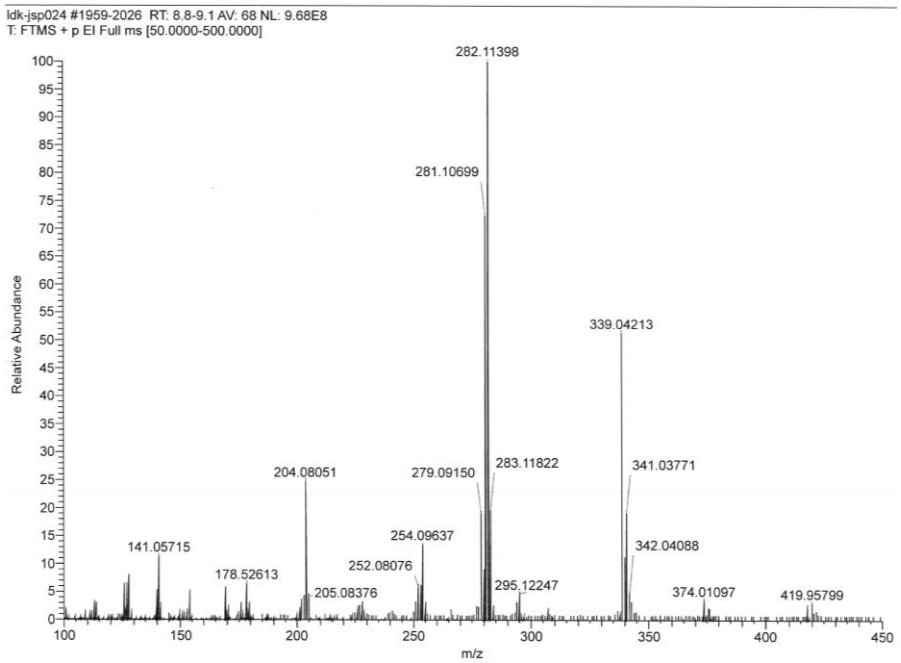

Figure 7-344 EI(+) mass spectrum (70eV) of [Ni(2Qu(Ph)Py)Br].

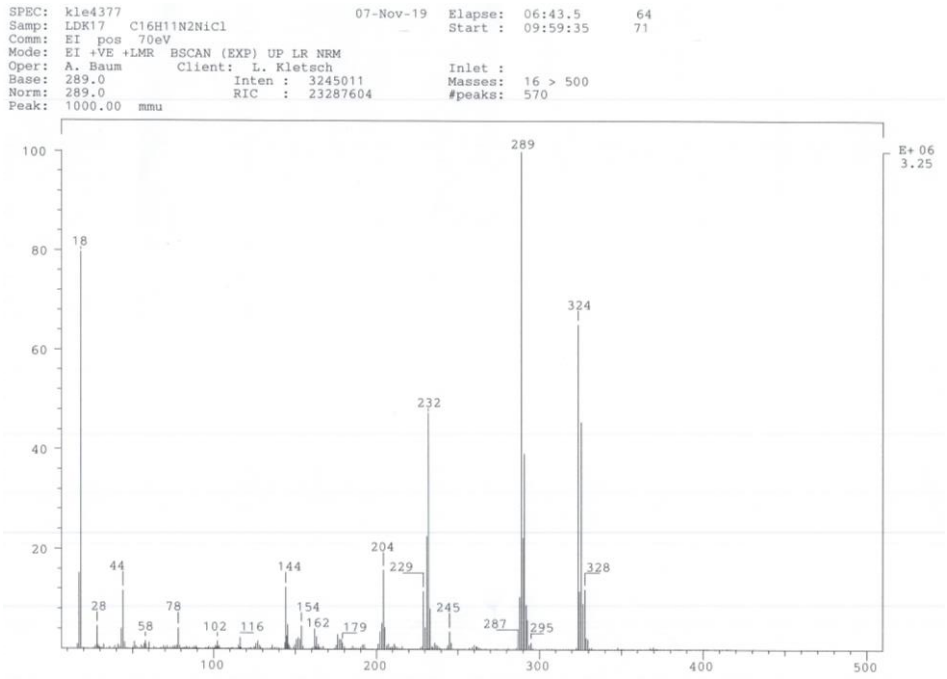

Figure 7-345 EI(+) mass spectrum (70eV) of [Ni(Py(Ph)Py)Cl].

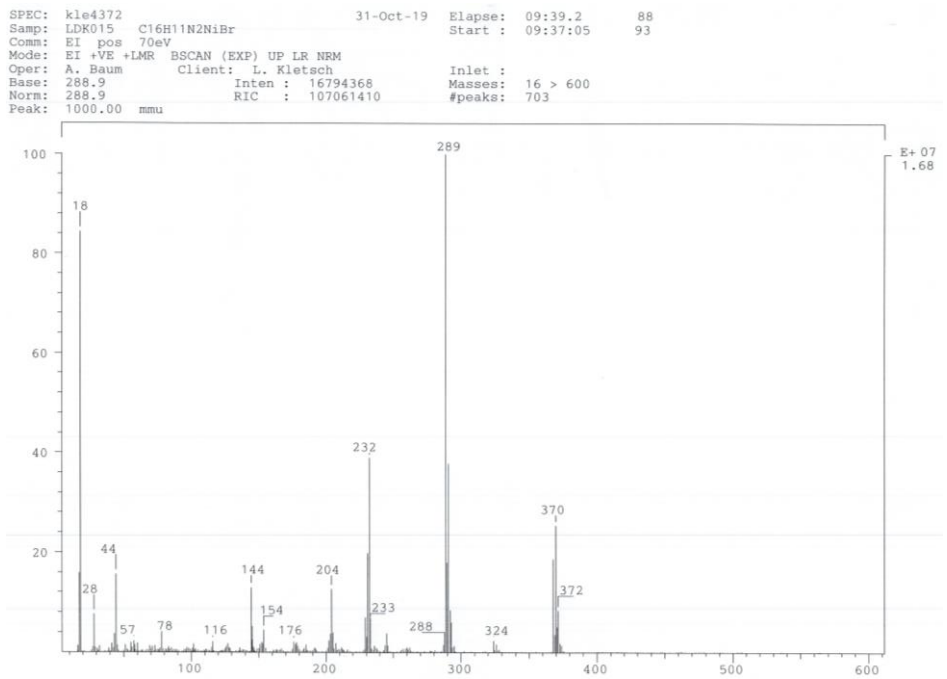

Figure 7-346 EI(+) mass spectrum (70eV) of [Ni(Py(Ph)Py)Br].

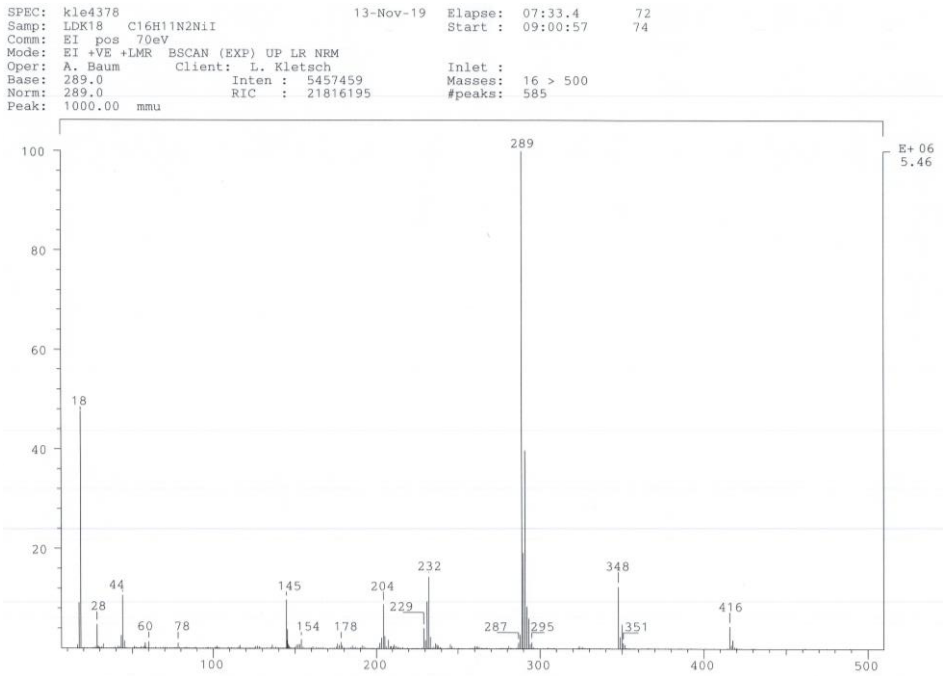

Figure 7-347 EI(+) mass spectrum (70eV) of [Ni(Py(Ph)Py)I].

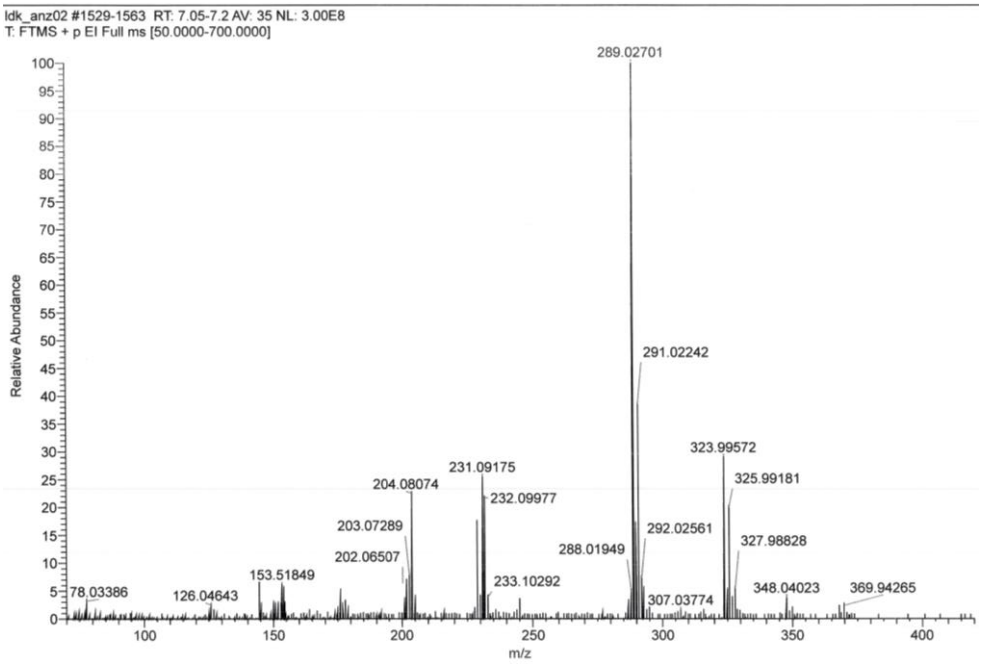

Figure 7-348 EI(+) mass spectrum (70eV) of [Ni(Py(Ph)Py)OAc].

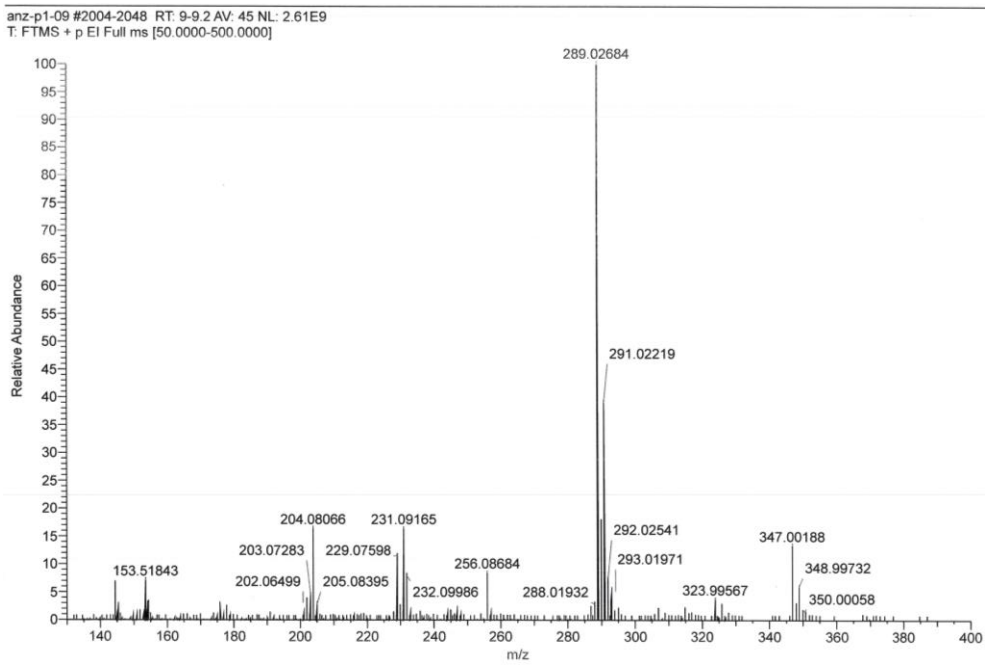

Figure 7-349 EI(+) mass spectrum (70eV) of [Ni(Py(Ph)Py)NCS].

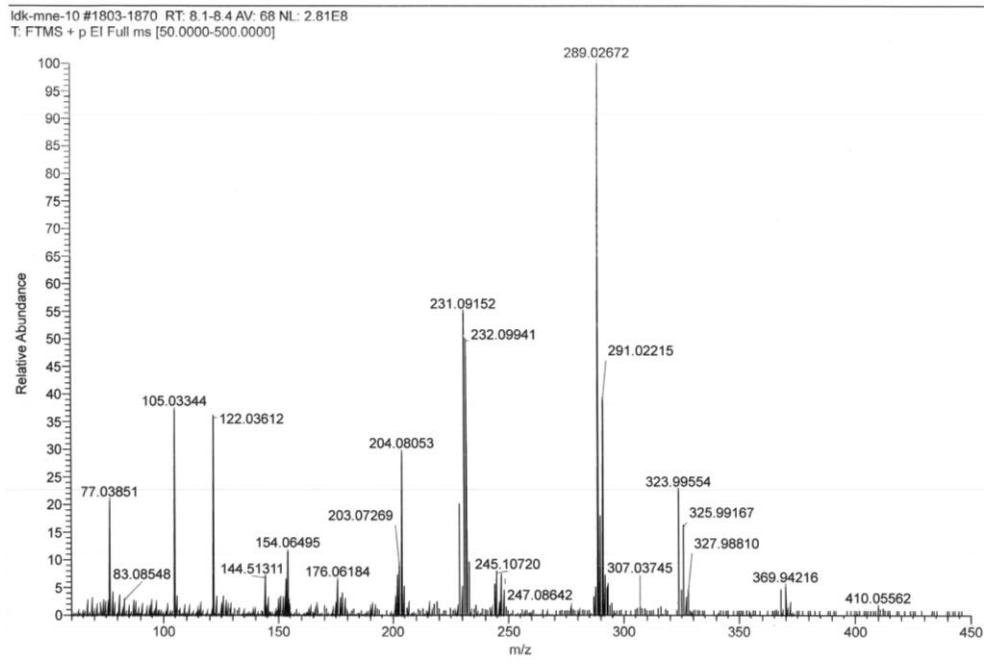

Figure 7-350 EI(+) mass spectrum (70eV) of [Ni(Py(Ph)Py)OBz].

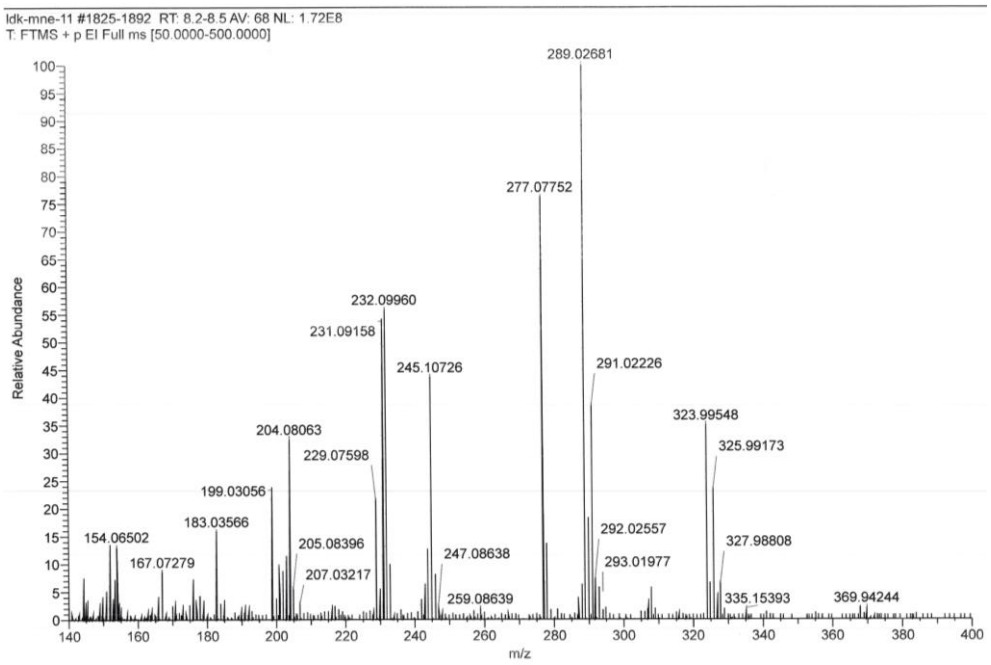

Figure 7-351 EI(+) mass spectrum (70eV) of [Ni(Py(Ph)Py)OPiv].

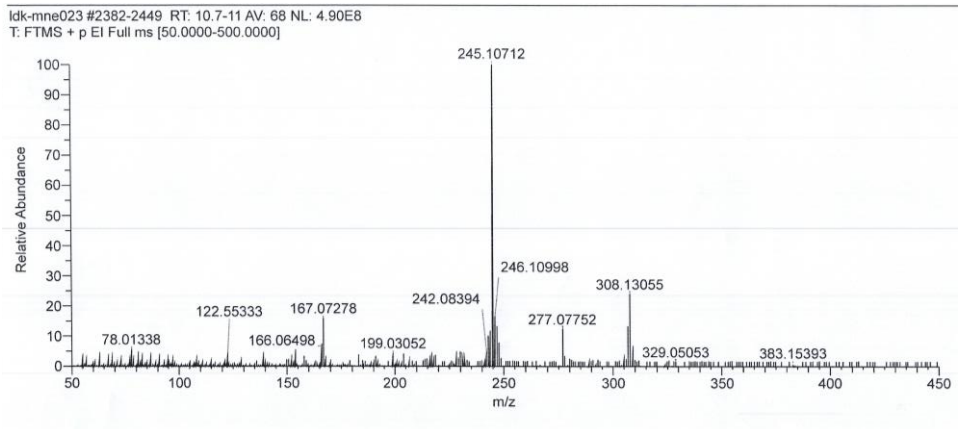

Figure 7-352 EI(+) mass spectrum (70eV) of [Ni(Py(Ph)Py)TFA].

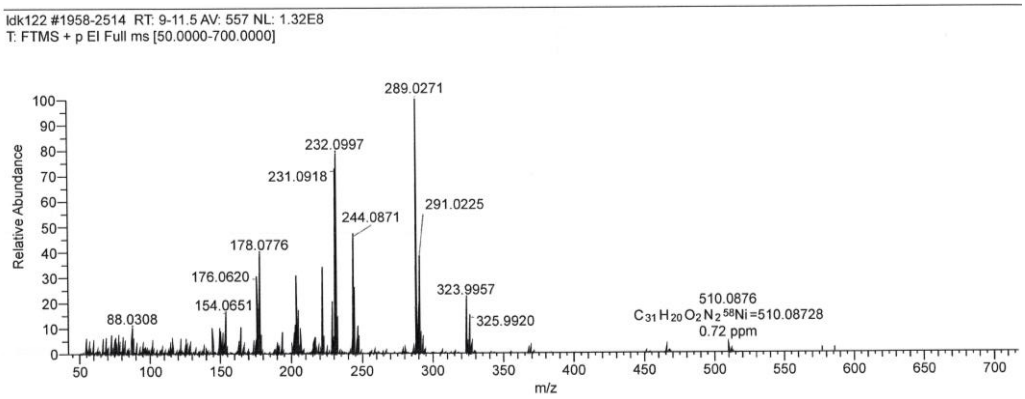

Figure 7-353 EI(+) mass spectrum (70eV) of [Ni(Py(Ph)Py)OOC-atc].

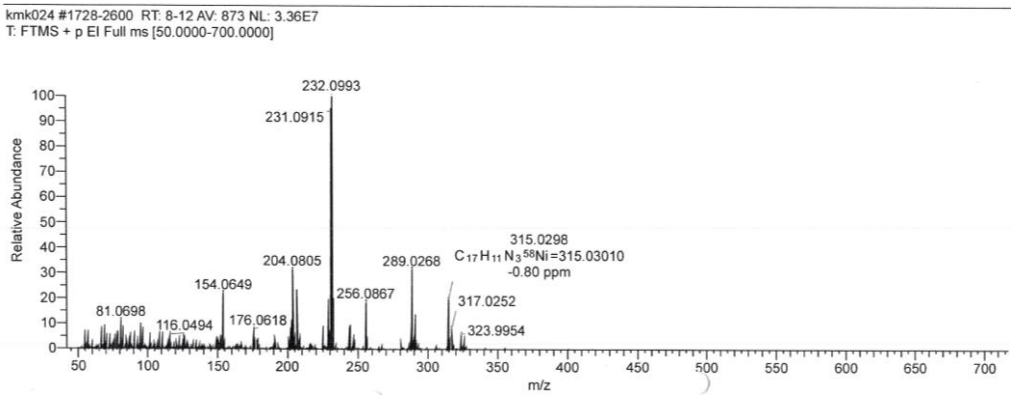

Figure 7-354 EI(+) mass spectrum (70eV) of [Ni(Py(Ph)Py)CN].

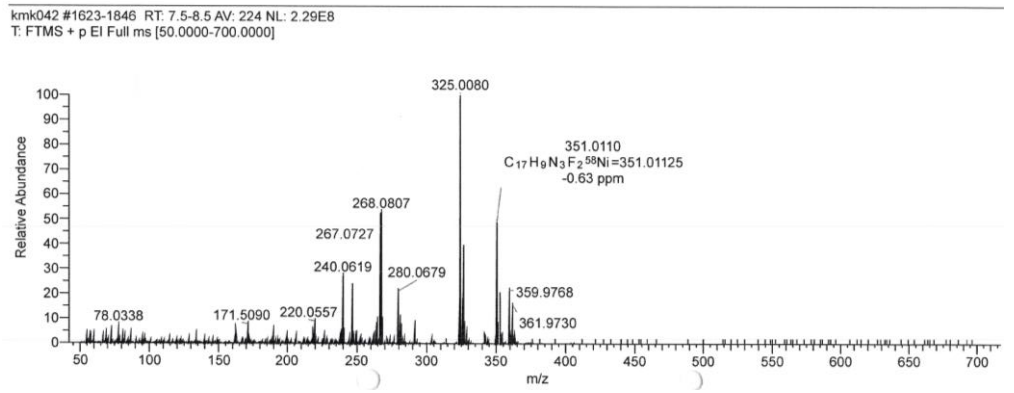

Figure 7-355 EI(+) mass spectrum (70eV) of [Ni(Py(4,6FPh)Py)CN].

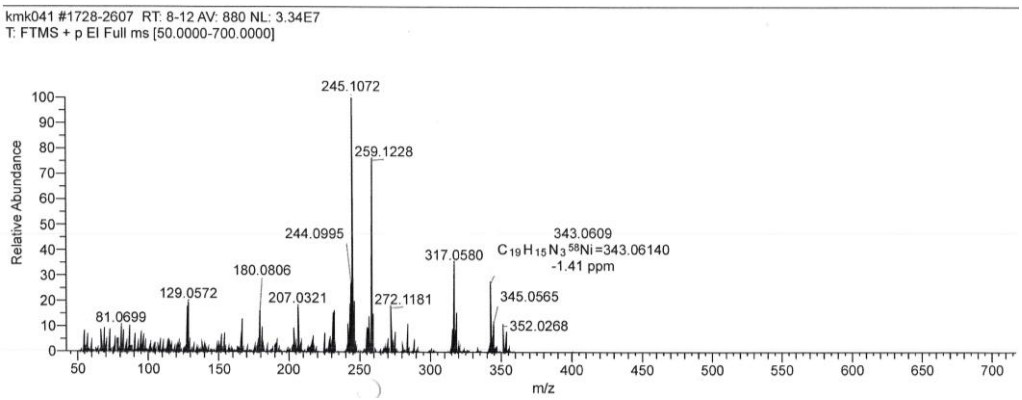

Figure 7-356 EI(+) mass spectrum (70eV) of [Ni(Py(4,6MePh)Py)CN].

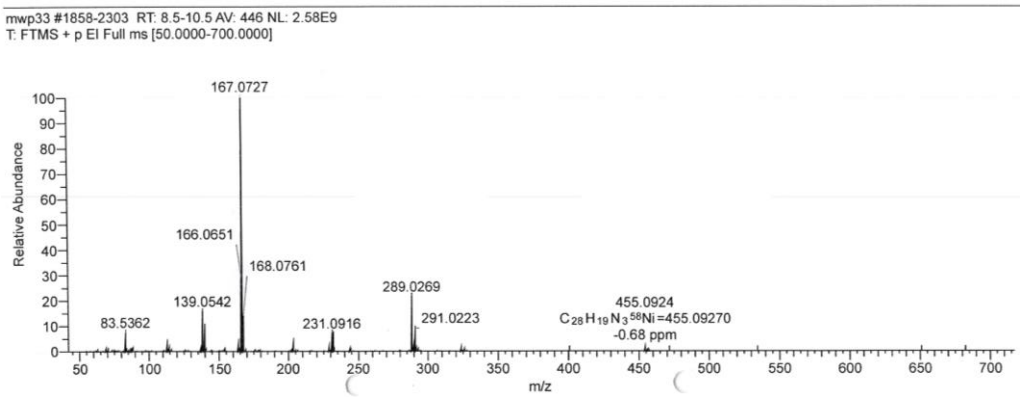

Figure 7-357 EI(+) mass spectrum (70eV) of [Ni(Py(Ph)Py)Carb].

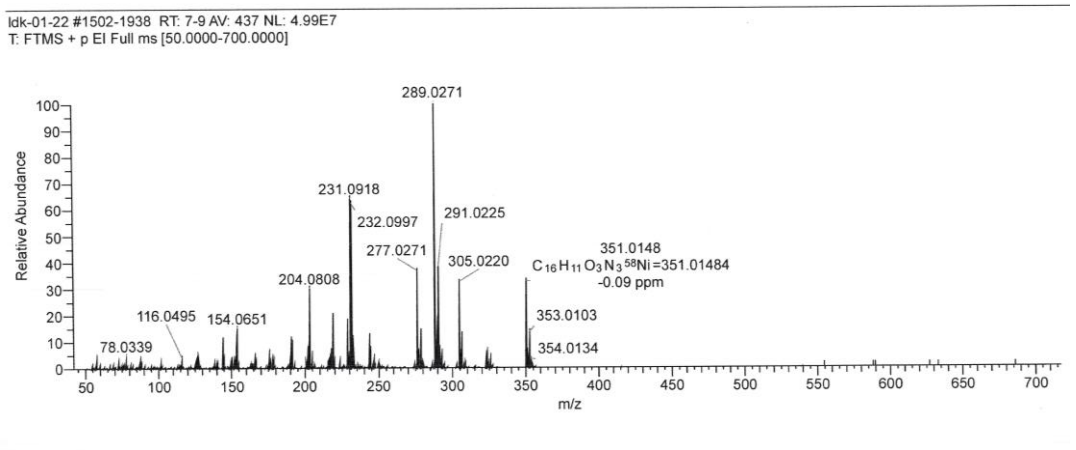

Figure 7-358 EI(+) mass spectrum (70eV) of [Ni(Py(Ph)Py)NO_3].

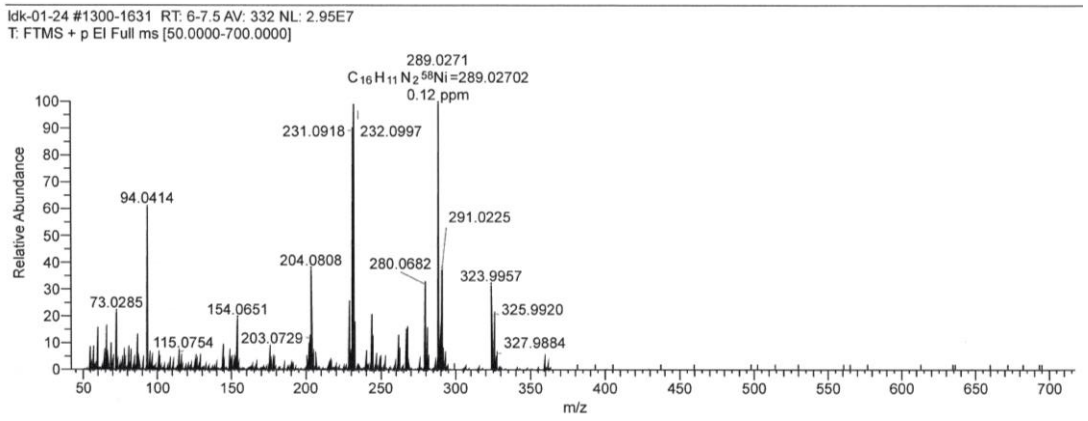

Figure 7-359 EI(+) mass spectrum (70eV) of [Ni(Py(Ph)Py)OPh].

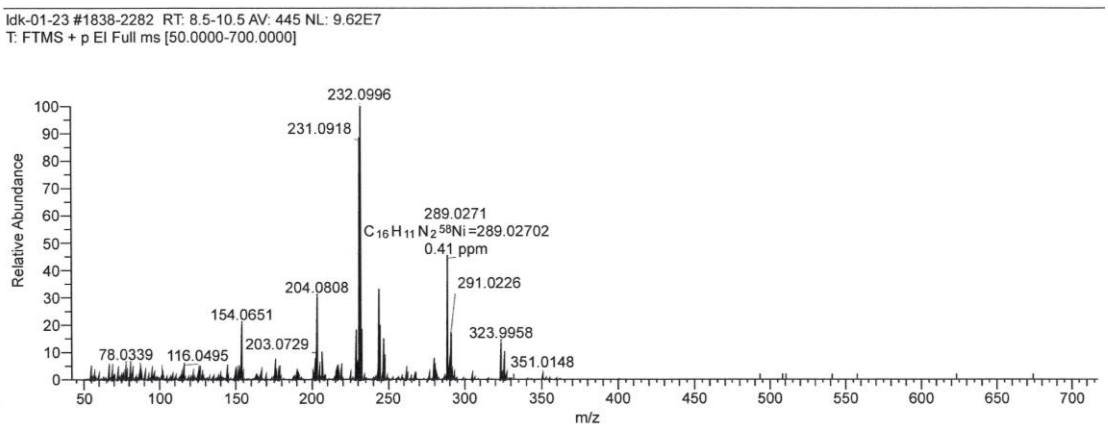

Figure 7-360 EI(+) mass spectrum (70eV) of [Ni(Py(Ph)Py)O*t*Bu].

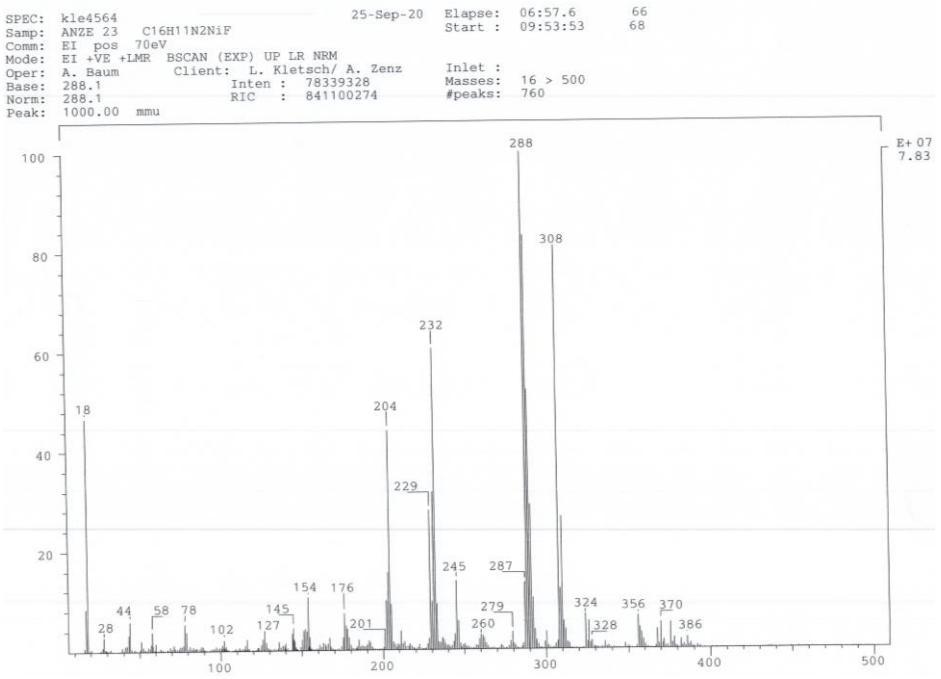

Figure 7-361 EI(+) mass spectrum (70eV) of [Ni(Py(Ph)Py)F].

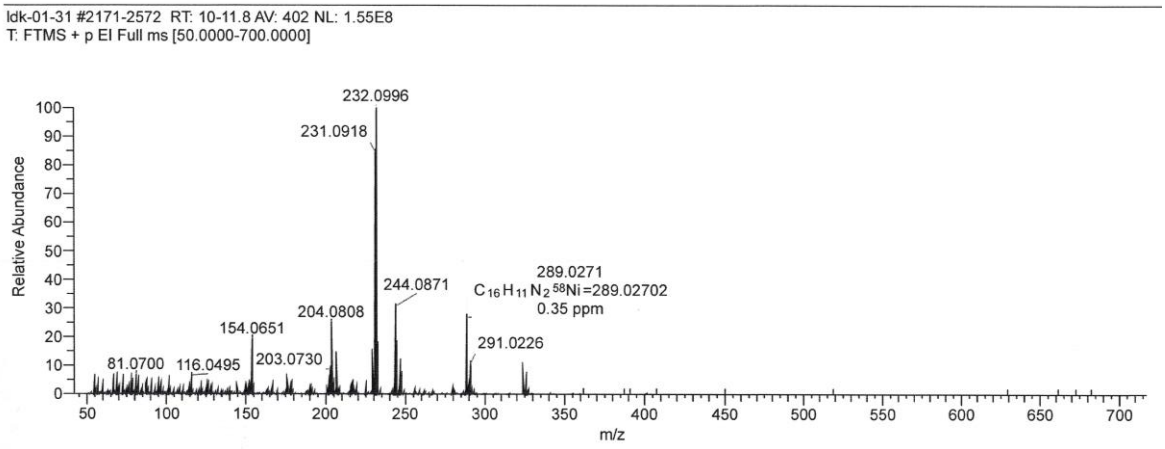

Figure 7-362 EI(+) mass spectrum (70eV) of [Ni(Py(Ph)Py)C_2F_5].

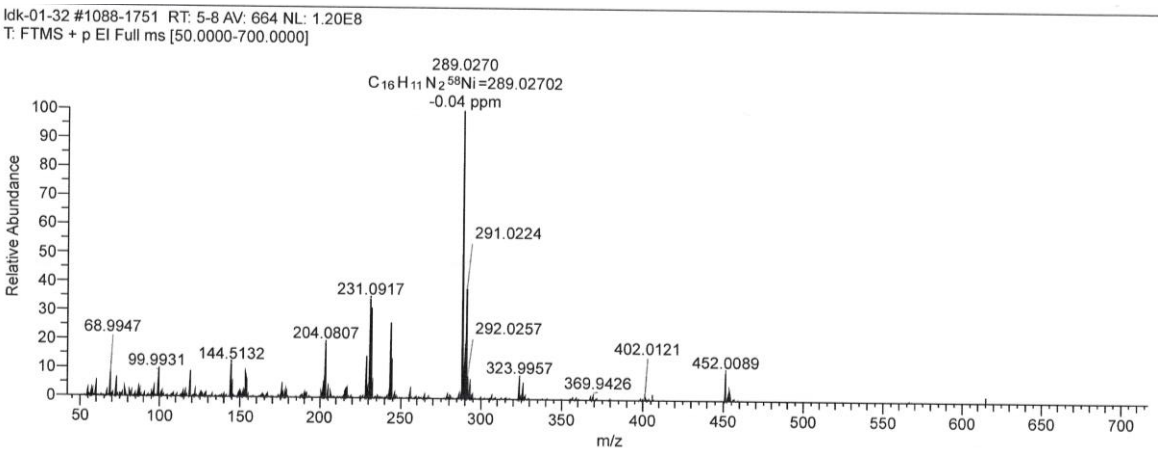

Figure 7-363 EI(+) mass spectrum (70eV) of [Ni(Py(Ph)Py)C_3F_7].

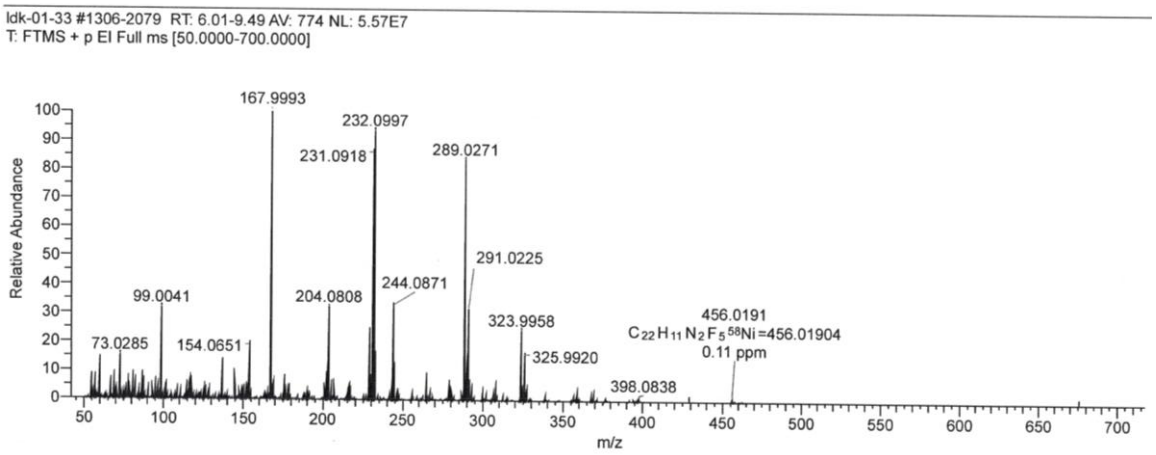

Figure 7-364 EI(+) mass spectrum (70eV) of [Ni(Py(Ph)Py)C_6F_5].

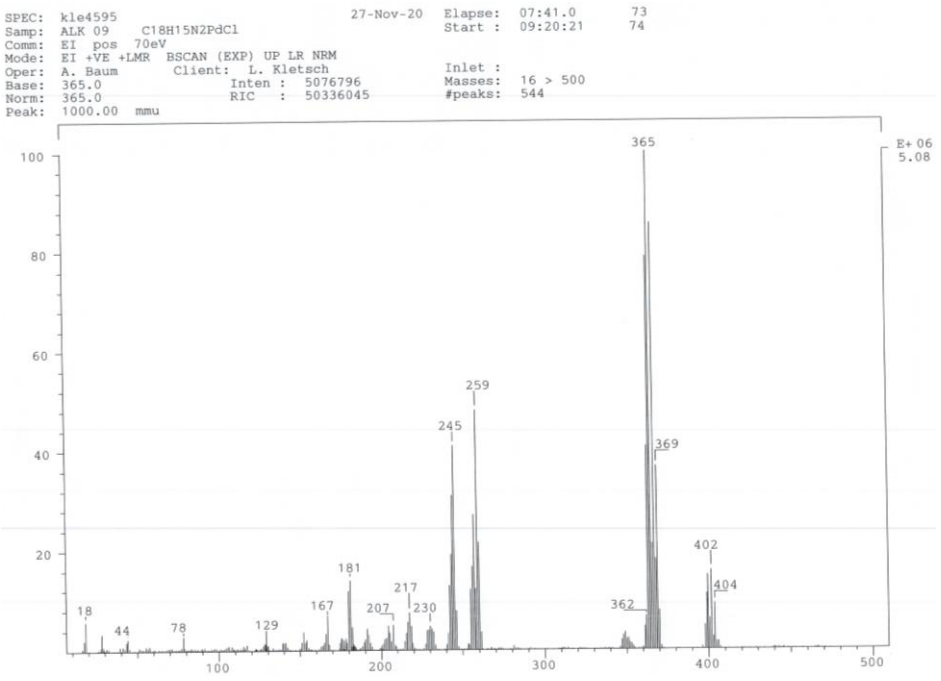

Figure 7-365 EI(+) mass spectrum (70eV) of [Pd(Py(4,6MePh)Py)Cl].

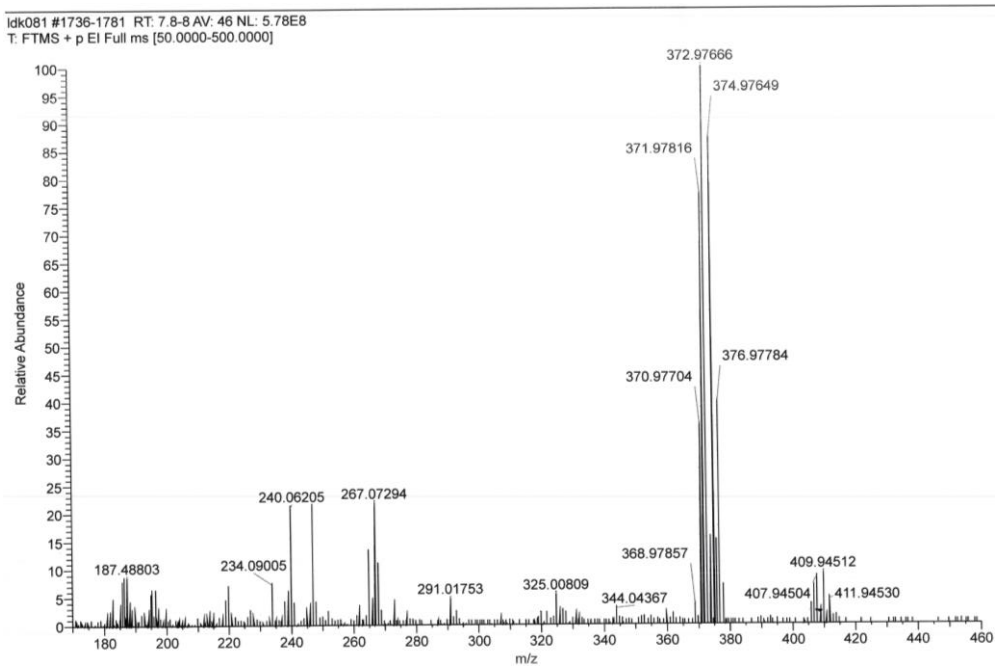

Figure 7-366 EI(+) mass spectrum (70eV) of [Pd(Py(4,6FPh)Py)Cl].

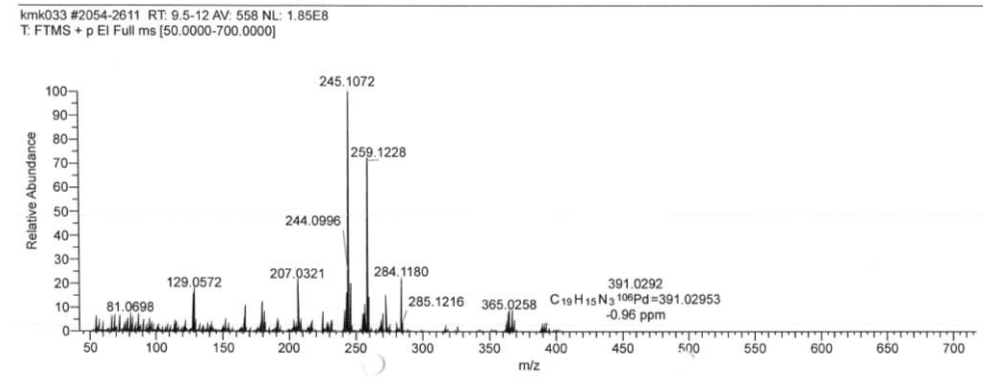

Figure 7-367 EI(+) mass spectrum (70eV) of [Pd(Py(4,6MePh)Py)CN].

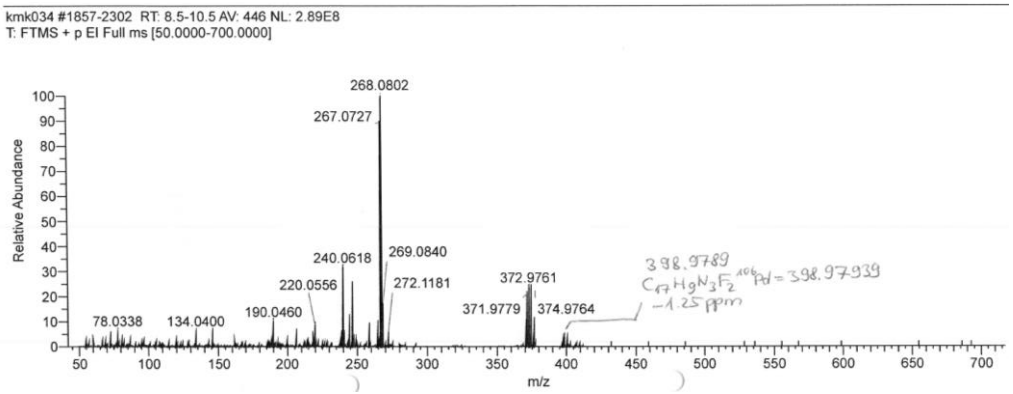

Figure 7-368 EI(+) mass spectrum (70eV) of [Pd(Py(4,6FPh)Py)CN].

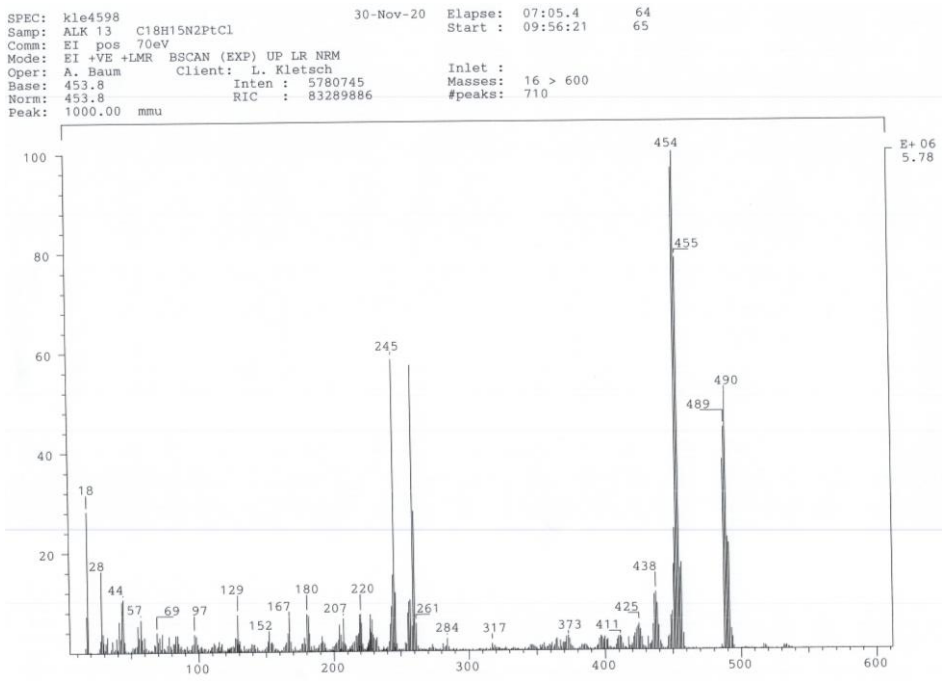

Figure 7-369 EI(+) mass spectrum (70eV) of [Pt(Py(4,6MePh)Py)Cl].

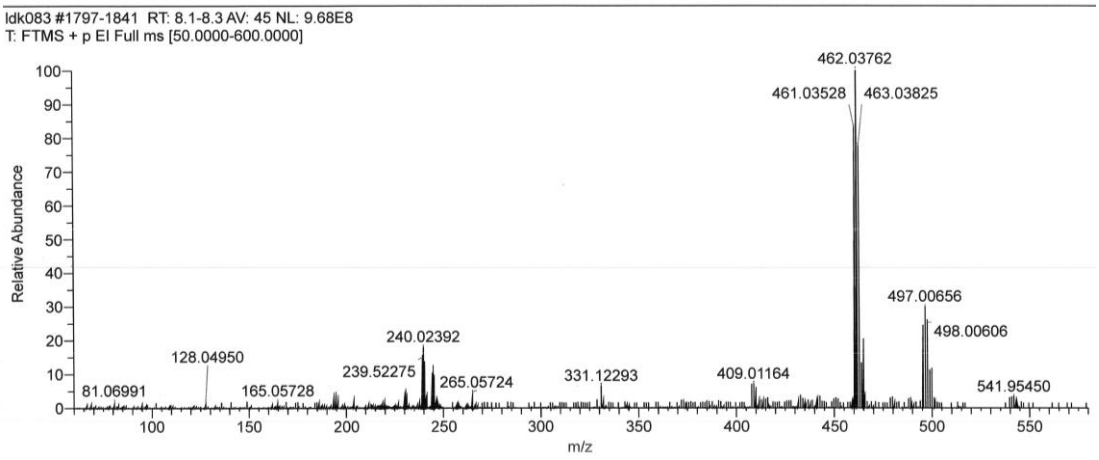

Figure 7-370 EI(+) mass spectrum (70eV) of [Pt(Py(4,6FPh)Py)Cl].

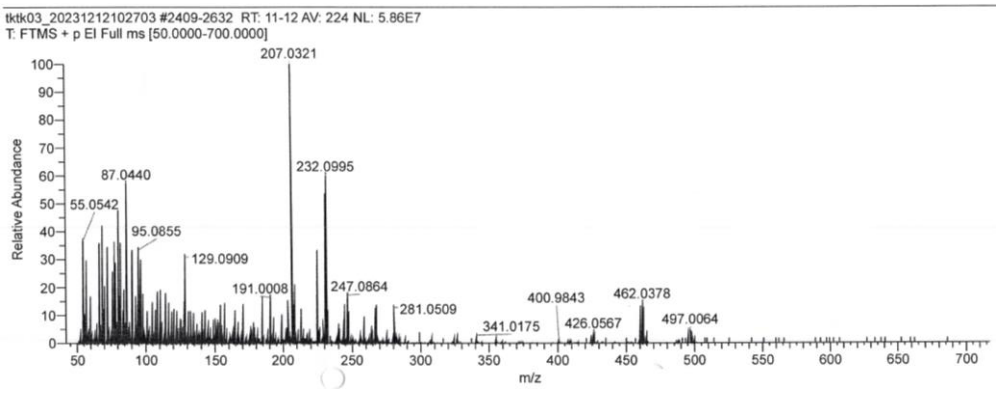

Figure 7-371 EI(+) mass spectrum (70eV) of [Pt(Py(Ph)Py)CN].

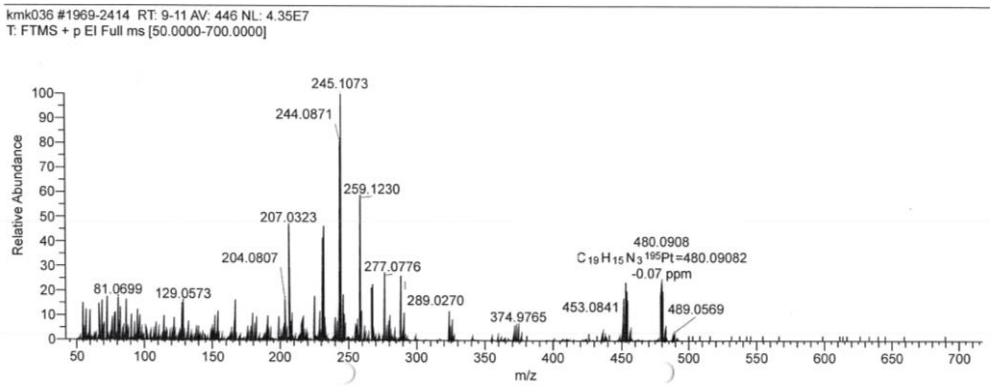

Figure 7-372 EI(+) mass spectrum (70eV) of [Pt(Py(4,6MePh)Py)CN].

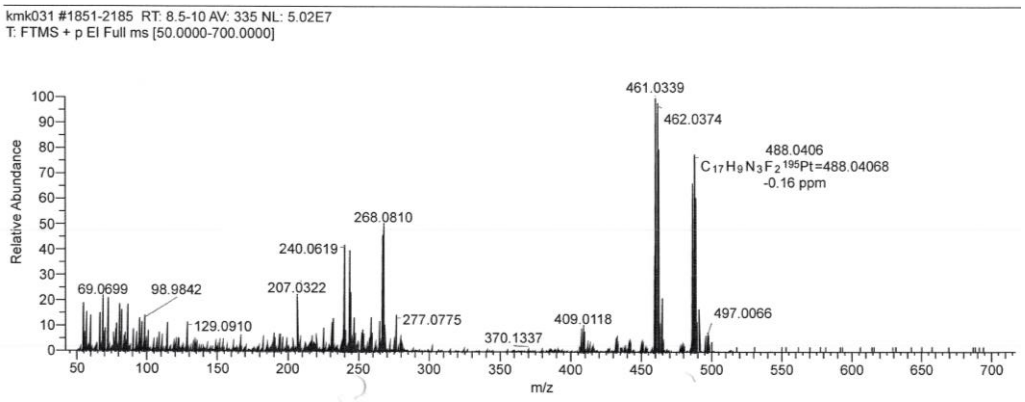

Figure 7-373 EI(+) mass spectrum (70eV) of [Pt(Py(4,6FPh)Py)CN].

7.3 Single Crystal XRD data

7.3.1 Py(5BuPhH)Py

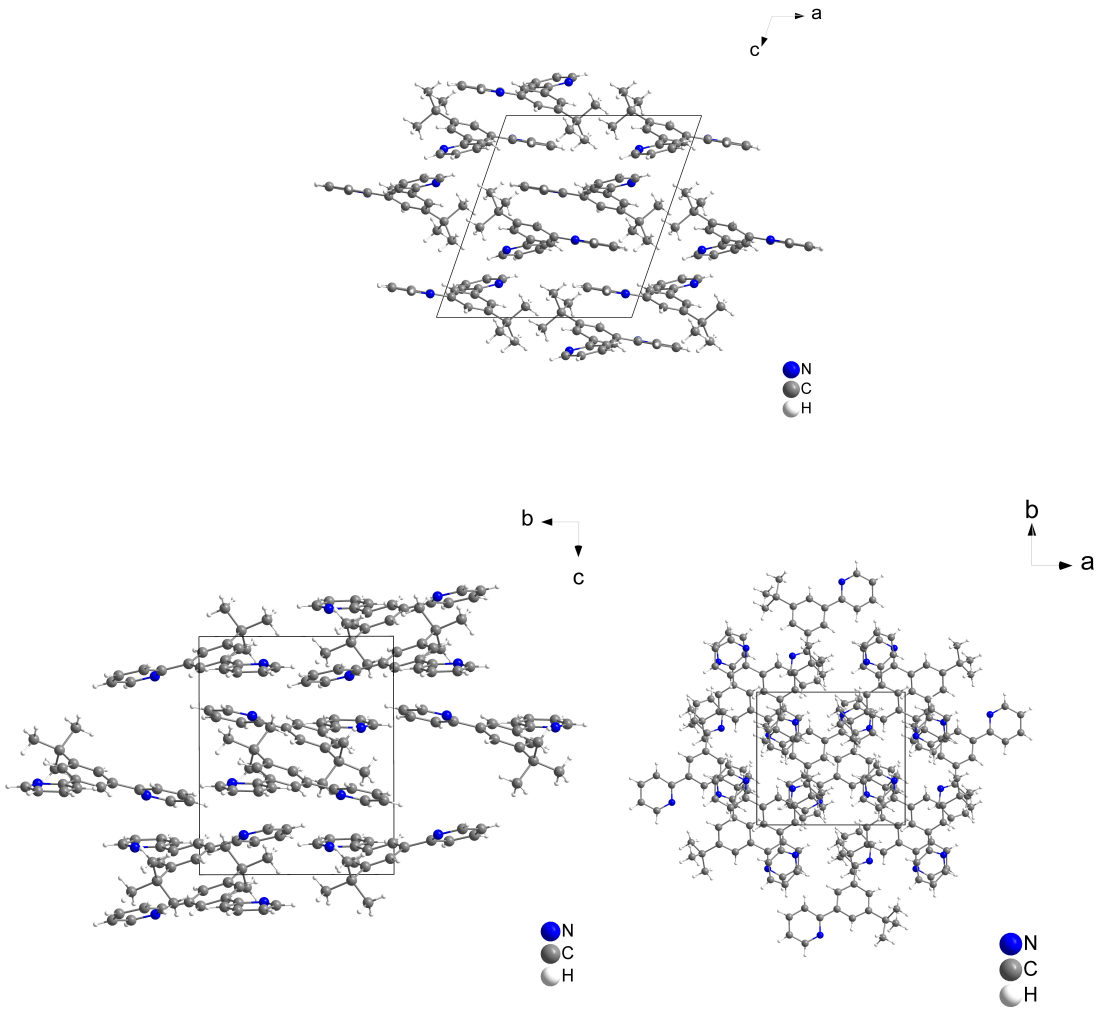

Figure 7-374 Crystal Structure of Py(5BuPhH)Py viewed along the crystallographic *a*-axis (bottom left), *b*-axis (top) and *c*-axis (bottom right).

Table 7-1 Crystal data and structure refinement for Py(5BuPhH)Py.

Identification code	Py(5BuPhH)Py
Empirical formula	$C_{20}H_{20}N_2$
Formula weight	288.38
Temperature/K	383.30
Crystal system	monoclinic
Space group	$P2_1/n$
a/Å	12.0960(4)
b/Å	10.2452(4)
c/Å	13.2431(5)
α/°	90
β/°	109.0740(10)
γ/°	90
Volume/Å^3	1551.06(10)
Z	4
ρ_{calc}g/cm^3	1.235

μ/mm^{-1}	0.073
F(000)	616.0
Radiation	MoKα (λ = 0.71073)
2Θ range for data collection/°	3.964 to 56.588
Index ranges	–16 ≤ h ≤ 16, –13 ≤ k ≤ 13, –17 ≤ l ≤ 17
Reflections collected	67917
Independent reflections	3820 [R_{int} = 0.0798, R_{sigma} = 0.0287]
Data/restraints/parameters	3820/0/203
Goodness-of-fit on F^2	1.093
Final R indexes [I>=2σ (I)]	R_1 = 0.0493, wR_2 = 0.1239
Final R indexes [all data]	R_1 = 0.0638, wR_2 = 0.1357
Largest diff. peak/hole / e Å^{-3}	0.41/–0.25

Table 7-2 Fractional Atomic Coordinates (×10^4) and Equivalent Isotropic Displacement Parameters (Å^2×10^3) for Py(5BuPhH)Py. U_{eq} is defined as 1/3 of the trace of the orthogonalized U_{IJ} tensor.

Atom	*x*	*y*	*z*	U(eq)
N1	7598.7(10)	7273.4(11)	3336.9(9)	17.6(3)
N2	4269.3(10)	1686.6(11)	3845.6(10)	19.4(3)
C11	5409.8(11)	3646.2(12)	3994.8(10)	14.9(3)
C7	6559.1(11)	5534.2(12)	3860.2(10)	14.6(3)
C10	6448.1(11)	2957.5(12)	4492.1(10)	15.8(3)
C9	7541.6(11)	3530.4(12)	4676.6(10)	14.8(3)
C3	6901.6(12)	9488.0(13)	3101.6(11)	20.0(3)
C8	7577.5(11)	4819.0(12)	4337.0(10)	15.1(3)
C6	6641.5(11)	6928.9(12)	3580.2(10)	14.8(3)
C5	5791.3(12)	7835.8(13)	3609.1(11)	17.7(3)
C1	5475.9(11)	4939.0(12)	3691.9(10)	15.8(3)
C13	3229.9(11)	3710.8(13)	3646.4(11)	18.8(3)
C4	5928.7(12)	9133.4(13)	3371.4(11)	20.0(3)
C12	4257.7(11)	3000.2(13)	3815.1(10)	15.5(3)
C17	8694.2(11)	2819.7(12)	5249.3(11)	16.0(3)
C2	7706.1(12)	8522.1(13)	3100.1(11)	19.5(3)
C19	9429.2(12)	3662.9(13)	6186.0(12)	21.3(3)
C16	3257.6(12)	1070.8(14)	3708.1(12)	22.7(3)
C14	2187.7(12)	3049.8(15)	3498.8(12)	22.0(3)
C15	2197.3(12)	1700.2(15)	3532.7(12)	22.9(3)
C20	8495.6(12)	1499.8(13)	5702.5(12)	22.5(3)
C18	9373.1(12)	2587.3(14)	4467.7(12)	21.9(3)

Table 7-3 Anisotropic Displacement Parameters (Å^2×10^3) for Py(5BuPhH)Py. The Anisotropic displacement factor exponent takes the form: $-2\pi^2[h^2a^{*2}U_{11}+2hka^*b^*U_{12}+\ldots]$.

Atom	U_{11}	U_{22}	U_{33}	U_{23}	U_{13}	U_{12}
N1	17.2(5)	15.8(5)	20.3(6)	2.6(4)	6.7(5)	0.5(4)
N2	19.1(6)	16.4(6)	24.7(6)	–2.1(4)	9.8(5)	–2.5(4)
C11	14.8(6)	15.1(6)	15.9(6)	–1.3(5)	6.5(5)	–0.9(4)
C7	17.2(6)	12.9(6)	14.7(6)	0.3(4)	6.7(5)	0.5(4)
C10	18.1(6)	12.5(6)	17.9(6)	1.0(5)	7.4(5)	–0.3(5)
C9	15.0(6)	14.6(6)	15.1(6)	0.7(5)	5.1(5)	1.7(4)
C3	24.1(7)	12.8(6)	20.5(7)	1.5(5)	3.8(5)	–1.1(5)
C8	14.0(6)	14.3(6)	17.8(6)	0.4(5)	6.5(5)	–0.6(4)

Atom	U_{11}	U_{22}	U_{33}	U_{23}	U_{13}	U_{12}
C6	16.1(6)	13.1(6)	14.1(6)	0.0(4)	3.6(5)	–0.4(4)
C5	17.1(6)	17.8(6)	18.9(6)	0.3(5)	7.0(5)	1.5(5)
C1	15.2(6)	15.8(6)	16.7(6)	0.0(5)	5.7(5)	1.6(5)
C13	17.2(6)	18.5(6)	21.0(7)	0.0(5)	6.6(5)	0.0(5)
C4	22.7(7)	15.3(6)	21.3(7)	0.2(5)	6.2(5)	5.1(5)
C12	15.5(6)	17.2(6)	14.6(6)	–1.1(5)	6.1(5)	–1.4(5)
C17	14.3(6)	13.8(6)	19.2(6)	2.2(5)	4.5(5)	0.0(4)
C2	18.3(6)	18.1(6)	22.1(7)	3.8(5)	6.4(5)	–1.9(5)
C19	18.7(6)	19.2(7)	22.8(7)	–0.3(5)	2.3(5)	0.5(5)
C16	23.4(7)	17.0(6)	30.4(8)	–3.1(5)	12.3(6)	–6.0(5)
C14	14.6(6)	26.6(7)	25.1(7)	–1.7(6)	7.0(5)	–0.3(5)
C15	17.1(6)	25.8(7)	26.8(7)	–4.5(6)	8.4(6)	–7.9(5)
C20	19.2(6)	16.8(7)	28.0(7)	7.5(5)	2.9(6)	–0.4(5)
C18	19.6(7)	23.2(7)	23.8(7)	2.6(5)	8.3(6)	5.6(5)

Table 7-4 Bond Lengths for Py(5BuPhH)Py.

Atom	Atom	Length/Å	Atom	Atom	Length/Å
N1	C6	1.3464(17)	C9	C17	1.5357(17)
N1	C2	1.3337(17)	C3	C4	1.385(2)
N2	C12	1.3463(17)	C3	C2	1.3883(19)
N2	C16	1.3354(17)	C6	C5	1.3957(18)
C11	C10	1.4029(18)	C5	C4	1.3886(19)
C11	C1	1.3938(17)	C13	C12	1.3944(18)
C11	C12	1.4900(17)	C13	C14	1.3874(18)
C7	C8	1.3945(17)	C17	C19	1.5346(19)
C7	C6	1.4877(17)	C17	C20	1.5299(18)
C7	C1	1.3954(17)	C17	C18	1.5355(19)
C10	C9	1.3937(17)	C16	C15	1.386(2)
C9	C8	1.3999(17)	C14	C15	1.383(2)

Table 7-5 Bond Angles for Py(5BuPhH)Py.

Atom	Atom	Atom	Angle/°	Atom	Atom	Atom	Angle/°
C2	N1	C6	117.73(11)	C4	C5	C6	119.16(12)
C16	N2	C12	117.91(12)	C11	C1	C7	120.56(12)
C10	C11	C12	119.91(11)	C14	C13	C12	119.29(13)
C1	C11	C10	119.10(12)	C3	C4	C5	118.96(12)
C1	C11	C12	120.98(11)	N2	C12	C11	116.05(11)
C8	C7	C6	119.75(11)	N2	C12	C13	121.79(12)
C8	C7	C1	119.15(12)	C13	C12	C11	122.15(12)
C1	C7	C6	121.05(11)	C19	C17	C9	108.96(11)
C9	C10	C11	121.54(12)	C19	C17	C18	109.63(11)
C10	C9	C8	117.92(11)	C20	C17	C9	112.29(11)
C10	C9	C17	122.91(11)	C20	C17	C19	107.71(11)
C8	C9	C17	119.17(11)	C20	C17	C18	108.33(11)
C4	C3	C2	117.93(12)	C18	C17	C9	109.87(11)
C7	C8	C9	121.69(11)	N1	C2	C3	124.14(12)
N1	C6	C7	116.38(11)	N2	C16	C15	124.04(13)
N1	C6	C5	122.07(12)	C15	C14	C13	119.06(13)
C5	C6	C7	121.51(11)	C14	C15	C16	117.91(13)

Table 7-6 Torsion Angles for Py(5BuPhH)Py.

A	B	C	D	Angle/°	A	B	C	D	Angle/°
N1	C6	C5	C4	0.5(2)	C6	C5	C4	C3	0.6(2)
N2	C16	C15	C14	0.0(2)	C1	C11	C10	C9	–0.86(19)
C11	C10	C9	C8	–0.81(19)	C1	C11	C12	N2	161.74(12)
C11	C10	C9	C17	178.07(12)	C1	C11	C12	C13	–19.50(19)
C7	C6	C5	C4	178.07(12)	C1	C7	C8	C9	–1.71(19)
C10	C11	C1	C7	1.30(19)	C1	C7	C6	N1	–152.88(12)
C10	C11	C12	N2	–19.34(18)	C1	C7	C6	C5	29.46(19)
C10	C11	C12	C13	159.42(13)	C13	C14	C15	C16	–0.4(2)
C10	C9	C8	C7	2.11(19)	C4	C3	C2	N1	0.3(2)
C10	C9	C17	C19	–126.14(13)	C12	N2	C16	C15	0.2(2)
C10	C9	C17	C20	–6.90(18)	C12	C11	C10	C9	–179.80(12)
C10	C9	C17	C18	113.74(14)	C12	C11	C1	C7	–179.78(12)
C8	C7	C6	N1	29.65(17)	C12	C13	C14	C15	0.6(2)
C8	C7	C6	C5	–148.01(13)	C17	C9	C8	C7	–176.81(12)
C8	C7	C1	C11	–0.04(19)	C2	N1	C6	C7	–178.90(12)
C8	C9	C17	C19	52.72(16)	C2	N1	C6	C5	–1.25(19)
C8	C9	C17	C20	171.96(12)	C2	C3	C4	C5	–1.1(2)
C8	C9	C17	C18	–67.41(15)	C16	N2	C12	C11	178.78(12)
C6	N1	C2	C3	0.8(2)	C16	N2	C12	C13	0.0(2)
C6	C7	C8	C9	175.82(12)	C14	C13	C12	N2	–0.4(2)
C6	C7	C1	C11	–177.53(12)	C14	C13	C12	C11	–179.11(13)

Table 7-7 Hydrogen Atom Coordinates (Å×10^4) and Isotropic Displacement Parameters (Å^2×10^3) for Py(5BuPhH)Py.

Atom	*x*	*y*	*z*	U(eq)
H10	6405.73	2098.53	4703.54	19
H3	7012.33	10346.25	2926.99	24
H8	8299.1	5208.15	4431.84	18
H5	5141.03	7574.32	3785.24	21
H1	4792.31	5408.97	3374.84	19
H13	3242.75	4618.19	3632.96	23
H4	5376.33	9754.62	3392.99	24
H2	8361.29	8760.97	2922.62	23
H19A	9611.42	4477.51	5918.47	32
H19B	10141.23	3213.09	6561.67	32
H19C	8994.86	3825.68	6663.82	32
H16	3265.06	163.48	3731.46	27
H14	1492.55	3507.57	3378.76	26
H15	1513.56	1230.11	3440.61	27
H20A	8075.94	1627.32	6197.3	34
H20B	9236.86	1098.8	6064.42	34
H20C	8049.34	945.05	5130.03	34
H18A	8928.55	2023.4	3901.5	33
H18B	10111.66	2186.73	4839.68	33
H18C	9503.49	3406.53	4173.2	33

7.3.2 Py(5PhPhH)Py

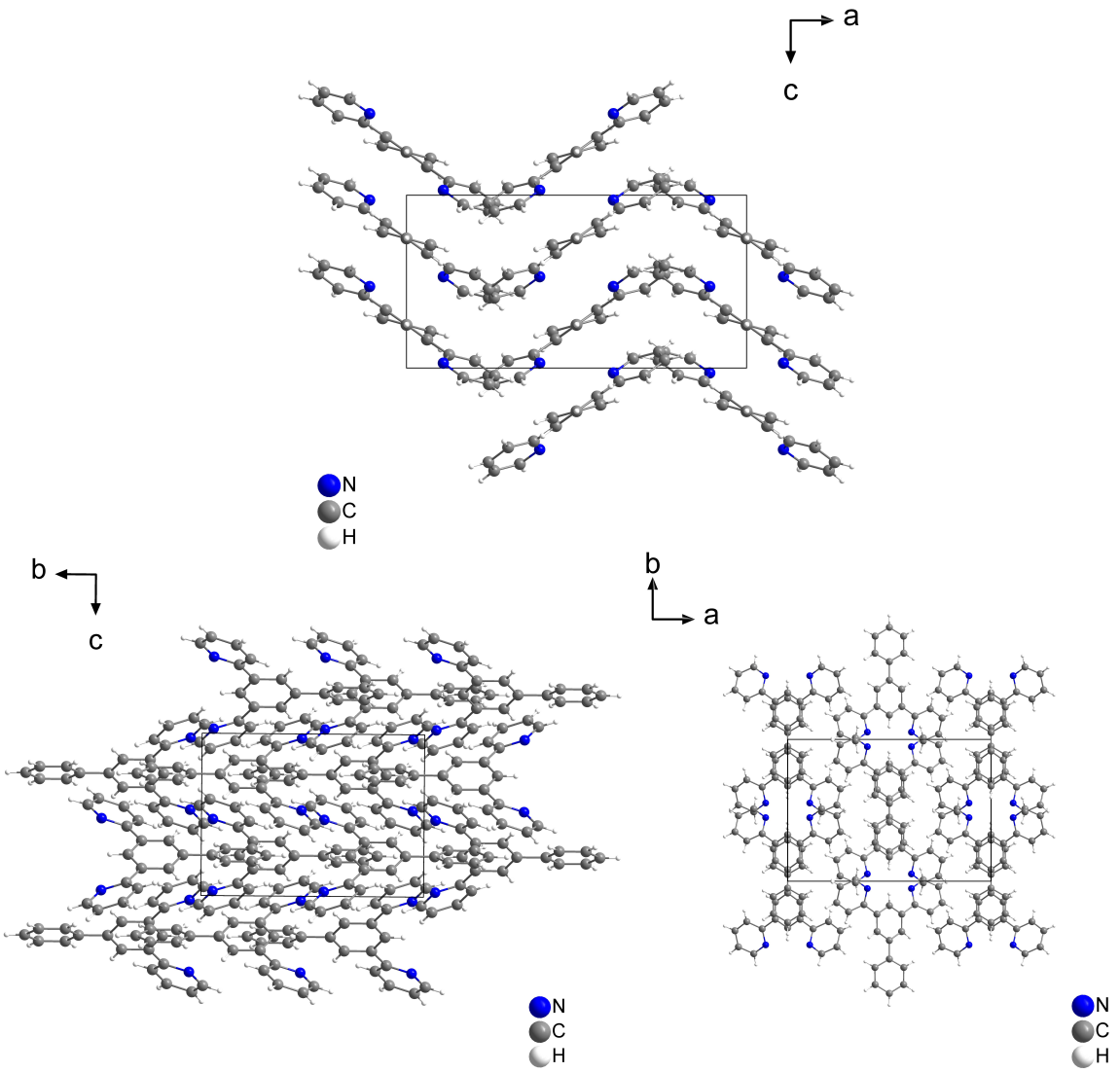

Figure 7-375 Crystal structure of Py(5PhPhH)Py viewed along the crystallographic *a*-axis (bottom left), *b*-axis (top) and *c*-axis (bottom right).

Table 7-8 Crystal data and structure refinement for Py(5PhPhH)Py.

Identification code	Py(5PhPhH)Py
Empirical formula	$C_{22}H_{16}N_2$
Formula weight	308.37
Temperature/K	293(2)
Crystal system	orthorhombic
Space group	*P*bcn
a/Å	16.2755(5)
b/Å	11.3410(3)
c/Å	8.2673(2)
α/°	90
β/°	90
γ/°	90
Volume/Å^3	1525.98(7)

Z	4
ρ_{calc}g/cm^3	1.342
μ/mm^{-1}	0.079
F(000)	648.0
Crystal size/mm^3	0.3 × 0.2 × 0.1
Radiation	MoKα (λ = 0.71073)
2Θ range for data collection/°	4.378 to 58.374
Index ranges	–22 ≤ h ≤ 22, –15 ≤ k ≤ 15, –10 ≤ l ≤ 11
Reflections collected	22441
Independent reflections	2064 [R_{int} = 0.0700, R_{sigma} = 0.0259]
Data/restraints/parameters	2064/0/112
Goodness-of-fit on F^2	1.179
Final R indexes [I>=2σ (I)]	R_1 = 0.0684, wR_2 = 0.1850
Final R indexes [all data]	R_1 = 0.0698, wR_2 = 0.1862
Largest diff. peak/hole / e Å^{-3}	0.31/–0.52

Table 7-9 Fractional Atomic Coordinates (×10^4) and Equivalent Isotropic Displacement Parameters (Å^2×10^3) for Py(5PhPhH)Py. U_{eq} is defined as 1/3 of the trace of the orthogonalized U_{IJ} tensor.

Atom	*x*	*y*	*z*	U(eq)
N1	6083.6(10)	9486.6(12)	5284(2)	37.4(4)
C1	5000	8282.0(17)	7500	25.1(4)
C7	5611.3(8)	7682.1(12)	6650.7(18)	24.3(3)
C8	5601.3(9)	6451.9(12)	6646.7(18)	26.0(3)
C5	7010.6(9)	7848.7(14)	5410(2)	29.3(4)
C6	6252.6(9)	8351.5(12)	5765.2(18)	25.3(3)
C11	4290.3(10)	3924.0(14)	7883(2)	31.3(4)
C9	5000	5828.0(17)	7500	25.0(4)
C10	5000	4514.2(18)	7500	26.8(4)
C2	6666.8(12)	10106.2(15)	4451(2)	38.8(4)
C4	7590.4(11)	8487.4(16)	4552(2)	36.7(4)
C13	5000	2096(2)	7500	45.3(7)
C12	4301.2(13)	2717.9(17)	7879(2)	43.1(5)
C3	7420.8(12)	9625.1(16)	4061(2)	39.2(4)

Table 7-10 Anisotropic Displacement Parameters (Å^2×10^3) for Py(5PhPhH)Py. The Anisotropic displacement factor exponent takes the form: $-2\pi^2[h^2a^{*2}U_{11}+2hka^*b^*U_{12}+\ldots]$.

Atom	U_{11}	U_{22}	U_{33}	U_{23}	U_{13}	U_{12}
N1	36.3(8)	29.0(7)	46.8(9)	0.2(6)	–2.9(6)	–0.5(5)
C1	24.8(9)	20.8(8)	29.7(10)	0	0.0(7)	0
C7	22.8(6)	23.3(6)	26.7(7)	1.1(5)	–0.1(5)	–0.9(5)
C8	24.5(6)	22.9(7)	30.6(7)	–1.2(5)	0.8(5)	1.1(5)
C5	26.0(7)	29.0(7)	32.9(8)	1.3(6)	2.9(5)	0.8(5)
C6	24.2(7)	24.6(7)	27.0(7)	–0.9(5)	0.4(5)	–1.8(5)
C11	30.0(7)	28.4(7)	35.4(8)	–4.0(6)	2.2(6)	–7.2(5)
C9	24.4(9)	20.7(8)	30.0(10)	0	–1.8(7)	0
C10	28.0(10)	22.1(9)	30.4(10)	0	–1.4(7)	0
C2	45.4(10)	27.1(7)	43.9(9)	5.0(6)	–9.4(8)	–4.0(7)
C4	28.3(8)	42.9(9)	39.0(9)	–0.1(7)	6.5(6)	–1.9(6)
C13	77(2)	19.4(9)	39.6(13)	0	–14.5(13)	0
C12	52.6(11)	37.8(9)	38.8(9)	0.2(7)	–3.7(8)	–20.9(8)
C3	40.4(9)	42.0(9)	35.3(8)	5.5(7)	2.9(7)	–14.5(7)

Table 7-11 Bond Lengths for Py(5PhPhH)Py.

Atom	Atom	Length/Å	Atom	Atom	Length/Å
N1	C6	1.3752(19)	C5	C4	1.385(2)
N1	C2	1.367(2)	C11	C10	1.3720(17)
C1	C7	1.3949(16)	C11	C12	1.368(2)
C1	C7[1]	1.3948(16)	C9	C10	1.490(3)
C7	C8	1.3953(19)	C2	C3	1.381(3)
C7	C6	1.4838(19)	C4	C3	1.381(3)
C8	C9	1.3986(17)	C13	C12	1.375(2)
C5	C6	1.390(2)	C13	C12[1]	1.375(2)

[1]1-X,+Y,3/2-Z

Table 7-12 Bond Angles for Py(5PhPhH)Py.

Atom	Atom	Atom	Angle/°	Atom	Atom	Atom	Angle/°
C2	N1	C6	119.21(15)	C8[1]	C9	C8	119.22(18)
C7[1]	C1	C7	121.62(18)	C8[1]	C9	C10	120.39(9)
C1	C7	C8	118.73(13)	C8	C9	C10	120.39(9)
C1	C7	C6	120.04(13)	C11[1]	C10	C11	121.6(2)
C8	C7	C6	121.24(13)	C11[1]	C10	C9	119.20(10)
C7	C8	C9	120.85(14)	C11	C10	C9	119.20(10)
C4	C5	C6	119.88(15)	N1	C2	C3	122.11(15)
N1	C6	C7	118.75(13)	C3	C4	C5	120.21(16)
N1	C6	C5	120.02(14)	C12[1]	C13	C12	118.2(2)
C5	C6	C7	121.23(13)	C11	C12	C13	121.64(17)
C12	C11	C10	118.45(16)	C4	C3	C2	118.56(16)

[1]1-X,+Y,3/2-Z

Table 7-13 Torsion Angles for Py(5PhPhH)Py.

A	B	C	D	Angle/°	A	B	C	D	Angle/°
N1	C2	C3	C4	–1.0(3)	C8	C9	C10	C11[1]	20.45(11)
C1	C7	C8	C9	–1.14(19)	C5	C4	C3	C2	0.3(3)
C1	C7	C6	N1	–23.8(2)	C6	N1	C2	C3	0.7(3)
C1	C7	C6	C5	156.64(13)	C6	C7	C8	C9	179.26(12)
C7[1]	C1	C7	C8	0.57(9)	C6	C5	C4	C3	0.6(3)
C7[1]	C1	C7	C6	–179.84(14)	C10	C11	C12	C13	–0.2(2)
C7	C8	C9	C8[1]	0.58(10)	C2	N1	C6	C7	–179.26(15)
C7	C8	C9	C10	–179.42(10)	C2	N1	C6	C5	0.3(2)
C8	C7	C6	N1	155.77(15)	C4	C5	C6	N1	–0.9(2)
C8	C7	C6	C5	–23.8(2)	C4	C5	C6	C7	178.64(15)
C8[1]	C9	C10	C11[1]	–159.55(11)	C12	C11	C10	C11[1]	0.08(12)
C8[1]	C9	C10	C11	20.45(11)	C12	C11	C10	C9	–179.92(12)
C8	C9	C10	C11	–159.55(11)	C12[1]	C13	C12	C11	0.09(12)

[1]1-X,+Y,3/2-Z

Table 7-14 Hydrogen Atom Coordinates (Å×10^4) and Isotropic Displacement Parameters (Å^2×10^3) for Py(5PhPhH)Py.

Atom	*x*	*y*	*z*	U(eq)
H1	4999.99	9102.04	7499.98	30
H8	5999.68	6041.49	6069.19	31
H5	7128.14	7084.99	5748.47	35
H11	3812.99	4334.3	8139.17	38
H2	6552.27	10876.4	4137.4	47
H4	8095.58	8148.72	4305.89	44
H13	5000.01	1275.69	7500.03	54
H12	3824.07	2308.72	8139.85	52
H3	7805.82	10058.17	3479.26	47

7.3.3 Py(4,5,6MeOPhH)Py

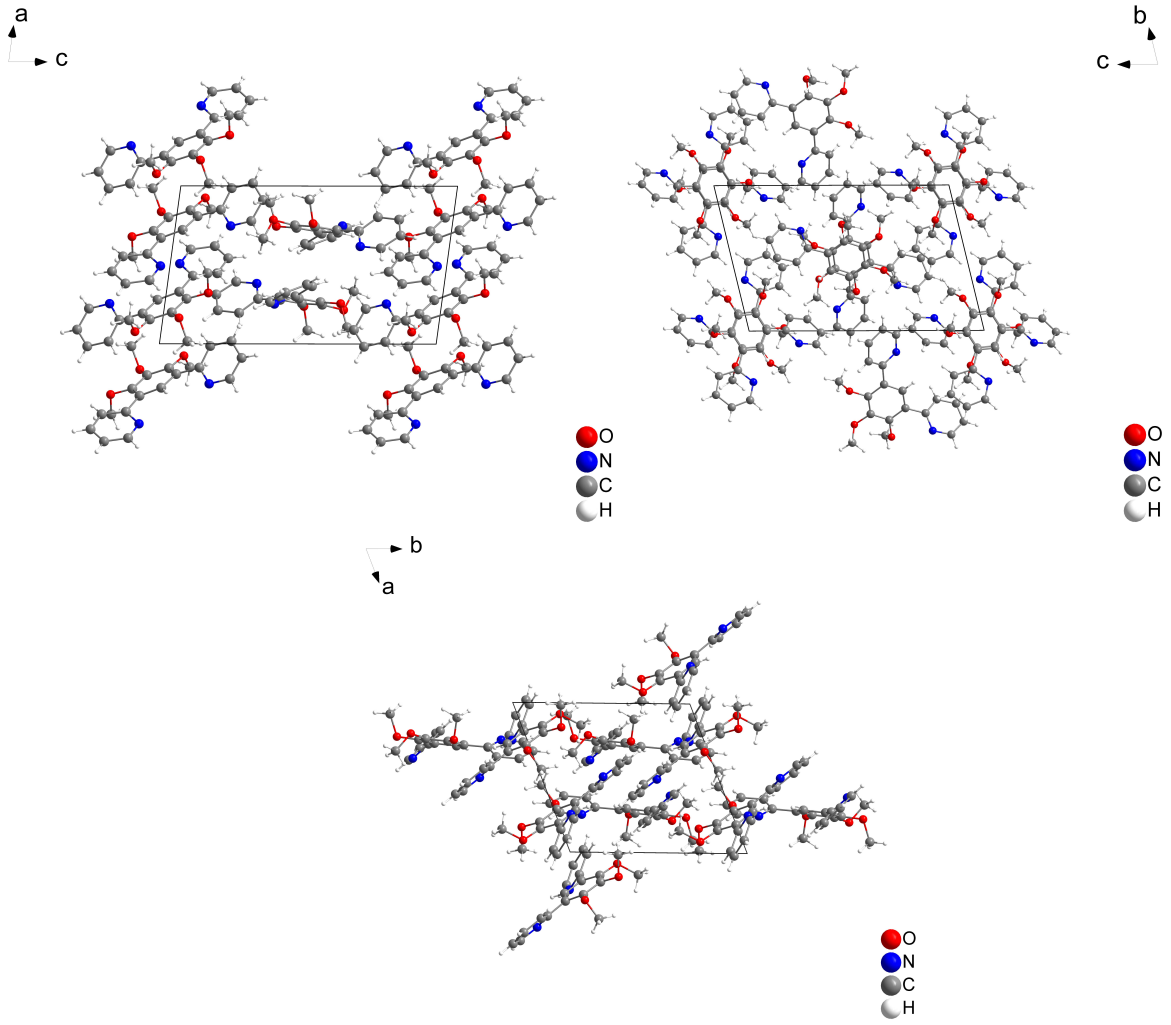

Figure 7-376 Crystal structure of Py(4,5,6MeOPhH)Py viewed along the crystallographic *a*-axis (top right), *b*-axis (top, left) and *c*-axis (bottom).

Table 7-15 Crystal data and structure refinement for Py(4,5,6MeOPhH)Py.

Identification code	2(Py(4,5,6MeOPhH)Py)
Empirical formula	$C_{19}H_{18}N_2O_3$
Formula weight	322.35

Temperature/K	100.0
Crystal system	triclinic
Space group	*P*1
a/Å	9.9774(9)
b/Å	11.2428(11)
c/Å	16.5898(17)
α/°	72.200(4)
β/°	76.003(4)
γ/°	65.595(3)
Volume/Å^3	1599.1(3)
Z	4
ρ_{calc}g/cm^3	1.339
μ/mm^{-1}	0.092
F(000)	680.0
Crystal size/mm^3	0.59 × 0.28 × 0.18
Radiation	MoKα (λ = 0.71073)
2Θ range for data collection/°	4.09 to 60.528
Index ranges	–14 ≤ h ≤ 13, –15 ≤ k ≤ 15, –23 ≤ l ≤ 23
Reflections collected	114489
Independent reflections	9416 [R_{int} = 0.0660, R_{sigma} = 0.0306]
Data/restraints/parameters	9416/0/440
Goodness-of-fit on F^2	1.120
Final R indexes [I>=2σ (I)]	R_1 = 0.0537, wR_2 = 0.1318
Final R indexes [all data]	R_1 = 0.0623, wR_2 = 0.1391
Largest diff. peak/hole / e Å^{-3}	0.91/–0.62

Table 7-16 Fractional Atomic Coordinates (×10^4) and Equivalent Isotropic Displacement Parameters (Å^2×10^3) for Py(4,5,6MeOPhH)Py. U_{eq} is defined as 1/3 of the trace of the orthogonalized U_{IJ} tensor.

Atom	*x*	*y*	*z*	U(eq)
O1	9238.5(9)	–2408.7(8)	10943.9(6)	19.32(18)
O2	8362.1(9)	–2206.2(8)	9419.4(6)	20.36(18)
O3	6780.6(9)	209.1(9)	8484.3(5)	18.31(17)
N1	7466.2(11)	859.8(10)	11994.5(6)	18.58(19)
N2	4928.2(12)	3506.3(10)	9656.0(7)	21.3(2)
C1	7214.3(12)	1210.9(11)	10282.3(7)	15.0(2)
C2	7781.4(13)	919.3(12)	12716.7(8)	21.1(2)
C3	9111.5(14)	116.3(12)	13040.4(8)	21.7(2)
C4	10170.2(13)	–799.8(12)	12593.3(8)	20.7(2)
C5	9862.5(12)	–889.0(11)	11846.4(7)	17.5(2)
C6	8493.6(12)	–36.0(11)	11563.2(7)	15.0(2)
C7	8084.4(11)	–15.6(11)	10754.4(7)	14.5(2)
C8	8457.6(11)	–1177.8(11)	10468.2(7)	15.6(2)
C9	8011.5(12)	–1073.8(11)	9705.7(7)	15.8(2)
C10	7148.3(11)	170.2(11)	9240.1(7)	15.1(2)
C11	6704.3(11)	1333.7(11)	9536.6(7)	14.35(19)
C12	5687.6(12)	2681.3(11)	9124.0(7)	15.8(2)
C13	5530.2(12)	3083.6(12)	8257.5(7)	18.5(2)
C14	4576.9(13)	4378.2(12)	7932.7(8)	21.3(2)
C15	3811.6(13)	5231.0(12)	8477.9(8)	22.1(2)
C16	4026.1(14)	4748.2(12)	9330.7(9)	24.2(2)
C17	8513.6(14)	–3365.8(12)	11213.3(9)	24.4(2)

Atom	*x*	*y*	*z*	U(eq)
C18	9844.0(17)	–2658.7(15)	8997.5(11)	34.9(3)
C19	5525.6(13)	–173.5(13)	8608.1(8)	21.8(2)
O4	2552.5(10)	5849.9(9)	6352.8(5)	19.37(17)
O5	2153.7(9)	3547.8(8)	6489.7(5)	18.77(17)
O6	2375.8(9)	2690.3(8)	5036.6(5)	17.41(17)
N3	2525.7(11)	8525.4(10)	3961.8(7)	18.6(2)
N4	3822.2(11)	3116.4(9)	3221.7(6)	17.24(19)
C20	2951.4(11)	5870.6(11)	4093.0(7)	14.5(2)
C21	2653.2(13)	9719.4(12)	3787.6(8)	20.7(2)
C22	3252.6(13)	10083.6(12)	4303.7(8)	21.2(2)
C23	3763.9(13)	9140.9(13)	5037.2(8)	20.7(2)
C24	3658.0(12)	7891.3(12)	5228.6(7)	17.2(2)
C25	3018.2(11)	7618.7(11)	4676.9(7)	14.5(2)
C26	2881.9(11)	6302.3(10)	4812.2(7)	14.14(19)
C27	2649.1(11)	5482.5(11)	5615.4(7)	14.9(2)
C28	2488.3(12)	4273.0(11)	5688.4(7)	15.2(2)
C29	2559.4(11)	3867.5(10)	4956.8(7)	14.5(2)
C30	2794.5(11)	4672.2(10)	4149.5(7)	14.09(19)
C31	2847.9(11)	4323.2(10)	3344.1(7)	14.19(19)
C32	1964.1(12)	5265.9(11)	2727.5(7)	17.8(2)
C33	2118.8(13)	4974.5(12)	1947.7(8)	20.6(2)
C34	3126.9(13)	3739.7(13)	1812.9(8)	21.3(2)
C35	3935.7(13)	2852.5(12)	2469.1(8)	20.0(2)
C36	1057.5(15)	6511.2(14)	6699.0(9)	27.7(3)
C37	3334.1(15)	2308.0(13)	6764.1(9)	26.7(3)
C38	857.4(13)	2801.2(13)	5282.4(9)	24.4(2)

Table 7-17 Anisotropic Displacement Parameters ($Å^2 \times 10^3$) for Py(4,5,6MeOPhH)Py. The Anisotropic displacement factor exponent takes the form: $-2\pi^2[h^2a^{*2}U_{11}+2hka^*b^*U_{12}+\ldots]$.

Atom	U_{11}	U_{22}	U_{33}	U_{23}	U_{13}	U_{12}
O1	17.8(4)	12.7(4)	26.1(4)	–1.3(3)	–7.5(3)	–4.0(3)
O2	20.3(4)	16.5(4)	25.6(4)	–10.3(3)	–1.5(3)	–5.0(3)
O3	19.5(4)	23.1(4)	15.5(4)	–5.9(3)	–2.5(3)	–9.8(3)
N1	18.0(4)	18.5(4)	17.4(4)	–4.7(4)	–3.6(3)	–3.8(3)
N2	24.6(5)	16.3(4)	21.5(5)	–5.3(4)	–8.4(4)	–2.5(4)
C1	14.7(4)	14.6(5)	15.6(5)	–3.2(4)	–2.8(4)	–5.1(4)
C2	23.5(5)	20.7(5)	17.4(5)	–5.2(4)	–3.6(4)	–5.7(4)
C3	26.3(6)	21.8(5)	19.1(5)	–2.2(4)	–8.5(4)	–9.6(4)
C4	18.6(5)	20.2(5)	23.3(6)	–1.3(4)	–8.9(4)	–6.6(4)
C5	14.6(5)	17.2(5)	20.6(5)	–3.6(4)	–3.3(4)	–5.8(4)
C6	15.3(4)	14.6(4)	15.6(5)	–2.3(4)	–3.0(4)	–6.4(4)
C7	12.6(4)	15.5(5)	15.6(5)	–3.2(4)	–2.6(3)	–5.1(4)
C8	12.7(4)	14.6(5)	18.0(5)	–2.7(4)	–2.6(4)	–4.1(4)
C9	15.2(4)	14.8(5)	17.8(5)	–6.0(4)	–0.6(4)	–5.2(4)
C10	14.0(4)	16.9(5)	15.3(5)	–4.8(4)	–1.3(4)	–6.3(4)
C11	14.1(4)	14.6(4)	14.0(5)	–2.7(4)	–2.1(3)	–5.3(4)
C12	15.8(4)	15.5(5)	16.5(5)	–1.9(4)	–4.2(4)	–6.4(4)
C13	17.2(5)	20.3(5)	16.3(5)	–1.7(4)	–3.3(4)	–6.7(4)
C14	18.5(5)	23.5(6)	19.4(5)	2.0(4)	–5.5(4)	–8.4(4)
C15	19.2(5)	16.9(5)	27.3(6)	0.9(4)	–8.3(4)	–5.4(4)
C16	26.4(6)	16.5(5)	27.2(6)	–5.8(4)	–10.0(5)	–1.4(4)

Atom	U_{11}	U_{22}	U_{33}	U_{23}	U_{13}	U_{12}
C17	26.7(6)	17.7(5)	28.8(6)	0.9(4)	–6.7(5)	–11.0(4)
C18	32.1(7)	28.3(7)	41.0(8)	–19.9(6)	12.9(6)	–9.2(5)
C19	19.7(5)	24.5(6)	25.8(6)	–8.9(5)	–5.6(4)	–9.0(4)
O4	24.2(4)	22.6(4)	14.6(4)	–6.6(3)	–3.9(3)	–9.5(3)
O5	21.4(4)	15.9(4)	15.2(4)	–0.7(3)	–1.5(3)	–5.8(3)
O6	17.6(4)	13.3(4)	22.2(4)	–5.5(3)	0.0(3)	–7.0(3)
N3	21.5(4)	15.0(4)	20.9(5)	–2.1(4)	–8.0(4)	–7.1(3)
N4	18.0(4)	15.1(4)	19.0(4)	–6.5(3)	–3.3(3)	–4.2(3)
C20	15.0(4)	14.6(5)	14.4(5)	–3.4(4)	–2.8(3)	–5.3(4)
C21	23.7(5)	15.4(5)	23.9(6)	–1.9(4)	–7.4(4)	–7.4(4)
C22	23.8(5)	18.0(5)	25.3(6)	–7.9(4)	–0.4(4)	–10.5(4)
C23	23.1(5)	26.5(6)	20.4(5)	–10.2(4)	–0.1(4)	–14.8(4)
C24	17.1(5)	21.2(5)	16.6(5)	–6.3(4)	–2.5(4)	–8.9(4)
C25	13.5(4)	14.6(4)	16.3(5)	–4.9(4)	–2.6(3)	–4.8(4)
C26	13.5(4)	13.7(4)	16.3(5)	–4.3(4)	–3.7(3)	–4.5(3)
C27	14.7(4)	16.0(5)	15.0(5)	–4.7(4)	–3.9(4)	–4.7(4)
C28	15.2(4)	14.4(5)	14.6(5)	–2.4(4)	–2.6(4)	–4.4(4)
C29	14.0(4)	12.1(4)	17.5(5)	–4.7(4)	–1.5(4)	–4.2(3)
C30	13.1(4)	13.3(4)	15.8(5)	–5.1(4)	–2.4(3)	–3.3(3)
C31	14.1(4)	13.7(4)	16.1(5)	–4.7(4)	–1.5(3)	–5.9(4)
C32	17.1(5)	15.7(5)	20.1(5)	–6.0(4)	–4.4(4)	–3.5(4)
C33	20.6(5)	22.1(5)	19.5(5)	–5.1(4)	–6.6(4)	–6.0(4)
C34	23.4(5)	24.6(6)	19.0(5)	–9.8(4)	–3.2(4)	–8.3(4)
C35	20.6(5)	18.4(5)	21.9(5)	–10.0(4)	–2.6(4)	–4.2(4)
C36	29.7(6)	31.2(7)	24.1(6)	–16.1(5)	2.9(5)	–9.8(5)
C37	27.6(6)	20.6(6)	23.0(6)	2.7(5)	–6.8(5)	–3.9(5)
C38	18.3(5)	21.3(5)	35.2(7)	–6.7(5)	–2.3(5)	–9.5(4)

Table 7-18 Bond Lengths for Py(4,5,6MeOPhH)Py.

Atom	Atom	Length/Å	Atom	Atom	Length/Å
O1	C8	1.3725(13)	O4	C27	1.3768(13)
O1	C17	1.4399(14)	O4	C36	1.4275(15)
O2	C9	1.3748(13)	O5	C28	1.3751(13)
O2	C18	1.4249(16)	O5	C37	1.4325(14)
O3	C10	1.3727(13)	O6	C29	1.3726(12)
O3	C19	1.4359(14)	O6	C38	1.4330(14)
N1	C2	1.3371(15)	N3	C21	1.3371(15)
N1	C6	1.3453(14)	N3	C25	1.3479(14)
N2	C12	1.3452(15)	N4	C31	1.3454(13)
N2	C16	1.3366(15)	N4	C35	1.3379(15)
C1	C7	1.3957(14)	C20	C26	1.3966(14)
C1	C11	1.3967(14)	C20	C30	1.3923(14)
C2	C3	1.3867(17)	C21	C22	1.3867(16)
C3	C4	1.3842(18)	C22	C23	1.3890(18)
C4	C5	1.3875(16)	C23	C24	1.3854(16)
C5	C6	1.3994(15)	C24	C25	1.3982(14)
C6	C7	1.4853(15)	C25	C26	1.4858(14)
C7	C8	1.4012(15)	C26	C27	1.3983(15)
C8	C9	1.3966(15)	C27	C28	1.3999(15)
C9	C10	1.4002(15)	C28	C29	1.3985(15)

Atom	Atom	Length/Å	Atom	Atom	Length/Å
C10	C11	1.3994(15)	C29	C30	1.3964(15)
C11	C12	1.4915(15)	C30	C31	1.4870(14)
C12	C13	1.3959(15)	C31	C32	1.3959(15)
C13	C14	1.3921(16)	C32	C33	1.3878(16)
C14	C15	1.3826(18)	C33	C34	1.3842(17)
C15	C16	1.3868(18)	C34	C35	1.3882(17)

Table 7-19 Bond Angles for Py(4,5,6MeOPhH)Py.

Atom	Atom	Atom	Angle/°	Atom	Atom	Atom	Angle/°
C8	O1	C17	115.25(9)	C27	O4	C36	112.91(9)
C9	O2	C18	112.93(10)	C28	O5	C37	114.15(9)
C10	O3	C19	112.51(9)	C29	O6	C38	112.70(8)
C2	N1	C6	118.05(10)	C21	N3	C25	118.17(10)
C16	N2	C12	118.18(10)	C35	N4	C31	117.12(10)
C7	C1	C11	123.05(10)	C30	C20	C26	122.62(10)
N1	C2	C3	123.58(11)	N3	C21	C22	123.79(11)
C4	C3	C2	118.28(11)	C21	C22	C23	117.65(11)
C3	C4	C5	119.18(10)	C24	C23	C22	119.73(10)
C4	C5	C6	118.81(10)	C23	C24	C25	118.67(11)
N1	C6	C5	122.10(10)	N3	C25	C24	121.98(10)
N1	C6	C7	114.99(9)	N3	C25	C26	114.99(9)
C5	C6	C7	122.88(10)	C24	C25	C26	122.99(10)
C1	C7	C6	118.34(9)	C20	C26	C25	118.04(10)
C1	C7	C8	118.41(10)	C20	C26	C27	117.79(10)
C8	C7	C6	123.14(10)	C27	C26	C25	124.14(9)
O1	C8	C7	119.85(10)	O4	C27	C26	121.04(10)
O1	C8	C9	120.56(10)	O4	C27	C28	118.34(10)
C9	C8	C7	119.58(10)	C26	C27	C28	120.62(10)
O2	C9	C8	120.23(10)	O5	C28	C27	118.57(10)
O2	C9	C10	118.84(10)	O5	C28	C29	120.92(10)
C8	C9	C10	120.87(10)	C29	C28	C27	120.34(10)
O3	C10	C9	117.97(9)	O6	C29	C28	119.81(10)
O3	C10	C11	121.63(10)	O6	C29	C30	120.37(9)
C11	C10	C9	120.39(10)	C30	C29	C28	119.82(10)
C1	C11	C10	117.58(10)	C20	C30	C29	118.81(10)
C1	C11	C12	118.11(9)	C20	C30	C31	118.30(9)
C10	C11	C12	124.29(10)	C29	C30	C31	122.87(9)
N2	C12	C11	114.45(10)	N4	C31	C30	117.70(9)
N2	C12	C13	121.73(10)	N4	C31	C32	122.40(10)
C13	C12	C11	123.82(10)	C32	C31	C30	119.81(9)
C14	C13	C12	119.17(11)	C33	C32	C31	119.30(10)
C15	C14	C13	119.04(11)	C34	C33	C32	118.72(11)
C14	C15	C16	118.06(11)	C33	C34	C35	118.02(11)
N2	C16	C15	123.80(12)	N4	C35	C34	124.40(10)

Table 7-20 Torsion Angles for Py(4,5,6MeOPhH)Py.

A	B	C	D	Angle/°	A	B	C	D	Angle/°
O1	C8	C9	O2	–0.54(16)	O4	C27	C28	O5	3.84(15)
O1	C8	C9	C10	176.64(10)	O4	C27	C28	C29	179.19(9)

A	B	C	D	Angle/°	A	B	C	D	Angle/°
O2	C9	C10	O3	–4.50(15)	O5	C28	C29	O6	–3.69(15)
O2	C9	C10	C11	176.61(10)	O5	C28	C29	C30	175.36(9)
O3	C10	C11	C1	–175.76(9)	O6	C29	C30	C20	178.94(9)
O3	C10	C11	C12	6.25(16)	O6	C29	C30	C31	0.51(15)
N1	C2	C3	C4	–0.18(19)	N3	C21	C22	C23	0.83(19)
N1	C6	C7	C1	33.15(14)	N3	C25	C26	C20	29.21(14)
N1	C6	C7	C8	–143.07(11)	N3	C25	C26	C27	–149.03(11)
N2	C12	C13	C14	0.84(17)	N4	C31	C32	C33	–1.99(17)
C1	C7	C8	O1	–176.24(9)	C20	C26	C27	O4	–179.31(9)
C1	C7	C8	C9	2.85(15)	C20	C26	C27	C28	–0.17(15)
C1	C11	C12	N2	–23.98(14)	C20	C30	C31	N4	126.32(11)
C1	C11	C12	C13	155.27(11)	C20	C30	C31	C32	–50.15(14)
C2	N1	C6	C5	–0.21(17)	C21	N3	C25	C24	–0.43(17)
C2	N1	C6	C7	–178.22(10)	C21	N3	C25	C26	–178.16(10)
C2	C3	C4	C5	–0.45(18)	C21	C22	C23	C24	–0.18(17)
C3	C4	C5	C6	0.72(17)	C22	C23	C24	C25	–0.69(17)
C4	C5	C6	N1	–0.40(17)	C23	C24	C25	N3	1.03(17)
C4	C5	C6	C7	177.45(10)	C23	C24	C25	C26	178.58(10)
C5	C6	C7	C1	–144.84(11)	C24	C25	C26	C20	–148.50(11)
C5	C6	C7	C8	38.94(16)	C24	C25	C26	C27	33.27(16)
C6	N1	C2	C3	0.51(18)	C25	N3	C21	C22	–0.53(18)
C6	C7	C8	O1	–0.01(16)	C25	C26	C27	O4	–1.07(16)
C6	C7	C8	C9	179.07(10)	C25	C26	C27	C28	178.07(10)
C7	C1	C11	C10	–2.69(16)	C26	C20	C30	C29	–0.05(16)
C7	C1	C11	C12	175.43(10)	C26	C20	C30	C31	178.45(9)
C7	C8	C9	O2	–179.62(10)	C26	C27	C28	O5	–175.33(9)
C7	C8	C9	C10	–2.44(16)	C26	C27	C28	C29	0.03(16)
C8	C9	C10	O3	178.29(9)	C27	C28	C29	O6	–178.93(9)
C8	C9	C10	C11	–0.61(16)	C27	C28	C29	C30	0.12(16)
C9	C10	C11	C1	3.09(15)	C28	C29	C30	C20	–0.10(15)
C9	C10	C11	C12	–174.90(10)	C28	C29	C30	C31	–178.53(9)
C10	C11	C12	N2	154.00(11)	C29	C30	C31	N4	–55.24(14)
C10	C11	C12	C13	–26.75(17)	C29	C30	C31	C32	128.28(11)
C11	C1	C7	C6	–176.68(10)	C30	C20	C26	C25	–178.16(9)
C11	C1	C7	C8	–0.28(16)	C30	C20	C26	C27	0.19(15)
C11	C12	C13	C14	–178.36(10)	C30	C31	C32	C33	174.31(10)
C12	N2	C16	C15	0.89(19)	C31	N4	C35	C34	0.44(18)
C12	C13	C14	C15	0.01(17)	C31	C32	C33	C34	1.40(18)
C13	C14	C15	C16	–0.38(18)	C32	C33	C34	C35	–0.03(18)
C14	C15	C16	N2	–0.1(2)	C33	C34	C35	N4	–0.95(19)
C16	N2	C12	C11	178.00(10)	C35	N4	C31	C30	–175.32(10)
C16	N2	C12	C13	–1.27(17)	C35	N4	C31	C32	1.05(16)
C17	O1	C8	C7	121.29(11)	C36	O4	C27	C26	95.49(12)
C17	O1	C8	C9	–57.79(14)	C36	O4	C27	C28	–83.67(13)
C18	O2	C9	C8	–80.45(14)	C37	O5	C28	C27	–111.00(12)
C18	O2	C9	C10	102.32(13)	C37	O5	C28	C29	73.67(13)
C19	O3	C10	C9	81.84(12)	C38	O6	C29	C28	75.35(13)
C19	O3	C10	C11	–99.28(12)	C38	O6	C29	C30	–103.70(12)

Table 7-21 Hydrogen Atom Coordinates (Å×10^4) and Isotropic Displacement Parameters (Å^2×10^3) for Py(4,5,6MeOPhH)Py.

Atom	*x*	*y*	*z*	U(eq)
H1	6956.99	1998.95	10477.3	18
H2	7054.39	1545.94	13024.98	25
H3	9291.44	193.03	13555.69	26
H4	11096.1	–1360.63	12795.39	25
H5	10568.46	–1517.78	11532.88	21
H13	6066.86	2481.37	7894.07	22
H14	4454.04	4671.4	7344.87	26
H15	3157.83	6121.73	8274.2	26
H16	3501.45	5334.1	9705.5	29
H17A	8899.41	–3970.25	10823.51	37
H17B	7441.39	–2888.79	11206.16	37
H17C	8706.78	–3889.64	11793.74	37
H18A	9975.36	–1952.39	8500.81	52
H18B	10034.05	–3466.05	8809.01	52
H18C	10541.93	–2868.73	9392.58	52
H19A	5284.37	–98.66	8051.69	33
H19B	4671.1	420.64	8915.51	33
H19C	5764.74	–1103.48	8941.69	33
H20	3112.1	6416.34	3543.2	17
H21	2313.54	10354.96	3280.92	25
H22	3311.36	10947.52	4160.7	25
H23	4184.52	9352.02	5406.16	25
H24	4012.86	7233	5724.67	21
H32	1264.1	6098.28	2840.57	21
H33	1543.96	5610.14	1514.63	25
H34	3261.36	3506.27	1286.9	26
H35	4615.48	2000.68	2377.63	24
H36A	590.95	7339.63	6285.42	42
H36B	1052.83	6729.71	7228.28	42
H36C	502.51	5918.3	6820.82	42
H37A	3618.93	1751.72	6351.82	40
H37B	2999.84	1830.22	7326.11	40
H37C	4190.98	2493.82	6802.2	40
H38A	238.33	3563.44	4887.36	37
H38B	526	2942.28	5863.66	37
H38C	769.28	1973.55	5264.21	37

7.3.4 [Ni(Py(5CF$_3$Ph)Py)Br]

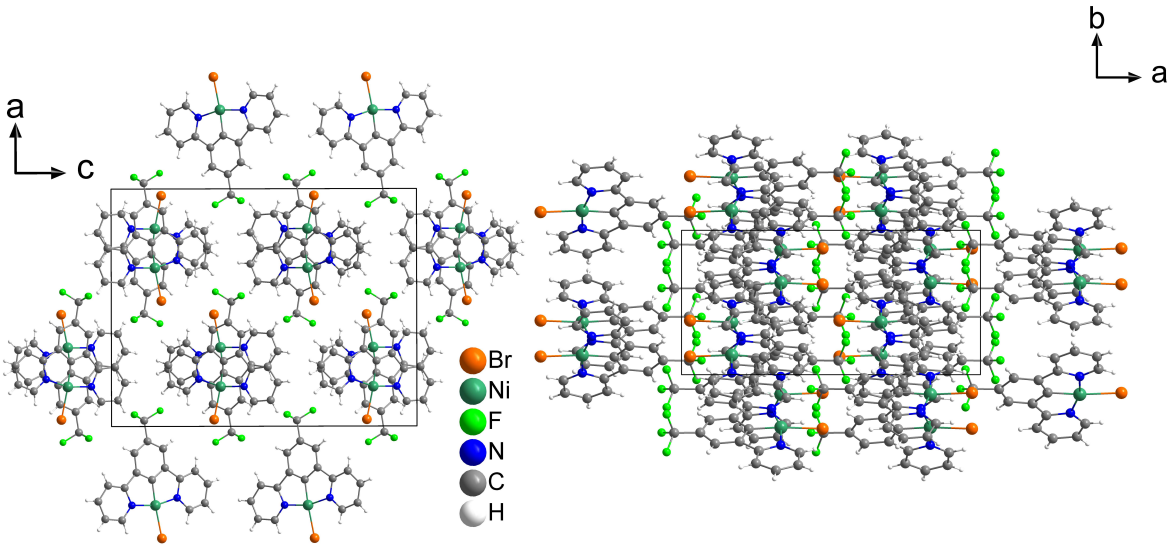

Figure 7-377 Crystal structure of [Ni(Py(5CF$_3$Ph)Py)Br] viewed along the crystallographic *b*-axis (left) and *c*-axis (right).

Table 7-22 Crystal data and structure refinement for [Ni(Py(5CF$_3$Ph)Py)Br].

Identification code	[Ni(Py(5CF$_3$Ph)Py)Br]
Empirical formula	$C_{17}H_{10}BrF_3N_2Ni$
Formula weight	437.89
Temperature/K	293(2)
Crystal system	orthorhombic
Space group	*P*bca
a/Å	16.7845(10)
b/Å	8.1115(4)
c/Å	21.5990(9)
α/°	90
β/°	90
γ/°	90
Volume/Å^3	2940.6(3)
Z	8
ρ_{calc}g/cm^3	1.978
μ/mm^{-1}	4.071
F(000)	1728.0
Crystal size/mm^3	0.2 × 0.3 × 0.3
Radiation	MoKα (λ = 0.71073)
2Θ range for data collection/°	3.772 to 53.752
Index ranges	–21 ≤ h ≤ 21, –10 ≤ k ≤ 10, –25 ≤ l ≤ 27
Reflections collected	31791
Independent reflections	3149 [R_{int} = 0.2621, R_{sigma} = 0.1094]
Data/restraints/parameters	3149/0/218
Goodness-of-fit on F^2	0.885
Final R indexes [I>=2σ (I)]	R_1 = 0.0547, wR_2 = 0.1234
Final R indexes [all data]	R_1 = 0.1256, wR_2 = 0.1529
Largest diff. peak/hole / e Å^{-3}	0.78/–0.82

Table 7-23 Fractional Atomic Coordinates (×10^4) and Equivalent Isotropic Displacement Parameters (Å^2×10^3) for [Ni(Py(5CF$_3$Ph)Py)Br]. U_{eq} is defined as 1/3 of the trace of the orthogonalized U_{IJ}.

Atom	*x*	*y*	*z*	U(eq)
Br1	9716.7(5)	6258.3(12)	6640.2(4)	45.0(3)
Ni1	8325.1(5)	6360.0(13)	6428.7(4)	31.6(3)
F3	4500(3)	4641(6)	5759(2)	50.0(12)
F1	4333(3)	5998(7)	6592(2)	58.4(14)
F2	4504(3)	7255(6)	5736(3)	60.4(15)
N2	8320(4)	5124(8)	5659(3)	33.6(14)
N1	8009(4)	7652(8)	7140(3)	32.1(14)
C7	6744(4)	6993(9)	6743(3)	29.6(15)
C12	7585(4)	4731(10)	5423(3)	32.3(17)
C2	8505(5)	8391(9)	7543(3)	34.5(17)
C10	6118(4)	5230(9)	5748(3)	33.1(17)
C9	5625(4)	5994(9)	6175(3)	32.3(17)
C1	7247(4)	6239(10)	6322(3)	32.1(15)
C13	7488(5)	3862(11)	4882(3)	34.0(16)
C14	8157(5)	3371(10)	4560(3)	40(2)
C11	6945(5)	5376(10)	5816(3)	33.7(17)
C6	7202(5)	7816(10)	7236(3)	35.4(17)
C8	5935(4)	6854(9)	6684(3)	34.2(17)
C15	8900(5)	3744(10)	4787(3)	38.8(17)
C5	6886(4)	8688(10)	7730(3)	35.6(16)
C17	4751(5)	5976(10)	6069(3)	36.6(18)
C3	8228(5)	9282(10)	8049(3)	39.2(19)
C16	8951(5)	4604(10)	5338(4)	39.6(19)
C4	7418(5)	9414(10)	8140(4)	39.6(19)

Table 7-24 Anisotropic Displacement Parameters (Å^2×10^3) for [Ni(Py(5CF$_3$Ph)Py)Br]. The Anisotropic displacement factor exponent takes the form: $-2\pi^2[h^2a^{*2}U_{11}+2hka^*b^*U_{12}+\ldots]$.

Atom	U_{11}	U_{22}	U_{33}	U_{23}	U_{13}	U_{12}
Br1	43.3(5)	52.5(5)	39.1(4)	–3.7(4)	–0.4(3)	3.0(4)
Ni1	37.3(5)	34.3(5)	23.1(4)	0.8(4)	0.4(4)	0.7(5)
F3	51(3)	47(3)	53(3)	–16(2)	–7(2)	2(2)
F1	44(3)	93(4)	39(3)	–15(3)	8(2)	–10(3)
F2	47(3)	49(3)	85(4)	24(3)	–13(3)	1(3)
N2	39(4)	34(4)	28(3)	6(3)	3(3)	1(3)
N1	39(4)	37(4)	20(3)	3(3)	–3(3)	–4(3)
C7	36(4)	29(4)	24(3)	6(3)	–1(3)	–4(3)
C12	44(4)	31(4)	21(4)	3(3)	5(3)	3(3)
C2	38(4)	35(4)	31(4)	3(3)	3(3)	5(4)
C10	41(4)	31(4)	27(4)	5(3)	–3(3)	0(3)
C9	35(4)	35(4)	28(4)	4(3)	–1(3)	4(3)
C1	36(4)	31(4)	30(3)	4(4)	3(3)	1(4)
C13	43(4)	27(4)	32(3)	–5(4)	–1(3)	2(3)
C14	61(5)	36(5)	24(3)	–8(3)	1(3)	7(4)
C11	46(4)	36(4)	20(3)	–1(3)	–2(3)	3(4)
C6	41(4)	36(4)	30(4)	9(3)	–4(3)	–2(4)
C8	37(4)	38(4)	28(4)	0(3)	1(3)	0(3)
C15	51(5)	31(4)	34(4)	–4(4)	16(3)	6(4)
C5	42(4)	39(4)	26(3)	–4(4)	–1(3)	1(4)

Atom	U_{11}	U_{22}	U_{33}	U_{23}	U_{13}	U_{12}
C17	43(4)	37(5)	29(4)	0(3)	1(3)	0(4)
C3	51(5)	38(4)	29(4)	–3(3)	–1(3)	–3(4)
C16	45(5)	40(5)	34(4)	5(3)	1(4)	–2(4)
C4	48(5)	43(5)	28(4)	–5(3)	2(3)	3(4)

Table 7-25 Bond Lengths for [Ni(Py(5CF_3Ph)Py)Br].

Atom	Atom	Length/Å	Atom	Atom	Length/Å
Br1	Ni1	2.3815(12)	C12	C13	1.375(10)
Ni1	N2	1.941(6)	C12	C11	1.465(10)
Ni1	N1	1.933(6)	C2	C3	1.390(10)
Ni1	C1	1.826(7)	C10	C9	1.385(10)
F3	C17	1.342(9)	C10	C11	1.400(11)
F1	C17	1.330(8)	C9	C8	1.403(10)
F2	C17	1.329(9)	C9	C17	1.484(10)
N2	C12	1.374(9)	C1	C11	1.393(10)
N2	C16	1.334(10)	C13	C14	1.379(10)
N1	C2	1.346(9)	C14	C15	1.374(11)
N1	C6	1.376(10)	C6	C5	1.385(10)
C7	C1	1.384(10)	C15	C16	1.383(11)
C7	C6	1.475(10)	C5	C4	1.388(10)
C7	C8	1.368(10)	C3	C4	1.378(11)

Table 7-26 Bond Angles for [Ni(Py(5CF_3Ph)Py)Br].

Atom	Atom	Atom	Angle/°	Atom	Atom	Atom	Angle/°
N2	Ni1	Br1	98.64(19)	C7	C1	Ni1	119.9(5)
N1	Ni1	Br1	97.81(18)	C7	C1	C11	121.0(7)
N1	Ni1	N2	163.5(3)	C11	C1	Ni1	119.1(5)
C1	Ni1	Br1	173.7(2)	C12	C13	C14	118.7(7)
C1	Ni1	N2	82.0(3)	C15	C14	C13	119.7(7)
C1	Ni1	N1	81.8(3)	C10	C11	C12	129.4(7)
C12	N2	Ni1	116.2(5)	C1	C11	C12	111.5(7)
C16	N2	Ni1	127.2(5)	C1	C11	C10	119.0(7)
C16	N2	C12	116.6(6)	N1	C6	C7	111.1(6)
C2	N1	Ni1	125.9(5)	N1	C6	C5	122.9(7)
C2	N1	C6	117.9(6)	C5	C6	C7	126.0(7)
C6	N1	Ni1	116.3(5)	C7	C8	C9	118.8(7)
C1	C7	C6	110.9(6)	C14	C15	C16	118.4(7)
C8	C7	C1	120.6(7)	C6	C5	C4	117.5(7)
C8	C7	C6	128.4(7)	F3	C17	C9	113.3(7)
N2	C12	C13	122.8(7)	F1	C17	F3	105.6(6)
N2	C12	C11	111.1(6)	F1	C17	C9	113.0(6)
C13	C12	C11	126.1(7)	F2	C17	F3	105.1(6)
N1	C2	C3	122.3(7)	F2	C17	F1	106.5(7)
C9	C10	C11	119.0(7)	F2	C17	C9	112.6(7)
C10	C9	C8	121.5(7)	C4	C3	C2	118.8(7)
C10	C9	C17	119.0(7)	N2	C16	C15	123.9(8)
C8	C9	C17	119.5(7)	C3	C4	C5	120.7(7)

Table 7-27 Torsion Angles for [Ni(Py(5CF$_3$Ph)Py)Br].

A	B	C	D	Angle/°	A	B	C	D	Angle/°
Ni1	N2	C12	C13	180.0(6)	C10	C9	C17	F2	–89.2(9)
Ni1	N2	C12	C11	0.7(8)	C9	C10	C11	C12	–178.2(7)
Ni1	N2	C16	C15	–179.1(6)	C9	C10	C11	C1	2.1(11)
Ni1	N1	C2	C3	–179.1(6)	C1	C7	C6	N1	1.6(9)
Ni1	N1	C6	C7	–2.4(8)	C1	C7	C6	C5	179.9(7)
Ni1	N1	C6	C5	179.2(6)	C1	C7	C8	C9	–2.8(11)
Ni1	C1	C11	C12	–2.2(9)	C13	C12	C11	C10	1.9(13)
Ni1	C1	C11	C10	177.6(6)	C13	C12	C11	C1	–178.4(8)
N2	Ni1	C1	C7	–178.2(6)	C13	C14	C15	C16	0.2(12)
N2	Ni1	C1	C11	2.1(6)	C14	C15	C16	N2	–1.3(12)
N2	C12	C13	C14	–0.5(12)	C11	C12	C13	C14	178.7(7)
N2	C12	C11	C10	–178.9(7)	C11	C10	C9	C8	–2.4(11)
N2	C12	C11	C1	0.9(9)	C11	C10	C9	C17	174.2(7)
N1	Ni1	C1	C7	–1.0(6)	C6	N1	C2	C3	0.7(11)
N1	Ni1	C1	C11	179.3(6)	C6	C7	C1	Ni1	0.0(8)
N1	C2	C3	C4	0.0(12)	C6	C7	C1	C11	179.7(7)
N1	C6	C5	C4	–0.3(12)	C6	C7	C8	C9	–179.3(7)
C7	C1	C11	C12	178.0(7)	C6	C5	C4	C3	1.0(12)
C7	C1	C11	C10	–2.2(11)	C8	C7	C1	Ni1	–177.1(6)
C7	C6	C5	C4	–178.4(7)	C8	C7	C1	C11	2.6(11)
C12	N2	C16	C15	1.4(11)	C8	C7	C6	N1	178.4(7)
C12	C13	C14	C15	0.6(12)	C8	C7	C6	C5	–3.3(13)
C2	N1	C6	C7	177.8(6)	C8	C9	C17	F3	–153.5(7)
C2	N1	C6	C5	–0.6(11)	C8	C9	C17	F1	–33.4(10)
C2	C3	C4	C5	–0.9(12)	C8	C9	C17	F2	87.4(8)
C10	C9	C8	C7	2.8(11)	C17	C9	C8	C7	–173.8(7)
C10	C9	C17	F3	29.9(10)	C16	N2	C12	C13	–0.5(11)
C10	C9	C17	F1	150.0(7)	C16	N2	C12	C11	–179.8(6)

Table 7-28 Hydrogen Atom Coordinates (Å×10^4) and Isotropic Displacement Parameters (Å^2×10^3) for [Ni(Py(5CF$_3$Ph)Py)Br].

Atom	*x*	*y*	*z*	U(eq)
H2	9051.4	8302.27	7481.31	41
H10	5903.84	4630.04	5421.38	40
H13	6981.4	3608.91	4735.43	41
H14	8105.43	2791.15	4190.54	48
H8	5597.39	7320.68	6977.04	41
H15	9357.48	3426.27	4575.18	47
H5	6338.69	8784.73	7784.2	43
H3	8583.23	9781.86	8320.59	47
H16	9455.51	4834.43	5494.79	47
H4	7225.58	9993.76	8479.76	48

7.3.5 [Ni(Py(5BuPh)Py)Br]

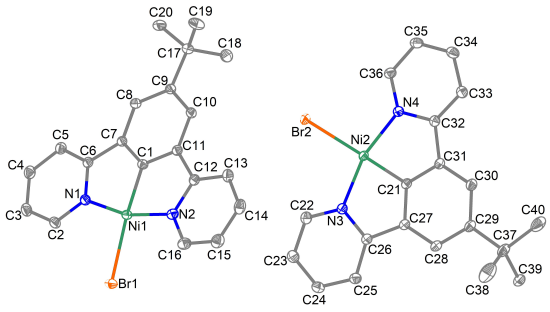

Figure 7-378 Asymmetric unit of [Ni(Py(5BuPh)Py)Br]. Ellipsoids are shown with a 50% probability. Hydrogen atoms are omitted for clarity.

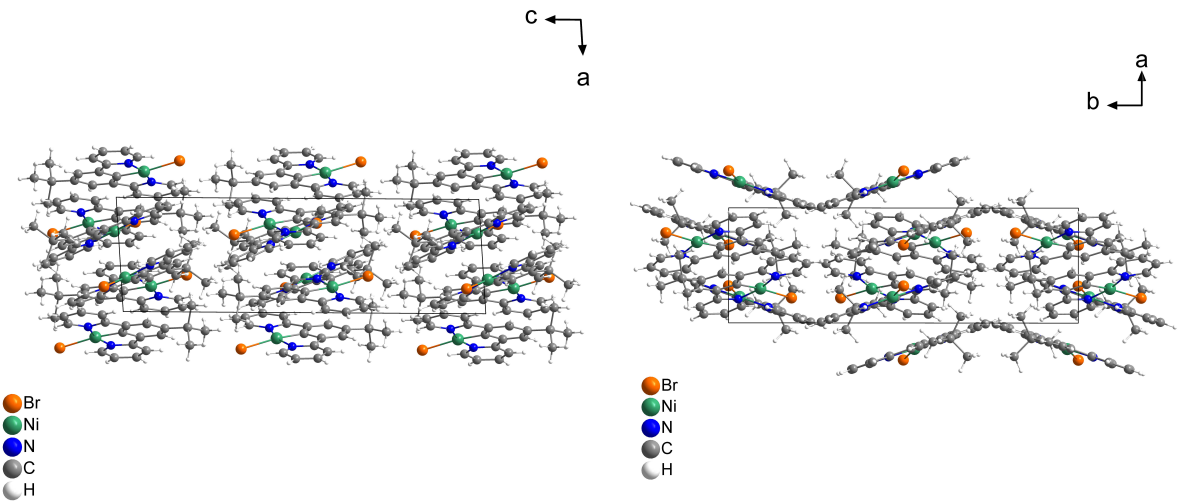

Figure 7-379 Crystal structure of [Ni(Py(5BuPh)Py)Br] viewed along the crystallographic *b*-axis (left) and *c*-axis (right).

Table 7-29 Crystal data and structure refinement for [Ni(Py(5BuPh)Py)Br].

Identification code	[Ni(Py(5BuPh)Py)Br]
Empirical formula	$C_{20}H_{19}BrN_2Ni$
Formula weight	425.99
Temperature/K	100.0
Crystal system	monoclinic
Space group	$P2_1/c$
a/Å	7.0878(4)
b/Å	21.5386(14)
c/Å	22.4093(15)
α/°	90
β/°	93.866(2)
γ/°	90
Volume/Å^3	3413.2(4)
Z	8
ρ_{calc}g/cm^3	1.658
μ/mm^{-1}	3.481
F(000)	1728.0
Crystal size/mm^3	0.22 × 0.11 × 0.04
Radiation	MoKα (λ = 0.71073)

2Θ range for data collection/°	4.104 to 70.192
Index ranges	–11 ≤ h ≤ 11, –34 ≤ k ≤ 34, –36 ≤ l ≤ 36
Reflections collected	249355
Independent reflections	15097 [R_{int} = 0.0671, R_{sigma} = 0.0266]
Data/restraints/parameters	15097/0/440
Goodness-of-fit on F^2	1.084
Final R indexes [I>=2σ (I)]	R_1 = 0.0291, wR_2 = 0.0627
Final R indexes [all data]	R_1 = 0.0386, wR_2 = 0.0663
Largest diff. peak/hole / e Å^{-3}	0.78/–0.87

Table 7-30 Fractional Atomic Coordinates (×10^4) and Equivalent Isotropic Displacement Parameters (Å^2×10^3) for [Ni(Py(5BuPh)Py)Br]. U_{eq} is defined as 1/3 of the trace of the orthogonalized U_{IJ} tensor.

Atom	*x*	*y*	*z*	U(eq)
Br1	6777.7(2)	–2.8(2)	3188.8(2)	19.64(3)
Br2	7829.3(2)	3202.2(2)	5487.8(2)	20.68(3)
Ni2	7022.0(2)	4093.9(2)	4889.0(2)	11.04(3)
Ni1	7744.2(2)	315.3(2)	4188.2(2)	11.57(3)
N4	7935.1(14)	4728.0(5)	5452.4(5)	11.87(17)
N1	7031.8(15)	–430.6(5)	4603.1(5)	12.44(17)
N3	5942.4(15)	3664.2(5)	4181.5(5)	12.51(17)
N2	8641.4(15)	1140.1(5)	4003.0(5)	13.54(18)
C32	7936.3(17)	5322.3(6)	5232.6(5)	12.29(19)
C11	8763.8(16)	1207.1(6)	5049.8(5)	11.85(19)
C31	7186.2(17)	5349.5(6)	4611.3(5)	12.10(19)
C6	7121.1(17)	–390.3(6)	5216.0(5)	12.22(19)
C8	7981.8(17)	445.1(6)	6010.5(5)	12.9(2)
C7	7781.2(16)	216.6(5)	5424.8(5)	11.50(19)
C27	5914.1(17)	4683.7(6)	3816.6(5)	12.09(19)
C1	8177.6(16)	597.9(6)	4951.5(5)	11.43(19)
C21	6636.9(16)	4766.8(6)	4402.8(5)	11.66(19)
C30	7017.5(18)	5860.8(6)	4227.1(6)	14.6(2)
C9	8548.5(17)	1059.2(6)	6118.4(5)	12.17(19)
C5	6597.6(18)	–882.9(6)	5567.8(6)	15.0(2)
C28	5744.1(17)	5191.4(6)	3430.8(6)	13.6(2)
C35	9188.5(19)	5115.1(7)	6401.4(6)	16.9(2)
C36	8545.5(18)	4636.4(6)	6025.7(6)	14.6(2)
C33	8606.4(18)	5817.0(6)	5582.7(6)	14.9(2)
C26	5474.5(17)	4034.0(6)	3695.3(5)	12.25(19)
C10	8945.5(17)	1439.3(6)	5632.4(5)	12.51(19)
C12	9056.1(17)	1520.5(6)	4486.4(5)	12.72(19)
C34	9236.0(19)	5710.7(6)	6173.9(6)	17.0(2)
C25	4670.1(18)	3788.6(6)	3162.7(6)	15.0(2)
C3	5961.4(19)	–1480.3(6)	4676.1(6)	17.0(2)
C2	6469.4(18)	–968.3(6)	4347.2(6)	15.4(2)
C29	6300.2(18)	5786.3(6)	3633.0(6)	14.1(2)
C24	4358(2)	3155.3(6)	3118.2(6)	17.5(2)
C4	6013.7(19)	–1434.3(6)	5292.3(6)	17.4(2)
C13	9694.8(19)	2124.0(6)	4416.6(6)	16.1(2)
C16	8901(2)	1364.2(7)	3454.4(6)	17.7(2)
C22	5608(2)	3051.8(6)	4131.5(6)	17.0(2)
C14	9926(2)	2348.7(6)	3845.8(7)	19.4(2)

Atom	*x*	*y*	*z*	U(eq)
C20	8362(2)	843.9(7)	7228.6(6)	18.6(2)
C17	8645.2(18)	1336.6(6)	6750.8(6)	14.6(2)
C15	9530(2)	1962.8(7)	3358.9(6)	20.4(2)
C23	4834(2)	2781.6(6)	3610.0(6)	19.3(2)
C39	4118(2)	6411.8(6)	2937.8(6)	19.4(2)
C37	6165(2)	6328.5(6)	3190.2(6)	18.7(2)
C18	7091(2)	1831.6(7)	6780.5(6)	20.7(3)
C19	10576(2)	1642.7(7)	6895.5(7)	22.2(3)
C40	6805(3)	6941.9(7)	3486.2(8)	31.1(4)
C38	7417(3)	6186.5(9)	2671.6(8)	34.0(4)

Table 7-31 Anisotropic Displacement Parameters ($Å^2×10^3$) for [Ni(Py(5BuPh)Py)Br]. The Anisotropic displacement factor exponent takes the form: $–2π^2[h^2a^{*2}U_{11}+2hka^*b^*U_{12}+…]$.

Atom	U_{11}	U_{22}	U_{33}	U_{23}	U_{13}	U_{12}
Br1	27.27(7)	18.71(6)	12.22(5)	–1.18(4)	–3.88(5)	–1.98(5)
Br2	35.68(8)	12.98(6)	12.96(5)	1.67(4)	–1.34(5)	6.59(5)
Ni2	12.50(7)	10.59(6)	10.01(6)	1.31(5)	0.67(5)	1.55(5)
Ni1	11.98(7)	12.27(7)	10.31(6)	–0.71(5)	–0.46(5)	0.07(5)
N4	11.0(4)	13.4(4)	11.3(4)	0.2(3)	1.4(3)	1.1(3)
N1	11.5(4)	12.0(4)	13.7(4)	–1.1(3)	–0.4(3)	0.7(3)
N3	12.8(4)	12.2(4)	12.6(4)	0.7(3)	0.9(3)	0.5(3)
N2	12.9(4)	15.6(4)	12.2(4)	0.9(3)	0.8(3)	0.3(4)
C32	10.6(5)	13.0(5)	13.5(5)	0.3(4)	2.3(4)	0.9(4)
C11	10.6(5)	12.3(5)	12.6(5)	0.1(4)	0.1(4)	0.5(4)
C31	11.1(5)	12.1(5)	13.1(5)	1.3(4)	0.9(4)	0.8(4)
C6	9.8(4)	12.5(5)	14.1(5)	–0.1(4)	–0.8(4)	1.6(4)
C8	13.0(5)	13.7(5)	11.8(5)	0.0(4)	0.0(4)	–0.3(4)
C7	10.6(4)	11.4(5)	12.4(5)	–0.2(4)	–0.5(4)	0.6(4)
C27	11.4(5)	13.0(5)	11.8(5)	1.3(4)	1.0(4)	0.7(4)
C1	9.8(4)	12.9(5)	11.5(4)	–0.9(4)	0.2(4)	0.2(4)
C21	10.4(4)	12.9(5)	11.7(5)	1.5(4)	1.1(4)	1.4(4)
C30	13.8(5)	13.1(5)	16.8(5)	2.1(4)	–0.3(4)	–0.6(4)
C9	11.3(5)	12.9(5)	12.1(5)	–0.4(4)	–0.6(4)	0.3(4)
C5	14.5(5)	13.4(5)	17.0(5)	1.2(4)	–0.2(4)	–0.3(4)
C28	13.0(5)	14.7(5)	12.8(5)	3.1(4)	0.0(4)	0.6(4)
C35	16.1(5)	21.3(6)	12.9(5)	–2.0(4)	–1.2(4)	1.4(4)
C36	14.8(5)	17.0(5)	11.9(5)	1.0(4)	0.9(4)	1.3(4)
C33	13.3(5)	14.7(5)	16.7(5)	–1.4(4)	0.8(4)	0.1(4)
C26	11.4(5)	13.6(5)	11.9(5)	1.0(4)	1.6(4)	0.9(4)
C10	12.6(5)	11.7(5)	13.2(5)	–1.1(4)	–0.1(4)	–0.5(4)
C12	11.5(5)	13.1(5)	13.6(5)	0.7(4)	1.0(4)	1.3(4)
C34	14.8(5)	19.1(6)	16.9(5)	–4.2(4)	–0.5(4)	–0.2(4)
C25	15.5(5)	16.5(5)	12.8(5)	0.2(4)	0.5(4)	0.3(4)
C3	16.1(5)	12.4(5)	22.4(6)	–2.3(4)	–1.2(4)	–0.9(4)
C2	14.5(5)	14.2(5)	17.3(5)	–3.6(4)	–1.5(4)	0.3(4)
C29	12.9(5)	14.0(5)	15.3(5)	4.5(4)	0.4(4)	–0.3(4)
C24	18.6(6)	18.4(6)	15.3(5)	–2.3(4)	–1.0(4)	–0.9(4)
C4	17.5(6)	13.2(5)	21.4(6)	1.7(4)	0.0(5)	–1.9(4)
C13	17.5(5)	13.5(5)	17.5(5)	0.6(4)	4.3(4)	0.5(4)
C16	19.2(6)	20.7(6)	13.5(5)	2.0(4)	2.1(4)	–0.2(5)
C22	19.8(6)	13.4(5)	17.6(5)	1.2(4)	0.0(4)	–0.7(4)

Atom	U_{11}	U_{22}	U_{33}	U_{23}	U_{13}	U_{12}
C14	21.7(6)	15.4(5)	21.9(6)	4.9(5)	6.7(5)	1.0(5)
C20	23.1(6)	20.9(6)	11.7(5)	0.5(4)	–0.5(4)	–0.3(5)
C17	15.6(5)	15.3(5)	12.7(5)	–1.6(4)	–0.8(4)	–0.7(4)
C15	23.5(6)	20.7(6)	17.6(6)	4.9(5)	5.4(5)	1.0(5)
C23	22.9(6)	14.5(5)	19.8(6)	–1.0(4)	–2.4(5)	–2.8(5)
C39	23.6(6)	15.7(5)	18.2(6)	3.7(4)	–4.8(5)	1.1(5)
C37	19.2(6)	16.4(5)	19.9(6)	8.4(4)	–1.7(5)	–2.0(4)
C18	24.6(6)	20.2(6)	17.3(6)	–3.0(5)	1.6(5)	5.6(5)
C19	20.9(6)	26.5(7)	18.8(6)	–5.6(5)	–1.8(5)	–7.5(5)
C40	34.6(8)	18.7(6)	37.4(9)	13.3(6)	–16.2(7)	–11.1(6)
C38	32.8(8)	37.8(9)	33.2(9)	20.7(7)	14.8(7)	5.1(7)

Table 7-32 Bond Lengths for [Ni(Py(5BuPh)Py)Br].

Atom	Atom	Length/Å	Atom	Atom	Length/Å
Br1	Ni1	2.3974(2)	C27	C21	1.3891(17)
Br2	Ni2	2.3902(2)	C27	C28	1.3942(17)
Ni2	N4	1.9410(11)	C27	C26	1.4552(17)
Ni2	N3	1.9475(11)	C30	C29	1.4018(18)
Ni2	C21	1.8227(12)	C9	C10	1.4059(17)
Ni1	N1	1.9401(11)	C9	C17	1.5353(17)
Ni1	N2	1.9412(11)	C5	C4	1.3886(18)
Ni1	C1	1.8222(12)	C28	C29	1.4065(18)
N4	C32	1.3716(16)	C35	C36	1.3885(19)
N4	C36	1.3423(16)	C35	C34	1.382(2)
N1	C6	1.3734(16)	C33	C34	1.3880(19)
N1	C2	1.3409(16)	C26	C25	1.3918(18)
N3	C26	1.3721(16)	C12	C13	1.3888(18)
N3	C22	1.3434(17)	C25	C24	1.3842(19)
N2	C12	1.3740(16)	C3	C2	1.3874(19)
N2	C16	1.3450(17)	C3	C4	1.382(2)
C32	C31	1.4576(17)	C29	C37	1.5313(18)
C32	C33	1.3880(18)	C24	C23	1.388(2)
C11	C1	1.3895(17)	C13	C14	1.3875(19)
C11	C10	1.3960(17)	C16	C15	1.386(2)
C11	C12	1.4586(17)	C22	C23	1.3855(19)
C31	C21	1.3857(17)	C14	C15	1.385(2)
C31	C30	1.3980(17)	C20	C17	1.5304(19)
C6	C7	1.4552(17)	C17	C18	1.5379(19)
C6	C5	1.3873(18)	C17	C19	1.5337(19)
C8	C7	1.3998(17)	C39	C37	1.532(2)
C8	C9	1.3985(17)	C37	C40	1.533(2)
C7	C1	1.3851(17)	C37	C38	1.539(2)

Table 7-33 Bond Angles for [Ni(Py(5BuPh)Py)Br].

Atom	Atom	Atom	Angle/°	Atom	Atom	Atom	Angle/°
N4	Ni2	Br2	98.25(3)	C31	C21	Ni2	119.42(9)
N4	Ni2	N3	163.62(4)	C31	C21	C27	120.86(11)
N3	Ni2	Br2	98.12(3)	C27	C21	Ni2	119.58(9)
C21	Ni2	Br2	174.30(4)	C31	C30	C29	120.35(12)

Atom	Atom	Atom	Angle/°	Atom	Atom	Atom	Angle/°
C21	Ni2	N4	81.91(5)	C8	C9	C10	119.14(11)
C21	Ni2	N3	81.74(5)	C8	C9	C17	121.47(11)
N1	Ni1	Br1	98.27(3)	C10	C9	C17	119.31(11)
N1	Ni1	N2	163.72(5)	C6	C5	C4	118.98(12)
N2	Ni1	Br1	97.98(3)	C27	C28	C29	120.28(11)
C1	Ni1	Br1	172.71(4)	C34	C35	C36	118.74(12)
C1	Ni1	N1	81.93(5)	N4	C36	C35	122.86(12)
C1	Ni1	N2	81.84(5)	C32	C33	C34	119.25(12)
C32	N4	Ni2	115.55(8)	N3	C26	C27	111.88(10)
C36	N4	Ni2	126.22(9)	N3	C26	C25	121.57(11)
C36	N4	C32	118.23(11)	C25	C26	C27	126.55(11)
C6	N1	Ni1	115.53(8)	C11	C10	C9	120.34(11)
C2	N1	Ni1	126.13(9)	N2	C12	C11	111.79(11)
C2	N1	C6	118.34(11)	N2	C12	C13	121.55(11)
C26	N3	Ni2	115.55(8)	C13	C12	C11	126.65(12)
C22	N3	Ni2	126.29(9)	C35	C34	C33	119.41(12)
C22	N3	C26	118.16(11)	C24	C25	C26	119.35(12)
C12	N2	Ni1	115.65(8)	C4	C3	C2	118.91(12)
C16	N2	Ni1	126.22(9)	N1	C2	C3	122.65(12)
C16	N2	C12	118.13(11)	C30	C29	C28	119.08(11)
N4	C32	C31	111.81(10)	C30	C29	C37	122.07(12)
N4	C32	C33	121.46(11)	C28	C29	C37	118.82(11)
C33	C32	C31	126.72(11)	C25	C24	C23	119.03(12)
C1	C11	C10	119.62(11)	C3	C4	C5	119.50(12)
C1	C11	C12	110.99(11)	C14	C13	C12	119.34(13)
C10	C11	C12	129.37(11)	N2	C16	C15	122.71(13)
C21	C31	C32	111.21(10)	N3	C22	C23	122.71(12)
C21	C31	C30	119.69(11)	C15	C14	C13	119.12(13)
C30	C31	C32	129.08(11)	C9	C17	C18	108.80(10)
N1	C6	C7	111.76(10)	C20	C17	C9	112.09(11)
N1	C6	C5	121.60(11)	C20	C17	C18	108.80(11)
C5	C6	C7	126.64(11)	C20	C17	C19	107.91(11)
C9	C8	C7	120.29(11)	C19	C17	C9	110.26(11)
C8	C7	C6	128.87(11)	C19	C17	C18	108.93(11)
C1	C7	C6	111.33(11)	C14	C15	C16	119.14(13)
C1	C7	C8	119.76(11)	C22	C23	C24	119.16(13)
C21	C27	C28	119.75(11)	C29	C37	C39	110.16(11)
C21	C27	C26	111.18(10)	C29	C37	C40	111.91(12)
C28	C27	C26	129.05(11)	C29	C37	C38	108.89(12)
C11	C1	Ni1	119.60(9)	C39	C37	C40	107.68(12)
C7	C1	Ni1	119.39(9)	C39	C37	C38	108.92(13)
C7	C1	C11	120.83(11)	C40	C37	C38	109.22(14)

Table 7-34 Torsion Angles for [Ni(Py(5BuPh)Py)Br].

A	B	C	D	Angle/°	A	B	C	D	Angle/°
Ni2	N4	C32	C31	1.47(13)	C1	C11	C12	N2	1.29(14)
Ni2	N4	C32	C33	–178.05(9)	C1	C11	C12	C13	–177.90(12)
Ni2	N4	C36	C35	179.67(10)	C21	C31	C30	C29	–0.12(18)
Ni2	N3	C26	C27	0.49(13)	C21	C27	C28	C29	–0.03(18)
Ni2	N3	C26	C25	–179.23(9)	C21	C27	C26	N3	–2.11(15)

A	B	C	D	Angle/°	A	B	C	D	Angle/°
Ni2	N3	C22	C23	–179.97(10)	C21	C27	C26	C25	177.60(12)
Ni1	N1	C6	C7	–1.05(13)	C30	C31	C21	Ni2	175.52(9)
Ni1	N1	C6	C5	178.07(9)	C30	C31	C21	C27	–0.19(18)
Ni1	N1	C2	C3	–179.24(10)	C30	C29	C37	C39	–122.55(14)
Ni1	N2	C12	C11	1.34(13)	C30	C29	C37	C40	–2.78(19)
Ni1	N2	C12	C13	–179.42(10)	C30	C29	C37	C38	118.06(15)
Ni1	N2	C16	C15	179.32(11)	C9	C8	C7	C6	–176.51(12)
N4	Ni2	C21	C31	3.06(9)	C9	C8	C7	C1	1.11(18)
N4	Ni2	C21	C27	178.83(10)	C5	C6	C7	C8	–2.1(2)
N4	C32	C31	C21	0.82(14)	C5	C6	C7	C1	–179.88(12)
N4	C32	C31	C30	–177.54(12)	C28	C27	C21	Ni2	–175.43(9)
N4	C32	C33	C34	–1.97(18)	C28	C27	C21	C31	0.27(18)
N1	Ni1	C1	C11	–177.67(10)	C28	C27	C26	N3	176.20(12)
N1	Ni1	C1	C7	–2.50(9)	C28	C27	C26	C25	–4.1(2)
N1	C6	C7	C8	176.96(12)	C28	C29	C37	C39	59.60(16)
N1	C6	C7	C1	–0.82(14)	C28	C29	C37	C40	179.37(13)
N1	C6	C5	C4	1.58(18)	C28	C29	C37	C38	–59.79(17)
N3	Ni2	C21	C31	–178.01(10)	C36	N4	C32	C31	–178.33(10)
N3	Ni2	C21	C27	–2.24(10)	C36	N4	C32	C33	2.14(17)
N3	C26	C25	C24	–0.96(19)	C36	C35	C34	C33	1.3(2)
N3	C22	C23	C24	–0.8(2)	C33	C32	C31	C21	–179.69(12)
N2	Ni1	C1	C11	3.54(9)	C33	C32	C31	C30	2.0(2)
N2	Ni1	C1	C7	178.71(10)	C26	N3	C22	C23	0.7(2)
N2	C12	C13	C14	–0.19(19)	C26	C27	C21	Ni2	3.05(14)
N2	C16	C15	C14	0.5(2)	C26	C27	C21	C31	178.76(11)
C32	N4	C36	C35	–0.54(18)	C26	C27	C28	C29	–178.21(12)
C32	C31	C21	Ni2	–3.02(14)	C26	C25	C24	C23	0.9(2)
C32	C31	C21	C27	–178.73(11)	C10	C11	C1	Ni1	174.73(9)
C32	C31	C30	C29	178.12(12)	C10	C11	C1	C7	–0.36(18)
C32	C33	C34	C35	0.18(19)	C10	C11	C12	N2	–176.93(12)
C11	C12	C13	C14	178.92(12)	C10	C11	C12	C13	3.9(2)
C31	C32	C33	C34	178.58(12)	C10	C9	C17	C20	–174.45(11)
C31	C30	C29	C28	0.35(19)	C10	C9	C17	C18	65.18(15)
C31	C30	C29	C37	–177.49(12)	C10	C9	C17	C19	–54.22(15)
C6	N1	C2	C3	0.60(18)	C12	N2	C16	C15	–1.3(2)
C6	C7	C1	Ni1	2.55(14)	C12	C11	C1	Ni1	–3.68(14)
C6	C7	C1	C11	177.66(11)	C12	C11	C1	C7	–178.78(11)
C6	C5	C4	C3	–0.17(19)	C12	C11	C10	C9	178.42(12)
C8	C7	C1	Ni1	–175.46(9)	C12	C13	C14	C15	–0.6(2)
C8	C7	C1	C11	–0.35(18)	C34	C35	C36	N4	–1.2(2)
C8	C9	C10	C11	0.41(18)	C25	C24	C23	C22	0.0(2)
C8	C9	C17	C20	8.81(17)	C2	N1	C6	C7	179.10(11)
C8	C9	C17	C18	–111.55(13)	C2	N1	C6	C5	–1.79(17)
C8	C9	C17	C19	129.04(13)	C2	C3	C4	C5	–1.0(2)
C7	C6	C5	C4	–179.44(12)	C4	C3	C2	N1	0.8(2)
C7	C8	C9	C10	–1.13(18)	C13	C14	C15	C16	0.5(2)
C7	C8	C9	C17	175.61(11)	C16	N2	C12	C11	–178.11(11)
C27	C28	C29	C30	–0.28(18)	C16	N2	C12	C13	1.12(18)
C27	C28	C29	C37	177.64(11)	C22	N3	C26	C27	179.90(11)
C27	C26	C25	C24	179.37(12)	C22	N3	C26	C25	0.18(18)
C1	C11	C10	C9	0.33(18)	C17	C9	C10	C11	–176.40(11)

Table 7-35 Hydrogen Atom Coordinates (Å×10^4) and Isotropic Displacement Parameters (Å^2×10^3) for [Ni(Py(5BuPh)Py)Br].

Atom	*x*	*y*	*z*	U(eq)
H8	7731.99	181.92	6336.05	15
H30	7390.89	6260.74	4369.33	18
H5	6637.96	–843.64	5990.75	18
H28	5250.68	5135.38	3029.68	16
H35	9588.3	5034.71	6807.19	20
H36	8537.16	4226.13	6181.23	17
H33	8633.78	6223.78	5419.65	18
H10	9339.56	1856.29	5700.95	15
H34	9695.41	6044.49	6419.81	20
H25	4338.25	4053.09	2832.94	18
H3	5583.73	–1856.21	4481.13	20
H2	6416.83	–999.95	3923.52	19
H24	3826.7	2979.17	2756.25	21
H4	5652.85	–1777.32	5525.56	21
H13	9970.56	2380.45	4756.22	19
H16	8642.99	1101.25	3118.45	21
H22	5915.5	2793.45	4467.67	20
H14	10350.22	2761.69	3789.74	23
H20A	7112.61	652.95	7155.19	28
H20B	8449.68	1038.77	7624.68	28
H20C	9341.34	524.46	7211.88	28
H15	9688.38	2106.74	2964.7	24
H23	4631	2345.88	3589.26	23
H39A	3661.19	6022.8	2752.92	29
H39B	4060.45	6742.56	2636.78	29
H39C	3321.46	6523.47	3262.32	29
H18A	7258.39	2149.56	6475.75	31
H18B	7174.98	2024.6	7177.45	31
H18C	5848.09	1636.15	6707.26	31
H19A	11569.29	1325.98	6900.4	33
H19B	10588.51	1842.99	7288.46	33
H19C	10802.87	1954.71	6590.26	33
H40A	6015.73	7032.9	3818.01	47
H40B	6678.3	7277.81	3191.15	47
H40C	8129.58	6907.24	3638.51	47
H38A	8734.72	6142.09	2827.98	51
H38B	7319.01	6527.38	2381.54	51
H38C	6993.19	5799.61	2475.24	51

7.3.6 [Ni(Py(4,6MePh)Py)Cl]

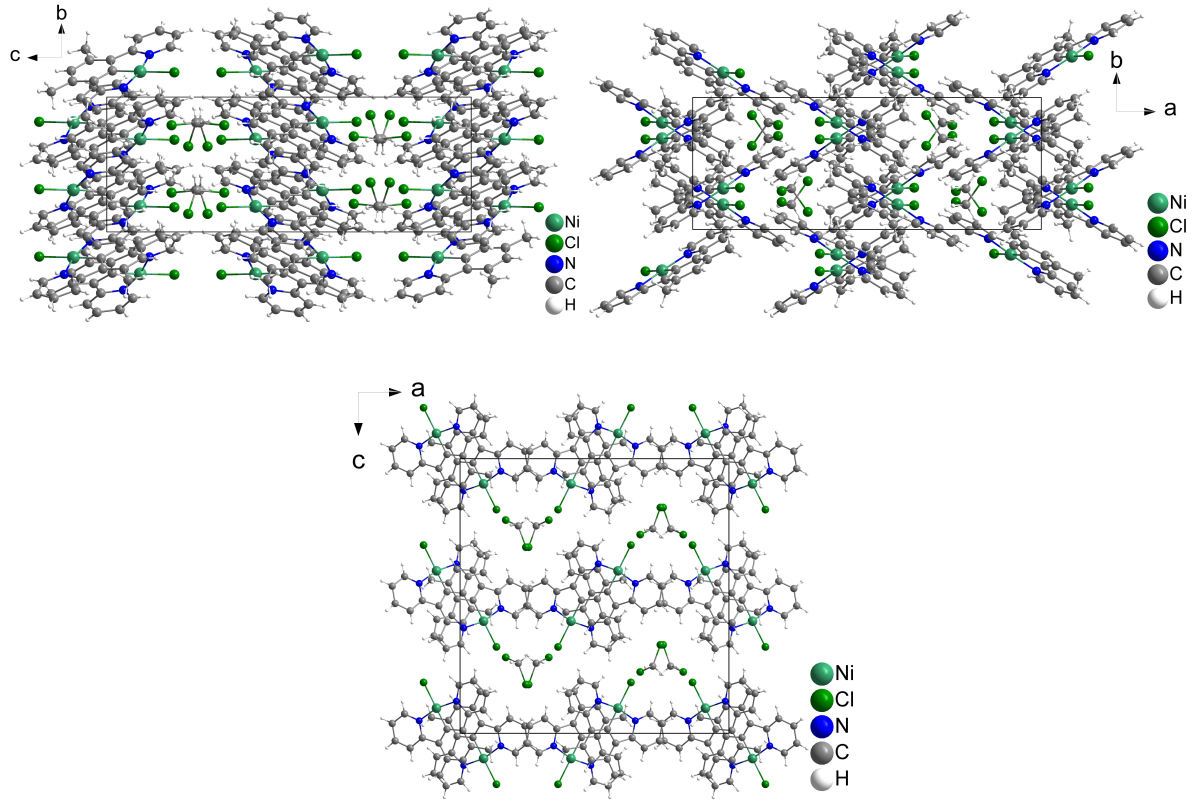

Figure 7-380 Crystal structure of [Ni(Py(4,6MePh)Py)Cl] · CH_2Cl_2 viewed along the crystallographic *a*-axis (top left), *b*-axis (bottom) and *c*-axis (top right).

Table 7-36 Crystal data and structure refinement for [Ni(Py(4,6MePh)Py)Cl] · CH_2Cl_2.

Identification code	[Ni(Py(4,6MePh)Py)Cl] · CH_2Cl_2
Empirical formula	$C_{19}H_{17}Cl_3N_2Ni$
Formula weight	438.40
Temperature/K	100.0
Crystal system	orthorhombic
Space group	*P*bca
a/Å	20.9923(9)
b/Å	7.9234(3)
c/Å	21.4048(9)
α/°	90
β/°	90
γ/°	90
Volume/Å^3	3560.3(3)
Z	8
ρ_{calc}g/cm^3	1.636
μ/mm^{-1}	1.544
F(000)	1792.0
Crystal size/mm^3	0.07 × 0.07 × 0.01
Radiation	MoKα (λ = 0.71073)

2Θ range for data collection/°	3.806 to 78.912
Index ranges	–37 ≤ h ≤ 37, –8 ≤ k ≤ 14, –38 ≤ l ≤ 38
Reflections collected	163303
Independent reflections	10641 [R_{int} = 0.2423, R_{sigma} = 0.1213]
Data/restraints/parameters	10641/0/229
Goodness-of-fit on F^2	1.039
Final R indexes [I>=2σ (I)]	R_1 = 0.0876, wR_2 = 0.1316
Final R indexes [all data]	R_1 = 0.1794, wR_2 = 0.1616
Largest diff. peak/hole / e Å^{-3}	1.19/–1.30

Table 7-37 Fractional Atomic Coordinates (×10^4) and Equivalent Isotropic Displacement Parameters (Å^2×10^3) for [Ni(Py(4,6MePh)Py)Cl] · CH_2Cl_2. U_{eq} is defined as 1/3 of the trace of the orthogonalized U_{IJ} tensor.

Atom	*x*	*y*	*z*	U(eq)
Ni1	5875.0(2)	3109.9(5)	4083.4(2)	11.61(8)
Cl1	6354.6(4)	3167.8(11)	3145.8(4)	21.88(15)
Cl32	7550.9(4)	2086.5(12)	1777.4(4)	26.08(18)
Cl31	8300.5(5)	3663.4(14)	2764.8(5)	34.8(2)
N2	5137.8(11)	1848(3)	3830.7(11)	14.1(4)
N1	6517.9(11)	4313(3)	4540.8(12)	13.1(4)
C1	5484.8(12)	3046(4)	4847.5(12)	11.0(4)
C2	5785.3(13)	3812(3)	5355.5(13)	12.2(5)
C6	4891.3(13)	2256(3)	4893.3(14)	12.6(5)
C15	6401.7(14)	4533(4)	5164.4(14)	13.8(5)
C4	4883.4(14)	3049(4)	5972.3(14)	16.5(5)
C5	4579.5(14)	2262(4)	5474.8(14)	14.2(5)
C21	5030.7(16)	1273(4)	3252.3(15)	19.4(6)
C25	4694.4(14)	1551(3)	4289.5(14)	13.6(5)
C3	5481.2(14)	3834(4)	5940.6(14)	15.5(5)
C11	7061.3(14)	4913(4)	4290.6(16)	17.5(6)
C24	4137.9(15)	672(4)	4148.8(16)	18.2(5)
C14	6852.1(15)	5352(4)	5534.4(16)	19.2(6)
C22	4485.4(16)	389(4)	3090.8(16)	22.0(6)
C8	3940.3(14)	1453(4)	5584.6(15)	18.2(6)
C13	7411.4(15)	5957(4)	5271.8(17)	21.2(6)
C23	4031.9(15)	84(4)	3546.8(17)	21.2(6)
C7	5749.9(16)	4598(4)	6522.5(15)	20.6(6)
C12	7519.3(16)	5747(4)	4640.0(17)	21.5(6)
C31	7833.2(17)	1899(5)	2553.3(15)	22.5(6)

Table 7-38 Anisotropic Displacement Parameters (Å^2×10^3) for [Ni(Py(4,6MePh)Py)Cl] · CH_2Cl_2. The Anisotropic displacement factor exponent takes the form: $-2\pi^2[h^2a^{*2}U_{11}+2hka^*b^*U_{12}+\ldots]$.

Atom	U_{11}	U_{22}	U_{33}	U_{23}	U_{13}	U_{12}
Ni1	10.51(14)	12.21(14)	12.10(15)	1.40(14)	1.24(13)	–0.50(14)
Cl1	19.7(3)	29.0(4)	17.0(3)	2.0(3)	5.2(3)	–3.1(3)
Cl32	26.8(4)	29.4(4)	22.1(4)	3.1(3)	–3.3(3)	–1.9(3)
Cl31	39.0(5)	39.1(5)	26.4(4)	2.9(4)	–10.6(4)	–8.6(4)
N2	13.1(10)	14.5(10)	14.6(10)	0.7(10)	–0.9(8)	1.0(9)
N1	8.9(9)	11.4(10)	18.9(11)	0.9(9)	1.1(8)	–0.2(8)
C1	10.6(10)	11.2(10)	11.2(10)	1.5(10)	1.0(8)	0.8(9)
C2	12.4(12)	10.9(10)	13.4(12)	2.2(9)	0.2(9)	1.9(9)

Atom	U_{11}	U_{22}	U_{33}	U_{23}	U_{13}	U_{12}
C6	10.3(11)	11.2(11)	16.2(13)	2.6(10)	–0.7(9)	–0.7(9)
C15	13.2(11)	10.9(11)	17.4(13)	1.7(10)	–1.2(10)	0.7(9)
C4	17.9(12)	18.1(12)	13.5(12)	3.9(12)	4.5(10)	6.6(11)
C5	13.6(11)	11.5(11)	17.5(13)	4.0(10)	3.3(10)	3.9(9)
C21	22.1(15)	22.6(14)	13.5(13)	–0.3(12)	–0.5(11)	–1.6(12)
C25	12.6(11)	11.1(11)	17.3(12)	2.4(10)	–1.6(10)	1.0(9)
C3	19.0(13)	13.7(11)	13.6(12)	2.5(11)	–0.7(11)	5.2(10)
C11	11.0(11)	14.1(12)	27.3(16)	2.0(12)	1.6(11)	0.0(10)
C24	13.5(11)	16.3(12)	25.0(15)	3.5(12)	–0.9(12)	–2.4(11)
C14	18.4(14)	15.4(12)	23.9(15)	0.3(12)	–6.7(12)	–0.8(11)
C22	24.5(15)	21.9(14)	19.8(15)	–2.8(13)	–7.7(12)	–0.9(13)
C8	14.1(12)	19.0(13)	21.5(14)	4.5(12)	4.9(11)	0.3(11)
C13	15.1(13)	15.6(13)	32.9(18)	–1.3(13)	–6.6(12)	–1.8(11)
C23	16.4(14)	17.6(13)	29.6(17)	0.0(12)	–8.5(12)	–1.9(11)
C7	25.3(16)	22.5(15)	13.9(13)	–1.3(12)	–1.0(11)	3.4(12)
C12	11.6(12)	13.5(12)	39.4(19)	–0.2(13)	2.4(13)	0.4(10)
C31	24.7(15)	25.7(15)	17.3(13)	6.0(14)	2.1(11)	4.8(14)

Table 7-39 Bond Lengths for [Ni(Py(4,6MePh)Py)Cl] · CH_2Cl_2.

Atom	Atom	Length/Å	Atom	Atom	Length/Å
Ni1	Cl1	2.2457(8)	C6	C5	1.406(4)
Ni1	N2	1.920(2)	C6	C25	1.467(4)
Ni1	N1	1.921(2)	C15	C14	1.394(4)
Ni1	C1	1.830(3)	C4	C5	1.389(4)
Cl32	C31	1.769(3)	C4	C3	1.402(4)
Cl31	C31	1.767(4)	C5	C8	1.506(4)
N2	C21	1.338(4)	C21	C22	1.386(5)
N2	C25	1.373(4)	C25	C24	1.393(4)
N1	C15	1.368(4)	C3	C7	1.495(4)
N1	C11	1.347(4)	C11	C12	1.386(5)
C1	C2	1.396(4)	C24	C23	1.388(5)
C1	C6	1.398(4)	C14	C13	1.387(5)
C2	C15	1.473(4)	C22	C23	1.385(5)
C2	C3	1.406(4)	C13	C12	1.381(5)

Table 7-40 Bond Angles for [Ni(Py(4,6MePh)Py)Cl] · CH_2Cl_2.

Atom	Atom	Atom	Angle/°	Atom	Atom	Atom	Angle/°
N2	Ni1	Cl1	96.91(8)	N1	C15	C14	119.5(3)
N2	Ni1	N1	165.54(11)	C14	C15	C2	128.3(3)
N1	Ni1	Cl1	97.49(8)	C5	C4	C3	125.0(3)
C1	Ni1	Cl1	179.58(10)	C6	C5	C8	123.5(3)
C1	Ni1	N2	82.91(11)	C4	C5	C6	117.8(3)
C1	Ni1	N1	82.68(11)	C4	C5	C8	118.7(3)
C21	N2	Ni1	125.0(2)	N2	C21	C22	122.8(3)
C21	N2	C25	119.3(3)	N2	C25	C6	111.9(2)
C25	N2	Ni1	115.7(2)	N2	C25	C24	120.0(3)
C15	N1	Ni1	115.81(19)	C24	C25	C6	128.1(3)
C11	N1	Ni1	124.6(2)	C2	C3	C7	125.2(3)
C11	N1	C15	119.6(3)	C4	C3	C2	116.3(3)

Atom	Atom	Atom	Angle/°	Atom	Atom	Atom	Angle/°
C2	C1	Ni1	118.8(2)	C4	C3	C7	118.5(3)
C2	C1	C6	122.9(3)	N1	C11	C12	122.8(3)
C6	C1	Ni1	118.3(2)	C23	C24	C25	120.2(3)
C1	C2	C15	110.5(2)	C13	C14	C15	120.3(3)
C1	C2	C3	119.6(3)	C23	C22	C21	118.7(3)
C3	C2	C15	129.9(3)	C12	C13	C14	119.6(3)
C1	C6	C5	118.4(3)	C22	C23	C24	119.1(3)
C1	C6	C25	111.1(3)	C13	C12	C11	118.2(3)
C5	C6	C25	130.5(3)	Cl31	C31	Cl32	111.10(19)
N1	C15	C2	112.2(2)				

Table 7-41 Torsion Angles for [Ni(Py(4,6MePh)Py)Cl] · CH_2Cl_2.

A	B	C	D	Angle/°	A	B	C	D	Angle/°
Ni1	N2	C21	C22	–179.0(2)	C2	C1	C6	C25	–179.5(3)
Ni1	N2	C25	C6	–1.1(3)	C2	C15	C14	C13	–180.0(3)
Ni1	N2	C25	C24	178.9(2)	C6	C1	C2	C15	–180.0(3)
Ni1	N1	C15	C2	–1.2(3)	C6	C1	C2	C3	–1.3(4)
Ni1	N1	C15	C14	178.2(2)	C6	C25	C24	C23	–179.6(3)
Ni1	N1	C11	C12	–178.7(2)	C15	N1	C11	C12	0.5(4)
Ni1	C1	C2	C15	–1.2(3)	C15	C2	C3	C4	179.0(3)
Ni1	C1	C2	C3	177.5(2)	C15	C2	C3	C7	–2.0(5)
Ni1	C1	C6	C5	–177.6(2)	C15	C14	C13	C12	0.2(5)
Ni1	C1	C6	C25	1.7(3)	C5	C6	C25	N2	178.9(3)
N2	Ni1	C1	C2	179.4(2)	C5	C6	C25	C24	–1.0(5)
N2	Ni1	C1	C6	–1.8(2)	C5	C4	C3	C2	0.2(4)
N2	C21	C22	C23	–0.1(5)	C5	C4	C3	C7	–178.9(3)
N2	C25	C24	C23	0.5(4)	C21	N2	C25	C6	179.5(3)
N1	Ni1	C1	C2	0.5(2)	C21	N2	C25	C24	–0.6(4)
N1	Ni1	C1	C6	179.3(2)	C21	C22	C23	C24	0.0(5)
N1	C15	C14	C13	0.7(4)	C25	N2	C21	C22	0.4(5)
N1	C11	C12	C13	0.4(5)	C25	C6	C5	C4	–179.5(3)
C1	C2	C15	N1	1.5(3)	C25	C6	C5	C8	1.0(5)
C1	C2	C15	C14	–177.9(3)	C25	C24	C23	C22	–0.2(5)
C1	C2	C3	C4	0.6(4)	C3	C2	C15	N1	–177.0(3)
C1	C2	C3	C7	179.6(3)	C3	C2	C15	C14	3.6(5)
C1	C6	C5	C4	–0.3(4)	C3	C4	C5	C6	–0.3(4)
C1	C6	C5	C8	–179.8(3)	C3	C4	C5	C8	179.2(3)
C1	C6	C25	N2	–0.4(3)	C11	N1	C15	C2	179.5(3)
C1	C6	C25	C24	179.7(3)	C11	N1	C15	C14	–1.0(4)
C2	C1	C6	C5	1.2(4)	C14	C13	C12	C11	–0.7(5)

Table 7-42 Hydrogen Atom Coordinates (Å×10^4) and Isotropic Displacement Parameters (Å^2×10^3) for [Ni(Py(4,6MePh)Py)Cl] · CH_2Cl_2.

Atom	*x*	*y*	*z*	U(eq)
H4	4670.11	3055.22	6363.73	20
H21	5341.8	1479.13	2939.11	23
H11	7133.63	4757.9	3856.28	21
H24	3829.96	474.53	4465.77	22
H14	6775.67	5497.28	5968.53	23
H22	4423.89	–0.91	2675.37	26

Atom	*x*	*y*	*z*	U(eq)
H8A	3626.23	1942.32	5298.47	27
H8B	3806.72	1653.02	6016.93	27
H8C	3972.05	235.21	5509.73	27
H13	7718.42	6511.96	5524.95	25
H23	3653.58	–518.31	3449.09	25
H7A	6125.45	3956.17	6654.54	31
H7B	5428.04	4568.49	6854.01	31
H7C	5872.14	5771.23	6440.42	31
H12	7896.98	6163.74	4450.19	26
H31A	7466.76	1802.39	2842.14	27
H31B	8091.84	859.27	2592.12	27

7.3.7 [Pd(Py(4,6MePh)Py)Cl]

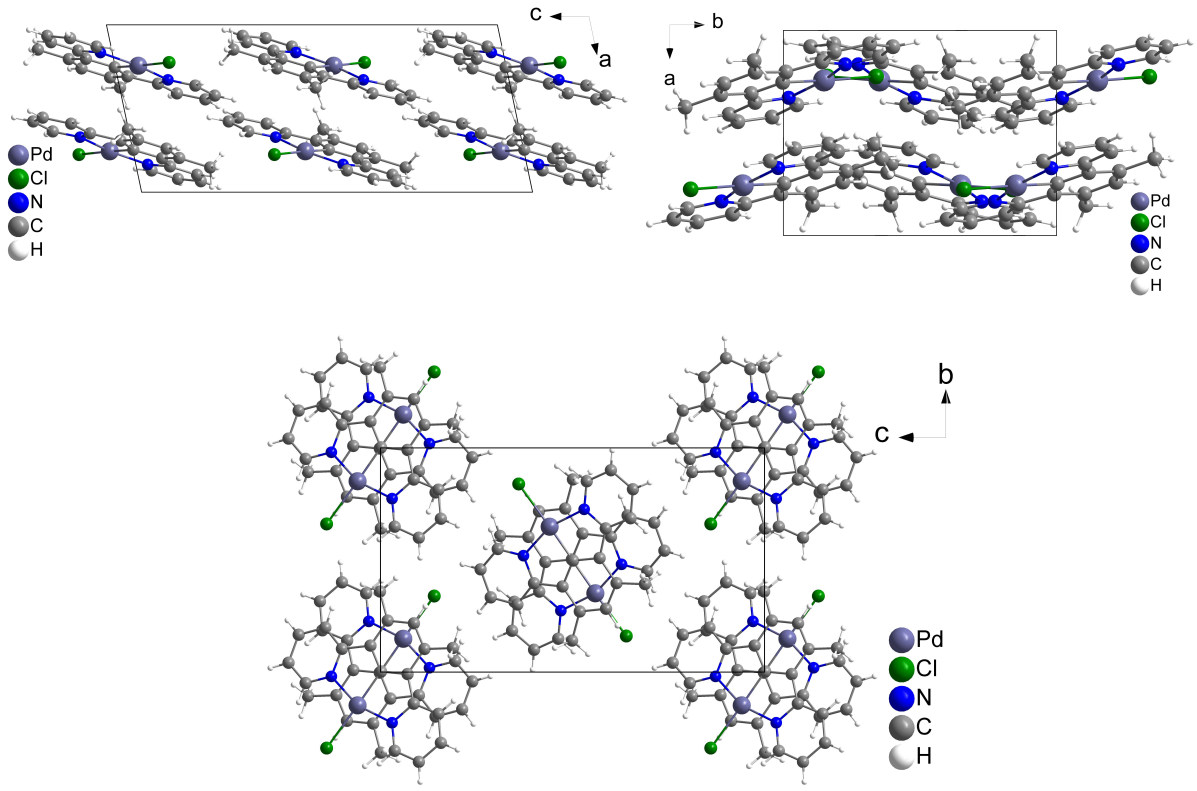

Figure 7-381 Crystal structure of [Pd(Py(4,6MePh)Py)Cl] viewed along the crystallographic *a*-axis (bottom), *b*-axis (top left) and *c*-axis (top right).

Table 7-43 Crystal data and structure refinement for [Pd(Py(4,6MePh)Py)Cl].

Identification code	[Pd(Py(4,6MePh)Py)Cl]
Empirical formula	$C_{18}H_{15}ClN_2Pd$
Formula weight	401.17
Temperature/K	100.0
Crystal system	monoclinic
Space group	$P2_1/c$
a/Å	7.9526(4)

b/Å	10.3875(6)
c/Å	18.2198(10)
α/°	90
β/°	101.889(2)
γ/°	90
Volume/Å^3	1472.81(14)
Z	4
ρ_{calc}g/cm^3	1.809
μ/mm^{-1}	1.438
F(000)	800.0
Crystal size/mm^3	0.409 × 0.194 × 0.164
Radiation	MoKα (λ = 0.71073)
2Θ range for data collection/°	5.234 to 84.208
Index ranges	–15 ≤ h ≤ 14, –19 ≤ k ≤ 19, –34 ≤ l ≤ 34
Reflections collected	115130
Independent reflections	10323 [R_{int} = 0.0216, R_{sigma} = 0.0108]
Data/restraints/parameters	10323/0/202
Goodness-of-fit on F^2	1.109
Final R indexes [I>=2σ (I)]	R_1 = 0.0142, wR_2 = 0.0395
Final R indexes [all data]	R_1 = 0.0145, wR_2 = 0.0397
Largest diff. peak/hole / e Å^{-3}	0.65/–0.72

Table 7-44 Fractional Atomic Coordinates (×10^4) and Equivalent Isotropic Displacement Parameters (Å^2×10^3) for [Pd(Py(4,6MePh)Py)Cl]. U_{eq} is defined as 1/3 of the trace of the orthogonalized U_{IJ} tensor.

Atom	*x*	*y*	*z*	U(eq)
Pd1	2441.7(2)	3514.7(2)	4405.2(2)	10.34(1)
Cl1	2245.5(2)	1608.2(2)	3599.2(2)	18.51(3)
N1	1655.1(6)	2738.7(5)	5303.3(3)	12.37(6)
N2	3288.0(6)	4806.9(5)	3723.2(3)	13.24(7)
C1	2534.0(6)	5024.9(5)	5015.7(3)	11.28(7)
C25	3515.1(7)	6037.3(5)	3998.2(3)	13.64(7)
C2	2029.4(6)	4911.0(5)	5706.8(3)	11.96(7)
C15	1539.9(7)	3590.1(5)	5865.8(3)	12.30(7)
C6	3078.0(7)	6181.0(5)	4741.0(3)	12.63(7)
C11	1297.9(9)	1487.1(6)	5371.2(4)	16.52(9)
C12	792.3(9)	994.7(7)	6000.4(4)	19.5(1)
C8	3747.5(10)	8595.2(6)	4988.5(5)	21.53(11)
C14	1036.1(8)	3137.3(7)	6511.1(3)	17.41(9)
C3	2043.9(7)	6030.0(6)	6146.9(3)	14.42(8)
C5	3137.9(7)	7295.8(5)	5189.6(3)	15.20(8)
C21	3630.9(8)	4511.1(7)	3053.4(3)	17.55(9)
C13	655.0(9)	1842.5(7)	6573.6(4)	19.97(10)
C24	4095.2(9)	6984.8(7)	3564.9(4)	19.71(10)
C22	4227.1(9)	5416.4(8)	2607.8(4)	21.77(11)
C23	4455.5(9)	6666.7(8)	2872.3(4)	22.88(12)
C7	1477.1(8)	6073.8(7)	6886.3(4)	19.39(10)
C4	2604.4(8)	7174.8(6)	5872.1(4)	16.49(8)

Table 7-45 Anisotropic Displacement Parameters ($Å^2×10^3$) for [Pd(Py(4,6MePh)Py)Cl]. The Anisotropic displacement factor exponent takes the form: $–2π^2[h^2a^{*2}U_{11}+2hka^*b^*U_{12}+…]$.

Atom	U_{11}	U_{22}	U_{33}	U_{23}	U_{13}	U_{12}
Pd1	11.86(2)	10.50(2)	8.90(2)	0.16(1)	2.73(1)	–0.22(1)
Cl1	27.98(7)	14.36(5)	13.48(5)	–2.77(4)	4.96(5)	–0.53(4)
N1	13.79(15)	12.48(15)	10.93(14)	0.68(12)	2.74(12)	–1.97(12)
N2	13.10(15)	15.63(17)	11.69(15)	2.39(13)	4.19(12)	0.82(13)
C1	11.29(15)	11.23(16)	11.32(16)	–0.07(13)	2.36(12)	–0.50(12)
C25	11.67(16)	14.57(18)	14.59(18)	3.95(15)	2.52(14)	–0.51(14)
C2	11.52(16)	13.50(17)	10.90(16)	–1.08(13)	2.46(13)	–0.18(13)
C15	11.67(16)	15.01(18)	10.43(16)	0.55(13)	2.77(13)	–0.84(13)
C6	11.92(16)	11.53(17)	14.11(18)	1.23(14)	1.90(13)	–0.53(13)
C11	20.2(2)	13.8(2)	15.4(2)	1.78(15)	3.18(17)	–3.87(16)
C12	21.6(2)	18.0(2)	18.8(2)	5.61(18)	3.87(18)	–4.82(18)
C8	21.9(3)	11.8(2)	29.2(3)	1.57(19)	1.4(2)	–1.71(17)
C14	19.0(2)	21.9(2)	12.78(18)	2.03(17)	6.55(16)	–0.99(18)
C3	13.15(17)	16.4(2)	13.25(18)	–3.45(15)	1.67(14)	1.29(15)
C5	13.99(18)	11.19(17)	19.0(2)	–0.05(15)	0.22(15)	–0.12(14)
C21	18.2(2)	22.5(2)	13.39(19)	3.12(17)	6.72(16)	2.78(18)
C13	20.4(2)	24.3(3)	16.4(2)	6.61(19)	6.39(18)	–2.7(2)
C24	19.2(2)	19.5(2)	20.6(2)	7.64(19)	4.52(18)	–3.40(18)
C22	20.2(2)	31.0(3)	15.9(2)	7.9(2)	7.95(18)	2.8(2)
C23	19.8(2)	29.0(3)	20.6(3)	11.9(2)	6.1(2)	–2.2(2)
C7	18.2(2)	25.3(3)	15.1(2)	–6.53(19)	4.43(17)	1.30(19)
C4	16.9(2)	13.27(19)	18.1(2)	–3.90(16)	0.86(16)	1.10(15)

Table 7-46 Bond Lengths for [Pd(Py(4,6MePh)Py)Cl].

Atom	Atom	Length/Å	Atom	Atom	Length/Å
Pd1	Cl1	2.45121(18)	C2	C3	1.4108(8)
Pd1	N1	2.0349(5)	C15	C14	1.3993(8)
Pd1	N2	2.0354(5)	C6	C5	1.4126(8)
Pd1	C1	1.9158(5)	C11	C12	1.3884(9)
N1	C15	1.3709(7)	C12	C13	1.3875(11)
N1	C11	1.3419(7)	C8	C5	1.5048(9)
N2	C25	1.3711(8)	C14	C13	1.3885(10)
N2	C21	1.3398(8)	C3	C7	1.5067(8)
C1	C2	1.4030(7)	C3	C4	1.3984(9)
C1	C6	1.4032(7)	C5	C4	1.3999(9)
C25	C6	1.4725(8)	C21	C22	1.3882(9)
C25	C24	1.3981(8)	C24	C23	1.3903(11)
C2	C15	1.4713(8)	C22	C23	1.3841(12)

Table 7-47 Bond Angles for [Pd(Py(4,6MePh)Py)Cl].

Atom	Atom	Atom	Angle/°	Atom	Atom	Atom	Angle/°
N1	Pd1	Cl1	99.765(15)	N1	C15	C2	113.16(4)
N1	Pd1	N2	161.30(2)	N1	C15	C14	119.08(5)
N2	Pd1	Cl1	98.935(15)	C14	C15	C2	127.74(5)
C1	Pd1	Cl1	178.272(16)	C1	C6	C25	112.93(5)
C1	Pd1	N1	80.72(2)	C1	C6	C5	118.12(5)
C1	Pd1	N2	80.59(2)	C5	C6	C25	128.95(5)
C15	N1	Pd1	115.13(4)	N1	C11	C12	122.40(6)

Atom	Atom	Atom	Angle/°	Atom	Atom	Atom	Angle/°
C11	N1	Pd1	124.32(4)	C13	C12	C11	117.95(6)
C11	N1	C15	120.53(5)	C13	C14	C15	119.98(6)
C25	N2	Pd1	115.27(4)	C2	C3	C7	124.35(6)
C21	N2	Pd1	124.04(4)	C4	C3	C2	117.58(5)
C21	N2	C25	120.69(5)	C4	C3	C7	118.07(5)
C2	C1	Pd1	117.92(4)	C6	C5	C8	124.66(6)
C2	C1	C6	123.95(5)	C4	C5	C6	117.40(5)
C6	C1	Pd1	118.12(4)	C4	C5	C8	117.94(6)
N2	C25	C6	113.08(5)	N2	C21	C22	122.38(7)
N2	C25	C24	118.94(6)	C12	C13	C14	120.05(6)
C24	C25	C6	127.98(6)	C23	C24	C25	119.93(7)
C1	C2	C15	113.05(5)	C23	C22	C21	117.92(6)
C1	C2	C3	118.05(5)	C22	C23	C24	120.15(6)
C3	C2	C15	128.90(5)	C3	C4	C5	124.87(5)

Table 7-48 Torsion Angles for [Pd(Py(4,6MePh)Py)Cl].

A	B	C	D	Angle/°	A	B	C	D	Angle/°
Pd1	N1	C15	C2	–0.48(6)	C25	C24	C23	C22	0.56(10)
Pd1	N1	C15	C14	–178.96(4)	C2	C1	C6	C25	–179.33(5)
Pd1	N1	C11	C12	178.88(5)	C2	C1	C6	C5	0.64(8)
Pd1	N2	C25	C6	–0.56(6)	C2	C15	C14	C13	–178.47(6)
Pd1	N2	C25	C24	179.96(4)	C2	C3	C4	C5	0.60(9)
Pd1	N2	C21	C22	–179.18(5)	C15	N1	C11	C12	0.36(9)
Pd1	C1	C2	C15	1.73(6)	C15	C2	C3	C7	–2.06(9)
Pd1	C1	C2	C3	–178.02(4)	C15	C2	C3	C4	178.69(5)
Pd1	C1	C6	C25	–0.27(6)	C15	C14	C13	C12	0.74(10)
Pd1	C1	C6	C5	179.70(4)	C6	C1	C2	C15	–179.22(5)
N1	C15	C14	C13	–0.24(9)	C6	C1	C2	C3	1.03(8)
N1	C11	C12	C13	0.14(10)	C6	C25	C24	C23	179.65(6)
N2	C25	C6	C1	0.53(7)	C6	C5	C4	C3	1.06(9)
N2	C25	C6	C5	–179.43(5)	C11	N1	C15	C2	178.17(5)
N2	C25	C24	C23	–0.96(9)	C11	N1	C15	C14	–0.30(8)
N2	C21	C22	C23	–0.48(10)	C11	C12	C13	C14	–0.68(10)
C1	C2	C15	N1	–0.73(7)	C8	C5	C4	C3	–178.41(6)
C1	C2	C15	C14	177.58(6)	C3	C2	C15	N1	178.99(5)
C1	C2	C3	C7	177.65(5)	C3	C2	C15	C14	–2.70(9)
C1	C2	C3	C4	–1.61(8)	C21	N2	C25	C6	–179.88(5)
C1	C6	C5	C8	177.80(6)	C21	N2	C25	C24	0.64(8)
C1	C6	C5	C4	–1.63(8)	C21	C22	C23	C24	0.14(10)
C25	N2	C21	C22	0.08(9)	C24	C25	C6	C1	179.96(6)
C25	C6	C5	C8	–2.23(9)	C24	C25	C6	C5	0.00(10)
C25	C6	C5	C4	178.33(5)	C7	C3	C4	C5	–178.70(6)

Table 7-49 Hydrogen Atom Coordinates (Å×10^4) and Isotropic Displacement Parameters (Å^2×10^3) for [Pd(Py(4,6MePh)Py)Cl].

Atom	*x*	*y*	*z*	U(eq)
H11	1394.43	917.22	4974.2	20
H12	547.9	104.62	6037.4	23
H8A	4911.07	8517.75	4892.2	32
H8B	3757.4	9194.82	5404.65	32

Atom	*x*	*y*	*z*	U(eq)
H8C	2971.03	8919.45	4537.67	32
H14	954.82	3715.6	6906.24	21
H21	3459.84	3650.64	2877.11	21
H13	299.95	1536.97	7009.19	24
H24	4242.84	7845.08	3743.57	24
H22	4470.75	5185.1	2136.13	26
H23	4859.46	7308.85	2579.88	27
H7A	315.93	5716.3	6823.98	29
H7B	1475.91	6968.1	7057.47	29
H7C	2270.99	5565.49	7258.25	29
H4	2624.71	7926.39	6170.92	20

7.3.8 [Ni(Pym(Ph)Pym)Br]

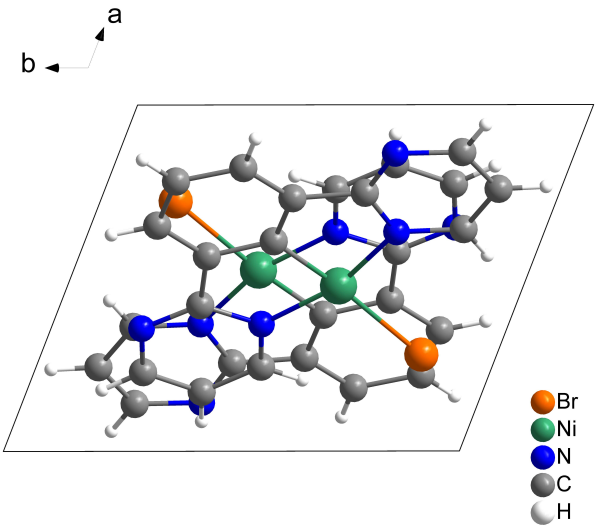

Figure 7-382 Crystal structure of [Ni(Pym(Ph)Pym)Br] viewed along the crystallographic *c*-axis.

Table 7-50 Crystal data and structure refinement for [Ni(Pym(Ph)Pym)Br].

Identification code	[Ni(Pym(Ph)Pym)Br]
Empirical formula	$C_{14}H_9BrN_4Ni$
Formula weight	371.87
Temperature/K	100.00
Crystal system	triclinic
Space group	$P\bar{1}$
a/Å	7.7380(6)
b/Å	9.6145(7)
c/Å	9.8063(6)
α/°	108.190(3)
β/°	106.069(3)
γ/°	104.167(3)
Volume/Å^3	620.66(8)
Z	2
ρ_{calc}g/cm^3	1.990
μ/mm^{-1}	4.774
F(000)	368.0

Crystal size/mm^3	0.06 × 0.03 × 0.03
Radiation	MoKα (λ = 0.71073)
2Θ range for data collection/°	4.734 to 56.564
Index ranges	–10 ≤ h ≤ 10, –12 ≤ k ≤ 12, –13 ≤ l ≤ 13
Reflections collected	34963
Independent reflections	3074 [R_{int} = 0.0472, R_{sigma} = 0.0234]
Data/restraints/parameters	3074/0/181
Goodness-of-fit on F^2	1.087
Final R indexes [I>=2σ (I)]	R_1 = 0.0288, wR_2 = 0.0713
Final R indexes [all data]	R_1 = 0.0320, wR_2 = 0.0730
Largest diff. peak/hole / e Å^{-3}	1.15/–0.49

Table 7-51 Fractional Atomic Coordinates (×10^4) and Equivalent Isotropic Displacement Parameters (Å^2×10^3) for [Ni(Pym(Ph)Pym)Br]. U_{eq} is defined as 1/3 of the trace of the orthogonalized U_{IJ} tensor.

Atom	*x*	*y*	*z*	U(eq)
Br1	7216.4(3)	8345.6(2)	10251.6(2)	17.43(8)
Ni1	5230.7(4)	5945.7(3)	8037.9(3)	12.98(9)
N2	6331(3)	4580(2)	8760(2)	14.3(4)
N1	3673(3)	6759(2)	6809(2)	14.2(4)
N4	6458(3)	1988(2)	7909(2)	16.7(4)
N3	1406(3)	6064(2)	4248(2)	16.0(4)
C11	5782(3)	3075(3)	7667(3)	13.8(4)
C10	4369(3)	2806(3)	6189(3)	14.0(4)
C6	2695(3)	4190(2)	4953(3)	13.1(4)
C5	2541(3)	5732(3)	5299(3)	13.6(4)
C1	3937(3)	4144(2)	6251(2)	12.7(4)
C8	2208(3)	1493(3)	3490(3)	15.8(4)
C14	7558(3)	4930(3)	10187(3)	16.9(4)
C7	1823(3)	2855(3)	3546(3)	15.1(4)
C12	7713(4)	2389(3)	9348(3)	18.7(5)
C3	2431(3)	8631(3)	6238(3)	17.7(4)
C4	1369(3)	7523(3)	4734(3)	16.9(4)
C2	3593(3)	8205(3)	7258(3)	16.4(4)
C9	3482(3)	1455(3)	4786(3)	14.9(4)
C13	8284(3)	3844(3)	10541(3)	18.0(4)

Table 7-52 Anisotropic Displacement Parameters (Å^2×10^3) for [Ni(Pym(Ph)Pym)Br]. The Anisotropic displacement factor exponent takes the form: $-2\pi^2[h^2a^{*2}U_{11}+2hka^*b^*U_{12}+\ldots]$.

Atom	U_{11}	U_{22}	U_{33}	U_{23}	U_{13}	U_{12}
Br1	20.68(13)	9.94(12)	12.89(12)	–1.05(8)	2.01(9)	3.79(9)
Ni1	15.97(15)	8.00(14)	10.42(14)	0.75(11)	2.60(11)	3.69(11)
N2	16.9(9)	9.3(8)	12.2(9)	1.3(7)	4.0(7)	3.3(7)
N1	15.4(9)	10.4(9)	13.8(9)	3.1(7)	5.2(7)	3.1(7)
N4	19.9(10)	13.3(9)	15.9(9)	4.8(7)	5.5(8)	7.5(8)
N3	18.3(9)	13.5(9)	15.0(9)	4.1(7)	5.6(7)	6.7(7)
C11	16.1(10)	8.7(9)	13.1(10)	1.5(8)	5.1(8)	3.3(8)
C10	16.1(10)	11.9(10)	13.6(10)	4.1(8)	6.0(8)	5.8(8)
C6	13.8(10)	9.2(9)	13.3(10)	1.9(8)	4.4(8)	3.5(8)
C5	13.9(10)	10.7(10)	14.2(10)	2.9(8)	6.2(8)	3.5(8)
C1	14.2(10)	7.7(9)	12.1(10)	1.2(8)	4.2(8)	2.1(8)

Atom	U_{11}	U_{22}	U_{33}	U_{23}	U_{13}	U_{12}
C8	19.2(11)	9.9(10)	13.0(10)	–0.1(8)	5.3(8)	4.1(8)
C14	18.9(11)	13.8(10)	13.9(10)	2.6(8)	5.0(9)	4.6(9)
C7	16.2(10)	13.2(10)	12.3(10)	2.6(8)	4.0(8)	4.5(8)
C12	22.7(12)	16.1(11)	18.9(11)	7.4(9)	7.2(9)	10.2(9)
C3	20.7(11)	13.0(10)	20.3(11)	6.3(9)	8.7(9)	7.4(9)
C4	18.3(11)	15.1(11)	17.8(11)	6.4(9)	6.2(9)	8.0(9)
C2	20.5(11)	10.4(10)	16.1(10)	3.1(8)	6.6(9)	5.2(8)
C9	18.9(11)	7.7(9)	15.0(10)	1.3(8)	6.5(8)	4.4(8)
C13	18.6(11)	18.3(11)	14.7(10)	6.0(9)	3.7(9)	6.8(9)

Table 7-53 Bond Lengths for [Ni(Pym(Ph)Pym)Br].

Atom	Atom	Length/Å	Atom	Atom	Length/Å
Br1	Ni1	2.3850(4)	C11	C10	1.454(3)
Ni1	N2	1.9352(19)	C10	C1	1.394(3)
Ni1	N1	1.9395(19)	C10	C9	1.406(3)
Ni1	C1	1.832(2)	C6	C5	1.457(3)
N2	C11	1.379(3)	C6	C1	1.387(3)
N2	C14	1.337(3)	C6	C7	1.401(3)
N1	C5	1.372(3)	C8	C7	1.400(3)
N1	C2	1.344(3)	C8	C9	1.393(3)
N4	C11	1.332(3)	C14	C13	1.390(3)
N4	C12	1.343(3)	C12	C13	1.382(3)
N3	C5	1.333(3)	C3	C4	1.380(3)
N3	C4	1.344(3)	C3	C2	1.384(3)

Table 7-54 Bond Angles for [Ni(Pym(Ph)Pym)Br].

Atom	Atom	Atom	Angle/°	Atom	Atom	Atom	Angle/°
N2	Ni1	Br1	97.54(6)	C9	C10	C11	129.5(2)
N2	Ni1	N1	163.73(8)	C1	C6	C5	111.19(19)
N1	Ni1	Br1	98.73(6)	C1	C6	C7	119.6(2)
C1	Ni1	Br1	173.14(7)	C7	C6	C5	129.2(2)
C1	Ni1	N2	81.98(9)	N1	C5	C6	112.02(19)
C1	Ni1	N1	81.88(9)	N3	C5	N1	125.3(2)
C11	N2	Ni1	115.79(15)	N3	C5	C6	122.7(2)
C14	N2	Ni1	127.49(16)	C10	C1	Ni1	118.92(17)
C14	N2	C11	116.72(19)	C6	C1	Ni1	119.13(16)
C5	N1	Ni1	115.57(15)	C6	C1	C10	121.7(2)
C2	N1	Ni1	127.73(16)	C9	C8	C7	121.5(2)
C2	N1	C5	116.70(19)	N2	C14	C13	121.6(2)
C11	N4	C12	116.7(2)	C8	C7	C6	119.0(2)
C5	N3	C4	116.4(2)	N4	C12	C13	122.6(2)
N2	C11	C10	111.72(19)	C4	C3	C2	117.6(2)
N4	C11	N2	125.0(2)	N3	C4	C3	122.6(2)
N4	C11	C10	123.3(2)	N1	C2	C3	121.3(2)
C1	C10	C11	111.39(19)	C8	C9	C10	119.2(2)
C1	C10	C9	119.1(2)	C12	C13	C14	117.3(2)

Table 7-55 Torsion Angles for [Ni(Pym(Ph)Pym)Br].

A	B	C	D	Angle/°	A	B	C	D	Angle/°
Ni1	N2	C11	N4	176.13(18)	C5	C6	C1	C10	–177.7(2)
Ni1	N2	C11	C10	–3.4(2)	C5	C6	C7	C8	179.3(2)
Ni1	N2	C14	C13	–178.13(18)	C1	C10	C9	C8	0.6(3)
Ni1	N1	C5	N3	–178.05(18)	C1	C6	C5	N1	0.7(3)
Ni1	N1	C5	C6	2.5(2)	C1	C6	C5	N3	–178.8(2)
Ni1	N1	C2	C3	178.82(17)	C1	C6	C7	C8	0.9(3)
N2	Ni1	C1	C10	–3.85(18)	C14	N2	C11	N4	–3.6(3)
N2	Ni1	C1	C6	–177.79(19)	C14	N2	C11	C10	176.8(2)
N2	C11	C10	C1	0.4(3)	C7	C6	C5	N1	–177.8(2)
N2	C11	C10	C9	178.7(2)	C7	C6	C5	N3	2.7(4)
N2	C14	C13	C12	1.1(4)	C7	C6	C1	Ni1	174.75(17)
N1	Ni1	C1	C10	178.18(19)	C7	C6	C1	C10	1.0(3)
N1	Ni1	C1	C6	4.24(18)	C7	C8	C9	C10	1.3(3)
N4	C11	C10	C1	–179.1(2)	C12	N4	C11	N2	2.6(3)
N4	C11	C10	C9	–0.8(4)	C12	N4	C11	C10	–177.9(2)
N4	C12	C13	C14	–2.2(4)	C4	N3	C5	N1	–0.9(3)
C11	N2	C14	C13	1.6(3)	C4	N3	C5	C6	178.5(2)
C11	N4	C12	C13	0.5(4)	C4	C3	C2	N1	–0.8(3)
C11	C10	C1	Ni1	3.0(3)	C2	N1	C5	N3	1.2(3)
C11	C10	C1	C6	176.8(2)	C2	N1	C5	C6	–178.27(19)
C11	C10	C9	C8	–177.6(2)	C2	C3	C4	N3	1.1(4)
C5	N1	C2	C3	–0.3(3)	C9	C10	C1	Ni1	–175.49(17)
C5	N3	C4	C3	–0.3(3)	C9	C10	C1	C6	–1.7(3)
C5	C6	C1	Ni1	–3.9(3)	C9	C8	C7	C6	–2.0(3)

Table 7-56 Hydrogen Atom Coordinates (Å×10^4) and Isotropic Displacement Parameters (Å^2×10^3) for [Ni(Pym(Ph)Pym)Br].

Atom	*x*	*y*	*z*	U(eq)
H8	1587.31	574.5	2546.34	19
H14	7943.56	5947.03	10978.84	20
H7	983.61	2872.84	2643.64	18
H12	8228.42	1641.66	9555.19	22
H3	2365.28	9650.36	6561.76	21
H4	581.33	7802.19	4014.43	20
H2	4350.75	8950.04	8296.78	20
H9	3747.77	528.24	4722.36	18
H13	9139.1	4092.34	11560.73	22

7.3.9 [Ni(2^{i}Qu(Ph)2^{i}Qu)Br]

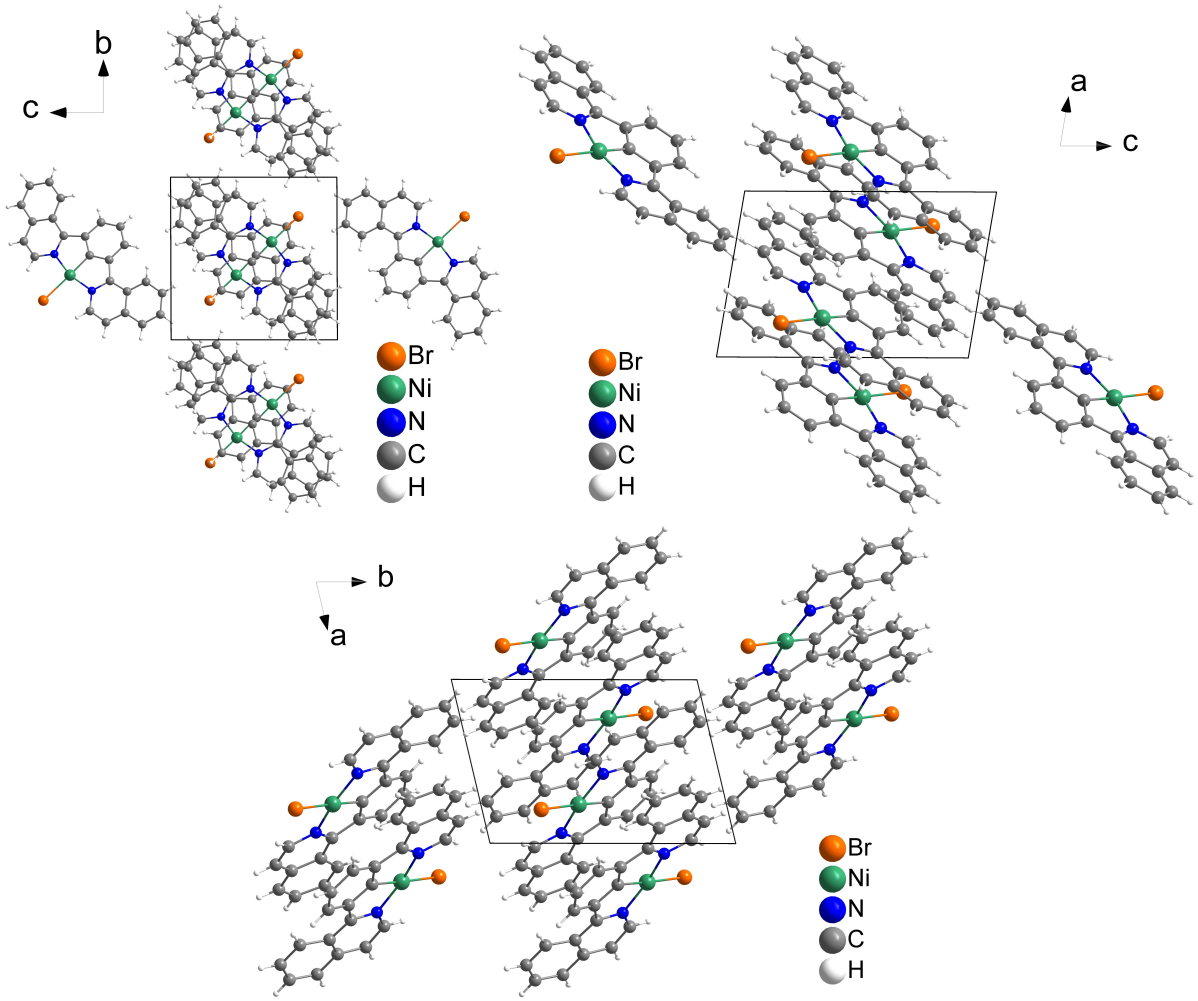

Figure 7-383 Crystal structure of [Ni(2^{i}Qu(Ph)2^{i}Qu)Br] viewed along the crystallographic *a*-axis (top left), *b*-axis (top right) and *c*-axis (bottom).

Table 7-57 Crystal data and structure refinement for [Ni(2^{i}Qu(Ph)2^{i}Qu)Br].

Identification code	[Ni(2^{i}Qu(Ph)2^{i}Qu)Br]
Empirical formula	$C_{24}H_{15}BrN_2Ni$
Formula weight	470.00
Temperature/K	103.00
Crystal system	triclinic
Space group	$P\bar{1}$
a/Å	7.5676(4)
b/Å	10.8971(6)
c/Å	10.9976(6)
α/°	87.515(2)
β/°	80.243(2)
γ/°	76.359(2)
Volume/Å^3	868.58(8)
Z	2
ρ_{calc}g/cm^3	1.797
μ/mm^{-1}	3.430
F(000)	472.0

Radiation	MoKα (λ = 0.71073)
2Θ range for data collection/°	5.368 to 61.026
Index ranges	–10 ≤ h ≤ 10, –15 ≤ k ≤ 15, 0 ≤ l ≤ 15
Reflections collected	9683
Independent reflections	9683 [R_{int} = 0.0428, R_{sigma} = 0.0277]
Data/restraints/parameters	9683/0/254
Goodness-of-fit on F^2	1.033
Final R indexes [I>=2σ (I)]	R_1 = 0.0362, wR_2 = 0.0857
Final R indexes [all data]	R_1 = 0.0470, wR_2 = 0.0916
Largest diff. peak/hole / e Å^{-3}	0.97/–0.76

Table 7-58 Fractional Atomic Coordinates (×10^4) and Equivalent Isotropic Displacement Parameters (Å^2×10^3) for [Ni(2^{i}Qu(Ph)2^{i}Qu)Br]. U_{eq} is defined as 1/3 of the trace of the orthogonalized U_{IJ} tensor.

Atom	*x*	*y*	*z*	U(eq)
Br1	2063.3(4)	7588.3(3)	2326.0(3)	24.50(8)
Ni1	2368.2(4)	6025.6(3)	3932.4(3)	12.04(8)
N1	626(3)	6988(2)	5244(2)	14.5(4)
C9	–941(3)	7027(3)	7364(2)	15.2(5)
N2	4243(3)	4729(2)	2993(2)	14.2(4)
C4	–1710(3)	8345(3)	7241(3)	16.7(5)
C5	–2851(4)	9041(3)	8267(3)	20.7(5)
C6	–3262(4)	8445(3)	9359(3)	22.8(6)
C7	–2587(4)	7129(3)	9468(3)	23.1(6)
C8	–1467(4)	6439(3)	8503(3)	19.9(5)
C10	301(3)	6384(2)	6338(2)	13.5(4)
C2	–231(4)	8233(3)	5129(3)	17.9(5)
C3	–1337(4)	8923(3)	6089(3)	20.0(5)
C11	1449(3)	5081(2)	6293(2)	14.0(4)
C12	1684(4)	4159(3)	7217(2)	17.7(5)
C13	3013(4)	3039(3)	6972(2)	20.1(5)
C14	4079(4)	2777(3)	5814(3)	17.9(5)
C15	3786(3)	3645(2)	4852(2)	14.0(4)
C1	2522(3)	4804(2)	5123(2)	13.4(4)
C24	5082(4)	4887(3)	1816(2)	17.3(5)
C23	6357(4)	3943(3)	1170(3)	18.2(5)
C22	6787(3)	2729(3)	1687(2)	16.0(5)
C17	5912(3)	2536(2)	2909(2)	14.6(5)
C16	4704(3)	3595(2)	3561(2)	13.8(4)
C21	8027(4)	1701(3)	1018(3)	20.4(5)
C20	8362(4)	520(3)	1529(3)	22.0(6)
C19	7439(4)	304(3)	2716(3)	21.5(5)
C18	6240(4)	1279(3)	3388(3)	18.2(5)

Table 7-59 Anisotropic Displacement Parameters (Å^2×10^3) for [Ni(2^{i}Qu(Ph)2^{i}Qu)Br]. The Anisotropic displacement factor exponent takes the form: $-2\pi^2[h^2a^{*2}U_{11}+2hka^*b^*U_{12}+\ldots]$.

Atom	U_{11}	U_{22}	U_{33}	U_{23}	U_{13}	U_{12}
Br1	28.25(15)	21.52(15)	19.21(14)	3.76(10)	–1.4(1)	0.66(10)
Ni1	12.94(14)	11.26(15)	11.19(15)	0.50(11)	–1.59(10)	–1.75(10)
N1	14.2(10)	14.6(10)	14.4(10)	0.5(8)	–2.1(7)	–3.0(7)
C9	13.2(11)	16.8(12)	15.3(11)	–2.2(9)	–2.2(9)	–2.8(9)

Atom	U_{11}	U_{22}	U_{33}	U_{23}	U_{13}	U_{12}
N2	15.2(10)	13.4(10)	13.8(10)	0.2(8)	–1.9(7)	–3.3(7)
C4	14.3(12)	16.8(12)	18.7(12)	–2.6(9)	–1.5(9)	–3.2(9)
C5	19.0(13)	18.3(13)	23.2(14)	–5.1(10)	–0.7(10)	–2.5(10)
C6	21.4(14)	24.5(14)	20.2(13)	–6.6(11)	0.3(10)	–2.4(10)
C7	22.6(14)	27.1(15)	17.1(13)	–1.1(11)	1.4(10)	–3.7(11)
C8	20.2(13)	19.6(13)	17.8(12)	2.2(10)	–0.2(10)	–2.8(10)
C10	13.8(11)	13.8(11)	13.3(11)	–0.2(9)	–3.0(8)	–3.4(8)
C2	18.4(13)	14.6(12)	19.0(12)	2.1(9)	–2.1(9)	–1.5(9)
C3	20.0(13)	15.1(12)	22.2(13)	0.5(10)	–0.9(10)	–0.9(9)
C11	14.7(12)	13.8(11)	13.5(11)	–0.2(9)	–2.1(8)	–3.2(8)
C12	21.8(13)	15.7(12)	14.0(11)	0.1(9)	–1.1(9)	–2.7(9)
C13	28.9(15)	15.8(13)	14.6(12)	2.2(9)	–3.3(10)	–3.7(10)
C14	21.9(13)	13.8(12)	16.8(12)	0.9(9)	–4.9(9)	–0.9(9)
C15	15.7(12)	12.7(11)	13.4(11)	–0.4(9)	–3.0(8)	–2.3(8)
C1	12.8(10)	13.4(11)	14.7(11)	–1.8(8)	–3.6(8)	–2.9(8)
C24	19.0(13)	17.6(12)	14.9(12)	1.4(9)	–1.0(9)	–5.2(9)
C23	18.9(13)	20.2(13)	14.8(12)	–1.0(10)	0.3(9)	–5.0(9)
C22	14.5(12)	17.9(12)	15.8(12)	–2.7(9)	–3.4(9)	–3.0(9)
C17	12.6(11)	15.3(11)	15.7(11)	–1.8(9)	–3.0(9)	–1.7(8)
C16	13.6(11)	13.6(11)	15.0(11)	–0.1(9)	–4.0(8)	–3.4(8)
C21	17.8(13)	22.9(14)	17.9(12)	–4.5(10)	–1.3(9)	–0.2(10)
C20	20.6(13)	21.6(14)	19.8(13)	–6.2(10)	–3.8(10)	4.3(10)
C19	24.2(14)	16.6(12)	22.3(13)	–2.1(10)	–7.2(10)	1.1(10)
C18	20.8(13)	15.9(12)	17.3(12)	–1.4(10)	–4.4(9)	–1.8(9)

Table 7-60 Bond Lengths for [Ni(2^{i}Qu(Ph)2^{i}Qu)Br].

Atom	Atom	Length/Å	Atom	Atom	Length/Å
Br1	Ni1	2.4012(4)	C2	C3	1.361(4)
Ni1	N1	1.937(2)	C11	C12	1.400(4)
Ni1	N2	1.939(2)	C11	C1	1.403(3)
Ni1	C1	1.824(3)	C12	C13	1.390(4)
N1	C10	1.360(3)	C13	C14	1.389(4)
N1	C2	1.369(3)	C14	C15	1.399(4)
C9	C4	1.426(4)	C15	C1	1.402(3)
C9	C8	1.422(4)	C15	C16	1.469(3)
C9	C10	1.430(3)	C24	C23	1.363(4)
N2	C24	1.364(3)	C23	C22	1.404(4)
N2	C16	1.357(3)	C22	C17	1.424(4)
C4	C5	1.425(4)	C22	C21	1.421(4)
C4	C3	1.405(4)	C17	C16	1.427(3)
C5	C6	1.365(4)	C17	C18	1.426(4)
C6	C7	1.411(4)	C21	C20	1.366(4)
C7	C8	1.368(4)	C20	C19	1.411(4)
C10	C11	1.477(3)	C19	C18	1.373(4)

Table 7-61 Bond Angles for [Ni(2^{i}Qu(Ph)2^{i}Qu)Br].

Atom	Atom	Atom	Angle/°	Atom	Atom	Atom	Angle/°
N1	Ni1	Br1	98.41(7)	C12	C11	C10	130.8(2)
N1	Ni1	N2	163.91(9)	C12	C11	C1	117.9(2)

Atom	Atom	Atom	Angle/°	Atom	Atom	Atom	Angle/°
N2	Ni1	Br1	97.58(7)	C1	C11	C10	111.1(2)
C1	Ni1	Br1	177.24(8)	C13	C12	C11	119.7(2)
C1	Ni1	N1	81.94(10)	C14	C13	C12	121.9(2)
C1	Ni1	N2	82.16(10)	C13	C14	C15	119.5(2)
C10	N1	Ni1	117.07(17)	C14	C15	C1	118.2(2)
C10	N1	C2	119.4(2)	C14	C15	C16	130.3(2)
C2	N1	Ni1	123.46(18)	C1	C15	C16	111.4(2)
C4	C9	C10	118.2(2)	C11	C1	Ni1	118.98(19)
C8	C9	C4	117.5(2)	C15	C1	Ni1	118.46(19)
C8	C9	C10	124.3(2)	C15	C1	C11	122.5(2)
C24	N2	Ni1	124.28(18)	C23	C24	N2	122.7(3)
C16	N2	Ni1	116.45(17)	C24	C23	C22	120.1(3)
C16	N2	C24	119.3(2)	C23	C22	C17	118.2(2)
C5	C4	C9	120.0(3)	C23	C22	C21	121.9(3)
C3	C4	C9	118.5(2)	C21	C22	C17	119.8(2)
C3	C4	C5	121.5(3)	C22	C17	C16	118.3(2)
C6	C5	C4	120.3(3)	C22	C17	C18	117.8(2)
C5	C6	C7	120.0(3)	C18	C17	C16	123.9(2)
C8	C7	C6	121.0(3)	N2	C16	C15	111.2(2)
C7	C8	C9	121.0(3)	N2	C16	C17	121.0(2)
N1	C10	C9	120.9(2)	C17	C16	C15	127.8(2)
N1	C10	C11	110.9(2)	C20	C21	C22	120.5(3)
C9	C10	C11	128.2(2)	C21	C20	C19	120.2(2)
C3	C2	N1	122.7(3)	C18	C19	C20	120.7(3)
C2	C3	C4	120.0(3)	C19	C18	C17	120.9(3)

Table 7-62 Torsion Angles for [Ni(2^{i}Qu(Ph)2^{i}Qu)Br].

A	B	C	D	Angle/°	A	B	C	D	Angle/°
Ni1	N1	C10	C9	178.94(18)	C2	N1	C10	C11	–176.2(2)
Ni1	N1	C10	C11	1.9(3)	C3	C4	C5	C6	176.9(3)
Ni1	N1	C2	C3	–174.6(2)	C11	C12	C13	C14	–2.6(4)
Ni1	N2	C24	C23	–178.0(2)	C12	C11	C1	Ni1	–175.65(19)
Ni1	N2	C16	C15	–6.1(3)	C12	C11	C1	C15	0.8(4)
Ni1	N2	C16	C17	172.97(18)	C12	C13	C14	C15	–1.6(4)
N1	Ni1	C1	C11	0.01(19)	C13	C14	C15	C1	5.3(4)
N1	Ni1	C1	C15	–176.5(2)	C13	C14	C15	C16	–179.7(3)
N1	C10	C11	C12	174.3(3)	C14	C15	C1	Ni1	171.49(19)
N1	C10	C11	C1	–1.8(3)	C14	C15	C1	C11	–4.9(4)
N1	C2	C3	C4	–3.1(4)	C14	C15	C16	N2	–168.7(3)
C9	C4	C5	C6	–2.1(4)	C14	C15	C16	C17	12.3(4)
C9	C4	C3	C2	–1.4(4)	C1	C11	C12	C13	3.0(4)
C9	C10	C11	C12	–2.5(5)	C1	C15	C16	N2	6.5(3)
C9	C10	C11	C1	–178.5(2)	C1	C15	C16	C17	–172.5(2)
N2	Ni1	C1	C11	177.5(2)	C24	N2	C16	C15	174.8(2)
N2	Ni1	C1	C15	0.9(2)	C24	N2	C16	C17	–6.1(4)
N2	C24	C23	C22	3.3(4)	C24	C23	C22	C17	–2.4(4)
C4	C9	C8	C7	–3.6(4)	C24	C23	C22	C21	176.3(3)
C4	C9	C10	N1	–5.1(4)	C23	C22	C17	C16	–2.5(4)
C4	C9	C10	C11	171.3(2)	C23	C22	C17	C18	174.9(2)
C4	C5	C6	C7	–1.3(4)	C23	C22	C21	C20	–177.4(3)

A	B	C	D	Angle/°	A	B	C	D	Angle/°
C5	C4	C3	C2	179.6(3)	C22	C17	C16	N2	6.9(4)
C5	C6	C7	C8	2.2(5)	C22	C17	C16	C15	–174.2(2)
C6	C7	C8	C9	0.3(4)	C22	C17	C18	C19	3.5(4)
C8	C9	C4	C5	4.4(4)	C22	C21	C20	C19	1.7(4)
C8	C9	C4	C3	–174.5(2)	C17	C22	C21	C20	1.2(4)
C8	C9	C10	N1	174.7(2)	C16	N2	C24	C23	1.0(4)
C8	C9	C10	C11	–8.8(4)	C16	C15	C1	Ni1	–4.4(3)
C10	N1	C2	C3	3.4(4)	C16	C15	C1	C11	179.2(2)
C10	C9	C4	C5	–175.7(2)	C16	C17	C18	C19	–179.2(3)
C10	C9	C4	C3	5.4(4)	C21	C22	C17	C16	178.8(2)
C10	C9	C8	C7	176.5(3)	C21	C22	C17	C18	–3.7(4)
C10	C11	C12	C13	–172.8(3)	C21	C20	C19	C18	–2.0(4)
C10	C11	C1	Ni1	1.0(3)	C20	C19	C18	C17	–0.7(4)
C10	C11	C1	C15	177.4(2)	C18	C17	C16	N2	–170.4(2)
C2	N1	C10	C9	0.8(4)	C18	C17	C16	C15	8.5(4)

Table 7-63 Hydrogen Atom Coordinates (Å×10^4) and Isotropic Displacement Parameters (Å^2×10^3) for [Ni(2^{i}Qu(Ph)2^{i}Qu)Br].

Atom	*x*	*y*	*z*	U(eq)
H5	–3328.48	9923.68	8190.8	25
H6	–4001.87	8915.19	10046.39	27
H7	–2914.28	6716.22	10222.12	28
H8	–1034.61	5553.95	8596.43	24
H2	–46.32	8631	4347.69	21
H3	–1856.85	9795.1	5979.96	24
H12	938.25	4299.23	8007.38	21
H13	3196.97	2435.08	7615.44	24
H14	5000.14	2014.09	5676.47	21
H24	4764.73	5687.89	1431.49	21
H23	6954.85	4105.51	368.75	22
H21	8627.18	1834.86	208.6	24
H20	9218.65	–156.52	1083.41	26
H19	7650.01	–524.62	3054.23	26
H18	5620.87	1115.51	4182.54	22

7.3.10 [Ni(2^{i}Qu(4,6FPh)2^{i}Qu)Br]

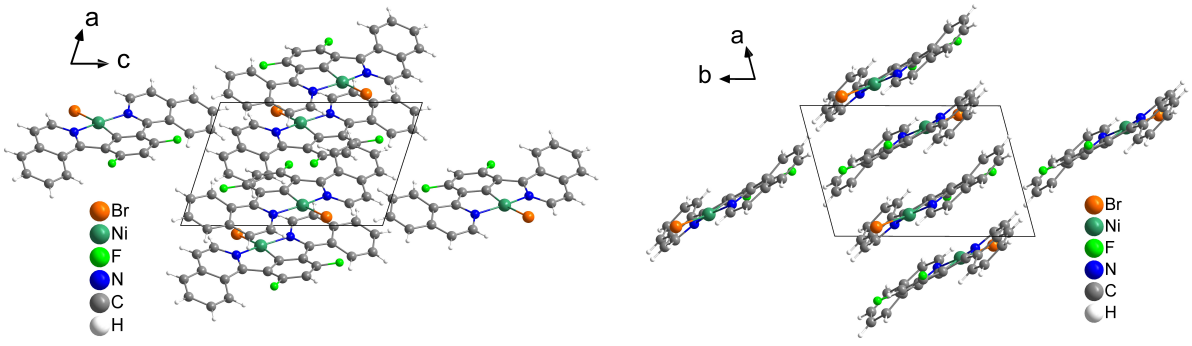

Figure 7-384 Crystal structure of [Ni(2^{i}Qu(4,6FPh)2^{i}Qu)Br] viewed along the crystallographic *b*-axis (left) and *c*-axis (right).

Table 7-64 Crystal data and structure refinement for [Ni(2^{i}Qu(4,6FPh)2^{i}Qu)Br].

Identification code	[Ni(2^{i}Qu(4,6FPh)2^{i}Qu)Br]
Empirical formula	$C_{24}H_{13}BrF_2N_2Ni$
Formula weight	505.98
Temperature/K	100.00
Crystal system	triclinic
Space group	$P\bar{1}$
a/Å	7.6925(5)
b/Å	10.8683(6)
c/Å	11.6319(7)
α/°	87.772(2)
β/°	72.098(2)
γ/°	75.008(2)
Volume/Å^3	893.02(9)
Z	2
ρ_{calc}g/cm^3	1.882
μ/mm^{-1}	3.359
F(000)	504.0
Crystal size/mm^3	0.30 × 0.05 × 0.01
Radiation	MoKα (λ = 0.71073)
2Θ range for data collection/°	3.884 to 56.72
Index ranges	–10 ≤ h ≤ 10, –14 ≤ k ≤ 14, –15 ≤ l ≤ 15
Reflections collected	55139
Independent reflections	4457 [R_{int} = 0.0614, R_{sigma} = 0.0260]
Data/restraints/parameters	4457/0/271
Goodness-of-fit on F^2	1.031
Final R indexes [I>=2σ (I)]	R_1 = 0.0332, wR_2 = 0.0832
Final R indexes [all data]	R_1 = 0.0419, wR_2 = 0.0875
Largest diff. peak/hole / e Å^{-3}	1.06/–0.47

Table 7-65 Fractional Atomic Coordinates (×10^4) and Equivalent Isotropic Displacement Parameters (Å^2×10^3) for [Ni(2^{i}Qu(4,6FPh)2^{i}Qu)Br]. U_{eq} is defined as 1/3 of the trace of the orthogonalized U_{IJ} tensor.

Atom	*x*	*y*	*z*	U(eq)
Br1	9311.4(4)	2194.8(2)	2919.2(2)	18.62(8)
Ni1	8351.4(4)	4002.4(3)	4287.8(3)	11.91(9)
F2	5047(2)	8724.1(14)	5610.2(14)	19.2(3)
F1	6985(2)	6130.3(15)	8461.6(14)	21.3(3)
N2	7598(3)	5286(2)	3228.8(19)	15.0(4)
N1	9095(3)	3144(2)	5602.7(19)	15.6(4)
C11	7302(4)	5085(2)	6596(2)	14.4(5)
C10	8327(3)	3757(2)	6702(2)	13.4(5)
C15	6272(4)	6484(2)	5050(2)	14.3(5)
C16	6444(3)	6419(2)	3755(2)	13.3(5)
C14	5692(4)	7509(2)	5893(2)	15.3(5)
C18	4088(4)	8449(2)	3548(2)	16.9(5)
C4	9940(4)	1913(2)	7594(2)	16.5(5)
C1	7147(3)	5307(2)	5431(2)	13.3(4)
C13	5888(4)	7366(2)	7038(2)	16.9(5)
C2	10342(4)	1969(2)	5472(2)	16.3(5)
C22	6320(4)	7180(2)	1766(2)	16.3(5)
C6	9288(4)	1772(3)	9753(2)	20.9(5)

Atom	*x*	*y*	*z*	U(eq)
C23	7660(4)	6032(3)	1261(2)	17.7(5)
C9	8573(4)	3113(2)	7762(2)	16.3(5)
C3	10853(4)	1368(2)	6413(2)	17.5(5)
C17	5613(4)	7368(2)	3049(2)	14.8(5)
C12	6702(4)	6168(2)	7368(2)	15.9(5)
C19	3415(4)	9327(2)	2810(3)	19.9(5)
C20	4205(4)	9186(3)	1538(3)	20.6(5)
C24	8196(4)	5109(2)	2002(2)	17.2(5)
C8	7481(4)	3564(3)	8961(2)	18.2(5)
C5	10298(4)	1275(3)	8615(2)	20.0(5)
C7	7834(4)	2905(3)	9931(2)	21.4(5)
C21	5622(4)	8127(3)	1022(3)	19.5(5)

Table 7-66 Anisotropic Displacement Parameters ($Å^2×10^3$) for [Ni(2^{i}Qu(4,6FPh)2^{i}Qu)Br]. The Anisotropic displacement factor exponent takes the form: $–2π^2[h^2a^{*2}U_{11}+2hka^*b^*U_{12}+…]$.

Atom	U_{11}	U_{22}	U_{33}	U_{23}	U_{13}	U_{12}
Br1	25.16(15)	11.89(13)	19.34(14)	–1.74(9)	–10.27(10)	–1.23(10)
Ni1	14.48(16)	8.30(15)	12.27(15)	–0.37(11)	–4.31(12)	–1.46(12)
F2	26.5(8)	9.0(7)	22.2(8)	0.0(6)	–10.1(6)	–1.8(6)
F1	31.8(9)	17.6(8)	16.4(7)	–1.4(6)	–11.2(7)	–4.9(7)
N2	16.2(10)	11.5(10)	15.9(10)	0.6(8)	–4.2(8)	–2.5(8)
N1	17.1(10)	13.6(10)	16.2(10)	0.5(8)	–5.1(8)	–4.3(8)
C11	14.7(11)	12.4(11)	15.4(11)	–1.0(9)	–3.1(9)	–3.8(9)
C10	13.8(11)	11.3(11)	15.3(11)	–0.5(9)	–4.2(9)	–3.6(9)
C15	15.9(11)	10.9(11)	17.2(12)	1.0(9)	–5.7(9)	–4.7(9)
C16	14.4(11)	9.9(11)	15.5(11)	–0.9(8)	–3.6(9)	–4.0(9)
C14	15.7(12)	9.9(11)	19.6(12)	0.7(9)	–4.9(10)	–2.7(9)
C18	19.9(12)	12.4(11)	19.6(12)	–1.4(9)	–7.8(10)	–4.0(10)
C4	19.2(12)	14.5(12)	19.0(12)	2.5(9)	–7.6(10)	–8.0(10)
C1	13.3(11)	11.2(11)	14.8(11)	–0.6(9)	–2.9(9)	–3.8(9)
C13	19.0(12)	12.8(12)	17.8(12)	–3.6(9)	–3.8(10)	–3.8(9)
C2	16.3(12)	13.7(12)	17.5(12)	0.5(9)	–4.4(10)	–2.5(9)
C22	18.5(12)	14.7(12)	18.9(12)	0.4(9)	–8.5(10)	–6.2(10)
C6	30.1(15)	19.4(13)	19.8(13)	8.3(10)	–11.8(11)	–13.8(11)
C23	21.6(13)	16.9(12)	13.8(11)	–0.4(9)	–3.9(10)	–5.4(10)
C9	18.0(12)	16.2(12)	17.7(12)	1.2(9)	–6.5(10)	–8.3(10)
C3	17.6(12)	12.8(12)	21.8(13)	0.6(9)	–5.6(10)	–3.9(10)
C17	17.8(12)	12.1(11)	16.6(12)	–0.3(9)	–7.2(10)	–5.4(9)
C12	19.1(12)	16.3(12)	13.0(11)	–1.2(9)	–4.8(9)	–5.9(10)
C19	21.2(13)	12.4(12)	27.7(14)	–0.4(10)	–10.7(11)	–3.0(10)
C20	27.3(14)	13.7(12)	26.6(14)	6.6(10)	–15.8(12)	–7.1(11)
C24	19.6(12)	13.2(12)	17.5(12)	–1.4(9)	–5.3(10)	–2.4(10)
C8	21.7(13)	15.4(12)	18.6(12)	1.8(9)	–5.8(10)	–7.6(10)
C5	26.0(14)	15.9(12)	22.8(13)	6.1(10)	–12.3(11)	–8.5(10)
C7	29.6(15)	21.6(13)	16.2(12)	–0.1(10)	–7.0(11)	–12.0(11)
C21	24.4(13)	15.8(12)	20.9(13)	1.8(10)	–9.5(11)	–6.7(10)

Table 7-67 Bond Lengths for [Ni(2^{i}Qu(4,6FPh)2^{i}Qu)Br].

Atom	Atom	Length/Å	Atom	Atom	Length/Å
Br1	Ni1	2.3894(4)	C14	C13	1.384(4)

Atom	Atom	Length/Å	Atom	Atom	Length/Å
Ni1	N2	1.920(2)	C18	C17	1.420(4)
Ni1	N1	1.920(2)	C18	C19	1.367(4)
Ni1	C1	1.829(2)	C4	C9	1.425(4)
F2	C14	1.352(3)	C4	C3	1.409(4)
F1	C12	1.353(3)	C4	C5	1.416(4)
N2	C16	1.356(3)	C13	C12	1.386(4)
N2	C24	1.363(3)	C2	C3	1.363(4)
N1	C10	1.351(3)	C22	C23	1.408(4)
N1	C2	1.366(3)	C22	C17	1.425(4)
C11	C10	1.475(3)	C22	C21	1.424(4)
C11	C1	1.403(3)	C6	C5	1.362(4)
C11	C12	1.396(3)	C6	C7	1.405(4)
C10	C9	1.434(3)	C23	C24	1.362(4)
C15	C16	1.473(3)	C9	C8	1.418(4)
C15	C14	1.400(3)	C19	C20	1.413(4)
C15	C1	1.407(3)	C20	C21	1.369(4)
C16	C17	1.436(3)	C8	C7	1.373(4)

Table 7-68 Bond Angles for [Ni(2^{i}Qu(4,6FPh)2^{i}Qu)Br].

Atom	Atom	Atom	Angle/˚	Atom	Atom	Atom	Angle/˚
N2	Ni1	Br1	97.97(7)	C3	C4	C5	121.6(2)
N1	Ni1	Br1	98.03(7)	C5	C4	C9	119.5(2)
N1	Ni1	N2	163.31(9)	C11	C1	Ni1	117.28(18)
C1	Ni1	Br1	168.21(8)	C11	C1	C15	125.0(2)
C1	Ni1	N2	82.65(10)	C15	C1	Ni1	117.48(18)
C1	Ni1	N1	82.66(10)	C14	C13	C12	119.2(2)
C16	N2	Ni1	116.84(17)	C3	C2	N1	122.7(2)
C16	N2	C24	120.1(2)	C23	C22	C17	118.8(2)
C24	N2	Ni1	123.10(17)	C23	C22	C21	121.3(2)
C10	N1	Ni1	116.99(17)	C21	C22	C17	119.9(2)
C10	N1	C2	119.7(2)	C5	C6	C7	120.3(2)
C2	N1	Ni1	123.31(18)	C24	C23	C22	119.7(2)
C1	C11	C10	111.8(2)	C4	C9	C10	117.6(2)
C12	C11	C10	132.2(2)	C8	C9	C10	124.2(2)
C12	C11	C1	115.3(2)	C8	C9	C4	118.1(2)
N1	C10	C11	110.4(2)	C2	C3	C4	119.3(2)
N1	C10	C9	120.6(2)	C18	C17	C16	124.2(2)
C9	C10	C11	129.0(2)	C18	C17	C22	118.2(2)
C14	C15	C16	132.4(2)	C22	C17	C16	117.6(2)
C14	C15	C1	115.1(2)	F1	C12	C11	122.0(2)
C1	C15	C16	111.6(2)	F1	C12	C13	115.4(2)
N2	C16	C15	110.7(2)	C13	C12	C11	122.5(2)
N2	C16	C17	120.3(2)	C18	C19	C20	121.3(3)
C17	C16	C15	129.0(2)	C21	C20	C19	119.9(2)
F2	C14	C15	122.1(2)	C23	C24	N2	122.5(2)
F2	C14	C13	115.1(2)	C7	C8	C9	120.6(3)
C13	C14	C15	122.5(2)	C6	C5	C4	120.6(3)
C19	C18	C17	120.4(2)	C8	C7	C6	120.6(3)
C3	C4	C9	118.9(2)	C20	C21	C22	120.0(3)

Table 7-69 Torsion Angles for [Ni(2^{i}Qu(4,6FPh)2^{i}Qu)Br].

A	B	C	D	Angle/°	A	B	C	D	Angle/°
Br1	Ni1	C1	C11	93.6(4)	C4	C9	C8	C7	4.7(4)
Br1	Ni1	C1	C15	–91.5(4)	C1	C11	C10	N1	9.0(3)
Ni1	N2	C16	C15	9.6(3)	C1	C11	C10	C9	–171.3(2)
Ni1	N2	C16	C17	–171.65(18)	C1	C11	C12	F1	–171.5(2)
Ni1	N2	C24	C23	–179.5(2)	C1	C11	C12	C13	4.3(4)
Ni1	N1	C10	C11	–9.9(3)	C1	C15	C16	N2	–7.4(3)
Ni1	N1	C10	C9	170.43(18)	C1	C15	C16	C17	173.9(2)
Ni1	N1	C2	C3	–179.8(2)	C1	C15	C14	F2	171.6(2)
F2	C14	C13	C12	–174.2(2)	C1	C15	C14	C13	–2.7(4)
N2	Ni1	C1	C11	–172.6(2)	C2	N1	C10	C11	170.0(2)
N2	Ni1	C1	C15	2.26(19)	C2	N1	C10	C9	–9.7(4)
N2	C16	C17	C18	165.6(2)	C22	C23	C24	N2	–5.4(4)
N2	C16	C17	C22	–11.9(4)	C23	C22	C17	C16	5.7(4)
N1	Ni1	C1	C11	–0.55(19)	C23	C22	C17	C18	–171.9(2)
N1	Ni1	C1	C15	174.3(2)	C23	C22	C21	C20	174.5(3)
N1	C10	C9	C4	12.2(4)	C9	C4	C3	C2	–3.2(4)
N1	C10	C9	C8	–164.6(2)	C9	C4	C5	C6	3.0(4)
N1	C2	C3	C4	6.1(4)	C9	C8	C7	C6	0.2(4)
C11	C10	C9	C4	–167.5(2)	C3	C4	C9	C10	–5.6(4)
C11	C10	C9	C8	15.7(4)	C3	C4	C9	C8	171.4(2)
C10	N1	C2	C3	0.4(4)	C3	C4	C5	C6	–174.6(3)
C10	C11	C1	Ni1	–4.5(3)	C17	C18	C19	C20	0.1(4)
C10	C11	C1	C15	–178.9(2)	C17	C22	C23	C24	2.5(4)
C10	C11	C12	F1	–1.5(4)	C17	C22	C21	C20	–3.3(4)
C10	C11	C12	C13	174.2(3)	C12	C11	C10	N1	–161.2(3)
C10	C9	C8	C7	–178.5(2)	C12	C11	C10	C9	18.4(5)
C15	C16	C17	C18	–15.8(4)	C12	C11	C1	Ni1	167.50(18)
C15	C16	C17	C22	166.7(2)	C12	C11	C1	C15	–6.9(4)
C15	C14	C13	C12	0.5(4)	C19	C18	C17	C16	178.2(2)
C16	N2	C24	C23	–0.8(4)	C19	C18	C17	C22	–4.4(4)
C16	C15	C14	F2	3.6(4)	C19	C20	C21	C22	–1.1(4)
C16	C15	C14	C13	–170.7(3)	C24	N2	C16	C15	–169.3(2)
C16	C15	C1	Ni1	2.2(3)	C24	N2	C16	C17	9.5(4)
C16	C15	C1	C11	176.6(2)	C5	C4	C9	C10	176.8(2)
C14	C15	C16	N2	160.9(3)	C5	C4	C9	C8	–6.2(4)
C14	C15	C16	C17	–17.8(5)	C5	C4	C3	C2	174.4(3)
C14	C15	C1	Ni1	–168.26(18)	C5	C6	C7	C8	–3.7(4)
C14	C15	C1	C11	6.2(4)	C7	C6	C5	C4	2.0(4)
C14	C13	C12	F1	174.7(2)	C21	C22	C23	C24	–175.3(2)
C14	C13	C12	C11	–1.3(4)	C21	C22	C17	C16	–176.4(2)
C18	C19	C20	C21	2.7(4)	C21	C22	C17	C18	6.0(4)

Table 7-70 Hydrogen Atom Coordinates (Å×10^{4}) and Isotropic Displacement Parameters (Å^{2}×10^{3}) for [Ni(2^{i}Qu(4,6FPh)2^{i}Qu)Br].

Atom	*x*	*y*	*z*	U(eq)
H18	3533.11	8564.42	4400.48	20
H13	5470.52	8080.17	7590.42	20
H2	10875.25	1553.23	4692.03	20
H6	9567.24	1349.92	10430.97	25

Atom	*x*	*y*	*z*	U(eq)
H23	8187.59	5901.81	408.24	21
H3	11814.79	589.52	6275.23	21
H19	2395.14	10045.74	3158.64	24
H20	3753.48	9824.61	1042.52	25
H24	9016.43	4311.58	1650.11	21
H8	6495.73	4330.2	9094.03	22
H5	11250.76	494.72	8504.84	24
H7	7088.42	3216.85	10728.97	26
H21	6138.67	8024.02	166.77	23

7.3.11 [Ni(2Qu(Ph)2Qu)Cl]

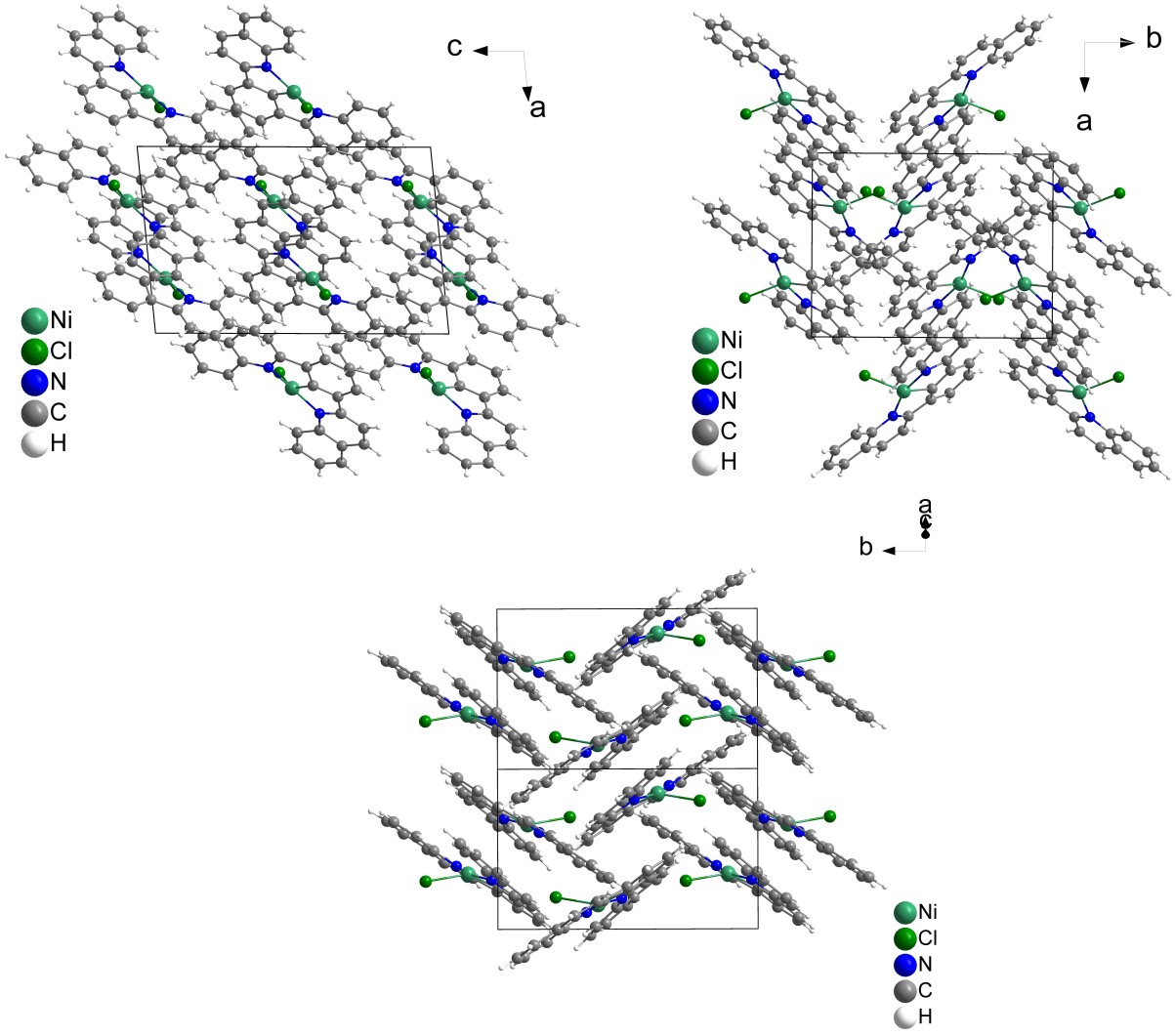

Figure 7-385 Crystal structure of [Ni(2Qu(Ph)2Qu)Cl] viewed along the crystallographic *b*-axis (top left), *c*-axis (top right) and viewed along the *a*-*c* face diagonal.

Table 7-71 Crystal data and structure refinement for [Ni(2Qu(Ph)2Qu)Cl].

Identification code	[Ni(2Qu(Ph)2Qu)Cl]
Empirical formula	$C_{24}H_{15}ClN_2Ni$
Formula weight	425.54

Temperature/K	100.0
Crystal system	monoclinic
Space group	$P2_1/c$
a/Å	9.5913(4)
b/Å	12.4899(5)
c/Å	14.9938(6)
α/°	90
β/°	95.7960(10)
γ/°	90
Volume/Å^3	1786.99(13)
Z	4
ρ_{calc}g/cm^3	1.582
μ/mm^{-1}	1.247
F(000)	872.0
Crystal size/mm^3	0.16 × 0.08 × 0.05
Radiation	MoKα (λ = 0.71073)
2Θ range for data collection/°	4.254 to 56.558
Index ranges	–12 ≤ h ≤ 12, –16 ≤ k ≤ 16, –19 ≤ l ≤ 19
Reflections collected	63244
Independent reflections	4419 [R_{int} = 0.0656, R_{sigma} = 0.0245]
Data/restraints/parameters	4419/0/253
Goodness-of-fit on F^2	1.094
Final R indexes [I>=2σ (I)]	R_1 = 0.0364, wR_2 = 0.0809
Final R indexes [all data]	R_1 = 0.0438, wR_2 = 0.0855
Largest diff. peak/hole / e Å^{-3}	0.70/–0.50

Table 7-72 Fractional Atomic Coordinates (×10^4) and Equivalent Isotropic Displacement Parameters (Å^2×10^3) for [Ni(2Qu(Ph)2Qu)Cl]. U_{eq} is defined as 1/3 of the trace of the orthogonalized U_{IJ} tensor.

Atom	*x*	*y*	*z*	U(eq)
Ni1	2933.5(3)	3846.9(2)	5526.8(2)	11.34(8)
Cl1	2091.3(5)	2226.6(4)	5912.7(3)	14.91(11)
N2	1821.3(18)	4760.1(14)	6264.2(12)	13.7(3)
N1	4280.1(18)	3406.0(15)	4674.1(12)	14.1(3)
C15	1786(2)	5789.6(17)	4960.7(15)	15.2(4)
C16	1258(2)	5628.0(17)	5829.3(14)	13.9(4)
C22	1856(2)	3557.4(18)	8505.3(15)	18.2(4)
C23	2208(2)	3757.5(17)	7653.8(15)	16.9(4)
C17	280(2)	6304.7(17)	6191.3(16)	17.3(4)
C11	3377(2)	4979.7(18)	3995.6(15)	15.7(4)
C1	2783(2)	5025.0(17)	4804.3(14)	14.6(4)
C14	1397(2)	6559.7(18)	4307.0(16)	17.8(4)
C19	502(2)	5219.2(17)	7518.1(15)	15.5(4)
C24	1509(2)	4572.4(16)	7129.2(14)	13.9(4)
C2	5175(2)	2534.3(18)	4732.2(15)	16.1(4)
C10	4274(2)	4050.9(17)	3949.0(15)	15.2(4)
C18	–118(2)	6086.5(17)	7021.9(16)	18.0(4)
C21	793(2)	4145.0(18)	8866.5(15)	18.7(4)
C7	6011(2)	2291.4(19)	4020.0(15)	19.4(5)
C12	3013(2)	5761.7(19)	3347.5(16)	19.3(4)
C8	5913(2)	2958(2)	3258.9(16)	23.1(5)
C9	5065(2)	3834(2)	3225.3(16)	20.6(5)

Atom	*x*	*y*	*z*	U(eq)
C3	5302(2)	1878.5(19)	5505.0(16)	19.9(5)
C13	2034(2)	6541.4(19)	3506.5(16)	19.9(5)
C20	147(2)	4971.6(18)	8389.1(15)	18.4(4)
C6	6904(3)	1389(2)	4097.1(16)	25.5(5)
C4	6167(3)	1000(2)	5553.0(18)	25.7(5)
C5	6960(3)	744(2)	4836.2(18)	29.8(6)

Table 7-73 Anisotropic Displacement Parameters ($Å^2×10^3$) for [Ni(2Qu(Ph)2Qu)Cl]. The Anisotropic displacement factor exponent takes the form: $–2π^2[h^2a^{*2}U_{11}+2hka^*b^*U_{12}+…]$.

Atom	U_{11}	U_{22}	U_{33}	U_{23}	U_{13}	U_{12}
Ni1	12.04(13)	9.68(13)	12.73(14)	–0.01(10)	3.39(9)	1.03(9)
Cl1	15.8(2)	10.9(2)	18.9(2)	–1.72(18)	5.87(18)	–1.13(17)
N2	12.8(8)	12.7(8)	15.7(9)	–2.0(7)	2.0(6)	–0.2(6)
N1	12.5(8)	15.0(8)	14.8(8)	–1.5(7)	1.9(6)	–0.9(7)
C15	13.9(10)	13.9(9)	17.5(10)	–0.6(8)	0.5(8)	–1.9(8)
C16	12.8(9)	11.7(9)	16.9(10)	–0.1(8)	0.2(8)	0.1(7)
C22	22.4(11)	13.4(10)	18.4(11)	1.7(8)	–0.2(8)	–2.6(8)
C23	17.1(10)	15.3(10)	18.3(11)	–2.7(8)	1.7(8)	1.0(8)
C17	18.7(10)	11.7(10)	21.4(11)	–0.1(8)	2.1(8)	2.6(8)
C11	14.5(10)	15.1(10)	17.5(10)	–0.8(8)	1.9(8)	–1.7(8)
C1	13.7(9)	13.5(9)	16.6(10)	–0.2(8)	1.7(8)	–1.8(8)
C14	15.6(10)	15.0(10)	22.7(11)	0.7(9)	1.0(8)	0.1(8)
C19	15.4(10)	12.5(9)	18.9(11)	–1.1(8)	3.8(8)	–1.1(8)
C24	15.8(10)	10.9(9)	15.0(10)	–1.9(8)	0.8(8)	–2.2(8)
C2	12.6(10)	16.7(10)	19.0(11)	–3.5(8)	1.4(8)	–0.2(8)
C10	14.8(10)	15.1(10)	15.7(10)	–1.2(8)	1.5(8)	–1.6(8)
C18	17.6(10)	13.9(10)	23.3(11)	–2.6(9)	5.6(8)	2.3(8)
C21	23.7(11)	18.2(10)	14.7(10)	–2.6(8)	3.7(8)	–4.4(9)
C7	17.4(10)	22.0(11)	18.2(11)	–7.8(9)	–0.7(8)	2.4(9)
C12	21.1(11)	19.8(11)	17.4(11)	1.7(9)	4.5(8)	–1.4(9)
C8	20.5(11)	30.3(13)	18.9(11)	–7.1(10)	3.4(9)	3.1(10)
C9	19.4(11)	26.1(12)	16.8(11)	–0.8(9)	4.4(8)	0.7(9)
C3	17.0(10)	18.9(11)	23.3(12)	–0.9(9)	0.5(8)	3.1(9)
C13	19.7(11)	19.1(11)	20.9(11)	6.4(9)	1.3(9)	–0.2(9)
C20	19.3(11)	17.8(10)	18.9(11)	–3.4(8)	5.6(8)	–0.9(8)
C6	22.5(12)	35.5(14)	17.9(11)	–11.1(10)	–0.7(9)	12.4(10)
C4	25.8(12)	23.0(12)	27.5(13)	2.7(10)	–1.0(10)	7.6(10)
C5	29.4(13)	30.3(14)	28.4(13)	–8.5(11)	–3.6(10)	17.1(11)

Table 7-74 Bond Lengths for [Ni(2Qu(Ph)2Qu)Cl].

Atom	Atom	Length/Å	Atom	Atom	Length/Å
Ni1	Cl1	2.2754(6)	C11	C10	1.450(3)
Ni1	N2	1.9746(18)	C11	C12	1.397(3)
Ni1	N1	1.9849(18)	C14	C13	1.401(3)
Ni1	C1	1.824(2)	C19	C24	1.428(3)
N2	C16	1.349(3)	C19	C18	1.411(3)
N2	C24	1.380(3)	C19	C20	1.417(3)
N1	C2	1.383(3)	C2	C7	1.431(3)
N1	C10	1.353(3)	C2	C3	1.414(3)
C15	C16	1.458(3)	C10	C9	1.412(3)

Atom	Atom	Length/Å	Atom	Atom	Length/Å
C15	C1	1.388(3)	C21	C20	1.368(3)
C15	C14	1.397(3)	C7	C8	1.408(3)
C16	C17	1.411(3)	C7	C6	1.414(3)
C22	C23	1.376(3)	C12	C13	1.390(3)
C22	C21	1.408(3)	C8	C9	1.361(3)
C23	C24	1.414(3)	C3	C4	1.373(3)
C17	C18	1.366(3)	C6	C5	1.366(4)
C11	C1	1.392(3)	C4	C5	1.414(4)

Table 7-75 Bond Angles for [Ni(2Qu(Ph)2Qu)Cl].

Atom	Atom	Atom	Angle/°	Atom	Atom	Atom	Angle/°
N2	Ni1	Cl1	98.37(5)	C15	C14	C13	118.8(2)
N2	Ni1	N1	160.80(8)	C18	C19	C24	119.0(2)
N1	Ni1	Cl1	100.82(6)	C18	C19	C20	121.7(2)
C1	Ni1	Cl1	149.28(7)	C20	C19	C24	119.2(2)
C1	Ni1	N2	81.48(9)	N2	C24	C23	120.62(19)
C1	Ni1	N1	81.88(9)	N2	C24	C19	120.51(19)
C16	N2	Ni1	113.95(14)	C23	C24	C19	118.8(2)
C16	N2	C24	118.43(18)	N1	C2	C7	120.7(2)
C24	N2	Ni1	127.50(14)	N1	C2	C3	120.6(2)
C2	N1	Ni1	128.14(15)	C3	C2	C7	118.7(2)
C10	N1	Ni1	113.71(14)	N1	C10	C11	113.10(19)
C10	N1	C2	118.14(18)	N1	C10	C9	123.0(2)
C1	C15	C16	111.27(19)	C9	C10	C11	123.9(2)
C1	C15	C14	119.7(2)	C17	C18	C19	119.5(2)
C14	C15	C16	129.1(2)	C20	C21	C22	119.9(2)
N2	C16	C15	112.63(18)	C8	C7	C2	118.9(2)
N2	C16	C17	123.0(2)	C8	C7	C6	121.9(2)
C17	C16	C15	124.4(2)	C6	C7	C2	119.2(2)
C23	C22	C21	121.1(2)	C13	C12	C11	119.7(2)
C22	C23	C24	120.0(2)	C9	C8	C7	119.7(2)
C18	C17	C16	119.3(2)	C8	C9	C10	119.4(2)
C1	C11	C10	111.80(19)	C4	C3	C2	120.5(2)
C1	C11	C12	118.8(2)	C12	C13	C14	121.3(2)
C12	C11	C10	129.3(2)	C21	C20	C19	120.6(2)
C15	C1	Ni1	117.96(16)	C5	C6	C7	120.7(2)
C15	C1	C11	121.6(2)	C3	C4	C5	120.6(2)
C11	C1	Ni1	118.02(16)	C6	C5	C4	120.2(2)

Table 7-76 Torsion Angles for [Ni(2Qu(Ph)2Qu)Cl].

A	B	C	D	Angle/°	A	B	C	D	Angle/°
Ni1	N2	C16	C15	–9.4(2)	C1	C11	C12	C13	–2.4(3)
Ni1	N2	C16	C17	171.34(17)	C14	C15	C16	N2	176.3(2)
Ni1	N2	C24	C23	12.2(3)	C14	C15	C16	C17	–4.5(4)
Ni1	N2	C24	C19	–169.59(15)	C14	C15	C1	Ni1	–164.48(17)
Ni1	N1	C2	C7	175.51(16)	C14	C15	C1	C11	–2.3(3)
Ni1	N1	C2	C3	–5.8(3)	C24	N2	C16	C15	174.12(18)
Ni1	N1	C10	C11	5.4(2)	C24	N2	C16	C17	–5.1(3)
Ni1	N1	C10	C9	–174.69(17)	C24	C19	C18	C17	–1.5(3)

A	B	C	D	Angle/°	A	B	C	D	Angle/°
Cl1	Ni1	C1	C15	76.9(2)	C24	C19	C20	C21	2.2(3)
Cl1	Ni1	C1	C11	–86.0(2)	C2	N1	C10	C11	–175.54(18)
N2	Ni1	C1	C15	–15.23(17)	C2	N1	C10	C9	4.4(3)
N2	Ni1	C1	C11	–178.07(18)	C2	C7	C8	C9	2.0(3)
N2	C16	C17	C18	0.5(3)	C2	C7	C6	C5	0.8(4)
N1	Ni1	C1	C15	174.39(18)	C2	C3	C4	C5	0.9(4)
N1	Ni1	C1	C11	11.55(17)	C10	N1	C2	C7	–3.4(3)
N1	C2	C7	C8	0.3(3)	C10	N1	C2	C3	175.3(2)
N1	C2	C7	C6	–179.4(2)	C10	C11	C1	Ni1	–11.6(2)
N1	C2	C3	C4	178.5(2)	C10	C11	C1	C15	–173.8(2)
N1	C10	C9	C8	–2.1(4)	C10	C11	C12	C13	174.5(2)
C15	C16	C17	C18	–178.6(2)	C18	C19	C24	N2	–3.1(3)
C15	C14	C13	C12	1.4(3)	C18	C19	C24	C23	175.1(2)
C16	N2	C24	C23	–171.85(19)	C18	C19	C20	C21	–178.1(2)
C16	N2	C24	C19	6.3(3)	C21	C22	C23	C24	0.7(3)
C16	C15	C1	Ni1	14.0(2)	C7	C2	C3	C4	–2.7(3)
C16	C15	C1	C11	176.21(19)	C7	C8	C9	C10	–1.2(4)
C16	C15	C14	C13	–178.4(2)	C7	C6	C5	C4	–2.8(4)
C16	C17	C18	C19	2.8(3)	C12	C11	C1	Ni1	165.78(17)
C22	C23	C24	N2	–178.0(2)	C12	C11	C1	C15	3.6(3)
C22	C23	C24	C19	3.8(3)	C12	C11	C10	N1	–173.8(2)
C22	C21	C20	C19	2.3(3)	C12	C11	C10	C9	6.3(4)
C23	C22	C21	C20	–3.8(3)	C8	C7	C6	C5	–178.9(2)
C11	C10	C9	C8	177.8(2)	C3	C2	C7	C8	–178.4(2)
C11	C12	C13	C14	–0.1(4)	C3	C2	C7	C6	1.9(3)
C1	C15	C16	N2	–2.0(3)	C3	C4	C5	C6	1.9(4)
C1	C15	C16	C17	177.2(2)	C20	C19	C24	N2	176.60(19)
C1	C15	C14	C13	–0.2(3)	C20	C19	C24	C23	–5.2(3)
C1	C11	C10	N1	3.3(3)	C20	C19	C18	C17	178.8(2)
C1	C11	C10	C9	–176.6(2)	C6	C7	C8	C9	–178.3(2)

Table 7-77 Hydrogen Atom Coordinates (Å×10^4) and Isotropic Displacement Parameters (Å^2×10^3) for [Ni(2Qu(Ph)2Qu)Cl].

Atom	*x*	*y*	*z*	U(eq)
H22	2338.52	3013.47	8855.65	22
H23	2920.88	3347.85	7418.53	20
H17	–97.29	6905.16	5861.11	21
H14	713.55	7086.29	4403.51	21
H18	–806.13	6515.38	7263.39	22
H21	523.97	3967.61	9441.04	22
H12	3433.79	5760.76	2800.35	23
H8	6437.09	2797.63	2770.94	28
H9	5006.52	4295.57	2719.29	25
H3	4785.68	2047.03	5994.76	24
H13	1791.45	7071.8	3063.65	24
H20	–545.69	5383.04	8643.92	22
H6	7470.51	1228.44	3630.27	31
H4	6233.8	560.13	6072.41	31
H5	7533.28	122.06	4868.66	36

7.3.12 [Ni(2Tz(Ph)2Tz)Cl]

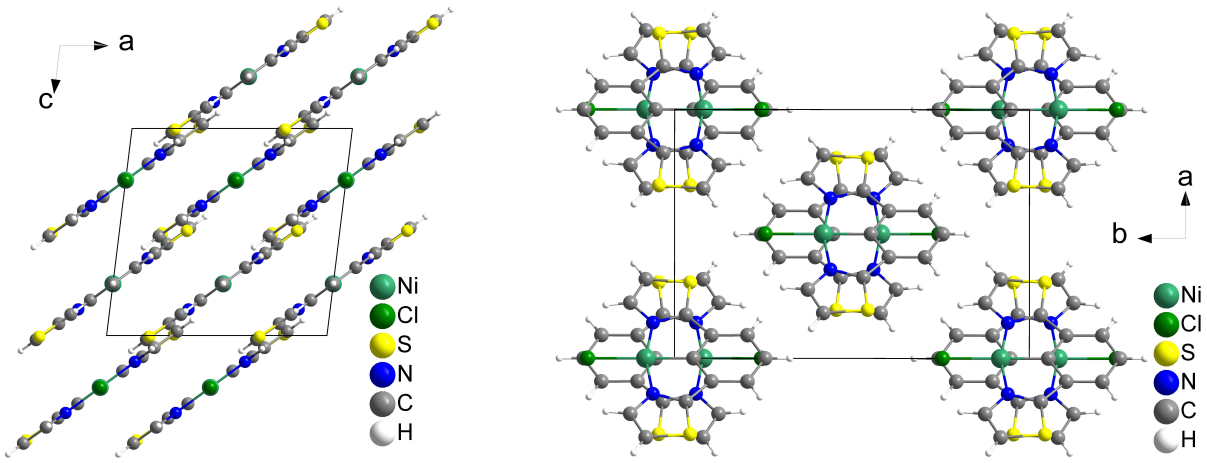

Figure 7-386 Crystal structure of [Ni(2Tz(Ph)2Tz)Cl] viewed along the crystallographic *b*- (left) and *c*-axis (right).

Table 7-78 Crystal data and structure refinement for [Ni(2Tz(Ph)2Tz)Cl].

Identification code	0.5[Ni(2Tz(Ph)2Tz)Cl]
Empirical formula	$C_6H_{3.5}Cl_{0.5}NNi_{0.5}S$
Formula weight	168.74
Temperature/K	100.0
Crystal system	monoclinic
Space group	*C*2/c
a/Å	9.6753(5)
b/Å	13.6967(7)
c/Å	9.1591(4)
α/°	90
β/°	97.015(2)
γ/°	90
Volume/Å^3	1204.68(10)
Z	8
ρ_{calc}g/cm^3	1.861
μ/mm^{-1}	2.156
F(000)	680.0
Crystal size/mm^3	0.22 × 0.11 × 0.04
Radiation	MoKα (λ = 0.71073)
2Θ range for data collection/°	5.18 to 77.242
Index ranges	–16 ≤ h ≤ 16, –24 ≤ k ≤ 24, –16 ≤ l ≤ 16
Reflections collected	43123
Independent reflections	3397 [R_{int} = 0.0508, R_{sigma} = 0.0222]
Data/restraints/parameters	3397/0/85
Goodness-of-fit on F^2	1.098
Final R indexes [I>=2σ (I)]	R_1 = 0.0278, wR_2 = 0.0682
Final R indexes [all data]	R_1 = 0.0312, wR_2 = 0.0703
Largest diff. peak/hole / e Å^{-3}	1.29/–0.66

Table 7-79 Fractional Atomic Coordinates (×10^4) and Equivalent Isotropic Displacement Parameters (Å^2×10^3) for [Ni(2Tz(Ph)2Tz)Cl]. U_{eq} is defined as 1/3 of the trace of the orthogonalized U_{IJ} tensor.

Atom	*x*	*y*	*z*	U(eq)
Ni1	5000	4191.5(2)	7500	10.11(5)
Cl1	5000	2546.6(3)	7500	18.22(7)
S1	8054.9(3)	5443.7(2)	4945.1(3)	16.38(6)
N1	6429.5(9)	4392.3(6)	6266.3(9)	12.37(13)
C5	5925.4(10)	6037.5(7)	6715.2(11)	12.36(14)
C4	6743.9(10)	5324.4(7)	6020.6(11)	12.67(15)
C7	5000	7554.4(11)	7500	16.4(2)
C1	5000	5535.9(10)	7500	11.63(19)
C2	7232.0(11)	3756.8(8)	5578.9(12)	14.93(16)
C3	8174.9(12)	4192.3(9)	4802.1(13)	17.41(18)
C6	5931.3(11)	7058.2(8)	6708.2(12)	15.51(16)

Table 7-80 Anisotropic Displacement Parameters (Å^2×10^3) for [Ni(2Tz(Ph)2Tz)Cl]. The Anisotropic displacement factor exponent takes the form: $-2\pi^2[h^2a^{*2}U_{11}+2hka^*b^*U_{12}+\ldots]$.

Atom	U_{11}	U_{22}	U_{33}	U_{23}	U_{13}	U_{12}
Ni1	10.89(7)	8.44(7)	11.36(7)	0	2.79(5)	0
Cl1	23.46(16)	10.21(12)	23.24(16)	0	11.89(13)	0
S1	13.44(10)	19.42(12)	17.04(11)	1.40(8)	4.97(8)	–2.27(8)
N1	12.7(3)	11.6(3)	13.0(3)	–0.4(2)	2.5(2)	0.4(2)
C5	12.5(3)	11.1(3)	13.3(3)	1.1(3)	0.8(3)	–0.7(3)
C4	11.9(3)	13.4(4)	12.7(3)	0.5(3)	1.7(3)	–0.9(3)
C7	18.9(6)	9.7(5)	20.0(6)	0	–0.3(5)	0
C1	12.1(5)	10.3(5)	12.6(5)	0	1.7(4)	0
C2	13.8(4)	16.0(4)	15.3(4)	–1.2(3)	3.3(3)	2.1(3)
C3	14.1(4)	21.2(5)	17.6(4)	–1.0(3)	4.7(3)	1.3(3)
C6	16.8(4)	12.0(4)	17.2(4)	2.1(3)	0.3(3)	–2.1(3)

Table 7-81 Bond Lengths for [Ni(2Tz(Ph)2Tz)Cl].

Atom	Atom	Length/Å	Atom	Atom	Length/Å
Ni1	Cl1	2.2529(4)	N1	C2	1.3698(13)
Ni1	N1	1.9097(9)	C5	C4	1.4522(14)
Ni1	N1^1	1.9097(9)	C5	C1	1.3956(12)
Ni1	C1	1.8414(14)	C5	C6	1.3980(15)
S1	C4	1.7062(10)	C7	C6^1	1.3998(13)
S1	C3	1.7240(12)	C7	C6	1.3998(13)
N1	C4	1.3379(14)	C2	C3	1.3612(16)

^{1}1-X,+Y,3/2-Z

Table 7-82 Bond Angles for [Ni(2Tz(Ph)2Tz)Cl].

Atom	Atom	Atom	Angle/˚	Atom	Atom	Atom	Angle/˚
N1^1	Ni1	Cl1	98.28(3)	C6	C5	C4	131.90(9)
N1	Ni1	Cl1	98.28(3)	N1	C4	S1	112.88(8)
N1	Ni1	N1^1	163.43(5)	N1	C4	C5	114.88(9)
C1	Ni1	Cl1	180.0	C5	C4	S1	132.23(8)
C1	Ni1	N1^1	81.72(3)	C6	C7	C6^1	121.91(13)
C1	Ni1	N1	81.72(3)	C5^1	C1	Ni1	119.49(6)

Atom	Atom	Atom	Angle/°	Atom	Atom	Atom	Angle/°
C4	S1	C3	90.59(5)	C5	C1	Ni1	119.49(6)
C4	N1	Ni1	115.66(7)	C5[1]	C1	C5	121.01(13)
C4	N1	C2	112.07(9)	C3	C2	N1	114.55(10)
C2	N1	Ni1	132.26(8)	C2	C3	S1	109.90(8)
C1	C5	C4	108.24(9)	C5	C6	C7	118.68(10)
C1	C5	C6	119.86(10)				

[1]1-X,+Y,3/2-Z

Table 7-83 Torsion Angles for [Ni(2Tz(Ph)2Tz)Cl].

A	B	C	D	Angle/°	A	B	C	D	Angle/°
Ni1	N1	C4	S1	178.60(5)	C1	C5	C4	S1	–178.89(7)
Ni1	N1	C4	C5	–1.03(11)	C1	C5	C4	N1	0.65(11)
Ni1	N1	C2	C3	–178.80(8)	C1	C5	C6	C7	0.13(13)
N1[1]	Ni1	C1	C5[1]	–0.44(5)	C2	N1	C4	S1	–0.59(11)
N1	Ni1	C1	C5	–0.44(5)	C2	N1	C4	C5	179.78(8)
N1[1]	Ni1	C1	C5	179.57(5)	C3	S1	C4	N1	0.62(8)
N1	Ni1	C1	C5[1]	179.56(5)	C3	S1	C4	C5	–179.83(10)
N1	C2	C3	S1	0.24(13)	C6	C5	C4	S1	1.20(18)
C4	S1	C3	C2	–0.48(9)	C6	C5	C4	N1	–179.26(10)
C4	N1	C2	C3	0.22(14)	C6	C5	C1	Ni1	179.94(7)
C4	C5	C1	Ni1	0.01(8)	C6	C5	C1	C5[1]	–0.06(7)
C4	C5	C1	C5[1]	–179.99(9)	C6[1]	C7	C6	C5	–0.06(7)
C4	C5	C6	C7	–179.97(9)					

[1]1-X,+Y,3/2-Z

Table 7-84 Hydrogen Atom Coordinates (Å×10^4) and Isotropic Displacement Parameters (Å^2×10^3) for [Ni(2Tz(Ph)2Tz)Cl].

Atom	*x*	*y*	*z*	U(eq)
H7	5000.01	8247.96	7500.02	20
H2	7138.16	3068.04	5639.49	18
H3	8805.32	3856.6	4261.5	21
H6	6554.91	7408.04	6176.6	19

7.3.13 [Ni(4Tz(Ph)4Tz)Cl]

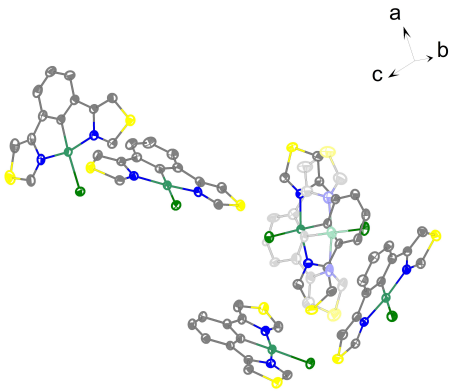

Figure 7-387 Asymmetric unit of [Ni(4Tz(Ph)4Tz)Cl]. Ellipsoids are shown with a 50% probability. Hydrogen atoms are omitted for clarity.

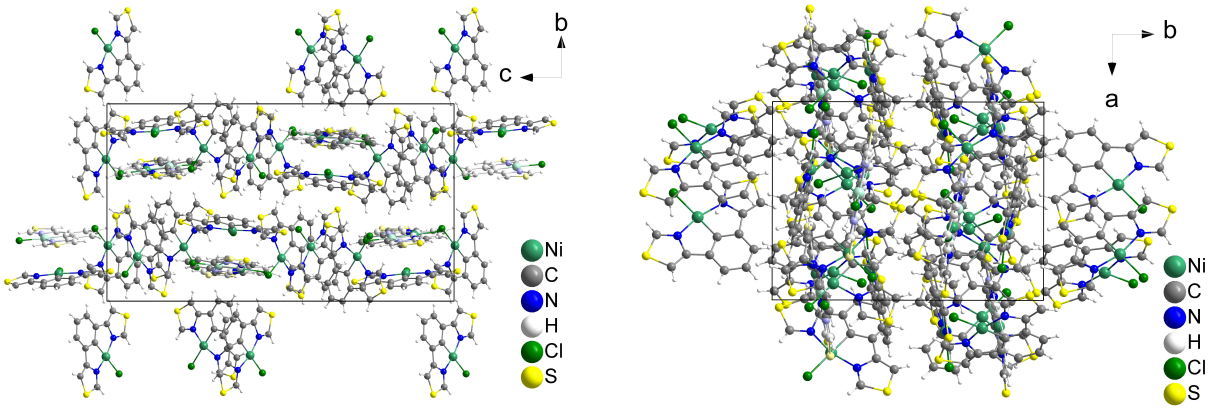

Figure 7-388 Crystal structure of [Ni(4Tz(Ph)4Tz)Cl] viewed along the crystallographic *a*- (left) and *c*-axis (right).

Table 7-85 Crystal data and structure refinement for [Ni(4Tz(Ph)4Tz)Cl].

Identification code	5[Ni(4Tz(Ph)4Tz)Cl]
Empirical formula	$C_{60}H_{35}Cl_5N_{10}Ni_5S_{10}$
Formula weight	337.48
Temperature/K	100.0
Crystal system	monoclinic
Space group	$P2_1/n$
a/Å	12.4902(6)
b/Å	16.8148(7)
c/Å	30.0903(12)
α/°	90
β/°	100.158(2)
γ/°	90
Volume/Å^3	6220.5(5)
Z	4
ρ_{calc}g/cm^3	1.802
μ/mm^{-1}	2.088
F(000)	3400.0
Crystal size/mm^3	0.2 × 0.1 × 0.3
Radiation	MoKα (λ = 0.71073)
2Θ range for data collection/°	2.75 to 61.998
Index ranges	–18 ≤ h ≤ 17, –24 ≤ k ≤ 24, –42 ≤ l ≤ 43
Reflections collected	265669
Independent reflections	19812 [R_{int} = 0.0786, R_{sigma} = 0.0395]
Data/restraints/parameters	19812/159/974
Goodness-of-fit on F^2	1.214
Final R indexes [I>=2σ (I)]	R_1 = 0.0484, wR_2 = 0.0944
Final R indexes [all data]	R_1 = 0.0710, wR_2 = 0.1042
Largest diff. peak/hole / e Å^{-3}	0.57/–0.79

Table 7-86 Fractional Atomic Coordinates (×10^4) and Equivalent Isotropic Displacement Parameters (Å^2×10^3) for [Ni(4Tz(Ph)4Tz)Cl]. U_{eq} is defined as 1/3 of the trace of the orthogonalized U_{IJ} tensor.

Atom	*x*	*y*	*z*	U(eq)
Ni1_1	8427.1(3)	3599.4(2)	6389.3(2)	17.52(8)
C4_1	9450(3)	3678.3(19)	5624.7(11)	18.3(6)
N1_1	8426(2)	3563.7(16)	5753.0(9)	18.5(5)
C1_1	9881(3)	3839.6(18)	6410.2(11)	18.8(6)

Atom	*x*	*y*	*z*	U(eq)
C5_1	10296(3)	3855.6(19)	6012.1(11)	19.8(6)
C2_1	7655(3)	3460.8(19)	5401.4(11)	21.5(6)
N2_1	8828(2)	3733.4(17)	7033.2(9)	21.6(6)
C9_1	10514(3)	4044(2)	6820.1(11)	22.4(7)
C3_1	9412(3)	3649(2)	5172.6(11)	22.8(7)
Cl1_1	6617.5(7)	3465.9(5)	6361.3(3)	23.00(16)
S1_1	8099.6(7)	3487.1(5)	4897.8(3)	24.11(17)
C10_1	9895(3)	4007(2)	7183.9(11)	24.9(7)
C6_1	11387(3)	4058(2)	6021.2(13)	25.4(7)
C7_1	12032(3)	4240(2)	6439.8(13)	28.1(8)
C8_1	11608(3)	4244(2)	6833.9(13)	28.2(8)
C12_1	8273(3)	3703(2)	7360.0(12)	29.4(8)
C11_1	10097(4)	4196(3)	7628.3(12)	35.2(9)
S2_1	8969.1(10)	4019.6(8)	7868.9(3)	42.2(3)
Ni1_2	5837.8(3)	7250.7(2)	5875.0(2)	16.41(8)
N1_2	6781(2)	6511.1(16)	6229.9(9)	18.4(5)
N2_2	5124(2)	8193.4(16)	5625.4(9)	18.8(5)
C1_2	6837(3)	7972.1(19)	6163.2(11)	19.2(6)
C4_2	7713(3)	6836(2)	6500.9(11)	19.7(6)
Cl1_2	4626.3(6)	6363.7(5)	5521.5(3)	20.14(15)
C10_2	5658(3)	8912.1(19)	5768.7(11)	20.8(6)
C5_2	7740(3)	7699(2)	6459.6(11)	21.0(6)
C9_2	6683(3)	8777.6(19)	6077.6(11)	21.4(6)
C12_2	4213(3)	8327(2)	5345.4(11)	21.6(6)
C2_2	6735(3)	5737(2)	6277.7(11)	21.8(7)
C11_2	5097(3)	9568(2)	5595.5(12)	23.4(7)
C3_2	8350(3)	6288(2)	6746.3(11)	24.3(7)
S2_2	3919.4(8)	9306.7(5)	5243.8(3)	24.75(18)
S1_2	7800.4(8)	5354.2(5)	6649.0(3)	25.28(18)
C8_2	7454(3)	9326(2)	6279.1(12)	26.1(7)
C6_2	8517(3)	8240(2)	6669.1(13)	28.7(8)
C7_2	8365(3)	9045(2)	6573.2(14)	31.5(8)
Ni1_3	–2660.7(3)	7817.2(2)	5028.8(2)	16.75(8)
C9_3	–1941(3)	6298.0(18)	5321.7(10)	17.2(6)
C1_3	–1696(3)	7101.9(19)	5346.6(10)	18.3(6)
N2_3	–3419(2)	6862.9(16)	4815.7(9)	18.5(5)
N1_3	–1591(2)	8570.2(16)	5302.6(9)	18.6(5)
C10_3	–2946(3)	6154.3(19)	5000.6(11)	18.7(6)
C5_3	–755(3)	7385.0(19)	5617.7(10)	18.8(6)
C4_3	–683(3)	8250.4(19)	5584.9(11)	20.6(6)
C8_3	–1244(3)	5754.6(19)	5581.6(11)	20.8(6)
C12_3	–4288(3)	6729(2)	4512.0(11)	21.1(6)
C6_3	–52(3)	6848(2)	5876.6(11)	21.6(7)
C7_3	–309(3)	6037(2)	5858.0(11)	22.1(7)
C11_3	–3499(3)	5492(2)	4830.8(12)	22.3(7)
C2_3	–1531(3)	9349(2)	5281.3(11)	22.5(7)
Cl1_3	–3849.6(7)	8685.1(5)	4651.9(3)	22.66(16)
S2_3	–4607.8(7)	5747.4(5)	4432.0(3)	24.02(17)
C3_3	57(3)	8804(2)	5766.8(12)	26.5(7)
S1_3	–380.8(8)	9739.6(5)	5595.3(3)	27.37(19)
Ni1_4	–3594.2(3)	7257.2(3)	2212.9(2)	18.34(9)
N2_4	–2858(2)	7854.9(17)	1819.7(9)	19.2(5)

Atom	*x*	*y*	*z*	U(eq)
C10_4	–2320(3)	7408(2)	1532.8(10)	19.3(6)
C1_4	–3107(3)	6412(2)	1914.5(11)	20.3(6)
C9_4	–2470(3)	6552(2)	1589.0(11)	20.9(6)
N1_4	–4215(2)	6424.3(17)	2519.7(9)	21.4(6)
C5_4	–3395(3)	5639(2)	2016.6(11)	21.4(7)
C12_4	–2749(3)	8620(2)	1760.1(11)	22.1(7)
C4_4	–4059(3)	5650(2)	2368.8(12)	23.3(7)
C8_4	–2104(3)	5916(2)	1358.9(11)	23.9(7)
C11_4	–1813(3)	7858(2)	1258.7(11)	25.1(7)
S2_4	–2002.6(8)	8850.0(5)	1353.1(3)	25.85(18)
C2_4	–4816(3)	6427(2)	2836.9(12)	26.5(7)
Cl1_4	–4138.8(7)	8304.3(5)	2571.2(3)	27.43(18)
C7_4	–2386(3)	5140(2)	1463.9(12)	27.5(8)
C6_4	–3028(3)	4996(2)	1788.9(13)	28.0(8)
C3_4	–4552(3)	5080(2)	2578.9(13)	29.3(8)
S1_4	–5230.7(8)	5504.9(6)	2972.1(4)	31.9(2)
N1_5	2701(4)	8496(3)	3684.8(12)	17.5(9)
N2_5	–186(3)	8166.9(19)	3866.5(12)	19.6(6)
Ni1_5	1319.6(5)	8358.4(4)	3860.2(2)	16.20(14)
C5_5	1613(4)	8339(3)	2956.8(15)	19.8(9)
C9_5	–217(4)	8045(2)	3078.9(14)	19.3(8)
C4_5	2704(3)	8486(2)	3217.7(12)	18.3(7)
C10_5	–818(5)	8002(7)	3446(4)	19.3(15)
Cl1_5	1822.7(17)	8538.1(14)	4605.1(5)	23.1(4)
C6_5	1291(3)	8223(2)	2494.8(13)	23.1(8)
C1_5	871(4)	8254(3)	3247(2)	19.2(10)
C12_5	–750(4)	8150(2)	4195.2(15)	24.7(8)
S1_5	4677.6(8)	8630.5(7)	3591.9(4)	26.0(2)
S2_5	–2089.9(11)	7934.5(9)	4018.1(5)	30.1(3)
C2_5	3690(3)	8559(2)	3915.2(13)	21.5(8)
C8_5	–548(4)	7900(3)	2620.9(18)	25.4(10)
C7_5	211(4)	7999(3)	2333.4(16)	25.7(9)
C3_5	3707(5)	8564(4)	3112.6(18)	26.7(12)
C11_5	–1887(3)	7855(3)	3470.6(17)	26.0(9)
C7_6	1720(40)	8550(30)	4689(17)	17(6)
C6_6	2450(20)	8558(17)	4398(10)	30(5)
N2_6	–1010(40)	8010(40)	3430(20)	25(7)
C8_6	686(19)	8318(15)	4580(8)	23(4)
Ni1_6	397(5)	8182(3)	3201.4(16)	25.6(12)
C12_6	–1890(20)	7888(16)	3220(12)	31(5)
C2_6	2320(30)	8500(20)	2787(12)	44(6)
C3_6	3640(30)	8670(20)	3477(14)	49(7)
N1_6	1860(30)	8419(16)	3112(11)	29(5)
C1_6	950(30)	8320(20)	3822(13)	21(5)
C10_6	–810(30)	8100(16)	3889(10)	28(4)
Cl1_6	–266(9)	8067(5)	2470(3)	31.7(18)
C11_6	–1720(30)	8010(30)	4062(16)	39(8)
S1_6	3666(10)	8683(8)	2927(4)	45(3)
C5_6	2090(20)	8462(13)	3940(9)	25(4)
C9_6	280(20)	8233(16)	4096(10)	28(5)
S2_6	–2829(7)	7854(5)	3569(3)	43(2)
C4_6	2640(40)	8520(30)	3544(15)	31(6)

Table 7-87 Anisotropic Displacement Parameters ($Å^2×10^3$) for [Ni(4Tz(Ph)4Tz)Cl]. The Anisotropic displacement factor exponent takes the form: $–2π^2[h^2a^{*2}U_{11}+2hka^*b^*U_{12}+…]$.

Atom	U_{11}	U_{22}	U_{33}	U_{23}	U_{13}	U_{12}
Ni1_1	17.4(2)	17.56(19)	17.07(18)	1.61(15)	1.66(15)	1.21(15)
C4_1	17.6(15)	15.3(14)	21.9(15)	–0.4(12)	3.0(12)	2.9(11)
N1_1	20.7(13)	15.4(12)	18.7(12)	–0.4(10)	1.5(10)	0.8(10)
C1_1	17.9(15)	13.6(13)	23.8(15)	2.3(12)	0.5(12)	1.5(11)
C5_1	19.1(15)	16.4(14)	22.8(15)	0.7(12)	1.0(12)	2.2(12)
C2_1	21.2(16)	18.3(15)	24.2(16)	–1.9(12)	1.4(13)	0.4(12)
N2_1	25.0(15)	21.1(14)	17.5(12)	2.5(10)	0.0(11)	3.9(11)
C9_1	23.9(17)	19.7(15)	21.3(15)	–1.1(12)	–2.3(13)	2.3(13)
C3_1	23.9(17)	23.6(16)	21.7(15)	–0.6(13)	6.6(13)	2.4(13)
Cl1_1	19.1(4)	24.4(4)	25.4(4)	2.8(3)	3.8(3)	–0.3(3)
S1_1	26.6(4)	26.9(4)	17.6(4)	–2.4(3)	0.5(3)	2.2(3)
C10_1	31.2(19)	22.4(16)	18.5(15)	1.5(13)	–2.4(13)	2.3(14)
C6_1	20.6(17)	22.2(16)	34.0(19)	2.1(14)	6.6(14)	0.5(13)
C7_1	18.2(17)	23.2(17)	40(2)	1.6(15)	–1.2(15)	–1.2(13)
C8_1	26.1(18)	24.1(17)	29.3(18)	–1.1(14)	–9.5(14)	–1.2(14)
C12_1	34(2)	31.8(19)	22.1(16)	7.4(14)	4.4(14)	8.6(16)
C11_1	45(2)	38(2)	19.0(16)	–0.9(15)	–5.7(16)	5.1(18)
S2_1	54.6(7)	53.9(7)	18.3(4)	3.8(4)	6.3(4)	12.3(6)
Ni1_2	18.34(19)	13.29(18)	17.23(18)	0.45(15)	2.08(15)	–0.12(15)
N1_2	19.5(13)	18.1(13)	18.1(12)	–0.1(10)	4.6(10)	1.0(10)
N2_2	23.2(14)	15.5(12)	17.3(12)	3.0(10)	2.5(10)	–0.5(10)
C1_2	20.1(15)	17.4(15)	21.1(15)	–1.9(12)	6.2(12)	–0.7(12)
C4_2	18.0(15)	22.7(16)	18.6(14)	0.0(12)	4.3(12)	1.0(12)
Cl1_2	19.0(4)	17.0(3)	23.5(4)	–2.2(3)	1.2(3)	–0.7(3)
C10_2	28.9(18)	14.0(14)	21.5(15)	1.6(12)	9.7(13)	0.9(13)
C5_2	20.8(16)	20.2(15)	22.2(15)	–2.2(12)	4.3(12)	–0.2(13)
C9_2	24.8(17)	17.4(15)	23.3(16)	–1.1(12)	7.9(13)	–0.6(13)
C12_2	27.6(18)	16.8(14)	21.3(15)	3.4(12)	6.8(13)	3.0(13)
C2_2	23.5(17)	17.5(15)	25.1(16)	2.0(12)	6.3(13)	1.0(13)
C11_2	28.8(18)	16.4(15)	25.0(16)	0.8(12)	5.0(14)	3.1(13)
C3_2	22.4(17)	27.7(17)	21.7(15)	0.1(13)	1.2(13)	4.1(14)
S2_2	29.2(5)	18.6(4)	26.1(4)	5.5(3)	4.2(3)	4.2(3)
S1_2	28.3(5)	20.4(4)	26.5(4)	5.1(3)	3.1(3)	5.8(3)
C8_2	29.1(19)	17.3(15)	32.9(18)	–3.5(14)	8.2(15)	–3.8(13)
C6_2	22.5(18)	26.4(18)	35.0(19)	–7.8(15)	–1.0(15)	–0.5(14)
C7_2	24.9(19)	26.0(18)	42(2)	–12.0(16)	2.0(16)	–5.9(15)
Ni1_3	16.82(19)	14.08(18)	18.47(18)	0.29(15)	0.73(15)	1.17(15)
C9_3	18.4(15)	16.9(14)	16.4(13)	2.0(11)	3.4(11)	1.5(12)
C1_3	20.1(15)	18.2(14)	17.0(13)	–0.1(11)	4.2(12)	1.7(12)
N2_3	17.3(13)	18.6(13)	19.6(12)	–1.4(10)	3.5(10)	–0.4(10)
N1_3	18.8(13)	16.2(12)	19.9(12)	–0.1(10)	1.2(10)	0.6(10)
C10_3	17.7(15)	16.0(14)	22.5(15)	1.6(12)	4.0(12)	1.4(12)
C5_3	22.3(16)	17.5(14)	15.9(13)	–1.0(11)	1.2(12)	0.7(12)
C4_3	22.2(16)	17.0(15)	21.2(15)	1.5(12)	–0.5(12)	2.1(12)
C8_3	25.2(17)	16.3(14)	21.4(15)	1.8(12)	5.2(13)	1.5(13)
C12_3	19.3(16)	19.5(15)	24.2(16)	0.1(12)	2.9(12)	0.5(12)
C6_3	22.3(16)	22.0(16)	18.4(14)	–0.1(12)	–2.0(12)	2.3(13)
C7_3	26.4(17)	19.0(15)	20.1(15)	2.4(12)	1.4(13)	5.2(13)
C11_3	21.2(16)	17.8(15)	27.4(16)	–0.4(13)	3.0(13)	1.7(12)

Atom	U_{11}	U_{22}	U_{33}	U_{23}	U_{13}	U_{12}
C2_3	25.4(17)	18.7(15)	21.2(15)	0.7(12)	–1.6(13)	–1.7(13)
Cl1_3	23.2(4)	18.0(3)	25.0(4)	1.2(3)	–0.7(3)	4.5(3)
S2_3	21.4(4)	19.0(4)	29.4(4)	–2.6(3)	–1.7(3)	–2.0(3)
C3_3	25.2(18)	21.9(16)	28.6(17)	–0.6(14)	–5.9(14)	–1.9(14)
S1_3	29.1(5)	18.1(4)	31.6(4)	0.6(3)	–3.8(4)	–3.5(3)
Ni1_4	16.49(19)	19.7(2)	18.03(18)	0.99(16)	1.00(15)	0.70(16)
N2_4	17.9(13)	21.3(13)	17.2(12)	0.7(10)	–0.4(10)	–0.3(11)
C10_4	18.3(15)	22.3(15)	16.3(14)	–0.7(12)	0.0(11)	–0.5(12)
C1_4	17.1(15)	20.7(15)	21.4(15)	2.0(12)	–1.6(12)	–0.9(12)
C9_4	21.4(16)	22.3(16)	17.2(14)	–1.2(12)	–1.6(12)	0.1(13)
N1_4	15.1(13)	25.4(14)	22.6(13)	5.1(11)	0.6(10)	1.4(11)
C5_4	15.8(15)	22.1(16)	24.4(16)	0.9(13)	–2.1(12)	–2.7(12)
C12_4	23.5(17)	19.6(15)	21.8(15)	0.0(12)	–0.2(13)	–1.6(13)
C4_4	16.5(15)	23.8(16)	28.2(17)	4.7(14)	0.0(13)	–0.1(13)
C8_4	23.0(17)	26.2(17)	20.7(15)	–5.3(13)	–1.4(13)	2.1(14)
C11_4	26.2(18)	28.6(18)	20.3(15)	0.1(13)	3.5(13)	–2.7(14)
S2_4	30.3(5)	22.9(4)	24.1(4)	3.1(3)	4.1(3)	–3.5(3)
C2_4	18.9(16)	32.6(19)	27.4(17)	8.9(15)	2.5(13)	4.1(14)
Cl1_4	29.1(4)	27.3(4)	26.9(4)	–0.1(3)	7.8(3)	6.4(3)
C7_4	26.9(18)	25.1(17)	28.5(18)	–6.2(14)	–0.4(14)	1.8(14)
C6_4	29.8(19)	19.2(16)	33.3(19)	–1.8(14)	1.3(15)	–3.0(14)
C3_4	22.7(18)	26.3(18)	39(2)	7.1(15)	4.9(15)	–0.6(14)
S1_4	24.0(5)	34.3(5)	39.1(5)	12.4(4)	9.8(4)	–0.4(4)
N1_5	18.5(17)	16.6(19)	17.0(17)	–2.6(17)	2.0(16)	0.1(12)
N2_5	19.4(17)	15.9(15)	23.9(17)	1.4(12)	5.4(14)	0.8(13)
Ni1_5	16.3(3)	15.9(3)	15.8(2)	–0.40(18)	1.2(2)	0.3(2)
C5_5	19(2)	19(2)	19.7(19)	0.8(17)	0.2(16)	–0.7(16)
C9_5	14.9(19)	18.0(18)	22.4(19)	5.0(15)	–3.8(16)	–0.1(15)
C4_5	20.5(19)	17.3(17)	16.7(17)	–2.1(13)	2.5(14)	0.0(14)
C10_5	12(3)	18(3)	26(2)	2.7(18)	–1(2)	1(2)
Cl1_5	29.2(8)	21.6(6)	16.9(7)	–3.2(5)	0.0(5)	0.8(5)
C6_5	26(2)	24.2(19)	18.5(17)	0.0(14)	1.8(15)	0.7(16)
C1_5	19(2)	17(2)	20(2)	1.7(15)	–1(2)	1(2)
C12_5	28(2)	18.1(18)	30(2)	0.3(16)	9.9(17)	2.6(15)
S1_5	17.2(5)	30.1(5)	30.2(5)	–1.3(4)	2.9(4)	–2.0(4)
S2_5	22.7(6)	26.9(6)	43.5(7)	2.9(5)	13.7(6)	1.1(5)
C2_5	20.5(19)	20.5(18)	22.5(18)	–2.8(15)	1.3(14)	–1.0(15)
C8_5	23(2)	24(2)	25(3)	4.6(19)	–5.7(19)	–1.9(18)
C7_5	29(3)	26(2)	18(2)	2.1(17)	–4.1(18)	0.7(19)
C3_5	26(2)	30(3)	25(3)	0(2)	7(2)	0.4(19)
C11_5	18(2)	23(2)	37(2)	6.6(19)	2.5(18)	–0.8(15)
C7_6	14(7)	10(10)	26(7)	0(6)	2(5)	3(6)
C6_6	16(7)	40(14)	36(7)	–4(6)	5(5)	–7(7)
N2_6	31(8)	13(16)	30(7)	8(6)	–3(5)	6(6)
C8_6	16(7)	27(11)	25(7)	0(6)	2(5)	0(6)
Ni1_6	36(3)	19.8(19)	21(2)	1.5(14)	5(2)	4(2)
C12_6	32(8)	16(11)	41(8)	3(7)	–6(6)	8(6)
C2_6	45(11)	42(17)	50(8)	5(7)	18(6)	–2(7)
C3_6	35(8)	52(19)	63(11)	–2(8)	16(6)	–6(8)
N1_6	36(8)	11(10)	42(7)	5(6)	9(5)	5(5)
C1_6	28(6)	8(11)	26(7)	6(5)	1(5)	2(6)
C10_6	29(6)	20(11)	33(7)	7(6)	–2(5)	–1(5)

Atom	U_{11}	U_{22}	U_{33}	U_{23}	U_{13}	U_{12}
Cl1_6	38(5)	29(4)	24(4)	1(3)	–7(3)	3(4)
C11_6	30(8)	50(20)	40(9)	4(7)	0(7)	–5(8)
S1_6	38(5)	41(6)	61(7)	–4(5)	21(5)	–4(4)
C5_6	27(6)	10(9)	38(6)	–2(5)	3(5)	–1(6)
C9_6	29(6)	26(12)	28(6)	3(5)	0(4)	–2(6)
S2_6	36(4)	36(4)	56(5)	–1(4)	6(3)	3(3)
C4_6	30(8)	21(16)	42(7)	2(6)	10(5)	2(7)

Table 7-88 Bond Lengths for [Ni(4Tz(Ph)4Tz)Cl].

Atom	Atom	Length/Å	Atom	Atom	Length/Å
Ni1_1	N1_1	1.916(3)	Ni1_4	N2_4	1.908(3)
Ni1_1	C1_1	1.851(3)	Ni1_4	C1_4	1.841(3)
Ni1_1	N2_1	1.927(3)	Ni1_4	N1_4	1.915(3)
Ni1_1	Cl1_1	2.2580(9)	Ni1_4	Cl1_4	2.2324(10)
C4_1	N1_1	1.413(4)	N2_4	C10_4	1.401(4)
C4_1	C5_1	1.459(4)	N2_4	C12_4	1.310(4)
C4_1	C3_1	1.354(4)	C10_4	C9_4	1.465(5)
N1_1	C2_1	1.311(4)	C10_4	C11_4	1.356(5)
C1_1	C5_1	1.387(5)	C1_4	C9_4	1.387(5)
C1_1	C9_1	1.386(4)	C1_4	C5_4	1.397(5)
C5_1	C6_1	1.400(5)	C9_4	C8_4	1.394(5)
C2_1	S1_1	1.704(4)	N1_4	C4_4	1.403(5)
N2_1	C10_1	1.407(5)	N1_4	C2_4	1.314(5)
N2_1	C12_1	1.300(5)	C5_4	C4_4	1.457(5)
C9_1	C10_1	1.449(5)	C5_4	C6_4	1.400(5)
C9_1	C8_1	1.400(5)	C12_4	S2_4	1.709(4)
C3_1	S1_1	1.722(4)	C4_4	C3_4	1.355(5)
C10_1	C11_1	1.354(5)	C8_4	C7_4	1.403(5)
C6_1	C7_1	1.404(5)	C11_4	S2_4	1.715(4)
C7_1	C8_1	1.382(6)	C2_4	S1_4	1.706(4)
C12_1	S2_1	1.708(4)	C7_4	C6_4	1.391(5)
C11_1	S2_1	1.720(5)	C3_4	S1_4	1.727(4)
Ni1_2	N1_2	1.905(3)	N1_5	Ni1_5	1.905(5)
Ni1_2	N2_2	1.906(3)	N1_5	C4_5	1.406(5)
Ni1_2	C1_2	1.844(3)	N1_5	C2_5	1.310(6)
Ni1_2	Cl1_2	2.2535(9)	N2_5	Ni1_5	1.911(4)
N1_2	C4_2	1.409(4)	N2_5	C10_5	1.395(10)
N1_2	C2_2	1.311(4)	N2_5	C12_5	1.312(5)
N2_2	C10_2	1.410(4)	Ni1_5	Cl1_5	2.2390(16)
N2_2	C12_2	1.311(4)	Ni1_5	C1_5	1.840(6)
C1_2	C5_2	1.387(5)	C5_5	C4_5	1.469(6)
C1_2	C9_2	1.386(4)	C5_5	C6_5	1.391(6)
C4_2	C5_2	1.458(5)	C5_5	C1_5	1.388(7)
C4_2	C3_2	1.349(5)	C9_5	C10_5	1.443(12)
C10_2	C9_2	1.461(5)	C9_5	C1_5	1.409(6)
C10_2	C11_2	1.359(5)	C9_5	C8_5	1.388(7)
C5_2	C6_2	1.396(5)	C4_5	C3_5	1.351(7)
C9_2	C8_2	1.392(5)	C10_5	C11_5	1.372(9)
C12_2	S2_2	1.704(3)	C6_5	C7_5	1.402(6)
C2_2	S1_2	1.705(4)	C12_5	S2_5	1.703(5)

Atom	Atom	Length/Å	Atom	Atom	Length/Å
C11_2	S2_2	1.711(4)	S1_5	C2_5	1.705(4)
C3_2	S1_2	1.717(4)	S1_5	C3_5	1.716(6)
C8_2	C7_2	1.396(5)	S2_5	C11_5	1.716(5)
C6_2	C7_2	1.390(5)	C8_5	C7_5	1.401(7)
Ni1_3	C1_3	1.846(3)	C7_6	C6_6	1.38(5)
Ni1_3	N2_3	1.915(3)	C7_6	C8_6	1.33(6)
Ni1_3	N1_3	1.918(3)	C6_6	C5_6	1.38(4)
Ni1_3	Cl1_3	2.2421(9)	N2_6	Ni1_6	2.01(6)
C9_3	C1_3	1.385(4)	N2_6	C12_6	1.18(6)
C9_3	C10_3	1.463(4)	N2_6	C10_6	1.38(7)
C9_3	C8_3	1.402(4)	C8_6	C9_6	1.46(4)
C1_3	C5_3	1.391(4)	Ni1_6	N1_6	1.94(3)
N2_3	C10_3	1.401(4)	Ni1_6	C1_6	1.89(4)
N2_3	C12_3	1.310(4)	Ni1_6	Cl1_6	2.218(10)
N1_3	C4_3	1.398(4)	C12_6	S2_6	1.71(4)
N1_3	C2_3	1.315(4)	C2_6	N1_6	1.22(4)
C10_3	C11_3	1.362(5)	C2_6	S1_6	1.69(4)
C5_3	C4_3	1.462(4)	C3_6	S1_6	1.66(4)
C5_3	C6_3	1.396(4)	C3_6	C4_6	1.33(6)
C4_3	C3_3	1.358(5)	N1_6	C4_6	1.49(5)
C8_3	C7_3	1.393(5)	C1_6	C5_6	1.42(4)
C12_3	S2_3	1.705(3)	C1_6	C9_6	1.29(5)
C6_3	C7_3	1.400(5)	C10_6	C11_6	1.34(5)
C11_3	S2_3	1.720(3)	C10_6	C9_6	1.41(4)
C2_3	S1_3	1.705(3)	C11_6	S2_6	1.86(4)
C3_3	S1_3	1.715(4)	C5_6	C4_6	1.48(5)

Table 7-89 Bond Angles for [Ni(4Tz(Ph)4Tz)Cl].

Atom	Atom	Atom	Angle/˚	Atom	Atom	Atom	Angle/˚
N1_1	Ni1_1	N2_1	164.38(13)	N2_4	Ni1_4	N1_4	164.73(13)
N1_1	Ni1_1	Cl1_1	97.77(9)	N2_4	Ni1_4	Cl1_4	96.05(9)
C1_1	Ni1_1	N1_1	82.44(13)	C1_4	Ni1_4	N2_4	82.36(14)
C1_1	Ni1_1	N2_1	82.02(14)	C1_4	Ni1_4	N1_4	82.38(14)
C1_1	Ni1_1	Cl1_1	173.10(10)	C1_4	Ni1_4	Cl1_4	178.16(11)
N2_1	Ni1_1	Cl1_1	97.46(9)	N1_4	Ni1_4	Cl1_4	99.22(9)
N1_1	C4_1	C5_1	111.8(3)	C10_4	N2_4	Ni1_4	115.8(2)
C3_1	C4_1	N1_1	113.3(3)	C12_4	N2_4	Ni1_4	132.5(3)
C3_1	C4_1	C5_1	134.7(3)	C12_4	N2_4	C10_4	111.7(3)
C4_1	N1_1	Ni1_1	115.3(2)	N2_4	C10_4	C9_4	111.8(3)
C2_1	N1_1	Ni1_1	133.0(2)	C11_4	C10_4	N2_4	113.7(3)
C2_1	N1_1	C4_1	111.7(3)	C11_4	C10_4	C9_4	134.5(3)
C5_1	C1_1	Ni1_1	119.2(2)	C9_4	C1_4	Ni1_4	119.6(3)
C9_1	C1_1	Ni1_1	119.1(3)	C9_4	C1_4	C5_4	121.1(3)
C9_1	C1_1	C5_1	121.5(3)	C5_4	C1_4	Ni1_4	119.4(3)
C1_1	C5_1	C4_1	111.0(3)	C1_4	C9_4	C10_4	110.4(3)
C1_1	C5_1	C6_1	119.9(3)	C1_4	C9_4	C8_4	119.9(3)
C6_1	C5_1	C4_1	129.1(3)	C8_4	C9_4	C10_4	129.6(3)
N1_1	C2_1	S1_1	113.9(3)	C4_4	N1_4	Ni1_4	115.6(2)
C10_1	N2_1	Ni1_1	115.2(2)	C2_4	N1_4	Ni1_4	132.8(3)
C12_1	N2_1	Ni1_1	132.6(3)	C2_4	N1_4	C4_4	111.6(3)

Atom	Atom	Atom	Angle/°	Atom	Atom	Atom	Angle/°
C12_1	N2_1	C10_1	111.7(3)	C1_4	C5_4	C4_4	110.5(3)
C1_1	C9_1	C10_1	111.4(3)	C1_4	C5_4	C6_4	119.5(3)
C1_1	C9_1	C8_1	119.1(3)	C6_4	C5_4	C4_4	130.0(3)
C8_1	C9_1	C10_1	129.5(3)	N2_4	C12_4	S2_4	113.7(3)
C4_1	C3_1	S1_1	110.5(3)	N1_4	C4_4	C5_4	112.1(3)
C2_1	S1_1	C3_1	90.52(16)	C3_4	C4_4	N1_4	113.9(3)
N2_1	C10_1	C9_1	111.8(3)	C3_4	C4_4	C5_4	134.0(4)
C11_1	C10_1	N2_1	113.3(4)	C9_4	C8_4	C7_4	119.0(3)
C11_1	C10_1	C9_1	134.8(4)	C10_4	C11_4	S2_4	110.4(3)
C5_1	C6_1	C7_1	118.2(3)	C12_4	S2_4	C11_4	90.44(17)
C8_1	C7_1	C6_1	121.7(3)	N1_4	C2_4	S1_4	114.0(3)
C7_1	C8_1	C9_1	119.6(3)	C6_4	C7_4	C8_4	121.3(3)
N2_1	C12_1	S2_1	114.3(3)	C7_4	C6_4	C5_4	119.3(3)
C10_1	C11_1	S2_1	110.5(3)	C4_4	C3_4	S1_4	110.2(3)
C12_1	S2_1	C11_1	90.11(19)	C2_4	S1_4	C3_4	90.39(19)
N1_2	Ni1_2	N2_2	164.41(12)	C4_5	N1_5	Ni1_5	116.0(3)
N1_2	Ni1_2	Cl1_2	97.45(9)	C2_5	N1_5	Ni1_5	132.8(3)
N2_2	Ni1_2	Cl1_2	97.82(9)	C2_5	N1_5	C4_5	111.2(4)
C1_2	Ni1_2	N1_2	82.28(13)	C10_5	N2_5	Ni1_5	115.1(4)
C1_2	Ni1_2	N2_2	82.46(13)	C12_5	N2_5	Ni1_5	132.2(3)
C1_2	Ni1_2	Cl1_2	179.59(11)	C12_5	N2_5	C10_5	112.7(5)
C4_2	N1_2	Ni1_2	115.9(2)	N1_5	Ni1_5	N2_5	164.55(15)
C2_2	N1_2	Ni1_2	132.4(2)	N1_5	Ni1_5	Cl1_5	98.80(12)
C2_2	N1_2	C4_2	111.6(3)	N2_5	Ni1_5	Cl1_5	96.64(12)
C10_2	N2_2	Ni1_2	115.4(2)	C1_5	Ni1_5	N1_5	82.2(2)
C12_2	N2_2	Ni1_2	133.5(2)	C1_5	Ni1_5	N2_5	82.4(2)
C12_2	N2_2	C10_2	111.1(3)	C1_5	Ni1_5	Cl1_5	177.35(19)
C5_2	C1_2	Ni1_2	119.4(2)	C6_5	C5_5	C4_5	129.5(4)
C9_2	C1_2	Ni1_2	119.7(3)	C1_5	C5_5	C4_5	109.9(4)
C9_2	C1_2	C5_2	120.9(3)	C1_5	C5_5	C6_5	120.4(4)
N1_2	C4_2	C5_2	111.5(3)	C1_5	C9_5	C10_5	109.6(5)
C3_2	C4_2	N1_2	113.5(3)	C8_5	C9_5	C10_5	130.4(5)
C3_2	C4_2	C5_2	135.0(3)	C8_5	C9_5	C1_5	119.9(5)
N2_2	C10_2	C9_2	112.1(3)	N1_5	C4_5	C5_5	111.7(4)
C11_2	C10_2	N2_2	113.2(3)	C3_5	C4_5	N1_5	113.5(4)
C11_2	C10_2	C9_2	134.7(3)	C3_5	C4_5	C5_5	134.6(4)
C1_2	C5_2	C4_2	110.8(3)	N2_5	C10_5	C9_5	113.4(5)
C1_2	C5_2	C6_2	119.8(3)	C11_5	C10_5	N2_5	112.8(8)
C6_2	C5_2	C4_2	129.3(3)	C11_5	C10_5	C9_5	133.8(8)
C1_2	C9_2	C10_2	110.3(3)	C5_5	C6_5	C7_5	118.4(4)
C1_2	C9_2	C8_2	120.3(3)	C5_5	C1_5	Ni1_5	120.1(4)
C8_2	C9_2	C10_2	129.4(3)	C5_5	C1_5	C9_5	120.6(5)
N2_2	C12_2	S2_2	114.5(3)	C9_5	C1_5	Ni1_5	119.2(4)
N1_2	C2_2	S1_2	113.8(3)	N2_5	C12_5	S2_5	113.4(4)
C10_2	C11_2	S2_2	111.0(3)	C2_5	S1_5	C3_5	90.0(2)
C4_2	C3_2	S1_2	110.6(3)	C12_5	S2_5	C11_5	90.8(2)
C12_2	S2_2	C11_2	90.16(17)	N1_5	C2_5	S1_5	114.4(3)
C2_2	S1_2	C3_2	90.48(17)	C9_5	C8_5	C7_5	118.5(5)
C9_2	C8_2	C7_2	118.4(3)	C8_5	C7_5	C6_5	122.1(4)
C7_2	C6_2	C5_2	118.8(3)	C4_5	C3_5	S1_5	110.9(4)
C6_2	C7_2	C8_2	121.9(3)	C10_5	C11_5	S2_5	110.3(5)
C1_3	Ni1_3	N2_3	82.33(13)	C8_6	C7_6	C6_6	125(4)

Atom	Atom	Atom	Angle/°	Atom	Atom	Atom	Angle/°
C1_3	Ni1_3	N1_3	82.29(13)	C7_6	C6_6	C5_6	120(3)
C1_3	Ni1_3	Cl1_3	179.02(11)	C12_6	N2_6	Ni1_6	130(5)
N2_3	Ni1_3	N1_3	164.29(12)	C12_6	N2_6	C10_6	122(6)
N2_3	Ni1_3	Cl1_3	97.57(9)	C10_6	N2_6	Ni1_6	108(3)
N1_3	Ni1_3	Cl1_3	97.86(8)	C7_6	C8_6	C9_6	115(3)
C1_3	C9_3	C10_3	110.6(3)	N2_6	Ni1_6	Cl1_6	97.2(19)
C1_3	C9_3	C8_3	119.8(3)	N1_6	Ni1_6	N2_6	168(2)
C8_3	C9_3	C10_3	129.6(3)	N1_6	Ni1_6	Cl1_6	94.4(10)
C9_3	C1_3	Ni1_3	119.4(2)	C1_6	Ni1_6	N2_6	83(2)
C9_3	C1_3	C5_3	121.4(3)	C1_6	Ni1_6	N1_6	85.5(15)
C5_3	C1_3	Ni1_3	119.2(2)	C1_6	Ni1_6	Cl1_6	177.8(11)
C10_3	N2_3	Ni1_3	115.5(2)	N2_6	C12_6	S2_6	111(4)
C12_3	N2_3	Ni1_3	132.7(2)	N1_6	C2_6	S1_6	114(3)
C12_3	N2_3	C10_3	111.7(3)	C4_6	C3_6	S1_6	110(3)
C4_3	N1_3	Ni1_3	115.8(2)	C2_6	N1_6	Ni1_6	136(3)
C2_3	N1_3	Ni1_3	132.7(2)	C2_6	N1_6	C4_6	111(4)
C2_3	N1_3	C4_3	111.5(3)	C4_6	N1_6	Ni1_6	113(3)
N2_3	C10_3	C9_3	112.0(3)	C5_6	C1_6	Ni1_6	116(3)
C11_3	C10_3	C9_3	134.6(3)	C9_6	C1_6	Ni1_6	117(3)
C11_3	C10_3	N2_3	113.4(3)	C9_6	C1_6	C5_6	127(3)
C1_3	C5_3	C4_3	110.9(3)	N2_6	C10_6	C9_6	117(4)
C1_3	C5_3	C6_3	119.3(3)	C11_6	C10_6	N2_6	112(4)
C6_3	C5_3	C4_3	129.9(3)	C11_6	C10_6	C9_6	132(3)
N1_3	C4_3	C5_3	111.8(3)	C10_6	C11_6	S2_6	105(3)
C3_3	C4_3	N1_3	113.7(3)	C3_6	S1_6	C2_6	93.0(18)
C3_3	C4_3	C5_3	134.5(3)	C6_6	C5_6	C1_6	114(3)
C7_3	C8_3	C9_3	118.9(3)	C6_6	C5_6	C4_6	133(3)
N2_3	C12_3	S2_3	114.2(3)	C1_6	C5_6	C4_6	113(3)
C5_3	C6_3	C7_3	119.4(3)	C1_6	C9_6	C8_6	118(3)
C8_3	C7_3	C6_3	121.2(3)	C1_6	C9_6	C10_6	115(3)
C10_3	C11_3	S2_3	110.5(3)	C10_6	C9_6	C8_6	126(3)
N1_3	C2_3	S1_3	114.0(3)	C12_6	S2_6	C11_6	89.6(19)
C12_3	S2_3	C11_3	90.22(16)	C3_6	C4_6	N1_6	112(4)
C4_3	C3_3	S1_3	110.4(3)	C3_6	C4_6	C5_6	136(4)
C2_3	S1_3	C3_3	90.38(17)	C5_6	C4_6	N1_6	112(4)

Table 7-90 Hydrogen Atom Coordinates (Å×10^4) and Isotropic Displacement Parameters (Å^2×10^3) for [Ni(4Tz(Ph)4Tz)Cl].

Atom	*x*	*y*	*z*	U(eq)
H2_1	6914.27	3378.86	5425.21	26
H3_1	10023.03	3709.56	5027.22	27
H6_1	11682.42	4071.77	5751.26	30
H7_1	12778.95	4362.87	6452.36	34
H8_1	12054.54	4382.45	7112.27	34
H12_1	7542.52	3519.59	7319.13	35
H11_1	10768.85	4398.58	7785.26	42
H12_2	3752.59	7910.65	5210.19	26
H2_2	6162.47	5419.68	6120.1	26
H11_2	5328.77	10099.54	5660.9	28
H3_2	9010.24	6401.95	6945.48	29
H8_2	7361.56	9878.57	6217.82	31

Atom	*x*	*y*	*z*	U(eq)
H6_2	9138.15	8060.41	6873.49	34
H7_2	8896.74	9413.58	6711.88	38
H8_3	–1406.69	5202.29	5569.32	25
H12_3	–4704.77	7142.7	4350.25	25
H6_3	593.58	7032.15	6063.46	26
H7_3	163.82	5673	6037.38	27
H11_3	–3299.61	4962.49	4920.07	27
H2_3	–2078.77	9666.65	5106.69	27
H3_3	724.03	8689.23	5961.65	32
H12_4	–3057.41	9011.59	1927.47	27
H8_4	–1670.89	6007.09	1134.2	29
H11_4	–1410.3	7653.4	1044.45	30
H2_4	–5002.94	6899.72	2978.34	32
H7_4	–2134.06	4703.53	1310.12	33
H6_4	–3215.88	4466.99	1855.61	34
H3_4	–4528.47	4525.96	2518.56	35
H6_5	1789.77	8293.37	2293.58	28
H12_5	–441.41	8247.7	4501.99	30
H2_5	3844.25	8564.1	4235.82	26
H8_5	–1271.6	7738.13	2505.15	30
H7_5	–14.32	7911.68	2018.82	31
H3_5	3854.39	8578.98	2813.66	32
H11_5	–2435.75	7727.73	3220.03	31
H7A_6	1967.38	8715	4991.06	20
H6A_6	3204.56	8632.36	4511.25	36
H8A_6	244.82	8216.45	4801.06	28
H12A_6	–2056.11	7818.57	2902.22	37
H2A_6	1947.04	8457.5	2483.38	53
H3A_6	4255.16	8750.51	3708.64	59
H11_6	–1791.38	8031.52	4371.73	47

Table 7-91 Atomic Occupancy for [Ni(4Tz(Ph)4Tz)Cl].

Atom	*Occupancy*	Atom	*Occupancy*	Atom	*Occupancy*
N1_5	0.8602(16)	N2_5	0.8602(16)	Ni1_5	0.8602(16)
C5_5	0.8602(16)	C9_5	0.8602(16)	C4_5	0.8602(16)
C10_5	0.8602(16)	Cl1_5	0.8602(16)	C6_5	0.8602(16)
H6_5	0.8602(16)	C1_5	0.8602(16)	C12_5	0.8602(16)
H12_5	0.8602(16)	S1_5	0.8602(16)	S2_5	0.8602(16)
C2_5	0.8602(16)	H2_5	0.8602(16)	C8_5	0.8602(16)
H8_5	0.8602(16)	C7_5	0.8602(16)	H7_5	0.8602(16)
C3_5	0.8602(16)	H3_5	0.8602(16)	C11_5	0.8602(16)
H11_5	0.8602(16)	C7_6	0.1398(16)	H7A_6	0.1398(16)
C6_6	0.1398(16)	H6A_6	0.1398(16)	N2_6	0.1398(16)
C8_6	0.1398(16)	H8A_6	0.1398(16)	Ni1_6	0.1398(16)
C12_6	0.1398(16)	H12A_6	0.1398(16)	C2_6	0.1398(16)
H2A_6	0.1398(16)	C3_6	0.1398(16)	H3A_6	0.1398(16)
N1_6	0.1398(16)	C1_6	0.1398(16)	C10_6	0.1398(16)
Cl1_6	0.1398(16)	C11_6	0.1398(16)	H11_6	0.1398(16)
S1_6	0.1398(16)	C5_6	0.1398(16)	C9_6	0.1398(16)
S2_6	0.1398(16)	C4_6	0.1398(16)		

7.3.14 [Ni(2Btz(Ph)2Btz)Cl]

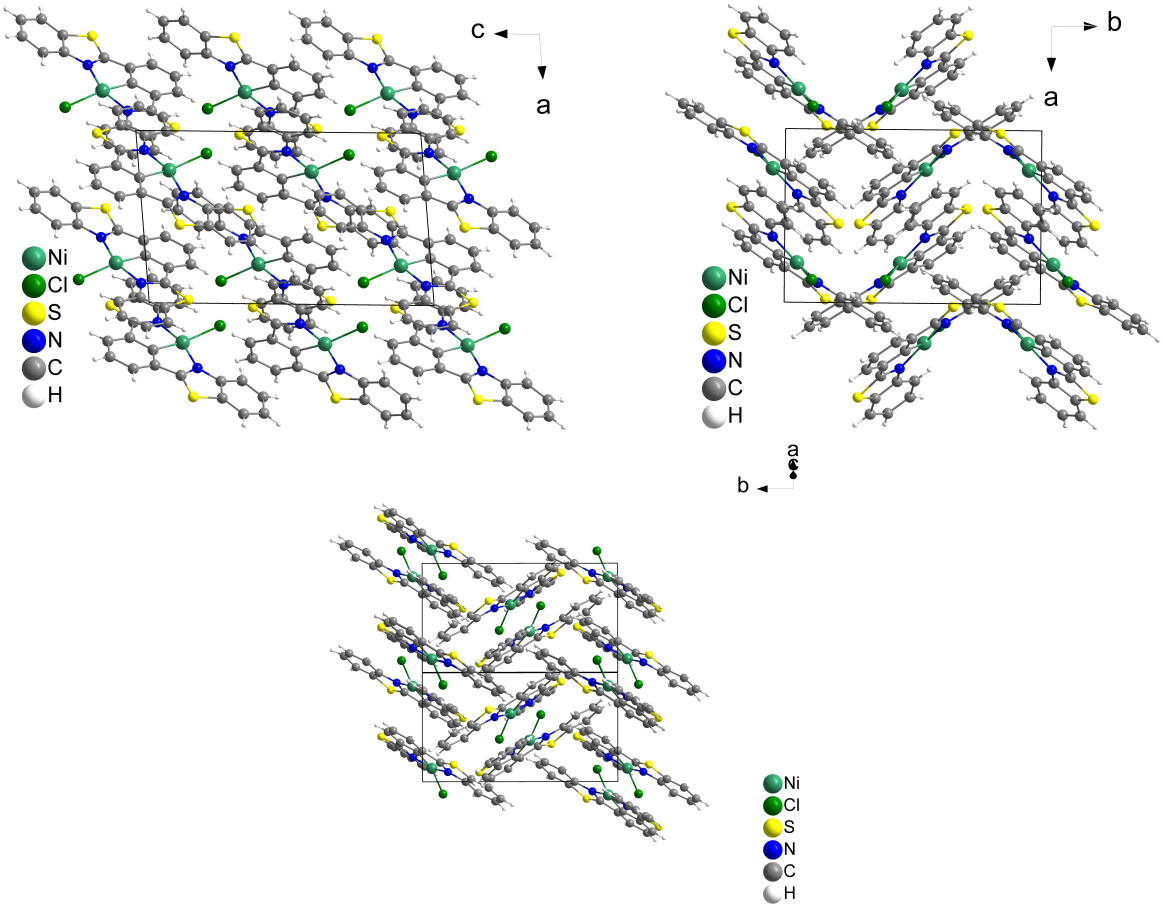

Figure 7-389 Crystal structure of [Ni(2Btz(Ph)2Btz)Cl] viewed along the crystallographic *b*- (top left) and *c*-axis (top right) and viewed along the *a*-*c* face diagonal.

Table 7-92 Crystal data and structure refinement for [Ni(2Btz(Ph)2Btz)Cl].

Identification code	[Ni(2Btz(Ph)2Btz)Cl]
Empirical formula	$C_{20}H_{11}ClN_2NiS_2$
Formula weight	437.59
Temperature/K	101.0
Crystal system	monoclinic
Space group	$P2_1/c$
a/Å	8.8717(3)
b/Å	13.0581(5)
c/Å	14.6499(6)
α/°	90
β/°	95.0680(10)
γ/°	90
Volume/Å^3	1690.52(11)
Z	4
ρ_{calc}g/cm^3	1.719
μ/mm^{-1}	1.559
F(000)	888.0
Crystal size/mm^3	0.11 × 0.05 × 0.03
Radiation	MoKα (λ = 0.71073)
2Θ range for data collection/°	4.186 to 55.754

Index ranges	–11 ≤ h ≤ 10, –14 ≤ k ≤ 17, –19 ≤ l ≤ 18
Reflections collected	18296
Independent reflections	3971 [R_{int} = 0.0579, R_{sigma} = 0.0432]
Data/restraints/parameters	3971/0/235
Goodness-of-fit on F^2	1.039
Final R indexes [I>=2σ (I)]	R_1 = 0.0354, wR_2 = 0.0729
Final R indexes [all data]	R_1 = 0.0462, wR_2 = 0.0810
Largest diff. peak/hole / e Å^{-3}	0.61/–0.35

Table 7-93 Fractional Atomic Coordinates (×10^4) and Equivalent Isotropic Displacement Parameters (Å^2×10^3) for [Ni(2Btz(Ph)2Btz)Cl]. U_{eq} is defined as 1/3 of the trace of the orthogonalized U_{IJ} tensor.

Atom	*x*	*y*	*z*	U(eq)
Ni1	2292.9(4)	5485.7(2)	3939.8(2)	14.42(9)
Cl1	1301.5(7)	6058.4(5)	2581.1(4)	19.03(14)
S2	5450.0(7)	2908.9(5)	3718.1(5)	19.40(15)
S1	189.7(7)	6598.3(5)	6369.6(4)	19.56(15)
N1	1131(2)	6304.5(16)	4765.5(14)	14.6(4)
N2	3773(2)	4529.2(16)	3489.2(14)	17.2(4)
C8	1152(3)	5915.4(19)	5607.0(16)	16.0(5)
C9	2044(3)	4994.3(19)	5781.4(17)	16.9(5)
C2	302(3)	7218.6(19)	4697.7(17)	16.3(5)
C1	2738(3)	4746.5(19)	4996.5(17)	16.5(5)
C13	3623(3)	3870.0(19)	4973.3(18)	17.8(5)
C14	4199(3)	3796.4(19)	4082.9(17)	17.4(5)
C12	3845(3)	3244(2)	5744.8(18)	20.6(5)
C7	–298(3)	7502(2)	5523.0(17)	18.1(5)
C3	34(3)	7851.3(19)	3933.5(17)	17.6(5)
C10	2259(3)	4379(2)	6562.1(18)	19.2(5)
C4	–791(3)	8737(2)	4004.0(19)	21.5(6)
C5	–1391(3)	8998(2)	4828.2(19)	24.4(6)
C11	3161(3)	3509(2)	6529.1(18)	21.1(6)
C20	4521(3)	4440.3(19)	2695.0(17)	17.4(5)
C6	–1143(3)	8391(2)	5592.8(18)	22.8(6)
C18	5405(3)	4944(2)	1260.1(18)	23.1(6)
C16	6408(3)	3398(2)	1992.3(18)	21.1(5)
C19	4478(3)	5124(2)	1956.2(17)	20.2(5)
C15	5498(3)	3587(2)	2699.9(18)	18.6(5)
C17	6355(3)	4086(2)	1272.6(19)	24.1(6)

Table 7-94 Anisotropic Displacement Parameters (Å^2×10^3) for [Ni(2Btz(Ph)2Btz)Cl]. The Anisotropic displacement factor exponent takes the form: –2π^2[h^{2}a*^{2}U_{11}+2hka*b*U_{12}+…].

Atom	U_{11}	U_{22}	U_{33}	U_{23}	U_{13}	U_{12}
Ni1	15.19(17)	12.20(17)	15.43(16)	0.93(12)	–1.09(12)	1.15(12)
Cl1	21.7(3)	18.2(3)	16.7(3)	0.8(2)	–1.4(2)	4.6(2)
S2	17.6(3)	13.9(3)	26.2(3)	–0.3(2)	–1.1(2)	1.7(2)
S1	21.2(3)	21.9(3)	15.2(3)	–1.5(2)	–0.5(2)	1.4(2)
N1	12.8(10)	13.9(10)	16.6(10)	–0.9(8)	–0.8(8)	–2.1(8)
N2	14.5(11)	16.4(11)	20.3(10)	–1.5(8)	–1.4(8)	0.2(8)
C8	15.2(13)	14.3(12)	17.8(12)	–2.0(9)	–2.4(9)	–3.6(9)
C9	16.4(13)	14.4(12)	18.6(12)	–0.1(10)	–5.0(9)	–3.5(9)

Atom	U_{11}	U_{22}	U_{33}	U_{23}	U_{13}	U_{12}
C2	13.9(12)	14.4(12)	20.1(12)	–2.9(10)	–1.1(9)	–2.6(9)
C1	13.8(12)	15.8(13)	18.7(12)	0.2(10)	–4.3(9)	–2.3(9)
C13	13.7(13)	14.4(13)	24.2(13)	0.0(10)	–3.9(10)	–3.2(9)
C14	14.4(13)	14.2(12)	22.6(13)	–1.7(10)	–2.9(10)	–2.7(9)
C12	18.3(13)	14.5(13)	27.8(14)	0.9(10)	–5.7(10)	0.9(10)
C7	16.7(13)	18.8(13)	18.3(12)	–1.1(10)	–1.6(10)	–2.5(10)
C3	19.2(13)	16.7(13)	17.1(12)	0.2(10)	2.9(10)	–1.5(10)
C10	16.6(13)	21.1(14)	19.2(12)	0.1(10)	–3.4(10)	–6.1(10)
C4	21.1(14)	17.4(13)	25.6(14)	3.5(11)	–0.4(11)	–0.4(10)
C5	24.3(15)	16.7(14)	31.6(15)	–6.1(11)	–0.3(11)	4.0(10)
C11	21.7(14)	19.1(14)	21.3(13)	6.3(10)	–5.1(10)	–2.2(10)
C20	14.8(13)	16.0(13)	20.9(12)	–7.1(10)	–1.9(9)	–0.9(9)
C6	23.8(15)	22.8(14)	21.4(13)	–6.5(11)	0.1(10)	3.0(11)
C18	22.1(14)	26.1(15)	20.5(13)	–3.1(11)	–2.1(10)	–1.8(11)
C16	16.5(13)	19.2(14)	27.5(14)	–7.0(11)	0.8(10)	–0.7(10)
C19	18.7(14)	19.5(13)	21.8(13)	–1.2(10)	–1.4(10)	–0.3(10)
C15	14.8(13)	16.3(13)	23.9(13)	–3.7(10)	–2.8(10)	–1.5(9)
C17	19.0(14)	27.6(15)	26.3(14)	–6.4(11)	5.0(11)	–3.5(11)

Table 7-95 Bond Lengths for [Ni(2Btz(Ph)2Btz)Cl].

Atom	Atom	Length/Å	Atom	Atom	Length/Å
Ni1	Cl1	2.2328(7)	C2	C3	1.395(3)
Ni1	N1	1.972(2)	C1	C13	1.390(4)
Ni1	N2	1.968(2)	C13	C14	1.446(4)
Ni1	C1	1.837(2)	C13	C12	1.394(4)
S2	C14	1.722(3)	C12	C11	1.390(4)
S2	C15	1.738(3)	C7	C6	1.390(4)
S1	C8	1.715(3)	C3	C4	1.377(4)
S1	C7	1.739(3)	C10	C11	1.392(4)
N1	C8	1.332(3)	C4	C5	1.404(4)
N1	C2	1.401(3)	C5	C6	1.374(4)
N2	C14	1.325(3)	C20	C19	1.401(4)
N2	C20	1.394(3)	C20	C15	1.411(3)
C8	C9	1.450(4)	C18	C19	1.385(4)
C9	C1	1.390(4)	C18	C17	1.401(4)
C9	C10	1.397(3)	C16	C15	1.391(4)
C2	C7	1.413(3)	C16	C17	1.383(4)

Table 7-96 Bond Angles for [Ni(2Btz(Ph)2Btz)Cl].

Atom	Atom	Atom	Angle/˚	Atom	Atom	Atom	Angle/˚
N1	Ni1	Cl1	100.32(6)	C1	C13	C14	108.8(2)
N2	Ni1	Cl1	97.79(6)	C1	C13	C12	120.1(2)
N2	Ni1	N1	161.84(9)	C12	C13	C14	131.0(2)
C1	Ni1	Cl1	164.89(8)	N2	C14	S2	115.88(19)
C1	Ni1	N1	81.55(10)	N2	C14	C13	116.2(2)
C1	Ni1	N2	81.32(10)	C13	C14	S2	127.9(2)
C14	S2	C15	89.35(12)	C11	C12	C13	118.9(2)
C8	S1	C7	89.73(12)	C2	C7	S1	110.08(19)
C8	N1	Ni1	113.29(17)	C6	C7	S1	128.0(2)

Atom	Atom	Atom	Angle/°	Atom	Atom	Atom	Angle/°
C8	N1	C2	110.8(2)	C6	C7	C2	121.9(2)
C2	N1	Ni1	135.90(17)	C4	C3	C2	119.4(2)
C14	N2	Ni1	113.46(17)	C11	C10	C9	118.5(2)
C14	N2	C20	111.0(2)	C3	C4	C5	120.8(2)
C20	N2	Ni1	135.51(18)	C6	C5	C4	121.0(3)
N1	C8	S1	115.94(19)	C12	C11	C10	121.8(2)
N1	C8	C9	116.3(2)	N2	C20	C19	127.6(2)
C9	C8	S1	127.73(19)	N2	C20	C15	113.5(2)
C1	C9	C8	108.8(2)	C19	C20	C15	118.8(2)
C1	C9	C10	120.3(2)	C5	C6	C7	118.0(2)
C10	C9	C8	130.9(2)	C19	C18	C17	121.4(3)
N1	C2	C7	113.5(2)	C17	C16	C15	118.0(3)
C3	C2	N1	127.8(2)	C18	C19	C20	118.9(3)
C3	C2	C7	118.8(2)	C20	C15	S2	110.18(19)
C9	C1	Ni1	119.79(19)	C16	C15	S2	127.5(2)
C9	C1	C13	120.3(2)	C16	C15	C20	122.2(2)
C13	C1	Ni1	119.5(2)	C16	C17	C18	120.6(3)

Table 7-97 Torsion Angles for [Ni(2Btz(Ph)2Btz)Cl].

A	B	C	D	Angle/°	A	B	C	D	Angle/°
Ni1	N1	C8	S1	178.99(11)	C2	N1	C8	S1	0.3(3)
Ni1	N1	C8	C9	1.9(3)	C2	N1	C8	C9	–176.8(2)
Ni1	N1	C2	C7	–178.18(18)	C2	C7	C6	C5	0.1(4)
Ni1	N1	C2	C3	1.2(4)	C2	C3	C4	C5	–1.4(4)
Ni1	N2	C14	S2	178.05(11)	C1	C9	C10	C11	–0.9(4)
Ni1	N2	C14	C13	–5.1(3)	C1	C13	C14	S2	175.29(19)
Ni1	N2	C20	C19	5.1(4)	C1	C13	C14	N2	–1.1(3)
Ni1	N2	C20	C15	–179.60(18)	C1	C13	C12	C11	0.4(4)
Ni1	C1	C13	C14	7.6(3)	C13	C12	C11	C10	0.3(4)
Ni1	C1	C13	C12	–173.53(19)	C14	S2	C15	C20	–1.39(19)
Cl1	Ni1	C1	C9	–92.9(4)	C14	S2	C15	C16	174.7(2)
Cl1	Ni1	C1	C13	79.4(4)	C14	N2	C20	C19	–173.4(2)
S1	C8	C9	C1	–174.68(19)	C14	N2	C20	C15	1.9(3)
S1	C8	C9	C10	6.0(4)	C14	C13	C12	C11	178.9(2)
S1	C7	C6	C5	180.0(2)	C12	C13	C14	S2	–3.4(4)
N1	Ni1	C1	C9	5.4(2)	C12	C13	C14	N2	–179.8(2)
N1	Ni1	C1	C13	177.7(2)	C7	S1	C8	N1	–0.5(2)
N1	C8	C9	C1	2.1(3)	C7	S1	C8	C9	176.3(2)
N1	C8	C9	C10	–177.2(2)	C7	C2	C3	C4	0.6(4)
N1	C2	C7	S1	–0.4(3)	C3	C2	C7	S1	–179.90(19)
N1	C2	C7	C6	179.4(2)	C3	C2	C7	C6	0.0(4)
N1	C2	C3	C4	–178.7(2)	C3	C4	C5	C6	1.5(4)
N2	Ni1	C1	C9	179.3(2)	C10	C9	C1	Ni1	173.76(18)
N2	Ni1	C1	C13	–8.4(2)	C10	C9	C1	C13	1.5(4)
N2	C20	C19	C18	174.5(2)	C4	C5	C6	C7	–0.9(4)
N2	C20	C15	S2	0.0(3)	C20	N2	C14	S2	–3.1(3)
N2	C20	C15	C16	–176.3(2)	C20	N2	C14	C13	173.7(2)
C8	S1	C7	C2	0.49(19)	C19	C20	C15	S2	175.75(19)
C8	S1	C7	C6	–179.4(3)	C19	C20	C15	C16	–0.6(4)
C8	N1	C2	C7	0.1(3)	C19	C18	C17	C16	–0.9(4)

A	B	C	D	Angle/°	A	B	C	D	Angle/°
C8	N1	C2	C3	179.5(2)	C15	S2	C14	N2	2.7(2)
C8	C9	C1	Ni1	–5.6(3)	C15	S2	C14	C13	–173.7(2)
C8	C9	C1	C13	–177.8(2)	C15	C20	C19	C18	–0.5(4)
C8	C9	C10	C11	178.3(2)	C15	C16	C17	C18	–0.3(4)
C9	C1	C13	C14	179.9(2)	C17	C18	C19	C20	1.3(4)
C9	C1	C13	C12	–1.3(4)	C17	C16	C15	S2	–174.7(2)
C9	C10	C11	C12	0.0(4)	C17	C16	C15	C20	1.0(4)

Table 7-98 Hydrogen Atom Coordinates (Å×10^4) and Isotropic Displacement Parameters (Å^2×10^3) for [Ni(2Btz(Ph)2Btz)Cl].

Atom	*x*	*y*	*z*	U(eq)
H12	4453.16	2646.38	5734.43	25
H3	416.54	7672.91	3369.34	21
H10	1798.76	4549.2	7103.54	23
H4	–956.37	9176.26	3488.27	26
H5	–1976.71	9603.83	4857.75	29
H11	3313.28	3086.42	7056.73	25
H6	–1537.44	8573.23	6152.59	27
H18	5395.94	5412.13	763.51	28
H16	7046.9	2813.16	2003.16	25
H19	3824.58	5701.06	1932.84	24
H17	6968.66	3976.15	782.13	29

7.3.15 [Ni(2Tz(Ph)Py)Br]

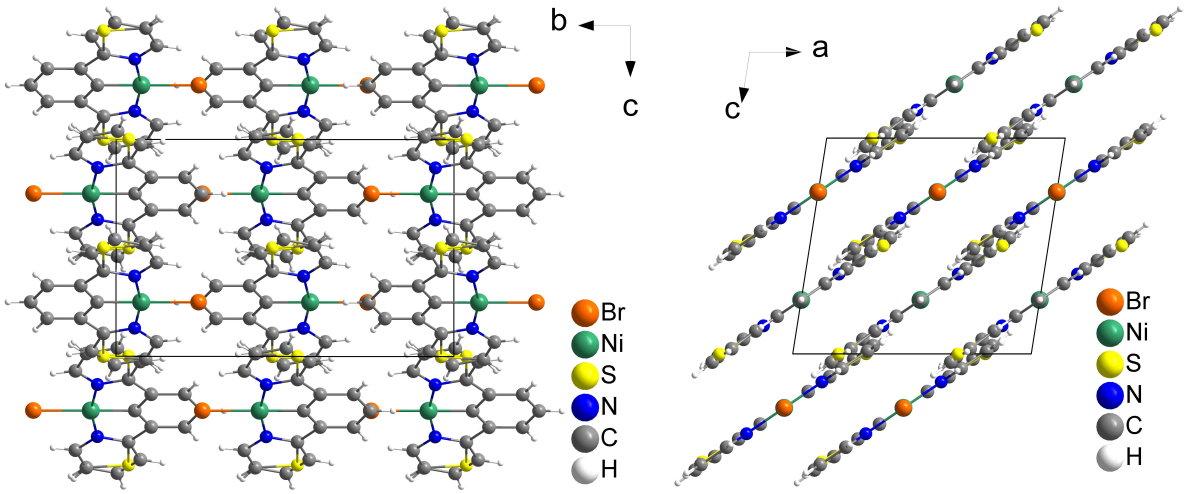

Figure 7-390 Crystal structure of [Ni(2Tz(Ph)Py)Br] viewed along the crystallographic *a*- (left) and *b*-axis (right).

Table 7-99 Crystal data and structure refinement for [Ni(2Tz(Ph)Py)Br].

Identification code	[Ni(2Tz(Ph)Py)Br].
Empirical formula	$C_7H_{4.5}Br_{0.5}NNi_{0.5}S_{0.5}$
Formula weight	187.96
Temperature/K	100.0
Crystal system	monoclinic
Space group	*C*2/c

a/Å	9.9854(4)
b/Å	14.0525(5)
c/Å	9.1400(3)
α/°	90
β/°	98.9600(10)
γ/°	90
Volume/Å^3	1266.87(8)
Z	8
ρ_{calc}g/cm^3	1.971
μ/mm^{-1}	4.833
F(000)	744.0
Crystal size/mm^3	0.19 × 0.05 × 0.02
Radiation	MoKα (λ = 0.71073)
2Θ range for data collection/°	5.046 to 56.586
Index ranges	–13 ≤ h ≤ 13, –18 ≤ k ≤ 18, –12 ≤ l ≤ 11
Reflections collected	18230
Independent reflections	1576 [R_{int} = 0.0399, R_{sigma} = 0.0181]
Data/restraints/parameters	1576/0/102
Goodness-of-fit on F^2	1.129
Final R indexes [I>=2σ (I)]	R_1 = 0.0232, wR_2 = 0.0489
Final R indexes [all data]	R_1 = 0.0253, wR_2 = 0.0497
Largest diff. peak/hole / e Å^{-3}	0.36/–0.64

Table 7-100 Fractional Atomic Coordinates (×10^4) and Equivalent Isotropic Displacement Parameters (Å^2×10^3) for [Ni(2Tz(Ph)Py)Br]. U_{eq} is defined as 1/3 of the trace of the orthogonalized U_{IJ} tensor.

Atom	*x*	*y*	*z*	U(eq)
Br1	5000	2555.8(2)	7500	19.63(9)
Ni1	5000	4254.8(2)	7500	13.56(9)
S1	8073.8(16)	5373.3(13)	4991.7(17)	19.4(3)
N1	6409.4(17)	4450.5(13)	6300.2(19)	18.4(3)
C1	5000	5560(2)	7500	20.9(6)
C5	6702(2)	5373.5(17)	6058(2)	24.0(5)
C9	7157(2)	3800.2(16)	5673(2)	21.7(4)
C4	5896(3)	6043.5(16)	6746(3)	26.6(5)
C8	8116(2)	4124.9(16)	4871(2)	21.0(4)
C3	5897(3)	7039.3(18)	6746(3)	43.4(8)
C2	5000	7524(2)	7500	49.4(13)
C6	7593(5)	5722(4)	5240(5)	18.8(9)
C7	8321(6)	5041(5)	4618(6)	20.7(11)

Table 7-101 Anisotropic Displacement Parameters (Å^2×10^3) for [Ni(2Tz(Ph)Py)Br]. The Anisotropic displacement factor exponent takes the form: $-2\pi^2[h^2a^{*2}U_{11}+2hka^*b^*U_{12}+\ldots]$.

Atom	U_{11}	U_{22}	U_{33}	U_{23}	U_{13}	U_{12}
Br1	24.21(16)	13.12(13)	23.83(16)	0	10.85(12)	0
Ni1	14.80(17)	12.51(17)	13.44(17)	0	2.39(13)	0
S1	17.2(7)	22.4(8)	19.5(7)	1.2(6)	6.1(5)	–2.3(6)
N1	16.6(8)	24.0(9)	14.1(8)	1.3(7)	0.2(7)	–3.8(7)
C1	28.6(16)	12.9(12)	17.4(14)	0	–8.6(12)	0
C5	22.9(11)	34.4(12)	12.9(9)	5.5(8)	–3.3(8)	–13.3(9)

Atom	U_{11}	U_{22}	U_{33}	U_{23}	U_{13}	U_{12}
C9	21.8(10)	23.8(10)	18.6(10)	1.8(8)	0.3(8)	–4.6(8)
C4	35.9(13)	18.5(10)	20.4(11)	4.1(8)	–11.6(9)	–6.6(9)
C8	18.8(10)	26.5(11)	18.2(10)	–0.2(8)	4.8(8)	3.1(8)
C3	66.7(19)	20.2(12)	31.8(14)	10.6(10)	–28.3(13)	–15.5(12)
C2	79(3)	10.3(14)	44(2)	0	–36(2)	0
C6	18(2)	19(2)	19(2)	1.6(18)	2.9(19)	–3.9(19)
C7	15(2)	28(3)	20(3)	0(2)	5.4(19)	0(2)

Table 7-102 Bond Lengths for [Ni(2Tz(Ph)Py)Br].

Atom	Atom	Length/Å	Atom	Atom	Length/Å
Br1	Ni1	2.3875(4)	C1	C4	1.389(3)
Ni1	N1	1.9337(17)	C5	C4	1.445(4)
Ni1	N1[1]	1.9337(17)	C5	C6	1.340(5)
Ni1	C1	1.834(3)	C9	C8	1.371(3)
S1	C5	1.800(3)	C4	C3	1.399(3)
S1	C8	1.759(3)	C8	C7	1.330(6)
N1	C5	1.355(3)	C3	C2	1.390(4)
N1	C9	1.362(3)	C6	C7	1.376(7)
C1	C4[1]	1.389(3)			

[1]1-X,+Y,3/2-Z

Table 7-103 Bond Angles for [Ni(2Tz(Ph)Py)Br].

Atom	Atom	Atom	Angle/°	Atom	Atom	Atom	Angle/°
N1	Ni1	Br1	98.18(5)	N1	C5	C4	113.78(19)
N1[1]	Ni1	Br1	98.18(5)	C4	C5	S1	139.30(19)
N1[1]	Ni1	N1	163.65(11)	C6	C5	N1	128.3(3)
C1	Ni1	Br1	180.0	C6	C5	C4	117.9(3)
C1	Ni1	N1	81.82(6)	N1	C9	C8	118.4(2)
C1	Ni1	N1[1]	81.82(5)	C1	C4	C5	110.0(2)
C8	S1	C5	93.53(12)	C1	C4	C3	119.3(3)
C5	N1	Ni1	115.05(15)	C3	C4	C5	130.6(3)
C5	N1	C9	115.27(19)	C9	C8	S1	105.84(17)
C9	N1	Ni1	129.68(15)	C7	C8	C9	123.7(3)
C4[1]	C1	Ni1	119.31(15)	C2	C3	C4	119.3(3)
C4	C1	Ni1	119.31(14)	C3[1]	C2	C3	121.4(3)
C4[1]	C1	C4	121.4(3)	C5	C6	C7	114.6(5)
N1	C5	S1	106.86(18)	C8	C7	C6	119.7(5)

[1]1-X,+Y,3/2-Z

Table 7-104 Torsion Angles for [Ni(2Tz(Ph)Py)Br].

A	B	C	D	Angle/°	A	B	C	D	Angle/°
Ni1	N1	C5	S1	177.73(10)	C1	C4	C3	C2	–0.1(3)
Ni1	N1	C5	C4	–0.1(2)	C5	S1	C8	C9	–2.38(17)
Ni1	N1	C5	C6	–177.8(3)	C5	N1	C9	C8	0.0(3)
Ni1	N1	C9	C8	–179.48(15)	C5	C4	C3	C2	179.67(19)
Ni1	C1	C4	C5	0.24(19)	C5	C6	C7	C8	–0.8(7)
Ni1	C1	C4	C3	–179.96(15)	C9	N1	C5	S1	–1.8(2)

A	B	C	D	Angle/°	A	B	C	D	Angle/°
S1	C5	C4	C1	–176.92(18)	C9	N1	C5	C4	–179.67(18)
S1	C5	C4	C3	3.3(4)	C9	N1	C5	C6	2.7(4)
N1[1]	Ni1	C1	C4[1]	–0.26(11)	C9	C8	C7	C6	3.3(7)
N1	Ni1	C1	C4[1]	179.74(11)	C4[1]	C1	C4	C5	–179.76(19)
N1[1]	Ni1	C1	C4	179.74(11)	C4[1]	C1	C4	C3	0.04(16)
N1	Ni1	C1	C4	–0.26(11)	C4	C5	C6	C7	–179.8(4)
N1	C5	C4	C1	–0.1(2)	C4	C3	C2	C3[1]	0.04(15)
N1	C5	C4	C3	–179.8(2)	C8	S1	C5	N1	2.43(17)
N1	C5	C6	C7	–2.2(6)	C8	S1	C5	C4	179.4(2)
N1	C9	C8	S1	1.9(2)	C6	C5	C4	C1	177.9(3)
N1	C9	C8	C7	–2.9(4)	C6	C5	C4	C3	–1.9(4)

[1]1-X,+Y,3/2-Z

Table 7-105 Hydrogen Atom Coordinates (Å×10^4) and Isotropic Displacement Parameters (Å^2×10^3) for [Ni(2Tz(Ph)Py)Br].

Atom	*x*	*y*	*z*	U(eq)
H9	7017.93	3137.39	5788.11	26
H8A	8685.33	3752.23	4356.24	25
H8B	8664.12	3669.77	4473.98	25
H3	6503.65	7380.7	6236.5	52
H2	5000	8199.8	7499.97	59
H6	7712.4	6384.47	5101.81	23
H7	8966.53	5225.77	4010.6	25

Table 7-106 Atomic Occupancy for [Ni(2Tz(Ph)Py)Br].

Atom	*Occupancy*	Atom	*Occupancy*	Atom	*Occupancy*
S1	0.5	H8A	0.5	H8B	0.5
C6	0.5	H6	0.5	C7	0.5
H7	0.5				

7.3.16 [Ni(4Tz(Ph)Py)Br]

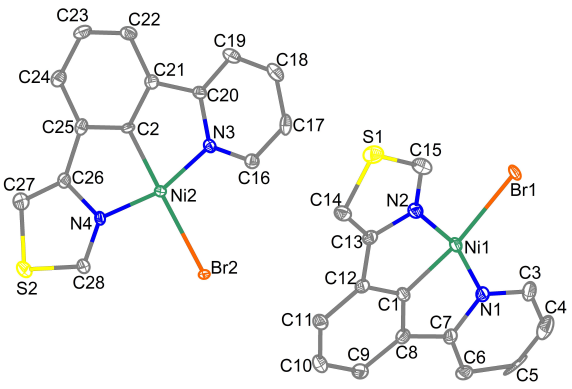

Figure 7-391 Asymmetric unit of [Ni(4Tz(Ph)Py)Br]. Ellipsoids are shown with a 50% probability. Hydrogen atoms are omitted for clarity.

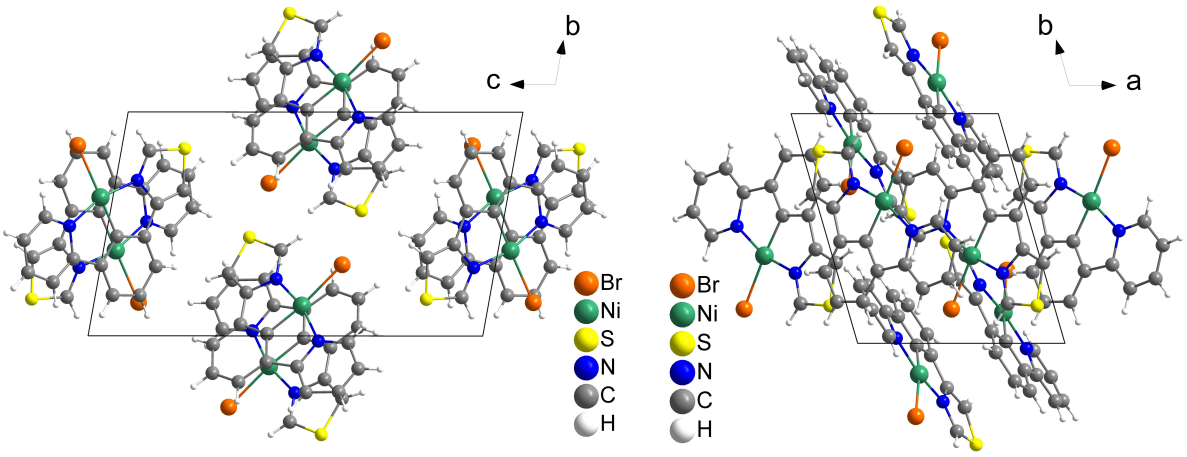

Figure 7-392 Crystal structure of [Ni(4Tz(Ph)Py)Br] viewed along the crystallographic *a*- (left) and *c*-axis (right).

Table 7-107 Crystal data and structure refinement for [Ni(4Tz(Ph)Py)Br].

Identification code	[Ni(4Tz(Ph)Py)Br]
Empirical formula	$C_{28}H_{18}Br_2N_4Ni_2S_2$
Formula weight	751.82
Temperature/K	100.0
Crystal system	triclinic
Space group	$P\bar{1}$
a/Å	8.4248(4)
b/Å	9.5962(5)
c/Å	16.4753(7)
α/°	96.821(2)
β/°	101.248(2)
γ/°	104.386(2)
Volume/Å^3	1245.66(10)
Z	2
ρ_{calc}g/cm^3	2.004
μ/mm^{-1}	4.916
F(000)	744.0
Crystal size/mm^3	0.15 × 0.03 × 0.02
Radiation	MoKα (λ = 0.71073)
2Θ range for data collection/°	4.452 to 60.11
Index ranges	–11 ≤ h ≤ 11, –13 ≤ k ≤ 13, –23 ≤ l ≤ 23
Reflections collected	54907
Independent reflections	7289 [R_{int} = 0.0672, R_{sigma} = 0.0400]
Data/restraints/parameters	7289/0/343
Goodness-of-fit on F^2	1.077
Final R indexes [I>=2σ (I)]	R_1 = 0.0527, wR_2 = 0.1148
Final R indexes [all data]	R_1 = 0.0637, wR_2 = 0.1204
Largest diff. peak/hole / e Å^{-3}	4.94/–2.65

Table 7-108 Fractional Atomic Coordinates (×10^4) and Equivalent Isotropic Displacement Parameters (Å^2×10^3) for [Ni(4Tz(Ph)Py)Br]. U_{eq} is defined as 1/3 of the trace of the orthogonalized U_{IJ} tensor.

Atom	*x*	*y*	*z*	U(eq)
Br2	4997.5(5)	8506.1(4)	1127.7(3)	13.02(10)
Br1	1780.6(6)	6818.1(6)	6113.8(3)	22.05(12)
Ni2	3271.9(6)	6183.3(5)	313.7(3)	8.46(11)

Atom	*x*	*y*	*z*	U(eq)
Ni1	2534.4(7)	8651.0(6)	5278.8(3)	12.54(12)
S2	813.4(15)	8360.0(13)	–1596.4(7)	18.5(2)
S1	4301.4(16)	5596.7(13)	3643.5(8)	22.1(2)
N4	2026(4)	6945(4)	–542(2)	9.8(6)
N3	4186(4)	4901(4)	967(2)	9.9(6)
N1	1931(4)	10228(4)	5857(2)	13.5(7)
N2	3295(5)	7459(4)	4506(2)	14.3(7)
C25	582(5)	4426(5)	–979(3)	11.9(7)
C7	1810(5)	11373(5)	5436(3)	13.4(8)
C20	3387(5)	3429(4)	723(3)	10.8(7)
C21	1968(5)	3155(5)	–9(3)	11.3(7)
C5	921(5)	12495(5)	6603(3)	21.2(11)
C13	3683(5)	8062(5)	3810(3)	13.6(8)
C26	718(5)	5911(5)	–1145(3)	11.5(7)
C1	2818(5)	9906(5)	4524(3)	12.8(8)
C8	2324(5)	11173(5)	4638(3)	13.5(8)
C12	3370(5)	9484(5)	3809(3)	13.0(8)
C17	6092(5)	4272(5)	2059(3)	15.0(8)
C2	1828(5)	4437(4)	–280(2)	10.2(7)
C16	5542(5)	5300(5)	1619(3)	12.5(7)
C23	–423(5)	1809(5)	–1124(3)	15.3(8)
C28	2197(5)	8268(5)	–712(3)	13.4(8)
C11	3467(6)	10391(5)	3205(3)	14.8(8)
C10	2951(6)	11659(5)	3320(3)	17.5(8)
C9	2361(6)	12061(5)	4019(3)	16.4(8)
C18	5280(6)	2828(5)	1810(3)	17.0(8)
C27	–75(6)	6490(5)	–1758(3)	16.3(8)
C19	3916(6)	2393(5)	1135(3)	15.9(8)
C6	1281(5)	12520(5)	5771(3)	15.6(8)
C15	3554(6)	6163(5)	4498(3)	20.4(9)
C24	–570(5)	3102(5)	–1400(3)	14.7(8)
C14	4266(6)	7216(5)	3282(3)	16.5(8)
C22	843(5)	1820(5)	–437(3)	13.9(8)
C3	1617(6)	10311(6)	6627(3)	20.4(9)
C4	1144(6)	11461(6)	6993(3)	26.8(11)

Table 7-109 Anisotropic Displacement Parameters ($Å^2×10^3$) for [Ni(4Tz(Ph)Py)Br]. The Anisotropic displacement factor exponent takes the form: $–2π^2[h^2a^{*2}U_{11}+2hka^*b^*U_{12}+…]$.

Atom	U_{11}	U_{22}	U_{33}	U_{23}	U_{13}	U_{12}
Br2	13.91(19)	8.99(18)	13.70(19)	1.29(14)	1.47(14)	0.47(14)
Br1	24.8(2)	24.5(2)	18.2(2)	13.38(18)	3.35(17)	6.15(19)
Ni2	9.4(2)	7.4(2)	8.5(2)	1.53(17)	1.92(17)	2.21(18)
Ni1	12.9(2)	13.4(3)	10.1(2)	4.58(19)	1.14(19)	1.7(2)
S2	25.2(6)	15.9(5)	15.9(5)	7.1(4)	3.5(4)	7.8(4)
S1	24.4(6)	17.6(5)	25.6(6)	1.2(4)	8.1(5)	7.6(4)
N4	12.0(15)	11.4(16)	6.5(14)	2.4(12)	3.0(12)	3.5(13)
N3	11.5(15)	10.7(15)	9.5(15)	3.2(12)	3.9(12)	4.8(12)
N1	10.7(16)	15.0(17)	11.1(16)	3.0(13)	–0.3(12)	–1.2(13)
N2	14.7(16)	14.0(17)	14.2(17)	3.9(13)	2.2(13)	4.5(14)
C25	9.2(17)	17(2)	8.9(17)	0.5(14)	4.2(14)	1.9(15)
C7	9.2(17)	15.3(19)	11.3(18)	1.6(15)	0.0(14)	–2.2(15)

Atom	U_{11}	U_{22}	U_{33}	U_{23}	U_{13}	U_{12}
C20	13.8(18)	9.5(17)	10.9(17)	2.4(14)	6.4(14)	3.4(14)
C21	11.9(17)	12.7(18)	10.8(17)	2.0(14)	6.7(14)	3.1(14)
C5	3.0(16)	20(2)	30(2)	–22.0(19)	–4.4(16)	3.7(15)
C13	12.0(18)	12.6(19)	13.2(19)	0.3(15)	1.1(15)	0.5(15)
C26	12.1(18)	14.3(19)	9.1(17)	1.5(14)	5.6(14)	3.4(15)
C1	9.3(17)	13.5(19)	11.7(18)	5.0(15)	–1.1(14)	–2.1(14)
C8	12.6(18)	13.7(19)	11.8(18)	0.3(15)	1.5(14)	1.6(15)
C12	11.4(18)	12.0(18)	12.3(18)	1.1(15)	0.9(14)	–0.9(15)
C17	9.0(17)	28(2)	8.1(17)	3.1(16)	1.8(14)	5.9(16)
C2	14.0(18)	5.7(16)	9.4(17)	–0.7(13)	4.0(14)	–0.2(14)
C16	11.3(18)	13.6(19)	12.5(18)	2.8(15)	3.7(14)	2.4(15)
C23	14.0(19)	11.0(18)	18(2)	–2.2(15)	5.0(16)	–0.5(15)
C28	17.0(19)	12.9(19)	10.4(18)	3.3(14)	3.6(15)	3.7(15)
C11	16.6(19)	15.0(19)	14.0(19)	4.4(15)	6.2(15)	3.7(16)
C10	19(2)	20(2)	15(2)	7.7(17)	4.4(16)	6.0(17)
C9	19(2)	13.9(19)	16(2)	2.5(16)	5.5(16)	3.0(16)
C18	21(2)	20(2)	18(2)	10.6(17)	9.6(17)	11.7(17)
C27	16(2)	18(2)	16(2)	3.7(16)	4.2(16)	6.5(17)
C19	19(2)	13.2(19)	20(2)	7.8(16)	7.3(17)	6.3(16)
C6	12.3(18)	12.9(19)	18(2)	1.1(16)	1.2(15)	–0.9(15)
C15	20(2)	17(2)	26(2)	8.0(18)	6.2(18)	5.2(17)
C24	12.1(18)	17(2)	13.4(19)	0.0(15)	2.2(15)	2.5(16)
C14	14.8(19)	15(2)	19(2)	5.4(16)	4.2(16)	2.5(16)
C22	16.5(19)	10.7(18)	16.5(19)	3.3(15)	8.6(16)	3.3(15)
C3	18(2)	26(2)	10.8(19)	1.5(17)	2.0(16)	–4.0(18)
C4	21(2)	38(3)	15(2)	–5(2)	6.5(18)	0(2)

Table 7-110 Bond Lengths for [Ni(4Tz(Ph)Py)Br].

Atom	Atom	Length/Å	Atom	Atom	Length/Å
Br2	Ni2	2.4083(7)	C7	C8	1.468(6)
Br1	Ni1	2.3981(7)	C7	C6	1.382(6)
Ni2	N4	1.916(3)	C20	C21	1.469(6)
Ni2	N3	1.931(3)	C20	C19	1.382(6)
Ni2	C2	1.838(4)	C21	C2	1.381(6)
Ni1	N1	1.920(4)	C21	C22	1.400(6)
Ni1	N2	1.917(4)	C5	C6	1.462(7)
Ni1	C1	1.839(4)	C5	C4	1.277(8)
S2	C28	1.706(4)	C13	C12	1.453(6)
S2	C27	1.730(5)	C13	C14	1.362(6)
S1	C15	1.734(5)	C26	C27	1.353(6)
S1	C14	1.734(5)	C1	C8	1.384(6)
N4	C26	1.407(5)	C1	C12	1.401(6)
N4	C28	1.311(5)	C8	C9	1.405(6)
N3	C20	1.377(5)	C12	C11	1.399(6)
N3	C16	1.345(5)	C17	C16	1.407(6)
N1	C7	1.382(6)	C17	C18	1.357(7)
N1	C3	1.342(6)	C23	C24	1.397(6)
N2	C13	1.403(6)	C23	C22	1.392(6)
N2	C15	1.314(6)	C11	C10	1.394(6)
C25	C26	1.463(6)	C10	C9	1.391(6)

Atom	Atom	Length/Å	Atom	Atom	Length/Å
C25	C2	1.397(6)	C18	C19	1.373(6)
C25	C24	1.398(6)	C3	C4	1.376(8)

Table 7-111 Bond Angles for [Ni(4Tz(Ph)Py)Br].

Atom	Atom	Atom	Angle/°	Atom	Atom	Atom	Angle/°
N4	Ni2	Br2	96.71(10)	C22	C21	C20	128.7(4)
N4	Ni2	N3	163.81(15)	C4	C5	C6	119.7(4)
N3	Ni2	Br2	99.37(11)	N2	C13	C12	111.8(4)
C2	Ni2	Br2	175.90(13)	C14	C13	N2	114.7(4)
C2	Ni2	N4	82.10(17)	C14	C13	C12	133.5(4)
C2	Ni2	N3	81.98(17)	N4	C26	C25	111.4(3)
N1	Ni1	Br1	100.05(11)	C27	C26	N4	114.0(4)
N2	Ni1	Br1	95.70(11)	C27	C26	C25	134.5(4)
N2	Ni1	N1	164.24(16)	C8	C1	Ni1	118.8(3)
C1	Ni1	Br1	171.43(13)	C8	C1	C12	121.9(4)
C1	Ni1	N1	81.91(18)	C12	C1	Ni1	119.0(3)
C1	Ni1	N2	82.45(18)	C1	C8	C7	111.4(4)
C28	S2	C27	90.4(2)	C1	C8	C9	119.4(4)
C14	S1	C15	90.3(2)	C9	C8	C7	129.3(4)
C26	N4	Ni2	116.1(3)	C1	C12	C13	111.0(4)
C28	N4	Ni2	132.4(3)	C11	C12	C13	130.0(4)
C28	N4	C26	111.4(3)	C11	C12	C1	118.9(4)
C20	N3	Ni2	116.2(3)	C18	C17	C16	119.8(4)
C16	N3	Ni2	126.5(3)	C25	C2	Ni2	119.8(3)
C16	N3	C20	117.3(4)	C21	C2	Ni2	119.1(3)
C7	N1	Ni1	116.4(3)	C21	C2	C25	121.1(4)
C3	N1	Ni1	126.0(3)	N3	C16	C17	121.9(4)
C3	N1	C7	117.6(4)	C22	C23	C24	121.2(4)
C13	N2	Ni1	115.7(3)	N4	C28	S2	114.2(3)
C15	N2	Ni1	132.6(3)	C10	C11	C12	118.9(4)
C15	N2	C13	111.7(4)	C9	C10	C11	122.3(4)
C2	C25	C26	110.5(4)	C10	C9	C8	118.6(4)
C2	C25	C24	119.5(4)	C17	C18	C19	119.2(4)
C24	C25	C26	129.9(4)	C26	C27	S2	110.1(3)
N1	C7	C8	110.9(4)	C18	C19	C20	119.7(4)
N1	C7	C6	121.3(4)	C7	C6	C5	117.1(4)
C6	C7	C8	127.9(4)	N2	C15	S1	113.5(4)
N3	C20	C21	111.2(3)	C23	C24	C25	119.1(4)
N3	C20	C19	122.1(4)	C13	C14	S1	109.8(3)
C19	C20	C21	126.7(4)	C23	C22	C21	119.2(4)
C2	C21	C20	111.5(4)	N1	C3	C4	122.7(5)
C2	C21	C22	119.8(4)	C5	C4	C3	121.4(5)

Table 7-112 Torsion Angles for [Ni(4Tz(Ph)Py)Br].

A	B	C	D	Angle/°	A	B	C	D	Angle/°
Ni2	N4	C26	C25	0.3(4)	C26	C25	C2	C21	–178.9(4)
Ni2	N4	C26	C27	–177.1(3)	C26	C25	C24	C23	179.1(4)
Ni2	N4	C28	S2	176.2(2)	C1	C8	C9	C10	–2.1(6)
Ni2	N3	C20	C21	0.2(4)	C1	C12	C11	C10	–2.3(6)

A	B	C	D	Angle/°	A	B	C	D	Angle/°
Ni2	N3	C20	C19	179.8(3)	C8	C7	C6	C5	–176.9(4)
Ni2	N3	C16	C17	179.3(3)	C8	C1	C12	C13	–175.4(4)
Ni1	N1	C7	C8	–4.8(4)	C8	C1	C12	C11	1.7(6)
Ni1	N1	C7	C6	175.8(3)	C12	C13	C14	S1	–178.9(4)
Ni1	N1	C3	C4	–178.1(4)	C12	C1	C8	C7	–179.7(4)
Ni1	N2	C13	C12	–1.7(5)	C12	C1	C8	C9	0.5(6)
Ni1	N2	C13	C14	178.3(3)	C12	C11	C10	C9	0.7(7)
Ni1	N2	C15	S1	–178.7(2)	C17	C18	C19	C20	–0.3(7)
Ni1	C1	C8	C7	6.7(5)	C2	C25	C26	N4	–1.9(5)
Ni1	C1	C8	C9	–173.1(3)	C2	C25	C26	C27	174.9(5)
Ni1	C1	C12	C13	–1.8(5)	C2	C25	C24	C23	–1.7(6)
Ni1	C1	C12	C11	175.4(3)	C2	C21	C22	C23	–1.0(6)
N4	Ni2	C2	C25	–2.1(3)	C16	N3	C20	C21	–178.2(3)
N4	Ni2	C2	C21	179.6(3)	C16	N3	C20	C19	1.5(6)
N4	C26	C27	S2	0.4(5)	C16	C17	C18	C19	–0.7(6)
N3	Ni2	C2	C25	–179.2(3)	C28	S2	C27	C26	–0.3(3)
N3	Ni2	C2	C21	2.5(3)	C28	N4	C26	C25	177.2(3)
N3	C20	C21	C2	1.7(5)	C28	N4	C26	C27	–0.3(5)
N3	C20	C21	C22	–179.3(4)	C11	C10	C9	C8	1.5(7)
N3	C20	C19	C18	0.0(6)	C18	C17	C16	N3	2.2(6)
N1	Ni1	C1	C8	–7.4(3)	C27	S2	C28	N4	0.1(4)
N1	Ni1	C1	C12	178.8(3)	C19	C20	C21	C2	–177.9(4)
N1	C7	C8	C1	–0.9(5)	C19	C20	C21	C22	1.1(7)
N1	C7	C8	C9	178.8(4)	C6	C7	C8	C1	178.4(4)
N1	C7	C6	C5	2.4(6)	C6	C7	C8	C9	–1.8(7)
N1	C3	C4	C5	2.5(8)	C6	C5	C4	C3	–4.1(7)
N2	Ni1	C1	C8	174.5(4)	C15	S1	C14	C13	–0.8(4)
N2	Ni1	C1	C12	0.7(3)	C15	N2	C13	C12	179.0(4)
N2	C13	C12	C1	2.1(5)	C15	N2	C13	C14	–1.0(6)
N2	C13	C12	C11	–174.6(4)	C24	C25	C26	N4	177.4(4)
N2	C13	C14	S1	1.2(5)	C24	C25	C26	C27	–5.9(8)
C25	C26	C27	S2	–176.3(4)	C24	C25	C2	Ni2	–176.5(3)
C7	N1	C3	C4	1.7(7)	C24	C25	C2	C21	1.7(6)
C7	C8	C9	C10	178.1(4)	C24	C23	C22	C21	1.0(6)
C20	N3	C16	C17	–2.6(6)	C14	S1	C15	N2	0.2(4)
C20	C21	C2	Ni2	–3.0(5)	C14	C13	C12	C1	–177.8(5)
C20	C21	C2	C25	178.7(4)	C14	C13	C12	C11	5.5(8)
C20	C21	C22	C23	–179.9(4)	C22	C21	C2	Ni2	177.9(3)
C21	C20	C19	C18	179.5(4)	C22	C21	C2	C25	–0.4(6)
C13	N2	C15	S1	0.4(5)	C22	C23	C24	C25	0.4(6)
C13	C12	C11	C10	174.2(4)	C3	N1	C7	C8	175.3(4)
C26	N4	C28	S2	0.1(5)	C3	N1	C7	C6	–4.1(6)
C26	C25	C2	Ni2	2.8(5)	C4	C5	C6	C7	1.8(6)

Table 7-113 Hydrogen Atom Coordinates (Å×10^4) and Isotropic Displacement Parameters (Å^2×10^3) for [Ni(4Tz(Ph)Py)Br].

Atom	*x*	*y*	*z*	U(eq)
H5	523.25	13245.12	6851.84	25
H17	7029.9	4588.8	2529.19	18
H16	6145.05	6304.4	1786.06	15
H23	–1199.32	905.46	–1410.59	18

Atom	*x*	*y*	*z*	U(eq)
H28	3020.03	9102.5	–371.58	16
H11	3876.63	10148	2724.99	18
H10	3004.45	12268.36	2906.05	21
H9	1992.03	12918.31	4076.19	20
H18	5650.53	2125.3	2100.31	20
H27	–986.89	5949.52	–2211.1	20
H19	3338.35	1385.59	951.81	19
H6	1155.73	13289.98	5473.16	19
H15	3350.62	5591.41	4919.19	24
H24	–1442.3	3081.55	–1867.91	18
H14	4601.67	7473.22	2788.95	20
H22	940.72	931.22	–260.71	17
H3	1725.36	9545.74	6931.11	25
H4	979.41	11485.22	7548.66	32

7.3.17 [Ni(2Btz(Ph)Py)Br]

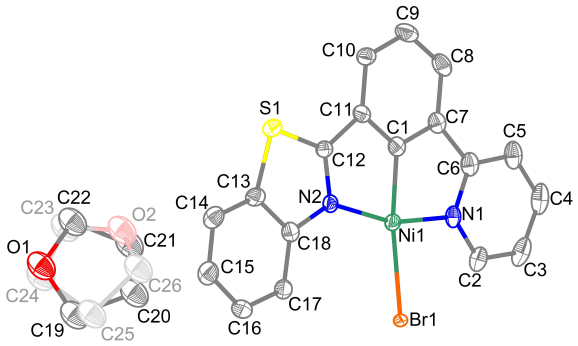

Figure 7-393 Asymmetric unit of [Ni(2Btz(Ph)Py)Br] · 0.5 THF. Ellipsoids are shown with a 50% probability. Hydrogen atoms are omitted for clarity.

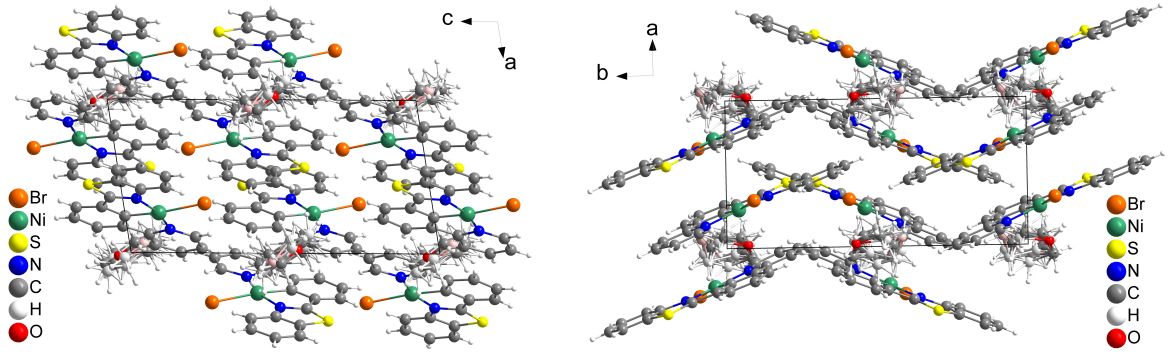

Figure 7-394 Crystal structure of [Ni(2Btz(Ph)Py)Br] · 0.5 THF viewed along the crystallographic *b*- (left) and *c*-axis (right).

Table 7-114 Crystal data and structure refinement for [Ni(2Btz(Ph)Py)Br] · 0.5 THF.

Identification code	[Ni(2Btz(Ph)Py)Br] · 0.5 THF
Empirical formula	$C_{20}H_{15}BrN_2NiO_{0.5}S$
Formula weight	462.02

Temperature/K	100.0
Crystal system	monoclinic
Space group	$P2_1/c$
a/Å	7.5738(2)
b/Å	15.2479(5)
c/Å	15.0726(5)
α/°	90
β/°	99.1900(10)
γ/°	90
Volume/Å^3	1718.31(9)
Z	4
ρ_{calc}g/cm^3	1.786
μ/mm^{-1}	3.584
F(000)	928.0
Crystal size/mm^3	0.29 × 0.02 × 0.02
Radiation	MoKα (λ = 0.71073)
2Θ range for data collection/°	3.824 to 55.752
Index ranges	–9 ≤ h ≤ 9, –20 ≤ k ≤ 20, –19 ≤ l ≤ 19
Reflections collected	32525
Independent reflections	4087 [R_{int} = 0.0651, R_{sigma} = 0.0346]
Data/restraints/parameters	4087/103/244
Goodness-of-fit on F^2	1.040
Final R indexes [I>=2σ (I)]	R_1 = 0.0414, wR_2 = 0.1021
Final R indexes [all data]	R_1 = 0.0511, wR_2 = 0.1100
Largest diff. peak/hole / e Å^{-3}	2.82/–0.52

Table 7-115 Fractional Atomic Coordinates (×10^4) and Equivalent Isotropic Displacement Parameters (Å^2×10^3) for [Ni(2Btz(Ph)Py)Br] · 0.5 THF. U_{eq} is defined as 1/3 of the trace of the orthogonalized U_{IJ} tensor.

Atom	*x*	*y*	*z*	U(eq)
Br1	3220.7(5)	5916.0(2)	7626.2(2)	22.25(12)
Ni1	2602.8(5)	5406.7(3)	6101.0(3)	15.91(12)
S1	4409.0(11)	6991.8(6)	3961.0(6)	19.46(18)
N1	1519(4)	4290.9(19)	6381(2)	18.9(6)
N2	3526(4)	6391.9(18)	5444.9(18)	16.4(5)
C11	2980(4)	5330(2)	4284(2)	17.9(6)
C12	3612(4)	6194(2)	4591(2)	16.3(6)
C2	1040(5)	4072(2)	7170(3)	25.3(8)
C7	1723(4)	4043(2)	4871(2)	20.0(7)
C1	2383(4)	4888(2)	4986(2)	18.8(7)
C18	4131(4)	7253(2)	5633(2)	18.9(7)
C17	4269(5)	7700(2)	6450(2)	20.7(7)
C16	4956(5)	8548(2)	6499(2)	25.8(8)
C9	2263(5)	4084(2)	3337(3)	26.5(8)
C6	1216(4)	3698(2)	5691(3)	22.7(7)
C13	4687(4)	7676(2)	4893(2)	20.5(7)
C15	5508(5)	8946(3)	5757(3)	28.8(8)
C10	2931(5)	4934(2)	3451(2)	20.8(7)
C8	1643(5)	3634(2)	4032(3)	25.3(8)
C3	294(5)	3263(3)	7317(3)	32.1(9)
C4	49(5)	2645(3)	6632(3)	32.5(9)
C5	511(5)	2878(3)	5814(3)	28.6(8)

Atom	*x*	*y*	*z*	U(eq)
C14	5368(5)	8530(3)	4952(3)	26.2(8)
O1	–310(40)	10701(11)	4653(13)	45.1(15)
C22	–750(40)	9919(14)	4130(12)	45.1(15)
C21	–610(40)	9166(11)	4804(15)	45.1(15)
C20	820(30)	9544(13)	5549(14)	45.1(15)
C19	140(40)	10493(13)	5575(14)	45.1(15)
O2	–580(30)	9209(10)	4553(10)	45.1(15)
C23	–1220(30)	9977(13)	4152(13)	45.1(15)
C26	250(60)	9276(15)	5435(17)	45.1(15)
C24	–750(30)	10708(11)	4861(14)	45.1(15)
C25	430(40)	10270(13)	5640(15)	45.1(15)

Table 7-116 Anisotropic Displacement Parameters ($Å^2 \times 10^3$) for [Ni(2Btz(Ph)Py)Br] · 0.5 THF. The Anisotropic displacement factor exponent takes the form: $-2\pi^2[h^2a^{*2}U_{11}+2hka^*b^*U_{12}+\ldots]$.

Atom	U_{11}	U_{22}	U_{33}	U_{23}	U_{13}	U_{12}
Br1	33.8(2)	18.47(18)	15.48(18)	0.15(12)	7.03(14)	0.52(13)
Ni1	15.7(2)	16.0(2)	15.8(2)	1.38(15)	1.91(16)	1.92(15)
S1	19.6(4)	22.0(4)	16.8(4)	1.2(3)	2.8(3)	–2.1(3)
N1	13.2(13)	17.1(14)	25.7(15)	4.5(11)	0.5(11)	2.6(10)
N2	16.2(13)	14.3(13)	17.6(14)	0.9(10)	–0.8(10)	1.4(10)
C11	13.8(15)	19.8(16)	19.0(16)	–2.4(12)	–1.0(12)	5.0(12)
C12	12.7(14)	19.8(16)	15.7(15)	–0.4(12)	0.5(12)	4.4(12)
C2	20.6(17)	24.8(19)	29.4(19)	9.4(15)	0.7(14)	0.3(14)
C7	13.3(15)	19.2(17)	25.8(18)	–0.1(13)	–1.5(13)	1.2(12)
C1	12.5(14)	20.4(16)	22.0(17)	–0.1(13)	–1.9(12)	3.6(12)
C18	14.1(15)	17.9(16)	22.6(17)	–0.8(13)	–3.5(12)	–1.1(12)
C17	21.2(16)	19.0(16)	21.4(17)	1.4(13)	1.6(13)	–0.1(13)
C16	32(2)	22.0(18)	22.4(18)	–4.4(14)	1.5(15)	–1.6(15)
C9	23.9(18)	28(2)	25.6(19)	–10.5(15)	–1.7(15)	2.7(14)
C6	13.1(15)	21.7(17)	31.0(19)	2.6(14)	–3.0(13)	1.8(13)
C13	16.8(15)	24.5(18)	18.3(16)	–1.3(13)	–2.7(12)	–0.4(13)
C15	33(2)	21.8(18)	30(2)	2.9(15)	0.4(16)	–8.7(15)
C10	18.6(16)	25.2(18)	17.7(16)	–1.7(13)	–0.4(13)	5.0(13)
C8	22.9(17)	16.8(17)	34(2)	–5.5(14)	–2.0(15)	–2.1(13)
C3	24.6(19)	33(2)	37(2)	18.4(17)	–0.3(16)	–2.9(16)
C4	20.5(18)	24.5(19)	50(3)	15.1(18)	–1.4(17)	–1.7(15)
C5	17.8(17)	21.7(18)	43(2)	6.4(16)	–4.1(15)	0.7(14)
C14	28.9(19)	24.2(19)	24.8(18)	5.1(14)	1.7(15)	–8.7(15)
O1	50(4)	33(3)	54(4)	–5(3)	16(3)	–5(2)
C22	50(4)	33(3)	54(4)	–5(3)	16(3)	–5(2)
C21	50(4)	33(3)	54(4)	–5(3)	16(3)	–5(2)
C20	50(4)	33(3)	54(4)	–5(3)	16(3)	–5(2)
C19	50(4)	33(3)	54(4)	–5(3)	16(3)	–5(2)
O2	50(4)	33(3)	54(4)	–5(3)	16(3)	–5(2)
C23	50(4)	33(3)	54(4)	–5(3)	16(3)	–5(2)
C26	50(4)	33(3)	54(4)	–5(3)	16(3)	–5(2)
C24	50(4)	33(3)	54(4)	–5(3)	16(3)	–5(2)
C25	50(4)	33(3)	54(4)	–5(3)	16(3)	–5(2)

Table 7-117 Bond Lengths for [Ni(2Btz(Ph)Py)Br] · 0.5 THF.

Atom	Atom	Length/Å	Atom	Atom	Length/Å
Br1	Ni1	2.4007(5)	C17	C16	1.392(5)
Ni1	N1	1.964(3)	C16	C15	1.393(5)
Ni1	N2	1.986(3)	C9	C10	1.392(5)
Ni1	C1	1.840(3)	C9	C8	1.394(6)
S1	C12	1.711(3)	C6	C5	1.384(5)
S1	C13	1.735(4)	C13	C14	1.398(5)
N1	C2	1.339(5)	C15	C14	1.359(5)
N1	C6	1.369(5)	C3	C4	1.389(6)
N2	C12	1.334(4)	C4	C5	1.380(6)
N2	C18	1.404(4)	O1	C22	1.440(14)
C11	C12	1.453(5)	O1	C19	1.413(13)
C11	C1	1.390(5)	C22	C21	1.525(13)
C11	C10	1.387(5)	C21	C20	1.543(13)
C2	C3	1.389(5)	C20	C19	1.538(13)
C7	C1	1.383(5)	O2	C23	1.369(17)
C7	C6	1.451(5)	O2	C26	1.382(17)
C7	C8	1.403(5)	C23	C24	1.547(15)
C18	C17	1.396(5)	C26	C25	1.549(16)
C18	C13	1.411(5)	C24	C25	1.514(16)

Table 7-118 Bond Angles for [Ni(2Btz(Ph)Py)Br] · 0.5 THF.

Atom	Atom	Atom	Angle/˚	Atom	Atom	Atom	Angle/˚
N1	Ni1	Br1	95.66(9)	C17	C18	C13	118.9(3)
N1	Ni1	N2	162.69(12)	C16	C17	C18	118.4(3)
N2	Ni1	Br1	101.64(8)	C17	C16	C15	121.3(3)
C1	Ni1	Br1	171.37(10)	C10	C9	C8	121.6(3)
C1	Ni1	N1	81.03(14)	N1	C6	C7	111.9(3)
C1	Ni1	N2	81.84(14)	N1	C6	C5	121.1(4)
C12	S1	C13	89.22(17)	C5	C6	C7	127.0(4)
C2	N1	Ni1	126.1(3)	C18	C13	S1	110.6(3)
C2	N1	C6	118.2(3)	C14	C13	S1	127.4(3)
C6	N1	Ni1	115.7(2)	C14	C13	C18	122.0(3)
C12	N2	Ni1	112.6(2)	C14	C15	C16	121.5(3)
C12	N2	C18	110.0(3)	C11	C10	C9	118.3(3)
C18	N2	Ni1	137.4(2)	C9	C8	C7	119.2(3)
C1	C11	C12	109.1(3)	C4	C3	C2	119.5(4)
C10	C11	C12	130.0(3)	C5	C4	C3	117.9(4)
C10	C11	C1	120.9(3)	C4	C5	C6	120.7(4)
N2	C12	S1	116.8(3)	C15	C14	C13	117.8(3)
N2	C12	C11	116.6(3)	C19	O1	C22	110.6(14)
C11	C12	S1	126.6(3)	O1	C22	C21	105.9(13)
N1	C2	C3	122.6(4)	C22	C21	C20	99.8(11)
C1	C7	C6	111.7(3)	C19	C20	C21	99.9(12)
C1	C7	C8	119.4(3)	O1	C19	C20	102.4(13)
C8	C7	C6	128.9(3)	C23	O2	C26	115.8(18)
C11	C1	Ni1	119.6(3)	O2	C23	C24	106.7(13)
C7	C1	Ni1	119.6(3)	O2	C26	C25	106.1(16)
C7	C1	C11	120.7(3)	C25	C24	C23	105.0(11)
N2	C18	C13	113.4(3)	C24	C25	C26	104.7(13)

Atom	Atom	Atom	Angle/°	Atom	Atom	Atom	Angle/°
C17	C18	N2	127.6(3)				

Table 7-119 Torsion Angles for [Ni(2Btz(Ph)Py)Br] · 0.5 THF.

A	B	C	D	Angle/°	A	B	C	D	Angle/°
Ni1	N1	C2	C3	–179.4(3)	C18	N2	C12	C11	–178.3(3)
Ni1	N1	C6	C7	–1.9(4)	C18	C17	C16	C15	–0.4(6)
Ni1	N1	C6	C5	177.9(3)	C18	C13	C14	C15	0.9(6)
Ni1	N2	C12	S1	–179.44(15)	C17	C18	C13	S1	179.4(3)
Ni1	N2	C12	C11	1.9(4)	C17	C18	C13	C14	–0.1(5)
Ni1	N2	C18	C17	0.6(6)	C17	C16	C15	C14	1.2(6)
Ni1	N2	C18	C13	178.9(2)	C16	C15	C14	C13	–1.4(6)
S1	C13	C14	C15	–178.6(3)	C6	N1	C2	C3	1.6(5)
N1	Ni1	C1	C11	–178.9(3)	C6	C7	C1	Ni1	2.4(4)
N1	Ni1	C1	C7	–2.7(3)	C6	C7	C1	C11	178.6(3)
N1	C2	C3	C4	1.0(6)	C6	C7	C8	C9	–177.9(3)
N1	C6	C5	C4	1.7(5)	C13	S1	C12	N2	0.2(3)
N2	Ni1	C1	C11	3.5(3)	C13	S1	C12	C11	178.6(3)
N2	Ni1	C1	C7	179.7(3)	C13	C18	C17	C16	–0.1(5)
N2	C18	C17	C16	178.1(3)	C10	C11	C12	S1	2.9(5)
N2	C18	C13	S1	1.0(4)	C10	C11	C12	N2	–178.6(3)
N2	C18	C13	C14	–178.6(3)	C10	C11	C1	Ni1	176.1(2)
C12	S1	C13	C18	–0.6(3)	C10	C11	C1	C7	–0.1(5)
C12	S1	C13	C14	178.9(3)	C10	C9	C8	C7	–1.0(5)
C12	N2	C18	C17	–179.2(3)	C8	C7	C1	Ni1	–176.7(3)
C12	N2	C18	C13	–0.8(4)	C8	C7	C1	C11	–0.6(5)
C12	C11	C1	Ni1	–3.3(4)	C8	C7	C6	N1	178.9(3)
C12	C11	C1	C7	–179.5(3)	C8	C7	C6	C5	–0.9(6)
C12	C11	C10	C9	179.4(3)	C8	C9	C10	C11	0.4(5)
C2	N1	C6	C7	177.2(3)	C3	C4	C5	C6	0.8(6)
C2	N1	C6	C5	–2.9(5)	O1	C22	C21	C20	–29(3)
C2	C3	C4	C5	–2.2(6)	C22	O1	C19	C20	26(3)
C7	C6	C5	C4	–178.4(3)	C22	C21	C20	C19	43(2)
C1	C11	C12	S1	–177.8(2)	C21	C20	C19	O1	–43(2)
C1	C11	C12	N2	0.6(4)	C19	O1	C22	C21	2(3)
C1	C11	C10	C9	0.2(5)	O2	C23	C24	C25	8(3)
C1	C7	C6	N1	–0.2(4)	O2	C26	C25	C24	13(5)
C1	C7	C6	C5	180.0(3)	C23	O2	C26	C25	–9(5)
C1	C7	C8	C9	1.1(5)	C23	C24	C25	C26	–12(3)
C18	N2	C12	S1	0.4(4)	C26	O2	C23	C24	1(4)

Table 7-120 Hydrogen Atom Coordinates (Å×10^4) and Isotropic Displacement Parameters (Å^2×10^3) for [Ni(2Btz(Ph)Py)Br] · 0.5 THF.

Atom	*x*	*y*	*z*	U(eq)
H2	1218.51	4485.49	7646.7	30
H17	3902.64	7431.36	6959.55	25
H16	5051.12	8861.65	7048.74	31
H9	2227.8	3803.4	2771.28	32
H15	5992.73	9521.59	5816.35	35
H10	3342.89	5235.31	2971.96	25
H8	1173.71	3057.9	3938.12	30

Atom	*x*	*y*	*z*	U(eq)
H3	–46.54	3134.03	7882.87	39
H4	–420.36	2080.73	6722.82	39
H5	342.57	2471.12	5330.81	34
H14	5721.11	8810.14	4445.03	31
H22A	92.68	9830.51	3700.16	54
H22B	–1980.33	9959.04	3789.54	54
H21A	–208.33	8616.93	4550.37	54
H21B	–1761.6	9061.61	5021.95	54
H20A	822.48	9240.58	6129.9	54
H20B	2029.36	9517.29	5381.49	54
H19A	–915.1	10530.29	5883.66	54
H19B	1089.83	10887.1	5880.04	54
H23A	–2527.86	9941.92	3959.76	54
H23B	–647.13	10095.91	3617.19	54
H26A	1438.8	8992.78	5515.24	54
H26B	–482.03	8989.53	5842.18	54
H24A	–107.76	11194.56	4615.8	54
H24B	–1847.24	10944.24	5052.97	54
H25A	25.83	10411.16	6215.55	54
H25B	1691.21	10462.13	5673.32	54

Table 7-121 Atomic Occupancy for [Ni(2Btz(Ph)Py)Br] · 0.5 THF.

Atom	*Occupancy*	Atom	*Occupancy*	Atom	*Occupancy*
O1	0.25	C22	0.25	H22A	0.25
H22B	0.25	C21	0.25	H21A	0.25
H21B	0.25	C20	0.25	H20A	0.25
H20B	0.25	C19	0.25	H19A	0.25
H19B	0.25	O2	0.25	C23	0.25
H23A	0.25	H23B	0.25	C26	0.25
H26A	0.25	H26B	0.25	C24	0.25
H24A	0.25	H24B	0.25	C25	0.25
H25A	0.25	H25B	0.25		

7.3.18 [Ni(3FPy(Ph)3FPy)Br]

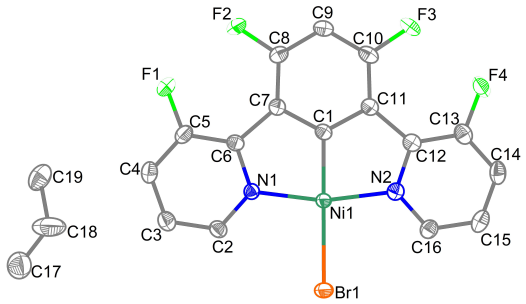

Figure 7-395 Asymmetric unit of [Ni(3FPy(4,6FPh)3FPy)Br] · 0.5 cHex. Ellipsoids are shown with a 50% probability. Hydrogen atoms are omitted for clarity.

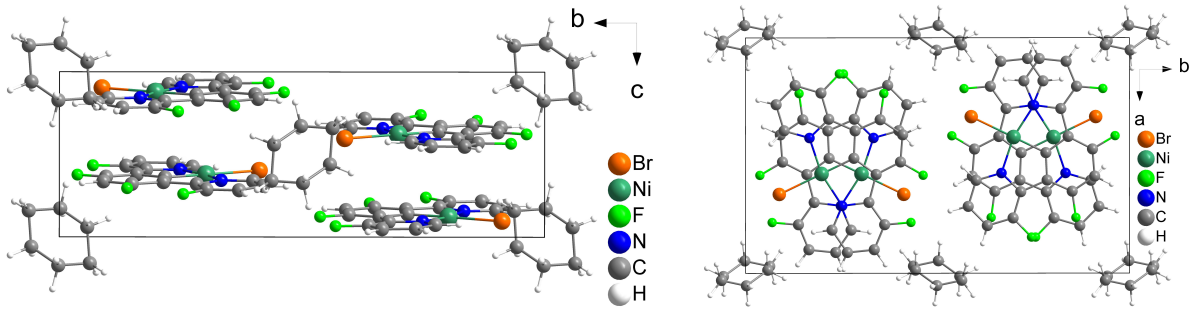

Figure 7-396 Crystal structure of [Ni(3FPy(4,6FPh)3FPy)Br] viewed along the crystallographic *a*- and *c*-axis.

Table 7-122 Crystal data and structure refinement for [Ni(3FPy(4,6FPh)3FPy)Br].

Identification code	[Ni(3FPy(4,6FPh)3FPy)Br] · 0.5 *c*Hex
Empirical formula	$C_{19}H_{13}BrF_4N_2Ni$
Formula weight	483.93
Temperature/K	103.00
Crystal system	monoclinic
Space group	$P2_1/c$
a/Å	12.1264(7)
b/Å	19.5518(11)
c/Å	6.7291(4)
α/°	90
β/°	98.604(2)
γ/°	90
Volume/Å^3	1577.47(16)
Z	4
ρ_{calc}g/cm^3	2.038
μ/mm^{-1}	3.814
F(000)	960.0
Crystal size/mm^3	0.52 × 0.02 × 0.02
Radiation	MoKα (λ = 0.71073)
2Θ range for data collection/°	3.984 to 56.584
Index ranges	–16 ≤ h ≤ 16, –26 ≤ k ≤ 26, –8 ≤ l ≤ 8
Reflections collected	33002
Independent reflections	3916 [R_{int} = 0.0504, R_{sigma} = 0.0286]
Data/restraints/parameters	3916/0/244
Goodness-of-fit on F^2	1.074
Final R indexes [I>=2σ (I)]	R_1 = 0.0356, wR_2 = 0.0891
Final R indexes [all data]	R_1 = 0.0487, wR_2 = 0.0954
Largest diff. peak/hole / e Å^{-3}	0.70/–0.70

Table 7-123 Fractional Atomic Coordinates (×10^4) and Equivalent Isotropic Displacement Parameters (Å^2×10^3) for [Ni(3FPy(4,6FPh)3FPy)Br]. U_{eq} is defined as 1/3 of the trace of the orthogonalized U_{IJ} tensor.

Atom	*x*	*y*	*z*	U(eq)
Br1	3351.1(3)	5879.2(2)	5966.6(5)	23.09(10)
Ni1	4219.8(3)	6979.3(2)	6220.6(6)	16.57(11)
F1	8468.9(18)	7446.6(12)	7398(4)	35.9(5)
N1	5747(2)	6666.4(13)	6571(4)	17.4(5)
C2	6056(3)	6005.3(17)	6606(5)	21.9(7)
F2	7636.6(17)	8603.4(11)	7049(3)	29.3(5)

Atom	*x*	*y*	*z*	U(eq)
N2	2865(2)	7515.9(14)	5933(4)	19.7(5)
C3	7163(3)	5799.4(18)	6903(5)	25.4(7)
F3	4161.7(19)	9625.7(10)	6231(3)	28.8(5)
C4	7979(3)	6295.6(19)	7169(5)	26.0(7)
F4	2158.1(19)	9307.4(11)	5661(3)	30.9(5)
C5	7657(3)	6966.9(18)	7122(5)	23.9(7)
C6	6542(3)	7167.4(16)	6799(5)	19.1(6)
C1	4882(3)	7822.5(16)	6385(5)	17.9(6)
C7	6049(3)	7854.8(16)	6681(5)	18.1(6)
C8	6522(3)	8507.3(17)	6790(5)	21.3(7)
C9	5881(3)	9092.7(17)	6638(5)	22.3(7)
C10	4727(3)	9036.4(16)	6352(5)	22.4(7)
C11	4196(3)	8402.8(16)	6216(5)	19.1(6)
C12	3008(3)	8212.9(17)	5928(5)	19.7(6)
C13	2063(3)	8622.3(18)	5690(5)	24.4(7)
C14	1000(3)	8351(2)	5478(5)	27.1(7)
C15	883(3)	7652(2)	5508(6)	28.2(8)
C16	1833(3)	7251.8(18)	5741(5)	23.0(7)
C17	10302(4)	5629(3)	6594(8)	49.3(12)
C18	10527(5)	4980(3)	6724(12)	76(2)
C19	10131(4)	5576(3)	4402(7)	40.3(10)

Table 7-124 Anisotropic Displacement Parameters ($Å^2×10^3$) for [Ni(3FPy(4,6FPh)3FPy)Br]. The Anisotropic displacement factor exponent takes the form: $–2π^2[h^2a^{*2}U_{11}+2hka^*b^*U_{12}+…]$.

Atom	U_{11}	U_{22}	U_{33}	U_{23}	U_{13}	U_{12}
Br1	23.07(17)	17.85(16)	27.32(19)	0.24(12)	0.39(13)	–3.89(12)
Ni1	16.5(2)	14.81(19)	17.9(2)	–0.13(15)	0.85(15)	–0.82(14)
F1	18.4(10)	32.1(12)	56.0(16)	–3.3(11)	1.5(10)	–4.6(9)
N1	17.0(13)	17.9(12)	16.9(13)	–0.3(10)	1.5(10)	0.3(10)
C2	23.8(17)	18.6(15)	22.5(17)	1.6(12)	0.9(13)	1.3(12)
F2	21.8(10)	28.2(11)	36.7(12)	–0.7(9)	0.5(9)	–8.1(8)
N2	20.1(13)	21.9(13)	16.6(13)	–1.5(10)	1.5(10)	–0.3(10)
C3	26.6(17)	23.4(16)	25.4(18)	0.8(13)	1.8(14)	4.0(14)
F3	37.4(12)	15.3(9)	33.7(12)	1.2(8)	5.7(9)	4.7(8)
C4	20.3(16)	31.6(18)	25.4(18)	–1.3(14)	1.0(13)	5.1(14)
F4	33.2(12)	22.0(10)	35.8(12)	–0.8(9)	–0.5(10)	9.4(9)
C5	17.7(15)	27.7(17)	26.0(18)	–3.1(14)	2.1(13)	–3.1(13)
C6	22.1(16)	17.6(14)	17.5(16)	1.3(12)	2.9(12)	–0.4(12)
C1	21.3(15)	16.7(14)	15.5(15)	0.8(11)	2.1(12)	0.5(12)
C7	19.5(15)	19.2(14)	15.4(15)	0.0(11)	1.6(12)	–0.1(12)
C8	20.8(16)	23.4(16)	19.5(16)	–1.5(13)	2.6(12)	–4.1(13)
C9	27.9(17)	17.9(15)	20.5(16)	–0.1(12)	2.2(13)	–3.3(13)
C10	32.1(18)	16.7(15)	18.2(16)	–0.6(12)	3.4(13)	1.5(13)
C11	22.5(16)	18.9(15)	15.2(15)	–0.4(12)	0.2(12)	0.6(12)
C12	24.2(16)	21.1(15)	13.7(15)	0.0(12)	2.4(12)	0.3(12)
C13	28.4(18)	24.7(16)	19.2(17)	0.7(13)	0.3(13)	5.2(14)
C14	22.5(17)	35.1(19)	22.2(17)	–3.1(14)	–1.8(13)	8.7(14)
C15	18.5(16)	40(2)	25.4(18)	–1.7(15)	1.5(13)	–0.3(15)
C16	21.0(16)	26.5(17)	21.3(17)	–1.5(13)	2.6(13)	–0.8(13)
C17	43(3)	50(3)	54(3)	–8(2)	5(2)	4(2)
C18	71(4)	35(3)	136(6)	–32(3)	64(4)	–22(3)

Atom	U_{11}	U_{22}	U_{33}	U_{23}	U_{13}	U_{12}
C19	29(2)	58(3)	33(2)	7(2)	–0.1(17)	–4.5(19)

Table 7-125 Bond Lengths for [Ni(3FPy(4,6FPh)3FPy)Br].

Atom	Atom	Length/Å	Atom	Atom	Length/Å
Br1	Ni1	2.3898(5)	C6	C7	1.468(4)
Ni1	N1	1.931(3)	C1	C7	1.400(4)
Ni1	N2	1.935(3)	C1	C11	1.401(4)
Ni1	C1	1.830(3)	C7	C8	1.397(4)
F1	C5	1.353(4)	C8	C9	1.379(5)
N1	C2	1.345(4)	C9	C10	1.388(5)
N1	C6	1.367(4)	C10	C11	1.393(5)
C2	C3	1.388(5)	C11	C12	1.472(5)
F2	C8	1.349(4)	C12	C13	1.388(5)
N2	C12	1.374(4)	C13	C14	1.381(5)
N2	C16	1.341(4)	C14	C15	1.375(6)
C3	C4	1.378(5)	C15	C16	1.382(5)
F3	C10	1.337(4)	C17	C18	1.298(7)
C4	C5	1.369(5)	C17	C19	1.462(7)
F4	C13	1.345(4)	C18	C19[1]	1.487(7)
C5	C6	1.392(5)			

[1]2-X,1-Y,1-Z

Table 7-126 Bond Angles for [Ni(3FPy(4,6FPh)3FPy)Br].

Atom	Atom	Atom	Angle/°	Atom	Atom	Atom	Angle/°
N1	Ni1	Br1	97.35(8)	C8	C7	C6	132.3(3)
N1	Ni1	N2	165.63(12)	C8	C7	C1	116.6(3)
N2	Ni1	Br1	97.01(9)	F2	C8	C7	122.0(3)
C1	Ni1	Br1	179.37(10)	F2	C8	C9	115.9(3)
C1	Ni1	N1	82.75(13)	C9	C8	C7	122.1(3)
C1	Ni1	N2	82.89(13)	C8	C9	C10	119.4(3)
C2	N1	Ni1	124.5(2)	F3	C10	C9	115.9(3)
C2	N1	C6	119.8(3)	F3	C10	C11	122.3(3)
C6	N1	Ni1	115.7(2)	C9	C10	C11	121.7(3)
N1	C2	C3	122.8(3)	C1	C11	C12	111.3(3)
C12	N2	Ni1	115.6(2)	C10	C11	C1	116.9(3)
C16	N2	Ni1	124.5(2)	C10	C11	C12	131.8(3)
C16	N2	C12	119.9(3)	N2	C12	C11	111.8(3)
C4	C3	C2	118.4(3)	N2	C12	C13	118.0(3)
C5	C4	C3	118.3(3)	C13	C12	C11	130.2(3)
F1	C5	C4	117.5(3)	F4	C13	C12	120.3(3)
F1	C5	C6	119.7(3)	F4	C13	C14	117.5(3)
C4	C5	C6	122.8(3)	C14	C13	C12	122.2(3)
N1	C6	C5	117.9(3)	C15	C14	C13	118.5(3)
N1	C6	C7	112.0(3)	C14	C15	C16	118.6(3)
C5	C6	C7	130.1(3)	N2	C16	C15	122.9(3)
C7	C1	Ni1	118.3(2)	C18	C17	C19	89.7(5)
C7	C1	C11	123.4(3)	C17	C18	C19[1]	126.1(7)
C11	C1	Ni1	118.3(2)	C17	C19	C18[1]	123.4(5)
C1	C7	C6	111.2(3)				

[1]2-X,1-Y,1-Z

Table 7-127 Torsion Angles for [Ni(3FPy(4,6FPh)3FPy)Br].

A	B	C	D	Angle/°	A	B	C	D	Angle/°
Ni1	N1	C2	C3	–178.6(3)	F4	C13	C14	C15	–179.8(3)
Ni1	N1	C6	C5	177.9(2)	C5	C6	C7	C1	–178.4(3)
Ni1	N1	C6	C7	–1.2(4)	C5	C6	C7	C8	2.2(6)
Ni1	N2	C12	C11	–1.9(3)	C6	N1	C2	C3	1.2(5)
Ni1	N2	C12	C13	178.9(2)	C6	C7	C8	F2	0.1(6)
Ni1	N2	C16	C15	–179.0(3)	C6	C7	C8	C9	180.0(3)
Ni1	C1	C7	C6	0.3(4)	C1	C7	C8	F2	–179.2(3)
Ni1	C1	C7	C8	179.8(2)	C1	C7	C8	C9	0.7(5)
Ni1	C1	C11	C10	179.9(2)	C1	C11	C12	N2	1.1(4)
Ni1	C1	C11	C12	0.1(4)	C1	C11	C12	C13	–179.8(3)
F1	C5	C6	N1	–178.6(3)	C7	C1	C11	C10	0.1(5)
F1	C5	C6	C7	0.5(6)	C7	C1	C11	C12	–179.6(3)
N1	Ni1	C1	C7	–0.8(3)	C7	C8	C9	C10	–0.5(5)
N1	Ni1	C1	C11	179.5(3)	C8	C9	C10	F3	179.6(3)
N1	C2	C3	C4	–0.2(5)	C8	C9	C10	C11	0.1(5)
N1	C6	C7	C1	0.6(4)	C9	C10	C11	C1	0.1(5)
N1	C6	C7	C8	–178.7(3)	C9	C10	C11	C12	179.7(3)
C2	N1	C6	C5	–1.9(5)	C10	C11	C12	N2	–178.5(3)
C2	N1	C6	C7	178.9(3)	C10	C11	C12	C13	0.6(6)
C2	C3	C4	C5	–0.1(5)	C11	C1	C7	C6	–180.0(3)
F2	C8	C9	C10	179.4(3)	C11	C1	C7	C8	–0.5(5)
N2	Ni1	C1	C7	178.8(3)	C11	C12	C13	F4	1.4(6)
N2	Ni1	C1	C11	–0.9(3)	C11	C12	C13	C14	–178.5(3)
N2	C12	C13	F4	–179.6(3)	C12	N2	C16	C15	0.8(5)
N2	C12	C13	C14	0.5(5)	C12	C13	C14	C15	0.1(5)
C3	C4	C5	F1	179.6(3)	C13	C14	C15	C16	–0.2(5)
C3	C4	C5	C6	–0.7(6)	C14	C15	C16	N2	–0.2(5)
F3	C10	C11	C1	–179.4(3)	C16	N2	C12	C11	178.3(3)
F3	C10	C11	C12	0.3(6)	C16	N2	C12	C13	–1.0(5)
C4	C5	C6	N1	1.7(5)	C18	C17	C19	C18[1]	45.4(7)
C4	C5	C6	C7	–179.3(3)	C19	C17	C18	C19[1]	–47.4(7)

[1]2-X,1-Y,1-Z

Table 7-128 Hydrogen Atom Coordinates (Å×10^4) and Isotropic Displacement Parameters (Å^2×10^3) for [Ni(3FPy(4,6FPh)3FPy)Br].

Atom	*x*	*y*	*z*	U(eq)
H2	5491.1	5664.56	6418.2	26
H3	7354.25	5328	6923.78	30
H4	8746.8	6174.71	7378.86	31
H9	6225.57	9530.22	6728.04	27
H14	364.08	8640.83	5315.52	33
H15	164.56	7448.03	5372.08	34
H16	1752.54	6768.69	5766.86	28
H17A	10937.73	5924.52	7141.75	59
H17B	9620.9	5757.36	7154.19	59
H18A	10566.26	4862.01	8163.45	91
H18B	11294.7	4932.45	6407.97	91

Atom	*x*	*y*	*z*	U(eq)
H19A	10882.18	5561.1	3995.39	48
H19B	9786.73	6011.87	3882.76	48

7.3.19 [Ni(3ClPy(Ph)3ClPy)Br]

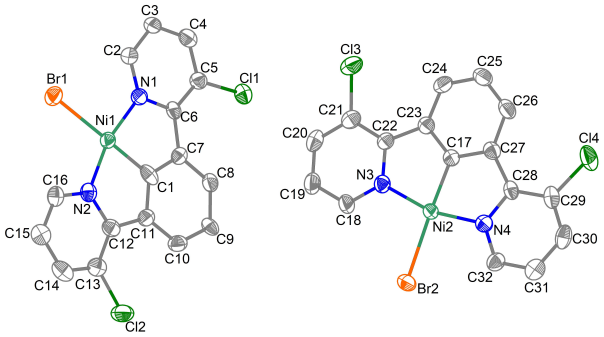

Figure 7-397 Asymmetric unit of [Ni(3ClPy(Ph)3ClPy)Br]. Ellipsoids are shown with a 50% probability. Hydrogen atoms are omitted for clarity.

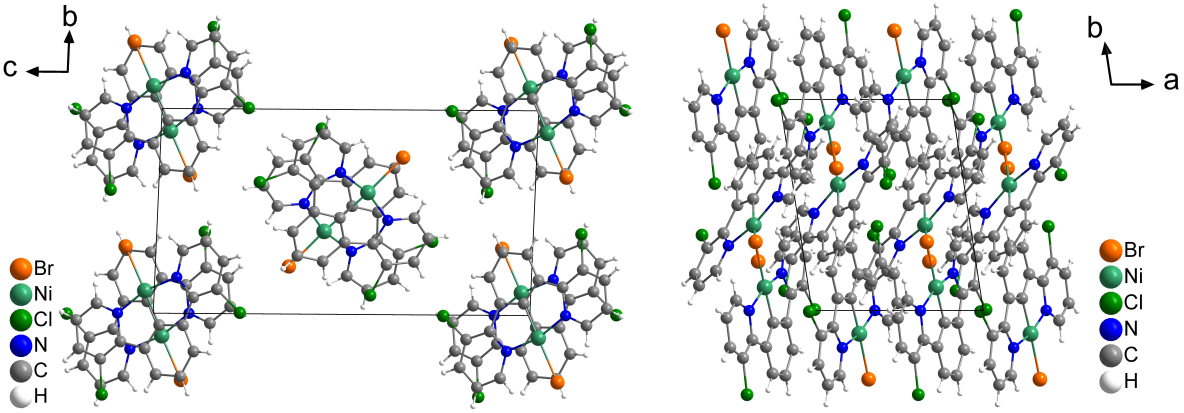

Figure 7-398 Crystal structure of [Ni(3ClPy(Ph)3ClPy)Br] viewed along the crystallographic *a*-axis (left) and *c*-axis (right).

Table 7-129 Crystal data and structure refinement for [Ni(3ClPy(Ph)3ClPy)Br].

Identification code	2[Ni(3ClPy(Ph)3ClPy)Br]
Empirical formula	$C_{16}H_9BrCl_2N_2Ni$
Formula weight	438.77
Temperature/K	293(2)
Crystal system	triclinic
Space group	$P\bar{1}$
a/Å	8.0719(5)
b/Å	9.9861(6)
c/Å	18.2862(11)
α/°	91.040(5)
β/°	97.112(5)
γ/°	98.510(5)
Volume/Å^3	1445.55(15)
Z	4
ρ_{calc}g/cm^3	2.016
μ/mm^{-1}	4.470
F(000)	864.0

Radiation	MoKα (λ = 0.71073)
2Θ range for data collection/°	4.126 to 58.386
Index ranges	–11 ≤ h ≤ 11, –13 ≤ k ≤ 13, –23 ≤ l ≤ 25
Reflections collected	15995
Independent reflections	7450 [R_{int} = 0.0593, R_{sigma} = 0.0759]
Data/restraints/parameters	7450/0/398
Goodness-of-fit on F^2	0.990
Final R indexes [I>=2σ (I)]	R_1 = 0.0442, wR_2 = 0.1013
Final R indexes [all data]	R_1 = 0.0947, wR_2 = 0.1326
Largest diff. peak/hole / e Å^{-3}	1.54/–1.04

Table 7-130 Fractional Atomic Coordinates (×10^4) and Equivalent Isotropic Displacement Parameters (Å^2×10^3) for [Ni(3ClPy(Ph)3ClPy)Br]. U_{eq} is defined as 1/3 of the trace of the orthogonalized U_{IJ} tensor.

Atom	*x*	*y*	*z*	U(eq)
Br1	2688.6(8)	–3254.6(6)	–811.2(3)	37.58(16)
Br2	2706.3(8)	7676.4(6)	3547.7(3)	36.54(15)
Ni1	2553.2(9)	–1098.7(7)	–250.4(3)	26.65(16)
Ni2	2639.0(8)	5954.6(6)	4441.8(3)	25.63(16)
Cl1	–167.7(19)	–47.9(15)	2297.4(7)	37.5(3)
Cl2	4548(2)	3985.2(15)	–1274.6(9)	46.3(4)
Cl3	–1420(2)	937.4(15)	4262.2(9)	46.6(4)
Cl4	5746(2)	6426(2)	7321.7(8)	52.8(4)
N4	4300(6)	6926(4)	5189(2)	29.2(9)
N2	3670(6)	7(5)	–949(2)	29.8(9)
N1	1439(6)	–1762(4)	581(2)	31.0(10)
N3	980(6)	4606(4)	3881(2)	29.9(9)
C9	2136(7)	3074(5)	789(3)	28.9(11)
C7	1601(6)	578(5)	803(3)	27.0(10)
C1	2374(6)	577(6)	173(3)	31.8(12)
C23	1296(7)	3513(5)	5001(3)	28.6(11)
C12	3747(7)	1392(6)	–839(3)	32.0(11)
C17	2432(6)	4712(5)	5157(3)	25.9(10)
C11	3005(7)	1723(5)	–188(3)	29.2(11)
C6	1080(7)	–788(5)	1043(3)	27.6(10)
C28	4471(7)	6337(5)	5858(3)	28.5(11)
C27	3412(7)	5003(6)	5847(3)	31.3(11)
C22	441(7)	3456(5)	4248(3)	27.7(10)
C10	2864(7)	2980(5)	135(3)	34.2(12)
C21	–737(7)	2434(6)	3863(3)	33.9(12)
C4	–107(7)	–2555(6)	1803(3)	34.5(12)
C3	263(8)	–3520(6)	1320(3)	35.4(12)
C2	1037(8)	–3069(6)	717(3)	34.4(12)
C8	1479(7)	1858(6)	1112(3)	31.6(11)
C5	321(7)	–1188(5)	1663(3)	30.8(11)
C16	4341(7)	–468(6)	–1516(3)	33.9(12)
C29	5559(7)	7035(6)	6443(3)	36.8(13)
C25	2135(8)	2849(6)	6240(3)	38.9(13)
C15	5052(8)	350(6)	–2035(3)	39.0(13)
C30	6501(7)	8269(6)	6340(3)	39.1(13)
C32	5247(7)	8120(6)	5093(3)	33.9(12)
C24	1139(8)	2586(5)	5562(3)	34.5(12)

Atom	*x*	*y*	*z*	U(eq)
C26	3248(8)	4031(6)	6389(3)	38.3(13)
C13	4450(7)	2244(6)	–1354(3)	34.4(12)
C20	–1369(8)	2586(6)	3140(3)	39.6(13)
C18	373(8)	4724(6)	3175(3)	36.6(13)
C19	–807(9)	3738(6)	2786(3)	44.4(15)
C31	6366(7)	8809(6)	5652(3)	38.3(13)
C14	5110(8)	1749(7)	–1945(3)	41.0(14)

Table 7-131 Anisotropic Displacement Parameters ($Å^2×10^3$) for [Ni(3ClPy(Ph)3ClPy)Br]. The Anisotropic displacement factor exponent takes the form: $–2π^2[h^2a^{*2}U_{11}+2hka^*b^*U_{12}+…]$.

Atom	U_{11}	U_{22}	U_{33}	U_{23}	U_{13}	U_{12}
Br1	44.7(4)	30.7(3)	37.3(3)	–4.6(2)	2.7(2)	8.2(2)
Br2	41.7(3)	36.2(3)	30.0(3)	8.5(2)	3.2(2)	0.5(2)
Ni1	28.8(4)	25.7(3)	25.0(3)	–0.4(2)	0.0(2)	5.5(3)
Ni2	27.8(4)	26.0(3)	23.0(3)	1.9(2)	2.1(2)	4.9(3)
Cl1	40.6(8)	42.7(7)	30.1(6)	–0.1(5)	5.8(5)	7.9(6)
Cl2	57.3(10)	34.1(7)	49.9(8)	10.0(6)	17.5(7)	4.9(7)
Cl3	49.0(9)	31.8(7)	56.1(9)	0.6(6)	7.4(7)	–3.6(7)
Cl4	52.5(10)	73.2(11)	28.3(7)	–0.4(7)	–6.2(6)	4.7(9)
N4	31(2)	29(2)	30(2)	1.1(17)	6.0(17)	9.9(19)
N2	27(2)	35(2)	28(2)	–1.1(17)	–0.6(17)	7(2)
N1	35(3)	27(2)	28(2)	2.2(17)	–4.7(18)	5.5(19)
N3	30(2)	31(2)	28(2)	–0.9(17)	–1.6(17)	5.9(19)
C9	31(3)	36(3)	23(2)	7(2)	3.9(19)	16(2)
C7	22(3)	27(2)	30(2)	–1.5(19)	–2.6(19)	5(2)
C1	17(3)	55(3)	23(2)	10(2)	–4.6(18)	9(2)
C23	31(3)	29(3)	28(2)	0.1(19)	6(2)	9(2)
C12	30(3)	35(3)	31(3)	5(2)	1(2)	7(2)
C17	25(3)	27(2)	27(2)	1.1(18)	3.7(19)	9(2)
C11	29(3)	27(2)	31(3)	0(2)	–1(2)	5(2)
C6	27(3)	34(3)	21(2)	1.1(19)	–2.9(18)	7(2)
C28	28(3)	36(3)	22(2)	–1.4(19)	–0.4(19)	10(2)
C27	35(3)	33(3)	28(2)	3(2)	4(2)	13(2)
C22	27(3)	26(2)	31(3)	–1.6(19)	6(2)	6(2)
C10	38(3)	27(3)	38(3)	5(2)	3(2)	6(2)
C21	32(3)	30(3)	42(3)	–1(2)	7(2)	9(2)
C4	27(3)	43(3)	30(3)	7(2)	–1(2)	–3(2)
C3	43(3)	31(3)	29(3)	6(2)	–2(2)	–1(2)
C2	43(3)	29(3)	30(3)	2(2)	2(2)	4(2)
C8	34(3)	35(3)	25(2)	–1(2)	0(2)	8(2)
C5	31(3)	31(3)	30(3)	3(2)	1(2)	4(2)
C16	32(3)	39(3)	31(3)	–5(2)	4(2)	6(2)
C29	34(3)	48(3)	28(3)	–7(2)	–1(2)	11(3)
C25	52(4)	37(3)	31(3)	8(2)	11(2)	15(3)
C15	34(3)	45(3)	39(3)	2(2)	5(2)	9(3)
C30	25(3)	49(3)	40(3)	–16(3)	–1(2)	3(3)
C32	31(3)	31(3)	38(3)	–1(2)	–1(2)	3(2)
C24	38(3)	24(2)	41(3)	–1(2)	9(2)	3(2)
C26	49(4)	43(3)	25(3)	4(2)	2(2)	17(3)
C13	28(3)	37(3)	37(3)	4(2)	2(2)	3(2)
C20	36(3)	37(3)	42(3)	–12(2)	–4(2)	4(3)

Atom	U_{11}	U_{22}	U_{33}	U_{23}	U_{13}	U_{12}
C18	46(4)	37(3)	25(3)	0(2)	–4(2)	10(3)
C19	54(4)	42(3)	33(3)	–7(2)	–8(3)	8(3)
C31	29(3)	40(3)	47(3)	–4(3)	6(2)	7(3)
C14	31(3)	57(4)	36(3)	13(3)	6(2)	9(3)

Table 7-132 Bond Lengths for [Ni(3ClPy(Ph)3ClPy)Br].

Atom	Atom	Length/Å	Atom	Atom	Length/Å
Br1	Ni1	2.3908(8)	C23	C17	1.398(8)
Br2	Ni2	2.3935(8)	C23	C22	1.457(7)
Ni1	N2	1.925(5)	C23	C24	1.400(7)
Ni1	N1	1.939(5)	C12	C11	1.451(7)
Ni1	C1	1.863(6)	C12	C13	1.396(8)
Ni2	N4	1.929(5)	C17	C27	1.405(7)
Ni2	N3	1.932(5)	C11	C10	1.403(7)
Ni2	C17	1.824(5)	C6	C5	1.391(7)
Cl1	C5	1.730(5)	C28	C27	1.471(8)
Cl2	C13	1.732(6)	C28	C29	1.401(8)
Cl3	C21	1.722(6)	C27	C26	1.404(8)
Cl4	C29	1.726(6)	C22	C21	1.401(8)
N4	C28	1.367(6)	C21	C20	1.377(8)
N4	C32	1.345(7)	C4	C3	1.384(8)
N2	C12	1.386(7)	C4	C5	1.394(8)
N2	C16	1.338(7)	C3	C2	1.384(8)
N1	C6	1.363(7)	C16	C15	1.386(8)
N1	C2	1.333(7)	C29	C30	1.378(9)
N3	C22	1.382(7)	C25	C24	1.389(8)
N3	C18	1.338(7)	C25	C26	1.375(9)
C9	C10	1.405(7)	C15	C14	1.397(9)
C9	C8	1.420(8)	C30	C31	1.375(9)
C7	C1	1.377(7)	C32	C31	1.378(8)
C7	C6	1.459(7)	C13	C14	1.379(8)
C7	C8	1.410(7)	C20	C19	1.375(9)
C1	C11	1.394(8)	C18	C19	1.383(9)

Table 7-133 Bond Angles for [Ni(3ClPy(Ph)3ClPy)Br].

Atom	Atom	Atom	Angle/°	Atom	Atom	Atom	Angle/°
N2	Ni1	Br1	97.45(13)	C10	C11	C12	130.9(5)
N2	Ni1	N1	165.15(18)	N1	C6	C7	112.4(4)
N1	Ni1	Br1	97.37(13)	N1	C6	C5	118.7(5)
C1	Ni1	Br1	178.10(15)	C5	C6	C7	128.9(5)
C1	Ni1	N2	82.9(2)	N4	C28	C27	112.0(4)
C1	Ni1	N1	82.3(2)	N4	C28	C29	118.9(5)
N4	Ni2	Br2	97.39(13)	C29	C28	C27	129.1(5)
N4	Ni2	N3	164.72(18)	C17	C27	C28	110.7(4)
N3	Ni2	Br2	97.88(13)	C26	C27	C17	117.9(5)
C17	Ni2	Br2	174.66(15)	C26	C27	C28	131.4(5)
C17	Ni2	N4	82.7(2)	N3	C22	C23	111.0(5)
C17	Ni2	N3	82.2(2)	N3	C22	C21	118.5(5)
C28	N4	Ni2	115.8(4)	C21	C22	C23	130.4(5)

Atom	Atom	Atom	Angle/°	Atom	Atom	Atom	Angle/°
C32	N4	Ni2	124.5(4)	C11	C10	C9	121.7(5)
C32	N4	C28	119.7(5)	C22	C21	Cl3	121.9(4)
C12	N2	Ni1	115.5(3)	C20	C21	Cl3	117.5(5)
C16	N2	Ni1	124.9(4)	C20	C21	C22	120.7(5)
C16	N2	C12	119.6(5)	C3	C4	C5	118.9(5)
C6	N1	Ni1	115.4(3)	C2	C3	C4	117.8(5)
C2	N1	Ni1	124.3(4)	N1	C2	C3	123.4(5)
C2	N1	C6	120.2(5)	C7	C8	C9	121.4(5)
C22	N3	Ni2	116.2(3)	C6	C5	Cl1	123.0(4)
C18	N3	Ni2	123.9(4)	C6	C5	C4	121.0(5)
C18	N3	C22	119.9(5)	C4	C5	Cl1	116.0(4)
C10	C9	C8	118.5(5)	N2	C16	C15	123.6(5)
C1	C7	C6	112.4(5)	C28	C29	Cl4	122.2(5)
C1	C7	C8	116.3(5)	C30	C29	Cl4	117.1(4)
C8	C7	C6	131.3(5)	C30	C29	C28	120.7(5)
C7	C1	Ni1	117.5(4)	C26	C25	C24	121.6(5)
C7	C1	C11	125.7(5)	C16	C15	C14	117.9(5)
C11	C1	Ni1	116.8(4)	C31	C30	C29	119.2(5)
C17	C23	C22	111.7(5)	N4	C32	C31	122.5(5)
C17	C23	C24	117.8(5)	C25	C24	C23	120.2(6)
C24	C23	C22	130.5(5)	C25	C26	C27	120.0(5)
N2	C12	C11	112.0(5)	C12	C13	Cl2	121.4(4)
N2	C12	C13	118.2(5)	C14	C13	Cl2	116.6(5)
C13	C12	C11	129.8(5)	C14	C13	C12	122.1(5)
C23	C17	Ni2	118.9(4)	C19	C20	C21	119.7(6)
C23	C17	C27	122.5(5)	N3	C18	C19	122.6(6)
C27	C17	Ni2	118.7(4)	C20	C19	C18	118.6(6)
C1	C11	C12	112.7(5)	C30	C31	C32	118.9(6)
C1	C11	C10	116.4(5)	C13	C14	C15	118.7(6)

Table 7-134 Torsion Angles for [Ni(3ClPy(Ph)3ClPy)Br].

A	B	C	D	Angle/°	A	B	C	D	Angle/°
Ni1	N2	C12	C11	2.2(6)	C12	N2	C16	C15	–3.4(8)
Ni1	N2	C12	C13	–176.2(4)	C12	C11	C10	C9	–177.9(5)
Ni1	N2	C16	C15	176.1(4)	C12	C13	C14	C15	0.8(9)
Ni1	N1	C6	C7	0.9(5)	C17	C23	C22	N3	0.1(6)
Ni1	N1	C6	C5	–178.3(4)	C17	C23	C22	C21	177.8(5)
Ni1	N1	C2	C3	179.0(4)	C17	C23	C24	C25	–2.2(7)
Ni1	C1	C11	C12	–1.4(6)	C17	C27	C26	C25	–1.0(8)
Ni1	C1	C11	C10	180.0(4)	C11	C12	C13	Cl2	0.2(9)
Ni2	N4	C28	C27	4.3(5)	C11	C12	C13	C14	179.8(5)
Ni2	N4	C28	C29	–175.1(4)	C6	N1	C2	C3	–0.4(9)
Ni2	N4	C32	C31	177.0(4)	C6	C7	C1	Ni1	1.4(6)
Ni2	N3	C22	C23	–0.8(5)	C6	C7	C1	C11	180.0(5)
Ni2	N3	C22	C21	–178.8(4)	C6	C7	C8	C9	177.8(5)
Ni2	N3	C18	C19	179.6(4)	C28	N4	C32	C31	–2.0(8)
Ni2	C17	C27	C28	0.3(6)	C28	C27	C26	C25	179.3(5)
Ni2	C17	C27	C26	–179.5(4)	C28	C29	C30	C31	–0.2(8)
Cl2	C13	C14	C15	–179.7(5)	C27	C28	C29	Cl4	–3.9(8)
Cl3	C21	C20	C19	–177.2(5)	C27	C28	C29	C30	177.8(5)

A	B	C	D	Angle/°	A	B	C	D	Angle/°
Cl4	C29	C30	C31	–178.6(4)	C22	N3	C18	C19	0.7(8)
N4	Ni2	C17	C23	–178.9(4)	C22	C23	C17	Ni2	0.7(6)
N4	Ni2	C17	C27	1.6(4)	C22	C23	C17	C27	–179.8(4)
N4	C28	C27	C17	–2.9(6)	C22	C23	C24	C25	178.2(5)
N4	C28	C27	C26	176.8(5)	C22	C21	C20	C19	1.6(9)
N4	C28	C29	Cl4	175.4(4)	C10	C9	C8	C7	2.3(8)
N4	C28	C29	C30	–2.9(8)	C21	C20	C19	C18	–0.8(9)
N4	C32	C31	C30	–1.2(8)	C4	C3	C2	N1	0.0(9)
N2	Ni1	C1	C7	–179.3(4)	C3	C4	C5	Cl1	–179.5(4)
N2	Ni1	C1	C11	2.0(4)	C3	C4	C5	C6	1.1(8)
N2	C12	C11	C1	–0.6(7)	C2	N1	C6	C7	–179.6(5)
N2	C12	C11	C10	177.8(5)	C2	N1	C6	C5	1.2(7)
N2	C12	C13	Cl2	178.3(4)	C8	C9	C10	C11	–2.2(8)
N2	C12	C13	C14	–2.2(8)	C8	C7	C1	Ni1	–179.9(4)
N2	C16	C15	C14	1.9(9)	C8	C7	C1	C11	–1.3(8)
N1	Ni1	C1	C7	–0.8(4)	C8	C7	C6	N1	–179.8(5)
N1	Ni1	C1	C11	–179.5(4)	C8	C7	C6	C5	–0.8(9)
N1	C6	C5	Cl1	179.1(4)	C5	C4	C3	C2	–0.3(8)
N1	C6	C5	C4	–1.6(8)	C16	N2	C12	C11	–178.2(5)
N3	Ni2	C17	C23	–0.9(4)	C16	N2	C12	C13	3.4(8)
N3	Ni2	C17	C27	179.6(4)	C16	C15	C14	C13	–0.6(9)
N3	C22	C21	Cl3	177.4(4)	C29	C28	C27	C17	176.4(5)
N3	C22	C21	C20	–1.3(8)	C29	C28	C27	C26	–3.9(9)
N3	C18	C19	C20	–0.4(9)	C29	C30	C31	C32	2.2(8)
C7	C1	C11	C12	–180.0(5)	C32	N4	C28	C27	–176.6(4)
C7	C1	C11	C10	1.4(8)	C32	N4	C28	C29	3.9(7)
C7	C6	C5	Cl1	0.1(8)	C24	C23	C17	Ni2	–178.9(4)
C7	C6	C5	C4	179.4(5)	C24	C23	C17	C27	0.5(7)
C1	C7	C6	N1	–1.4(6)	C24	C23	C22	N3	179.7(5)
C1	C7	C6	C5	177.6(5)	C24	C23	C22	C21	–2.6(9)
C1	C7	C8	C9	–0.6(8)	C24	C25	C26	C27	–0.7(8)
C1	C11	C10	C9	0.4(8)	C26	C25	C24	C23	2.4(8)
C23	C17	C27	C28	–179.2(4)	C13	C12	C11	C1	177.6(6)
C23	C17	C27	C26	1.1(7)	C13	C12	C11	C10	–4.1(10)
C23	C22	C21	Cl3	–0.1(8)	C18	N3	C22	C23	178.1(5)
C23	C22	C21	C20	–178.9(5)	C18	N3	C22	C21	0.1(7)

Table 7-135 Hydrogen Atom Coordinates (Å×10^4) and Isotropic Displacement Parameters (Å^2×10^3) for [Ni(3ClPy(Ph)3ClPy)Br].

Atom	*x*	*y*	*z*	U(eq)
H9	2084.61	3914.4	1006.03	35
H10	3262.86	3770	–90.35	41
H4	–631.73	–2814.7	2214.15	41
H3	–0.22	–4440.31	1398.72	43
H2	1290.61	–3710.47	390.38	41
H8	957.22	1907.65	1535.29	38
H16	4330.89	–1398.31	–1564.38	41
H25	2047.12	2208.56	6601.73	47
H15	5475.71	–20.93	–2429.86	47
H30	7219.45	8731.45	6729.95	47
H32	5142.64	8495.49	4630.5	41

Atom	x	y	z	U(eq)
H24	365.98	1793.12	5481.88	41
H26	3892.67	4187.97	6848.35	46
H20	–2172.44	1913.62	2891.67	48
H18	759.18	5501.05	2935.55	44
H19	–1212.35	3850.61	2296.11	53
H31	7019.14	9625.62	5566.51	46
H14	5584.56	2335.5	–2278.59	49

7.3.20 [Ni(Py(Ph)Py)Carb]

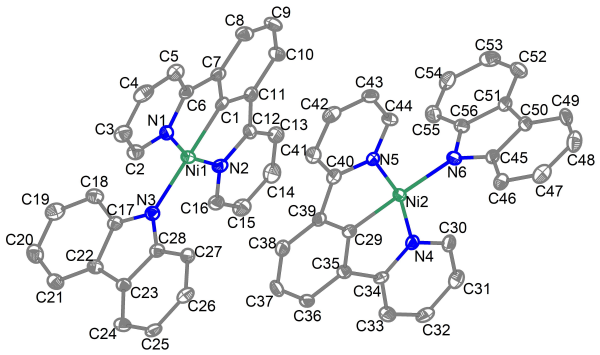

Figure 7-399 Asymmetric unit of [Ni(Py(Ph)Py)Carb]. Ellipsoids are shown with a 50% probability. Hydrogen atoms are omitted for clarity.

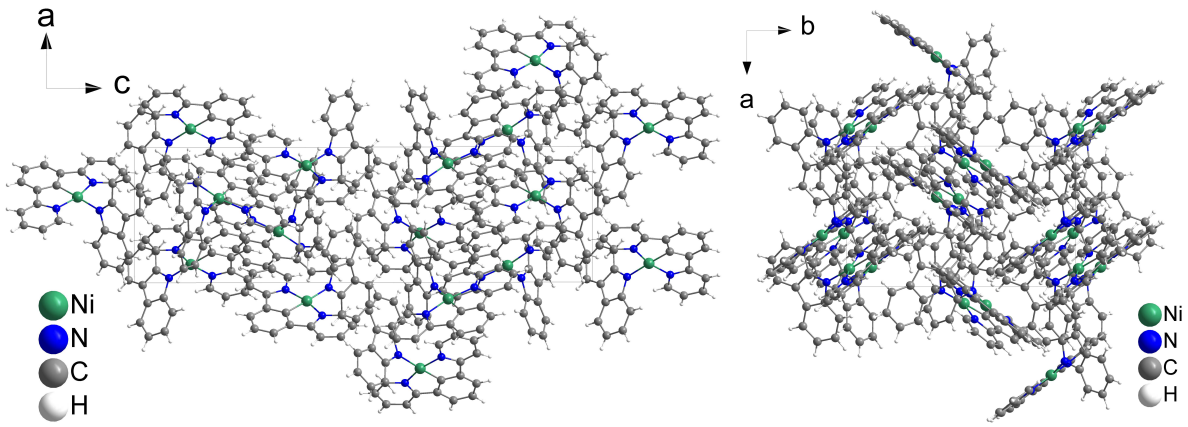

Figure 7-400 Crystal structure of [Ni(Py(Ph)Py)Carb] viewed along the crystallographic *b*- (left) and *c*-axis (right).

Table 7-136 Crystal data and structure refinement for [Ni(Py(Ph)Py)Carb].

Identification code	[Ni(Py(Ph)Py)Carb]
Empirical formula	$C_{56}H_{38}N_6Ni_2$
Formula weight	912.34
Temperature/K	100.0
Crystal system	orthorhombic
Space group	$P2_12_12_1$
a/Å	9.0665(3)
b/Å	14.8314(5)
c/Å	30.7378(11)
α/°	90
β/°	90
γ/°	90

Volume/Å^3	4133.3(2)
Z	4
ρ_{calc}g/cm^3	1.466
μ/mm^{-1}	0.961
F(000)	1888.0
Crystal size/mm^3	0.3 × 0.3 × 0.3
Radiation	MoKα (λ = 0.71073)
2Θ range for data collection/°	3.816 to 54.206
Index ranges	–11 ≤ h ≤ 10, –19 ≤ k ≤ 19, –35 ≤ l ≤ 39
Reflections collected	33940
Independent reflections	8961 [R_{int} = 0.0775, R_{sigma} = 0.0756]
Data/restraints/parameters	8961/0/577
Goodness-of-fit on F^2	1.031
Final R indexes [I>=2σ (I)]	R_1 = 0.0419, wR_2 = 0.0769
Final R indexes [all data]	R_1 = 0.0608, wR_2 = 0.0862
Largest diff. peak/hole / e Å^{-3}	0.40/–0.34
Flack parameter	0.015(9)

Table 7-137 Fractional Atomic Coordinates (×10^4) and Equivalent Isotropic Displacement Parameters (Å^2×10^3) for [Ni(Py(Ph)Py)Carb]. U_{eq} is defined as 1/3 of the trace of the orthogonalized U_{IJ} tensor.

Atom	*x*	*y*	*z*	U(eq)
Ni2	3640.1(7)	3922.9(3)	6236.1(2)	13.60(13)
Ni1	1231.3(7)	5119.9(3)	8150.9(2)	13.72(13)
N5	4486(4)	4631(2)	6700.1(12)	13.9(8)
N3	299(4)	4118(2)	8449.9(13)	15.9(9)
N1	2355(4)	5574(2)	8638.4(12)	15.2(8)
N2	377(4)	4940(2)	7578.8(12)	16.2(8)
N6	4636(4)	4512(2)	5756.4(13)	16.3(8)
N4	2570(4)	3028(2)	5902.7(12)	15.8(9)
C17	–1161(5)	4054(3)	8569.2(14)	15.4(9)
C35	1886(5)	2591(3)	6609.0(15)	15.5(10)
C39	3109(5)	3599(3)	7114.5(15)	15.2(10)
C28	971(5)	3348(3)	8611.1(14)	15.1(10)
C29	2775(5)	3333(3)	6692.8(15)	15.1(10)
C12	803(5)	5546(3)	7266.7(15)	15.5(10)
C50	6492(5)	4982(3)	5287.3(14)	16.6(10)
C34	1766(5)	2423(3)	6143.6(15)	14.8(10)
C44	5394(5)	5336(3)	6649.8(16)	18.1(10)
C45	6102(5)	4408(3)	5640.5(14)	16.1(10)
C23	–61(5)	2778(3)	8823.9(15)	14.6(10)
C53	3377(6)	6466(3)	4869.9(17)	25.9(12)
C27	2468(6)	3123(3)	8606.5(15)	17.6(10)
C24	418(6)	1974(3)	9014.5(16)	18.2(11)
C11	1826(5)	6221(3)	7436.2(15)	16.4(10)
C7	3107(5)	6601(3)	8102.0(16)	15.6(10)
C25	1891(5)	1744(3)	8999.0(16)	19.2(11)
C26	2909(5)	2328(3)	8800.2(16)	19.2(10)
C6	3264(5)	6295(3)	8551.3(16)	16.2(10)
C30	2585(6)	2951(3)	5468.6(16)	20.2(11)
C43	6016(5)	5790(3)	6995.4(15)	20.1(11)
C54	2304(6)	6158(3)	5161.1(16)	24.2(11)

Atom	*x*	*y*	*z*	U(eq)
C56	4071(5)	5160(3)	5480.3(14)	17.8(10)
C22	–1448(5)	3247(3)	8808.3(15)	16.8(9)
C3	3233(6)	5579(3)	9372.5(16)	22.8(11)
C36	1282(6)	2112(3)	6960.3(14)	17.4(10)
C40	4134(5)	4363(3)	7114.1(15)	15.6(10)
C51	5153(6)	5468(3)	5181.0(15)	18.2(10)
C42	5700(5)	5504(3)	7413.5(17)	20.9(11)
C52	4791(6)	6130(3)	4876.7(16)	25.4(11)
C49	7923(5)	4981(3)	5124.8(16)	21.9(11)
C21	–2837(5)	3088(3)	8981.4(16)	19.5(11)
C2	2346(5)	5242(3)	9042.0(16)	20.2(10)
C55	2650(6)	5508(3)	5468.1(16)	21.9(11)
C18	–2301(5)	4674(3)	8499.5(16)	20.6(11)
C38	2516(5)	3119(3)	7464.5(16)	19.7(11)
C1	2127(5)	6069(3)	7871.3(15)	15.2(10)
C31	1808(6)	2274(3)	5250.9(17)	22.3(11)
C37	1604(5)	2385(3)	7379.2(16)	20.1(11)
C47	8581(6)	3868(3)	5661.2(16)	24.6(11)
C20	–3939(6)	3722(3)	8920.2(16)	24.6(11)
C46	7167(5)	3850(3)	5829.4(15)	18.4(10)
C19	–3677(6)	4503(3)	8675.8(15)	24.3(11)
C41	4747(5)	4784(3)	7474.0(15)	18.4(10)
C10	2509(6)	6938(3)	7222.5(17)	20.6(11)
C8	3805(6)	7319(3)	7887.4(16)	21.3(10)
C5	4184(5)	6650(3)	8868.1(16)	20.0(11)
C13	321(6)	5464(3)	6842.8(17)	22.1(11)
C14	–618(6)	4766(3)	6729.4(16)	24.7(11)
C16	–529(5)	4269(3)	7468.1(16)	19.6(11)
C32	1004(6)	1664(3)	5492.9(16)	22.4(11)
C4	4156(6)	6287(3)	9280.5(17)	26.1(12)
C15	–1039(6)	4159(3)	7046.8(16)	23.4(11)
C33	982(5)	1740(3)	5941.1(16)	21.4(11)
C9	3490(6)	7478(3)	7452.9(17)	24.5(12)
C48	8958(6)	4433(3)	5309.0(16)	27.5(12)

Table 7-138 Anisotropic Displacement Parameters ($Å^2 \times 10^3$) for [Ni(Py(Ph)Py)Carb]. The Anisotropic displacement factor exponent takes the form: $-2\pi^2[h^2a^{*2}U_{11}+2hka^*b^*U_{12}+\ldots]$.

Atom	U_{11}	U_{22}	U_{33}	U_{23}	U_{13}	U_{12}
Ni2	14.7(3)	12.8(3)	13.2(3)	0.7(2)	0.9(3)	–1.5(2)
Ni1	13.8(3)	12.1(3)	15.2(3)	1.5(2)	–1.3(3)	–0.6(2)
N5	15(2)	12.6(19)	14(2)	–1.1(15)	1.1(16)	1.2(15)
N3	18(2)	15(2)	15(2)	0.5(16)	–0.4(17)	0.4(17)
N1	15(2)	15.2(19)	16(2)	1.5(16)	1.1(16)	2.1(16)
N2	14.8(19)	12.5(18)	21(2)	–0.5(17)	–1.1(16)	2.1(16)
N6	16(2)	14.4(18)	18(2)	1.9(16)	0.9(17)	–0.8(16)
N4	16(2)	15.2(19)	16(2)	–0.3(16)	1.7(17)	3.3(16)
C17	20(2)	15(2)	12(2)	–3.6(17)	–3(2)	–3(2)
C35	15(2)	13(2)	18(3)	3.4(18)	1(2)	3.0(18)
C39	16(2)	13(2)	17(3)	1.0(18)	1.6(19)	5.9(18)
C28	20(3)	14(2)	11(2)	–2.6(17)	–3.2(19)	–1.8(19)
C29	16(2)	12(2)	18(3)	0.7(18)	1.5(19)	3.3(19)

Atom	U_{11}	U_{22}	U_{33}	U_{23}	U_{13}	U_{12}
C12	14(2)	16(2)	17(3)	4.5(19)	3.1(19)	4.1(18)
C50	22(2)	17(2)	11(2)	–5.3(18)	2.1(19)	–7(2)
C34	16(2)	10(2)	18(3)	–3.0(18)	–0.9(19)	0.8(17)
C44	20(2)	13(2)	21(3)	0.4(19)	1(2)	–4.1(19)
C45	17(2)	15(2)	17(2)	–4.5(18)	3(2)	–3(2)
C23	16(2)	13(2)	15(3)	–2.4(19)	–2(2)	–2.9(18)
C53	39(4)	17(2)	22(3)	4(2)	–7(2)	3(2)
C27	22(3)	17(2)	13(2)	–1.1(19)	1(2)	–1(2)
C24	26(3)	15(2)	14(3)	1.7(19)	–4(2)	–4(2)
C11	18(2)	16(2)	16(3)	–0.4(19)	2.0(19)	3.2(19)
C7	15(2)	12(2)	20(3)	–1.1(19)	0(2)	2.8(18)
C25	26(3)	11(2)	20(3)	–2.1(19)	–1(2)	4(2)
C26	22(3)	17(2)	19(3)	–4(2)	–5(2)	5.7(19)
C6	12(2)	13(2)	24(3)	–3.6(19)	2.7(19)	1.5(17)
C30	19(3)	22(2)	20(3)	–4(2)	5(2)	1(2)
C43	20(3)	13(2)	26(3)	–1.1(19)	1(2)	–2.3(19)
C54	30(3)	24(3)	18(3)	–2(2)	0(2)	9(2)
C56	27(3)	15(2)	11(2)	–0.2(18)	–0.5(19)	–4(2)
C22	15(2)	16(2)	19(2)	–1.4(19)	–2(2)	–4(2)
C3	31(3)	21(3)	17(3)	–2(2)	–4(2)	2(2)
C36	17(2)	12(2)	22(3)	1.6(17)	3(2)	1(2)
C40	17(2)	17(2)	14(2)	–1.0(18)	–2.4(19)	3.8(19)
C51	23(3)	16(2)	16(3)	–4.7(19)	4(2)	–2(2)
C42	19(2)	19(2)	25(3)	–6(2)	–6(2)	3(2)
C52	36(3)	21(3)	18(3)	1(2)	4(2)	–9(2)
C49	20(2)	25(3)	21(3)	–6(2)	9(2)	–10(2)
C21	17(2)	20(2)	22(3)	0(2)	–1(2)	–5(2)
C2	22(2)	17(2)	21(3)	1(2)	–1(2)	1(2)
C55	22(3)	24(3)	20(3)	0(2)	2(2)	–1(2)
C18	21(3)	17(2)	23(3)	3(2)	–2(2)	0(2)
C38	19(3)	20(2)	20(3)	–1(2)	3(2)	3(2)
C1	15(2)	11(2)	20(3)	–0.6(19)	3.8(19)	7.2(19)
C31	24(3)	26(3)	17(3)	–5(2)	–1(2)	4(2)
C37	19(3)	21(2)	20(3)	7(2)	7(2)	1(2)
C47	18(2)	27(2)	28(3)	–9(2)	–6(2)	3(2)
C20	17(3)	30(3)	27(3)	–2(2)	2(2)	–6(2)
C46	21(2)	21(2)	14(2)	–5(2)	–1.3(19)	0(2)
C19	20(2)	22(2)	30(3)	–1(2)	–6(3)	4(2)
C41	20(2)	20(2)	15(2)	3(2)	–2(2)	6(2)
C10	26(3)	15(2)	21(3)	7(2)	3(2)	3(2)
C8	16(2)	16(2)	32(3)	–2(2)	0(2)	–4(2)
C5	16(2)	21(2)	23(3)	–4(2)	–3(2)	–0.4(19)
C13	26(3)	20(2)	19(3)	2(2)	2(2)	3(2)
C14	27(3)	32(3)	15(3)	–3(2)	–5(2)	1(2)
C16	17(2)	16(2)	25(3)	0(2)	2(2)	2(2)
C32	24(3)	16(2)	27(3)	–8(2)	–3(2)	0(2)
C4	31(3)	22(3)	26(3)	–10(2)	–7(2)	2(2)
C15	21(3)	23(2)	26(3)	–7(2)	–4(2)	–4(2)
C33	19(3)	19(2)	26(3)	0(2)	2(2)	–4(2)
C9	27(3)	16(2)	31(3)	7(2)	6(2)	–3(2)
C48	19(3)	38(3)	26(3)	–13(2)	5(2)	–6(2)

Table 7-139 Bond Lengths for [Ni(Py(Ph)Py)Carb].

Atom	Atom	Length/Å	Atom	Atom	Length/Å
Ni2	N5	1.930(4)	C23	C22	1.438(6)
Ni2	N6	1.937(4)	C53	C54	1.398(7)
Ni2	N4	1.938(4)	C53	C52	1.376(7)
Ni2	C29	1.830(5)	C27	C26	1.381(6)
Ni1	N3	1.941(4)	C24	C25	1.380(7)
Ni1	N1	1.933(4)	C11	C1	1.383(6)
Ni1	N2	1.940(4)	C11	C10	1.395(6)
Ni1	C1	1.838(5)	C7	C6	1.460(7)
N5	C44	1.340(6)	C7	C1	1.384(6)
N5	C40	1.371(6)	C7	C8	1.404(6)
N3	C17	1.377(6)	C25	C26	1.406(7)
N3	C28	1.386(6)	C6	C5	1.386(6)
N1	C6	1.377(6)	C30	C31	1.397(7)
N1	C2	1.335(6)	C43	C42	1.384(7)
N2	C12	1.371(6)	C54	C55	1.385(7)
N2	C16	1.335(6)	C56	C51	1.420(6)
N6	C45	1.385(6)	C56	C55	1.388(7)
N6	C56	1.381(6)	C22	C21	1.387(6)
N4	C34	1.372(6)	C3	C2	1.389(7)
N4	C30	1.339(6)	C3	C4	1.372(7)
C17	C22	1.429(6)	C36	C37	1.381(6)
C17	C18	1.400(6)	C40	C41	1.387(6)
C35	C29	1.389(6)	C51	C52	1.395(7)
C35	C34	1.456(7)	C42	C41	1.386(7)
C35	C36	1.404(6)	C49	C48	1.365(7)
C39	C29	1.388(6)	C21	C20	1.385(7)
C39	C40	1.465(6)	C18	C19	1.383(7)
C39	C38	1.397(6)	C38	C37	1.392(7)
C28	C23	1.421(6)	C31	C32	1.379(7)
C28	C27	1.397(7)	C47	C46	1.382(7)
C12	C11	1.460(6)	C47	C48	1.411(7)
C12	C13	1.380(7)	C20	C19	1.402(7)
C50	C45	1.424(6)	C10	C9	1.391(7)
C50	C51	1.449(7)	C8	C9	1.386(7)
C50	C49	1.390(6)	C5	C4	1.377(7)
C34	C33	1.386(6)	C13	C14	1.385(7)
C44	C43	1.378(6)	C14	C15	1.381(7)
C45	C46	1.398(7)	C16	C15	1.385(7)
C23	C24	1.398(6)	C32	C33	1.383(7)

Table 7-140 Bond Angles for [Ni(Py(Ph)Py)Carb].

Atom	Atom	Atom	Angle/˚	Atom	Atom	Atom	Angle/˚
N5	Ni2	N6	97.57(16)	C52	C53	C54	121.3(5)
N5	Ni2	N4	164.31(16)	C26	C27	C28	118.7(5)
N6	Ni2	N4	98.03(16)	C25	C24	C23	119.9(5)
C29	Ni2	N5	82.15(18)	C1	C11	C12	111.0(4)
C29	Ni2	N6	177.35(19)	C1	C11	C10	119.5(4)

Atom	Atom	Atom	Angle/°	Atom	Atom	Atom	Angle/°
C29	Ni2	N4	82.18(19)	C10	C11	C12	129.5(4)
N1	Ni1	N3	97.41(16)	C1	C7	C6	111.8(4)
N1	Ni1	N2	163.95(16)	C1	C7	C8	118.8(4)
N2	Ni1	N3	98.63(16)	C8	C7	C6	129.5(4)
C1	Ni1	N3	179.5(2)	C24	C25	C26	119.9(5)
C1	Ni1	N1	82.13(19)	C27	C26	C25	121.6(5)
C1	Ni1	N2	81.83(18)	N1	C6	C7	111.5(4)
C44	N5	Ni2	125.7(3)	N1	C6	C5	121.2(4)
C44	N5	C40	118.5(4)	C5	C6	C7	127.3(4)
C40	N5	Ni2	115.8(3)	N4	C30	C31	122.2(5)
C17	N3	Ni1	126.7(3)	C44	C43	C42	118.8(4)
C17	N3	C28	105.7(4)	C55	C54	C53	120.4(5)
C28	N3	Ni1	127.5(3)	N6	C56	C51	111.5(4)
C6	N1	Ni1	115.8(3)	N6	C56	C55	128.3(4)
C2	N1	Ni1	126.1(3)	C55	C56	C51	120.3(4)
C2	N1	C6	118.1(4)	C17	C22	C23	105.3(4)
C12	N2	Ni1	115.6(3)	C21	C22	C17	120.3(4)
C16	N2	Ni1	125.4(3)	C21	C22	C23	134.3(4)
C16	N2	C12	119.0(4)	C4	C3	C2	118.6(5)
C45	N6	Ni2	126.3(3)	C37	C36	C35	119.1(4)
C56	N6	Ni2	127.5(3)	N5	C40	C39	111.9(4)
C56	N6	C45	106.0(4)	N5	C40	C41	121.1(4)
C34	N4	Ni2	115.3(3)	C41	C40	C39	127.0(4)
C30	N4	Ni2	125.5(3)	C56	C51	C50	105.8(4)
C30	N4	C34	119.2(4)	C52	C51	C50	134.3(5)
N3	C17	C22	111.7(4)	C52	C51	C56	119.9(5)
N3	C17	C18	128.6(4)	C43	C42	C41	119.3(4)
C18	C17	C22	119.7(4)	C53	C52	C51	119.0(5)
C29	C35	C34	111.1(4)	C48	C49	C50	119.6(5)
C29	C35	C36	119.0(4)	C20	C21	C22	119.2(4)
C36	C35	C34	129.8(4)	N1	C2	C3	122.9(4)
C29	C39	C40	110.9(4)	C54	C55	C56	119.2(5)
C29	C39	C38	119.4(4)	C19	C18	C17	119.0(4)
C38	C39	C40	129.7(4)	C37	C38	C39	118.8(5)
N3	C28	C23	111.4(4)	C11	C1	Ni1	119.3(4)
N3	C28	C27	128.3(4)	C11	C1	C7	122.0(4)
C27	C28	C23	120.2(4)	C7	C1	Ni1	118.7(3)
C35	C29	Ni2	119.0(4)	C32	C31	C30	118.6(5)
C39	C29	Ni2	119.2(3)	C36	C37	C38	122.0(4)
C39	C29	C35	121.6(4)	C46	C47	C48	121.6(5)
N2	C12	C11	112.3(4)	C21	C20	C19	120.8(5)
N2	C12	C13	120.9(4)	C47	C46	C45	118.3(5)
C13	C12	C11	126.8(4)	C18	C19	C20	121.0(5)
C45	C50	C51	105.1(4)	C42	C41	C40	119.3(4)
C49	C50	C45	120.3(4)	C9	C10	C11	118.9(5)
C49	C50	C51	134.5(4)	C9	C8	C7	119.3(5)
N4	C34	C35	112.3(4)	C4	C5	C6	119.2(5)
N4	C34	C33	120.5(4)	C12	C13	C14	119.9(5)
C33	C34	C35	127.2(4)	C15	C14	C13	118.6(5)
N5	C44	C43	122.9(4)	N2	C16	C15	122.1(5)
N6	C45	C50	111.6(4)	C31	C32	C33	119.5(5)
N6	C45	C46	128.5(4)	C3	C4	C5	120.0(5)

Atom	Atom	Atom	Angle/°	Atom	Atom	Atom	Angle/°
C46	C45	C50	119.9(4)	C14	C15	C16	119.5(4)
C28	C23	C22	105.8(4)	C32	C33	C34	120.0(5)
C24	C23	C28	119.7(4)	C8	C9	C10	121.6(4)
C24	C23	C22	134.3(4)	C49	C48	C47	120.3(5)

Table 7-141 Torsion Angles for [Ni(Py(Ph)Py)Carb].

A	B	C	D	Angle/°	A	B	C	D	Angle/°
Ni2	N5	C44	C43	–176.9(4)	C45	N6	C56	C51	0.9(5)
Ni2	N5	C40	C39	–2.7(5)	C45	N6	C56	C55	–179.4(5)
Ni2	N5	C40	C41	176.0(3)	C45	C50	C51	C56	0.8(5)
Ni2	N6	C45	C50	–176.5(3)	C45	C50	C51	C52	179.0(5)
Ni2	N6	C45	C46	1.9(7)	C45	C50	C49	C48	–0.7(7)
Ni2	N6	C56	C51	177.0(3)	C23	C28	C27	C26	2.0(7)
Ni2	N6	C56	C55	–3.4(7)	C23	C24	C25	C26	1.4(7)
Ni2	N4	C34	C35	0.3(5)	C23	C22	C21	C20	176.4(5)
Ni2	N4	C34	C33	–178.6(3)	C53	C54	C55	C56	–0.6(7)
Ni2	N4	C30	C31	178.6(4)	C27	C28	C23	C24	–2.4(7)
Ni1	N3	C17	C22	–176.3(3)	C27	C28	C23	C22	174.0(4)
Ni1	N3	C17	C18	1.1(7)	C24	C23	C22	C17	178.0(5)
Ni1	N3	C28	C23	177.9(3)	C24	C23	C22	C21	1.1(10)
Ni1	N3	C28	C27	1.8(7)	C24	C25	C26	C27	–1.9(7)
Ni1	N1	C6	C7	3.5(5)	C11	C12	C13	C14	177.8(5)
Ni1	N1	C6	C5	–176.5(3)	C11	C10	C9	C8	0.1(8)
Ni1	N1	C2	C3	177.2(4)	C7	C6	C5	C4	178.3(4)
Ni1	N2	C12	C11	–0.5(5)	C7	C8	C9	C10	–0.5(8)
Ni1	N2	C12	C13	177.1(3)	C6	N1	C2	C3	–1.4(7)
Ni1	N2	C16	C15	–176.7(4)	C6	C7	C1	Ni1	0.0(5)
N5	Ni2	C29	C35	–177.5(4)	C6	C7	C1	C11	–178.7(4)
N5	Ni2	C29	C39	–2.1(4)	C6	C7	C8	C9	179.3(5)
N5	C44	C43	C42	0.4(7)	C6	C5	C4	C3	0.5(7)
N5	C40	C41	C42	1.7(7)	C30	N4	C34	C35	179.0(4)
N3	C17	C22	C23	–1.6(5)	C30	N4	C34	C33	0.2(7)
N3	C17	C22	C21	175.9(4)	C30	C31	C32	C33	0.3(7)
N3	C17	C18	C19	–175.3(4)	C43	C42	C41	C40	0.3(7)
N3	C28	C23	C24	–178.9(4)	C54	C53	C52	C51	0.1(7)
N3	C28	C23	C22	–2.5(5)	C56	N6	C45	C50	–0.4(5)
N3	C28	C27	C26	177.8(4)	C56	N6	C45	C46	178.0(4)
N1	Ni1	C1	C11	–179.8(4)	C56	C51	C52	C53	–0.7(7)
N1	Ni1	C1	C7	1.5(3)	C22	C17	C18	C19	1.9(7)
N1	C6	C5	C4	–1.8(7)	C22	C23	C24	C25	–174.5(5)
N2	Ni1	C1	C11	0.5(4)	C22	C21	C20	C19	1.9(7)
N2	Ni1	C1	C7	–178.2(4)	C36	C35	C29	Ni2	176.9(3)
N2	C12	C11	C1	0.9(5)	C36	C35	C29	C39	1.6(7)
N2	C12	C11	C10	179.5(5)	C36	C35	C34	N4	–177.6(5)
N2	C12	C13	C14	0.6(7)	C36	C35	C34	C33	1.2(8)
N2	C16	C15	C14	–0.8(7)	C40	N5	C44	C43	1.5(7)
N6	C45	C46	C47	–179.0(4)	C40	C39	C29	Ni2	1.2(5)
N6	C56	C51	C50	–1.1(5)	C40	C39	C29	C35	176.5(4)
N6	C56	C51	C52	–179.6(4)	C40	C39	C38	C37	–177.2(4)
N6	C56	C55	C54	–179.7(4)	C51	C50	C45	N6	–0.2(5)

A	B	C	D	Angle/°	A	B	C	D	Angle/°
N4	Ni2	C29	C35	1.5(4)	C51	C50	C45	C46	–178.8(4)
N4	Ni2	C29	C39	176.9(4)	C51	C50	C49	C48	179.0(5)
N4	C34	C33	C32	–0.1(7)	C51	C56	C55	C54	–0.1(7)
N4	C30	C31	C32	–0.3(7)	C52	C53	C54	C55	0.6(8)
C17	N3	C28	C23	1.5(5)	C49	C50	C45	N6	179.5(4)
C17	N3	C28	C27	–174.6(4)	C49	C50	C45	C46	0.9(6)
C17	C22	C21	C20	–0.1(7)	C49	C50	C51	C56	–179.0(5)
C17	C18	C19	C20	–0.2(7)	C49	C50	C51	C52	–0.8(9)
C35	C34	C33	C32	–178.8(4)	C21	C20	C19	C18	–1.8(7)
C35	C36	C37	C38	–0.3(7)	C2	N1	C6	C7	–177.8(4)
C39	C40	C41	C42	–179.8(4)	C2	N1	C6	C5	2.2(6)
C39	C38	C37	C36	0.7(7)	C2	C3	C4	C5	0.3(7)
C28	N3	C17	C22	0.1(5)	C55	C56	C51	C50	179.2(4)
C28	N3	C17	C18	177.5(4)	C55	C56	C51	C52	0.7(7)
C28	C23	C24	C25	0.7(7)	C18	C17	C22	C23	–179.3(4)
C28	C23	C22	C17	2.4(5)	C18	C17	C22	C21	–1.8(6)
C28	C23	C22	C21	–174.5(5)	C38	C39	C29	Ni2	–176.5(3)
C28	C27	C26	C25	0.2(7)	C38	C39	C29	C35	–1.2(7)
C29	C35	C34	N4	0.8(5)	C38	C39	C40	N5	178.4(5)
C29	C35	C34	C33	179.6(4)	C38	C39	C40	C41	–0.2(8)
C29	C35	C36	C37	–0.9(7)	C1	C11	C10	C9	0.7(7)
C29	C39	C40	N5	1.0(5)	C1	C7	C6	N1	–2.2(5)
C29	C39	C40	C41	–177.6(5)	C1	C7	C6	C5	177.7(4)
C29	C39	C38	C37	0.0(7)	C1	C7	C8	C9	0.2(7)
C12	N2	C16	C15	0.8(7)	C31	C32	C33	C34	–0.2(7)
C12	C11	C1	Ni1	–0.9(5)	C46	C47	C48	C49	0.1(7)
C12	C11	C1	C7	177.8(4)	C10	C11	C1	Ni1	–179.7(3)
C12	C11	C10	C9	–177.8(5)	C10	C11	C1	C7	–1.0(7)
C12	C13	C14	C15	–0.6(7)	C8	C7	C6	N1	178.6(5)
C50	C45	C46	C47	–0.7(6)	C8	C7	C6	C5	–1.4(8)
C50	C51	C52	C53	–178.7(5)	C8	C7	C1	Ni1	179.2(3)
C50	C49	C48	C47	0.2(7)	C8	C7	C1	C11	0.6(7)
C34	N4	C30	C31	0.0(7)	C13	C12	C11	C1	–176.5(5)
C34	C35	C29	Ni2	–1.7(5)	C13	C12	C11	C10	2.1(8)
C34	C35	C29	C39	–177.0(4)	C13	C14	C15	C16	0.7(7)
C34	C35	C36	C37	177.4(5)	C16	N2	C12	C11	–178.3(4)
C44	N5	C40	C39	178.7(4)	C16	N2	C12	C13	–0.7(6)
C44	N5	C40	C41	–2.6(6)	C4	C3	C2	N1	0.2(7)
C44	C43	C42	C41	–1.3(7)	C48	C47	C46	C45	0.2(7)

Table 7-142 Hydrogen Atom Coordinates (Å×10^4) and Isotropic Displacement Parameters (Å^2×10^3) for [Ni(Py(Ph)Py)Carb].

Atom	*x*	*y*	*z*	U(eq)
H44	5618.43	5532.51	6363.18	22
H53	3123.46	6916.14	4663.13	31
H27	3168.56	3510.55	8472.74	21
H24	–269.08	1586.96	9154.42	22

Atom	*x*	*y*	*z*	U(eq)
H25	2217.38	1191.17	9122.4	23
H26	3925.51	2171.48	8799.14	23
H30	3143.71	3370.24	5303.13	24
H43	6649.78	6290.29	6947.36	24
H54	1332.48	6396.25	5148.3	29
H3	3200.85	5325.86	9656.13	27
H36	659.79	1606.89	6910.5	21
H42	6131.69	5797.69	7656.79	25
H52	5510	6345.1	4677.3	30
H49	8178.24	5359.65	4887.2	26
H21	–3030.01	2550.48	9139.85	23
H2	1704.49	4752.73	9106.07	24
H55	1924.5	5303.2	5667.84	26
H18	–2132.14	5204.43	8333.54	25
H38	2730.91	3290.84	7755.42	24
H31	1832.26	2234.54	4942.45	27
H37	1189.69	2062.12	7616.54	24
H47	9315.64	3491.02	5785.75	29
H20	–4884.39	3625.84	9045.32	29
H46	6925.72	3468.01	6067.18	22
H19	–4455	4921.83	8630.57	29
H41	4515.03	4581.64	7759.15	22
H10	2306.17	7055.67	6924.64	25
H8	4485.23	7692.53	8038.44	26
H5	4825.57	7137.19	8801.58	24
H13	633.29	5885.53	6628.98	27
H14	–964.61	4705.19	6439.2	30
H16	–834.39	3853.35	7685.34	24
H32	469.82	1195.84	5352.73	27
H4	4775.58	6527.24	9501.18	31
H15	–1673.11	3670.25	6976.63	28
H33	428.7	1324.18	6110.27	26
H9	3956.96	7967.31	7308.74	29
H48	9937.99	4431.19	5199.39	33

7.3.21 [Ni(Py(Ph)Py)CN]

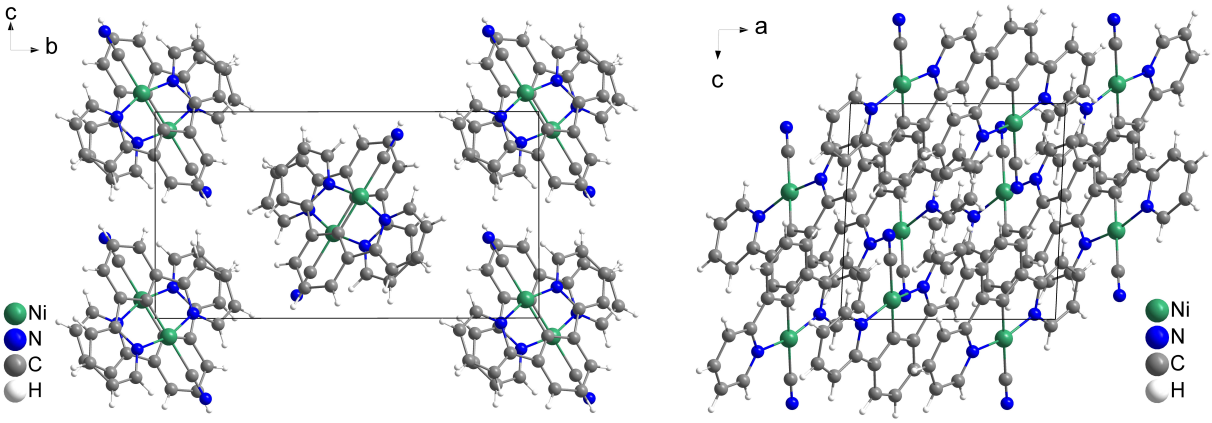

Figure 7-401 Crystal structure of [Ni(Py(Ph)Py)CN] viewed along the crystallographic *a*- (left) and *b*-axis (right).

Table 7-143 Crystal data and structure refinement for [Ni(Py(Ph)Py)CN].

Identification code	[Ni(Py(Ph)Py)CN]
Empirical formula	$C_{17}H_{11}N_3Ni$
Formula weight	316.00
Temperature/K	100.0
Crystal system	monoclinic
Space group	$P2_1/n$
a/Å	8.8536(6)
b/Å	16.4635(9)
c/Å	8.8635(5)
α/°	90
β/°	92.670(2)
γ/°	90
Volume/Å^3	1290.55(13)
Z	4
ρ_{calc}g/cm^3	1.626
μ/mm^{-1}	1.497
F(000)	648.0
Crystal size/mm^3	0.2 × 0.2 × 0.2
Radiation	MoKα (λ = 0.71073)
2Θ range for data collection/°	4.948 to 71.356
Index ranges	–14 ≤ h ≤ 14, –26 ≤ k ≤ 26, –14 ≤ l ≤ 14
Reflections collected	103118
Independent reflections	5974 [R_{int} = 0.0809, R_{sigma} = 0.0309]
Data/restraints/parameters	5974/0/190
Goodness-of-fit on F^2	1.113
Final R indexes [I>=2σ (I)]	R_1 = 0.0370, wR_2 = 0.0756
Final R indexes [all data]	R_1 = 0.0508, wR_2 = 0.0871
Largest diff. peak/hole / e Å^{-3}	0.59/–0.56

Table 7-144 Fractional Atomic Coordinates (×10^4) and Equivalent Isotropic Displacement Parameters (Å^2×10^3) for [Ni(Py(Ph)Py)CN]. U_{eq} is defined as 1/3 of the trace of the orthogonalized U_{IJ} tensor.

Atom	*x*	*y*	*z*	U(eq)
Ni1	2639.4(2)	5348.5(2)	5894.3(2)	11.13(5)
N1	4020.8(14)	5988.4(7)	4763.8(13)	12.2(2)
N2	1217.5(14)	4534.1(7)	6497.7(14)	13.0(2)
N3	2930.8(18)	6310.9(9)	8898.2(16)	21.2(3)
C12	1563.5(16)	4092.7(9)	4019.2(16)	13.6(2)
C13	825.0(16)	3956.1(9)	5434.0(16)	13.7(2)
C2	2808.2(17)	5956.7(9)	7775.5(17)	15.6(2)
C3	4803.7(17)	6637.3(9)	5290.1(16)	14.1(2)
C8	3325.9(16)	5022.0(9)	2913.3(16)	13.0(2)
C7	4212.7(16)	5746.2(9)	3303.0(16)	13.2(2)
C1	2495.9(16)	4771.4(8)	4123.7(16)	12.8(2)
C17	603.5(17)	4490.7(9)	7857.2(17)	15.5(2)
C10	2295.2(19)	3900.0(10)	1465.2(17)	18.0(3)
C5	5968.8(17)	6828.2(9)	2939.2(18)	16.1(2)
C4	5791.4(17)	7068.2(9)	4421.3(17)	15.2(2)
C11	1458.7(18)	3650.0(9)	2672.8(18)	17.3(3)
C16	–403.3(18)	3882.4(10)	8221.0(18)	17.3(3)
C9	3225.6(18)	4587.2(10)	1561.0(17)	17.3(3)
C6	5163.8(17)	6165.2(9)	2367.3(17)	16.1(2)
C14	–163.7(18)	3328.7(10)	5749.5(18)	17.6(3)
C15	–784.1(18)	3293.2(10)	7156.7(19)	18.2(3)

Table 7-145 Anisotropic Displacement Parameters (Å^2×10^3) for [Ni(Py(Ph)Py)CN]. The Anisotropic displacement factor exponent takes the form: $-2\pi^2[h^2a^{*2}U_{11}+2hka^*b^*U_{12}+\ldots]$.

Atom	U_{11}	U_{22}	U_{33}	U_{23}	U_{13}	U_{12}
Ni1	12.34(8)	11.13(8)	9.96(8)	–1.04(6)	0.77(5)	0.36(6)
N1	13.3(5)	12.2(5)	11.1(5)	–1.1(4)	–0.4(4)	1.8(4)
N2	13.1(5)	13.2(5)	12.6(5)	0.0(4)	0.2(4)	1.0(4)
N3	24.8(7)	20.9(6)	18.2(6)	–3.9(5)	3.8(5)	–0.6(5)
C12	13.4(5)	13.7(6)	13.6(5)	–0.8(4)	–0.6(4)	0.9(4)
C13	12.3(5)	13.8(5)	14.8(6)	0.8(4)	–1.2(4)	1.4(4)
C2	16.5(6)	15.1(6)	15.5(6)	1.1(5)	2.7(5)	0.5(5)
C3	15.1(6)	12.8(5)	14.4(6)	–0.5(4)	0.2(5)	–0.2(4)
C8	13.1(5)	14.3(6)	11.6(5)	–1.6(4)	0.0(4)	1.2(4)
C7	12.8(5)	14.2(6)	12.6(5)	0.0(4)	0.6(4)	1.6(4)
C1	13.6(5)	12.5(5)	12.1(5)	–1.5(4)	–0.5(4)	2.3(4)
C17	16.9(6)	15.3(6)	14.3(6)	1.6(5)	2.0(5)	1.4(5)
C10	21.3(7)	18.5(6)	14.2(6)	–5.8(5)	–0.5(5)	0.1(5)
C5	16.6(6)	14.3(6)	17.6(6)	2.9(5)	3.6(5)	0.5(5)
C4	15.8(6)	12.4(5)	17.5(6)	0.8(5)	0.6(5)	0.2(5)
C11	18.4(6)	15.9(6)	17.3(6)	–4.4(5)	–2.6(5)	–1.5(5)
C16	16.7(6)	18.0(6)	17.4(6)	4.8(5)	2.9(5)	0.7(5)
C9	19.1(6)	20.2(7)	12.6(6)	–3.7(5)	0.9(5)	0.8(5)
C6	17.0(6)	17.8(6)	13.6(6)	0.6(5)	3.1(5)	1.3(5)
C14	17.9(6)	15.7(6)	18.9(6)	0.4(5)	–1.3(5)	–2.7(5)
C15	17.4(6)	15.6(6)	21.5(7)	5.1(5)	0.6(5)	–1.7(5)

Table 7-146 Bond Lengths for [Ni(Py(Ph)Py)CN].

Atom	Atom	Length/Å	Atom	Atom	Length/Å
Ni1	N1	1.9297(13)	C3	C4	1.387(2)
Ni1	N2	1.9317(13)	C8	C7	1.460(2)
Ni1	C2	1.9448(15)	C8	C1	1.391(2)
Ni1	C1	1.8339(14)	C8	C9	1.395(2)
N1	C3	1.3451(19)	C7	C6	1.392(2)
N1	C7	1.3729(18)	C17	C16	1.389(2)
N2	C13	1.3727(19)	C10	C11	1.392(2)
N2	C17	1.3467(19)	C10	C9	1.400(2)
N3	C2	1.154(2)	C5	C4	1.388(2)
C12	C13	1.458(2)	C5	C6	1.387(2)
C12	C1	1.390(2)	C16	C15	1.384(2)
C12	C11	1.398(2)	C14	C15	1.387(2)
C13	C14	1.391(2)			

Table 7-147 Bond Angles for [Ni(Py(Ph)Py)CN].

Atom	Atom	Atom	Angle/˚	Atom	Atom	Atom	Angle/˚
N1	Ni1	N2	163.67(5)	C1	C8	C7	110.94(12)
N1	Ni1	C2	97.99(6)	C1	C8	C9	119.71(14)
N2	Ni1	C2	98.34(6)	C9	C8	C7	129.35(14)
C1	Ni1	N1	81.88(6)	N1	C7	C8	111.80(12)
C1	Ni1	N2	81.79(6)	N1	C7	C6	121.52(13)
C1	Ni1	C2	179.52(7)	C6	C7	C8	126.67(13)
C3	N1	Ni1	125.61(10)	C12	C1	Ni1	119.40(11)
C3	N1	C7	118.25(13)	C12	C1	C8	121.37(13)
C7	N1	Ni1	116.13(10)	C8	C1	Ni1	119.23(11)
C13	N2	Ni1	116.00(10)	N2	C17	C16	122.43(14)
C17	N2	Ni1	125.45(10)	C11	C10	C9	121.68(14)
C17	N2	C13	118.55(13)	C6	C5	C4	119.42(14)
C1	C12	C13	110.81(13)	C3	C4	C5	118.82(14)
C1	C12	C11	119.46(14)	C10	C11	C12	119.06(14)
C11	C12	C13	129.72(14)	C15	C16	C17	119.07(14)
N2	C13	C12	111.98(13)	C8	C9	C10	118.71(14)
N2	C13	C14	121.22(14)	C5	C6	C7	119.16(14)
C14	C13	C12	126.79(14)	C15	C14	C13	119.42(14)
N3	C2	Ni1	178.85(15)	C16	C15	C14	119.30(14)
N1	C3	C4	122.80(14)				

Table 7-148 Torsion Angles for [Ni(Py(Ph)Py)CN].

A	B	C	D	Angle/˚	A	B	C	D	Angle/˚
Ni1	N1	C3	C4	179.43(11)	C7	C8	C1	Ni1	–0.11(16)
Ni1	N1	C7	C8	–1.25(15)	C7	C8	C1	C12	180.00(13)
Ni1	N1	C7	C6	179.13(11)	C7	C8	C9	C10	179.48(15)
Ni1	N2	C13	C12	–1.20(15)	C1	C12	C13	N2	0.82(17)
Ni1	N2	C13	C14	178.58(11)	C1	C12	C13	C14	–178.93(14)
Ni1	N2	C17	C16	–179.36(11)	C1	C12	C11	C10	0.1(2)
N1	Ni1	C1	C12	179.45(12)	C1	C8	C7	N1	0.86(17)
N1	Ni1	C1	C8	–0.44(11)	C1	C8	C7	C6	–179.54(14)
N1	C3	C4	C5	0.8(2)	C1	C8	C9	C10	–0.6(2)

A	B	C	D	Angle/°	A	B	C	D	Angle/°
N1	C7	C6	C5	1.9(2)	C17	N2	C13	C12	179.14(13)
N2	Ni1	C1	C12	–0.43(11)	C17	N2	C13	C14	–1.1(2)
N2	Ni1	C1	C8	179.68(12)	C17	C16	C15	C14	–0.6(2)
N2	C13	C14	C15	1.0(2)	C4	C5	C6	C7	–1.1(2)
N2	C17	C16	C15	0.6(2)	C11	C12	C13	N2	–179.64(15)
C12	C13	C14	C15	–179.22(14)	C11	C12	C13	C14	0.6(3)
C13	N2	C17	C16	0.3(2)	C11	C12	C1	Ni1	–179.69(11)
C13	C12	C1	Ni1	–0.10(17)	C11	C12	C1	C8	0.2(2)
C13	C12	C1	C8	179.79(13)	C11	C10	C9	C8	0.9(2)
C13	C12	C11	C10	–179.44(15)	C9	C8	C7	N1	–179.23(14)
C13	C14	C15	C16	–0.2(2)	C9	C8	C7	C6	0.4(3)
C3	N1	C7	C8	178.28(12)	C9	C8	C1	Ni1	179.98(11)
C3	N1	C7	C6	–1.3(2)	C9	C8	C1	C12	0.1(2)
C8	C7	C6	C5	–177.66(14)	C9	C10	C11	C12	–0.6(2)
C7	N1	C3	C4	0.0(2)	C6	C5	C4	C3	–0.3(2)

Table 7-149 Hydrogen Atom Coordinates (Å×10^4) and Isotropic Displacement Parameters (Å^2×10^3) for [Ni(Py(Ph)Py)CN].

Atom	*x*	*y*	*z*	U(eq)
H3	4674.6	6807.71	6299.93	17
H17	868.99	4891.03	8594.53	19
H10	2232.97	3596.62	552.71	22
H5	6635.99	7115.68	2321.74	19
H4	6336.69	7519.67	4833.5	18
H11	825.56	3184.94	2583.27	21
H16	–824.67	3870.87	9187.09	21
H9	3778.24	4754.3	721.6	21
H6	5260.11	5998.97	1349.93	19
H14	–412.06	2927.91	5007.74	21
H15	–1463.18	2868.98	7387.12	22

7.3.22 [Ni(Py(4,6FPh)Py)CN]

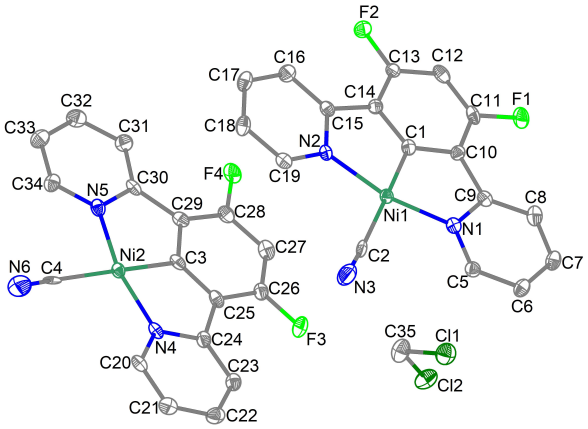

Figure 7-402 Asymmetric unit of 2 [Ni(Py(4,6FPh)Py)CN] · CH_2Cl_2. Ellipsoids are shown with a 50% probability. Hydrogen atoms are omitted for clarity.

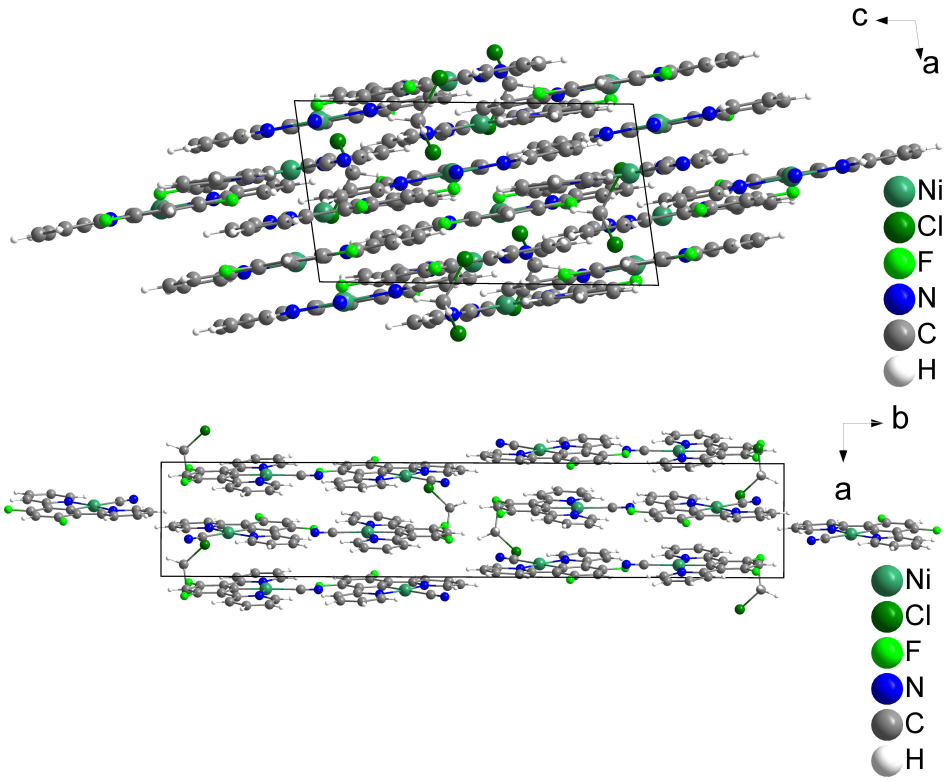

Figure 7-403 Crystal structure of 2 [Ni(Py(4,6FPh)Py)CN] · CH_2Cl_2 viewed along the crystallographic *b*- (top) and *c*-axis (bottom).

Table 7-150 Crystal data and structure refinement for 2 [Ni(Py(4,6FPh)Py)CN] · CH_2Cl_2.

Identification code	2 [Ni(Py(4,6FPh)Py)CN] · CH_2Cl_2
Empirical formula	$C_{35}H_{20}Cl_2F_4N_6Ni_2$
Formula weight	788.89
Temperature/K	100.0
Crystal system	monoclinic
Space group	$P2_1/n$
a/Å	6.6847(5)
b/Å	36.052(3)
c/Å	12.3884(11)
α/°	90
β/°	98.516(3)
γ/°	90
Volume/Å^3	2952.7(4)
Z	4
ρ_{calc}g/cm^3	1.775
μ/mm^{-1}	1.522
F(000)	1592.0
Crystal size/mm^3	0.23 × 0.05 × 0.003
Radiation	MoKα (λ = 0.71073)
2Θ range for data collection/°	4.02 to 55.754
Index ranges	–8 ≤ h ≤ 8, –47 ≤ k ≤ 47, –16 ≤ l ≤
Reflections collected	16 89016
Independent reflections	7045 [R_{int} = 0.0901, R_{sigma} = 0.0433]
Data/restraints/parameters	7045/0/443
Goodness-of-fit on F^2	1.117
Final R indexes [I>=2σ (I)]	R_1 = 0.0587, wR_2 = 0.1056
Final R indexes [all data]	R_1 = 0.0778, wR_2 = 0.1135
Largest diff. peak/hole / e Å^{-3}	0.56/–0.58

Table 7-151 Fractional Atomic Coordinates (×10^4) and Equivalent Isotropic Displacement Parameters (Å^2×10^3) for 2 [Ni(Py(4,6FPh)Py)CN] · CH_2Cl_2. U_{eq} is defined as 1/3 of the trace of the orthogonalized U_{IJ} tensor.

Atom	*x*	*y*	*z*	U(eq)
Ni1	1161.6(8)	3921.6(2)	4600.6(4)	12.71(12)
Ni2	3921.2(8)	6683.9(2)	5628.4(4)	13.17(12)
Cl1	6336.9(17)	4582.6(3)	9385.8(9)	27.9(2)
Cl2	2220.8(18)	4295.7(3)	8882.4(9)	28.3(2)
F1	815(4)	2544.6(6)	3454(2)	22.5(5)
F4	3272(4)	5375.3(6)	3924(2)	22.1(5)
F2	–222(4)	3429.0(7)	650.7(19)	20.6(5)
F3	4469(4)	5447.0(7)	7746(2)	23.5(5)
N1	1526(5)	3512.0(9)	5598(3)	14.0(7)
N4	4521(5)	6638.7(9)	7203(3)	14.2(7)
N2	742(5)	4229.4(9)	3316(3)	13.6(6)
N5	3333(5)	6582.0(9)	4077(3)	16.0(7)
C4	3879(6)	7246.6(11)	5537(3)	11.3(7)
C2	1547(6)	4334.3(11)	5689(3)	14.7(8)
C24	4569(6)	6282.6(11)	7611(3)	15.8(8)
C1	810(6)	3547.9(11)	3582(3)	14.3(8)
C25	4228(6)	6011.2(10)	6734(3)	15.2(8)
C14	440(6)	3645.8(11)	2492(3)	14.0(8)
C13	159(6)	3357.0(11)	1739(3)	13.8(7)
N3	1735(6)	4557.9(12)	6216(3)	30.7(9)
C15	452(6)	4046.6(11)	2331(3)	14.3(8)
C5	1900(6)	3539.1(11)	6694(3)	15.6(8)
C26	4195(6)	5622.8(11)	6765(3)	17.1(8)
C29	3563(6)	5974.3(11)	4742(3)	15.4(8)
C10	959(6)	3183.2(11)	3949(3)	14.2(8)
C34	2996(6)	6836.8(11)	3275(3)	17.8(8)
C9	1399(6)	3159.7(11)	5137(3)	14.8(8)
N6	3866(7)	7528.5(13)	5513(3)	36.9(10)
C23	4928(6)	6217.4(11)	8723(3)	17.4(8)
C28	3566(6)	5589.1(11)	4835(3)	16.8(8)
C19	798(6)	4602.8(11)	3317(3)	16.6(8)
C11	678(6)	2908.2(10)	3155(3)	16.6(8)
C33	2544(6)	6743.2(12)	2187(3)	21.3(9)
C12	260(6)	2986.0(11)	2054(3)	17.7(8)
C3	3914(6)	6174.0(10)	5716(3)	15.1(8)
C18	628(6)	4806.1(11)	2358(3)	19.5(9)
C20	4900(6)	6921.4(11)	7913(3)	17.0(8)
C30	3224(6)	6215.5(11)	3781(3)	15.2(8)
C27	3858(6)	5408.8(11)	5835(3)	18.8(8)
C22	5298(6)	6514.3(12)	9440(3)	21.3(9)
C17	367(6)	4622.9(11)	1370(4)	20.5(9)
C16	258(6)	4240.0(12)	1361(3)	18.9(8)
C32	2451(6)	6372.9(12)	1892(4)	21.6(9)
C21	5311(6)	6870.7(12)	9033(3)	19.4(8)
C31	2790(6)	6104.1(12)	2700(3)	19.1(8)
C7	2102(6)	2882.7(11)	6909(3)	19.2(8)

Atom	*x*	*y*	*z*	U(eq)
C8	1706(6)	2847.0(12)	5789(4)	19.6(9)
C6	2179(6)	3232.2(11)	7367(3)	18.5(8)
C35	3950(7)	4635.1(13)	8570(4)	27.1(10)

Table 7-152 Anisotropic Displacement Parameters ($Å^2×10^3$) for 2 [Ni(Py(4,6FPh)Py)CN] · CH_2Cl_2. The Anisotropic displacement factor exponent takes the form: $–2π^2[h^2a^{*2}U_{11}+2hka^*b^*U_{12}+…]$.

Atom	U_{11}	U_{22}	U_{33}	U_{23}	U_{13}	U_{12}
Ni1	14.4(2)	9.5(2)	14.3(2)	–0.16(19)	2.55(19)	–0.48(19)
Ni2	14.2(2)	9.0(2)	16.4(3)	–0.32(19)	2.55(19)	–0.31(19)
Cl1	26.8(6)	29.7(6)	25.4(6)	–0.1(5)	–1.8(4)	–1.0(5)
Cl2	31.2(6)	31.4(6)	22.6(5)	3.7(4)	4.9(4)	–7.9(5)
F1	28.1(13)	10.8(11)	27.9(14)	–1.1(10)	1.2(11)	–0.5(10)
F4	28.1(14)	11.8(11)	25.6(13)	–6.8(10)	1.5(10)	–0.6(10)
F2	25.0(13)	21.2(12)	14.7(12)	–1.6(9)	0.0(10)	1.7(10)
F3	28.8(14)	16.8(12)	24.2(13)	7.7(10)	2.1(11)	–0.6(10)
N1	11.5(15)	12.9(16)	17.5(17)	–0.7(13)	1.5(13)	–1.7(12)
N4	10.5(15)	11.0(15)	21.2(17)	–3.3(13)	2.8(13)	0.7(12)
N2	13.8(16)	10.8(15)	16.1(16)	0.4(13)	1.9(13)	1.8(12)
N5	12.1(16)	14.0(16)	22.2(18)	1.6(13)	3.2(13)	0.6(12)
C4	8.9(16)	20(2)	4.7(16)	–8.1(14)	1.5(13)	–4.1(15)
C2	10.2(18)	14.2(19)	20(2)	10.1(17)	3.1(15)	2.0(15)
C24	13.6(18)	14.7(19)	19(2)	2.3(15)	2.7(15)	0.8(15)
C1	9.9(17)	13.3(18)	20(2)	3.1(15)	4.6(15)	–1.2(14)
C25	9.3(17)	12.7(19)	24(2)	–1.5(15)	2.7(15)	0.6(14)
C14	12.0(18)	14.2(18)	16.5(19)	1.9(15)	4.2(15)	–0.6(14)
C13	13.2(18)	15.1(19)	12.9(18)	–1.4(15)	1.7(14)	1.8(15)
N3	32(2)	33(2)	27(2)	11.5(19)	5.5(18)	1.4(18)
C15	11.0(18)	13.9(18)	18(2)	–0.9(15)	2.7(15)	0.5(14)
C5	16.8(19)	14.3(19)	15.6(19)	–1.5(15)	1.8(15)	–0.1(15)
C26	14.2(19)	14.8(19)	23(2)	4.1(16)	5.4(16)	1.0(15)
C29	13.9(19)	13.2(19)	20(2)	–3.9(15)	5.1(15)	–2.2(14)
C10	12.6(18)	16.1(19)	13.7(19)	1.7(15)	1.5(15)	0.2(15)
C34	16(2)	16.8(19)	21(2)	4.7(16)	3.6(16)	–3.5(15)
C9	12.2(18)	14.6(18)	17.2(19)	–2.1(15)	1.2(15)	0.0(14)
N6	41(3)	43(3)	27(2)	0(2)	4.6(19)	5(2)
C23	15.4(19)	15.1(19)	22(2)	3.0(16)	3.9(16)	–1.0(15)
C28	15.8(19)	13.8(19)	21(2)	–4.3(16)	1.9(16)	–0.9(15)
C19	15.4(19)	15.5(19)	19(2)	–2.2(16)	4.0(15)	–0.2(15)
C11	14.6(19)	8.5(17)	27(2)	–0.3(16)	3.7(16)	1.0(14)
C33	20(2)	24(2)	20(2)	3.1(17)	2.3(17)	–4.6(17)
C12	14.1(19)	13.9(19)	25(2)	–7.1(16)	1.4(16)	–0.2(15)
C3	11.2(18)	13.2(18)	22(2)	–3.3(15)	5.7(15)	0.9(14)
C18	20(2)	14.1(19)	23(2)	4.3(16)	–0.9(17)	–1.9(16)
C20	15.1(19)	13.8(19)	22(2)	–4.2(16)	3.6(16)	2.5(15)
C30	13.4(19)	12.1(18)	21(2)	–4.0(15)	4.2(15)	2.3(14)
C27	14.0(19)	13.6(19)	29(2)	–0.1(16)	2.6(17)	–3.2(15)
C22	18(2)	30(2)	15(2)	–0.7(17)	0.1(16)	1.4(17)
C17	20(2)	17(2)	23(2)	6.8(17)	0.8(17)	–2.3(16)
C16	18(2)	21(2)	18(2)	0.7(16)	0.9(16)	–0.9(16)
C32	22(2)	24(2)	19(2)	–5.5(17)	0.5(17)	–2.5(17)
C21	15(2)	23(2)	20(2)	–3.5(17)	1.2(16)	–1.4(16)

Atom	U_{11}	U_{22}	U_{33}	U_{23}	U_{13}	U_{12}
C31	22(2)	17(2)	19(2)	–1.6(16)	3.4(16)	–2.4(16)
C7	21(2)	13.3(19)	23(2)	5.3(16)	2.9(17)	–3.7(16)
C8	14.9(19)	16(2)	27(2)	3.6(17)	0.8(17)	–1.7(15)
C6	18(2)	21(2)	16(2)	3.1(16)	–1.5(16)	–1.4(16)
C35	31(3)	21(2)	27(2)	2.9(18)	–3.8(19)	–5.3(19)

Table 7-153 Bond Lengths for 2 [Ni(Py(4,6FPh)Py)CN] · CH_2Cl_2.

Atom	Atom	Length/Å	Atom	Atom	Length/Å
Ni1	N1	1.917(3)	C25	C26	1.401(5)
Ni1	N2	1.926(3)	C25	C3	1.378(6)
Ni1	C2	1.999(5)	C14	C13	1.391(5)
Ni1	C1	1.837(4)	C14	C15	1.459(5)
Ni2	N4	1.939(3)	C13	C12	1.392(5)
Ni2	N5	1.939(4)	C15	C16	1.378(6)
Ni2	C4	2.032(4)	C5	C6	1.382(5)
Ni2	C3	1.841(4)	C26	C27	1.378(6)
Cl1	C35	1.768(5)	C29	C28	1.394(5)
Cl2	C35	1.765(5)	C29	C3	1.395(5)
F1	C11	1.362(4)	C29	C30	1.464(6)
F4	C28	1.356(4)	C10	C9	1.460(5)
F2	C13	1.360(4)	C10	C11	1.389(5)
F3	C26	1.358(5)	C34	C33	1.379(6)
N1	C5	1.347(5)	C9	C8	1.385(6)
N1	C9	1.390(5)	C23	C22	1.390(6)
N4	C24	1.379(5)	C28	C27	1.387(6)
N4	C20	1.346(5)	C19	C18	1.386(6)
N2	C15	1.375(5)	C11	C12	1.380(6)
N2	C19	1.347(5)	C33	C32	1.383(6)
N5	C34	1.347(5)	C18	C17	1.378(6)
N5	C30	1.370(5)	C20	C21	1.386(6)
C4	N6	1.017(6)	C30	C31	1.388(6)
C2	N3	1.033(6)	C22	C21	1.381(6)
C24	C25	1.456(5)	C17	C16	1.382(6)
C24	C23	1.383(6)	C32	C31	1.388(6)
C1	C14	1.382(5)	C7	C8	1.379(6)
C1	C10	1.390(5)	C7	C6	1.379(6)

Table 7-154 Bond Angles for 2 [Ni(Py(4,6FPh)Py)CN] · CH_2Cl_2.

Atom	Atom	Atom	Angle/°	Atom	Atom	Atom	Angle/°
N1	Ni1	N2	164.79(14)	N1	C5	C6	122.6(4)
N1	Ni1	C2	98.45(14)	F3	C26	C25	119.4(4)
N2	Ni1	C2	96.73(14)	F3	C26	C27	118.1(3)
C1	Ni1	N1	82.48(15)	C27	C26	C25	122.5(4)
C1	Ni1	N2	82.34(15)	C28	C29	C3	116.4(4)
C1	Ni1	C2	179.05(16)	C28	C29	C30	131.1(4)
N4	Ni2	N5	164.26(14)	C3	C29	C30	112.5(3)
N4	Ni2	C4	98.00(14)	C1	C10	C9	112.2(3)
N5	Ni2	C4	97.74(14)	C11	C10	C1	116.6(4)
C3	Ni2	N4	81.89(16)	C11	C10	C9	131.2(4)

Atom	Atom	Atom	Angle/°	Atom	Atom	Atom	Angle/°
C3	Ni2	N5	82.38(16)	N5	C34	C33	122.9(4)
C3	Ni2	C4	179.02(16)	N1	C9	C10	110.6(3)
C5	N1	Ni1	125.5(3)	C8	C9	N1	120.6(4)
C5	N1	C9	118.1(3)	C8	C9	C10	128.8(4)
C9	N1	Ni1	116.4(3)	C24	C23	C22	119.6(4)
C24	N4	Ni2	116.0(3)	F4	C28	C29	119.9(4)
C20	N4	Ni2	125.8(3)	F4	C28	C27	117.4(3)
C20	N4	C24	118.2(3)	C27	C28	C29	122.7(4)
C15	N2	Ni1	116.2(2)	N2	C19	C18	122.0(4)
C19	N2	Ni1	125.1(3)	F1	C11	C10	119.8(4)
C19	N2	C15	118.7(3)	F1	C11	C12	117.4(3)
C34	N5	Ni2	126.1(3)	C12	C11	C10	122.7(4)
C34	N5	C30	117.6(4)	C34	C33	C32	119.3(4)
C30	N5	Ni2	116.3(3)	C11	C12	C13	117.8(4)
N6	C4	Ni2	178.5(4)	C25	C3	Ni2	118.5(3)
N3	C2	Ni1	176.8(4)	C25	C3	C29	123.7(4)
N4	C24	C25	111.0(3)	C29	C3	Ni2	117.8(3)
N4	C24	C23	121.0(4)	C17	C18	C19	119.4(4)
C23	C24	C25	127.9(4)	N4	C20	C21	123.0(4)
C14	C1	Ni1	118.0(3)	N5	C30	C29	111.1(3)
C14	C1	C10	123.7(4)	N5	C30	C31	122.2(4)
C10	C1	Ni1	118.2(3)	C31	C30	C29	126.7(4)
C26	C25	C24	130.7(4)	C26	C27	C28	118.0(4)
C3	C25	C24	112.5(3)	C21	C22	C23	119.5(4)
C3	C25	C26	116.8(4)	C18	C17	C16	119.1(4)
C1	C14	C13	116.8(4)	C15	C16	C17	120.0(4)
C1	C14	C15	112.5(3)	C33	C32	C31	119.2(4)
C13	C14	C15	130.7(4)	C22	C21	C20	118.5(4)
F2	C13	C14	120.6(3)	C30	C31	C32	118.9(4)
F2	C13	C12	117.1(3)	C6	C7	C8	119.2(4)
C14	C13	C12	122.4(4)	C7	C8	C9	120.1(4)
N2	C15	C14	110.8(3)	C7	C6	C5	119.3(4)
N2	C15	C16	120.9(4)	Cl2	C35	Cl1	111.4(2)
C16	C15	C14	128.2(4)				

Table 7-155 Torsion Angles for 2 [Ni(Py(4,6FPh)Py)CN] · CH_2Cl_2.

A	B	C	D	Angle/°	A	B	C	D	Angle/°
Ni1	N1	C5	C6	–178.9(3)	C14	C1	C10	C9	178.8(3)
Ni1	N1	C9	C10	–1.2(4)	C14	C1	C10	C11	–1.2(6)
Ni1	N1	C9	C8	177.9(3)	C14	C13	C12	C11	–0.8(6)
Ni1	N2	C15	C14	2.6(4)	C14	C15	C16	C17	–178.0(4)
Ni1	N2	C15	C16	–176.1(3)	C13	C14	C15	N2	178.6(4)
Ni1	N2	C19	C18	175.2(3)	C13	C14	C15	C16	–2.8(7)
Ni1	C1	C14	C13	–179.3(3)	C15	N2	C19	C18	–1.7(6)
Ni1	C1	C14	C15	1.7(4)	C15	C14	C13	F2	–1.6(6)
Ni1	C1	C10	C9	–0.2(4)	C15	C14	C13	C12	178.0(4)
Ni1	C1	C10	C11	179.8(3)	C5	N1	C9	C10	179.2(3)
Ni2	N4	C24	C25	2.5(4)	C5	N1	C9	C8	–1.8(5)
Ni2	N4	C24	C23	–178.3(3)	C26	C25	C3	Ni2	179.5(3)
Ni2	N4	C20	C21	179.7(3)	C26	C25	C3	C29	0.4(6)

A	B	C	D	Angle/°	A	B	C	D	Angle/°
Ni2	N5	C34	C33	–178.6(3)	C29	C28	C27	C26	–1.3(6)
Ni2	N5	C30	C29	0.8(4)	C29	C30	C31	C32	178.0(4)
Ni2	N5	C30	C31	179.2(3)	C10	C1	C14	C13	1.7(6)
F1	C11	C12	C13	–178.7(3)	C10	C1	C14	C15	–177.3(4)
F4	C28	C27	C26	178.8(3)	C10	C9	C8	C7	–179.8(4)
F2	C13	C12	C11	178.9(3)	C10	C11	C12	C13	1.3(6)
F3	C26	C27	C28	179.6(3)	C34	N5	C30	C29	–178.2(3)
N1	Ni1	C1	C14	–179.4(3)	C34	N5	C30	C31	0.2(6)
N1	Ni1	C1	C10	–0.3(3)	C34	C33	C32	C31	0.8(6)
N1	C5	C6	C7	0.9(6)	C9	N1	C5	C6	0.7(6)
N1	C9	C8	C7	1.3(6)	C9	C10	C11	F1	–0.3(6)
N4	Ni2	C3	C25	2.0(3)	C9	C10	C11	C12	179.7(4)
N4	Ni2	C3	C29	–178.8(3)	C23	C24	C25	C26	–0.9(7)
N4	C24	C25	C26	178.3(4)	C23	C24	C25	C3	179.9(4)
N4	C24	C25	C3	–0.9(5)	C23	C22	C21	C20	1.6(6)
N4	C24	C23	C22	–1.6(6)	C28	C29	C3	Ni2	–180.0(3)
N4	C20	C21	C22	–1.1(6)	C28	C29	C3	C25	–0.8(6)
N2	Ni1	C1	C14	–0.3(3)	C28	C29	C30	N5	179.0(4)
N2	Ni1	C1	C10	178.8(3)	C28	C29	C30	C31	0.7(7)
N2	C15	C16	C17	0.5(6)	C19	N2	C15	C14	179.8(3)
N2	C19	C18	C17	0.8(6)	C19	N2	C15	C16	1.1(6)
N5	Ni2	C3	C25	–178.3(3)	C19	C18	C17	C16	0.8(6)
N5	Ni2	C3	C29	0.9(3)	C11	C10	C9	N1	–179.2(4)
N5	C34	C33	C32	–0.8(6)	C11	C10	C9	C8	1.9(7)
N5	C30	C31	C32	–0.2(6)	C33	C32	C31	C30	–0.3(6)
C24	N4	C20	C21	–0.8(6)	C3	C25	C26	F3	–179.1(3)
C24	C25	C26	F3	1.7(6)	C3	C25	C26	C27	–0.3(6)
C24	C25	C26	C27	–179.5(4)	C3	C29	C28	F4	–178.8(3)
C24	C25	C3	Ni2	–1.2(5)	C3	C29	C28	C27	1.3(6)
C24	C25	C3	C29	179.7(4)	C3	C29	C30	N5	–0.1(5)
C24	C23	C22	C21	–0.3(6)	C3	C29	C30	C31	–178.4(4)
C1	C14	C13	F2	179.7(3)	C18	C17	C16	C15	–1.4(6)
C1	C14	C13	C12	–0.6(6)	C20	N4	C24	C25	–177.1(3)
C1	C14	C15	N2	–2.7(5)	C20	N4	C24	C23	2.1(6)
C1	C14	C15	C16	175.9(4)	C30	N5	C34	C33	0.3(6)
C1	C10	C9	N1	0.9(5)	C30	C29	C28	F4	2.1(7)
C1	C10	C9	C8	–178.1(4)	C30	C29	C28	C27	–177.8(4)
C1	C10	C11	F1	179.6(3)	C30	C29	C3	Ni2	–0.7(4)
C1	C10	C11	C12	–0.3(6)	C30	C29	C3	C25	178.4(4)
C25	C24	C23	C22	177.5(4)	C8	C7	C6	C5	–1.3(6)
C25	C26	C27	C28	0.8(6)	C6	C7	C8	C9	0.2(6)

Table 7-156 Hydrogen Atom Coordinates (Å×10^4) and Isotropic Displacement Parameters (Å^2×10^3) for 2 [Ni(Py(4,6FPh)Py)CN] · CH_2Cl_2.

Atom	*x*	*y*	*z*	U(eq)
H5	1974.25	3778.69	7016.29	19
H34	3072.9	7092.04	3467.23	21
H23	4923.01	5971.09	8995.02	21
H19	960.32	4730.6	3994.59	20
H33	2299.37	6931.09	1645.33	26
H12	47.16	2792.81	1528.22	21

Atom	*x*	*y*	*z*	U(eq)
H18	689.84	5069.27	2380.96	23
H20	4884.82	7166.94	7633.52	20
H27	3825.97	5145.8	5876.81	23
H22	5539.77	6472.39	10205.82	26
H17	264.31	4757.86	705.78	25
H16	48.68	4110.23	686.12	23
H32	2157.6	6303.44	1145.27	26
H21	5595.51	7076.62	9509.4	23
H31	2726.49	5848.09	2515.81	23
H7	2318.36	2669.04	7360.09	23
H8	1644.81	2607.65	5465.19	23
H6	2422.21	3261.48	8137.12	22
H35A	3407.13	4884.81	8690.53	33
H35B	4109.03	4614.83	7790.65	33

7.3.23 [Ni(Py(4,6MePh)Py)CN]

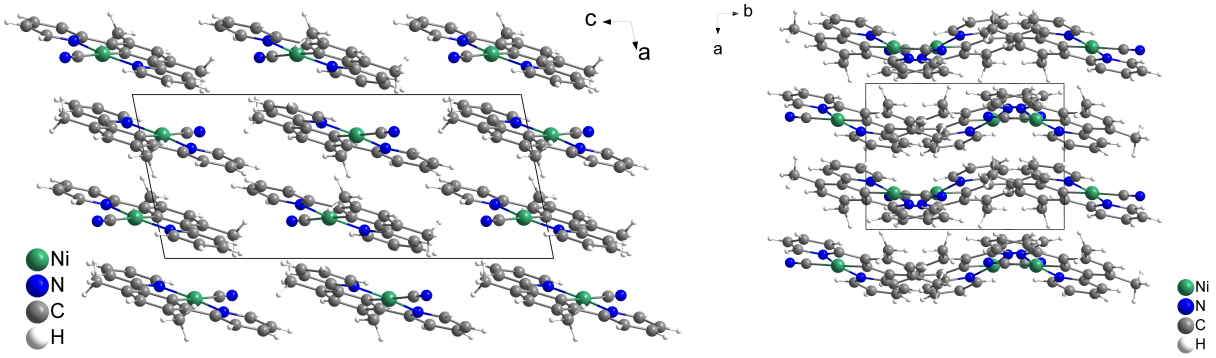

Figure 7-404 Crystal structure of [Ni(Py(4,6MePh)Py)CN] viewed along the crystallographic *b*- (left) and *c*-axis (right).

Table 7-157 Crystal data and structure refinement for [Ni(Py(4,6MePh)Py)CN].

Identification code	[Ni(Py(4,6MePh)Py)CN]
Empirical formula	$C_{19}H_{15}N_3Ni$
Formula weight	344.05
Temperature/K	100.0
Crystal system	monoclinic
Space group	$P2_1/c$
a/Å	7.7996(5)
b/Å	10.4099(7)
c/Å	18.1779(13)
α/°	90
β/°	101.199(2)
γ/°	90
Volume/Å^3	1447.82(17)
Z	4
ρ_{calc}g/cm^3	1.578
μ/mm^{-1}	1.342
F(000)	712.0
Crystal size/mm^3	0.02 × 0.01 × 0.01

Radiation	MoKα (λ = 0.71073)
2Θ range for data collection/°	4.53 to 56.696
Index ranges	–10 ≤ h ≤ 9, –13 ≤ k ≤ 13, –24 ≤ l ≤ 24
Reflections collected	42922
Independent reflections	3607 [R_{int} = 0.0720, R_{sigma} = 0.0305]
Data/restraints/parameters	3607/0/210
Goodness-of-fit on F^2	1.096
Final R indexes [I>=2σ (I)]	R_1 = 0.0344, wR_2 = 0.0730
Final R indexes [all data]	R_1 = 0.0488, wR_2 = 0.0837
Largest diff. peak/hole / e Å^{-3}	0.65/–0.39

Table 7-158 Fractional Atomic Coordinates (×10^4) and Equivalent Isotropic Displacement Parameters (Å^2×10^3) for [Ni(Py(4,6MePh)Py)CN]. U_{eq} is defined as 1/3 of the trace of the orthogonalized U_{IJ} tensor.

Atom	*x*	*y*	*z*	U(eq)
Ni1	7517.0(4)	3588.3(3)	5559.5(2)	14.28(9)
N1	8282(2)	2831.7(18)	4719.6(10)	15.6(4)
N2	6717(2)	4751.3(18)	6235.6(10)	16.3(4)
C2	7667(3)	1994(2)	6208.3(13)	18.5(5)
C13	6489(3)	6006(2)	6008.7(13)	16.6(4)
C12	6919(3)	6196(2)	5263.6(13)	16.2(4)
C8	7968(3)	4965(2)	4292.6(12)	15.0(4)
C7	8440(3)	3641(2)	4141.8(12)	15.3(4)
C1	7455(3)	5055(2)	4985.7(12)	14.8(4)
C3	8631(3)	1573(2)	4662.0(13)	19.3(5)
C11	6867(3)	7317(2)	4832.5(13)	17.9(4)
N3	7732(4)	1169(3)	6541.9(14)	39.6(6)
C6	8965(3)	3156(2)	3501.9(13)	19.8(5)
C9	7981(3)	6083(2)	3862.3(13)	17.2(4)
C5	9327(3)	1863(2)	3457.4(14)	22.4(5)
C4	9155(3)	1059(2)	4041.0(14)	21.9(5)
C10	7413(3)	7217(2)	4144.5(13)	18.7(4)
C18	8576(3)	6127(2)	3119.1(13)	21.7(5)
C17	6380(3)	4409(2)	6905.0(13)	19.9(5)
C16	5805(3)	5275(3)	7384.3(14)	23.9(5)
C19	6257(3)	8609(2)	5055.7(14)	22.5(5)
C14	5938(3)	6910(2)	6477.4(13)	21.4(5)
C15	5586(3)	6535(3)	7163.0(14)	24.7(5)

Table 7-159 Anisotropic Displacement Parameters (Å^2×10^3) for [Ni(Py(4,6MePh)Py)CN]. The Anisotropic displacement factor exponent takes the form: $-2\pi^2[h^2a^{*2}U_{11}+2hka^*b^*U_{12}+\ldots]$.

Atom	U_{11}	U_{22}	U_{33}	U_{23}	U_{13}	U_{12}
Ni1	16.97(14)	13.43(14)	12.81(14)	–0.21(11)	3.83(10)	0.72(11)
N1	15.0(9)	16.8(9)	14.8(9)	–1.6(7)	2.1(7)	1.4(7)
N2	13.6(8)	19.2(9)	16.3(9)	–1.9(7)	3.0(7)	–0.2(7)
C2	19.5(11)	21.4(12)	15.7(11)	–11.2(9)	5.8(9)	–3.6(9)
C13	11.2(9)	19.6(11)	18.1(11)	–2.5(8)	0.5(8)	0.8(8)
C12	13.0(9)	16.2(11)	18.9(10)	–1.7(8)	2.1(8)	0.0(8)
C8	12.7(9)	16.3(10)	15.5(10)	–1.7(8)	1.9(8)	–1.1(8)
C7	12.1(9)	18.3(10)	15.2(10)	–0.6(8)	1.9(8)	–0.1(8)
C1	12.6(9)	17.8(10)	13.3(10)	0.1(8)	0.6(8)	–0.1(8)
C3	19.2(11)	15.8(11)	21.9(11)	0.5(9)	1.9(9)	2.9(9)

Atom	U_{11}	U_{22}	U_{33}	U_{23}	U_{13}	U_{12}
C11	15.2(10)	14.2(10)	23.0(11)	–3.2(9)	0.5(9)	0.2(8)
N3	52.8(16)	39.2(15)	28.1(13)	–6.0(11)	11.6(11)	3.9(12)
C6	21.3(11)	23.0(12)	16.0(11)	–3.2(9)	5.7(9)	–0.5(9)
C9	13.2(10)	21.3(11)	16.3(10)	1.9(8)	1.0(8)	–1.3(8)
C5	20.7(11)	26.6(12)	20.0(11)	–8.5(9)	4.7(9)	–0.2(9)
C4	19.8(11)	19.5(11)	25.6(12)	–6.8(9)	2.7(9)	3.4(9)
C10	17.8(11)	16.8(11)	20.1(11)	2.7(9)	0.3(9)	–0.8(8)
C18	20.9(11)	25.0(12)	20.3(11)	6.1(9)	6.3(9)	0.3(9)
C17	19.6(11)	24.9(12)	15.4(10)	–2.1(9)	4.1(9)	–3.6(9)
C16	21.2(11)	34.3(14)	17.2(11)	–4.5(10)	6.5(9)	–2.1(10)
C19	22.4(11)	15.3(10)	29.1(12)	–1.8(10)	3.7(9)	3.2(9)
C14	19.4(11)	22.0(12)	22.5(12)	–7.5(9)	3.3(9)	1.3(9)
C15	20.3(11)	33.4(14)	20.5(11)	–10.4(10)	4.0(9)	3.6(10)

Table 7-160 Bond Lengths for [Ni(Py(4,6MePh)Py)CN].

Atom	Atom	Length/Å	Atom	Atom	Length/Å
Ni1	N1	1.9134(19)	C8	C1	1.398(3)
Ni1	N2	1.9142(19)	C8	C9	1.404(3)
Ni1	C2	2.026(3)	C7	C6	1.400(3)
Ni1	C1	1.845(2)	C3	C4	1.381(3)
N1	C7	1.371(3)	C11	C10	1.401(3)
N1	C3	1.346(3)	C11	C19	1.508(3)
N2	C13	1.371(3)	C6	C5	1.381(3)
N2	C17	1.342(3)	C9	C10	1.393(3)
C2	N3	1.047(3)	C9	C18	1.512(3)
C13	C12	1.471(3)	C5	C4	1.378(4)
C13	C14	1.392(3)	C17	C16	1.387(3)
C12	C1	1.386(3)	C16	C15	1.373(4)
C12	C11	1.402(3)	C14	C15	1.383(3)
C8	C7	1.466(3)			

Table 7-161 Bond Angles for [Ni(Py(4,6MePh)Py)CN].

Atom	Atom	Atom	Angle/˚	Atom	Atom	Atom	Angle/˚
N1	Ni1	N2	164.54(8)	N1	C7	C8	111.79(18)
N1	Ni1	C2	97.80(8)	N1	C7	C6	120.0(2)
N2	Ni1	C2	97.67(8)	C6	C7	C8	128.2(2)
C1	Ni1	N1	82.40(9)	C12	C1	Ni1	118.70(16)
C1	Ni1	N2	82.15(9)	C12	C1	C8	123.1(2)
C1	Ni1	C2	178.08(9)	C8	C1	Ni1	118.24(16)
C7	N1	Ni1	116.54(15)	N1	C3	C4	122.5(2)
C3	N1	Ni1	124.17(16)	C12	C11	C19	124.6(2)
C3	N1	C7	119.3(2)	C10	C11	C12	117.1(2)
C13	N2	Ni1	116.66(15)	C10	C11	C19	118.3(2)
C17	N2	Ni1	124.04(17)	C5	C6	C7	119.8(2)
C17	N2	C13	119.3(2)	C8	C9	C18	124.0(2)
N3	C2	Ni1	179.5(3)	C10	C9	C8	117.4(2)
N2	C13	C12	111.48(19)	C10	C9	C18	118.6(2)
N2	C13	C14	119.8(2)	C4	C5	C6	119.7(2)
C14	C13	C12	128.7(2)	C5	C4	C3	118.8(2)

Atom	Atom	Atom	Angle/°	Atom	Atom	Atom	Angle/°
C1	C12	C13	111.02(19)	C9	C10	C11	124.4(2)
C1	C12	C11	119.2(2)	N2	C17	C16	122.7(2)
C11	C12	C13	129.8(2)	C15	C16	C17	118.3(2)
C1	C8	C7	111.01(19)	C15	C14	C13	119.9(2)
C1	C8	C9	118.7(2)	C16	C15	C14	119.9(2)
C9	C8	C7	130.3(2)				

Table 7-162 Torsion Angles for [Ni(Py(4,6MePh)Py)CN].

A	B	C	D	Angle/°	A	B	C	D	Angle/°
Ni1	N1	C7	C8	–0.2(2)	C7	C8	C1	Ni1	1.5(2)
Ni1	N1	C7	C6	–178.93(16)	C7	C8	C1	C12	–179.2(2)
Ni1	N1	C3	C4	179.00(17)	C7	C8	C9	C10	178.4(2)
Ni1	N2	C13	C12	0.2(2)	C7	C8	C9	C18	–1.9(4)
Ni1	N2	C13	C14	–178.92(16)	C7	C6	C5	C4	0.5(4)
Ni1	N2	C17	C16	179.82(17)	C1	C12	C11	C10	–1.7(3)
N1	Ni1	C1	C12	179.37(18)	C1	C12	C11	C19	177.9(2)
N1	Ni1	C1	C8	–1.29(17)	C1	C8	C7	N1	–0.8(3)
N1	C7	C6	C5	–0.3(3)	C1	C8	C7	C6	177.8(2)
N1	C3	C4	C5	–0.1(4)	C1	C8	C9	C10	–2.3(3)
N2	Ni1	C1	C12	–0.18(17)	C1	C8	C9	C18	177.4(2)
N2	Ni1	C1	C8	179.16(18)	C3	N1	C7	C8	178.58(19)
N2	C13	C12	C1	–0.3(3)	C3	N1	C7	C6	–0.2(3)
N2	C13	C12	C11	–179.9(2)	C11	C12	C1	Ni1	179.99(16)
N2	C13	C14	C15	–1.4(3)	C11	C12	C1	C8	0.7(3)
N2	C17	C16	C15	–0.5(4)	C6	C5	C4	C3	–0.4(4)
C13	N2	C17	C16	0.0(3)	C9	C8	C7	N1	178.6(2)
C13	C12	C1	Ni1	0.3(2)	C9	C8	C7	C6	–2.8(4)
C13	C12	C1	C8	–178.97(19)	C9	C8	C1	Ni1	–177.95(16)
C13	C12	C11	C10	177.9(2)	C9	C8	C1	C12	1.4(3)
C13	C12	C11	C19	–2.5(4)	C18	C9	C10	C11	–178.4(2)
C13	C14	C15	C16	0.9(4)	C17	N2	C13	C12	–179.95(19)
C12	C13	C14	C15	179.6(2)	C17	N2	C13	C14	0.9(3)
C12	C11	C10	C9	0.7(3)	C17	C16	C15	C14	0.0(4)
C8	C7	C6	C5	–178.8(2)	C19	C11	C10	C9	–178.9(2)
C8	C9	C10	C11	1.3(3)	C14	C13	C12	C1	178.7(2)
C7	N1	C3	C4	0.3(3)	C14	C13	C12	C11	–0.9(4)

Table 7-163 Hydrogen Atom Coordinates (Å×10^4) and Isotropic Displacement Parameters (Å^2×10^3) for [Ni(Py(4,6MePh)Py)CN].

Atom	*x*	*y*	*z*	U(eq)
H3	8511.49	1017.81	5063.71	23
H6	9070.77	3714.57	3099.83	24
H5	9692.67	1529.28	3026.46	27
H4	9393.48	166.85	4016.6	26
H10	7395.59	7973.2	3850.71	22
H18A	9764.9	5782.03	3181.6	33
H18B	8563.99	7017.63	2944.12	33
H18C	7785.45	5608.72	2750.07	33
H17	6541.64	3536.88	7056.99	24
H16	5568.9	5002.83	7853.49	29

Atom	*x*	*y*	*z*	U(eq)
H19A	5074.27	8527.76	5159.28	34
H19B	6247.08	9222.6	4646.24	34
H19C	7051.57	8914.72	5506.57	34
H14	5803.4	7784.06	6326.5	26
H15	5193.08	7148.24	7480.18	30

7.3.24 [Pd(Py(4,6MePh)Py)CN]

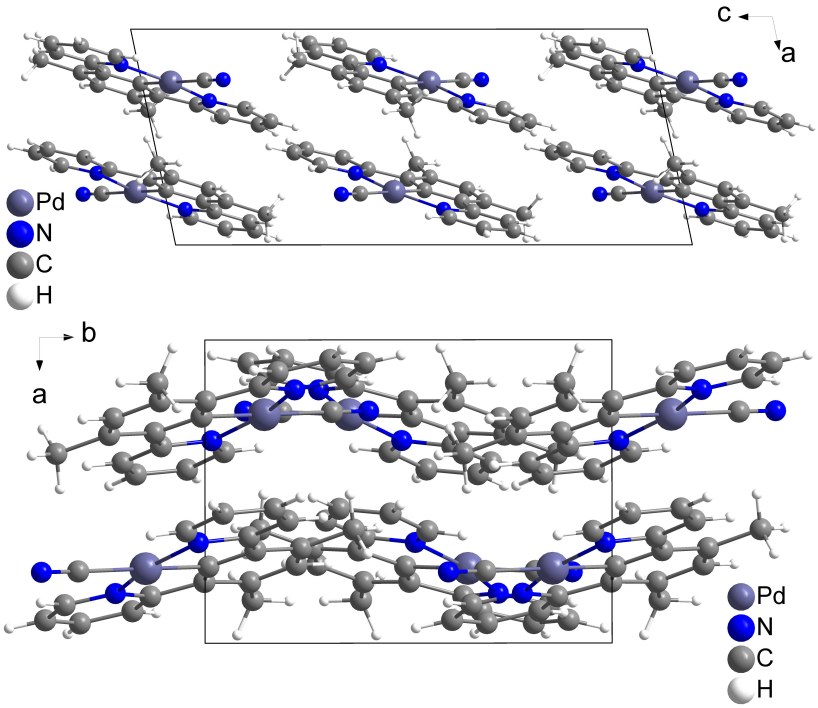

Figure 7-405 Crystal structure of [Pd(Py(4,6MePh)Py)CN] viewed along the crystallographic *b*- (top) and *c*-axis (bottom).

Table 7-164 Crystal data and structure refinement for [Pd(Py(4,6MePh)Py)CN].

Identification code	[Pd(Py(4,6MePh)Py)CN]
Empirical formula	$C_{19}H_{15}N_3Pd$
Formula weight	391.74
Temperature/K	100.0
Crystal system	monoclinic
Space group	$P2_1/c$
a/Å	7.8883(3)
b/Å	10.3760(4)
c/Å	18.4881(7)
α/°	90
β/°	101.7700(10)
γ/°	90
Volume/Å^3	1481.42(10)
Z	4
ρ_{calc}g/cm^3	1.756
μ/mm^{-1}	1.255
F(000)	784.0
Crystal size/mm^3	0.1 × 0.1 × 0.2
Radiation	MoKα (λ = 0.71073)
2Θ range for data collection/°	4.5 to 63.012

Index ranges	–11 ≤ h ≤ 11, –15 ≤ k ≤ 15, –26 ≤ l ≤ 26
Reflections collected	42103
Independent reflections	4865 [R_{int} = 0.0249, R_{sigma} = 0.0146]
Data/restraints/parameters	4865/0/211
Goodness-of-fit on F^2	1.076
Final R indexes [I>=2σ (I)]	R_1 = 0.0201, wR_2 = 0.0476
Final R indexes [all data]	R_1 = 0.0235, wR_2 = 0.0499
Largest diff. peak/hole / e Å^{-3}	0.79/–0.72

Table 7-165 Fractional Atomic Coordinates (×10^4) and Equivalent Isotropic Displacement Parameters (Å^2×10^3) for [Pd(Py(4,6MePh)Py)CN]. U_{eq} is defined as 1/3 of the trace of the orthogonalized U_{IJ} tensor.

Atom	*x*	*y*	*z*	U(eq)
Pd1	2463.1(2)	3541.7(2)	4439.6(2)	13.24(4)
N1	1644.8(14)	2796.2(11)	5329.0(6)	14.9(2)
N2	3320.2(14)	4834.3(11)	3765.6(6)	16.1(2)
C8	2024.4(16)	4981.6(12)	5716.2(7)	14.3(2)
N3	2346(2)	978.1(14)	3413.5(8)	30.2(3)
C12	3060.0(17)	6234.9(13)	4757.1(7)	15.6(2)
C7	1544.7(16)	3655.5(12)	5881.8(7)	14.6(2)
C13	3500.8(16)	6078.5(14)	4024.3(7)	16.4(2)
C9	2018.1(17)	6107.5(14)	6141.6(7)	16.3(2)
C1	2527.1(16)	5082.7(12)	5034.0(7)	13.8(2)
C3	1263.4(18)	1546.6(13)	5402.9(8)	18.4(2)
C2	2375.1(19)	1880.2(15)	3778.1(8)	20.3(3)
C11	3126.1(17)	7356.1(13)	5191.9(8)	17.2(2)
C14	4042.7(18)	7029.9(15)	3583.8(8)	21.6(3)
C6	1060.3(18)	3214.7(14)	6524.8(8)	19.2(2)
C4	764.3(19)	1070.3(15)	6027.6(8)	21.5(3)
C16	4273.1(19)	5442.9(17)	2666.1(8)	24.4(3)
C15	4431(2)	6702.0(16)	2909.5(9)	24.9(3)
C19	3748(2)	8652.5(13)	4986.4(9)	22.5(3)
C10	2586.2(17)	7246.6(13)	5864.4(8)	18.3(2)
C5	660.8(19)	1922.0(15)	6592.2(8)	21.1(3)
C18	1427.0(19)	6169.6(14)	6866.1(8)	19.8(3)
C17	3693.8(18)	4535.9(15)	3109.3(8)	20.6(3)

Table 7-166 Anisotropic Displacement Parameters (Å^2×10^3) for [Pd(Py(4,6MePh)Py)CN]. The Anisotropic displacement factor exponent takes the form: –2π^2[h^{2}a*^{2}U$_{11}$+2hka*b*U$_{12}$+…].

Atom	U_{11}	U_{22}	U_{33}	U_{23}	U_{13}	U_{12}
Pd1	14.31(5)	13.40(5)	12.17(5)	–0.03(3)	3.10(3)	–0.39(3)
N1	14.8(5)	15.1(5)	14.8(5)	1.5(4)	2.8(4)	–1.5(4)
N2	14.8(5)	18.6(5)	15.2(5)	2.8(4)	4.0(4)	0.6(4)
C8	13.1(5)	14.7(5)	14.9(5)	0.0(4)	2.8(4)	–0.6(4)
N3	46.3(8)	23.3(6)	22.2(6)	–3.4(5)	9.7(6)	–3.2(6)
C12	13.6(5)	16.5(6)	16.5(6)	1.8(4)	2.3(4)	–0.4(4)
C7	12.8(5)	16.0(6)	14.7(5)	0.9(4)	2.0(4)	–0.3(4)
C13	12.8(5)	18.6(6)	17.6(6)	3.4(5)	2.4(4)	0.4(4)
C9	14.4(5)	18.2(6)	15.5(6)	–1.0(5)	1.2(4)	1.7(5)
C1	13.0(5)	14.1(5)	13.8(5)	–0.8(4)	1.8(4)	0.0(4)
C3	20.1(6)	15.1(6)	19.6(6)	0.1(5)	3.3(5)	–2.6(5)

Atom	U_{11}	U_{22}	U_{33}	U_{23}	U_{13}	U_{12}
C2	24.6(6)	20.4(6)	16.5(6)	0.8(5)	5.6(5)	–0.5(5)
C11	14.8(5)	14.3(6)	21.1(6)	1.5(5)	0.4(4)	–0.2(4)
C14	20.4(6)	22.4(7)	22.0(7)	6.5(5)	4.1(5)	–2.4(5)
C6	20.3(6)	21.4(6)	16.7(6)	1.3(5)	6.0(5)	–0.7(5)
C4	22.1(6)	18.4(6)	23.9(7)	4.3(5)	4.4(5)	–4.1(5)
C16	22.2(6)	34.7(8)	17.8(6)	5.9(6)	7.8(5)	3.5(6)
C15	20.6(6)	32.0(8)	22.8(7)	11.9(6)	6.0(5)	–1.2(6)
C19	22.9(6)	14.6(6)	29.1(7)	2.1(5)	3.6(5)	–2.4(5)
C10	18.1(6)	15.7(6)	19.7(6)	–2.5(5)	0.7(5)	0.7(5)
C5	20.8(6)	23.5(7)	20.1(6)	6.1(5)	6.8(5)	–1.8(5)
C18	20.5(6)	22.1(6)	17.1(6)	–3.4(5)	4.5(5)	0.6(5)
C17	19.6(6)	26.1(7)	17.0(6)	1.2(5)	5.9(5)	3.2(5)

Table 7-167 Bond Lengths for [Pd(Py(4,6MePh)Py)CN].

Atom	Atom	Length/Å	Atom	Atom	Length/Å
Pd1	N1	2.0376(11)	C12	C11	1.4090(19)
Pd1	N2	2.0378(11)	C7	C6	1.3978(19)
Pd1	C1	1.9350(13)	C13	C14	1.4009(19)
Pd1	C2	2.1067(15)	C9	C10	1.398(2)
N1	C7	1.3707(17)	C9	C18	1.5070(19)
N1	C3	1.3443(17)	C3	C4	1.385(2)
N2	C13	1.3740(18)	C11	C19	1.5067(19)
N2	C17	1.3419(17)	C11	C10	1.399(2)
C8	C7	1.4756(18)	C14	C15	1.385(2)
C8	C9	1.4088(18)	C6	C5	1.389(2)
C8	C1	1.4011(18)	C4	C5	1.383(2)
N3	C2	1.151(2)	C16	C15	1.379(2)
C12	C13	1.4746(19)	C16	C17	1.385(2)
C12	C1	1.3986(18)			

Table 7-168 Bond Angles for [Pd(Py(4,6MePh)Py)CN].

Atom	Atom	Atom	Angle/˚	Atom	Atom	Atom	Angle/˚
N1	Pd1	N2	160.49(5)	N2	C13	C14	118.82(13)
N1	Pd1	C2	100.34(5)	C14	C13	C12	127.85(13)
N2	Pd1	C2	99.17(5)	C8	C9	C18	124.66(13)
C1	Pd1	N1	80.28(5)	C10	C9	C8	117.30(12)
C1	Pd1	N2	80.21(5)	C10	C9	C18	118.04(12)
C1	Pd1	C2	179.12(5)	C8	C1	Pd1	118.04(9)
C7	N1	Pd1	115.51(9)	C12	C1	Pd1	118.25(10)
C3	N1	Pd1	124.23(10)	C12	C1	C8	123.71(12)
C3	N1	C7	120.23(12)	N1	C3	C4	122.44(13)
C13	N2	Pd1	115.43(9)	N3	C2	Pd1	179.09(14)
C17	N2	Pd1	124.23(10)	C12	C11	C19	124.70(13)
C17	N2	C13	120.34(12)	C10	C11	C12	117.23(12)
C9	C8	C7	128.84(12)	C10	C11	C19	118.06(13)
C1	C8	C7	112.84(11)	C15	C14	C13	119.98(15)
C1	C8	C9	118.31(12)	C5	C6	C7	119.91(13)
C1	C12	C13	112.77(12)	C5	C4	C3	118.16(13)
C1	C12	C11	118.41(12)	C15	C16	C17	117.99(14)

Atom	Atom	Atom	Angle/°	Atom	Atom	Atom	Angle/°
C11	C12	C13	128.81(12)	C16	C15	C14	120.30(14)
N1	C7	C8	113.31(11)	C9	C10	C11	124.96(13)
N1	C7	C6	119.25(12)	C4	C5	C6	120.00(13)
C6	C7	C8	127.43(12)	N2	C17	C16	122.54(14)
N2	C13	C12	113.33(12)				

Table 7-169 Torsion Angles for [Pd(Py(4,6MePh)Py)CN].

A	B	C	D	Angle/°	A	B	C	D	Angle/°
Pd1	N1	C7	C8	1.15(14)	C9	C8	C7	N1	177.77(12)
Pd1	N1	C7	C6	–177.50(10)	C9	C8	C7	C6	–3.7(2)
Pd1	N1	C3	C4	177.86(10)	C9	C8	C1	Pd1	–178.12(9)
Pd1	N2	C13	C12	0.98(14)	C9	C8	C1	C12	1.42(19)
Pd1	N2	C13	C14	–178.41(10)	C1	C8	C7	N1	–1.53(16)
Pd1	N2	C17	C16	179.96(11)	C1	C8	C7	C6	176.99(13)
N1	C7	C6	C5	–1.0(2)	C1	C8	C9	C10	–2.56(18)
N1	C3	C4	C5	0.0(2)	C1	C8	C9	C18	176.77(12)
N2	C13	C14	C15	–1.7(2)	C1	C12	C13	N2	–0.73(16)
C8	C7	C6	C5	–179.46(13)	C1	C12	C13	C14	178.59(13)
C8	C9	C10	C11	1.3(2)	C1	C12	C11	C19	177.09(12)
C12	C13	C14	C15	178.97(13)	C1	C12	C11	C10	–2.37(18)
C12	C11	C10	C9	1.2(2)	C3	N1	C7	C8	179.33(12)
C7	N1	C3	C4	–0.1(2)	C3	N1	C7	C6	0.67(19)
C7	C8	C9	C10	178.18(12)	C3	C4	C5	C6	–0.3(2)
C7	C8	C9	C18	–2.5(2)	C11	C12	C13	N2	178.66(13)
C7	C8	C1	Pd1	1.26(14)	C11	C12	C13	C14	–2.0(2)
C7	C8	C1	C12	–179.20(12)	C11	C12	C1	Pd1	–179.33(9)
C7	C6	C5	C4	0.8(2)	C11	C12	C1	C8	1.14(19)
C13	N2	C17	C16	0.1(2)	C15	C16	C17	N2	–1.4(2)
C13	C12	C1	Pd1	0.14(15)	C19	C11	C10	C9	–178.30(13)
C13	C12	C1	C8	–179.40(12)	C18	C9	C10	C11	–178.06(12)
C13	C12	C11	C19	–2.3(2)	C17	N2	C13	C12	–179.19(12)
C13	C12	C11	C10	178.26(12)	C17	N2	C13	C14	1.42(19)
C13	C14	C15	C16	0.5(2)	C17	C16	C15	C14	1.0(2)

Table 7-170 Hydrogen Atom Coordinates (Å×10^4) and Isotropic Displacement Parameters (Å^2×10^3) for [Pd(Py(4,6MePh)Py)CN].

Atom	*x*	*y*	*z*	U(eq)
H3	1339.03	968.64	5012.2	22
H14	4144	7899.71	3747.45	26
H6	1004.36	3798.2	6915.21	23
H4	500.31	182.95	6067.1	26
H16	4553.31	5204.82	2208.38	29
H15	4806.98	7347.45	2613.47	30
H19A	4903.53	8562.5	4873.73	34
H19B	3800.55	9251.36	5400.27	34
H19C	2944.48	8986.68	4551.59	34
H10	2607.17	8003.87	6154.91	22
H5	316.59	1623.21	7026.17	25
H18A	268	5791.96	6806.36	30
H18B	1392.3	7070.65	7021.38	30

Atom	x	y	z	U(eq)
H18C	2236.31	5686.61	7241.9	30
H17	3555.64	3669.14	2942.25	25

7.3.25 [Ni(Py(Ph)Py)NO$_3$]

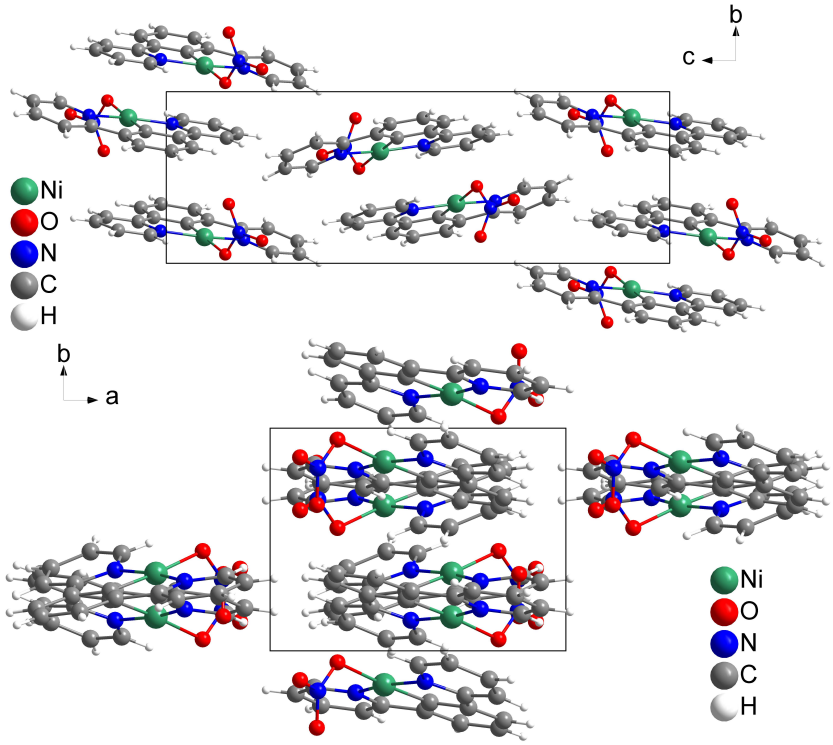

Figure 7-406 Crystal structure of [Ni(Py(Ph)Py)NO$_3$] viewed along the crystallographic *a*- (top) and *c*-axis (bottom).

Table 7-171 Crystal data and structure refinement for [Ni(Py(Ph)Py)NO$_3$].

Identification code	[Ni(Py(Ph)Py)NO$_3$]
Empirical formula	$C_{16}H_{11}N_3NiO_3$
Formula weight	351.99
Temperature/K	150.0
Crystal system	monoclinic
Space group	$P2_1/c$
a/Å	9.4575(9)
b/Å	7.0258(7)
c/Å	20.911(2)
α/°	90
β/°	99.352(3)
γ/°	90
Volume/Å^3	1371.0(2)
Z	4
ρ_{calc}g/cm^3	1.705
μ/mm^{-1}	1.435
F(000)	720.0
Crystal size/mm^3	0.4 × 0.1 × 0.1
Radiation	MoKα (λ = 0.71073)
2Θ range for data collection/°	6.346 to 49.37
Index ranges	–8 ≤ h ≤ 9, –8 ≤ k ≤ 8, –16 ≤ l ≤ 24
Reflections collected	4426

Independent reflections	1995 [R_{int} = 0.0370, R_{sigma} = 0.0559]
Data/restraints/parameters	1995/0/208
Goodness-of-fit on F^2	1.001
Final R indexes [I>=2σ (I)]	R_1 = 0.0393, wR_2 = 0.0821
Final R indexes [all data]	R_1 = 0.0622, wR_2 = 0.0905
Largest diff. peak/hole / e Å^{-3}	0.46/–0.38

Table 7-172 Fractional Atomic Coordinates (×10^4) and Equivalent Isotropic Displacement Parameters (Å^2×10^3) for [Ni(Py(Ph)Py)NO$_3$]. U_{eq} is defined as 1/3 of the trace of the orthogonalized U_{IJ} tensor.

Atom	*x*	*y*	*z*	U(eq)
Ni1	3858.2(5)	6523.9(6)	5757.8(2)	23.7(2)
O1	2278(3)	5517(4)	6171.0(12)	32.9(7)
N1	2892(3)	6878(4)	4885.4(14)	21.9(8)
N2	5240(3)	6373(4)	6536.8(14)	23.1(8)
O3	1581(3)	8450(4)	6242.3(14)	47.2(8)
N3	1616(4)	6796(5)	6440.9(17)	31.6(9)
O2	1014(3)	6311(4)	6901.9(15)	54.1(9)
C6	3744(4)	7426(5)	4443.5(18)	21.8(9)
C11	6704(4)	7531(5)	5818.4(18)	22.8(9)
C1	5398(4)	7313(5)	5414.4(17)	20.2(9)
C5	3167(4)	7695(5)	3803.3(19)	27.8(10)
C10	7894(5)	8119(5)	5559(2)	28.8(10)
C12	6597(4)	7002(5)	6490.5(18)	23.5(9)
C16	5016(4)	5639(5)	7108.5(18)	28.5(9)
C9	7743(4)	8457(5)	4895.1(19)	27.8(10)
C14	7409(5)	6285(5)	7602.6(19)	34.9(11)
C2	1492(4)	6646(5)	4680.7(19)	25.6(9)
C7	5239(4)	7672(5)	4748.5(17)	22.1(9)
C13	7669(4)	7020(5)	7018.4(19)	31.6(10)
C15	6071(5)	5544(6)	7640.5(18)	33.1(10)
C8	6431(4)	8245(5)	4493.7(19)	26.7(10)
C4	1720(5)	7437(5)	3597.5(19)	30.6(10)
C3	867(5)	6921(5)	4041.7(19)	31.6(11)

Table 7-173 Anisotropic Displacement Parameters (Å^2×10^3) for [Ni(Py(Ph)Py)NO$_3$]. The Anisotropic displacement factor exponent takes the form: –2π^2[h^{2}a*^{2}U$_{11}$+2hka*b*U$_{12}$+…].

Atom	U_{11}	U_{22}	U_{33}	U_{23}	U_{13}	U_{12}
Ni1	23.1(4)	28.1(3)	20.8(3)	–0.7(2)	6.4(2)	–0.6(2)
O1	32.2(18)	38.7(16)	30.8(16)	–6.3(14)	14.2(14)	–1.1(13)
N1	19(2)	24.3(17)	22.1(18)	–4.0(13)	3.8(17)	1.3(14)
N2	25(2)	23.5(16)	22.7(18)	–3.1(14)	9.4(16)	0.6(14)
O3	48(2)	44.1(18)	50(2)	–10.5(16)	8.9(17)	1.6(16)
N3	19(2)	47(2)	28(2)	–8.4(19)	2.1(18)	–6.4(18)
O2	43(2)	88(3)	36.4(19)	–8.2(17)	22.9(18)	–9.6(17)
C6	25(3)	19.6(18)	22(2)	–4.3(17)	8(2)	4.4(17)
C11	24(3)	21.0(19)	25(2)	0.8(17)	8(2)	3.6(18)
C1	17(2)	20.0(18)	24(2)	–4.7(16)	6.7(19)	2.6(16)
C5	32(3)	25(2)	27(2)	–2.8(18)	6(2)	2.1(18)
C10	22(3)	26(2)	38(3)	–4.1(18)	6(2)	0.0(17)
C12	21(3)	22(2)	29(2)	–6.4(16)	7(2)	1.2(16)

Atom	U_{11}	U_{22}	U_{33}	U_{23}	U_{13}	U_{12}
C16	32(3)	32(2)	23(2)	–0.7(19)	11(2)	–0.2(19)
C9	20(2)	30(2)	37(2)	2.6(19)	15(2)	1.8(18)
C14	39(3)	38(2)	26(2)	–6.4(19)	–2(2)	5(2)
C2	23(3)	26.0(19)	28(2)	–5.5(18)	6(2)	–1.0(18)
C7	23(3)	23.2(19)	21(2)	–3.4(17)	7(2)	5.6(17)
C13	28(3)	35(2)	31(2)	–2.9(19)	3(2)	–0.4(18)
C15	43(3)	37(2)	21(2)	–0.1(19)	10(2)	0(2)
C8	32(3)	27(2)	24(2)	2.7(17)	14(2)	5.0(18)
C4	38(3)	30(2)	21(2)	–3.9(18)	–1(2)	6(2)
C3	26(3)	36(2)	32(2)	–6.7(18)	0(2)	0.1(18)

Table 7-174 Bond Lengths for [Ni(Py(Ph)Py)NO_3].

Atom	Atom	Length/Å	Atom	Atom	Length/Å
Ni1	O1	1.975(3)	C11	C10	1.390(5)
Ni1	N1	1.919(3)	C11	C12	1.473(5)
Ni1	N2	1.918(3)	C1	C7	1.399(5)
Ni1	C1	1.812(4)	C5	C4	1.379(5)
O1	N3	1.278(4)	C10	C9	1.392(5)
N1	C6	1.376(5)	C12	C13	1.372(5)
N1	C2	1.334(5)	C16	C15	1.370(5)
N2	C12	1.376(5)	C9	C8	1.389(5)
N2	C16	1.350(4)	C14	C13	1.385(5)
O3	N3	1.233(4)	C14	C15	1.382(5)
N3	O2	1.244(4)	C2	C3	1.384(5)
C6	C5	1.374(5)	C7	C8	1.383(5)
C6	C7	1.463(5)	C4	C3	1.374(5)
C11	C1	1.388(5)			

Table 7-175 Bond Angles for [Ni(Py(Ph)Py)NO_3].

Atom	Atom	Atom	Angle/°	Atom	Atom	Atom	Angle/°
N1	Ni1	O1	100.67(13)	C10	C11	C12	129.3(4)
N2	Ni1	O1	93.91(12)	C11	C1	Ni1	119.1(3)
N2	Ni1	N1	165.39(14)	C11	C1	C7	121.8(4)
C1	Ni1	O1	175.57(14)	C7	C1	Ni1	119.1(3)
C1	Ni1	N1	82.68(15)	C6	C5	C4	120.2(4)
C1	Ni1	N2	82.72(15)	C11	C10	C9	118.8(4)
N3	O1	Ni1	113.7(2)	N2	C12	C11	111.0(3)
C6	N1	Ni1	115.8(2)	C13	C12	N2	121.5(3)
C2	N1	Ni1	125.7(3)	C13	C12	C11	127.5(4)
C2	N1	C6	118.6(3)	N2	C16	C15	122.7(4)
C12	N2	Ni1	115.9(2)	C8	C9	C10	121.4(4)
C16	N2	Ni1	126.2(3)	C15	C14	C13	119.1(4)
C16	N2	C12	117.9(3)	N1	C2	C3	122.6(4)
O3	N3	O1	120.1(4)	C1	C7	C6	110.6(3)
O3	N3	O2	121.9(4)	C8	C7	C6	131.0(3)
O2	N3	O1	117.9(4)	C8	C7	C1	118.3(4)
N1	C6	C7	111.7(3)	C12	C13	C14	119.5(4)
C5	C6	N1	120.6(3)	C16	C15	C14	119.2(4)
C5	C6	C7	127.7(4)	C7	C8	C9	120.2(4)

Atom	Atom	Atom	Angle/°	Atom	Atom	Atom	Angle/°
C1	C11	C10	119.5(3)	C3	C4	C5	119.1(4)
C1	C11	C12	111.1(3)	C4	C3	C2	118.9(4)

Table 7-176 Torsion Angles for [Ni(Py(Ph)Py)NO_3].

A	B	C	D	Angle/°	A	B	C	D	Angle/°
Ni1	O1	N3	O3	27.0(4)	C11	C10	C9	C8	0.9(5)
Ni1	O1	N3	O2	–153.3(3)	C11	C12	C13	C14	–173.3(3)
Ni1	N1	C6	C5	179.1(2)	C1	C11	C10	C9	–0.7(5)
Ni1	N1	C6	C7	–1.5(3)	C1	C11	C12	N2	1.9(4)
Ni1	N1	C2	C3	–179.8(3)	C1	C11	C12	C13	179.3(3)
Ni1	N2	C12	C11	–4.4(3)	C1	C7	C8	C9	–0.2(5)
Ni1	N2	C12	C13	178.0(3)	C5	C6	C7	C1	178.4(3)
Ni1	N2	C16	C15	178.5(3)	C5	C6	C7	C8	1.1(6)
Ni1	C1	C7	C6	3.3(4)	C5	C4	C3	C2	–1.1(5)
Ni1	C1	C7	C8	–179.0(2)	C10	C11	C1	Ni1	179.5(2)
N1	Ni1	C1	C11	177.1(3)	C10	C11	C1	C7	–0.1(5)
N1	Ni1	C1	C7	–3.3(3)	C10	C11	C12	N2	–175.8(3)
N1	C6	C5	C4	0.7(5)	C10	C11	C12	C13	1.6(6)
N1	C6	C7	C1	–1.0(4)	C10	C9	C8	C7	–0.5(5)
N1	C6	C7	C8	–178.3(3)	C12	N2	C16	C15	1.6(5)
N1	C2	C3	C4	0.6(5)	C12	C11	C1	Ni1	1.5(4)
N2	Ni1	C1	C11	–3.1(3)	C12	C11	C1	C7	–178.1(3)
N2	Ni1	C1	C7	176.5(3)	C12	C11	C10	C9	176.9(3)
N2	C12	C13	C14	3.9(5)	C16	N2	C12	C11	172.8(3)
N2	C16	C15	C14	2.3(6)	C16	N2	C12	C13	–4.7(5)
C6	N1	C2	C3	0.5(5)	C2	N1	C6	C5	–1.1(5)
C6	C5	C4	C3	0.5(5)	C2	N1	C6	C7	178.3(3)
C6	C7	C8	C9	176.9(3)	C7	C6	C5	C4	–178.6(3)
C11	C1	C7	C6	–177.2(3)	C13	C14	C15	C16	–3.1(5)
C11	C1	C7	C8	0.5(5)	C15	C14	C13	C12	0.2(5)

Table 7-177 Hydrogen Atom Coordinates (Å×10^4) and Isotropic Displacement Parameters (Å^2×10^3) for [Ni(Py(Ph)Py)NO_3].

Atom	*x*	*y*	*z*	U(eq)
H5	3767.05	8060.54	3501.61	33
H10	8794.42	8288.25	5828.97	35
H16	4089.84	5168.37	7143.29	34
H9	8555.24	8841.59	4713	33
H14	8140.01	6290.62	7972.47	42
H2	900.35	6277.92	4985.63	31
H13	8582.73	7531.79	6983.25	38
H15	5885.48	4976.3	8030.77	40
H8	6351.94	8493.29	4042.73	32
H4	1317.41	7612.14	3154.75	37
H3	–135.78	6756.52	3912.29	38

7.3.26 [Ni(Py(Ph)Py)OPh]

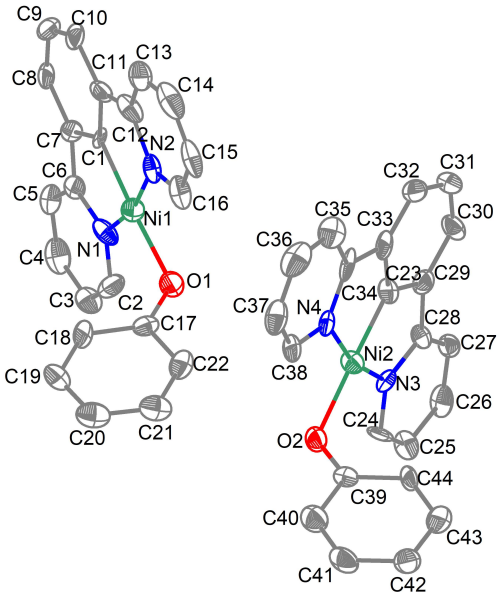

Figure 7-407 Asymmetric unit of 2[Ni(Py(Ph)Py)OPh]. Ellipsoids are shown with a 50% probability. Hydrogen atoms are omitted for clarity.

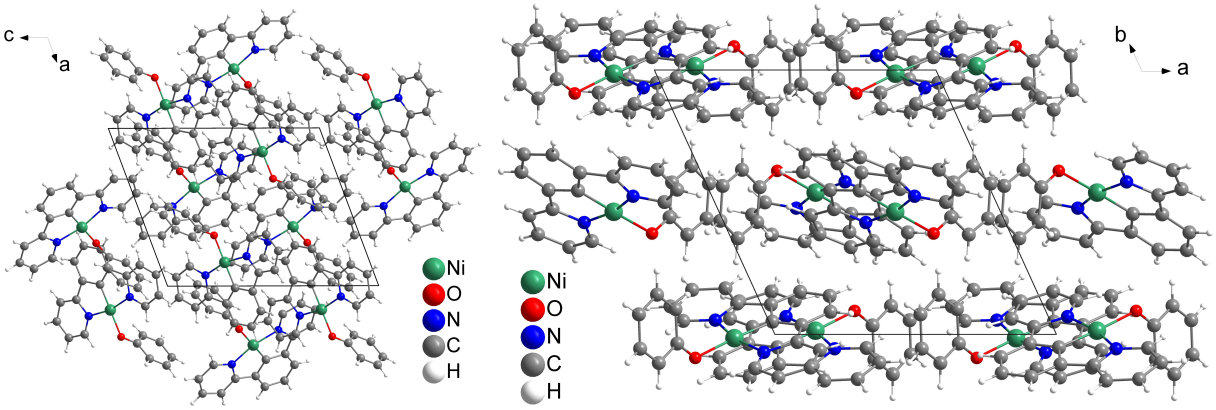

Figure 7-408 Crystal structure of 2[Ni(Py(Ph)Py)OPh] viewed along the crystallographic *b*- (left) and *c*-axis (right).

Table 7-178 Crystal data and structure refinement for 2[Ni(Py(Ph)Py)OPh].

Identification code	2[Ni(Py(Ph)Py)OPh]
Empirical formula	$C_{22}H_{16}N_2NiO$
Formula weight	383.08
Temperature/K	150.0
Crystal system	triclinic
Space group	$P\bar{1}$
a/Å	11.7795(10)
b/Å	11.7960(11)
c/Å	13.9308(12)
α/°	97.886(3)
β/°	105.937(3)
γ/°	110.959(3)
Volume/Å^3	1677.3(3)
Z	4
ρ_{calc}g/cm^3	1.517
μ/mm^{-1}	1.170

F(000)	792.0
Crystal size/mm^3	0.2 × 0.1 × 0.1
Radiation	MoKα (λ = 0.71073)
2Θ range for data collection/°	5.564 to 41.068
Index ranges	–11 ≤ h ≤ 11, –11 ≤ k ≤ 11, –13 ≤ l ≤ 13
Reflections collected	16069
Independent reflections	3362 [R_{int} = 0.1002, R_{sigma} = 0.0964]
Data/restraints/parameters	3362/0/469
Goodness-of-fit on F^2	1.095
Final R indexes [I>=2σ (I)]	R_1 = 0.0574, wR_2 = 0.1237
Final R indexes [all data]	R_1 = 0.1003, wR_2 = 0.1365
Largest diff. peak/hole / e Å^{-3}	0.57/–0.36

Table 7-179 Fractional Atomic Coordinates (×10^4) and Equivalent Isotropic Displacement Parameters (Å^2×10^3) for 2[Ni(Py(Ph)Py)OPh]. U_{eq} is defined as 1/3 of the trace of the orthogonalized U_{IJ} tensor.

Atom	*x*	*y*	*z*	U(eq)
Ni2	3742.1(11)	5363.1(10)	6994.5(8)	25.3(4)
Ni1	8501.6(11)	9858.1(10)	6871.0(8)	26.0(4)
O2	2731(6)	6184(5)	7382(4)	29.8(16)
O1	6790(6)	9112(5)	6899(5)	31.0(16)
N3	2802(7)	4775(6)	5541(5)	21.6(18)
N4	4961(7)	5768(6)	8352(6)	26.6(19)
N1	8113(9)	10541(7)	5731(5)	29(2)
N2	9318(8)	9325(6)	8015(5)	27.0(19)
C28	3186(8)	4030(8)	4972(7)	22(2)
C30	4992(9)	3206(8)	5390(7)	31(2)
C34	5871(9)	5262(8)	8437(7)	29(3)
C27	2561(9)	3525(8)	3937(7)	25(2)
C33	5701(9)	4540(8)	7428(7)	28(2)
C23	4664(9)	4558(8)	6650(8)	27(2)
C39	1844(9)	5567(9)	7741(6)	21(2)
C6	9159(9)	11168(8)	5445(7)	25(2)
C7	10342(9)	11130(8)	6061(7)	24(2)
C17	6385(9)	9656(9)	7545(7)	27(2)
C29	4307(9)	3880(8)	5635(7)	28(2)
C1	10118(8)	10485(8)	6834(7)	24(2)
C5	8990(10)	11744(8)	4646(6)	26(2)
C11	11097(10)	10356(8)	7524(7)	29(2)
C26	1509(10)	3775(8)	3426(7)	34(3)
C3	6743(10)	11061(9)	4412(7)	32(2)
C8	11586(10)	11610(8)	6030(7)	31(3)
C22	5414(9)	8922(9)	7863(7)	34(3)
C24	1781(9)	4994(8)	5045(7)	27(2)
C31	5999(9)	3190(8)	6147(8)	35(3)
C10	12342(10)	10857(8)	7497(7)	31(2)
C18	6878(9)	10960(9)	7950(7)	30(2)
C44	1191(9)	4253(8)	7465(7)	25(2)
C12	10671(11)	9714(8)	8254(7)	31(3)
C19	6457(10)	11502(10)	8634(8)	39(3)
C2	6963(10)	10513(8)	5220(7)	34(3)
C25	1128(9)	4527(8)	3990(7)	32(3)

Atom	*x*	*y*	*z*	U(eq)
C16	8744(10)	8716(8)	8594(7)	35(3)
C37	5890(10)	6697(9)	10176(8)	39(3)
C9	12568(9)	11458(9)	6748(9)	41(3)
C21	4983(10)	9462(11)	8543(8)	37(3)
C42	–98(9)	4298(10)	8555(7)	38(3)
C20	5495(10)	10761(11)	8929(8)	42(3)
C35	6793(10)	5496(9)	9368(8)	39(3)
C43	237(9)	3634(9)	7849(7)	39(3)
C4	7783(12)	11687(9)	4131(7)	41(3)
C32	6375(9)	3857(8)	7182(8)	34(3)
C15	9426(13)	8377(8)	9421(7)	42(3)
C38	4993(9)	6468(8)	9225(8)	34(3)
C41	548(10)	5615(10)	8835(7)	39(3)
C13	11340(10)	9405(9)	9060(8)	43(3)
C40	1496(10)	6225(9)	8446(7)	37(3)
C36	6796(10)	6213(10)	10251(8)	47(3)
C14	10730(14)	8748(10)	9659(8)	49(3)

Table 7-180 Anisotropic Displacement Parameters ($Å^2×10^3$) for 2[Ni(Py(Ph)Py)OPh]. The Anisotropic displacement factor exponent takes the form: $–2π^2[h^2a^{*2}U_{11}+2hka^*b^*U_{12}+…]$.

Atom	U_{11}	U_{22}	U_{33}	U_{23}	U_{13}	U_{12}
Ni2	27.5(8)	26.3(8)	23.2(8)	5.1(6)	7.7(6)	13.8(6)
Ni1	27.0(8)	26.3(8)	25.5(8)	6.7(6)	10.7(6)	10.7(6)
O2	33(4)	22(4)	36(4)	4(3)	18(3)	10(3)
O1	36(4)	28(4)	36(4)	11(3)	20(3)	14(3)
N3	16(5)	19(5)	23(5)	5(4)	6(4)	0(4)
N4	24(5)	12(4)	33(5)	0(4)	8(4)	0(4)
N1	44(6)	30(5)	19(5)	3(4)	11(5)	25(5)
N2	39(6)	15(5)	22(5)	0(4)	9(4)	9(4)
C28	30(6)	19(6)	19(6)	9(5)	9(5)	13(5)
C30	43(7)	26(6)	39(7)	12(5)	28(6)	20(6)
C34	29(7)	14(6)	13(7)	–1(5)	–12(5)	–8(5)
C27	28(6)	22(6)	29(7)	8(5)	14(5)	11(5)
C33	32(7)	13(6)	35(7)	13(5)	11(6)	1(5)
C23	34(7)	18(6)	37(7)	21(5)	16(6)	13(5)
C39	21(6)	31(7)	9(5)	–1(5)	0(5)	14(6)
C6	30(7)	22(6)	23(6)	–2(5)	16(6)	9(5)
C7	25(7)	24(6)	24(6)	0(5)	17(5)	8(5)
C17	20(6)	32(7)	38(7)	25(6)	12(5)	14(6)
C29	26(6)	23(6)	33(7)	4(5)	15(5)	4(5)
C1	13(6)	12(6)	29(6)	–17(5)	6(5)	–5(5)
C5	36(7)	22(6)	12(5)	2(5)	6(5)	5(5)
C11	26(7)	25(6)	31(7)	–6(5)	1(6)	16(6)
C26	45(7)	27(6)	19(6)	–4(5)	10(6)	6(5)
C3	37(7)	34(6)	27(6)	12(5)	6(5)	21(6)
C8	32(7)	12(6)	47(7)	8(5)	20(6)	4(5)
C22	31(7)	29(6)	30(7)	5(5)	4(6)	5(6)
C24	25(6)	32(6)	40(7)	13(5)	17(6)	24(5)
C31	30(7)	30(7)	51(8)	11(6)	18(6)	18(5)
C10	22(7)	17(6)	35(7)	1(5)	–7(5)	3(5)
C18	34(7)	17(7)	41(7)	18(5)	20(6)	5(5)

Atom	U_{11}	U_{22}	U_{33}	U_{23}	U_{13}	U_{12}
C44	31(6)	15(6)	25(6)	–4(5)	10(5)	8(5)
C12	47(8)	32(7)	16(6)	4(5)	1(6)	28(6)
C19	43(8)	33(7)	47(7)	4(6)	18(6)	23(6)
C2	21(7)	37(7)	34(7)	–2(6)	12(6)	3(5)
C25	38(7)	29(6)	18(6)	1(5)	–4(5)	16(5)
C16	57(7)	22(6)	29(6)	8(5)	19(6)	16(6)
C37	43(8)	26(6)	26(7)	2(5)	–1(6)	2(6)
C9	21(7)	29(7)	61(8)	–11(6)	17(6)	2(5)
C21	40(7)	50(9)	39(7)	26(6)	23(6)	26(6)
C42	29(7)	37(8)	39(7)	–5(5)	9(5)	12(6)
C20	40(8)	57(9)	42(7)	21(7)	17(6)	29(7)
C35	44(7)	37(7)	33(7)	14(6)	11(6)	14(6)
C43	29(7)	33(7)	42(7)	–3(6)	5(6)	7(6)
C4	63(9)	32(7)	22(6)	3(5)	13(7)	17(6)
C32	24(6)	29(6)	53(8)	17(6)	13(6)	12(5)
C15	73(10)	19(6)	34(7)	8(5)	15(7)	22(6)
C38	34(7)	17(6)	41(7)	–8(5)	11(6)	5(5)
C41	42(7)	42(8)	31(7)	–5(6)	9(6)	25(6)
C13	40(7)	28(7)	45(8)	–13(6)	7(7)	11(6)
C40	40(7)	37(7)	36(7)	6(6)	14(6)	19(6)
C36	36(8)	48(8)	36(8)	19(6)	–6(6)	5(6)
C14	74(10)	35(7)	37(7)	5(6)	4(7)	34(7)

Table 7-181 Bond Lengths for 2[Ni(Py(Ph)Py)OPh].

Atom	Atom	Length/Å	Atom	Atom	Length/Å
Ni2	O2	1.918(6)	C6	C5	1.386(11)
Ni2	N3	1.909(7)	C7	C1	1.430(12)
Ni2	N4	1.907(7)	C7	C8	1.385(12)
Ni2	C23	1.792(9)	C17	C22	1.389(12)
Ni1	O1	1.904(6)	C17	C18	1.402(12)
Ni1	N1	1.896(7)	C1	C11	1.354(12)
Ni1	N2	1.929(7)	C5	C4	1.377(12)
Ni1	C1	1.798(9)	C11	C10	1.385(12)
O2	C39	1.310(10)	C11	C12	1.443(13)
O1	C17	1.322(10)	C26	C25	1.376(11)
N3	C28	1.376(10)	C3	C2	1.383(12)
N3	C24	1.344(10)	C3	C4	1.376(12)
N4	C34	1.387(11)	C8	C9	1.390(12)
N4	C38	1.356(10)	C22	C21	1.375(12)
N1	C6	1.387(11)	C24	C25	1.383(11)
N1	C2	1.332(11)	C31	C32	1.408(12)
N2	C12	1.416(11)	C10	C9	1.372(12)
N2	C16	1.318(10)	C18	C19	1.372(12)
C28	C27	1.357(11)	C44	C43	1.389(12)
C28	C29	1.474(12)	C12	C13	1.359(13)
C30	C29	1.391(11)	C19	C20	1.365(13)
C30	C31	1.362(12)	C16	C15	1.407(12)
C34	C33	1.461(12)	C37	C38	1.369(12)
C34	C35	1.360(12)	C37	C36	1.366(13)
C27	C26	1.401(12)	C21	C20	1.391(12)

Atom	Atom	Length/Å	Atom	Atom	Length/Å
C33	C23	1.402(12)	C42	C43	1.399(12)
C33	C32	1.389(12)	C42	C41	1.403(12)
C23	C29	1.392(12)	C35	C36	1.392(13)
C39	C44	1.401(11)	C15	C14	1.364(13)
C39	C40	1.405(12)	C41	C40	1.387(13)
C6	C7	1.441(12)	C13	C14	1.385(13)

Table 7-182 Bond Angles for 2[Ni(Py(Ph)Py)OPh].

Atom	Atom	Atom	Angle/°	Atom	Atom	Atom	Angle/°
N3	Ni2	O2	98.4(3)	C8	C7	C6	131.6(9)
N4	Ni2	O2	96.3(3)	C8	C7	C1	118.1(8)
N4	Ni2	N3	165.2(3)	O1	C17	C22	119.8(9)
C23	Ni2	O2	178.2(3)	O1	C17	C18	124.1(9)
C23	Ni2	N3	82.1(4)	C22	C17	C18	116.1(9)
C23	Ni2	N4	83.2(4)	C30	C29	C28	130.4(9)
O1	Ni1	N2	96.4(3)	C30	C29	C23	120.2(9)
N1	Ni1	O1	97.7(3)	C23	C29	C28	109.4(8)
N1	Ni1	N2	166.0(4)	C7	C1	Ni1	118.1(7)
C1	Ni1	O1	177.1(3)	C11	C1	Ni1	120.9(8)
C1	Ni1	N1	83.8(4)	C11	C1	C7	121.0(9)
C1	Ni1	N2	82.2(4)	C4	C5	C6	120.2(9)
C39	O2	Ni2	117.7(5)	C1	C11	C10	120.4(9)
C17	O1	Ni1	122.5(6)	C1	C11	C12	112.0(9)
C28	N3	Ni2	116.4(6)	C10	C11	C12	127.6(9)
C24	N3	Ni2	125.3(6)	C25	C26	C27	119.0(9)
C24	N3	C28	118.3(7)	C4	C3	C2	117.7(9)
C34	N4	Ni2	115.7(6)	C7	C8	C9	119.4(9)
C38	N4	Ni2	126.1(7)	C21	C22	C17	121.1(9)
C38	N4	C34	118.2(8)	N3	C24	C25	122.6(8)
C6	N1	Ni1	115.3(6)	C30	C31	C32	121.2(9)
C2	N1	Ni1	126.4(7)	C9	C10	C11	119.3(9)
C2	N1	C6	118.3(8)	C19	C18	C17	123.0(9)
C12	N2	Ni1	114.2(6)	C43	C44	C39	122.2(8)
C16	N2	Ni1	126.0(7)	N2	C12	C11	110.7(8)
C16	N2	C12	119.7(8)	C13	C12	N2	118.7(9)
N3	C28	C29	111.1(8)	C13	C12	C11	130.5(11)
C27	C28	N3	121.5(8)	C20	C19	C18	119.8(9)
C27	C28	C29	127.4(8)	N1	C2	C3	123.9(9)
C31	C30	C29	119.9(9)	C26	C25	C24	118.9(9)
N4	C34	C33	111.0(8)	N2	C16	C15	121.8(10)
C35	C34	N4	120.8(9)	C36	C37	C38	118.9(10)
C35	C34	C33	128.2(10)	C10	C9	C8	121.7(9)
C28	C27	C26	119.7(8)	C22	C21	C20	121.2(9)
C23	C33	C34	110.8(9)	C43	C42	C41	117.0(9)
C32	C33	C34	129.3(9)	C19	C20	C21	118.8(9)
C32	C33	C23	119.9(9)	C34	C35	C36	119.6(10)
C33	C23	Ni2	119.2(7)	C44	C43	C42	121.3(9)
C29	C23	Ni2	120.8(7)	C3	C4	C5	120.0(9)
C29	C23	C33	119.8(8)	C33	C32	C31	119.0(9)
O2	C39	C44	123.9(8)	C14	C15	C16	118.8(10)

Atom	Atom	Atom	Angle/°	Atom	Atom	Atom	Angle/°
O2	C39	C40	120.0(9)	N4	C38	C37	122.5(9)
C44	C39	C40	116.1(9)	C40	C41	C42	121.3(9)
N1	C6	C7	112.5(8)	C12	C13	C14	121.3(10)
C5	C6	N1	119.9(8)	C41	C40	C39	122.1(9)
C5	C6	C7	127.6(9)	C37	C36	C35	120.0(9)
C1	C7	C6	110.2(8)	C15	C14	C13	119.5(10)

Table 7-183 Torsion Angles for 2[Ni(Py(Ph)Py)OPh].

A	B	C	D	Angle/°	A	B	C	D	Angle/°
Ni2	O2	C39	C44	–29.0(10)	C33	C23	C29	C30	–1.2(13)
Ni2	O2	C39	C40	151.1(6)	C23	C33	C32	C31	–0.1(13)
Ni2	N3	C28	C27	177.8(6)	C39	C44	C43	C42	–1.7(14)
Ni2	N3	C28	C29	–1.9(9)	C6	N1	C2	C3	0.8(12)
Ni2	N3	C24	C25	–179.1(6)	C6	C7	C1	Ni1	1.2(9)
Ni2	N4	C34	C33	1.7(9)	C6	C7	C1	C11	–178.5(7)
Ni2	N4	C34	C35	179.6(7)	C6	C7	C8	C9	178.4(8)
Ni2	N4	C38	C37	178.7(7)	C6	C5	C4	C3	0.2(13)
Ni2	C23	C29	C28	3.6(10)	C7	C6	C5	C4	179.8(8)
Ni2	C23	C29	C30	–176.6(6)	C7	C1	C11	C10	0.5(12)
Ni1	O1	C17	C22	–152.1(6)	C7	C1	C11	C12	178.1(7)
Ni1	O1	C17	C18	27.7(11)	C7	C8	C9	C10	–0.7(13)
Ni1	N1	C6	C7	2.3(8)	C17	C22	C21	C20	0.5(14)
Ni1	N1	C6	C5	–177.5(6)	C17	C18	C19	C20	–1.5(14)
Ni1	N1	C2	C3	177.9(6)	C29	C28	C27	C26	–179.6(8)
Ni1	N2	C12	C11	–3.8(8)	C29	C30	C31	C32	–0.6(13)
Ni1	N2	C12	C13	178.8(6)	C1	Ni1	N1	C6	–1.3(6)
Ni1	N2	C16	C15	–179.3(6)	C1	Ni1	N1	C2	–178.6(7)
Ni1	C1	C11	C10	–179.1(6)	C1	C7	C8	C9	–0.5(12)
Ni1	C1	C11	C12	–1.6(10)	C1	C11	C10	C9	–1.7(13)
O2	C39	C44	C43	–178.7(8)	C1	C11	C12	N2	3.4(10)
O2	C39	C40	C41	179.0(8)	C1	C11	C12	C13	–179.7(9)
O1	Ni1	N1	C6	–178.8(5)	C5	C6	C7	C1	177.7(8)
O1	Ni1	N1	C2	4.0(7)	C5	C6	C7	C8	–1.2(14)
O1	C17	C22	C21	179.3(8)	C11	C10	C9	C8	1.9(13)
O1	C17	C18	C19	–178.8(8)	C11	C12	C13	C14	–178.2(9)
N3	Ni2	C23	C33	–179.1(7)	C8	C7	C1	Ni1	–179.8(6)
N3	Ni2	C23	C29	–3.7(7)	C8	C7	C1	C11	0.6(12)
N3	C28	C27	C26	0.8(13)	C22	C17	C18	C19	1.0(13)
N3	C28	C29	C30	179.3(8)	C22	C21	C20	C19	–0.9(14)
N3	C28	C29	C23	–0.9(10)	C24	N3	C28	C27	0.1(12)
N3	C24	C25	C26	2.2(13)	C24	N3	C28	C29	–179.5(7)
N4	Ni2	C23	C33	2.3(7)	C31	C30	C29	C28	–179.0(9)
N4	Ni2	C23	C29	177.7(7)	C31	C30	C29	C23	1.2(13)
N4	C34	C33	C23	0.0(10)	C10	C11	C12	N2	–179.3(8)
N4	C34	C33	C32	–177.7(8)	C10	C11	C12	C13	–2.3(16)
N4	C34	C35	C36	2.4(13)	C18	C17	C22	C21	–0.5(13)
N1	Ni1	C1	C7	0.0(6)	C18	C19	C20	C21	1.4(14)
N1	Ni1	C1	C11	179.7(7)	C44	C39	C40	C41	–0.9(13)
N1	C6	C7	C1	–2.2(9)	C12	N2	C16	C15	–3.3(12)
N1	C6	C7	C8	179.0(8)	C12	C11	C10	C9	–178.9(8)

A	B	C	D	Angle/°	A	B	C	D	Angle/°
N1	C6	C5	C4	–0.4(12)	C12	C13	C14	C15	1.6(14)
N2	Ni1	N1	C6	–2.1(15)	C2	N1	C6	C7	179.8(7)
N2	Ni1	N1	C2	–179.3(9)	C2	N1	C6	C5	–0.1(11)
N2	Ni1	C1	C7	179.9(7)	C2	C3	C4	C5	0.4(13)
N2	Ni1	C1	C11	–0.5(7)	C16	N2	C12	C11	179.7(7)
N2	C12	C13	C14	–1.5(13)	C16	N2	C12	C13	2.4(12)
N2	C16	C15	C14	3.4(13)	C16	C15	C14	C13	–2.4(14)
C28	N3	C24	C25	–1.7(12)	C42	C41	C40	C39	1.1(14)
C28	C27	C26	C25	–0.3(13)	C35	C34	C33	C23	–177.7(9)
C30	C31	C32	C33	0.0(13)	C35	C34	C33	C32	4.6(15)
C34	N4	C38	C37	0.6(12)	C43	C42	C41	C40	–1.5(13)
C34	C33	C23	Ni2	–1.9(10)	C4	C3	C2	N1	–0.9(13)
C34	C33	C23	C29	–177.3(8)	C32	C33	C23	Ni2	176.1(6)
C34	C33	C32	C31	177.5(8)	C32	C33	C23	C29	0.7(12)
C34	C35	C36	C37	–1.2(14)	C38	N4	C34	C33	–179.9(7)
C27	C28	C29	C30	–0.3(15)	C38	N4	C34	C35	–2.1(12)
C27	C28	C29	C23	179.5(8)	C38	C37	C36	C35	–0.3(14)
C27	C26	C25	C24	–1.2(13)	C41	C42	C43	C44	1.7(13)
C33	C34	C35	C36	179.9(9)	C40	C39	C44	C43	1.2(12)
C33	C23	C29	C28	178.9(7)	C36	C37	C38	N4	0.6(14)

Table 7-184 Hydrogen Atom Coordinates (Å×10^4) and Isotropic Displacement Parameters (Å^2×10^3) for 2[Ni(Py(Ph)Py)OPh].

Atom	*x*	*y*	*z*	U(eq)
H30	4756.68	2756.65	4694.37	37
H27	2834.98	3004.39	3561.51	30
H5	9707.55	12178.48	4453.11	31
H26	1065.59	3429.37	2702.05	41
H3	5903.4	11007.71	4062.77	38
H8	11766.73	12037.63	5523.41	37
H22	5041.92	8032.37	7607.19	41
H24	1495.89	5489.25	5435.8	32
H31	6455.77	2720.22	5974.2	42
H10	13033.03	10786.04	7993.12	37
H18	7533.1	11493.37	7740.89	36
H44	1407.57	3769.32	7001.22	30
H19	6832.72	12390.14	8901.06	46
H2	6250.43	10090.84	5423.79	41
H25	427.63	4722.68	3658.43	38
H16	7844.93	8498.48	8449.37	42
H37	5881.85	7183.91	10774.67	46
H9	13418.36	11779.4	6719.97	49
H21	4322.64	8937.92	8752.72	44
H42	–733	3875.69	8831.98	45
H20	5181.61	11125.25	9390.7	51
H35	7431.76	5171.55	9414.85	47
H43	–197.5	2742.65	7626.54	47
H4	7669.11	12079.18	3582.1	49
H32	7078.76	3839.38	7704.34	41
H15	8986.77	7898.86	9807.37	50
H38	4369.09	6811.72	9174.05	41

Atom	*x*	*y*	*z*	U(eq)
H41	331.28	6097.12	9299.98	46
H13	12244.32	9643.6	9216.25	52
H40	1923.18	7117.63	8662.1	45
H36	7427.21	6365.53	10904.41	57
H14	11216.22	8558.05	10230.07	59

7.3.27 [Ni(Py(Ph)Py)O*t*Bu]

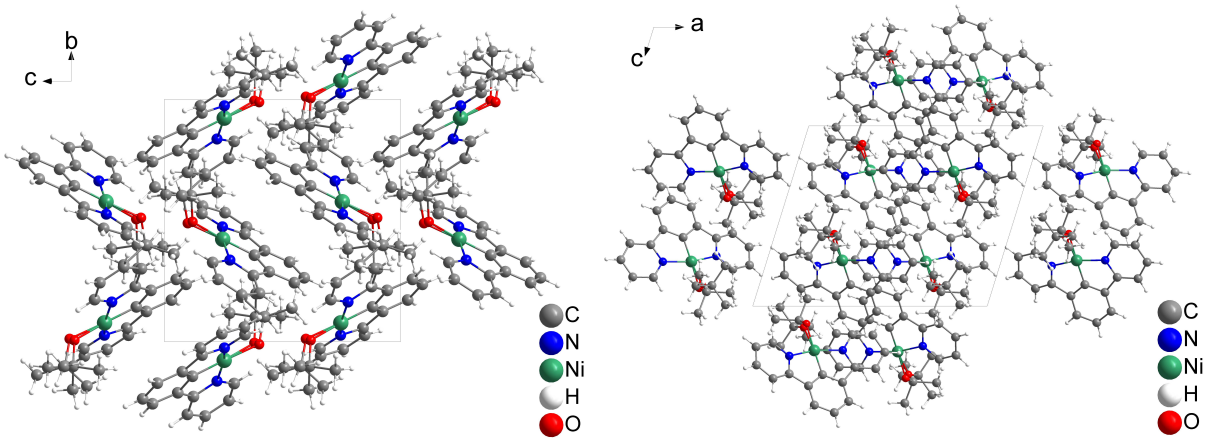

Figure 7-409 Crystal structure of [Ni(Py(Ph)Py)O*t*Bu] viewed along the crysallographic *a*- (left) and *b*-axis (right).

Table 7-185 Crystal data and structure refinement for [Ni(Py(Ph)Py)O*t*Bu].

Identification code	[Ni(Py(Ph)Py)O*t*Bu]
Empirical formula	$C_{20}N_2NiOH_{20}$
Formula weight	363.09
Temperature/K	150(2)
Crystal system	monoclinic
Space group	$P2_1/c$
a/Å	14.9647(10)
b/Å	11.7733(8)
c/Å	12.0344(8)
α/°	90
β/°	107.280(2)
γ/°	90
Volume/Å^3	2024.6(2)
Z	4
ρ_{calc}g/cm^3	1.191
μ/mm^{-1}	0.965
F(000)	760.0
Radiation	MoKα (λ = 0.71073)
2Θ range for data collection/°	5.164 to 50.71
Index ranges	–18 ≤ h ≤ 18, –14 ≤ k ≤ 14, –14 ≤ l ≤ 14
Reflections collected	24164
Independent reflections	3702 [R_{int} = 0.0868, R_{sigma} = 0.0723]
Data/restraints/parameters	3702/154/263
Goodness-of-fit on F^2	1.122
Final R indexes [I>=2σ (I)]	R_1 = 0.0763, wR_2 = 0.1249
Final R indexes [all data]	R_1 = 0.1023, wR_2 = 0.1351
Largest diff. peak/hole / e Å^{-3}	0.45/–0.35

Table 7-186 Fractional Atomic Coordinates (×10^4) and Equivalent Isotropic Displacement Parameters (Å^2×10^3) for [Ni(Py(Ph)Py)O*t*Bu]. U_{eq} is defined as 1/3 of the trace of the orthogonalized U_{IJ} tensor.

Atom	*x*	*y*	*z*	U(eq)
C1	6118(3)	3567(4)	6187(4)	26.1(11)
N2	5575(3)	4738(3)	7541(3)	26.3(9)
Ni1	6788.5(4)	4226.3(5)	7532.2(5)	26.8(2)
C6	5158(3)	3755(4)	5760(4)	27.2(11)
C12	4835(3)	4443(4)	6594(4)	27.2(11)
C4	5108(4)	2635(4)	4081(4)	32.2(12)
C16	5382(4)	5286(4)	8412(4)	33.7(12)
C13	3927(4)	4737(4)	6524(4)	34.0(12)
C2	6563(3)	2885(4)	5567(4)	27.3(11)
C5	4644(3)	3283(4)	4701(4)	29.1(11)
C7	7547(3)	2728(4)	6230(4)	30.1(11)
C3	6060(3)	2432(4)	4498(4)	31.4(12)
N1	7782(3)	3366(3)	7226(3)	31.5(10)
C11	8175(4)	1993(5)	5974(5)	42.2(14)
C14	3760(4)	5325(4)	7432(5)	39.3(13)
C15	4494(4)	5598(4)	8386(5)	39.6(13)
C8	8659(4)	3267(5)	7955(5)	42.2(14)
C9	9320(4)	2568(5)	7731(5)	53.6(16)
C10	9062(4)	1924(5)	6725(6)	55.3(17)
O1_1	7478(15)	4889(12)	9009(17)	34(4)
C1_1	7836(7)	6011(10)	9206(8)	40(3)
C2_1	7304(10)	6836(12)	8281(11)	66(4)
C3_1	8859(7)	6028(10)	9264(11)	56(3)
C4_1	7774(8)	6383(9)	10398(8)	68(3)
O1_2	7540(20)	4945(18)	8810(30)	29(5)
C1_2	7984(11)	6018(14)	8855(12)	35(4)
C2_2	8819(12)	6069(18)	9934(13)	64(6)
C3_2	7310(17)	6980(20)	8880(20)	89(9)
C4_2	8289(11)	6176(13)	7763(11)	58(5)

Table 7-187 Anisotropic Displacement Parameters (Å^2×10^3) for [Ni(Py(Ph)Py)O*t*Bu]. The Anisotropic displacement factor exponent takes the form: $-2\pi^2[h^2a^{*2}U_{11}+2hka^*b^*U_{12}+\ldots]$.

Atom	U_{11}	U_{22}	U_{33}	U_{23}	U_{13}	U_{12}
C1	37(3)	18(2)	25(3)	5(2)	10(2)	–2(2)
N2	36(2)	21(2)	22(2)	2.1(17)	9.4(19)	–2.6(18)
Ni1	28.9(3)	24.2(3)	25.5(3)	–1.6(3)	5.5(2)	–1.6(3)
C6	39(3)	18(2)	25(3)	3(2)	11(2)	–2(2)
C12	37(3)	19(2)	26(3)	1(2)	9(2)	0(2)
C4	43(3)	28(3)	20(3)	–2(2)	2(2)	–6(2)
C16	49(3)	28(3)	26(3)	0(2)	13(2)	4(2)
C13	34(3)	27(3)	38(3)	1(2)	7(2)	–3(2)
C2	37(3)	20(2)	27(3)	2(2)	13(2)	–6(2)
C5	30(3)	21(2)	32(3)	3(2)	3(2)	–2(2)
C7	35(3)	27(3)	32(3)	–1(2)	15(2)	–3(2)
C3	43(3)	21(2)	33(3)	–3(2)	15(2)	–3(2)
N1	30(2)	30(2)	35(2)	0.6(19)	10(2)	–1.2(19)

Atom	U_{11}	U_{22}	U_{33}	U_{23}	U_{13}	U_{12}
C11	39(3)	40(3)	49(4)	–4(3)	15(3)	–4(3)
C14	35(3)	37(3)	50(4)	–1(3)	19(3)	11(3)
C15	53(4)	34(3)	36(3)	–5(2)	21(3)	7(3)
C8	34(3)	42(3)	47(3)	–4(3)	7(3)	–4(3)
C9	28(3)	67(4)	61(4)	–9(3)	4(3)	9(3)
C10	41(4)	56(4)	71(4)	–11(3)	21(3)	10(3)
O1_1	47(8)	31(5)	18(5)	–8(4)	–1(5)	–4(4)
C1_1	41(5)	34(5)	39(6)	–13(4)	3(5)	–2(4)
C2_1	59(8)	35(7)	83(9)	14(7)	–9(7)	–12(6)
C3_1	42(6)	43(6)	80(9)	–24(7)	14(6)	–10(4)
C4_1	75(8)	65(7)	64(6)	–38(5)	23(6)	–10(6)
O1_2	27(8)	28(7)	31(12)	1(6)	8(7)	4(6)
C1_2	45(10)	17(7)	34(7)	–8(6)	–4(6)	–1(6)
C2_2	64(11)	65(13)	47(9)	–12(11)	–9(8)	–21(9)
C3_2	69(14)	38(10)	160(30)	–6(17)	39(17)	16(10)
C4_2	66(11)	52(10)	49(8)	–6(7)	10(7)	–30(8)

Table 7-188 Bond Lengths for [Ni(Py(Ph)Py)O*t*Bu].

Atom	Atom	Length/Å	Atom	Atom	Length/Å
C1	Ni1	1.807(5)	C2	C3	1.389(6)
C1	C6	1.392(6)	C7	N1	1.369(6)
C1	C2	1.393(6)	C7	C11	1.379(7)
N2	Ni1	1.916(4)	N1	C8	1.349(6)
N2	C12	1.377(6)	C11	C10	1.368(7)
N2	C16	1.334(6)	C14	C15	1.370(7)
Ni1	N1	1.924(4)	C8	C9	1.374(7)
Ni1	O1_1	1.934(18)	C9	C10	1.382(8)
Ni1	O1_2	1.82(3)	O1_1	C1_1	1.419(10)
C6	C12	1.478(6)	C1_1	C2_1	1.513(11)
C6	C5	1.393(6)	C1_1	C3_1	1.512(10)
C12	C13	1.380(6)	C1_1	C4_1	1.529(10)
C4	C5	1.388(7)	O1_2	C1_2	1.424(13)
C4	C3	1.383(7)	C1_2	C2_2	1.512(13)
C16	C15	1.371(7)	C1_2	C3_2	1.522(13)
C13	C14	1.377(7)	C1_2	C4_2	1.525(13)
C2	C7	1.463(7)			

Table 7-189 Bond Angles for [Ni(Py(Ph)Py)O*t*Bu].

Atom	Atom	Atom	Angle/°	Atom	Atom	Atom	Angle/°
C6	C1	Ni1	120.0(4)	N1	C7	C2	111.4(4)
C6	C1	C2	119.9(4)	N1	C7	C11	121.6(5)
C2	C1	Ni1	120.0(4)	C11	C7	C2	126.9(5)
C12	N2	Ni1	116.6(3)	C4	C3	C2	119.1(5)
C16	N2	Ni1	125.6(3)	C7	N1	Ni1	116.3(3)
C16	N2	C12	117.6(4)	C8	N1	Ni1	125.3(4)
C1	Ni1	N2	82.21(19)	C8	N1	C7	118.1(4)
C1	Ni1	N1	81.8(2)	C10	C11	C7	118.8(5)
C1	Ni1	O1_1	177.4(5)	C15	C14	C13	119.6(5)

Atom	Atom	Atom	Angle/°	Atom	Atom	Atom	Angle/°
C1	Ni1	O1_2	174.7(9)	C14	C15	C16	119.1(5)
N2	Ni1	N1	162.64(17)	N1	C8	C9	122.7(5)
N2	Ni1	O1_1	96.7(7)	C8	C9	C10	118.1(5)
N1	Ni1	O1_1	99.0(7)	C11	C10	C9	120.7(5)
O1_2	Ni1	N2	101.2(11)	C1_1	O1_1	Ni1	126.9(12)
O1_2	Ni1	N1	95.3(11)	O1_1	C1_1	C2_1	112.7(11)
C1	C6	C12	110.3(4)	O1_1	C1_1	C3_1	110.3(11)
C1	C6	C5	120.1(4)	O1_1	C1_1	C4_1	107.4(11)
C5	C6	C12	129.6(5)	C2_1	C1_1	C4_1	109.9(9)
N2	C12	C6	110.8(4)	C3_1	C1_1	C2_1	109.2(10)
N2	C12	C13	121.5(4)	C3_1	C1_1	C4_1	107.2(9)
C13	C12	C6	127.7(4)	C1_2	O1_2	Ni1	127.3(19)
C3	C4	C5	121.7(4)	O1_2	C1_2	C2_2	109.0(15)
N2	C16	C15	123.1(5)	O1_2	C1_2	C3_2	110.6(16)
C14	C13	C12	119.0(5)	O1_2	C1_2	C4_2	109.7(15)
C1	C2	C7	110.1(4)	C2_2	C1_2	C3_2	109.8(14)
C3	C2	C1	120.2(5)	C2_2	C1_2	C4_2	110.6(13)
C3	C2	C7	129.6(4)	C3_2	C1_2	C4_2	107.0(13)
C4	C5	C6	118.9(4)				

Table 7-190 Hydrogen Atom Coordinates (Å×10^4) and Isotropic Displacement Parameters (Å^2×10^3) for [Ni(Py(Ph)Py)O*t*Bu].

Atom	*x*	*y*	*z*	U(eq)
H4	4762.47	2323.44	3351.84	39
H16	5884.43	5467.91	9083.33	40
H13	3424.55	4537.69	5859.93	41
H5	3988.34	3403.17	4408.41	35
H3	6365.3	1989.27	4059.91	38
H11	7996.12	1542.25	5288.05	51
H14	3140.18	5538.85	7397.1	47
H15	4387.82	5998.66	9019.96	48
H8	8825.91	3699.83	8653.09	51
H9	9935.94	2527.82	8251.52	64
H10	9504.8	1429.14	6553.86	66
H2A_1	7168.27	6477.99	7513.85	98
H2B_1	7684.25	7518.35	8302.04	98
H2C_1	6716.23	7046.9	8428.79	98
H3A_1	9193.65	5438.04	9802.24	84
H3B_1	9126.01	6772.79	9538.85	84
H3C_1	8919.6	5883.24	8487.43	84
H4A_1	7116.52	6498.31	10358.13	102
H4B_1	8118.67	7095.83	10624.67	102
H4C_1	8046.98	5795.06	10974.68	102
H2A_2	8607.72	5983.43	10626.23	96
H2B_2	9134.92	6802.23	9963.72	96
H2C_2	9254.68	5454.36	9911.06	96
H3A_2	6706.6	6835.81	8291.93	134
H3B_2	7568.35	7699.16	8699.82	134
H3C_2	7220.26	7024.07	9648.91	134
H4A_2	8751.47	5593.86	7740.15	86
H4B_2	8568.69	6930.77	7775.85	86
H4C_2	7744.27	6105.87	7072.73	86

Table 7-191 Atomic Occupancy for [Ni(Py(Ph)Py)O*t*Bu].

Atom	*Occupancy*	Atom	*Occupancy*	Atom	*Occupancy*
O1_1	0.618(9)	C1_1	0.618(9)	C2_1	0.618(9)
H2A_1	0.618(9)	H2B_1	0.618(9)	H2C_1	0.618(9)
C3_1	0.618(9)	H3A_1	0.618(9)	H3B_1	0.618(9)
H3C_1	0.618(9)	C4_1	0.618(9)	H4A_1	0.618(9)
H4B_1	0.618(9)	H4C_1	0.618(9)	O1_2	0.382(9)
C1_2	0.382(9)	C2_2	0.382(9)	H2A_2	0.382(9)
H2B_2	0.382(9)	H2C_2	0.382(9)	C3_2	0.382(9)
H3A_2	0.382(9)	H3B_2	0.382(9)	H3C_2	0.382(9)
C4_2	0.382(9)	H4A_2	0.382(9)	H4B_2	0.382(9)
H4C_2	0.382(9)				

7.3.28 [Ni(Py(Ph)Py)C_2F_5]

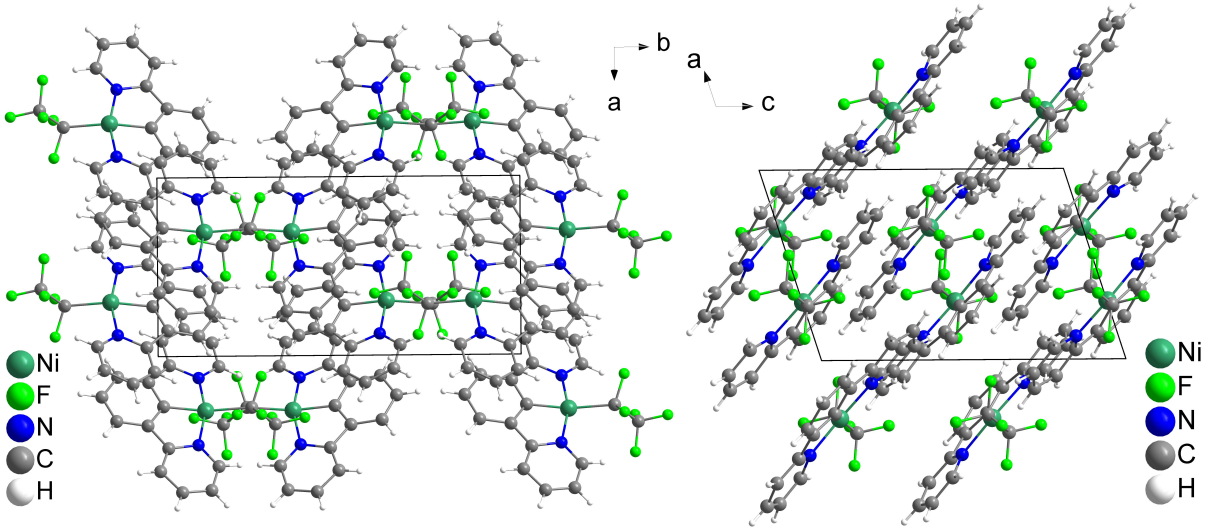

Figure 7-410 Crystal structure of [Ni(Py(Ph)Py)C_2F_5] viewed along the crystallographic *c*- (left) and *b*-axis (right).

Table 7-192 Crystal data and structure refinement for [Ni(Py(Ph)Py)C_2F_5].

Identification code	[Ni(Py(Ph)Py)C_2F_5]
Empirical formula	$C_{18}H_{11}F_5N_2Ni$
Formula weight	409.00
Temperature/K	150.0
Crystal system	monoclinic
Space group	$P2_1/c$
a/Å	8.1443(5)
b/Å	15.7664(10)
c/Å	12.3871(8)
α/°	90
β/°	107.846(2)

γ/°	90
Volume/Å^3	1514.05(17)
Z	4
ρ_{calc}g/cm^3	1.794
μ/mm^{-1}	1.342
F(000)	824.0
Crystal size/mm^3	0.2 × 0.1 × 0.1
Radiation	MoKα (λ = 0.71073)
2Θ range for data collection/°	5.168 to 55.15
Index ranges	–10 ≤ h ≤ 10, –20 ≤ k ≤ 20, –16 ≤ l ≤ 16
Reflections collected	22760
Independent reflections	3493 [R_{int} = 0.0709, R_{sigma} = 0.0651]
Data/restraints/parameters	3493/0/235
Goodness-of-fit on F^2	1.030
Final R indexes [I>=2σ (I)]	R_1 = 0.0434, wR_2 = 0.0796
Final R indexes [all data]	R_1 = 0.0852, wR_2 = 0.0919
Largest diff. peak/hole / e Å^{-3}	0.47/–0.35

Table 7-193 Fractional Atomic Coordinates (×10^4) and Equivalent Isotropic Displacement Parameters (Å^2×10^3) for [Ni(Py(Ph)Py)C_2F_5]. U_{eq} is defined as 1/3 of the trace of the orthogonalized U_{IJ} tensor.

Atom	*x*	*y*	*z*	U(eq)
Ni1	6940.7(5)	6295.7(2)	4977.0(3)	18.24(12)
F2	6723(2)	7839.3(11)	3739.8(13)	28.7(4)
F1	8860(2)	7833.8(11)	5323.6(14)	28.8(4)
F4	4476(2)	8128.4(12)	4946.1(16)	36.4(5)
F3	6565(2)	8122.8(11)	6506.1(14)	35.5(5)
F5	6536(3)	9026.4(11)	5211.5(16)	40.0(5)
N2	5031(3)	6092.1(15)	3599.4(19)	19.7(6)
N1	8787(3)	6108.7(15)	6393(2)	19.0(6)
C12	6129(4)	4704.6(18)	3928(2)	19.5(7)
C1	7193(4)	5138.2(18)	4865(2)	19.6(7)
C11	6392(4)	3844.6(19)	3807(3)	25.5(7)
C2	7126(4)	7566(2)	4877(2)	20.6(7)
C6	10867(4)	5106(2)	7479(2)	23.8(7)
C13	4849(4)	5272.4(19)	3197(2)	22.0(7)
C7	9489(4)	5310.1(18)	6544(2)	19.0(6)
C8	8558(4)	4731.8(18)	5643(2)	19.3(7)
C5	11517(4)	5697(2)	8319(3)	27.0(8)
C3	9420(4)	6668(2)	7237(2)	22.2(7)
C9	8861(4)	3878.4(18)	5503(3)	24.5(7)
C17	3831(4)	6653(2)		23.6(7)
C16	2495(4)	6449(2)	2084(2)	26.8(8)
C10	7761(4)	3440(2)	4594(3)	25.9(7)
C14	3568(4)	5043(2)	2215(2)	26.9(7)
C15	2378(4)	5643(2)	1648(3)	30.4(8)
C4	10749(4)	6487(2)	8201(3)	25.5(8)
C18	6184(4)	8215.9(19)	5381(3)	24.2(7)

Table 7-194 Anisotropic Displacement Parameters ($Å^2×10^3$) for [Ni(Py(Ph)Py)C_2F_5]. The Anisotropic displacement factor exponent takes the form: $–2π^2[h^2a^{*2}U_{11}+2hka^*b^*U_{12}+…]$.

Atom	U_{11}	U_{22}	U_{33}	U_{23}	U_{13}	U_{12}
Ni1	17.5(2)	17.2(2)	18.6(2)	–0.39(18)	3.36(15)	–0.41(18)
F2	33.5(11)	28.2(10)	22.0(9)	5.4(8)	5.2(8)	–5.1(8)
F1	19.0(10)	29.8(11)	34.3(10)	2.3(9)	3.6(8)	–6.3(8)
F4	20.6(11)	39.1(12)	45.3(12)	–6.6(10)	3.9(9)	4.5(9)
F3	42.1(12)	38.2(12)	25.4(10)	–0.2(9)	9.3(9)	12.6(10)
F5	54.4(13)	16.7(10)	45.5(12)	–0.6(9)	10.2(10)	–0.8(9)
N2	18.7(14)	20.5(14)	21.2(13)	1.1(11)	8.2(11)	–1.5(11)
N1	18.3(13)	17.0(14)	22.5(13)	0.2(10)	7.5(11)	–0.9(10)
C12	22.2(17)	19.2(16)	18.7(15)	–1.4(13)	8.8(13)	–3.8(13)
C1	19.8(17)	17.4(16)	23.3(16)	0.6(13)	9.3(13)	–2.9(13)
C11	27.4(18)	25.6(19)	26.7(17)	–7.6(14)	13.4(15)	–8.8(14)
C2	15.4(16)	25.7(17)	16.1(15)	2.1(13)	–1.8(13)	–4.2(13)
C6	19.8(17)	23.5(17)	27.5(17)	7.4(14)	6.4(14)	3.2(14)
C13	21.0(17)	28.1(18)	17.8(15)	–1.8(14)	7.2(13)	–4.9(14)
C7	18.7(16)	17.9(16)	21.7(16)	2.3(13)	8.1(13)	–0.6(13)
C8	17.9(16)	18.4(16)	23.9(16)	0.9(13)	9.9(13)	–1.2(13)
C5	18.0(17)	34(2)	25.8(17)	5.0(15)	2.2(14)	0.6(15)
C3	22.8(17)	20.8(16)	22.6(16)	–1.0(14)	6.2(14)	0.4(14)
C9	23.9(18)	19.5(18)	32.6(18)	4.0(14)	12.4(15)	0.1(13)
C17	17.6(17)	27.9(18)	24.5(17)	3.8(14)	5.2(14)	–3.6(14)
C16	21.0(17)	37(2)	19.8(16)	9.2(15)	2.6(14)	–2.6(15)
C10	33.2(19)	16.4(16)	32.0(17)	–2.6(14)	15.7(16)	–1.9(14)
C14	26.9(18)	32.1(19)	22.8(16)	–5.3(15)	9.3(15)	–9.2(15)
C15	26.4(18)	46(2)	15.8(16)	–0.2(15)	1.4(14)	–12.6(17)
C4	25.3(18)	23.8(19)	22.3(17)	–2.0(13)	–0.3(14)	–2.0(14)
C18	21.5(18)	20.2(18)	26.7(18)	–1.1(14)	1.0(14)	–1.8(14)

Table 7-195 Bond Lengths for [Ni(Py(Ph)Py)C_2F_5].

Atom	Atom	Length/Å	Atom	Atom	Length/Å
Ni1	N2	1.951(2)	C12	C13	1.460(4)
Ni1	N1	1.952(2)	C1	C8	1.386(4)
Ni1	C1	1.847(3)	C11	C10	1.391(4)
Ni1	C2	2.014(3)	C2	C18	1.524(4)
F2	C2	1.413(3)	C6	C7	1.382(4)
F1	C2	1.414(3)	C6	C5	1.376(4)
F4	C18	1.337(3)	C13	C14	1.386(4)
F3	C18	1.340(3)	C7	C8	1.460(4)
F5	C18	1.340(3)	C8	C9	1.388(4)
N2	C13	1.377(4)	C5	C4	1.382(4)
N2	C17	1.342(4)	C3	C4	1.373(4)
N1	C7	1.371(3)	C9	C10	1.388(4)
N1	C3	1.344(4)	C17	C16	1.378(4)
C12	C1	1.395(4)	C16	C15	1.373(4)
C12	C11	1.388(4)	C14	C15	1.381(4)

Table 7-196 Bond Angles for [Ni(Py(Ph)Py)C_2F_5].

Atom	Atom	Atom	Angle/°	Atom	Atom	Atom	Angle/°
N2	Ni1	N1	161.68(10)	C5	C6	C7	120.1(3)
N2	Ni1	C2	99.47(11)	N2	C13	C12	112.0(2)

Atom	Atom	Atom	Angle/°	Atom	Atom	Atom	Angle/°
N1	Ni1	C2	98.84(11)	N2	C13	C14	122.1(3)
C1	Ni1	N2	81.30(11)	C14	C13	C12	126.0(3)
C1	Ni1	N1	81.12(11)	N1	C7	C6	121.7(3)
C1	Ni1	C2	164.92(11)	N1	C7	C8	111.9(2)
C13	N2	Ni1	116.08(19)	C6	C7	C8	126.4(3)
C17	N2	Ni1	127.0(2)	C1	C8	C7	111.2(3)
C17	N2	C13	116.8(2)	C1	C8	C9	119.8(3)
C7	N1	Ni1	115.78(19)	C9	C8	C7	129.1(3)
C3	N1	Ni1	127.3(2)	C6	C5	C4	118.3(3)
C3	N1	C7	116.9(2)	N1	C3	C4	123.5(3)
C1	C12	C13	111.0(3)	C10	C9	C8	119.2(3)
C11	C12	C1	119.4(3)	N2	C17	C16	123.2(3)
C11	C12	C13	129.5(3)	C15	C16	C17	119.7(3)
C12	C1	Ni1	119.5(2)	C9	C10	C11	121.3(3)
C8	C1	Ni1	119.3(2)	C15	C14	C13	119.3(3)
C8	C1	C12	120.9(3)	C16	C15	C14	118.7(3)
C12	C11	C10	119.3(3)	C3	C4	C5	119.3(3)
F2	C2	Ni1	111.46(18)	F4	C18	F3	106.8(3)
F2	C2	F1	101.4(2)	F4	C18	F5	106.4(2)
F2	C2	C18	102.2(2)	F4	C18	C2	111.0(2)
F1	C2	Ni1	110.97(18)	F3	C18	F5	106.0(2)
F1	C2	C18	101.9(2)	F3	C18	C2	111.5(2)
C18	C2	Ni1	126.0(2)	F5	C18	C2	114.8(3)

Table 7-197 Torsion Angles for [Ni(Py(Ph)Py)C_2F_5].

A	B	C	D	Angle/°	A	B	C	D	Angle/°
Ni1	N2	C13	C12	1.9(3)	C1	C12	C11	C10	–2.9(4)
Ni1	N2	C13	C14	–178.7(2)	C1	C12	C13	N2	1.2(3)
Ni1	N2	C17	C16	–178.3(2)	C1	C12	C13	C14	–178.2(3)
Ni1	N1	C7	C6	176.4(2)	C1	C8	C9	C10	–1.5(4)
Ni1	N1	C7	C8	–6.2(3)	C11	C12	C1	Ni1	175.9(2)
Ni1	N1	C3	C4	–178.8(2)	C11	C12	C1	C8	3.2(4)
Ni1	C1	C8	C7	7.1(3)	C11	C12	C13	N2	–178.7(3)
Ni1	C1	C8	C9	–173.7(2)	C11	C12	C13	C14	1.9(5)
Ni1	C2	C18	F4	–60.1(3)	C2	Ni1	C1	C12	–90.0(5)
Ni1	C2	C18	F3	58.8(3)	C2	Ni1	C1	C8	82.7(5)
Ni1	C2	C18	F5	179.27(19)	C6	C7	C8	C1	177.1(3)
F2	C2	C18	F4	68.1(3)	C6	C7	C8	C9	–2.1(5)
F2	C2	C18	F3	–173.0(2)	C6	C5	C4	C3	–2.6(5)
F2	C2	C18	F5	–52.5(3)	C13	N2	C17	C16	–2.0(4)
F1	C2	C18	F4	172.7(2)	C13	C12	C1	Ni1	–4.1(3)
F1	C2	C18	F3	–68.4(3)	C13	C12	C1	C8	–176.7(2)
F1	C2	C18	F5	52.1(3)	C13	C12	C11	C10	177.0(3)
N2	Ni1	C1	C12	4.1(2)	C13	C14	C15	C16	–0.5(4)
N2	Ni1	C1	C8	176.9(2)	C7	N1	C3	C4	2.4(4)
N2	C13	C14	C15	–3.4(4)	C7	C6	C5	C4	0.4(4)
N2	C17	C16	C15	–1.7(5)	C7	C8	C9	C10	177.7(3)
N1	Ni1	C1	C12	178.9(2)	C8	C9	C10	C11	1.7(4)
N1	Ni1	C1	C8	–8.3(2)	C5	C6	C7	N1	3.3(4)
N1	C7	C8	C1	–0.2(3)	C5	C6	C7	C8	–173.7(3)

A	B	C	D	Angle/°	A	B	C	D	Angle/°
N1	C7	C8	C9	–179.4(3)	C3	N1	C7	C6	–4.7(4)
N1	C3	C4	C5	1.2(5)	C3	N1	C7	C8	172.8(2)
C12	C1	C8	C7	179.7(2)	C17	N2	C13	C12	–174.8(2)
C12	C1	C8	C9	–1.0(4)	C17	N2	C13	C14	4.6(4)
C12	C11	C10	C9	0.5(4)	C17	C16	C15	C14	3.0(4)
C12	C13	C14	C15	175.9(3)					

Table 7-198 Hydrogen Atom Coordinates (Å×10^4) and Isotropic Displacement Parameters (Å^2×10^3) for [Ni(Py(Ph)Py)C$_2$F$_5$].

Atom	*x*	*y*	*z*	U(eq)
H11	5645.5	3535.52	3192.75	31
H6	11367.16	4556.93	7542.24	29
H5	12469.3	5564.86	8963.37	32
H3	8922.05	7218.31	7163.17	27
H9	9809.38	3597.5	6022.25	29
H17	3907.18	7218.48	3316.24	28
H16	1658.11	6864.28	1729.28	32
H10	7948.1	2852.71	4509.02	31
H14	3509.74	4479.66	1934.66	32
H15	1496.36	5499.66	970.26	37
H4	11135.63	6901.37	8780.57	31

7.3.29 [Ni(Py(Ph)Py)NCS]

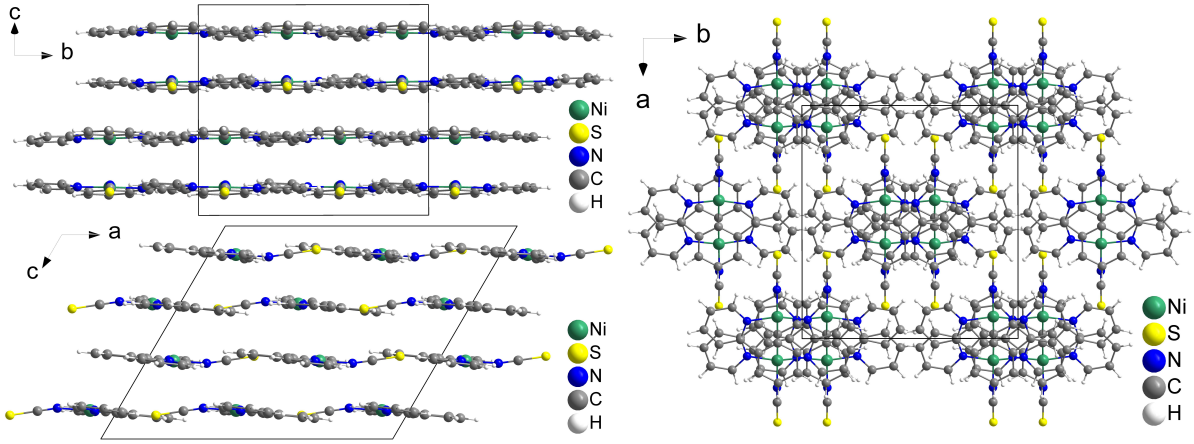

Figure 7-411 Crystal structure of [Ni(Py(Ph)Py)NCS] viewed along the crystallographic *a*- (top left), *b*- (bottom left) and *c*-axis (right).

Table 7-199 Crystal data and structure refinement for [Ni(Py(Ph)Py)NCS].

Identification code	[Ni(Py(Ph)Py)NCS]
Empirical formula	$C_{17}H_{11}N_3NiS$
Formula weight	348.06
Temperature/K	100.00
Crystal system	monoclinic
Space group	*C*2/c
a/Å	16.9632(7)
b/Å	13.5861(6)
c/Å	14.3464(5)
α/°	90
β/°	120.2810(10)

γ/°	90
Volume/Å^3	2855.2(2)
Z	8
ρ_{calc}g/cm^3	1.619
μ/mm^{-1}	1.503
F(000)	1424.0
Crystal size/mm^3	0.3 × 0.3 × 0.2
Radiation	MoKα (λ = 0.71073)
2Θ range for data collection/°	4.088 to 56.606
Index ranges	–22 ≤ h ≤ 22, –18 ≤ k ≤ 18, –19 ≤ l ≤ 16
Reflections collected	27709
Independent reflections	3506 [R_{int} = 0.0385, R_{sigma} = 0.0210]
Data/restraints/parameters	3506/0/199
Goodness-of-fit on F^2	1.056
Final R indexes [I>=2σ (I)]	R_1 = 0.0239, wR_2 = 0.0631
Final R indexes [all data]	R_1 = 0.0269, wR_2 = 0.0648
Largest diff. peak/hole / e Å^{-3}	0.35/–0.29

Table 7-200 Fractional Atomic Coordinates (×10^4) and Equivalent Isotropic Displacement Parameters (Å^2×10^3) for [Ni(Py(Ph)Py)NCS]. U_{eq} is defined as 1/3 of the trace of the orthogonalized U_{IJ} tensor.

Atom	*x*	*y*	*z*	U(eq)
Ni1	5936.1(2)	3850.6(2)	6339.6(2)	13.72(6)
S1	8591.5(3)	3853.0(3)	6114.8(3)	26.44(9)
N2	5753.5(7)	2449.3(8)	6290.7(8)	16.1(2)
N1	5804.4(7)	5255.5(8)	6354.7(8)	16.0(2)
N3	7105.8(8)	3835.0(8)	6446.6(10)	20.4(2)
C1	4809.1(9)	3866.8(9)	6198.8(10)	15.3(2)
C12	4953.0(9)	2143.8(10)	6219.1(9)	16.5(2)
C11	4383.0(8)	2978.6(10)	6153.6(9)	16.1(2)
C6	4994.4(9)	5583.3(10)	6240.4(9)	16.7(2)
C7	4395.8(9)	4767.0(10)	6141.5(9)	16.4(2)
C16	6340.9(9)	1763.5(10)	6332.4(10)	19.4(3)
C13	4757.3(10)	1151.5(10)	6215.0(11)	21.1(3)
C8	3525.1(9)	4785.5(11)	6019.0(10)	20.6(3)
C5	4822.1(10)	6581.6(10)	6254.3(10)	21.1(3)
C17	7729.1(9)	3839.7(9)	6311.7(11)	17.5(2)
C10	3518.8(9)	2988.1(11)	6049.8(10)	19.9(3)
C2	6437.5(9)	5923.1(10)	6483.0(10)	19.0(3)
C3	6308.8(10)	6927.2(10)	6528.0(11)	22.4(3)
C14	5384.2(10)	456.5(10)	6289.3(11)	24.8(3)
C9	3100.0(9)	3891.9(11)	5979.5(11)	22.3(3)
C4	5492.5(10)	7258.8(10)	6416.8(11)	24.1(3)
C15	6183.7(10)	762.0(11)	6339.6(11)	24.4(3)

Table 7-201 Anisotropic Displacement Parameters (Å^2×10^3) for [Ni(Py(Ph)Py)NCS]. The Anisotropic displacement factor exponent takes the form: $-2\pi^2[h^2a^{*2}U_{11}+2hka^*b^*U_{12}+\ldots]$.

Atom	U_{11}	U_{22}	U_{33}	U_{23}	U_{13}	U_{12}
Ni1	13.06(9)	14.02(10)	15.06(9)	0.56(5)	7.80(7)	0.36(6)
S1	21.53(17)	26.38(19)	39.8(2)	6.62(14)	21.64(16)	4.36(13)
N2	16.3(5)	17.9(5)	13.5(5)	0.2(4)	7.1(4)	0.6(4)

Atom	U_{11}	U_{22}	U_{33}	U_{23}	U_{13}	U_{12}
N1	17.8(5)	16.8(5)	12.5(5)	0.1(4)	7.0(4)	0.0(4)
N3	18.3(5)	19.9(6)	24.1(6)	1.8(4)	11.6(5)	1.2(4)
C1	14.6(6)	19.5(6)	11.7(5)	0.3(4)	6.5(4)	0.3(4)
C12	17.1(6)	19.6(6)	12.0(5)	0.8(4)	6.7(5)	–0.8(5)
C11	16.2(6)	19.1(6)	11.8(5)	0.6(4)	6.2(4)	–0.1(5)
C6	19.2(6)	19.2(6)	10.8(5)	0.9(4)	6.9(5)	2.9(5)
C7	18.2(6)	19.0(6)	11.6(5)	0.3(4)	7.2(5)	2.5(5)
C16	19.1(6)	19.8(7)	19.1(6)	–0.8(5)	9.3(5)	1.4(5)
C13	23.1(7)	20.9(7)	19.6(6)	0.5(5)	11.1(5)	–3.4(5)
C8	18.7(6)	26.6(7)	16.5(6)	0.9(5)	8.8(5)	6.2(5)
C5	26.8(7)	20.3(6)	15.5(6)	0.5(5)	10.2(5)	5.2(5)
C17	17.2(6)	13.7(6)	20.9(6)	1.7(4)	9.0(5)	1.0(5)
C10	17.3(6)	26.1(7)	16.4(6)	0.0(5)	8.4(5)	–3.5(5)
C2	20.3(6)	19.7(6)	14.9(6)	–0.5(5)	7.2(5)	–2.7(5)
C3	26.8(7)	18.7(6)	17.5(6)	–2.5(5)	8.0(5)	–5.7(5)
C14	32.4(8)	15.5(6)	26.1(7)	0.2(5)	14.4(6)	–1.7(5)
C9	15.3(6)	32.5(8)	19.6(6)	0.0(5)	9.2(5)	0.6(5)
C4	34.7(7)	16.1(6)	18.2(6)	–0.7(5)	10.9(6)	1.6(6)
C15	26.9(7)	18.5(7)	27.0(7)	–0.1(5)	12.8(6)	4.9(6)

Table 7-202 Bond Lengths for [Ni(Py(Ph)Py)NCS].

Atom	Atom	Length/Å	Atom	Atom	Length/Å
Ni1	N2	1.9245(11)	C12	C13	1.3877(18)
Ni1	N1	1.9231(12)	C11	C10	1.3970(18)
Ni1	N3	1.9115(12)	C6	C7	1.4614(18)
Ni1	C1	1.8185(13)	C6	C5	1.3897(19)
S1	C17	1.6240(14)	C7	C8	1.3970(18)
N2	C12	1.3734(16)	C16	C15	1.387(2)
N2	C16	1.3433(17)	C13	C14	1.386(2)
N1	C6	1.3732(16)	C8	C9	1.398(2)
N1	C2	1.3455(17)	C5	C4	1.388(2)
N3	C17	1.1670(19)	C10	C9	1.397(2)
C1	C11	1.3912(18)	C2	C3	1.3882(19)
C1	C7	1.3913(18)	C3	C4	1.387(2)
C12	C11	1.4623(18)	C14	C15	1.385(2)

Table 7-203 Bond Angles for [Ni(Py(Ph)Py)NCS].

Atom	Atom	Atom	Angle/˚	Atom	Atom	Atom	Angle/˚
N1	Ni1	N2	164.75(5)	C1	C11	C10	119.31(12)
N3	Ni1	N2	97.66(5)	C10	C11	C12	129.67(12)
N3	Ni1	N1	97.58(5)	N1	C6	C7	111.70(11)
C1	Ni1	N2	82.36(5)	N1	C6	C5	121.32(12)
C1	Ni1	N1	82.39(5)	C5	C6	C7	126.96(12)
C1	Ni1	N3	178.47(5)	C1	C7	C6	110.90(11)
C12	N2	Ni1	115.88(9)	C1	C7	C8	119.50(12)
C16	N2	Ni1	125.63(9)	C8	C7	C6	129.59(12)
C16	N2	C12	118.49(12)	N2	C16	C15	122.65(13)
C6	N1	Ni1	115.82(9)	C14	C13	C12	119.27(13)

Atom	Atom	Atom	Angle/°	Atom	Atom	Atom	Angle/°
C2	N1	Ni1	125.54(9)	C7	C8	C9	118.71(13)
C2	N1	C6	118.64(12)	C4	C5	C6	119.27(13)
C17	N3	Ni1	167.76(12)	N3	C17	S1	179.48(14)
C11	C1	Ni1	119.14(10)	C9	C10	C11	118.95(13)
C11	C1	C7	121.69(12)	N1	C2	C3	122.37(13)
C7	C1	Ni1	119.16(10)	C4	C3	C2	119.03(13)
N2	C12	C11	111.54(11)	C15	C14	C13	119.55(13)
N2	C12	C13	121.29(12)	C10	C9	C8	121.82(13)
C13	C12	C11	127.17(12)	C3	C4	C5	119.34(13)
C1	C11	C12	111.02(11)	C14	C15	C16	118.71(13)

Table 7-204 Torsion Angles for [Ni(Py(Ph)Py)NCS].

A	B	C	D	Angle/°	A	B	C	D	Angle/°
Ni1	N2	C12	C11	2.17(13)	C12	N2	C16	C15	–2.05(18)
Ni1	N2	C12	C13	–177.78(10)	C12	C11	C10	C9	–178.58(12)
Ni1	N2	C16	C15	177.17(10)	C12	C13	C14	C15	–1.6(2)
Ni1	N1	C6	C7	0.66(13)	C11	C1	C7	C6	178.25(11)
Ni1	N1	C6	C5	179.04(9)	C11	C1	C7	C8	–0.98(19)
Ni1	N1	C2	C3	–177.40(9)	C11	C12	C13	C14	–179.67(12)
Ni1	C1	C11	C12	–0.72(14)	C11	C10	C9	C8	–0.5(2)
Ni1	C1	C11	C10	179.75(9)	C6	N1	C2	C3	1.48(18)
Ni1	C1	C7	C6	–1.61(14)	C6	C7	C8	C9	–177.78(12)
Ni1	C1	C7	C8	179.16(9)	C6	C5	C4	C3	2.01(19)
N2	Ni1	C1	C11	1.51(10)	C7	C1	C11	C12	179.42(11)
N2	Ni1	C1	C7	–178.62(11)	C7	C1	C11	C10	–0.11(19)
N2	C12	C11	C1	–0.97(15)	C7	C6	C5	C4	176.32(12)
N2	C12	C11	C10	178.51(12)	C7	C8	C9	C10	–0.5(2)
N2	C12	C13	C14	0.3(2)	C16	N2	C12	C11	–178.54(10)
N2	C16	C15	C14	0.8(2)	C16	N2	C12	C13	1.52(18)
N1	Ni1	C1	C11	–178.27(11)	C13	C12	C11	C1	178.97(12)
N1	Ni1	C1	C7	1.59(10)	C13	C12	C11	C10	–1.6(2)
N1	C6	C7	C1	0.52(15)	C13	C14	C15	C16	1.1(2)
N1	C6	C7	C8	179.65(12)	C5	C6	C7	C1	–177.75(12)
N1	C6	C5	C4	–1.80(18)	C5	C6	C7	C8	1.4(2)
N1	C2	C3	C4	–1.24(19)	C2	N1	C6	C7	–178.33(10)
C1	C11	C10	C9	0.86(19)	C2	N1	C6	C5	0.06(17)
C1	C7	C8	C9	1.28(19)	C2	C3	C4	C5	–0.55(19)

Table 7-205 Hydrogen Atom Coordinates (Å×10^4) and Isotropic Displacement Parameters (Å^2×10^3) for [Ni(Py(Ph)Py)NCS].

Atom	*x*	*y*	*z*	U(eq)
H16	6885.88	1972.56	6357.89	23
H13	4199.5	950.95	6161.91	25
H8	3227.48	5393.25	5963.7	25
H5	4251.81	6798.17	6153.69	25
H10	3220.59	2389.17	6027.39	24
H2	6992.51	5699.17	6545.02	23
H3	6773.12	7380.53	6633.38	27
H14	5266.41	–225.03	6305.55	30
H9	2510.04	3899.98	5902.66	27

Atom	*x*	*y*	*z*	U(eq)
H4	5393.14	7942.64	6451.59	29
H15	6616.13	295.04	6378.36	29

7.3.30 [Ni(Py(Ph)Py)OBz]

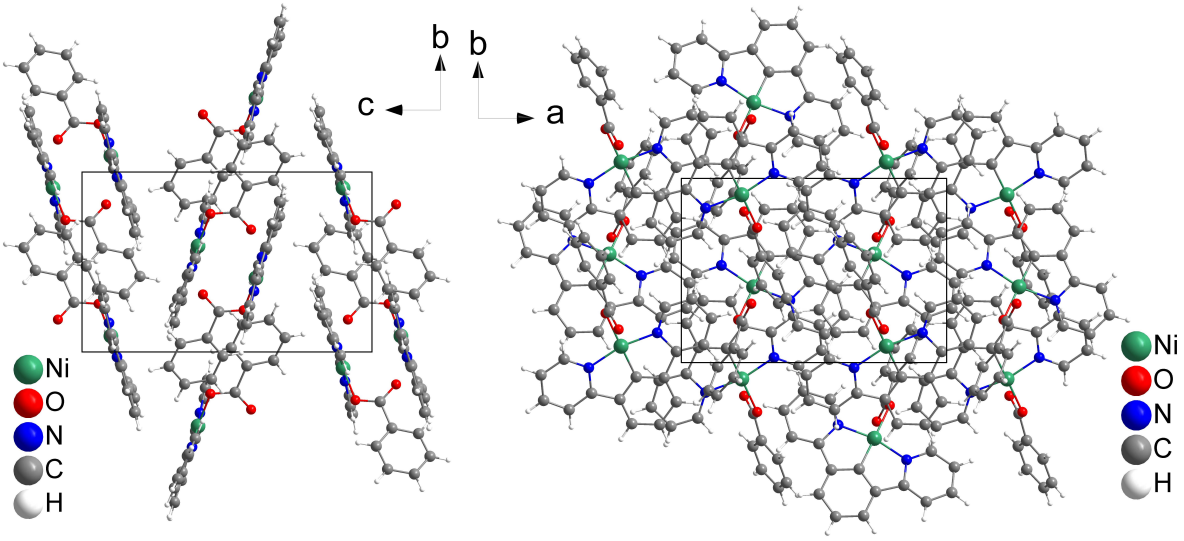

Figure 7-412 Crystal structure of [Ni(Py(Ph)Py)OBz] viewed along the crystallographic *a*- (left) and *c*-axis (right).

Table 7-206 Crystal data and structure refinement for [Ni(Py(Ph)Py)OBz].

Identification code	[Ni(Py(Ph)Py)OBz]
Empirical formula	$C_{23}H_{16}N_2NiO_2$
Formula weight	411.09
Temperature/K	100.00
Crystal system	monoclinic
Space group	$P2_1/n$
a/Å	13.2713(5)
b/Å	9.1026(4)
c/Å	14.8552(7)
α/°	90
β/°	98.744(2)
γ/°	90
Volume/Å^3	1773.70(13)
Z	4
ρ_{calc}g/cm^3	1.539
μ/mm^{-1}	1.116
F(000)	848.0
Crystal size/mm^3	0.78 × 0.38 × 0.19
Radiation	MoKα (λ = 0.71073)
2Θ range for data collection/°	4.468 to 68.712
Index ranges	–21 ≤ h ≤ 18, –14 ≤ k ≤ 14, –23 ≤ l ≤ 23
Reflections collected	75522
Independent reflections	7366 [R_{int} = 0.0448, R_{sigma} = 0.0236]
Data/restraints/parameters	7366/0/253
Goodness-of-fit on F^2	1.059
Final R indexes [I>=2σ (I)]	R_1 = 0.0322, wR_2 = 0.0869

Final R indexes [all data]	R_1 = 0.0340, wR_2 = 0.0879
Largest diff. peak/hole / e Å^{-3}	1.43/–0.50

Table 7-207 Fractional Atomic Coordinates (×10^4) and Equivalent Isotropic Displacement Parameters (Å^2×10^3) for [Ni(Py(Ph)Py)OBz]. U_{eq} is defined as 1/3 of the trace of the orthogonalized U_{IJ} tensor.

Atom	*x*	*y*	*z*	U(eq)
Ni1	2725.2(2)	4110.5(2)	4002.1(2)	12.83(4)
O1	2143.5(7)	2322.6(9)	4426.4(6)	17.54(14)
O2	2633.1(8)	3198.6(10)	5830.0(6)	23.83(17)
N2	4089.9(7)	3381.6(10)	4067.4(6)	13.51(14)
N1	1508.7(7)	5277.4(10)	3793.5(6)	15.43(15)
C17	2272.3(7)	2240.1(11)	5281.1(7)	14.55(16)
C1	3297.1(8)	5776.5(11)	3631.9(7)	13.78(16)
C12	4812.5(8)	4396.7(11)	3915.9(7)	13.41(15)
C6	1614.4(8)	6660.6(12)	3452.1(7)	15.83(17)
C16	4384.1(8)	1990.0(11)	4255.9(7)	16.33(17)
C7	2681.1(8)	6998.0(11)	3395.8(7)	15.39(16)
C11	4350.1(8)	5820.9(10)	3650.4(7)	13.65(16)
C8	3128.6(9)	8312.8(12)	3172.2(8)	18.39(18)
C9	4185.4(9)	8357.7(12)	3189.6(8)	18.62(18)
C15	5395.6(9)	1550.6(12)	4327.8(8)	18.27(18)
C13	5838.7(8)	4026.1(12)	4004.0(7)	16.21(17)
C19	2301.1(9)	465.8(12)	6605.1(7)	17.16(17)
C20	1981.6(9)	–798.3(13)	6999.2(8)	19.09(19)
C5	770.1(9)	7552.6(13)	3188.5(8)	20.04(19)
C10	4806.5(9)	7131.2(12)	3428.0(7)	16.61(17)
C2	576.5(9)	4812.8(13)	3908.2(8)	19.08(19)
C14	6133.3(9)	2586.6(13)	4217.2(8)	18.09(18)
C18	1986.6(8)	771.0(11)	5682.7(7)	14.34(16)
C22	1041.7(10)	–1510.9(14)	5536.4(8)	22.0(2)
C23	1368.5(9)	–230.9(13)	5146.5(7)	18.33(18)
C4	–194.2(9)	7049.3(15)	3297.8(8)	23.2(2)
C21	1335.0(10)	–1779.7(13)	6461.2(8)	21.4(2)
C3	–291.9(9)	5671.0(15)	3677.0(9)	22.9(2)

Table 7-208 Anisotropic Displacement Parameters (Å^2×10^3) for [Ni(Py(Ph)Py)OBz]. The Anisotropic displacement factor exponent takes the form: $-2\pi^2[h^2a^{*2}U_{11}+2hka^*b^*U_{12}+\ldots]$.

Atom	U_{11}	U_{22}	U_{33}	U_{23}	U_{13}	U_{12}
Ni1	13.40(6)	11.62(6)	13.46(6)	2.21(4)	2.01(4)	–1.02(4)
O1	20.3(3)	16.3(3)	15.9(3)	2.1(3)	2.2(3)	–3.9(3)
O2	32.4(5)	18.6(4)	20.4(4)	–3.3(3)	3.6(3)	–9.5(3)
N2	15.1(3)	11.9(3)	13.7(3)	1.1(3)	2.6(3)	–0.6(3)
N1	15.7(3)	16.8(4)	13.7(3)	1.0(3)	2.0(3)	0.3(3)
C17	10.3(3)	16.7(4)	18.0(4)	–5.5(3)	6.6(3)	–5.0(3)
C1	16.7(4)	12.0(4)	12.7(4)	1.6(3)	2.3(3)	–1.0(3)
C12	15.5(4)	12.2(4)	12.7(4)	–0.4(3)	2.7(3)	–1.4(3)
C6	18.3(4)	16.6(4)	12.4(4)	1.1(3)	1.7(3)	2.3(3)

Atom	U_{11}	U_{22}	U_{33}	U_{23}	U_{13}	U_{12}
C16	18.5(4)	12.3(4)	18.5(4)	2.1(3)	3.7(3)	0.1(3)
C7	19.5(4)	13.8(4)	12.7(4)	2.1(3)	1.7(3)	0.9(3)
C11	16.6(4)	11.8(4)	12.6(4)	1.0(3)	2.6(3)	–1.3(3)
C8	24.8(5)	13.4(4)	16.6(4)	3.5(3)	2.1(4)	0.7(4)
C9	25.6(5)	13.2(4)	17.2(4)	3.2(3)	3.8(4)	–3.1(4)
C15	19.7(4)	14.8(4)	20.6(4)	1.9(3)	4.1(4)	2.4(3)
C13	15.7(4)	16.6(4)	16.8(4)	–1.0(3)	3.7(3)	–1.0(3)
C19	20.0(4)	16.6(4)	14.8(4)	–0.1(3)	2.2(3)	–0.1(3)
C20	23.0(5)	19.8(5)	14.8(4)	3.7(3)	3.9(4)	1.7(4)
C5	22.5(5)	21.7(5)	15.6(4)	1.8(4)	1.9(4)	7.0(4)
C10	20.4(4)	14.2(4)	15.5(4)	1.1(3)	3.8(3)	–4.1(3)
C2	15.9(4)	23.1(5)	18.4(4)	–0.4(4)	3.0(3)	–0.6(4)
C14	17.1(4)	18.8(4)	18.6(4)	–0.4(3)	3.3(3)	2.1(3)
C18	14.3(4)	14.5(4)	14.5(4)	0.0(3)	2.8(3)	–0.9(3)
C22	23.6(5)	22.1(5)	19.7(5)	2.6(4)	1.2(4)	–9.6(4)
C23	20.2(4)	18.6(4)	15.7(4)	1.2(3)	1.0(3)	–5.5(4)
C4	19.9(5)	29.7(6)	19.4(5)	–1.2(4)	1.1(4)	8.2(4)
C21	24.4(5)	20.1(5)	20.2(5)	4.8(4)	4.8(4)	–4.3(4)
C3	16.5(4)	30.2(6)	21.9(5)	–2.8(4)	3.1(4)	2.6(4)

Table 7-209 Bond Lengths for [Ni(Py(Ph)Py)OBz].

Atom	Atom	Length/Å	Atom	Atom	Length/Å
Ni1	O1	1.9467(8)	C16	C15	1.3893(15)
Ni1	N2	1.9174(9)	C7	C8	1.3984(15)
Ni1	N1	1.9180(9)	C11	C10	1.3998(14)
Ni1	C1	1.8181(10)	C8	C9	1.3994(17)
O1	C17	1.2574(13)	C9	C10	1.4009(16)
O2	C17	1.2395(13)	C15	C14	1.3869(16)
N2	C12	1.3747(13)	C13	C14	1.3902(15)
N2	C16	1.3424(13)	C19	C20	1.3864(16)
N1	C6	1.3725(14)	C19	C18	1.3983(15)
N1	C2	1.3425(14)	C20	C21	1.4016(17)
C17	C18	1.5351(15)	C5	C4	1.3919(18)
C1	C7	1.3930(14)	C2	C3	1.3915(17)
C1	C11	1.3942(15)	C18	C23	1.3930(15)
C12	C11	1.4625(14)	C22	C23	1.3992(16)
C12	C13	1.3898(15)	C22	C21	1.3915(17)
C6	C7	1.4633(16)	C4	C3	1.389(2)
C6	C5	1.3909(15)			

Table 7-210 Bond Angles for [Ni(Py(Ph)Py)OBz].

Atom	Atom	Atom	Angle/˚	Atom	Atom	Atom	Angle/˚
N2	Ni1	O1	96.45(4)	N2	C16	C15	122.32(10)
N2	Ni1	N1	164.85(4)	C1	C7	C6	110.73(9)
N1	Ni1	O1	98.62(4)	C1	C7	C8	119.26(10)
C1	Ni1	O1	178.42(4)	C8	C7	C6	130.00(10)
C1	Ni1	N2	82.49(4)	C1	C11	C12	110.97(9)
C1	Ni1	N1	82.47(4)	C1	C11	C10	119.24(9)
C17	O1	Ni1	112.16(7)	C10	C11	C12	129.80(10)
C12	N2	Ni1	115.86(7)	C7	C8	C9	118.77(10)
C16	N2	Ni1	125.42(7)	C8	C9	C10	122.07(10)

Atom	Atom	Atom	Angle/°	Atom	Atom	Atom	Angle/°
C16	N2	C12	118.71(9)	C14	C15	C16	119.10(10)
C6	N1	Ni1	115.91(7)	C12	C13	C14	119.20(10)
C2	N1	Ni1	125.05(8)	C20	C19	C18	120.92(10)
C2	N1	C6	118.93(10)	C19	C20	C21	119.23(10)
O1	C17	C18	116.15(9)	C6	C5	C4	119.38(11)
O2	C17	O1	127.00(10)	C11	C10	C9	118.66(10)
O2	C17	C18	116.81(10)	N1	C2	C3	122.45(11)
C7	C1	Ni1	119.07(8)	C15	C14	C13	119.26(10)
C7	C1	C11	122.01(9)	C19	C18	C17	119.96(9)
C11	C1	Ni1	118.78(7)	C23	C18	C17	120.46(9)
N2	C12	C11	111.44(9)	C23	C18	C19	119.50(10)
N2	C12	C13	121.29(9)	C21	C22	C23	119.82(11)
C13	C12	C11	127.26(9)	C18	C23	C22	120.08(10)
N1	C6	C7	111.58(9)	C3	C4	C5	119.25(11)
N1	C6	C5	121.08(10)	C22	C21	C20	120.40(10)
C5	C6	C7	127.32(10)	C4	C3	C2	118.83(11)

Table 7-211 Torsion Angles for [Ni(Py(Ph)Py)OBz].

A	B	C	D	Angle/°	A	B	C	D	Angle/°
Ni1	O1	C17	O2	6.49(15)	C12	N2	C16	C15	1.82(16)
Ni1	O1	C17	C18	–171.10(7)	C12	C11	C10	C9	179.72(10)
Ni1	N2	C12	C11	–5.24(11)	C12	C13	C14	C15	0.66(16)
Ni1	N2	C12	C13	175.68(8)	C6	N1	C2	C3	1.29(17)
Ni1	N2	C16	C15	–177.37(8)	C6	C7	C8	C9	178.42(11)
Ni1	N1	C6	C7	–5.14(11)	C6	C5	C4	C3	0.65(18)
Ni1	N1	C6	C5	173.55(8)	C16	N2	C12	C11	175.49(9)
Ni1	N1	C2	C3	–174.76(9)	C16	N2	C12	C13	–3.59(15)
Ni1	C1	C7	C6	–2.96(12)	C16	C15	C14	C13	–2.37(17)
Ni1	C1	C7	C8	175.55(8)	C7	C1	C11	C12	–179.80(9)
Ni1	C1	C11	C12	4.47(12)	C7	C1	C11	C10	0.17(15)
Ni1	C1	C11	C10	–175.55(8)	C7	C6	C5	C4	–179.64(11)
O1	C17	C18	C19	166.39(10)	C7	C8	C9	C10	–0.33(17)
O1	C17	C18	C23	–17.11(15)	C11	C1	C7	C6	–178.68(9)
O2	C17	C18	C19	–11.46(15)	C11	C1	C7	C8	–0.16(16)
O2	C17	C18	C23	165.05(11)	C11	C12	C13	C14	–176.56(10)
N2	Ni1	C1	C7	178.27(9)	C8	C9	C10	C11	0.34(17)
N2	Ni1	C1	C11	–5.88(8)	C13	C12	C11	C1	179.73(10)
N2	C12	C11	C1	0.71(12)	C13	C12	C11	C10	–0.25(18)
N2	C12	C11	C10	–179.26(10)	C19	C20	C21	C22	1.92(19)
N2	C12	C13	C14	2.36(16)	C19	C18	C23	C22	1.88(17)
N2	C16	C15	C14	1.15(17)	C20	C19	C18	C17	174.60(10)
N1	Ni1	C1	C7	0.19(8)	C20	C19	C18	C23	–1.94(17)
N1	Ni1	C1	C11	176.05(9)	C5	C6	C7	C1	–173.55(11)
N1	C6	C7	C1	5.04(13)	C5	C6	C7	C8	8.14(19)
N1	C6	C7	C8	–173.27(11)	C5	C4	C3	C2	–2.16(18)
N1	C6	C5	C4	1.89(17)	C2	N1	C6	C7	178.45(9)
N1	C2	C3	C4	1.21(18)	C2	N1	C6	C5	–2.86(15)
C17	C18	C23	C22	–174.64(11)	C18	C19	C20	C21	0.04(17)
C1	C7	C8	C9	0.23(16)	C23	C22	C21	C20	–2.0(2)
C1	C11	C10	C9	–0.26(15)	C21	C22	C23	C18	0.05(19)

Table 7-212 Hydrogen Atom Coordinates (Å×10^4) and Isotropic Displacement Parameters (Å^2×10^3) for [Ni(Py(Ph)Py)OBz].

Atom	*x*	*y*	*z*	U(eq)
H16	3882.81	1280.72	4343.26	20
H8	2722.81	9159.87	3011.46	22
H9	4491.25	9247.87	3034.88	22
H15	5579.59	553.95	4450.98	22
H13	6332.86	4747.88	3919.5	19
H19	2739.77	1134.01	6966.83	21
H20	2198.44	–997.12	7626.51	23
H5	850.86	8496.55	2936.22	24
H10	5523	7187.67	3438.57	20
H2	507.27	3862.8	4156.4	23
H14	6832.1	2315.48	4286.37	22
H22	620.58	–2194.74	5170.67	26
H23	1168.72	–44.81	4515.37	22
H4	–779.04	7641.45	3115.22	28
H21	1095.58	–2633.47	6729.6	26
H3	–940.15	5320.63	3776.7	27

7.3.31 [Ni(Py(Ph)Py)TFA]

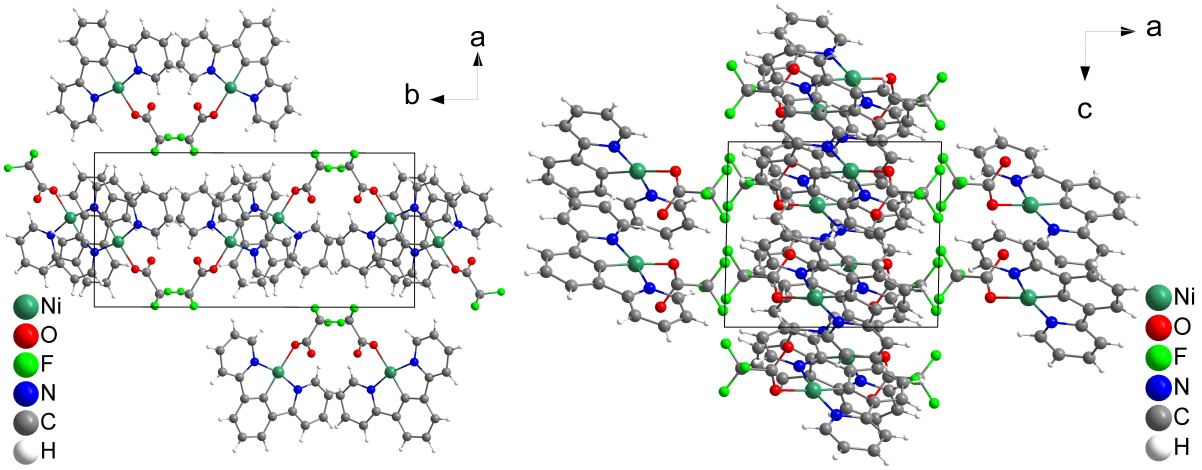

Figure 7-413 Crystal structure of [Ni(Py(Ph)Py)TFA] viewed along the crystallographic *c*- (left) and *b*-axis (right).

Table 7-213 Crystal data and structure refinement for [Ni(Py(Ph)Py)TFA].

Identification code	[Ni(Py(Ph)Py)TFA]
Empirical formula	$C_{18}H_{11}F_3N_2NiO_2$
Formula weight	403.00
Temperature/K	100.00
Crystal system	monoclinic
Space group	$P2_1/c$
a/Å	9.4616(3)
b/Å	19.6594(7)
c/Å	8.2274(2)
α/°	90
β/°	91.2160(10)
γ/°	90

Volume/Å^3	1530.03(8)
Z	4
ρ_{calc}g/cm^3	1.749
μ/mm^{-1}	1.318
F(000)	816.0
Crystal size/mm^3	0.4 × 0.2 × 0.05
Radiation	MoKα (λ = 0.71073)
2Θ range for data collection/°	4.144 to 56.61
Index ranges	–12 ≤ h ≤ 12, –26 ≤ k ≤ 26, –10 ≤ l ≤ 10
Reflections collected	41961
Independent reflections	3799 [R_{int} = 0.0843, R_{sigma} = 0.0350]
Data/restraints/parameters	3799/0/235
Goodness-of-fit on F^2	1.061
Final R indexes [I>=2σ (I)]	R_1 = 0.0453, wR_2 = 0.1114
Final R indexes [all data]	R_1 = 0.0578, wR_2 = 0.1191
Largest diff. peak/hole / e Å^{-3}	1.50/–0.56

Table 7-214 Fractional Atomic Coordinates (×10^4) and Equivalent Isotropic Displacement Parameters (Å^2×10^3) for [Ni(Py(Ph)Py)TFA]. U_{eq} is defined as 1/3 of the trace of the orthogonalized U_{IJ} tensor.

Atom	*x*	*y*	*z*	U(eq)
Ni1	5773.4(4)	4252.5(2)	6584.8(4)	14.73(12)
O1	7551(2)	3724.3(11)	6597(3)	25.2(5)
F3	8996(2)	2294.8(11)	7826(3)	48.5(6)
N1	6449(2)	4992.9(12)	7901(3)	14.8(4)
N2	4656(3)	3642.6(12)	5263(3)	17.2(5)
O2	6992(2)	3221.1(13)	8917(3)	33.4(6)
F2	9916(2)	3126.5(14)	9108(3)	53.9(7)
F1	9955(3)	3100.1(16)	6521(4)	65.6(9)
C17	7748(3)	3369.5(14)	7675(4)	19.7(6)
C7	4057(3)	5302.2(14)	7632(3)	16.3(5)
C6	5449(3)	5459.9(14)	8348(3)	15.2(5)
C11	2910(3)	4435.3(15)	5962(3)	17.8(5)
C1	4111(3)	4709.9(14)	6704(3)	16.0(5)
C5	5794(3)	5996.2(14)	9383(3)	17.3(5)
C8	2778(3)	5646.6(15)	7771(3)	19.7(6)
C12	3247(3)	3806.6(14)	5089(3)	16.9(5)
C4	7183(3)	6069.7(14)	9941(3)	19.4(6)
C16	5149(3)	3093.1(14)	4502(3)	20.1(6)
C13	2339(3)	3410.3(16)	4146(3)	22.0(6)
C2	7792(3)	5077.7(14)	8431(3)	17.3(5)
C14	2862(3)	2846.7(16)	3349(4)	24.6(6)
C3	8195(3)	5609.4(15)	9440(4)	19.7(6)
C15	4284(3)	2684.1(15)	3525(4)	22.9(6)
C9	1574(3)	5375.2(16)	7002(4)	21.7(6)
C10	1618(3)	4769.4(16)	6117(3)	21.0(6)
C18	9156(3)	2962.3(17)	7768(4)	27.4(7)

Table 7-215 Anisotropic Displacement Parameters (Å^2×10^3) for [Ni(Py(Ph)Py)TFA]. The Anisotropic displacement factor exponent takes the form: $-2\pi^2[h^2a^{*2}U_{11}+2hka^*b^*U_{12}+\ldots]$.

Atom	U_{11}	U_{22}	U_{33}	U_{23}	U_{13}	U_{12}
Ni1	13.82(18)	15.07(18)	15.29(19)	0.43(13)	0.02(12)	1.12(13)

Atom	U_{11}	U_{22}	U_{33}	U_{23}	U_{13}	U_{12}
O1	24.4(11)	25.3(11)	26.1(11)	–9.8(9)	8.5(9)	–6.5(9)
F3	41.8(13)	24.9(11)	78.6(18)	–0.1(11)	0.1(12)	10.5(9)
N1	15.4(11)	14.6(11)	14.5(11)	1.3(8)	1.8(8)	0.5(8)
N2	20.2(12)	17.7(11)	13.7(11)	3.9(9)	–0.5(8)	–1.5(9)
O2	26.6(12)	35.5(13)	38.5(14)	9.2(11)	12.5(10)	4.7(10)
F2	32.1(12)	65.7(17)	63.1(17)	–12.0(13)	–21.1(11)	5.3(11)
F1	41.9(14)	86(2)	70.5(18)	39.0(16)	32.3(13)	35.1(14)
C17	4.7(11)	15.9(13)	38.2(17)	–22.2(13)	–10.3(10)	7.1(9)
C7	17.3(13)	18.2(13)	13.5(12)	4.6(10)	1.9(10)	0.4(10)
C6	16.7(12)	16.2(12)	12.9(12)	4.8(10)	2.5(9)	–0.2(10)
C11	18.9(13)	21.3(13)	13.1(12)	5.0(10)	–0.5(10)	–0.2(10)
C1	16.1(12)	17.6(13)	14.3(12)	4.7(10)	0.8(9)	0.5(10)
C5	18.0(13)	17.7(13)	16.2(13)	1.1(10)	2.8(10)	1.5(10)
C8	19.6(14)	21.1(14)	18.4(13)	3.7(11)	1.7(10)	6.0(11)
C12	19.9(13)	18.2(13)	12.6(12)	5.7(10)	0.1(10)	–1.0(10)
C4	23.8(14)	15.4(13)	19.0(14)	0.6(10)	0.8(11)	–2.9(11)
C16	25.2(14)	17.1(13)	18.0(13)	2.6(11)	–1.0(11)	–1.4(11)
C13	23.6(14)	25.4(15)	16.9(13)	4.5(11)	–2.9(11)	–6.0(12)
C2	16.0(13)	18.5(13)	17.4(13)	1.6(10)	0.9(10)	1.1(10)
C14	31.8(16)	22.7(15)	19.0(14)	3.3(12)	–4.1(12)	–10.3(12)
C3	17.6(13)	21.0(14)	20.5(14)	2.9(11)	–2.4(10)	0.0(11)
C15	31.9(16)	17.9(14)	18.8(14)	1.3(11)	–0.3(11)	–1.2(12)
C9	15.3(13)	30.4(16)	19.4(14)	5.1(12)	–0.4(10)	6.3(11)
C10	16.8(13)	29.0(16)	17.2(13)	6.4(11)	–1.5(10)	–0.2(11)
C18	19.8(15)	28.3(16)	34.0(17)	3.8(13)	0.4(12)	3.5(12)

Table 7-216 Bond Lengths for [Ni(Py(Ph)Py)TFA].

Atom	Atom	Length/Å	Atom	Atom	Length/Å
Ni1	O1	1.977(2)	C7	C1	1.394(4)
Ni1	N1	1.916(2)	C7	C8	1.394(4)
Ni1	N2	1.921(2)	C6	C5	1.389(4)
Ni1	C1	1.817(3)	C11	C1	1.387(4)
O1	C17	1.140(4)	C11	C12	1.468(4)
F3	C18	1.322(4)	C11	C10	1.396(4)
N1	C6	1.374(3)	C5	C4	1.391(4)
N1	C2	1.344(4)	C8	C9	1.397(4)
N2	C12	1.377(4)	C12	C13	1.385(4)
N2	C16	1.338(4)	C4	C3	1.386(4)
O2	C17	1.293(4)	C16	C15	1.391(4)
F2	C18	1.343(4)	C13	C14	1.384(5)
F1	C18	1.316(4)	C2	C3	1.383(4)
C17	C18	1.555(4)	C14	C15	1.387(4)
C7	C6	1.464(4)	C9	C10	1.397(4)

Table 7-217 Bond Angles for [Ni(Py(Ph)Py)TFA].

Atom	Atom	Atom	Angle/°	Atom	Atom	Atom	Angle/°
N1	Ni1	O1	97.03(9)	C10	C11	C12	129.8(3)
N1	Ni1	N2	165.33(10)	C7	C1	Ni1	119.0(2)

Atom	Atom	Atom	Angle/°	Atom	Atom	Atom	Angle/°
N2	Ni1	O1	97.64(9)	C11	C1	Ni1	119.1(2)
C1	Ni1	O1	176.09(11)	C11	C1	C7	121.8(3)
C1	Ni1	N1	82.69(11)	C6	C5	C4	119.3(3)
C1	Ni1	N2	82.68(12)	C7	C8	C9	118.6(3)
C17	O1	Ni1	116.8(2)	N2	C12	C11	111.5(2)
C6	N1	Ni1	115.79(18)	N2	C12	C13	120.9(3)
C2	N1	Ni1	125.39(19)	C13	C12	C11	127.6(3)
C2	N1	C6	118.8(2)	C3	C4	C5	119.2(3)
C12	N2	Ni1	115.65(19)	N2	C16	C15	122.1(3)
C16	N2	Ni1	125.2(2)	C14	C13	C12	119.5(3)
C16	N2	C12	119.1(2)	N1	C2	C3	122.3(3)
O1	C17	O2	131.9(3)	C13	C14	C15	119.3(3)
O1	C17	C18	118.6(3)	C2	C3	C4	119.2(3)
O2	C17	C18	109.4(3)	C14	C15	C16	119.0(3)
C1	C7	C6	110.8(2)	C10	C9	C8	121.9(3)
C8	C7	C6	129.8(3)	C11	C10	C9	119.0(3)
C8	C7	C1	119.5(3)	F3	C18	F2	105.6(3)
N1	C6	C7	111.7(2)	F3	C18	C17	114.5(3)
N1	C6	C5	121.1(2)	F2	C18	C17	111.1(3)
C5	C6	C7	127.2(3)	F1	C18	F3	107.5(3)
C1	C11	C12	111.0(2)	F1	C18	F2	106.5(3)
C1	C11	C10	119.2(3)	F1	C18	C17	111.2(3)

Table 7-218 Torsion Angles for [Ni(Py(Ph)Py)TFA].

A	B	C	D	Angle/°	A	B	C	D	Angle/°
Ni1	O1	C17	O2	2.6(4)	C6	C5	C4	C3	0.6(4)
Ni1	O1	C17	C18	–177.92(19)	C11	C12	C13	C14	177.1(3)
Ni1	N1	C6	C7	–2.9(3)	C1	C7	C6	N1	1.0(3)
Ni1	N1	C6	C5	176.1(2)	C1	C7	C6	C5	–177.8(3)
Ni1	N1	C2	C3	–177.1(2)	C1	C7	C8	C9	1.6(4)
Ni1	N2	C12	C11	0.8(3)	C1	C11	C12	N2	1.5(3)
Ni1	N2	C12	C13	179.1(2)	C1	C11	C12	C13	–176.7(3)
Ni1	N2	C16	C15	–178.2(2)	C1	C11	C10	C9	0.6(4)
O1	C17	C18	F3	–121.7(3)	C5	C4	C3	C2	–1.7(4)
O1	C17	C18	F2	118.8(3)	C8	C7	C6	N1	–179.5(3)
O1	C17	C18	F1	0.4(4)	C8	C7	C6	C5	1.6(5)
N1	Ni1	C1	C7	–2.4(2)	C8	C7	C1	Ni1	–178.1(2)
N1	Ni1	C1	C11	–177.9(2)	C8	C7	C1	C11	–2.7(4)
N1	C6	C5	C4	1.6(4)	C8	C9	C10	C11	–1.7(4)
N1	C2	C3	C4	0.6(4)	C12	N2	C16	C15	0.6(4)
N2	Ni1	C1	C7	178.7(2)	C12	C11	C1	Ni1	–3.4(3)
N2	Ni1	C1	C11	3.1(2)	C12	C11	C1	C7	–178.8(2)
N2	C12	C13	C14	–0.9(4)	C12	C11	C10	C9	–178.9(3)
N2	C16	C15	C14	–0.7(4)	C12	C13	C14	C15	0.8(4)
O2	C17	C18	F3	57.9(4)	C16	N2	C12	C11	–178.1(2)
O2	C17	C18	F2	–61.6(3)	C16	N2	C12	C13	0.2(4)
O2	C17	C18	F1	180.0(3)	C13	C14	C15	C16	0.0(4)
C7	C6	C5	C4	–179.6(3)	C2	N1	C6	C7	178.4(2)
C7	C8	C9	C10	0.5(4)	C2	N1	C6	C5	–2.7(4)
C6	N1	C2	C3	1.5(4)	C10	C11	C1	Ni1	177.0(2)

A	B	C	D	Angle/°	A	B	C	D	Angle/°
C6	C7	C1	Ni1	1.4(3)	C10	C11	C1	C7	1.5(4)
C6	C7	C1	C11	176.8(2)	C10	C11	C12	N2	–178.9(3)
C6	C7	C8	C9	–177.8(3)	C10	C11	C12	C13	2.9(5)

Table 7-219 Hydrogen Atom Coordinates (Å×10^4) and Isotropic Displacement Parameters (Å^2×10^3) for [Ni(Py(Ph)Py)TFA].

Atom	*x*	*y*	*z*	U(eq)
H5	5087.89	6309.18	9705.62	21
H8	2725.61	6057.24	8374.78	24
H4	7436.02	6430.91	10656.65	23
H16	6120.04	2978.55	4631.92	24
H13	1365.71	3524.4	4047.19	26
H2	8488.18	4761.39	8100.52	21
H14	2252.76	2573.89	2687.1	29
H3	9153.63	5658.47	9785.23	24
H15	4660.71	2299.27	2986.86	27
H9	699.58	5609.37	7083.75	26
H10	781.37	4587.62	5628.02	25

7.4 Cyclic Voltammetry

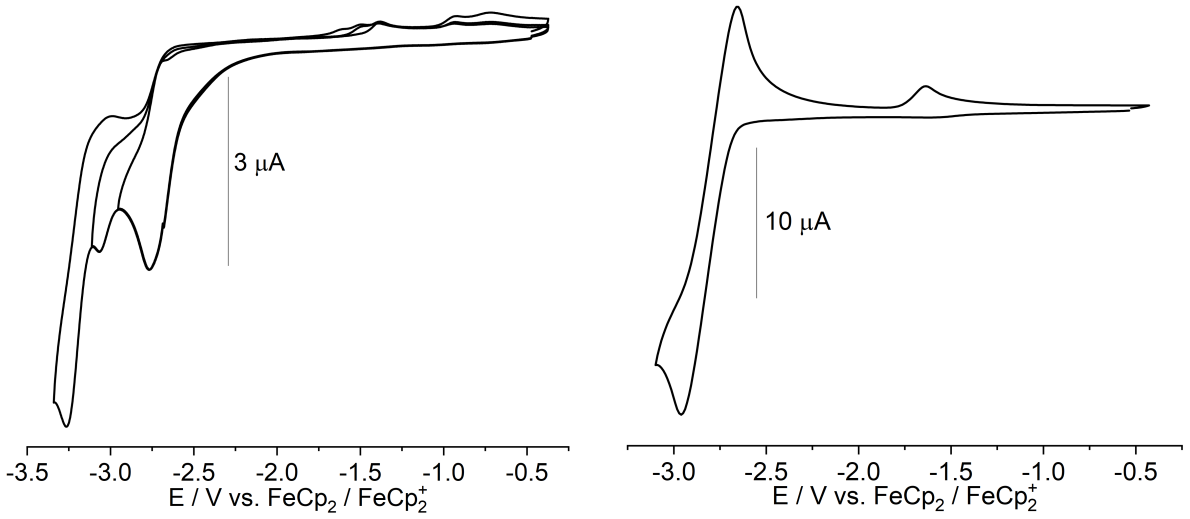

Figure 7-414 Cyclic voltammograms of Py(5PhPhH)Py (left) and Py(5MeOPhH)Py (right) in 0.1M *n*Bu$_4$NPF$_6$ / THF at a feed rate of 100 mV/s.

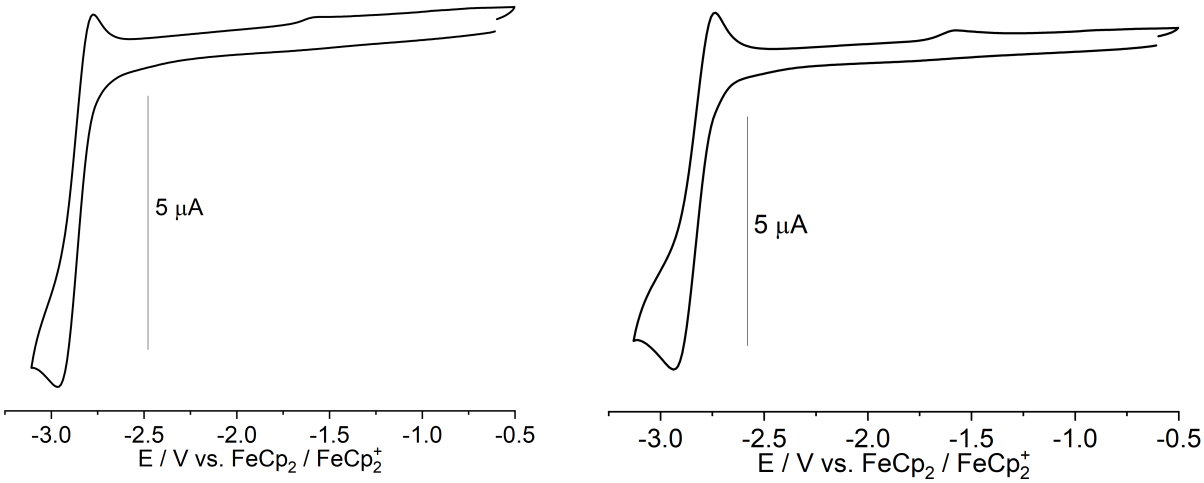

Figure 7-415 Cyclic voltammograms of Py(5BuPhH)Py (left) and Py(5MePhH)Py (right) in 0.1M nBu$_4$NPF$_6$ / THF at a feed rate of 100 mV/s.

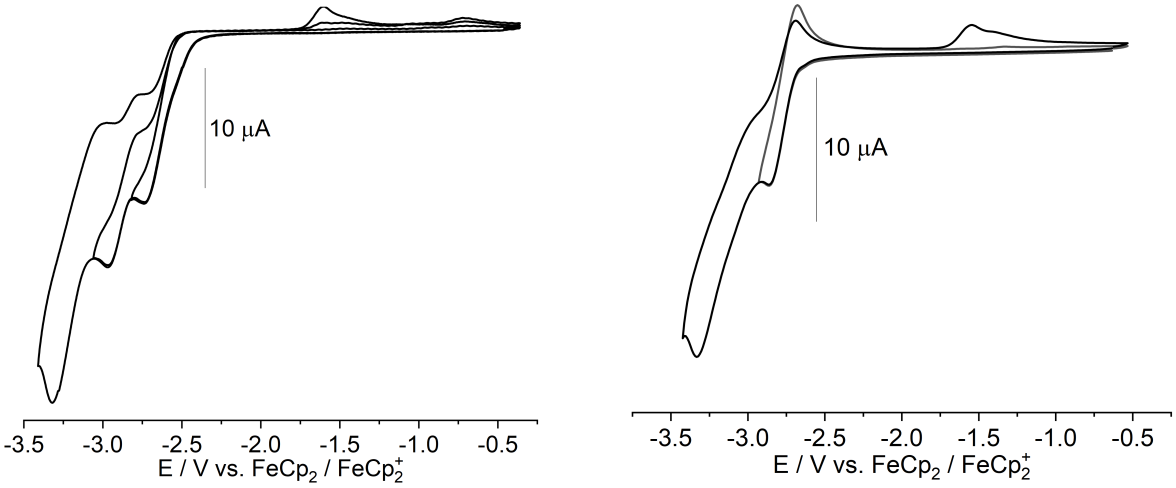

Figure 7-416 Cyclic voltammograms of Py(5CF$_3$PhH)Py (left) and Py(4FPhH)Py (right) in 0.1M nBu$_4$NPF$_6$ / THF at a feed rate of 100 mV/s.

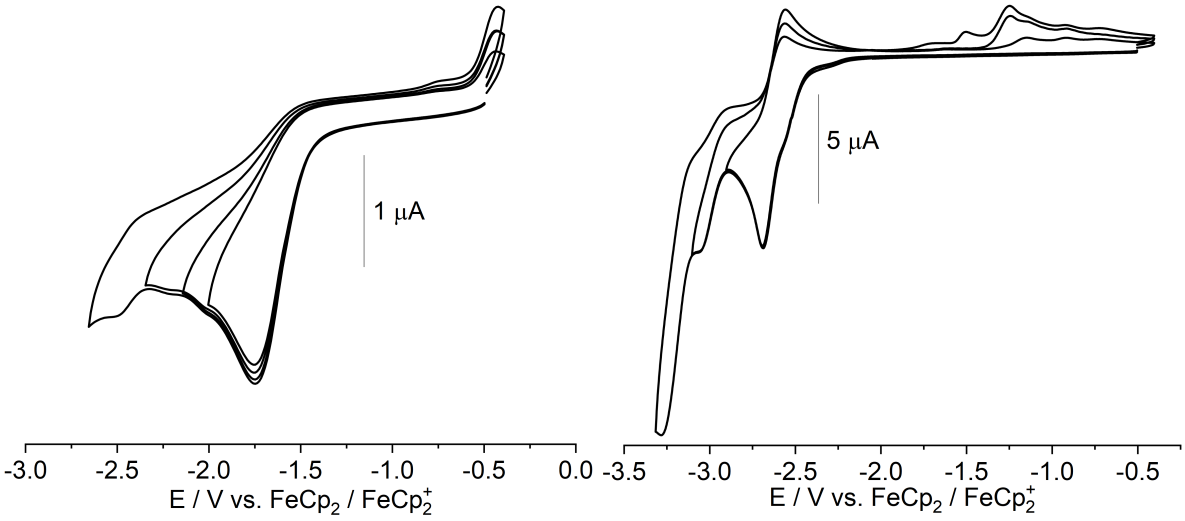

Figure 7-417 Cyclic voltammograms of Py(4,6MePhH)Py in 0.1M nBu$_4$NPF$_6$ / CH_2Cl_2 (left) and Py(PyH)Py in 0.1M nBu$_4$NPF$_6$ / THF (right) at a feed rate of 100 mV/s.

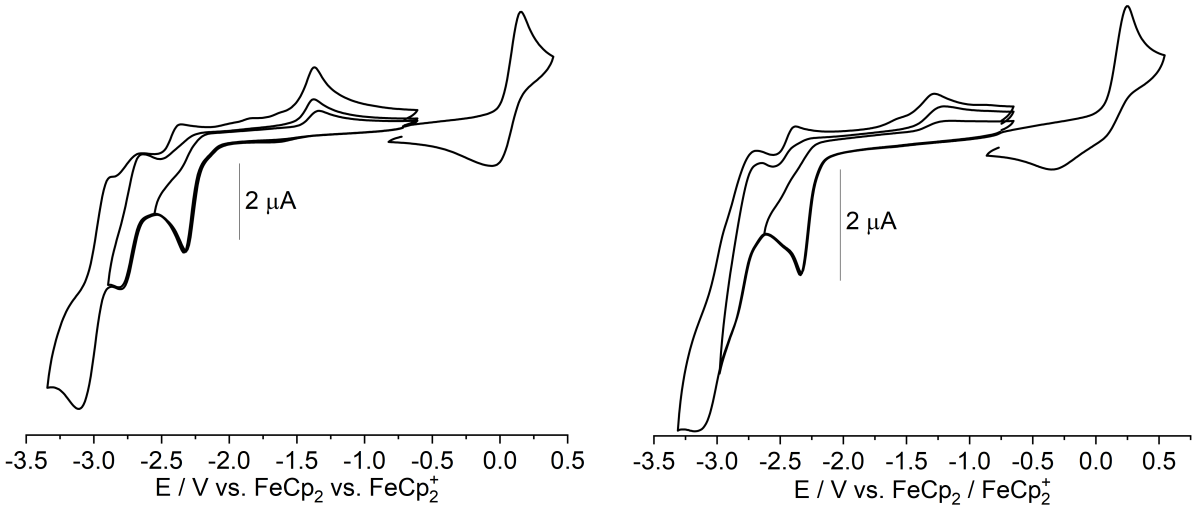

Figure 7-418 Cyclic voltammograms of [Ni(Py(5MeOPh)Py)Br] (left) and [Ni(Py(5BuPh)Py)Br] (right) in 0.1M *n*Bu_4NPF_6 / THF at a feed rate of 100 mV/s.

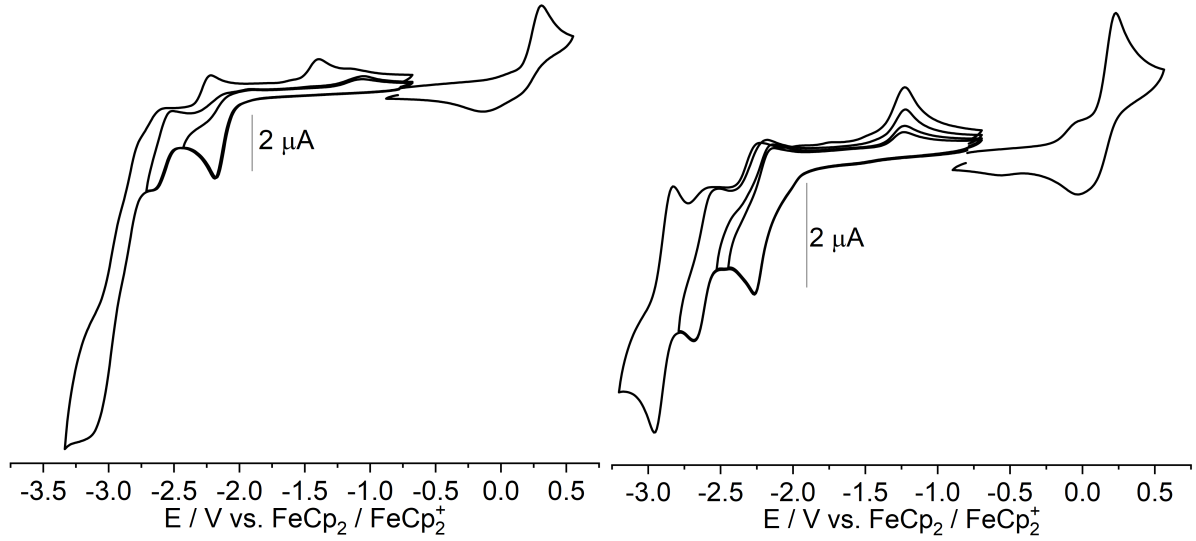

Figure 7-419 Cyclic voltammograms of [Ni(Py(5CF_3Ph)Py)Br] (left) and [Ni(Py(5FPh)Py)Br] (right) in 0.1M *n*Bu_4NPF_6 / THF at a feed rate of 100 mV/s.

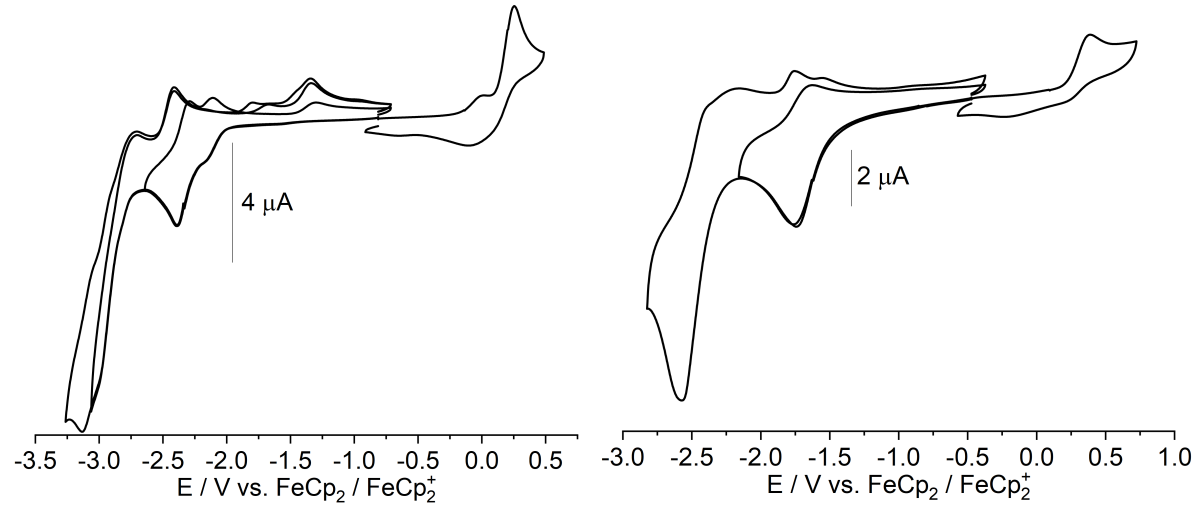

Figure 7-420 Cyclic voltammograms of [Ni(Py(4,5,6MeOPh)Py)Br] (left) and [Ni(Py(5NO_2Ph)Py)Br] (right) in 0.1M *n*Bu_4NPF_6 / THF at a feed rate of 100 mV/s.

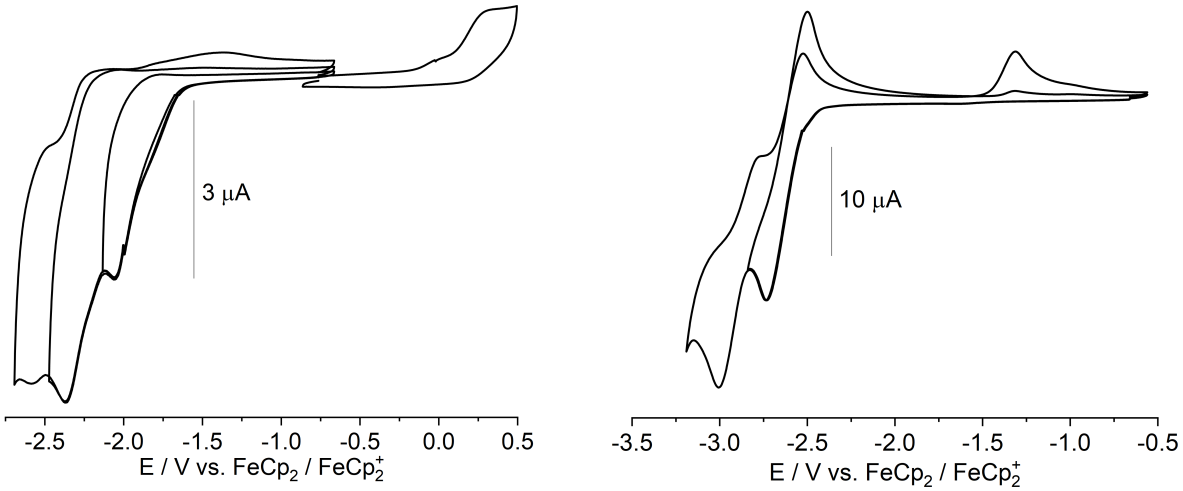

Figure 7-421 Cyclic voltammogram of [Ni(Py(Py)Py)Br] (left) and Pym(PhH)Pym (right) in 0.1M nBu$_4$NPF$_6$ / THF at a feed rate of 100 mV/s.

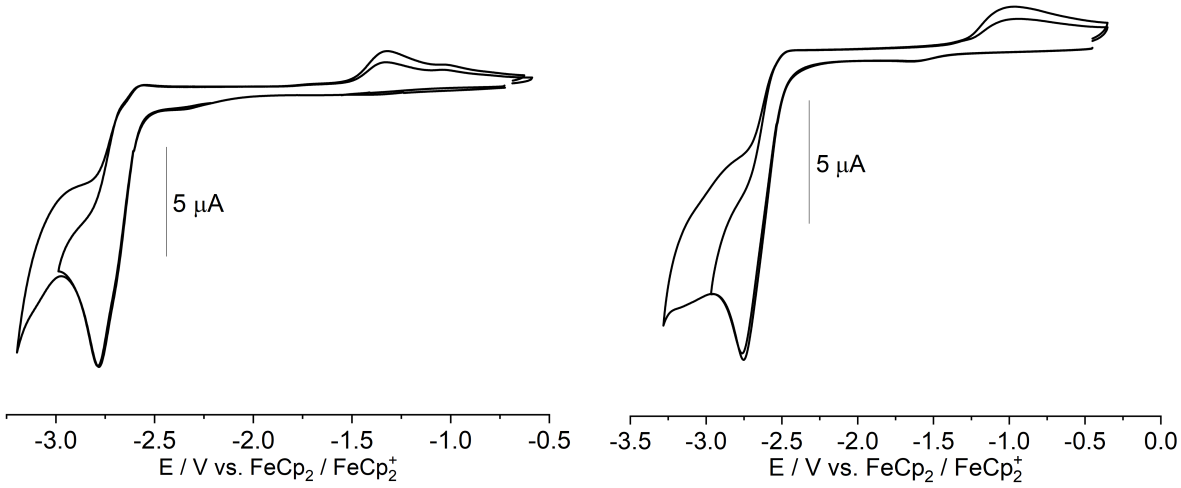

Figure 7-422 Cyclic voltammogram of 2^{i}Qu(PhH)2^{i}Qu (left) and 2^{i}Qu(4,6FPhH)2^{i}Qu (right) in 0.1M nBu$_4$NPF$_6$ / THF at a feed rate of 100 mV/s.

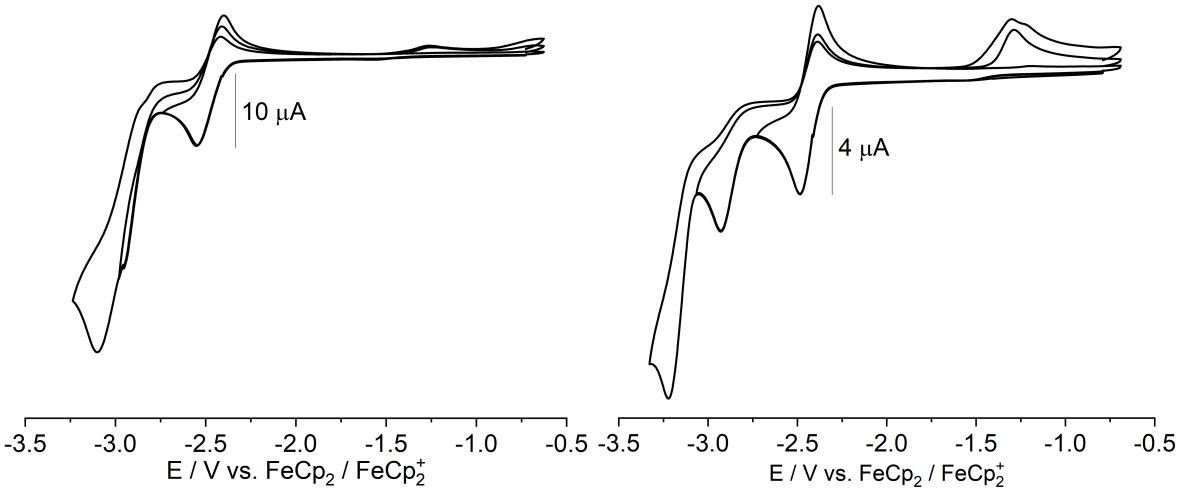

Figure 7-423 Cyclic voltammogram of 2Qu(PhH)Py (left) and 2Btz(PhH)Py (right) in 0.1M nBu$_4$NPF$_6$ / THF at a feed rate of 100 mV/s.

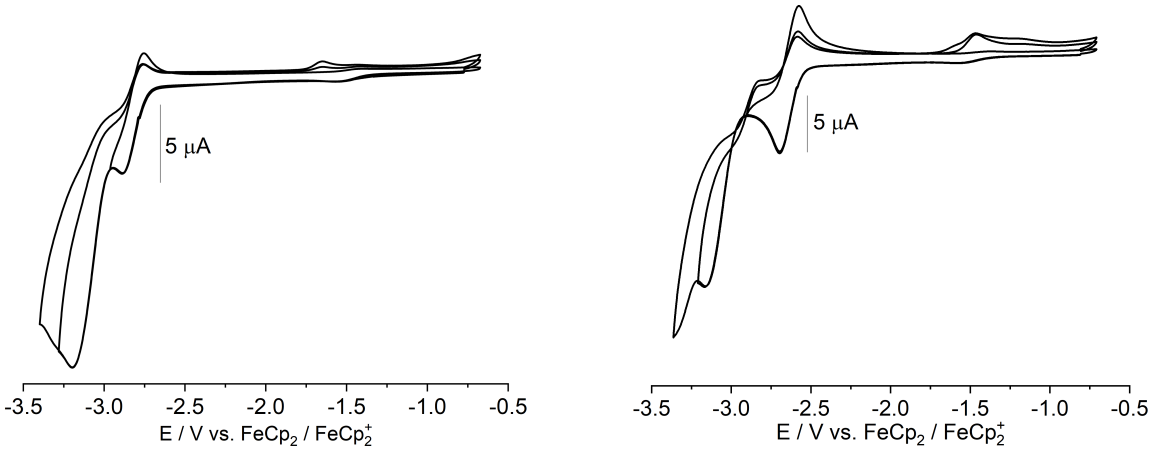

Figure 7-424 Cyclic voltammogram of 4Tz(PhH)Py (left) and 2Tz(PhH)Py (right) in 0.1M nBu$_4$NPF$_6$ / THF at a feed rate of 100 mV/s.

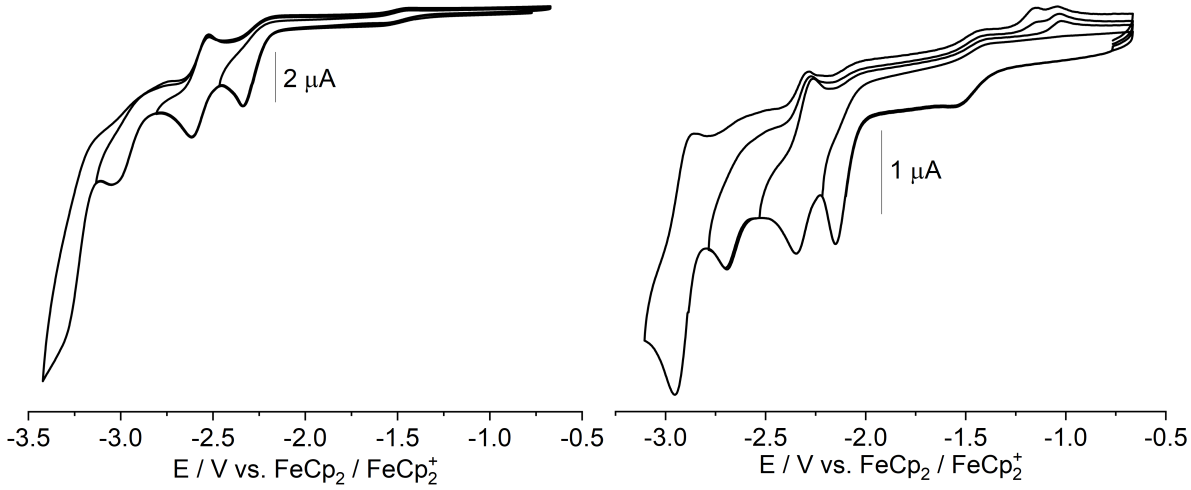

Figure 7-425 Cyclic voltammogram of 2Tz(PhCl)2Tz (left) and 2Btz(PhCl)2Btz (right) in 0.1M nBu$_4$NPF$_6$ / THF at a feed rate of 100 mV/s.

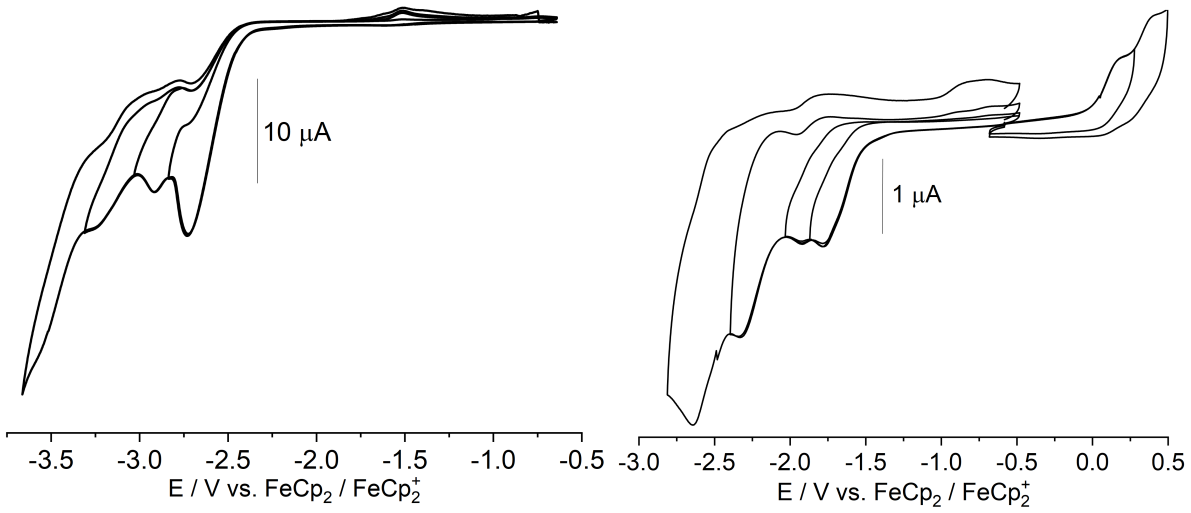

Figure 7-426 Cyclic voltammogram of 3ClPy(PhH)3ClPy (left) and [Ni(Pz(Ph)Pz)Br] (right) in 0.1M nBu$_4$NPF$_6$ / THF at a feed rate of 100 mV/s.

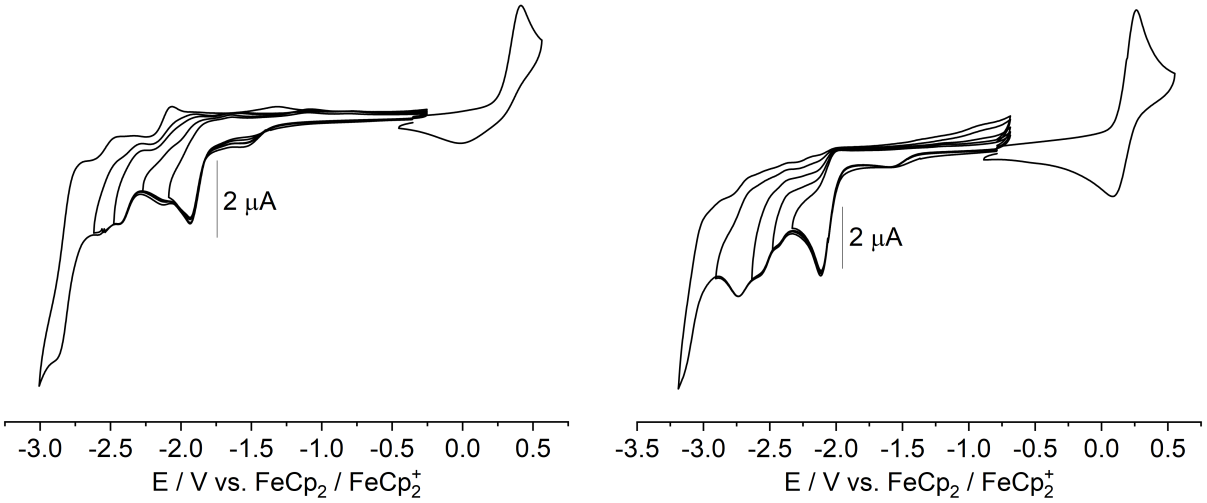

Figure 7-427 Cyclic voltammogram of [Ni(3FPy(4,6FPh)3FPy)Br] (left) and [Ni(2Tz(Ph)2Tz)Cl] (right) in 0.1M nBu$_4$NPF$_6$ / THF at a feed rate of 100 mV/s.

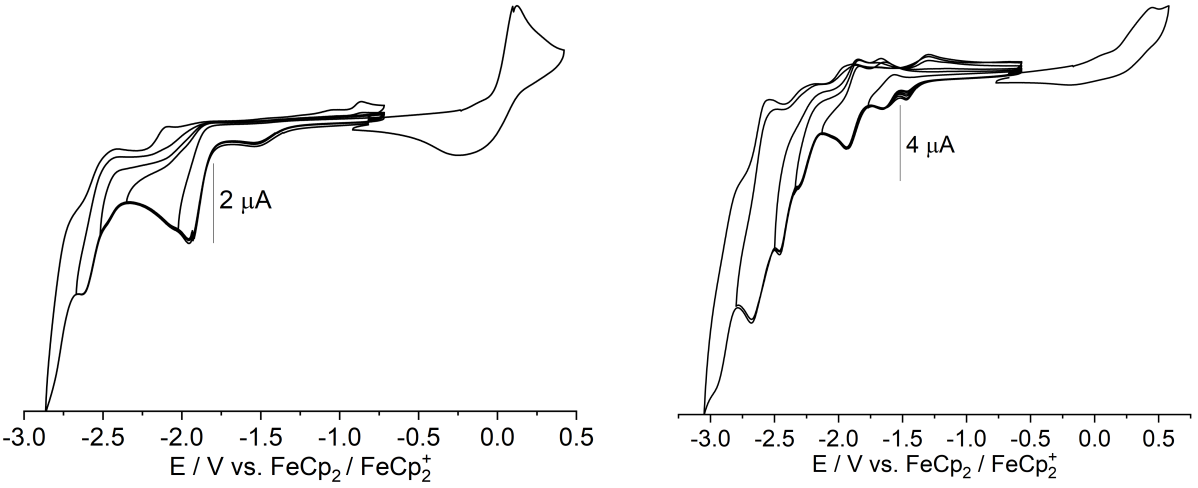

Figure 7-428 Cyclic voltammogram of [Ni(2Btz(Ph)Py)Br] (left) and [Ni(2^{i}Qu(4,6FPh)2^{i}Qu)Br] (right) in 0.1M nBu$_4$NPF$_6$ / THF at a feed rate of 100 mV/s.

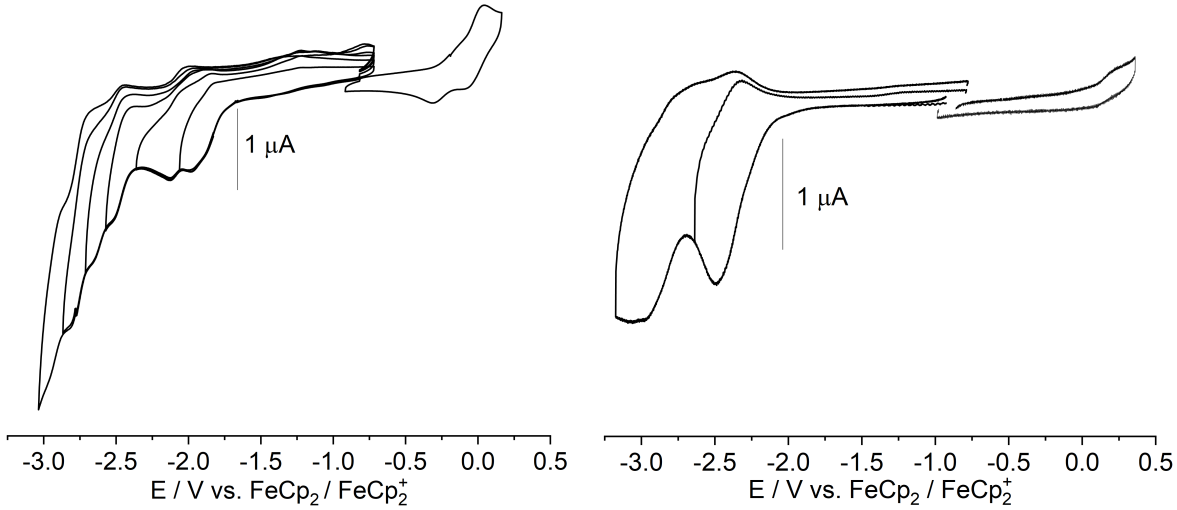

Figure 7-429 Cyclic voltammogram of [Ni(2Qu(Ph)Py)Br] (left) and [Ni(Py(Ph)Py)C$_2$F$_5$] (right) in 0.1M nBu$_4$NPF$_6$ / THF at a feed rate of 100 mV/s.

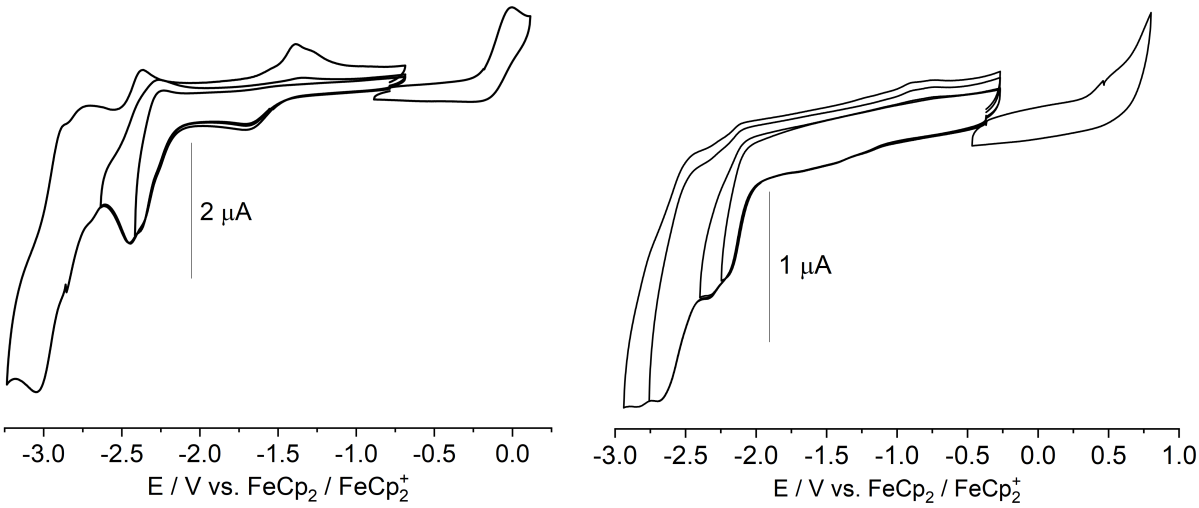

Figure 7-430 Cyclic voltammogram of [Ni(Py(Ph)Py)OAc] (left) and [Pt(Py(Ph)Py)CN] (right) in 0.1M nBu$_4$NPF$_6$ / THF at a feed rate of 100 mV/s.

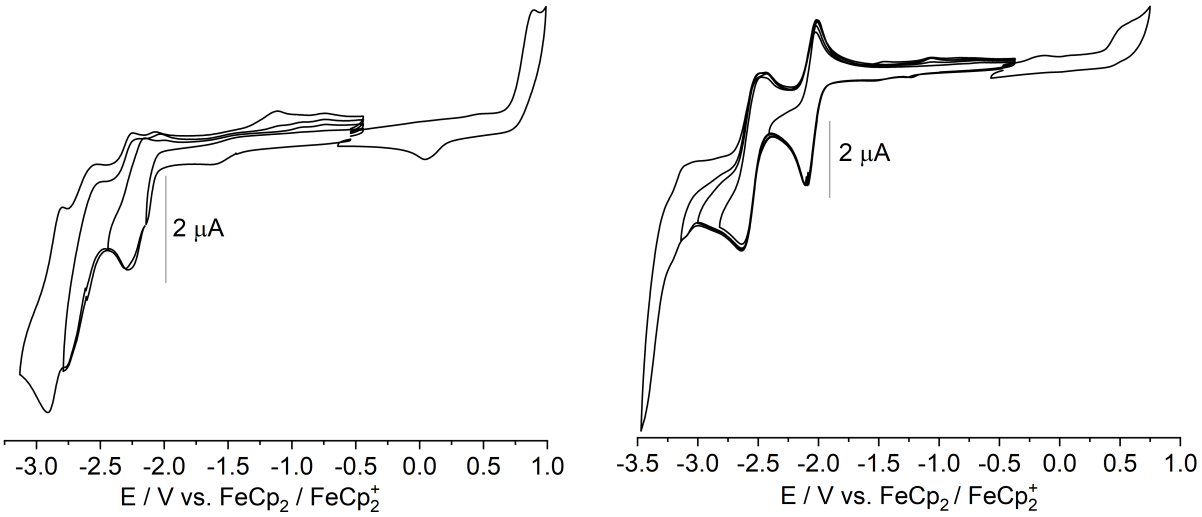

Figure 7-431 Cyclic voltammogram of [Pd(Py(4,6FPh)Py)Cl] (left) and [Pt(Py(4,6FPh)Py)Cl] (right) in 0.1M nBu$_4$NPF$_6$ / THF at a feed rate of 100 mV/s.

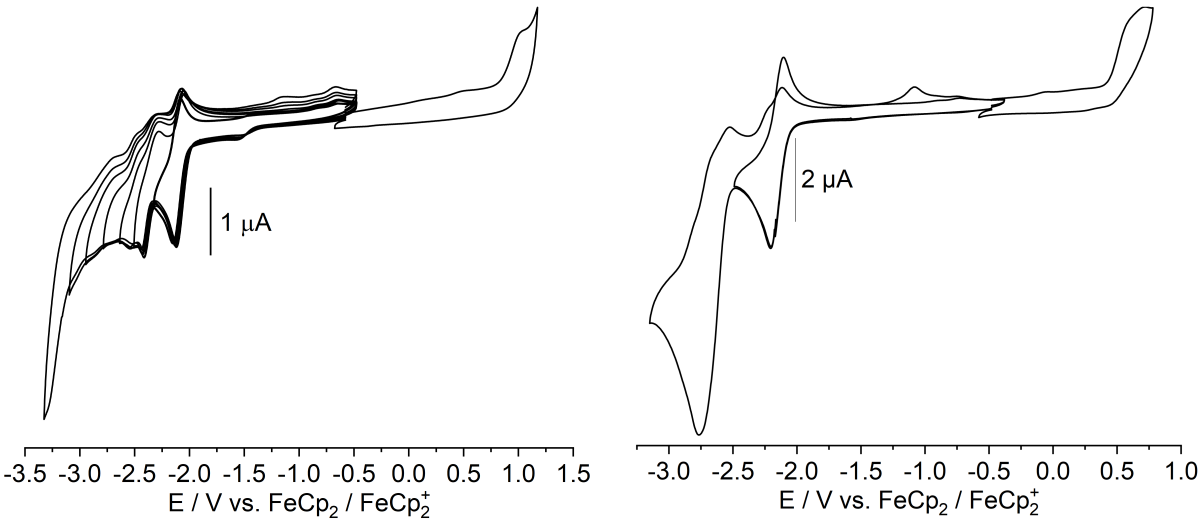

Figure 7-432 Cyclic voltammogram of [Pd(Py(4,6FPh)Py)CN] (left) and [Pt(Py(4,6FPh)Py)CN] (right) in 0.1M nBu$_4$NPF$_6$ / THF at a feed rate of 100 mV/s.

7.5 UV/vis Spectra

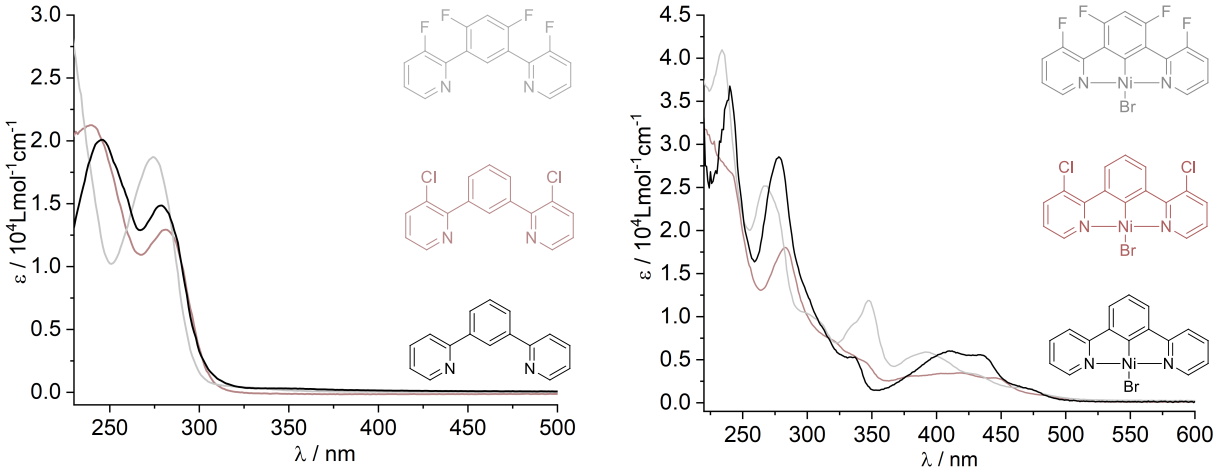

Figure 7-433 UV/vis spectra of 3FPy(4,6FPhH)3FPy and 3ClPy(PhH)3ClPy and their corresponding Ni(II) bromido complexes in comparison to the standard ligand Py(PhH)Py, respectively the standard complex [Ni(Py(Ph)Py)Br] measured in THF at rt.

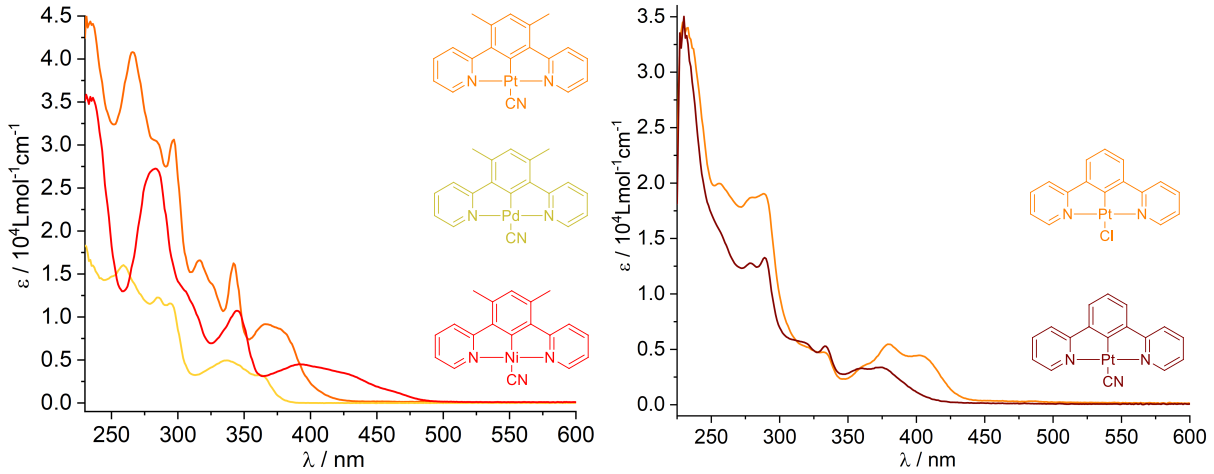

Figure 7-434 Left: UV/vis spectra of [M(Py(4,6MePh)Py)CN] (M = Ni (red), Pd (yellow) and Pt (orange)). Right: UV/vis spectra of [Pt(Py(Ph)Py)CN] and its chlorido precursor. All spectra were measured in CH_2Cl_2 at rt.

Erklärung zur Dissertation

gemäß der Promotionsordnung vom 12. März 2020

„Hiermit versichere ich an Eides statt, dass ich die vorliegende Dissertation selbstständig und ohne die Benutzung anderer als der angegebenen Hilfsmittel und Literatur angefertigt habe. Alle Stellen, die wörtlich oder sinngemäß aus veröffentlichten und nicht veröffentlichten Werken dem Wortlaut oder dem Sinn nach entnommen wurden, sind als solche kenntlich gemacht. Ich versichere an Eides statt, dass diese Dissertation noch keiner anderen Fakultät oder Universität zur Prüfung vorgelegen hat; dass sie - abgesehen von unten angegebenen Teilpublikationen und eingebundenen Artikeln und Manuskripten - noch nicht veröffentlicht worden ist sowie, dass ich eine Veröffentlichung der Dissertation vor Abschluss der Promotion nicht ohne Genehmigung des Promotionsausschusses vornehmen werde. Die Bestimmungen dieser Ordnung sind mir bekannt. Darüber hinaus erkläre ich hiermit, dass ich die Ordnung zur Sicherung guter wissenschaftlicher Praxis und zum Umgang mit wissenschaftlichem Fehlverhalten der Universität zu Köln gelesen und sie bei der Durchführung der Dissertation zugrundeliegenden Arbeiten und der schriftlich verfassten Dissertation beachtet habe und verpflichte mich hiermit, die dort genannten Vorgaben bei allen wissenschaftlichen Tätigkeiten zu beachten und umzusetzen. Ich versichere, dass die eingereichte elektronische Fassung der eingereichten Druckfassung vollständig entspricht."

Teilpublikationen:

1. „Luminescence of Ni(II), Pd(II), and Pt(II) complexes [M(Me_2dpb)Cl] obtained from C–H activation of 1,5-di(2-pyridyl)–2,4-dimethylbenzene (Me_2dpbH)", L. Kletsch, R. Jordan, A. S. Köcher, S. Buss, C. A. Strassert, A. Klein, *Molecules* **2021**, *26*, 5051 (1–20). DOI: 10.3390/molecules26165051.

2. "C–H Metalation of Terpyridine-Stereoisomers with Ni(II), Pd(II), and Pt(II)", L. Payen, L. Kletsch, T. Lapic, M. Wickleder, A. Klein, *Inorganics* **2023**, *11*, 174. DOI: 10.3390/inorganics11040174.

Köln, 05.05.2024, Lukas Daniel Kletsch

Datum, Name und Unterschrift

Curriculum Vitae

Personal Data

Name	Lukas Daniel Kletsch
Date / Place of Birth	23. November 1994, Cologne, Germany
Nationality	German

Education

08/2001 – 07/2005	Peter-Petersen-**Grundschule**, Cologne
08/2005 – 06/2013	Rhein-**Gymnasium**, Cologne
10/2009 – 04/2010	Participant of „**Schüler an der Universität“** – Module Participation „Inorganic Chemistry“ including a practical training at the Chempark Leverkusen

Higher Education

10/2013 – 03/2017	**Bachelor of Science** in Chemistry at University of Cologne, Grade: 1.9 **Bachelorthesis**: α-Diimin-Nickel(II) Komplexe mit elektronenarmen Aryl-coliganden (Prof. Dr. A. Klein)
04/2017 – 03/2020	**Master of Science** in Chemistry at University of Cologne, Grade: 1.4 **Masterthesis**: C–H Activation for Cyclometalated Nickel(II) Complexes with a Tridentate Carbanionic N^C^N-Ligand (Prof. Dr. A. Klein)
10/2013 – 03/2020	**Scholarship** - Talent Program from Cusanuswerk e.V.

Ph. D. Studies

06/2020 – 07/2024	**Ph. D. Studies** at the Institute for Inorganic Chemistry at University of Cologne under Supervision of Prof. Dr. Axel Klein Topic: Tridentate N^C^N Ligands in Organonickel(II) Complexes for C–C Cross coupling Catalysis **Scholarship** - Talent Program from Cusanuswerk e.V.
07/2022	**Head of Conference** at the 5th Ligand Design Workshop 2022 in Cologne, Germany
06/2023 – 10/2023	**Research Stay** at Lehigh University, PA, USA for Application Test in a Collaboration with Prof. Dr. D. A. Vicic

Professional Occupation

07/2013 – 09/2013	**Working Student** at Polymaterials AG, Chempark Leverkusen Germany
09/2019 – 03/2024	**Research / Teaching Assistant** at Cologne University for Prof. Dr. A. Klein

Conference Presentations

02.03.2020	**16th KCT in Freiburg, Germany. Awarded Poster**: C–H Activation for Cyclometalated Ni(II) Complexes with Tridentate N^C^N Ligands: [Ni(PyPhPy)X] (X = Cl, Br, I) and its Spectroscopical and Electrochemical Properties
26.07.2021	**4th Ligand Design Workshop in Cologne, Germany – Presentation:** Tridentate N^C^N Ligands in Organonickel(II) Complexes for C–C Cross Coupling Catalysis and Luminescent Applications
27.02.2024	**18th KCT in Innsbruck, Austria – Presentation:** Tridentate N^C^N Ligands in Cyclometalated Ni(II) Complexes for C–C Cross Coupling Catalysis

8 Publications

1. Cyclometalated Ni(II) complexes [Ni(N^C^N)X] of the tridentate 2,6-di(2-pyridyl)-phenide ligand, L. Kletsch, G. Hörner, A. Klein, *Organometallics* **2020**, *39*, 2820−2829. DOI: 10.1021/acs.organomet.0c00355.

2. „Luminescence of Ni(II), Pd(II), and Pt(II) complexes [M(Me_2dpb)Cl] obtained from C–H activation of 1,5-di(2-pyridyl)–2,4-dimethylbenzene (Me_2dpbH)", L. Kletsch, R. Jordan, A. S. Köcher, S. Buss, C. A. Strassert, A. Klein, *Molecules* **2021**, *26*, 5051 (1–20). DOI: 10.3390/molecules26165051.

3. "On the Role of the X Coligands in Cyclometalated [Ni(Phbpy)X] Complexes (HPhbpy = 6-phenyl–2,2'-bipyridine), N. Vogt, A. Sandleben, L. Kletsch, S. Schäfer, M. T. Chin, D. A. Vicic, G. Hörner, A. Klein, *Organometallics* **2021**, *40*, 1776−1785. DOI: 10.1021/acs.organomet.1c00237.

4. „Switching from energy transfer to electron transfer photocatalysis (PenT – PET): an unexpected oxidative cleavage of cyclobutanes alters the product composition with irradiation time, J. Lefarth, A. Haseloer, L. Kletsch, A. Klein, J. Neudörfl, A. G. Griesbeck, *Chem. Commun.* **2022**, *58*, 12999–13002. DOI: 10.1039/D2CC04693H.

5. "Hydrido nickel(II) complexes [Ni(C^N^N)H] and [Ni(N^C^N)H] with cyclometalated C^N^N or N^C^N ligands", L. Kletsch, L. Payen, A. Fiorentino, G. Hörner, B. Blom, D. Romano, A. Klein, *Organometallics* **2023**, *42*, 2206–2215. DOI: 10.1021/acs.organomet.3c00191.

6. "C–H Metalation of Terpyridine-Stereoisomers with Ni(II), Pd(II), and Pt(II)", L. Payen, L. Kletsch, T. Lapic, M. Wickleder, A. Klein, *Inorganics* **2023**, *11*, 174. DOI: 10.3390/inorganics11040174.

7. Luminescent Platinum(II) Complexes with a Tridentate Caffeine-Based NHC-Pincer Ligand: Synthesis, Electrochemistry and Photophysics, O. Bysewski, N. Klosterhalfen, R. Jordan, L. Kletsch, A. Winter, A. Klein, B. Dietzek-Ivansic, U. S. Schubert, *Eur. J. Inorg. Chem.* **2024**, 27, e202300620. DOI: https://doi.org/10.1002/ejic.202300620.

8. Cyanido-bridged diplatinum(II) complexes: ligand and solvent effect on aggregation and luminescence, V. V. Khistiaeva, S. Buss, T. Eskelinen, P. Hirva, N. Kinnunen, J. Friedel, L. Kletsch, A. Klein, C. A. Strassert, I. O. Koshevoy, *Chem. Sci.*, **2024,** *15*, 4005–4018. DOI: https://doi.org/10.1039/D3SC06941A.

9. Nickel Perfluoroalkyl Complexes Supported by Simple Acetate Co-Ligands C. M. Ravidas, S. Shreiber, L. Kletsch, A. Klein, D. A. Vicic, *Organometallics* **2024**, *43,* 6, 706–712. DOI: https://doi.org/10.1021/acs.organomet.4c00029.